Sea Ice

Second Edition

Edited by

David N. Thomas[*] **and Gerhard S. Dieckmann**[†]
[*]School of Ocean Sciences, College of Natural Sciences,
Bangor University, UK
[†]Alfred Wegener Institute for Polar and Marine Research,
Bremerhaven, Germany

This page intentionally left blank

Sea Ice

As in the previous edition of this work, this book is dedicated to all the ships' crews, air support teams, field station/base crews and the myriad of other people associated with the logistic support that makes sea ice research possible. Albeit beautiful, these are hostile parts of planet Earth in which to work and we are mindful of those who have lost their lives in the pursuit of scientific endeavour and excellence. Beyond our colleagues our families and friends have had to come to terms with us being at the *ends of the earth*, often for long periods of time. In most cases they never get to experience, first hand, the wonders we have seen and it is only right that this book is also dedicated to them.

Antarctic fast ice floes breaking up (pen and ink by David Thomas, 2007). We of course are driven by scientific curiosity to understand the processes that drive the physics, biology and geology of frozen oceans and seas. We are also partially drawn to these regions because of the extreme beauty and mystery of these isolated realms. Have a look at: Buckland, D., MacClip, A. & Parkinson, S. (Eds.) (2006) *Burning Ice: Art & Climate Change.* Cape Farewell Press, London, and Faithfull, S. (2006) *Ice Blink: An Antarctic Essay.* Book Works & The Arts Catalyst, London.

Sea Ice

Second Edition

Edited by

David N. Thomas[*] and Gerhard S. Dieckmann[†]
[*]School of Ocean Sciences, College of Natural Sciences,
Bangor University, UK
[†]Alfred Wegener Institute for Polar and Marine Research,
Bremerhaven, Germany

Contents

Contributors

David G. Ainley
H.T. Harvey & Associates, 983 University Avenue, Los Gatos, CA 95118. USA

Leanne K. Armand
Australian Antarctic Division and Antarctic Climate and Ecosystems Cooperative Research Centre (ACE CRC), Private Bag 80, c/o University of Tasmania, Sandy Bay, Tasmania 7001. Australia
(New address: Climate Risk CORE – Department of Biological Sciences, Macquarie University, North Ryde, NSW, 2109. Australia)

Kevin R. Arrigo
Department of Geophysics, Mitchell Building, Stanford University, Stanford, CA 94305-2215. USA

Bodil A. Bluhm
School of Fisheries & Ocean Sciences, University of Alaska Fairbanks, P.O. Box 757220, Fairbanks, AK 99775-7220. USA

Mark A. Brandon
Department of Earth Sciences, The Open University, Walton Hall, Milton Keynes, MK7 6AA. UK

David A. Caron
Department of Biological Sciences, University of Southern California, 3616 Trousdale Parkway, Los Angeles, CA 90089-0371. USA

Josefino C. Comiso
Cryospheric Sciences Branch, Code 614.1, NASA Goddard Space Flight Center, Greenbelt, MD 20771. USA

Finlo R. Cottier
Scottish Association for Marine Science, Dunstaffnage Marine Laboratory, Oban, Argyll, PA37 1QA. UK

Jody W. Deming
School of Oceanography, University of Washington, Campus Box 357940, Seattle, WA 98195-7940. USA

Gerhard S. Dieckmann
Alfred Wegener Institute for Polar & Marine Research, Am Handelshafen 12, D-27570 Bremerhaven. Germany

Hajo Eicken
Geophysical Institute, University of Alaska Fairbanks, P.O. Box 757320, Fairbanks, AK 99775-7320. USA

Rebecca J. Gast
Department of Biology, Woods Hole Oceanographic Institution, Woods Hole, MA 02543. USA

Rolf R. Gradinger
School of Fisheries & Ocean Sciences, University of Alaska Fairbanks, P.O. Box 757220, Fairbanks, AK 99775-7220. USA

Mats A. Granskog
Norwegian Polar Institute, Polar Environmental Centre, 9296 Tromsø. Norway.

Christian Haas
Department of Earth & Atmospheric Sciences, 1-26 Earth Sciences Building, University of Alberta, Edmonton, Alberta. T6G 2E3. Canada

Hartmut H. Hellmer
Alfred Wegener Institute for Polar & Marine Research, Bussestrasse, D-27570 Bremerhaven. Germany

Hermanni Kaartokallio
Finnish Environment Institute, P.O. Box 140, FI-00251 Helsinki. Finland

Harri Kuosa
Tvärminne Zoological Station, University of Helsinki, J.A. Palménin tie 260, FI-10900 Hanko. Finland

Amy Leventer
Department of Geology, Colgate University, 13 Oak Drive, Hamilton, NY-13346. USA

Michael P. Lizotte
Department of Biology & Microbiology, University of Wisconsin Oshkosh, 800 Algoma Boulevard, Oshkosh WI 54901. USA

Robert A. Massom
Australian Antarctic Division and Antarctic Climate and Ecosystems Cooperative Research Centre (ACE CRC), Private Bag 80, c/o University of Tasmania, Sandy Bay, Tasmania 7001. Australia

Christine Michel
Freshwater Institute, 501 University Crescent, Winnipeg, Manitoba, R3T 2N6. Canada

Thomas Mock
School of Environmental Sciences, University of East Anglia, Norwich, NR4 7TJ. UK

Frank Nilsen
The University Centre in Svalbard (UNIS), P.O. Box 156, N-9171 Longyearbyen. Norway

Stathys Papadimitriou
School of Ocean Sciences College of Natural Sciences, Bangor University, Menai Bridge, Anglesey LL59 5AB. UK

Chris Petrich
Geophysical Institute, University of Alaska Fairbanks, 903 Koyukuk Drive, P.O. Box 757320, Fairbanks, AK 99775-7320. USA

Sigrid B. Schnack-Schiel
Alfred Wegener Institute for Polar & Marine Research, Columbusstr. D-27568 Bremerhaven. Germany

Ian Stirling
Wildlife Research Division, Science & Technology Branch, Environment Canada, 5320 122 Street NW, Edmonton, AB T6H 3S5. Canada

Matthew Sturm
USA-CRREL-Alaska, P.O. Box 35170, Ft. Wainwright, Alaska 99703-0170. USA

David N. Thomas
School of Ocean Sciences, College of Natural Sciences, Bangor University, Menai Bridge, Anglesey LL59 5AB. UK

Cynthia T. Tynan
Associated Scientists at Woods Hole, P.O. Box 438, West Falmouth, MA 02574. USA

John S. Wettlaufer
Geophysics and Physics, Yale University, New Haven, CT 06520-8109. USA

This page intentionally left blank

Foreword

The study of sea ice, as the authors of the first chapter have detailed, has had a lengthy history although it is notable that until recent times, it has not been particularly unified. In the past, sea ice research fell between glaciology and oceanography as a physical science discipline, and, other than the ice cover entombing the ocean from life activity during winter, sea ice research did not have very much involvement from the life sciences. This paradigm has changed in the last 40 years, and, in my own involvement with sea ice science, I have been privileged to watch and participate in the explosive growth in its study and in its broadening perspective to include climate, whole ecosystems and biogeochemistry with important interactive features that affect marine processes in completely unique and important ways.

Some serendipity is involved with everyone's career path: My first encounter with career fate was in being assigned to the US Army Cold Regions Research and Engineering Laboratory (CRREL), Hanover NH, USA when drafted into military service in 1968. After my 2 years of service, I became a physical scientist in the Snow and Ice Branch, in the same branch as Willy Weeks, one of the few, but probably the leading sea ice scientist in the world at that time. Andrew Assur, who first developed the phase diagram for sea ice, was also Chief Scientist of the laboratory then. After going with Willy on two field trips to the Arctic, I got a US National Science Foundation project on an icebreaker trip to the Antarctic in 1977 to make perhaps the first measurements of the modern era to look specifically at the properties of drifting pack ice in the Antarctic. On that trip we found features unique to Antarctic pack ice, such as a lack of melt ponds on the surface of summer ice, in contrast to Arctic summer sea ice. We also measured sea ice thicknesses in the Weddell Sea that were much higher than previously assumed, commensurate with the thickness of Arctic multiyear pack ice. The most important discovery however was due to another piece of serendipity. On board was a marine biology team from Texas A&M University, conducting water column primary productivity measurements. They were not finding much, and I happened to mention to two of them, Satoru Taguchi and Kurt Buck, that during helicopter flights to sample ice, we were seeing a lot of 'green and yellowish brown stuff' in the ice, and were they interested in that? Of course they were! So they started to measure chlorophyll levels in ice core samples and from these first measurements we found that, again unlike Arctic ice, there was measurable biology in every sample. We also found internal sea ice communities, rather different from the bottom communities seen in Arctic ice, and that there were some identifiable relationships between the ice physics and the sea ice biology.

On our next trip in 1980, Kurt Buck and I further looked into the physical–biological relationships in sea ice. We were joined by David Garrison, who happened to be aboard

as a member of the physical oceanography sampling team from University of California Santa Cruz. Together we discovered that newly forming frazil and pancake ice, found in much greater quantities in the Antarctic than the Arctic, could concentrate algae by physical mechanisms: Concentrations within the ice were several times the relatively low levels found in the water column. Dave and Kurt continued to work together and extended their work on sea ice after that trip.

Later in that same year, Cornelius (Neal) Sullivan of University of Southern California started his work in McMurdo Sound fast ice looking at the ice biology. His time in McMurdo overlapped with that of Willy Weeks and Tony Gow from CRREL who were conducting work on physical properties of the sea ice and a remote sensing program. They assisted Neal in looking at the physical side of the sea ice samples and, through this beginning, Neal and I also began to collaborate. Several graduate students of Neal's (including chapter authors of this book, Kevin Arrigo and Mike Lizotte) got their start in sea ice work through this program at McMurdo Sound.

Another major development took place with the beginning of the Alfred Wegener Institute (AWI) in Germany. The first winter cruise into the Antarctic drifting pack ice since Shackleton's Endurance (1915–1916), was conducted on AWI's research vessel Polarstern in 1986. I joined a team that included Gerhard Dieckmann (co-editor), Hajo Eicken, Rob Massom and Joey Comiso (chapter authors here). The group at AWI, in conjunction with university groups in Germany, continued to develop and initiated both laboratory and field work on sea ice physics and biology. So, the number of people involved in jointly looking at sea ice from several fronts, specifically for the Antarctic, started to undergo geometric growth through the 1980s, with important interdisciplinary linkages between the physics and biology being an early feature of those collaborations. These collaborations replaced the isolated and sporadic disciplinary efforts that had taken place in earlier times.

A key unifying development of the field took place when a Scientific Committee on Oceanic Research (SCOR) Working Group (WG 86 on Sea Ice Ecology) was organized in 1987. This group brought together many of the key workers in this new field of sea ice ecology for the first time for both the Arctic and the Antarctic systems. We put together two papers that provided definitions and terminology for sea ice habitat (Horner et al., 1992) and some estimates of the contribution of sea ice biology as a carbon source for the world ocean (Legendre et al., 1992). Both papers gave some coherence and general application of the importance of sea ice as a habitat and ecological niche and tied together the work in the Arctic and the Antarctic.

During this era we proposed the start of a new series of biennial Gordon Research Conferences on Polar Marine Science, with sea ice ecology as the theme of the first GRC in 1997. As I write, we have just held the seventh in the series with David Thomas (Editor) as Chair. Sea ice, particularly in its interdisciplinary study and connections, has been a feature of every GRC since the first. The GRC on Polar Marine Science, which continues with its core principles of being interdisciplinary, international and both Arctic and Antarctic in its outlook, has been key in building the community of scientists involved with interdisciplinary work on sea ice and has contributed measurably to the growth and unification of the field of sea ice science.

It has been extraordinarily satisfying to me to have contributed in the early stages of this work and to be still involved with this now large and diverse group of scientists, all contributing to understanding one of the most important earth and life science systems of our time.

This book reflects the explosive growth in the field of sea ice science, continuing now at a seemingly exponential rate, even since the first edition in 2003. The number of chapters has increased to 15, with 6 completely new chapters. All other chapters have been heavily revised and updated, including some with new authors or additional co-authors. All chapters, in their extensive reference lists, reflect the recent development of the field with only a few references (less than ten out of hundreds in most chapters) from prior to 1980. With the high number of citations after 2003, the book gives the new information that has come out in the past few years and further validates the need for the new version of the book at this time.

Chapter 1 provides an overview of the importance of sea ice: The changes, particularly in Arctic sea ice summer extent, that have taken place since the first edition in 2003, with record lows seen in 2007 and 2008, are pointed out here as revising the prediction of the disappearance of summer sea ice before 2050. New public awareness of the impact of climate change on polar bears, the possible exploitation of Arctic waters for natural resources and increasing political actions on territorial claims are all new realities associated with the impact of sea ice decline and give new rationales for this book at this time.

Chapter 2 on the growth structure and properties of sea ice sets the stage for how the large-scale behaviour of sea ice in its response to climate forcing and the micro-scale behaviour derived from ice growth and structure are linked together. It is important to see both, the role of sea ice in the environment, and the ways in which the microscopic properties evolve and eventually upscale to the continuum properties important for climate. Ultimately this sub-millimetre scale is the habitat for microscopic life that is detailed in several other chapters, so these properties are fundamental to the structure of the biological environment and provide the substrates for biogeochemical processes. This chapter provides the key physics for these other discussions.

Chapter 3 on sea ice and oceanography is one of the very few, if not the only, review of polar oceanography that accounts effectively for the varying, but central, roles of sea ice on ocean water mass properties, in both the Arctic and Antarctic. The explosion in information from new technologies like AUVs, and particularly Ice Tethered Profilers (Arctic) and use of CTD's mounted on elephant seals in the Antarctic are new exciting findings described here also.

In Chapter 4 on ice thickness, recent Arctic ice thickness data shows that abrupt thinning also coincided with the minimum summer extent period of 2007, primarily due to replacement of multiyear with first-year ice in the north pole region. Later data (April) however still showed a significant thinning feature related to delayed ice growth, so thinner ice in the Arctic is now the norm rather than the previous thicker multiyear ice.

Chapter 5 on snow and sea ice is a comprehensive and thorough examination of the peculiarities of snow on sea ice that both points out the unique behaviour, even control, that snow cover exhibits on sea ice. The authors describe how these properties and processes vary between the Arctic and Antarctic and at many different time and space scales.

Chapter 6 thoroughly updates the trends in large-scale variations in sea ice extent/area from satellite imagery which have been changing dramatically since the time of the first edition in 2003. Shown are the drastic changes in Arctic summer ice extents with all time lows in 2007 and 2008 and the accelerating decline of multiyear ice, now decreasing at 11–12% per decade. The counter trend in the Antarctic, a slight overall increase with large regional decreases and increases counterbalancing each other, appears related to circulation anomalies that may also be connected to effects on large-scale circulation patterns (e.g. SAM and ENSO) from the increased size of the ozone hole and greenhouse warming of the atmosphere.

Chapter 7 on sea ice bacteria and viruses describes the important role these hitherto unstudied organisms play in the sea ice ecosystem. Recent investigations have revealed a large number of previously unknown species. Given these discoveries, a sobering assessment is made that the heavily understudied multiyear ice in the Arctic may disappear and cause extinction of species before we even have a chance to identify them.

Chapter 8 on primary production and sea ice points out that despite lower rates of primary production by sea ice algae compared to phytoplankton, they are virtually the sole source of fixed carbon for higher trophic levels in ice-covered waters. They have been shown to sustain a wide variety of organisms, including krill, throughout the winter months when other sources of food are lacking. Recent information on gene sequencing of polar alga have shown that large percentages of their genes have no assigned function and many of their genes seem to be species-specific. Further work on these lineages is expected to reveal new information on how these organisms are adapted to their extreme environment.

Chapter 9 on heterotrophic protists associated with sea ice points out that within the last quarter century, not only has work shown the high metabolic activity of sea ice microalgae and bacteria, but that an increasingly large and diverse assemblage of major consumers of alga and bacteria, the heterotrophic protists, are found in sea ice. Application of DNA sequencing has resulted in radical and frequent changes in the evolutionary relationships among these organisms.

Chapter 10, on sea ice meio- and macrofauna, describes the diverse group of metazoans that live in either permanent association with sea ice (autochthonous fauna) or temporary association (allochthonous fauna). Those permanently associated with sea ice are constrained by the features of the micro-scale of sea ice (Chapter 2), particularly the size constraints and the extreme temperature and salinity features that are sometimes encountered. The temporary associates such as Antarctic krill, form a key component of the diet of many of the top trophics (mammals and birds) so form important links in the polar ecosystem.

Chapter 11 describes sea ice as a critical habitat for marine mammals and birds. The authors point out that, along with the polar bear and the emperor penguin as the 'charismatic mega-fauna' of the polar regions possibly affected by sea ice decline under climate change, that there are a host of other mammals and birds, including the Narwhal and Bowhead whales in the Arctic, and Crabeater, Leopard, Weddell and Ross seals in the Antarctic, that are similarly ice-obligate. An even larger number are ice-associated, and have evolved adaptations to exploit sea–ice habitat.

Chapter 12 is on biogeochemistry of sea ice and reviews the important links between the chemical and biological environments within sea ice, and is perhaps the newest study area of the sea ice system. While driven by processes at the most minute scales of molecular interaction, the ramifications of understanding the biogeochemistry cycles are wide-reaching, impacting on problems such as the carbon dioxide uptake and release through and within sea ice, both by organic and inorganic processes; DMS production and release to the atmosphere and ocean and the mediation of biological processes by trace nutrients, such as iron, within the sea ice and water columns affected by sea ice.

Chapter 13 is on paleo sea ice distribution and the reconstruction of ice extent from the geological record. It is an in-depth but very understandable review of both techniques and reconstructions of paleo sea ice distributions for both the Arctic and Antarctic. It includes the important revision of the Last Glacial Maximum (LGM) Antarctic ice extent in summer to a value between today's summer minimum and winter maximums, rather than at the

current winter maximum for LGM summer minimum as previously inferred. Important new techniques are also explained, including some nice aides for the non-specialist such as drawing clearly the distinction between calendar years before present and carbon dated years before present. The context for current climate change in the Arctic is illustrated particularly well, and how dramatic an event it will be for the pending loss of summer ice, as if (or when) it occurs, it will be a singular event in the geologic history of the Arctic Ocean over many millions of years.

Chapter 14 on sea ice in non-polar regions is a comprehensive review of non-polar seas' ice covers and their very recent investigations, as all but one citation are post-1980. An introduction to seas such as the Aral, Azov, Baltic, Sea of Okhotsk, Hudson's Bay and others show the basics of both the ice characteristics in each and recent response to man-made activities, e.g. the Aral Sea has been divided into two separate water bodies because of river diversions. The importance of these areas economically is illustrated with dynamic ice covers affecting offshore petroleum development, shipping and fishing in significant ways and with new responses to climate change with dramatic further effects on their ecosystems expected as well.

In Chapter 15, on sea ice and astrobiology, insight is given on the processes that have led to the evolution of sea ice organisms on earth, with their special adaptations of Extracellular Polymeric Substrates (EPS) and Antifreeze Proteins (AFP) and associations of cellular life with the particular physics and chemistry of ice surfaces characterized by 'premelting'. These adaptations are analogues to those that may have had also to take place elsewhere for life to evolve in icy planets such as Europa or on the past surface of Mars. Understanding of the physics, biogeochemistry and biology of sea ice are perhaps the best terrestrial analogues to these suggested astrobiological processes.

The authors have thoroughly explained the recent findings and subtleties of the various topics without oversimplifying them. Each chapter is both thorough and understandable, comprehensively referenced, a difficult feat accomplished to provide the background necessary for all of us to gain the understanding to continue to advance sea ice science in a comprehensive way: Much work has been done but much remains.

Because of the central role of sea ice in the climate system under global warming, and the threat to ice-obligate species with decreasing levels of sea ice available as habitat, knowledge of how the sea ice system operates is crucially important to understand. In the past, I may have only wanted this book as a specialist in the field. Now, I need it, and others in and outside of the field will also find it of similar crucial importance. For all of us, I thank the authors and editors for providing new understanding of difficult topics and a high service to our science.

Stephen F. Ackley

Geological Sciences Department, University of Texas at San Antonio,
One UTSA Circle, San Antonio, TX 78249. USA

References

Horner, R., Ackley, S.F., Dieckmann, G.S. et al. (1992) Ecology of sea ice biota – 1. Habitat, terminology, and methodology. *Polar Biology*, **12**, 417–427.

Legendre, L, Ackley, S. F., Dieckmann, G.S. et al. (1992) Ecology of sea ice biota: 2. Global significance. *Polar Biology*, **12**, 429–444.

This page intentionally left blank

1 The Importance of Sea Ice: An Overview

Gerhard S. Dieckmann and Hartmut H. Hellmer

1.1 Introduction

A few years ago, researchers modelling the fate of Arctic sea ice under global warming saw a good chance that the ice could disappear, in summertime at least, by the end of the 21st century. Then talk swung to summer ice not making it past mid-century. Now, after watching Arctic sea ice shrink back in 2007 to a startling record-low area and followed by an almost identical retreat in 2008, scientists are worried that 2050 may be over-optimistic (Fig. 1.1; Kerr, 2007; Fetterer et al., 2008). Never before in recent history has sea ice been in the focus
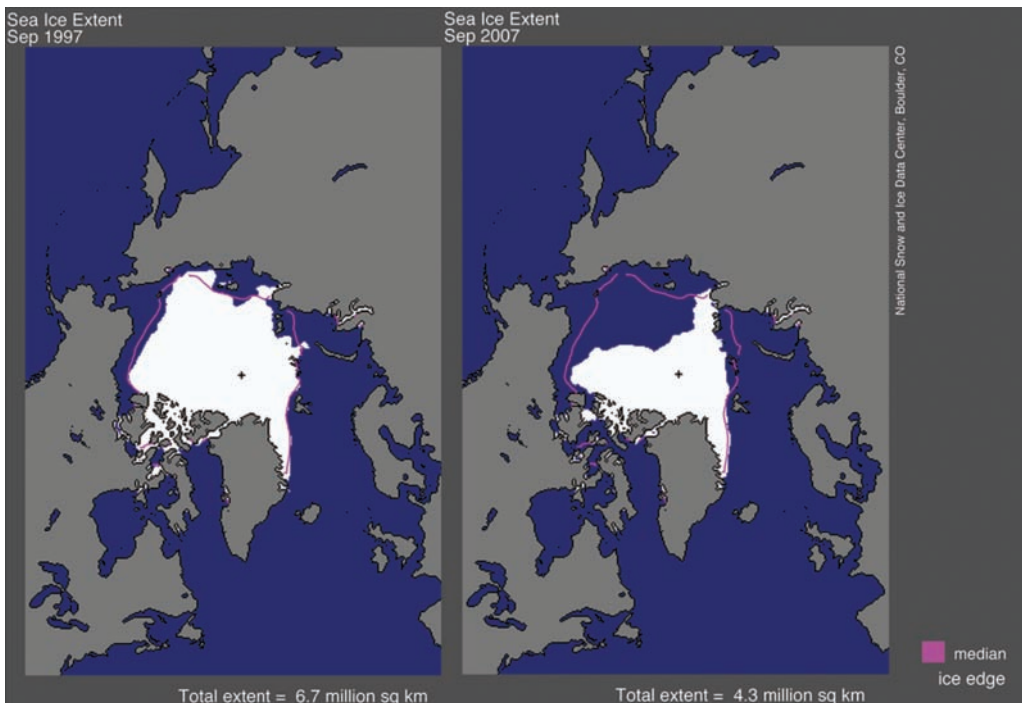

Fig. 1.1 Difference between the minimum Arctic sea ice extent in September 1997 and 2007 compared to the median recorded ice edge. Image courtesy of National Snow and ice Data Center, Boulder, Colorado.

of human interest as much as in the past decade. At the time of writing, both the North West Passage and North East Passage have become navigable for ocean freighters because of the disappearing sea ice. The research ice-breaker Polarstern traversed both passages without really having to break ice on an Arctic expedition in September and October 2008.

The possible implications and feedback mechanisms of these dramatic changes are not yet fully understood. Just one example, for instance, is that the shrinking sea ice cover is expected to cause an increase in primary production by as much as three times that of 10 years ago, with unforeseeable consequences for the Arctic marine ecosystem (Arrigo et al., 2008b). These are alarming signs of climate change and that is why sea ice has, in the last few years, become the focus of the media, drawing increasing attention from the general public. The rapid decline in the Arctic is thus of major concern to all of us, with implications not only for climate and ecosystems, but for mankind too, in more ways than one.

Disappearance of sea ice is giving prospects of new sea routes, of new resources such as gas and oil, and is already initiating new territorial claims. Is the prospect of a disappearing sea ice cover really so disconcerting? Should we not be relieved that an apparently hostile and useless hindrance to shipping and fishing is vanishing? It is an aim of this book to provide answers to these questions as well as to show the reader why and how sea ice affects climate, ocean circulation, polar ecosystems and us, and how these in turn affect sea ice.

Sea ice is a substrate, which after the initial freezing of sea water is profoundly modified by the interaction of physical, biological and chemical processes. Sea ice becomes a heterogeneous, semi-solid matrix in its simplest form resembling a sponge. Oceanic, atmospheric and continental inputs all influence its formation, consolidation and subsequent melt when the ice returns to water. Probably the most important property of sea ice is, despite it being solid, its density is less than sea water, and therefore floats and acts as a blanket on the cold ocean.

During the course of a year, tremendous areal expanses of sea water in the Arctic, the Southern Ocean, and also the Baltic, Caspian and Okhotsk Seas (Chapters 6 and 14) undergo a cycle of freezing and melting. In winter, sea ice covers an area of up to 7% of the earth's surface, and as such is clearly one of the largest biomes on earth.

With the exception of the Inuit, who over several thousand years adapted to a life closely associated with Arctic sea ice, for most humans sea ice, until the turn of the last century, was simply a hostile environment and an obstruction to the navigation of sea routes, fishing grounds and the hunting of birds and mammals (Thomas et al., 2008; Weeks, 1998; McGhee, 2006). It is only during the past 200 years, and mostly within the past 100 years, that adventurous expeditions have visited the polar oceans and our understanding of the significance of sea ice in a global context has begun to develop.

Today we know that the annual cycle of sea ice formation and degradation not only plays a pivotal role in governing the global climate, but also influences processes in the oceans down to the abyss. The life cycles of marine plants and animals ranging from micro-organisms to whales, and even humans, are also influenced by the large-scale cycles of ice formation. Sea ice is recognized as a fundamental component of system earth, which cannot be ignored in the large-scale environmental discussions and the predictions of future climate conditions as has become increasingly apparent in the last decade.

Recently, disturbing headlines from the high latitudes regarding the impacts of ozone holes, collapsing ice sheets and rapidly declining sea ice cover indicate that climate change is indeed underway at a rate not envisaged even a few years ago. The seeming inevitability of shrinking

ice on the Arctic Ocean, for instance, would infer a threat to the indigenous way of life of local human communities, hard times ahead for Arctic birds and mammals including the polar bears (Turner et al., 2006; Kerr, 2007). In the Antarctic, changes in sea ice extent and distribution of sea ice cover are not so evident with the exception of the Antarctic Peninsula where significant warming has become apparent. The difference arising obviously from a weak response to increasing greenhouse gases and a cooling of the Antarctic stratosphere due to the ozone hole – and/or a reduced cloud cover which might mask the greenhouse gas-induced warming. On the other hand, ecological changes in krill and whale feeding, which seem to have severely affected local seabird populations (Croxall et al., 2002; Atkinson et al., 2004), are attributed to signs of global climate change.

Sea ice research spans many modern scientific disciplines including, among others, geophysics, glaciology, geology, chemistry, oceanography, biogeochemistry and numerous branches of biology, and recently in particular, molecular biology. Knowledge of all the processes associated with sea ice is important for climate researchers wanting to understand interactions pertinent for the polar regions and also for global-scale climate. Present-day sea ice research ranges from molecular studies to the composition and structure of the ice itself, to that of the elements and the micro-organisms living within the ice, through to scales many orders of magnitude greater up to the monitoring of the ice cover from space (Fig. 1.1).

Modern ice breakers, as well as stations on the peripheries of Antarctica or the Arctic, greatly facilitate the access to sea ice, even during seasons when in the past ice and weather conditions prohibited effective work. During the past 60 years, these facilities have greatly enhanced the chances for regional meso-scale studies on the development and growth of sea ice and the dynamics of pack ice fields. These include investigations into the physicochemical interactions between the atmosphere, ice and underlying water, as well as into the fauna and flora living within or in close association with sea ice (Chapters 2, 4, 10 and 11). Geologists use information gathered from sediment cores in areas beneath past and present sea ice cover, obtained by ice breaker, to reconstruct the earth's history, particularly that of the sea ice extent (Chapter 13), whilst glaciologists are looking for proxies for sea ice extent in ice cores from continental ice (Abram et al., 2007).

On a larger scale, airborne equipment used from helicopters or light airplanes provides information on heat exchange, floe distribution and sea ice thickness as well as on the distribution of birds and mammals. Floats, submarines and remotely operated or autonomous vehicles are the latest tools to be used for obtaining insight into the underside topography of sea ice fields, ice thickness and the behaviour of animals under the ice (Brierley & Thomas, 2002). New technologies have been harnessed to investigate the fluxes of organic matter from sea ice to benthic communities, as well as investigating the seasonal dynamics and growth of these communities.

Constantly improving remote-sensing technology and new satellite sensors (Chapters 4 and 6) enable high-resolution, large-scale monitoring of the ice cover, surface roughness, dynamics and thickness on a seasonal and inter-annual basis. This information is being compiled to validate numerical models that reconstruct and forecast the behaviour and role of sea ice with regard to past and present climate change, as well as enabling assessment of its large-scale ecological significance (Chapters 6 and 8). Global positioning technology allows the tracking of birds and animals, including seals and polar bears, and their seasonal migrations associated with sea ice. Sophisticated suites of information such as diving depths, water temperature and salinity, and foraging behaviour can be transmitted

daily over many months enabling a far greater understanding of animal behaviour in sea ice-covered regions than has ever been possible before (Wilson et al., 2007; Chapter 11). Recently, oceanographic sensors and cameras mounted on mammals have provided information of the ice underside and related hydrography (Watanabe et al., 2006; Charrassin et al., 2008; Chapter 3).

This chapter provides a brief overview of the importance of sea ice. It spans the historical development of sea ice research and the expansion in research interests through to the current state-of-the-art issues and new perspectives that are receiving increasing attention.

1.2 Historical aspects of sea ice exploration

For obvious reasons, the historical development of sea ice research differs greatly between the northern and southern hemispheres. A detailed chronological account is beyond the scope of this chapter and is more fully covered by Fogg (1992), Martin (1996), Weeks (1998) and McGhee (2006). Excerpts have been extracted from these works to compile the brief summary that follows.

In both hemispheres, it was probably the biology associated with sea ice that led to human's interest, association and confrontation with this hostile environment. Around the Arctic, Baltic and Caspian Seas, humans have inhabited coastal areas for millennia, living off the animals closely associated with sea ice, and adapting their lifestyles and migrations to the seasonal fluctuations in sea ice cover. In the Antarctic, it was the whalers and sealers of the 19th century who first encountered sea ice during the pursuit of their prey.

The first records of sea ice date back to reports in the Baltic, and near Greenland, when Irish monks crossed *Mare Concretum* during their voyages to Iceland. These journeys actually took place in approximately 795 AD (Weeks, 1998). In about 1070, Adam of Bremen described both Iceland and Greenland as well as sea ice. Two hundred years later, a book containing descriptions of sea ice was written by the priest Ivarr Bodde. There is a detailed report with a map showing the crossing of sea ice on the Baltic Sea prepared by Olaus Magnus Gothus in 1539, whilst expedition reports containing general descriptions of sea ice in the Arctic, such as those of Martin Frobisher, date back to 1576 (Weeks, 1996). Because of the general expansion of ocean trade routes during the later 18th century, interest increased in finding a route that offered faster passage between Europe and the Orient. One of the most notable expeditions during that time was the Great Northern Expedition which started in 1733 under the command of Vitus Bering, who concluded in 1774 that the route was probably not navigable with the ships available at that time.

The 19th century began with a series of expeditions established mainly to clarify the existence of a north-west or north-east passage. The best known are the expeditions of Ross in 1818, 1829–33, William Edward Parry and Franklin in 1845. By 1870, the first scientific papers on the properties and variations in sea ice conditions had started to appear (Tomlinson, 1871; Petterson, 1883), as had reports on the first sea ice experiments (Buchanan, 1874). Ehrenberg (1841, 1853) was the first to describe diatoms from Arctic sea ice, after which many papers followed describing diatoms and organisms in sea ice (Dickie, 1880; Cleve, 1883; summarized by Horner, 1985; Thomas et al., 2008). Probably the most epic voyage with a scientific background at the end of the 19th century was that of Nansen on the *Fram*. This voyage initiated the beginning of modern sea ice geophysics.

Sea ice research in the 20th century was governed by political, logistical, as well as scientific enterprise interrupted by the two world wars. At the forefront of 20th century, research was on the engineering and the development of metal ice-breaking ships. The first, the *Yermak*, was actually built for Admiral Makarov in 1898 and used for the first sea ice research programme in the summer of 1901, with the additional intention of discovering the northern sea route. In 1927, Malmgren published his doctoral thesis on sea ice growth and property observations carried out during the drift of the *Maud* between 1918 and 1925. This probably made him the first true student of sea ice geophysics (Weeks, 1998).

The Russians were very active in sea ice research even prior to and during World War II. Particularly noteworthy is the book on Arctic ice by Zubov (1945). Other pioneering work on sea ice during this period was conducted by Tsurikov who developed the first geometric model for the variation in sea ice strength with changes in the gas and brine volumes. Usachev (1949) reviewed work that had been carried out on sea ice algae. Western scientists were evidently not active during the period up to 1945, although Ringer, a Dutch chemist, worked on phase relationships in sea water and brines in 1906, only publishing his work in German in 1926. Other scientists involved in sea ice research at that time were Whitman, Barnes, Smith, Crary and Ewing, the last among them later becoming the Chief Scientist for the US IGY (International Geophysical Year 1 in 1957–1958) Programme in the Antarctic (Weeks, 1998).

After World War II, sea ice research increased markedly. Emphasis changed from that of finding appropriate sea routes and facing the challenges that sea ice posed to shipping to other priorities. These were in part directed by the then developing political 'cold war' with the consequences for the missile race, submarine strategy, Arctic offshore oil exploration, remote sensing, the role of sea ice in global climate and the transfer of pollutants via sea ice.

The first mention of the Antarctic continent is that of Aristotle in 322 bc who described, an as yet unknown, extreme southern region *Antarktikos*. The name was derived from 'opposite the Bear', *Arktos* being the Great Bear (or Big Dipper) constellation above the North Pole (Martin, 1996). Yet while the ancient Greeks only imagined the continent, the first human to actually encounter the Antarctic may well have been a 7th century Raratongan traveller, Ui-te-Rangiara, who according to Polynesian legend is said to have 'sailed south to a place of bitter cold where white rock-like forms grew out of a frozen sea'. However, the actual recorded discovery and exploration of Antarctica dates back to just 200 years.

Voyages into sub-Antarctic waters began in the 16th and 17th centuries. The first recorded crossing of the Antarctic Circle and encounter with sea ice was in 1773 by British Captain James Cook who described that there must be 'a tract of land at the Pole that is the source of all the ice that is spread over this vast Southern Ocean'. Cook reached 71°S, a higher latitude than anyone before him. These voyages were followed by a period when American and British sealers travelled south encountering sea ice during their pursuit of seals (Fogg, 1992).

Scientific expeditions followed in the wake of the sealing parties. From the late 1830s onwards, investigations into the earth's magnetic fields encouraged expeditions to set out to locate the South Magnetic Pole. The Frenchman Dumont d'Urville and the American Charles Wilkes searched for the South Magnetic Pole in 1840. The following year, James Clark Ross of Great Britain sailed into the Ross Sea on HMS *Erebus* and HMS *Terror* on an unsuccessful expedition to determine the approximate position of the South Magnetic Pole. He was successful, however, in charting unknown territory and was probably the first to show a scientific interest in the sea ice. In fact, Joseph Hooker, the young naturalist on

board HMS *Erebus*, investigated the discoloured sea ice they often encountered and which was first thought to contain volcanic ash. Hooker's examination of the melted ice samples showed this discoloration to be made by diatoms.

From then onwards, almost every expedition to the Antarctic resulted in scientific work being carried out, often including sea ice studies. Among the most significant were the descriptions of Antarctic sea ice by Drygalski (1904) which he recorded during the expedition of the *Gauss*. Wright and Priestley, who were members of Scott's last expedition, reported their interesting observations of sea ice both in the Journals and Reports of Scott's last expedition and in a classic book entitled *Glaciology* in 1922. A subsequent expedition, which provided new insight into the understanding of sea ice, was that of Shackleton between 1914 and 1917 published by Wordie (1921).

With the advent of new technology and scientific interest, the past 75 years have resulted in an almost exponential expansion in sea ice research, not only in the sense of reports and papers published, but also in the numbers of countries supporting sea ice research and scientists participating in expeditions, workshops and dedicated sea ice symposia. Sea ice research is of great international importance, and present-day sea ice campaigns tend to bring scientists from many countries together in order to consolidate their efforts in a truly multi- and inter-disciplinary research focus. Recent and current internationally co-ordinated programmes include ISPOL, SHEBA, SIMBA, ASPECT, SIPEX, some in the framework of the International Polar Year (IPY) 2007/09.

1.3 Sea ice influence on ocean and atmosphere

Sea ice can be thought of as a thin blanket covering the ocean surface which controls, but is also controlled by, the fluxes of heat, moisture and momentum across the ocean–atmosphere interface. Because it is relatively thin, sea ice is vulnerable to small perturbations within the ocean and/or the atmosphere, which significantly change the extent and thickness of the polar ice cover. Both, in turn, have a major influence on the state of the ocean and the atmosphere. Due to this complex interaction between key components of the earth's climate system, sea ice has become one, if not the most important, component in the research of the past, present and future climate.

Sea ice extent and thickness are controlled by the growth/decay and drift of the ice cover. They are therefore linked to thermodynamic and dynamic processes in the ocean and the atmosphere (and the sea ice). Cooling of the ocean surface below the freezing temperature, which ranges from 0°C for freshwater to −1.9°C for salty Antarctic shelf waters, initiates the formation of sea ice. The growth rate, and later the age, determines how much brine is expelled to the ocean (Chapters 2 and 3), causing a densification of the surface waters.

For both hemispheres, these waters primarily correspond to shelf waters, indicating that on earth the continental shelves are the prime location for sea ice formation. In contrast to the Arctic where relatively fresh surface waters, due to river run-off, buffer most of the salt input in autumn, brine rejection in the Southern Ocean causes deep convection, a cooling and salt enrichment of the marginal stable shelf water column. At salinities greater than 34.46, these waters have the potential to initiate deep and bottom water formation during mixing with open ocean components at various locations of the Antarctic continental shelf break (Gill, 1973).

Along most of Antarctica's periphery, the interplay of katabatic winds, tides, and currents maintains, in some regions all year round, narrow (hundreds of metres to a few kilometres) polynyas in which surface waters are exposed to cold air transported from high elevations of Antarctica's interior to the coast. Based on satellite data, 13 major coastal polynyas produce ~10% of Southern Ocean sea ice at rates of up to 5 cm per day, though covering only ~1% of the maximum ice area (Tamura et al., 2008). They are called *latent* heat polynyas because of the heat the surface water gains from the formation of ice crystals. This is the only heat available, but it is insufficient for melting sea ice because shelf convection transports only very limited, if any, heat from the depth to the surface (shelf waters are characterized by near-surface freezing temperatures). Therefore, it is the action of external forces (wind and tides) that mainly maintains low ice concentrations close to the Antarctic coastline.

The route high salinity shelf water takes on the shelf determines its modification in the mixing process and its contribution to the formation of new bottom water. Observations from the southern Weddell Sea are presented here, but the types of processes described are applicable to all broad continental shelves fringed by large ice shelves:

(1) A direct route towards the continental shelf break results in the mixing with warmer open ocean components forming Weddell Sea Deep Water (WSDW) and Weddell Sea Bottom Water (WSBW) at the slope front (Foster & Carmack, 1976).

(2) A sloping shelf topography towards the south induces high salinity shelf water to flow into the ice shelf cavity participating in the sub-ice shelf circulation.

(3) Interaction with the deep ice shelf base initiates melting and possibly freezing, and the formation of a meltwater plume. This is less saline and, with temperatures below surface freezing, is defined as Ice Shelf Water (ISW). If bottom topography allows, ISW might reach the continental shelf break where mixing with deep waters of circumpolar origin again results in the formation of WSBW (Foldvik et al., 1985).

It has been speculated that the latter route might be sensitive to climate shifts, and related changes in the sea ice cover will have consequences for the ice shelf mass balance and the characteristics of the meltwater plume (Nicholls, 1997). In return, the basal melt has an influence on the stability of the shelf water column and thus on deep convection with consequences for sea ice thickness – a reduction of freshwater from underneath the ice shelves causes a thicker sea ice cover (Hellmer, 2004). The spreading of the new bottom water is confined to the Weddell Basin, while the new deep water is able to escape through gaps in the confining ridges. Outside the Weddell Sea, this water mass is historically called Antarctic Bottom Water which has been observed in the Atlantic as far as 40°N.

The most famous *sensible* heat polynya is the Weddell polynya. Initiated by the heat of warm deep waters, at its maximum it has exposed nearly 250,000 km² of ice-free ocean to the winter atmosphere in the eastern Weddell Sea. It occurred most impressively during the mid-1970s (Carsey, 1980). Thin ice and/or low ice concentration are common winter conditions in the vicinity of Maud Rise, a seamount at 65°S, 2.5°E which rises from the 5000 m deep abyssal plain to within 1600 m of the ocean surface. Interaction of ocean currents and tides with the steep bottom topography is assumed to trigger a complex regional circulation pattern which transports warm deep waters of circumpolar origin to the near surface. For a short period of time, the winter heat fluxes associated with this upwelling can be almost 200 W m^{-2} with an areal average of 25 W m² (Muench et al., 2001). Under

the perennial pack of the western Weddell Sea, however, heat fluxes are as low as 3 W m² (Lytle & Ackley, 1996). This is similar to the 2 W m⁻² in the central Arctic Ocean where a *sensible* heat polynya has not occurred up to now. Although ocean processes might initiate the polynya's onset, a persistent wind resulting from the interaction of the ice-free ocean with the atmosphere seems necessary to keep the area clean of ice, as indicated by results from a sea ice–mixed layer model coupled with a simple atmosphere (Timmermann et al., 1999). However, for the better understanding of the processes related to the onset, maintenance and disappearance of a polynya, further small-scale field studies accompanied by high-resolution numerical models combining atmosphere, sea ice and ocean processes are necessary.

As in the coastal polynya, sea ice formation and the resulting densification of the surface layer initiate open ocean convection which can affect a water column up to 4000 m thick (Gordon, 1978). As a result, most of the underlying deep water is cooled with consequences for deep and bottom water ventilating the world ocean abyss. For example, the cooling of the bottom layer of the Argentine Basin in the late 1980s has been related to the cooling of the deep Weddell Sea during the polynya years of the 1970s (Coles et al., 1996). Similar open ocean convection sites influenced by sea ice related processes exist in the northern hemisphere, namely the Greenland and Labrador Seas where the parent water masses of the North Atlantic Deep Water (NADW) are formed. NADW dominates the lower stratum of the Atlantic Ocean and has a global distribution by feeding the deep waters of the Antarctic Circumpolar Current.

A sensitivity of the NADW formation process to changes in the Arctic sea ice cycle was assumed for the period of the Great Salinity Anomaly (Lazier, 1980). In the late 1960s, a lens of freshwater caused by enhanced sea ice export through the Fram Strait travelled south with the boundary current influencing both the Greenland and Labrador Seas. Nowadays, open ocean convection in the North Atlantic is thought to be controlled by the atmospheric circulation, which might be influenced by anomalous Arctic sea ice conditions (Dickson et al., 1996). Further changes in the Nordic Seas are likely to occur due to the rapid thinning of sea ice in the Arctic Transpolar Drift (Haas et al., 2008) and thus a reduced surface freshwater export through Fram Strait.

In the central Arctic Ocean, convection is restricted to the upper 50–100 m due to the strong stratification of the water column. The deeper layers are renewed by advection of water masses of Atlantic origin entering through the Fram Strait and across the Barents Sea. Although these waters became warmer in the past decade (Schauer et al., 2008), an influence on the sea ice cover can be excluded due to the strong Arctic halocline, which restricts convection to the upper 50–100 m. The inflow is still modified due to the admixture of cold and saline waters from the shallow continental shelf as the deep water flows anticlockwise with the gyre circulations that dominate the three Arctic basins (Rudels et al., 1994). Finally, these deep waters escape from the Arctic Ocean, again through the Fram Strait (sill depth ~2500 m), into the Greenland and Norwegian Seas to contribute either there, or further downstream, to deep water formation. However, due to a sill depth of 600–800 m at the Greenland-Scotland Ridge, only the upper deep waters of Arctic origin are able to continue towards the Labrador Sea.

The influence of sea ice on the atmosphere is manifold, covering a wide range of physical processes, and spatial and temporal scales. Primarily, sea ice, and the snow cover it sustains, prevents the ocean from heating the lower atmosphere due to turbulent fluxes across the interface. A cooler atmosphere is also supported by a high surface albedo in summer and the emission of long-wave radiation in winter. The former reduces the absorption of short-wave solar radiation (absent in winter) that would otherwise warm (and melt) the ice or the ocean

surface. The latter cools the snow and ice surfaces which in turn extract heat from the air blown across the interface. The winter cooling, however, can be mitigated by the existence of clouds, resulting from evaporation in ice-free areas, that effectively trap long-wave radiation. In summer, the warming of the atmosphere due to clouds might be less because a denser cloud cover reduces the incoming solar radiation.

All of these factors illustrate a positive feedback mechanism, initiated by a climatic warming, that was predicted to lead to a reduced extent and thickness of the polar ice cover. Sensitivity studies with a thermodynamic sea ice model revealed that the summer Arctic ice cover would completely disappear with a 3–5°C increase in air temperature or a 15–20% decrease in albedo (Maykut & Untersteiner, 1971). Despite the fact that this model did not include the relevant ice dynamics that might enhance an ice retreat, because thinner ice is more compressible, the prediction has come true.

The influence of the sea ice on the dynamics of the atmosphere is concentrated on the atmospheric boundary layer. The exchange of momentum due to turbulent processes primarily controls the sea ice drift on timescales of 1 day and more; ocean currents dominate the sea ice motion on timescales of more than 1 month (Kottmeier & Sellmann, 1996). Among other things, polar field experiments are designed to determine drag coefficients used to parameterize the transfers of heat, moisture and momentum in atmosphere and sea ice models. The state-of-the-art sea ice models take numerous parameters into consideration including different ice classes, thermodynamics based on a one-dimensional heat diffusion equation applied to multiple layers, an elastic-viscous-plastic rheology, a snow cover, sea water flooding due to the suppression of the ice-snow interface, the formation of superimposed ice, the treatment of brine pockets and biology. This information is all coupled to circulation models of different complexity for the atmosphere and the ocean.

The deep and bottom waters produced by the polar oceans form part of the global thermohaline circulation. Therefore, sea ice processes contribute to the driving of the global distribution of water mass characteristics, the ventilation of the deep world ocean, and the transport of natural and anthropogenic substances (tracers) from the ocean surface to the abyss where these can be stored for centuries. The latter is of climatic relevance in the view of increasing concentrations of greenhouse gases in the atmosphere, which are assumed to have caused the 0.5 K increase in global temperatures during the last century (Jones et al., 1999).

The Arctic warming, as the consequence of a change in the wind pattern, is thought to be responsible for the rapid reduction in summer extent of the Arctic ice cover during the past two decades (Chapter 6). Since the warming predominately affects the perennial ice cover, it is not surprising that during the same period Arctic mean ice drafts also declined by 42% (Wadhams, 2001). The trend continued reaching an unprecedented and stronger than predicted (by the climate models) minimum summer sea ice extent in 2007, which only slightly recovered in 2008 (Fetterer et al., 2008). So far, feedback mechanisms, and the consequences of an ice-free summer Arctic Ocean on the climate of the northern hemisphere and beyond, are still speculative. Further research is necessary to understand the complex climate system of which sea ice is one key component.

In the Arctic, despite a large interannual variability, negative trends are becoming obvious while such changes are minor in the Antarctic where sea ice is more influenced by alternating anomalies propagating around Antarctica as part of the Antarctic Circumpolar Wave (ACW) (White & Peterson, 1996; Chapter 6) and/or by zonally non-symmetric (non-annular) fluctuations related to the dominant atmospheric variability known as the Southern Annular Mode (SAM) (Lefebvre et al., 2004). The ACW seems to be linked to the El Niño Southern

Oscillation (ENSO) cycle, indicating a control on the sea ice conditions far beyond the limits of the polar southern hemisphere.

1.4 Similarities and differences between Arctic and Antarctic sea ice

Apart from the fact that global climate change causes a different response of sea ice in the Arctic from that in the Antarctic, there are other fundamental differences between sea ice of both polar regions. The most significant being that the Arctic is a closed basin surrounded by land with only one deep passage through which water can be readily exchanged with the rest of the world ocean. In contrast, the Antarctic Ocean is circumpolar and surrounded by the Indian, Atlantic and Pacific Oceans.

Shelf seas in the Arctic take up about one-third of the ocean area with a depth below 100 m while the mean ocean depth is 1800 m (Wadhams, 2000). In a broader sense, the Arctic encompasses estuaries, gulfs and bays such as Hudson Bay or smaller seas such as the Sea of Okhotsk and the White Sea. At the time of its maximum advance (February and March), sea ice covers the entire Arctic Ocean extending from the North Pole to about 44°N in the Sea of Japan, while in September it has reached its minimum (Chapters 6 and 14; Fig. 1.2).

This may be one reason why Antarctic annual sea ice has a much higher amplitude and year-to-year variability (Table 1.1). Sea ice here occurs between about 55° and 75°S. In the Antarctic, the continental shelves are comparatively narrow, and so the Antarctic pack ice zone is largely over ocean basins between 4000 and 6500 m depth.

Ice growth and melting in both polar regions are governed by the same energy fluxes, but several factors differ considerably between the hemispheres. The most notable is the oceanic heat flux, estimated to be about 3–4 W m^{-2} in the Arctic (Krishfield & Perovich, 2005), whereas the average annual flux in many parts of the Southern Ocean may be as high as 30 W m^{-2} (Lytle et al., 2000). More than half of the Arctic sea ice is multi-year ice (Table 1.1), whereas
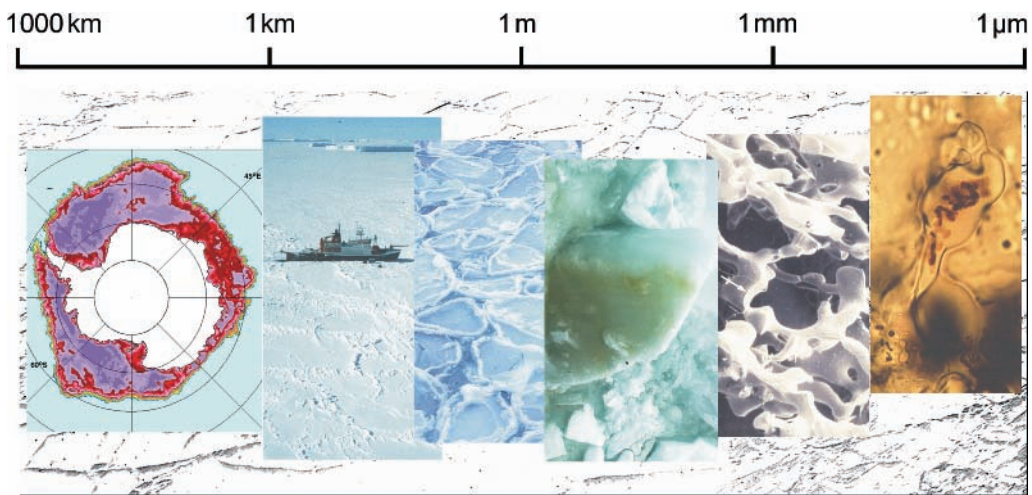

Fig. 1.2 Research on sea ice spans several orders of magnitude, from the molecular and microscopic level to satellite images taken from space. Shown from left to right are diatoms in a brine pocket, cast of brine channel system, sea ice floe tainted brown by diatoms, pancake ice, the ice breaker RV Polarstern in a pack ice field and satellite image of Antarctic sea ice cover in September.

in the Southern Ocean multi-year ice only constitutes a small fraction predominantly covering the western Weddell Sea and as patches of fast ice in embayments along the Antarctic coast (Table 1.1).

In the Arctic, sea ice is affected by considerable terrestrial input, due to river run-off in the form of sediment and/or suspension freezing of bottom sediments. Pollution of sea ice

Table 1.1 Selected examples of differences between Arctic and Antarctic sea ice.

Feature	Arctic	Antarctic
Maximum extent	15.7×10^6 km² (February–March) (Chapter 6)	18.8×10^6 km² (September) (Chapter 6)
Minimum extent	4.3×10^6 km² (September) (Chapter 6)	3.6×10^6 km² (February) (Chapter 6)
Drift velocities	1.7–8.7 km/day (Pavlov & Pavlova, 2007)	>20 km/day (Heil & Allison, 1999)
Mean thickness	1976: 5 m (Wadhams, 2000) 2007: 1.27 m first year and 1.81 m second year (Haas et al., 2008)	0.5–0.6 m (Wadhams, 2000)
Annual ice cover (first-year ice)	7×10^6 km²: <50% (Comiso, Chapter 6)	15.5×10^6 km²: >80% (Comiso, Chapter 6)
Latitudinal range	90°N to 44°N	55°S to 75°S
Multi-year ice	9×10^6 km² (Gloersen et al., 1992) (Chapter 6)	3.5×10^6 km² (Chapter 6)
Extent of land-fast ice	Not known	5% (0.8×10^6 km²) (Fedotov et al., 1998)
Annual average heat flux	3–4 W m^{-2} (Krishfield & Perovich, 2005)	5–30 W m^{-2} (Lytle et al., 2000); 10–50 W m^{-2} sometimes exceeding 100 (Muench et al., 2001)
Platelet ice	Sporadic Freshwater under floes	Common under fast ice (Gow et al., 1998)
Polynyas	Coastal	Large, open ocean
Melt ponds	Significant feature	Insignificant feature
Superimposed ice	Present (Chapters 4 and 5)	Significant (Chapters 4 and 5)
Flooding	Not extensive	Extensive
Sea ice residence time	<1–7 years	<1–2 years
Texture	5–20% frazil (Tucker et al., 1987)	50–60% frazil (Lange et al., 1989)
Salinity	Generally low	Higher
Pollution	Riverine and aeolian	Insignificant aeolian
Sediment inclusion	Considerable	Insignificant
Precipitation of calcium carbonate	No record	Extensive: as ikaite crystals (Dieckmann et al., 2008; Chapter 12)
Top predators	Polar bear, polar fox	Leopard seal
Seals	Walrus; ringed, harp, bearded and hooded seal	Weddell seal, crabeater seal, Ross seal, fur seal
Flightless birds	None (except moulting)	Emperor and Adélie penguins
Fish	Arctic cod (*Boreogadus saida*)	Broadhead fish (*Pagothenia borchgrevinki*)
Key crustaceans	Amphipods	Krill (*Euphausia superba*)
Nematodes	Several species, common	One record (Blome & Riemann, 1999)
Nudibranchs	No record	*Tergipes antarcticus* (Kiko et al., 2008)

in the Arctic can be considerable and is either aeolian or also due to terrestrial and riverine run-off resulting from the proximity of industrial centres (Chapters 12 and 13). In contrast, Antarctic sea ice can still be considered pristine, with terrestrial input playing an insignificant role and only found where strong winds may blow dust from exposed rocks or nunataks onto the sea ice. Aeolian pollution through industrial input is also of minor significance; however, signs of elevated PCB (polychlorinated biphenyls) have been found in birds and seals associated with sea ice.

Many other differences between Arctic and Antarctic sea ice exist, some of which are summarized in Table 1.1. They range from structural and textural differences, such as the composition of different ice textures, to differences in the salt regime, heat flux and the biology.

One major difference with regard to sea ice growth and development is the occurrence and role of platelet ice along the Antarctic coastline, a feature not observed in the Arctic. Platelet ice formation occurs within the water column and is associated with super cooled water usually derived from the contact of warmer deep water with the base of ice shelves. They are either formed underneath or in front of the ice shelves as well as under an existing fast or pack ice cover where super cooled water exists (Dieckmann et al., 1986). Platelets, however, also aggregate under ice shelves where with time, they consolidate and end up as marine ice which amalgamates with the overlying floating ice shelf and thus has a considerable impact on the dynamics of these ice shelves (Kipfstuhl et al., 1992).

Green icebergs, frequently observed in the Southern Ocean, represent remnants of calved icebergs containing marine ice. When platelets accrue under sea ice, usually fast ice, they add to the growth and thickness of the ice by congealing due to freezing from the top (Chapter 2). They also aggregate loosely under fast or pack ice, forming an important habitat for a highly productive and uniquely adapted microbial community comprising organisms, which appear to live exclusively in this habitat. This microbial community is one of the most productive sea ice communities and provides food for pelagic zooplankton species such as a copepods and amphipods which are associated with the platelets in large numbers (Chapter 10 and Fig. 1.3). It is also considered to be an important source of food for the benthos on the coastal shelf, particularly since platelet ice is a high latitude feature of the Antarctic coastline, which is covered by sea ice for a period of up to 7 months. Although the extent of platelet ice formation is unknown, it is expected to occur around the continent wherever there are floating ice shelves.

Apart from features and differences pertaining directly to sea ice, such as described above, the biology associated with sea ice in the Arctic and Antarctic has many similarities but also large differences. In fact, several plant and animal species are cosmopolitan. Whales such as the Minke frequent the pack ice of both the Arctic and the Antarctic, yet the two hemispheres do not share the same seal species (Chapter 11). While the polar bear is the top predator on Arctic sea ice, an equivalent predator is missing from Antarctic sea ice, although the leopard seal occupies a similar niche, living off penguins and other seals.

Many different seal species associated with sea ice occur in both polar regions where they have a very similar function in the food web. Many birds, both endemic and migratory, frequent the sea ice fields in both polar regions, but the most significant difference being the flightless penguins in the Antarctic which are missing in the Arctic (Chapter 11).

Notable differences exist between the fish associated with the sea ice. The most important species in the Arctic is the Arctic cod (*Boreogadus saida*), while in Antarctica it is the broadhead fish (*Pagothenia borchgrevinki*). These species occupy similar niches, often living

Fig. 1.3 Platelet ice with microalgae growing on the edges and being grazed by amphipods. Image courtesy of Bjørn Gulliksen.

amongst ice crystals, and have developed almost identical antifreeze proteins in response to similar environmental conditions although they are genetically unrelated (Chapter 10).

Another major difference between Arctic and Antarctic sea ice associated organisms is found in the crustaceans. The Antarctic krill (*Euphausia superba*) is the pivotal crustacean, in terms of biomass, associated with sea ice. It is adapted to live off the micro-algae growing on the peripheries of ice floes as well as in the water column (Chapter 10). Although krill species occur in the Arctic, they do not reach the biomass reported in Antarctic waters and *E. superba* is absent from the Arctic. Amphipods are not that frequently found in Antarctic sea ice, with the exception of platelet ice, whereas in the Arctic they are the most dominant crustaceans associated with sea ice.

Smaller metazoans and protozoans such as copepods, ciliates, nematodes, turbellarians and foraminifers have been found in the sea ice of both hemispheres. An example is the planktonic foraminifer, *Neogloboquadrina pachyderma*, which has been found by many studies in large numbers in Antarctic but has rarely in Arctic sea ice. On the other hand, there is only one record of nematodes from sea ice in the Antarctic (Blome & Riemann, 1999), whereas they are commonly found in Arctic sea ice. The same applies to rotifers, often found in large numbers in Arctic sea ice, but which have not yet been recorded in Antarctic sea ice (Chapter 10).

There are well over 100 diatom species that are commonly found to live within the brine channel labyrinth of sea ice. Some of the important diatom species, such as *Fragilariopsis cylindrus* and *F. curta*, are bipolar and constitute important representatives in the sea ice of both polar oceans. Other species such as *Melosira arctica* have a central role in the Arctic sea ice ecosystem only.

Many of the similar, as well as different, features pertaining to sea ice relate to the geological history of the poles. The bipolar occurrence of the same organisms in sea ice is often found

in those that are able to migrate long distances, such as some birds and whales, or in the case of smaller planktonic organisms, those that are transported by ocean currents. However, some conundrums, such as the occurrence of the large numbers of krill in Antarctica and not in the Arctic, still need to be clarified.

1.5 Implications for astrobiology and future natural resource exploitation

Sea ice as a proxy for extraterrestrial systems

During the past 15 years, sea ice has received increasing interest as a proxy for extraterrestrial systems and the search for life in other parts of our solar system (Chapter 15). The fact that the earth's ice-covered poles appear to closely resemble those of other planets such as Mars or Jupiter's moons, Europa and Ganymede, makes ice, particularly sea ice, a possible proxy to assess and compare the suitability of extraterrestrial life (Chyba & Phillips, 2001). Based on the understanding of life processes on earth, some scientists argue that analogically life on another planet or moon might exist if four conditions are met (McKay, 2000):

(1)   The presence of water or a similar solvent to enable biochemical activity.
(2)   The availability of carbon, nitrogen, phosphorus and sulphur.
(3)   Environmental stability.
(4)   Energy to maintain biochemical processes.

   Since sea ice appears to be an ideal terrestrial analogy, scientists are focusing on the psychrophilic environmental conditions and constraints for organisms living within. One theory is that life may have originated under just such conditions (Deming, 2002; Soare & Green, 2002). Because of its brine network, sea ice has the capacity to retain liquid pockets containing nutrients and organic resources down to −35°C. Metabolic activity, such as respiration and functional protein synthesizing machinery, has been detected at −20°C in sea ice. This, combined with the further evidence that bacteria live at the interface between crystal and liquid (Junge et al., 2001), indicates that the eutectic interface between solid and liquid phases of water may well be a biochemical crucible for life (Deming, 2002). In particular, these ideas are enhanced by the findings that freezing improves and enhances important biomolecular reactions (Vajda, 1999).
   Although these are possible analogues for the conditions that may have sustained primitive life on earth, countless questions concerning the origin of life and antecedent pre-biotic conditions remain unresolved (Levy & Miller, 1998). Despite the tantalizing lure to compare the brown colourations observed on Europa's surface to diatom-coloured sea ice, these ice systems, tens to hundreds of kilometres thick, are substantially different to the 1–10 m thick ice that we know from our polar oceans. Surface water or near-surface water required for photosynthesis or sub-surface energetic conditions required for chemosynthesis have also not yet been discerned in this extraterrestrial system. With the intense radiation acting on the extraterrestrial ice, if life forms do exist, or have existed in the past, it seems that they will be quite unlike those that dominate sea ice found on earth today (Thomas & Dieckmann, 2002).

Use of ice organisms for novel biotechnologies

Because organisms, particularly bacteria and micro-algae living within the sea ice, have a high degree of biochemical and physiological adaptation to cold and changeable salinity conditions, they have a high potential for biotechnological applications (Russell, 1997; Cavicchioli et al., 2002; Thomas & Dieckmann, 2002; Raymond et al., 2007; Chapter 8). Adaptation to a permanently cold environment includes the optimization of basic cell processes necessary for growth and survival. These can be summarized into three categories: enzyme function, nutrient transport and cell membrane function. The adaptations of cellular processes in each of these areas represent potential biotechnology products for exploitation (Cavicchioli et al., 2002; Raymond et al., 2007).

Two such examples are the production of polyunsaturated fatty acids (PUFAs) and the production of cold-active enzymes by bacteria and diatoms from Antarctic sea ice (Thomas & Dieckmann, 2002). A critical metabolic requirement at low temperatures is the maintenance of functional membranes. The fatty acid composition of membrane phospholipids regulates the degree of fluidity (Russell & Nichols, 1999). Therefore, an increase in PUFAs is required to retain membrane fluidity at low temperatures. This approach may lead to new ways of manufacturing these fatty acids for the expanding market in these compounds as dietary supplements for humans, livestock and fish. To this day, PUFAs have remained as a natural product due to the synthetic difficulty of reproducing the methylene interrupted double bond sequence by industrial chemistry. Their significance to animals and humans lies in their biological activity, as precursors for groups of nutritionally important compounds and as essential cellular components (Meyer et al., 1999). Interest in the production of PUFAs from alternative sources for use in aquaculture feeds and human health supplements has fuelled recent research into the molecular biology of PUFA production in sea ice organisms (Mock & Kroon, 2002a,b).

Cold-active or cold-adapted enzymes are produced by organisms existing in permanently cold habitats located in polar zones, at high altitudes or in the deep sea. These enzymes provide opportunities to study the adaptation of life to low temperature and also the potential for biotechnological exploitation (Morita et al., 1997; Deming, 2002; Thomas & Dieckmann, 2002; Amils et al., 2007). Applications exist in a range of industries for cold-active enzyme applications, e.g. cleaning agents, leather processing, degradation of xenobiotic compounds in cold climes, food processing (fermentation, cheese manufacture, bakery, confectionery, meat tenderization) and molecular biology (Amils et al., 2007; Margesin et al., 2007). Cold-active enzymes typically have maximal catalytic activity at temperatures below 40°C and usually display some degree of thermolability. Recent research has focused on determining the structural characteristics that confer cold adaptation in enzymes (Amils et al., 2007). Individual enzyme types possess different structural strategies to gain overall increased flexibility, suggesting that protein folding has a critical role in conferring activity at low temperature. Preliminary data have been obtained for a variety of psychrophilic and psychrotolerant (cold-tolerant) enzymes from Antarctic bacterial isolates from sea ice indicating that they are good sources of cold-active enzymes (Nichols et al., 1999).

In addition to enzyme applications and PUFA production, cold-adapted archaea, bacteria and eukaryotes have wide-ranging biotechnological applications. These range from sources of cryoprotectants, bioremediation of oil spills, frost protection, and low-temperature waste treatment (Cavicchioli et al., 2002). The vastness of sea ice extent, and the diversity of

abiotic regimes that are found within the sea ice zone, clearly promise tremendous potential for the discovery of novel low-temperature extremophiles and their exploitation for future biotechnological applications.

1.6 Recent advances and perspectives

As we become increasingly aware of the tremendous influence sea ice has on global processes, particularly climate, it is not surprising that scientific interest is steadily growing and making rapid advances in all disciplines. Possibly one of the most crucial and pressing issues is whether the observed changes in Arctic sea ice cover are part of some natural cycle or represent a climatic regime change in which the feedbacks associated with the presence of a sea ice cover play an important role. It is not yet really understood what connections exists between what is happening in the Arctic or Antarctic and other changes both inside and outside the polar regions. These questions will hopefully be answered with the advent of new remote-sensing technology and the development of improved models. Cryosat, for instance, is a 3-year radar altimetry mission, scheduled for launch in 2009, to determine variations in the thickness of the earth's continental ice sheets and marine ice cover. Its primary objective is to test the prediction of thinning Arctic ice due to global warming.

There are still fundamental problems with sea ice dynamical models that prevent their useful application in Global Circulation Models (GCMs). Parameter tuning is required because current sea ice models do not resolve physical processes below grid sizes of 20 km. Such tuning can, at best, provide a good fit to reality over limited periods of time. Accurate simulation over decadal and longer timescales requires models with parameters that can be independently assessed, although ice thickness remains a largely uncertain parameter (Chapters 4 and 6).

The lack of sub-20 km scale model physics is compounded by the fact that, because ice floes are of typically 0.1–10 km^2, the continuity assumption of existing models breaks down for smaller scales. Therefore, the observed discontinuities in properties such as ice velocity, thickness and motion cannot be represented. Although these problems have been recognized for almost three decades, recent advances in numerical climate prediction make the study of the impact of improved sea ice physics especially relevant (Chapter 2). There is a need to include comprehensive, elastic–viscous–plastic models of sea ice rheology. Further improvements to sea ice dynamical models require fundamental advances in understanding sub-grid scale physics down to the microstructure of sea ice. However, here too considerable advances are being made. Meso-scale ice thickness is being obtained with airborne EM (electromagnetic) instrumentation and upward looking sonars (ULS) either tethered to the sea floor or deployed in submarines (Chapter 4).

Recent improvements in analytical techniques, with the development of *in situ* earthmagnetic field NMR spectroscopy as a particularly interesting example, hold considerable promise in resolving some of the microstructural issues (Chapter 2). Further down the scale, the eutectic interface between the solid and liquid phases of water in sea ice can be studied with sophisticated microscope technology being developed to examine micro-scale processes within sea ice (Junge et al., 2001; Deming, 2002; Chapter 7).

The ecological significance of sea ice in the polar regions, whilst recognized as being considerable, is still difficult to assess because of logistical constraints and problems encountered in the methodology to investigate the heterogeneous and multiple ecological niches of the ice.

Remote-sensing technology using ocean colour satellites such as the Sea-viewing Wide Field-of-view Sensor (SeaWiFS) and long time series of sea ice concentration data from microwave sensors, available from the National Snow and Ice Data Center, one of eight NASA Distributed Active Archive Centers (DAACs), enable the examination of how variations in sea ice cover affect primary production associated with a retreating or advancing ice edge (Arrigo et al., 2008a). Long-term records of environmental effects due to sea ice dynamics are scarce and incomplete. Yet these are essential to interpret correctly the observed fluctuations in krill, bird and animal populations (Croxall et al., 2002).

Large-scale under-ice surveys of organisms associated with the sea ice, particularly krill, using remotely operated or autonomous underwater vehicles, have improved our understanding of the relationship between krill and sea ice cover (Brierley et al., 2002). Biogeochemical processes, and the growth and survival of organisms within the ice or at the sea ice peripheries, are difficult to study without interfering or destroying the ice itself. The latest designs in microelectrodes and optodes are being successfully developed to avoid these problems and to measure parameters such as oxygen, nutrients and light in brine channels or the skeletal layer of sea ice (Mock et al., 2002; Chapters 8 and 12). As mentioned before, the psychrophilic sea ice organisms, particularly bacteria and diatoms, are being investigated and screened using molecular biological techniques to understand their adaptation and potential use in biotechnology (Feller and Gerday, 1997).

The progress which has been made in obtaining physical, ecological and biogeochemical data on sea ice has benefited the first attempts to model and estimate primary production of sea ice, particularly in the Antarctic (Chapter 8). Yet despite these advances, sea ice research is often comparable to the proverbial 'needle in a haystack'. If we consider the field experiments and measurements, we come to the conclusion that only a very small proportion and area of the total sea ice cover has been investigated. The total number of cores extracted for physical and biological investigations probably does not even amount to more than a few hundred thousand, covering an area of only a few square kilometres. We use the data acquired in this manner to extrapolate, well knowing that sea ice samples taken only a few centimetres apart may differ tremendously in their fundamental properties.

We have a good knowledge of the fundamentals of chemistry and physics leading to the first crystals of ice. However, do we understand the chemical changes that take place from the point of freezing to the time of melting within the sea ice matrix, especially when there is extensive growth of biological assemblages which can be highly variable in composition.

Today more than ever, sea ice in the Arctic is receiving attention because of the search and quest for oil. The exploration and drilling for oil is known to be hazardous and often devastating to the environment. In the case of sea ice this is even more acute. The consequences of accidental oil spill in cold regions will clearly be far reaching. However, it is still unclear as to how oil will react with sea ice and how the sea ice biota and associated ecology will be affected. Preliminary studies have been conducted, but our understanding about the recovery of sea ice ecosystems following massive oil spill events still remains highly speculative. There is therefore a need to increase our awareness and to expand our research activities on sea ice in order to answer the many open questions. Increasingly we need to realize that with the expanding human population and the ever-widening quest for resources, sea ice will more than ever constitute a challenge to scientists and environmentalists alike.

Despite an overwhelming wealth of information that has been gathered over the past 200 years, sea ice still remains a largely unexplored realm. This is largely due to its inaccessibility, its complexity and extreme heterogeneity. Sea ice research remains a costly enterprise because

of the specialized logistics essential for any fieldwork campaign. Most of our knowledge is derived from the summer months with very little direct information or data during the winter. More information is required on small- and large-scale processes. Longer time-series are required to understand seasonal and annual variations in the many processes that interact to make sea ice the complex, yet fascinating, substratum so important in a global context.

References

Abram, N.J., Mulvaney, R., Wolff, E.W. & Mudelsee, M. (2007) Ice core records as sea ice proxies: an evaluation from the Weddell Sea region of Antarctica. *Journal of Geophysical Research*, **112**, D15101, 10.1029/2006JD008139.

Amils, R., Ellis-Evans, C., & Hinghofer-Szalkay, H.G. (2007) *Life in Extreme Environments*. Springer-Verlag, Berlin, Germany.

Arrigo, K.R., van Dijken, G.L. & Bushinsky, S. (2008a) Primary production in the Southern Ocean, 1997–2006. *Journal of Geophysical Research*, **113**, C08004, 10.1029/2007JC004551.

Arrigo K.R., van Dijken, G.L. & Pabi, S. (2008b) Impact of a shrinking Arctic ice cover on marine primary production. *Geophysical Research Letters*, **35**, L19603, 10.1029/2008GL035028.

Atkinson, A., Siegel, V., Pakhomov, E. & Rothery, P. (2004) Long-term decline in krill stock and increase in salps within the Southern Ocean. *Nature*, **432**, 100–103.

Blome, D. & Riemann, F. (1999) Antarctic sea ice nematodes, with description of *Geomonhystera glaciei* sp. nov. (Monhysteridae). *Mitteilungen aus dem Hamburgischen Zoologischen Museum und Institut*, **96**, 15–20.

Brierley, A.S. & Thomas, D.N. (2002) On the ecology of Southern Ocean pack ice. *Advances in Marine Biology*, **43**, 173–278.

Brierley, A.S., Fernandes, P.G., Brandon, M.A., et al. (2002) Antarctic krill under sea ice: elevated abundance in a narrow band just south of ice edge. *Science*, **295**, 1890–1892.

Buchanan, J.Y. (1874) Some observations on sea-water ice. *Proceedings of the Royal Society London*, **22**, 431–432.

Carsey, F.D. (1980) Microwave observation of the Weddell Polynya. *Monthly Weather Review*, **108**, 2032–2044.

Cavicchioli, R., Siddiqui, K.S., Andrews, D. & Sowers, K.R. (2002) Low-temperature extremophiles and their applications. *Current Opinion in Biotechnology*, **13**, 253–261.

Charrassin, J.-B., Hindell, M., Rintoul, S.R., et al. (2008) Southern Ocean frontal structure and sea ice formation rates revealed by elephant seals. *Proceedings of the National Academy of Sciences of the USA*, **105**, 11634–11639.

Chyba, F.F. & Phillips, C.B. (2001) Possible ecosystems and the search for life on Europa. *Proceedings of the National Academy of Sciences of the USA*, **98**, 801–804.

Cleve, P.T. (1883) Diatoms collected during the expedition of the Vega. *Vega Expeditions*, Vetenskap Iakttagelsen, Stockholm, **3**, 455–542.

Coles, V.J., McCartney, M.S., Olson, D.B. & Smethie, W.M. Jr. (1996) Changes in Antarctic Bottom Water properties in the western South Atlantic in the late 1980s. *Journal of Geophysical Research*, **101**, 8957–8970.

Croxall, J., Trathan, P.N. & Murphy, E.J. (2002) Environmental change and Antarctic seabird populations. *Science*, **297**, 1510–1514.

Deming, J.W. (2002) Psycrophiles and polar regions. *Current Opinion in Microbiology*, **5**, 301–309.

Dickie, G. (1880) On the algae found during the Arctic Expedition. *Botanical Journal of the Linnean Society, London*, **17**, 6–12.

Dickson, R., Lazier, J., Meincke, K., Rhines, P. & Swift, J. (1996) Long-term coordinated changes in the convective activity of the North Atlantic. *Progress in Oceanography*, **38**, 241–295.

Dieckmann, G., Rohardt, G., Hellmer, H. & Kipfstuhl, J. (1986) The occurrence of ice platelets at 250 m depth near the Filchner Ice Shelf and its significance for sea ice biology. *Deep-Sea Research Part 1*, **33**,141–148.

Dieckmann, G.S., Nehrke, G., Papadimitriou, S., et al. (2008) Calcium carbonate as ikaite crystals in Antarctic sea ice. *Geophysical Research Letters*, **35**, L08501, 10.1029/2008GL033540.

Drygalski, E. (1904) *Zum Kontinent des eisigen Südens – Deutsche Südpolarexpedition – Fahrten und Forschungen des 'Gaub' 1901–1903*. Verlag Georg Reimer, Berlin.

Ehrenberg, C.G. (1841) Nachtrag zu dem Vortrage über Verbreitung und Einfluss des mikroskipischen Lebens in Süd- und Nordamerika. *Berichte über die zur Bekanntmachung geeigneten Verhandlung der Königlich-Preussischen Akademie der Wissenschaften zu. Berlin*, **1841**, 201–209.

Ehrenberg, C.G. (1853) Über neue Anschauungen des kleinstein nördlichen Polarlebens. *Berichte über die zur Bekanntmachung geeigneten Verhandlung der Königlich-Preussischen Akademie der Wissenschaften zu. Berlin*, **1853**, 522–529.

Fedotov, V.I., Cherepanov, N.V. & Tyshko, K.P. (1998) Some features of the growth, structure and metamorphism of East Antarctic landfast ice. In: *Antarctic Sea Ice: Physical Processes, Interactions and Variability* (Ed. M.O. Jeffries), American Geophysical Union, Washington, DC. *Antarctic Research Series*, **74**, 343–354.

Feller, G. & Gerday, C. (1997) Psychrophilic enzymes – molecular basis of cold adaptation. *Cellular and Molecular Life Sciences*, **53**, 830–841.

Fetterer, F., Knowles, K., Meier, W. & Savoie, M. (2002, updated 2008). *Sea Ice Index*. National Snow and Ice Data Center Boulder, CO, USA.

Fogg, G.E. (1992) *A History of Antarctic Science*. Studies in Polar Research, Cambridge University Press, Cambridge.

Foldvik, A., Gammelsrød, T. & Tørresen, T. (1985) Circulation and water masses on the southern Weddell Sea shelf. In: *Oceanology of the Antarctic Continental Shelf* (Ed. S.S. Jacobs), American Geophysical Union, Washington, DC. *Antarctic Research Series*, **43**, 5–20.

Foster, T.D. & Carmack, E.C. (1976) Frontal zone mixing and Antarctic bottom water formation in the southern Weddell Sea. *Deep-Sea Research*, **23**, 301–317.

Gill, A.E. (1973) Circulation and bottom water production in the Weddell Sea. *Deep-Sea Research*, **20**, 111–140.

Gloersen P., Campbell, W.J., Cavalieri, D.J., Comiso, J.C., Parkinson, C.L. & Zwally, H.J. (1992) *Arctic and Antarctic Sea Ice, 1978–1987: Satellite Passive Microwave Observations and Analysis*. NASA Special Publication, **511**, 289 pp. National Aeronautics and Space Administration, Washington, DC.

Gordon, A.L. (1978) Deep Antarctic convection west of Maud Rise. *Journal of Physical Oceanography*, **8**, 600–612.

Gow, A.J., Ackley, S.F. & Govoni, J.W. (1998) Physical and structural properties of land-fast ice in McMurdo Sound, Antarctica. In: *Antarctic Sea Ice: Physical Processes, Interactions and Variability* (Ed. M.O. Jeffries), American Geophysical Union, Washington, DC. *Antarctic Research Series*, **74**, 355–374.

Haas, C., Pfaffling, A., Hendricks, S., Rabenstein, L., Etienne, J.-L. & Rigor, I. (2008) Reduced ice thickness in Arctic Transpolar Drift favours rapid ice retreat. *Geophysical Research Letters*, **35**, L17501, 10.1029/ 2008GL034457.

Heil, P. & Allison, I. (1999) The pattern and variability of Antarctic sea ice drift in the Indian Ocean and western Pacific sectors. *Journal of Geophysical Research*, **104**, 789–15,802.

Hellmer, H.H. (2004) Impact of Antarctic ice shelf melting on sea ice and deep ocean properties. *Geophysical Research Letters*, **31**, L10307, 10.1029/2004GL019506.

Horner, R.A. (Ed.) (1985) *Sea Ice Biota*. CRC Press, Boca Raton, FL.

Jones, P.D., New, M., Parker, D.E., Martin, S. & Rigor, I.G. (1999) Surface air temperature and its changes over the past 150 years. *Reviews in Geophysics*, **37**, 173–199.

Junge, K., Krembs, C., Deming, J., Stierle, A. & Eicken, H. (2001) A microscopic approach to investigate bacteria under *in situ* conditions in sea ice samples. *Annals of Glaciology*, **33**, 304–310.

Kerr, R.A. (2007) Is battered Arctic Sea Ice down for the count? *Science*, **318**, 33–34.

Kiko, R., Kramer, M., Spindler, M. & Wägele, H. (2008) *Tergipes antarcticus* (Gastropoda, Nudibranchia): distribution, life cycle, morphology, anatomy and adaptation of the first mollusk known to live in Antarctic sea ice. *Polar Biology*, **31**, 1383–1395.

Kipfstuhl, J., Dieckmann, G., Oerter, H., Hellmer, H. & Graf, W. (1992) The origin of green icebergs in Antarctica. *Journal of Geophysical Research*, **97**, 20319–20324.

Kottmeier, C. & Sellmann, L. (1996) Atmospheric and oceanic forcing of the Weddell Sea ice motion. *Journal of Geophysical Research*, **101**, 20809–20824.

Krishfield, R.A. & Perovich, D.K. (2005) Spatial and temporal variability of oceanic heat flux to the Arctic ice pack. *Journal of Geophysical Research*, **110**, C07021, 10.1029/2004JC002293.

Lange, M.A., Ackley, S.F., Wadhams, P., Dieckmann, G.S. & Eicken, H. (1989) Development of sea ice in the Weddell Sea, Antarctica. *Annals of Glaciology*, **12**, 92–96.

Lazier, J. (1980) Oceanographic conditions at ocean weather ship *Bravo*, 1964–1974. *Atmosphere and Ocean*, **18**, 227–238.

Lefebvre, W., Goosse, H., Timmermann, R. & Fichefet, T. (2004) Influence of the Southern Annular Mode on the sea ice-ocean system. *Journal of Geophysical Research*, **109**, 10.1029/2004JC002403.

Levy, M. & Miller, S.L. (1998) The stability of the RNA bases: implications for the origin of life. *Proceedings of the National Academy of Sciences USA*, **95**, 7933–7938.

Lytle, V.I. & Ackley, S.F. (1996) Heat flux through sea ice in the western Weddell Sea: convective and conductive transfer processes. *Journal of Geophysical Research*, **101**, 8853–8868.

Lytle, V.I., Massom, R., Bindoff, A., Worby, A. & Allison, I. (2000) Winter-time heat flux to the underside of East Antarctic pack ice. *Journal of Geophysical Research*, **105**, 28759–28770.

McGhee, R. (2006) *The last Imaginary Place: A Human History of the Arctic World*. Oxford University Press, Oxford.

McKay, C.P. (2000) The deep biosphere: lessons for planetary exploration. In: *Subsurface Microbiology and Biogeochemistry* (Eds J.K. Fredrickson & M. Fletcher), pp. 315–328. John Wiley & Sons, New York.

Margesin, R., Schinner, F., Marx, J.-C. & Gerday, C. (2007) *Psychrophiles: From Biodiversity to Biotechnology*. Springer Verlag GmbH, Berlin.

Martin, S. (1996) *A History of Antarctica*. State Library of New South Wales Press, Sydney.

Maykut, G.A. & Untersteiner, N. (1971) Some results from a time dependent thermodynamic model of sea ice. *Journal of Geophysical Research*, **76**, 1550–1575.

Meyer, B.J., Tsivis, E., Howe, P.R.C., Tapsell, L. & Calvert, G.D. (1999) Polyunsaturated fatty acid content of foods: differentiating between long and short chain omega-3 fatty acids. *Food Australia*, **51**, 82–95.

Mock, T. & Kroon, B.M.A. (2002a) Photosynthetic energy conversion under extreme conditions. I. Important role of lipids as structural modulators and energy sink under N-limited growth in Antarctic sea ice diatoms. *Phytochemistry*, **61**, 41–51.

Mock, T. & Kroon, B.M.A. (2002b) Photosynthetic energy conversion under extreme conditions. II. The significance of lipids at low temperature and low irradiances in Antarctic sea ice diatoms. *Phytochemistry*, **61**, 53–60.

Mock, T., Dieckmann, G.S., Haas, C., et al. (2002) Micro-optodes in sea ice: a new approach to investigate oxygen dynamics during sea ice formation. *Aquatic Microbial Ecology*, **29**, 297–306.

Morita, Y., Nakamura, T., Hasan, Q., Murakami, Y., Yokoyama, K. & Tamiya, E. (1997) Cold-active enzymes from cold-adapted bacteria. *Journal of the American Oil Chemists Society*, **74**, 441–444.

Muench, R.D., Morison, J.M., Padman, L., et al. (2001) Maud Rise revisited. *Journal of Geophysical Research*, **106**, 2423–2440.

Nicholls, K.W. (1997) Predicted reduction in basal melt rates of an Antarctic ice shelf in a warmer climate. *Nature*, **388**, 460–462.

Nichols, D.S., Sanderson, K., Bowman, J., et al. (1999) Developments with Antarctic microorganisms: PUFA, culture collections, bioactivity screening and cold adapted enzymes. *Current Opinions in Biotechnology*, **10**, 240–246.

Pavlov, V.K. & Pavlova, O.A. (2007) Increasing sea ice drift velocities in the Arctic Ocean, 1979–2005. *Geophysical Research Abstracts*, **9**, 07124.

Petterson, O. (1833) On the properties of water and ice. *Vega Expeditions*, Vetenskap Iakttagelsen, Stockholm, **3**, 249–323.

Raymond, J.A., Fritsen, C. & Shen, K. (2007) An ice-binding protein from an Antarctic sea ice bacterium. *FEMS Microbiology Ecology*, **61**, 214–221.

Rudels, B., Jones, E.P., Anderson, L.G. & Kattner, G. (1994) On the intermediate depth waters of the Arctic Ocean. In: *The Polar Oceans and Their Role in Shaping the Global Environment* (Eds O.M. Johannessen, R.D. Muench & J.E. Overland), American Geophysical Union, Washington, DC. *Geophysical Monograph*, **85**, 33–46.

Russell, N.J. (1997) Psychrophilic bacteria – molecular adaptations of membrane lipids. *Comparative Biochemistry and Physiology*, **118**, 489–493.

Russell, N.J. & Nichols, D.S. (1999) Polyunsaturated fatty acids in marine bacteria – a dogma rewritten. *Microbiology*, **145**, 767–779.

Schauer, U., Beszczynska-Möller, A., Walczowski, W., Fahrbach, E., Piechura, J. & Hansen, E. (2008) Variation of measured heat flow through the Fram Strait between 1997 and 2006. In: *Arctic–Subarctic Ocean Fluxes: Defining the Role of the Northern Seas in Climate* (Eds R.R. Dickson, J. Meincke & P. Rhines), pp. 65–85. Springer-Verlag, Dordrecht.

Soare, R.J. & Green, D.M. (2002) The habitability of Europa: a cautionary note. *EOS, Transactions of the American Geophysical Union*, **83**, 231.

Tamura, T., Ohshima, K.I. & Nihashi, S. (2008) Mapping of sea ice production for Antarctic coastal polynyas. *Geophysical Research Letters*, **35**, L07606, 10.1029/2007GL032903.

Thomas, D.N. & Dieckmann, G.S. (2002) Antarctic sea ice – a habitat for extremophiles. *Science*, **295**, 641–644.

Thomas, D.N., Fogg, G.E., Convey, P., et al. (2008) *The Biology of Polar Regions*. Oxford University Press, Oxford.

Timmermann, R., Lemke, P. & Kottmeier, C. (1999) Formation and maintenance of a polynya in the Weddell Sea. *Journal of Physical Oceanography*, **29**, 1251–1264.

Tomlinson, C. (1871) *Frozen Stream: Formation and Properties of Ice*. SPCK, London.

Tucker, W.B., Gow, A.J. & Weeks, W.F. (1987) Physical properties of summer sea ice in the Fram Strait. *Journal of Geophysical Research*, **92**, 6787–6803.

Turner, J., Lachlan-Cope, T.A., Colwell, S., Marshall, G.J. & Connolley, W.M. (2006) Significant warming of the Antarctic winter troposphere. *Science*, **311**, 1914–1917.

Usachev, P.I. (1949) The microflora of polar ice. *Transactions of the Institute Okeanology, Akademii Nauk SSSR*, **3**, 216 pp. (in Russian).

Vajda, T. (1999) Cryo-bioorganic chemistry: molecular interactions at low temperature. *Cellular and Molecular Life Sciences*, **56**, 398–414.

Wadhams, P. (2000) *Ice in the Ocean*. Gordon and Breach Science Publishers, Amsterdam.

Wadhams, P. (2001) Sea ice: variations in extent and thickness. In: *Encyclopedia of Ocean Sciences* (Eds J.H. Steele & K.K. Turekian), pp. 2582–2599. Academic Press, San Diego, CA.

Watanabe, Y., Bornemann, H., Liebsch, N., et al. (2006) Seal-mounted cameras detect invertebrate fauna on the underside of an Antarctic ice shelf. *Marine Ecology Progress Series*, **309**, 297–300.

Weeks, W.F. (1998) On the history of research on sea ice. In: *Physics of Ice-Covered Seas*, Vol. 1 (Ed. M. Leppäranta), pp. 1–24, University of Helsinki Press, Helsinki, Finland.

White, W.B. & Peterson, R.G. (1996) An Antarctic circumpolar wave in surface pressure, wind, temperature, and sea ice extent. *Nature*, **380**, 699–702.

Wilson, R., Liebsch, N., Davis, I., et al. (2007). All at sea with animal tracks; methodological and analytical solutions for the resolution of movement. *Deep-Sea Research Part II*, **54**, 193–210.

Wordie, J.M. (1921) Shackleton Antarctic Expedition, 1914–1917: the natural history of pack ice as observed in the Weddell Sea. *Transactions of the Royal Society of Edinburgh*, **52**, 795–829.

Wright, I.P. & Priestley, R.E. (1922) *Glaciology. British (Terra Nova) Antarctic Expedition 1910–1913*. Harrison & Sons, London.

Zubov, N.N. (1945) *Arctic Ice*. US Navy Electronics Laboratory, San Diego, CA (originally published in Russian by Izdatelstvo Glasevmorputi in 1943).

2 Growth, Structure and Properties of Sea Ice

Chris Petrich and Hajo Eicken

2.1 Introduction

The substantial reduction in summer Arctic sea ice extent observed in 2007 and 2008 and its potential ecological and geopolitical impacts generated a lot of attention by the media and the general public. The remote-sensing data documenting such recent changes in ice coverage are collected at coarse spatial scales (Chapter 6) and typically cannot resolve details finer than about 10 km in lateral extent. However, many of the processes that make sea ice such an important aspect of the polar oceans occur at much smaller scales, ranging from the submillimetre to the metre scale. An understanding of how large-scale behaviour of sea ice monitored by satellite relates to and depends on the processes driving ice growth and decay requires an understanding of the evolution of ice structure and properties at these finer scales, and is the subject of this chapter.

As demonstrated by many chapters in this book, the macroscopic properties of sea ice are often of most interest to studies of the interaction between sea ice and its environment. They are defined as the continuum properties averaged over a specific volume (Representative Elementary Volume) or mass of sea ice. The macroscopic properties are determined by the microscopic structure of the ice, i.e. the distribution, size and morphology of ice crystals and inclusions. The challenge is to see both the forest, i.e. the role of sea ice in the environment, and the trees, i.e. the way in which the constituents of sea ice control key properties and processes. In order to understand and project how the forest will respond to changes in its environment, we have to understand the life cycle of its constituents, the trees. Here, we will follow a bottom-up approach, starting with the trees, characterizing microscopic properties and processes and how they determine macroscopic properties, to give us better view of the forest as a whole.

In following this approach, we will build up from the submillimetre scale and conclude with the larger scales shown in Fig. 2.1. In the process, we use the term 'microscopic' not to describe an absolute scale, but rather the range of scales at which the different component phases can be clearly distinguished. By averaging over the individual, microscopic component phases, one arrives at a macroscopic representation of the material where the specific properties of the microscopic component phases are subsumed in a single, bulk parameter. This approach requires a microstructural model of the medium.

Sea ice would not be sea ice without the salt. In fact, take away the salt and we are left with lake ice, differing in almost all aspects that we discuss in this chapter. The microscopic and
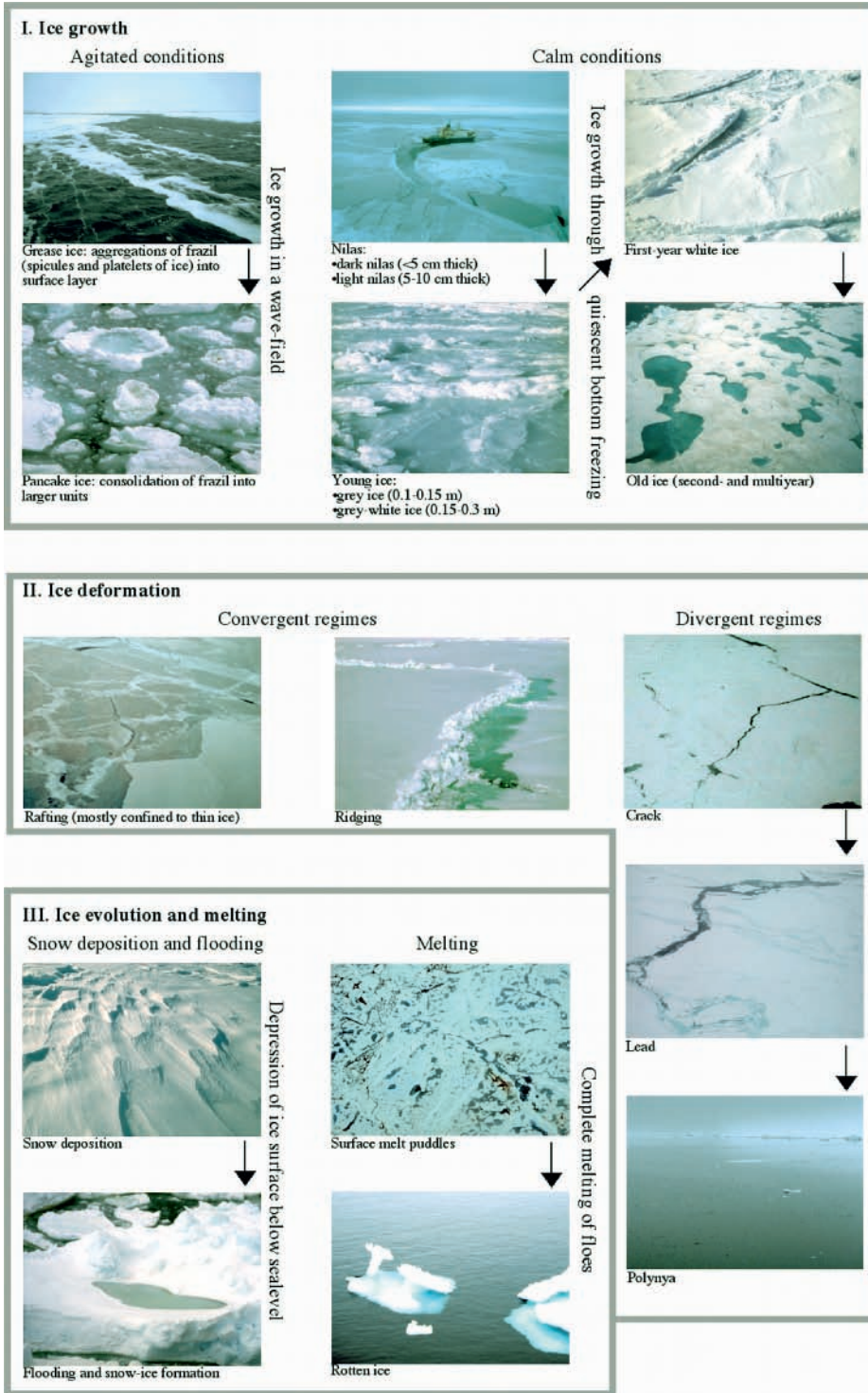
Fig. 2.1   Ice types pack ice features and growth, melt and deformation processes.
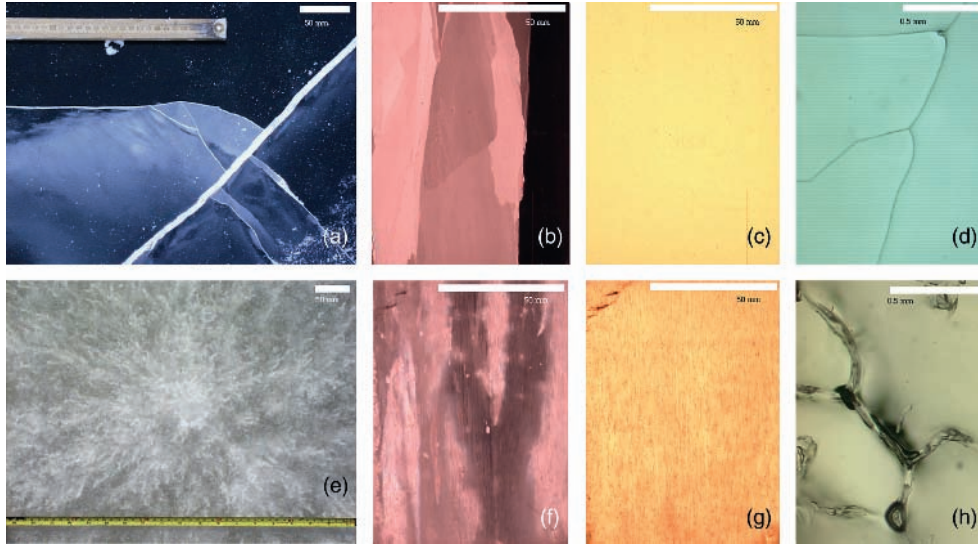
Fig. 2.2 Surface appearance and microstructure of winter lake ice (Imikpuk Lake, top, panels a–d) and sea ice (Chukchi Sea fast ice, bottom, panels e–h) near Barrow, Alaska. The bright features apparent in the lake ice are cracks that penetrate all the way to the bottom of the ice cover (close to 1 m thick), the clear, uncracked ice appears completely black (a, top). The sea ice surface photograph (e) shows a network of brine channels that join into a few feeder channels. Panels b, c, f and g show photographs of vertical thin sections from the two ice covers, with b and f recorded between crossed polarizers, highlighting different ice crystals in different colours. Panels c and g show the same section as b and f in plain transmitted light, demonstrating the effect of brine inclusions on transparency of the ice. Panels d and h are photomicrographs showing the typical pore structure at a temperature of $-5°C$ (lake ice) and $-15°C$ (sea ice), with few thin inclusions along grain boundaries in lake ice (d) and a network of thicker brine inclusions in sea ice (h).

macroscopic redistribution of ions opens the path to understanding all other macroscopic properties of sea ice. We will therefore start in Section 2.2 by looking at the influence of ions on ice growth at the scale of individual ice crystals, both in sea ice growing under rough and quiescent conditions. We will continue in Section 2.3 by looking at the dynamic feedback system between fluid dynamics and pore volume, both microscopically and at the continuum scale. We will point out that our knowledge is far from being exhaustive in this fundamental aspect. However, armed with a basic understanding of crystal structure, phase equilibria and pore structure, we can shed light on ice optical, dielectric and thermal properties, and macroscopic ice strength in Section 2.4. One of the most discussed aspects of sea ice is its presence or absence. We will look at the growth and energy budget of sea ice, and touch on deformation and decay processes in Section 2.5.

Lake ice versus sea ice

As a way of illustrating how the aspects discussed above are intertwined in nature, and as an example of the manner in which ice growth, microstructure and properties manage to affect important processes up to regional scales, consider the following example.

The photographs in Fig. 2.2 show the surface of snow-free lake ice and sea ice in late spring near Barrow, Alaska. Despite comparable thickness and growth conditions, the lake ice, due to its high transparency, appears much darker than the sea ice. This is also expressed

in a large difference in albedo (the fraction of the incident short-wave radiation reflected from a surface, Section 2.4), such that more than three-quarters of the incoming short-wave irradiative flux penetrates the lake ice surface and the underlying water, compared with less than half for the sea ice cover. This has substantial consequences for the heat budget of the ice cover and the water beneath. The fact that the albedo of sea ice is typically higher than that of open water by a factor of up to 10 gives rise to the so-called ice-albedo feedback: a perturbation in the surface energy balance resulting in a decrease in ice extent due to warming may amplify since the reduction in ice extent in turn increases the amount of solar energy absorbed by the system (Curry et al., 1995). Under natural conditions, this contrast is affected by snow deposition in winter which increases albedo, at least prior to the onset of ice surface melt, and by the drainage of meltwater from lake ice, potentially bringing up albedo later in the melt season. For low-albedo lake ice, this effect is less pronounced.

What is the cause underlying these contrasts? As the thin-section photographs in Fig. 2.2 demonstrate, lake ice is nearly devoid of millimetre and submillimetre liquid inclusions, whereas sea ice can contain more than 10 mm^{-3}. Hence, while light passes through the clear lake ice with only minor attenuation along its path, much of the light entering sea ice is scattered back towards the surface. This explains both the high albedo and lack of transparency of thicker sea ice samples.

This contrast in ice properties and appearance is only partly explained by the difference in salinity between lake and sea water. Microscopically, at the scale of brine inclusions and below, lake ice grows differently from sea ice, with the interface between liquid and solid being planar rather than lamellar as is the case with sea ice. Hence, typically more than 99.9% of the impurities such as ions dissolved in lake water are expelled from the ice cover. In sea ice, brine is trapped between the lamellae at the bottom of the ice, allowing for a retention of between 10 and 40% of the ions in the ice.

While the differences in bulk ice properties such as albedo or optical extinction coefficient are immediately obvious from these images, the physical features and processes responsible for these differences only reveal themselves to the microscopic approach, as exemplified by the thin-section images depicting individual inclusions (Fig. 2.2). In the sections below, we will consider in more detail how microstructure and microphysics are linked to sea ice growth and evolution, and how both in turn determine the properties of the ice cover as a whole.

2.2 Ions in the water: sea ice microstructure and phase diagram

Crystal structure of ice Ih

The characteristic properties of sea ice and its role in the environment are governed by the crystal lattice structure of ice Ih, in particular its resistance to incorporate sea salt ions. Depending on pressure and temperature, water ice can appear in more than a dozen different modifications. At the Earth's surface, freezing of water under equilibrium conditions results in the formation of the modification ice Ih, with the 'h' indicating crystal symmetry in the hexagonal system. Throughout this chapter, the term 'ice' refers to ice Ih.

The water molecules (H_2O) in ice Ih are arranged tetrahedrally around each other, with a sixfold rotational symmetry apparent in the so-called basal plane (Fig. 2.3). The principal crystallographic axis (referred to either as the corresponding unit vector [0001] or simply as
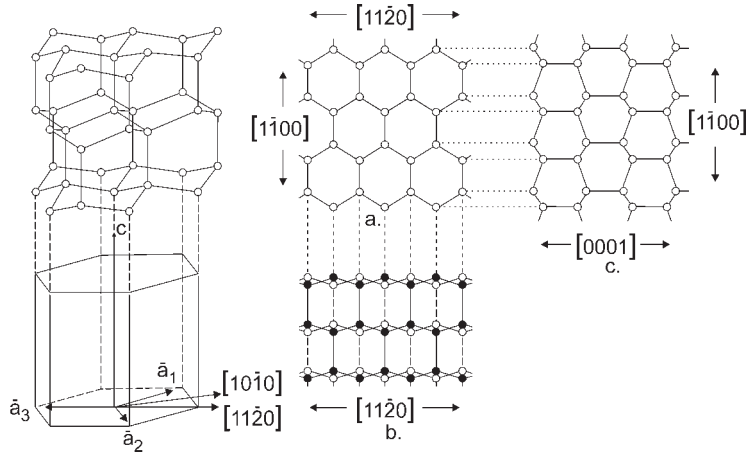
Fig. 2.3 Crystal structure of ice Ih (from Weeks & Ackley, 1986). The *c*-axis is indicated at left and right, the center panels correspond to a view along (top) and normal (bottom) to the *c*-axis.

the *c*-axis) is normal to the basal plane and corresponds to the axis of maximum rotational symmetry (Fig. 2.3). The interface of the basal plane is smooth at the molecular level. The basal plane is defined by the crystal *a*-axes, and the crystal faces perpendicular to this plane are rough at the molecular level. The different interface morphologies result in different interface kinetics and are responsible for a pronounced anisotropy in growth rates. For example, the higher growth rates in the basal plane lead to the development of individual frazil ice crystals with thickness-to-width ratios on the order of 1:10 to 1:100 (Hobbs, 1974). Another key aspect of the ice crystal structure is the fact that the packing density of water molecules in ice, and hence its material density, is lower than in the liquid. In the liquid state, water molecules are arranged as hydrate shells surrounding impurities (e.g. sea salt ions) owing to the strong polarity of the water molecule. However, accommodation of sea salt ions is greatly restricted in the ice crystal lattice (Fig. 2.3). Only very few species of ions and molecules are incorporated in the ice crystal in appreciable quantities (either replacing water molecules or filling voids) owing to constraints on size and electric charge. Among them are fluorine and ammonium ions and some gases. However, the major ions present in sea water (Na^+, K^+, Ca^{2+}, Mg^{2+}, Cl^-, SO_4^{2-}, CO_3^{2-}) are not incorporated into the ice crystal lattice and are rejected by the advancing ice–water interface during crystal growth. This has very important consequences for the microstructure and properties of sea ice, as part of the salt is retained in liquid inclusions in the solid ice matrix while a larger fraction is rejected into the underlying water column. Both of these processes and their implications will be discussed in the next paragraph and in Sections 2.3 and 2.4.

Columnar ice microstructure and texture

As ice grows and the ice–water interface advances downwards into the melt, salt ions are rejected from the ice. The salt builds up ahead of the advancing interface, increasing the salinity of a thin layer of a few millimetres to a few centimetres in thickness. The resulting gradient in salt concentration leads to diffusion of salt away from the interface towards the less saline ocean. Thermodynamic equilibrium dictates that the interface itself is at the
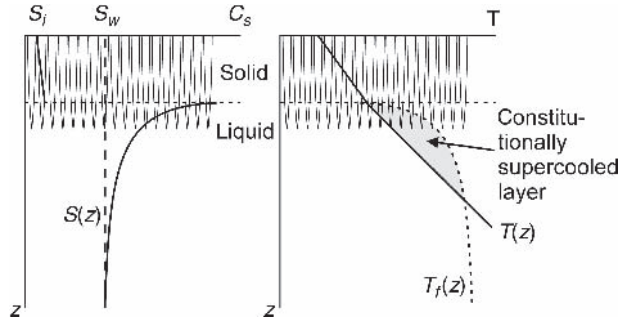
Fig. 2.4 Schematic of the lamellar ice–water interface (skeletal layer) and the corresponding salinity (left) and temperature (right) gradients. The freezing temperature profile is shown as a dashed line at right, with a constitutionally supercooled layer bounded by the actual temperature gradient and the salinity-dependent freezing-point curve.

respective melting/freezing point. Since the freezing point decreases with increasing salinity, an increase in salt concentration goes along with a drop in temperature. This leads to a heat flux from the ocean towards the now colder interface.

At the same time, the higher density (equation 2.9) of the more saline brine in contact with the ice bottom can also lead to enhanced transport of brine through convection (Niedrauer & Martin, 1979; Wettlaufer et al., 1997). In a simplified approach, the effects of turbulent convective transport and molecular diffusion can be subsumed in an 'effective' diffusion coefficient. However, heat transport through this convective boundary layer from the warmer ocean to the colder interface is still faster than the transport of ions away from the enriched interface to the ocean. As a result, a thin layer is established ahead of the interface that is cooled below the freezing point of the ocean but only slightly enriched in salinity above the ocean level. This layer is said to be *constitutionally supercooled* since its temperature is below the freezing point of the brine (Fig. 2.4).

It is this constitutional supercooling that distinguishes the growth of lake ice from that of sea ice and helps explain their respective characteristic properties. Any small (submillimetre) perturbation of a planar ice–water interface that protrudes into the constitutionally supercooled zone finds itself at a growth advantage, since heat is not only conducted upwards and away from the ice–water interface, but the supercooled water layer also provides a non-negligible heat sink. Considering that ice grows fastest in the basal plane, crystals with horizontal *c*-axes quickly outgrow crystals with *c*-axes off the horizontal in a process termed geometric selection (see below). The salt rejected by a protrusion contributes to a freezing point reduction of the brine along the protrusion boundaries. Consequently, such perturbations can grow into ordered patterns of lamellar bulges at the ice–water interface (for a full quantitative analysis of constitutional supercooling and its impact on ice microstructure, see Weeks & Ackley, 1986; Wettlaufer, 1998). In its most pronounced manifestation, this process of localized, non-linear heat and salt dissipation leads to the so-called dendritic growth with a complex interface typical of, for example, snowflakes. In the case of sea ice, the morphology of the interface is mostly reported to be lamellar or cellular (Figs 2.4 and 2.5) rather than fully dendritic. For brackish ice grown from water with very low salinities (details given in Weeks & Ackley, 1986; Weeks & Wettlaufer, 1996), a planar interface remains stable throughout the growth process, resulting in rejection of the bulk of the impurities and low porosities.

The growth of individual ice platelets into supercooled water is also observed in the vicinity of Antarctic ice shelves (Jeffries et al., 1993; Leonard et al., 2006) and under Arctic sea
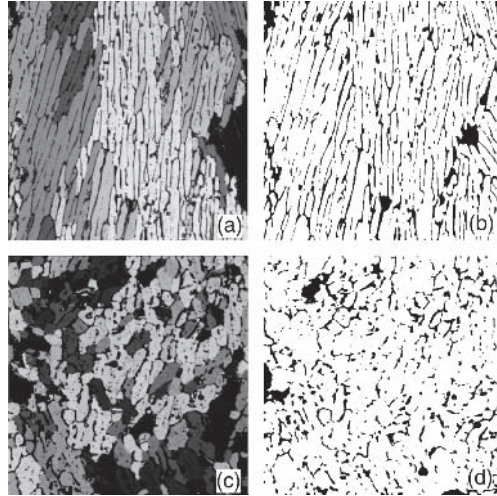
Fig. 2.5 Horizontal thin-section photographs of columnar sea ice grown in a large ice tank (Hamburg Environmental Test Basin, INTERICE experiments) in the absence of an under-ice current (a, b; porosity 0.154, mean pore area 0.096 mm^2) and with a current speed of 0.16 m s^{-1} (c, d; porosity 0.138, mean pore area 0.077 mm^2). Images a and c have been recorded between crossed polarizers (section is 20 mm wide), with grain boundaries apparent as transitions in grey shades due to different interference colours. Images b and d show the same section with pores indicated in black, based on processing of images recorded in incident light.

ice that is separated from the ocean by a meltwater lens (Notz et al., 2003). Characteristic of the resulting crystal fabric are comparatively large platelets whose c-axes deviate from the horizontal seemingly at random. The process of their formation is poorly understood; one hypothesis is that they are seeded by frazil crystals that formed in the supercooled water.

When fully developed, as in the case of ordinary columnar sea ice (Fig. 2.6), the lamellar interface consists of submillimetre-thick blades of ice, separated by narrow films of brine, so called brine layers. The transitional layer, demarcated by ice volume fractions tending towards zero at its lower end and with a transition to laterally interconnected ice lamellae at a porosity of about 30% at its upper end is commonly referred to as the skeletal layer. This thin, low- to zero-strength layer is subjected to a significant advective exchange between ocean water and brine from the interior of the sea ice (Section 2.3).

As evident from Fig. 2.4, the arrays of brine layers between ice blades extend all the way up into the ice sheet. If we were to consider the fate of the skeletal layer in a thickening ice cover with time, we would in essence be following a trajectory in the phase diagram shown in Fig. 2.7 (though for a smaller bulk salinity). As more ice is added underneath the layer under consideration, its temperature drops and the fraction of liquid decreases while ice is added onto the ice blades. Eventually, the ice lamellae join up and consolidate into lower-porosity sea ice. During this consolidation process, brine is being lost from the ice as discussed in more detail in Section 2.3. Though not rigorously accurate, the principle process is the reverse of the warming sequence depicted in Fig. 2.8.

During ice growth, the basic patterns of the grain and pore microstructure, i.e. the size and orientation of crystals and the layer spacing of pores, remain essentially unchanged from that laid down in the skeletal layer. This is illustrated in Fig. 2.5, which shows horizontal thin sections of two different varieties of columnar ice grown under the same conditions except for a difference in the under-ice current. Ice grown in the absence of externally
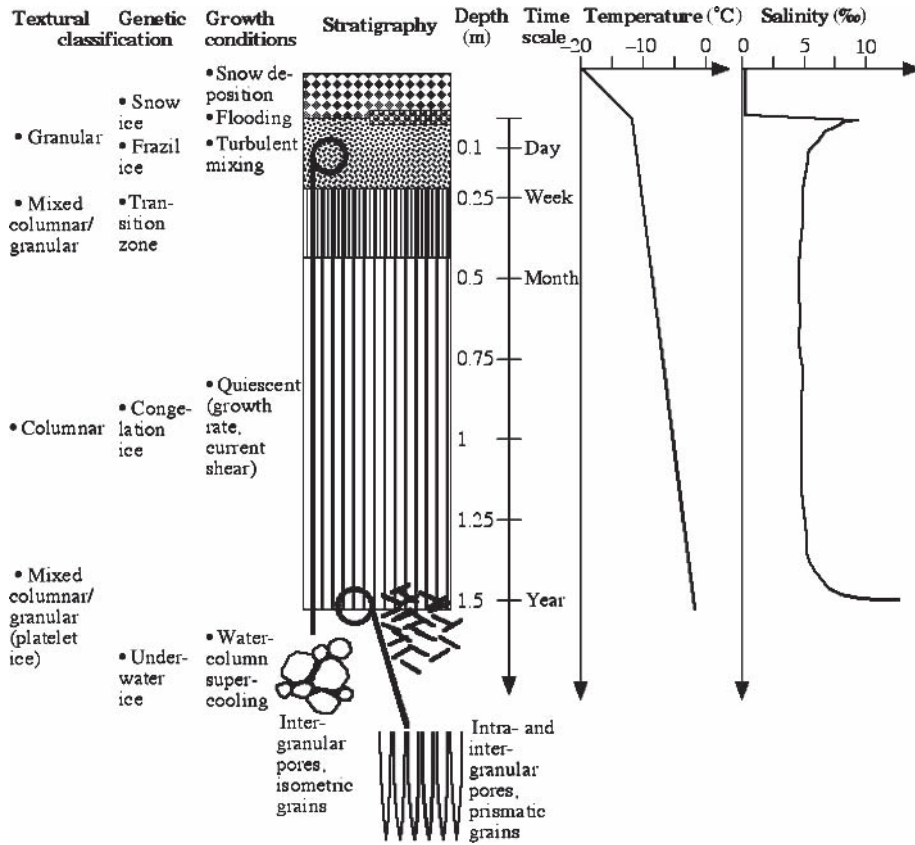
**Fig. 2.6** Schematic summarizing the main ice textures, growth conditions and timescales, and typical winter temperature and salinity profiles for first-year sea ice.
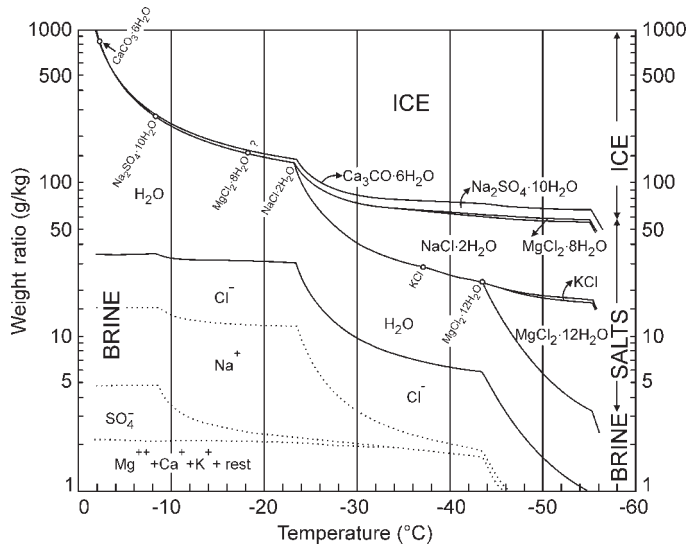

Fig. 2.7 Phase diagram of sea ice from Assur (1960). The different curves indicate the mass fraction of solid ice (top), salts (middle) and liquid brine (bottom) present in a closed volume of standard seawater at different temperatures.
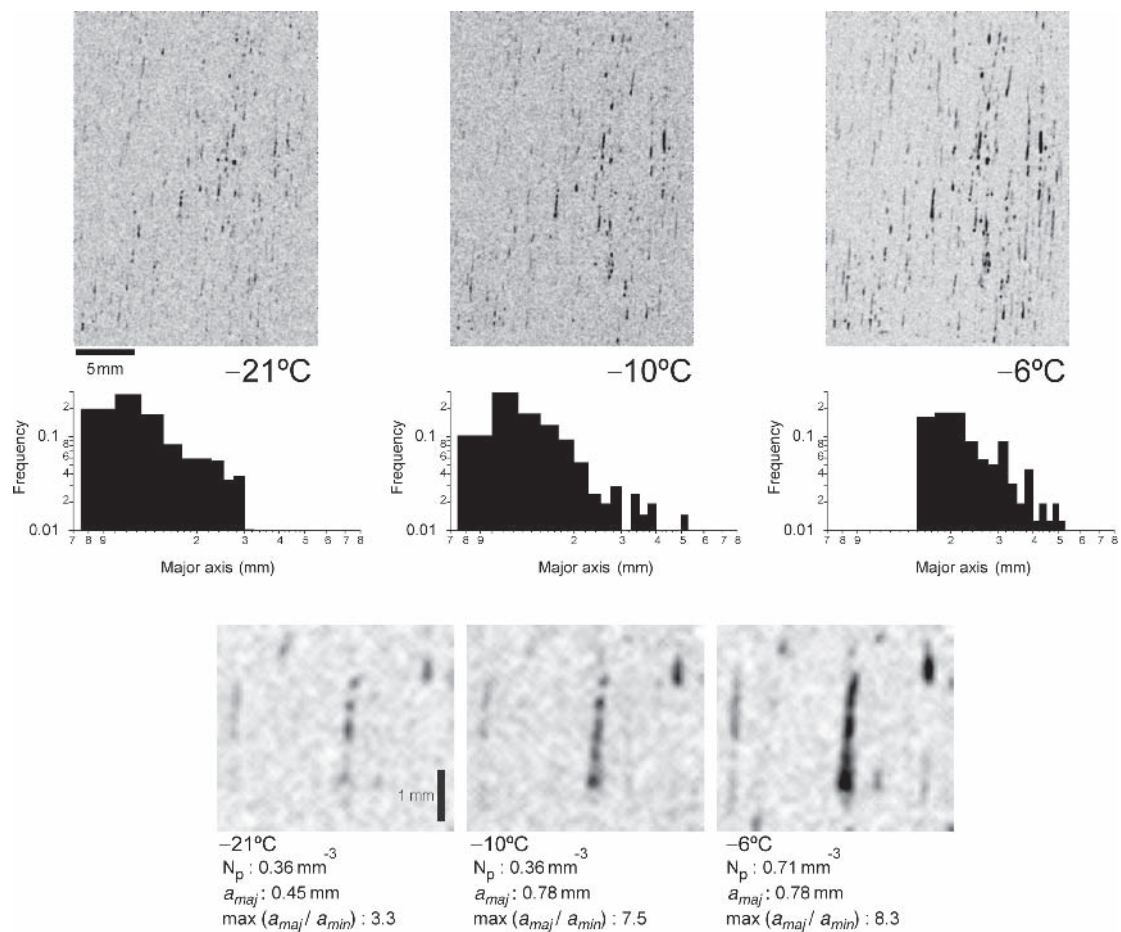
Fig. 2.8 Thermal evolution of fluid inclusions in first-year sea ice obtained near Barrow, Alaska (0.13–0.16 m depth, sample obtained in March 1999 and maintained at *in situ* temperatures after sampling up until experiment; for details see Eicken et al., 2000) as studied with MRI techniques. The upper three panels show a vertical cross section through the sample as it is warmed, with pores appearing dark. The middle panels show the size distribution of the major pore axes a_{maj} (upper 10-percentile), indicating enlarging and merging of pores in the vertical. The change in pore size, morphology (as indicated by the maximum ratio between major and minor pore axis length $max(a_{maj}/a_{min})$) and number density N_p is apparent in the lower panels, which show a smaller subset of pores at 0.15 m depth.

imposed currents exhibits the typical lamellar substructure, with rows of brine layers within individual crystals, and remnants of the liquid separating individual blades of ice within the skeletal layer. Along grain boundaries, the size and shape of pores is more heterogeneous, with brine tubes and channels of several millimetres in diameter apparent in the lower right of Fig. 2.5b. The arrangement, shape and size of crystals on the scale of a thin section such as those in Fig. 2.5 are typically referred to as the texture of the ice. The ice grown in a current ($0.16 \, \mathrm{m \, s^{-1}}$ measured 0.5 m below the ice bottom) also exhibits a grain substructure delineated by pores, but the degree of parallel alignment of pores and the aspect ratios of individual inclusions are very different, as are the grain sizes (Fig. 2.5c,d). This is a result of the fact that the thickness and degree of supercooling of the constitutionally supercooled zone, as well as the thickness of the skeletal layer, depend on a variety of factors, such as the ice-growth rate, the salinity of the underlying water and, as illustrated here, the magnitude of currents enhancing transport away from the ice.

The impact of currents, though not all that well understood quantitatively, has been shown to have dramatic effects on the orientation of individual ice lamellae and the crystals they are constituting. Independent of under-ice currents, in growing sea ice (Fig. 2.6), the number of grains with horizontal c-axes increases rapidly downwards, such that the vast majority of crystals exhibit horizontal c-axes and vertically oriented ice lamellae below 20 cm from the top of the columnar ice layer (Weeks & Wettlaufer, 1996). This is interpreted to be the result of 'geometric selection' during the growth process, such that crystals with ice lamellae tilted more into the vertical (c-axis horizontal) are at a growth advantage and displace lamellae of a more horizontal orientation during the thickening of an ice cover. Further, c-axes tend to be parallel in the presence of a unidirectional under-ice current (Weeks & Wettlaufer, 1996). It appears that salt transport away from the interface is enhanced for crystals with lamellae oriented perpendicular (c-axes parallel) to the current, providing them with a growth advantage that eventually results in the dominance of c-axes parallel to the current (Langhorne & Robinson, 1986). Both of these processes result in a pronounced anisotropy of the ice cover.

A further, important aspect of the lamellar substructure is the observation that the width of ice lamellae, and hence the spacing of brine layers, exhibits a dependence on growth rate. Nakawo and Sinha (1984) demonstrated this for Arctic sea ice, where the down-core reduction in growth rate (see Section 2.5) closely corresponded to an increase in the brine layer spacing a_0. Typically, a_0 is in the order of a few tenths of a millimetre. However, in what is probably the oldest sea ice sampled to date, grown at rates of a few centimetres per year, Zotikov et al., (1980) found brine layer spacings of several millimetres.

In spite of contributing only marginally to the total mass of sea ice, the skeletal layer harbours one of the greatest concentrations of phytoplankton in the world's oceans by providing a habitat for diatoms and other microorganisms, and in turn grazers (Smith et al., 1990; see also Chapters 8–10). As algae depend not only on sunlight but also on nutrients for photosynthetic activity, in many areas, the most active layer of ice organisms is found within the bottom few centimetres of the ice cover, where high porosities and permeabilities and the proximity of the ocean reservoir provide a sufficient influx of inorganic nutrients and gas exchange (Chapters 7, 8 and 12). At the same time, this layer offers some protection from the largest grazers (Chapter 10) and presents photosynthetic organisms with a foothold at the top of the water column where irradiative fluxes are highest (Eicken, 1992b).

Granular ice microstructure and texture

Salinity of ocean water is measured in practical salinity units and is discussed in more detail below. The practical salinity scale is valid for constant sea water composition and is based on conductivity ratios measured in the salinity interval from 2 to 42.

The freezing point of sea water with a salinity of 34 is at $-1.86°C$ due to the freezing point depression by the dissolved inorganic salts (see below). Pure sea water lacks solid impurities that can act as nuclei for ice crystal formation and can be cooled substantially below the freezing point without ice formation (supercooling). However, maximum supercoolings observed in the oceans are typically less than 0.1 K owing to the abundant presence of impurities upon which nucleation of ice crystals takes place (Fletcher, 1970).

In contrast to lake or brackish water, the temperature of the density maximum is not above the freezing point of sea water. A body of sea water above the freezing point cooled from the surface will experience convective overturning (colder surface water is replaced by warmer water displaced at depth owing to buoyancy) until the entire upper water layer (mixed layer) is at the freezing point. This mixing process is usually supported by wind and waves. In a lake of zero salinity, the water has its maximum density at 4°C. Once the entire water column has cooled to this temperature, the surface waters stratify and ice forms as soon as the very surface layer is at the freezing point while denser, warmer water remains underneath.

The combination of a mixed layer and the action of wind stress at the ocean surface only rarely allows for quiescent initial formation of ice typical of lakes. Rather, ice crystals form throughout the upper water layers and are kept in suspension until a surface layer of ice slush builds up, reducing mixing agitated by wind. The ice crystals forming in the water take the shape of needles, spicules or platelets, often intertwined into aggregates and are known as frazil ice (Figs 2.2 & 2.5). Individual crystals are typically a few to a few tens of millimetres across and less than a millimetre in thickness (Weeks & Ackley, 1986). Following further freezing and consolidation of this surface slush layer composed of frazil ice, the microstructure and texture of the ice change as layer upon layer is added to the bottom of the ice sheet through quiescent growth of the so-called congelation ice (columnar ice, Fig. 2.6). The stratigraphy of such a 'typical' ice cover, as revealed through analysis of vertical core sections, consists of a sequence of granular ice (a few tens of centimetres at most in the Arctic, but substantially more in other, more dynamic environments such as the Antarctic), with isomeric or prismatic crystals (see detailed descriptions in Weeks & Ackley 1986; Tyshko et al., 1997), followed by a transitional layer that is underlain by columnar ice, composed of vertically elongated prismatic crystals that can grow to several centimetres in diameter and tens of centimetres in length (Fig. 2.6, see above for details).

Frazil ice

Whereas congelation growth of sea ice with columnar texture typically dominates in the Arctic, frazil growth resulting in granular textures is also common, in particular in the Southern Ocean. Growth of individual platelets and needles of frazil in a supercooled water column differs from growth of congelation ice insofar as both heat and salt have to be transported away from the interface into the surrounding ocean water. Consequently, beyond a certain size, individual frazil crystals also develop rough, dendritic surfaces as a result

of solute build-up. Frazil growing in the turbulent uppermost metres of the ocean has the tendency to aggregate into floes of crystals that are capable of sweeping particulates and biota from the water column, carrying them to the surface as a layer of frazil or grease ice accumulates (Reimnitz et al., 1990; Smedsrud, 2001; Chapter 8). Despite its abundance, some aspects of frazil growth are not that well understood, including the inherent 'stickiness' attributed to its role in enhancing concentrations of biota in Antarctic sea ice or the conditions governing the growth of larger ice platelets at greater depths in water parcels supercooled through interaction with the melting Antarctic ice shelves (Bombosch, 1998). The latter process is capable of generating large volumes of crystals that contribute both to the mass balance of the ice shelves as well as the coastal sea ice, where one finds platelets as large as 10 cm across and a few millimetres thick floating towards the surface and accumulating in layers of several metres thickness.

Another aspect of frazil growth that is currently not well understood is the actual consolidation of loose masses of frazil crystals, with ice volume fractions between about 10 and 30% into solid granular sea ice. Evidence from oxygen stable-isotope (Chapter 3) and salinity measurements of individual crystals and layers of granular ice suggests that the consolidation process is a combination of downward freezing of voids among the mesh of frazil crystals and transformations in the size distribution and morphology of the crystals themselves. This is similar to what has been observed to occur in water-saturated snow slush (Eicken, 1998). Further studies are required to elucidate the specific processes and resultant heat and salt fluxes, since frazil ice growth is a key process in the interaction of ocean and atmosphere.

Formation of sea ice

In the Antarctic higher wind speeds, the effects of ocean swell penetrating from higher latitudes and the larger number of openings in the pack greatly favour the formation of frazil ice, which can constitute as much as 60–80% of the total ice thickness in some regions (Lange et al., 1989; Jeffries et al., 1994). The ice edge advances northwards from the Antarctic continent by as much as 2500 km from austral autumn through spring (Chapter 6). This dynamic ice-growth environment favours growth of frazil ice and leads to the predominance of the so-called pancake ice (Fig. 2.8). Pancake ice forms through accretion of frazil crystals into centimetre-sized floes of ice that in turn accrete into decimetre-sized pans of ice. Under the action of wind and ocean swell that penetrate deep into the sea ice zone, these pans bump and grind against one another, resulting in a semi-consolidated ice cover composed of ice discs with raised edges that are from a few centimetres to more than 10 cm thick. These pancakes eventually congeal into larger units (Wadhams et al., 1987). Once the ice cover has consolidated into a continuous, solid sheet or large floes with snow accumulated on top, only characteristic surface roughness features ('stony fields' or 'rubble ice') betray its dynamic origins. However, stratigraphic analysis of ice cores clearly demonstrates that the ice cover is largely composed of individual pancakes, often tilted or stacked in multiplets on top of one another. The interstices between the individual pancakes eventually consolidate through a combination of frazil growth and freezing of congelation ice (Lange et al., 1989). Typically, these processes account for ice thicknesses of up to 0.5 m (Wadhams et al., 1987; Worby et al., 1998).

In the Arctic, recent reductions in perennial ice extent (Chapters 4 and 6) may now increasingly favour the formation of frazil ice. The limited data available to date does suggest an increase in the proportion of granular ice compared to previous studies (Perovich et al., 2008), but more observations are needed to confirm these early indications. In the past, most of the ice cover was composed of congelation ice (Weeks & Ackley, 1986).

Phase relations in sea ice

Unlike Zn and Cu in brass alloys, sea salts and ice do not form a solid solution in which the constituents intermingle in different proportions. Hence, the question arises as to what exactly is the fate of ions in freezing sea water. In order to fully address this problem, one needs to consider the physicochemical phase relations of an idealized or somewhat simplified sea water system. Sodium and chloride ions (Na^+, Cl^-) account for roughly 85%, sulphate ions (SO_4^{2-}) for 8% and magnesium, calcium and potassium for another 6% of the mass of salts dissolved in sea water. Owing to the predominance of sodium and chloride ions in sea water, many aspects of sea ice properties and structure can already be observed in a simple sodium chloride solution. More sophisticated representations of sea water typically take into account Na^+, K^+, Ca^{2+}, Mg^{2+}, Cl^-, SO_4^{2-} and CO_3^{2-}. In his classical study of the phase relations in sea ice, Assur (1960) assumed a constant 'standard' composition for sea ice. While such an approach is inadequate for geochemical studies (Marion & Grant, 1997; Chapter 12) and does present problems with ice that is strongly desalinated or grown in isolated basins, it is sufficient to predict the most important characteristics of sea ice behaviour upon cooling or warming.

Figure 2.7, taken from Assur's work, serves to illustrate the key aspects of the phase relations in sea ice. In a closed system (i.e. the mass fraction of all components is constant) of sea water of salinity 34, cooled below the freezing point at −1.86°C, one would observe a steady increase in the ice fraction as the temperature is lowered, assuming that the individual phases are in thermodynamic equilibrium at all times. As the salts dissolved in sea water are not incorporated into the ice crystal lattice (see above), their concentration in the remaining brine increases steadily. At the same time, the freezing point of the brine decreases, coevolving with the increasing salinity of the liquid phase. At a temperature of −5°C, the ice mass fraction in the system amounts to 65% and the salinity of the brine in equilibrium with the ice has risen to 87. At −8.2°C, the concentration of salts has increased to the point that the solution is supersaturated with respect to sodium sulphate, a major component of sea water, resulting in the onset of mirabilite precipitation ($Na_2SO_4 \cdot 10H_2O$, Fig. 2.7). If one were to continue lowering the temperature of the system, mirabilite would continue to precipitate in the amounts specified in Fig. 2.7. Other salts precipitating during the freezing of sea water include ikaite ($CaCO_3 \cdot 6H_2O$), about whose distribution and mineralogy in sea ice little is known (Dieckmann et al., 2008), as well as hydrohalite ($NaCl \cdot 2H_2O$). The latter is predicted to start precipitating at −22.9°C, with roughly 90% of the precipitable sodium chloride present as hydrohalite at −30°C (Fig. 2.7). While the mass fraction of brine drops below 8% at −30°C, even at the lowest temperatures typically encountered in sea ice (around −40°C), a small but non-negligible liquid fraction remains. The presence of unfrozen water even at these low temperatures has important consequences, in particular for the survival of microorganisms overwintering in sea ice (Chapters 7 and 8).

Originally, the saltiness of ocean water was defined as the ratio of the mass of dissolved material to the mass of the solution. However, the mass of dissolved material is difficult to measure by evaporation since many crystalline salts are bound with water, and volatile components may evaporate during heating. A simplified approach has been followed since the beginning of last century exploiting the fact that ocean water around the world is of almost uniform composition. For most of the last century, the concentration of Cl⁻ ions has been measured by titration and scaled linearly to salinity (sometimes quoted as ppt or ‰). This relationship is sensitive to the composition of the sea water used for calibration and was corrected slightly in the 1960s. With the advent of conductivity meters, an accurate and even more convenient way opened up for salinity measurements. Today, the ocean salinity is defined by the ratio of the electrical conductivity of a solution to the conductivity of a reference solution, and converted to a practical salinity scale with an equation given by UNESCO (1978). As such, it is independent of chlorinity and mass of dissolved material. Salinity is defined as a dimensionless quantity; however, *practical salinity unit* (psu) is sometimes used as a unit to denote the use of the practical salinity scale.

The differences between the definitions of salinity are insignificant for most aspects of sea ice, with growth at the scale of individual ice crystals being a potential exception. The ocean salinity is only defined for one specific composition (Copenhagen Seawater), salinities between 2 and 42, and at temperatures above −2°C (UNESCO, 1978). However, sea ice bulk salinities of old ice and brine salinities are often well below and above this range, respectively, and the composition of dissolved ions in sea ice changes significantly with temperature. As discussed in the next section, brine salinity is usually calculated from bulk salinity. Considering the limited range of applicability of the practical salinity scale, care must be taken if brine salinity is to be measured directly.

2.3 Desalination and pore microstructure

Salinity profiles of growing and melting sea ice

In a pioneering study, Malmgren (1927)[1] studied the salinity evolution of Arctic first-year sea ice during the course of winter and into the summer melt season (Fig. 2.9). In this section, we will briefly consider the processes responsible for the characteristic C-shape of the salinity profile of young and first-year ice as well as the reduction in surface salinities during the first melt season in an ice floe's evolution. The importance of understanding the evolution of an ice cover's salinity profile is rooted in the central role temperature and salinity play with respect to ice porosity and pore microstructure. The majority of large-scale sea ice models currently assume constant ice salinity, thus depriving the simulated ice cover of an important response mechanism to changes in the atmospheric or oceanic boundary conditions.

The importance of these processes is illustrated by comparing the first-year winter sea ice salinity profile in Fig. 2.9 with that of summer or multiyear sea ice. As dictated by the phase relationships (Fig. 2.7), the transition from winter to summer sea ice generally corresponds to a change in the direction of the conductive heat flux through an ice floe from being directed upwards to being directed downwards (cf. Fig. 2.10).
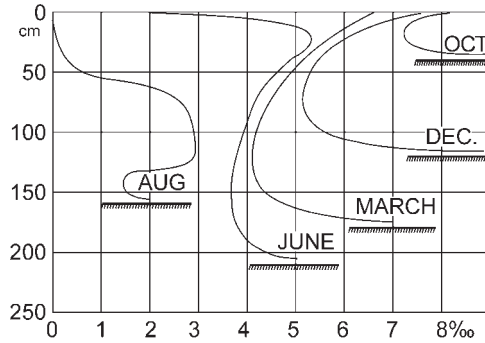
Fig. 2.9 Evolution of sea-ice salinity profiles (from Malmgren, 1927). Note the characteristic C-shape of the young and first-year ice salinity profile and the reduction in surface salinity due to meltwater flushing with the onset of summer melt.
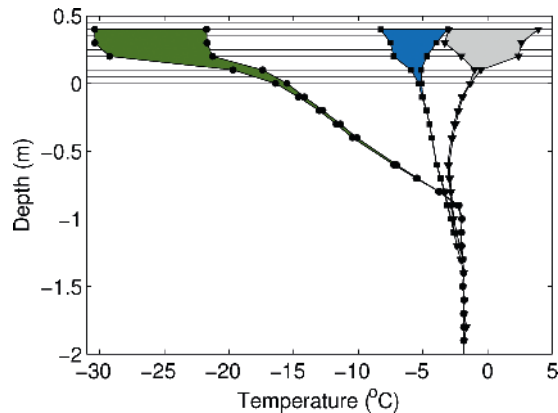

Fig. 2.10 Vertical temperature profiles measured with a thermistor probe frozen into the ice in Barrow, 2008. Positive depths are snow and air, negative depths are sea ice and ocean. Profiles show the temperature range encountered over a 24-hour period in mid February (day 45, circles), mid-May (day 135, squares) and at the end of May (day 150, triangles).

Origin of brine movement in growing sea ice

The microscopic exclusion of ions from a growing ice crystal leads to a local increase in brine salinity but it does not change the local bulk salinity. However, observations clearly show that the bulk salinity of growing first-year sea ice (typically 4–6) is only a fraction of the bulk salinity of the ocean water (around 33) (Fig. 2.9). The reduction of the bulk salinity, i.e. the removal of ions from sea ice, is due to a combination of molecular diffusion and advection in pore network and ocean, and turbulence at the sea ice–ocean transition. A special case is the migration of individual brine pockets in a temperature gradient due to solute diffusion (see Weeks & Ackley, 1986); it is significant on a microscopic level, and its impacts on these scales are still not well understood. However, it has been shown to be of little or no significance for the overall evolution of salinity profiles in winter. We can understand desalination of growing sea ice in idealized scenarios (e.g. neglecting turbulence at the sea ice–ocean interface) on the basis of advection alone.

Advection through growing sea ice is driven by three processes: a net hydrostatic pressure, typically due to the density difference between brine in sea ice and ocean; pressure fluctuations at the sea ice interface, e.g. from under-ice shear flow; and a small contribution due to volume expansion during freezing (brine expulsion). Simplifying the discussion, we will focus on the influence of the hydrostatic pressure. Feltham et al., (2002) have considered the impact of under-ice shear flow.

For a start, we treat sea ice according to the effective medium approach; we assume that the brine films and pores in sea ice are interconnected and that no dominant channels exist; fish-tank bubbler stones have this microstructure. In growing sea ice, we find a temperature gradient from the warmest ice at the ocean to the coldest ice at the upper surface (Fig. 2.10). Thus, brine salinity and brine density will increase towards the upper surface if the system is in thermodynamic equilibrium. This configuration is hydrostatically unstable, and a small perturbation in the density field will tend to grow and drive advective flow (called natural convection). The flow is retarded by the dynamic fluid viscosity μ and the ice permeability Π, which depends on the pore microstructure. Furthermore, perturbations are countered by the phase change that takes place during the flow and the resulting change in brine density. The rate of this change is related to the thermal diffusivity of the ice α_{si} and a characteristic distance Δh. A Rayleigh number can be defined for a homogeneous porous medium (Worster & Wettlaufer, 1997),

$$\mathrm{Ra} = \frac{g \Delta\rho \, \Pi \, \Delta h}{\mu \alpha_{si}} \qquad\qquad \text{(Equation 2.1)}$$

where $\Delta\rho$ is the density difference across the vertical distance Δh and g is the acceleration due to gravity. In order for natural convection to take place in a porous medium, the Rayleigh number has to exceed a critical value Ra_c (see Nield & Bejan 1998 for values). Wettlaufer et al., (1997) demonstrated in idealized laboratory experiments that brine release from growing saltwater ice set in only after the thickness of the ice exceeded a threshold. However, there are no direct observations of a critical Rayleigh number in naturally growing sea ice to date, and it is unclear under what conditions this might be observable given the variety of growth conditions discussed in the previous section.

Brine movement and bulk salinity

Mass conservation dictates that the volume of brine leaving the sea ice due to advection is balanced by brine entering the sea ice from the ocean (we neglect effects due to the density difference between ice and water here). This leads to a turbulent sea ice–ocean interface flux (i.e. an advective flux with no net direction), and there is one attempt to estimate its magnitude experimentally (Wakatsuchi & Ono, 1983). Apart from its relation to the brine flux, the volume flux from ocean into the ice determines the flux of nutrients, which is of particular relevance for biological processes (Chapters 7–10 and 12).

Within sea ice, a downward flow increases the local bulk salinity and porosity and ultimately leads to the formation of brine channels. Locally, brine is replaced by more saline brine from above, thereby increasing the bulk salinity. Since the more saline brine is superheated (i.e. above the freezing point) due to warming from the surrounding ice, it will partially dissolve surrounding ice to attain thermodynamic equilibrium, thereby increasing the porosity.

Brine leaving through channels is detectable as distinct brine plumes (streamers) in the under-lying water (Wakatsuchi, 1983; Dirakev et al., 2004). From stability analysis, it is expected that brine channels develop as a consequence of convection inside the porous medium, i.e. brine also moving upwards through the porous medium as part of the development process of channels (Worster & Wettlaufer, 1997). An upward-directed flow of brine leads to a reduction of the local bulk salinity and decrease of porosity. Niedrauer and Martin (1979) found in labo-ratory experiments that downward flow follows a cusp-shape pattern that terminates in brine channels. Consistent with this general pattern of bulk salinity distribution, Cottier et al., (1999) found in high-resolution salinity measurements that the bulk salinity is highest in the presence of brine channels and somewhat lower in between. The salinity difference between the brine leaving the sea ice and the brine entering the sea ice is the cause for the net desalination of sea ice that gives rise to the characteristic bulk salinity profiles (Fig. 2.9).

The rate of bulk desalination becomes insignificant with increasing distance from the sea ice–ocean interface. This gives rise to a quasi–steady state salinity, also termed stable salinity (Nakawo & Sinha, 1981). Two processes have been put forward to explain when bulk flow and desalination cease during cooling. On the one hand, based on continuum fluid dynamics considerations, the permeability of the sea ice may reach values too low to sustain natural convection, similar to arguments leading to equation 2.1. One the other hand, based on percolation considerations, the sea ice may develop pores that are dis-connected from regular fluid motion and therefore retain their salt content until the melt season (see below). There is currently no compelling experimental or theoretical evidence to determine which explanation describes the process in sea ice best. In numerical continuum fluid dynamics simulations of cracks that refreeze in two directions (top-down and inwards form the sides), Petrich et al., (2007) found that they needed to allow for a separation of the pore space to obtain steady-state salinity profiles. However, simulating ordinary uni-directionally forming sea ice, Petrich et al., (2009) obtained steady-state salinity profiles using the continuum approach without special considerations for the sea ice microstruc-ture. Either way, desalination is confined to a few centimetres at the bottom of growing sea ice (Figs 2.4 and 2.6).

Textbook bulk salinity profiles such as the ones in Fig. 2.9 show systematic characteristics (Eicken, 1992b) such as the typical C-shape during growth and seem to be predictable from the environmental conditions during growth (see below; Cox & Weeks, 1988). However, there is a considerable amount of variability between cores taken in proximity (Weeks & Lee, 1962). This variability has been attributed to pores and channels that are large compa-red to the sample size (Bennington, 1967; Cottier et al., 1999).

Development of the pore microstructure during growth and melt

In spite of its importance for optical properties, there is still no quantitative and complete description of the evolution of the pore microstructure during freezing and melt. However, we can link observations and hypotheses to understand the general process in a piecemeal approach. Here, we focus on sea ice with columnar rather than granular texture.

The ice microstructure is lamellar close to the ocean, and individual ice lamellae are intersper-sed by liquid brine films. The separation of the lamellae is typically around 0.3–0.5 mm. As the sea ice cools or desalinates, the lamellae grow thicker at the expense of the brine films and interconnect by forming bridges, presumably at porosities between 0.1 and 0.3 (see also

(a) $T = -15°C$, $\phi = 0.033$ (b) $T = -6°C$, $\phi = 0.075$ (c) $T = -3°C$, $\phi = 0.143$
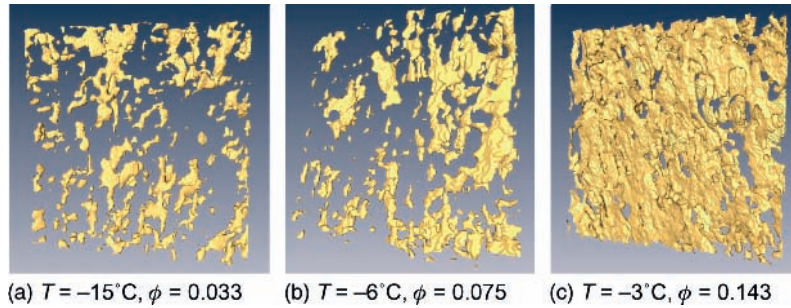
Fig. 2.11   X-ray microtomography images of brine layers in sea-ice single crystals as a function of temperature. Note how the sample porosity (f) and connectivity increase as it is warmed (Golden et al., 2007).

discussion of Fig. 2.11). Horizontal sections of this ice reveal inclusions ranging over several orders of magnitude in size (Perovich & Gow, 1996). What appears as large, high-aspect ratio inclusions in these images is the brine film narrowed by the ice bridges between lamellae. The bridges themselves are interspersed with smaller inclusions at all scales. All inclusions get smaller upon further cooling or desalination, and the narrowed brine films separate into even narrower films and terminate vertically. There is likely to be some form of residual connectivity throughout this pore space at least while volume expansion during freezing creates enough pressure to push brine though the matrix. In addition to the pores between the lamellae, brine channels form that mark the preferred pathways of downward-moving brine during desalination. They are usually vertical (Fig. 2.12). Their diameter can exceed the lamellae spacing, and evidence is inconclusive as to what extent the lamellar structure affects the development of brine channels. Brine channels are supplied with brine through the pore network that formed between the lamellae (Lake & Lewis, 1970; Niedrauer & Martin, 1979). However, the direction of flow in brine channels can reverse and oscillations between inflowing and outflowing brine have been observed (Lake & Lewis, 1970; Eide & Martin, 1975). Because brine flowing upwards into channels is less saline, it supports the disintegration into pores and close-off of the open end, called necking (Eide & Martin, 1975). Inclusions resembling disintegrated feeder channels are sometimes found leading towards brine channels (Lake & Lewis, 1970). They tend to be inclined around 45° and appear mostly in the upper part of sea ice. Overall, brine inclusions in cold sea ice show a characteristic distribution of length-to-width ratios (Light et al., 2003).

Porous materials tend to show a well-defined porosity threshold below which the pores are largely disconnected and above which percolation is possible through the pore network. This percolation threshold is around 0.3 but can be substantially different, e.g. if the distribution of pores is systematic rather than statistically random (values in excess of 0.7 are observed in certain types of volcanic rocks). The percolation threshold is lowered if the porous medium contains an excluded volume, e.g. solid foreign bodies like precipitated crystals commonly observed in volcanic rocks. Experimental observations have long given rise to the notion that the sea ice bulk salinity is effectively steady at porosities below 0.05–0.07 (Cox & Weeks, 1988; Arrigo et al., 1993). Percolation theory has been suggested as an explanation (Golden et al., 1998) that is consistent with the fabric of sea ice (Petrich et al., 2006). However, desalination of growing ice is largely due to natural convection that relies on a fluid permeability of sufficient magnitude (see above). An apparent porosity threshold for steady bulk salinity of the same magnitude is expected from continuum fluid dynamics
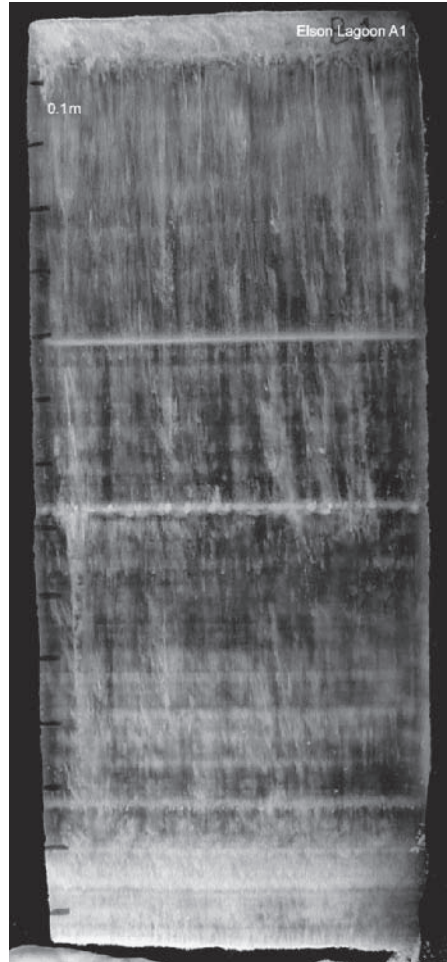
Fig. 2.12 Photograph of a slab of sea ice obtained from sea ice of approximately 1.4 m thickness near Barrow, Alaska (photo courtesy of D.M. Cole). Note the distinct horizontal layering as well as the parallel rows of vertical brine channels (shown in horizontal cross-section in Fig. 2e).

regardless of the connectivity of the microstructure (Petrich et al., 2009). Either way, the actual nature of this critical transition and its dependence on the microstructure of the ice are currently not well known.

The brine inclusions enlarge upon warming during the melt season and form new pathways for brine and meltwater. The slow redistribution of salinity in conjunction with a drive towards thermodynamic equilibrium leads to the widening of brine channels that form preferred pathways thereafter. Often, this secondary pore space contains longer and bigger channels than the primary pore space of growing sea ice.

Brine movement during melt

The most prominent form of brine movement during the melt season is flushing of surface meltwater (Untersteiner, 1968). Since the density of ice is lower than the density of water, the

surface of free-floating sea ice of thickness H protrudes above the water level by a distance h_f called freeboard,

$$h_f = H \left(\frac{\rho_{sw} - \rho_{si}}{\rho_{si}} \right)$$ (Equation 2.2)

If the sea ice is sufficiently permeable, then the hydrostatic pressure of brine and meltwater (melting snow and surface ice melt) above the ocean level can result in significant transport through the ice both vertically and laterally. Studies involving different tracers have demonstrated that the vertical and lateral transport of meltwater varies with season as a function of ice permeability. As much as a quarter of the meltwater produced annually at the surface of Arctic sea ice can be retained in pores within the ice cover (Eicken et al., 2002).

Meltwater flushing leads to desalination throughout the ice. It results in extremely low bulk salinities of Arctic multiyear sea ice (typically around 2–3) and the characteristic linear increase in ice salinity from values close to 0 at the surface to a few per mille in the lower ice layers (Fig. 2.9). Both lateral and vertical fluxes add to the heat and salt budget of the ocean (Lytle & Ackley, 1996; Eicken et al., 2002; Section 2.5).

Permeability of sea ice

Fluid moving though sea ice experiences a resistance that is due to both microscopic obstacles in the flow path (which lead to its tortuosity) and due to viscous drag along the pore walls. The reciprocal of resistivity is permeability Π, measured in m². Its magnitude is similar to that of the cross-sectional area of an individual duct if we assume that the porous medium is a close-packed bundle of ducts. The volume flux q through a homogeneous porous medium can be described by Dacry's law,

$$q = -\frac{\Pi}{\mu} \frac{\partial p}{\partial x}$$ (Equation 2.3)

where μ is the dynamic viscosity and $\partial p / \partial x$ is the pressure gradient in the direction of flow. The permeability tensor is generally anisotropic in sea ice, i.e. its components depend on the direction of flow, due to the anisotropic crystal fabric and pore structure providing the highest permeability in the vertical direction. In aligned sea ice, differences of about 1 order of magnitude seem to be typical (Freitag & Eicken, 2003). While the permeability of the open ocean is infinite, we can expect that the permeability at the bottom of the skeletal sea ice layer remains finite even as the porosity approaches 1: the regularly spaced ice lamellae, no matter how thin, will exert drag forces on the brine moving past.

A possible permeability–porosity relationship for growing sea ice that is consistent with field measurements (Freitag, 1999; Eicken et al., 2004), geometric consideration based on flow between parallel plates (Petrich et al., 2009) and effective medium theory (Golden et al., 2007) is:

$$\Pi = \Pi_0 \left(\frac{V_b}{V} \right)^3$$ (Equation 2.4)

where Π_0 is of the order of 2×10^{-8} m^2 and V_b/V is the brine volume (porosity) of the ice. The value of Π_0 depends on whether we consider one component of the permeability tensor in unidirectional flow or an equivalent isotropic permeability for multidimensional flow. The equivalent isotropic permeability is usually the geometric mean of the individual component, and an isotropic value of $\Pi_0 = 10^{-8}$ m^2 leads to good experimental agreement in computational fluid dynamics simulations (Petrich et al., 2009). Owing to the development of secondary pore space during melt (e.g. large brine channels), the permeability–porosity relationship will likely depend on the history of the ice. In fact, it is unclear if the presence of large brine channels still allows us to describe fluid flow through the porous matrix in a meaningful way with only one parameter (permeability). Rather, the dynamics may be better treated as flow through fractured porous media.

Sea ice salinity parameterizations

One of the key characteristics of sea ice is its bulk salinity because with it the porosity can be calculated under changing temperature. It is theoretically possible to simulate sea ice growth down to the pore scale in multidimensional numerical simulations, given enough time and computational power. However, this is impractical, and there are a few attempts to find more practical ways to predict the bulk salinity on the basis of environmental conditions. A rigorously derived and broadly applicable parameterization remains to be found.

Cox & Weeks (1988) presented a forward-explicit model on the basis of their laboratory experiments of sea ice desalination during growth. They separated the desalination process into an initial phase of rapid desalination within the skeletal layer ('initial segregation', determined from the ice-growth rate), followed by a relatively steady rate of desalination termed gravity drainage (determined from temperature gradient and porosity) and a small contribution due to brine expulsion. In this model, gravity drainage is set to cease when the porosity falls below 0.05. The initial segregation is expressed by a segregation coefficient that follows a functional form borrowed from planar rather than lamellar interfaces. Although relatively successful in predicting the bulk salinity profile, this approach seems to be difficult to transfer to stable oxygen isotope fractionation (Eicken, 1998). Refinement of the model and comparison with oxygen stable-isotope tracer data indicate that the salinity profile in individual floes depends strongly on the date of ice-growth onset, the ocean heat flux as well as snow accumulation and, in particular, surface flooding (Eicken, 1992a; Maksym & Jeffries, 2000). This model is frequently employed owing to its simplicity, its ability to approximate observed salinity profiles and presumably lack of alternatives.

However, it has been observed that the steady-state bulk salinity appears to be correlated with the growth rate (Nakawo & Sinha, 1981). Measurements and fluid dynamics simulations can be fitted with a power law over a wide range of growth rates (Kovacs, 1996; Petrich et al., 2006). Unfortunately, there is currently no theoretical or experimental backing for the choice of a power law. The expression from Petrich et al., (2009) yielded good correspondence between growth rate ν and steady-state bulk salinity S_{si} data in Barrow, Alaska, 2008 (Fig. 2.13),

$$\frac{S_{si}}{S_0} = 0.14 \left(\frac{\nu}{1.35 \times 10^{-7} \text{ ms}^{-1}} \right)^{0.33} \qquad \text{(Equation 2.5)}$$
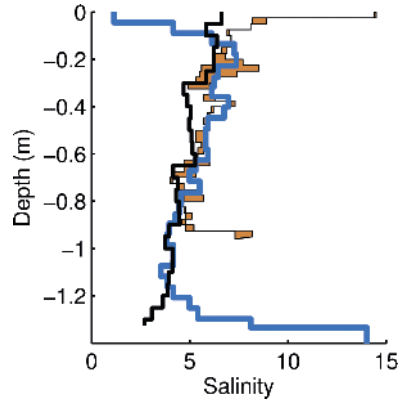
Fig. 2.13 Bulk salinity profiles measured in Barrow, Alaska at the end of May (thick line), and two profiles measured 2 m apart in early February (thin lines, difference between profiles is shaded). The solid black line is the expectation based on Equation 2.5 with growth rate from Fig. 2.25.

where the sea water salinity was $S_0 = 33$. The bulk salinity data expected from equation 2.5 are compared with three salinity cores in Fig. 2.13. The history of growth rates v of the ice was inferred from a degree-day model (Section 2.5), and the actual growth conditions were closely monitored only after a thickness of 0.65 m had been reached. The bulk salinity profile is generally well reproduced from 0.65 m to 1.1 m even though the growth rate is estimated without taking into account important atmospheric conditions (snow depth, wind speed) and oceanic conditions (under-ice currents, storms). We can only speculate about the origin of significant discrepancies between the two February cores at 30 cm, and the discrepancy between expectation and actual measurement around 40 cm. The salinities at the bottom of the cores are elevated since the ice was still actively desalinating (5 cm in early February, 20 cm in late May); the core in late May shows first signs of flushing in the upper 15 cm (see Section 2.5 for melt conditions).

Phase fractions and microstructural evolution

A phase diagram, such as that shown in Fig. 2.7, in itself contains no direct information on the (microscopic) configuration of individual phases within the system, i.e. its microstructure. In the case of natural sea ice, the latter depends on two principal factors, the growth environment and the boundary conditions at the advancing ice–water interface at the time of growth (Fig. 2.5), and the *in situ* temperature and chemical composition of the ice horizon under consideration. This second controlling factor leads to a temperature-dependent porosity and is of prime importance for a wide range of ice properties considered in Section 2.4. Owing to the stark contrast in physical properties between ice, brine, salts and gas inclusions, knowledge of their relative volume fraction can provide us with a first-order estimate of the bulk (macroscopic) properties of sea ice. For example, the mechanical strength of sea ice depends strongly on the relative brine and gas volume fraction, because these two phases effectively have no strength.

A specific example of the microstructural evolution of sea ice as a function of temperature is given in Fig. 2.8, which shows the relative volume fraction and microstructure of elongated pores in a core sample of columnar sea ice. The data for these images were

obtained using magnetic resonance imaging (MRI) of samples at the indicated temperature. This permitted the microstructural evolution of brine-filled pores to be followed without disturbing or destroying the sample. One particular challenge common to most studies of ice microstructure and properties is the strong dependence of the relative liquid pore volume on temperature. Commonly, samples are cooled to temperatures below −20°C immediately after sampling to avoid loss of brine from the sample. As evident in Figs 2.7 and 2.8, such temperature changes strongly affect the pore microstructure. Hence, it requires either special sampling and sample preparation techniques or non-destructive methods, such as MRI, to actually obtain insight into the pore microstructure at the *in situ* temperature (Eicken et al., 2000).

As the sample is warmed from its *in situ* temperature, at which it was maintained for the entire period after sampling, the brine volume fraction increases as prescribed by the phase relations. At the same time, however, the size, morphology and connectivity of pores evolve, with pores visibly linking up at warmer temperatures (−6°C, Fig. 2.8). This process of inter-connecting pores of reasonable size as the temperature increases above a critical threshold (for a given salinity) is an important aspect of microstructural evolution and of great importance for sea ice transport properties, such as permeability. In a recent study that combines different modelling approaches and high-resolution X-ray microtomography, Golden et al., (2007) have further examined these linkages between pore connectivity and permeability. The X-ray microtomography data clearly show how sheets of brine that segregated into disjunct, isolated pores at low temperatures start to link up at higher temperatures (Fig. 2.11). It is important to note that these microtomography images and more detailed data on pore morphology and connectivity derived from them illustrate that the classic pore-space model developed by Assur (see discussion in Section 2.4) is not sufficient for modelling of ice transport properties.

Temperature and salinity as state variables

From the phase relations (as summarized in Fig. 2.7), it follows that the relative volume fraction of brine depends solely on the ice temperature, T, and its bulk salinity, S_{si}, provided the volume is isothermal and in thermodynamic equilibrium, and given the pressure (usually atmospheric) and composition of the brine (usually 'standard' composition). The salinity of the brine, S_b, contained within such an ice volume would similarly be prescribed by the phase relations (see also Fig. 2.8). Hence, temperature and salinity of the ice are the prime controlling or state variables governing not only the phase fractions but, as outlined below, a whole host of other physical properties. Here, use of the term 'state variable' occurs in a very loose sense, as formulation of a true equation of state for sea ice has been elusive to date. For deeper insight into the problem and recent progress, see Feistel & Hagen (1998).

The thermodynamic coupling between these different variables is a key aspect of sea ice as a geophysical material and a habitat. Any temperature change directly affects the porosity and pore microstructure of the ice as well as the salinity and chemical composition of the brine. Direct measurement of these properties in the field is difficult. Commonly, the *in situ* brine volume fraction and other properties are derived from the bulk salinity of an ice sample and its *in situ* temperature. The latter can be measured by inserting temperature probes into freshly drilled holes in a core or with sensors frozen into the ice. The bulk salinity is typically obtained by dividing an ice core into sections, melting these in the lab and then deriving the salinity from electrolytical conductivity measurements. Ideally, one would also measure the

density of a sea ice sample, ρ_{si}, in order to estimate the air volume fraction V_a/V. In fresh ice, it is typically much smaller than the brine volume fraction, but it can be substantial in multiyear or deteriorated ice (Timco & Frederking, 1996).

From the data compiled by Assur (1960) for the phase relations[2] and on the basis of the continuity equations for a multiphase sea ice mixture, Cox & Weeks (1983) derived a rather useful set of equations describing the brine volume fraction as a function of ice temperature and salinity. Thus, the brine volume fraction is derived as:

$$\frac{V_b}{V} = \left(1 - \frac{V_a}{V}\right)\frac{(\rho_i/1000)S_{si}}{F_1(T) - (\rho_i/1000)S_{si}F_2(T)}$$ (Equation 2.6)

The density of pure ice is given as:

$$\rho_i = 917 - 0.1403\,T$$ (Equation 2.7)

with ρ_i in kg m^{-3} and T in °C. $F_1(T)$ and $F_2(T)$ are empirical polynomial functions $F_i(T) = a_i + b_iT + c_iT^2 + d_iT^3$, based on the phase relations. The coefficients for different temperature intervals are listed in Table 2.1. The brine salinity can be approximated for temperatures above −23°C as:

$$S_b = \left(1 - \frac{54.11}{T}\right)^{-1} \times 1000$$ (Equation 2.8)

The relationships in equations 2.6 and 2.8 give rise to *the rule of fives*: in first-year sea ice that formed from ocean water (rather than less saline brackish water), we expect the bulk salinity to be around $S_{si} = 5$; in this case, the porosity is 5% if the ice temperature is near $T = -5$°C. The phase relationship equation 2.6 is illustrated in Fig. 2.14 in the absence of air. Note that the porosity of cold ice is generally small. The brine density ρ_b in kg m^{-3} depends on brine salinity S_b according to:

$$\rho_b = 1000 + 0.8\,S_b$$ (Equation 2.9)

Equations 2.6–2.9 thus provide us with a simple tool to derive key quantities for a wide range of physical, biological and chemical studies of sea ice.

Table 2.1 Coefficients for functions $F_1(T)$ and $F_2(T)$ for different temperature intervals. From Cox & Weeks (1983) and Leppäranta & Manninen (1988).

T, °C	a_1	b_1	c_1	d_1
$0 \geq T > -2$	−0.041221	−18.407	0.58402	0.21454
$-2 \geq T \geq -22.9$	−4.732	−22.45	−0.6397	−0.01074
$-22.9 > T \geq -30$	9899	1309	55.27	0.7160

| T, °C	a_2	b_2	c_2	d_2
$0 \geq T > -2$	0.090312	−0.016111	1.2291×10^{-4}	1.3603×10^{-4}
$-2 \geq T \geq -22.9$	0.08903	−0.01763	-5.330×10^{-4}	-8.801×10^{-6}
$-22.9 > T \geq -30$	8.547	1.089	0.04518	5.819×10^{-4}
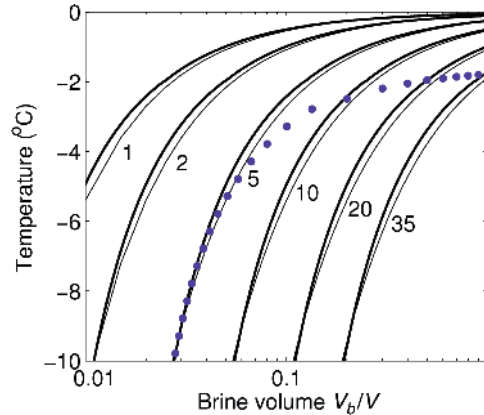
Fig. 2.14   Relationship between brine volume fraction and temperature T for various values of bulk sea ice salinity S_{si}. The thick line is after Cox & Weeks (1983), the thin line follows the linearized relationship $V_b/V = mS_{si}/T$ with $m = -0.054$ K. The dots are an artist's impression of a possible desalination pathway in growing sea ice.

Caveats and limitations

In arguing the case for the overriding importance of temperature and salinity in determining ice properties, one needs to be aware of some important limitations and knowledge gaps that may, at least in some cases, invalidate the approach outlined above. In contrast to the assumption that the system under investigation is of constant chemical composition and at thermodynamic equilibrium with respect to its bulk composition, microstructural studies and geochemical analysis indicate that chemical fractionation cannot always be ignored. Consequently, microscopically, the fluid composition in sea ice may deviate significantly from its bulk composition, impacting phase evolution, pore microstructure and dependent properties. Such deviations from the evolution of a microscopically homogeneous system are potentially also of great significance for biological processes within the ice cover. Recent improvements in analytical techniques, with development of *in situ* earth magnetic field NMR (nuclear magnetic resonance) spectroscopy as a particularly interesting example (Callaghan et al., 1999), and advances in geochemical modelling of aqueous solutions at low temperatures (Spencer et al., 1990; Marion & Grant, 1997) hold considerable promise for resolving some of these issues. Geochemical modelling is particularly useful, as it allows us to easily treat systems of different chemical composition, whereas the empirical approach outlined above is only valid for a single system of a given, standard composition.

2.4 Physical properties

Thermal conductivity

The thermal properties control the amount of heat transferred through the ice cover and determine its response to variations in surface or bottom forcing. The conductive heat flux through an ice cover, F_c, is given by the product of sea ice thermal conductivity, λ_{si}, and the temperature gradient, dT/dz:

$$F_c(z) = -\lambda_{si}\left(\frac{dT}{dz}\right)_z$$

(Equation 2.10)

The thermal conductivity of pure ice as a function of temperature is given by Yen et al., (1991) as:

$$\lambda_i = 1.16 \text{ W m}^{-1} \text{ K}^{-1}(1.91 - 8.66 \times 10^{-3} \, T + 2.97 \times 10^{-5} \, T^2) \qquad \text{(Equation 2.11)}$$

with T in °C. At 0°C, λ_i is approximately 2.0 W m^{-1} K^{-1}. The thermal conductivity of brine, on the other hand, is lower by a factor of roughly 4, and can be approximated by:

$$\lambda_b = 0.4184 \text{ W m}^{-1} \text{ K}^{-1}(1.25 + 0.030 \, T + 0.00014 \, T^2) \qquad \text{(Equation 2.12)}$$

with T in °C (Yen et al., 1991). Thus, the volume fraction of brine as well as its microstructural arrangement exert a significant influence on the bulk (i.e. macroscopic) sea ice thermal conductivity. Schwerdtfeger (1963) and Ono (1968) developed a model for the thermal conductivity of sea ice on the basis of the thermal properties of the pure end members, ice and brine, and assumptions about the ice microstructure. For vertically oriented, parallel lamellar brine inclusions, one arrives at the following dependence of λ_{si} on brine volume (no gas inclusions) in direction parallel to the lamellae:

$$\lambda_{si} = \lambda_i - (\lambda_i - \lambda_b)\frac{S_{si}\rho_{si}}{m\rho_b T^2} \qquad \text{(Equation 2.13)}$$

with sea ice salinity S_{si}, bulk sea ice and brine densities ρ_{si} and ρ_b, respectively, temperature T (in °C) and $m < 0$, the slope of the phase boundary in the phase diagram (Fig. 2.7). Note that the fraction in equation 2.13 is a function of the porosity of the ice (cf. Section 2.3). Hence, in this physical configuration, the magnitude of λ_{si} does not depend on the actual size or distribution of the inclusions but only on their mass fraction. Ono and Schwerdtfeger also considered the impact of spherical gas inclusions on λ_{si}. These are typically of minor importance in first-year ice, as gas volume fractions are mostly an order of magnitude lower than those of brine.

Untersteiner introduced a simple parameterization as a function of ice temperature, T, and salinity, S_{si}, that has been employed in some ice-growth models (Maykut, 1986):

$$\lambda_{si} = \lambda_i + 0.13\frac{S_{si}}{T^2} \qquad \text{(Equation 2.14)}$$

Both equations 2.13 and 2.14 are functionally identical to the continuum approach in Section 2.3, which postulates for porosity V_b/V in thermodynamic equilibrium,

$$\lambda_{si} = \lambda_i + (\lambda_b - \lambda_i)\frac{V_b}{V} \qquad \text{(Equation 2.15)}$$

Recently, accurate measurements of the thermal conductivity of sea ice have been performed by Pringle et al., (2007). They give the thermal conductivity as:

$$\lambda_{si} = \frac{\rho_{si}}{\rho_i}\left(2.11 - 0.011 \, T + 0.09\frac{S}{T} - \frac{\rho_{si} - \rho_i}{1000}\right) \text{W m}^{-1} \text{ K}^{-1} \qquad \text{(Equation 2.16)}$$

with T in °C, and ρ_{si} and ρ_i the densities of sea ice and pure ice, respectively, in kg m^{-3}.

Specific heat capacity and latent heat of fusion and of sea ice

The specific heat capacity 'c' describes the relationship between an amount of energy δQ added to a system of mass M and the temperature change dT it experiences:

$$\delta Q = Mc\, dT \qquad \text{(Equation 2.17)}$$

Since a temperature change of sea ice is always accompanied by a phase transition, the apparent heat capacity of sea ice, c_{si}, is larger than the heat capacity of pure ice, c_i. Given an expression for the apparent heat capacity of sea ice, temperature changes of sea ice can be calculated conveniently from equation 2.17.

Malmgren (1927) introduced an expression for the sea ice heat capacity as a function of heat capacities of ice, brine and water, and latent heat released owing to phase transition under the assumption of thermodynamic equilibrium and constant bulk salinity. Ono (1967) simplified the expression of Malmgren by assuming a linear relationship between brine salinity and temperature for $T > -8.2°C$ (the onset of mirabilite precipitation), yet allowed for a temperature dependence of the heat capacity of ice and water. The most significant terms in his result are:

$$c_{si} = c_i + \beta T - m_m L \frac{S_{si}}{T^2} \qquad \text{(Equation 2.18)}$$

where he used $c_i = 2.11$ kJ kg^{-1} K^{-1} for the specific heat capacity of ice at 0°C, $\beta = 7.5$ J kg^{-1} K^{-2} as temperature coefficient of the heat capacity of ice; L = 333.4 kJ kg^{-1} for the latent heat of fusion of freshwater and $m_m = -0.05411$ K for the slope of the liquid. S_{si} is the bulk salinity of sea ice and T the temperature in °C.

Previously, Untersteiner (1961) proposed an empirical relationship for the heat capacity of sea ice:

$$c_{si} = 2.11 \text{ kJ kg}^{-1} \text{ K}^{-1} + 17.2 \text{ kJ K kg}^{-1} \frac{S_{si}}{T^2} \qquad \text{(Equation 2.19)}$$

which is in line with Ono's result.

It is instructive to trace the origin of this relationship. The specific heat capacity at constant pressure can be expressed in terms of enthalpy (internal energy) H as:

$$c_{si} = \frac{1}{M}\left(\frac{dH}{dT}\right)_P \qquad \text{(Equation 2.20)}$$

where M is the mass containing H. Including sensible heat of liquid and ice, and the latent heat,

$$H = M\left[c_w T f_m + c_i T(1 - f_m) - (1 - f_m)L\right] \qquad \text{(Equation 2.21)}$$

where c_w and c_i are the specific heat capacity of liquid and ice, respectively (assumed to be temperature independent), and f_m is the liquid mass fraction in thermodynamic equilibrium:

$$f_m = m_m \frac{S_{si}}{T} \qquad \text{(Equation 2.22)}$$

We keep the bulk sea ice salinity S_{si} fixed, insert equation 2.22 into equation 2.21 and differentiate following equation 2.20 to obtain:

$$c_{si} = c_i - m_m L \frac{S_{si}}{T^2}$$

(Equation 2.23)

Equation 2.23 is in line with the result of both Ono and Untersteiner. Perhaps surprisingly, the heat capacity of sea ice does not explicitly depend on the heat capacity of the liquid. This is due to the assumptions of a linear phase relationship and constant bulk salinity: thereby, the sensible heat term of the liquid in equation 2.21 is independent of temperature, i.e. the heat contained in the (variable) liquid mass remains constant. We should emphasize that the equations given for the specific heat capacity apply to the case of constant bulk salinity only. Making the bulk salinity a function of temperature, we can estimate that the effective heat capacity during initial desalination of sea ice (i.e. while the temperature drops from −2°C to −5°C) can amount to twice the value calculated from equations 2.18 and 2.19. In this case, it may be more practical to follow an approach based on the effective latent heat of fusion of sea ice discussed below.

As is evident from equation 2.19 and from Fig. 2.15 showing measurements of c_{si} as a function of temperature, the specific heat capacity increases substantially above about −5°C. This increase implies that it takes substantially more energy to warm an ice cover by 1 K at a temperature close to the freezing point of sea water than at, say, −10°C. Ignoring the contribution of latent heat in raising or lowering the temperature of a sea ice volume has important ramifications. For example, in large-scale sea ice or climate models this would significantly overestimate the amount of ice thinning or lateral melting.
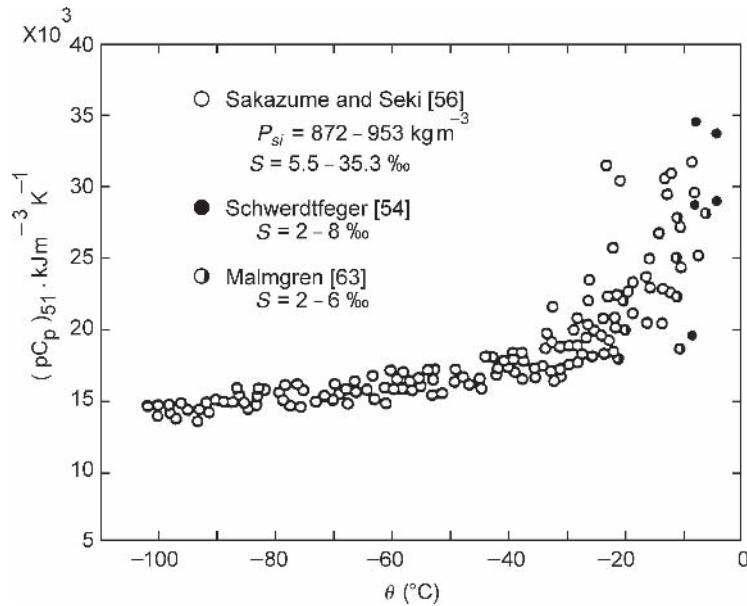

Fig. 2.15   Effective specific heat capacity of sea ice Cp (shown as product of Cp with ice density ρ) as a function of temperature θ in °C. Reproduced with kind permission from Springer Science + Business Media. From Fukusako (1990).

The diffusive propagation of a temperature signal in sea ice can be determined from the heat transfer equation, describing the change in temperature with time dT/dt in terms of c_{si}, λ_{si} and ρ_i. In one dimension,

$$\rho_i c_{si} \frac{dT}{dt} = \frac{\partial}{\partial z}\left[\lambda_{si}\frac{\partial T}{\partial z}\right] \qquad \text{(Equation 2.24)}$$

Note that while equation 2.24 is energy conserving, it does not account for density differences between liquid and solid, which induce brine movement or vapour bubble formation during temperature change. For a medium of homogeneous thermal properties,

$$\frac{dT}{dt} = \frac{\lambda_{si}}{\rho_i c_{si}}\frac{\partial^2 T}{\partial z^2} \qquad \text{(Equation 2.25)}$$

The term $(\lambda_{si}/c_{si}\rho_i)$ is commonly referred to as the ice thermal diffusivity and indicates the rate at which a temperature fluctuation propagates through the ice. It is over an order of magnitude larger in cold ice than near the ice–ocean interface.

The specific heat capacity of sea ice is a useful concept to calculate the temperature change within the ice without the need to consider porosity changes and latent heat explicitly. Similarly, a latent heat of fusion of sea ice can be derived to facilitate the calculation of growth and ablation rates without the need to consider porosity and sensible heat explicitly (Bitz & Lipscomb, 1999; Section 2.5). In this sense, the latent heat of fusion of sea ice can be defined as the temperature integral of the specific heat capacity. This is the difference between the enthalpy of sea ice at a given temperature and salinity and the enthalpy when all the ice is melted at temperature $T_F = m_m S_{si}$. Thus,

$$-L_{si}M = H(T, S_{si}) - H(T_F, S_{si}) \qquad \text{(Equation 2.26)}$$

and using equations 2.21 and 2.22, we find:

$$L_{si} = L - c_i T + c_i m_m S_{si} - m_m L \frac{S_{si}}{T} \qquad \text{(Equation 2.27)}$$

Equation 2.27 contains the dominant terms of the expression derived by Ono (1967) that he obtained from integrating his result for the specific heat capacity of sea ice from temperature T to the melting point of sea ice of bulk salinity S_{si}. The most significant contributions are:

$$L_{si} = \left(333.4 - 2.11\,T - 0.114 S_{si} + 18.1\frac{S_{si}}{T}\right)\text{kJ kg}^{-1} \qquad \text{(Equation 2.28)}$$

The latent heat of fusion of sea ice takes into account both the reduction of the latent heat due to finite porosity and the transfer of sensible heat between brine and ice. For example, the amount of sensible and latent heat required to completely melt sea ice amounts to 246 kJ kg^{-1} at a temperature of $T = -2°C$ and a salinity of $S_{si} = 10$.

While equations 2.27 and 2.28 apply only to melting sea ice, the effective latent heat for freezing ice can be obtained similarly if we assume $T_F = m_m S_0$ for the initial liquid of salinity S_0. The result is:

$$L_{si} = L - c_i T + c_i m_m S_{si} - m_m L \frac{S_{si}}{T} + c_w m_m (S_0 - S_{si}) \qquad \text{(Equation 2.29)}$$

Comparing equations 2.27 and 2.29, we see that the effective latent heat of fusion of sea ice is about 2% smaller during freezing of ocean water than it is during melting; freezing sea ice gets an energy head start equivalent to the amount of heat required to cool the liquid mass from the freezing point of the melt in equation 2.27 (i.e. $m_m S_{si}$) to the freezing point of ocean water in equation 2.29 (i.e. $m_m S_0$). Applications for both sea ice latent heat and heat capacity are given in Section 2.5.

A further problem inherent in the approaches commonly taken in modelling the thermal properties of sea ice relates to the practical definition of the melting point of sea ice. The freezing point of sea ice is typically defined as the highest temperature at which ice formation is observed. However, a corresponding definition for the melting point as the lowest temperature at which melting is observed is problematic since a liquid phase is present in sea ice down to temperatures as low as $-55°C$ (Fig. 2.7). Thus, with a continuous increase in brine volume fraction as temperatures are increased from typical sea ice winter minima to summer values, sea ice is technically melting on a microscopic level at all times.

Macroscopically, on the scale of an individual ice floe, 'melting' typically implies the disintegration of the entire ice volume. For this to happen, the temperature of the ice has to be raised well above the freezing point of the ocean since the bulk salinity of sea ice is significantly lower than the sea water salinity. Minuscule though these temperature differences appear to be, the fact that they are associated with substantial amounts of heat that has to be provided in order to warm up the ice means they can have dramatic impacts on model performance and the heat budget of the polar regions. Currently, we are far from understanding these issues, either on microscopic, macroscopic or larger scales.

Radiative transfer in sea ice

The thin-section photographs in Fig. 2.2 and the different ice types shown in Fig. 2.1 provide some indication of the complexity of the topic of radiative transfer between atmosphere, ice and ocean. The amount of light scattered back from the ice cover (as measured in the albedo, α), the amount absorbed within the ice column and the fraction that ultimately penetrates into the ocean depend on the relative contribution of absorption and scattering along the path of individual photons (Perovich, 1998). In pure ice, free of gas or brine inclusions (some types of lake ice actually being acceptable approximations of such ice, Fig. 2.2), the attenuation of light passing through the ice can be described through Beer's law (also called Bouguer–Lambert's law). The transmittance T of light travelling parallel to the z-direction through a slab of thickness z_0 is:

$$T(\lambda) = \frac{I(z_0, \lambda)}{I(0, \lambda)} = \exp(-\kappa_a z_0) \qquad \text{(Equation 2.30)}$$

where $I(z, \lambda)$ is the spectral radiance at wavelength λ, and κ_a is the wavelength-dependent absorption coefficient. The reciprocal of the absorption coefficient is the absorption mean free path or penetration depth. The absorption coefficient in ice and water increases several orders of magnitude from 500 to 1500 nm.

Owing to the ample presence of inclusions in sea ice, the effect of scattering has to be considered. Scattering in ice and snow is strongly forward peaked, i.e. the distance over which light deflects significantly from its path is much longer than the distance between individual scatterers. We can combine the effect of the density of scatterers and the forward peakedness

in an effective scattering coefficient κ_s. The scattering coefficient is independent of wavelength since the scattering elements are much larger than the wavelength of light. Combining absorption and scattering, an extinction coefficient κ is defined (Perovich, 1990):

$$\kappa(\lambda) = \sqrt{\kappa_a^2 + 2\kappa_a\kappa_s} \qquad \text{(Equation 2.31)}$$

Equation 2.31 simplifies to $\kappa(\lambda) \approx \kappa_a + \kappa_s$ if $\kappa_s \ll \kappa_a$. Generally, scattering increases the effective path length of light on its traverse through the ice and therefore reduces the transmittance. However, scattering also deflects light, which gives rise to albedo. We can understand the most fundamental optical characteristics of sea ice with a relatively simple two-stream model (Grenfell, 1979). In addition to light travelling in the direction of the incident rays, $I_\downarrow$ (which is a combination of the incident (direct) light and diffusely scattered light), a two-stream model includes (diffusely scattered) light travelling in the opposite direction, $I_\uparrow$. For a single homogeneous slab of thickness z_0 subjected to incident light $I_\downarrow(0, \lambda)$ at $z = 0$ and to reflected light $I_\uparrow(z_0, \lambda) = \alpha_b I_\downarrow(z_0, \lambda)$ at $z = z_0$, the solution inside the slab can be written as:

$$\frac{I_\downarrow(z,\lambda)}{I_\downarrow(0,\lambda)} = \frac{1 - g\,\exp\left[-2\kappa(z_0 - z)\right]}{1 - g\,\exp(-2\kappa\,z_0)}\,\exp(-\kappa z) \qquad \text{(Equation 2.32)}$$

and

$$\frac{I_\uparrow(z,\lambda)}{I_\downarrow(0,\lambda)} = \frac{1 - \dfrac{g}{\alpha_\infty^2}\,\exp\left[-2\kappa(z_0 - z)\right]}{1 - g\,\exp(-2\kappa\,z_0)}\,\alpha_\infty\,\exp(-\kappa z) \qquad \text{(Equation 2.33)}$$

provided that $\kappa_a > 0$. Here,

$$g(\lambda) = \frac{\alpha_\infty^2 - \alpha_b\alpha_\infty}{1 - \alpha_b\alpha_\infty} \qquad \text{(Equation 2.34)}$$

where α_b is the spectral albedo beneath the slab (at $z = z_0$), and α_∞ is defined as:

$$\alpha_\infty(\lambda) = \frac{\kappa_a + \kappa_s - \kappa}{\kappa_s} \qquad \text{(Equation 2.35)}$$

Equation 2.35 is the spectral albedo of the slab at infinite thickness.

Hence, the spectral transmittance $I_\downarrow(z_0, \lambda)/I_\downarrow(0, \lambda)$ through the slab is:

$$T(\lambda) = \frac{1 - g}{1 - g\,\exp(-2\kappa\,z_0)}\,\exp(-\kappa\,z_0) \qquad \text{(Equation 2.36)}$$

and the spectral reflectance $I_\uparrow(0, \lambda)/I_\downarrow(0, \lambda)$ of the slab is:

$$R(\lambda) = \alpha_\infty\,\frac{1 - \dfrac{g}{\alpha_\infty^2}\,\exp(-2\kappa\,z_0)}{1 - g\,\exp(-2\kappa\,z_0)} \qquad \text{(Equation 2.37)}$$
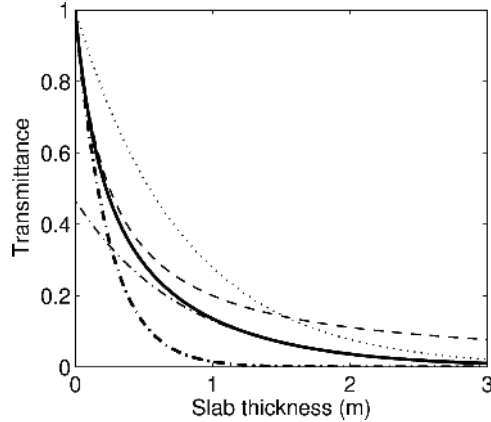
Fig. 2.16   Spectral transmittance through a homogeneous slab of thickness z_0 with absorption ($\kappa_a = 0.2$ m^{-1}) and multiple scattering ($\kappa_s = 4$ m^{-1}); light enters the slab from one side only ($\alpha_b = 0$), surface reflection is not considered. Prediction based on two-stream model Equation (2.36) (solid line); expectations based on Beer's law using extinction coefficient Equation (2.31) (dotted line); thick-slab limit of Equation (2.36), i.e. exponential with constant factor (thin dash-dotted line); Beer's law using $\kappa = \kappa_a + \kappa_s$ (thick dash-dotted line); assuming scattering only, Equation (2.38) (dashed line).

The spectral albedo beneath a slab of sea ice is generally $\alpha_b = 0$ unless biota are present.

Figure 2.16 compares the qualities of extinction due to scattering and absorption based on Beer's law and the two-stream model. The transmittance at the bottom of a homogeneous slab of sea ice ($\kappa_a \approx 0.2$ m^{-1}, $\kappa_s \approx 4$ m^{-1}, $\alpha_b = 0$) is shown as a function of slab thickness z_0. Initially, the transmittance is bounded from below by $[(\kappa_a + \kappa_s)z_0]$, (i.e. assuming scattering has the effect of absorption), and from above by:

$$T(\lambda) = [1 + (1 - \alpha_b)\kappa_s z_0]^{-1} \qquad \text{(Equation 2.38)}$$

which is the transmittance from the two-stream model in the absence of absorption ($\kappa_a = 0$). While equation 2.38 is a good approximation for a thin slab, finite absorption leads to a noticeable discrepancy in thicker slabs. There, the net transmission is proportional to exp $(-\kappa z_0)$ (equation 2.36).

More accurate calculations generally require detailed knowledge of the microstructure of the ice and numerical approaches. Owing to the wavelength dependence of absorption, the wavelength-integrated irradiance depends on the spectral composition of the incoming solar radiation, which strongly depends on cloudiness and other factors (Grenfell & Maykut, 1977).

The amount of scattering depends on the contrast in refractive indices between the host medium and inclusions, which in the case of sea ice explains the disproportionate importance of gas and precipitated salt inclusions for the scattering of light. While the Beer/Bouguer–Lambert approach is limited in its application, it does allow for reasonable estimates of short-wave attenuation in sea ice. Owing to its computational simplicity, it is still widely employed to derive the extent of solar heating of individual ice layers (Perovich, 1998). Moreover, it may be more practical for applications with larger numbers of scatterers other than simple air or brine inclusions, such as in bio-optical models of sea ice (Arrigo & Sullivan, 1994; Chapter 8). More sophisticated approaches to the solution of the radiative transfer equation are those of Grenfell (1991), Jin et al., (1994) and those summarized in Perovich (1998). However, as apparent from Fig. 2.17, such approaches also require a more sophisticated
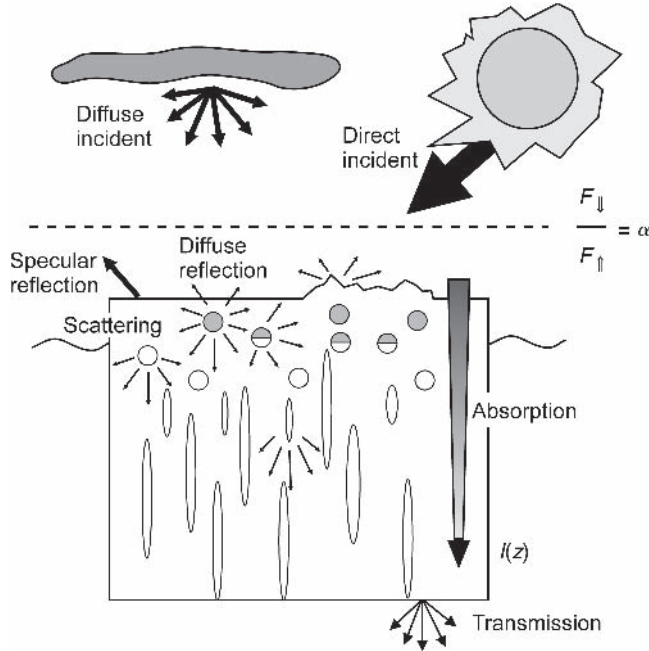
Fig. 2.17   Schematic depiction of sea-ice radiative transfer processes (modified from Perovich (1998)).

treatment of the ice microstructure, specifically those of brine, gas and salt inclusions. Such data are only now starting to become available (Light et al., 2003; Golden et al., 2007; Pringle et al., 2009) and it will require further efforts to develop a fully coupled optical/microstructural/heat transfer model of sea ice.

Sea ice albedo

The albedo of snow and sea ice is primarily due to scattering within the bulk of the material rather than due to surface reflectance alone. The spectral albedo of a sea ice cover is defined as the fraction of the incident irradiance that emerges from the surface:

$$\alpha(\lambda) = \frac{F \Uparrow (0,\lambda)}{F \Downarrow (0,\lambda)}$$
(Equation 2.39)

The total (all-wavelength) albedo, α_t, is then given by the integral over the entire range of the solar short-wave spectrum (commonly taken as 400–1500 nm; Perovich, 1998),

$$\alpha_t = \frac{\int \alpha(\lambda) F \Downarrow (0,\lambda)\, d\lambda}{\int F \Downarrow (0,\lambda)\, d\lambda}$$
(Equation 2.40)

As shown in Fig. 2.17, α is determined both by the combined effect of specular reflection and scattering at the surface and by scattering and absorption in the volume of the ice. Hence, the albedo depends strongly on the ice interior structure, which has been hinted at in Section 2.2 and is clearly apparent in Fig. 2.2. In contrast to lake ice with few inclusions and low-albedo, snow-free sea ice with numerous brine inclusions has a significantly higher albedo. The number of brine inclusions acting as scatterers correlates with the thickness

of the ice cover (Fig. 2.17), such that one typically observes a pronounced increase in ice albedo with an increase in ice thickness (equation 2.37). This phenomenon is implicit in the nomenclature of thin ice types, identified as dark and light nilas, grey, grey-white and white ice (Figs 2.1 and 2.18). Bulk scattering is also responsible for the high albedo of snow, rendering thin snow layers partially translucent. However, the dependence of snow albedo on snow thickness is less obvious on sea ice because the underlying sea ice has a relatively high albedo itself.

The range of albedo associated with the polar ice pack spans almost the entire range of albedo of different planetary surfaces (Fig. 2.18). Values increase during the course of the ice-growth season as the ice cover thickens and snow accumulates. In summer, the trend in surface albedo is the opposite, with values dropping to about 0.65 for snow-free bare multiyear ice and decreasing to well below 0.5 for ponded multiyear ice (Fig. 2.19). Whereas the stark contrast in albedo of the open versus the ice-covered ocean is an important driver of ice-albedo feedback processes (Section 2.5), even the less drastic differences in albedo between different degrees of melt-pond coverage are of considerable importance. Model results suggest that Arctic sea ice is highly sensitive to changes in surface albedo. A difference in the degree of ponding, typically ranging between 10 and 50% areal coverage corresponding to albedos $\alpha > 0.6$ and $\alpha < 0.5$, respectively, would be critical for the stability and potential disappearance of the perennial ice pack (Steele & Flato, 2000).

Despite the importance of large-scale albedo variations, few, if any, models are currently able to fully predict the summer evolution of ice albedo. However, spurred by computational advances and recent field measurements aimed at providing key data, several efforts are underway to include more realistic physical models of albedo evolution in large-scale sea ice
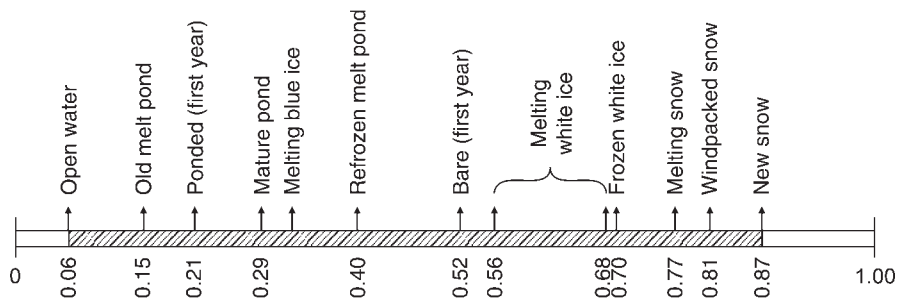

Fig. 2.18   Range of albedo of different ice pack surfaces (from Perovich, 1998).
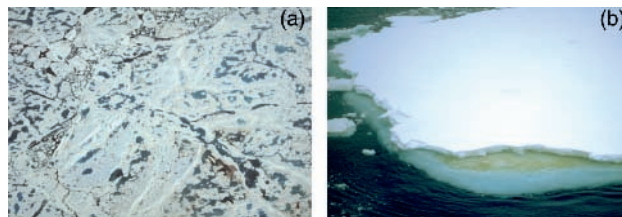

Fig. 2.19   Surface of summer Arctic sea ice, aerial photograph, several hundred metres wide (a). Summer Antarctic sea ice, ship-based photograph, approximately 20 m wide (b). Note the high albedo of snow-free, well-drained surface ice and the low albedo of the melt ponds in (a). The brown discolouration of the ice visible at freeboard level in (b) is due to high concentrations of sea ice algae in an infiltration layer (see Chapters 7, 8 & 9).

and climate models. The key challenge that remains to be addressed is the ability to predict the changing pond fractions and depths, and their impact on the ice albedo. The vast majority of large-scale sea ice models and global circulation models (GCMs) is currently prescribing ice albedo through some type of parameterization scheme that links the surface albedo to the air or surface temperature or introduces a time-dependent albedo that varies during the course of the melt season.

Dielectric properties of sea ice

The dielectric properties of sea ice govern the propagation and attenuation of electromagnetic waves that in turn determine both the optical properties of sea ice and sea ice signatures in remote-sensing data sets (Chapter 6). For a detailed treatment of electromagnetic wave propagation in lossy dielectric media, see Schanda (1986) and Hallikainen and Winebrenner (1992).

For an electromagnetic wave propagating in z-direction at the time t, the electric field, E_x, in the x-direction is given by:

$$E_x = E_0 \cos(\omega t - kz) \qquad \text{(Equation 2.41)}$$

where E_0 is the field at $z = 0$, k is the wave number and ω the angular frequency. Maxwell's equations yield the speed of wave propagation (v) in a medium with the relative electric permittivity, ε, and relative magnetic permeability, μ, as:

$$v = \frac{c}{\sqrt{\varepsilon\mu}} \qquad \text{(Equation 2.42)}$$

with the speed of light in terms of the permittivity and permeability of free space:

$$c = \frac{1}{\sqrt{\varepsilon_0\mu_0}} \qquad \text{(Equation 2.43)}$$

The relative (dimensionless) permittivity ε, also referred to as the dielectric constant, is a complex variable for a medium in which electromagnetic waves are absorbed (a so-called lossy medium), such that,

$$\varepsilon = \varepsilon' - i\varepsilon'' = \varepsilon'(1 - i \tan \delta) \qquad \text{(Equation 2.44)}$$

where i denotes the complex part of the permittivity and $i^2 = -1$; ε' describes the contrast with respect to free space ($\varepsilon'_{air} = 1$) and $\tan \delta$ is the so-called loss tangent.

In a non-polar medium, ε' and ε'' are constants, whereas in substances in which the molecules exhibit a permanent dipole moment (e.g. water), ε' and ε'' are frequency dependent because resonance affects wave decay. Ionic impurities present in sea water and brine also affect the propagation of electromagnetic waves, such that ε'' depends on the conductivity σ (Fig. 2.20):

$$\varepsilon'' = \frac{\sigma}{\varepsilon_0\omega} \qquad \text{(Equation 2.45)}$$

Ignoring scattering and assuming a homogeneous medium, one can assess the penetration depth, δ_p, of electromagnetic radiation of a given frequency as:

$$\delta_p = \frac{1}{\kappa_a} = \frac{\sqrt{\varepsilon'}}{\kappa_0\varepsilon''} \qquad \text{for } \varepsilon' << \varepsilon'' \qquad \text{(Equation 2.46)}$$
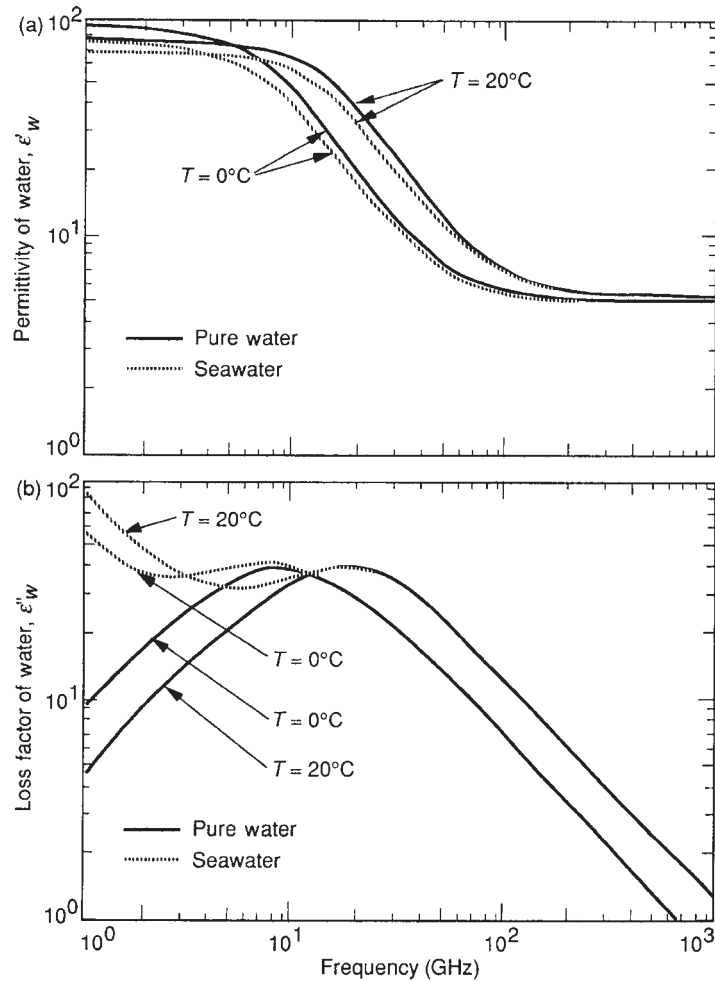
Fig. 2.20 Permittivity (top, a) and loss factor (bottom, b) for pure water and sea water at microwave frequencies (Hallikainen & Winebrenner, 1992).

The attenuation of electromagnetic waves can be described in simplified terms by an extinction coefficient κ, with separate contributions by absorption, κ_a, and scattering, κ_s. Despite its gross simplification of radiative transfer, the concept of a penetration depth can help in the interpretation of remote-sensing data, such as radar or passive-microwave imagery (Chapter 6). Thus, it is of particular relevance for remote sensing of the oceans and sea ice that the dielectric loss factor ε'' of water varies by more than 1 order of magnitude in the 1–100 GHz frequency range. Furthermore, at frequencies below 10 GHz, ε'' differs by as much as 1 order of magnitude for freshwater and sea water or brine, owing to the impact of ionic impurities on wave decay. Hence, penetration depths at typical radar or passive-microwave frequencies are in the order of millimetres to centimetres in sea water. For pure, cold ice, ε' is constant at 3.17 for frequencies between 10 MHz and 1000 GHz, whereas ε'' is up to several orders of magnitude smaller than that of water. Consequently, one can derive the dielectric properties of sea ice from the properties of its constituent phases on the
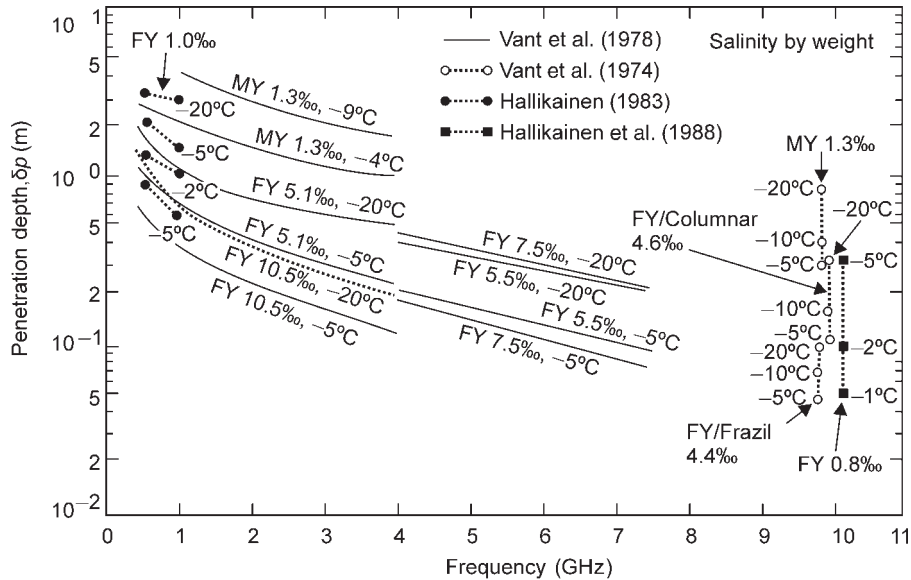
Fig. 2.21 Penetration depth at microwave frequencies for different types of first-year (FY) and multiyear (MY) sea ice (Hallikainen & Winebrenner, 1992).

basis of an underlying microstructural model (Stogryn, 1987) specifying the shape, size and distribution of brine inclusions as well as their volume fraction. Rather than describing ice microstructure in highly idealized terms such as the Stogryn model, Lin et al., (1988) have derived the emissivity of sea ice at microwave frequencies on the basis of a stochastic representation of sea ice microstructure. In this approach, the subparallel arrangement of brine layers within individual ice crystals (Figs 2.4 and 2.5) is rendered in terms of the autocorrelation length of the two-dimensional autocorrelation function.

In simpler, empirical approaches, ε has been parameterized as a function of the fractional brine volume (Hallikainen & Winebrenner, 1992), which in turn is determined by the temperature and salinity of the ice (Section 2.3). The extent to which temperature and ice salinity dominate the penetration depth is illustrated in Fig. 2.21. At temperatures of around −5°C, radar waves can thus penetrate several tens of centimetres to more than a metre into low-salinity multiyear ice, whereas penetration depths in saline first-year ice are only in the order of a few centimetres at most. Under such conditions, the radar backscatter signatures of multiyear ice are dominated by volume scattering from gas bubbles and brine inclusions. In first-year and young sea ice, ice surface scattering predominates and radar backscatter coefficients are mostly determined by the surface roughness of the ice. This allows for discrimination of generally smooth first-year ice and multiyear sea ice in radar satellite imagery. Owing to the polarization and frequency dependence of the dielectric properties (Fig. 2.21), more sophisticated multifrequency and multipolarization instruments can be of considerable use in distinguishing between different ice types. The same principles apply to thermal emission at microwave frequencies from different ice types and form the basis for commonly employed algorithms in discriminating between first- and multiyear sea ice in passive-microwave data (Chapter 4).

Macroscopic ice strength

Ice strength – at least on the macroscopic level as manifest, e.g. in a uniaxial compressive strength test commonly employed in studying the mechanical properties of sea ice (Richter-Menge, 1992) – is typically defined as the peak stress, σ_{max}, sustained by a sample when a load is applied. In simplified terms, σ corresponds to the magnitude of the force, F, applied per unit area, A:

$$\sigma = \frac{F}{A} \qquad\qquad \text{(Equation 2.47)}$$

For an ideal elastic response, the strain ε resulting from a given stress σ is proportional to σ, with Young's modulus E as the proportionality constant,

$$\sigma = E\varepsilon \qquad\qquad \text{(Equation 2.48)}$$

Here, strain $\varepsilon = (l - l_0)/l_0$ is defined as the relative change in linear dimension that a body experiences as it is stretched or compressed from l_0 to l. For elastic deformation, the body fully recovers from a given strain in the way an ideal spring would (Fig. 2.22a). Upon
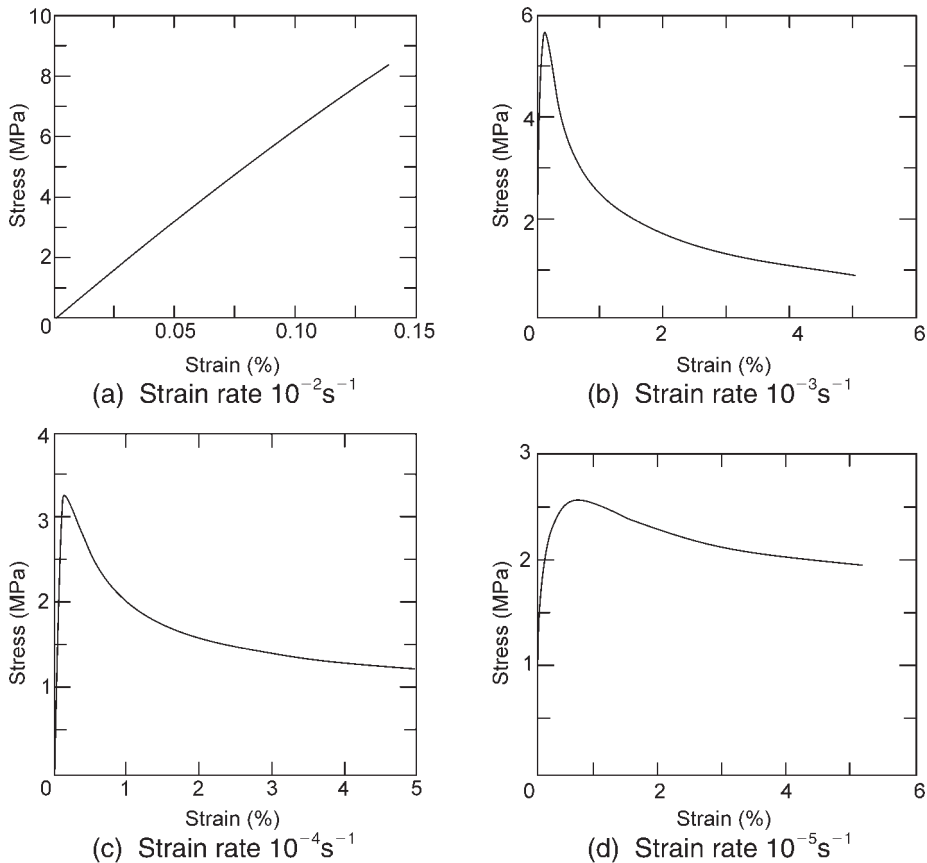

Fig. 2.22 Stress–strain curves for uniaxial compression tests of granular sea ice carried out at –10°C at different strain rates (Richter-Menge, 1992); see text for details. Reproduced with kind permission of the Department of Civil and Environmental Engineering, University of Alberta, Canada.

reaching the yield stress σ_{max}, the sample fails catastrophically, by releasing the stored elastic energy mostly in the form of kinetic energy and sound. This process is referred to as brittle failure. The same mode of failure is experienced by a glass that shatters as it is dropped to the floor. Unlike glass, however, sea ice typically responds to a given stress not only through elastic but also through viscous (non-recoverable) deformation. For a Newtonian liquid, the latter is characterized by a linear relation between stress, σ, and strain rate, $d\varepsilon/dt$, with the viscosity of the medium η as the proportionality constant,

$$\sigma = \eta \frac{d\varepsilon}{dt} \qquad \text{(Equation 2.49)}$$

Hence, deformation of natural sea ice is often best described by a model that takes into account both elastic and viscous strain components (Mellor, 1986). Equation 2.49 implies a connection between the magnitude of the stress and the strain rate. In fact, as evident from Fig. 22a–d, the deformation of natural sea ice samples at different strain rates conforms with such a visco-elastic model, with the peak stress σ_{max} reduced by a factor of 3 as the strain rate is dropped from 10^{-2} s^{-1} to 10^{-5} s^{-1}. Also note that at smaller strain rates (Fig. 2.22b–d), the ice exhibits ductile failure and is still capable of supporting a load after attaining σ_{max}, in contrast with the brittle failure shown in Fig. 2.22a.

It requires a highly sophisticated approach to translate these results from laboratory experiments into the real world, in which the load could be applied by a person stepping on fairly thin, young ice, with the strain rate dictated by the speed at which the foot is set down on the ice surface. Nevertheless, on the basis of this knowledge, one could devise a strategy of how to best cross a very thin, young sea ice cover if one absolutely had to. First, one would not want to apply the full load fast enough to induce catastrophic brittle failure, as this would result in the person breaking through the ice without much of a warning (i.e. prior deflection of the ice sheet, see Fig. 2.22a). If strain rates were small enough to induce deformation in a ductile mode, then one would experience the ice giving way underneath after initially appearing quite strong (at least for strain rates corresponding to the transitional brittle–ductile regime characteristic of Fig. 2.22b) and, as long as the load would be reduced fast enough, the ice sheet would not fail (i.e. break).

Contrived though this example may appear, polar bears venturing out on nilas (≤ 10 cm thick) have been observed to make intuitive use of the physics underlying such different sea ice failure modes. Thus, in ambling across the thin ice, the bear sets down each foot just long enough for the peak stress to be surpassed (at the associated strain rates in the order of a few seconds at most) and then lifts it again to place it ahead on yet unstrained ice. Indigenous hunters, such as the Iñupiat of northern Alaska, employ a similar strategy in crossing stretches of ice that would never support a person's weight if stationary for more than a few seconds at most. As the thin, warm ice flexes and is depressed below sea level, brine and sea water forced upwards through the ice onto the surface provide a visible indicator of the amount of accumulated strain.

The deformation process itself and the accommodation of strain on a microscopic level can be quite complicated. Thus, the solid ice matrix experiences deformation of atomic bonds, slip along microcracks, movement of grain boundaries and other processes (Schulson, 1999). It is the combination of all of these individual, microscopic processes that determines the macroscopic response of the ice cover. Hence, the microstructure of the ice plays an important role in determining both ice strength and mode of failure (Schulson, 1999). The contrasting properties of lake and sea ice have already been considered in Section 2.1, and

similar contrasts hold for ice deformation. Thus, for typical stresses and strain rates, the response of lake ice to an imposed loading is almost exclusively elastic, with failure occurring catastrophically in a brittle mode. This gives no advance warning to anybody who is about to break through the ice as the yield stress coincides with the complete failure of the material, similar to breaking glass. On the other hand, the lack of brine inclusions, which do not contribute to the overall strength of the material, is responsible for a somewhat higher strength of thin lake ice as compared to sea ice, which in the case of nilas can contain as much as 20% liquid-filled pores.

The actual macroscopic strength (i.e. the yield stress σ_{max}, see Fig. 2.22) of a sample or volume of sea ice is to a large extent controlled by the volume fraction of gas, V_a/V, and brine, V_b/V, both of which do not contribute to the mechanical strength of the material. As shown in an analysis by Assur (1960) (see summary in Weeks & Ackley (1986)), it is thus the ice cross-sectional area $(1 - \psi)$ (with ψ referred to as the 'plane porosity') that determines the magnitude of the *in situ* stress and hence the macroscopic yield stress, σ_{max}, such that,

$$\sigma_{max} = (1 - \psi)\sigma_0 \qquad \text{(Equation 2.50)}$$

where σ_0 would correspond to the strength of ice with all characteristics of sea ice but zero porosity. On the basis of Assur's (1960) pore model (Fig. 2.23), one can now derive the cross-sectional area of brine inclusions (assuming $V_a/V = 0$) in the vertical plane along which an ice sheet will typically fail under natural conditions. As shown in detail by Weeks & Ackley (1986), assuming the brine cell geometry outlined in Fig. 2.23, an expression can be derived for ψ in terms of the platelet spacing, a_0, the minor and major radii of an ellipsoidal inclusion, r_a and r_b, spaced b_0 apart in the direction of the ice lamellae, and a vertical separation of inclusions of length g by g_0 such that equation 2.50 can be evaluated as:

$$\sigma_{max} = \left(1 - 2\sqrt{\frac{r_b}{r_a}\frac{g}{g_0}\frac{a_0}{b_0}\frac{V_b}{V}}\right)\sigma_0 \qquad \text{(Equation 2.51)}$$

A model of this form is commonly assumed to govern the porosity and pore-shape dependence of ice strength, although some recent work suggests more complex relationships, as illustrated in Fig. 2.11 and discussed in Section 2.3 above. Apart from the stress-bearing, effective cross-sectional area, strength is also highly dependent on the nucleation and propagation of cracks that ultimately lead to failure. The latter depend strongly on other microstructural parameters, such as grain size or preferred alignment of crystals (Schulson, 1999). On the scale of an individual ice floe, the bending of an ice sheet results in a vertical stress/strain distribution such that maximum tensile stress is found at the top of a flexing ice sheet, with σ decreasing to zero in the interior of the ice sheet and maximum compressive stress found at a point opposite the crest in the ice. As sea ice is stronger in compression than tension by a factor of 2–4, the ice typically fails by cracks developing at the outer surface that is in tension with the crack propagating into the interior of the ice sheet. At the same time, it is the colder, less porous and hence stronger layers that determine the overall strength of an ice sheet (Fig. 2.6). Ice strength is a property of sea ice that, probably unlike few others, is highly dependent on the scale at which it is being considered. Thus, at the scale of the ice pack, ice strength mostly is only in the order of tens to hundreds of kPa, whereas it is typically above 1 MPa in laboratory-scale experiments.
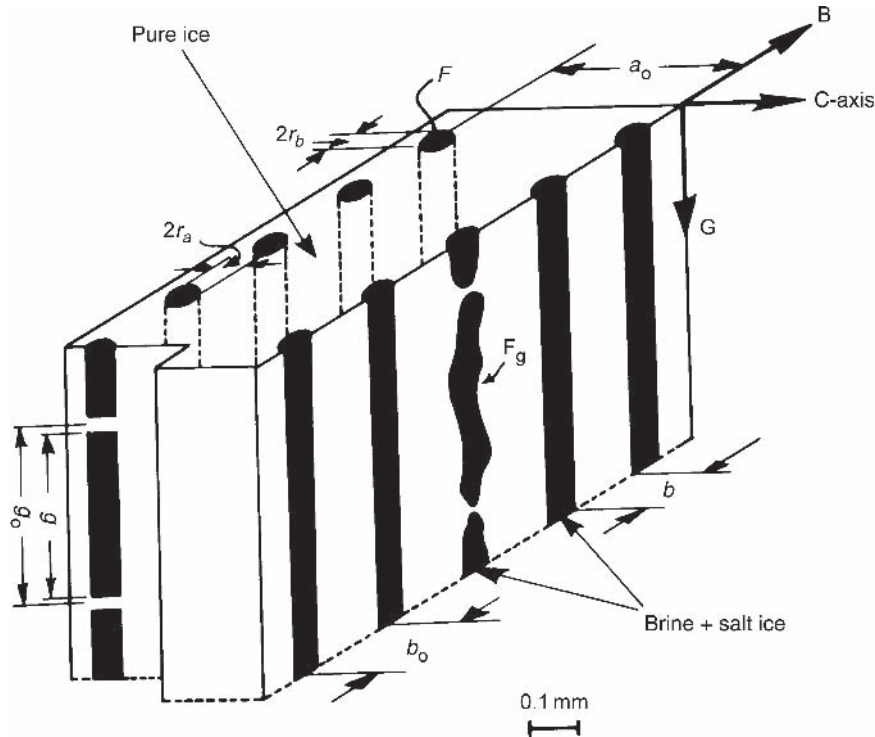
Fig. 2.23   Pore microstructural model by Assur (1960).

2.5 Sea ice–growth models, deformation and melt

The role of the snow cover in sea ice growth

Though it typically accounts for less than 10% of the total mass of ice in the polar seas, the snow cover plays a major role in the heat budget of sea ice. First, snow albedos are consistently higher than those of bare sea ice (Fig. 2.18, Section 2.4 and Chapter 5). More importantly, snow is a good insulator, as the thermal conductivity of snow is generally lower than that of sea ice by roughly 1 order of magnitude. The low thermal conductivity is determined by both snow texture and density. The air content is large and results in a snow density around 300 kg m^{-3}. However, most of the variability is related to the metamorphic state of the snow layer (Sturm et al., 2002). The bulk thermal conductivity of snow typically ranges between 0.1 and 0.4 W m^{-1} K^{-1}, as compared to roughly 2 W m^{-1} K^{-1} for sea ice (Massom et al., 2001; Sturm et al., 2002). Even a few centimetres of deposition on 0.5-m ice can impede ice growth by reducing the conductive heat flux, F_c (equation 2.10), by as much as 50%. At the same time, the sensitivity of the ice cover to changes in the oceanic heat flux increases (equation 2.52). In the Antarctic, where snow depths on sea ice reach several tens of centimetres and more than a metre in some regions (Jeffries et al., 1994), model simulations show that snow deposition approximately halves the ice thickness in the Weddell Sea and East Antarctica. Another consequence of snow deposition on sea ice is a reduction in the amount of short-wave radiation entering into the ice and underlying water, and a temperature increase

in the upper sea ice layers. Both have important ramifications for overall ice properties and the role of sea ice as a habitat for microorganisms (Chapters 7–9).

In most cases, snow-covered ice grows to be thinner than snow-free ice. However, once the load of a thicker snow cover is sufficient to depress the ice surface below the sea surface, sea water and brine may percolate either vertically or laterally through the ice cover (Maksym & Jeffries, 2000). Such sea water flooding shifts the locale of ice growth from the bottom of the ice cover to its top surface and the bottom of the snow pack. The ensuing increase in the conductive heat flux, F_c (equation 2.10), allows more ice to grow per unit area and time than would be possible through freezing at the ice bottom.

In the Arctic, snow depths in relation to ice thickness are rarely high enough to allow for surface flooding and snow ice formation. In the Antarctic, however, an overall thinner ice cover and higher snow accumulation rates result in widespread occurrence of this phenomenon, with more than 50% of the surface flooded in some areas (Eicken et al., 1994; Jeffries et al., 1994; Worby et al., 1998). This has important consequences for sea ice remote sensing as it substantially changes the dielectric properties of sea ice and hence its signature in active- and passive-microwave remote-sensing data sets (Chapter 6). Similarly, sea ice ecology is also strongly affected by this process (Chapter 8; see infiltration layer community in Fig. 2.19b).

As the flooded snow refreezes, the microstructural traces of its meteoric origin are often obliterated and it becomes exceedingly difficult to distinguish such snow ice from similarly fine-grained consolidated frazil ice. Here, the stark contrast in the stable-isotope signatures of snow, which is greatly depleted in the heavy isotopes of oxygen (^{18}O) and hydrogen (D), and ice grown from sea water with its stable, undepleted composition, can help determine the total contribution of precipitation (often referred to as meteoric ice) to the total ice thickness (Eicken et al., 1994; Chapter 3). Numerous studies in the Southern Ocean have established that snow ice (the frozen mixture of snow and sea water and/or brine) is exceedingly common, accounting for between a few per cent to more than 50% of the total ice thickness. The actual meteoric ice fraction is generally less than 20%. Both small- and large-scale model simulations (Fichefet & Morales Maqueda, 1999; Maksym & Jeffries, 2000; Powell et al., 2005) indicate snow ice formation to be important on the global scale as well.

Snow ice formation may also help prevent the complete removal of sea ice from areas with high oceanic heat fluxes, F_w. For example, in the eastern Weddell Sea, bottom topography and local hydrography result in winter values of F_w in excess of 100 W m^{-2} for extended periods of time (McPhee et al., 1996). In the mid-1970s, this region was the site of a vast polynya that persisted for several years (Chapters 4 and 6). Considering that such high heat fluxes would halt ice growth and induce bottom melt even in mid-winter, one wonders how an ice cover can survive at all in this region. Observations during the ANZFLUX study (McPhee et al., 1996) demonstrated that level ice of several tens of centimetre thickness does in fact melt at rates of several centimetres per day in the area during intervals of high oceanic heat flux. At the surface of the ice, buffered against the oceanic heat by the ice layers below, snow ice growth seems to be able to compensate for the intermittent substantial bottom ice losses.

Heat budget of sea ice during growth

The fact that in the Southern Ocean, level, undeformed ice typically grows to less than 0.7 m thickness within a single year, compared to as much as 1.8 m in the Arctic (Chapter 4), leads us to the question as to what exactly controls the thickness that an ice floe can attain through

freezing of sea water onto its bottom. We will limit ourselves to the discussion of sea ice during the growth season in this section, where solar short-wave radiation is negligible.

The ice-growth rate is determined by the energy balance at the lower boundary, i.e. the ice bottom. Here, the conductive heat flux out of the interface into the ice, F_c, and the oceanic heat flux, F_w, from the underlying water into the interface are balanced by the release or uptake of latent heat, L_{si}, during freezing or melting, i.e. thickness change dH/dt (dH/d$t >$ 0 during freezing):

$$-F_c + F_w + \rho_i L_{si} \frac{\mathrm{d}H}{\mathrm{d}t} = 0 \qquad\qquad \text{(Equation 2.52)}$$

where ρ_i is the density of ice.

The sign of a flux is a matter of convention; when considering the energy balance at one interface only, usually all fluxes are defined as either positive or negative if they are directed away from the interface; however, we consider fluxes between two interfaces and within the bulk in this section. For the sake of consistency, we define fluxes as positive if heat flows upwards towards the atmosphere.

In the absence of an oceanic heat flux, the ice cover would thicken as long as heat is removed through the ice to the atmosphere. Without radiative transfer of energy into the ice, this is the case as long as the surface temperature of the ice is less than the freezing point of sea water at the lower interface. However, the ocean underlying the ice typically contains a reservoir of heat that is either remnant from solar heating of the mixed layer in summer (Maykut & McPhee, 1995) or due to transfer of heat from deeper water layers. In the Arctic, where the amount of heat transported into the polar basin and entrained into the surface mixed layer from below the halocline is comparatively small, F_w amounts to a few W m^{-2} in most regions (Steele & Flato, 2000). In the North American Arctic, where advection of heat is minimal, the seasonal cycle of F_w is almost exclusively controlled by the absorption of solar short-wave radiation in the upper ocean, which is transferred to the ice bottom later in the season (Maykut & McPhee, 1995).

In the Antarctic, ocean heat flow can be in the order of several tens of W m^{-2} (Martinson & Iannuzzi, 1998). As a result, even an ice cover that is cooled substantially from the atmosphere in winter may only grow to a maximum thickness that is determined by the balance of ocean and conductive heat flow, $F_c = F_w$. Measurements of ice thickness and surface hydrography indicate that this maximum (winter equilibrium) thickness is in the order of 0.5–0.7 m (Wadhams et al., 1987; Martinson & Iannuzzi, 1998). As shown below, such estimates can also be obtained from simple analytical modelling.

In areas where oceanic heat fluxes can episodically increase to several hundred W m^{-2} owing to convective exchange with a deeper ocean well above freezing (McPhee et al., 1996), an ice cover can thin significantly, or vanish entirely, by melting from below. Such extended areas where the ocean is ice free even in mid-winter are referred to as polynyas. The vast Weddell Sea polynya of the 1970s is the most prominent example of open water maintained through active melting and heating of the surface ocean. Alternatively, polynyas can also form dynamically, with strong, steady winds pushing ice away from a coastline or stretches of land-fast ice.

Oceanic heat and heat released by freezing is transferred to the upper surface of the ice cover and ultimately released to the atmosphere. The rate at which heat can be extracted is determined by the energy balance at the upper surface of the ice floe as well as the snow and

ice thermal properties. For a surface at steady temperature, conservation of energy requires that the heat fluxes out of and into the surface be balanced:

$$(1 - \alpha)F_r - I_0 + F_L \Downarrow + F_L \Uparrow + F_s + F_e - F_c + F_m = 0 \qquad \text{(Equation 2.53)}$$

Here, the individual heat flux terms are: incoming solar short-wave flux, F_r (with ice albedo, α, indicating the ratio between incident and reflected short-wave energy for a given ice surface); the short-wave flux penetrating into the ice/water, I_0; the incoming long-wave flux, $F_L\Downarrow$; the outgoing long-wave flux, $F_L\Uparrow$; the turbulent atmospheric sensible and latent heat fluxes F_s and F_e, respectively; the heat flux due to melting of ice at the surface, F_m (in the Arctic typically only relevant during the summer after the ice surface starts to melt) and the conductive heat flux from the interior of the snow/ice, F_c. Equation 2.53 is formulated with positive fluxes transporting heat upwards for consistency within this section. Details on the surface energy balance can be found in Maykut (1986) and Steele & Flato (2000).

   While a detailed discussion of the magnitude of all these terms is given in Maykut (1986) or Persson et al., (2002), over Arctic multiyear ice, the net radiation balance typically does not drop below -50 W m^{-2} during winter and has its maximum in July at just over 100 W m^{-2}. The other fluxes range between a few and tens of W m^{-2}.

   The surface and bottom heat balances are coupled through conductive heat exchange F_c with the snow and ice in between. The energy balance in sea ice is for conductive heat transfer and absorption of short-wave radiation,

$$\frac{\partial H}{\partial t} = \rho_i c_{si} \frac{\partial T}{\partial t} = \frac{\partial}{\partial z}\left(\lambda_{si} \frac{\partial T}{\partial z}\right) - \frac{\partial F_{sw}}{\partial z} \qquad \text{(Equation 2.54)}$$

where F_{sw} is the radiative short-wave flux (for the definition of enthalpy, see equation 2.21); the energy balance for snow is similar. In steady state ($dT/dt = 0$) and in the absence of radiative heat input ($dF_{sw}/dz = 0$), the conductive heat flux is constant throughout sea ice; i.e. F_c is equal at both interfaces. Simplified models that couple both interfaces are discussed next.

Simple models of sea ice growth

A rigorous mathematical treatment of the problem of ice growth requires numerical techniques because the individual terms in the surface energy balance (equation 2.54) depend either directly or indirectly on surface and air temperatures in a non-linear fashion, and the thermal properties in equation 2.54 are temperature dependent. Nevertheless, as demonstrated more than a century ago by Stefan (Leppäranta, 1993), through some simplifications it is actually possible to arrive at fairly accurate predictions of ice growth. Such simple, so-called degree-day models can also help us in understanding key aspects of the heat budget of sea ice and are therefore discussed in more detail below. The principal aim of ice-growth modelling is to evaluate the growth rate dH/dt of sea ice as a function of time. The temperature at the ice–ocean interface is at the freezing point T_w, and we assume the oceanic heat flux F_w to be known (Fig. 2.24). The conductive heat flux at the bottom of the ice is largely determined by the heat flux to the atmosphere. At the interface with the atmosphere, one finds that net long-wave radiative fluxes can be described as a function of surface and air temperature. Likewise, the turbulent heat fluxes F_s and F_e depend on air and surface temperature
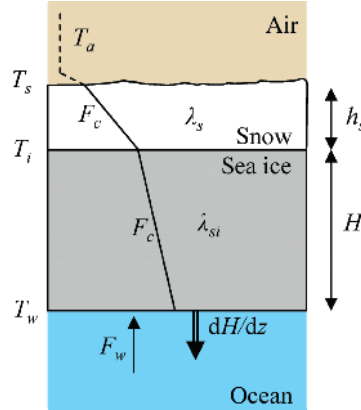
Fig. 2.24   Illustration of the two-layer model of sea ice growth.

(for a discussion of the latent heat flux F_e, see Andreas et al., 2002). As a first approximation, the net atmospheric flux can be linearized with respect to the temperature difference between air and surface, i.e. the magnitude of the net atmospheric flux F_a increases with temperature difference between surface and air:

$$F_a = -k(T_a - T_s) + F_a^0(T_a, T_s, ...)$$ (Equation 2.55)

where k is an effective heat transfer coefficient between surface and atmosphere, and the flux F_a^0 is usually set to 0. Owing to the large ratio between latent and sensible heat stored in sea ice, sea ice grows so slowly that the ice temperature profile adjusts to the increasing ice thickness quasi-instantaneously (Carslaw & Jaeger, 1986). Hence, the temperature profile is linear in the absence of solar heating (e.g. in winter) and rapid temperature fluctuations, provided the thermal conductivity λ_{si} is homogeneous in the ice. Temperature profiles in sea ice are indeed linear during much of the growth season. This is illustrated in Fig. 2.10. Considering the two-layer system of snow and ice with continuity in temperature and heat flux throughout snow and sea ice (Fig. 2.24), the net conductive heat flux is:

$$F_a = F_c = -\frac{T_a - T_w}{\dfrac{1}{k} + \dfrac{H}{\lambda_{si}} + \dfrac{h_s}{\lambda_s}}$$ (Equation 2.56)

where H and h_s are the thickness of sea ice and snow, respectively, and λ_{si} and λ_s are the respective thermal conductivities. Since $\lambda_s \approx 0.1 \lambda_{si}$, we see that even a layer of snow that is thin with respect to sea ice thickness H can have a profound influence on the heat flux.

Equating equation 2.56 with the energy balance at the ice bottom (equation 2.52), we find:

$$\frac{dH}{dt}\rho_i L_{si} = -\frac{T_a - T_w}{\dfrac{1}{k} + \dfrac{H}{\lambda_{si}} + \dfrac{h_s}{\lambda_s}} - F_w$$ (Equation 2.57)

This equation is suitable for numerical modelling if a time series of air temperature, snow depth and oceanic heat flux are known. However, further approximations are commonly made to allow ice thickness estimates solely based on the air temperature history: we assume the absence of an oceanic heat flux, that the atmospheric heat transfer coefficient k is constant with time and that the snow thickness increases with time proportionally to the ice thickness following:

$$h_s = r_s H \qquad \text{(Equation 2.58)}$$

where r_s is the constant of proportionality (note that we would expect surface flooding if r_s exceeds approximately 0.3). Integrating equation 2.57 over time, we find that the ice thickness evolves according to:

$$H^2 + \frac{2\lambda_{si}}{k}\left(1 + \frac{\lambda_{si}}{\lambda_s}r_s\right)^{-1} H = \frac{2\lambda_{si}}{\rho_i L_{si}}\left(1 + \frac{\lambda_{si}}{\lambda_s}r_s\right)^{-1}\int -(T_a - T_w)dt \qquad \text{(Equation 2.59)}$$

For the special case of a known and constant surface temperature, i.e. $k \to \infty$ and constant T_a, and absence of snow, i.e. $r_s = 0$, equation 2.59 reduces to the solution of the Stefan problem,

$$H^2 = \frac{2\lambda_{si}(T_w - T_a)}{\rho_i L_{si}}t \qquad \text{(Equation 2.60)}$$

This is the result of the most fundamental growth model of sea ice that states that the thickness of ice increases with the square root of time.

Commonly, the term

$$\theta = \int_0^{t_e}(T_w - T_a)dt \qquad \text{(Equation 2.61)}$$

in equation 2.59 is computed for discrete time steps $\Delta t = 1$ day; θ is then referred to as the number of freezing-degree days, a variable easily derived from standard meteorological observations. Reasonable accuracy can be achieved by deriving the factors in equation 2.59 empirically, typically from a time series of ice thickness and air temperatures for a given location. One such approach is that by Anderson (1961) with ice thickness given as:

$$H^2 + 5.1H = 6.7\theta \qquad \text{(Equation 2.62)}$$

where H and θ are in cm and °C days, respectively (the coefficients in equation 2.62 are consistent with $r_s \approx 0.13$ and $k \approx 45$ W m^{-2} K^{-1}).

As indicated by the quadratic nature of equation 2.59, ice growth slows as the ice cover thickens with time. As a consequence, differences in thickness between ice floes formed at different stages in winter tend to diminish with time. In the absence of ocean (or solar) heat fluxes into the ice, and without any summer melt, there would be no limiting thickness for sea ice growth. However, since the oceanic heat flux, F_w, is rarely 0, at some point the ice thickness reaches a limiting, maximum value for which the conductive heat flux out of the

ice bottom equals that of the oceanic heat flux into it (equation 2.52) and all ice growth stops. From equations 2.57 and 2.58, the magnitude of this limiting or equilibrium thickness, H_{eq}, is given by:

$$H_{eq} = -\lambda_{si} \frac{T_a - T_w}{F_w} \left(1 + \frac{\lambda_{si}}{\lambda_s} r_s\right)^{-1}$$
(Equation 2.63)

For typical Antarctic conditions, with $T_a - T_w = -20$ K, $\lambda_{si} = 2.0$ W m^{-1} K^{-1} and $F_w = 20$ W m^{-2}, $\lambda_{si}/\lambda_i = 10$, and $r_s = 0.3$ (i.e. flooding) the limiting thickness is 0.5 m, suggesting that the ocean does in fact limit the growth of level ice. In the Arctic, F_w is typically smaller by an order of magnitude and the limiting thickness greatly exceeds what can be achieved within a single year of ice growth.

Figure 2.25 shows a comparison between the Anderson model and measurements: it is evident that the impact of a snow cover on the ice thickness evolution is substantial. A simple degree-day model following equation 2.59, $H^2 + 25H = 7.3\theta$ ($r_s = 0.08$, $\lambda_{si}/\lambda_i = 6.7$, $k = 10$ Wm^{-2}K^{-1}), was used to describe the development of sea ice thickness from mid-December to June. Varying the parameter r_s, estimates are obtained for the thickness evolution without snow cover ($r_s = 0$) and with a snow cover deep enough to cause flooding ($r_s = 0.3$).

The importance of ice deformation

In discussing the impact of climate variability and change on the state of the polar sea ice covers, one needs to consider more than thickening or thinning of the ice cover through ice growth or melt. Deformation of the ice cover through rafting and ridging of floes (Fig. 2.1) not only accounts for the thickest ice observed in the polar oceans, it also provides a mechanism for rapid thickening in cases where freezing rates at the ice bottom are approaching 0. The complex interplay of different deformation processes and their overall impact on the ice thickness distribution are the topic of Chapter 4. Here it suffices to state that predicting the response of an ice cover to changes in the meteorological and oceanographic boundary
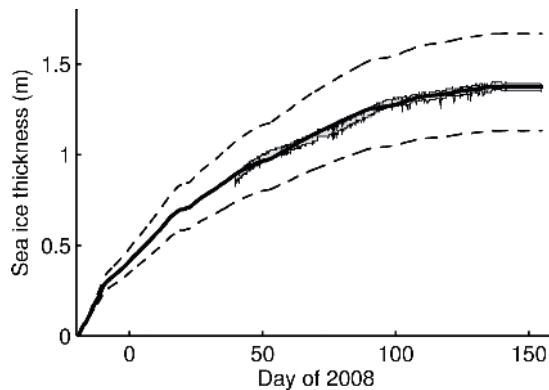

Fig. 2.25   Sea ice thickness in Barrow as function of time based on a degree-day model (thick line), and estimates of thickness development without snow and with heavy snow load (dashed lines, see text for details). Thickness measurements from an acoustic sounder are indicated by a stripe of width 4 cm from day 45 onwards. Air temperatures are based on measurements 2 m above ground (courtesy Atmospheric Radiation Measurement (ARM) Program).

conditions requires an assessment of both the static component of ice growth and melt, as well as the dynamic component of thickening through rafting or ridging. Deformation processes are particularly important in a warming climate, as they may be capable of compensating for some of the thinning due to decreased ice growth and increased ice melt.

Sea ice melt

As has been demonstrated above, ice melts at the bottom whenever the oceanic heat flux into the ice–water interface exceeds the conductive heat flux out of the interface. For sea water of constant salinity, the interface temperature is not subject to change but remains constant at the ice melting/freezing point of, for example, $-1.86°C$ for a salinity of 34. At the upper surface of sea ice, temperatures are typically much lower in winter, such that a net heat flux into the ice cover does not immediately result in melting of the entire ice matrix, but initially in warming of the ice cover (see temperature profile in Fig. 2.10 at the end of May). Warming of sea ice is also associated with melting, but on a microscopic scale, not at the scale of the ice thickness. Typically, this warming is accompanied by a reduction in ice salinity, with the surface layer of sea ice approaching zero salinity as a result of surface warming and snow melt that flush salt downwards through the ice cover (Untersteiner, 1968).

While the linkage between surface salinity, ice temperature and microscopic melt is complicated, warming eventually raises the temperature to the bulk melting point of ice. This input of heat into the surface layer results in a reduction in ice thickness through surface ablation. In contrast with bottom melt, surface melt generates liquid water above sea level, and the subsequent fate of this meltwater plays an important role in the energy and mass balance of the ice cover as a whole. Typically, in the Arctic, a quarter of this water is retained in surface melt ponds (Eicken et al., 2002), resulting in a significant decrease in surface albedo (apparent in Fig. 2.19a). As much as half of the meltwater percolates downwards into the ice, flushing out salt in the process, with the rest running off into the upper ocean.

While surface melting is the dominant ablation process in the Arctic, accounting for a loss of between 0.3 and 1 m of ice from the surface of the perennial ice in the central Arctic, recent studies indicate that bottom melt is increasing in importance: as much as 0.5 m of level ice was melted off the bottom in a single season (McPhee et al., 1998; Perovich et al., 2003). Only a minor fraction of bottom melt can be explained by transfer of heat from the deeper ocean into the surface layer, with most of it supplied by solar heating.

Decreasing ice concentrations and ice extent over the Arctic Ocean in the 1990s and 2000s have resulted in an increase in the amount of solar short-wave energy stored in the upper ocean and released during the latter part of the summer melt season (Perovich et al., 2007). In combination with atmospheric warming and shifts in ice circulation, these changes are believed to be underlying observations of a thinning of the Arctic ice pack (Rothrock et al., 1999) and, if continuing unabated, may result in significant shrinkage and eventual complete disappearance of the perennial Arctic sea ice (Stroeve et al., 2007).

Currently, much of the Arctic ice cover survives summer melt, with subsequent surface melting and winter accretion resulting in a gradual thickening of the ice cover. The rate of winter ice growth at the bottom decreases with ice thickness (see equation 2.57), whereas the amount of surface and bottom melt does not. Consequently, at some point, perennial sea ice reaches a maximum equilibrium thickness for which the amount of summer melt

is compensated by the amount of winter ice growth. While the concept of an equilibrium thickness is highly idealized since it neglects, among other things, interseasonal and interannual variability in atmospheric and oceanic forcing or ice properties, it is of substantial value in discussing the impacts of variability in the forcing.

Numerical simulations by Maykut and Untersteiner indicate that ice attained equilibrium thickness between 2.5 and 3 m thick at the onset of summer melt (Maykut, 1986). These model results were obtained for atmospheric forcing data representative of the 1960s to the 1980s and recent observations indicate that equilibrium thickness may have substantially decreased (Perovich et al., 2003; Chapter 4). Among other factors, such as the depth of the snow cover, the magnitude of the oceanic heat flux plays a prominent role in determining the equilibrium thickness. Maykut and Untersteiner's model results suggest that the perennial ice vanishes for $F_w = 7$ W m^{-2}, with only seasonal ice remaining in the Arctic Ocean.

By contrast, the surfaces of Antarctic sea ice floes appear almost unchanged during the summer months (Fig. 2.17b), as most of the melting takes place along their margins and bottom, due to heat transfer from the deeper ocean and absorption of solar radiation in surface waters. The lack of ice surface ablation and development of melt ponds, characteristic of the Arctic ice pack, is commonly explained by a combination of a colder, drier atmosphere in the Antarctic that effectively cools the ice surface even during summer (Andreas & Ackley, 1981) along with smaller concentrations of surface impurities in Antarctic snow and ice as compared with the Arctic. Nevertheless, recent observations of melt ponding, both on sea ice (Drinkwater & Xiang, 2000) and on floating ice shelves of the Antarctic Peninsula, raise the question as to whether the Antarctic ice pack can also be subject to extensive surface melt and the associated drastic reductions in surface albedo under a variable or changing climate regime.

Conclusion

This chapter started out with an introduction to the importance of the scale of observation in the study of sea ice. As to be expected, focus on a particular process or phenomenon often leads to the danger of not seeing the forest for the trees or failing to see the trees that make up a forest. In sea ice research, both instances happen on a regular basis, and the authors of the chapter are not exempt from falling into this trap. At the same time, however, methodological innovations and advances in our understanding of sea ice as a material and a large-scale phenomenon have now opened the door to studies that are cognizant of both the vast forest and the particulars of each tree. For example, computational limitations have prevented physically realistic representations of sea ice processes in climate models. This may now be changing and there is increasing interest and ability by modellers to incorporate the finer details of ice growth and ice properties into these models. Similarly, the increasing sophistication of field research methods and the realization of the importance of key sea ice processes in a global context have prompted a number of investigations that are seeking to bridge the gaps between the microscopic, macroscopic and the regional scales. Much has changed in the world of sea ice in the half decade or so that passed between the publishing of the first and second editions of this book and it appears like this trend of increasing interest in the polar sea ice covers is likely to continue.

End notes

1 Malmgren's work and fate may also serve to illustrate how scientific investigation, exploration and the incalculable were intertwined in the early 20th century (and arguably continue to be so to some extent). Finn Malmgren's thorough and groundbreaking study of sea ice properties was prompted by Harald Sverdrup who had suggested this work as a project to at least gain something out of the unplanned freezing in of Roald Amundsen's vessel *Maud* during the Northeast Passage expedition of 1922–25. Malmgren's experience and scientific prowess predestined him to be one of the key participants in Nobile's ill-fated airship expedition to the North Pole, where Malmgren perished in the ice pack on a trek to reach the Svalbard archipelago.

2 The data assembled by Assur originate mostly from the first half of the 20th century but have been verified to some extent by nuclear magnetic resonance studies of the liquid volume fraction (Richardson, 1976). Nevertheless, some cautions apply.

References

Anderson, D.L. (1961) Growth rate of sea ice. *Journal of Glaciology*, **3**, 1170–1172.

Andreas, E.L. & Ackley, S.F. (1981) On the differences in ablation seasons of the Arctic and Antarctic sea ice. *Journal of Atmospheric Science*, **39**, 440–447.

Andreas, E.L., Guest, P.S., Persson, P.O.G. et al. (2002), Near-surface water vapour over polar sea ice is always near ice saturation. *Journal of Geophysical Research*, **107**, 8033, 10.1029/2000JC000411.

Andreas, E.L., Guest, P.S., Persson, P.O.G. et al. (2002), Near-surface water vapor over polar sea ice is always near ice saturation. *Journal of Geophysical Research*, **107**, 8033, 10.1029/2000JC000411.

Arrigo, K.R., Kremer, J.N. & Sullivan, C.W. (1993) A simulated Antarctic fast ice ecosystem. *Journal of Geophysical Research*, **98**, 6929–6946.

Arrigo, K.R. & Sullivan, C.W. (1994). A high resolution bio-optical model of microalgal growth: tests using sea ice algal community time-series data. *Limnology and Oceanography*, **39**, 609–631.

Assur, A. (1960) Composition of sea ice and its tensile strength. *SIPRE Research Report*, **44**.

Bennington, K.O. (1967) Desalination features in natural sea ice. *Journal of Glaciology*, **48**, 845–857.

Bitz, C.M. & Lipscomb, W.H. (1999) An energy-conserving thermodynamic model of sea ice. *Journal of Geophysical Research*, **104** (C7), 15,667–15,677.

Bombosch, A. (1998) Interactions between floating ice platelets and ocean water in the southern Weddell Sea. In: *Ocean, Ice, and Atmosphere: Interactions at the Antarctic Continental Margin* (Ed. S.S. Jacobs). American Geophysical Union, Washington. *Antarctic Research Series*, **75**, 257–266.

Callaghan, P.T., Dykstra, R., Eccles, C.D., Haskell, T.G. & Seymour, J.D. (1999) A nuclear magnetic resonance study of Antarctic sea ice brine diffusivity. *Cold Regions Science and Technology*, **29**, 153–171.

Carslaw, H.S. & Jaeger, J.C. (1986) *Conduction of Heat in Solids*. Oxford University Press.

Cottier, F., Eicken, H. & Wadhams, P. (1999) Linkages between salinity and brine channel distribution in young sea ice. *Journal of Geophysical Research*, **104**, 15859–15871.

Cox, G.F.N. & Weeks, W.F. (1983) Equations for determining the gas and brine volumes in sea ice samples. *Journal of Glaciology*, **29**, 306–316.

Cox, G.F.N. & Weeks, W.F. (1988) Numerical simulations of the profile properties of undeformed first-year sea ice during the growth season. *Journal of Geophysical Research*, **93**, 12449–12460.

Curry, J.A., Schramm, J.L. & Ebert, E.E. (1995) Sea ice-albedo climate feedback mechanism. *Journal of Climate*, **8**, 240–247.

Dieckmann, G.S., Nehrke, G., Papadimitriou, S. et al. (2008) Calcium carbonate as ikaite crystals in Antarctic sea ice. *Geophysical Research Letters*, **35**, L08501,10.1029/2008GL033540.

Dirakev, S.N., Poyarkov, S.G. & Chuvil'chikov, S.I. (2004) Laboratory modeling of small-scale convection under a growing ice cover in winter Arctic leads. *Oceanology*, **44**, 62–70.

Drinkwater, M.R. & Xiang, L. (2000) Seasonal to interannual variability in Antarctic Sea ice surface melt. *IEEE Transactions of Geosciences & Remote Sensing*, **38**, 1827–1842.

Eicken, H. (1992a) The role of sea ice in structuring Antarctic ecosystems. *Polar Biology*, **12**, 3–13.

Eicken, H. (1992b) Salinity profiles of Antarctic sea ice: field data and model results. *Journal of Geophysical Research*, **97**, 15545–15557.

Eicken, H. (1998) Factors determining microstructure, salinity and stable-isotope composition of Antarctic sea ice: deriving modes and rates of ice growth in the Weddell Sea. In: *Antarctic Sea Ice Physical Processes, Interactions and Variability* (Ed. M.O. Jeffries). American Geophysical Union, Washington. *Antarctic Research Series*, **74**, 89–122.

Eicken, H., Lange, M.A., Hubberten, H.-W. & Wadhams, P. (1994) Characteristics and distribution patterns of snow and meteoric in the Weddell Sea and their contribution to the mass balance of sea ice. *Annales Geophysicae*, **12**, 80–93.

Eicken, H., Bock, C., Wittig, R., Miller, H. & Poertner, H.-O. (2000) Nuclear magnetic resonance imaging of sea ice pore fluids: methods and thermal evolution of pore microstructure. *Cold Regions Science and Technology*, **31**, 207–225.

Eicken, H., Krouse, H.R., Kadko, D. & Perovich, D.K. (2002) Tracer studies of pathways and rates of meltwater transport through Arctic summer sea ice. *Journal of Geophysical Research*, **107**, 10.1029/2000JC000583.

Eicken, H., Grenfell, T.C., Perovich, D.K., Richter-Menge, J.A. & Frey, K. (2004) Hydraulic controls of summer Arctic pack ice albedo. *Journal of Geophysical Research*, **109**, C08007, 10.1029/2003JC001989.

Eide, L.I. & Martin, S. (1975) The formation of brine drainage features in young sea ice. *Journal of Glaciology*, **14**, 137–154.

Feltham, D.L., Worster, M.G. & Wettlaufer, J.S. (2002) The influence of ocean flow on newly forming sea ice. *Journal of Geophysical Research*, **107**, 3009, 10.1029/2000JC000559.

Feistel, R. & Hagen, E. (1998) A Gibbs thermodynamic potential for sea ice. *Cold Regions Science and Technology*, **28**, 83–142.

Fichefet, T. & Morales Maqueda, M.A. (1999) Modelling the influence of snow accumulation and snow-ice formation on the seasonal cycle of the Antarctic sea ice cover. Climate Dynamics, **15**, 251–268.

Fletcher, N.H. (1970) *The Chemical Physics of Ice*. Cambridge University Press, Cambridge.

Freitag, J. (1999) The hydraulic properties of Arctic sea ice – Implications for the small-scale particle transport (in German). *Reports on Polar Research*, **325**, 1–150.

Freitag, J. & Eicken, H. (2003) Meltwater circulation and permeability of Arctic summer sea ice derived from hydrological field experiments. *Journal of Glaciology*, **49**, 349–358.

Fukusako, S. (1990) Thermophysical properties of ice, snow and sea ice. *International Journal of Thermophysics*, **11**, 353–372.

Golden, K.M., Ackley, S.F. & Lytle, V.I. (1998) The percolation phase transition in sea ice. *Science*, **282**, 2238–2241.

Golden, K.M., Eicken, H., Heaton, A.L., Miner, J., Pringle, D.J. & Zhu, J. (2007) Thermal evolution of permeability and microstructure in sea ice, *Geophysical Research Letters*, **34**, L16501, 10.1029/2007GL030447.

Grenfell, T.C. (1979) The effects of ice thickness on the exchange of solar radiation over the polar oceans. *Journal of Glaciology*, **22**, 305–320.

Grenfell, T.C. (1991) A radiative transfer model for sea ice with vertical structure variations. *Journal of Geophysical Research*, **96**, 16991–17001.

Grenfell, T.C. & Maykut, G.A. (1977) The optical properties of ice and snow in the Arctic Basin. *Journal of Glaciology*, **18**, 445–463.

Hallikainen, M. & Winebrenner, D.P. (1992) The physical basis for sea ice remote sensing. In: *Microwave remote sensing of sea ice* (Ed. F.D. Carsey). American Geophysical Union, Washington. *Geophysical Monograph*, **68**, 29–46.

Hobbs, P.V. (1974) *Ice Physics*. Clarendon Press, Oxford.

Jeffries, M.O., Weeks, W.F., Shaw, R. & Morris, K. (1993) Structural characteristics of congelation and platelet ice and their role in the development of Antarctic land-fast sea ice. *Journal of Glaciology*, **39**, 223–238.

Jeffries, M.O., Shaw, R.A., Morris, K., Veazey, A.L. & Krouse, H.R. (1994) Crystal structure, stable isotopes (d18O), and development of sea ice in the Ross, Amundsen, and Bellingshausen seas, Antarctica. *Journal of Geophysical Research*, **99**, 985–995.

Jin, Z., Stamnes, K., Weeks, W.F. & Tsay, S.-C. (1994) The effect of sea ice on the solar energy budget in the atmosphere-sea ice ocean system: a model study. *Journal of Geophysical Research*, **99**, 25281–25294.

Kovacs, A. (1996) Sea ice: Part I. Bulk salinity versus ice floe thickness. *CRREL Report 96-7*.

Lake, R.A. & Lewis, E.L. (1970) Salt rejection by sea ice during growth. *Journal of Geophysical Research*, **75**, 583–597.

Lange, M.A., Ackley, S.F., Wadhams, P., Dieckmann, G.S. & Eicken, H. (1989) Development of sea ice in the Weddell Sea, Antarctica. *Annals of Glaciology*, **12**, 92–96.

Langhorne, P.J. & Robinson, W.H. (1986) Alignment of crystals in sea ice due to fluid motion. *Cold Regions Science and Technology*, **12**, 197–215.

Leonard, G.H., Purdie, C.R., Langhorne, P.J., Haskell, T.G., Williams, M.J.M. & Frew, R.D. (2006) Observations of platelet ice growth and oceanographic conditions during the winter of 2003 in McMurdo Sound, Antarctica. *Journal of Geophysical Research*, **111**, C04012, 10.1029/2005JC002952

Leppäranta, M. (1993) A review of analytical models of sea ice growth. *Atmosphere–Ocean*, **31**, 123–138.

Leppäranta, M. & Manninen, T. (1988) The brine and gas content of sea ice with attention to low salinities and high temperatures. *Finnish Institute of Marine Research Internal Report 88-2*, Helsinki.

Light, B., Maykut, G.A. & Grenfell, T.C. (2003) Effects of temperature on the microstructure of first-year Arctic sea ice. *Journal of Geophysical Research*, **108**, 3051, 10.1029/2001JC000887.

Lin, F.C., Kong, J.A., Shin, R.T., Gow, A.J. & Arcone, S.A. (1988) Correlation function study for sea ice. *Journal of Geophysical Research*, **93**, 14055–14063.

Lytle, V.I. & Ackley, S.F. (1996) Heat flux through sea ice in the western Weddell Sea: convective and conductive transfer processes. *Journal of Geophysical Research*, **101**, 8853–8868.

McPhee, M.G., Ackley, S.F., Guest, P. et al. (1996) The Antarctic Zone Flux Experiment. *Bulletin of the American Meteorological Society*, **77**, 1221–1232.

McPhee, M.G., Stanton, T.P., Morison, J.H. & Martinson, D.G. (1998) Freshening of the upper ocean in the central Arctic: Is perennial sea ice disappearing? *Geophysical Research Letters*, **25**, 1729–1732.

Maksym, T. & Jeffries, M.O. (2000) A one-dimensional percolation model of flooding and snow ice formation on Antarctic sea ice. *Journal of Geophysical Research*, **105**, 26313–26331.

Malmgren, F. (1927) On the properties of sea ice. Norwegian North Pole Expedition "Maud" 1918–1925, **1**, 1–67.

Marion, G.M. & Grant, S.A. (1997) Physical chemistry of geochemical solutions at subzero temperatures. *CRREL Special Report*, 97-10, 349–356.

Martinson, D.G. & Iannuzzi, R.A. (1998) Antarctic ocean–ice interaction: implications from ocean bulk property distributions in the Weddell Gyre. In: *Antarctic Sea Ice: Physical Processes, Interactions and Variability* (Ed. M.O. Jeffries). American Geophysical Union, Washington. Antarctic Research Series, **74**, 243–271.

Massom, R.A., Eicken, H., Haas, C. et al. (2001) Snow on Antarctic sea ice. *Reviews in Geophysics*, **39**, 413–445.

Maykut, G.A. (1986) The surface heat and mass balance. In: *The geophysics of sea ice* (Ed. N. Unter-
steiner), pp. 395–463. Martinus Nijhoff Publishers, Dordrecht (NATO ASI B146).

Maykut, G.A. & McPhee, M.G. (1995) Solar heating of the Arctic mixed layer. *Journal of Geophysical Research*, **100**, 24691–24703.

Mellor, M. (1986) Mechanical behavior of sea ice. In: *The geophysics of sea ice* (Ed. N. Untersteiner), pp. 165–281. Martinus Nijhoff Publishers, Dordrecht (NATO ASI B146).

Nakawo, M. & Sinha, N.K. (1981) Growth rate and salinity profile of first-year sea ice in the high Arctic. *Journal of Glaciology*, **27**, 315–330.

Nakawo, M. & Sinha, N.K. (1984) A note on brine layer spacing of first-year sea ice. *Atmosphere–Ocean*, **22**, 193–206.

Niedrauer, T.M. & Martin, S. (1979) An experimental study of brine drainage and convection in young sea ice. *Journal of Geophysical Research*, **84**, 1176–1186.

Nield, D.A. & Bejan, A. (1998) *Convection in Porous Media*. Springer-Verlag, New York.

Notz, D., McPhee, M.G., Worster, M.G., Maykut, G.A., Schlünzen, K.H. & Eicken, H. (2003) Impact of underwater-ice evolution on Arctic summer sea ice. *Journal of Geophysical Research*, **108**, 3223, 10.1029/2001JC00173.

Ono, N. (1967) Specific heat and heat of fusion of sea ice. In: *Physics of Snow and Ice Volume 1* (Ed. H. Oura), pp. 599–610. Institute of Low Temperature Science, Sapporo, Japan.

Ono, N. (1968) Thermal properties of sea ice: IV, thermal constants of sea ice (in Japanese). *Low Temperature Science Series A*, **26**, 329–349.

Perovich, D.K. (1990) Theoretical estimates of light reflection and transmission by spatially complex and temporally varying sea ice covers. *Journal of Geophysical Research*, **95**, 9557–9567.

Perovich, D.K. (1998) Optical properties of sea ice. In: *Physics of ice-covered seas Volume 1* (Ed. M. Leppäranta), pp. 195–230. University of Helsinki, Helsinki.

Perovich, D.K. & Gow, A.J. (1996) A quantitative description of sea ice inclusions. *Journal of Geophysical Research*, **101**, 18,327–18,343.

Perovich, D.K., Grenfell, T.C., Richter-Menge, J.A., Light, B., Tucker III, W.B. & Eicken, H. (2003) Thin and thinner: sea ice mass balance measurements during SHEBA. *Journal of Geophysical Research*, **108**, 8050, 10.1029/2001JC001079.

Perovich, D.K., Light, B., Eicken, H., Jones, K.F., Runciman, K. & Nghiem, S.V. (2007) Increasing solar heating of the Arctic Ocean and adjacent seas, 1979–2005: attribution and role in the ice-albedo feedback. *Geophysical Research Letters*, **34**, L19505, 10.11029/12007/GL031480.

Perovich, D.K., Grenfell, T.C., Light, B. et al. (2008) Trans-polar observations of the morphological properties of Arctic sea ice. *Journal of Geophysical Research*, 10.1029/2008JC004949.

Persson, P.O.G., Fairall, C.W., Andreas, E.L., Guest, P.S. & Perovich, D.K. (2002) Measurements near the Atmospheric Surface Flux Group tower at SHEBA: near-surface conditions and surface energy budget. *Journal of Geophysical Research*, **107**, 10.1029/2000JC000705.

Petrich, C., Langhorne, P.J. & Sun, Z.F. (2006) Modelling the interrelationships between permeability, effective porosity and total porosity in sea ice. *Cold Regions Science and Technology*, **44**, 131–144.

Petrich, C., Langhorne, P.J. & Haskell, T.G. (2007) Formation and structure of refrozen cracks in land-fast first-year sea ice. *Journal of Geophysical Research*, **112**, C04006, 10.1029/2006JC003466.

Petrich, C., Langhorne, P.J. & Eicken, H. (2009) Salinity development in growing sea ice.

Pringle, D.J., Eicken, H., Trodahl, H.J. & Backstrom, L.G.E. (2007) Thermal conductivity of landfast Antarctic and Arctic sea ice. *Journal of Geophysical Research*, **112**, C04017, 10.1029/2006JC003641.

Pringle, D.J., Miner, J.E., Eicken, H. & Golden, K.M. (2009) Pore-space percolation in sea ice single crystals.

Powell, D.C., Markus, T. & Stössel, A. (2005) Effects of snow depth forcing on Southern Ocean sea ice simulations. *Journal of Geophysical Research*, **110**, C06001, 10.1029/2003JC002212.

Reimnitz, E., Kempema, E.W., Weber, W.S., Clayton, J.R. & Payne, J.R. (1990) Suspended-matter scavenging by rising frazil ice. *CRREL Monograph*, **90-1**, 97–100.

Richter-Menge, J.A. (1992) Compressive strength of frazil sea ice. *Proceeding of the IAHR Symposium on Ice, Banff, Alberta*, **2**, 1065–1074.

Rothrock, D.A., Yu, Y. & Maykut, G.A. (1999) Thinning of the Arctic sea ice cover. *Geophysical Research Letters*, **26**, 3469–3472.

Schanda, E. (1986) *Physical Fundamentals of Remote Sensing*. Springer-Verlag, Berlin.

Schulson, E.M. (1999) The structure and mechanical behavior of ice. *JOM*, **51**, 21–27.

Schwerdtfeger, P. (1963) The thermal properties of sea ice. *Journal of Glaciology*, **4**, 789–807.

Smedsrud, L.H. (2001) Frazil-ice entrainment of sediment: large-tank laboratory experiments. *Journal of Glaciology*, **47**, 461–471.

Smith, R.E.H., Harrison, W.G., Harris, L.R. & Herman, A.W. (1990) Vertical fine structure of particulate matter and nutrients in sea ice of the high Arctic. *Canadian Journal of Fisheries and Aquatic Science*, **47**, 1348–1355.

Spencer, R.J., Møller, N. & Weare, J.H. (1990) The prediction of mineral solubilities in natural waters: a chemical equilibrium model for the Na–K–Ca–Mg–Cl–SO4–H2O system at temperatures below 25°C. *Geochimica et Cosmochimica Acta*, **54**, 575–590.

Steele, M. & Flato, G.M. (2000) Sea ice growth, melt, and modeling: a survey. In: *The Freshwater Budget of the Arctic Ocean* (Ed. E.L. Lewis), pp. 549–587. Kluwer Academic Publishers, Dordrecht.

Stogryn, A. (1987) An analysis of the tensor dielectric constant of sea ice at microwave frequencies. *IEEE Transactions on Geoscience & Remote Sensing*, **GE-25**, 147–158.

Stroeve, J., Holland, M.M., Meier, W., Scambos, T. & Serreze, M. (2007) Arctic sea ice decline: faster than forecast. *Geophysical Research Letters*, **34**, L09501, 09510.01029/02007GL029703.

Sturm, M., Perovich, D.K. & Holmgren, J. (2002) Thermal conductivity and heat transfer through the snow on the ice of the Beaufort Sea. *Journal of Geophysical Research*, **107**, 10.1029/2000JC000409.

Timco, G.W. & Frederking, R.M.W. (1996) A review of sea ice density. *Cold Regions Science and Technology*, **24**, 1–6.

Tyshko, K.P., Fedotov, V.I. & Cherepanov, I.V. (1997) Spatio-temporal variability of the Arctic seas' ice cover structure. In: *Sea ice* (Eds. I.E. Frolov & V.P. Gavrilo), pp. 191–213. Gidrometeoizdat, St. Petersburg.

UNESCO (1978) *Eighth Report of the Joint Panel on Oceanographic Tables and Standards UNESCO Technical Papers in Marine Science 28*. UNESCO, Paris.

Untersteiner, N. (1961) On the mass and het budget of Arctic sea ice. *Archive für Meteorologie Geophysik Bioklimatologie Series A*, **12**, 151–182.

Untersteiner, N. (1968) Natural desalination and equilibrium salinity profile of perennial sea ice. *Journal of Geophysical Research*, **73**, 1251–1257.

Wakatsuchi, M. (1983) Brine exclusion process from growing sea ice. *Low Temperature Science*, **A33**, 29–65.

Wadhams, P., Lange, M.A. & Ackley, S.F. (1987) The ice thickness distribution across the Atlantic sector of the Antarctic ocean in midwinter. *Journal of Geophysical Research*, **92**, 14535–14552.

Wakatsuchi, M. & Ono, N. (1983) Measurements of salinity and volume of brine excluded from growing sea ice. *Journal of Geophysical Research*, **88**, 2943–2951.

Weeks, W.F. & Lee, O.S. (1962) The salinity distribution in young sea ice. *Arctic*, **15**, 92–108.

Weeks, W.F. & Ackley, S.F. (1986) The growth, structure and properties of sea ice. In: *The Geophysics of Sea Ice* (Ed. N. Untersteiner), pp. 9–164. Plenum Press, New York (NATO ASI B146).

Weeks, W.F. & Wettlaufer, J.S. (1996) Crystal orientations in floating ice sheets. In: *The Johannes Weertman Symposium* (Eds. R.J. Arsenault, D. Cole, T. Gross, G. Kostorz, P.K. Liaw, S. Parameswaran & H. Sizek), pp. 337–350. The Minerals, Metals and Materials Society, Warrendale, Pennsylvania.

Wettlaufer, J. (1998) Introduction to crystallization phenomena in natural and artificial sea ice. In: *Physics of Ice-Covered Seas, Volume 1* (Ed. M. Leppäranta), pp. 105–194. University of Helsinki Press, Helsinki.

Wettlaufer, J.S., Worster, M.G. & Huppert, H.E. (1997) Natural convection during solidification of an alloy from above with application to the evolution of sea ice. *Journal of Fluid Mechanics*, **344**, 291–316.

Worby, A.P., Massom, R.A., Allison, I., Lytle, V.I. & Heil, P. (1998) East Antarctic sea ice: a review of its structure, properties and drift. In: *Antarctic Sea Ice Physical Processes, Interactions and Variability* (Ed. M.O. Jeffries). American Geophysical Union, Washington. *Antarctic Research Series*, **74**, 41–67.

Worster, M.G. & Wettlaufer, J.S. (1997) Natural convection, solute trapping, and channel formation during solidification of saltwater. *Journal of Physical Chemistry B*, **101**, 6132–6136.

Yen, Y.C., Cheng, K.C. & Fukusako, S. (1991) Review of intrinsic thermophysical properties of snow, ice, sea ice, and frost. In: *Proceedings 3rd International Symposium on Cold Regions Heat Transfer, Fairbanks, AK, June 11–14, 1991* (Ed. J.P. Zarling & S.L. Faussett), pp. 187–218. University of Alaska, Fairbanks.

Zotikov, I.A., Zagorodnov, V.S. & Raikovsky, J.V. (1980) Core drilling through the Ross Ice Shelf (Antarctica) confirmed basal freezing. *Science*, **207**, 1463–1465.

This page intentionally left blank

3 Sea Ice and Oceanography

Mark A. Brandon, Finlo R. Cottier and Frank Nilsen

3.1 Introduction

The study of sea ice and oceanography can sometimes be regarded as peripheral to the study of the world's oceans. But it is now clear that when sea ice is formed in the polar regions, water masses are transformed locally by relatively small-scale processes and these make a significant contribution to the entire global ocean circulation (Schmitz, 1995). At the simplest level, the generation and decay of sea ice moves buoyancy. When ice is formed, brine is released causing the density of the surface waters to increase; the upper water column becomes unstable, causing convection and mixing with a resulting modification of the water properties. When the ice melts, the addition of freshwater restratifies and stabilizes the water column, inhibiting vertical mixing. These two processes, ice formation and ice melt, combined with the regional bathymetry, contribute to the driving of the global thermohaline circulation.

It is important to note that the processes of formation and melt, whilst being dominated by seasonal forcing, can occur at any time of the year. For example, at the edge of the Antarctic continent, katabatic winds can cause small-scale ice generation even in summer. Similarly, at the edge of the winter extreme of sea ice extent, the ice is decaying and melting. Sea ice can also provide mechanical stirring of the upper water column because of the rough under-ice topography. Turbulence is generated as the ice and ocean move relative to each other (icebergs provide the same effect only on a larger scale) which can have an important influence on polar waters with marginal stability.

Despite their remoteness the study of the physics and biology of polar oceans has extended back to almost the foundation of the subject of oceanography. It was, for example, Fridtjof Nansen on the Arctic drift of the *Fram* (1893–1896) who first noted that the sea ice does not drift in the direction of the wind, but is in fact deflected to the right in the northern hemisphere because of the rotation of the Earth (Nansen, 1897). This was developed by the Swedish mathematician Vagn Ekman into the formulation of the Ekman Spiral (Ekman, 1905) which is fundamental to physical oceanography. Similar important work was accomplished in the early Antarctic expeditions such as the biological sampling on the Scottish National Antarctic Expedition (1902–04) (Scottish National Antarctic Expedition, 1907), and Edward Nelson's tidal measurements on Scott's last Antarctic expedition (Huxley, 1913). As the scope of environmental research has increased over the last few decades, a look at the contents page of virtually any physical oceanographic journal will confirm the current importance of polar work.

In the open ocean, the most challenging conditions which prevent working aboard research ships are generally caused by storms and swell. In sea ice, ship-based work has additional practical considerations and constraints. However, once within the ice cover, certain aspects of ship activity can be easier than in the open ocean because the sea ice rapidly damps out short-period waves. The biggest difficulties are then caused by the drift of sea ice. Whilst a modern research ship can generally clear an area of open water for sampling with ease, ice convergence caused by strong winds in a distant region can cause problems. The second factor is that the presence of thick sea ice and icebergs can prevent sampling in important regions such as within boundary currents. The final and perhaps most obvious point is that in general, because most sea ice-covered areas are undersampled and because satellite-derived bathymetry is not available outside ±72° latitude (Smith & Sandwell, 1997), the location of the most useful sampling regions are not known *a priori*. All of these factors lead to circumstances where sampling strategies are liable to rapid and frequent change.

Whilst it is can be straightforward for a ship to maintain an open water area, doing so can often mean running the ship's thrusters. This of course vigorously mixes the surface waters and precludes studies of properties of the ice–ocean boundary layer. For this reason, minimizing such disturbance has always been important, with the most obvious method being to move away from a ship and to use the ice itself as the sampling platform. Pioneered by Nansen from the *Fram* during its drift (Nansen, 1897), sampling across the Arctic Basin on drifting sea ice became increasingly important in latter half of the 20th century. The first such drift was by four Russians who were deployed by aeroplane at the North Pole and then drifted in the pack from May 1937 to February 1938. They recorded 38 hydrographic stations in a drift of over 1300 miles through Fram Strait and as far south as Scoresby Sund before being recovered by ship (Papanin, 1940). Oceanographic data collected using these techniques increased as Soviet drifting stations continued throughout the 20th century and they were joined by American occupations of the drifting ice shelf T3, or 'Fletchers Island' (Crary et al., 1952; Koenig et al., 1952). Indeed, strategic considerations have meant that since the late 1950s there has been continued nuclear submarine presence in the Arctic. But it is only in the last decades that data from – and even the direct use of – nuclear submarines as hydrographic platforms have become available (Morison et al., 1998). In more recent times, drifting ice camps have become focussed on particular processes such as the Lead Experiment (LEADEX) which investigated the oceanic and atmospheric boundary layer in early 1992 (The LEADEX Group, 1993), and ships such as the *Des Grosielliers* have been again, like *Fram* in the 19th century, deliberately frozen into the pack to drift and perform experiments such as the Surface Heat Budget of the Arctic Ice Station experiment (SHEBA) (Macdonald et al., 2002). Most recently, the schooner *Tara* was frozen into the Arctic north of the Laptev Sea in September 2006 and crossed the Arctic Ocean conducting measurements of the ice, ocean and atmospheric conditions for the DAMOCLES project (Developing Arctic Modeling and Observing Capabilities for Long-term Environmental Studies) before leaving the ice via Fram Strait in July 2008 (Gascard et al., 2008).

In contrast, the Antarctic has been relatively undersampled and large areas are still devoid of any data. The only intentional drifting ice station comparable to the Arctic efforts was Ice Station Weddell in 1992 (ISW-1) that followed a track similar to that of Shackleton's doomed *Endurance* in 1915. This experiment provided, as we shall see below, hugely important hydrographic data in the perennially ice-covered region of the Weddell Sea (Muench & Gordon, 1995). More recently, there have been drifting ship experiments such as the Antarctic

Zone Flux Experiment in the Weddell Sea (McPhee et al., 1996) and the ISPOL drift of the German ship *Polarstern* in the Weddell Sea in 2006 (Hellmer et al., 2008).

There have been many excellent works on polar oceanography (Smith, 1990a,b; Smith & Grebmeier, 1995), and in this chapter, we stress the importance of the coupled nature of sea ice and oceanography. This will not be an exhaustive treatise covering all ice–ocean inter-actions, but instead will focus on selected examples from both polar regions that illustrate how sea ice and oceanography are each able to modify and influence the properties and processes of the other. The chapter is structured as follows: Section 3.2 will present a sim-plified description of the general ocean circulation of the Arctic and Antarctic and highlight areas that are important for the rest of the chapter. Section 3.3 will concentrate on the Arctic halocline and Section 3.4 will focus on polynyas and the process of making very dense water in the shallow shelf seas in the polar regions. In Section 3.5, we will discuss how the dense waters formed in Section 3.4 cascade down the continental slope to form deep and interme-diate waters of the global oceans. In Section 3.6, we discuss the use of isotopes as tracers in polar regions, and finally in Section 3.7, we will provide a brief review of future technologies that may significantly increase the volume and geographic coverage of data available for polar oceanography.

3.2 General oceanographic description

The two polar regions differ in their regional geography. The most obvious difference is that the Arctic Ocean is a landlocked sea (Fig. 3.1a) and at first glance the region appears relatively isolated from the rest of the planet. There are three topographic gaps which con-nect the Arctic to the global ocean, by far the deepest and most significant being Fram Strait between the archipelago of Svalbard and Greenland where water depths are over 3000 m. The two smaller but still important gaps are the Bering Strait between North America and Asia, and the numerous channels between the Arctic Ocean and Baffin Bay through the Canadian archipelago. There are also three distinct deep basins (the Canada Basin, the Amundsen Basin and the Nansen Basin) separated by active mid-ocean ridges (Sohn et al., 2008). North of Greenland and North America, there is no significant continental shelf and water depths rapidly reach over 2000 m. On the eastern hemisphere, there is a large shallow region of generally less than 500 m depth which was covered with glacial ice sheets during the great ice ages. The proximity of this shallow region to the large Eurasian land mass is important for, as we shall see below, the formation the Arctic halocline and polynyas.

The seasonal sea ice cover in the Arctic varies from ~15.5 million km^2 in the northern winter decreasing to ~6 million km^2 in the summer. Although in the northern hemisphere the continuing retreat of the Arctic summer sea ice extent has become an annual news event (Serreze et al., 2007; Stroeve et al., 2007). This means that every year approximately 9.5 million km^2 of ocean is seasonally ice covered. The general circulation of the Arctic Ocean consists of a cyclonic gyre over the Canada Basin called the Beaufort Gyre, a strong flow of polar surface waters out of the basin on the west of Fram Strait from the Transpolar Drift and a strong flow of warm salty Atlantic Waters (AWs) into the Arctic Basin on the east of Fram Strait and across the shallow Barents Sea (Carmack, 1990). The distribution of these water masses in the Arctic basins is seen partially in the sea ice distribution of Fig. 3.1a: the heat supplied from the AWs in the Barents Sea means that the winter ice edge is much further
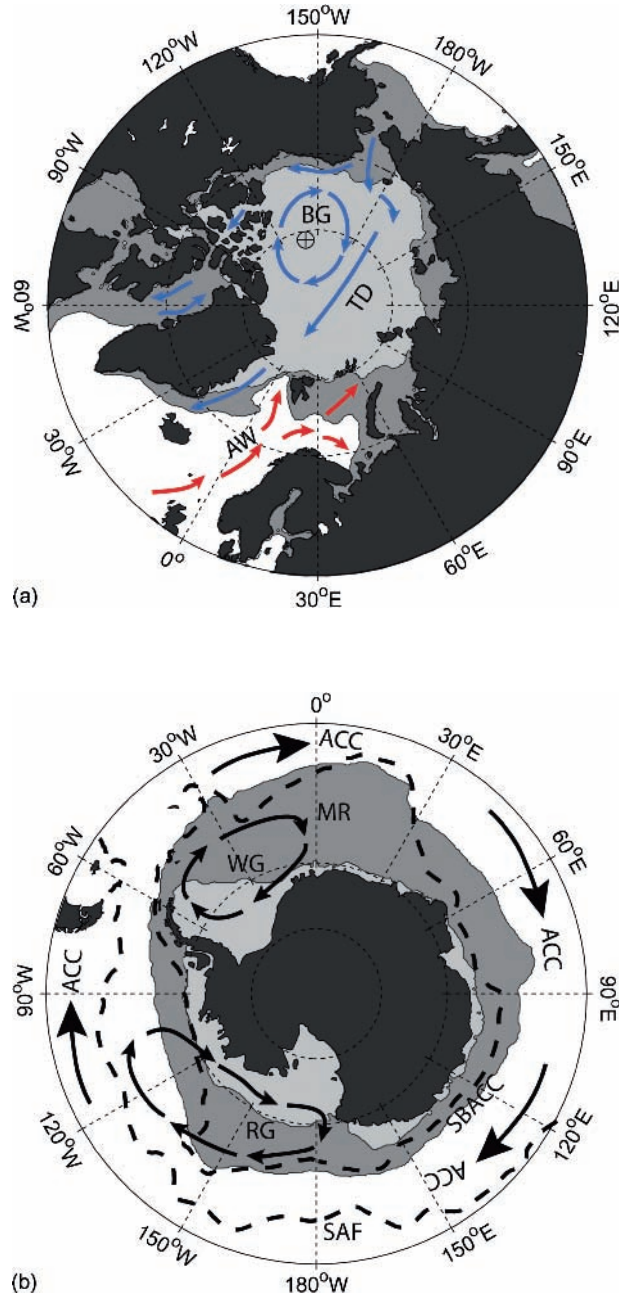
Fig. 3.1 (**a**) The Arctic region. The location for the CTD station shown in Fig. 3.2 is shown as the circle with a cross in it. Blue arrows represent cold currents and red arrows the inflowing Atlantic Water. BG – the Beaufort Gyre, TD – the Transpolar Drift, AW- Atlantic Water. (**b**) The Antarctic region. The location of the two ocean fronts that delineate the Antarctic Circumpolar Current (ACC) are labelled SAF for the sub-Antarctic Front and the SBACC for the Southern Boundary of the ACC. Arrows represent the schematic circulation direction, WG – the Weddell Gyre, RG – the Ross Gyre and MR the location of Maud Rise. In both figures the darker grey shows the mean maximum winter ice extent from 1979-2007 (February in the Arctic and September in the Antarctic), and the lighter grey the minimum summer ice extent (September in the Arctic and February in the Antarctic), with the data in both cases being from the SMMI satellite sensors.

north than in the western Atlantic Ocean, and the perennial ice cover is limited to the region north of Greenland and North America.

In complete contrast, the Antarctic consists of a central land mass surrounded by deep oceans (Fig. 3.1b). North of the continent, the Antarctic Circumpolar Current (ACC) circumnavigates in a clockwise direction and is delineated by strong and continuous ocean fronts (Orsi et al., 1995), the most pronounced being the Sub-Antarctic Front (SAF) and Polar Front which mark the northern boundary of the ACC. Further south, as surface gradients of temperature and salinity become smaller, the ACC is delineated by the Southern Boundary to the ACC (SBACC) (Orsi et al., 1995). South of the ACC, there is evidence of an anticlockwise coastal current (Tchernia and Jeannin, 1980; Heywood et al., 1998) but there is currently – generally because of sea ice preventing sampling – insufficient data to say whether this is continuous around the continent. There are two large cyclonic gyres south of the ACC in the Weddell and Ross seas, which are, as we shall note below, globally important for the production of bottom waters (Orsi et al., 1999). The annual variation in sea ice extent in Antarctica is much greater than in the Arctic. In February, there is a minimum in sea ice extent of typically $\sim$3 million km² with ice restricted to coastal regions with larger areas in the Weddell Sea and the south east Pacific sector of the Antarctic. At the height of the austral winter, ice extent increases to almost 19 million km² – a total range of more than 1.5 times as great as the Arctic seasonal change. Unlike the Arctic, there has not been a relentless downward trend of summer sea ice extent in the Antarctic, although there have been regional changes in the distribution of sea ice extent, particularly to the west of the Antarctic Peninsula. Indeed, there is a very slight positive trend in both sea ice extent and area (Comiso & Nishio, 2008). Having briefly introduced both polar regions and an overview of their oceanographic and sea ice characteristics, we now consider one particular oceanographic feature that demonstrates the close coupling between ice and ocean – the Arctic halocline.

3.3 The Arctic halocline

As noted above, the growth and retention of Arctic sea ice is intimately linked to the oceanographic structures beneath it. A vertical profile of salinity from the central Arctic Ocean shows a strong halocline located at depths between 50 and 200 m (Fig. 3.2a), and it is this that plays a vital role in maintaining an ice cover. This salinity-stratified layer of water marks the transition between two water masses: the cold, fresh Polar Surface Water (PSW) and the warm, saline AW that is present throughout much of the Arctic Basin. It was Nansen (1897) who first realized that beneath the halocline 'this warmer and more strongly saline water must clearly originate from the warmer current of the Atlantic Ocean'. Whilst there is a rapid increase in salinity with depth within the halocline, the temperature remains almost isothermal, and usually very close to the freezing point. This gives rise to its widely accepted name of the Cold Halocline Layer (CHL).

At low temperatures, the density of sea water is determined primarily by salinity – as seen by the almost vertical orientation of the potential density lines in the potential temperature salinity (TS) plot of Fig. 3.2b. Hence, the steep halocline defines a strong density gradient (or pycnocline) between the PSW and the AW. Consequently, one of the critical roles that the halocline plays in Arctic oceanography is to inhibit the upward mixing of the warm AW
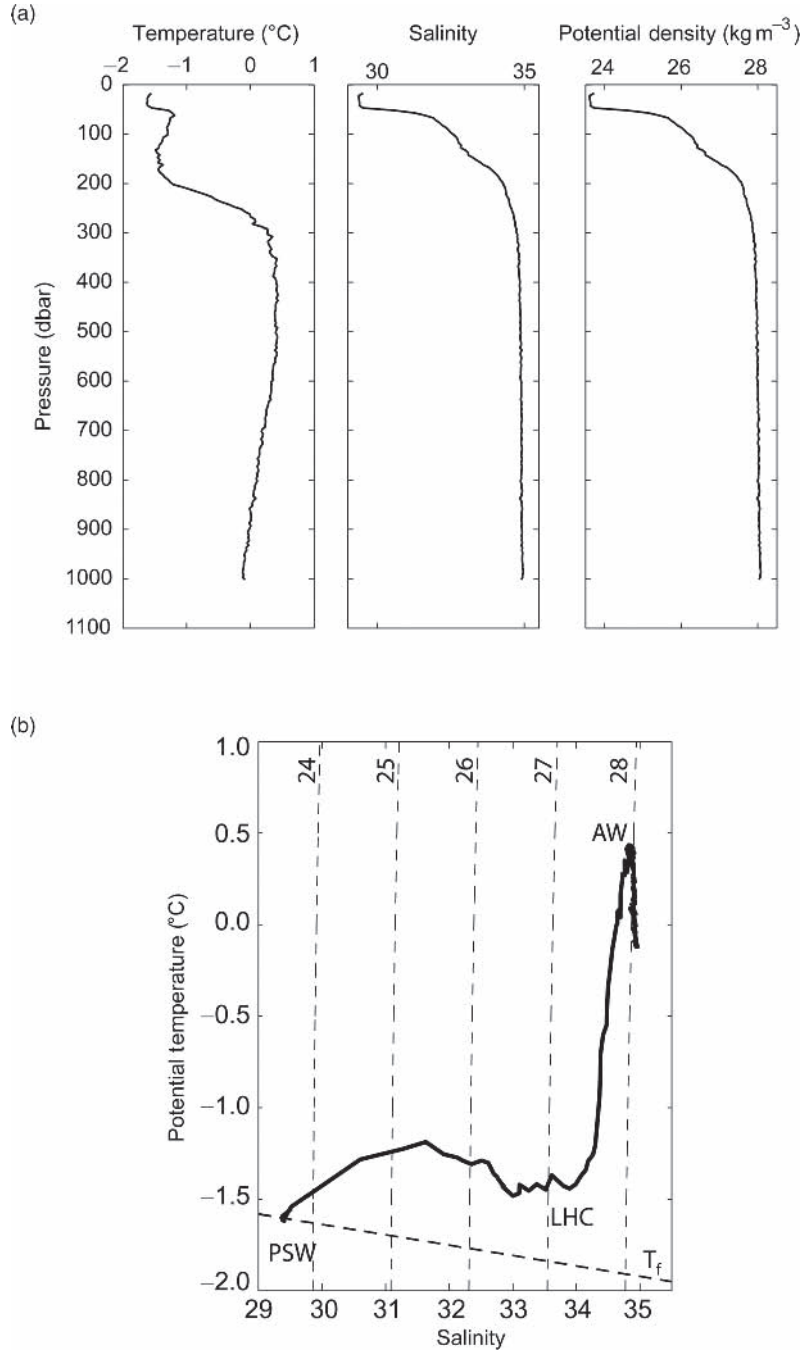
Fig. 3.2 A CTD station showing the upper 1000 m of the water column from the central Arctic Ocean (81° 10'N, 138° 52W marked on Figure 3.1a) recorded by the submarine USS Pogy in September 1996). (a) profiles of the temperature, salinity and potential density against pressure. (b) a potential temperature – salinity plot of the same data in 3.2a. The surface freezing line is shown as a dashed line labelled T_f. The near vertical dashed lines are lines of potential density referenced to the surface in units of kg m^{-3}.

into the PSW by virtue of the steep density gradient. This reduces the ocean heat flux from the AW to the surface, promotes winter sea ice growth and ultimately helps maintain the sea ice cover. In those regions of the Arctic where a CHL is not well developed, e.g. around the Svalbard margin, enhanced ocean heat flux in winter to the surface can be sufficient to prevent the formation of sea ice (Cottier et al., 2007) and can be appreciated by the area of open water to the west of Svalbard during winter shown in Fig. 3.1a. Above the cold halocline, the PSW forms an upper mixed layer with some of the freshest waters in the world ocean ($S < 31$) which derive from river outflow, the relatively fresh Bering Sea inflow, excess precipitation and freshwater addition through sea ice melt. Techniques to differentiate the contribution of each source of freshwater are discussed below in Section 3.6.

Temperatures in the PSW are generally at or close to the surface freezing point and these fresh cold source waters are mixed below the sea ice and become trapped above the strong density gradient at the CHL. The properties of the PSW layer are then maintained via the annual melt-freeze cycle. Sea ice growth in winter is limited because of the insulating capacity of the ice cover. Hence, the volume of brine that is released is also limited, being insufficient to break down the CHL through convection driven by ice growth; so ultimately, the heat from the AW layer below is not released into the upper waters.

An obvious question to ask is: What is the origin of the CHL? Figure 3.2b shows a TS plot of the Arctic waters where the PSW and AW layers are clearly identifiable, one as a cold fresh layer (in this case with potential temperature $\sim-1.5°C$, salinity ~29.5) and one as a relatively warm salty layer (potential temperature $\sim0.4°C$, salinity ~34.9). But between these two water masses is a sharp kink in the TS curve. If the CHL was simply a product of mixing between the PSW and the AW, then there would be a straight mixing line between the two water masses (Kikuchi et al., 2004). Clearly, as Fig. 3.2b shows, this is not the case and we must look for an alternative explanation. The location of this kink in the TS curve defines the Lower Halocline Water (LHW), which is the most saline water within the CHL at or close to the surface freezing point. Identifying the origin of the CHL is tied to the formation mechanism of the LHW and has given rise to a number of explanations. Here, we briefly review some of these explanations and the role that sea ice plays.

Advection mechanism

One of the earliest mechanisms proposed identified the marginal shelf seas surrounding the Amundsen and Nansen basins (collectively referred to as the 'Eurasian Basin') as the source of the halocline waters (Aagaard et al., 1981). Winter ice formation on the shelves, particularly in areas of sea ice divergence, would lead to high rates of brine production and, as we shall describe in more detail below, increase the shelf water salinity. These cold, saline waters would then advect laterally from the shelf break entering the central Arctic Basin below the PSW to form LHW. By implication, any removal of ice from the shelves through wind stress will enhance the rates of brine release. Latterly, there have been numerous studies that have tried to interpret the contribution of brine-enriched shelf waters to the CHL (Cavalieri & Martin, 1994; Rudels et al., 1996). However, one problem with this mechanism is that the differing salinity characteristics of the shelf waters compared to those of the LHW in the Eurasian Basin are such that LHW could only form in the Barents Sea. Here, the shelf waters are of high enough salinity through mixing with the more saline AW, to actually intrude at the depth of the LHW (Steele & Boyd, 1998).

Another difficulty, revealed by analysis of the LHW temperature relative to the freezing point, suggests that advective formation is rare at most shelf sites in the Eastern Arctic (Kikuchi et al., 2004). However, nutrients can be an important indicator for the source of CHL waters and in some regions enhanced levels of nutrients suggest water from the adjacent shelves is carrying resuspended biogenic material (Jones & Anderson, 1986). An example being the high silicate found in the upper halocline in the Canada Basin (Mathis et al., 2007). However, this most likely only occurs in coastal polynya regions and in years of intense ice production.

Convection mechanism

A more generally workable mechanism for the formation of LHW invokes winter convection processes (Rudels et al., 1996). Figure 3.3 illustrates schematically the steps in this mechanism and the effect that each step has in the TS distribution. The first stage involves the inflow of warm saline AW into the Nansen Basin through the Fram Strait and Barents Sea. This is called the upstream condition in Fig. 3.3a because such TS profiles would be found upstream of the main modification processes. When the northward-flowing AW encounters sea ice at Fram Strait and in the Barents Sea, melting occurs and a surface 'wedge' of fresher water is created that is well-mixed and at near-freezing temperatures. In Fig. 3.3a, the surface layer is termed pre-existing Surface Water (pSW) below which is the remaining warm salty core of AW. At this point in TS space, the curve simply shows a straight line between these two end members (Fig. 3.3a).
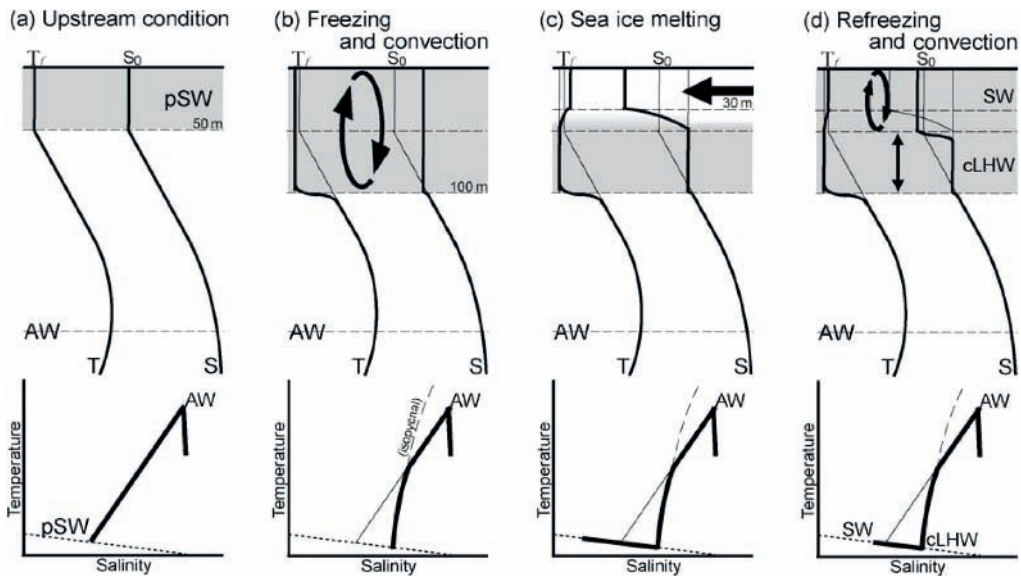
Fig. 3.3 Schematic of the formation process of the cold halocline through convection processes. The upper panel shows typical temperature and salinity profiles from before ice generation processes to the end product. The lower panel shows the θ-S corresponding to the upper panels with the dotted lines indicating the surface freezing point. From Kikuchi (2004). Distribution of Convective Lower Halocine Water in the eastern Arctic ocean. JGR Oceans (109). Reproduced with kind permission from the American Geophysical Union.

Further downstream, perhaps north of the Barents Sea, the second stage involves winter ice formation. Brine release gives rise to an unstable convective situation to form an approximately 100 m deep mixed layer with increased salinity and with temperatures at the surface freezing point. The increase in salinity and departure of the mixed layer from the pSW–AW mixing line is shown in the TS curve (Fig. 3.3b). In the following spring and summer, sea ice melt decreases the salinity at the surface forming a shallow seasonal halocline (Steele & Boyd, 1998). Figure 3.3c shows that this is represented in TS space as an extension of the less dense surface water towards lower salinity along the surface freezing point line. There is further brine release during ice formation in the following winter to produce instabilities and mixing down to the permanent pycnocline as shown in Fig. 3.3d. This cycle of melt and freezing can occur several times and create LHW through convective processes. A schematic of the resulting TS curve shown in the final panel of Fig. 3.3d.

A modification to this mechanism, called the 'advective–convective' mechanism, was described by Steele and Boyd (1998). They proposed a later addition of low salinity shelf water into the surface layer to cap the LHW formed by convection in the second stage (Fig. 3.3b) and create surface freezing temperatures in the winter mixed layer. Such a mechanism is likely to occur at many Arctic shelf locations, particularly north of the Kara and Laptev Seas where low salinity shelf waters are formed by outflow from the major rivers of the Lena, Yenisey and Ob. Whilst this addition of shelf waters is not essential to the formation of LHW, it is a process by which the CHL can be strengthened by increasing the vertical salinity gradient.

In the description of these two processes (advection and convection), a conflict arises (Steele & Boyd, 1998): Are the shelf waters salty (required by advection) or fresh (required by convection)? The possibility that the shelf waters could exhibit a seasonal cycle of being salty in winter and fresh in summer is ruled out because the only shelf in the eastern Arctic that could be regarded as salty (with $S > 33$) is the Barents Sea. The Siberian shelves eastwards of Kara Sea are all relatively fresh even in winter (Aagaard et al., 1981). Overall, the range of salinities of shelf waters means that the formation and subsequent modification of the CHL varies regionally within the Arctic and the halocline is clearly not a static vertical thermohaline transition.

Some indication of the variation in the process leading to formation of LHW can be found by examining conductivity-temperature-depth (CTD) data from sections across the Arctic shelves and into the central basins. Data from such a section in the Nansen Basin is shown in the TS plot in Fig. 3.4 (Woodgate et al., 2001). In this example, the origin of the LHW is determined from the thermal signature. In the convective process, the LHW is near to its freezing point as the convection is driven by the brine released through freezing. In advection, the temperature of the halocline need not necessarily be at the surface freezing point. Offshore, the TS data show LHW close to surface freezing point, which is indicative of formation through convection. Inshore, the TS data show that the LHW is warmer and saltier, which is indicative of a shelf origin and thus an advective source. In this example, shelf processes maintain the CHL within the boundary current, whilst in deeper water convection is predominant.

The changes that have occurred in the Arctic in relation to the sea ice cover and the underlying oceanography have been well documented (Polyakov et al., 2005; Serreze & Francis, 2006; Drobot et al., 2008; Walsh, 2008). One example is the variation in the extent of the CHL across the Arctic, starting first with its decline and then the subsequent recovery. Whilst
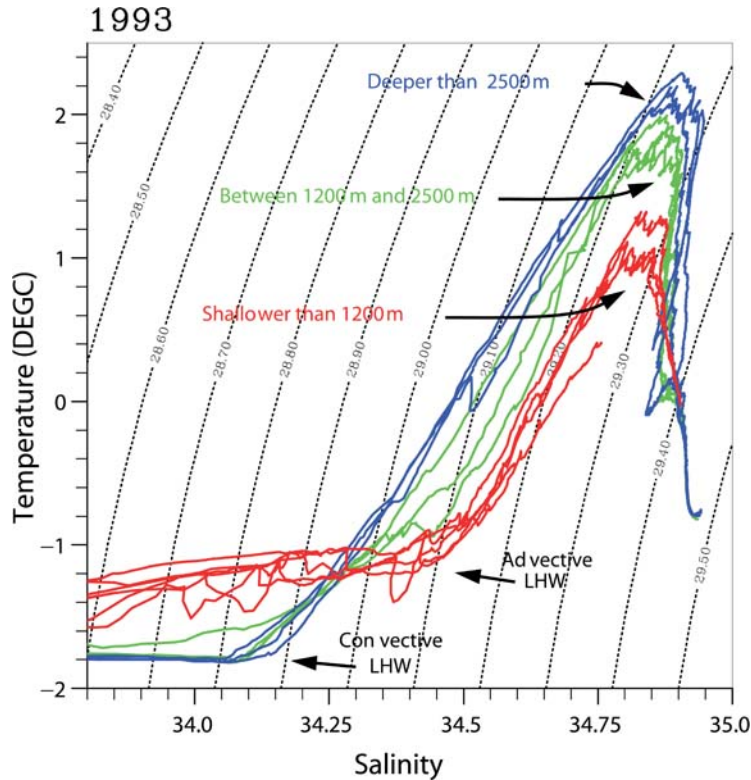
Fig. 3.4 Curves of *in situ* temperature versus salinity for a CTD section running north from the Siberian shelf into the Eurasian Basin at 118°E recorded in 1993. Red profiles are the six stations closest to the continental shelf (water depth <1200m), blue curves are for deepest stations (water depth was >2500m). Green profiles are for three stations at intermediate depths showing characteristics of both deep and shallow stations. Dotted lines are isopycnals referenced to 290 db. Reprinted from Deep Sea Research. Woodgate et al. (2001) The Arctic Ocean Boundary Current along the Eurasian Slope and the adjacent Lomosov Ridge. With permission from Elsevier.

it has long been regarded as a robust feature in Arctic Oceanography, there has been extensive discussion of the CHL weakening and the implications for sea ice melt as the heat stored within the AW becomes mixed into the surface waters (Jones et al., 2008). The 'strength' of the halocline can be quantified by the salinity at its upper boundary; a high salinity in this location would represent a weak gradient or poorly developed halocline, a low salinity the reverse. By this measure, the CHL in the early 1990s was observed to weaken or retreat from the Eurasian Basin, across the Lomonosov Ridge and into the Makarov Basin (a small basin between the Nansen and Canada basins). Steele and Boyd (1998) proposed that the cause of this retreat was a change in the 'injection' point of fresher shelf water, being located further eastwards. This change in oceanographic conditions may have been linked to the atmospheric circulation which has also been shown to vary during the same time period.

The pattern of large-scale atmospheric circulation is represented by the Arctic Oscillation (AO) index, which is indicative of the strength of the Polar vortex in the northern hemisphere. An increasing AO index is associated with a more cyclonic circulation over the Arctic, whilst a low AO index represents an anticyclonic state. During the early 1990s and the period when the CHL was observed to weaken or retreat, the AO index increased and then subsequently

decreased after the mid-1990s. The more cyclonic atmospheric circulation in the early to mid-1990s would tend to deflect the sea ice and the shelf waters to the east. Consequently, the 'injection point' of the fresh shelf waters from the Kara and Laptev would also shift eastwards from the Amundsen Basin and into the Makarov Basin (Johnson & Polyakov, 2001). By the mid-1990s, the transport of low salinity shelf water into the Eurasian Basin had effectively shut down. This was followed in the latter part of the decade by a partial recovery as the CHL strengthened in some areas (Boyd et al., 2002). Subsequently, Morison et al. (2006) have shown that in the central Arctic, the conditions have returned to the climatological state before the change of the 1990s and that the weakening of the CHL was partially correlated with the AO.

As already noted, the CHL is important in isolating the underlying warm AW from the surface waters and sea ice, and in fact one definition for the presence of a CHL is that the winter oceanic heat flux is zero (Steele & Boyd, 1998). Clearly, any erosion or weakening of the CHL will increase the potential for enhanced mixing of warm AW into the surface layer. The result will be increased ocean heat flux and a significant impact on the sea ice cover: both the thickness of winter growth and the total period for growth will be reduced. Steele and Boyd (1998) used a simple one-dimensional ocean model to quantify the potential impact on winter ice formation under conditions of a weakened CHL by using temperature and salinity profiles derived from field data and a surface mixing term. Applying a thermohaline structure representative of a weak CHL, the wintertime ocean heat flux to the underside of the sea ice increased from a presumed winter value of 0 W m^{-2} to 2 W m^{-2}. To put this increase in context, the average heat flux generated during the short Arctic summer months can be up to 5 W m^{-2}. Therefore, an enhanced winter heat flux could account for up to an additional 40% of the annual average ocean heat flux. This addition to the annual ocean heat flux term could switch the sea ice growth–melt condition from one of net freezing to one of net melting in certain regions.

The effect of enhanced winter ocean heat fluxes on ice thickness can be estimated by equating the ocean heat flux ΔF_w to a decrease in the freezing rate Δh (Steele & Boyd, 1998). So, $\Delta h = -\Delta F_w / \rho_i L_i$, where $\rho_i = 910$ kg m^{-3} is the sea ice density and $L_i = 3 \times 10^5$ J kg^{-1} is the latent heat of fusion for sea ice. Applying different values of ΔF_w, one can estimate the potential reductions in ice growth. For example, ΔF_w values of 0.5, 1.0 and 3.0 W m^{-2} yield reductions in the ice-growth rate of 6, 12 and 35 cm year^{-1}. This represents a significant proportion of the net winter ice growth, which is typically in the range 30–90 cm year^{-1}. There would also be a substantial impact on the equilibrium ice thickness of multiyear ice, and Maykut and Untersteiner (1971) showed in a one-dimensional model that increasing the ocean heat flux by 1.5 W m^{-2} reduced the equilibrium thickness from 3 to 2 m. Whilst this may seem at first extreme, Giles et al. (2008) have reported rapid ice thickness changes of 0.5 m, and these are perhaps linked to changes in ocean heat flux.

A comparison of a strong or weak CHL in terms of the changes in heat flux and sea ice growth demonstrates how strong stratification prevents the convecting surface layer from breaking through to the AW layer (Björk et al., 2002). With a weakened halocline, the convection creates a much deeper winter mixed layer of 120 m compared to just 40 m for a strong CHL. This deeper layer would penetrate into the AW and produce a larger oceanic heat flux during winter and early spring, peaking at 9 W m^{-2}. Initial ice thickness turns out to be an important parameter in determining the impact of enhanced ocean heat flux on annual ice growth. Under conditions of a weakened CHL and initial ice thicknesses of 3.0,

2.0 and 1.0 m, the annual ice growth with increased heat fluxes would be reduced by 0.25, 0.5 and 0.84 m respectively. Clearly, this gives the potential for a positive feedback with a reduced initial ice thickness, leading to a rapid decrease in sea ice thickness. However, the problem is complex and requires a full dynamic–thermodynamic model in which there are other ice–ocean feedback mechanisms at play. In order to understand the longer-term effect of the CHL on sea ice growth, we also need to consider ice advection and ice residence time in the Arctic Basin.

The annual sea ice export from the Arctic Ocean into the Barents Sea provides an example of such an ice–ocean feedback mechanism. It is highly variable and at its maximum is approximately 20% of that exported through the Fram Strait (Kwok et al., 2005). An enhanced ice export into the Barents Sea constitutes an increase in freshwater flux such that the Barents Sea shelf waters will cool and freshen as the ice is melted by the branch of warm AW that crosses into it (Fig. 3.1a). As these fresher shelf waters leave the Barents Sea and flow into the Nansen Basin, they will tend to strengthen the CHL by increasing the salinity gradient between the PSW and the AW. As discussed, this then suppresses the ocean heat flux from the AW to the surface, promoting winter sea ice formation. Therefore, melting of sea ice exported from one region of the Arctic can increase ice growth in other regions through the effect of changing the salinity of surface waters (Woodgate et al., 2001).

Such relationships between oceanography and sea ice are well illustrated through observations in the Pacific sector of the Arctic (Shimada et al., 2006). Here, the spatial patterns of sea ice reduction in extent, concentration and thickness have mirrored the distribution of relatively warm Pacific Summer Water, suggesting a causal link. Pacific Summer Water originates in the Bering Sea and it contributes to the upper portion of the halocline in the southern Canada Basin. But the sea ice variability is also closely linked to the large-scale atmospheric circulation indicated by the AO. In the late 1980s, the AO index was increasing which correlated with a reduction in sea ice. However, since the mid-1990s as the AO index has decreased, sea ice concentration in the Pacific sector has continued to reduce at an accelerated rate. Clearly, as Morison et al. (2006) showed, atmospheric variability alone only partially explains these changes in ice cover.

The mechanism proposed by Shimada et al. (2006) combines both the atmospheric driver of the AO and the increased temperature of Pacific Summer Water. Figure 3.5a shows clearly that towards the end of the satellite record, sea ice concentration along the shelf in winter has greatly reduced in the Chukchi and Beaufort Seas when compared with the mean for the whole period. This decline in concentration, associated with an increase in the temperature of Pacific Summer Water, allowed more efficient coupling between the atmosphere and the upper ocean due to a reduction of the internal stress in the ice. The result is shown in Fig. 3.5b – indicating that the sea ice velocity anomaly in winter has increased. This effect was to reverse the flow of Pacific Summer Water which would normally enter the Arctic as a buoyancy-driven current and flow eastwards following the shelf slope. Instead, the anticyclonic circulation of the atmosphere was transferred to the ocean so that the heat within the Pacific Summer Water was delivered into the central Arctic Basin. The enhanced heat content of this water mass in Fig. 3.5c is clear when compared with the Environmental Working Group Arctic Atlas data. The result is shown in Fig. 3.5d, where the extra heat delays the onset of winter ice formation and alters the balance between winter growth and summer melt, leading to further acceleration of ice loss. The positive feedback between the ocean and the atmosphere illustrated in Fig. 3.5 could contribute to a catastrophic change in Arctic sea ice cover.
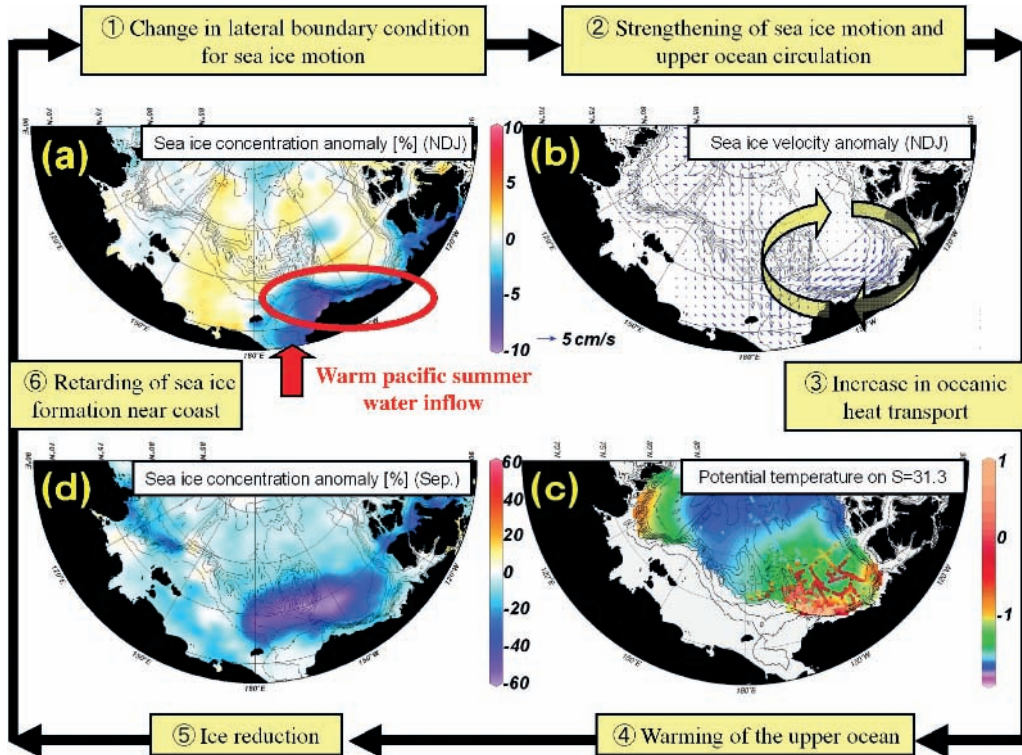
Fig. 3.5 The feedback system in the Canada Basin as proposed by Shimada et al. (2006). (a) Sea ice concentration anomaly for November to January (this is the mean concentration from the period 1997-2003 minus the mean concentration from the period 1979-1997). The concentration is greatly reduced in the shelf regions, (b) sea ice velocity anomaly derived from the same time periods as (a) showing that the anti-cyclonic circulation has increased into the central Arctic Basin. (c) The potential temperature on the isohaline layer S=31.3. The background colour is the climatology from the EWG Arctic Ocean Atlas and dotted circles are from measurements for the period 1998–2004. Clearly the dots on the shelf are up to 2°C warmer than the atlas data. (d) sea ice concentration anomaly for September derived from concentration (1998-2003) minus the concentration (1979-1997) showing that in summer the ice concentration is greatly reduced particularly over the shelf region. From Shimada et al. (2006) Pacific ocean inflow. Geophysical Research Letters 33. Reproduced with kind permission.

The Arctic halocline represents a strong oceanographic control on sea ice formation and decay operating over seasonal and interannual timescales, and there is no similar Antarctic analogue. In contrast, polynyas are a mechanism where sea ice formation has one of the greatest impacts on ocean salinity and they operate at timescales of weeks to months and are present and important in both hemispheres.

3.4 Polynyas

The word polynya originates from a Russian term for 'ice hole' and is defined by the World Meteorological Organisation as 'any non-linear shaped opening enclosed in (sea) ice' (WMO, 1970). They can be persistent and recurring regions with open water and/or a reduced ice concentration in the seasonal sea ice zone in locations where a more consolidated and thicker

ice cover would be climatologically expected (Smith et al., 1990; Martin, 2001). In area, they range in size from tens to tens of thousands of square kilometres and tend to appear recurrently at fixed geographical locations. While the reoccurrence of open water at specific locations suggests that the processes that cause them are regionally robust, the timing, duration and size of the open water area may display large interannual variation ultimately because of the general interannual variability in air–ice–ocean interaction processes (Morales Maqueda et al., 2004). The importance of polynyas for global processes like deep-water formation and gas ventilation is unquestionable, and they respond sensitively to thermodynamic and dynamic forcing by both the ocean and atmosphere. They are also ecologically important polar oases that enable birds and mammals to overwinter in high latitudes and encourage enhanced primary production in spring (Smith & Barber, 2007).

Ocean-to-atmosphere heat fluxes through a polynya are several orders of magnitude greater than those through the surrounding winter pack ice, so they dominate regional heat budgets and can even influence the atmospheric circulation (Gallèe, 1997). Such immense heat fluxes inevitably lead to high salt fluxes with the result that polynyas play a key role in coupling atmospheric heat loss to the overall ice-mass balance. Ultimately, the salt production may lead to deep-water formation (Shcherbina et al., 2003; Skogseth et al., 2005a; Smedsrud, 2005; Williams et al., 2008). For comprehensive reviews on polynyas, Smith et al. (1990) and Morales Maqueda et al. (2004) are good starting points. The recently published book by Smith and Barber (2007) built on these reviews and introduced a practical polynya classification based on the forcing mechanisms that will be partly adopted in this section (Williams et al., 2007).

Traditionally, polynyas have been divided into two classes: sensible-heat polynyas which are thermally driven through convection and latent-heat polynyas which are mechanically driven through ice-divergence. Sensible-heat polynyas are typically formed in regions of upwelling, vigorous vertical mixing or where there is a strong interaction between ocean currents and topographic features. They are called sensible because the heat that is transferred from the ocean to the atmosphere causes the water temperature to decrease and thus a reduction of the sensible heat content of the surface waters. But before heat can be brought to the surface to form a sensible-heat polynya, some form of preconditioning has to occur for free convection to start. For example, the cyclonic circulation around the Maud Rise (Fig. 3.1b) acts as preconditioning for the occasional formation of the Maud Rise Polynya (Martinson et al., 1981; Akitomo et al., 1995; McPhee, 2000). There is generally some ice motion into the polynya area which then melts. Because of this, the size of a sensible-heat polynya is limited to the dimensions of the flux of warm water to the surface and dependent on the rate of melting being greater than the rate of ice advection into it.

Locations where warm water comes to the surface in winter can therefore be regions of low ice concentration, or have thin ice rather than open water. An example of a sensible-heat polynya is the forced-convection polynya called Whaler's Bay Polynya to the north of Spitsbergen which forms close to the ice edge over the shelf break of the Eurasian Basin. This polynya is highly variable (January open water area ~35,000 km²) and its formation is due to heat advected to the ice edge by the West Spitsbergen Current (WSC) around the north coast of the archipelago. Upon encountering the southward-moving pack ice, the eastward-flowing current melts ice to form the Bay through a strong mixing of cold surface water with warm AW transported at a depth of 200–300 m (Aagaard et al., 1987). So tidal forcing and vertical velocity shear supply turbulent energy to overcome the ambient stratification.

Brine rejection by ice formation may cause penetrative free convection and also be part of the vertical heat transport mechanism in the Bay.

Latent-heat polynyas require a divergent sea ice cover. They, therefore, tend to form adjacent to coastlines swept by offshore winds (called coastal or shore polynyas) or downwind or down current of land-fast ice, glacier tongues or grounded icebergs (called flaw polynyas). They are called latent-heat polynyas because the energy that is lost from the ocean stems from the removal of latent heat from the water so that it can freeze. New ice that forms in the open water is carried away by the forcing mechanism so an area of open water is maintained. The temperature of the water within a latent-heat polynya stays at the surface freezing point and there is no change in its sensible-heat content. It is only the ice-divergence through wind stress or ocean currents which maintain the open water. Therefore, the polynya size is governed by the balance of ice formation and export: accumulation of frazil ice tends to make the polynya narrower, whereas offshore wind-forcing of the pack ice tends to make it wider.

As surface waters are already at the freezing point, strong cold winds promote high rates of sea ice formation and at the same time continually advect the new ice away as it forms. This results in substantially higher net ice production rates than would be measured in open regions in the ice cover away from such winds. Indeed, latent-heat polynyas have often been described as the 'ice factories' of the pack ice zone. One recent study in the Antarctic has estimated that polynyas could be responsible for 10% of the entire Southern Ocean sea ice production (Tamura et al., 2008). Consequently, there is a high rate of brine release into the underlying water column. This means that the water column in a mechanically forced latent-heat polynya experiences a very efficient water mass transformation, and they are relatively common in parts of the Arctic and Antarctic (Martin & Cavalieri, 1989; Renfrew et al., 2002). The continental shelf areas of the Arctic constitute more than 50% of the total area of the Arctic Ocean (Jakobsson, 2002), and along the 2×10^5 km coastal margin, there are many coastal (mainly flaw) polynyas on the shallow continental shelves. Brine rejection associated with ice formation at these locations results in brine-enriched shelf waters, making these latent-heat polynyas, as noted above, important contributors to the CHL of the Arctic Ocean (Aagaard et al., 1981; Martin & Cavalieri, 1989; Winsor & Björk, 2000).

Away from the coasts in the central Arctic Ocean, leads and polynyas occupy only ~1% of the total pack ice area; however, the volume of ice they produce is similar to the volume formed below all the Arctic multiyear ice during winter (Morales Maqueda et al., 2004). Thus, case studies for understanding and documentation of the ice production and brine formation are important. Such a case study is in Storfjorden, in Svalbard, which is one of the few areas in the easily accessible Barents Sea where there is a recurrent wind-driven polynya which forms brine-enriched shelf waters (Skogseth et al., 2008). Once formed in the polynya, this dense water can, if the density excess permits, flow down the continental slope into the deep Norwegian Sea and northwards along the eastern slope of Fram Strait towards the Arctic Ocean (Schauer & Fahrbach, 1999; Fer et al., 2003). Although relatively small, it is estimated that this polynya alone supplies between 5% and 20% of the all the newly formed dense water which enters the Arctic Ocean (Skogseth et al., 2005b).

The product of polynyas and ice growth on continental shelves is generally dense, brine-enriched bottom water which, as noted above, will be more dense than water found off-the-shelf. This means that after formation, the brine-enriched water will tend to spill over the shelf edge and descend down the shelf slope to greater depths. This process, a form of

near-bottom gravity current, is referred to as cascading (Shapiro et al., 2003), and such gravity currents occur all over the world and are globally important (Ivanov et al., 2004).

3.5 Cascades

Cascades of dense, brine-enriched water are commonly found in the Arctic and Antarctic (Ivanov et al., 2004). The contribution of dense water from cascades, as discussed above, helps the maintenance of the CHL, and they are a primary means of ventilating intermediate and deep waters in the Arctic (Backhaus et al., 1997); as such, they are an important component in the machinery of the Atlantic Meridional Overturning circulation. In the Antarctic, cascades of dense shelf water have the potential to reach the bottom of the continental slope and to form Antarctic Bottom Water (AABW) (Baines & Condie, 1998). In addition, because of the relatively rapid transport from shallow to deep waters, the cascades represent an important exchange process between the shelves and the deep ocean for both the nutrient fluxes and carbon cycling.

The process of cascading progresses through three distinct stages: the formation of brine-enriched waters; the transport of the dense water down the continental slope as a complex three-dimensional plume and finally the mixing of the cascade with deep waters (Shapiro et al., 2003). Prior to formation of the denser waters, the initial shelf waters must be homogenized or very weakly stratified. Mixing of the water column to achieve this homogenization can be through thermal convection (i.e. cooling is the main driving force) or haline convection (i.e. through ice formation and associated brine release) – the latter process is particularly effective in coastal polynyas maintained by cold offshore winds. In a previously ice-free area, such very large ocean–atmosphere heat fluxes, of the order of 1000 W m^{-2} (Brandon & Wadhams, 1999), will induce thermal convection – the early stages of which will not in general penetrate into the bottom waters. There will be a net upward heat and salt transport as warmer and more saline waters are mixed towards the surface with the result that the warmer surface waters will inhibit ice formation initially. Only when the surface water reaches the surface freezing temperature will ice begin to form, and brine release will then drive deeper convection. As the haline convection penetrates to greater depths, the upward heat flux once again increases. This will tend to inhibit further ice growth, setting up a negative feedback between the ice and the ocean as brine release is moderated and the efficacy of haline convection reduces. Consequently, the existence of a polynya or large amounts of sea ice production in shelf areas does not necessarily mean that dense bottom waters will be formed. Once the water column has been preconditioned and the existing thermal reservoir reduced by these processes, a further period of atmospheric cooling will produce a very different hydrographic outcome.

Further, convective mixing will drive the release of the remaining heat, and as temperatures throughout the water column approach freezing point, new sea ice formation starts with an accompanying release of brine. Salinities increase and convection shifts from thermal to haline buoyancy forcing. The initial thermal reservoir in shallow shelf waters is less than in that found in deeper waters, making it possible to generate a greater density increase. This is because after depletion of the thermal reservoir, salinification will only increase the density of the waters, not drive convection to release more heat.

The periodic and generally localized brine-enriched waters produced by polynyas and shelf convection are denser than the surrounding water so they will collapse, because of

gravity, to form a pool of dense water. This pool will then take some period of time to reach the shelf edge as it flows down the gently sloping relatively flat shelves. There can be a substantial interval between dense water formation and the initiation of a cascade as the dense water spills over the shelf edge.

Once over the shelf break, the density of the plume will undergo continual modification as it cascades down the shelf slope accelerating under gravity and entraining and mixing with the surrounding ambient waters (Baines & Condie, 1998). The plume density changes on its journey, leading to a modification of its descent rate and shape through bed friction. The entrainment process also has the effect of transporting ambient water properties rapidly to depth. For example, a cold saline plume in the Arctic that entrains warm saline AW will effectively cause a net downward flux of both heat and salt. If it is not dense enough to travel all the way to the sea floor, the cascade will leave the slope and spread isopycnally into the ambient basin water at an equilibrium depth determined by both the original properties of the plume water and its final density. However, a rapidly descending plume can resuspend and entrain sediments, increasing the negative buoyancy. In this case, as the plume reaches its equilibrium depth, the entrained sediment is deposited giving rise to sediment accumulation at the bottom of continental slopes if the cascade was dense enough to reach the seabed or, if the cascade was not dense enough, intermediate depth nephloid layers. Once the initial density instability has been set up, the cold source waters can sometimes penetrate to greater depths. This is simply due to the thermobaric effect whereby the compressibility of sea water increases with decreasing temperature, thus enhancing the density contrast (Thorkildsen & Haugan, 1999). Therefore, through all these processes, the cascading waters have the potential to penetrate, and therefore ventilate, waters at greater depth than simple convective mixing.

The depth that a cascade can descend is of course dependent upon its initial TS properties that are created by the cooling and salinification processes. At the shelf break, the contrast in TS properties will be most extreme compared with the ambient water offshore. In polar oceans, the vertical thermohaline structure of the water column makes the relative contribution of temperature or salinity gradients to the cascading process a function of the depth of the shelf. Essentially, water in the surface mixed layer is generally very cold and fresh and because the haline contraction coefficient β is $\sim$30 times more important than the thermal expansion coefficient α in controlling the density (see e.g. the relatively vertical potential density lines in the potential temperature and salinity plots in Figs. 3.2 and 3.4), the largest contribution to the density contrast between the cascade and the ambient water is through changes in salinity. Figure 3.6 shows that this is the case down to depths of $\sim$150 m. In deeper waters, there is usually a warmer and more saline water mass. For deeper shelves, this means that there will be a greater modification required to actually create water dense enough to cascade with the result that the salinity contrast between the cascade and the ambient water is diminished. So at depths >200 m, Fig. 3.6 shows that the density difference that drives the cascade is through the temperature gradient and not salinity (Ivanov et al., 2004).

An example of a very clear cascade off the eastern side of the Antarctic Peninsula is shown in Fig. 3.7. The potential temperature distribution along the CTD section shows a clear thin layer of cold water cascading down the shelf break which was associated with high on-shelf salinities and was presumed to be spreading into the deep waters at the edge of the Weddell Gyre (Muench & Gordon, 1995). The horizontal density gradient between the waters on the shallow shelf and the ambient waters in the deep basin drives the cascade down the shelf. With a shelf depth of approximately 500 m, we should expect, from Fig. 3.6, the temperature

difference to be the controlling factor. Indeed, temperatures at sea floor on shelf are $< -1.9°C$ which is over 2°C cooler than waters at comparable depths off-shelf, whilst salinities both on- and off-shelf at 500 m depth were comparable (Muench & Gordon, 1995). In cascades, typical values for the density difference at the shelf break can be up to 0.4 kg m^{-3}, which can be achieved in almost all cascading locations around the world through cooling in winter and the formation of a horizontal temperature gradient (Shapiro et al., 2003; Ivanov et al., 2004). In ice-covered waters, this gradient can be greatly enhanced by the salinification of the water through brine released during sea ice formation, and for shallow shelves, the density difference between the cold and saline on-shelf and the offshore waters can be as great as to 2 kg m^{-3}.

A key water mass in the global ocean circulation is AABW, which is formed close to the continent and in the seasonal and perennially sea ice-covered regions of Antarctica (Fig. 3.1b). However, the actual formation method of this important water mass is not clear (Orsi et al., 1999). A very cold salty variety of high-salinity shelf water (HSSW) is formed through salt rejection from ice growth on the shallow coastal regions in a process similar to that described above. The water formed is dense enough to cascade to the sea floor, but the conversion of HSSW to AABW as it cascades down the continental slope and entrains the ambient water mass remains undetermined (see e.g. Foster & Carmack, 1976; Foldvik et al., 2004 for proposed alternatives; Gordon et al., 2004).

In the Arctic, the required combination of shallow shelves and sea ice formation makes the vast Eurasian and Siberian shelves coast prime region for cascading events (Ivanov et al.,
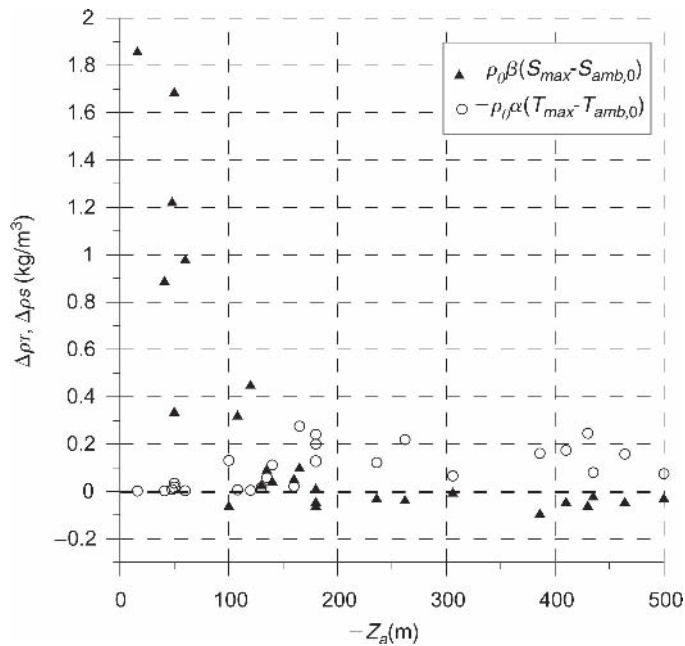
Fig. 3.6 The contribution to density contrast in a cascade by temperature: $\Delta \rho T/\rho_0 = -\alpha(T_a - T_d)$ (open circles) and by salinity $\Delta \rho S/\rho_0 = \beta(S_a - S_d)$ (filled triangles) versus the depth of maximum water density in shallow polar seas Z_a. The subscript "a" represents the maximum within the cascade, "d" represents the properties at the same depth as "a", but in ambient water outside the cascade. Reprinted from Progress in Oceanography, Ivanov et al (2004). Cascades of dense water around the world ocean. Progress in Oceanography. With permission from Elsevier.

2004). Of the Arctic shelf regions, the Barents Sea is the most active cascading region, which can be attributed to three distinct factors. First, as Fig. 3.1a shows, proximity to AW means that overall there is a higher salinity of the resident water masses. Second, there are numerous banks with depths less than 100 m separated by channels of >300 m depth. Third, the local meteorological forcing means that there are relatively high ocean–atmosphere heat fluxes that lead to high rates of ice formation. In some areas of the Barents Sea, e.g. the western Novaya Zemlya shelf, it is estimated that up to 10 m of ice can form annually (Winsor & Björk, 2000). The product of all these factors is the formation of Barents Sea Bottom Water (BSBW), a cold and highly saline water that once formed on the shallow banks, cascades into the deeper water of the Arctic Ocean through the relatively deep canyons that open into
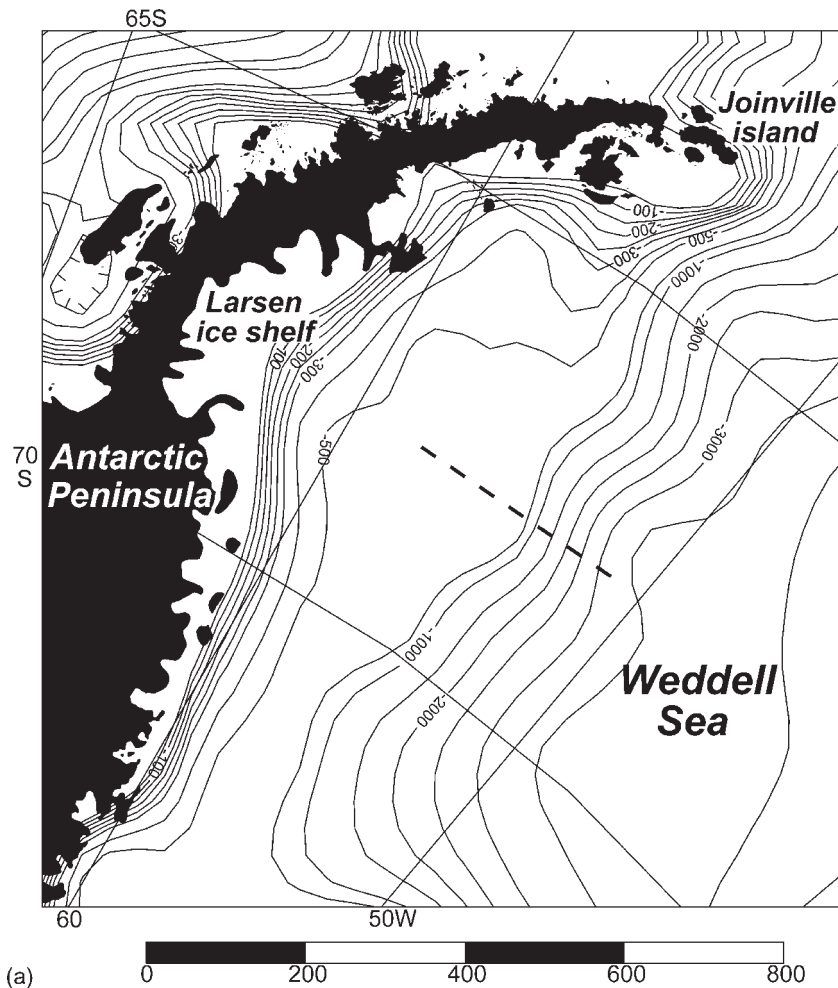
Fig. 3.7 Cascading off the Weddell Sea break on the edge of the eastern side of the Antarctic Peninsula. (a) Sea bed topography and location of the CTD section shown as a dashed line. Note the bathymetry is poorly known, (b) The potential temperature distribution along the CTD section shown above recorded in 1992. The cold shelf waters are measured in a thin cascade down the shelf break. Reprinted from Progress in Oceanography, Ivanov et al (2004). Cascades of dense water around the world ocean. Progress in Oceanography. With permission from Elsevier.
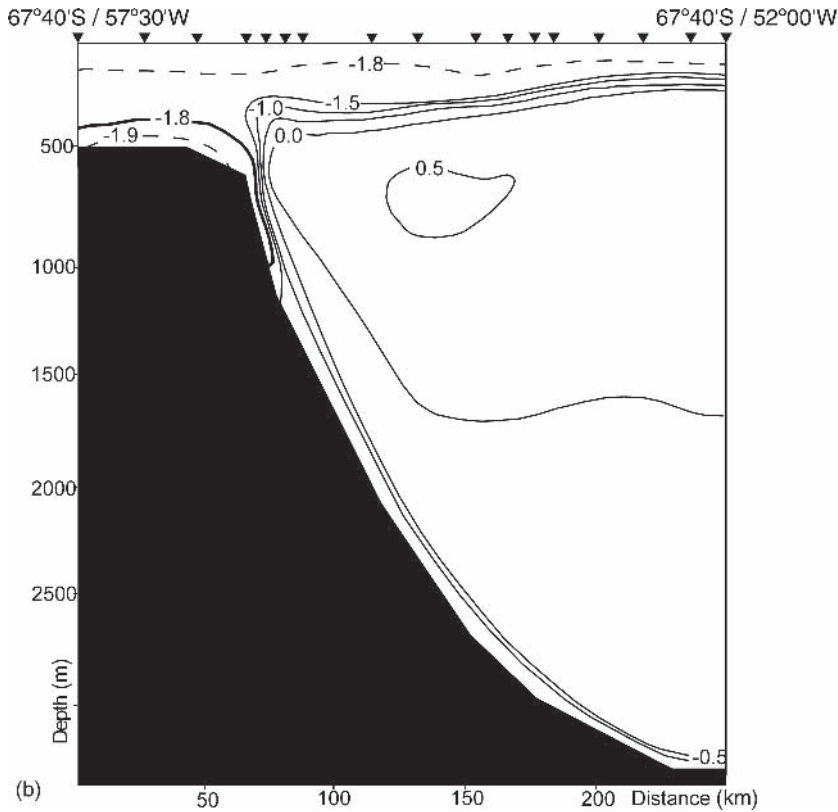
Fig. 3.7   (*Continued*)

the Nansen Basin including the St Anna Trough and the Franz-Victoria Channel. There are similar active cascading areas in the shallow Chukchi Sea where dense water cascades into the Barrow Canyon although in general it is often very difficult to routinely observe active cascades as they are usually intermittent in their formation in both time and space.

In the preceding sections, we have described and illustrated many processes where sea ice growth and melt are occurring. Add to this the inputs from precipitation and rivers, and the balance of source waters and modification processes can become complex. Any technique that enables the determination of the origins of these waters has particular utility.

3.6 The use of isotopes

The formation and melt of sea ice leaves a characteristic signature on the local water masses – a change in salinity being the most obvious. For example, the brine-enriched waters that are a precursor to shelf cascades and the distinctive summer freshwater cap in polar CTD profiles are readily observed. However, normal oceanographic processes such as mixing and overturning of the water column can eliminate what was a once a clear salinity signal of sea ice influence. In addition, in the Arctic, sea ice melt is obviously not the only significant freshwater source: Seasonal river discharge across the Siberian and Canadian shelves (Yang et al., 2002)

is important in the salinity balance of these regions as well as fresher water entering from the Pacific Ocean through the Bering Strait. Consequently, it can prove extremely difficult to tease out the relative contribution of sea ice in modifying the hydrography of these waters. One particularly useful technique is by measuring the isotopic composition of the sea water using the differing ratio of two common oxygen isotopes found in the water molecule.

The most dominant isotope of oxygen in water is ^{16}O, whereas ^{18}O is much less common. The ratio of these two oxygen isotopes in a sample will vary depending on the source owing to the differing energies required in the evaporation and condensation processes (Bigg & Rohling, 2000). For example, river water is derived from precipitation – and the moisture for this came from evaporation. As water evaporates, some of the heavier ^{18}O in the source water is left behind, so the precipitation-derived river water is depleted in ^{18}O compared to the ocean. Of course, should precipitation fall as snow and turn to glacial ice, it too will be depleted in ^{18}O. This means that as rivers flow into the seas or glacial ice melts and the water is freshened by a proportion of meteoric water, a sample of such ocean water will also be depleted in ^{18}O. Fundamentally, the isotopic composition of an ocean water sample can be used to determine the source waters, and through a combination of salinity and isotopic data, the relative proportions of the source waters can be determined.

The isotopic composition of water is usually given in the delta (δ) notation, which is the ratio of the two dominant oxygen isotopes (^{18}O/^{16}O) in the sample compared to the ratio of an international standard called Vienna Mean Standard Ocean Water (VMSOW) (although called ocean water, this standard has salinity 0). It is defined as:

$$\delta^{18}O = \left\{ \frac{^{18}O/_{^{16}O_{sample}}}{^{18}O/_{^{16}O_{VMSOW}}} - 1 \right\} \times 1000 \,(‰)$$

and standard water would have a δ^{18}O value of 0. As well as showing a variation in temperature and salinity, water samples will also have a range of δ^{18}O with both positive (i.e. enriched in ^{18}O) and negative values (depleted in ^{18}O), and the δ^{18}O values can, as Fig. 3.8 demonstrates, be represented in a graph that depicts the mixing between two sources of water (Bauch et al., 1995; Yamamoto et al., 2002). On top of this simple linear mixing line, the formation of sea ice has a marked effect which causes a departure from the straight line (Meredith et al., 2008). During freezing, although there is a clear increase in water salinity, the fractionation of the stable oxygen isotopes is minimal, hence the δ^{18}O of sea ice is close to that of sea water (Lehmann & Siegenthaler, 1991). Therefore, brine initially released from sea ice will also have approximately the same δ^{18}O value as the source water. As sea ice melts, it represents a relatively freshwater source, but because the δ^{18}O signature is similar to ocean water, the isotopic composition will remain approximately constant although the overall salinity will change. This fact means that the effects of sea ice melt and river discharge/glacial melt can be distinguished from each other based on their isotopic composition and the departure from the straight line.

In addition, because like salinity, δ^{18}O is a conservative property that is not changed by chemical or biological processes, it can be used with salinity in a series of mass-balance equations to determine the relative proportions of water derived from oceanic, meteoric
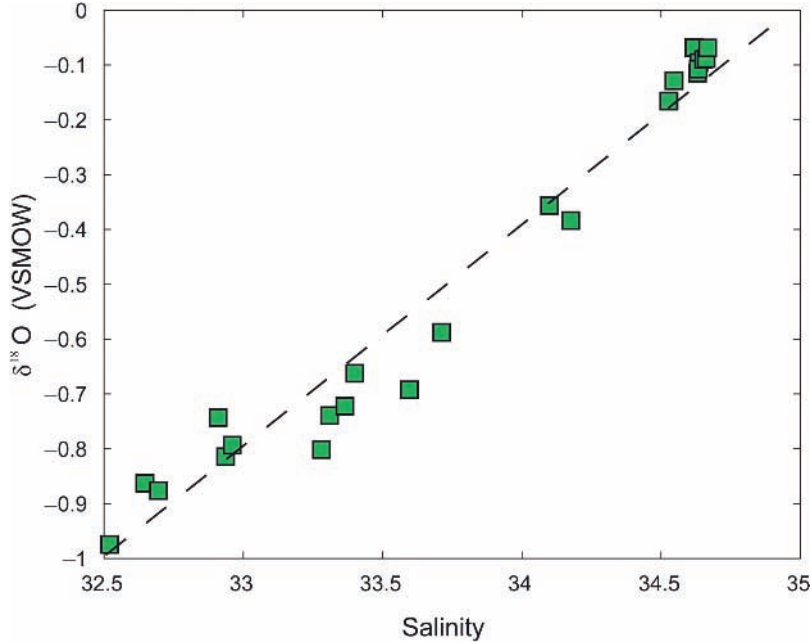
Fig. 3.8 Salinity-δ¹⁸O relationship for coastal waters of Antarctica recorded at Rothera Research Station showing the influence of ACC water (high salinity, high δ¹⁸O) and samples diluted with glacial melt (low salinity, low δ¹⁸O).

and sea ice sources (Östlund & Hut, 1984). In essence, the fraction (f) of each of the three sources must add up to 1.

$$f_{ice} + f_{ocean} + f_{meterotic} = 1$$

and the salinity of each component scaled by its fractional composition must add up to the salinity of the sample:

$$f_{ice} \, S_{ice} + f_{ocean} S_{ocean} + f_{meterotic} S_{meteoric} = S_{sample}$$

And finally,

$$f_{ice} \, \delta_{ice} + f_{ocean} \delta_{ocean} + f_{meterotic} \delta_{meteoric} = \delta_{sample}$$

where δ is the δ¹⁸O value of that component of the system. An example of this technique is the estimation of the relative freshwater contributions from meteoric sources and sea ice to the water masses in Fram Strait (Meredith et al., 2001). Here, the isotopic signature of each component was δ_{ice} = 2.1‰, δ_{ocean} = 0.3‰ and $\delta_{meteoric}$ = −21‰, and the waters of the East Greenland Current were shown to have a negative fraction of sea ice melt, which corresponds to inferred ice growth (as this is effectively removing freshwater from the ocean). Meredith et al. (2001) estimated that it would take 11 m of sea ice formation to create the isotopic and salinity signals observed in Fram Strait. Another example is Meredith et al. (2008), who derived a time series of sea ice production using δ¹⁸O from a hydrographic time series collected year round at an Antarctic research station.

Oxygen isotope analysis is extremely useful, but it is just one tracer technique that can be used to determine the source waters that contribute to the water mass composition. Another tracer commonly used in conjunction with $\delta^{18}O$ measurements is barium, which can be used to differentiate between the different river inputs and Pacific Water input (Ekwurzel et al., 2001; Taylor et al., 2003).

With so many remaining questions about the interaction of the sea ice cover with the polar oceans, it is clear that it will continue to be an area of study that brings great reward. However, the fundamental problem noted in Section 3.1 remains – to paraphrase, how to actually sample the regions effectively? In the final section (3.7), we review recent technological advances that offer great hope.

3.7 Future sampling technology

The challenging conditions presented by the polar regions have meant that they have always been the place where technological advances have been pioneered, from Nansen bottles through to the latest development of autonomous underwater vehicles (AUVs) (Brierley et al., 2002; Wadhams et al., 2006). However, some of the latest developments in open water sampling such as Argo buoys and gliders have limited polar use because of the lack of easy access to open water needed for data return. In addition, technologies such as AUVs still require a ship platform for deployment and recovery and they operate for relatively short durations. The perfect polar sampling instrument would be easy to deploy, operate for long periods of time and move through the region, sampling as it went and return the data back via satellite. In fact, one could consider such an instrument as a modern analogue of the *Fram* and the established technique of manned drifting stations. The first successful deployments of such an instrument were the introduction of the Arctic Ice Ocean Environment Buoy (IOEB) in the early 1990s. This instrument consisted of a surface package deployed on the ice measuring meteorological parameters with a mooring string with fixed oceanographic sensors beneath the ice to measure hydrographic properties and thermistor chains frozen into the ice measuring ice growth and melt. As the IOEB drifted through the Arctic, data was sent back by satellite and unique oceanic heat flux and internal wave observations were made (Perovich et al., 1989; Plueddemann, 1992).

As technologies have developed, the IOEB has evolved into Ice-tethered profilers (ITPs). These are similar packages to the IOEB but instead of fixed sensors on a mooring beneath the buoy, the unit has a fixed line 500–800 m long beneath the ice – with a sensor package profiling up and down the line at programmed time intervals; the vertical sampling resolution is approximately 25 cm (Doherty et al., 1999). Essentially, the instruments drift with the ice making hydrographic profiles whilst sending the data back in near-real time by satellite. Their reliability has proved generally very good, and to date 30 units have been deployed in the Arctic (Fig. 3.9). The most successful unit (ITP1) lasted for almost 2 years from 2005 to 2007 on a drift of almost 5000 km, and it made over 2000 hydrographic profiles. The data that these buoys provide can be put to all the standard uses of through-the-ice polar hydrography. For example, Timmermans et al. (2008) used data from five ITPs and established that they drifted over 21 shallow anticyclonic eddies in the Canada Basin with horizontal dimensions comparable to the Rossby Radius of deformation. Such
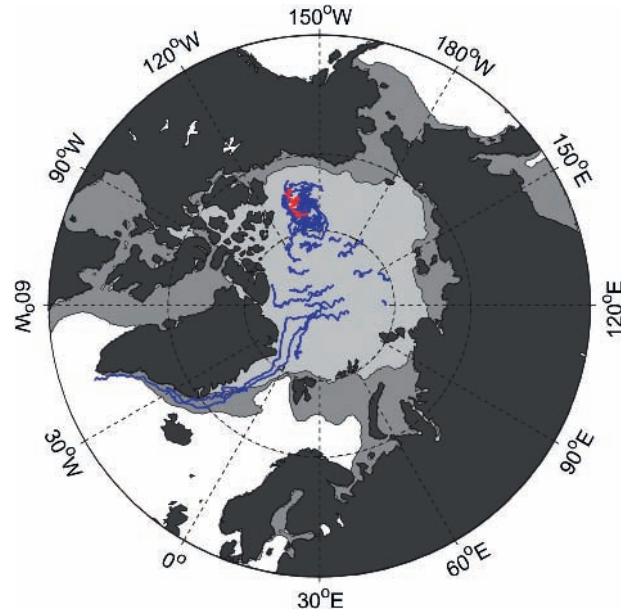
Fig. 3.9 The drift tracks of 30 ITP's deployed in the Arctic up to September 2008. The tracks of the buoys trace out both the Beaufort Gyre and the Transpolar Drift (Figure 3.1a). Inertial oscillations can be seen in the longer tracks. The grey shading is the ice cover as in Figure 3.1. Data from the red ITP track is shown in Fig. 3.10.
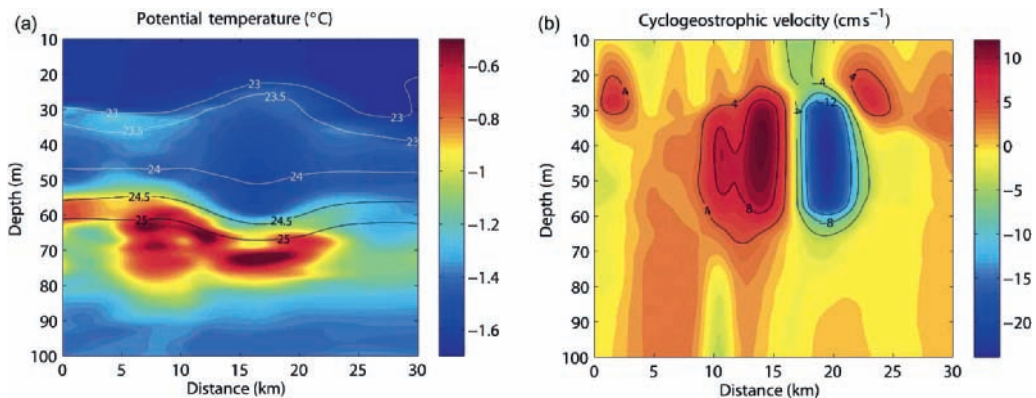

Fig. 3.10   (a) Sections of potential temperature with potential density superimposed across a typical eddy observed by Timmermans et al. (2008) using 13 profiles collected in just over 3 days from ITP 3. (b) The cyclogeostrophic velocity through the same eddy shown in (A). The track of the buoy from which this data come from is shown red in Fig. 3.9. From Timmermans et al. (2008). Copyright (2008) American Meteorological Society.

shallow anticyclonic eddies have been known about for many years from drifting ice camps (Manley & Hunkins, 1985), but the sampling resolution Timmermans et al. (2008) show is impressive. Figure 3.10a shows a typical eddy identified from 13 CTD profiles from ITP 3 (sampling at four profiles per day). There is the expected divergence in isopycnals (and reduced vertical stratification) just beneath the mixed layer at the centre of a cold anticyclonic eddy, and much warmer water just beneath it. Figure 3.10b shows the rotation in the eddy

derived from dynamic heights referenced to 300 m. At approximately 3 km from its centre, this eddy has a rotation velocity of $\sim$20 cm s^{-1} superimposed on an overall background drift of 1–2 cm s^{-1}. Timmermans et al. (2008) suggested on the basis of ITP data that such eddies have a lifetime of at least 6 months and are clearly endemic to the Canada Basin. Whilst currently undersampled, they could be important for the overall heat transfer within the CHL. Clearly, the continued use of ITPs in the Arctic is going to be a major step forward in data collection and availability, and hence understanding. There are currently no ITPs deployed in the Antarctic where shorter deployment durations would be expected, except at some particular sites such as the Weddell Gyre. This is due to the drift of the surface package within a sea ice cover that experiences large seasonal variation (Fig. 3.1b). There is also the additional difficulty because the initial deployment of such packages still involves visiting what are often very remote regions. Also, the sparse knowledge of the bathymetry in many regions means that there is a risk of undersampling the water column or even snagging the fixed line on the bottom.

There is however an intriguing possibility for obtaining data in polar regions provided by sensors deployed on animals. Although the precise sampling path cannot be controlled, the use of animals as a platform for oceanographic measurements fulfils many of the desirable characteristics of the perfect sampling instrument: ease of deployment, long duration, roaming behaviour and satellite data transmission. Many species of both birds and mammals have been equipped with small CTD sensor packages in the last decades and have provided unprecedented data coverage in the polar regions. For example, in the Arctic, Lydersen et al. (2002) deployed satellite-linked CTD loggers on two beluga whales close to Svalbard and collected more than 500 CTD profiles in the previously noted important Storfjorden region in up to 90% ice cover. Similar success was provided with 11 tagged ringed seals collecting over 2300 CTD profiles in the Norwegian and Russian Arctic within ice covers of 90–100% (Lydersen et al., 2004). In the Antarctic, Bost et al. (2004) showed that King penguins tagged on the relatively accessible sub-Antarctic Crozet archipelago transited more than 1500 km south (46°S to $\sim$60°S), and spent approximately a quarter of their entire foraging time throughout the southern winter within the Antarctic marginal ice zone, perhaps to exploit the high biomass (Brierley et al., 2002). There is a clear opportunity to equip such penguins with CTD sensors.

Greater success has been demonstrated with CTD sensors attached to various species of Antarctic seal – although the choice of species is critical because some species, e.g. leopard seals, stay relatively close to one location whereas others range over wide areas (Costa et al., 2008). Perhaps, the most exciting current research is using data from the wide-ranging southern ocean elephant seal. Charrassin et al. (2008) showed 58 animals tagged at various sub-Antarctic islands provided over 8000 CTD profiles to mean depth 500 m south of 60°S – a data set that is more than 9 times bigger than the ship and float data set for the same time period. Over 4500 of these profiles were within the sea ice cover in the austral autumn and winter – a number that is more than 30 times the size of the conventional in-ice autumn winter data set (Fig. 3.11). Charrassin et al. (2008) demonstrated that it is possible to map circumpolar frontal position with the seal data, but the real advance is from data within the ice. They created four pseudo-hydrographic time series from tagged animals that remained close to one location within the ice.

Figure 3.12 shows one such time series created from 200 CTD profiles collected within an approximately 1° area adjacent to the continental shelf and constantly within 80 $\pm$24% ice concentration (the location is the yellow star on Fig. 3.11). The layer thickness of water
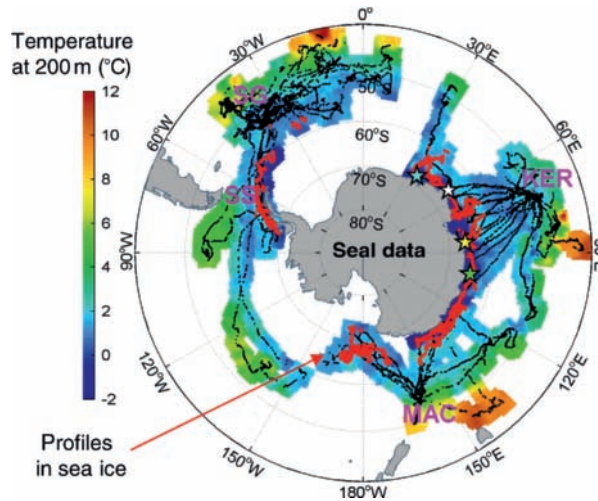
Fig. 3.11   The temperature at 200 m depth collected by elephant seals equipped with CTD –Satellite Relay Data Loggers at South Georgia (SG), the South Shetland (SS), Kerguelen, (KER), and Macquarie (MAC) islands. Red tracks indicate profiles collected within sea ice. The coloured stars indicate the locations of time series collected by four different seals within the sea ice cover. The data from the seal at 84°E marked by the yellow star is shown in Figure 3.12. Reproduced from Charrassin (2008) Southern Ocean Frontal Structure and Sea-ice Formation Rates Revealed by Elephant Seals. Proceedings of the National Academy of Sciences of the United States 105 (33) 11634 -11639. © 2008, National Academy of Sciences, U.S.A.

with temperature $< -1.8°C$ increases over the record from ~15 m in March to over 300 m by mid-May, which is associated with a steady increase in salinity and thickness of the mixed layer. Such a record is similar to human-derived CTD time series on the west of the Antarctic Peninsula as winter ice grows (Meredith et al., 2004). By making the assumption that salinification of the surface waters above 100 m was entirely due to salt rejection during sea ice formation, Charrassin et al. (2008) derived an ice generation rate for the time series of 2.4 cm day^{-1}, and overall there would need to be 1.12 m of ice generated to account for the observation in Fig. 3.12. Such an estimate is entirely reasonable given the seasonal nature of the ice cover in this location (Fig. 3.1b) and it is a perfect demonstration of the potential usefulness of data provided by the wide-ranging elephant seals. The main issue is clearly that, as Fig. 3.11 shows, both the Weddell Sea and almost the entire south east Pacific sector are not sampled at all. Biuw et al. (2007)[1] showed that some satellite-tracked elephant seals do transit the Pacific 'gap' in Fig. 3.11 but were presumably not instrumented with CTDs, though no seals entered the Weddell Sea. There is some evidence to suggest that seals tagged at King George Island (SS on Fig. 3.11) actually do transit to the southern Weddell Sea, but perhaps, as Fig. 3.1b suggests, elephant seals generally stay out of the oldest sea ice in the Antarctic. It is not unreasonable to imagine that such data gaps could be filled by tagging e.g. crabeater seals, which remain in the southern Weddell Sea for their whole life cycle.

Tagged mammals offer a powerful sampling alternative to traditional ship-based or moored observations. The major difficulty is clearly the unpredictable nature of the sample path, such that there is uncertainty about the prospect of achieving repeat sections. To some extent, this can be overcome by careful selection of particular animal groups that undertake annual migration over similar routes and regions at predictable times of the year. However, it is worth noting that a similarly uncontrollable sampling methodology has not been
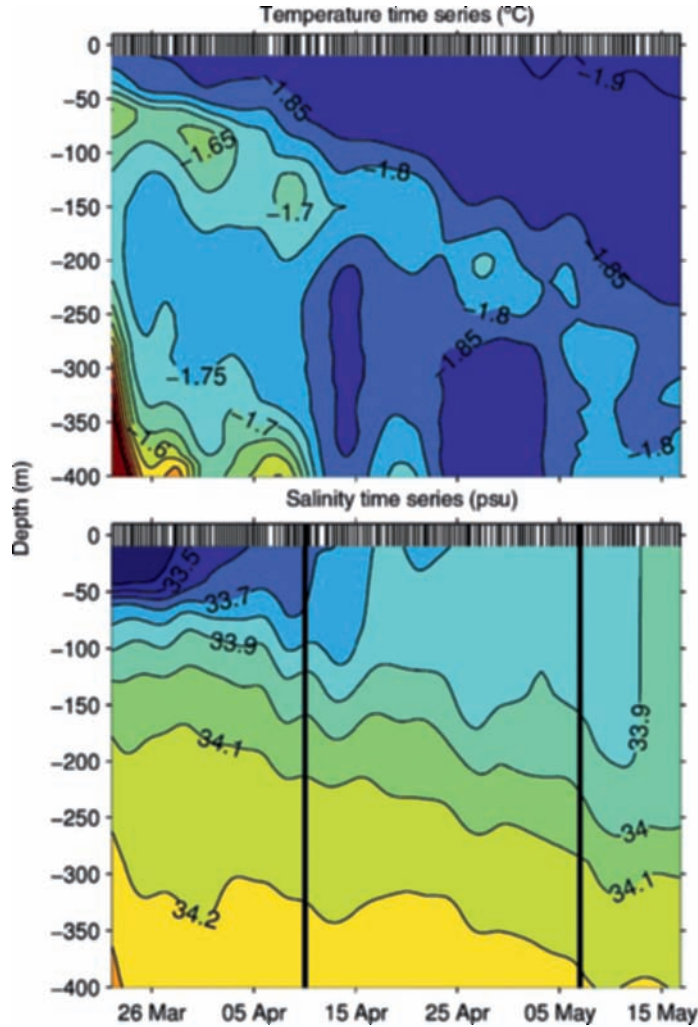
Fig. 3.12 A pseudo temperature and salinity time series collected by an elephant sea from April–May 2004 close to 84°E (yellow star on Fig. 3.11). Small bars at the top of each panel represent the time of the profiles. The solid lines on 10th April and 7th May are period over which the ice growth estimates were made. Reproduced from Charrassin (2008) Southern Ocean Frontal Structure and Sea-ice Formation Rates Revealed by Elephant Seals. Proceedings of the National Academy of Sciences of the United States 105 (33) 11634 -11639. © 2008, National Academy of Sciences, U.S.A.

detrimental to the scientific output from the extremely successful Argo float array. Tagging of marine mammals therefore represents a valuable collaboration between physical oceanography and zoology.

3.8 Summary and conclusions

In this chapter, we have briefly reviewed some areas of polar oceanography where there is a close connection or interaction between the ocean and the sea ice. The range of interactions has included the modification of salt and heat budgets, feedback mechanisms (both positive

and negative) and the chemical signatures they leave on the water masses. We finished by highlighting two potentially very useful sampling technologies that can significantly increase the size of the current data sets.

In all cases, we stress that there is a two-way response whereby the presence or absence of sea ice has a profound effect on the oceanography, and oceanographic structures have a critical role in modifying or maintaining the sea ice cover. In the Arctic, we are in an era of rapid changes in the ice cover and in the Antarctic there remain fundamental challenges in the observation and characterization of the shelf processes. Both regions present scientific and technological challenges to quantify and predict the ice–ocean coupling that can fundamentally alter the global oceanographic processes. We are now standing on the brink of an exciting era with an armoury of techniques to take up these challenges. The use of AUVs, gliders, drifters, mammals and chemical tracers will all play their part in our future investigations of the interactions between sea ice and oceanography.

Acknowledgements

End note

1 Biuw et al. (2007) present data from 85 elephant seals and there is a partial overlap with the data from the 58 seals presented in Charrassin et al. (2008).

References

Aagaard, K., Coachman, L.K. & Carmack, E. (1981) On the halocline of the Arctic ocean. *Deep-Sea Research Part I*, **28**, 529–545.

Aagaard, K., Foldvik, A. & Hillman, S.R. (1987) The West Spitsbergen Current – disposition and water mass transformation. *Journal of Geophysical Research*, **92** (C4), 3778–3784.

Akitomo, K., Awaji, T. & Imasato, N. (1995) Open-ocean deep convection in the Weddell Sea – 2-dimensional numerical experiments with a nonhydrostatic model. *Deep-Sea Research Part I*, **42** (1), 53–73.

Backhaus, J.O., Fohrmann, H., Kampf, J. & Rubino, A. (1997) Formation and export of water masses produced in Arctic shelf polynyas – process studies of oceanic convection. *Ices Journal of Marine Science*, **54**, 366–382.

Baines, P.G. & Condie, S. (1998) Observations and modelling of Antarctic downslope flows: a review. In: *Ocean*, *Ice and Atmosphere: Interactions at the Antarctic Continental Margin* (Eds. S.S. Jacobs & R. Weiss), pp. 29–49. American Geophysical Union, Washington, DC.

Bauch, D., Schlosser, P. & Fairbanks, R.G. (1995) Fresh-water balance and the sources of deep and bottom waters in the arctic-ocean inferred from the distribution of $H_2^{18}O$. *Progress in Oceanography*, **35**, 53–80.

Bigg, G.R. & Rohling, E.J. (2000) An oxygen isotope data set for marine waters. *Journal of Geophysical Research*, **105**, 8527–8535.

Biuw, M., Boehme, L., Guinet, C. et al. (2007) Variations in behavior and condition of a Southern Ocean top predator in relation to in situ oceanographic conditions. *Proceedings of the National Academy of Sciences of the USA*, **104**, 13705–13710.

Björk, G., Söderkvist, J., Winsor, P., Nikolopoulos, A. & Steele, M. (2002) Return of the cold halocline layer to the Amundsen Basin of the Arctic Ocean: implications for the sea ice mass balance. *Geophysical Research Letters*, **29**, 10.1029/2001gl014157.

Bost, C.A., Charrassin, J.B., Clerquin, Y., Ropert-Coudert, Y. & Le Maho, Y. (2004) Exploitation of distant marginal ice zones by king penguins during winter. *Marine Ecology Progress Series*, **283**, 293–297.

Boyd, T.J., Steele, M., Muench, R.D. & Gunn, J.T. (2002) Partial recovery of the Arctic Ocean halocline. *Geophysical Research Letters*, **29**, 10.1029/2001gl014047.

Brandon, M.A. & Wadhams, P. (1999) The near surface hydrography beneath the Odden ice tongue. *Deep-Sea Research Part II*, **46**, 1301–1318.

Brierley, A.S., Fernandes, P. G., Brandon, M.A. et al. (2002) Antarctic krill under sea ice: elevated abundance in a narrow band just south of ice edge. *Science*, **295**, 1890–1892.

Carmack, E.C. (1990) Large-scale physical oceanography of polar oceans. In: *Polar Oceanography, Part A: Physical Science* (Ed. W.O Smith, Jr.), pp 171–222. Academic Press, San Diego.

Cavalieri, D.J. & Martin, S. (1994) The contribution of Alaskan, Siberian, and Canadian coastal polynyas to the cold halocline layer of the Arctic-Ocean. *Journal of Geophysical Research*, **99**, 18343–18362.

Charrassin, J.B., Hindell, M., Rintoul, S.R. et al. (2008) Southern Ocean frontal structure and sea ice formation rates revealed by elephant seals. *Proceedings of the National Academy of Sciences of the USA*, **105**, 11634–11639.

Comiso, J.C. & Nishio, F. (2008) Trends in the sea ice cover using enhanced and compatible AMSR-E, SSM/I, and SMMR data. *Journal of Geophysical Research*, **113**, 10.1029/2007jc004257.

Costa, D.P., Klinck, J. M., Hofmann, E.E., Dinniman, M.S. & Burns, J.M. (2008) Upper ocean variability in west Antarctic Peninsula continental shelf waters as measured using instrumented seals. *Deep-Sea Research Part II*, **55**, 323–337.

Cottier, F.R., Nilsen, F., Inall, M. E., Gerland, S., Tverberg, V. & Svendsen, H. (2007) Wintertime warming of an Arctic shelf in response to large-scale atmospheric circulation. *Geophysical Research Letters*, **34**, 10.1029/2007gl029948.

Crary, A.P., Cotell, R.D. & Sexton, T.F. (1952) Preliminary report on scientific work on 'Fletcher's Ice Island', T3. *Arctic*, **5**, 211–223.

Doherty, K.W., Frye, D.E., Liberatore, S.P. & Toole, J.M. (1999) A moored profiling instrument. *Journal of Atmospheric and Oceanic Technology*, **16**, 1816–1829.

Drobot, S., Stroeve, J., Maslanik, J.A., Emery, W., Fowler, C. & Kay, J. (2008) Evolution of the 2007–2008 Arctic sea ice cover and prospects for a new record in 2008. *Geophysical Research Letters*, **35**, L19501, 10.1029/2008GL035316.

Ekman, V.W. (1905) On the influence of the Earth's rotation on ocean currents. *Arkiv för Matematik, Astronomi och Fysik*, 2, 1–52.

Ekwurzel, B., Schlosser, P., Mortlock, R.A., Fairbanks, R.G. & Swift, J.H. (2001) River runoff, sea ice meltwater, and Pacific water distribution and mean residence times in the Arctic Ocean. *Journal of Geophysical Research*, **106**, 9075–9092.

Fer, I., Skogseth, R., Haugan, P.M. & Jaccard, P. (2003) Observations of the Storfjorden overflow. *Deep-Sea Research Part I*, **50**, 1283–1303.

Foldvik, A., Gammelsrod, T., Osterhus, S. et al. (2004) Ice shelf water overflow and bottom water formation in the southern Weddell Sea. *Journal of Geophysical Research*, 109, 10.1029/2003jc002008.

Foster, T.D. & Carmack, E.C. (1976) Frontal zone mixing and Antarctic bottom water formation in southern Weddell Sea. *Deep-Sea Research*, **23**, 301–317.

Gallèe, H. (1997) Air–sea interactions over Terra Nova Bay during winter: simulation with a coupled atmosphere–polynya model. *Journal of Geophysical Research,* **102**, 13835–13849.

Gascard, J.-C., Festy, J., Le Goff, H. et al. (2008) Exploring Arctic transpolar drift during recent dramatic sea ice retreat. *EOS Transactions, American Geophysical Union*, **89**, 21–22.

Giles, K.A., Laxon, S.W. & Ridout, A.L. (2008) Circumpolar thinning of Arctic sea ice following the 2007 record ice extent minimum. *Geophysical Research Letters*, **35**, 10.1029/2008GL035710.

Gordon, A.L., Zambianchi, E., Orsi, A. et al. (2004) Energetic plumes over the western Ross Sea continental slope. *Geophysical Research Letters*, **31**, 10.1029/2004gl020785.

Hellmer, H.H., Schröder, M., Haas, C., Dieckmann, G.S. & Spindler, M. (2008) The ISPOL Drift Experiment. *Deep-Sea Research Part II*, **55**, 913–917.

Heywood, K. J., Locarnini, R.A., Frew, R.D., Dennis, P.F. & King, B.A. (1998) Transport and water masses of the Antarctic Slope Front system in the eastern Weddell Sea. In: *Ocean, Ice and Atmosphere: Interactions at the Antarctic Continental Margin* (Eds. S.S. Jacobs & R. Weiss), pp. 203–214. American Geophysical Union, Washington, DC.

Huxley, L. (1913) *Scott's Last Expedition: Vol II Being the reports of the journeys & Scientific Work Undertaken by Dr E.A Wilson and the Surviving Members of the Expedition*. Smith, Elder & Co., London.

Ivanov, V.V., Shapiro, G.I., Huthnance, J.M., Aleynik, D.L. & Golovin, P.N. (2004) Cascades of dense water around the world ocean. *Progress in Oceanography*, **60**, 47–98.

Jakobsson, M. (2002) Hypsometry and volume of the Arctic Ocean and its constituent seas. *Geochemistry Geophysics Geosystems*, **3**, 10.1029/2001gc000302.

Johnson, M.A. & Polyakov, I.V. (2001) The Laptev Sea as a source for recent Arctic Ocean salinity changes. *Geophysical Research Letters*, **28**, 2017–2020.

Jones, E.P. & Anderson, L.G. (1986) On the origin of the chemical-properties of the Arctic-Ocean halocline. *Journal of Geophysical Research*, **91**, 759–767.

Jones, E.P., Anderson, L.G., Jutterstrom, S., Mintrop, L. & Swift, J.H. (2008) Pacific freshwater, river water and sea ice meltwater across Arctic Ocean basins: Results from the 2005 Beringia Expedition. *Journal of Geophysical Research*, **113**, 10.1029/2007jc004124.

Kikuchi, T., Hatakeyama, K. & Morison, J.H. (2004) Distribution of convective Lower Halocline Water in the eastern Arctic Ocean. *Journal of Geophysical Research*, **109**, 10.1029/2003jc002223.

Koenig, L.S., Greenaway, K.R., Dunbar, M. & Hattersley-Smith, G. (1952) Arctic ice islands. *Arctic*, **5**, 66–103.

Kwok, R., Maslowski, W. & Laxon, S.W. (2005) On large outflows of Arctic sea ice into the Barents Sea. *Geophysical Research Letters*, **32**, 10.1029/2005gl024485.

Lehmann, M. & Siegenthaler, U. (1991) Equilibrium oxygen-isotope and hydrogen-isotope fractionation between ice and water. *Journal of Glaciology*, **37**, 23–26.

Lydersen, C., Nøst, O. A., Lovell, P. et al. (2002) Salinity and temperature structure of a freezing Arctic fjord – monitored by white whales (*Delphinapterus leucas*). *Geophysical Research Letters*, **29**, 10.1029/2002gl015462.

Lydersen, C., Nøst, O.A., Kovacs, K.M. & Fedak, M.A. (2004) Temperature data from Norwegian and Russian waters of the northern Barents Sea collected by free-living ringed seals. *Journal of Marine Systems*, **46**, 99–108.

Macdonald, R.W., Mclaughlin, F.A. & Carmack, E.C. (2002) Fresh water and its sources during the SHEBA drift in the Canada Basin of the Arctic Ocean. *Deep-Sea Research Part I*, **49**, 1769–1785.

McPhee, M.G. (2000) Marginal thermobaric stability in the ice-covered upper ocean over Maud Rise. *Journal of Physical Oceanography*, **30**, 2710–2722.

McPhee, M.G., Ackley, S.F., Guest, P. et al. (1996) The Antarctic Zone flux experiment. *Bulletin of the American Meteorological Society*, **77**, 1221–1232.

Manley, T.O. & Hunkins, K. (1985) Mesoscale Eddies of the Arctic Ocean. *Journal of Geophysical Research*, **90**, 4911–4930.

Martin, S. & Cavalieri, D.J. (1989) Contributions of the Siberian shelf polynyas to the Arctic Ocean intermediate and deep-water. *Journal of Geophysical Research*, **94**, 12725–12738.

Martin, S. (2001) Polynyas. In: *Encyclopedia of Ocean Sciences* (Eds. J.H. Steel, K.K. Turekian & S.A. Thorpe), pp. 2241–2247. Academic Press, London.

Martinson, D.G., Killworth, P.D. & Gordon, A.L. (1981) A convective model for the Weddell polynya. *Journal of Physical Oceanography*, **11**, 466–488.

Mathis, J.T., Pickart, R.S., Hansell, D.A., Kadko, D. & Bates, N.R. (2007) Eddy transport of organic carbon and nutrients from the Chukchi Shelf: Impact on the upper halocline of the western Arctic Ocean. *Journal of Geophysical Research*, **112**, 10.1029/2006jc003899.

Maykut, G.A. & Untersteiner, N. (1971) Some results from a time-dependent thermodynamic model of sea ice. *Journal of Geophysical Research*, **76**, 1550–1575.

Meredith, M., Heywood, K., Dennis, P. et al. (2001) Freshwater fluxes through the western Fram Strait. *Geophysical Research Letters*, **28**, 1615–1618.

Meredith, M.P., Renfrew, I.A., Clarke, A., King, J.C. & Brandon, M.A. (2004) Impact of the 1997/98 ENSO on upper ocean characteristics in Marguerite Bay, western Antarctic Peninsula. *Journal of Geophysical Research*, **109**, 10.1029/2003jc001784.

Meredith, M.P., Brandon, M.A., Wallace, M.I. et al. (2008) Variability in the freshwater balance of northern Marguerite Bay, Antarctic Peninsula: Results from δ^{18}O. *Deep-Sea Research Part II*, **55**, 309–322.

Morales Maqueda, M.A.M., Willmott, A.J. & Biggs, N.R.T. (2004) Polynya dynamics: a review of observations and modeling. *Reviews of Geophysics*, **42**, 10.1029/2002rg000116.

Morison, J., Steele, M. & Andersen, R. (1998) Hydrography of the upper Arctic Ocean measured from the nuclear submarine USS Pargo. *Deep-Sea Research Part I*, **45**, 15–38.

Morison, J., Steele, M., Kikuchi, T., Falkner, K. & Smethie, W. (2006) Relaxation of central Arctic Ocean hydrography to pre-1990s climatology. *Geophysical Research Letters*, **33**, 10.1029/2006gl026826.

Muench, R.D. & Gordon, A.L. (1995) Circulation and transport of water along the western Weddell Sea margin. *Journal of Geophysical Research*, **100**, 18503–18515.

Nansen, F. (1897) *Farthest North*. Archibald Constable and Company, Westminster.

Orsi, A.H., Johnson, G.C. & Bullister, J.L. (1999) Circulation, mixing, and production of Antarctic Bottom Water. *Progress in Oceanography*, **43**, 55–109.

Orsi, A.H., Whitworth, T. & Nowlin, W.D. (1995) On the meridional extent and fronts of the Antarctic circumpolar current. *Deep-Sea Research Part I*, **42**, 641–673.

Östlund, H.G. & Hut, G. (1984) Arctic Ocean water mass balance from isotope data. *Journal of Geophysical Research*, **89**, 6373–6381.

Papanin, I. (1940) *Life on an Ice Floe*. Hutchinson & Company, London.

Perovich, D.K., Tucker, W.B. & Krishfield, R.A. (1989) Oceanic heat-flux in the Fram Strait measured by a drifting buoy. *Geophysical Research Letters*, **16**, 995–998.

Plueddemann, A.J. (1992) Internal wave observations from the Arctic environmental drifting buoy. *Journal of Geophysical Research*, **97**, 12619–12638.

Polyakov, I.V., Beszczynska, A., Carmack, E.C. et al. (2005) One more step toward a warmer Arctic. *Geophysical Research Letters*, **32**, 10.1029/2005gl023740.

Renfrew, I.A., King, J.C. & Markus, T. (2002) Coastal polynyas in the southern Weddell Sea: variability of the surface energy budget. *Journal of Geophysical Research*, **107**, 10.1029/2000jc000720.

Rudels, B., Anderson, L.G. & Jones, E.P. (1996) Formation and evolution of the surface mixed layer and halocline of the Arctic Ocean. *Journal of Geophysical Research – Oceans*, **101**, 8807–8821.

Schauer, U. & Fahrbach, E. (1999) A dense bottom water plume in the western Barents Sea: downstream modification and interannual variability. *Deep-Sea Research Part I*, **46**, 2095–2108.

Schmitz, W.J. (1995) On the interbasin-scale thermohaline circulation. *Reviews of Geophysics*, **33**, 151–173.

Scottish National Antarctic Expedition (1907) *Report of the scientific results of the voyage of S.Y. "Scotia" during the years 1902, 1903, and 1904: under the leadership of William S. Bruce*. The Scottish Oceanographical Laboratory, Edinburgh.

Shapiro, G.I., Huthnance, J.M. & Ivanov, V.V. (2003) Dense water cascading off the continental shelf. *Journal of Geophysical Research – Oceans*, **108**, 10.1029/2002jc001610.

Shcherbina, A.Y., Talley, L.D. & Rudnick, D.L. (2003) Direct observations of North Pacific ventilation: Brine rejection in the Okhotsk Sea. *Science*, **302**, 1952–1955.

Shimada, K., Kamoshida, T., Itoh, M. et al. (2006) Pacific Ocean inflow: influence on catastrophic reduction of sea ice cover in the Arctic Ocean. *Geophysical Research Letters*, **33**, 10.1029/2005gl025624.

Serreze, M.C. & Francis, J.A. (2006) The Arctic on the fast track of change. *Weather*, **61**, 65–69.

Serreze, M.C., Holland, M.M. & Stroeve, J. (2007) Perspectives on the Arctic's shrinking sea ice cover. *Science*, **315**, 1533–1536.

Skogseth, R., Haugan, P.M. & Jakobsson, M. (2005a) Watermass transformations in Storfjorden. *Continental Shelf Research*, **25**, 667–695.

Skogseth, R., Fer, I. & Haugan, P.M. (2005b) Dense-water production and overflow from an Arctic Coastal Polynya in Storfjorden. In: *The Nordic Seas: An Integrated Perspective* (Eds. H. Drange, T. Dokken, T. Furevik, R. Gerdes & W. Berger), pp. 73–88. American Geophysical Union, Washington, DC.

Skogseth, R., Smedsrud, L.H., Nilsen, F. & Fer, I. (2008) Observations of hydrography and downflow of brine-enriched shelf water in the Storfjorden polynya, Svalbard. *Journal of Geophysical Research – Oceans*, **113**, 10.1029/2007jc004452.

Smedsrud, L.H. (2005) Warming of the deep water in the Weddell Sea along the Greenwich meridian: 1977–2001. *Deep-Sea Research Part I*, **52**, 241–258.

Smith Jr., W.O. (1990a) *Polar Oceanography, Part A: Physical Science*. Academic Press, London.

Smith Jr., W.O. (1990b) *Polar Oceanography, Part B Chemistry, Biology, and Geology*. Academic Press, London.

Smith Jr., W.O. & Barber, D.G. (2007) *Polynyas: Windows to the World*. Elsevier, Amsterdam.

Smith Jr., W.O. & Grebmeier, J.M. (1995) *Arctic Oceanography: Marginal Ice Zones and Continental Shelves*. American Geophysical Union. Washington, DC.

Smith, S.D., Muench, R.D. & Pease, C.H. (1990) Polynyas and leads – an overview of physical processes and environment. *Journal of Geophysical Research – Oceans*, **95**, 9461–9479.

Smith, W.H.F. & Sandwell, D.T. (1997) Global sea floor topography from satellite altimetry and ship depth soundings. *Science*, **277**, 1956–1962.

Sohn, R.A., Willis, C., Humphris, S. et al. (2008) Explosive volcanism on the ultraslow-spreading Gakkel ridge, Arctic Ocean. *Nature*, **453**, 1236–1238.

Steele, M. & Boyd, T. (1998) Retreat of the cold halocline layer in the Arctic Ocean. *Journal of Geophysical Research – Oceans*, **103**, 10419–10435.

Stroeve, J., Holland, M.M., Meier, W., Scambos, T. & Serreze, M. (2007) Arctic sea ice decline: faster than forecast. *Geophysical Research Letters*, **34**, 10.1029/2007gl029703.

Tamura, T., Ohshima, K.I. & Nihashi, S. (2008) Mapping of sea ice production for Antarctic coastal polynyas. *Geophysical Research Letters*, **35**, 10.1029/2007gl032903.

Taylor, J.R., Falkner, K.K., Schauer, U. & Meredith, M. (2003) Quantitative considerations of dissolved barium as a tracer in the Arctic Ocean. *Journal of Geophysical Research – Oceans*, **108**, 10.1029/2002jc001635.

Tchernia, P. & Jeannin, P.F. (1980) Observations on the Antarctic east wind drift using tabular icebergs tracked by satellite NIMBUS-F (1975–1977). *Deep-Sea Research Part I*, **27**, 467–474.

The LEADEX Group (1993) The LEADEX Experiment. *EOS Transactions, American Geophysical Union*, **74**, 393.

Thorkildsen, F. & Haugan, P.M. (1999) Modeling of deep-water renewal through cold convective plumes. *Deep-Sea Research Part II*, **46**, 1357–1383.

Timmermans, M.L., Toole, J., Proshutinsky, A., Krishfield, R. & Plueddemann, A. (2008) Eddies in the Canada Basin, Arctic Ocean, observed from ice-tethered profilers. *Journal of Physical Oceanography*, **38**, 133–145.

Wadhams, P., Wilkinson, J.P. & McPhail, S.D. (2006) A new view of the underside of Arctic sea ice. *Geophysical Research Letters*, **33**, 10.1029/2005gl0251331.

Walsh, J.E. (2008) Climate of the Arctic Marine Environment. *Ecological Applications*, **18** (2), S3–S22.

Williams, G.D., Bindoff, N.L., Marsland, S.J. & Rintoul, S.R. (2008) Formation and export of dense shelf water from the Adelie Depression, East Antarctica. *Journal of Geophysical Research – Oceans*, **113**, 10.1029/2007jc004346.

Williams, W.J., Carmack, E.C. & Ingram, R.G. (2007) Physical oceanography of polynyas. In: *Polynyas: Windows to the World* (Eds. W.O. Smith Jr. & D.G. Barber), pp. 55–85. Elsevier Oceanography Series, Amsterdam.

Winsor, P. & Björk, G. (2000) Polynya activity in the Arctic Ocean from 1958 to 1997. *Journal of Geophysical Research – Oceans*, **105**, 8789–8803.

WMO (1970) *WMO Sea Ice Nomenclature*. World Meteorological Organisation, Geneva.

Woodgate, R.A., Aagaard, K., Muench, R.D. et al. (2001) The Arctic Ocean boundary current along the Eurasian slope and the adjacent Lomonosov Ridge: water mass properties, transports and transformations from moored instruments. *Deep-Sea Research Part I*, **48**, 1757–1792.

Yamamoto, M., Watanabe, S., Tsunogai, S. & Wakatsuchi, M. (2002) Effects of sea ice formation and diapycnal mixing on the Okhotsk Sea intermediate water clarified with oxygen isotopes. *Deep-Sea Research Part I*, **49**, 1165–1174.

Yang, D.Q., Kane, D.L., Hinzman, L.D., Zhang, X.B., Zhang, T.J. & Ye, H.C. (2002) Siberian Lena River hydrologic regime and recent change. *Journal of Geophysical Research – Atmospheres*, **107**, 10.1029/2002jd002542.

This page intentionally left blank

4 Dynamics versus Thermodynamics: The Sea Ice Thickness Distribution

Christian Haas

4.1 Introduction

Changes of sea ice coverage are commonly taken as an indicator for climate change. Since 30 years, the area of the Arctic and Southern oceans covered by sea ice is routinely monitored by satellite radiometers (Chapter 6). These observations show that the ice coverage of the Arctic Ocean strongly declines during summer, with an average rate of –11.1% per decade. However, in 2007 and 2008, this trend was drastically exceeded when sea ice extent reduced to record lows of only 4.13 and 4.52 km^2, less than 20% of previous summers, and raising concerns that the Arctic Ocean might become ice-free during summers within the next few decades. However, winter ice coverage of the Arctic Ocean decreases at a much slower pace of only −2.8% per decade. And in contrast to the Arctic, sea ice coverage of the Southern Ocean increases slightly, with 0.6% and 3.4% per decade in the winter and summer, respectively.

The sea ice decline in the Arctic is much more rapid than predicted by any of the Intergovernmental Panel for Climate Change (IPCC) climate models (Stroeve et al., 2007). This demonstrates our limited understanding of the processes of sea ice growth and melt, and ice motion and deformation. For a full understanding of the areal changes, additional information on ice thickness is required, but is largely missing up to the date of this writing. This chapter will discuss the importance of ice thickness information, the most frequently used ice thickness measurement techniques and results from observations of long-term, interannual and seasonal thickness variations.

In Chapter 2, it was described how sea ice initially forms from open water and subsequently grows into an ice cover, or in other terms, how sea ice grows thermodynamically. One of the basic concepts is that the ice grows thicker, the colder the air is due to the establishment of greater temperature gradients in the ice, and higher freezing rates. Vice versa, it would follow that as a consequence of climate warming, the polar sea ice cover would become thinner. However, another process contributes to the sea ice thickness distribution: Due to its relative thinness – some decimetres to a few metres – sea ice floating over deep water is subject to winds and currents which steadily move the ice around, i.e. the ice cover drifts. As a result, it breaks up into floes interspersed by open water leads. With changing drift directions and speeds, the ice floes will be pushed together and collide with each other. If the resulting forces in the ice become too large, it will finally break. The resulting ice

fragments and blocks will be pushed onto, and below, the edges of the floes forming the so-called pressure ridges (Fig. 4.1).

Obviously, such dynamically formed ridges are much thicker than the adjacent, thermodynamically grown undeformed level ice. In terms of a statistical approach, this discussion shows that it is important to take into account different ice thickness classes (from thin to thick ice), and that a certain mean ice thickness can be attained by many different arrangements of thin and thick ice. As a consequence, it is quite difficult to interpret ice thickness data for indications of climate warming or cooling. This will be illustrated in later sections of this chapter.

Figure 4.2 shows three thickness profiles of ice floes of different developmental stage obtained in the western Weddell Sea, Antarctica: thin first-year ice, thick first-year ice and second-year ice. In general, the figure shows that the ice becomes thicker with increasing age. Note that the thickness of these ice floes is also comparable to typical first- and second-year thicknesses in the Arctic, which is hardly seen in other regions of the Southern Ocean. However, the figure also demonstrates the increasing degree of deformation and accumulation of deformed ice the ice floes undergo while becoming older. With the thin first-year ice, the original, uniform level ice thickness can well be seen and represents the thermodynamic growth since the first formation of the ice sheet. Ice thicknesses are less uniform with the thicker first-year ice, but the most frequent level ice thickness of 2.5 m can still be seen. The second-year floe is composed almost exclusively of deformed ice. Note that also snow thickness increases with increasing age of the ice in these Antarctic examples.

The ultimate variable to assess the shrinking or growing of the global sea ice cover is ice volume, i.e. the mathematical product of areal ice coverage and ice thickness. In contrast to ice thickness, sea ice coverage can be monitored reasonably well from space using satellites (Chapter 6). However, from the discussion above, it follows that as long as the ice thickness is unknown, the observed recent changes of ice coverage reported in that chapter are difficult to interpret in terms of overall ice volume and climate signals. These changes are mainly due to a retreat or advance of the ice edge in certain regions. It should be noted, however, that the location of the ice edge is a result of an equilibrium between ice drift, new ice formation and melting, i.e. atmospheric heat flux (including air temperature) and ocean heat flux.
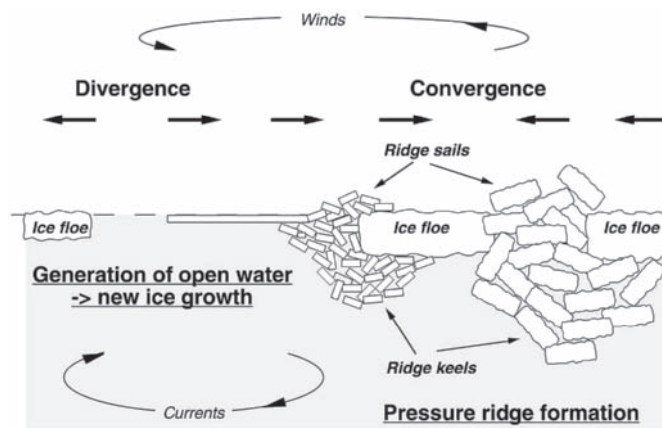
Fig. 4.1 Illustration of the processes that dynamically (i.e. by divergent or convergent ice motion and deformation) modify the ice thickness distribution.
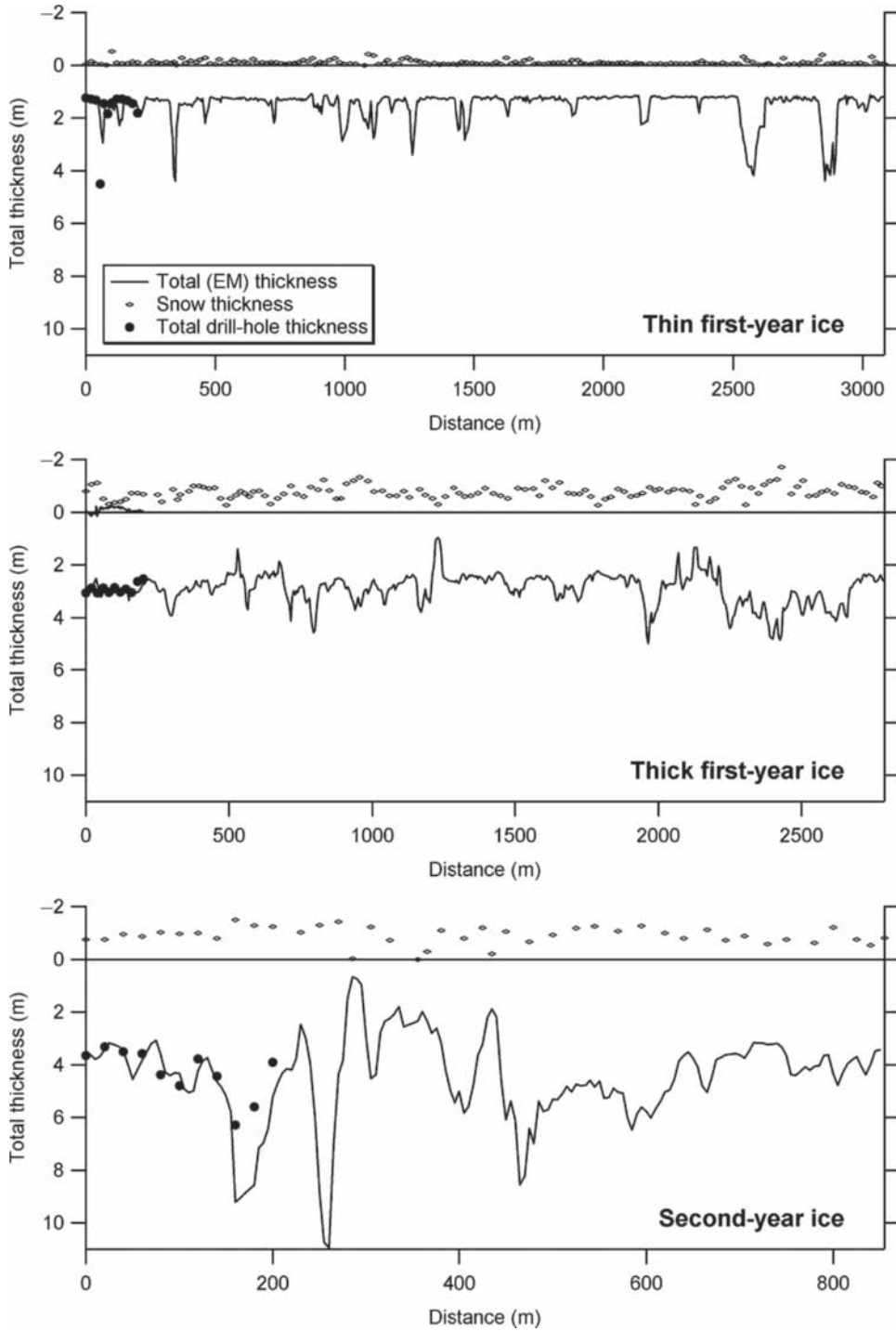
Fig. 4.2 Thickness profiles of (a) thin first-year, (b) thick first-year and (c) second-year ice floes in the Weddell Sea obtained by ground-based EM sounding and drilling. The graphs show total (ice plus snow) thickness plotted downwards from $Z = 0$, and snow thickness plotted upwards, to give an approximate representation of the surface and bottom morphology. Note the different horizontal scales and number of measurements shown in each panel.

Particularly, the latter is a function of the velocity and heat content of ocean currents, whose origin usually is in non-polar latitudes. Prominent examples are the West Spitzbergen and Barents Sea branches of the Norwegian Current, which are the northward extensions of the Gulf Stream. Due to these complexities of the air–ice–ocean system, even the retreat of an ice edge is not necessarily linked to an overall decrease of ice volume.

This chapter presents the physical and statistical approaches used to understand and simulate the ice thickness distribution on a local and regional scale, as well as what is known about the global distribution of ice thicknesses. Different methods to determine ice thickness are presented, as well as some recent results of observations of the variability and trends of sea ice thickness in certain regions.

4.2 The sea ice thickness distribution

Statistical description

Figure 4.3 shows aerial photographs of typical ice regimes of first-year ice in the Weddell Sea, heavily deformed multiyear ice in the Lincoln Sea north of Ellesmere Island, Canada, and second-year ice at the North Pole in summer. The photos show obvious differences of the morphology of the ice. These also represent differences in thickness, as the floating ice is generally in isostatic equilibrium and higher surface elevations indicate regions of deeper drafts and thicker ice. Large level areas of first-year ice (Fig. 4.3a) indicate a uniform thickness distribution, with only few ridges contributing to thicker ice. In contrast, the heavily deformed multiyear ice (Fig. 4.3b) comprises extensive regions of thick pressure ridges. The ice is generally much thicker, but there are also few regions of thinner ice which forms occasionally in leads opening between the thick multiyear ice floes. In contrast, in summer, strong surface melting occurs even at the North Pole, and the ice surface is then extensively covered with melt ponds (Fig. 4.3c). These cause local thinning and therefore contribute to a general roughening of the ice. The modes of second-year thickness distributions (Fig. 4.3c) are therefore often broader than the modes of first-year ice (Fig. 4.3a). When leads open between floes in summer, they do not refreeze for a while, introducing regions with zero ice thickness.

The thickness distribution is defined as a probability density function (PDF) $g(h)$ of the areal fraction of ice with a certain ice thickness in a certain region R (Thorndike et al., 1975). The PDF of ice thickness $g(h)$ is given by:

$$g(h) \, \mathrm{d}h = \mathrm{d}A(h, h + \mathrm{d}h)/R$$

where $\mathrm{d}A(h, h + \mathrm{d}h)$ is the areal fraction of a region R covered with ice of thickness between h and $(h + \mathrm{d}h)$. In practice, the thickness distribution is mostly obtained along linear profiles, and $\mathrm{d}A$ and R are one-dimensional, with R as the total length of the profile. $g(h)$ is derived by dividing a frequency histogram of ice thickness data by the bin-width ($\mathrm{d}h$). Thus, its dimension is m^{-1}. The advantage of using a PDF instead of a normal frequency distribution is that the numerical value of each thickness bin is independent of the bin-width used in calculating the histogram. This may be required if numerical values of thickness histograms are to be compared with other distributions, or are used to parameterize the thickness distribution in numerical equations for computer models. For most practical applications, it is sufficient to calculate the frequency distribution and to give results in fractions or as percentages.
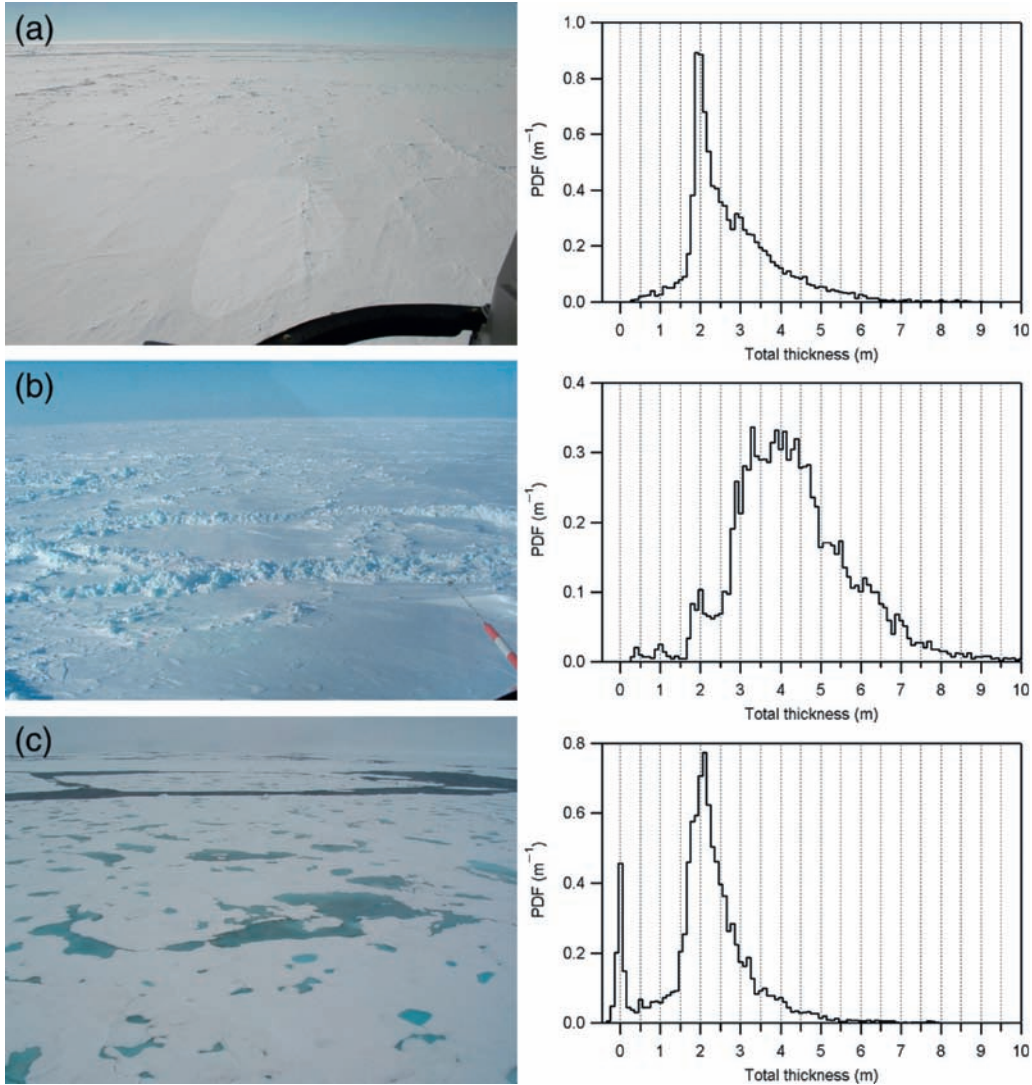
Fig. 4.3 Aerial photographs of typical sea ice types and conditions, and graphs of their corresponding ice thickness distributions (given as probability density functions – PDFs – of total (ice plus snow) thickness): (a) first-year ice in the Weddell Sea, (b) heavily deformed multiyear ice in the Lincoln Sea and (c) second-year ice at the North Pole in summer.

Figure 4.3 also includes the ice thickness distributions of the ice regimes depicted in the aerial photos, typical of ice thickness distributions in general. The distributions are dominated by one or several modes originating from the most frequently occurring thickness classes. Mostly, the modal thicknesses represent the thickness of level ice, as this covers the largest areal fractions of any given sea ice region. The uniformity of the level ice thickness in Fig. 4.3a results in a very narrow, sharp mode of 1.9 m (Table 4.1). The mixture of floes of different multiyear age accumulated over the years results in blurred modes of between 4.3 and 4.9 m in the example of Fig. 4.3b. In addition, newly formed ice in leads and polynyas

Table 4.1   Mean and modal ice thickness of profiles in Fig. 4.2.

	Mean ± SD	Mode
Fig. 4.2a	1.5 ± 0.6 m	1.2 m
Fig. 4.2b	2.9 ± 0.6 m	2.5 m
Fig. 4.2c	4.4 ± 1.7 m	3.6 m
Fig. 4.3a	2.8 ± 1.1 m	1.9 m
Fig. 4.3b	4.3 ± 1.5 m	0.4, 1.0, 2.0, 3.3, 3.9 m
Fig. 4.3c	2.2 ± 1.1 m	0.0, 2.1 m

causes modes at thicknesses of 0.4, 1.0 and 2.0 m. The presence of open water as in Fig. 4.3c introduces a mode or delta function at a thickness of $h = 0.0$ m. The long tails of the distributions represent the amount and thickness of pressure ridges. Ice thicker than 6 m is abundant in the multiyear ice regime of the Lincoln Sea (Fig. 4.3b), while it is almost absent in the younger ice regimes of the Weddell Sea and North Pole (Fig. 4.3a,c). As a consequence, there is quite some difference between the modal and mean thickness of any ice regime, and it is important to consider the kind of thickness value when interpreting the results of thickness observations. Table 4.1 compares modal and mean thicknesses of the thickness profiles shown in Fig. 4.2 and of the thickness distributions shown in Fig. 4.3. Depending on the degree of deformation, pressure ridges can contribute as much as 30–80% to the total ice volume of a floe or ice field. Therefore, there have been extensive efforts to statistically describe the occurrence and thickness of ridges. After identifying ridges by means of certain criteria from a thickness profile, not only the thickness distributions, but also spacing distributions can be calculated. Interestingly, the tails of both thickness and spacing distributions behave systematically, and can be well described by means of exponential or log-normal functions such as:

$$n(h) = A \exp(-Bh)$$

where $n(h)$ is the thickness or spacing distribution and A and B are coefficients derived from the mean thicknesses and spacings (Wadhams, 1994). However, it should be noted that there is some dispute as to which statistical function really fits best (Wadhams, 1994). Fortunately, this seems to be of little practical importance.

Modelling changes of the ice thickness distribution

As mentioned earlier, understanding and predicting the ice thickness distribution requires consideration of both thermodynamic as well as dynamic processes (Fig. 4.1). The temporal development of the ice thickness distribution $\partial g/\partial t$ can be written as (Thorndike et al., 1975):

$$\partial g/\partial t = -\partial(fg)/\partial h + \mathrm{div}(\nu g) + \Phi$$

Three terms contribute to this equation (Fig. 4.4): $f(h,x,t) = dh/dt$ is the thermodynamic growth or melt rate of ice of thickness h at a location x and time t. ν is the ice drift velocity vector, and Φ is the so-called redistribution function.
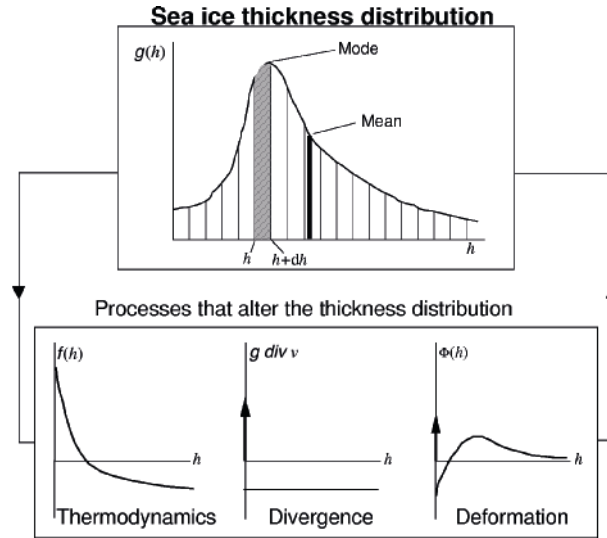
Fig. 4.4 Illustration of the contribution of the different terms and processes in equation 4.1 to the ice thickness distribution.

Thermodynamics

The thermodynamic growth term of equation 4.1 has been described in detail in Chapter 2. It should be noted again, however, that it is dependent on ice thickness itself, i.e. that thin ice grows faster than thick ice due to steeper temperature gradients. On the other hand, thermodynamic growth implies that thick ice exceeding a certain equilibrium thickness (e.g. pressure ridges) will melt, even in winter, if the oceanic heat flux exceeds the (generally low) heat flow through thick, insulating ice. The heat conductivity of snow ranges between 0.11 and 0.35 W m^{-1} K^{-1} depending on its density and grain structure (see Chapter 5). This is only one-seventh or less of the heat conductivity of sea ice. Therefore, the presence of snow significantly reduces ice growth and the equilibrium ice thickness.

Divergence and advection

The second term in equation 4.1 represents ice-divergence and advection due to ice motion. As mentioned earlier, the ice is subject to external forces, mainly due to wind and current action (see equation 4.2 below). These forces cause the ice to drift. Away from the coast or other obstacles, the ice will drift freely, and drift direction and speed are closely related to the geostrophic wind. By comparing the motion of drifting buoys deployed on ice floes with geostrophic wind fields, it has been shown that ice in the Arctic drifts at 1% of the mean wind speed, and with an angle of 18° to the right (Colony & Thorndike, 1984; Serreze et al., 1989). For the Weddell Sea, these numbers are 1.6% and 10–15° to the left, respectively (Kottmeier et al., 1992).

   Divergence within the ice generates cracks, leads, or polynyas with open water where new ice will form. Thus, for a certain region, divergence removes ice of finite thickness and causes a delta signal at zero thickness in the thickness distribution (Fig. 4.4).

Deformation/convergence

The last term in equation 4.1 is the redistribution function describing how thin ice is deformed and transformed into thicker ice classes in the case of ice convergence and deformation. It is the most critical term to realistically model the temporal development of the thickness distribution. It is also the most unknown term, since it depends very much on fracture mechanics, and is very dependent on factors like small-scale ice properties, friction between ice blocks among each other as well as at the snow and ice interfaces, and deformation energy and lengths. A very promising approach to ridge formation modelling has been presented by Hopkins (1994) using a dynamic ridge growth model, where the fate of single ice blocks was computed as a function of external forces. However, thin ice will generally deform more easily than thick ice.

On a regional scale, the large-scale spatial thickness distribution is obtained by solving a momentum balance equation considering the main forces acting on a unit area of the sea ice cover:

$$\mathrm{M}\, a = \tau_a + \tau_w + F_C + F_i + F_t, \qquad\qquad \text{(Equation 4.2)}$$

where the force of mass M times the acceleration a balances the sum of the air and water drags τ_a and τ_w, the Coriolis force F_C, internal ice forces F_i and of the force due to sea surface tilt F_t. Usually, the first two terms are most dominant by more than an order of magnitude. For every model grid cell, mean ice thickness is derived by solving equation 4.2 for ice motion, and distributing the ice volume drifted into a cell equally over the cell area assuming mass conservation. Clearly, as with the redistribution term in equation 4.1, ice strength and rheology are of great importance here. The first models involving plastic or viscous-plastic rheologies were developed by Hibler (1979) and Coon (1980). The rheology describes a viscous flow of an ice field, with plastic deformation once ice concentration and internal ice forces exceed a certain threshold. While these first models prescribed the atmospheric and oceanic forces acting on the ice, today complex coupled atmosphere–ice–ocean models exist (Zhang et al., 2000; Timmermann et al., 2002; Köberle and Gerdes, 2003; Rinke et al., 2003; Gerdes and Köberle, 2007; Holland et al., 2006).

Melting

Melting commences once the surface energy budget becomes positive. The excess energy is consumed by the latent heat of fusion needed for melting (Chapter 2). Thus, the thermo-dynamic term in equation 4.1 (thickness balance) just becomes negative. A meteorological consequence is, e.g., that even in summer, air temperatures hardly become positive over ice surfaces.

On large scales, melting patterns correspond to large-scale meteorological conditions and to ocean heat flux regimes. However, even more than with freezing (see above), on small scales melt rates depend critically on the ice thickness distribution itself, and are different for different thickness classes and ice types (Perovich et al., 2003). The heat flux through pressure ridges is lower than through level ice because of their greater thickness. Consequently, they would melt faster. As their keels protrude far down into the water, they might even reach into warmer water. More importantly, ridge keels contribute to the roughness of the

ice underside, thereby increasing upward turbulent fluxes of heat. The flanks of ridge sails are exposed more normally to the incident solar radiation than ridge crests, as solar elevation is low in polar regions. Therefore, melting can be expected to be higher on the flanks. Although the variations of melt rates might seem to be rather small, they can contribute to significantly different thickness changes in the course of the ablation season.

Much stronger differences in melt rates exist on small thickness classes, i.e. on level ice (Perovich et al., 2003; Eicken et al., 2004). Snow and ice melt water primarily accumulates at topographic low points to form melt ponds. Even small amounts of snow wetting, and the formation of melt ponds, significantly reduce surface albedo. Typical surface albedos are 0.8 for snow, 0.6 for bare ice and 0.15–0.3 for melt ponds. Thus, once formed, melt ponds absorb more energy than the neighbouring snow or bare ice, thereby increasing local melt rates. Throughout the summer, the surface of melt ponds falls down to sea level, and vertical pond walls form reaching deep into the floe. This positive feedback causes significant changes to the ice thickness distribution of level ice, as it contributes to an increase in surface roughness. This is also demonstrated in the thickness distribution shown in Fig. 4.3c, where melt ponding has caused a roughening of the ice and led to a widening of the dominant mode of the distribution.

The discussion in this section shows that many factors are responsible for shaping the ice thickness distribution. Thinning, for instance, can result from melting, but also from advection of thinner ice into a certain region. Therefore, any interpretation or forecast of changes of the ice thickness distribution in terms of climate change has to take into account both thermodynamic and dynamic processes. This will be highlighted later with the discussion of observations of seasonal, interannual and decadal variations (Section 4.4).

Global sea ice thickness distributions

Figure 4.5 shows maps of mean ice drift and thickness in the Arctic and Southern oceans, as derived from two coupled ice–ocean models operated at the Alfred Wegener Institute (North Atlantic Ocean Sea Ice Model [NAOSIM], Köberle & Gerdes, 2003; and the Bremerhaven Regional Ice–Ocean Simulations [BRIOS], Timmermann et al., 2002). Both models have a three-dimensional multilayer ocean model coupled to a dynamic–thermodynamic sea ice model with a viscous-plastic rheology (Hibler, 1979; see above).

It becomes immediately obvious that Arctic sea ice is generally thicker than its counterpart in the Southern Ocean. In the model simulations, most Arctic ice is thicker than 2 m. In contrast, hardly any ice grows as thick in the Southern Ocean. These hemispheric contrasts are due to at least five main differences in the thermodynamic and dynamic boundary conditions of ice growth in the Arctic and Southern oceans:

(1) *Ocean heat flux*: One fundamental difference between the Arctic and Southern oceans is the occurrence of a fresh mixed layer in the Arctic overlying a strong pycnocline. This layer is fed by the inflow of freshwater from large rivers, mainly from the Siberian continent. The Arctic Ocean receives approximately 10% of the world river run-off. The fresh mixed layer is very stable and prohibits any significant heat fluxes from the much warmer Atlantic water underneath. A typical value for the ocean heat flux in the Arctic Ocean is 4 W m^{-2}. The 'Atlantic layer' at a depth of 200–300 m is 1–2°C warm.
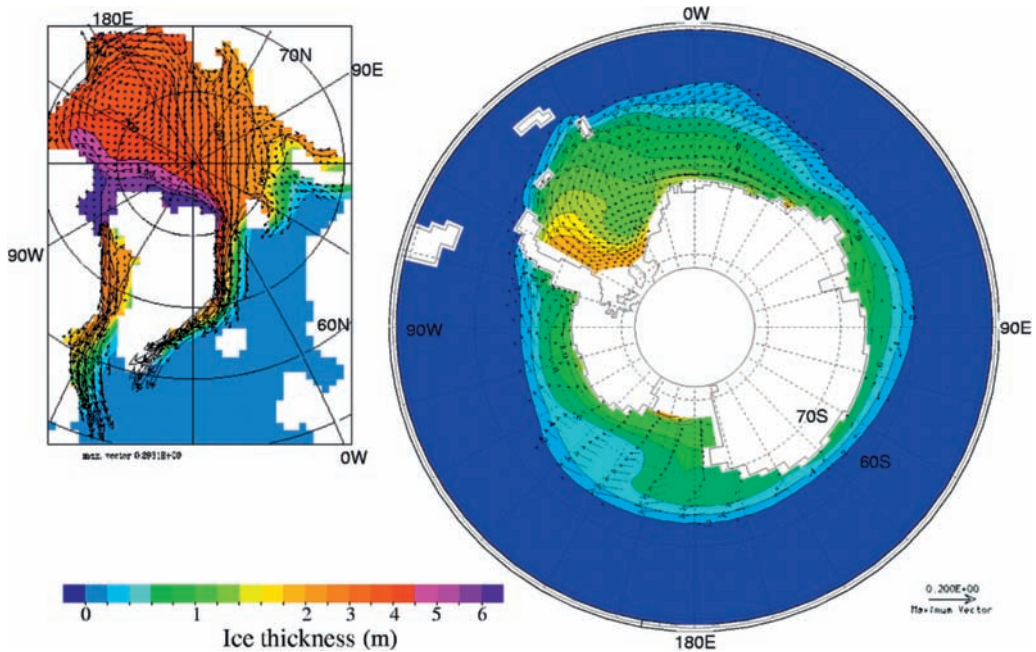
Fig. 4.5 Maps of the Arctic and Southern oceans, showing model results of mean ice drift speed and direction (vectors) as well as mean ice thickness (colours), calculated for the winters of 1985–93. (a) Köberle & Gerdes (2003). (b) Timmermann et al. (2002). Note that the thickness intervals are irregular.

This heat would be sufficient to melt all ice during summer (Barry et al., 1993). In the Southern Ocean, no rivers enter the seas. Therefore, the mixed layer is much saltier and not well stratified. Mean ocean heat fluxes amount to about 40 W m^{-2}.

(2) *Snow thickness*: With a thermal conductivity between 0.11 and 0.35 W m^{-1} K^{-1} (Massom et al., 2001), snow is a strong thermal insulator. Therefore, ice with a thick snow cover grows slower than if the snow were thin. The Arctic Ocean is surrounded by large continents and mean snow thickness reaches only about 0.3 m in spring (Warren et al., 1999). In contrast, Antarctic sea ice is usually covered by thick snow. On perennial ice in the Pacific sector or in the western Weddell Sea mean snow thickness can be larger than 0.5 m (Massom et al., 2001). This is due to the fact that the sea ice areas are completely surrounded by oceans, which provide a permanent moisture source. In the South, sea ice may collect the snow blown off the continental ice shelves. As a consequence of the thick snow and high ocean heat fluxes, Antarctic ice may melt at its underside even during winter, because the temperature gradients through the ice are only small.

(3) *Ice age*: Most ice in the Arctic Ocean drifts for 3–6 years (Colony & Thorndike, 1984) until it leaves the Basin through the Fram Strait where it melts further south. The older an ice field becomes, the more deformation events it will experience, where it thickens by the accumulation of pressure ridges. This dynamic thickening is accompanied by passing through several winters where the ice can also thicken by thermodynamic growth until it reaches an equilibrium thickness. In contrast, most Antarctic ice melts during summer. Thus, it rarely becomes older than 1 year, and only few regions with

perennial ice exist in the western Weddell Sea and southern Bellingshausen, Amundsen and Ross Seas.

(4) *Divergence versus convergence*: As mentioned above, the Arctic Ocean is surrounded by continents, and thus ice motion is confined by coasts where the ice converges and thickens by deformation. In contrast, ice drift around Antarctica is mostly divergent (Kottmeier et al., 1992), with a northerly drift component towards the surrounding open oceans. Divergence causes the opening of polynyas and leads, and the addition of thin new ice to the thickness distribution.

(5) *Latitude*: Most of the ice in the Arctic is at latitudes north of 70°N, whereas in the southern hemisphere most ice extends into much lower latitudes, as far north as 55°S. Thus, air temperatures, total incoming solar radiation and the length of the summer season are generally lower in the Arctic than in the Southern Ocean. However, the Antarctic ice sheet is a giant cold reservoir, and the sea ice region is well isolated from lower latitudes by the atmospheric and oceanic flow regimes of the Circumantarctic Current so that warm and moist air advection are not as important as they are for the Arctic. Due to these, strong surface melting rarely occurs on sea ice in the Southern Ocean (Nicolaus et al., 2006). This is in stark contrast to conditions in the Arctic, where strong surface melting occurs in summer even at the North Pole at much higher latitudes than in the Antarctic.

The order of these points is arbitrary and does not include any ranking between the most important and less important factors. The final ice thickness depends on the magnitude of, and interrelation between, these different aspects. Clearly, both dynamic and thermodynamic factors are responsible for the hemispheric differences.

The maps in Fig. 4.5 also show large regional thickness variations within each hemisphere itself. These are primarily a result of ice motion and deformation. As between 30% and 80% of the volume of an ice field is contained within pressure ridges, the mean thickness of a region is more dependent on the number and thickness of ridges than on the thickness of level ice. In other words, for the overall ice volume within a certain region, dynamics is more important than thermodynamics. Therefore, on a regional scale, the average ice thickness distribution is determined by the prevailing atmospheric circulation regimes, which are responsible for mean ice motion and the dominant drift directions. Where the ice drifts against, or shears along a coast, there will be strong ice pressure, and the ice will become heavily deformed. As a result, the mean thickness in regions with mean drift convergence is larger than in regions with mean divergence, where thin new ice is permanently generated and exported.

The arrows in Fig. 4.5 show the dominant drift patterns which develop as the result of the prevailing atmospheric circulation. Although the ice motion is presented only for winter in the figure, this is also representative for the average annual conditions. In the Arctic, mainly two drift systems exist. The Beaufort Gyre is an anticyclonic gyre in the Canada Basin north of the Canadian Archipelago and Alaska. It is caused by quasi-permanent high-atmospheric pressure over the Beaufort Sea. The Beaufort Gyre can transport ice floes for a couple of years before they are exported into the Transpolar Drift. This is the other prominent drift system, which transports ice from the source regions on the Siberian Shelves within about 2–3 years across the North Pole into the Fram Strait and the East Greenland Current, where it finally melts. The Transpolar Drift is mainly driven by low-pressure systems passing from the North Atlantic into the Barents and Kara Seas.
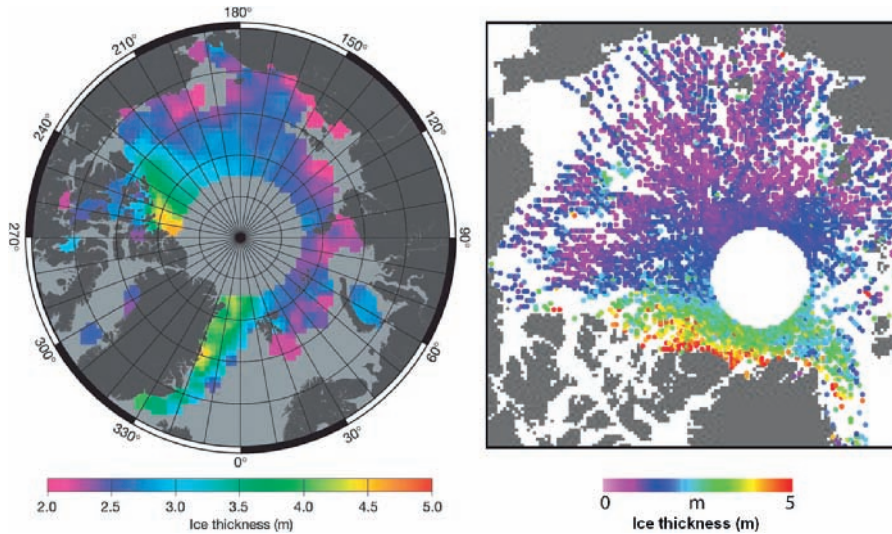
Fig. 4.6 Arctic sea ice thickness maps derived from satellite altimetry. Left: Average October–March ice thickness for the period 1993–2001 obtained from ERS radar altimetry (Laxon et al., 2003). Right: Mean ice thickness in October and November 2006 from ICESat laser altimetry (Kwok and Cunningham, 2008). See Section 4.3 for description of methods.

On average, these drift patterns push the ice against the coasts of northern Greenland and the Canadian Archipelago. Consequently, as a result of strong convergence and deformation, the thickest ice is found in these regions. Mean maximum thicknesses range between 6 and 8 m, mainly resulting from the large spatial density of ridges. Another region with predominantly convergent conditions can be seen in the East Siberian and Chukchi Seas. If the Beaufort Gyre is very strongly developed, ice is pushed against the coast of the New Siberian Islands.

The youngest and thinnest ice is found along the Siberian Shelf, where prominent polynyas occur and from where ice is permanently exported into the Transpolar Drift. The modelled basin-scale thickness distribution is in general agreement with submarine sonar measurements collected over many years over most of the Arctic Ocean (Bourke & Garret, 1987). It is also well represented in recent thickness maps derived from satellite altimetry (Fig. 4.6, see Section 4.3 for a description of methods).

Figure 4.5 shows that the thickest ice in Antarctica occurs close to the continent, in accordance with the greatest latitude and with the vicinity to the coast where it is sporadically compressed. The most prominent feature, however, is the thickest ice in the southern and western Weddell Sea. On the one hand, this is one of a few regions possessing perennial ice. On the other hand, it is a region where ice drift is directed towards the coast, and subsequently much deformation occurs. The so-called Weddell Gyre is caused by low average sea level pressure over the central Weddell Sea. It should be noted that both the Beaufort Gyre and the Weddell Gyre rotate clockwise. However, due to the Coriolis force, this results in ice convergence within the gyre centre on the northern hemisphere, whereas clockwise circulation results in net divergence inside the gyre in the south. The great thickness in the western Weddell Sea is therefore caused by ice motion away from the divergent gyre centre, with the Antarctic Peninsula acting as an obstacle for the ice drift.
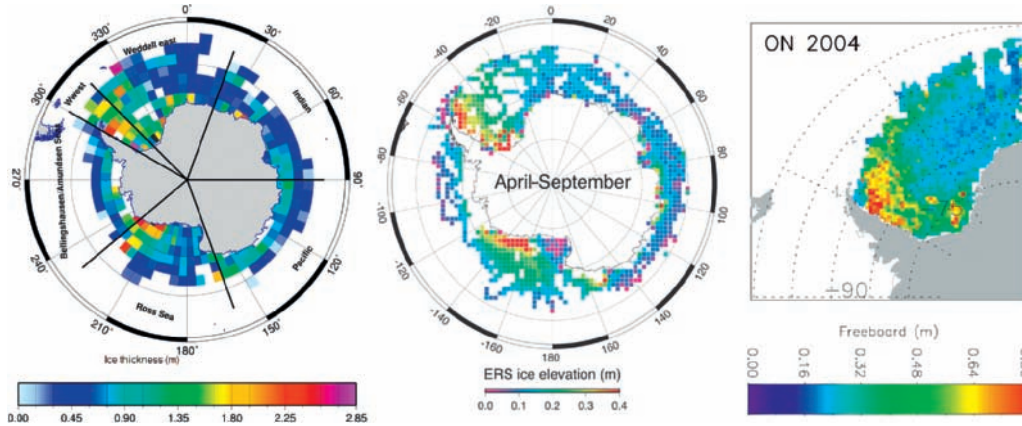
Fig. 4.7 Antarctic sea ice thickness maps derived from visual observations and satellite altimetry. Left: Mean ice thickness from ship-based visual observations performed between 1981 and 2005 (Worby et al., 2008). Centre: Mean ice freeboard measured by ERS radar altimetry between April and September 1995–2002 (Giles et al., 2008). Right: Mean snow freeboard observed by ICESat laser altimetry in October and November 2004 (Zwally et al., 2008).

In contrast to the Arctic, regional ice thickness distributions in the Antarctic are less well known, because only few systematic measurements have been performed. The use of military nuclear submarines is prohibited by the Antarctic Treaty. However, thickness maps derived from visual observations and satellite altimetry show similar patterns (Fig. 4.7) as those computed by the model.

It should be noted that the drift systems and thickness distributions shown in Fig. 4.5 represent long-term average conditions. There is large seasonal, interannual and decadal variability superimposed on these mean patterns, which is also obvious by comparisons with the satellite data in Figs. 4.6 and 4.7, and which will be highlighted later in Section 4.4.

4.3 Measurement techniques

While extent and concentration of sea ice can be measured with sufficient accuracy by satellites from space, determining its thickness is much more involved, even from aircraft or while standing on the ice. This is due to its relative thinness, which is a challenge for any geophysical measurement technique. Therefore, most methods are indirect measurements, which derive thickness from a related variable which is actually measured instead.

The traditional direct method of ice thickness measurement is to drill a hole into the ice by hand or with a gas- or battery-driven motor. The thickness is measured with a ruler lowered into the hole. This technique is described in detail by Haas & Druckenmiller (2009). It is also the only method allowing determination of the thickness of the ice and snow, as well as ice draft and freeboard (the depth of the ice underside below the water level and the height of the snow/ice-interface above the water level, respectively) with one measurement and at the same time. Although drilling is tedious, and only limited data can be gathered in a short

time, most thickness information about the relatively thin Antarctic sea ice still comes from drill-hole measurements (Lange & Eicken, 1991; Worby et al., 1996). Only recently have moored upward looking sonars (ULS) and electromagnetic (EM) methods as well as satellite altimetry (see below) been applied in Antarctica.

There are also a number of studies involving video recording of ice floes broken by an icebreaker. The broken ice fragments are often moved side-up against the ship's hull, revealing their cross profile. From the video footage, the thickness can then be manually retrieved. Some studies have shown reasonable agreement of level ice thickness estimates compared with data derived from other methods (Lensu & Haas, 1998). Similarly, ice thickness can be determined just visually while ice breaking. A coordinated, systematic collection of visual ice observations has been compiled by the international Antarctic Sea Ice Processes and Climate (ASPeCt) program (Worby et al., 2008).

Other direct thickness measurements would be pulse radar or ultrasonic sounding where the travel time of a signal through the ice is measured. For sufficient resolution and accuracy, the small thickness requires short radar or sound wavelengths of only some decimetres. However, these high-frequency signals suffer from the heterogeneity of sea ice due to salt inclusions, fractures and rafted ice blocks. These lead to strong signal scatter on the one hand, and to highly variable signal propagation velocities, which must be known to calculate thickness from travel time. Recent new technology developments have led to the design of broadband, continuous-wave frequency-modulated (CWFM) radars for snow and ice thickness measurements, which may improve some of the issues related to absorption and resolution (Kanagaratnam et al., 2007; Holt et al., 2008).

The following sections provide short overviews of the methods most commonly applied today, and which have resulted in the most abundant thickness data so far. More detailed descriptions of these and other techniques including data examples are given by Haas and Druckenmiller (2009).

Submarine and moored ULSs

So far, most thickness data have been obtained by means of upward-looking sonar (ULS) or ice profiling sonars (IPS) mounted either on military nuclear submarines (Bourke & Garret, 1987; Rothrock et al., 1999; Wadhams & Davis, 2000; Rothrock et al., 2008) or on oceanographic moorings (Strass & Fahrbach, 1998; Vinje et al., 1998; Harms et al., 2001, Melling & Riedel, 2004; Melling et al., 2005). With this method, estimates of draft are obtained, i.e. of the depth of the ice underside below the water level, which is a reasonable proxy for ice thickness. The instruments measure the travel time, t, of a sonar pulse transmitted by the ULS and reflected back from the ice bottom (Fig. 4.8). Additionally, the depth of the sonar beneath the water level, z, and the sound velocity, v, in the water must be known. Then, ice draft, d, is calculated according to

$$d = z - v * t/2$$

The depth of the ULS is derived from pressure sensors, whose signals are also dependent on air pressure. The sound velocity profile is either assumed constant with a certain sound speed or taken from a mixed layer model (Strass & Fahrbach, 1998). This can become quite complicated in the case of strong water stratification or when the measurements are performed close to ocean frontal zones. A plausibility test for the depth measurement or the
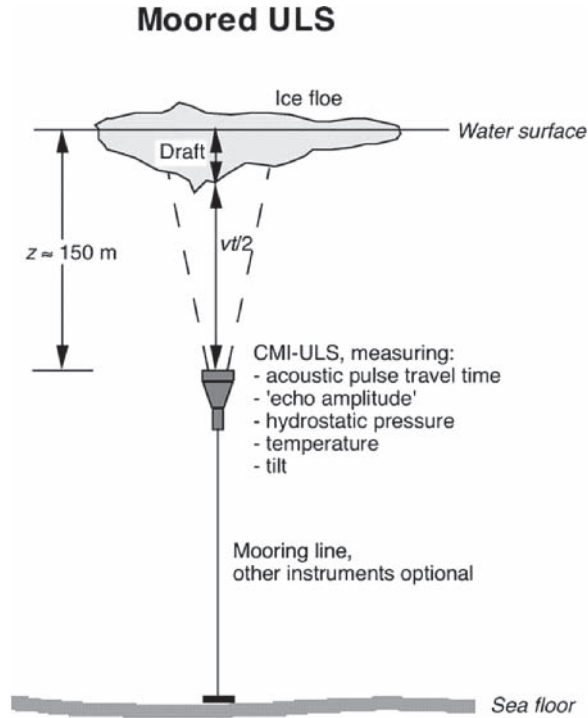
Fig. 4.8   Illustration of ULS ice thickness measurements from an oceanographic mooring. Adapted from Strass and Fahrbach (1998)

sound velocity profile can be performed when profiling open leads with ice thickness zero. Then, the measured sonar distance must equal the ULS depth.

Ice thickness, h, is calculated from draft, d, by assuming isostatic equilibrium, a certain snow depth, z_s, and water, ice and snow densities ρ_w, ρ_i and ρ_s:

$$h = (\rho_w\, d - \rho_s\, z_s)\, /\, \rho_i \qquad\qquad\qquad\qquad \text{(Equation 4.3)}$$

The values for ice and snow density, as well as snow depth, are reasonably well known so that only small errors arise for h.

Due to the problems of assuming the correct sound velocity profiles and ULS depth, estimates of the accuracy of absolute level ice thickness measurements range between 0.05 m (Strass & Fahrbach, 1998) and 0.25 m (Rothrock & Wensnahan, 2007). However, an ULS is very sensitive to pressure ridge keels, and their depth relative to the level ice bottom can be very well determined.

Submarines allow for long-range, basin-scale transects for determining the ice thickness profile. However, so far, submarine surveys have only been performed in conjunction with military cruises. This means they provide only snapshots of the ice thickness distribution, because the transects are not performed in a systematic manner. As a consequence, measurements often have to be corrected for seasonal variability before they can be compared with each other (Rothrock et al., 2008). Some improvement was achieved with the SCICEX

missions, the Scientific Ice Expeditions of the US navy between 1995 and 1999. These cruises were dedicated to meeting scientific goals, and a small number of scientists were allowed onboard the submarines. Meanwhile, Autonomous Underwater Vehicles (AUVs) are being developed, and they may provide an alternative for the use of submarines in the near future (Wadhams et al., 2006; Dowdeswell et al., 2008). They can also be used in Antarctica, where the operation of military, nuclear submarines is prohibited by the Antarctic Treaty.

ULSs mounted on oceanographic moorings provide long time series of ice thickness in a single location. These allow studying the temporal development of the ice thickness distribution, e.g. in the course of the growing season (Melling & Riedel, 2004). Transects can be achieved if several moorings are simultaneously operated across a certain region, as current arrays in Fram Strait (Vinje et al., 1998) or the Weddell Sea (Strass & Fahrbach, 1998; Harms et al., 2001). The thickness distribution between single moorings can then be interpolated. Combined with ice drift velocity data retrieved from satellite imagery or buoys, mooring data allow for the calculation of ice volume fluxes, Q, according to:

$$Q = v\,h$$

where v is ice velocity and h is ice thickness.

While moored ULS can provide very valuable continuous data, the operation of the instruments at water depths of 50–150 m for periods of one, or more, years is still a technological challenge. Similarly, the recovery of the instruments is often difficult, or instruments may be lost, e.g. as a result of commercial trawl fishing. Therefore, the success rate of moored ULS measurements is only about 70%. Moorings cannot be deployed in shallow waters, where they might be destroyed by ridge keels or icebergs.

Electromagnetic induction sounding

In contrast to high-frequency EM techniques employing radar wavelengths low-frequency, frequency-domain electromagnetic induction (EMI) sounding has become a widely applied method. Typical operating frequencies are between 10 and 100 kHz. The technique is usually employed in geophysical problems related to the mapping of ore or groundwater deposits on land. With EM sounding, the mean or apparent electrical underground conductivity is determined. Sea ice is almost an electrical insulator with low electrical conductivities between 0 and 50 mS m^{-1} (milli-siemens per metre). In contrast, cold sea water with a salinity of 32 has a conductivity of 2500 mS m^{-1}. Consequently, the overall apparent conductivity of the underground decreases with increasing ice thickness, i.e. the more ice occupies the half-space underneath the EM instrument.

The subsurface apparent conductivity is measured by means of two coils, one transmitter and one receiver coil (Fig. 4.9). The transmitter generates a primary EM field which induces eddy currents in the underground. As induction is dependent on the conductivity of the material, the field penetrates through the sea ice almost unaffectedly, and eddy currents are mainly induced in the sea water just below the ice bottom. These eddy currents in turn generate a secondary EM field, whose amplitude and phase are measured with the receiver coil. The secondary field amplitude and phase are primarily dependent on the distance between the eddy currents at the water surface and the coils. This distance is equivalent to ice
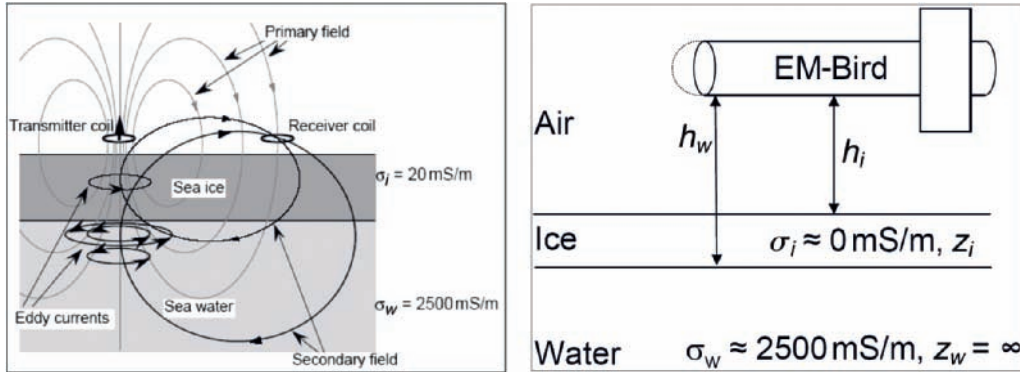
Fig. 4.9   Left: Principle of EM ice thickness sounding, showing the generation of a primary field by a transmitter coil and induction of a secondary field, whose strength and phase are measured by a receiver coil. Right: If an EM instrument is operated above the ice, ice thickness Z_i is obtained from the difference of measurements of the instrument's height above the water and above the ice surface, h_w and h_i, respectively (Haas et al., 2008b). h_i is usually determined with a laser altimeter. Note that Z_i corresponds to the total thickness, i.e. the sum of ice plus snow thickness.

thickness, if the instrument is lying on the ice. Apparent conductivity is calculated from the imaginary part of the secondary field. Comparison with drill-hole measurements yielded the empirical equation:

$$h = 7.81 - 1.09 \ln(\sigma_a - 62.5) \qquad\qquad\qquad \text{(Equation 4.4)}$$

for the calculation of ice thickness h from apparent conductivity σ_a using a Geonics EM-31 instrument (Haas et al., 1997). Similar equations have been derived by Haas & Eicken (2001) and Eicken et al. (2001), with slightly varying coefficients due to different modal thicknesses in the respective study regions.

The Geonics-EM31 is most widely used for sea ice thickness measurements and has a coil spacing of 3.66 m with an operating frequency of 9.8 kHz. For instruments with other frequencies and coil spacings, different equations would have to be developed. The equations can also be derived by numerical EM forward modelling, computing the EM response to a layered half-space (Anderson, 1979). More involved equations can be calculated from two- or three-dimensional EM models, which can also represent pressure ridges (Liu & Becker, 1990).

Figure 4.2 has already shown two examples of ground-based EM profiles. These were obtained by pulling an EM instrument installed on a sledge over the ice. Comparison with drill-hole measurements reveals a good agreement within ± 0.1 m over level ice. However, there is quite some disagreement over deformed ice. As the induced eddy currents possess a finite lateral extent, the resulting ice thickness estimate is some average over a certain area, called the 'footprint'. Estimates of the footprint diameter range between 3.7 and 10 times the distance between the EM instrument and the water surface, depending on the instrument configuration (Kovacs et al., 1995; Reid et al., 2006). Consequently, EM measurements

underestimate the maximum thickness of deformed ice such as ridge keels, because the induced eddy currents are also affected by the occurrence of water within and adjacent to deformed ice structures. The maximum thickness of pressure ridges can be underestimated by as much as 50%.

EM measurements are hardly affected by seasonally varying ice properties, because these do not affect ice conductivity very much (Haas et al., 1997). However, surface flooding or the occurrence of sea water-filled gap layers due to rafting or internal melting can lead to underestimates of ice thickness by EM sounding if they are not detected (Haas, 1998; Uto et al., 2006).

An advantage of the EM technique is that it can be applied also from above the ice without any ground contact. In this case, the EM measurement determines the distance h_w between the EM sensor and the water surface or ice underside, respectively (Fig. 4.9). The height h_i of the instrument above the ice surface can be measured with a laser or sonar range finder. Ice thickness is then obtained by subtracting h_i from h_w. This principle is widely applied from ships and aircrafts. However, it is important to note that the ice thickness thus obtained is the total, i.e. snow plus ice thickness, as the laser or sonar range finders do not penetrate into the snow cover.

Ship-borne measurements, performed from onboard icebreakers while steaming through the ice, can yield regional ice thickness information. They have been carried out under a variety of conditions primarily in thinner ice, allowing straight cruise tracks (Haas, 1998; Haas et al., 1999b, Reid et al., 2003; Uto et al., 2006). In addition, when performed in front of a ship or from another structure like a lighthouse or bridge pillar, these measurements can provide instant ice thickness information required for ship performance or ice load studies (Haas et al., 1999b; Haas & Jochmann, 2003). However, ship-based measurements are obviously limited by the ice itself since ships cannot penetrate the thickest ice. More importantly, most ships follow the route of least resistance, which is the one with the thinnest or absent ice. Therefore, representative information on regional ice thickness distributions can only be obtained on dedicated, scientific cruises.

The ultimate goal of EM sounding is to perform systematic, large-scale surveys using aircraft. Airborne sensors have been deployed from helicopters or fixed-wing aircrafts (Kovacs et al., 1987; Kovacs & Holladay, 1990; Prinsenberg & Holladay, 1993; Multala et al., 1996). Currently, two different types of helicopter systems are in operation: a towed instrument called an 'EM-Bird' (Haas et al., 2008b), and a system where the shell is hard mounted at the nose of the helicopter, the so-called 'IcePic' (Prinsenberg et al., 2002; Peterson et al., 2008). Extensive comparisons with drill-hole measurements and theoretical considerations have shown that the accuracy of these measurements over level ice is better than 10 cm (Pfaffling et al., 2007), but it is still unclear how ridge cross sections compare with results from other methods (Haas & Jochmann, 2003).

The EM-birds of the German Alfred Wegener Institute and of the University of Alberta in Canada operate at frequencies of 3.6 and 112 kHz, and have a maximum coil spacing of 2.7 m with an overall length of 3.4 m (Fig. 4.10). The bird is towed under a helicopter with a 20-m cable and operated 15–20 m above the ice surface. Its size and small weight of only 100 kg allow shipping to remote Arctic sites, operation by any kind of helicopter and deployment from small helicopter decks of icebreakers.

As can be seen from equation 4.4, the EM response decreases exponentially with increasing instrument height. Therefore, airborne systems must fly low and have to have very good

Fig. 4.10   The Alfred Wegener Institute's EM-bird with its towing helicopter in the background on an ice floe in the Arctic (photo by S. Goebell).

signal-to-noise ratios to be able to resolve even small signal changes. This is particularly challenging for systems as small as the EM-bird or IcePic.

Figure 4.11 shows two typical examples of ice thickness profiles obtained by helicopter-borne EM sounding. The profiles are superimposed on Synthetic Aperture Radar (SAR) imagery acquired by the European Space Agency's (ESA) Envisat satellite, which give an overview of the general ice conditions at the time of the helicopter flights. The data over the Lincoln Sea were obtained on May 14, 2005 (Fig. 4.11, left) (Haas et al., 2006). A mixture of darker first-year ice and brighter multiyear ice is visible on the SAR image. Their different ice thicknesses are well represented by the EM data, which also shows an ice thickness of 0 m over a bright-appearing polynya at the mouth of Nares Strait. First-year ice thicknesses ranged between 1 and 2.5 m, while the multiyear ice thickness mostly exceeded 4 m. Similarly, ice thicknesses and SAR backscatter delineate different ice regimes of heavily deformed first- and second-year ice and level, young first-year ice in the northwestern Weddell Sea between September 19 and October 10, 2006 (Fig. 4.11, right). The heavily deformed ice with high backscatter in the right part of the image had mean thicknesses of more than 3 m in the south, and was thinning northward, probably as a result of divergence and melting, which both affect the mean thickness. The first-year ice between the band of heavily deformed ice and the Antarctic Peninsula originated from a polynya in the Larsen A and B bays in the southwestern corner of the image. It had modal thicknesses of up to 1.5 m, with mean thicknesses of 2 m and more. However, a strong gradient towards the refrozen polynya was observed, where mean ice thicknesses only amounted to around 0.5 m.

As a by-product of ship-based and airborne EM measurements, the surface profile of the ice is obtained from the laser data. This provides information on surface roughness and pressure ridge statistics (von Saldern et al. 2006; Peterson et al. 2008). The laser measurements could thus partially compensate for the lack of accuracy of EM data over pressure ridges, if relationships between the height of ridges and their overall thickness could be established. At the very least, ice regimes can be described by their EM-derived distinct level ice thickness and the laser-estimated amount of ridged ice.
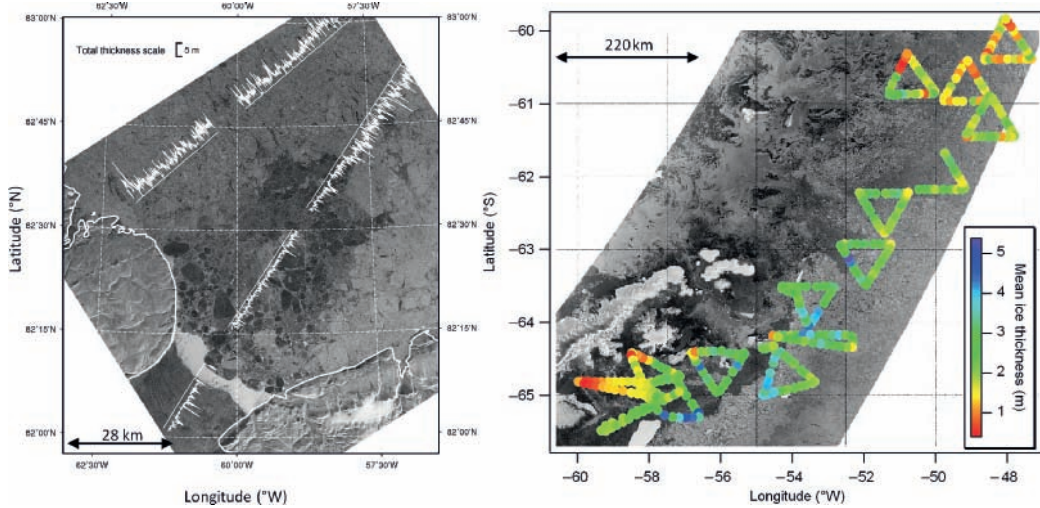
Fig. 4.11 Typical examples of thickness profiles obtained by helicopter-borne EM sounding, and comparison with satellite SAR images. Left: Ice thickness and ice conditions in the Lincoln Sea on 14 May 2005 (Haas et al., 2006) and (right) in the northwestern Weddell Sea between 19 September and 10 October 2006, with the SAR image showing ice conditions on 19 September. Coloured dots show mean ice thickness in 8-km long profile sections. Note the different scales of maps

The laser altimeter surveys of EM systems, or independent laser altimeter measurements, can be combined with differential GPS to accurately determine the altitude of the laser system over a reference surface like the water surface. Then, the freeboard of the ice can be estimated, and can be used as a measure of ice thickness (Hvidegaard & Forsberg, 2002). The estimation of ice thickness from airborne or satellite altimetric measurements of freeboard will be discussed in the next section.

Satellite altimetry

Significant progress has been made in recent years with the application of satellite laser and radar altimetry for the retrieval of ice freeboard or snow surface elevation, and for the estimation of ice thickness from those (Laxon et al., 2003; Kwok et al., 2004; Giles et al., 2008; Kwok & Cunningham, 2008; Zwally et al., 2008). Figures 4.6 and 4.7 have already given examples of surface elevation and ice thickness maps of the Arctic and Southern oceans thus obtained. Figure 4.12 compares ICESat surface elevation and reflectivity with ice conditions revealed on a SAR image. With satellite altimeters, the distance between the satellite and the surface of the earth is measured. Relative surface height differences between the ice and water are observed to estimate sea ice freeboard or surface elevation. The calculation of ice thickness from these measurements relies on several assumptions about snow thickness and density, as well as the densities of ice and snow.

Two different kinds of altimeters are employed. The ESA's ERS and Envisat satellites carry Ku-band (e.g. 13.8 GHz) radar altimeters, while NASA's ICESat operates a laser altimeter. These are generally different in their penetration characteristics for snow and sea ice, and
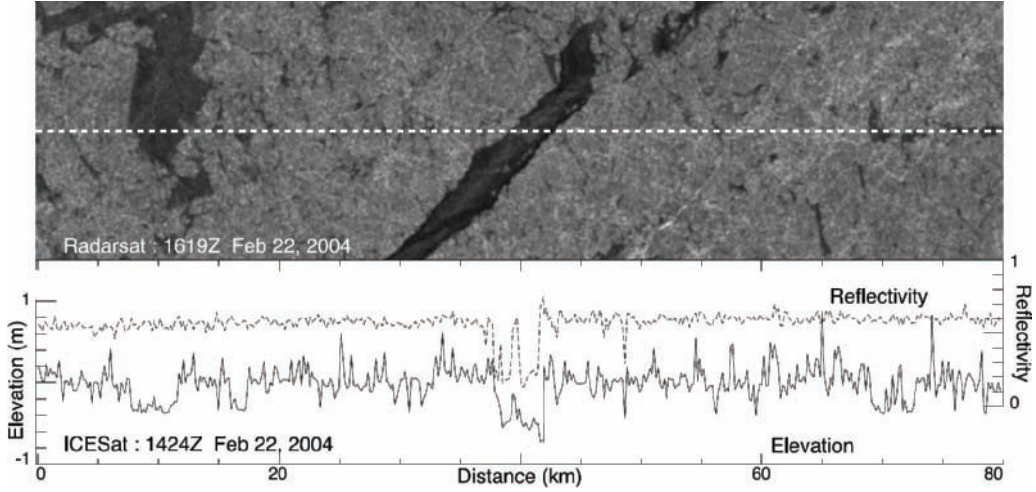
Fig. 4.12   Example of 80-km long ICESat profile from the Arctic Ocean and comparison with near-coincident Radarsat SAR image (Kwok et al., 2006). The ICESat track is shown on the SAR image as white dashed line. Lower panel shows the elevation (solid, centred around mean) and reflectivity profiles (dashed).

in their spatial resolution. Penetration characteristics are particularly important for sea ice measurements. While the near-infrared wavelengths of lasers do not penetrate into snow and ice and are scattered at the upper snow surface, radar altimeter wavelengths penetrate the snow to some degree, and the reflections are generally believed to originate from the snow/ ice-interface (Laxon et al., 2003). Therefore, with laser altimeters, the elevation of the snow surface Z_{se} is obtained, while with radar altimeters the freeboard Z_{fb} of the ice is retrieved. Accordingly, different equations for the calculation of ice thickness Z_i are applied, which result from Archimedes Law and the general isostasy of the ice:

For laser altimetry:
$$z_i = \left(\frac{\rho_w}{\rho_w - \rho_i}\right) z_{se} - \left(\frac{\rho_w - \rho_s}{\rho_w - \rho_i}\right) z_s \qquad \text{(Equation 4.5a)}$$

For radar altimetry:
$$z_i = \left(\frac{\rho_w}{\rho_w - \rho_i}\right) z_{fb} - \left(\frac{\rho_s}{\rho_w - \rho_i}\right) z_s \qquad \text{(Equation 4.5b)}$$

with the densities ρ_w, ρ_i, and ρ_s of water, ice and snow, respectively, and snow thickness Z_s.

   With typical densities of $\rho_w = 1024$ kg m^{-3}, $\rho_i = 925$ kg m^{-3} and $\rho_s = 300$ kg m^{-3}, the first term in these equations implies an approximately tenfold amplification of freeboard uncertainties for the calculation of ice thickness for both methods. However, it is also important to note that the second terms are different, resulting in a stark difference in the sensitivity of thickness retrievals to uncertainties in snow thickness. The term is approximately 7 for laser altimetry and approximately 3 for radar altimetry. Therefore, snow thickness uncertainties in laser altimeter data contribute to more than twice as large uncertainties in retrieved ice thicknesses than in radar altimeter data.

A comprehensive analysis of the sensitivity of ice thickness calculations according to equation 4.5 to uncertainties in snow and ice properties has been performed by Kwok & Cunningham (2008). Results show that the overall uncertainty of thickness retrievals from altimetry can be reduced to less than 0.7 to 0.5 m.

However, another challenge of altimeter measurements of ice freeboard and surface elevation is the retrieval of the local water level, which is required as a reference. Small-scale sea surface height variations occur due to tides and currents, unknown geoid undulations, and temporal variations due to weather-related surface pressure changes. Therefore, measurements rely on the occurrence of open water regions within the pack ice which can be used as tie-points for the reconstruction of the water level. Echo shape and amplitude information of the laser and radar signals are used to support the detection of tie-points (Kwok et al., 2006). Figure 4.12 shows that low elevations often coincide with low reflectivity, indicative of open water or a refreezing lead. The presence of the lead is confirmed by the SAR image. However, note that only the central lead is clearly identifiable in the reflectivity data. Larger errors can be introduced in the freeboard retrievals if tie-points cannot be clearly and frequently detected.

Altimetric measurements are essentially one-dimensional along the satellite track. ICESat performs a measurement every 170 m with a footprint diameter of 70 m. The ERS radar altimeter obtained a measurement every 330 m, but with a footprint of several kilometres due to the nature of the pulse-limited radar altimeter signals. Therefore, large regions of the earth surface including the poles are not covered by satellite altimeters at all. There are trade-offs between orbit inclination, repeat orbit intervals and ground coverage. For example, higher across-track coverage can be achieved with longer repeat intervals, but then temporal changes cannot be so well resolved. A typical orbit repeat period is 30 days. More frequent measurements are only performed at crossover locations of descending and ascending orbits. In addition, the uncertainty of individual point measurements can be large, and sufficient accuracy is only obtained with significant spatial and temporal averaging.

Validation of altimetric ice thickness measurements is difficult due to the footprint of the methods and the variable ice conditions in-between. It is still not clear if the retrieved freeboard values actually represent the mean freeboard, modal freeboard or maximum freeboard within the footprint. Although radar signals might penetrate through fresh, cold snow unaffectedly, there are indications that this assumption is not valid for older and metamorphic snow.

Some of the problems of conventional radar altimetry related to the footprint size and orbit configuration will be overcome by ESA's CryoSat mission to be launched in late 2009. In contrast to previous altimeter missions, which were designed to map the world's oceans, CryoSat is dedicated to observations of sea ice and ice sheet thickness, and will therefore operate with a high inclination of 92°, allowing observations to as far as 88° North and South. Its only payload is a Synthetic-Aperture Interferometric Radar Altimeter (SIRAL) (Wingham et al., 2004). With synthetic-aperture processing, multiple, coherent measurements of the same surface location are taken at by different beams at different viewing angles while the satellite passes over that location. These measurements can later be reconstructed and stacked, thereby increasing the along-track resolution and decreasing the along-track footprint to approximately 250 m. With this reduced footprint size, it will be much better possible to distinguish between measurements over ice and water, thereby improving the identification of tie-points and reconstruction of the water level for better freeboard measurements.

Other satellite methods

Except altimeters, most other satellite sensors are imaging instruments, which provide areal information about specific surface properties rather than any information from inside the ice or its underside. However, these surface properties can be used to identify the type and age of the ice, which can serve as a proxy for ice thickness.

Thin ice has a warmer surface than thick ice as long as it is not yet snow covered, and its surface temperature decreases with increasing thickness. Therefore, it is well separable from thicker ice by means of thermal infrared techniques. Yu & Rothrock (1996) have suggested an algorithm based on thermal channels of the Advanced Very High Resolution Radiometer (AVHRR) sensor to obtain the thickness of snow-free ice up to 0.5 m thick with a spatial resolution of 1.1 km. These observations are particularly valuable over the thin ice regions of polynyas. The method has been refined and adapted to data of the Moderate Resolution Imaging Spectroradiometer (MODIS) instrument with higher spatial resolution of 250 m by Kwok et al. (2007), as shown in Fig. 4.13. Note that the surface air temperature
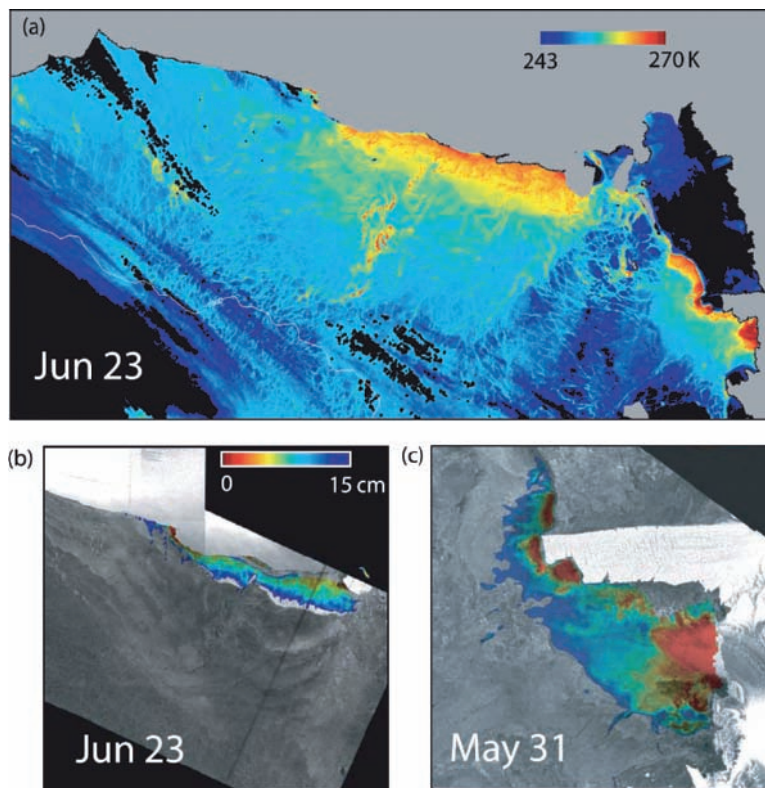
Fig. 4.13   Three examples of ice surface temperature fields and thin ice thickness (0–15 cm) derived from MODIS data in the Ross Sea, Antarctica (Kwok et al., 2007). (a) Ice surface temperature of the Ross Sea region (23 June). Note that part of the image is covered by cloud obscuring the view to the ice surface, indicated by black colour. (b,c) MODIS-derived ice thickness at the Ross Sea (23 June) and Terra Nova Bay (31 May), and polynyas overlaid on near-coincident SAR images. The MODIS IST is at 1-km resolution; the SAR data resolution is degraded to match that of MODIS

has to be known for the application of these algorithms, which are taken from numerical reanalysis data or weather stations. Applicability of these algorithms is also limited to cloud-free situations.

Similarly, microwave brightness temperatures as observed by passive microwave sensors are affected by surface temperature. Measurements of different channels of the Special Sensor Microwave/Imager (SSM/I) and Advanced Microwave Scanning Radiometer (AMSR) have been combined to derive thin ice thicknesses up to 0.2 m over various polynyas in the Arctic and Antarctic (Martin et al., 2004; Kwok et al., 2007). These measurements are not affected by clouds, but have a lower spatial resolution of between 12 and 25 km.

Microwave emissivity, absorption and scattering are also sensitive to varying properties of the surface of thicker ice. These are mainly dependent on the ice and snow salinity and small-scale surface roughness. As shown in Chapter 2, large changes of surface salinity occur in first-year ice once it experiences its first melting season. The salt drains into deeper layers or is flushed by melt water. The pores widen considerably and brine is replaced by air. Therefore, second- and multiyear ice are characterized by lower microwave emissivities and higher radar backscatter coefficients than first-year ice. Consequently, mapping of regions with low brightness temperatures or high radar backscatter can provide estimates on the relative amount of thick multiyear and thin first-year ice. Using low-resolution, Ku-band backscatter data from the QuikScat satellite, Kwok (2004, 2007) and Nghiem et al. (2007) have demonstrated the decreasing amount of multiyear ice in the Arctic as one component of the present rapid change (see below). However, quantitative thickness information or thickness distributions cannot be obtained from these data.

SAR imagery of the ESA's ERS-1&2 and Envisat satellites, as well as of the Canadian RADARSAT-1&2 satellites, provides the same qualitative differentiation between thin and thick ice, and can well distinguish between regions of first- and multiyear ice. This was already demonstrated with the examples in Figs 4.11, 4.12 and 4.13 above. The high horizontal resolution of 12–75 m is sufficient to resolve leads and to partially identify ridges or ridge zones. These features have different backscattering properties than the surrounding ice. Leads are covered by open water or thin new ice, which is rapidly thickening. They may also be recognizable by their linear extended shape, and the saline ice is easily distinguished by its lower backscatter compared with the surrounding older ice. However, frost flowers, rafting or multiple scattering over very thin ice can also cause high backscatter of leads. Kwok et al. (1999) have developed the so-called Radarsat Geophysical Processor System (RGPS) which tracks leads in successive SAR images and computes their thickness distribution by means of a thermodynamic model. RGPS also computes the thickening of the new ice by deformation if leads close under convergent drift conditions. The overall thickness distribution, including thick floes, is difficult to obtain though.

The number of ridges and the degree of deformation are relative measures of ice thickness. Ridge sails consist of piled ice blocks with arbitrarily tilted sidewalls. These provide a number of interfaces pointing normally to the incident radar signal. Thus, backscatter is higher than from the surrounding level ice. In addition, ridge backscatter can also rise by increased volume scattering, as aged ridge blocks become more weathered and porous. Therefore, single large ridges can be seen in SAR images. However, smaller ridges also contribute to the mean backscatter of a certain image pixel. There are indications that the backscatter distribution of a certain region includes information on the amount of ridges in this region (Haas et al., 1999a; Karvonen et al., 2004).

4.4 Ice thickness variability

Decadal thickness variability in the Arctic

As outlined above, the thickness distributions shown in Fig. 4.5 represent 9-year average fields. Although average conditions over even longer-time periods look similar (Bourke & Garret, 1987), on timescales of years and decades, the thickness distribution shows large interannual and decadal variability, and longer-term trends. Most spectacular observations of changes of the Arctic ice cover have been published by Rothrock et al. (1999). They compared submarine sonar data obtained in 28 regions of the Arctic Ocean during the period 1958–76 with those gathered in the same regions between 1993 and 1997. In all regions, a decrease in the mean draft was observed (Fig. 4.14). On average, there was a 1.3 m decrease from a mean draft of 3.1 m in the earlier period to a mean draft of 1.8 m in the 1990s, equivalent to a reduction of 42% of ice thickness. The thinning was most pronounced in the Siberian Arctic and Nansen Basin, where the average decrease of draft was 1.8 m. Although their results indicated a continued thinning in some regions during the 1990s, the study essentially only compared two distinct periods (1958–76 and 1993–97) with each other. Therefore, it is unclear if the results are an indication of a trend or just represent two arbitrary samples of a varying parameter.

Figure 4.15 shows the mean annual ice volume in the Arctic from 1948 to 1999 as simulated with a dynamic–thermodynamic ice–ocean model (Rothrock & Zhang, 2005). The figure clearly shows that there are large decadal ice volume fluctuations of as much as 5×10^3 km^3 around a mean volume of 22.5×10^3 km^3. The data in fact show a marked thinning of about 37% between the 1960s and the 1990s, i.e. the period covered by Rothrock et al. (1999). However, for the complete model period, only a small decrease of ice volume
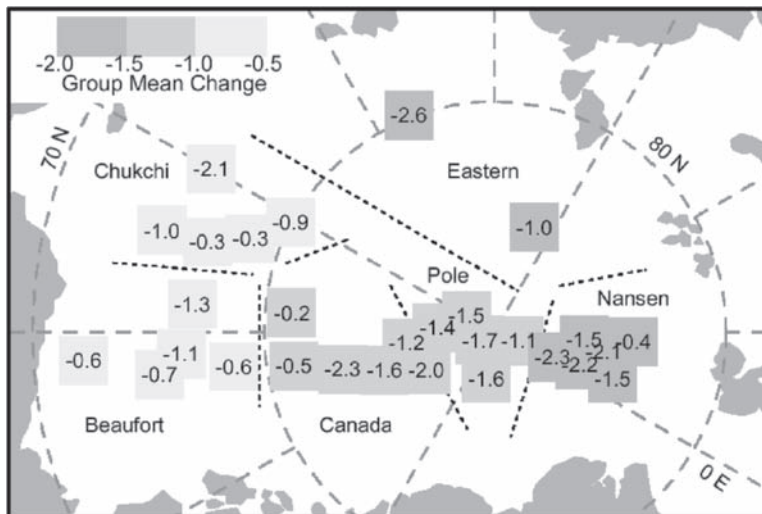
Fig. 4.14   Map of the Arctic showing the regions of coincident submarine tracks in 1958–76 and 1993–97. Numbers indicate the ice thickness difference between the two periods. From Rothrock et al. (1999)
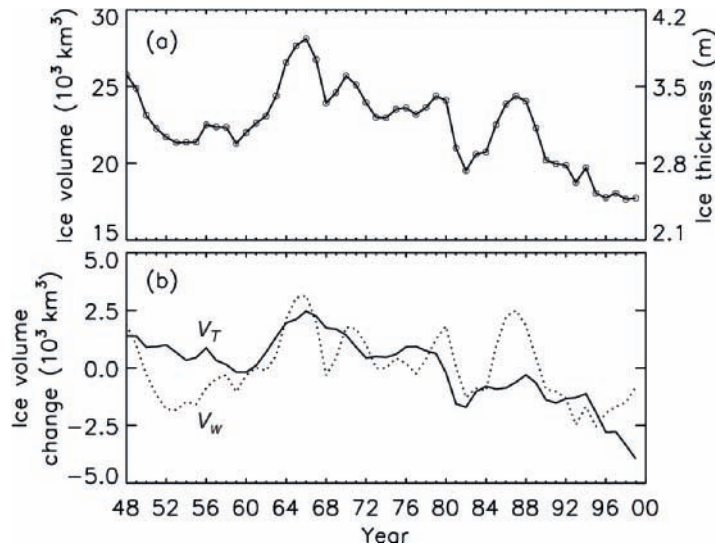
Fig. 4.15 (a) Modelled ice volume within the Arctic Ocean 1948–99 (Rothrock & Zhang, 2005). The 52-year mean annual ice-covered area of 6.91×106 km^2 is used to convert volume to an approximate thickness scale on the right axis. (b) Wind-forced volume change $V_w(t)$ (dotted line) and the temperature-forced component $V_T(t)$ (solid line), as defined in the text.

of -4% per decade was obtained. The model results indicate that this decrease is unevenly distributed over different regions of the Arctic. The largest decrease was obtained from the East Siberian Sea and central Arctic, whereas the regions north off the Canadian Archipelago showed slightly increasing ice thicknesses.

The causes for the modeled variability and trends are further examined in Fig. 4.15b, which shows a separation between the impacts of changes in wind forcing and temperature forcing. V_w represents ice volume changes due purely to variations in wind forcing, and V_T due to variations of only thermal forcing. V_w was calculated by retaining the interannually varying winds, but by using only the long-term average annual cycle of air temperatures. V_T was similarly obtained by using variable temperatures and constant, average winds. Figure 4.15b shows that V_w contributes approximately two-thirds of the total ice volume variability. It does not possess any clear trend. However, V_T shows less variability but a clear trend. In conclusion, these results suggest that the changes observed over the past couple of decades are the result of strong interannual variability mainly due to variable winds, which are superimposed on a longer-term trend of decreasing ice volume due to warming temperatures.

Tucker et al. (2001) compared complementary submarine draft measurements performed between off Alaska and the North Pole between 1985 and 1988 with data from the same transects obtained in 1992–94. During this short period, mean ice drafts decreased by 1.5 m. Again, it remains unclear if this represents just some variability or an actual trend. The data are in agreement with the ice volume time series presented in Fig. 4.15. However, Tucker et al. (2001) took a step further in relating their results to changes in the ice drift regime. While the Beaufort Gyre was well developed in the 1980s, it weakened considerably in the

1990s. This led to stronger ice-divergence and to less production of thick, deformed ice. The different circulation regimes also resulted in shorter residence times of the ice in the Canadian Basin, and therefore less time to accumulate deformed ice.

The relationships between ice thickness changes and different circulation regimes observed by Tucker et al. (2001) are thoroughly demonstrated by a coupled dynamic–thermodynamic ice–ocean model of Zhang et al. (2000) for the period 1979–96. This period was characterized by two distinct circulation regimes during 1979–88 and 1989–96, respectively. These different circulation regimes are characterized by high and low North Atlantic Oscillation (NAO) and Arctic Oscillation (AO) indices, parameters derived from the difference and variability of sea level pressure in the Arctic and at lower latitudes (Hurrel, 1995; Thompson & Wallace, 1998). The period 1979–88 was characterized by low NAO and AO indices, and therefore high sea level pressure over the central Arctic, while the period 1989–96 was characterized by high NAO and AO indices and low sea level pressure. Figure 4.16a,b shows the mean sea level pressure contours and modelled ice velocity fields for both periods. Figure 4.16c,d shows the anomalies of ice velocity fields based on the differences between the 1979–88 and 1989–96 fields and the mean field of 1979–96, respectively. The latter period (1989–96) was characterized by smaller pressure gradients and a weaker Beaufort Gyre, which had also retreated more towards the Canadian Coast. Essentially, the anomaly fields show reversed conditions, with an anticyclonic circulation anomaly in 1979–88 and a cyclonic anomaly in 1989–96. Figure 4.17 shows the corresponding thickness anomalies, derived from the difference of the thickness fields in 1979–88 and in 1989–96. There was strong thinning in the East Siberian Sea (up to –2.5 m) and the central Arctic, whereas ice thickness increased in the Beaufort Sea and off the Canadian and Alaskan coasts. Ice volume decreased by 28% in the eastern Arctic and simultaneously increased by 16% in the western Arctic. Overall, in the whole Arctic it decreased by only 6% between 1979–88 and 1989–96. Note that the thickness measurements reported by Rothrock et al. (1999) and Tucker et al. (2001) were mostly in the regions of modelled thickness decrease and were consistent with these model results.

The results of Zhang et al. (2000) show that the ice thickness changes between 1979 and 1996 can almost exclusively be attributed to changes in the circulation regimes. This mainly led to different amounts of ice exported from the western into the eastern Arctic. The study therefore shows that on shorter timescales dynamics are far more important than thermodynamics in shaping the overall thickness distribution in the Arctic, in agreement with the results shown in Fig. 4.15. Similar results were found by Holloway and Sou (2002).

However, Zhang et al. (2000) also clearly demonstrate that thermodynamics plays an important role in modifying the dynamically caused differences, both through negative and positive feedback mechanisms. The different circulation regimes also caused differences in the ice concentration fields. Between 1979–88 and 1989–96, there was a decrease of mean ice concentration in the eastern Arctic and an increase in the western Arctic, which were most pronounced during summer. The positive feedback was the higher absorption of incident solar radiation in the mixed layer due to an overall decrease of surface albedo caused by larger areas of open water. This led to enhanced lateral and bottom melting and to a later onset of freezing, consequently enhancing the thinning. However, due to the thinner ice and more open water, freezing rates during winter were also higher, and therefore ice growth increased. The net ice production remained almost constant under the different circulation regimes.
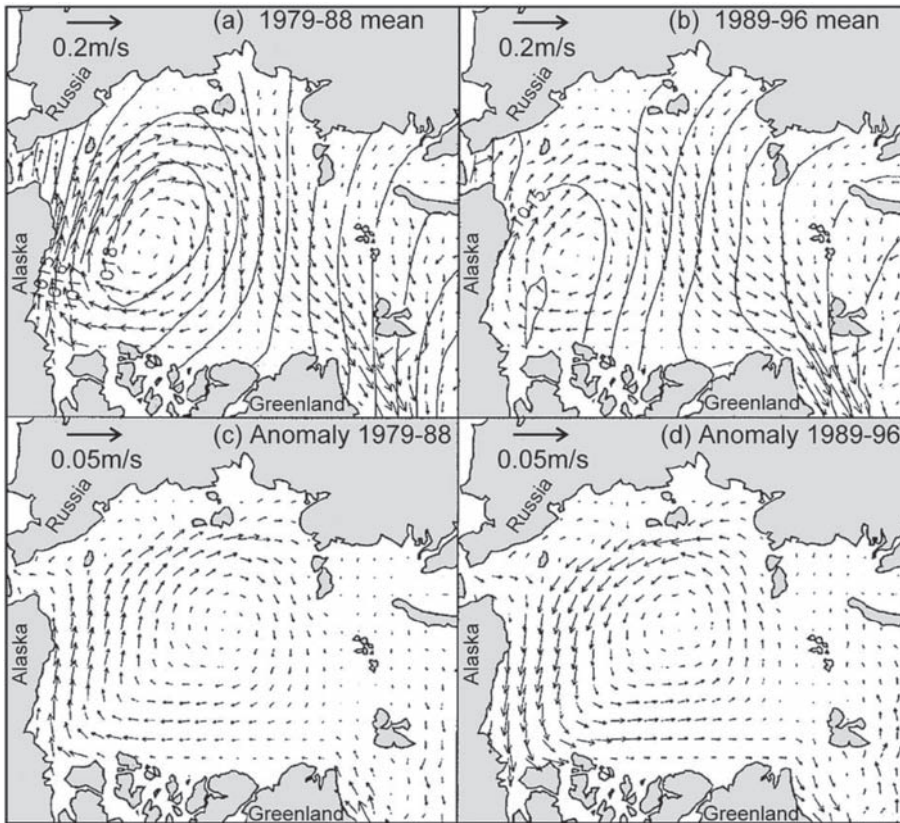
Fig. 4.16 Simulated mean ice velocity fields and annual mean sea level pressure contours for (a) 1979–88 and (b) 1989–96 (Zhang et al., 2000). Anomaly fields of ice velocity based on the differences (c) between the 1979–88 mean and the 1979–96 mean and (d) between the 1989–96 mean and the 1979–96 mean.
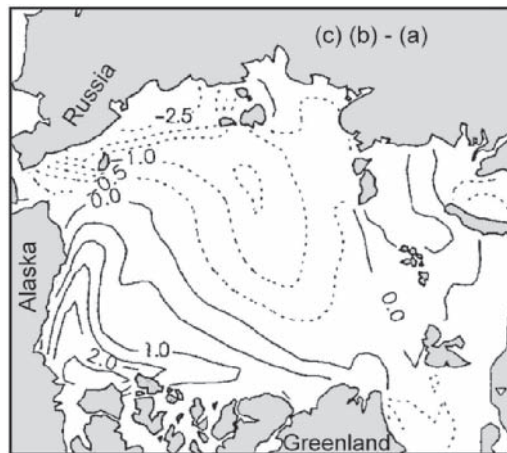
Fig. 4.17 Difference between the simulated ice thickness fields for 1979–88 and 1989–96. From Zhang et al. (2000)

Cyclonic and anticyclonic circulation regimes were shown to follow each other with periods of 7–15 years (Proshutinsky & Johnson, 1997). Therefore, it is quite likely that these also cause simultaneous long-term ice volume changes such as those shown in Fig. 4.15. This high level of dynamically caused variability makes the detection of temperature-induced climate changes very complicated.

Present day, interannual thickness variability

Superimposed on the decadal thickness variations are large seasonal and interannual thickness variations. Only a few studies have had the opportunity to make repeated surveys in the same region over a couple of years. Among those are moored ULS measurements, e.g. in the Weddell Sea (Strass & Fahrbach, 1998; Harms et al., 2001), the Beaufort Sea (Melling & Riedel, 1995, 2004) and the Fram Strait (Vinje et al., 1998). The latter study showed that the ice volume flux through Fram Strait is well explained by changes of the NAO, and thus possesses a pronounced interannual variability.

On the contrary, results of satellite radar altimetry measurements by Laxon et al. (2003) showed the importance of changes of thermodynamic boundary conditions for the interannual thickness variability. They observed anomalies of mean winter ice thickness over the whole Arctic Basin between 1993 and 2001, which compared well with observations of the melt season length in the respective previous summer obtained from passive microwave satellite measurements. Thickness change from one year to the other correlated well with the length of the melt season in-between. A possible explanation of this observation might be that changes in circulation which would redistribute ice from one region of the Arctic Ocean to another are averaged out if observations over the whole Arctic are considered, and therefore thermodynamic changes would be more dominant.

However, large ice thickness changes were observed by means of EM sounding in the Laptev Sea in the summers of 1993, 1995 and 1996, and demonstrated the close interrelation between dynamic and thermodynamic processes (Haas & Eicken, 2001). With mean and modal thicknesses of 1.8 and 1.25 m, ice thickness was minimal in 1995. It was maximal in 1996, when the mean and modal thickness amounted to 2.0 and 1.85 m. Mean and modal thicknesses were intermediate in 1993, with values of 1.85 and 1.75 m, respectively. There was strong, intermediate and no melt pond coverage in 1995, 1993 and 1996, respectively. Satellite data showed that the ice coverage of the Laptev Sea assumed a record minimum in 1995, and a record maximum in 1996, since satellite observations began in 1978.

The interannual differences could be well explained by the prevailing mean atmospheric circulation during July and August in each of the three summers, which was 'normal' in 1993, but was characterized by high pressure over the central Arctic in 1995, and a deep low centred over the North Pole in 1996. The situation in 1995 favoured the northward advection of the ice edge, and the inflow of warm air from the south, which caused strong surface melt. In contrast, the low pressure over the North Pole in 1996 resulted in strong cyclonic geostrophic air and ice circulation. This moved the ice into the marginal seas, causing high ice coverage, and prevented the advection of warm air from the South, preventing surface melting. The result showed the importance of the strength and location of the summer cyclonic atmospheric circulation pattern for the advection of ice and occurrence of surface melt. It is also remarkable that ice thicknesses in 1996 were maximal despite a late onset of autumn freeze-up in 1995, which occurred 3 weeks later than on average due

to the storage of heat in the water. However, it is not clear whether the thick ice in 1996 was due to stronger than normal ice growth or just due to the absence of summer melt. This is a problem of interpreting end-of-summer ice thicknesses, since it remains unclear if reduced (increased) thicknesses are due to reduced (increased) winter growth or increased (decreased) summer melt.

The extreme situation of 1995 and 1996 might provide an example of how a year with maximum ice coverage can be reached even after a minimum year. As much as special atmospheric conditions have favoured the rapid summer ice decline between 2006 and 2007 (Stroeve et al., 2008), a similar situation as in 1996 could still contribute to an at least partial recovery of Arctic ice conditions in the coming years.

Another presently observed consequence of circulation changes in the Arctic Ocean is the reduction of the amount of perennial and old ice (Kwok, 2007; Maslanik et al., 2007; Nghiem et al., 2007). These observations are based on satellite backscatter and emissivity measurements in more recent times, and on the tracking of buoys deployed by the International Arctic Buoy Program since the 1970s and utilization of numerical weather reanalysis data (Rigor & Wallace, 2004). The changes of ice age are an indication of overall reduced ice volume. However, they also complicate the interpretation of observations of actual thickness changes. Figure 4.18 shows maps of the locations of ground-based and airborne EM thickness profiles obtained during summer in the region of the North Pole during six sporadic measurement campaigns between 1991 and 2007 (Haas et al., 2008a). The resulting thickness distributions are shown in the right part of the figure. It can be seen that modal thicknesses decreased from 2.5 m in 1991 to 1.9 m in 2001 and 2.2 m in 2004. In the summer of 2007, modal thickness was only 0.9 m, i.e. 53% less than in 2001. Mean thicknesses decreased at similar rates (Haas et al., 2008a). The decreasing modal thicknesses indicate a general increase of heat fluxes towards the ice. However, the maps in Fig. 4.18 also show that the large thinning observed in 2007 was accompanied by a replacement of older ice by first-year ice. In fact, in the summer of 2007, the region of the North Pole was only covered by first-year ice for the first time since ice age information is available. In April 2007, the region was still covered by second-year ice. However, Fig. 4.18 shows that also the second-year ice modal thickness was only 1.65 m after seasonal adjustment, i.e. 20% less than in the summer of 2001.

These results demonstrate that the replacement of older ice by first-year ice is accompanied by abrupt thinning, which is superimposed on general trends of thermodynamically induced thinning trends. In the summer of 2007, the first-year ice in the region of the North Pole was so thin that only slightly more thinning in coming years could soon result in an ice-free North Pole during summer.

Seasonal thickness variability

Apart from decadal and interannual variations, ice thickness is also subject to a strong seasonal cycle, which is superimposed on the lower-period changes, and which often exceeds longer-term changes in amplitude. The seasonal cycle results from prevailing thickening during the winter and from thinning during the summer, both through bottom and surface melt. The latter is most prominent in the Arctic, and results in the formation of melt ponds. Therefore, knowledge of the seasonal cycle, and of interannual variations of it, are important for the interpretation of thickness changes in general.

For example, an ice thickness change from one summer to the next can be the result of reduced freezing in the preceding winter, or of increased melting in the actual summer when
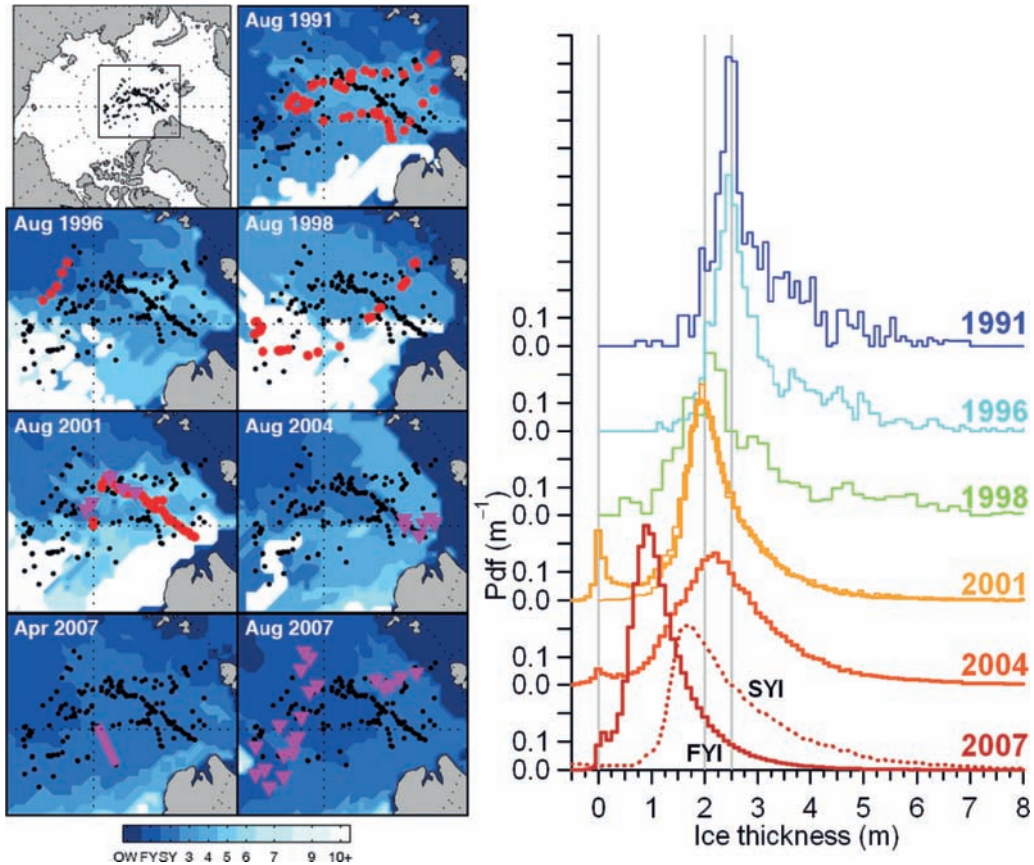
Fig. 4.18 Late summer ice age (left) and thickness (right) in the region of the North Pole between 1991 and 2007 (Haas et al., 2008a). Thicknesses were obtained by means of ground-based (thin lines, red circles) and HEM sounding (thick lines, magenta triangles). The second-year ice (SYI) distribution obtained in April 2007 was seasonally adjusted by 0.7 m to represent summer conditions. From Haas et al. (2008a).

the measurements have been performed, or both. If measurements are performed in different seasons, they will have to be compensated for the seasonal cycle before they are comparable. For example, Rothrock et al.'s (1999) submarine measurements have been performed both in late spring and early summer, and in late summer/early fall. All these measurements (Fig. 4.14) were seasonally adjusted to September 15 by means of a seasonal cycle computed with an ice–ocean model of the Arctic Ocean. That model indicated a mean seasonal thickness cycle of 1.5 m between April and September 15, the seasonal minimum. Obviously, questions arise whether it is appropriate to use a model of the whole Arctic Ocean for the correction of observations which were mainly performed in the central Arctic Ocean, and if the amplitude of seasonal changes is uniform over large regions.

  In a more recent study, Rothrock et al. (2008) separated the seasonal cycle from the submarine data themselves by means of multiple regression. The annual cycle of mean ice thickness in the central Arctic Ocean has a maximum on 30 April and a minimum on 30 October with a peak-to-trough amplitude of 1.12 m, i.e. less than computed with the model in their earlier study.

Again, this mean cycle comprises both dynamic and thermodynamic components. As discussed above and shown by Perovich et al. (2003), the thermodynamic component of the seasonal cycle can be as high as obtained by Rothrock et al. (2008) for the mean, and varies strongly between different ice types and geographical regions. Typical, maximum winter growth rates can be estimated from first-year ice modal thicknesses in various regions of the Arctic, and can be as high as or higher than 2 m per winter (Haas & Eicken, 2001). Melling & Riedel (1996) and Strass & Fahrbach (1998) show time series of the development of level ice drafts observed by ULS.

A comparison of summer bottom and surface melt rates between 1994 and 2007 in the Beaufort Sea and in the region of the North Pole is shown in Fig. 4.19 (Perovich et al., 2008). These observations were made from autonomous ice mass balance buoys (IMB) (Richter-Menge et al., 2006) that drifted with the ice pack. These buoys are equipped with acoustic range finders placed above the ice surface and below the ice bottom, and provide information on snow accumulation and melt as well as ice growth and decay. The average annual surface melt in the Beaufort Sea is 0.64 m, greater than near the North Pole region, where it is only 0.26 m. These differences are primarily due to the greater incident solar radiation at the lower latitude of the Beaufort Sea. In most years, surface melt exceeds bottom melt. Both top and bottom melting exhibit interannual variability.

Despite the extreme ice cover retreat during 2007, the amount of surface melt in both regions was not significantly different in 2007 compared to earlier years. Bottom melting at the North Pole in 2007 was also comparable to earlier years. However, there was a dramatic increase in bottom melting in the Beaufort sector in 2007. This strong bottom melting was accompanied by very low ice concentrations in the region of that particular IMB (Perovich et al., 2008). Calculations indicate that this supported solar heating of the upper ocean, which was the primary source of heat for this observed enhanced bottom melting.
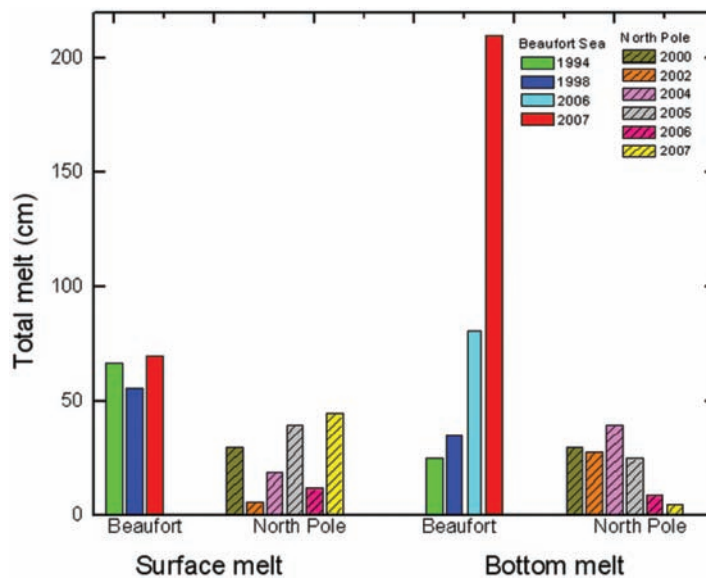
Fig. 4.19   Observations of total surface and bottom melting in different years in the Beaufort Sea and North Pole regions. From Perovich et al. (2008).

The increase in the open water fraction resulted in a 500% positive anomaly in solar heat input to the upper ocean, triggering an ice–albedo feedback and contributing to the accelerating ice retreat. This is again an example for the close interrelationship between thermodynamic and dynamic processes. The strong bottom melt was primarily triggered by dynamically induced reductions in ice concentration. Only then could the thermodynamic ice–albedo feedback become efficient.

Haas et al. (2008c) have studied the seasonal development of surface melting in the Weddell Sea. During a 5-week drift phase as part of the Ice Station Polarstern (ISPOL) project of the German icebreaker RV Polarstern in December 2004 (Hellmer et al., 2006), snow and ice thickness changes were measured to obtain similar data as was previously available from the Arctic. However, during the observation period, there was hardly any thinning of the ice, and the originally 0.2–0.5 m thick snow thinned only by 0.2 m. This is remarkable when compared with conditions in the Arctic, where the strongest surface ablation is observed during the corresponding month of June (Perovich et al., 2003), and at much higher latitudes (77°N) than where the ISPOL measurements were made (67°S). Overall, the slow melting rates observed during ISPOL are one reason for the general absence of melt ponds on Antarctic sea ice. They are caused by the special climatic conditions dominated by the cold Antarctic continent and the rareness of events of warm air advection from the North. Andreas and Ackley (1982), Nicolaus et al. (2006) and Vihma et al. (2009) show observations and calculations of the surface heat balance of Antarctic sea ice, and demonstrate the importance of upward turbulent heat fluxes as the dominant component for the prevention of strong surface melt.

4.5 Conclusion and outlook

This chapter has shown that the sea ice thickness distribution is a result of complicated thermodynamic and dynamic processes, which can also be closely interacting. There are many feedbacks involved in changes of ice thickness, and therefore the reasons for observed changes are not always clear at first sight. The deviations between climate predictions and observed changes are largely due to an under-representation of these processes in the models. Ice thickness research requires multidisciplinary approaches including model, field and remote-sensing studies.

Field studies are always limited by their restricted spatial and temporal coverage. This can be partially compensated by satellite measurements, which can also provide information on the regional redistribution of ice thickness. Completely new insights have now been possible with laser and radar altimetry data of ICESat, and ERS and Envisat, respectively. These showed the potential, but also the uncertainties of those measurements. Another milestone will be reached with the dedicated CryoSat mission. However, there is an urgent need to validate those satellite data, and to improve auxiliary data, particularly of sea surface height and snow thickness and density. Accurate and extensive underwater, airborne and *in situ* measurements are required for this validation. At present, satellite measurements are rather experimental than operational, and therefore their continuity is not guaranteed.

The optimum ice thickness observing system would therefore consist of a hierarchy of measurements at different scales and with different accuracies: ULS moorings at key sites

like the big flux gates can provide continuous but local observations. These can be complemented by airborne surveys or underwater AUV measurements between mooring sites or along other transects to provide information on possible thickness gradients, which is required to estimate ice volume fluxes. Airborne campaigns or icebreaker cruises should also provide opportunities for extensive *in situ* measurements of snow thickness and density, and for a few validation measurements with the highest accuracy. On much larger scales, but probably with less accuracy, satellites would provide continuous and Arctic-wide data, whose uncertainty could nevertheless be reduced by means of the validation measurements.

Another problem of validation is the comparability among all data sets, as they obtain thicknesses with different spatial resolution, and with varying accuracy over different thickness classes. Cross-calibrations are urgently required between EM and ULS measurements to provide a broad statistical database for comparison and to be able to develop correction functions for various ice types and conditions. Both methods are complementary, as they obtain their most accurate estimates either for level or for deformed ice. Few approaches have already been made, but a proper analysis has not been successful due to technical and/or weather problems. Similarly, although airborne EM measurements might provide the best compromise between ease of use and accuracy, their range is limited so far. The recent Pole-Airship project of French explorer Jean-Louis Etienne tried to use an airship as a potential alternative platform for Arctic-wide EM measurements, but failed due to an airship crash during test flights in southern France. A hovercraft is now under development for Arctic-wide operations, which is also equipped with an EM thickness system. However, it too has some range issues to solve. The ultimate platform might be the Basler BT67 airplane of the German Alfred Wegener Institute. This plane can operate an EM-bird, and a first Arctic survey has successfully been performed in April 2009.

The examples in this book were mostly of large scales and from the central Arctic Ocean, as they had primarily been motivated by climate research aspects. However, shrinking and thinning sea ice has also fundamental consequences for the eco- and human systems of the Arctic. The ice is an important habitat and hunting and resting platform for a wide variety of organisms including Polar bears. However, it is also used by the human population of the Arctic for travel and hunting. On the contrary, it is an obstacle for shipping and offshore operations in polar waters. An understanding of short- and long-term ice thickness changes is required for these activities as well. It might even be more difficult to provide the proper thickness measurements and observation strategies, as most problems are of a local nature, and require continuous and small-scale measurements, and often fewer resources may be available for individual sites (Haas & Druckenmiller, 2009).

References

Anderson, W.L. (1979) Computer Program. Numerical integration of related Hankel transforms of orders 0 and 1 by adaptive digital filtering. *Geophysics*, **44**, 1287–1305.

Andreas, E.L. & Ackley, S.F. (1982) On the differences in ablation seasons of Arctic and Antarctic sea ice. *Journal of Atmospheric Science*, **39**, 440–447.

Barry, R.G., Serreze, M.C., Maslanik, J.A. & Preller, R.H. (1993) The Arctic sea ice climate system: observations and modeling. *Reviews of Geophysics*, **31**, 397–422.

Bourke, R.H. & Garrett, R.P. (1987) Sea ice thickness distribution in the Arctic Ocean. *Cold Regions Science and Technology*, **13**, 259–280.

Colony, R. & Thorndike, A.S. (1984) An estimate of the mean field of Arctic sea ice motion. *Journal of Geophysical Research*, **89**, 10623–10629.

Coon, M.D. (1980) A review of AIDJEX modelling. In: *Sea Ice Processes and Models* (Ed. R.S. Pritchard), pp. 12–27. University of Washington Press, Seattle, Washington.

Dowdeswell, J.A., Evans, J., Mugford, R. et al. (2008) Autonomous underwater vehicles (AUVs) and investigations of the ice–ocean interface: deploying the Autosub AUV in Antarctic and Arctic waters. *Journal of Glaciology*, **54**, 661-672.

Eicken, H., Tucker, W.B. & Perovich, D.K. (2001) Indirect measurements of the mass balance of summer Arctic sea ice with an electromagnetic induction technique. *Annals of Glaciology*, **33**, 194–200.

Eicken, H., Grenfell, T.C., Perovich, D.K., Richter-Menge, J.A. & Frey, K. (2004) Hydraulic controls of summer Arctic pack ice albedo. *Journal of Geophysical Research*, **109**, C08007, 10.1029/2003JC001989.

Gerdes, R. & Köberle, C. (2007) Comparison of Arctic sea ice thickness variability in IPCC climate of the 20th century experiments and in ocean–sea ice hindcasts. *Journal of Geophysical Research*, **112**, C04S01, 10.1029/2006JC003616.

Giles, K.A., Laxon, S.W. & Worby, A.P. (2008) Antarctic sea ice elevation from satellite radar altimetry. *Geophysical Research Letters*, **35**, L03503, doi:10.1029/2007GL031572.

Haas, C. (1998) Evaluation of ship-based electromagnetic-inductive thickness measurements of summer sea ice in the Bellingshausen and Amundsen Sea. *Cold Regions Science and Technology*, **27**, 1–16.

Haas, C. & Druckenmiller, M. (2009) Ice thickness and roughness measurements. In: *Sea Ice Handbook*. (Eds. Eicken, H., Gradinger, R., Salganek, M., Shirasawa, K., Perovich, D. & Lepparanta, M.). University of Alaska Fairbanks Press.

Haas, C. & Eicken, H. (2001) Interannual variability of summer sea ice thickness in the Siberian and Central Arctic under different atmospheric circulation regimes. *Journal of Geophysical Research*, **106**, 4449–4462.

Haas, C. & Jochmann, P. (2003) Continuous EM and ULS thickness profiling in support of ice force measurements. In: *Proceedings of the 17th International Conference on Port and Ocean Engineering under Arctic Conditions, POAC ´03, Trondheim, Norway, Vol. 2* (Eds. S. Loeset, B. Bonnemaire & M. Bjerkas), pp. 849–856. Department of Civil and Transport Engineering, Norwegian University of Science and Technology NTNU, Trondheim, Norway.

Haas, C., Gerland, S., Eicken, H. & Miller, H. (1997) Comparison of sea ice thickness measurements under summer and winter conditions in the Arctic using a small electromagnetic induction device. *Geophysics*, **62**, 749–757.

Haas, C., Liu, Q. & Martin, T. (1999a) Retrieval of Antarctic sea ice pressure ridge frequencies from ERS SAR imagery by means of in-situ laser profiling and usage of a neural network. *International Journal of Remote Sensing*, **2**, 3111–3123.

Haas, C., Rupp, K.-H. & Uuskallio, A. (1999b) Comparison of along track EM ice thickness profiles with ship performance data. In: *Proceedings of the 15th International Conference on Port and Ocean Engineering Under Arctic Conditions (POAC '99), Espoo, Finland, August 23–27, Vol. 1* (Eds. J. Tuhkuri & K. Riska), pp. 343–353. Helsinki University of Technology, Ship Laboratory, Helsinki, Finland.

Haas, C., Hendricks, S. & Doble, M. (2006) Comparison of the sea ice thickness distribution in the Lincoln Sea and adjacent Arctic Ocean in 2004 and 2005. *Annals of Glaciology*, **44**, 247–252.

Haas, C., Pfaffling, A., Hendricks, S., Rabenstein, L., Etienne, J.-L. & Rigor, I. (2008a) Reduced ice thickness in Arctic Transpolar Drift favors rapid ice retreat. *Geophysical Research Letters*, **35**, L17501, 10.1029/2008GL034457.

Haas, C., Lobach, J., Hendricks, S., Rabenstein, L. & Pfaffling, A. (2008b) Helicopter-borne measurements of sea ice thickness, using a small and lightweight, digital EM system. *Journal of Applied Geophysics*, 10.1016/j.jappgeo.2008.05.005.

Haas, C., Nicolaus, M., Willmes, S., Worby, A. & Flinspach, D. (2008c) Sea ice and snow thickness and physical properties of an ice floe in the western Weddell Sea and their changes during spring warming. *Deep-Sea Research Part II*, **55**, 963–974.

Harms, S., Fahrbach, E. & Strass, V.H. (2001) Sea ice transports in the Weddell Sea. *Journal of Geophysical Research*, **106**, 9057–9073.

Hellmer, H.H., Dieckmann, G.S., Haas, C. & Schröder, M. (2006) Sea ice feedbacks observed in western Weddell Sea. *EOS Transactions*, **87**, 173.

Hibler, W.D., III (1979) A dynamic thermodynamic sea ice model. *Journal of Physical Oceanography*, **7**, 987–1015.

Holland, M.M., Bitz, C.M. & Tremblay, B. (2006) Future abrupt reductions in the summer Arctic sea ice. *Geophysical Research Letters*, **33**, L23503, 10.1029/2006GL028024.

Holloway, G. & Sou, T. (2002) Has Arctic sea ice rapidly thinned? *Journal of Climate*, **15**, 1691–1701.

Holt, B., Kanagaratnam, P., Gogineni, S.P., Ramasami, V.C., Mahoney, A. & Lytle, V. (2008) Sea ice thickness measurements by ultrawideband penetrating radar: first results. *Cold Regions Science and Technology*, 10.1016/ j.coldregions.2008.04.007.

Hopkins, M.A. (1994) On the ridging of intact lead ice. *Journal of Geophysical Research*, **99**, 16351–16360.

Hurrel, J.W. (1995) Decadal trends in the North Atlantic Oscillation: regional temperatures and precipitation. *Science*, **269**, 676–679.

Hvidegaard, S.M. & Forsberg, R. (2002) Sea ice thickness from airborne laser altimetry over the Arctic Ocean north of Greenland. *Geophysical Research Letters*, **29**, 1952, 10.1029/2001GL014474.

Kanagaratnam, P., Markus, T., Lytle, V., Heavey, B., Jansen, P., Prescott, G. & Gogineni, S.P. (2007) Ultrawideband radar measurements of thickness of snow over sea ice. *IEEE Transactions on Geoscience and Remote Sensing*, **45**, 2715–2724.

Karvonen, J., Similä, M., Haapala, J., Haas, C. & Mäkynen, M. (2004) Comparison of SAR data and operational sea ice products to EM ice thickness measurements in the Baltic Sea. *Proceedings, IEEE International Geoscience and Remote Sensing Symposium (IGARSS'04), Anchorage, Alaska. (IGARSS)*, **5**, 3021–3024.

Köberle, C. & Gerdes, R. (2003) Mechanisms determining the variability of Arctic sea ice conditions and export. *Journal of Climate*, **16**, 2843–2858.

Kottmeier, C., Olf, J., Frieden, W. & Roth, R. (1992) Wind forcing and ice motion in the Weddell Sea region. *Journal of Geophysical Research*, **97**, 20373–20382.

Kovacs, A. & Holladay, J.S. (1990) Sea ice thickness measurements using a small airborne electromagnetic sounding system. *Geophysics*, **55**, 1327–1337.

Kovacs, A., Valleau, N.C. & Holladay, J.S. (1987) Airborne electromagnetic sounding of sea ice thickness and subice bathymetry. *Cold Regions Science and Technology*, **14**, 289–311.

Kovacs, A., Holladay, J.S. & Bergeron, C.J.J. (1995) The footprint/altitude ratio for helicopter electromagnetic sounding of sea ice thickness: comparison of theoretical and field estimates. *Geophysics*, **60**, 374–380.

Kwok, R. (2004) Annual cycles of multiyear sea ice coverage of the Arctic Ocean: 1999–2003. *Journal of Geophysical Research*, **109**, C11004, 10.1029/2003JC002238.

Kwok, R. (2007) Near zero replenishment of the Arctic multiyear sea ice cover at the end of 2005 summer. *Geophysics Research Letters*, **34**, L05501, 10.1029/2006GL028737.

Kwok, R. & Cunningham, G.F. (2008) ICESat over Arctic sea ice: estimation of snow depth and ice thickness. *Journal of Geophysical Research*, **113**, C08010, 10.1029/2008JC004753.

Kwok, R., Cunningham, G.F. & Yueh, S. (1999) Area balance of the Arctic Ocean perennial ice zone: October 1996–April 1997. *Journal of Geophysical Research*, **104**, 25747–25759.

Kwok, R., Zwally, H.J. & Yi, D. (2004) ICESat observations of Arctic sea ice: a first look. *Geophysical Research Letters*, **31**, L16401, 10.1029/2004GL020309.

Kwok, R., Cunningham, G.F., Zwally, H.J. & Yi, D. (2006) ICESat over Arctic sea ice: interpretation of altimetric and reflectivity profiles. *Journal of Geophysical Research*, **111**, C06006, 10.1029/2005JC003175.

Kwok, R., Comiso, J.C., Martin, S. & Drucker, R. (2007) Ross Sea polynyas: response of ice concentration retrievals to large areas of thin ice. *Journal of Geophysical Research*, **112**, C12012, 10.1029/2006JC003967.

Lange, M.A. & Eicken, H. (1991) The sea ice thickness distribution in the northwestern Weddell Sea. *Journal of Geophysical Research*, **96**, 4821–4837.

Laxon, S., Peacock, N. & Smith, D. (2003) High interannual variability of sea ice thickness in the Arctic region. *Nature*, **425**, 947–950, 10.1038/nature02050.

Lensu, M. & Haas, C. (1998) Comparison of ice thickness from ship based video and field data. In: *Ice in Surface Waters* (Ed. H.T. Shen), pp. 225–230. Proceedings of the 14th International Symposium on Ice, Potsdam, New York. Balkema, Rotterdam.

Liu, G. & Becker, A. (1990) Two-dimensional mapping of sea ice keels with airborne electromagnetic. *Geophysics*, **55**, 239–248.

Martin, S., Drucker, R., Kwok, R. & Holt, B. (2004) Estimation of the thin ice thickness and heat flux for the Chukchi Sea Alaskan coast polynya from Special Sensor Microwave/Imager data, 1990–2001. *Journal of Geophysical Research*, **109**, C10012, 10.1029/2004JC002428.

Maslanik, J.A., Fowler, C., Stroeve, J., Drobot, S., Zwally, J., Yi, D. & Emery, W. (2007) A younger, thinner Arctic ice cover: Increased potential for rapid, extensive sea ice loss. *Geophysical Research Letters*, **34**, L24501, 10.1029/2007GL032043.

Massom, R.A., Eicken, H., Haas, C. et al. (2001) Snow on Antarctic Sea Ice. *Reviews of Geophysics*, **39**, 413–445.

Melling, H. & Riedel, D.A. (1995) The underside topography of sea ice over the continental shelf of the Beaufort Sea in the winter of 1990. *Journal of Geophysical Research*, **100**, 13,641–13,653.

Melling, H. & Riedel, D.A. (1996) Development of seasonal pack ice in the Beaufort Sea during the winter of 1991–1992: a view from below. *Journal of Geophysical Research*, **101**, 11,975–11,991.

Melling, H. & Riedel, D.A. (2004) Draft and movement of pack ice in the Beaufort Sea: a time-series presentation April 1990–August 1999. *Canadian Technical Reports on Hydrographic Oceanic Science*, **238**, 24 pp.

Melling, H., Riedel, D.A. & Gedalof, Z. (2005) Trends in the draft and extent of seasonal pack ice, Canadian Beaufort Sea. *Geophysical Research Letters*, **32**, L24501, 10.1029/2005GL024483.

Multala, J., Hautaniemi, H., Oksama, M., Leppäranta, M., Haapala, J., Herlevi, A., Riska, K. & Lensu, M. (1996) An airborne electromagnetic system on a fixed wing aircraft for sea ice thickness mapping. *Cold Regions Science and Technology*, **24**, 355–373.

Nghiem, S.V., Rigor, I.G., Perovich, D.K., Clemente-Colón, P., Weatherly, J.W. & Neumann, G. (2007) Rapid reduction of Arctic perennial sea ice. *Geophysical Research Letters*, **34**, L19504, 10.1029/2007GL031138.

Nicolaus, M., Haas, C., Bareiss, J. & Willmes, S. (2006) A model study of differences of snow thinning on Arctic and Antarctic first-year sea ice during spring and summer. *Annals of Glaciology*, **44**, 146–153.

Perovich, D.K., Grenfell, T.C., Richter-Menge, J.A., Light, B., Tucker III, W.B. & Eicken, H. (2003) Thin and thinner: sea ice mass balance measurements during SHEBA. *Journal of Geophysical Research*, **108**, 8050, 10.1029/2001JC001079.

Perovich, D.K., Richter-Menge, J.A., Jones, K.F. & Light, B. (2008) Sunlight, water, and ice: extreme Arctic sea ice melt during the summer of 2007. *Geophysical Research Letters*, **35**, L11501, 10.1029/2008GL034007.

Peterson, I.K., Prinsenberg, S.J. & Holladay, J.S. (2008) Observations of sea ice thickness, surface roughness and ice motion in Amundsen Gulf. *Journal of Geophysical Research*, **113**, C06016, 10.1029/2007JC004456.

Pfaffling, A., Haas, C. & Reid, J.E. (2007) A direct helicopter EM sea ice thickness inversion, assessed with synthetic and field data. *Geophysics*, **72**, F127– F137.

Prinsenberg, S.J. & Holladay, J.S. (1993) Using air-borne electromagnetic ice thickness sensor to validate remotely sensed marginal ice zone properties. In: *Proceedings of the 12th International Conference on Port and Ocean Engineering under Arctic Conditions (POAC '93), Hamburg, 1993, Vol. 2* (Eds. J. Schwarz & K.V. Evers), pp. 936–948. Hamburgische Schiffbau-Versuchsanstalt, Hamburg.

Prinsenberg, S.J., Holladay, J.S. & Lee, J. (2002) Measuring ice thickness with EISFlowTM, a fixed-mounted helicopter electromagnetic-laser system. In: *Proceedings of the Twelfth (2002) International Offshore and Polar Engineering Conference May 26–31, 2002, Vol. 1*, pp. 737–740, Kitakyushu, Japan.

Proshutinsky, A.Y. & Johnson, M.A. (1997) Two circulation regimes of the wind-driven Arctic Ocean. *Journal of Geophysical Research*, **102**, 12493–12514.

Reid, J.E., Worby, A.P., Vrbancich, J. & Munro, A.I.S (2003) Shipborne electromagnetic measurements of Antarctic sea ice thickness. *Geophysics*, **68**, 1537–1546, 10.1190/1.1620627.

Reid, J.E., Pfaffling, A. & Vrbancich, J. (2006) Airborne electromagnetic footprints in 1D earths. *Geophysics*, **71**, G63–G72.

Richter-Menge, J.A., Perovich, D.K., Elder, B.C., Claffey, K., Rigor, I. & Ortmeyer, M. (2006) Ice mass balance buoys: a tool for measuring and attributing changes in the thickness of the Arctic sea ice cover. *Annals of Glaciology*, **44**, 205–210.

Rigor, I.G. & Wallace, J.M. (2004) Variations in the age of Arctic sea ice and summer sea ice extent. *Geophysical Research Letters*, **31**, L09401, 10.1029/2004GL019492.

Rinke, A., Gerdes, R., Dethloff, K. et al. (2003) A case study of the anomalous Arctic sea ice conditions during 1990: insights from coupled and uncoupled regional climate model simulations. *Journal of Geophysical Research*, **108**, 4275, 10.1029/2002JD003146.

Rothrock, D.A. & Wensnahan, M. (2007) The accuracy of sea ice drafts measured from U.S. Navy submarines. *Journal of Atmospheric and Oceanic Technology*, 10.1175/JTECH2097.1.

Rothrock, D.A. & Zhang, J. (2005) Arctic Ocean sea ice volume: what explains its recent depletion? *Journal of Geophysical Research*, **110**, C01002, 10.1029/2004JC002282.

Rothrock, D.A., Yu, Y. & Maykut, G.A. (1999) Thinning of the Arctic sea ice cover. *Geophysical Research Letters*, **26**, 3469–3472.

Rothrock, D.A., Percival, D.B. & Wensnahan, M. (2008) The decline in arctic sea ice thickness: separating the spatial, annual, and interannual variability in a quarter century of submarine data. *Journal of Geophysical Research*, **113**, C05003, 10.1029/2007JC004252.

Saldern, C., von, Haas, C. & Dierking, W.(2006) Parameterisation of Arctic sea ice surface roughness for application in ice type classification. *Annals of Glaciology*, **44**, 224–230.

Serreze, M.C., McLaren, A.S. & Barry, R.G. (1989) Seasonal variations of sea ice motion in the Transpolar Drift Stream. *Geophysical Research Letters*, **16**, 811–814.

Strass, V.H. & Fahrbach, E. (1998) Temporal and regional variation of sea ice draft and coverage in the Weddell Sea obtained from Upward Looking Sonars. In: *Antarctic Sea Ice: Physical Processes, Interactions and Variability* (Ed. M.O. Jeffries). American Geophysical Union, Washington, D.C. *Antarctic Research Series*, **74**, 123–140.

Stroeve, J., Holland, M.M., Meier, W., Scambos, T. & Serreze, M. (2007) Arctic sea ice decline: faster than forecast. *Geophysical Research Letters*, **34**, L09501, 10.1029/2007GL029703.

Stroeve, J., Serreze, M., Drobot, S. et al. (2008) Arctic Sea Ice Extent Plummets in 2007. *EOS Transactions American Geophysical Union*, **89** (2), 13.

Thompson, D.W.J. & Wallace, J.M. (1998) The Arctic Oscillation signature in the wintertime geopotential height and temperature fields. *Geophysical Research Letters*, **25**, 1297–1300.

Thorndike, A.S., Rothrock, D.A., Maykut, G.A. & Colony, R. (1975) The thickness distribution of sea ice. *Journal of Geophysical Research*, **80**, 4501–4513.

Timmermann, R., Beckmann, A. & Hellmer, H.H. (2002) Simulations of ice-ocean dynamics in the Weddell Sea. I: model configuration and validation. *Journal of Geophysical Research*, **107**, 3024, 10.1029/2000JC000741.

Tucker, W.B., III, Weatherly, J.W., Eppler, D.T., Farmer, L.D. & Bentley, D.L. (2001) Evidence for rapid thinning of sea ice in the western Arctic Ocean at the end of the 1980s. *Geophysical Research Letters*, **28**, 2851–2854.

Uto, S., Toyota, T., Shimoda, H., Tateyama, K. & Shirasawa, K. (2006) Ship-borne electromagnetic induction sounding of sea ice thickness in the southern Sea of Okhotsk. *Annals of Glaciology*, **44**, 253–260.

Vihma et al. (2009) ISPOL Journal of Geophysical Research, in press.{AQ1}

Vinje, T., Nordlund, N. & Kvambekk, A. (1998) Monitoring ice thickness in Fram Strait. *Journal of Geophysical Research*, **103**, 10437–10450.

Wadhams, P. (1994) Sea ice thickness changes and their relation to climate. In: *The Polar Oceans and Their Role in Shaping the Global Environment* (Eds. O.M. Johannessen, R.D. Muench & J.E. Overland). American Geophysical Union, Washington, DC. *Geophysical Monograph*, **85**, 337–362.

Wadhams, P. & Davis, N.R. (2000) Further evidence of ice thinning in the Arctic Ocean. *Geophysical Research Letters*, **27**, 3973–3975.

Wadhams, P., Wilkinson, J.P. & McPhail, S.D. (2006) A new view of the underside of Arctic sea ice. *Geophysical Research Letters*, **33**, L04501, 10.1029/2005GL025131.

Warren, S.G., Rigor, I.G., Untersteiner, N., Radionov, V.F., Bryazgin, N.N., Aleksandrov, Y.I. & Colony, R. (1999) Snow depth on Arctic sea ice. *Journal of Climate*, **12**, 1814–1829.

Wingham, D.J., Phalippou, L., Mavrocordatos, C. & Wallis, D. (2004) The mean echo and echo cross product from a beamforming interferometric altimeter and their application to elevation measurement. *IEEE Transactions of Geoscience and Remote Sensing*, **42**, 2305–2323.

Worby, A.P., Jeffries, M.O., Weeks, W.F., Morris, K. & Jaña, R. (1996) The thickness distribution of sea ice and snow cover during late winter in the Bellingshausen and Amundsen Seas, Antarctica. *Journal of Geophysical Research*, **101**, 28441–28455.

Worby, A.P., Geiger, C.A., Paget, M.J., Van Woert, M.L., Ackley, S.F.& DeLiberty, T.L. (2008) Thickness distribution of Antarctic sea ice. *Journal of Geophysical Research*, **113**, C05S92, 10.1029/2007JC004254.

Yu, Y. & Rothrock, D.A. (1996) Thin ice thickness from satellite thermal imagery. *Journal of Geophysical Research*, **101** (C11), 25,753–25,766.

Zhang, J., Rothrock, D. & Steele, M. (2000) Recent changes in Arctic sea ice: the interplay between ice dynamics and thermodynamics. *Journal of Climate*, **13**, 3099–3114.

Zwally, H.J., Yi, D., Kwok, R. & Zhao, Y. (2008) ICESat measurements of sea ice freeboard and estimates of sea ice thickness in the Weddell Sea. *Journal of Geophysical Research*, **113**, C02S15, 10.1029/2007JC004284.

This page intentionally left blank

5 Snow and Sea Ice

Matthew Sturm and Robert A. Massom

5.1 Introduction

Most sea ice older than a few days is covered with snow. The snow modifies the physical, climatic and biological impact of the ice, and it alters the processes that take place involving the ice. In large measure, this is due to the snow's superb insulative properties, its high albedo and its role as a source of freshwater to the ocean when it melts. As a result, snow is an integral component in polar atmosphere-ice-ocean interactions and is a key determinant of the structure of high-latitude marine ecosystems (Ledley, 1991; Eicken, 1992; Granberg, 1998). Its presence complicates the interpretation and retrieval of sea ice geophysical parameters from satellite data (Lubin & Massom, 2006), and from a human perspective, the snow on the ice affects travel and hunting conditions during subsistence activities (Gearheard et al., 2006). It also reduces the ice-breaking efficiency of icebreakers. Moreover, snow in the Arctic entrains and transports contaminants such as soot (Grenfell et al., 2002) and mercury (Douglas et al., 2008). In short, understanding snow on sea ice is crucially important.

In this chapter, we review our current knowledge of the sea ice snow cover. The emphasis here is on polar regions, although snow is also a key component of other ice-covered seas, e.g. the Sea of Okhotsk (Toyota et al., 2007). The overall aim of the chapter is to show that the snow cover exhibits variability and heterogeneity in thickness and physical properties over a range of spatial and temporal scales – and that this variability has a direct bearing on the overall impact of the snow. Nonetheless, we show that certain large-scale patterns do occur, and that there are distinct differences between Arctic and Antarctic sea ice snow cover. Detailed information on the techniques used to measure snow on sea ice is beyond the scope of this chapter, and the reader is referred to Sturm (2009). Throughout, snow type is described according to the *International Classification for Snow on the Ground* (Colbeck et al., 1990).

Roots: a short history of snow on sea ice studies

Ancient and intrepid sailors who entered the pack ice more than 2000 years ago were undoubtedly the first observers to note that sea ice is usually covered by snow, though it is uncertain how much attention they paid to this detail. The first recorded account is of Pytheas, a Greek from Massilia, who sailed a bireme northwest of Scotland in 325 B.C., encountering pack ice
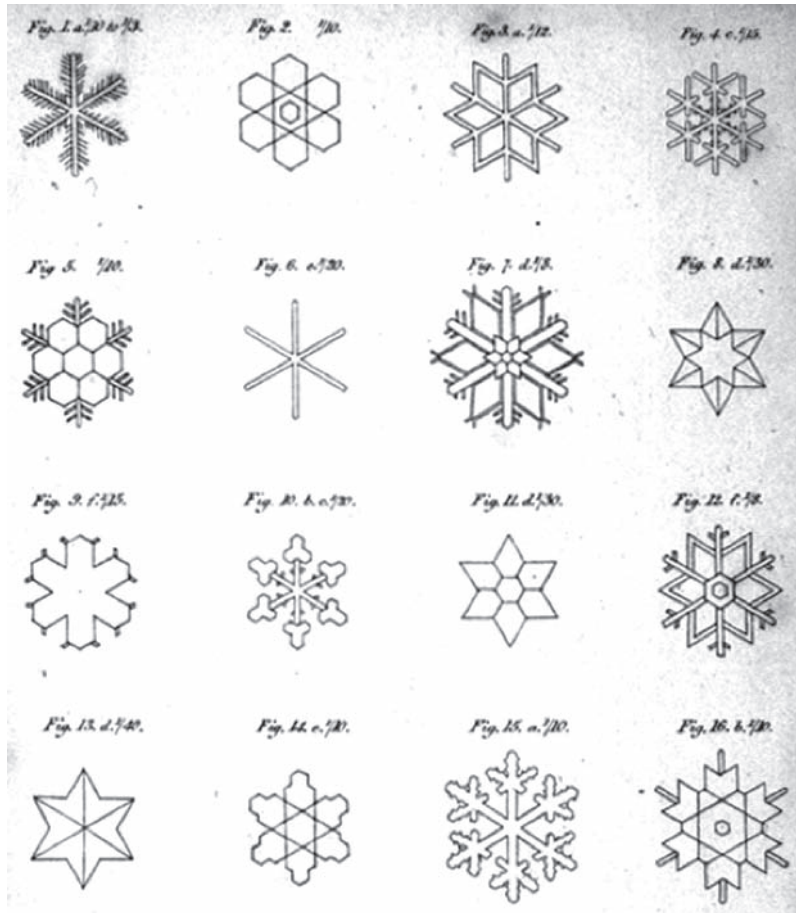
Fig. 5.1   Snowflakes observed by Captain William Scoresby while whaling near Greenland, 1810–1820. From Scoresby (1820), p. 588, Plate VIII.

southeast of Iceland (Mowat, 1960). There were undoubtedly other early voyages, but the next recorded run-in with the ice seems to be that of the Celtic priest, Brendan, who sailed a leather curragh not only to Iceland and Greenland, but also to Jan Mayen Island, all in 550 A.D. In his extensive travels, Brendan must surely have noted that until late in the summer, the ice floes were covered by snow. By the 1550s, mariners were plying the Northeast Passage up and around Scandinavia and Russia for purposes of trading, and occasionally they were forced to winter over on the northern coast. During those dull and interminable dark winters, they would have had an excellent first-hand look at the snow, as well as plenty of time to make observations on the snow cover, but if they did so, no accounts have survived. The first proof of attention to snow on Arctic sea ice we have found is the work of William Scoresby (1820), a whaling captain from England who travelled extensively in the Arctic waters near Greenland (Fig. 5.1). Scoresby was one of a legion of navigators who tried to find and sail through the Northwest Passage (Cooke & Holland, 1978).

The search for the Northwest Passage continued until 1906 and is recounted in several books including *Ordeal by Ice* (Mowat, 1960) and *Arctic Grail* (Berton, 1989). Voyages

Table 5.1   Iñupiaq words for snow features (cf. Webster & Zibell, 1970).

Akillukkak	Soft snow behind a drift
Apun	Snow cover; snow (generic)
Aluktinniq	Windswept snow-free area on the ice
Avoorik	A whaleback drift
Kamoruk	A long snowdrift useful for navigation
Katagagnatuaq	Deep melting snow or wet slushy area (a snow swamp)
Kiyokluk	An 'anvil-head' drift or sastrugi
Katikronuk	Migrating dunes, still soft and eroding by the wind
Isrriqutit	Diamond dust or ice crystals in the air
Masayyak	Snow damp enough to stick, as in making snowballs
Natigvik	Low drifting snow, no higher than the knee
Nataovuoaluka	Saltating and suspended snow in a full-on blizzard
Nutagak	Fresh powder snow
Nutaak	Soft snow
Nutagun	New/fresh snow covering a hole in the ice
Pukak	Basal snow that has metamorphosed into depth hoar
Kayuktak	Ripple marks on the snow surface
Silliq	Hard, icy snow
Silliqruk	Old icy snow, extra hard

venturing south to the Antarctic ice pack started with Captain Cook's epic journey in 1773 (Beaglehole, 1974). Here again, explorers encountered sea ice, and snow on the ice. We are indebted to these intrepid explorers, who braved the sea ice, and snow, in fragile ships, pushing back both the geographic and scientific frontiers.

Snow on ice in northern cultures

Nonetheless, we must look to northern indigenous cultures for the earliest in-depth knowledge of the sea ice snow. There are about 75 words for snow and snow features in Iñupiaq, the Inuit language spoken in northern Alaska (Webster & Zibell, 1970; with additions by Sturm, unpublished data). A similar list exists for Inuktitut, the language of Greenland and eastern Canada. There is good reason to believe that this language is hundreds if not thousands of years old, suggesting these cultures had an appreciation of many of the features and subtleties of snow on ice that would not be learned by western science until the late 20th century. Table 5.1 lists some Iñupiaq words that demonstrate knowledge of key properties and processes that take place in the snow and that we discuss in this chapter.

5.2 The intimate and complex relationship between snow and sea ice

Snow has an intimate yet complex relationship with sea ice. They share a common origin in a cold climate, but while the sea ice requires only below-freezing ocean temperatures to form,

the snow cover needs three conditions to be met:

(1) Low temperatures to ensure that precipitation comes as snow, sleet or hail.
(2) Precipitation.
(3) An existing ice cover with sufficient bearing capacity to support the fallen snow.

Regarding this last requirement, much initially depends on the sequence of weather events in autumn, when sea ice is beginning to form. If the weather is cold and dry, then rapid thermodynamic sea ice growth will occur, undeterred by the strong insulating properties of a snow cover. When snow subsequently falls, it will accumulate on a relatively dry substrate that is thick enough to support it. This results in a dry and non-saline snow cover. With cold but damp weather, on the other hand, snowfall is likely to coincide with the initial sea ice formation. Snow accumulating on newly forming sea ice will significantly slow its thermodynamic growth rate (Maykut & Untersteiner, 1971), and is more likely to become damp/wet, by (1) wicking brine upwards from the newly formed ice surface and/or (2) by depressing the thin ice below sea level, causing flooding. Both of these processes result in a snow cover that has a wet, saline base. The subsequent evolution of both dry and wet snow covers is intimately connected to that of the underlying ice, coupled by strong heat and moisture exchange between the two layers. This interaction, along with highly variable weather events (cycling of storms with cold periods), plus more slowly acting seasonal cycles, determines whether the snow will remain dry or wet. Ocean heat flux also comes into play in Antarctica in particular (Martinson & Iannuzzi, 1998) via its effect on the snow:ice thickness ratio.

Two key equations, linked by snow depth, density and thermal conductivity, govern the most important aspects of the interplay between snow and ice. Their simplicity belies the myriad of trajectories that can be taken by the snow sea ice system. The first equation describes the isostatic balance between floating ice and an overburden of snow, assuming that the ice is in hydrostatic equilibrium (Fig. 5.2):

$$f = h_i \left(\rho_w - \rho_i \right) - h_s \rho_s \qquad \text{(Equation 5.1a)}$$

where h is thickness, f is the ice freeboard, ρ is density and the subscripts w, i and s refer to seawater, ice and snow respectively. Equation 5.1a states that ice freeboard is controlled by the difference between the ice buoyancy (first term on the right-hand side) and the weight of the snow (second term). Snow flooding occurs when f is negative, or when:

$$h_s \geq h_i \left\{ \frac{\rho_w - \rho_i}{\rho_s} \right\} \qquad \text{(Equation 5.1b)}$$

Approximate mean values of ρ_w, ρ_i and ρ_s are 1000, 900 and 300 kg m^{-3}, respectively, suggesting that if the snow depth:ice thickness ratio exceeds 1:3, then seawater flooding will potentially occur. As discussed later, flooding depends on availability of conduits between the ocean and ice surface, which in turn depends on the ice temperature, the salinity, and/or state of deformation. A key point is that flooding diminishes the insulative capacity of the snow. Water-saturated snow conducts heat far better than dry snow, resulting (under freezing conditions) in a rapid refreezing of the *snow-slush* to form *snow-ice*. In this manner, sea ice formation can, paradoxically, occur in the presence of a thick insulative snow cover, and at the ice
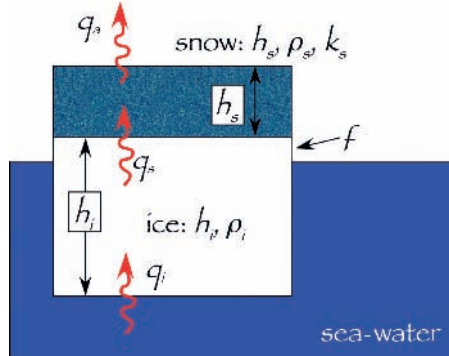
Fig. 5.2 Schematic of a sea ice floe covered by a snow cover. The symbols are defined in the text. The red lines indicate heat flow, which here is assumed to be only in the vertical direction, and hence must be equal at all levels along a vertical pathway i.e. $q_a = q_s$. q_i, the heat flux from the ocean, is assumed to be zero, with all heat loss up through the ice converted into ice growth at the base of the existing ice.

surface rather than its base. Flooding and snow–ice formation, which are much more common in the Antarctic than Arctic, are discussed in greater detail in Section 5.6 and Chapter 2.

The second equation describes the relationship between sea ice growth and heat loss (q):

$$\frac{dh_i}{dt} = \frac{1}{\rho_i L_i} \left\{ -k_s \frac{\Delta T_s}{h_s} \right\}$$ (Equation 5.2a)

where t is time, k_s is the bulk thermal conductivity of the snow, ΔT_s is the vertical temperature drop across a snow cover that is h_s thick and ρ_i and L_i are the density and the latent heat of fusion of ice (Pounder, 1965). This simple equation for ice growth assumes that the heat flow through the ice equals the heat flow through the snow, and that there is no significant heat flow to the bottom of the ice from the ocean below (i.e. q_i in Fig. 5.2 is zero).

Sturm et al. (1997) developed a relationship between thermal conductivity (W m^{-1} K^{-1}) and snow density (kg m^{-3}):

$$k_s = 0.138 - 0.00101\rho_s + 0.000003233\rho_s^2$$ (Equation 5.2b)

which when substituted into equation 5.2a links ice growth directly to snow density, and inversely to snow depth. For a fixed temperature drop across the snow pack, the denser the snow, or the thinner the snow pack, the faster the rate of ice growth. Of course, as the ice gets thicker, the snow–ice interface temperature will decrease, and the temperature difference across the snow pack (ΔT_s) will be reduced, slowing the rate of ice growth. Snow thermal conductivity is discussed in more detail in Section 5.5.

The interactions described in equations 5.1 and 5.2 have been explored in numerous models (e.g. Saloranta, 2000; Maksym & Jeffries, 2000). Table 5.2 suggests why this linked behaviour is both endlessly fascinating and confoundedly difficult to pin down. Bear in mind that 'deeper' snow here is relative to the sea ice thickness (i.e. is more than 1/3 the ice thickness), not an absolute measure of snow depth.

Despite many exceptions to the rule, we suggest that the central Arctic Basin is predominantly a 'dry' ice-snow system in which the snow depth is rarely sufficient to 'sink' the ice

Table 5.2 Simplified interactions of Equations 5.1 and 5.2.

	Primary Effect	Result 1	Result 2	Result 3
Equation 5.1				
Denser snow	More flooding	More snow-ice	Larger ΔT_s	More congelation ice
Deeper snow	More flooding	More snow-ice	Larger ΔT_s	More congelation ice
Equation 5.2				
Denser snow	More heat conduction	More congelation ice	Less flooding	Less snow-ice
Deeper snow	Less heat conduction	Less congelation ice	More flooding	More snow-ice

(apart from the marginal seas) (Perovich et al., 1988), while the Antarctic is largely a 'wet' ice-snow system where the snow often exceeds the buoyancy of the ice. This contrast has its origin in the diametrically different geographical settings and environmental conditions of the two polar regions, which result in fundamentally different sea ice conditions (see Chapter 1, also Lubin & Massom, 2006). The Antarctic sea ice zone is predominantly seasonal, about 80% first-year ice (FYI) that melts back each summer, compared to less than 50% FYI for the Arctic (Chapter 6) – although the extent of Arctic multiyear ice (MYI) is dropping dramatically (Maslanik et al., 2007). The overall impact of these hemispheric differences on the temporal evolution of the two snow covers is elaborated upon in Section 5.4, which also describes the dramatic switch that takes place in spring when the Arctic system shifts from 'dry' to 'wet'. When that happens, melt ponds cover up to 60% of the Arctic ice surface in spring (Eicken et al., 2004): such ponds are largely absent from Antarctic sea ice (Andreas & Ackley, 1981).

5.3 General characteristics of snow on ice

Snowflakes

The raw material from which the snow cover on the sea ice is built comes from snowflakes, those falling gems of exquisite symmetry that have fascinated humans for thousands of years (see Fig. 5.1). Snowflakes have been the subject of numerous books (Nakaya, 1954), and several snowflake classification systems have been proposed (LaChapelle, 1992). As many as 80 snowflake types have been identified, but these can be subdivided into two basic classes: (1) those with hexagonal symmetry and euhedral crystalline forms and (2) those with amorphous forms. The former class includes sector plates, stellar dendrites (Fig. 5.3a: the 'classic' six-armed snowflake of Christmas decorations), columns and needles. The latter class includes graupel, ice pellets and hail.

Snow metamorphism

With respect to the sea ice snow cover, however, it hardly matters which class or type of snowflake falls. What is important are: (1) the amount that falls, (2) the rate of snow accumulation and (3) whether the snow falls with or without wind. This is because once deposited, snowflakes quickly lose their original form through the action of wind, gravitational and thermal
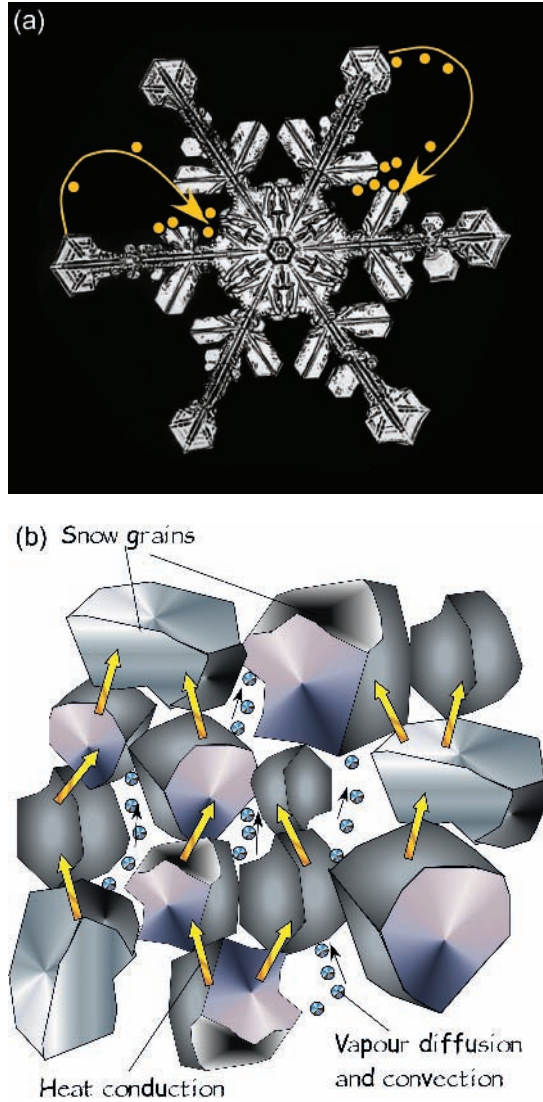
Fig. 5.3 (a) A stellar dendrite (branched snowflake), showing schematically how vapour diffusion driven by the Kelvin (curvature) Effect, leads to a net transfer of water molecules (yellow circles) from branch points to cusps near the centre of the snowflake (snowflake by C. Bentley, http://snowflakebentley.com/snowflakes.htm). (b) Macroscopic temperature gradients across the snow pack produce a net upward flux of water molecules (small circles) through the sea ice snow cover, accreting on the lower side of grains, sublimating from the upper sides and changing the size and shape of the grains. The yellow arrows indicate heat flow by conduction through the ice network of grains. The black arrows indicate heat flow produced by the vapour flux. Drawing by M. Sturm.

effects. The wind breaks and fragments snowflakes, creating sharp-pointed shards that sinter (bond) rapidly. Gravity-driven settling further breaks off fragile snowflake arms and compacts the snow. The surface curvature of these fragments drives a net movement of water molecules from snowflake branch tips to cusps (negative curvature), rounding the grains (the Kelvin Effect: see Fig. 5.3a). Temperature gradients across the snow pack drive a diffusive flux of

Table 5.3 Four types of metamorphic pathways for snow on sea ice. Resultant snow conditions are given in italics.

Type 1	Type 2	Type 3	Type 4
Destructive metamorphism[1]	Constructive metamorphism[1]	Wind metamorphism	Wet snow metamorphism
Equi-temperature metamorphism (ET)[2]	Temperature gradient metamorphism (TG)[2]		
Equilibrium growth[3]	Kinetic growth[3]		
Grains become rounded	*Grains become faceted and striated*	*Small shard-like grains with percussive features result*	*Rounded grains with water films result, and can refreeze*

[1]Seligman, 1936 & von Eugster, 1950
[2]Sommerfeld, 1970
[3]Colbeck, 1982

vapour from the base of the snow upwards, creating more rounding or, if the temperature gradient is strong enough, faceted crystalline grains (Fig. 5.3b). In short, in as little as a few hours, the original snowflakes are often replaced by new forms through metamorphic transitions. These changes impact snow grain size, density and thermal conductivity, as well as optical and electromagnetic properties, as the snow cover evolves (see Section 5.5).

Four basic metamorphic pathways have been identified, though several interchangeable sets of terms have been used to describe two of these pathways (Table 5.3). One pathway (*destructive metamorphism*, *equi-temperature* [*ET*], or *equilibrium growth*) produces rounded grains when temperatures are below freezing, but temperature gradients are low. Another pathway (*constructive metamorphism*, *temperature gradient* [*TG*], or *kinetic growth*) produces faceted ornate grains that grow rapidly when a strong temperature gradient is imposed on the snow cover. Two other pathways are *wind metamorphism*, which produces small fragmented grains that sinter (bond) strongly, and *wet snow metamorphism*, which takes place when liquid water is introduced to the snow cover by above-freezing temperatures or rain.

Changing from one metamorphic pathway to another is common: once snow is deposited on the ice, it will frequently move down one pathway, then another, then switch to yet a third (and so on) as the ambient conditions change. For example, new snow may fall, followed by a brief thaw during which time the snowflakes will begin to melt. Liquid water will collect at the interstices of the grains, the grains will round and the whole mass may refreeze into an icy layer. Alternately, after the new snow falls, the wind speed may increase sufficiently to transport the flakes, breaking and fracturing them as they bound along the ice surface. Next, the weather may turn cold, and the wind-driven grains will seize up into a hard wind slab. Under freezing conditions, the sea ice surface will remain warm relative to the air owing to its proximity to seawater at a temperature near $-1.8°C$, so a strong temperature gradient will be set up across the snow. This gives rise to kinetic growth, leading to the formation of depth hoar (described below). Such cyclical metamorphic transitions occur in marginal ice zones in general, over much of the whole Antarctic sea ice zone throughout the winter and in the central Arctic ice pack in the 'shoulder' seasons (autumn and spring).

Snow grain types

Each type of metamorphic pathway, or combination of pathways, produces snow grains with distinct characteristics. *The International Classification for Snow on the Ground*
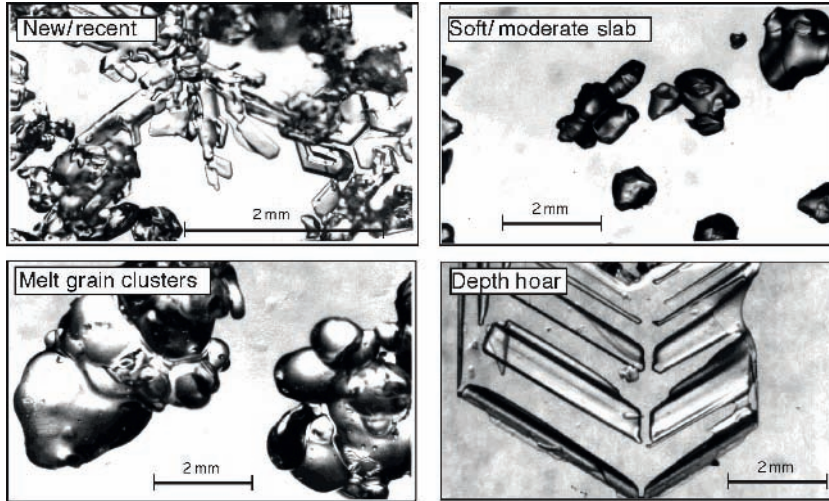
Fig. 5.4   Four common types of snow grains found on sea ice. From Sturm et al. (1998). Reproduced by permission of American Geophysical Union. Copyright 1998 American Geophysical Union.

(Colbeck et al., 1990), and its replacement (Fierz et al., 2008), provide comprehensive descriptions of these grains as well as pictures of each type. Six types are typically found on sea ice (both Arctic and Antarctic: Massom et al., 2001; Sturm et al., 2002a). These are:

1.   New and recent snow
2.   Fine-grained snow
3.   Wind slab
4.   Faceted grains including depth hoar
5.   Icy layers
6.   Damp/wet snow and slush

Micrographs of four of the most common types on sea ice are shown in Fig. 5.4.

New/recent snow

New snow is generally defined as having fallen within the last 24 hours, and is always at the top of the snow pack. Recent snow may retain features of new snow (i.e. snowflake forms) for days to weeks, and is often found deeper in the snow pack. The density and grain size of this type of snow largely reflects conditions during and immediately after deposition. In the absence of wind, gravitational settlement is the primary metamorphic force acting on the snow, with the amount of newly fallen snow (i.e. the overburden) determining the settlement rate and the density. Kojima (1966) has modelled the settling of the snow as a viscous fluid, where the viscosity is highly dependent on the snow density. As the snow densifies, it becomes more viscous and therefore settles and compacts ever more slowly. This results in a characteristic exponential settling curve that depends on the initial density of the snow. Table 5.4 lists the range of densities of new and recent snow.

Table 5.4 New and recent snow densities (after McKay & Gray, 1981).

Snow Type	Density (kg m^{-3})
Wild snow (still falling)	10–30
New snow	50–65
Recent snow	70–90
New snow with wind	60–80

Fine-grained snow

Fine-grained snow is frequently a default identification when (1) snow grains are small (<1 mm), (2) they show neither obvious characteristics of the initial snowflakes nor indications of wind action and (3) they have no facets or other obvious characteristics of kinetic growth (Table 5.3). The density of a fine-grained layer of snow rarely exceeds 350 kg m^{-3}. One source of possible confusion in identifying fine-grained snow is that a wind slab, while in the process of being formed, will be both fine-grained and soft, but within 24 hours of being deposited, the wind slab will sinter (see below) into a hard cohesive unit, while the fine-grained snow will not. In practice, older wind slab cannot be penetrated by a finger.

Wind slab

Strong (>8 m s^{-1} at 10m height) winds both during and following snowfall events (Massom et al., 1997) produce significant mechanical fragmentation and compaction of the snow, which creates medium- to high-density hard layers known as *wind slabs* (Seligman, 1936; Benson & Sturm, 1993). This snow type is characterized by very small snow grains (0.1–0.5 mm) that are well bonded, has low permeability and is ideal snow for constructing igloos. The wind transports snow grains by saltation and suspension (Pomeroy & Gray, 1995). Saltation, which is also a mechanism that transports sand grains in the desert, occurs because the wind speed 0.1–0.5 m above the snow surface is greater than at the surface itself. Grains ejected upwards by grain–grain collisions get accelerated by the faster wind, sustaining the transport process. When the wind finally ceases, a layer of small fragmented grains will remain, and will sinter into a hard mass. Sintering is a process in which a fine-grained material is brought to a temperature that is within a few tens of degrees of its melting point, then allowed to cool (German, 1996). Volume diffusion during the heating and cooling transfers molecules to the cusps formed where sharp-pointed grains touch each other, bonding the material into a solid mass. Many of the parts in a cell phone are produced this way. Snow sinters in large measure because it is often within 20°C of its melting temperature. In general, the finer the grains, and closer the temperature is to the freezing point, the harder the resulting wind slab. In some cases, these slabs can become so hard they cannot be shovelled, but have to be cut with a saw.

Faceted grains including depth hoar

Temperature gradients produce water vapour density gradients that lead to snow grain growth (Fig. 5.3b). When the gradients exceed ~25°C m^{-1} (e.g. a drop of 10°C from the ice surface to the top of a 0.4-m-deep snow pack) (Akitaya, 1974), faceted grains will grow.

Fig. 5.5   A depth hoar cluster from the base of a snow cover that formed over an ice surface. Note the euhedral (geometric) shapes, the striae, and the razor-sharp edges indicating rapid, kinetic growth. The clear crystal in the foreground is about 11 mm across.

The facets and other euhedral and ornate growth structures (see Figs 5.4 and 5.5) form because the growth is limited by crystallographic growth mechanisms rather than vapour supply. The resulting crystals are beautiful and distinctive. Both Arctic and Antarctic sea ice snow covers exceed the critical gradients for most of the winter (Massom et al., 2001; Sturm et al., 2001). Exceptionally strong temperature gradients exist in autumn when the ice is new, the ice surface temperature is near-freezing and the snow cover is thin (<0.2 m). Sturm et al. (2001) found gradients exceeding 100°C m^{-1}, four times the critical gradient. This is the reason that the basal layers of snow are often metamorphosed into large (3–10 mm) faceted grains called depth hoar. Depth-hoar formation also forms under dense icy layers, due in part to their high thermal conductivity (Sturm et al., 1997) and the fact that these layers impede upward vapour flow (Colbeck, 1991).

There is a continuum of faceted grains. When kinetic (or TG) growth begins, the first grains that form are small rounded grains (<1 mm) with a few incipient facets. With increasing time (and higher-temperature gradients), fully faceted grains, then hollow skeletal grains, or striaed pyramidal cups, can form (1–8 mm). These can be at the base of the snow (depth hoar), at the surface (surface hoar) or beneath an ice lens or layer. Eventually, complex and ornate grain clusters like those shown in Fig. 5.5 will develop. By mid-winter, layers composed of grains like those in Fig. 5.5 will have undergone total recrystallization. In fact, Sturm and Benson (1997) found that the winter vapour flux was 10 times greater than needed to achieve the apparent growth rates, suggesting that the grains in the pack recrystallized several times over.

Icy layers

Icy layers and ice lenses in the snow are prevalent during all seasons in both Arctic and Antarctic snow covers, but are common in the Antarctic. They form in several ways. Above-freezing temperatures (thaws) can produce liquid water at the snow surface, while sleet/rain can introduce water into the pack even if the temperature is slightly below freezing

(Massom et al., 1997; Sturm et al., 1998). The water will either penetrate into the snow pack in discreet pipes (this happens if the snow is well below freezing) (Wankiewicz, 1978) or move downwards as a planar wetting front (if the snow is isothermal at 0°C). In both cases, multiple internal ice lenses and layers can be formed in a single thaw or rain-on-snow event. The telltale sign of this occurrence is that several ice layers will be connected by vertical percolation columns. Two other mechanisms have also been proposed to explain the formation of thin (<0.5 mm) ice layers: (1) wind glazing due to kinetic heating of the snow surface by wind-driven (saltating) drift snow (Goodwin, 1990) and (2) radiation effects (in spring–summer) (Colbeck, 1991). Our direct experience has been that virtually all Arctic wind glaze layers we have examined could be traced back to episodes of thaw, rain-on-snow or freezing mist (*minniq* in Iñupiaq). In the Antarctic, we have observed minor topographic perturbations like hoarfrost 'flowers' transformed into icy rippled and 'nubbly' layers consisting of irregular lumps of ice, 0.01–0.02 m high and spaced every few centimetres, but again only when liquid water was present in the air (Sturm et al., 1998). Wind-blasted, upwind faces of sastrugi and dunes are particularly susceptible to icy crust formation (Massom et al., 1997).

Although icy layers in total represent only a small fraction of the total snow cover thickness on sea ice, they play an inordinately large role in the evolution of the snow pack. For example, less than 3% of the snow on East Antarctic sea ice comprised icy layers in winter 1995 (Massom et al., 1998), but these layers effectively 'locked' the snow in place and reduced wind erosion and sublimation losses. Similar results have been observed in the Arctic (Sturm et al., 2002a). The wind crusts and ice layers also intercept meltwater migrating downwards in percolation columns (Colbeck, 1991), even in winter (Jeffries et al., 1997; Sturm et al., 1998). Where intercepted, this meltwater will spread out laterally and can create quite thick (~30 mm) icy layers. Such features have a significant effect on polarization in microwave remote sensing (Garrity, 1992). These horizontal ice layers also form largely impermeable barriers to the upward flux of water vapour, leading to enhanced depth-hoar formation underneath them (Colbeck, 1991; Massom et al., 2001).

Damp/wet snow and slush

The introduction of liquid water, either fresh or saline, into the snow pack produces a predictable change in grain size and shape. Colbeck et al. (1990) present a general classification of liquid water content in snow: dry when the percentage of liquid water is 0%, moist when it is less than 3%, wet at 3–8%, very wet at 8–15% and saturated (slush) at greater than 15%. An alternate system recognizes two wetting regimes: a low-water regime in which the pore spaces between snow grains are still air-filled and connected, and the liquid water is found as a meniscus at grain junctions (*pendular regime*), and a high-water regime where the water films are continuous and air spaces are isolated bubbles within the water film (*funicular regime*). Denoth (1982) indicates that the transition between regimes occurs when the water content exceeds 7%. Regardless of which water regime is in force, the net result is that the snow grains become rounded. The initial rounding should not be mistaken for melting. By definition, water-surrounded grains are isothermal at 0°C, a condition highly conducive to volume diffusion as well as the destruction of sharp-edged features like those in Fig. 5.5. Low water content metamorphism produces clusters of rounded crystals held
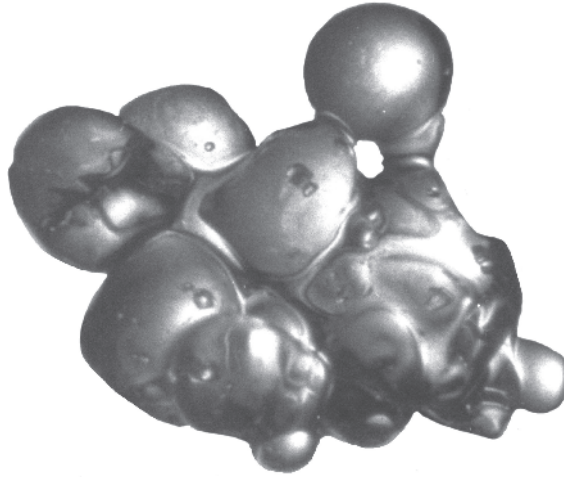
Fig. 5.6   A melt-grain cluster showing the rounded grains and thick ice-to-ice bonds typical of low to moderately wet snow (now refrozen). The cluster is ~10 mm across.

together (after refreezing) by large ice-to-ice bonds (Colbeck, 1986) (Fig. 5.6). High water content metamorphism and subsequent freezing leads to rounded melt-freeze particles, whereby individual crystals are frozen into a solid polycrystalline grain. Melt-grain clusters up to 10 mm across have been observed in Antarctic in all seasons but mainly in summer (Haas et al., 2001), and in the Arctic in spring. These large clusters have a strong microwave signature (see Section 5.7).

   The most extreme stage of wet metamorphism is slush. In slush, the ice grains are no longer bonded to one another, and may not even be in contact. The grains are oblate ellipsoids, very beautiful and regular. Slush on sea ice can be fresh (as when a melt pond is formed) or saline (when the slush is due to seawater flooding). In the latter case, capillary 'wicking' of seawater can wet/dampen the snow to a height of 0.1–0.2 m above a saturated (slush) layer (see Figure 6 in Massom et al., 2001).

Metamorphic pathways

While the 'pure' outcome of each of the individual metamorphic pathways shown in Table 5.3 is distinctive and differentiable snow grains, actual metamorphic trajectories are often more complex, producing grains with compound characteristics. For example, new snow falling on the sea ice might first undergo kinetic growth (TG metamorphism), becoming faceted or, if the negative temperature gradients prevail longer, striated and faceted. If the temperature rises and reduces the temperature gradient across the snow, equilibrium (TG) metamorphism will be initiated, and the faceted grains will begin to round. With time, the grains may become fully rounded. If the temperature rises further (to above freezing), then melt-grain clusters, or perhaps even slush, will form. If the air temperature drops, strengthening the temperature gradient across the snow cover, then kinetic growth will start again. These complex trajectories are traced out schematically in Fig. 5.7.
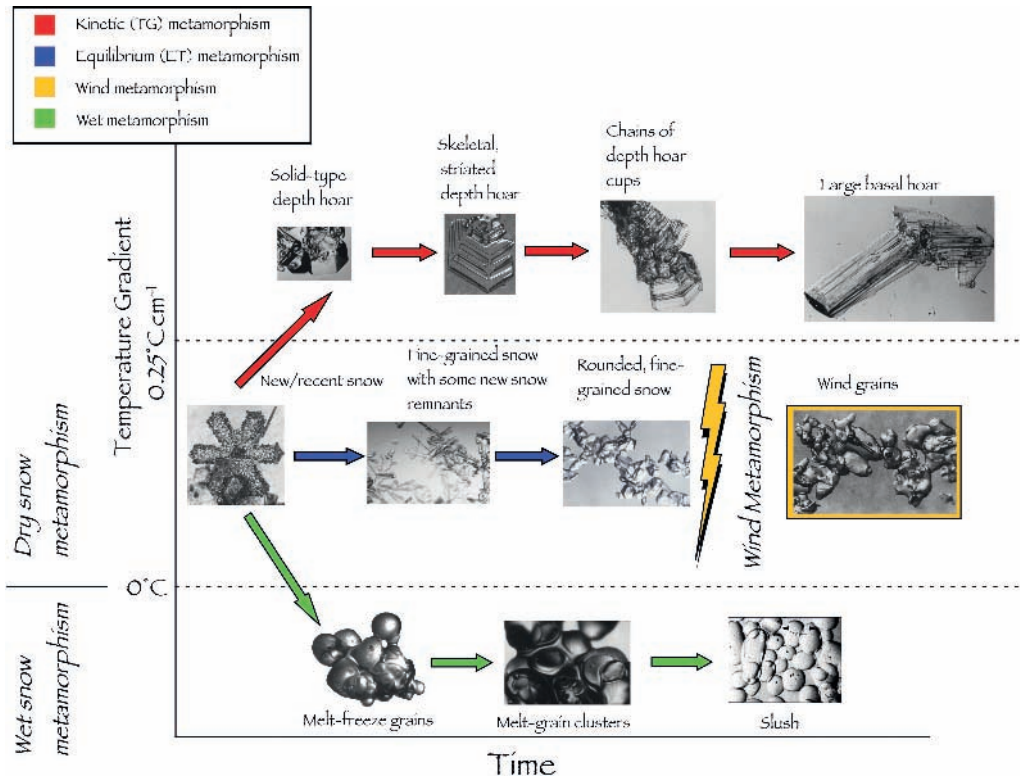
Fig. 5.7 Metamorphic pathways for snow grains under different environmental conditions. Cross-connections are not shown to avoid clutter, but virtually all nodes in the figure could be interconnected.

Snow layering and salinity

Snow grains are the building blocks of snow layers, while layers are the fundamental components of the snow cover. They are easy to recognize, but harder to define. Typically, grain size, shape and multigrain structures (see Fig. 5.7: *chains of depth hoar*) differ from one layer to another, comprising a suite of differences that leads to visually distinct units with sharp boundaries (Fig. 5.8). The sources of these differences are the weather and time. Each layer has a different depositional history and follows a unique post-depositional metamorphic trajectory. In the absence of wind transport, melting or significant ice topography, snow layers will be planar and laterally continuous, but on sea ice this is rare. More often, within wind-generated features such as ripple marks, sastrugi and dunes, the layers taper. For example, all three of the layers in Fig. 5.8a are tapered because they were deposited or reworked by the wind into long whaleback-shaped dunes. One reason layers are important is that the physical and thermal properties of the snow are assigned to layers, with bulk properties often being computed from individual layer values as a weighted average.

There are no simple rules for connecting snow-layer characteristics to weather events, but the connection is strong. Of the eight layers making up the snow cover on the sea ice of the Chukchi Sea during project SHEBA (Surface Heat Budget of the Arctic, Perovich et al., 1999) shown in Fig. 5.9, six formed during combined snowfall and wind transport events,
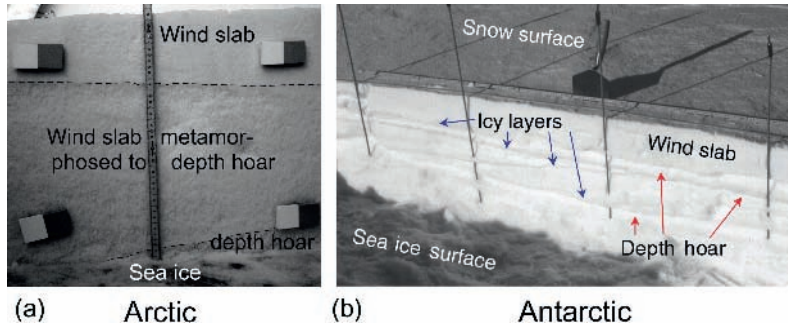
Fig. 5.8 (a) The snow cover on sea ice in the Chukchi Sea off the coast of Barrow, Alaska, photographed using near-infrared photography (Mätzl and Schneebeli, 2006). The grey and white markers are Spectralon, a material of known reflectance. The snow is 0.43 m deep. (b) Photograph of cross-section through a typical winter snow cover (depth 0.25 m) from the Amundsen Sea, Antarctica, September 1994, showing distinct layering (from Massom et al., 2001). Reproduced by permission of American Geophysical Union. Copyright 2001 American Geophysical Union.
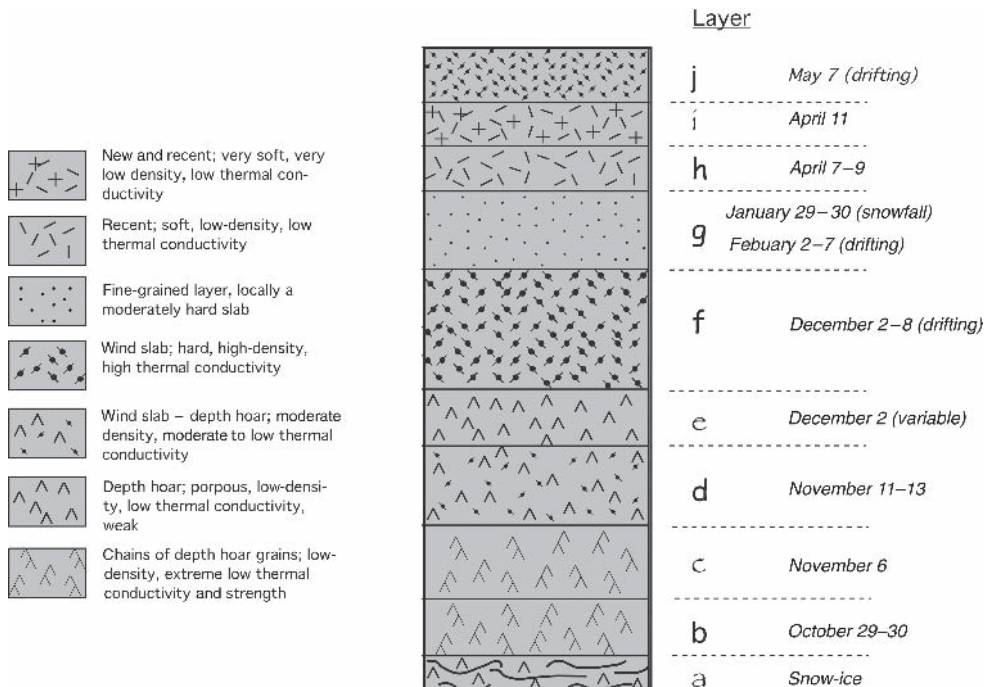
Fig. 5.9 Generalized snow stratigraphy column for the SHEBA area, 1997–1998. Symbols follow the Colbeck et al. (1990) snow classification. Dates indicate the approximate time of layer deposition (see Fig. 5.10). The thin layer of snow ice (a) was in this case formed from snow that had fallen on wet ice prior to the experiment. From Sturm et al. (2002a). Reproduced by permission of American Geophysical Union. Copyright 2002 American Geophysical Union.

while two formed from snowfall without significant wind (see Fig. 5.10). Significant dry snow transport takes place when 10-m wind speeds are in excess of 8 m s^{-1} (Andreas & Claffey, 1995) – a threshold often exceeded over Antarctic sea ice in particular (Massom et al., 2001). Precipitation seems to be the one necessary ingredient for layer formation. Our experience has been that wind transport events alone cannot produce layers (although they
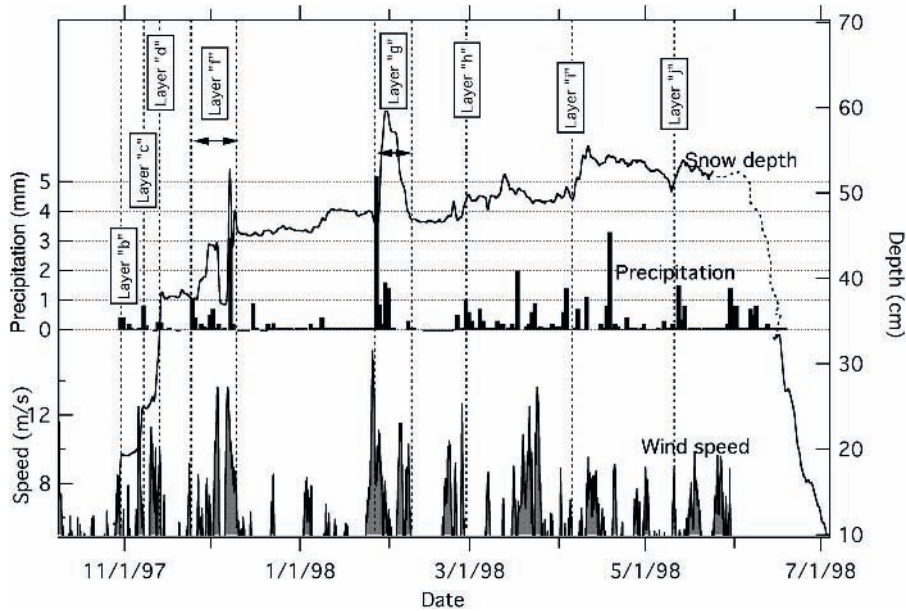
Fig. 5.10 Snow layer formation during the winter of 1997–1998 on the sea ice during Project SHEBA (Chukchi Sea) as determined from correlation of weather records with the snow depth measured at a sonic sounder site (dark line). Layer descriptors correspond to layers shown in Fig. 5.9. In total, the record contained ~30 precipitation events and at least 26 contiguous periods when wind speed was sufficient to transport unconsolidated new snow. From Sturm et al. (2002a). Reproduced by permission of American Geophysical Union. Copyright 2002 American Geophysical Union.

can and do erode existing layers of snow). An episode of winds in excess of 12 m s^{-1} with no snow layer formation in late March shown in Fig. 5.10 bears this out.

Wind is therefore crucial to the formation of snow layers and the development and evolution of the snow cover on the sea ice. Wind transport generally produces heterogeneity in snow depth distribution and properties, rather than homogeneity (Fig. 5.11). A whole continuum of drift forms have been identified (Doumani, 1966), ranging from ripple marks a few centimetres high to dunes that can be 0.75 m high and ~20 m long. The wind produces both depositional and erosional features. Depositional features include dunes (of various shapes and orientations), barchans (crescent-shaped dunes with the horns pointing downwind) and drift aprons (Fig. 5.11, bottom). The latter form in the lee of ice blocks and pressure ridges (Adolphs, 1999; Tin & Jeffries, 2001). Because wind directions change and ice floes rotate, these aprons often occur on both sides of pressure ridges, while dunes 'cross bed'. Barchans form in large fields on wide expanses of undeformed flat FYI (Massom et al., 2001) or during erosional events. Erosional features include sastrugi (dunes sculpted into fluted forms), pitting and areas of ice swept free of snow. In cross section in a snow pit, both erosional and depositional drift features appear as layers that pinch and swell at a variety of scales.

Another salient snow feature, particularly in the Antarctic, is the presence of saline and moist basal layers (even in the absence of seawater flooding). Brine that occurs on the surface of the ice, due to its upward expulsion during initial stages of ice formation (Perovich &
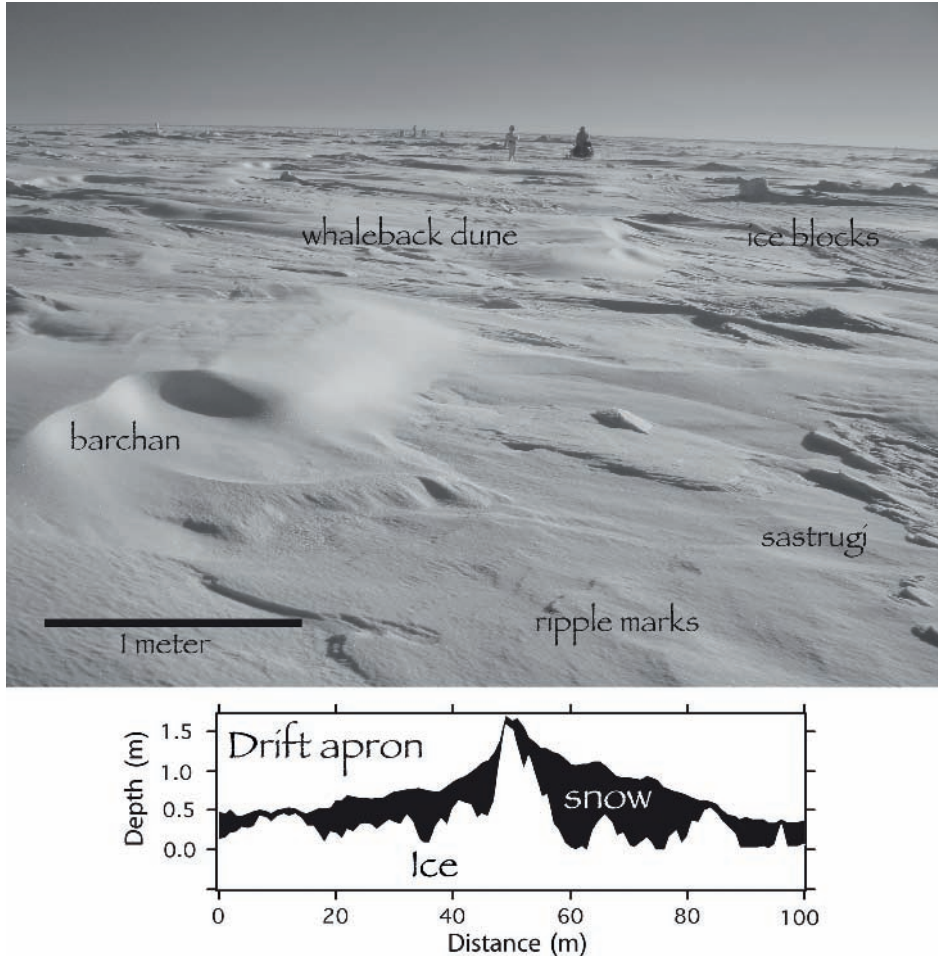
Fig. 5.11 Snow drift features common on sea ice. The near-infrared photograph is from the sea ice near Barrow, Alaska, but could easily have been taken in Antarctica. The cross section at the bottom shows a drift apron in the lee of a 1.5 m ice ridge in the Chukchi Sea (0 m on the *y*-axis is sea level). Comparable drifts occur on Antarctic sea ice (see Sturm et al., 1998; Fig. 5.9).

Richter-Menge, 1994), is wicked up into the snow by capillary suction. High salinities (>10) can occur up to 0.2 m in the snow cover, but are mainly found in the bottom 0.05 m, as shown in Massom et al. (2001: Figure 11). Brine supply depends on ice temperature, which is in turn affected by snow depth and properties once the ice acquires a snow cover, while seawater supply is also determined by freeboard (see Sections 5.2 and 5.6). Measurements indicate that mean salinities of the bottom 30 mm of Antarctic snow range from 13 to 24. However, Massom et al. (1998) report considerable lateral variability in salinity values. Salinities ranged from 4.7 to 34.8 across a smooth, unridged first-year floe. Lower 'background' salinities (1) that are found higher in the snow column are likely the result of blowing snow, which has wicked salt and/or sea spray from adjacent leads and polynyas during strong wind events.

Table 5.5   Mean bulk snow salinities from various Antarctic sea ice experiments, as a function of region and season. After Massom et al. (2001). Modified with permission from American Geophysical Union.

Sector	Season (Year)	Snow Salinity	Range, salinity	N	Reference
Indian & W Pacific Oceans					
75–150°E	Spring (1994)	8.8 ± 13.3	0.1–66.4	41	Worby & Massom (1995)
139–141°E, 144–150°E	Autumn (1993)	8.4 ± 13.5	0.1–47.1	51	Worby & Massom (1995)
138–142°E	Winter (1995)	8.5 ± 10.6	0.1–54.5	202	Massom et al. (1998)
Bellingshausen, Amundsen & Ross Seas					
75–110°W	Autumn–winter (1993)	8.7 ± 10.6	0.2–36.3	84	Jeffries et al. (1994)
165–180°W	Autumn–winter (1995)	8.7 ± 10.2	0.02–39.8	193	Jeffries & Morris (2001)
175°E–175°W	Autumn–winter (1998)	13.1 ± 18.5	0.01–91.8	179	Jeffries & Morris (2001)
109–171°W	Winter–spring (1994)	2.6 ± 6.5	0.1–40.5	333	Jeffries et al. (1997)
70–130°W	Late summer (1994)	0.02 ± 0.08	0.0–0.36	37	Sturm et al. (1998)
Weddell Sea					
0–55°W	Spring (1989)	4	0.0–41.9	87	Haas et al. (1996)
20–55°W	Late summer (1997)	0.15 ± 0.8	0.0–8.6	130	Eicken et al. (1994)
5°E–55°W	Autumn–winter (1992)	2.6	–	–	Haas et al. (1998)
0–50°W	Winter (1997)	8.7±10.7	0.0–48.8	189	Lytle & Ackley (1992) Massom et al. (1997)

Particularly high snow basal salinities (>34) can occur when frost flowers are incorporated into the base of the snow cover (Perovich & Richter-Menge, 1994; Massom et al., 1997). Frost flowers, which form extensive carpets on nilas in both Arctic and Antarctic sea ice covers under calm clear and cold atmospheric conditions, attain salinities as high as 110 (Drinkwater & Crocker, 1988; Alvarez-Aviles et al., 2008). Enhanced snow salinities depress the snow melting point, leading to a persistent dampness even at lower temperatures. This dampness is tangible: even at −10°C, a snowball can be made from saline snow at the base of the snow cover. Mean bulk snow salinities measured in Antarctica are compiled in Table 5.5.

5.4 The temporal evolution of the snow pack

Arctic

Recent time series observations acquired on MYI during the SHEBA experiment (Sturm et al., 2002a) provide insight into the temporal evolution of the arctic sea ice snow cover. These results are thought to be representative of most of the central Arctic Basin – excluding the eastern Arctic where greater winter snowfall rates and snow depths occur (Serreze & Maslanik, 1997). The SHEBA snow cover initially built up in October and November, attaining near-maximum depth (0.34 m) by mid-December (Fig. 5.10). From then until snowmelt onset in late May, the

depth and properties changed little. Snowmelt was rapid, eradicating the snow in less than 20 days (Fig. 5.10). This seasonal pattern is similar to that described for the Arctic Basin by Warren et al. (1999) from Russian drifting ice camp observations and closely matches earlier observations from the Beaufort Sea (Untersteiner, 1961).

The SHEBA snow cover comprised three basic snow types, namely (1) depth hoar (Figs. 5.9 and 5.10, layers b, c, d and e); (2) wind slab (layers f, g and j) or (3) recent (layers h and i). Strong snow temperature gradients in early winter metamorphosed layers b through d into the depth hoar, while diurnal temperature cycling in April and May produced near-surface kinetic growth (Birkeland, 1998) comprising small (0.5 mm) faceted crystals in the upper layers. The snow layers were produced by 10 fairly discreet weather events (defined as continuous periods of precipitation, wind, or wind plus precipitation). Most events were short-lived (<24 hours), although multiday storms were responsible for the formation of the two most prominent layers (wind slabs f and g). The combined time for all the key weather events constituted only 6% of the entire winter. These results emphasize the critical dependence of snow cover properties on the timing of snowfall and wind events, and in particular, they highlight the crucial importance of early winter storms in the development of the snow cover.

Cold dry conditions lasted at SHEBA from November until May, during which time the albedo of the snow remained uniformly high (0.8–0.9) (Perovich et al., 2002). Moderate warming over the April–May period led to an increase in snow grain size accompanied by a gradual decrease in albedo. Though brief, a rainfall event in late May had an immediate effect, resulting in rapid grain-size coarsening to ~1 mm, and a reduction in albedo from 0.8 to 0.7. The snow melt onset proper occurred on SHEBA in late May, marking the start of a period of abrupt changes in snow properties. Snow albedo continued to decrease to about 0.5 and exhibited more spatial variability as the melt phase proceeded. Eventually, the ice surface was transformed into a mosaic of bare ice and melt ponds (characteristic in summer). The winter snow cover preconditioned the ice prior to the melt, with the ponds forming in the hollows between drifts (Eicken et al., 2004). The return to below-freezing temperatures (dry cold conditions) and new snow accumulation by the end of August (the onset of autumn freeze-up) led to an increase in albedo, with average values returning to their spring-time maxima (0.8–0.9) and exhibiting spatial uniformity by the end of September. The reader is referred to Grenfell and Perovich (2004) for similar information on the spatial and seasonal evolution of coastal Arctic snow and sea ice near Barrow (Alaska), and Iacozza and Barber (2001) for ablation patterns over first-year Canadian ice.

Antarctic

Unfortunately, similar information on snow cover evolution over an annual cycle of Antarctic sea ice is lacking, although seasonal patterns can be pieced together from data collected during various field campaigns, albeit campaigns separated in space and time (reviewed through 2000 in Massom et al., 2001). While there are many fundamental similarities to the evolution of the Arctic sea ice snow cover, a number of standout features differentiate the evolution of the Antarctic snow–ice system, most notably a lack of wholesale snow melt, and the absence of surface melt ponds in summer (Andreas & Ackley, 1981), along with the widespread year-round occurrence of icy layers and basal flooding/dampness.

These differences may be largely explained by the weather (combined in the case of flooding with contrasting oceanic and sea ice conditions). Owing to the constant passage of storms around the circumpolar Southern Ocean (Simmonds et al., 2003), weather conditions over the Antarctic sea ice zone are highly dynamic and variable, with heavy snowfall accompanied by strong wind events and warmer temperatures, followed by calmer colder events between storms. Changes in air temperature before, during and after wind events are often large and abrupt, including melt episodes in winter such as one described below. The more dynamic nature of the Antarctic weather cycles is noticeable in the snow stratigraphy (Fig. 5.8b), which typically has more layers, and more melt features, than its Arctic counterpart (Fig. 5.8a).

Proportions of the six main snow types described in Section 5.3 and observed on seven Antarctic cruises are given in Table 5.6. As in the Arctic, wind slab and depth hoar form a large proportion of the snow cover in autumn and winter. Relatively high air temperatures and persistent winds during snowfall account for the relative abundance of soft to moderate slab (Sturm et al., 1998), although the occurrence of hard slabs is substantially lower than in the Arctic where wind conditions are similar but there are significantly lower temperatures (Benson & Sturm, 1993). Depth-hoar and faceted snow types account for up to 55% of the snow cover. Newly deposited snow quickly undergoes rapid depth-hoar formation owing to the ready availability of moisture at the snow base and the strong temperature gradients (Massom et al., 1998). In fact, the largest percentage of faceted snow and depth hoar has been observed in autumn–early spring, possibly linked to larger snow temperature gradients at this time (Massom et al., 2001).

The large proportion of icy snow (ranging from 9% to 46%) observed in all seasons reflects both the high incidence of melt-freeze events, the frequency of high winds in the case of crust formation and the impact of moisture (brine and seawater) incursion from below (Sturm et al., 1998; Massom et al., 2001). Sturm et al. (1998) observed an increase in the proportion of icy snow with increasing proximity to the ice edge during winter–spring cruises (consistent with increasing temperature), and an increase in depth hoar with increasing southerly latitude. The other snow types exhibited no such correlations.

Flooding and snow–ice formation in Antarctic appears to vary seasonally, but with regional differences. Lower percentages of snow-ice are observed early in the winter (Sturm et al., 1998; Massom et al., 2001). With time (and more snowfall), these percentages increase. Come summer, more extensive ice surface flooding is observed (Drinkwater & Lytle, 1997), most likely due to large rates of basal ice melt due to high oceanic heat fluxes (Martinson & Iannuzzi, 1998) combined with the retention of thick snow in perennial ice regions, e.g. the western Weddell Sea and eastern Ross Sea (Morris & Jeffries, 2001). An exception to this pattern seems to be the West Antarctic Peninsula (WAP) sector, which represents a 'warm end member' in terms of snow and ice properties and flooding/snow–ice formation (Perovich et al., 2004; Massom et al., 2006). According to Perovich et al. (2004), optimal conditions for snow–ice formation (sufficient snow, thin ice and cold temperatures for slush freezing) only occur in WAP in late autumn–early winter. Although heavy snowfall and flooding continue through mid- to late winter, slightly warmer air temperatures and increased snow depth (insulation) can prevent slush from freezing.

As the result of the aggressive formation rate of snow-ice in Antarctic, there is a large apparent discrepancy between measured snow accumulation and the snow depth on Antarctic sea ice (Maksym & Markus, 2008). Jeffries et al. (2001), for example suggest that almost

Table 5.6 Snow cover characteristics during selected sea ice field campaigns in Antarctic. After Massom et al. (2001). Modified with permission from American Geophysical Union.

Season Region	Spring 1994 East Antarctic	Spring 1994 Amundsen/Ross	Autumn 1993 East Antarctic	Autumn–winter 1995 Ross	Winter 1995 East Antarctic	Winter-spring 1994 Bellingshausen/ Amundsen	Winter-spring 1995 Bellingshausen/Ross
No. of snow pits	10	164	16	73	46	58	45
% Icy	10	20	18	26	18	9	46
% New and recent	16	14	12	8	23	30	4
% Soft–moderate slab	11	23	7	10	8	–	13
% Hard slab	7	6	11	0	9	–	0
% Faceted/depth hoar	9	31	48	47	39	55	29
% Slush	54	6	4	9	3	6	8
Mean depth, m	0.15	0.28	0.17	0.24	0.13	0.2	0.22
Mean temperature gr., °C m^{-1}	–	−23	−66	−82	−47	−41	−44
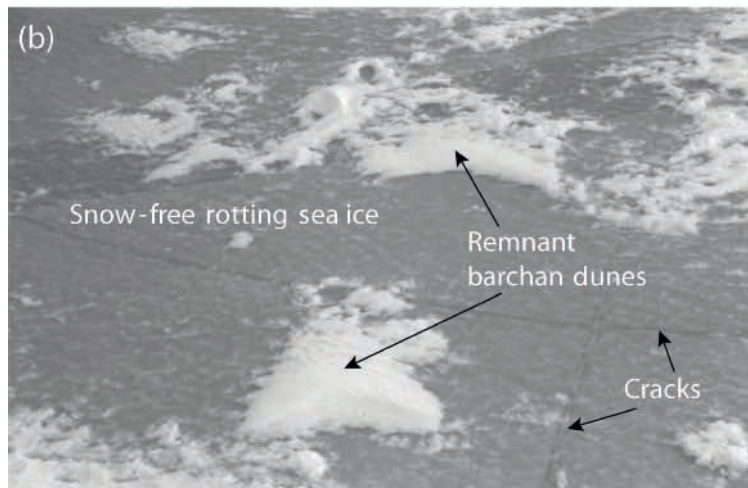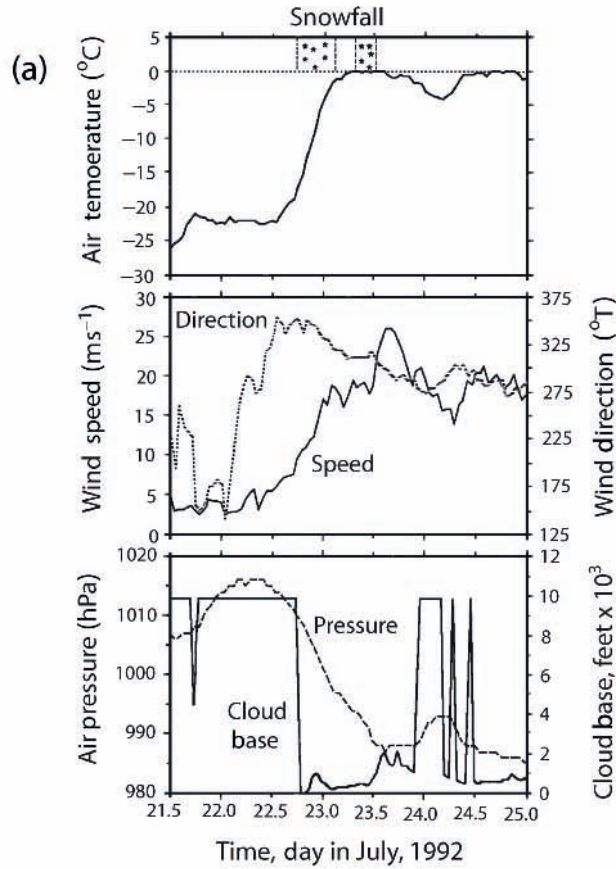
Fig. 5.12 (a) Near-surface meteorological variables measured from R/V Polarstern while drifting with the pack ice in the NW Weddell Sea (at ∼61ºS, 43ºW), July 21–25, 1992. (b) Photograph taken on July 25, 1992, showing extensive snowmelt (nearly complete removal) associated with synoptic warm air advection. The surviving high-density barchan dune in the foreground is ∼5 m across. From Massom et al. (2001). Reproduced by permission of American Geophysical Union. Copyright 2001 American Geophysical Union.

half the snow on ice in the Pacific sector of Antarctic is eventually converted into snow-ice, a point discussed further in Section 5.6.

The remarkable June transformation of the snow–ice system in the central Arctic converts high-albedo snow cover into low-albedo melt ponds in a few short weeks (Perovich et al., 2002). No similar transformation takes place in Antarctica. Satellite-based studies indicate that seasonal surface melt is relatively short-lived and is neither spatially nor temporally contiguous (Drinkwater & Liu, 2000), with albedo values remaining relatively high throughout the summer (see Section 5.5). Moreover, Antarctic ice melts largely from the bottom up, due to relatively large ocean heat fluxes (Martinson & Iannuzzi, 1998) and cool and windy ambient conditions (Andreas & Ackley, 1981). As a result, the summer Antarctic snow cover remains largely intact on the greater than 4×10^6 km^2 of ice that remain in February in the Amundsen, western Weddell and eastern Ross Seas (see Chapter 6). This intact snow cover retards summer surface ablation (Eicken et al., 1995), in sharp contrast to what takes place in the Arctic. Textural studies show that strong snow melting does occur (Haas et al., 2001; Morris & Jeffries, 2001), but not enough to completely remove the snow cover, while melt ponds are rare. This strong summer snow melt is reflected in sharp decreases in snow salinity in summer (Table 5.5), and the widespread occurrence of superimposed ice where snow meltwater refreezes on to the ice surface. Haas et al. (2001) attribute the latter to a seasonal reversal in the snow temperature gradient.

Also in sharp contrast to the central Arctic, in the Antarctic there are episodic incursions of warm maritime air over the ice pack that can cause almost complete snow melt (ephemeral removal) even in winter. The dramatic impact of one such episode, in the NW Weddell Sea in July 1992 (Massom et al., 1997), is documented in Fig. 5.12. An increase in temperature from −22°C to 0°C over a 12-hour period was followed by 3 days of periodic rain and sleet. The end result was a layer of slush on rotting sea ice with a pitted, porous grey surface, but no melt ponds (due to drainage through enlarged centimetre-scale brine channels). A return to freezing conditions occurred a few days later, with new snowfall subsequently obscuring the refrozen melt surface. Such events can affect much of the circumpolar Antarctic sea ice zone, although they are more prevalent in the marginal ice zone and sectors where the ice attains lower latitudes.

5.5 Snow pack properties

Grain size

Grain size is intimately associated with snow type (see Section 5.3, also Colbeck et al., 1990). Typical grain sizes by snow type for Antarctic winter conditions are given in Table 5.7. As noted in Section 5.3, there is a substantial difference in size between new/recent snow and wind slab (fine-grained), and well-developed depth hoar (generally the largest grains – see Fig. 5.5). Melt clusters typically account for the intermediate sizes. Within a given snow column (pit) in winter, grain size typically increases with depth, as a result of the stratigraphic sequence (Sturm et al., 1998). Moreover, grain size distributions exhibit bimodality if the snow has been subjected to wetting, e.g. a substantial number of grains far exceed the mean size if ice lenses are present.

Table 5.7   Mean grain size and density of the main snow types on the sea ice of the Amundsen and Ross Seas (grain size is taken here to be the longest dimension). After Sturm et al. (1998). Modified with permission from The American Geophysical Union.

Snow type	Grain size, mm	Number of samples (Snow pits)	Snow density kg m^{-3}
New/recent snow	1.1 ± 0.6	2	310
Soft–moderate wind slab	1.2 ± 0.4	21	340
Hard wind slab	0.9 ± 0.3	4	410
Depth hoar	2.0 ± 0.9	29	290
Melt clusters	1.3 ± 0.6	8	350

Table 5.8   Mean snow grain size measured in snow pits in Antarctica, derived from sources given in the reference column. After Massom et al. (2001). Modified with permission from American Geophysical Union.

Sector	Season (Year)	Grain size, mm	Range, mm	N	Reference
Indian & W Pacific Oceans					
75–150°E	Spring (1994)	1.7 ± 0.8	0.05–4.0	17	Worby and Massom (1995)
139–141°E, 144–150°E	Autumn (1993)	1.5 ± 1.5	0.05–10.0	54	Worby and Massom (1995)
138–142°E	Winter (1995)	1.6 ± 1.2	0.01–10.0	167	Massom et al. (1998)
Bellingshausen, Amundsen, Ross Seas					
70–130°W	Late summer (1994)	2.5 ± 1.0	1.0–4.0	11	Haas et al. (2001)
109–171°W	Winter–spring (1994)	1.6 ± 0.7	0.8–3.6	49	Sturm et al. (1998)
Weddell Sea					
20–55°W	Late summer (1997)	2.9 ± 1.2	0.5–10.0	129	Haas et al. (2001)
0–50°W	Winter (1992)	2.7 ± 3.1	0.2–10.0	90	Massom et al. (1997)

Regional estimates of mean Antarctic grain size by season are presented in Table 5.8. They vary over a narrow range (1.5–2.9 mm) and are spatially and temporally similar. With the exception of the Weddell Sea winter cruise of 1992 (characterized by both significant melt episodes and a large proportion of depth hoar/faceted snow), summer mean grain sizes are larger than values at other times of year due to the preponderance of coarse grain clusters and icy layers within the snow cover. These clearly reflect the strong internal melt and refreeze cycling conditions that occur episodically throughout the year but which predominate in summer (Hass et al., 2001).

In the Arctic, there have been relatively few studies on grain size, and none by season. Sturm et al. (2006) sieved snow to measure the size and found that wind slabs had mean grain sizes of 1 mm or less, while depth hoar ranged from 5 to 7 mm. Because these are the two most frequent types of snow in the Arctic snow cover, it is safe to conclude that grain sizes fall generally into these two size classes.

Density and snow-water equivalent

Snow density, which is typically measured by weighing a known volume of snow, is correlated with snow thermal conductivity (see next section), air permeability, and optical and microwave properties. Accurate knowledge of this key parameter is also required to derive sea ice thickness from satellite altimeter data. Density, along with depth, also determines the snow–water equivalent (SWE), which is an important component of the ocean freshwater budget. Density measurements can be made either on individual layers or as a bulk measurement by coring through all the layers, which is usually done when the primary interest is to determine the SWE.

As with grain size (to which it is closely related), the density of snow layers constantly evolves, though in general the trajectory is one of increasing density with time. Layer densities can range from less than 100 kg m^{-3} for new snow (Table 5.4) to as much as 760 kg m^{-3} for icy layers (Sturm et al., 1998). Mean values from the Amundsen and Ross Seas in Antarctica for several types of snow are given in Tables 5.7 and 5.9, with snow cover bulk density values from a number of Antarctic cruises listed in Table 5.8. Warren et al. (1999, Figure 11) found similar bulk density values for the Arctic Ocean. The highest reported mean density (391 kg m^{-3}) was measured in late summer, reflecting the predominance of icy snow at this time of year (Haas et al., 2001). Unfortunately, the density of snow columns containing substantial icy snow tends to be underestimated owing to difficulties in sampling very hard layers. A typical wintertime frequency distribution from the Indian Ocean sector of the Antarctic pack shows a mode at 300–350 kg m^{-3} with a minor peak at ~700 kg m^{-3} for the icy layers, while another from the Weddell Sea exhibits less spread and a lower mode (250–300 kg m^{-3}) as a result of a greater depth-hoar contribution (Figure 8 in Massom et al., 2001).

Substantial horizontal variability occurs on small scales, i.e. across and between individual floes. In East Antarctica in August 1995, e.g., average bulk densities ranged from 240 to 600 kg m^{-3} (Massom et al., 1998). On the large scale and as a rule of thumb, however, representative average bulk snow density can be roughly predicted from the sequence of prevailing weather conditions, if known. Low-density snow (200–300 kg m^{-3}) predominates for cold dry conditions; for warm, windy conditions, medium/high density (350–500 kg m^{-3}) and for melt-refreeze conditions, high density (400–700 kg m^{-3}).

SWE is the product of depth and bulk density. A map of SWE for the Arctic Ocean has been compiled by applying two-dimensional quadratic fits to Soviet drifting station measurements of SWE (Warren et al., 1999), and is shown in Fig. 5.13. The average SWE derived from these data at the peak of the seasonal cycle (mid-May) is 11 cm. In effect, this represents 9 months of solid precipitation (sum of all snowfall, rime and frost deposition, minus sublimation) minus an unknown amount lost by drifting into leads. Sturm et al. (2002a) determined that because the mean Arctic snow bulk density varies over a narrow range, snow depth can be converted to SWE with reasonable accuracy using a fixed value for the bulk density (340 kg m^{-3} [$n = 357$]). Their estimate of average SWE for the central Beaufort Sea was 11.6 cm, quite similar to the value of Warren et al. (1999). Unfortunately, similar peak SWE estimates for the Antarctic are not available, and if they were, would likely vary by region. Efforts to remotely sense SWE have been reported by Barber et al. (2003).
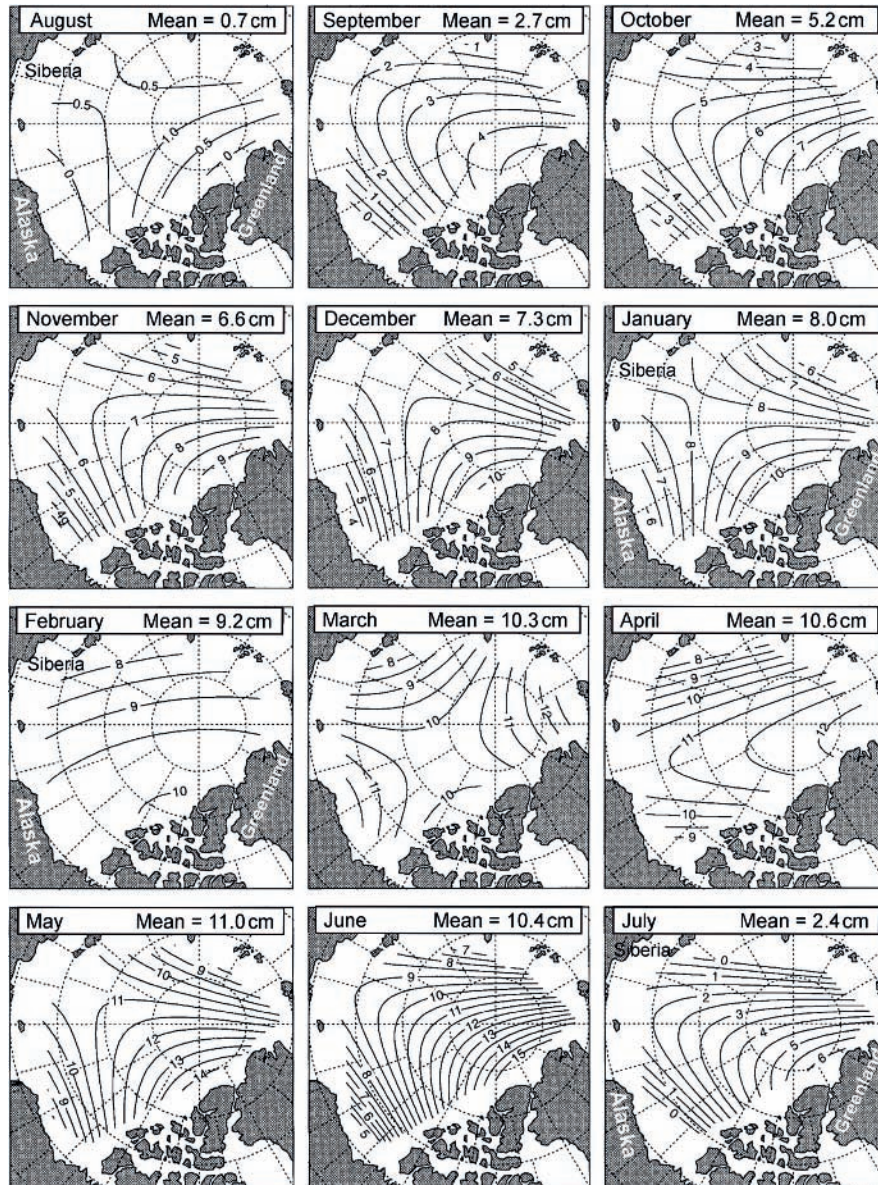
Fig. 5.13   Mean snow-water equivalent (SWE) for 1954–1991 on Arctic multi-year ice at measured drifting stations for each month, in cm's of liquid equivalent depth. After Warren et al. (1999). Reproduced by permission of American Meteorological Society. Copyright 1999 American Meteorological Society.

Thermal properties

There are three thermal properties of importance for the snow cover, all of which are inter-related: thermal conductivity (k_s), thermal diffusivity (λ_s) and the volumetric heat capacity ($\rho c)_s$. Thermal conductivity indicates the rate at which heat flows through a material. For snow, the transfer mechanisms include (1) molecular conduction through the solid network of ice grains (Fig. 5.3b); (2) the transfer of heat across pore spaces as water vapour sublimates
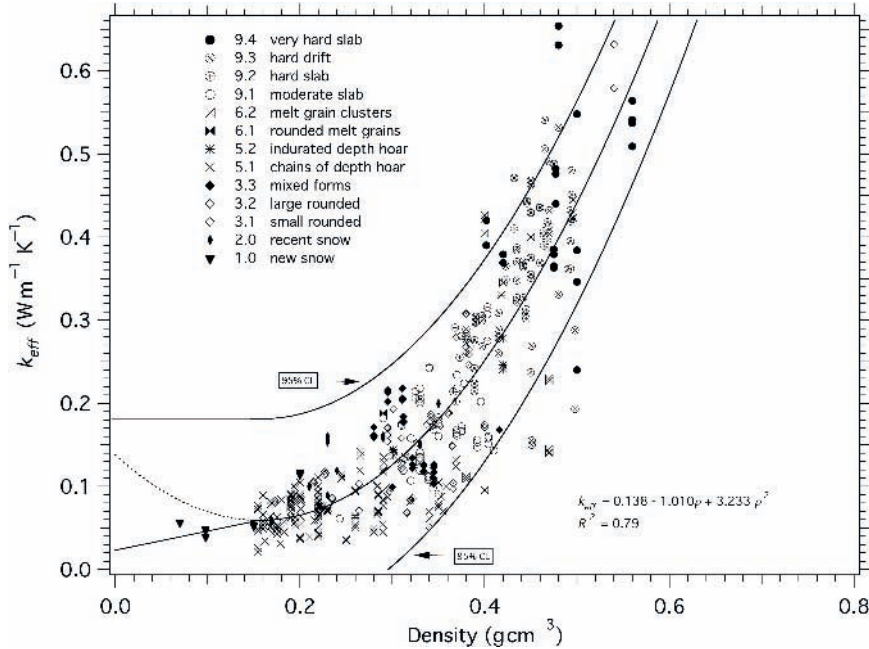
Fig. 5.14   The thermal conductivity of snow as a function of density and snow type from Sturm et al. (1997). Reproduced from the Journal of Glaciology with permission of the International Glaciological Society.

from a lower grain and condenses on a higher one (Fig. 5.3b) and (3) the convective movement of air through the pore spaces in the snow (driven by natural air buoyancy or by surface winds) (Sturm, 1991; Waddington & Harder, 1996). Because the second two transfer mechanisms are not strictly conductive, it is customary to report the *effective thermal conductivity* of the snow (k_{eff}), a value that includes all three mechanisms. k_{eff} varies with snow density and snow type (Fig. 5.14), as well as slightly with temperature. Values range from about 0.1 to 0.6 W m^{-1} K^{-1} (Sturm et al., 1997, 1998). Typical values used in global climate and sea ice models are about 0.3 W m^{-1} K^{-1}. The lowest and highest values of k_{eff} are found in layers of depth hoar and hard wind slab, respectively. These are the two most prevalent types of snow found on the Arctic sea ice, with depth-hoar layers comprising 36–51% of all layers, and wind slab comprising 35–58% (Sturm et al., 2006). In the Antarctic, depth hoar is also prevalent (up to 55% – see Table 5.6), but wind slab is a more minor component of the snow cover (13–29%) (Massom et al., 2001). These two thermally dissimilar types of snow can be converted into the other type by wind (which can happen in as little as a day) or by kinetic growth (which takes days to weeks).

   The most frequent use of thermal conductivity measurements is to compute the heat flow through the snow (q_s):

$$q_s = -k_{eff} \frac{\partial T}{\partial z} \qquad \qquad \text{(Equation 5.3)}$$

where T is temperature and z is the vertical coordinate with zero at the ice surface and positive values up. The negative sign accounts for the fact that a negative temperature gradient ($\partial T/\partial z$), which prevails most of the winter, produces a positive (upward) flux of heat. In practice, $\partial T/\partial z$ is often approximated by $\Delta T/h_s$. It is also often assumed that q_s is equal

to q_i (Fig. 5.2). Equation 5.3 can then be used to describe the rate of heat loss from the ice, which can be compared to the thickening of the ice by congelation growth (with allowance made for oceanic heat flow). When this is done (Sturm et al., 2001, 2002b), it is often found that k_{eff} determined for small samples of snow is too low to balance measured changes in ice thickness by thermodynamic growth, a finding that suggests that other heat flow mechanisms are operating or that the flow is not solely one dimensional. Numerous empirical relationships between snow density and thermal conductivity have been suggested, including the following by Sturm et al. (1997) (see also equation 5.2a):

$$k_{eff} = 0.138 - 0.00101\rho_s + 0.000003233\rho_s^2 \quad (150 \leq \rho_s \leq 8600 \text{ kg m}^{-3}) \quad \text{(Equation 5.4)}$$

Thermal diffusivity describes the rate at which temperature waves propagate through a material. For snow, this rate is a balance (ratio) between the heat flow and the volumetric heat capacity, a product of the snow density and the specific heat capacity of the snow (c_s), such that:

$$\lambda_s = \frac{k_{eff}}{(\rho c)_s} \quad \text{(Equation 5.5)}$$

where $(\rho c)_s$ is the volumetric heat capacity of the snow. This is primarily the heat capacity of the ice fraction of the snow (the air having very little heat capacity), but is given in full by:

$$(\rho c)_s = (\rho c)_i (1 - \varphi) + (\rho c)_a (\varphi) \quad \text{(Equation 5.6)}$$

where φ is the snow porosity, and the subscripts 'i' and 'a' indicate the ice and air components of the snow respectively. The heat capacity of the ice fraction $(\rho c)_i$ is 1.805×10^6 J m^{-3} K^{-1}, about 1000 times higher than the heat capacity of the air in the snow $(\rho c)_a$, which is 1.507×10^3 J m^{-3} K^{-1}, so the right-hand term can be dropped from equation 5.6. Also, $1 - \varphi$ can be approximated by the snow density divided by the density of ice (~917 kg m^{-3}), allowing equation 5.6 to be rewritten as:

$$\lambda_s = 0.000508 \frac{k_{eff}}{\rho_s} \quad \text{(Equation 5.7)}$$

Thermal diffusivity predicted by equation 5.7 ranges from 2×10^{-7} to 5×10^{-7} m^2 s^{-1}, decreasing with snow density and increasing with thermal conductivity. Thermal diffusivity values are chiefly used in computing the time it takes a change in temperature to propagate through the snow cover. This can be estimated from h_s^2 / λ_s, which for snow 0.25 m deep of moderate density would take about 2.5 days. Thermal convection, wind pumping and breaks in the snow cover accelerate the rate, but even with this acceleration, it can be seen that the snow has a major buffering effect on ice temperatures.

Optical properties

The optical properties of snow and sea ice are inextricably related to their physical structure and state (Perovich, 1996, 2001), with physical changes in the snow resulting in changes in the reflection, transmission and absorption of incident electromagnetic radiation (EMR). Understanding these physical–optical interactions and their evolution/change over time and

space is of critical importance from a number of perspectives. These include global climate change (most notably via the ice–albedo feedback mechanism) (Kellogg, 1971), sea ice thermodynamics (see Chapter 2), ice algal production (including potentially harmful effects of ultraviolet (UV) radiation [0.28–0.4 μm]) and remote sensing of snow cover and sea ice properties (Chapter 6) (Lubin & Massom, 2006).

At solar wavelengths, radiative transfer in snow is primarily governed by scattering and absorption (Fig. 15.15; Warren, 1982; Perovich, 2001, 2003). *Scattering* refers to the multiple reflection of EMR off surfaces or particles/scattering centres, and is characterized by the scattering coefficient (a measure of the amount of scattering) and a phase function describing the angular distribution of scattered light. Scattering coefficients for dry snow are large and approximately constant with wavelength. *Absorption* refers to the loss of energy from EMR as it propagates through an absorbing medium, and/or is a measure of the ability of a surface to absorb incident radiation (primarily determined by its dielectric properties) (Warren et al., 2006). It is characterized by the *absorption coefficient*, which is a measure of the amount of absorption per unit length. Following Warren (1984), absorption for ice (snow) is strong in the UV at wavelengths of less than 0.17 μm, very weak in the visible (0.4–0.73 μm) and moderate in the near-IR (0.73–1.3 μm). As a result, snow albedo is much lower in the near-IR than in the visible. It follows that near-IR solar irradiance plays a key role in snow (and ice) melt. Whereas visible light penetrates deeply into thick dry snow owing to minimal absorption, this is not the case in the near-IR, where strong absorption of radiation occurs in the upper few millimetres of the snow (Warren, 1982, 1984). The absorption spectrum for liquid water largely parallels that of ice from the UV to near-IR. The combination of scattering and absorption is referred to as *attenuation* (or *extinction*).

The best-known and studied optical property of snow on sea ice is its *albedo* (or reflectance). *Reflectance* is defined as the ratio of the intensity of radiation reflected by a target (surface) to that of the radiation incident upon it, and is the primary variable measured by optical remote-sensing systems. Strictly speaking, albedo is defined as the integral of the ratio of reflected to incoming radiation over all angles as a function of solar zenith angle (θ_0), wavelength (λ), viewing zenith angle and viewing azimuth angle, and is usually given as spectral albedo (a function of λ and θ_0). Differences between albedo and reflectance can be as great as a factor of 3 over snow (Nolin & Frei, 2001), depending on properties such as surface roughness, but are normally much closer to a factor of 1. An increase in small-scale snow surface roughness in the form of dunes, e.g., alters the normal forward-scattering pattern of a flat snow surface in terms of its bidirectional reflectance characteristics (Warren et al., 1998). Regarding θ_0, snow albedo increases as the Sun nears the horizon (Warren, 1982). Albedo is also affected by the presence/absence of cloud cover (Warren, 1982; Perovich et al., 2002).

Snow on sea ice is a mixture of ice, air and water. Owing to the preponderance of small grains at the snow–air interface, snow is a highly scattering medium. This, combined with the dielectric properties of ice, result in a high albedo at visible wavelengths (Perovich, 2001). Snow depth affects reflectance/albedo only when the snow is shallow and in the visible spectrum. Snow effectively becomes semi-infinite at near-IR wavelengths when its depth exceeds ~3 cm (Zhou et al., 2003). As a result, only a thin snow layer can raise the albedo of sea ice considerably (Allison et al., 1993). For example, Weller (1968) reported that the addition of just 2–3 cm of snowfall on snow-free thick Antarctic first-year fast ice doubled the broadband solar albedo from 0.42 to 0.88. Snow is such an effective scattering medium that
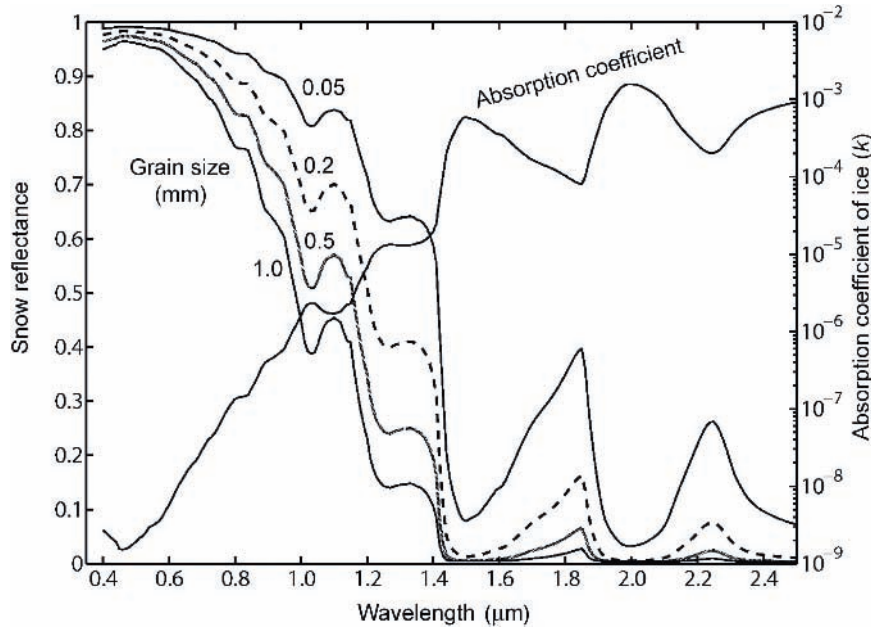
Fig. 5.15 Spectral reflectivity of clean, deep snow for a range of snow grain sizes from new, fine snow to coarse snow, as calculated by the Wiscombe & Warren (1980) model. Also shown is the absorption coefficient of ice on the right-hand, logarithmic axis (data from Warren, 1984). Snow reflectivity is most sensitive to grain size at wavelengths where absorption is moderate. Figure courtesy of J. Dozier, University of California, Santa Barbara (USA).

a continuous snow cover will dominate the surface albedo of the ice. Even small differences in albedo translate to large impacts on surface energy balance and snow melt calculations (Nolin & Frei, 2001). Moreover, albedo is a dominant control of the radiation balance at the snow/ice surface, and an indicator of physical properties of the snow in terms of grain size, snow thickness and liquid–water content.

At visible wavelengths, the spectral albedo and reflectance of snow are sensitive to snow depth, whereas the near-IR albedo is strongly sensitive to grain size (which is why we use near-IR photography: see Fig. 5.8a) and less so to solar zenith angle (Warren & Wiscombe, 1980). In other words, snow density can be neglected when estimating these parameters from snow properties. Regarding dependence on grain size, snow spectral reflectance decreases with an increase in the latter (Fig. 5.15). Grain-size enlargement by snow metamorphism can thus lead to a decrease in albedo, i.e. generally as the snow ages the albedo goes down (Warren, 1982). Grain enlargement by both depth-hoar formation and by melt-refreeze cycling (producing multiple clusters) therefore reduces the albedo and reflectance.

The direct impact on snow reflectance/albedo of the presence of liquid water at less than 10% by volume is minimal at visible and near-IR wavelengths, as the absorption of water is similar to that of ice in this spectral region (Green et al., 2002). However, liquid water, either in the form of snow meltwater or brine/seawater, has an indirect effect on snow optical properties by causing ice-air interfaces transform into ice–water interfaces and snow grains to cluster. This leads to an increase in effective grain size (Colbeck, 1986), with the net effect of significantly reducing scattering and decreasing reflectance/albedo at near-IR wavelengths – an effect that remains when the wet snow refreezes (Dozier et al., 1981).

In regions of floe flooding, waterlogging of the lower snow horizons reduces the effective snow thickness, which has much the same effect as melting snow (Brandt et al., 2005), i.e. it lowers the albedo.

An additional factor affecting the optical properties of snow on coastal Arctic sea ice is the presence of impurities such as soot, which are highly absorbing in the visible spectrum. As a result, the visible (but not near-IR) albedo is sensitive to small amounts of such impurities (Warren & Wiscombe, 1980), and there is often sufficient soot present in Arctic snow (precipitated from Arctic haze) to lower the spectrally averaged albedo by 1–2% (Warren & Clarke, 1986), although this effect is spatially variable (Grenfell et al., 2002). While pristine snow at the South Pole has an albedo of 0.98 (Grenfell et al., 1994), that of similar cold dry snow on coastal fast ice at Barrow (Alaska) is substantially lower, e.g. 0.9 (Perovich et al., 1998) – due to the relatively large concentration of particulates (soot and other material) in the latter.

Transmittance, or the fraction of incident irradiance transmitted though the snow cover, is another important optical property that depends upon the physical composition and state of the snow cover – most notably on grain size and density (Zhou et al., 2003). This is a key determinant of the intensity and spectral composition of photosynthetically active radiation (PAR, 0.4–0.7 μm) available to ice algae for photosynthesis, the impact of UV light on biota living within and/or under the ice and the shortwave energy available for snow/ice ablation (Perovich, 2003). The dominant effect of snow depth on variability in transmission of solar radiation through ice-covered oceans is based on the fact that snow albedos can be almost twice as large as those of bare thick sea ice (Grenfell & Maykut, 1977), while spectral extinction coefficients for snow are more than an order of magnitude larger than those for ice (Warren, 1982). Transmittance through the ice during SHEBA increased by 6 orders of magnitude over a period of only a few weeks from early June, as a direct consequence of the initial switch from a dry to wet (melting) snow followed by a major decrease in snow depth (Fig. 5.10).

Application of an UV radiative transfer model to Antarctic sea ice by Perovich (1993) highlighted the fact that snow is particularly effective at reducing UV transmittance by absorption, e.g. UV-B is reduced by about 2 orders of magnitude by a 0.1-m-thick snow cover. A further important finding was that sea ice covered with snow reduces the transmission of harmful irradiance more than it does the biologically beneficial PAR. Similar findings have been reported for Arctic conditions by Perovich (2001).

5.6 Snow depth distribution

Snow depth (h_s) and its variability is a crucial measurement for a number of reasons. Relatively minor changes in snow depth have a disproportionately large impact on the surface heat flux compared to changes in ice thickness (Lytle et al., 2000). Snow depth is also a key factor in maintaining a high surface albedo in the spring (Brandt et al., 2005), which can have a strong impact on the timing of the annual ice melt (Eicken et al., 1995). In the Antarctic summer, snow depth is also thought to play a role in the retention of snow-covered sea ice in certain regions (Massom et al., 2006). As noted earlier, a thick snow cover is also a major contributor to the mass balance of the Antarctic ice pack via snow–ice formation (Maksym & Jeffries, 2000), and in the Arctic, snowdrifts determine the location of melt

ponds (Eicken et al., 2004). Moreover, small variations in h_s have a major impact on total PAR available to intra- and sub-ice algal communities (Iacozza & Barber, 1999) as a result of the exponential nature of PAR extinction. While snow properties and layer characteristics are important, knowing the snow depth distribution is probably the single most frequently used measurement of the snow cover.

Despite this, we have a surprisingly limited understanding of the global thickness distribution of snow on the sea ice because of:

(i)   The vast extent of the ice.
(ii) The seasonal, year-to-year, and spatial variability of the snow (making it difficult to obtain comparable measurements).
(iii) The fact that remote sensing of snow depth remains problematic.

Figure 5.10 depicts a typical seasonal pattern of snow build-up and melt in the Arctic Ocean. Snow depth increases rapidly at first, then more slowly, to attain a maximum thickness in 1997/1998 of 0.5 m. Often, there is a significant secondary increase in depth in March or April, before rapid melt occurs in spring. Depending on when measurements are made, there can appear to be large year-to-year variations in depth that may not be real, and such variations seem to be the rule even when it is possible to account for seasonal changes in h_s. Colony et al. (1998), examining seasonal data from Russian Arctic sea ice stations, found that the snow depth could vary by ± 0.1 m ($\pm 1\sigma$) from the multiyear mean (0.1–0.3 m) at virtually anytime during the winter, a coefficient of variation that ranges up to 100%. Similarly, Warren et al. (1999), analysing multiyear data from the Russian North Pole Station 22 (NP-22), found that during a 4-year period, the peak in h_s varied by more than a factor of 2 (from 0.38 to 0.80 m), and that the pattern of snow cover build-up was quite different from one year to the next. Similar findings come from the Bellingshausen Sea in Antarctica (Perovich et al., 2004).

On top of temporal variability, spatial variation in h_s can be considerable. Figure 5.16 (bottom) depicts a map of snow depth distribution over a 25×200 m area of Chukchi Sea ice, derived from 11,531 depth measurements acquired by snow radar. We also hand-probed the snow depth and used a laser level to determine the elevation of both the snow and ice surface of a portion of the area (Fig. 5.16, upper left). The depth varied by a factor of 5, with maximum and minimum depths often adjacent. Homogeneous patches of snow tended to be between no more than 50 m in extent (Sturm et al., 2002a). These results highlight that single depth measurements can be almost meaningless. The measurements also show that the roughness characteristics of the underlying sea ice play a key role in determining h_s even when that roughness is of only moderate amplitude. As a result, the type of ice, whether it is FYI or MYI, is a good predictor of the snow depth distribution, at least in the central Arctic (Iacozza & Barber, 1999; Sturm et al., 2002a). Of course, the age of a floe also has a direct bearing on the mean h_s, with younger floes potentially missing older snow layers because the floe age post-dates the snow depositional event. The last key factor in the snow depth distribution is the wind, which through snow transport and redistribution, produces localized variability that interacts with the variability due to ice roughness (Wadhams et al., 1987; Massom et al., 1997, 1998; Sturm et al., 1998). The result of all these mechanisms is a complex blanket of snow that varies across a cascade of scales.
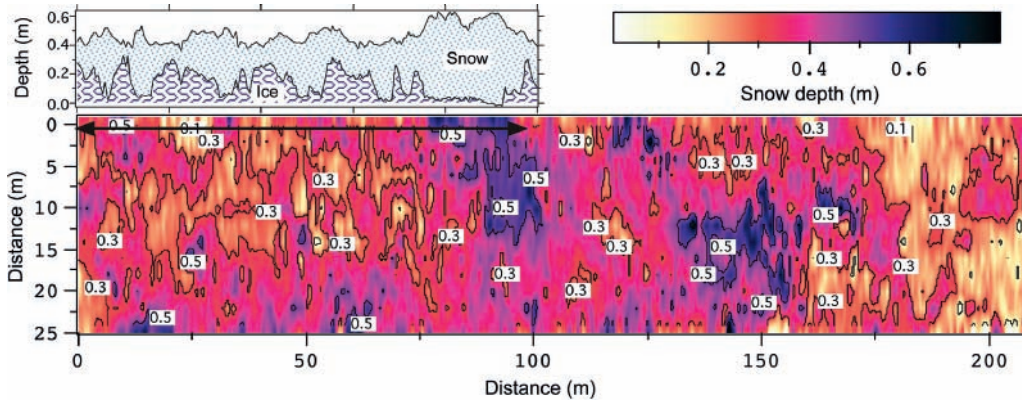
Fig. 5.16 The snow depth distribution on the ice of the Chukchi Sea at SHEBA. The colour indicates the snow depth, which due to both surface undulations in the snow (drifts, barchans, sastrugi) and variations in ice surface roughness. The cross section in the upper left corner suggests that at least half of the depth variations are due to ice micro-topography. From Sturm et al. (2002a). Reproduced by permission of American Geophysical Union. Copyright 2002 American Geophysical Union.

Global or hemispheric snow on ice

At the largest, or hemispheric, scale, there appears to be little significant difference in measured snow depth between the Arctic and the Antarctic. Massom et al. (2001) (Table 5.1) compiled depth statistics from 42 studies in all sectors of Antarctica for summer, autumn, winter and spring seasons ($n = 69,273$). A wide range of depths were reported, with a mean value of 0.21 m. When only late winter and spring values are used, the mean value was 0.20 m ($n = 45,374$). No comparable compilation for Arctic sea ice snow depths exists, but based on a number of studies (Table 5.10) using only March or April (spring) values, the mean snow depth for the Arctic was 0.29 m ($n = 38,000$). By comparison, Toyota et al. (2007) observed a mean snow depth of 0.10 m on the lower-latitude sea ice in the Sea of Okhotsk (they also found that 78% of the snow was depth hoar).

It should be borne in mind that because of snow–ice formation, the Antarctic–Arctic snow depth comparison is misleading. As discussed earlier, flooding of the snow/ice interface is a common occurrence in Antarctica, due in large part to the combined effects of high precipitation rates and a relatively thin seasonal ice cover (resulting from net ice divergence and relatively high ocean heat fluxes). The snow depth (h_s) is often sufficient to exceed the conditions required for negative freeboard (equation 5.1b), at which time flooding occurs by the lateral incursion of seawater from floe margins or vertically up through the ice via cracks or brine drainage channels (Maksym & Jeffries, 2000). Seawater infiltration via the latter is strongly dependent on ice temperature and salinity, which is regulated by the snow, with channels tending to interconnect to form conduits between the ocean and ice surface if levels of −5°C and 5 psu respectively have been attained (Golden et al., 1998). These thresholds are frequently exceeded in Antarctica, although flooding does not always accompany negative freeboard, e.g. under cold conditions (Massom et al., 2001). Moreover, flooding can also occur by wave-ice interaction and deformation processes (Massom et al., 1997). The overall outcome is that over 50% of the Antarctic sea ice surface can be flooded by seawater in some regions

Table 5.9 Snow densities (mean and standard deviation) measured over Antarctic sea ice, derived from sources given in the reference column. After Massom et al. (2001). Modified with permission from American Geophysical Union.

Sector	Season (Year)	Snow density, kg m^{-3}	Range, kg m^{-3}	N	Reference
Indian & W Pacific Oceans					
139–141°E, 144–150°E	Autumn (1993)	390 ± 170	120–660	55	Worby and Massom (1995)
138–142°E	Winter (1995)	360 ± 110	120–760	170	Massom et al. (1998)
110–120°E	Winter–spring (2003)	319	125–735	188	Massom (unpublished data, 2003)
Bellingshausen, Amundsen, Ross Seas					
95–165°W	Autumn (1992)	340 ± 80	99–543	134	Jeffries et al. (1994)
165–180°W	Autumn–winter (1995)	350 ± 80	240–817	73	Sturm et al. (1998)
75–110°W	Winter–spring (1993)	247 ± 210	108–467	210	Jeffries et al. (1997)
109–171°W	Winter–spring (1994)	360 ± 40	300–440	255	Sturm et al. (1998)
80–110°W, 155–180°W	Winter–spring (1995)	380 ± 80	290–480	45	Sturm et al. (1998)
70–130°W	Late summer (1994)	391 ± 71	212–518	37	Haas et al. (1996)
Weddell Sea					
5°E–55°W	Autumn–winter (1992)	290	200–600	–	Lytle (unpublished data, 2001)
0–50°W	Winter (1992)	320	180–670	132	Massom et al. (1997)
0–55°W	Spring (1989)	290 ± 70	110–550	206	Eicken et al. (1994)
20–57°W	Late summer (1997)	349 ± 72	130–496	130	Haas et al. (1998)

Table 5.10 Snow depths from the Arctic Basin, derived from sources given in the reference column.

Area	Mean (m)	n	Reference
Central Arctic Basin	0.34	Thousands	Colony et al. (1998)
Central Arctic Basin	0.34	Thousands	Warren et al. (1999)
Canadian Archipelago	0.23–0.29 (FYI)	2756	Iacozza and Barber (1999)
Canadian Archipelago	0.24–0.35 (MYI)	2048	Iacozza and Barber (1999)
Canadian Archipelago	0.23	dozens	Iacozza and Barber (2001)
Beaufort Sea	0.34	21,169	Sturm et al. (2002a)
Beaufort Sea	0.21	1906	Sturm et al. (2006)
AVERAGE	**0.29**	**About 38,000**	

(Eicken et al., 1994; Jeffries et al., 1994), this estimate being based on limited *in situ* observations. Such flooding is rare in the Arctic, although it may play a significant role in marginal seas such as the Greenland Sea (Perovich et al., 1988). As a result, snow depths measured in the Antarctic almost certainly underestimate the actual snowfall, since a substantial component of the initial snow will have been converted into snow-ice (and therefore not measured).

Table 5.11 shows that the percentage of *in situ* measurements showing negative ice freeboard on various Antarctic cruises varied from 11 to 51%, and was paralleled in the percentage of slush occurrence. When not negative, the freeboard of Antarctic FYI is typically at or close to zero (Jeffries et al., 1998), implying that little additional snow accumulation is required to cause flooding. Sturm et al. (1998) suggest that there is a 'self-balancing' mechanism in snow–ice formation, whereby negative freeboards are in general likely to be short-lived phenomena, as snow-ice will form shortly after flooding and will re-establish the isostatic balance and produce a zero freeboard. The contribution of snow-ice to the overall sea ice mass balance is negligible in the Arctic, due to the thicker ice relative to h_s (Chapter 2).

Regional distribution of snow depth

Information on regional variations in h_s has been presented for the Arctic Ocean by Warren et al. (1999). There the deepest snow is found north of Greenland and the eastern Canadian Archipelago, with depth decreasing towards Wrangell Island and Siberia. In Antarctica, we must combine the distribution of h_s measurements with the distribution of snow-ice. On the basis of the rather limited suite of *in situ* observations available (collated in Massom et al., 2001), maximum snow depths in the circumpolar Antarctic sea ice zone appear to occur in the Bellingshausen, Amundsen and Ross Sea sectors, due largely to high precipitation rates in these regions and the presence in the latter two sectors of MYI. In the Weddell Sea, a large contrast is noted between the NW and SE in winter (Lange & Eicken, 1991; Massom et al., 1997), with thicker snow to the west of ~35°W in the western limb of the Weddell Gyre, which contains a significant proportion of MYI.

The contrast in the ice, snow and freeboard conditions in Antarctica versus the Arctic is evident from a comparison of probability distributions from (1) Marguerite Bay in Antarctica (August–September 2002) (Perovich et al., 2004) and (2) a US Navy Ice Camp in the Beaufort Sea in the Arctic Basin (March, 2003) (Sturm et al., 2006) (Fig. 5.17). The Arctic ice, which was both FYI and MYI, was 3–4 times thicker than the Antarctic ice. Much more of it had been scoured bare of snow, though the mean snow depth was not radically different than the value from Antarctica. Freeboard was not explicitly measured at Navy Ice Camp, but no negative freeboard was observed, with observations from nearby suggesting consistent positive freeboard of 8–10 cm – compared to a mean of 4.5 cm in Marguerite Bay (where 17% of the freeboard measurements were negative).

The relatively few observations over Antarctic fast ice show minimal snow accumulation in the near-coastal zone due to removal by strong and persistent katabatic winds (Table 2 in Massom et al., 2001). Work in Lützow-Holm Bay in East Antarctica shows a significant increase in h_s on fast ice with increasing distance offshore, due to diminution in the strength of the katabatic winds (Kawamura et al., 1997). Analyses to date suggest that snow-ice makes only a moderate contribution to the sea ice mass balance in the Weddell Sea (Eicken et al., 1994) and East Antarctica (Worby et al., 1998). By contrast, snow-ice appears to make a significant contribution to sea ice thickening in the eastern and western Pacific sectors

Table 5.11 Percentage of drilled holes and snow pits with negative freeboard and slush, and the proportion of snow-ice measured in sea ice core analyses, from various studies around Antarctica, derived from sources given in the reference column. After Massom et al. (2001). Modified with permission from American Geophysical Union.

Sector	Season (Year)	% Pits w/slush (n)	% f ≤0 m (n)	Mean hs/hi (n)	% Snow-ice
Indian & W Pacific Oceans					
136–138°E	Early spring (1991)[1]	–	–	0.37 (7)	30
64–106°E	Late spring (1991)[1]	–	–	0.10 (39)	18
62–102°E	Spring (1992)[1]	–	39 (23)	0.07 (67)	23
75–150°E	Spring (1994)[1]	40 (10)	35 (54)	0.18 (106)	–
139–141°E, 144–150°E	Autumn (1993)[1]	53 (17)	11 (134)	0.09 (186)	9
138–142°E	Winter (1995)[2]	29 (46)	18 (577)	0.19 (584)	–
Bellingshausen, Amundsen & Ross Seas					
66–68°W	Winter (2001)[3]	–	52 (488)	0.26 (488)	15
66–68°W	Winter (2002)[3]	–	20 (564)	0.20 (564)	–
165–180°W	Autumn–winter (1995)[4]	36 (73)	29 (3671)	0.21/0.31	25 (15/38)
175°E–175°W	Autumn–winter (1998)[5]	0 (43)	17 (3253)	0.18 (3253)	12 (7/25)
80–110°W, 155–180°W	Winter–spring (1995)[6]	51 (45)	34 (4025)	0.32 (4176)	–
75–110°W	Winter–spring (1993)[7]	35	18	0.29	24
109–171°W	Winter–spring (1994)[8]	46 (165)	51 (2227)	0.35	38
70–130°W	Late summer (1997)[9]	12 (170)	17 (170)	–	–
Weddell Sea					
0–55°W	Winter–spring (1989)[10]	50	40	0.27 (5339)	8
7°E–5°W	Winter (1986)[11]	–	17	0.18 (4238)	–
0–50°W	Winter (1982)[12]	–	11.5 (468)	0.14 (386)	–
46–54°W	Spring (1988)[13]	–	15	0.23 (1553)	–
45–55°W	Summer (1992)[14]	30–50 (~100 holes)	–	–	–

[1]Worby and Massom (1995)
[2]Massom et al. (1998)
[3]Perovich et al. (2004)
[4]Jeffries & Adolphs (1997); Sturm et al. (1998); Jeffries et al. (1998)
[5]Jeffries et al. (2001); Morris and Jeffries (2001)
[6]Sturm et al. (1998)
[7]Jeffries et al. (1997)
[8]Sturm et al. (1998); Jeffries et al. (1998)
[9]Haas et al. (1996)
[10]Ackley et al. (1990); Lange et al. (1990)
[11]Wadhams et al. (1987)
[12]Massom et al. (1997)
[13]Eicken et al. (1994)
[14]Drinkwater and Lytle (1997)
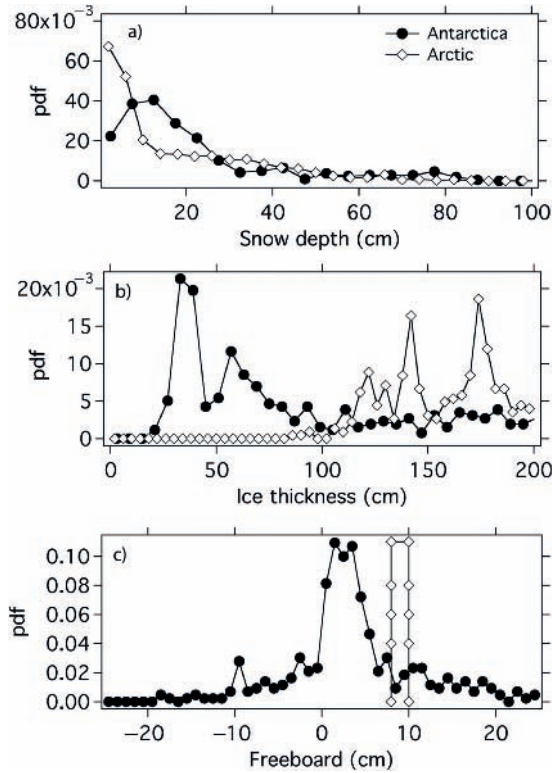
Fig. 5.17 Probability distributions of (a) snow depth, (b) ice thickness and (c) freeboard determined from survey profiles in Marguerite Bay (Antarctica) and in the Beaufort Sea (Arctic Basin). Antarctic data courtesy of Don Perovich, CRREL, USA.

(Jeffries et al., 1997, 1998). Latitudinal variability has also been noted in the western Ross Sea (Jeffries & Adolphs, 1997), with the percentage of snow ice encountered in the inner pack being less than half that in the outer pack (Table 5.10).

A promising recent development has been an algorithm to derive global estimates of snow depth over sea ice from time series of satellite passive-microwave brightness temperature (T_b) data, specifically from the NASA Aqua Advanced Microwave Scanning Radiometer-Earth Observing System (AMSR-E). Details of the technique are given in Comiso et al. (2003). In short, snow depth is determined from the spectral gradient ratio of T_b data from the 18.7 and 36.5 GHz channels (vertical polarization), using coefficients derived from regression analysis of coincident *in situ* snow depth measurements and T_b data and correcting for ice concentration. In effect, the algorithm is based on the enhanced scattering efficiency at 36.5 GHz compared to 18.7 GHz (Comiso et al., 2003) and the assumption of an increase in microwave scattering with increasing snow depth. Vertical polarization channel data are used in preference to horizontal polarization owing to their lower sensitivity to snow layering (Armstrong et al., 1993). Snow thicker than 0.5 m cannot be detected using the current algorithm, owing to the limited penetration depth at the frequencies used, and snow depth retrievals cannot be carried out over Arctic MYI, as the microwave signature of the latter can resemble that of snow on FYI (Comiso et al., 2003). Marginal ice zones are also excluded, and the algorithm is only effective under dry snow conditions. Example images are shown in Fig. 5.18.
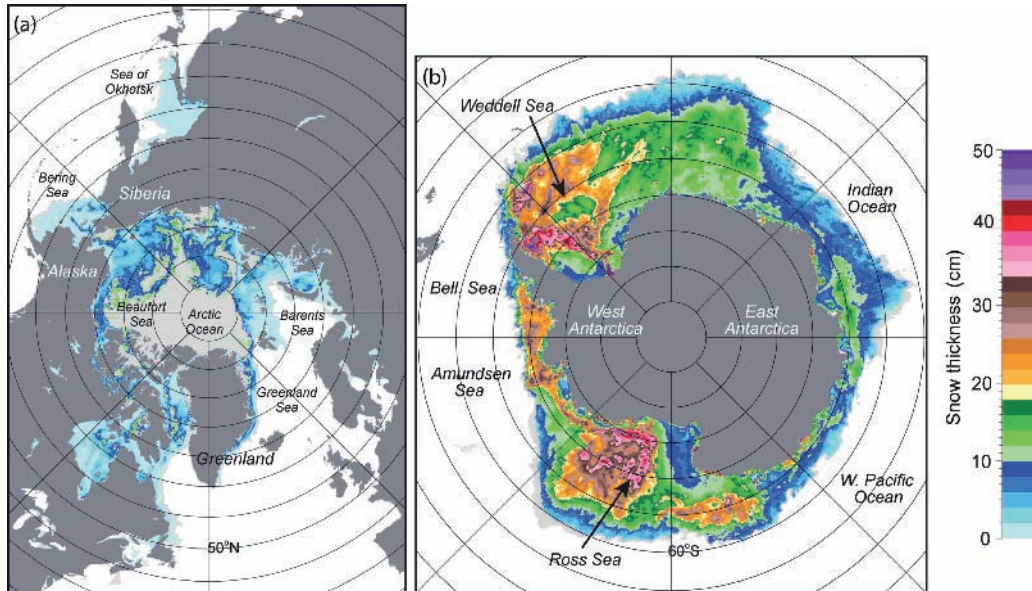
Fig. 5.18   Maps of snow depth on sea ice for (a) the Arctic (on March 15 2007), and (b) the Antarctic (on September 17, 2007), retrieved from AMSR-E brightness temperature and derived ice-concentration data. Note that MYI is masked out (light grey) in the Arctic. Images courtesy of Thorsten Markus, NASA Goddard Space Flight Center, USA.

The AMSR-E snow depth products are routinely available from the US National Snow and Ice Data Centre (http://nsidc.org) as 5-day running averages, in order to minimize variability in weather, snow grain size and snow density. They date back to 2002, mapped at 12.5-km resolution to a standard polar stereographic grid for direct comparison with the coincident AMSR-E sea ice concentration and temperature products. Unfortunately, recent validation campaigns suggest that this product underestimates actual snow depth by as much as a factor of 2–3 (Worby et al., 2008), due primarily to ice surface roughness effects (Stroeve et al., 2006). Work is underway to improve the accuracy, possibly by incorporating ice surface roughness information acquired on a similar scale by satellite radar scatterometers. Moreover, Powell et al. (2006) show that the accuracy of snow depth retrievals from passive-microwave data could be improved by taking into account the observed variability of snow pack properties (e.g. density and grain size) and sea ice emissivity, although this is not a simple task. However, although absolute accuracy of the current AMSR-E snow depth product is an issue, it provides considerable insight into large-scale spatial patterns of snow depth variability that correspond to similar patterns in ice type and age. Taken at face value, the AMSR-E snow maps (Fig. 5.18) indicate the deepest snow near the Antarctic Peninsula, and overall, deeper snow in Antarctica than in the Arctic. In fact, the maps indicate that the snow cover in the Arctic is surprisingly shallow and homogeneous.

Floe-scale distribution of snow depth, and surface roughness characteristics

The close relationship between ice roughness and snow depth has been shown for both Arctic and Antarctic sea ice snow packs in numerous cross sections measured of the snow (Sturm et al., 1998; Iacozza & Barber, 1999, Figure 4; Sturm et al., 2006). These cross sections are
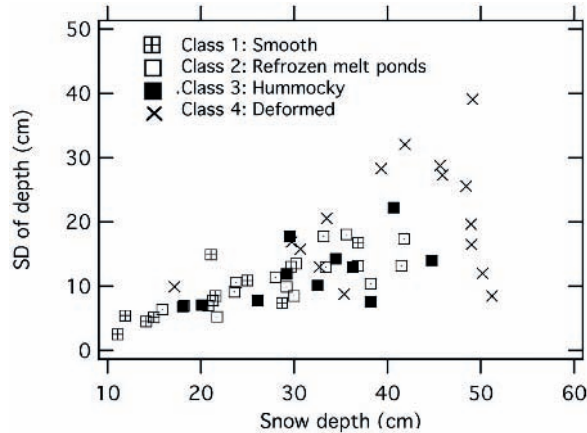
Fig. 5.19   Snow depth and standard deviation of snow depth (SD) by ice type for snow on sea ice in the Chukchi Sea at SHEBA (Sturm et al., 2002a). Reproduced by permission of American Geophysical Union. Copyright 2002 American Geophysical Union.

somewhat qualitative, but analysis by Sturm et al. (2002a) has shown good discrimination of snow depth and snow variance by ice type, at least in the Arctic (Fig. 5.19).

Recently, semi-variogram analysis has been applied to *in situ* measurements of snow depth in order to understand the spatial distribution of snow at scales ranging from metres to a kilometre (Sturm et al., 1998; Iacozza & Barber, 1999). Sturm et al. (1998) reported snow structural lengths for the Amundsen, Bellingshausen and Ross Seas of 3–70 m. Average values ranged from 12.7 m in August–September 1995, through 22 m in September–October 1994, to 23.3 m in May–June 1995. These values compared with a structure length range of ~4–6 m for the underlying ice surface, indicating that the addition of snow increased the floe topographic relief, but tends to 'smooth out' the higher frequency (i.e. rougher) ice surface. Sturm et al., (1998) concluded that any ice surface roughness feature with a relief of greater than 0.2 m 'nucleated' a significant snow surface feature. In the Arctic, semi-variograms were used to analyse snow cover with similar results. Snow structural lengths ranged from about 5 to 35 m (Iacozza & Barber, 1999), and 20–50 m (Sturm et al., 2002a), where the range was fairly constant with ice type, but the amplitude of the features increased with increasing deformation of the ice. Most recently (Sturm et al., 2006), for snow on the ice of the Beaufort Sea, ranges of 7–120 m were found, again with the amplitude increasing with ice roughness (deformation), but the range seemingly independent of the degree of deformation.

By smoothing the ice surface, snow greatly modifies both the ice–air drag coefficient, to affect the degree of coupling between ice and atmosphere, and the bulk transfer coefficients for latent and sensible heat (Andreas & Claffey, 1995). These authors further show the surface drag coefficient to be critically dependent on the alignment of the dominant snowdrift pattern relative to the mean wind direction.

5.7 Remote-sensing considerations

Interpretation of satellite microwave data (both active and passive) acquired over frozen oceans is complicated by the fact that the snow cover evolves through time to make a

variable and at times first-order contribution to the observed remote-sensing signature – depending on its age, structural characteristics and state. As a result, unambiguous interpretation of satellite data, and accurate inference of key geophysical quantities from the data, e.g. ice concentration, requires understanding of the interaction of EMR with the snow (and ice) layers, and its dependency on both physical and electromagnetic properties of snow and ice and satellite instrument parameters, e.g. wavelength, polarization and incidence angle. Detailed treatment of this complex field is beyond the scope of this chapter – see Chapter 2, Hallikainen & Winebrenner (1992), Lewis et al. (1994), Lubin & Massom (2006), Rees (2005) and Tucker et al. (1992) for more in-depth information on snow (and sea ice) physical properties relevant to remote sensing, and Lubin and Massom (2006) for snow and ice variables derived from satellite data. However, certain fundamental relationships are of key importance and will be outlined here. Here we concentrate on snow properties relevant to microwave and thermal infrared (TIR) remote sensing, as optical properties relevant to visible, near-IR remote sensing are covered in Chapter 2 and Section 5.5.

Major determinants of the relative contributions of the various EMR–surface interactions (i.e. reflection, absorption, transmission and scattering) are the dielectric (material) and scattering (geometrical) properties of the snow and underlying ice cover (Hallikainen & Winebrenner, 1992; Rees, 2005). Dielectric properties of the snow and ice substrate determine the propagation and attenuation of electromagnetic waves and govern both its optical and microwave properties (and remote-sensing signature). Scattering of EMR from a surface depends upon its dielectric constant, the geometry of the scattering centres and its roughness properties. The dielectric constant of snow is basically determined by the dielectric properties of ice, ice particle shape and snow density. For dry snow, the real part of the dielectric constant mainly depends on its density, while the imaginary part (which governs the amount of absorption) is minimal but moderately dependent on temperature (Hallikainen et al., 1986). Owing to the low absorption in dry snow, propagation of visible, near-IR and microwave radiation at wavelengths exploited by satellite remote sensing is typically dominated by volume scattering (multiple reflection off surfaces/layers or particles/scattering centres). The contribution in this case is largely dependent on the dimension of the scatterers (snow grains and internal layers/dielectric discontinuities) relative to wavelength of the radiation. In the microwave, it increases at frequencies >~37 GHz for passive systems and >5 GHz (C-band) for radars (Drinkwater, 1995; Barber et al., 1998). The decrease in passive-microwave emission and increase in radar backscatter with increasing grain size is greater at horizontal than vertical polarization (Armstrong et al., 1993).

Dry snow plays an indirect role in remote sensing by affecting the dielectric constant of the snow–ice interface. The insulative snow cover increases the temperature of this interface, which increases the brine volume in the lower snow horizons. This creates a 'dielectrically rough' interface. Variations in snow/ice temperature and associated surface salinity can result in large dielectric fluctuations (Shokr & Barber, 1994).

As with snow physical properties, there is a marked seasonal evolution in snow electromagnetic properties, with major differences between the Arctic and Antarctic. Particularly dramatic changes occur in the Arctic in response to the seasonal physical changes described in Section 5.4. In late spring, thaw-freeze cycles lead to diurnal and semi-diurnal fluctuations in microwave backscatter and emission (Grenfell and Lohanick, 1985; Barber et al., 1992; Eppler et al., 1992). At the onset of spring melt proper, the appearance of a small amount

of liquid water in the snow (i.e. 2–3% by volume) leads to an abrupt increase in microwave absorption and decrease in penetration depth (Hallikainen & Winebrenner, 1992). Surface rather than volume scattering then dominates to typically reduce radar backscatter (Onstott, 1992). For passive-microwave sensing, wet snow emissivity approaches unity to act like a black body, leading to a large frequency- and polarization-dependent increase in the observed brightness temperature (Eppler et al., 1992). For this reason, the snow contribution in late spring–summer dominates to effectively mask backscatter and emissivity contrasts that occur under colder dryer conditions between the underlying ice types, e.g. Arctic MYI and FYI (Comiso & Kwok, 1996). For radars, this impact is greatest at higher frequencies (Hallikainen & Winebrenner, 1992). In contrast, the subsequent formation of melt ponds significantly lowers the sea ice microwave emissivity to cause significant ice-concentration underestimates from satellite data (Comiso & Kwok, 1996). In autumn, refreezing and drying of the surface plus new snow accumulation lead to a recovery of backscatter to winter levels (Beaven & Gogineni, 1994) and a decrease in microwave emissivity.

Satellite remote-sensing techniques have been developed to exploit such abrupt changes in snow microwave signature to map and monitor large-scale spatio-temporal patterns in seasonal snow cover melt and refreezing. These techniques, using mainly passive microwave, SAR and radar scatterometer data, are described in detail in Lubin and Massom (2006). An example is given in Fig. 5.20. Given the close correlation between large-scale sea ice backscatter behaviour and air temperature in the Arctic Ocean from spring to autumn (Jeffries et al., 1997), variability in snow melt/freeze-up onset and length of the annual melt season may also be a sensitive bellwether of climate change/variability. However, issues remain regarding application in Antarctica due to the probable impact of flooding on melt detection accuracy using microwave techniques.

Seasonal changes in snow electromagnetic properties are generally less pronounced for Antarctic sea ice, where there is less contrast in the microwave signatures of FYI and MYI than in the Arctic (Comiso et al., 1992; Drinkwater, 1995) and snow basal wetness is common through the year (Massom et al., 2001). However, rapid backscatter increases are seen in Antarctic perennial ice regions November–December due to superimposed-ice formation (Haas et al., 2001), with abrupt though ephemeral signal changes occurring year-round due to strong warm air incursion and snow melt (wetting) episodes followed by refreezing a few days later (Drinkwater et al., 1995) (e.g. Fig. 5.12). The summer-time backscatter increase is in marked contrast to the summer decline in Arctic backscatter noted above, related to the different snow conditions. A slow Antarctic backscatter decline from March onwards then corresponds to the transition to flood-freeze cycle processes (Morris et al., 1998). At this time, flooding may also be responsible for masking the passive-microwave signature of Antarctic MYI (Comiso et al., 1992).

Regarding snow electromagnetic properties in the TIR region (important deriving snow surface temperature maps from satellite TIR data) (Lubin & Massom, 2006), emissivity is largely insensitive to snow grain size, liquid–water content (at least up to 20% of the total particle volume), density, impurities, depth or temperature over the range typically encountered (Dozier & Warren, 1982). In the atmospheric water vapour window exploited by satellite sensors i.e. 8–14 μm, values for dry snow are typically 0.965–0.995 (with an angular dependence) (Warren, 1982), whereas that of sea ice is typically 0.98 (Rees, 2005). This is in stark contrast to the wide range of snow (and sea ice) emissivities at microwavelengths (Comiso et al., 1992).
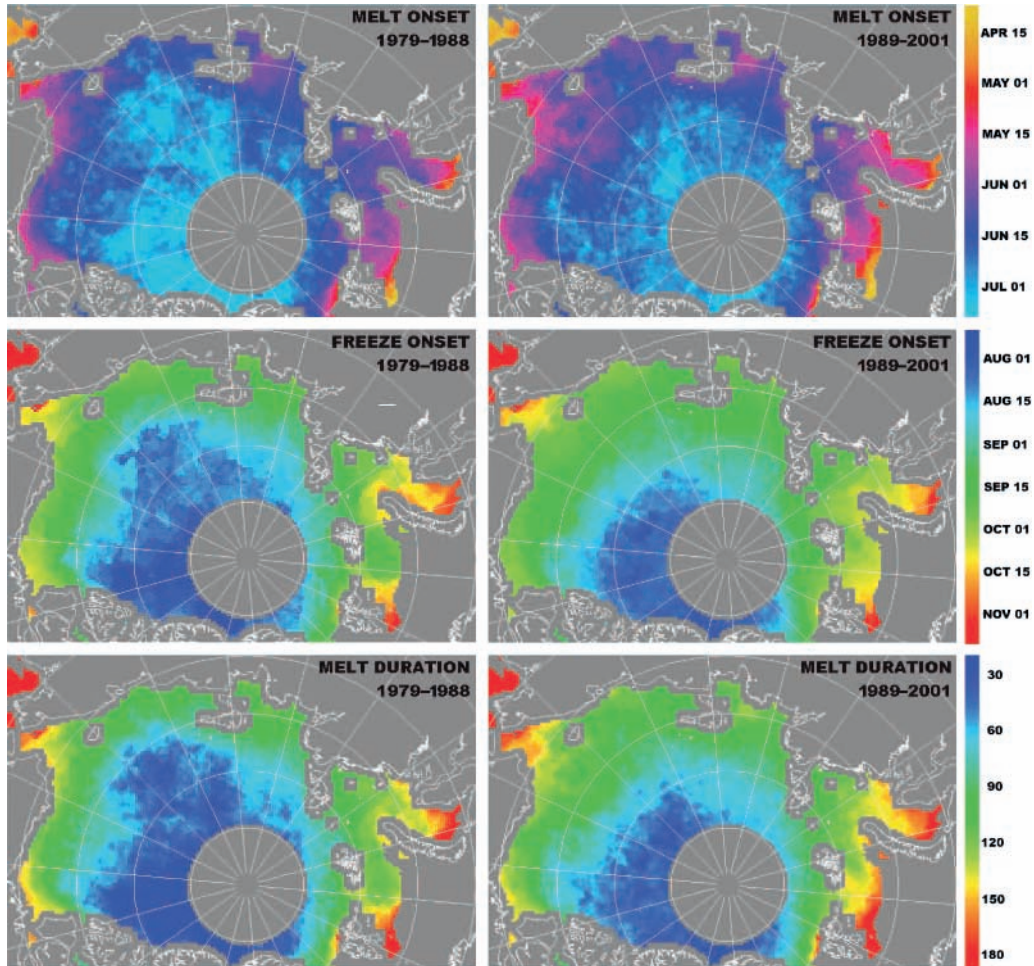
Fig. 5.20   Maps of average sea ice melt onset date, freeze onset date and melt season duration in the Arctic Ocean and surrounding seas during the low-index Arctic Oscillation (AO) period (1979–1988) and high-index AO period (1989–2001). These were estimated using coincident satellite passive-microwave brightness temperature data and buoy-derived surface air temperature data (Rigor et al., 2000). From Belchansky et al. (2004). Reproduced by permission of American Meteorological Society, Copyright 2004 American Meteorological Society.

5.8 Ecological significance of snow

Snow has a number of important yet contrasting ecological roles in ice-covered oceans, and at all trophic levels. On the one hand, it insulates the ice from large and cyclical synoptic-scale changes in air temperature while maintaining a relatively high ice temperature (Massom et al., 1997). This in turn affects the microstructure, salinity and permeability of the ice, thereby influencing space available for colonization by microorganisms and nutrient transport within the ice (Chapters 7, 8 and 10). In addition, extensive seawater flooding due in large part to snow 'loading' seeds the snow/ice interface with nutrients, algae and other microorganisms to form productive 'infiltration' algal communities (Ackley & Sullivan,

1994). This effect is compounded in the vicinity of pressure ridges, due to ice surface buckling and enhanced wind-blown snow accumulation there (Massom et al., 2001). Snow also strongly impacts primary productivity and biological activity within and under the sea ice in spring–summer by regulating the intensity and spectral composition of downwelling PAR (Mundy et al., 2007) and by contributing to the pulse of freshwater (upon melting) that stabilizes the mixed layer each spring (see Chapter 8). Even minor variations in snow depth can have a major impact on total transmitted PAR due to the exponential nature of PAR extinction (Iacozza & Barber, 1999). Another important factor is that snow-covered sea ice dramatically decreases the penetration of potentially harmful UV radiation into the ice cover and upper ocean, as discussed in Section 5.5. In addition, snow on sea ice accumulates iron in the form of aerosols deposited from the atmosphere. Although miniscule, levels may be sufficient to play a role in stimulating phytoplankton growth when released into the water column by melt, e.g. in Antarctic shelf waters (Edwards and Sedwick, 2001).

By affecting phytoplankton (primary) productivity, snow further plays a role in atmospheric composition by affecting the release by ice algal communities of dimethylsulfoniopropionate (DMSP) into the atmosphere (Curran & Jones, 2000). This is of considerable climatic significance, in that DMSP is a precursor of dimethylsulphide (DMS), which is the main source of ocean-derived sulphates and thus affects cloud-condensation nuclei and solar insolation (Chapters 8 & 12) (Liss et al., 2004). It follows that any significant change in sea ice and associated snow cover distribution and conditions will potentially affect climate via this path by driving changes in sea ice algal production and distribution.

In the Arctic, snow thickness distribution during winter and spring is an important factor determining habitat selection by predators at the apex of the food chain such as the ringed seal (*Phoca hispida*) and polar bear (*Ursus maritimus*, Chapter 11). Thick snowdrifts on the sea ice, for example are required by ringed seals for the construction of birthing and resting lairs. Moreover, the snow (and ice) must remain sufficiently stable for the critical 6-week lactation period, and insufficient snowfall prior to breeding and/or the effect on the snow cover of anomalously high temperatures or rainfall in spring can also leave the seals subject to increased exposure and predation by polar bears (Stirling & Smith, 2004). Snow cover is also an important component of polar bear habitat in that it too provides insulation and cover for young polar bears, with a proportion of the bear population building their maternity dens on multiyear sea ice (Derocher et al., 2004). Changing snow cover and sea ice conditions have potentially dire consequences for these magnificent creatures (see Chapter 11).

5.9 The outlook

The most profound immediate change related to snow on sea ice is likely to be the disappearance of MYI from the Arctic Basin (Maslanik et al., 2007). Without MYI, snow arriving early in the winter is more likely to fall into the ocean. Snow arriving later will fall on considerably thinner ice with the potential of altering the Arctic sea ice from a 'dry' snow system into a 'wet' system with more extensive snow–ice formation. As we noted earlier, an alteration of this sort could easily have ramifications in many areas, including the formation of melt ponds in the summer (which currently is widespread in the Arctic, but might be altered). Of course, the loss of MYI has profound implications for global climate and Arctic biota.

The next largest impact is likely to come from climate-driven changes in the amount and type of precipitation that falls on the ice. This will have a major impact on the thickness distribution and properties of snow on the sea ice covers of both hemispheres. Precipitation changes will be accompanied by changes in wind strength and patterns. The latter will also affect sea ice roughness characteristics, which in turn impact patterns of snow accumulation in a windy environment. Temperature and wind changes combined will further affect snow metamorphism processes, to influence key snow properties such as the size and shape of grains and snow density – and *ipso facto* – surface albedo and snow thermal conductivity. To reiterate, snow plays a dominant role in controlling the amount of energy that reaches and penetrates the ice in the form of solar radiation, and any marked change/trend in snow thickness distribution and properties will have a complex and major impact on the sea ice surface energy budget and atmosphere-ice-ocean interactions.

This is likely to be particularly true in Antarctica. Because of snow-ice formation, snow plays a dominant role in controlling the Antarctic sea ice mass balance, so knowledge of its behaviour, distribution and variability is crucial for understanding the climatic response in this region. Yet, the region remains perhaps one of the least well-known parts of the cryosphere. The ability to accurately monitor the snow depth of this region from space would be an invaluable step forward in our understanding. However, such measurements are complicated by a variety of small-scale processes that occur within the snow cover. Worse still, the ubiquitous conversion of snow to ice means that measurements of snow depth may underestimate total snow accumulation of by as much as a half.

In spite of its overall significance (as discussed above), snow is still treated in a coarse and often simplistic fashion in coupled ice–ocean–atmosphere and global circulation models (Lemke et al., 1997). We recognize that this is in part due to the complexity of the snow, and snow–ice interactions, as well as (until recently) lack of in-depth knowledge of snow characteristics and their spatio-temporal variability. The need to include the observed spatio-temporal variability of snow on sea ice in improved parameterizations of mass and energy exchange processes nested within regional and global models is a critical issue, yet represents a major challenge to modellers (Sturm et al., 2002a). Equally challenging, yet essential for future progress, is improved ability to remotely sense snow depth, SWE and other key properties. While considerable work is still being done in this area, as long as remote sensing is problematic, large-scale modelling of the snow on ice will be difficult. In the past, these difficulties might have been more readily accepted, but in the light of recent decreases in Arctic sea ice and snow cover, and the potential acceleration of the temperature-albedo feedback mechanism, it is time for renewed and redoubled efforts to understand and better monitor the snow cover on the ice.

Acknowledgements

References

Ackley, S.F. & Sullivan, C.W. (1994) Physical controls on the development and characteristics of Antarctic sea ice biological communities – a review and synthesis. *Deep-Sea Research*, **41**, 1583–1604.

Ackley, S. F., Lange, M.A. & Wadhams, P. (1990) Snow cover effects on Antarctic sea ice thickness. *CRREL Monograph,* **90-1**, 16–21.

Adolphs, U. (1999) Roughness variability of sea ice and snow cover thickness profiles in the Ross, Amundsen, and Bellingshausen Seas. *Journal of Geophysical Research*, **10**, 13577–13591.

Akitaya, E. (1974) Studies on depth hoar. *Contributions from the Institute of Low Temperature Science*, Series A, **26**, 1–67.

Allison, I., Brandt, R.E. & Warren, S.G. (1993) East Antarctic sea ice: Albedo, thickness distribution, and snow cover. *Journal of Geophysical Research*, **98**, 12,417–12,429.

Alvarez-Aviles, L., Simpson, W.R., Douglas, T.A., Sturm, M., Perovich, D.K. & Domine, F. (2008) Frost flower chemical composition during growth and its implications for aerosol production and bromine activation. *Journal of Geophysical Research Atmospheres*, **113**, 10.1029/2008JD010277.

Andreas, E.L. & Ackley, S.F. (1981) On the difference in ablation seasons of Arctic and Antarctic sea ice. *Journal of Atmospheric Science*, **39**, 440–447.

Andreas, E.L. & Claffey, K.J. (1995) Air-ice drag coefficients in the western Weddell Sea 1. Values deduced from profile measurements. *Journal of Geophysical Research*, **100**, 4821–4831.

Armstrong, R.L., Chang, A., Rango, A. et al. (1993) Snow depth and grain-size relationships with relevance for passive microwave studies. *Annals of Glaciology*, **17**, 171–176.

Barber, D.G., LeDrew, E.F., Flett, D.G., Shokr, M. & Falkingham, J. (1992) Seasonal and diurnal variations in SAR signatures of sea ice. *IEEE Transactions on Geoscience Remote Sensing*, **30**, 638–642.

Barber, D.G., Fung, A.K. Grenfell, T.C. et al. (1998) The role of snow on microwave emission and scattering over first-year sea ice. *IEEE Transactions on Geoscience and Remote Sensing*, **36**, 1750–1763.

Barber, D.G., Iacozza, J. & Walker, A.E. (2003) Estimation of snow water equivalent using microwave radiometry over Arctic first-year sea ice. *Hydrologic Processes*, **17**, 3503–3517.

Beaglehole, J.C. (1974) *The Life of Captain James Cook*. Stanford University Press, Stanford, USA.

Beaven, S.G. & Gogineni, S.P. (1994) Shipborne radar backscatter measurements from Arctic sea ice during the fall freeze-up. *Remote Sensing Reviews*, **9**, 3–25.

Belchansky, G.I., Douglas, D.C. & Platonov, N.G. (2004) Duration of the Arctic sea ice melt season: regional and interannual variability, 1979–2001. *Journal of Climate*, **17** (1), 67–80.

Benson, C.S. & M. Sturm, M. (1993) Structure and wind transport of seasonal snow on the Arctic slope of Alaska. *Annals of Glaciology*, **18**, 261–267.

Berton, P. (1989) *The Arctic Grail: The Quest for the North West Passage and the North Pole, 1818–1909*, 672 pp. Anchor Canada.

Birkeland, K. (1998) Terminology and predominant processes associated with the formation of weak layers of near-surface faceted crystals in the mountain snowpack. *Arctic and Alpine Research*, **30**, 193–199.

Brandt, R.E., Warren, S.G., Worby, A.P. & Grenfell, T.C. (2005) Surface albedo of the Antarctic sea ice zone. *Journal of Climate*, **18**, 3606–3622.

Colbeck, S.C. (1982) An overview of seasonal snow metamorphism. *Reviews of Geophysics and Space Physics*, **20**, 45–61.

Colbeck, S.C. (1986) Statistics of coarsening in water-saturated snow. *Acta Metallurgica*, **34**, 347–352.

Colbeck, S.C. (1991) The layered character of snow covers. *Reviews of Geophysics*, **29**, 81–96.

Colbeck, S., Akitaya, E., Armstrong, R. et al. (1990) *International Classification for Seasonal Snow on the Ground*. International Commission for Snow and Ice, World Data Center A for Glaciology, University of Colorado, Boulder, CO, USA.

Colony, R., Radionov, V. & Tanis, F.J. (1998) Measurements of precipitation and snowpack at Russian North Pole drifting stations. *Polar Record*, **34**, 3–14.

Comiso, J.C. & Kwok, R. (1996) Surface and radiative characteristics of the summer Arctic sea ice cover from multi-sensor satellite observations. *Journal of Geophysical Research*, **101**, 28,397–28,416.

Comiso, J.C., Grenfell, T.C., Lange, M. et al. (1992) Microwave remote sensing of the Southern Ocean ice cover. In: *Microwave Remote Sensing of Sea Ice* (Ed. F.D. Carsey), pp. 243–259. American Geophysical Union, Washington, DC.

Comiso, J.C., Cavalieri, D.J. & Markus, T. (2003) Sea ice concentration, ice temperature, and snow depth, using AMSR-E data. *IEEE Transactions on Geoscience and Remote Sensing*, **41**, 243–252.

Cooke, A. & Holland, C. (1978) *The Exploration of Northern Canada: 500-1920 A Chronology*, 549 pp. The Arctic History Press, Toronto.

Curran, M.A.J. & Jones, G.B. (2000) Dimethylsulphide in the Southern Ocean: seasonality and flux. *Journal of Geophysical. Research*, **105**, 20451–20459.

Denoth, A. (1982) Effect of grain geometry on electrical properties of snow at frequencies up to 100 MHz. *Journal of Applied Physics*, **53**, 7496–7501.

Derocher, A.E., Lunn, N.J. & Stirling, I. (2004) Polar bears in a warming climate. *Integrative & Comparative Biology*, **44**, 163–176.

Douglas, T.A., Sturm, M., Simpson, W.R. et al. (2008) The influence of snow and ice crystal formation and accumulation on mercury deposition to the Arctic. *Environmental Science & Technology*, **42**, 1542–1551.

Doumani, G.A. (1966) Surface structures in snow. In: *International Conference on Low Temperature Science: I. Physics of Snow and Ice*, pp. 1119–1136. Sapporo, Japan.

Dozier, J. & Warren, S.G. (1982) Effect of viewing angle on the infrared brightness temperature of snow. *Water Resources Research*, **18**, 1424–1434.

Dozier, J., Schneider, S.R. & McGinnis Jr., D.F. (1981) Effects of grain size and snowpack water equivalence on visible and near-infrared satellite observations of snow. *Water Resources Research*, **17**, 1213–1221.

Drinkwater, M.R. (1995) Airborne and satellite SAR investigations of sea ice surface characteristics. In: *Oceanographic Applications of Remote Sensing* (Eds. M. Ikeda & F.W. Dobson), pp. 339–357. CRC Press, Boca Raton, Florida.

Drinkwater, M.R. & Crocker, G.B. (1988) Modeling changes in the dielectric and scattering properties of young snow-covered sea ice at GHz frequencies. *Journal of Glaciology*, **34**, 274–282.

Drinkwater, M.R. & Liu, X. (2000) Seasonal to interannual variability in Antarctic sea ice surface melt. *IEEE Transactions on Geoscience Remote Sensing*, **38**, 1827–1842.

Drinkwater, M.R. & Lytle, V.I. (1997) ERS-1 radar and field-observed characteristics of autumn freeze-up in the Weddell Sea. *Journal of Geophysical Research*, **102**, 12,593–12,608.

Drinkwater, M.R., Hosseinmostafa, R. & Gogineni, P. (1995) C-band backscatter measurements of winter sea ice in the Weddell Sea, Antarctica. *International Journal of Remote Sensing*, **16**, 3365–3389.

Edwards, R. & Sedwick, P. (2001) Iron in east Antarctic snow: Implications for atmospheric iron deposition and algal production in Antarctic waters. Geophysical Research Letters, **28** (20), 3907–3910.

Eicken, H. (1992) The role of sea ice in structuring Antarctic ecosystems. *Polar Biology*, **12**, 3–13.

Eicken, H., Lange, M.A., Hubberten, H.-W. & Wadhams, P. (1994) Characteristics and distribution patterns of snow and meteoric ice in the Weddell Sea and their contribution to the mass balance of sea ice. *Annales Geophysicae*, **12**, 80–93.

Eicken, H., Fischer, H. & Lemke, P. (1995) Effects of the snow cover on Antarctic sea ice and potential modulation of its response to climate change. *Annals of Glaciology*, **21**, 369–376.

Eicken, H., Grenfell, T.C., Perovich, D.K. et al. (2004) Hydraulic controls of summer Arctic pack ice albedo. *Journal of Geophysical Research*, **109**, C08007, 10.1029/2003JC001989.

Eppler, D.T., Farmer, L.D., Lohanick, A.W. et al. (1992) Passive microwave signatures of sea ice. In: *Microwave Remote Sensing of Sea Ice* (Ed. F.D. Carsey), pp. 47–71. American Geophysical Union, Washington DC.

von Eugster, H.P. (1950) On the Form and Metamorphosis of Snow. *Report 113*. Institute for Snow and Avalance Research, Davos, Switzerland.

Fierz, C., Armstrong, R.L., Durand, Y. et al. (2008) IACS International classification for seasonal snow on the ground. In: *Technical Documents in Hydrology*. International Association of Cryospheric Sciences/UNESCO.

Garrity, C. (1992) Characterization of snow on floating ice and case studies of brightness temperature changes during the onset of melt. In: *Microwave Remote Sensing of Sea Ice* (Ed. F.D. Carsey), pp. 313–326. American Geophysical Union, Washington, DC, USA.

Gearheard, S., Matumeak, W., Angutikjuaq, I. et al. (2006) "It's not that simple": a collaborative comparison of sea ice environments, their uses, observed changes, and adaptations in Barrow, Alaska, USA, and Clyde River, Nunavut, Canada. *Ambio*, **35**, 203–211.

German, R.M. (1996) *Sintering Theory and Practice*, 550 pp. John Wiley & Sons, Inc., New York.

Golden, K.M., Ackley, S.F. & Lytle, V.I. (1998) The percolation phase transition in sea ice. *Science*, **282**, 2238–2241.

Goodwin, I.D. (1990) Snow accumulation and surface topography in the katabatic zone of eastern Wilkes Land, Antarctica. *Antarctic Science*, **2**, 235–242

Granberg, H. (1998) Snow cover on sea ice. In: *Physics of Ice-Covered Seas* (Ed. M. Leppäranta), pp. 605–649. Helsinki University Press, Helsinki, Finland.

Green, R.O., Dozier, J., Roberts, D.A. & Painter, T.H. (2002) Spectral snow reflectance models for grain-size and liquid-water fraction in melted snow for the solar-reflected spectrum. *Annals of Glaciology*, **34**, 71–73.

Grenfell, T.C. & Lohanick, A.W. (1985) Temporal variations of the microwave signature of sea ice during the late spring and early summer near Maud Bay NWT. *Journal of Geophysical Research*, **90**, 5063–5074.

Grenfell, T.C. & Maykut, G.A. (1977) The optical properties of ice and snow in the Arctic basin. *Journal of Glaciology*, **18**, 445–463.

Grenfell, T.C. & Perovich, D.K. (2004) Seasonal and spatial evolution of albedo in a snow-ice-land-ocean environment. *Journal of Geophysical Research*, **109**, C01001, 10.1029/2003JC001866.

Grenfell, T.C., Warren, S.G. & Mullen, P.C. (1994) Reflection of solar radiation by the Antarctic snow surface at ultraviolet, visible, and near-infrared wavelengths. *Journal of Geophysical Research*, **99**, 18669–18684.

Grenfell, T.C., Light, B. & Sturm, M. (2002) Spatial distribution and radiative effects of soot in the snow and sea ice during the SHEBA experiment. *Journal of Geophysical Research*, **107**, 8032, 10.1029/2002JC000414.

Haas, C., Rebhan, H., Thomas, D.N. & Viehoff, T. (1996) Sea ice. In: *The Expedition ANTARK-TIS-XI/3 of RV "Polarstern" in 1994* (Eds. H. Miller & H. Grobe), pp. 29–43. Reports on Polar Research, 188/96.

Haas, C., Thomas, D.N., Steffens, M. et al. (1998) Physical and biological investigations of sea ice. In: *The Expedition ANTARKTIS-XIV of RV "Polarstern" in 1997*, *Report of Leg ANT-XIV/3* (Eds. W. Jokat & H. Oerter), pp. 18–30. Reports on Polar Research, 267/98.

Haas, C., Thomas, D.N. & J. Bareis, J. (2001) Surface properties and processes of perennial Antarctic sea ice in summer. *Journal of Glaciology*, **47**, 623–625.

Hallikainen, M. & Winebrenner, D.P. (1992) The physical basis for sea ice remote sensing. In: *Microwave Remote Sensing of Sea Ice* (Ed. F.D. Carsey), pp. 29–46. American Geophysical Union, Washington, DC, USA.

Hallikainen, M., Ulaby, F.T. & Abdelrazik, M. (1986). Dielectric properties of snow in the 3 to 37 GHz range. *IEEE Transactions on Antennas and Propagation*, **AP-34**, 1329–1339.

Iacozza, J. & Barber, D.G. (1999) An examination of the distribution of snow on sea ice. *Atmosphere–Ocean*, **37**, 21–51.

Iacozza, J. & Barber, D.G. (2001) Ablation patterns of snow cover over smooth first-year sea ice in the Canadian Arctic. *Hydrological Processes*, **15**, 3359–3569.

Jeffries, M.O. & Adolphs, U. (1997) Early winter snow and ice thickness distribution, ice structure and development of the western Ross Sea pack ice between the ice edge and the Ross Ice Shelf. *Antarctic Science*, **9**, 188–200.

Jeffries, M.O., Veazey, A.L., Morris, K. & Krouse, H.R. (1994) Depositional environment of the snow cover on West Antarctic pack-ice floes. *Annals of Glaciology*, **20**, 33–38.

Jeffries, M.O., Worby, A.P., Morris, K. Weeks, W.F., Hurst-Cushing, B., Jana, R.A. & Krouse, H.R. (1997) Late winter snow and ice characteristics of first-year floes in the Bellingshausen and Amundsen Seas, Antarctica. Results of investigations during R. V. *Nathaniel B. Palmer* cruise NBP 93-5 in August and September 1993. *Report UAG-R-325*. Geophysical Institute, University of Alaska, USA.

Jeffries, M.O., Hurst-Cushing, B., Krouse, H.R. & Maksym, T. (1998) The role of snow in the thickening and mass budget of first-year floes in the eastern Pacific sector of the Antarctic pack ice. *Report UAG-R-327*. Geophysical Institute, University of Alaska Fairbanks, USA.

Jeffries, M.O., Krouse, H.R., Hurst-Cushing, B. & Maksym, T. (2001) Snow-ice accretion and snow-cover depletion on Antarctic first-year sea ice floes. *Annals of Glaciology*, **33**, 51–60.

Kawamura, T., Ohshima, K., Takizawa, T. & Ushio, S. (1997) Physical, structural and isotopic characteristics and growth processes of fast ice in Lützow-Holm Bay, Antarctica. *Journal of Geophysical Research*, **102**, 334–355.

Kellogg, W.W. (1973) Climatic feedback mechanisms involving the polar regions. In: *Climate of the Arctic: Twenty-Fourth Alaska Science Conference* (Eds. G. Weller & S.A. Bowling), pp. 111–116. Geophysical Institute, University of Alaska, USA.

Kojima, K. (1966) Densification of seasonal snow cover. In: *Physics of Snow and Ice*, pp. 929–951. Institute of Low Temperature Science, Saporro, Japan.

LaChapelle, E.R. (1992) *Field Guide to Snow Crystals*. International Glaciological Society, Cambridge, UK.

Lange, M.A. & Eicken, H. (1991) The sea ice thickness distribution in the northwestern Weddell Sea. *Journal of Geophysical Res*earch, **96**, 4821–4837.

Lange, M.A., Schlosser, P., Ackley, S.F., Wadhams, P. & Dieckmann, G.S. (1990) ^{18}O concentrations in sea ice of the Weddell Sea, Antarctica. *Journal of Glaciol*ogy, **36**, 315–323.

Ledley, T.S. (1991) Snow on sea ice: competing effects in shaping climate. *Journal of Geophysical Research*, **96**, 17,195–17,208.

Lemke, P., Hibler III, W.D., Flato, G.M., Harder, M. & Kreyscher, M. (1997) On the improvement of sea ice models for climate simulations: the Sea Ice Model Intercomparison Project. *Annals of Glaciology*, **25**, 183–187.

Lewis, E.O., Livingstone, C.E., Garrity, C. & Rossiter, J.R. (1994) Properties of snow and ice. In: *Remote Sensing of Sea Ice and Icebergs* (Eds. S. Haykin, E.O. Lewis, R.K. Raney & J.R. Rossiter), pp. 21–96. John Wiley and Sons, New York.

Liss, P.S., Chuck, A.L., Turner, S.M. & Watson, A.J. (2004) Air–sea gas exchange in Antarctic waters. *Antarctic Science*, **16**, 517–529.

Lubin, D. & Massom, R.A. (2006) *Polar Remote Sensing. Volume 1: Atmosphere and Polar Oceans*, 756 pp. Praxis/Springer, Chichester & Berlin.

Lytle, V.I. & Ackley, S.F. (1992) Snow properties and surface elevation profiles in the Western Weddell Sea (NBP92–2). *Antarctic Journal of the US.*, *XXVII*, **5**, 93–94.

Lytle, V.I., Massom, R., Bindoff, N., Worby, A.P. & Allison, I. (2000) Wintertime heat flux to the underside of East Antarctic pack ice. *Journal of Geophysical Research*, **105**, 28,759–28,769.

McKay, G.A. & Gray, D.M. (1981) The distribution of snowcover. In: *Handbook of Snow: Principles, Processes, Management and Use* (Eds. D.M. Gray & D.H. Male), pp. 153–190. Pergamon, Oxford.

Maksym, T. & Jeffries, M.O. (2000) A one-dimensional percolation model of flooding and snow-ice formation on Antarctic sea ice. *Journal of Geophysical Research*, **105**, 26313–26331.

Maksym, T. & Markus, T. (2008) Antarctic sea ice thickness and snow-to-ice conversion from atmospheric reanalysis and passive microwave snow depth *Journal of Geophysical Research*, **113**, C02S12, 10.1029/2006JC004085.

Martinson, D.G. & Iannuzzi, R.A. (1998) Antarctic ocean–ice interaction: implications from ocean bulk property distributions in the Weddell Gyre. In: *Antarctic Sea Ice: Physical Processes, Interactions and Variability* (Ed. M.O. Jeffries), pp. 243–271. American Geophysical Union, Washington, DC, USA.

Maslanik, J.A., Fowler, C., Stroeve, J., Drobot, S., Zwally, J., Yi, D. & W. Emery, W. (2007) A younger, thinner Arctic ice cover: increased potential for rapid, extensive sea ice loss. *Geophysical Research Letters*, **34** (L24501), 10.1029/2007GL032043.

Massom, R.A., Drinkwater, M.R. & Haas, C. (1997) Winter snow cover on sea ice in the Weddell Sea. *Journal of Geophysical Research*, **102**, 1101–1117.

Massom, R.A., Lytle, V.I., Worby, A.P. & Allison, I. (1998) Winter snow cover variability on East Antarctic sea ice. *Journal of Geophysical Research*, **103**, 24,837–24,855.

Massom, R.A., Eicken, H., Haas, C. et al. (2001) Snow on Antarctic sea ice. *Reviews of Geophysics*, **39**, 413–445.

Massom, R.A., Stammerjohn, S.E., Smith, R.C. et al. (2006) Extreme anomalous atmospheric circulation in the West Antarctic Peninsula region in austral spring and summer 2001/2, and its profound impact on sea ice and biota. *Journal of Climate*, **19**, 3544–3571.

Mätzl, M. & Schneebeli, M. (2006) Measuring specific surface area of snow by near-infrared photography. *Journal of Glaciology*, **52**, 558–564.

Maykut, G.A. & Untersteiner, N. (1971) Some results from a time-dependent thermodynamic model of sea ice. *Journal of Geophysical Research*, **76**, 1550–1575.

Morris, K. & Jeffries, M.O. (2001) Seasonal contrasts in snow-cover characteristics on Ross Sea ice floes. *Annals of Glaciology*, **33**, 61–68.

Morris, K. Jeffries, M.O. & Li, S. (1998) Sea ice characteristics and seasonal variability of ERS-1 backscatter in the Bellingshausen Sea. In: *Antarctic Sea Ice: Physical Processes, Interactions and Variability* (Ed. M.O Jeffries), pp. 213–242. American Geophysical Union, Washington, DC, USA.

Mowat, F. (1960) *Ordeal by Ice: The Search for the Northwest Passage (Volume I of the Top of the World Trilogy)*, 428 pp. McClelland and Stewart, Toronto.

Mundy, C.J., Ehn, J.K., Barber, D.G. & Michel, C. (2007) Influence of snow cover and algae on the spectral dependence of transmitted irradiance through Arctic landfast first-year sea ice. *Journal of Geophysical Research*, **112**, C03007, 10.1029/2006JC003683.

Nakaya, U. (1954) *Snow Crystals*. Harvard University Press, Boston, USA.

Nolin, A.W. & A. Frei, A. (2001) Remote sensing of snow and snow albedo characterization for climate simulations. In: *Remote Sensing and Climate Simulations: Synergies and Limitations, Advances in Global Change Research* (Eds. M. Beniston & M.M. Verstraete), pp. 159–180. Kluwer Academic Publishers, Dordrecht and Boston.

Onstott, R.G. (1992) SAR and scatterometer signatures of sea ice. In: *Microwave Remote Sensing of Sea Ice* (Ed. F.D. Carsey), pp. 73–104. American Geophysical Union, Washington, DC, USA.

Perovich, D.K. (1993) A theoretical model of ultraviolet light transmission through Antarctic sea ice. *Journal of Geophysical Research*, **98**, 22,579–22,587.

Perovich, D.K. (1996) The optical properties of sea ice. *US Army Cold Regions Research and Engineering Laboratory (CRREL) Report 96-1*. Hanover, NH, USA.

Perovich, D.K. (2001) UV radiation and optical properties of sea ice and snow. In: *UV-Radiation and Arctic Ecosystems* (Ed. D. Hessen), pp. 73–89. Springer-Verlag, Heidelberg.

Perovich, D.K. (2003) Complex yet translucent, the optical properties of sea ice. *Physica B, Condensed Matter*, **338**, 107–114.

Perovich, D.K. & Richter-Menge, J. (1994) Surface characteristics of lead ice, *Journal of Geophysical Research*, **99**, 16341–16350.

Perovich, D.K., Gow, A.J. & Tucker III, W.B. (1988) Physical properties of snow and ice in the winter marginal ice zone of Fram Strait. In: *Proceedings of IGARSS'88 Symposium, Edinburgh, Scotland*, pp. 1119–1123. ESA SP-284, European Space Agency, Noordwijk, Netherlands.

Perovich, D.K., Roesler, C.S. & Pegau, W.S. (1998) Variability in Arctic sea ice optical properties. *Journal of Geophysical Research*, **103**, 1193–1208.

Perovich, D.K., Andreas, E.L., Curry, J.A. et al. (1999) Year on ice gives climate insights. *Eos, Transactions of the American Geophysical Union*, **80**, 481–486.

Perovich, D.K., Grenfell, T.C., Light, B. & Hobbs, P.V. (2002) The seasonal evolution of Arctic sea ice albedo. *Journal of Geophysical Research*, 10.1029/2000JC000438.

Perovich, D.K., Elder, B.C., Claffey, K.J. et al. (2004) Winter sea ice properties in Marguerite Bay, Antarctica. *Deep-Sea Research Part II*, **51**, 2023–2039.

Pomeroy, J.W. & Gray, D.M. (1995) *Snowcover Accumulation, Relocation and Management*, pp. 144. National Hydrology Research Institute, Saskatoon, Canada.

Pounder, E.R. (1965) *Physics of Ice*. Pergamon Press, Oxford.

Powell, D.C., Markus, T., Cavalieri, D.J. et al. (2006) Microwave signatures of snow on sea ice: modeling. *IEEE Transactions on Geoscience and Remote Sensing*, **44**, 3091–3102.

Rees, W.G. (2005) *Remote Sensing of Snow and Ice*. CRC Press, Boca Raton, FL.

Rigor, I.G., Colony, R.L. & Martin, S. (2000). Variations in surface air temperature observations in the Arctic 1979–97. *Journal of Climate*, **13**, 896–914.

Saloranta, T.M. (2000) Modeling the evolution of snow, snow ice and ice in the Baltic Sea. *Tellus*, **52A**, 93–108.

Scoresby, W. (1820) *An Account of the Arctic Regions With a History and Description of the Northern Whale-Fishery*, 651 pp. Archibald Constable and Co., Edinburgh.

Seligman, G. (1936) *Snow Structure and Ski Fields*. International Glaciological Society, Cambridge.

Serreze, M.C. & Maslanik, J.A. (1997) Arctic precipitation as represented in the NCEP/NCAR reanalysis. *Annals of Glaciology*, **25**, 429–433.

Shokr, M.E. & Barber, D.G. (1994) Temporal evolution of physical and dielectric properties of sea ice and snow during the early melt season: observations from SIMS '90 experiment. *Journal of Glaciology*, **40**, 16–30.

Simmonds, I., Keay, K. & Lim, E.-P. (2003) Synoptic activity in the seas around Antarctica. *Monthly Weather Review*, **131**, 272–288.

Sommerfeld, R.A. (1970) The classification of snow metamorphism. *Journal of Glaciology*, **9**, 3–17.

Stirling, I. & Smith, T.G. (2004) Implications of warm temperatures, and an unusual rain event for the survival of ringed seals on the coast of Southeastern Baffin Island. *Arctic*, **57**, 59–67.

Stroeve, J.C., Markus, T., Maslanik, J.A. et al. (2006) Impact of surface roughness on AMSR-E sea ice products. *IEEE Transactions on Geoscience and Remote Sensing*, **44**, 3103–3117.

Sturm, M. (1991) The role of thermal convection in heat and mass transport in the subarctic snow cover. *USA-CRREL. Report 91-19*.

Sturm, M. (2009) Field techniques for snow observations on sea ice. In: *Sea Ice Handbook*. (Eds. Eicken, H., Gradinger, R., Salganek, M., Shirasawa, K., Perovich, D. & Lepparanta, M.). University of Alaska Fairbanks Press.

Sturm, M. & Benson, C.S. (1997) Vapor transport, grain growth and depth hoar development in the subarctic snow. *Journal of Glaciology*, **43**, 42–59.

Sturm, M., Holmgren, J., König, M. & Morris, K. (1997) The thermal conductivity of seasonal snow. *Journal of Glaciology*, **43**, 26–41.

Sturm, M., Morris, K. & Massom, R. (1998) The winter snow cover of the West Antarctic pack ice: its spatial and temporal variability. In: *Antarctic Sea Ice Physical Processes, Interactions and Variability* (Ed. M.O. Jeffries), pp. 1–18. American Geophysical Union, Washington, DC.

Sturm, M., Holmgren, J. & Perovich, D.K. (2001) Spatial variations in the winter heat flux at SHEBA: estimates from snow–ice interface temperatures. *Annals of Glaciology*, **33**, 213–220.

Sturm, M., Holmgren, J. & Perovich, D.K. (2002a) Winter snow cover on the sea ice of the Arctic Ocean at the surface heat budget of the Arctic Ocean (SHEBA): temporal evolution and spatial variability. *Journal of Geophysical Research*, **107**, 10.1029/2000JC000400.

Sturm, M., Perovich, D.K. & Holmgren, J. (2002b) Thermal conductivity and heat transfer through the snow and ice of the Beaufort Sea. *Journal of Geophysical Research*, **107**, 10.1029/2000JC000409, 8043.

Sturm, M., Maslanik, J.A., Perovich, D.K. et al. (2006) Snow depth and ice thickness measurements from the Beaufort and Chukchi Seas collected during the AMSR-Ice03 Campaign. *IEEE Transactions on Geoscience and Remote Sensing*, **44**, 3009–3020.

Tin, T. & Jeffries, M.O. (2001) Sea ice thickness and roughness in the Ross Sea, Antarctica. *Annals of Glaciology*, **33**, 187–193.

Toyota, T., Takatsuji, S., Tateyama, K., Naoki, K. & Ohshima, K.I. (2007) Properties of sea ice and overlying snow in the Southern Sea of Okhotsk. *Journal of Oceanography*, **63**, 393–411.

Tucker, W.B., Perovich, D.K., Gow, A.J., Weeks, W.F. & Drinkwater, M.R. (1992) Physical properties of sea ice relevant to remote sensing. In: *Microwave Remote Sensing of Sea Ice* (Ed. F.D. Carsey), pp. 9–28. American Geophysical Union, Washington, DC.

Untersteiner, N. (1961) On the mass and heat budget of Arctic sea ice. *Archiv für Geophysiks und Bioklimatologie*, **A12**, 151–182.

Waddington, E.D. & Harder, S.L. (1996), The effects of snow ventilation on chemical concentrations. In: *NATO ASI Series: Chemical Exchange between the Atmosphere and Polar Snow* (Eds. E.W. Wolff & R.C. Bales), pp. 403–451. Springer-Verlag, Berlin.

Wadhams, P., Lange, M. & Ackley, S.F. (1987) The ice thickness distribution across the Atlantic sector of the Antarctic Ocean in mid-winter. *Journal of Geophysical Research*, **92**, 14535–14552.

Wankiewicz, A. (1978) A review of water movement in snow. In: *Modeling of Snow Cover Runoff*, (Eds. S.C. Colbeck & M. Ray), pp. 222–237. U.S. Army CRREL, Hanover, New Hampshire.

Warren, S.G. (1982) Optical properties of snow. *Reviews of Geophysics & Space Physics*, **20**, 67–89.

Warren, S.G. (1984) Optical constants of ice from the ultraviolet to the microwave. *Applied Optics*, **23**, 1206–1225.

Warren, S.G. & Clarke, A.D. (1986) Soot from Arctic haze: radiative effects on the Arctic snowpack. *Glaciological Data*, **18**, 73–77.

Warren, S.G. & Wiscombe, W.J. (1980) A model for the spectral albedo of snow. II: snow containing atmospheric aerosols. *Journal of Atmospheric Science*, **37**, 2734–2745.

Warren, S.G., Brandt, R.E. & O'Rawe Hinton, P. (1998) Effect of surface roughness on bidirectional reflectance of Antarctic snow. *Journal of Geophysical Research*, **103**, 25789–25807.

Warren, S.G., Rigor, I.G., Untersteiner, N. et al. (1999) Snow depth on Arctic sea ice. *Journal of Climate*, **12**, 1814–1829.

Warren, S.G., Brandt, R.E. & Grenfell, T.C. (2006) Visible and near-ultraviolet absorption spectrum of ice from transmission of solar radiation into snow. *Applied Optics*, **45**, 5320–5334.

Webster, D.H. & Zibell, W. (1970) *Iñupiat Eskimo Dictionary*. Summer Institute of Linguistics, Fairbanks, Alaska.

Weller, G.E. (1968) The heat budget and heat transfer processes in Antarctic plateau ice and sea ice. *ANARE Publication 102*, 155 pp. Australian Antarctic Division, Melbourne, Australia.

Wiscombe, W.J. & Warren, S.G. (1980) A model for the spectral albedo of snow. I. Pure snow. *Journal Atmospheric Sciences*, **37**, 2712–2733.

Worby, A.P. & Massom, R.A. (1995) The structure and properties of sea ice and snow cover in East Antarctic pack ice. *Antarctic CRC Research Report 7*. Antarctic CRC, Hobart, Australia.

Worby, A.P., Massom, R.A., Allison, I., Lytle, V.I. & Heil, P. (1998) East Antarctic sea ice: a review of its structure, properties and drift. In: *Antarctic Sea Ice Physical Processes, Interactions and Variability* (Ed. M.O. Jeffries), pp. 41–68, American Geophysical Union, Washington, DC.

Worby, A.P., Markus, T., Steer, A.D., Lytle, V.I. & Massom, R.A. (2008) Evaluation of AMSR-E snow depth product over East Antarctic sea ice using in situ measurements and aerial photography. *Journal of Geophysical Research*, **113**, C05S94, 10.1029/2007JC004181.

Zhou, X., Li, S. & Stamnes, K. (2003) Effects of vertical inhomogeneity on snow spectral albedo and its implication for optical remote sensing of snow. *Journal of Geophysical Research*, **108**, 4738, 10.1029/2003JD003859.

6 Variability and Trends of the Global Sea Ice Cover

Josefino C. Comiso

6.1 Introduction

At high latitudes, the global oceans are covered by vast blankets of sea ice, the extent of which range any one time between 16.6×10^6 and 27.5×10^6 km². This corresponds to a significant fraction (3–6%) of the total surface area of the earth. In the Arctic region, the ice cover doubles its size from summer to winter, while in the Antarctic the corresponding value is fivefold (Zwally et al., 1983; Parkinson et al., 1987; Gloersen et al., 1992). The sea ice cover is thus one of the most expansive and most seasonal geophysical parameters on the earth's surface, second only to the more variable and less predictable snow cover. The presence or absence of sea ice affects the atmosphere and the ocean, and therefore the climate, in many ways. For example, as an insulating material, it limits the flow of heat between the ocean and atmosphere. Also, on account of its high albedo, a high fraction of solar radiation is kept from being directly absorbed by the surface and is instead reflected back to the atmosphere. It is because of such ice–albedo feedback effect between surface and atmosphere that climate change signals are expected to be amplified in polar regions (Budyko, 1966). Modelling studies have in fact indicated that the amplification can be as high as 3–5 times that of global signals (Holland & Bitz, 2003) in the Arctic region.

The direct impact of the sea ice cover on the ocean is well known and equally significant. For example, the process of growth and decay of sea ice causes vertical and/or horizontal redistribution of salt in the ocean. During ice formation, brine rejection causes enhanced salinity of the underlying ocean and this process can initiate vertical convection and/or the formation of bottom water. Conversely, during ice retreat, low-salinity meltwater is introduced and causes the upper layer of the ocean to be stratified and vertically stable. The latter is conducive for phytoplankton growth and thereby increases the productivity of the region (Sullivan et al., 1993; Smith & Comiso, 2008). Large sensible-heat polynyas and other sea ice features within the ice pack, such as the Odden ice tongue, have been discovered and associated with deep ocean convection (Gordon & Comiso, 1988; Comiso & Gordon, 1998; Gordon et al., 2007). Latent-heat polynyas, which are usually near coastal regions and caused primarily by strong katabatic winds, have also been observed as the key source of the high-salinity bottom water that is involved in global thermohaline circulation (Zwally et al., 1985; Comiso & Gordon, 1998; Markus et al., 1998; Massom et al., 1999).

The large-scale variability in the sea ice cover has been studied previously using satellite passive-microwave data (Bjørgo et al., 1997; Stammerjohn & Smith, 1997; Parkinson et al.,

1999; Zwally et al., 2002). In-depth analysis of the state of the sea ice cover is important, especially in light of recent reports of the declining ice extent in the Arctic (Johannessen et al., 1999; Cavalieri et al., 1997) and in parts of the Antarctic (Jacobs & Comiso, 1997; Kwok & Comiso, 2002a). But the most intriguing change that has been observed from satellite data is the rapid decline in the perennial ice cover (Comiso, 2002). Even more remarkable is the observed dramatic decline in the perennial ice in 2007 (Comiso et al., 2008) followed by a similarly low value in 2008 as will be reported in this chapter. The perennial ice in 2007 was observed to be not only a record low, but also was 27% lower than the previous lowest value in 2005 and 38% lower than climatological average (Comiso et al., 2008). Meanwhile, large changes in the thickness distribution of the Arctic sea ice cover during the last few decades have been reported using submarine sonar data (Rothrock et al., 1999; Wadhams & Davis, 2000). Such changes will be discussed in greater detail in another chapter of this book (Chapter 4), but more detailed studies are needed to better understand the climate system in the region.

In this chapter, the large-scale variability of the sea ice cover as described in the previous edition of this book is updated using a newly generated sea ice concentration data as described by Comiso & Nishio (2008). The new data has been enhanced to be compatible and in good agreement with the more accurate but much shorter AMSR-E data set. The merits of this data set and how it differs from others were discussed in detail by Comiso & Steffen (2001) and Comiso & Nishio (2008). In this chapter, I hope to:

(a)   Provide a quantitative assessment of the large-scale characteristics of global sea ice.
(b)   Assess the state of the ice cover and trends with emphasis on recent changes.
(c)   Give insights into the mechanisms of change and evaluate the future of the ice cover.

A key parameter that is relevant and directly associated with the variability of the sea ice cover is surface temperature. Co-registered and concurrent satellite surface temperature data are used to understand the last of these four objectives.

Analysis of an updated data set is important because of large interannual variability and the rapidly changing state of the sea ice cover. There have also been some inconsistencies in previous reports. For example, a report by Kukla and Gavin (1981) of a rapidly declining Antarctic ice cover was associated with greenhouse warming, while a subsequent and more comprehensive study by Zwally et al. (1983) showed inconclusive trends. More recent reports that made use of data with twice the record length used previously have shown positive but relatively modest trends (Cavalieri et al., 1997; Zwally et al., 2002). The discrepancies are mainly due to the different record lengths of data utilized and differences in associated statistical errors. Different results are also usually obtained when different techniques are used to derive geophysical products from the same set of satellite data (Comiso et al., 1997; Stammerjohn & Smith, 1997; Comiso & Steffen, 2001; Parkinson & Comiso, 2008), but differences are relatively minor and the general conclusions are usually the same as long as data from the same time period are utilized in the analysis.

6.2 Satellite observations

Detailed studies of the global sea ice cover have been made possible by the advent of satellite data that provide comprehensive areal coverage at a relatively high temporal resolution. The

use of satellite data for sea ice studies has been discussed in numerous publications (Shuchman & Onstott, 1990; Carsey, 1992; Lubin & Massom, 2008). The satellite sensors used for sea ice studies can be divided into visible, infrared and microwave sensors. The visible sensors detect radiations at wavelengths ranging approximately from 0.5 to 1 μm, while infrared sensors detect radiation from 3 μm to 15 μm. At these wavelengths, both sensors are sensitive to clouds with the infrared sensor providing useful data during both day and night, while the visible sensor provides useful data during daytime only. The persistence of clouds in the polar regions limits the suitability of these two sensors for continuous large-scale variability studies of the sea ice cover. However, they usually have very high spatial resolutions and can be extremely useful for mesoscale studies when taken during cloud-free conditions. The microwave sensors operate at wavelengths from millimetres to metres, and provide day/night almost all weather monitoring of the sea ice cover. In recent years, radar altimeters and laser profilers have also been used to study the freeboard and hence the thickness distribution of the sea ice cover (Laxon et al., 2003; Kwok et al, 2007; Zwally et al., 2008).

Passive- and active-microwave systems have been the more popular techniques for studying the characteristics and variability of the sea ice cover because of ability to monitor the surface continuously, independent of weather and cloud cover conditions. For large-scale variability and trend studies, passive-microwave data have been the primary tool because of a relatively long, comprehensive and consistent historical record. Also, they are usually dual polarized and multifrequency systems that can discriminate the major ice types and minimize retrieval ambiguities. An apparent weakness of passive-microwave data is the coarse spatial resolution (about 25×25 km), which makes such data difficult to use for detecting small spatial features in the ice cover, such as leads, ridges and ice bands. To partly overcome this weakness, the percentage of ice (called ice concentration) within each satellite grid element is calculated using a mixing algorithm, that takes advantage of the high contrast of the emissivity of ice and open water. The time series data started with the Nimbus-5/Electrically Scanning Microwave Radiometer (ESMR) which is a one-channel system (at 19 GHz) that provided useful data from late 1972 to 1976. This was followed by the Nimbus-7/Scanning Multichannel Microwave Radiometer (SMMR) which is a 10-channel system and provided useful data from November 1978 to August 1987. The successor to the SMMR is the series of DMSP/Special Scanning Microwave Imager (SSM/I) sensor that has provided useful data from July 1987 to the present. In addition, the EOS-Aqua/Advanced Microwave Scanning Radiometer (AMSR-E) was launched in May 2002 and has been providing higher resolution data at a wider spectral range than the SSM/I system. The true spatial distribution of the sea ice cover was revealed for the first time by ESMR which provided the data set used in the first assessment of the seasonal and interannual variability of the global sea ice cover (Zwally et al., 1983; Parkinson et al., 1987). Because of many gaps in the data stream and larger error because the sensor had only one channel, the ESMR data set has usually not been used for time series studies. What has been used are data from SMMR (November 1978–July 1987), SSM/I (August 1987 to the present) and AMSR-E (June 2002 to the present). The compatibility of these data sets has been analysed using data during overlap periods and for optimum consistency, the entire data set has been updated and enhanced using AMSR-E data as the baseline as reported by Comiso & Nishio (2008).

Maps of the two hemispheres at high latitudes showing some of the areas of interest and the vast difference in the distribution of land and oceans are presented in Fig. 6.1a,b. Each of these maps also shows difference maps of monthly climatologies in February and September
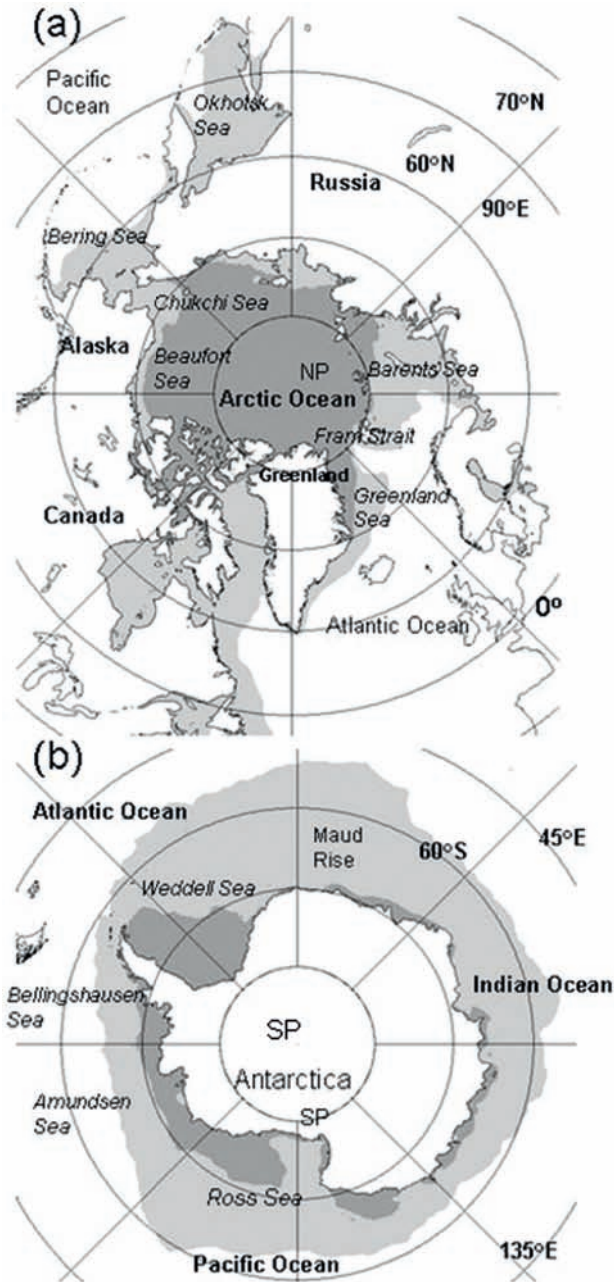
Fig. 6.1 Location maps for (a) northern hemisphere and (b) southern hemisphere. Average locations of the sea ice cover during maximum and minimum extents are shown in light grey and dark grey respectively.

to illustrate the extent and locations of the sea ice cover during summer and winter. In both images, the seasonal ice cover is shown in light grey while the perennial ice is shown as darker grey. The perennial ice regions are shown to be much more extensive in the northern than in the southern hemisphere while the seasonal ice cover is substantially more extensive
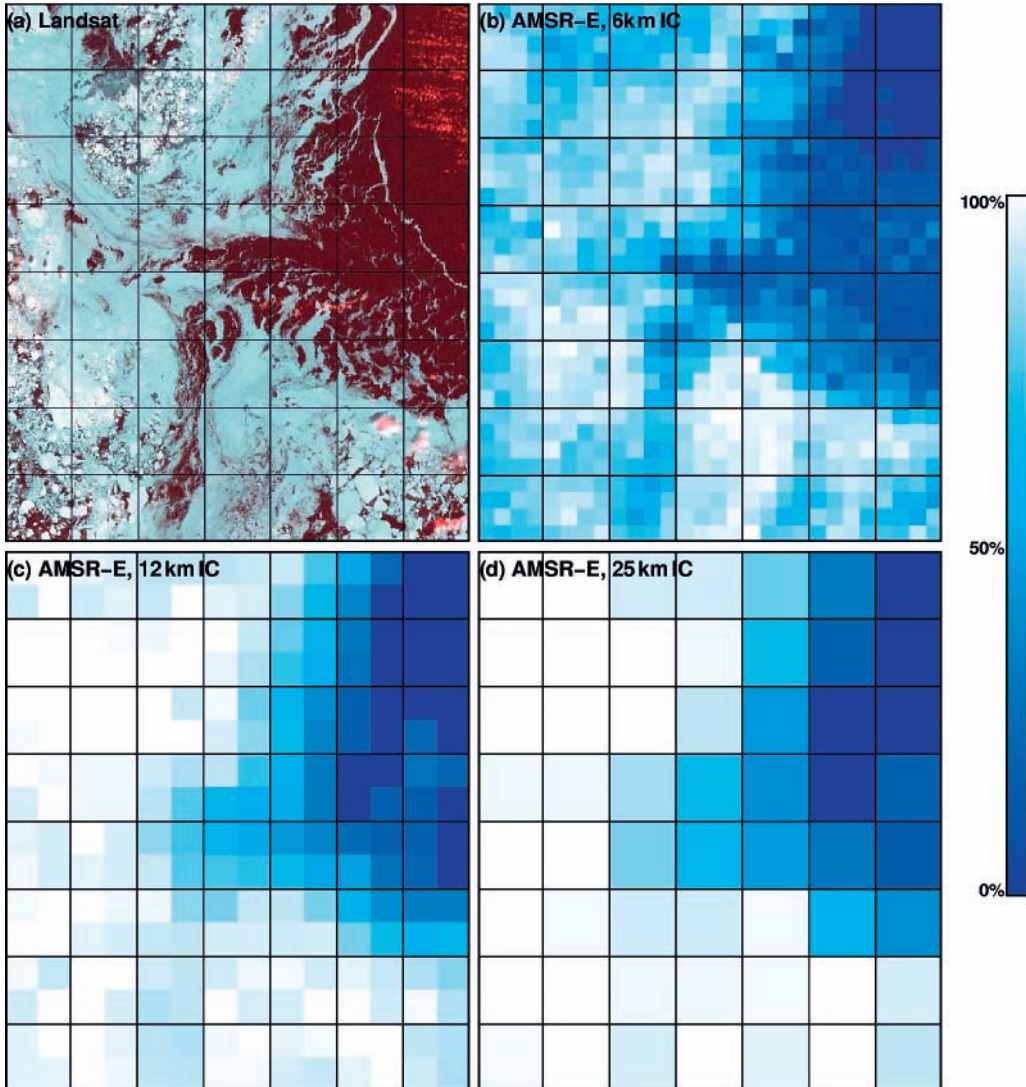
Fig. 6.2 Sea ice cover in the Okhotsk Sea from (a) Landsat-7 0.6 μm data and ice concentrations derived from AMSR-E at (b) 6.25 km resolution using the 89 GHz channels; (c) 12.5 km resolution using the standard algorithm and (d) 25 km resolution using the standard algorithm.

in the southern than in the northern hemisphere. The sea ice cover also goes further towards lower latitudes in the northern hemisphere than in the southern hemisphere.

When the weather and conditions are right, high-resolution visible data provide good, and spatially detailed, characterization of the ice cover. A good example of the kind of information available from such data for sea ice process studies is provided by the image in Fig. 6.2a, as recorded by the Landsat-7/Thematic Mapper. The image was taken on 11 March 2003 at the Sea of Okhotsk, and depicts some features of the ice cover that is difficult to capture with the coarser resolution data. During this time period of ice growth, small platelets and needles, called frazil ice, are usually formed in supercooled water, and through wave action

and wind, the ice particles accumulate at the surface to form grease ice, shuga and small pancakes (Ackley, 1996; Chapter 2). The spatial pattern of the ice cover shows a highly dynamic region with the apparent thermodynamic ice growth modified by wind, waves and tides, resulting in the complex distribution of all forms of new ice. The image in Fig. 6.2b represents ice concentration distributions at the same location and approximately the same time as observed by the EOS-Aqua/AMSR-E which operates at six different wavelengths and resolutions ranging from about 6 km for the 89 GHz sensor to 50 km for the 6.8 GHz sensor. Figure 6.2b shows data derived from the dual-polarized 89 GHz sensor only and provide the optimal resolution afforded by the sensor. It is apparent that many of the interesting features depicted by the Landsat image are captured by the AMSR-E sensor. What is not captured are the fine structures in the distribution such as the ice bands along the ice edges and the ice floe size distribution. But overall, the spatial distribution of sea ice including the areas of divergence, as observed by the Landsat image, is basically reproduced in the 89 GHz, 6.25 km image. The standard algorithm used for deriving ice concentration makes use of the 37 GHz and 18.7 GHz channels of AMSR-E as discussed by Comiso and Nishio (2008). The ice concentrations are derived at resolutions of 12.5 and 25 km, as depicted in Fig. 6.2c,d, one to match the resolution of the 37 GHz radiometer and the other to match that of the 18.7 GHz radiometer. In these two images, many of the spatial features provided by the Landsat image are basically gone and the ice cover is depicted in terms of different percentages of ice concentration. It should be noted, however, that for the parameter of interest in large-scale sea ice studies (i.e. ice concentration), the results of regression analysis indicate that the ice concentrations from AMSR-E 6.25 km, 12.5 km and 25 km data agree well with the Landsat-7 data with correlation coefficients of greater than 0.9 and RMS error of about 10%.

The physical characteristics of the sea ice cover from micro- to macroscales have been discussed extensively in the literature (Weeks & Ackley, 1986; Tucker et al., 1992; Ackley, 1996; Chapter 2). The radiation emitted by the surface and detected by the satellite sensor is closely linked to the physical characteristics of the surface through an electrical property called emissivity. Together with surface temperature, the surface emissivity determines the brightness temperature that is observed by satellite sensors and converted to sea ice concentration. To illustrate how the global sea ice cover is revealed by high-resolution microwave (6.25 km) data, ice concentration maps for the northern hemisphere during minimum and maximum ice cover extents in 2008 and the southern hemisphere during minimum extent in 2008 and maximum extent in 2007 are presented in Fig. 6.3. The set of images depicts some of the mesoscale characteristics of the ice cover that are usually not captured by standard ice concentration data because of the lack of adequate spatial resolution. The images are able to depict some of the spatial details within the ice pack including the presence of big leads and vast ice floes and some of the uniques features of the marginal ice zones. Also, the highly dynamic nature of the ice cover becomes more apparent as areas of divergence and convergence compared to previous images derived from passive-microwave data (e.g. Gloersen et al., 1992); such images clearly provide more information. However, interpretation of such images requires some care because of aforementioned high sensitivity of the 89 GHz radiation to atmospheric and snow cover effects. Although the images in Fig. 6.3 represent derived ice concentration maps, the values are sometimes erroneous because of the variability of the effective emissivity of sea ice at 89 GHz. When the conditions are right (e.g. cloud-free as in Fig. 6.2), the data provides valuable information, but even in other conditions, ability to detect leads, polynyas and large ice floes can be very useful even if the retrieved ice concentration value is biased.
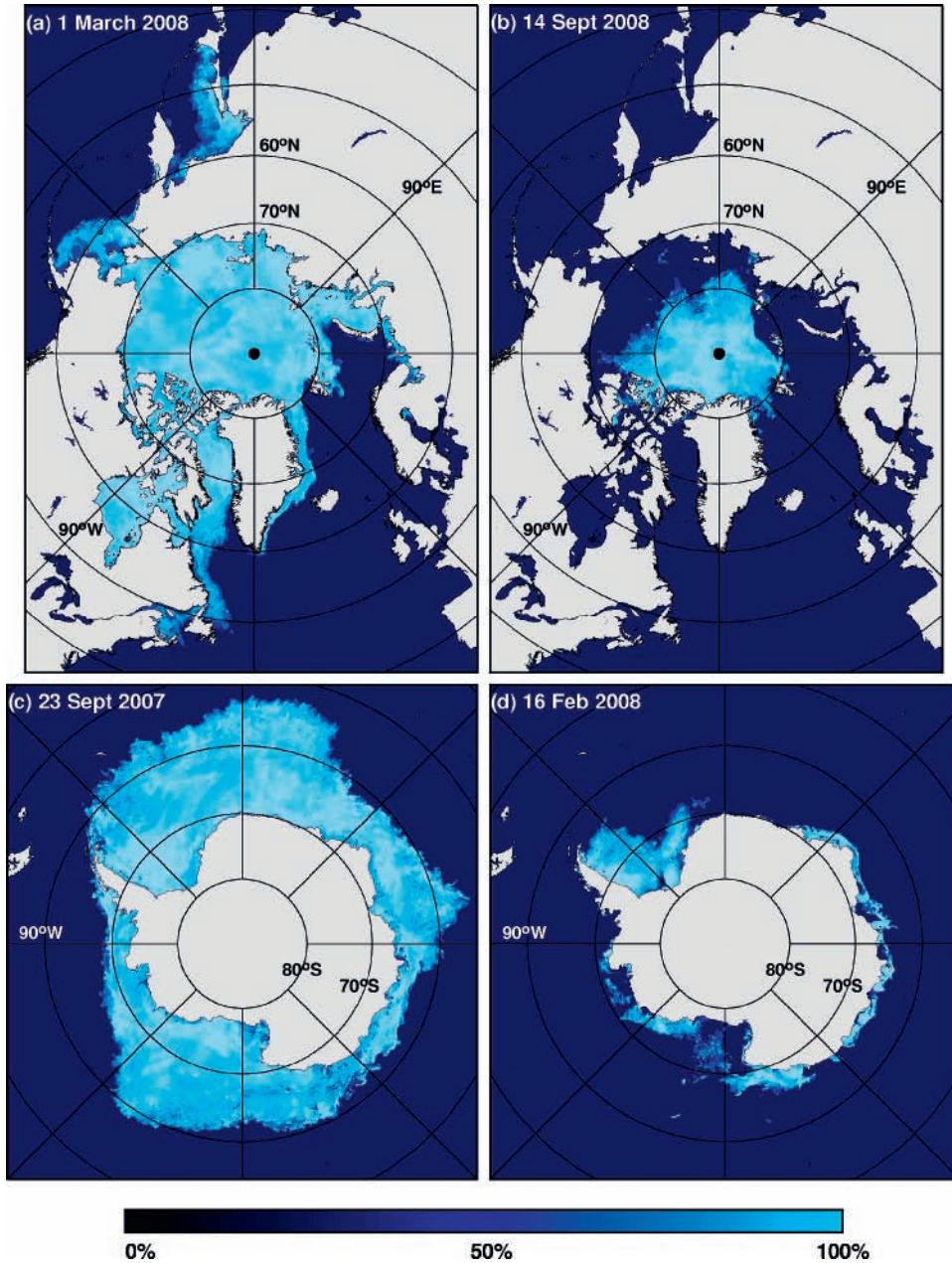
Fig. 6.3 Sea ice concentration maps as derived from the 89 GHz AMSR-E data at 6.5 km resolution during (a) maximum ice extent and (b) minimum ice extent in the northern hemisphere in 2008 and during (c) maximum ice extent and (d) minimum ice extent in the southern hemisphere in 2007 and 2008, respectively.

It is apparent that geographical considerations play an important role in the distribution of sea ice. In the northern hemisphere, the Arctic Ocean is surrounded by land that limits the advance of sea ice to lower latitudes. During maximum extent in winter, the ice cover is shown to be fragmented with the largest fraction in the Arctic Basin and the rest in the Canadian

Archipelago, the peripheral seas and bays. In this hemisphere, the sea ice cover is observed as far south as 44°N in the Okhotsk Sea and as far south as 46°N in the Labrador Sea (Fig. 6.3a). In the summer, the ice cover is basically confined mainly to the Arctic Basin (Fig. 6.3b). On the other hand, the Antarctic continent serves as the limit of sea ice to the south with the highest latitude being about 78°S in the southern hemisphere but no apparent limit at lower latitudes. The sea ice cover is shown as a contiguous ring surrounding Antarctica in winter (Fig. 6.3c) and covering a significant part of the Indian, Pacific and Atlantic oceans. During minimum extent at the end of the summer (Fig. 6.3d), the ice cover is fragmented and located mainly in the western Weddell Sea, the Bellingshausen Sea, the Amundsen Sea and parts of the Ross Sea. The mesoscale features are also more complex in the southern hemisphere indicating a more active and dynamic sea ice cover than in the northern hemisphere.

The spatial changes in ice concentration reflect primarily changes in the fraction of open water and the physical properties of the ice cover. During the growth period in autumn, large areas covered by new ice have intermediate values in the visible channel (see Fig. 6.2a) because of the relatively low reflectivity of new ice (Allison, 1981; Massom, 1991; Chapter 5). The same surfaces also have low brightness temperatures and hence relatively low concentration because of lower microwave emissivity for new ice than the thicker ice types (Grenfell et al., 1994). Conversely, during the onset of melt, the emissivity of the surface becomes very high as the snow starts to melt (Eppler et al., 1992) and in some areas the passive microwave provides higher concentration than actual observations. It is important to note that with conventional algorithms, intermediate values of ice concentration in the microwave data do not strictly represent the fraction of ice cover within the data element but could reflect the presence of newly formed ice (as in leads and polynyas), especially in autumn and winter. Since open water in leads and polynyas is covered by ice of some form within hours of formation in autumn and winter, this is also a more useful way of quantifying the ice cover compared to an ice–no ice discrimination schemes that would show near-100% ice cover in practically all regions during growth stages (Comiso & Steffen, 2001). But while the 12.5 and 25 km data provides consistent information about the ice cover, there are times when the values disagree with those provided by the 6.25 km data. For example, in the images shown in Fig. 6.3, there are features in the middle of the ice pack that indicate relatively low concentration ice but are not observed as such in the standard ice concentration data. Comparative analyses done with simultaneously observed visible channel data from MODIS onboard the same satellite for such cases have indicated better agreement between MODIS and the 12.5 km data than between MODIS and the 6.25 km data.

For studies that require high spatial resolution irrespective of weather and time, Synthetic Aperture Radar (SAR) data which has a resolution of about 35 m can be very useful. Ice floes and ridges are recognizable within the ice pack at this resolution, but in some areas, especially near the ice edge, the interpretation of the data is difficult and sometimes ambiguous. With the use of time series of images, some of these ambiguities can be resolved, but such type of data is not always available. The SAR data has been useful for deriving other parameters such as the drift of sea ice and the thickness of seasonal ice (Kwok et al., 1998). A problem in terms of the use of the SAR data for global studies is the paucity of data and the lack of sufficient spatial and temporal coverage.

The other active microwave systems available that provide less resolution but more comprehensive coverage are the scatterometers such as the QuickSCAT (Drinkwater & Lytle, 1997; Nghiem et al., 2007), and the radar altimeter (Fetterer et al., 1992; Laxon et al., 2003).

The data coverage and resolution are similar to those from passive microwave but more research is needed to accurately interpret the data, and algorithms have to be developed to retrieve geophysical parameters.

6.3 Spatial and temporal variations of the sea ice cover

The growth and decay of sea ice is primarily a response of the ocean surface to changes in atmospheric and environmental conditions from one season to another. For the two hemispheres, the growth periods are expected to be out of phase by 6 months to correspond to the well-defined period between summer and winter. Two parameters have been used when using satellite data to quantify the sea ice cover. One is sea ice extent, which is defined as the integrated sum of the areas of all data elements with at least 15% ice cover, and the other is ice area, which is the sum of the actual ice areas (i.e. ice concentration multiplied by the area of the data element). To illustrate how the sea ice cover typically changes in extent during an annual cycle, monthly climatologies were generated from 30 years of historical passive-microwave data and the results are presented in Fig. 6.4. The highest and lowest monthly values during the satellite period are indicated by the upper and lower lines, respectively. It is clear that the seasonal distributions of the ice cover in the two hemispheres are considerably different. In the northern hemisphere, the ice cover distribution is approximately symmetrical in that the growth period takes almost as long as the decay period. In the southern hemisphere, however, the growth season takes about 7 months while the decay period takes only 5 months. The difference can be partly attributed to the large contrast in the geographical and environmental conditions in the two hemispheres as discussed earlier. In particular, the retreat of sea ice in the Antarctic is accelerated by direct intrusions of warm water from lower latitudes and ice break-ups cause by the penetration of large ocean waves. In the Arctic, the presence of surrounding land boundaries minimizes such effects. On the other hand, the presence of land at the lower latitudes that cools fast during autumn and winter leads to a cold environment during this time period and causes the ice extent to reach its maximum value at a relatively faster rate and to form farther to the south. Meanwhile, the relatively warm ocean that surrounds the ice cover in the Antarctic acts to moderate the growth of sea ice while the presence of the cold Antarctic continent may partly influence the lengthening of the growth season in the region.

In the northern hemisphere, the mean monthly extents, represented by data points along the middle line in Fig. 6.4a, are shown to vary on the average from a minimum of 6.8×10^6 km^2 during the beginning of the freeze-up period (September) to about 15.2 km^2 during the beginning of the melt period (March). The corresponding values in the southern hemisphere (Fig. 6.4b, solid line) are 3.0×10^6 km^2 (in February) and 18.3×10^6 km^2 (in September), respectively. Note that although the minimum values for sea ice in the northern hemisphere are greater than that in the southern hemisphere, the effective polar albedo in the latter is much greater than that of the former because of the presence of the snow-covered Antarctic continent which has a total area of about 14×10^6 km^2. Except for glaciers and Greenland, much of the snow-covered areas over land in the northern hemisphere are gone by summer. Thus, interannual changes in the sea ice cover during summer, when the solar insolation is high, are more critical in terms of ice–albedo feedback effects in the northern hemisphere than in the southern hemisphere.
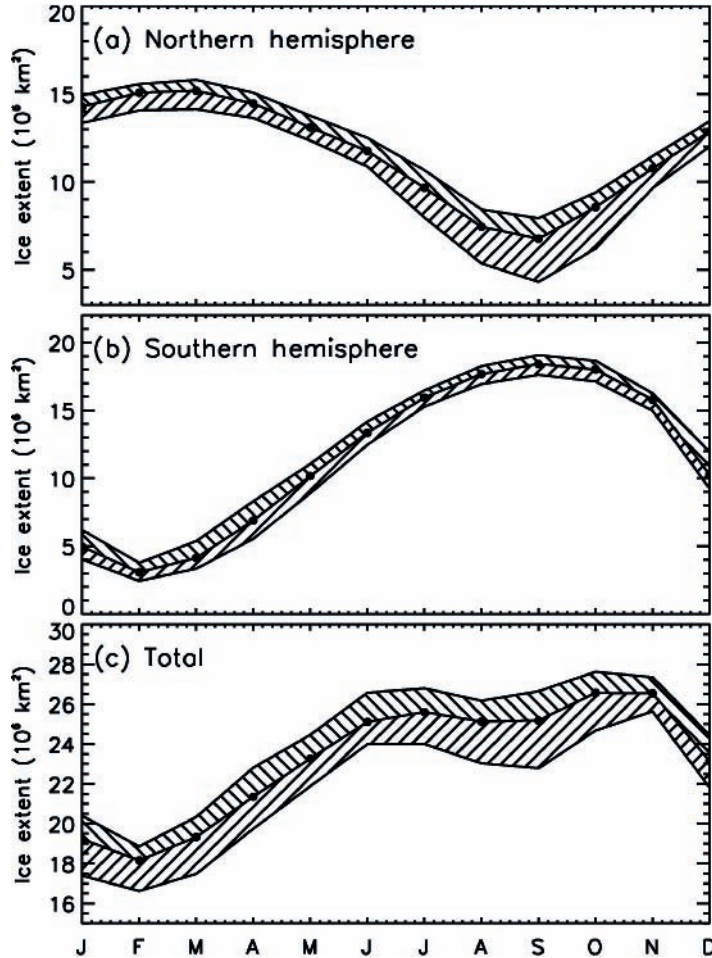
Fig. 6.4 Climatological seasonal variations derived from the monthly means from 1979 through 2007 in (a) the northern hemisphere, (b) the southern hemisphere and (c) combined northern and southern hemisphere. The data points in closed circles in the middle line represent the climatological means, while the top and bottom lines represent the highest and lowest monthly values for each month during the 30-year period.

It is apparent that the high and low monthly values represented by the upper and lower lines, respectively, do not differ from the average values (middle line) by the same amount. The deviations are largest during the summer and early autumn in the northern hemisphere when the difference of low and average values is more than two times larger than the difference of the high and average values. Such discrepancies are true for all months in the northern hemisphere except in April, May and June when the deviations are practically equal. This phenomenon is consistent with a declining ice cover in the Arctic region. In the southern hemisphere, the deviations of the high values from the average are more similar to the deviation of low values from the average. However, there are a few months like December and January when the deviations of high values from the average are larger than the deviations of low values from the average. This reflects the general trend towards a slightly higher extent in the ice cover in the Antarctic.

For completeness, the climatological monthly global sea ice cover, which is basically the sum of data in Fig. 6.4a,b, is presented in Fig. 6.4c. The plot shows that at any one time, the extent of the average total ice cover ranges from about 18.1×10^6 to 26.6×10^6 km^2. The upper and lower curves represent basically the upper and lower limits of the total monthly ice extent and can be as low as 16.6×10^6 km^2 and as high as 27.5×10^6 km^2. The low values occur in February during austral summer in the Antarctic and winter in the Arctic, while the high values occur in November which is spring in the Antarctic and autumn in the Arctic. The date for the high values occurs later in the year in part because of the effect of the seasonal asymmetry in growth and decay of the Antarctic ice cover. The seasonality of the total sea ice cover is in part associated with the higher extents in the Antarctic region compared to those in the Arctic region in the winter and vice versa in the summer. It is interesting to note that despite large hemispherical differences in ice cover distributions, the total area is almost constant from June through November.

The observed growth and decay patterns of the sea ice cover do not normally match expected variations during the different seasons. To illustrate seasonal patterns and how they change with time, average extents of the sea ice cover during the different seasons for each year from 1979 to 2008 are presented in Fig. 6.5. The months associated with each season are as follows: (a) December, January and February for winter; (b) March, April and May for spring; (c) June, July and August for summer and (d) September, October and November for autumn. It is interesting that the plots in Fig. 6.5 show basically only two ice seasons: a high ice extent season in winter and spring and a low extent season in summer and autumn. However, such classification is not so meaningful since winter and spring cannot be combined together since one is an ice growth season while the other is a melt season; similarly for summer and autumn. In the northern hemisphere, only small interannual changes are apparent during winter (closed circles) and spring (squares), especially during the 1990–2008 period, but during summer (diamonds) and autumn (triangles), significant interannual changes are evident (Fig. 6.5a). It is interesting to note that the season with the lowest value is autumn and not summer. The summer averages are shown to be consistently higher than those of autumn because the latter includes September which is the month of minimum extent and the growth process in October and November is usually slow. The extents in autumn are on the average about 2×10^6 km^2 lower than those of summer while the extents are almost identical during winter and spring. In the northern hemisphere, the average extent in spring is usually slightly higher than that of winter because the date of maximum extent normally occurs in March and the decay of sea ice is not so rapid in April and May. On the other hand, the extent of the ice cover in December is low compared to those of the other months in winter and spring.

In the southern hemisphere, the seasons are similarly represented but there is a phase difference of 6 months. It is apparent that in this hemisphere, the average extent in spring is generally higher than those of winter by an average of about 2×10^6 km^2. The main reason is the slow seasonal growth of ice with the highest extent occurring in September. It is also apparent that unlike the other hemisphere, the average extents in austral autumn are higher than those of the austral summer with the difference averaging by about 1×10^6 km^2.

The sea ice extents in spring are normally higher than those of winter in part because of the time lag between the occurrence of freeze-up temperature and the production of sea ice. While the seasons are determined by temperature change associated with the orbital parameters of the earth in relation to the sun (i.e. spring is defined to coincide with the occurrence
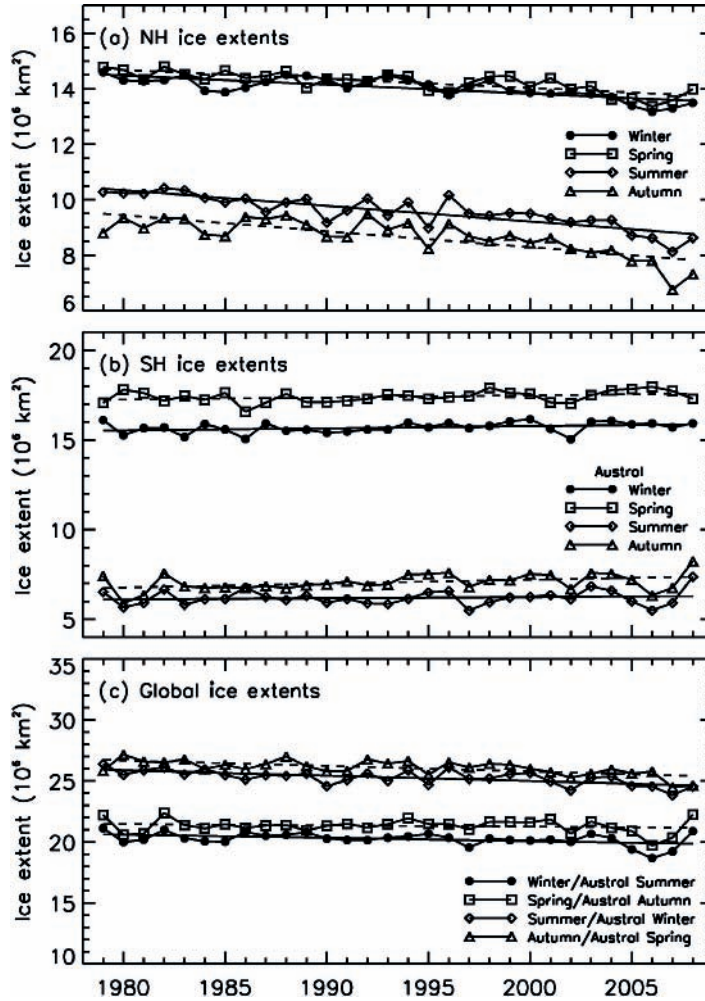
Fig. 6.5 Ice extent averages during the winter, spring, summer and autumn in (a) the northern hemisphere, (b) the southern hemisphere and (c) the two hemispheres. Dashed and solid lines show trends in extent from 1979 to 2008 for each season (see Tables 6.1 and 6.2).

the equinox on March 20 and the winter with the occurrence of the solstice on December 21), it takes some time for the upper layer of the ocean to get cold enough to enable the formation of sea ice. Also, sea ice continues to form long after the surface temperature reaches minimum values, and this period extends beyond the period formally defined as winter. The relative values for the different seasons are different for the two hemispheres mainly because of differences in growth and decay patterns. The global extents during each season shown in Fig. 6.5c indicate very similar values in winter and spring and also between summer and autumn. Because of the larger seasonality of the sea ice cover in the southern hemisphere than that of the northern hemisphere, the season with the highest values is consistently the austral spring while the season with the lowest values is the austral summer.
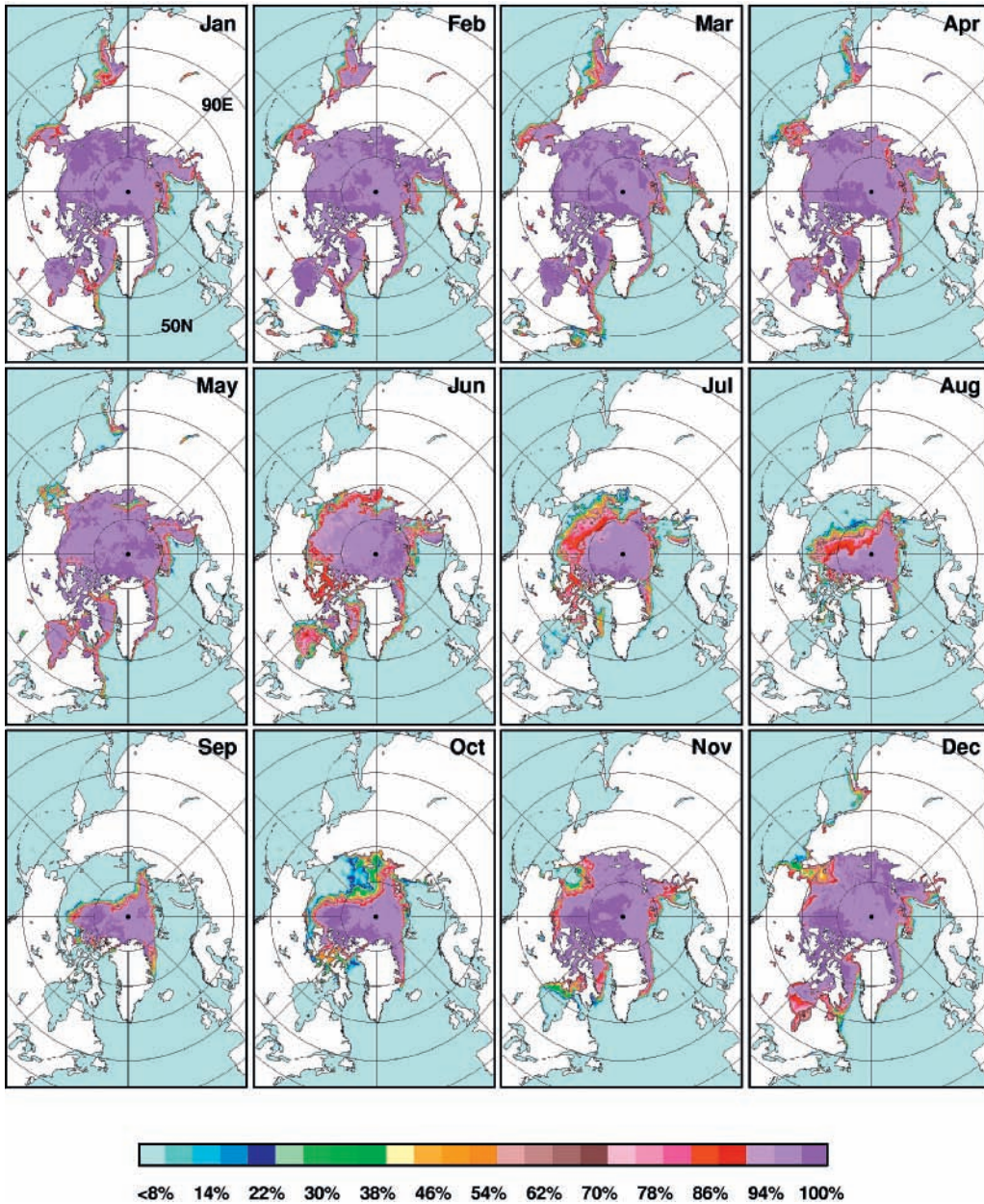
Fig. 6.6   Colour-coded ice concentration monthly averages in the northern hemisphere from January to December 2007 as derived from the 12.5 km AMSR-E standard ice data.

Ice Cover in the Arctic region

To illustrate how the sea ice cover changes spatially with season on a month-to-month basis, colour-coded monthly maps of sea ice concentrations in 2007 are presented in Fig. 6.6. We use the 12.5 km data set to provide better spatial details (than standard historical data) and

data for 2007 to show how the sea ice cover looks like in recent years. The set of images depicts the distribution of the sea ice cover in the northern hemisphere during different stages of formation. In January, February and March, the sea ice cover is shown to go as far south as 44ºN in the Pacific Ocean region (Okhotsk Sea) and 45ºN in the Atlantic Ocean (Labrador Sea). It also covers other seas and bays in the Pacific and Atlantic oceans including the Hudson Bay, the Gulf of Bothnia (near Finland) and northern Japan Sea. In the spring, sea ice retreats to the north and in July and August, the wide band of low concentration ice in the western region reflects a relatively fast moving ice ice during the period. Although the concentration may be high in the inner pack, the monthly averaging usually produces relatively low concentration values when ice advances or retreats rapidly and low or zero concentration values are averaged with high concentration values for some data elements during the month. By the end of summer in September, there is sea ice only in the Arctic Basin, Greenland Sea and a small part of the Canadian Archipelago. In October, a large area of low concentration ice in the western region is also apparent, indicating a rapidly advancing sea ice cover. By December, the Arctic Basin is basically completely covered by sea ice. The extent of the sea ice cover on 14 September 2007 was the lowest observed during the satellite era and during this time, the Canadian Archipelago was basically ice-free and open for navigation.

The basic data set used for studying the seasonal and the interannual variability in the ice cover has been the historical data set that combines SMMR and SSM/I data and covers the period from November 1978 to the present. This sea ice data set has been enhanced to be compatible with AMSR-E data set as described in Comiso and Nishio (2008). The historical data are initially generated as daily averages of ice concentrations mapped onto a polar stereographic grid with a 25 × 25 km resolution. The data therefore provide good temporal resolution and at the same time consistent information from 1979 to the present. Monthly averages of ice extent and ice area from 1979 to 2008 are presented in Fig. 6.7a,b, with data from SMMR, SSM/I and AMSR-E plotted in different colours. Although AMSR-E data provide the most accurate estimates, they are not used in the analysis of the time series because they cause a small negative bias (see overlap period from 2002 to 2008) in the estimates of ice extent and to a lesser degree, ice area. Such bias has been attributed to the higher resolution of AMSR-E compared to those of SMMR and SSM/I and has also been identified by Worby and Comiso (2004). The distributions for both ice extent and actual ice area are coherent and show similar patterns. The peak values are also shown to have much less interannual variability than the minimum values, especially in the 1990s. Relatively low values in the minimum ice extent (Fig. 6.7a) are apparent in 1995, 2002, 2005 and 2007 while relatively high values are shown for 1992, 1994, 1996 and 2001. In the ice area plot (Fig. 6.7b), the minimum values during these years appear even relatively lower. This is partly because of relatively lower average concentrations which in turn may be due to more divergence during these later years. The latter is consistent with more storms that may be associated with a declining surface level pressure as reported by Walsh et al. (1996).

The colour-coded anomaly maps for February, presented in Fig. 6.8, provide the means to assess large-scale and regional changes in the ice cover from one year to another during a winter month. Positive anomalies are shown in the colour-coded maps as greys, greens or blues while negative anomalies are in oranges, purples and reds. The yearly climatology used for deriving the yearly anomalies is the same data used in Fig. 6.4. It is apparent that the February anomalies are generally close to zero in the Arctic Basin as expected since this
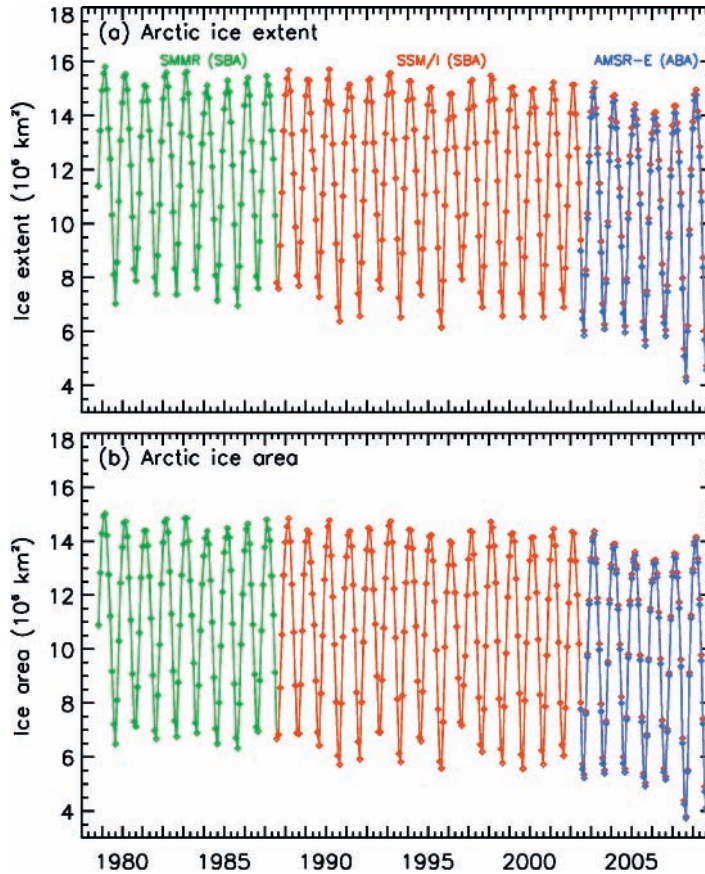
Fig. 6.7 Monthly averages of (a) ice extent and (b) actual ice area in the northern hemisphere for each month from November 1978 through September 2008. Data from SMMR, SSM/I and AMSR-E are plotted separately in green, red and blue, respectively. Updated from Comiso and Nishio (2008).

region is covered by consolidated ice every year. Among the regions where large interannual changes are evident are the Okhotsk Sea and the Bering Sea in the Pacific Ocean region and the Barents Sea, Greenland Sea and Baffin Bay in the Atlantic Ocean region. Some teleconnections between these two seas have been observed (Cavalieri & Parkinson, 1987) with negative anomalies in one sea occurring concurrently with positive anomalies in the other. A negative anomaly at the Sea of Okhotsk and a positive anomaly at the Bering Sea are shown to occur concurrently in 1979, 1982, 1985 and 2001. A positive anomaly at the Sea of Okhotsk and a negative anomaly at the Bering Sea were also concurrent in 1984, 1991 and 1997. The anomalies were mainly negative in both regions in 1980, 1983, 1990 and 2002 and were mainly positive in both regions in 1996, 2005 and to a lesser degree in 2006 and 2007. During other years, almost equal mixtures of positive and negative anomalies are apparent in both seas. These results show that the teleconnection between the two seas is not strong. Similar analysis has been applied in the other seas such as between Barents Sea and Greenland Sea and between Barents Sea and Bering Sea. Again, no orderly or periodic patterns are apparent. What is most remarkable is the occurrence of dominantly negative
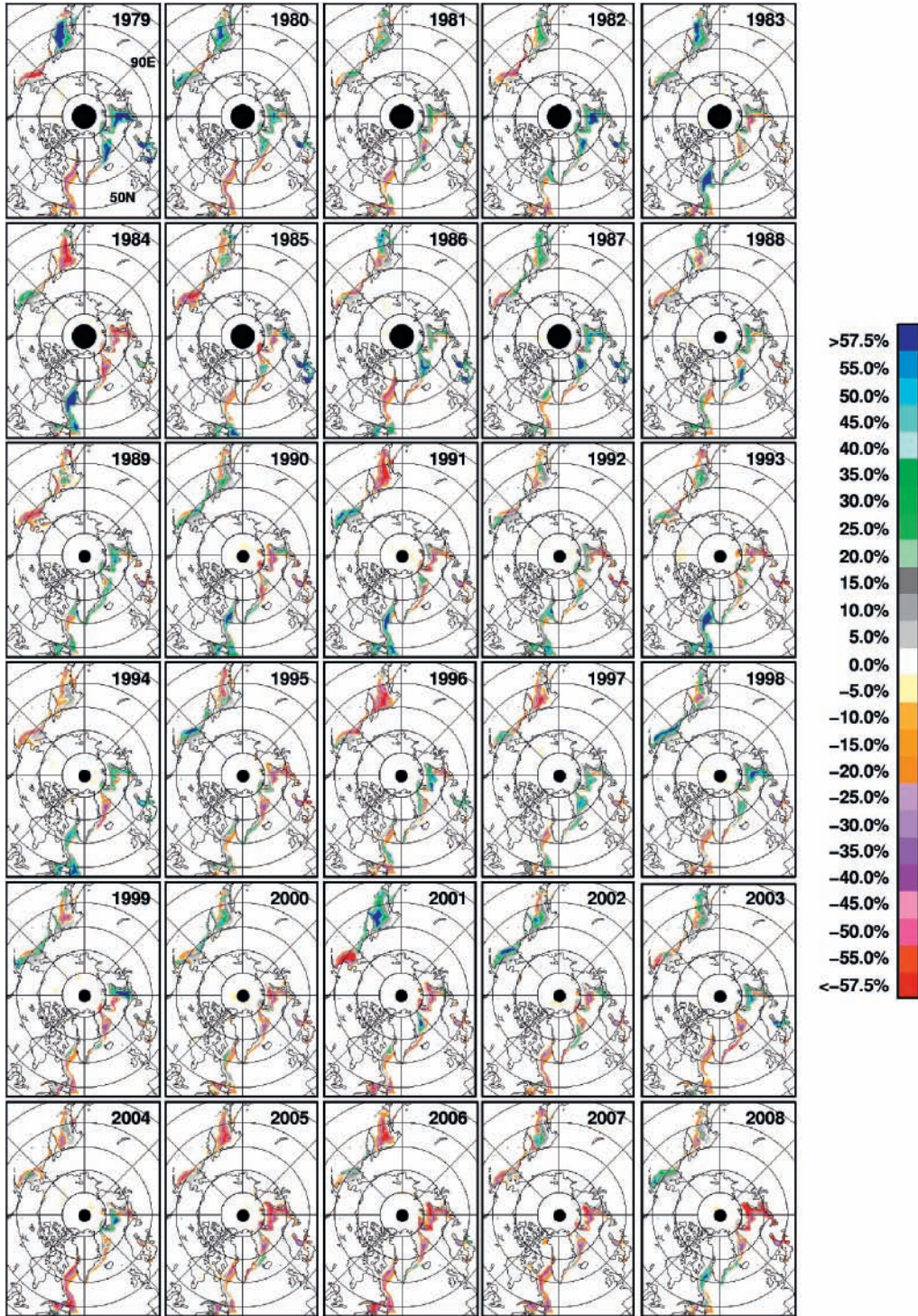
Fig. 6.8 Colour-coded ice concentration monthly anomaly maps for each February from 1979 to 2008 in the northern hemisphere.
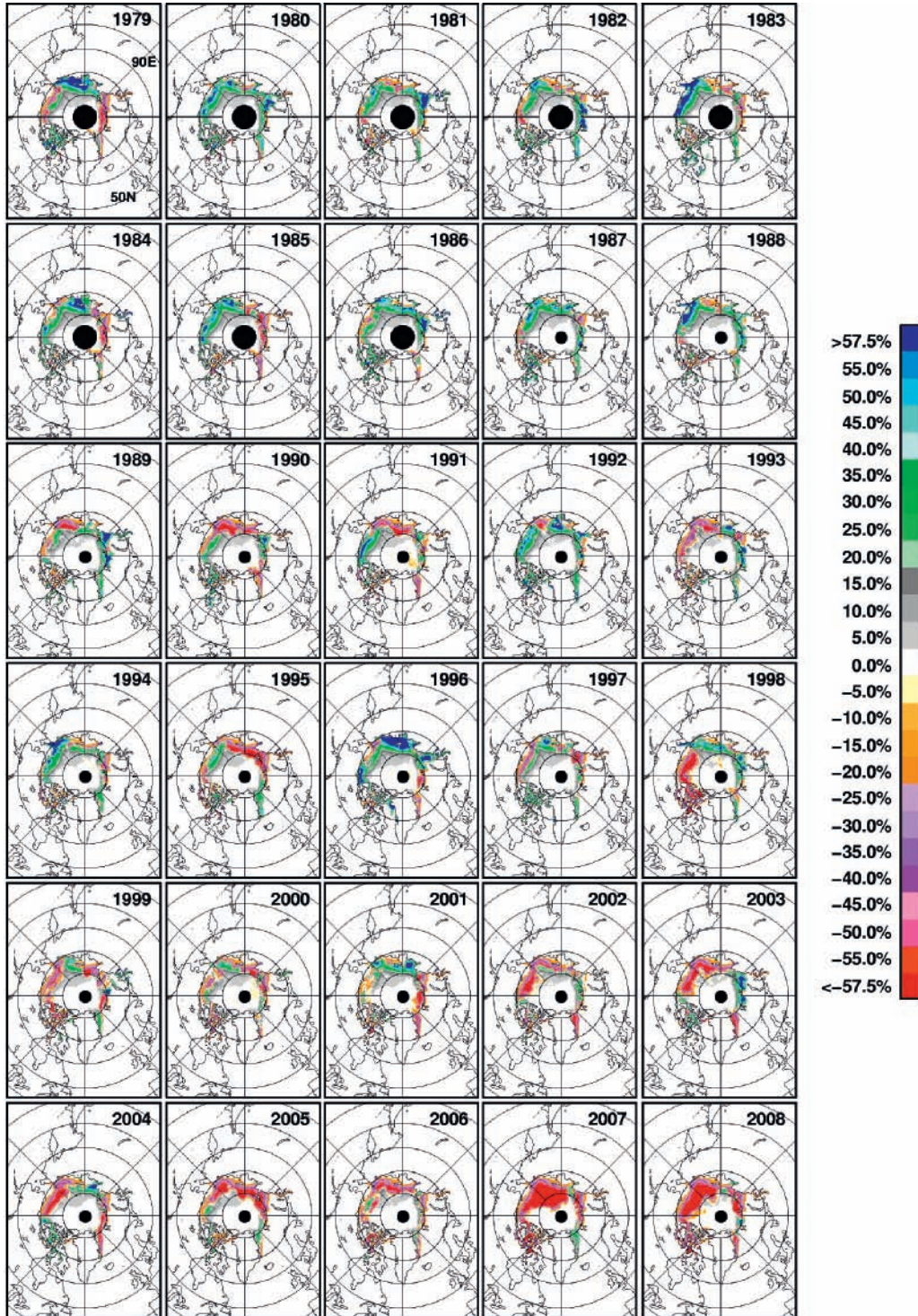
Fig. 6.9 Colour-coded ice concentration monthly anomaly maps for each September from 1979 to 2008 in the northern hemisphere.

anomalies in 2004, 2005, 2006 and 2007. In 2008, negative anomalies were not as strong in part because of positive anomalies in the Bering Sea and Baffin Bay. This was caused by significant cooling in the region due to a relatively strong La Niña in late 2007 and early 2008.

A similar set of anomaly maps but for September are presented in Fig. 6.9 to illustrate the interannual changes in the ice cover during the end of the summer. The September maps show a decadal shift in the anomalies with the maps in the 1980s being dominated by negative anomalies, the maps in the 1990s were mixtures of negative and positive anomalies while the maps in the 2000s being dominated by positive anomalies. There are some exceptions with the maps for 1990, 1993, 1995 and 1998 being mainly positive while those for 1992, 1996 and 2001 being mainly negative. It is, however, apparent that the anomaly maps in 2007 and also 2008 were not just dominantly positive but also indicative of an unusually large decline in the ice cover. The ice that survived the summer melt is often referred to as perennial ice and consists mainly of the thick multiyear ice floes which have been the mainstay of the Arctic ice cover. This ice type has been reported previously as being in a rapid decline (Comiso, 2002; Comiso et al., 2008; Stroeve et al., 2007).

Ice Cover in the Antarctic region

The seasonal variability of the sea ice cover in the southern hemisphere is depicted by the colour-coded ice concentration maps for each month in 2007 from January to December (Fig. 6.10). The images change from one season to another. January is a time period when the sea ice cover decays very rapidly, and as explained earlier, the monthly ice concentration values could be averages of data that vary from near 100% ice at the beginning of the month to near 0% ice cover at the end. A good example of such occurrences is the large area of low concentration ice in the Ross Sea at around 200ºE and 70ºS. The month with the lowest average ice extent in 2007 is February, although the actual day of minimum ice extent could sometimes occur in March. During this month, a large fraction of the coastal areas around the continent is ice free. Ice freeze-up usually starts in March and during this period, much of the ice-free coastal areas gets covered by sea ice. The inner pack is usually highly consolidated, and wide bands of different concentrations along the ice edges (e.g. 10ºW–40ºW) in April, May and June are manifestations of rapid advances of sea ice in the region during the month. Maximum ice cover is not reached until September but the retreat is slow in October, and it is not until November when the sea ice cover starts to decline rapidly. As indicated earlier, it takes 7 months to reach maximum extent and only 5 months to reach minimum extent. The distribution of the sea ice cover is almost symmetric during austral winter and autumn except for a sharp corner at around 140ºW in the Ross Sea. This feature appears almost every year in approximately the same spot, suggesting that it is an oceanographic effect and influenced by the bathymetry in the region. There is indeed a rise in the vicinity, causing a semi-linear ice edge from 155ºE and 220ºE. In December, it is apparent that the sea ice cover is breaking up not just at the ice margin but also in the coastal areas and sometimes in the middle as in the Maud Rise area. Again, areas of relatively low ice concentrations during this period are usually where ice had been retreating or melting the fastest.

Monthly plots of ice extents and ice area in the southern hemisphere for the period from 1979 through 2008 are presented in Fig. 6.11, and it is apparent that the ice cover is more seasonal in this region than in the northern hemisphere (Fig. 6.6). The data from SMMR, SSM/I and AMSR-E are plotted again in green, red and blue, respectively, to show that the
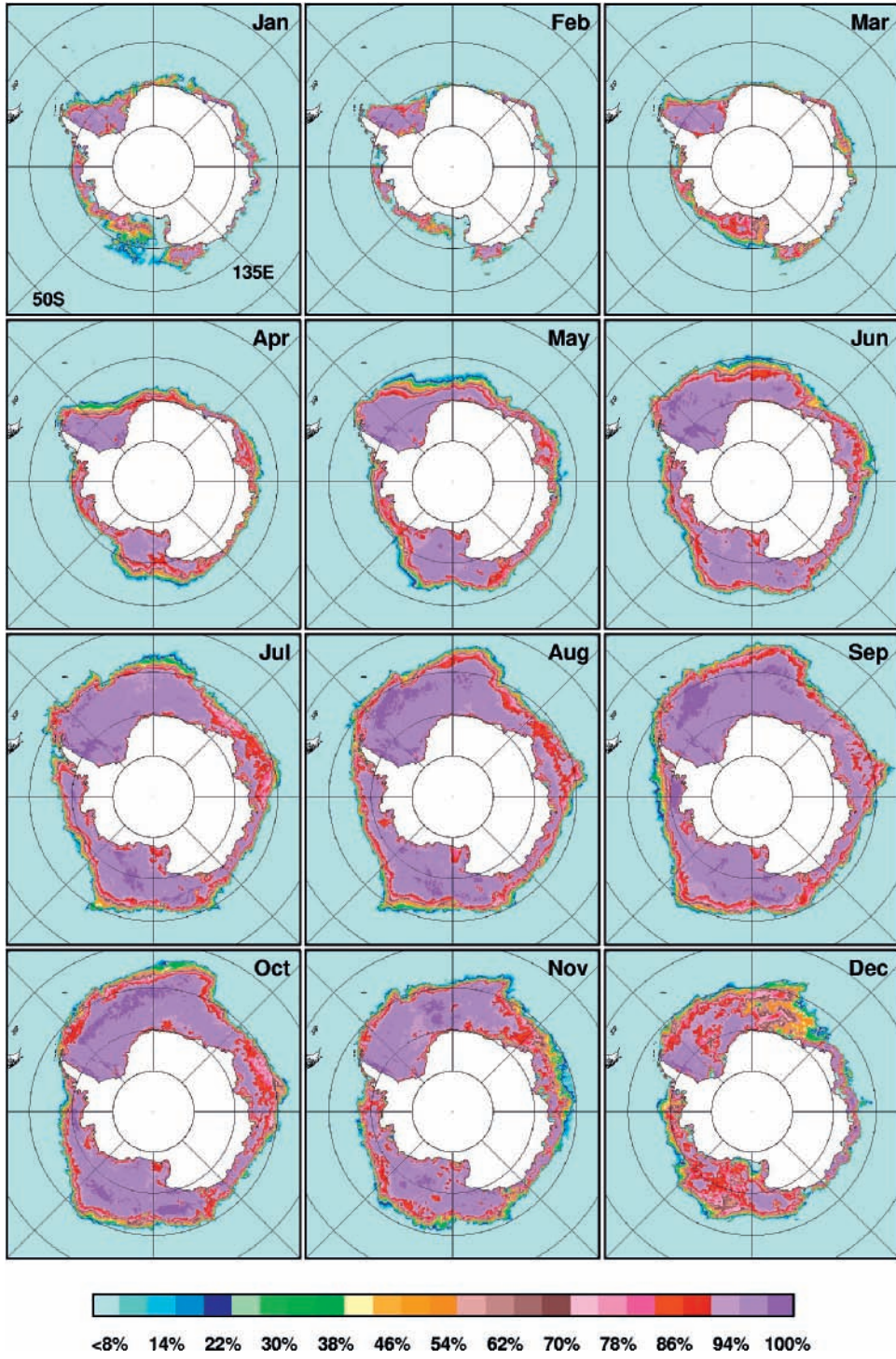
Fig. 6.10 Colour-coded ice concentration monthly averages in the southern hemisphere from January to December 2007 as derived from the 12.5-km AMSR-E standard ice data.
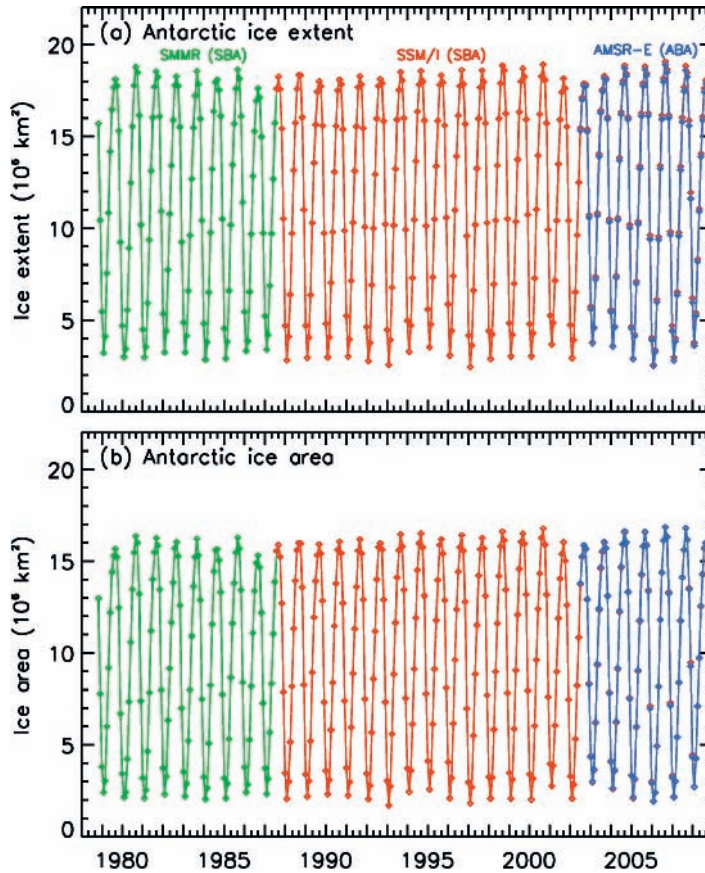
Fig. 6.11   Monthly averages of (a) ice extent and (b) actual ice area in the southern hemisphere for each month from November 1978 through September 2008. Data from SMMR, SSM/I and AMSR-E are plotted separately in green, red and blue, respectively. Updated from Comiso and Nishio (2008).

retrievals from the different sensors provide similar results. The monthly extents and area from all three sensors show variability that ranges from about 3×10^6 km² to 19×10^6 km² and from about 2×10^6 km² to 17×10^6 km², for ice extent and ice area, respectively. Significant interannual variability in maximum and minimum values are also apparent from the time record. During the period of overlap, the AMSR-E values are shown to be slightly less than those of the SSM/I values, reflecting the same bias associated with resolution as in the northern hemisphere. Again, because of this bias, the time series analysis will be done using SMMR and SSM/I data only. The ice extent and ice area are shown to have very similar distributions but sometimes, there are deviations especially in the summer when changes from one year to another are different (e.g. 1986 and 1987), likely associated with storms or changes in atmospheric circulation.

Colour-coded anomaly maps for each month of September from 1979 through 2008, as presented in Fig. 6.12, illustrate how the winter ice cover has been changing during the last 30 years. The anomaly maps for this winter month are defined by the patterns of alternate negative and positive anomalies along the periphery of the sea ice cover that surrounds the continent. From one year to another these patterns tend to move around, propagating like
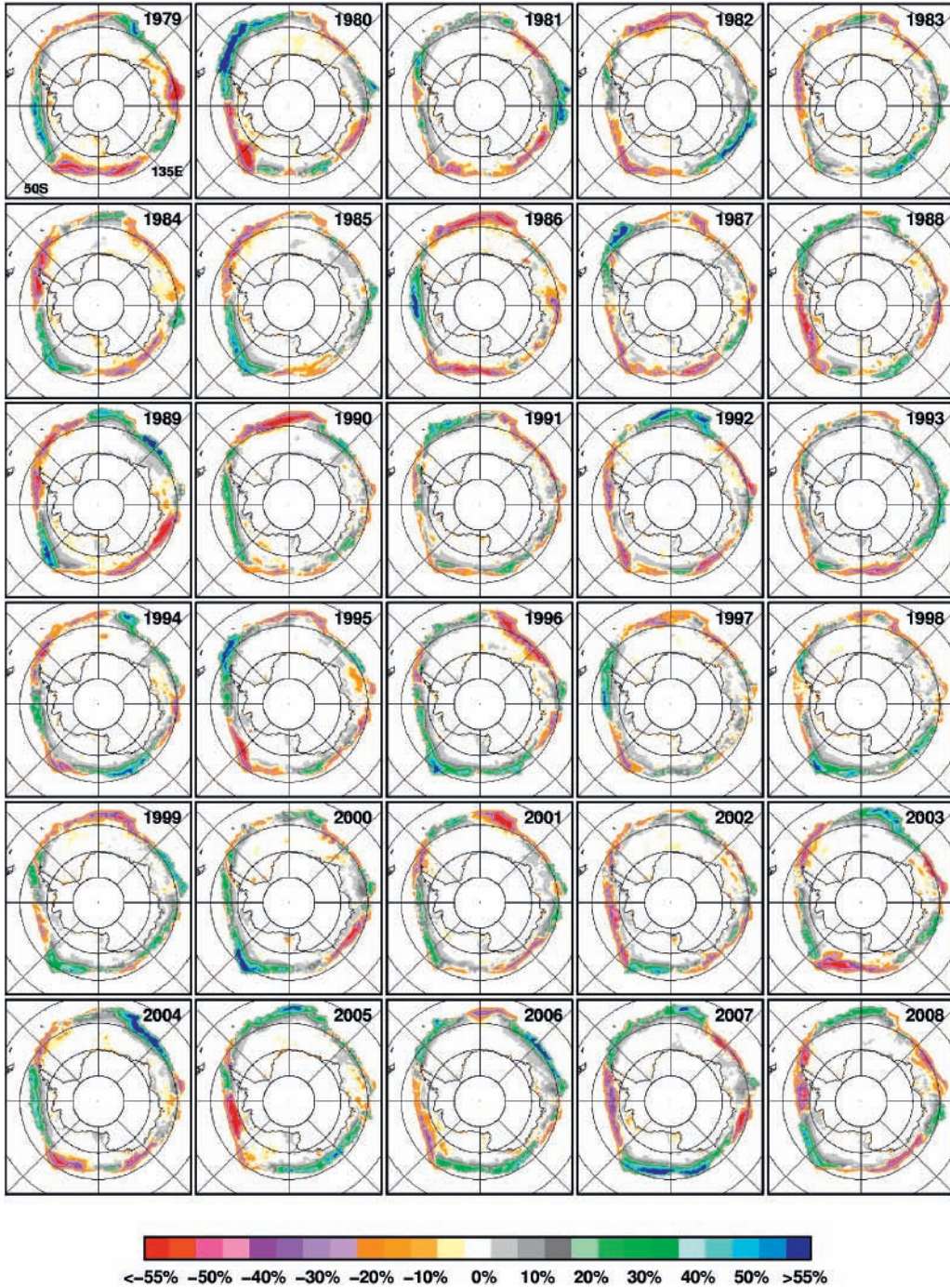
Fig. 6.12 Colour-coded ice concentration monthly anomaly maps for each September from 1979 to 2008 in the southern hemisphere.

a wave, and has been referred to as the Antarctic Circumpolar Wave (ACW) (White & Peterson, 1996). The period of propagation has been estimated to be about 8−10 years with a revisit time of 4−5 years at every point, assuming a wave number 2 or mode-2 pattern. Such wave number would lead to two sequences of negative and positive anomalies around the continent. A quick inspection of the anomaly images indicates that there are indeed some such patterns in 1982, 1985, 1987, 1988, 1989 and 2007, but as shown for the other years, this is not always the case. During some years, the pattern appears more like a mode-3 pattern as in 1979, 1984, 1994, 1995, 2001, 2003, 2006 and 2008. During other years, the wave number or mode is not well defined. White and Peterson (1996) also described the ACW as an ice edge phenomenon. The anomaly patterns in Fig. 6.12 indicate that the effect goes farther into the ice pack and could even be deeper into the pack as was illustrated by Comiso (2000) using surface temperature data.

A similar set of anomaly maps but for the month of February from 1979 to 2008 are presented in Fig. 6.13. The anomalies show that the exact location of the summer ice cover moves around from one year to another. The ACW pattern is difficult to detect from these maps because much of coastal areas becomes free of sea ice during the summer season. The main areas with sea ice cover during the period are the Western Weddell, Bellingshausen, Amundsen and Ross Seas. The summer ice is thus located basically on either sides of the Antarctic Peninsula. There are some years when positive anomalies were dominant in the Western Weddell Sea as in 1991, 1995, 2003 and 2004 and some years when negative anomalies were dominant as in 1985 and 1999. In the Bellingshausen/Amundsen Seas region, positive anomalies were quite dominant in 1979, most of the 1980s, 2001 and 2005, while negative anomalies were dominant in most of the 1990s and in 2003, 2004, 2007 and 2008. On the other hand, in the Ross Sea, negative anomalies were dominant in 1979, 1980, 1984, 1991, 1993, 1997 and 2005, while positive anomalies were dominant in 1986, 1987, 1998, 1999, 2001, 2003, 2004, 2007 and 2008. These results are consistent with high interannual variability in the ice cover in these two regions but show patterns that are also consistent with a decreasing sea ice cover in the Bellingshausen/Amundsen Seas and an increasing sea ice cover in the Ross Sea (Jacobs & Comiso, 1997; Kwok & Comiso, 2002b).

6.4 Hemispherical and regional trends

Trends in the Arctic Region

To quantitatively evaluate interannual changes, monthly anomalies in ice extents for the entire hemisphere and the various sectors in the Arctic region (as described in Gloersen et al., 1992; Parkinson et al., 1999) are presented in Fig. 6.14 for the 1979−2008 period. Each data point in the anomaly plots is the difference of the value for each month and that of the monthly climatology. Monthly anomaly data are used instead of yearly data to assess interannual variability and trends because they provide more information about temporal changes and better statistical accuracy for the trends. Monthly data are not used for this purpose because of large seasonal fluctuations that make it difficult to identify changes and to estimate interannual trends accurately.

A plot of the monthly anomalies for the entire northern hemisphere is presented in Fig. 6.14a, and it is apparent that the abnormally low and high values stand out better in
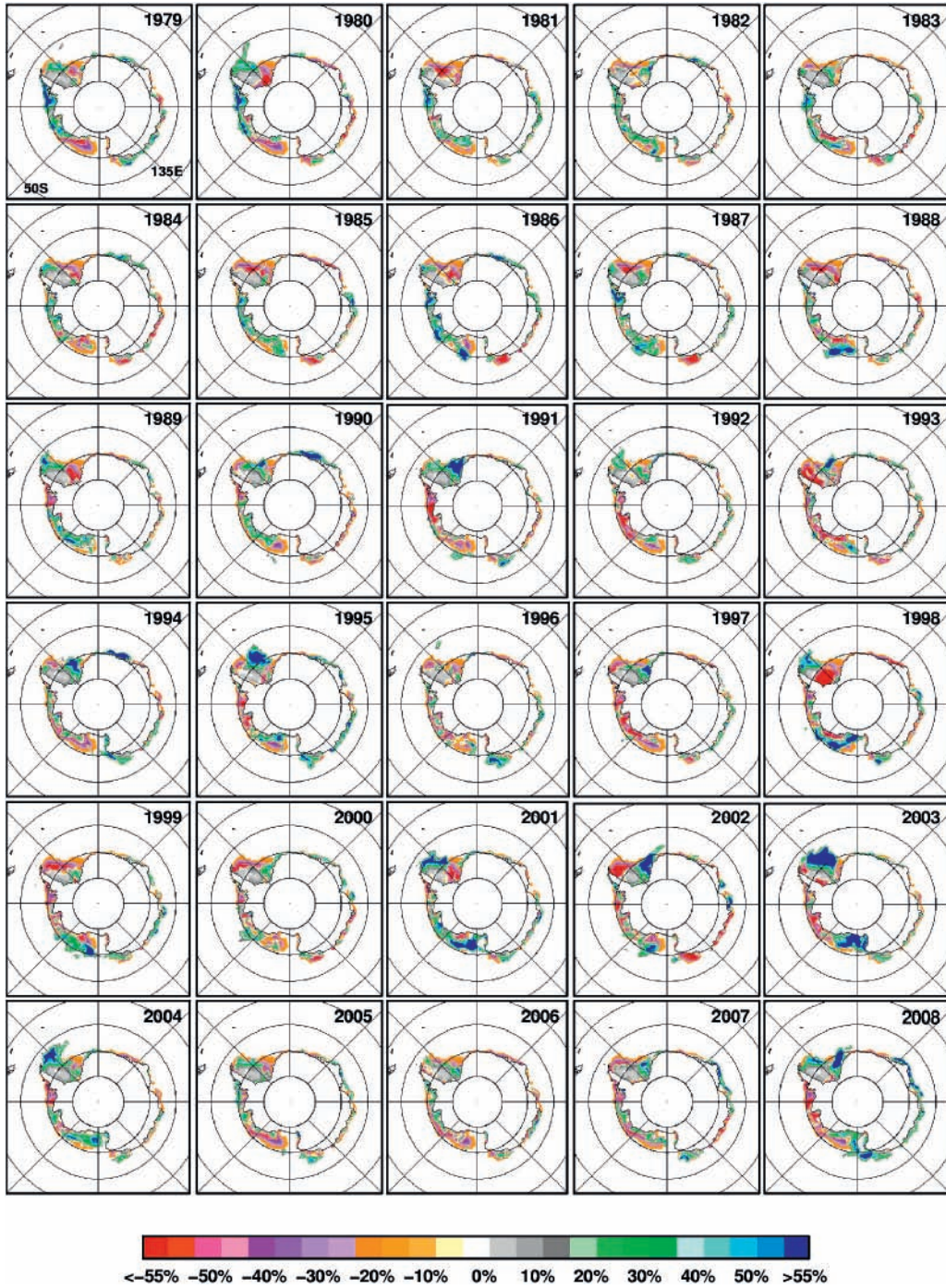
Fig. 6.13 Colour-coded ice concentration monthly anomaly maps for each February from 1979 to 2008 in the southern hemisphere.
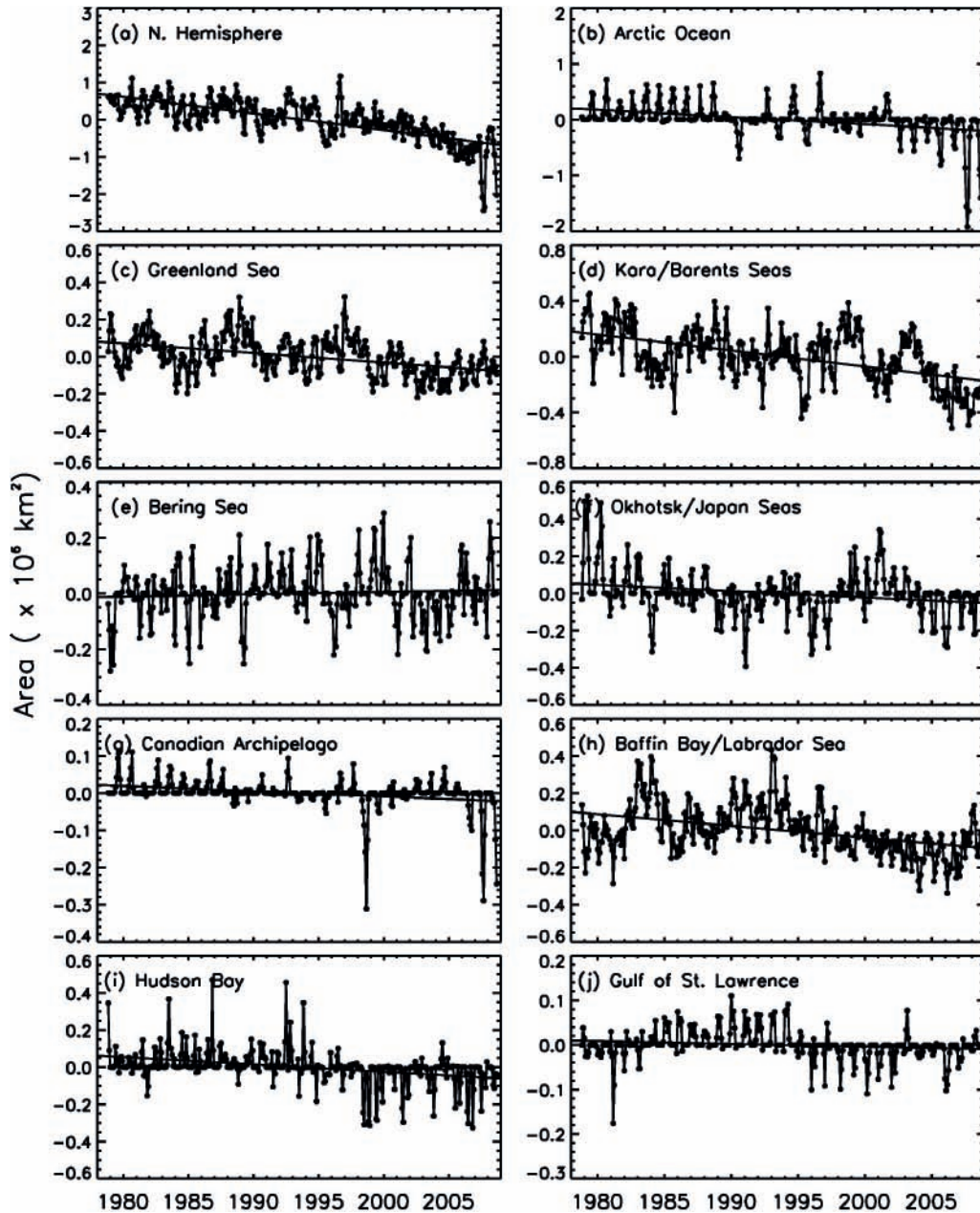
Fig. 6.14 Monthly averages of ice extents from daily data in (a) entire northern hemisphere; (b) Arctic Ocean sector; (c) Greenland Sea sector; (d) Kara/Barents Seas sector; (e) Bering Sea; (f) Okhotsk/Japan Seas; (g) Canadian Archipelago; (h) Baffin Bay/Labrador Sea; (i) Hudson Bay and (j) Gulf of St Lawrence sector. Updated from Comiso and Nishio (2008).

these plots than in the raw monthly data shown in Fig. 6.7. It is interesting to note that an abnormally low value in 1995 is followed by an abnormally high value in 1996 and subsequently, the ice cover started to show consistent declines after that ending with two dramatic drops in ice cover in the summer of 2007 and 2008. Before 1996, significant interannual

fluctuations in the anomalies are apparent but there is no obvious trend if the low value in 1995 is excluded. In the Arctic sector, the anomalies are usually close to zero if not zero during the winter because the region is completely covered by sea ice during the period, but the anomalies are significantly different from zero only during spring, summer and autumn (Fig. 6.14b). Note that the anomalies are generally positive in the 1980s and mainly negative in the 1990s, the exceptions being 1992, 1994 and 1996. This suggests that the distribution pattern of the ice cover changed significantly from one decade to another.

In the 2000s, except for the relatively slight positive anomalies in 2000 and 2001, the anomalies were all negatives from 2002 to the present, indicating persistent decline in the sea ice cover. The anomalies in the Greenland Sea sector (Fig. 6.14c) show some periodic variability with a period of about 7–8 years from 1979 to 1997 but after 1997, the distribution appears uniform. A cyclical pattern is apparently associated with the formation of the Odden, as described by Toudal et al. (1999). The frequency of Odden formation went down dramatically after 1997. In the Kara and Barents Seas, the ice variability (Fig. 6.14d) is similar to that of the Greenland Sea, although a cyclical pattern is not as apparent. In this sector, significant decreases occurred in 1985, 1992, 1995, 2000 and 2006 whereas increases occurred in most other years. An overall decline in the ice cover in this region, however, is apparent. The magnitude of the interannual variability of the sea ice anomalies in the Bering and Okhotsk Seas (Fig. 6.14e,f) are similar but with opposite trends. The anomalies in the Bering Sea were mainly negative in the 1980s, mainly positive in the 1990s and mainly negative in the 2000s but not negative enough to overcome the previously strong positive trend. In the Okhotsk Sea, the anomalies were strongly positive in the early 1980s, mainly negative in the 1990s and except for positive anomalies from 1999 to 2002, the anomalies in the 2000s have been negative.

In the Canadian Archipelago, the anomalies in extent were generally small except for the big declines in 1998, 2007 and 2008. During these years, the regions were almost or basically ice-free during the summer. Although the anomalies were generally positive from 2000 to 2005, the distribution shows a declining ice cover in the region. In the Baffin Bay/Labrador Sea region, some periodicities in the fluctuations of the anomalies (Fig. 6.14h) are apparent with the period much shorter in the 1980s than in the 1990s and 2000s. From 2000 to 2007, the anomalies were dominantly negative. In the Hudson Bay (Fig. 6.14i), the anomalies were primarily positive from 1979 to 1997 and after that, it was primarily negative. Since the region is usually covered completely by ice in winter, the negative anomalies mean delayed freeze-up period and early melt. In the Gulf of St Lawrence (Fig. 6.14j), there is a suggestion of a strong periodicity with the anomalies being mainly negative up to 1984, mainly positive from 1984 to 1994 and mainly negative from 1995 to 2007. It is apparent that there is a lack of coherence in the variability of the anomaly distributions at the different regions. The peaks and the dips generally do not occur at the same time in the different regions, and periodicities, when they occur, are usually out of phase from each other. The lack of coherence is partly the result of a complex atmospheric circulation system in the Arctic climate system.

Overall, negative trends of varying degree of significance are observed in all sectors, except for the Bering Sea sector in which the ice cover has been increasing but at much more moderate rate than previously reported. Quantitative estimates of trends in ice extent and ice area in the northern hemisphere and the various sectors are presented in Table 6.1. For data from January 1979 to September 2008, the trend of ice extent in the entire northern hemisphere is $-3.8 \pm 0.2\%$ per decade. This is higher than previous estimates (Bjorgo et al.,

Table 6.1　Trends in extent and area in the northern hemisphere.

Sector/season	Trend in extent km²/yr (%/decade)	Error in extent km²/yr (%/decade)	Trend in area km²/yr (%/decade)	Error in area km²/yr (%/decade)
Northern hemisphere	−45,200 (−3.8)	2,270 (0.2)	−49,100 (−4.5)	2,140 (0.2)
Arctic Ocean	−13,300 (−2.0)	1,570 (0.2)	−16,200 (−2.5)	1,670 (0.3)
Greenland Sea	−5,150 (−7.8)	567 (0.9)	−4,610 (−8.6)	479 (0.9)
Kara/Barents Seas	−11,700 (−9.1)	1,010 (0.8)	−12,100 (−10.6)	962 (0.8)
Bering Sea	864 (2.9)	528 (1.8)	479 (2.0)	471 (2.0)
Okhotsk/Japan Seas	−3,400 (−9.0)	689 (1.8)	−3,690 (−12.0)	667 (2.2)
Canadian Archipelago	−1,440 (−2.0)	231 (0.3)	−1,840 (−2.8)	250 (0.4)
Baffin Bay/Labrador Sea	−6,300 (−8.0)	741 (0.9)	−6,210 (−9.1)	675 (1.0)
Hudson Bay	−4,050 (−5.1)	518 (0.6)	−4,190 (−5.7)	471 (0.6)
Gulf of St Lawrence	−626 (−10.8)	185 (3.2)	−629 (−14.8)	160 (3.8)
Maximum	−34,500 (−2.2)	6,290 (0.4)	−36,010 (−2.5)	6,150 (0.4)
Minimum	−73,900 (−11.3)	11,300 (1.7)	−72,500 (−12.5)	9,560 (1.7)
Winter	−32,880 (−2.3)	5,220 (0.4)	−37,720 (−2.8)	4,700 (0.3)
Spring	−32,790 (−2.3)	5,000 (0.3)	−36,240 (−2.7)	4,860 (0.4)
Summer	−56,900 (−5.9)	6,670 (0.7)	−61,180 (−7.2)	6,720 (0.8)
Autumn	−56,890 (−6.5)	8,770 (1.0)	−59,910 (−7.4)	8,250 (1.0)

1997; Parkinson et al., 1999) because of consistently strong negative anomalies in the last decade. In the central Arctic Ocean region, the trend is −2.0 ± 0.2% per decade, which is a more modest decline rate than that for the entire northern hemisphere. The low rate is not unexpected since this sector is fully ice covered which means no change during winter and early spring months. The plot in Fig. 6.14b indicates spikes associated with changes in the spring, summer and autumn which are shown to be mainly positive in the 1980s, a mixture of positives and negatives in the 1990s and mainly negative in the 2000s. The negative trend appears to be primarily influenced by unusually low ice extent events in 2002–2008.

The trends in other sectors are varied with the only positive trend occurring in the Bering Sea at 2.9 ± 1.8% per decade. This positive trend reflects increases in the winter ice cover in the region despite decreases in the ice cover in the adjacent (Arctic) region. Also, towards the south-west of this region at the Okhotsk Sea, the ice cover is changing significantly more but with opposite sign, with the trend being −9.0 ± 1.8% per decade. In the latter, the trend would have been even more negative were it not for the relatively strong recovery during the years 1997–2002. Other regions with strong negative trends are the Greenland Sea, the Kara/Barents Seas, Baffin Bay/Labrador Sea and the Gulf of St Lawrence with trends of −7.8 ± 0.9% per decade, −9.1 ± 0.8% per decade, −8.0 ± 0.9 % per decade and −10.8 ± 3.2% per decade, respectively. The trend at Hudson Bay is −5.0 ± 0.7 % per decade, as expected, since the anomalies are mainly positive in the first 20 years and mainly negative in the last decade. The trend at the Canadian Archipelago is also significant at −2.0 ± 0.3% per decade but this is mainly due to a big drop in the ice cover in the region in 1998, 2007 and 2008. Despite the strong trends in the seasonal ice regions around the Arctic Basin, the contributions from these regions are relatively minor when the trend for the entire hemisphere is considered because the coverages are small compared to that of the Arctic Ocean which has a relatively modest

trend. The apparent cyclic patterns in these seas that are not in phase with each other make the contributions from these seas less predictable. However, the anomalies in extent appear to be consistently negative in many regions in at least part of the last decade.

While the trend of ice cover in the entire northern hemisphere is controlled by trends in both the Arctic and the peripheral seas, the most important trend of interest is actually that associated with the central Arctic. The northern hemisphere has smaller seasonal amplitude than the southern hemisphere because of the presence of extensive and thick multiyear ice cover in the central Arctic. Ice that survives the summer is often referred to as the perennial ice cover, which consists mainly of the relatively thick multiyear ice floes that survive the melt season. The extent and area of the perennial ice cover can be inferred by finding the minimum value for each year from the time series of daily data. The yearly record of the minimum extents of the ice cover for each year from 1979 to 2000 is shown together with that of maximum extent in Fig. 6.15. The trends in maximum ice values for both extent and ice area are -2.2 ± 0.4 and $-2.5 \pm 0.4\%$ per decade, respectively, and are only a little less than those of the entire hemisphere (Fig. 6.14a, Table 6.1). The trends in minimum ice cover, however, are $-11.3 \pm 1.7\%$ per decade and $-12.5 \pm 1.7\%$ per decade for ice extent and ice
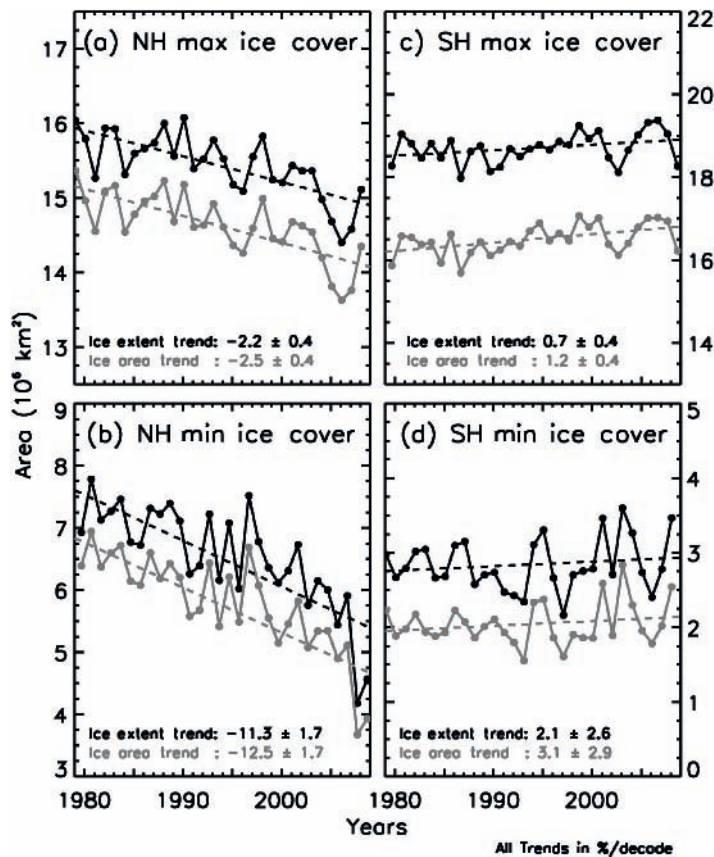
Fig. 6.15 Plots of (a) maximum ice extent and ice area, (b) minimum extents and ice areas in the northern hemisphere, and (c) maximum ice extents and ice areas, and (d) minimum ice extents and ice areas in the southern hemisphere from 1979 to 2008.

area, respectively (Fig. 6.15b, Table 6.1). Such large negative trends (about five times higher than maximum trends) indicate that the perennial ice cover has continued to shrink at an even higher rate than that reported previously (Comiso, 2002) and updated in recent years (Comiso et al., 2008; Stroeve et al., 2007). The results are consistent with trends in the multi-year ice cover as inferred from winter passive-microwave data (7% per decade) as previously reported by Johannessen et al. (1999). Using QuickScat data, Nghiem et al. (2007) also cited rapid decline in the multiyear ice fraction since 1999. The results are also consistent with reports by Rothrock et al. (1999) and Wadhams and Davis (2000) that made use of submarine sonar data and indicated that the average ice thickness in the 1990s is significantly less than averages collected in the previous decades. The issues associated with ice thickness and its variability are addressed in Chapter 4.

Trends in the Antarctic region

The time series monthly ice extent anomalies for the entire hemisphere and the various sectors, as presented in Fig. 6.16, show more quantitatively how the sea ice cover in the southern ocean has been changing. The anomalies for the entire hemisphere (Fig. 6.16a) indicate a highly variable sea ice cover that fluctuates in yearly anomalies by as much as 1×10^6 km^2. The anomalies fluctuated highly but almost randomly in the first 7 years, became almost steady and uniform in the next 7 years and went through a semi-periodic increase and decrease with a period of about 5 years after that. Conspicuously, the time series show a big negative anomaly in the beginning (1980) and a big positive anomaly in the end (2008), making the net trend more positive than what can be inferred from an almost uniform distribution. The monthly anomalies in the various sectors are shown to have very different patterns, none of which is similar to that of the entire hemisphere. This is in part because the ice edges go through cycles of advances and retreats as discussed earlier and in part because of the ACW. As indicated earlier, the cycles are not very regular as illustrated in the plot for the Weddell Sea sector. In this sector, there are peaks in 1980, 1989, 1993, 1995, 1998, 2001, 2003 and 2008 while there are dips in 1981, 1986, 1991, 1999 and 2002. Some periodic variations can be detected in the Indian Ocean which has peaks in 1984, 1989, 1994, 2000 and 2006 and dips in 1980, 1987, 1992, 1996, 2002 and 2008. The plot for the West Pacific Sector is shown to have a peak in 1983 and a big dip in 1989 but nothing significant after that except for a mild dip in 2002. The Ross Sea Sector plot has a broad peak in 1986 and narrow peaks in 1996, 1999 and 2008 and dips in 1980, 1986, 1992, 1996 and 2005. The plot for the Bellingshausen–Amundsen Seas sector appears a little periodic with peaks in 1982, 1987, 1991, 1996 and 2002 and dips in 1983, 1988, 1992, 1998 and 2007. A phase shift in the anomaly pattern between the two most periodic regions (i.e. Indian Ocean and the Bellingshausen/Amundsen Seas Region) is approximately 2–3 years and a revisit time of about 5–6 years can be inferred. This would be approximately consistent with the ACW but it is not clear why the other sectors are not showing similar patterns. For the ACW to be a propagating wave going around the circumpolar region, all sectors should be affected in a similar manner. Some insights into the problem has been proposed by Yuan and Li (2008) who hypothesized that the pattern is affected by the strong influence of the wave-3 pattern and other phenomena such as the Pacific South American Pattern (PSA) and the Antarctic Dipole Pattern (ADP). The impact on the ice cover of the El Niño Southern Oscillation (ENSO) during the years of 1983, 1988, 1992 and 1998 has also been cited may many investigators (Ledley & Huang,
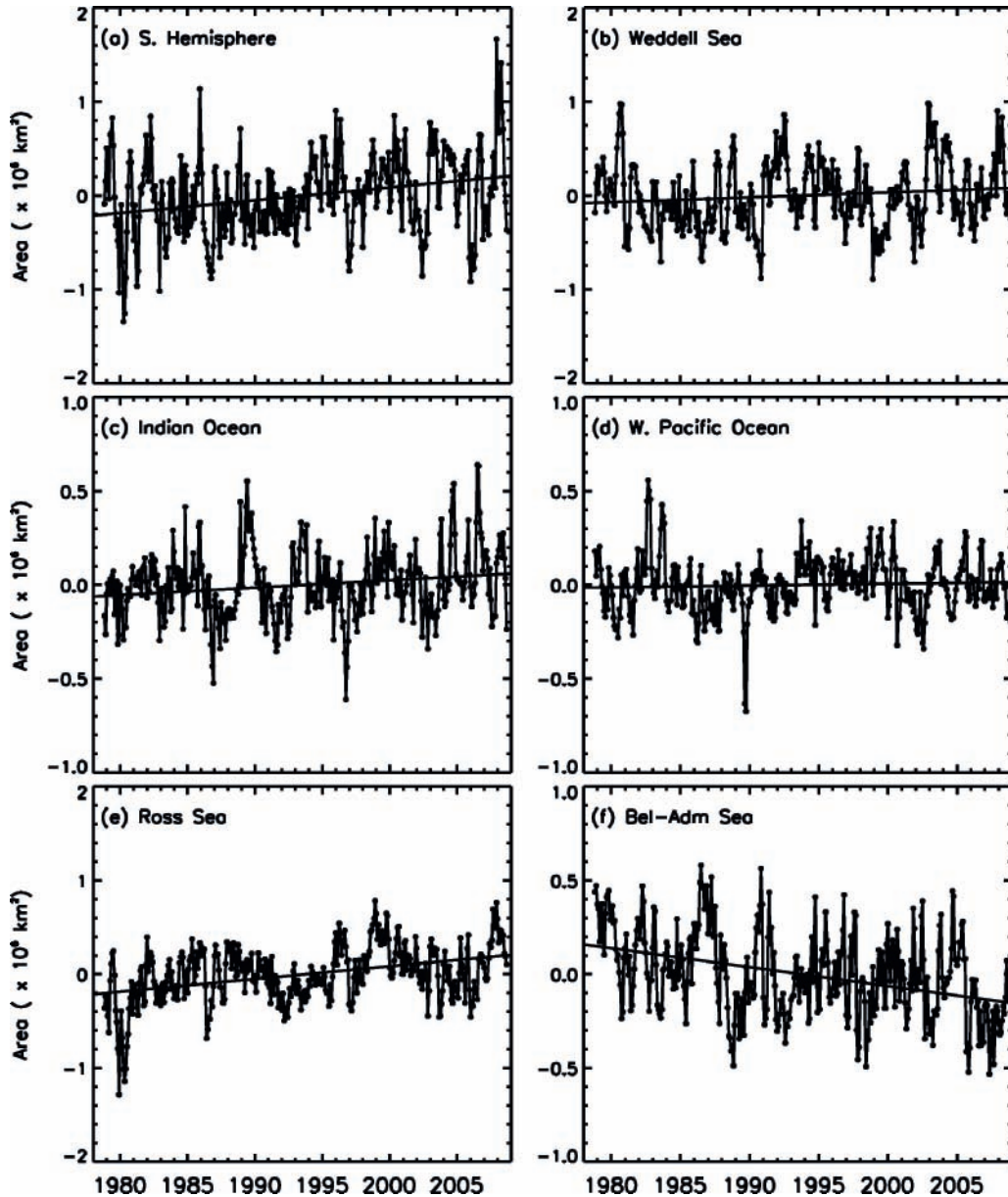
Fig. 6.16   Monthly averages of daily ice extents of the (a) entire southern hemisphere; (b) Weddell Sea; (c) Indian Ocean; (d) West Pacific Ocean; (e) Ross Sea and (f) Bellingshausen/Amundsen Seas. Updated from Comiso and Nishio (2008).

1997; Paterson & White, 1998; Kwok & Comiso, 2002a). The patterns are relatively irregular at times because the atmospheric circulation in the region is complex and driven by many factors, some of which are regional in origin. For example, in the Weddell Sea, a large positive anomaly in 1981 was followed by a negative anomaly in the subsequent summer, while a negative anomaly in 1991 was followed by 2 years of positive anomalies. Other anomalous patterns have also been cited in the literature (Hanna, 2001).

Quantitative estimates of the trends of sea ice extent and area in the southern hemisphere and the various sectors are provided in Table 6.2. The trends in the southern hemisphere are generally more modest and not as indicative of drastic changes such as those in the northern hemisphere. However, it is interesting to note that the trends are mainly positive, albeit relatively low. The result of analysis of data from the 30-year period shows a small but significant trend in ice extent of $1.2 \pm 0.2\%$ per decade for the entire southern hemisphere (Table 6.2). This is slightly more than the $1.0 \pm 0.4\%$ per decade reported by Zwally et al. (2002) for the 1979–2000 period. The trends in extent are similarly small but significant at 1.2 ± 0.5 and $2.1 \pm 0.6\%$ per decade at the Weddell Sea and Indian Ocean, respectively. In the Western Pacific Ocean sector, the trend is insignificant at $0.8 \pm 0.7\%$ per decade. In the last two sectors, the trends are quite substantial with opposite signs of $4.9 \pm 0.6\%$ per decade and $-7.1 \pm 0.9\%$ per decade at the Ross Sea and Bellingshausen/Amundsen Seas sectors, respectively. Since the two sectors are adjacent to each other, it appears that the opposite trends in the two sectors are partly caused by advection of ice from one sector to the other. However, the Antarctic Peninsula that is adjacent to the Bellingshausen/Amundsen Seas sector has been an area of climate anomaly described by King (1994) and Jacobs & Comiso (1997). The low extents in the region has also been associated with low sea level pressure in the region that results in increased northerly flow to the west of the Antarctic Peninsula (Lefebvre et al., 2004). Also, the Ross Sea region has been associated with influences of ENSO (Ledley & Huang, 1997) and the continental area adjacent to it has been experiencing some cooling during the last two decades (Comiso, 2000). Changes in the pattern of the Southern Annular Mode (SAM) during this period (Thompson & Solomon, 2002; Stammerjohn et al., 2008) may also cause stronger southerly winds over the Ross Ice Shelf, causing more persistent coastal polynyas and more ice. It is also postulated that the enhanced winds are caused by increased vorticity in the West Antarctic region that is in part caused by the ozone hole. The increased ice production in the continental shelf area also has an important role since the region is regarded as one of the primary source of bottom water formation (Zwally et al., 1985; Gordon et al., 2007). Note that the trends in ice area for the entire hemisphere are

Table 6.2 Trends in extent and area in the southern hemisphere.

Sector/season	Trend in extent km²/yr (%/decade)	Error in extent km²/yr (%/decade)	Trend in area km²/yr (%/decade)	Error in area km²/yr (%/decade)
Southern hemisphere	13,1600 (1.2)	2,520 (0.2)	19,100 (1.9)	2,360 (0.2)
Weddell Sea	5,400 (1.2)	2,140 (0.5)	7,130 (1.9)	1,920 (0.5)
Indian Ocean	3,970 (2.1)	1,080 (0.6)	3,920 (2.5)	998 (0.6)
Western Pacific Ocean	1,000 (0.8)	895 (0.7)	2,500 (2.7)	758 (0.8)
Ross Sea	13,800 (4.9)	1,700 (0.6)	13,700 (5.7)	1,520 (0.6)
Bellingshausen/Amundsen Seas	−10,300 (−7.1)	1,290 (0.9)	−8,120 (−6.8)	1,130 (0.9)
Maximum	13,260 (0.7)	7,320 (0.4)	20,400 (1.2)	6,650 (0.4)
Minimum	5,650 (2.0)	7,456 (2.6)	6,300 (3.1)	6,010 (2.9)
Winter	12,140 (0.8)	6,190 (0.4)	19,990 (1.4)	5,910 (0.4)
Spring	12,870 (0.7)	6,350 (0.4)	18,470 (1.2)	6,350 (0.4)
Summer	6,420 (1.0)	8,820 (1.4)	9,660 (2.1)	7,520 (1.6)
Autumn	21,980 (3.1)	9,400 (1.3)	27,430 (4.7)	9,070 (1.5)

slightly higher, indicating the effects of changing atmospheric circulation and the calving of two big icebergs in 2000 and 2002.

The trends of maximum ice extents for each year in the southern hemisphere are similar but greater than that inferred from the monthly time series, being $0.7 \pm 0.4\%$ per decade and $1.2 \pm 0.4\%$ per decade for ice extent and ice area, respectively. The trends of minimum values for each year are even more positive but insignificant at 2.0 ± 2.6 and $3.1 \pm 2.9\%$ per decade for ice extent and ice area, respectively. It appears that the rate of decline is strongest in the summer and early autumn as in the Arctic but the values are much more modest and the errors are larger because of a much lower extent of ice in the summer.

6.5 Seasonal trends in extents, ice concentration and surface temperature

Seasonal averages of sea ice extents and ice areas were presented earlier in Fig. 6.5 and it is apparent that the seasonality of the sea ice cover in the two hemispheres are very different. In the northern hemisphere, the average extents of sea ice in winter and spring have very similar magnitudes while they vary significantly in summer and autumn. In the southern hemisphere, the average extents are quite different in winter and spring while they are similar, though slightly different, in summer and autumn. The most remarkable differences of the seasonal distributions for the two hemispheres, however, are in the magnitude and sign of the trends as given in Tables 6.1 and 6.2. In the northern hemisphere, the trends in ice extent are all negative at -2.3, -2.3, -5.9 and -6.5% per decade for winter, spring, summer and autumn, respectively. On the other hand, the trends are all positive in the southern hemisphere at 0.8, 0.7, 1.0 and 3.1 % per decade for winter, spring, summer and autumn, respectively. The differences in the trends for the ice area are even bigger, as indicated in Tables 6.1 and 6.2. The distributions for the yearly seasonal values are similar for both ice extent and ice area but the trends in ice area provide a better assessment of the change in volume and hence the mass, if the average thickness and the density of the sea ice cover are known. The seasonal trends in winter and spring are shown to be relatively low and approximately equal and similar to that for maximum extent (see Table 6.1) in the northern hemisphere. These results indicate that the farthest extents of the sea ice cover in this hemisphere have not changed much during the last 30 years. In summer and autumn, the trends are considerably higher (more than two times), indicating that the key changes in the Arctic region are occurring during these two seasons.

In the southern hemisphere, the trends are also about the same during austral winter, spring and summer at 0.8, 0.7 and 1.0% per decade, respectively, while they are significantly higher at 3.1% per decade during the austral autumn. Again, the ice cover has not been changing much in winter as in the northern hemisphere and the key changes occur during summer and autumn. Since the seasons are out of phase by about 6 months, the large changes in ice cover do not occur concurrently in the two hemispheres. This suggests that in terms of atmospheric (or oceanic) forcing on the sea ice cover, the greatest impacts occur in summer and autumn regardless of hemisphere. It is intriguing that the signs for the trend are generally different for the two hemispheres.

To gain insights into the spatial pattern of the changes in the ice cover, the trend in ice concentration in each data element was estimated for the period 1981–2007 for each season,

using the yearly seasonal averages, and for the northern hemisphere, the results are presented in Fig. 6.17. A negative trend in ice concentration for a certain area generally means less sea ice cover in this area in recent years than in previous years. Overall, negative trends are dominant for all seasons, consistent with the aforementioned decline of sea ice in the Arctic region. In winter and spring, the only areas that have positive trends are the Bering Sea and parts of the Okhotsk Sea. In the summer, the trends are practically all negative with the unusually high trends occurring in the Beaufort Sea and Barents Sea where considerable decline of sea ice has been observed in the last decade. In autumn, the trend is highest in the Beaufort Sea which is the site where the perennial ice has retreated the most in recent years.

The decline in the sea ice cover over the 30-year satellite data period can be due to a number of factors including changes in sea level pressure and surface wind patterns (Walsh &
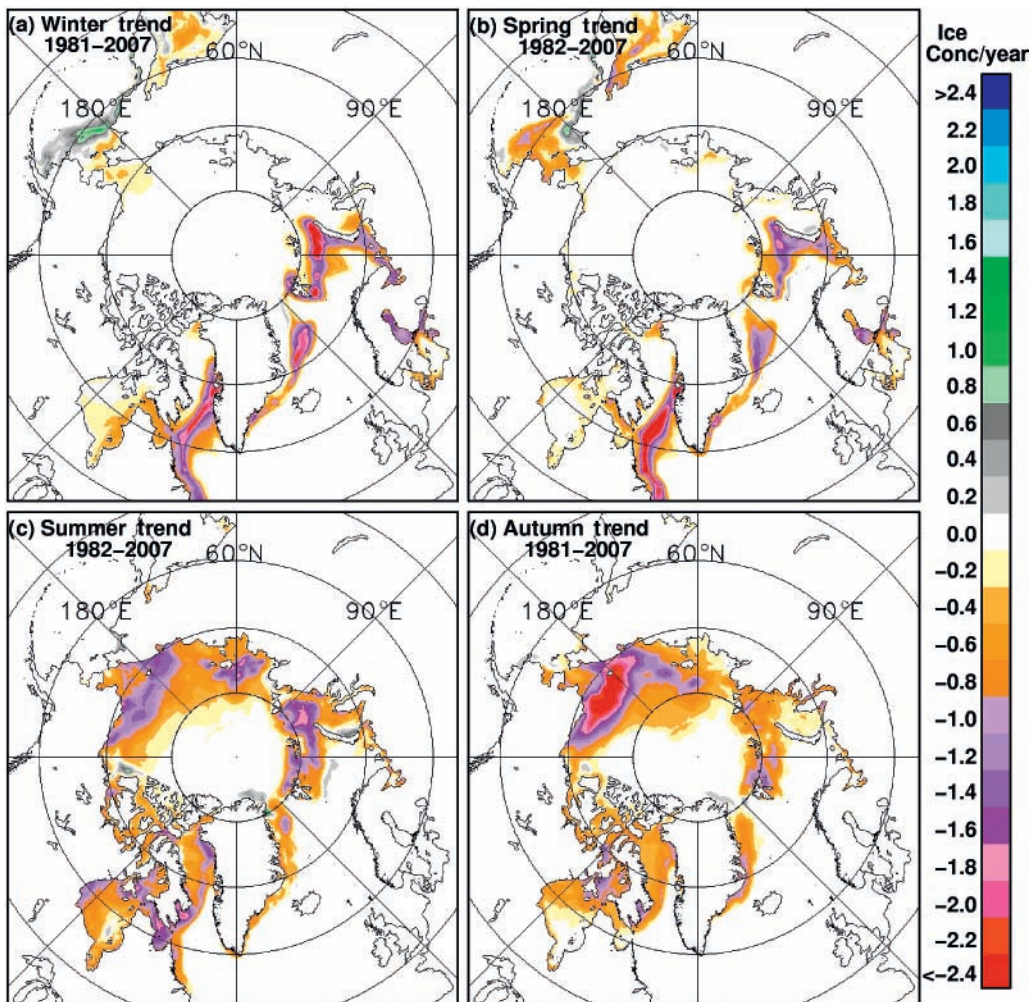
Fig. 6.17   Trends of average ice concentration in the northern hemisphere for each season in (a) winter (1981–2007), (b) spring (1982–2007), (c) summer (1982–2007) and (d) autumn (1981–2007).

Johnson, 1979) and changing surface temperatures (Comiso, 2003). The direct effect of increasing surface temperature on the sea ice cover is of interest in light of contentious debates about the warming impact of increasing antrophogenic greenhouse gases in the atmosphere. To get an idea about the relationship of surface tempature with the sea ice cover, we make use of available surface temperature data from 1981 to 2007 which is derived from NOAA/AVHRR data as described in Comiso (2003). The ice concentration trend maps were constructed for the same period as available surface temperature data for an even match of the coverage of the two data sets. Trend maps for surface temperatures in the northern hemisphere for each season over the period 1981–2007 are presented in Fig. 6.18. The trend maps show overall warming in all seasons, but it is surprising that during winter, large areas in the Bering Sea and over land in the Russian region show negative trends (Fig. 6.14a). It is apparent that in the Bering Sea, the negative trends in temperature appear in approximately in the same area where positive trends in the sea ice cover (Fig. 6.13a) have been observed.
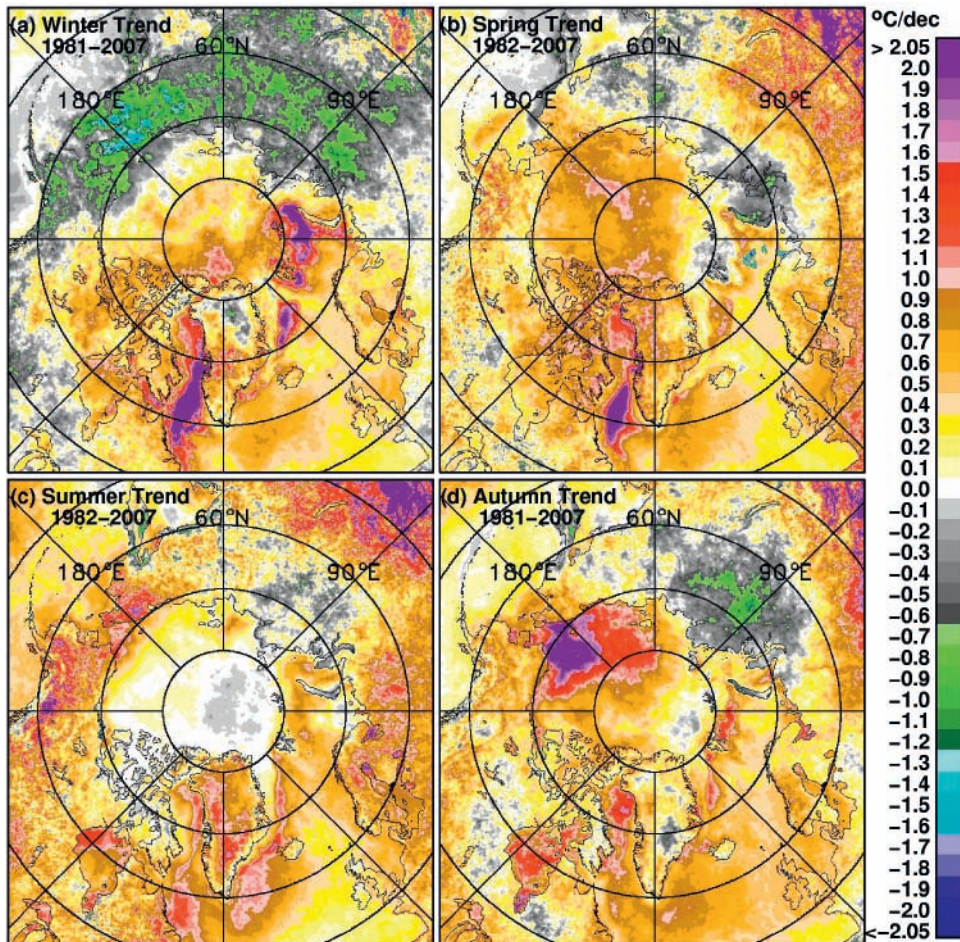
Fig. 6.18 Trends in surface temperatures in the northern hemisphere for each season in (a) winter (1981–2007), (b) spring (1982–2007), (c) summer (1982–2007) and (d) autumn (1981–2007).

This suggests that the changes in sea ice cover are connected to the changes in surface temperature. The impact of the negative trend over land is difficult to assess since during this time period, the ice cover in the Arctic Basin is consistently fully consolidated. The cooling in some areas in winter and spring also indicates that overall, the changes in surface temperature during this period are relatively modest. This is likely the reason why the trends in the sea ice cover in winter and spring are not as high as in the summer and autumn.

In the southern hemisphere, similar sets of trend maps in sea ice cover are presented in Figs 6.19 and 6.20. The patterns of trends for sea ice are quite interesting at least for the winter and spring seasons (Fig. 6.19a,b) because negative and positive trends are again alternating around the circumpolar region along the ice edges like those of the winter anomalies as cited earlier. It is like a mode-2 system with positive trends at around the top (0ºE) and bottom (180ºE) of the image and negative trends along the left (270ºE) and right side (120ºE)of the image. The negative pattern to the west of the Antarctic Peninsula is consistent with the
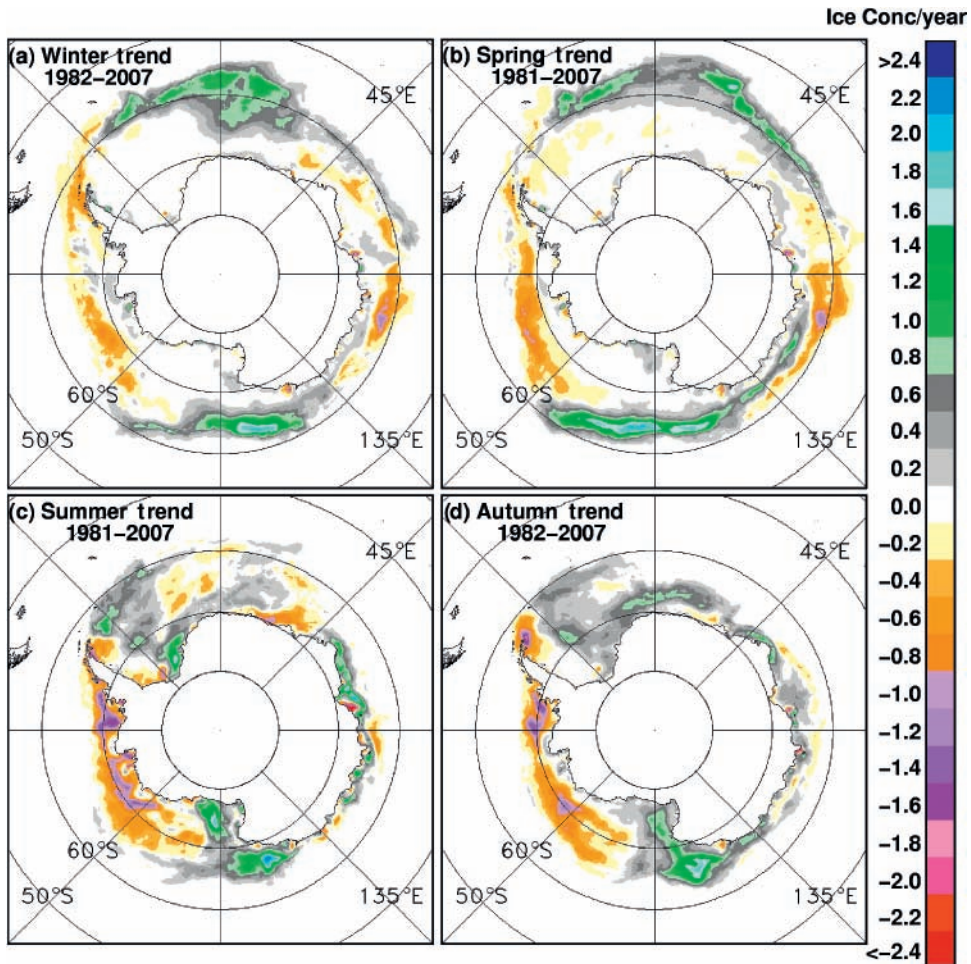
Fig. 6.19   Trends of average ice concentration in southern hemisphere for each season in (a) winter (1982–2007), (b) spring (1981–2007), (c) summer (1981–2007) and (d) autumn (1982–2007).

climate anomaly in the area as previously observed (Jacob & Comiso, 1997) and the retreat of sea ice in the region. The positive trend in the Ross Sea has also be identified previously (Kwok & Comiso, 2002b). However, it appears that the positive trend in the Eastern Weddell Sea and negative trend at 90°E are relatively strong and persist for at least two seasons of the year. In summer, the negative trends at the Bellingshause/Amundsen Seas and the positive trends at the Ross Sea become stronger while those in other areas become unpredictable because of the rapid decline of the sea ice cover. In autumn, the winter pattern appears to be reproduced except at 90°E where only a small area of negative anomaly is present. Overall, however, these results are consistent with the observed positive trends in ice extent and area for the entire region and a negative trend in the Bellingshausen/Amundsen Seas region.

The seasonal trends in surface temperature in the southern hemisphere are presented in Fig. 6.20, and although the patterns are not as well organized as those for the sea ice cover, there are some similarities. For example, along the vertical line at 0°E and 180°E and between 55°S and 6°S, the trends in winter and spring are mainly negative or cooling in these
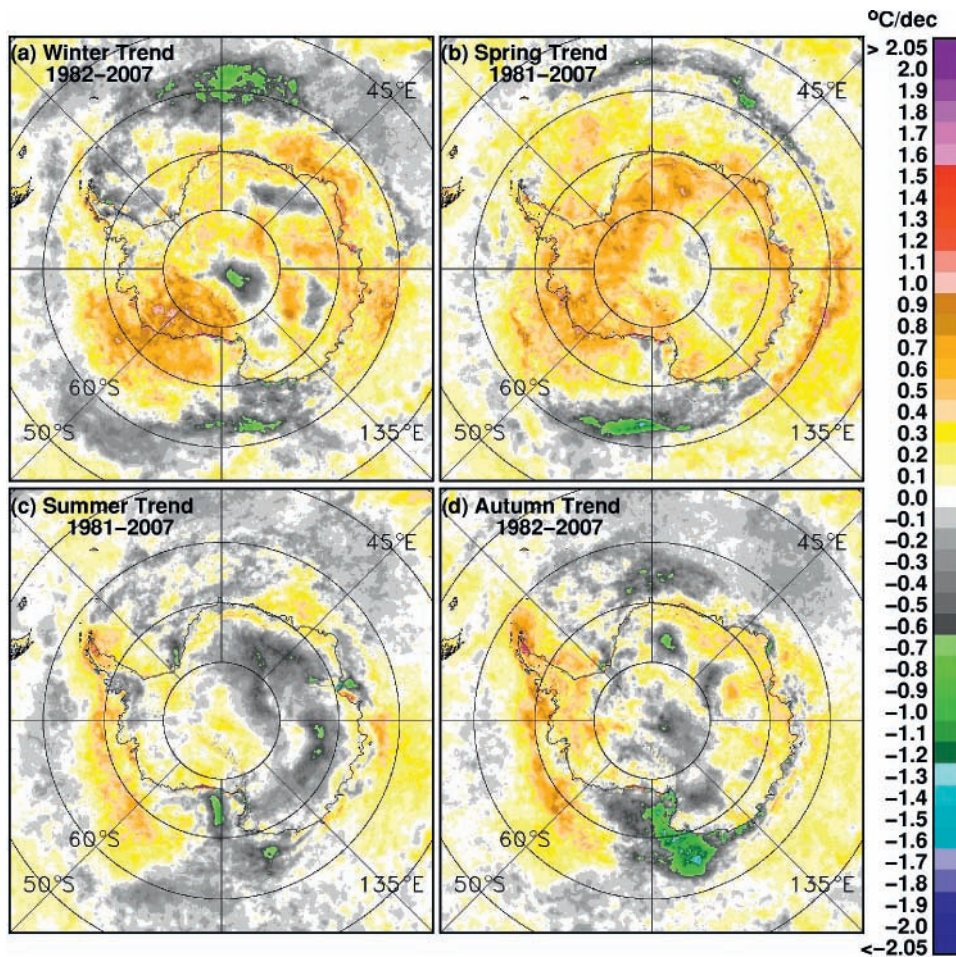
Fig. 6.20 Trends in average surface temperatures in the southern hemisphere for each season in (a) winter (1982–2007), (b) spring (1981–2007), (c) summer (1981–2007) and (d) autumn (1982–2007).

regions. This is again consistent with the positive trend in sea ice concentration in the same regions. Conversely, near 90ºE and 270ºE, at around 55ºS, the trends in surface temperature are mainly positive and consistent with the negative trends in ice concentration as revealed by Fig. 6.19. In the summer and autumn, the trends in surface temperature at the Bellings-hausen/Amundsen Sea regions are clearly positive and therefore consistent with the observed negative trends in sea ice concentration shown in Fig. 6.19. Cooling at the Ross Sea is also apparent and this is consistent with the very positive trends in sea ice concentration during the same period.

The overall changes in the sea ice cover in the polar regions over the last 30 years as obser-ved by satellite data can be summarized using the monthly average plots presented in Fig. 6.21. Five-year averages of monthly ice extent and ice area are presented in different colours to indicate the progression of the coverage of the sea ice cover during the first 25 years of satellite data. Single-year averages for 2005 through 2008 are also provided to show how the ice cover during the recent years compare with historical data. In the Arctic, the progression of the ice decline especially during the summer is vividly illustrated with the 1980–1984 average (purple line) showing the highest values. The 1985 average (blue line) is shown to be almost the same as that of the 1980–1984 average, indicating a relatively stable sea ice cover in the first decade. The data for 1990–1994 (green) and for 1995–1999 (orange) are also very similar but show relatively lower values than those for the first decade. The data for 2000–2004 (red) show even lower value, indicating a significant drop from the previous decades. Yearly data from 2005 to 2008 all show lower values than the 2000–2004 average values with 2007 exhibiting the
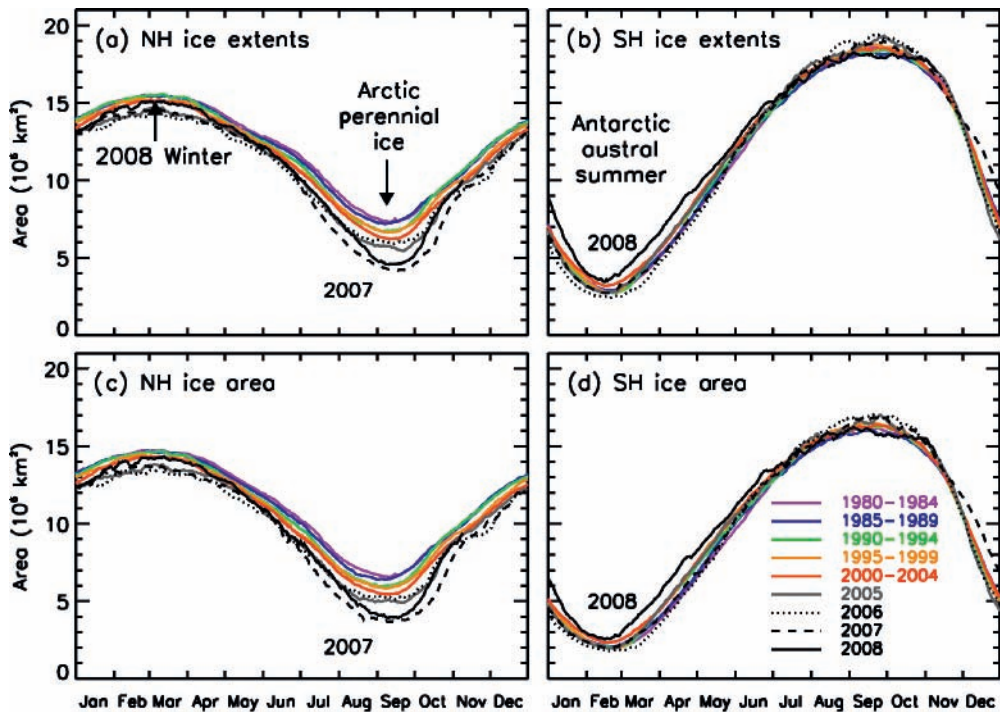
Fig. 6.21 Daily averages over 5 years in (a) ice extent and (b) ice area in the northern hemisphere and (c) ice extent and (d) ice area in the southern hemisphere. Updated from Comiso et al. (2008).

lowest values in the summer months while the 2008 data show higher values than the other three in winter but almost as low as the 2007 value at the end of the summer.

It is apparent that the changes during the winter are not as drastic as those in the summer months and although the data for 2008 during this time is almost the same as those of the 2000–2004 average, the values for 2005, 2006 and 2007 are significantly lower during the winter period. In the southern hemisphere, the 5-year averages are much more similar and it is only the 2000–2004 average that stands out to be almost consistently higher than the others. The individual year average for 2008 shows significantly higher values than any of the others in the summer and autumn following high values for 2007 in the previous spring, but in winter, it was almost average. Also, the 2006 monthly extents and areas are shown to be the lowest in the summer but about the highest in the winter. The data is consistent with a positive trend in the ice cover in the southern hemisphere.

6.6 Summary

Global climate change is expected to be amplified in polar regions because of feedback effects associated with the high albedo of ice and snow. A global warming of 0.6 K has been observed during the last century (Jones et al., 1999) and an enhanced trend in surface temperature has been reported for the last 50 years. In the Arctic, the climate signal is expected to be amplified and indeed the rate of warming during the last 25 years of satellite observations in the region has indicated that inside the Arctic circle, the warming rate is about 0.6 K per decade (Comiso et al., 2008). Such rate of warming is now observed in terms of other Arctic parameters such as sea ice, snow, glaciers ice sheets and permafrost, all acting in concert to the effects of higher temperatures than normal. On the other hand, cooling has been observed in the Antarctic region and the sea ice cover has been expanding in the process as discussed in this chapter. Such unexpected scenario in light of global warming has been studied and results have indicated that it can happen under warming atmospheric and oceanic conditions. Also, studies of long-term records from the 1950s to the present using reconstructed surface temperatures have revealed significant warming in the region during the last 60 years (Steig et al., 2009). Meanwhile, the ozone hole has been regarded as one of the culprits of current conditions in the Antarctic region.

Globally, the sea ice cover is shown to have a negative trend in the northern hemisphere and a positive but more modest trend in the southern hemisphere. Regression analysis yields overall trends in the northern hemisphere of $-3.8 \pm 0.2\%$ and $-4.5 \pm 0.2\%$ per decade, in ice extent and ice area respectively, but there are regions like the Bering Sea with positive trends in extent of about $2.9 \pm 1.8\%$ per decade. The rate of decline in extent is strongest in the summer at $-6.6 \pm 1.0\%$ per decade and weakest in the winter at $-2.3 \pm 0.4\%$ per decade. The most remarkable result as obtained from satellite data, however, is the rapid decline of the Arctic perennial sea ice cover, the rate of decline being -11.3 ± 1.7 per decade and $-12.5 \pm 1.7\%$ per decade for ice extent and ice area, respectively. Such result is an update to what has been reported elsewhere (Comiso et al., 2008; Stroeve et al., 2007) and is especially important because the perennial ice cover consists mainly of the thick multiyear ice floes that are the mainstay of the Arctic sea ice cover. The perennial ice basically controlled the thickness distribution of ice in the Arctic Basin and has kept ship navigation in the Arctic very limited in the past. The decline rate of the perennial ice is so large that we will likely lose this ice type

during this century (Serreze et al., 2007). Among the key reasons for the rapid decline is the ice–albedo feedback which in effect causes a warming in the upper layer of the Arctic Ocean. Some evidence that the temperature of the Arctic Ocean has been increasing has in fact already been reported (Gunn & Muench, 2001). Such loss of the perennial ice would mean profound changes in the Arctic including having a blue ocean in summer and a very different Arctic environment. With the surface temperature increasing as indicated, longer melt seasons will occur, leading to thinner ice and therefore decreasing ice volume (Hakkinen & Mellor, 1990).

In the southern hemisphere, the seasonal variability of the sea ice cover is high but the interannual changes have been more modest than in the Arctic. Alternating negative and positive ice concentration anomalies occur around the periphery of the ice-covered region that appears to propagate as a wave, often referred to as the ACW, going in a clockwise direction around the continent. The year-to-year changes in the anomaly patterns are, however, not always in line with that expected from the ACW, as described by White and Paterson (1996), suggesting a relatively complex and unpredictable circulation patterns in the Antarctic region. The trends in the Antarctic sea ice cover are surprisingly positive at 1.2 ± 0.2% per decade and 2.0 ± 0.2% per decade, for ice extent and ice area, respectively. While, counter-intuitively, a positive trend for the Antarctic ice cover during a scenario of global warming has actually been predicted (Manabe et al., 1992) the mechanism that would cause such a positive trend has not been adequately understood. Also, trend results in the Bellingshausen/Amundsen Seas sector show a relatively strong negative decline at −6.7 ± 1.0% per decade which has been previously reported and assumed part of an abnormal climate in the region that includes the Antarctic Peninsula. The relatively high rate of decline is compensated for by a positive trend in the Ross Sea and other regions. The good correlation of ENSO indices with climate anomalies in these regions, as observed by Kwok & Comiso (2002a), suggests that the sea ice anomalies may be in part influenced by recent ENSO episodes. It is also interesting that the trends in ice concentration in winter and spring are most significant near the edges and follow a pattern of positive and negative anomalies. Such a pattern suggests that trends currently detected in the southern hemisphere may be influenced by a periodic pattern (e.g. ACW, SAM or ENSO). Such patterns would produce negative or positive trends depending on which part of the cycle is at the beginning or end. To overcome such a bias, longer data records would be needed. Indeed, some studies that make use of reconstructed temperature series for the time period from the 1950s to the present (Steig et al., 2009) show warming trends in the Antarctic compared to what has been previously inferred from data sets with shorter records (Comiso, 2000; Doran et al., 2002). Such a positive trend is consistent with the observed decline in the ice cover from the 1950s and 1960s to the present as inferred from ship and whaling data sets by De la Mare (1997). While analysis of whaling data has its problems, including the possible inconsistency in the identification of the ice edge (Ackley et al., 2003), the correlation of the reported trend in ice edge location with surface-temperature trend is intriguing. It is obvious that further studies are needed before we can say with confidence what the Antarctic sea ice cover will look like in the future.

Acknowledgements

References

Ackley, S.F. (1996) Sea ice. In: *Encyclopedia of Applied Physics*. VCH Publishers, Inc., New York.

Ackley, S.F., Wadhams, P., Comiso, J.C. & Worby, A. (2003) Decadal decrease of Antarctic sea ice extent from whaling records revisited on the basis of historical and modern sea ice records. *Polar Research*, **22**, 10–25.

Allison, I. (1981) Antarctic sea ice growth and oceanic heat flux. *International Association of Hydrological Sciences, Publication*, **131**, 161–170.

Bjørgo, E., Johannessen, O.M. & Miles, M.W. (1997) Analysis of merged SSMR-SSMI time series of Arctic and Antarctic sea ice parameters 1978–1995. *Geophysical Research Letters*, **24**, 413–416.

Budyko, M.I. (1966) Polar ice and climate. In: *Proceedings of the Symposium on the Arctic Heat Budget and Atmospheric Circulation* (Ed. J.O. Fletcher), pp. 3–32. RM 5233-NSF. Rand Corporation, Santa Monica, California.

Carsey, F.D. (Ed.) (1992) *Microwave Remote Sensing of Sea Ice*. American Geophysical Union, Washington, DC. *Geophysical Monograph*, **68**.

Cavalieri, D.J. & Parkinson, C.L. (1987) On the relationship between atmospheric circulation and the fluctuations in the sea ice extents of the Bering and Okhotsk seas. *Journal of Geophysical Review*, **92**, 7141–7162.

Cavalieri, D.J., Gloersen, P., Parkinson, C., Comiso, J.C. & Zwally, H.J. (1997) Observed hemispheric asymmetry in global sea ice changes. *Science*, **278**, 1104–1106.

Comiso, J.C. (2000) Variability and trends in Antarctic surface temperatures from in situ and satellite infrared measurements. *Journal of Climate*, **13**, 1674–1696.

Comiso, J.C. (2002) A rapidly declining perennial sea ice cover in the Arctic. Geophysical Research Letters, **29**, 1029/2002GL015650.

Comiso, J.C. (2003) Warming trends in the Arctic. *Journal of Climate*, **16**, 3498–3510.

Comiso, J.C. & Gordon, A.L (1998) Interannual variabilities of summer ice minimum, coastal polynyas, and bottom water formation in the Weddell Sea. In: *Antarctic Sea Ice*: *Physical Properties and Processes* (Ed. M.O. Jeffries), American Geophysical Union, Washington, DC. *Antarctic Research Series*, **74**, 293–315.

Comiso, J.C. & Nishio, F. (2008) Trends in the sea ice cover using enhanced and compatible AMSR-E, SSM/I, and SMMR data. *Journal of Geophysical Research*, **113**, C02S07, 10.1029/2007JC004257.

Comiso, J.C. & Steffen, K. (2001) Studies of Antarctic sea ice concentrations from satellite data and their applications. *Journal of Geophysical Research*, **106**, 31362–31385.

Comiso, J.C., Cavalieri, D.J., Parkinson, C.L. & Gloersen, P. (1997) Passive microwave algorithms for sea ice concentrations. *Remote Sensing of the Environment*, **60**, 357–384.

Comiso, J.C., Parkinson, C.L., Gersten, R. & Stock, L. (2008) Accelerated decline in the Arctic sea ice cover. *Geophysical Research Letters*, **35**, L01703, 10.1029/2007GL031972.

De la Mare, W.K. (1997) Abrupt mid-twentieth-century decline in Antarctic sea ice extent from whaling records. *Nature*, **389**, 57–60.

Doran, P.T., Priscu, J.C., Lyons, W.B. et al. (2002) Antarctic temperature cooling and terrestrial ecosystem response. *Nature*, **415**, 517–520.

Drinkwater, M.R. & Lytle, V.I. (1997) ERS 1 radar and field-observed characteristics of autumn freeze-up in the Weddell Sea. *Journal of Geophysical Research*, **102**, 12593–12608.

Eppler, D., Anderson, M.R., Cavalieri, D.J. et al. (1992) Passive microwave signatures of sea ice. In: Microwave Remote Sensing of Sea Ice (Ed. F.D. Carsey), American Geophysical Union, Washington, DC. *Geophysical Monograph*, **68**, 47–71.

Fetterer, F.M., Drinkwater, M.R., Jezek, K.C., Laxon, S.W.C., Onstoot, R.G. & Ulander, L.M.H. (1992) Sea ice altimetry. In: Microwave Remote Sensing of Sea Ice (Ed. F.D. Carsey), American Geophysical Union, Washington, DC. *Geophysical Monograph*, **68**, 111–135.

Gloersen, P., Campbell, W.J., Cavalieri, D.J., Comiso, J.C., Parkinson, C.L. & Zwally, H.J. (1992) *Arctic and Antarctic Sea Ice, 1978–1987: Satellite Passive Microwave Observations and Analysis*. National Aeronautics and Space Administration, Washington, DC. NASA *Special Publication*, **511**, 289 pp.

Gordon, A.L. & Comiso, J.C. (1988) Polynyas in the Southern Ocean. *Scientific American*, 256, 90–97.

Gordon, A.L., Visbeck, M. & Comiso, J.C. (2007) A possible link between the Weddell Polynya and the Southern Annular Mode. *Journal of Climate*, **20**, 2558–2571.

Grenfell, T.C., Comiso, J.C., Lange, M.A., Eicken, H. & Wenshahan, M.R. (1994) Passive microwave observations of the Weddell Sea during austral winter and early spring. *Journal of Geophysical Research*, **99**, 9995–10010.

Gunn, J.T. & Muench, R.D. (2001) Observed changes in Arctic Ocean temperature structure over the past half decade. *Geophysical Research Letters*, **28**, 1035–1038.

Hakkinen, S. & Mellor, G.L. (1990) One hundred years of Arctic ice cover variations as simulated by a one-dimentional, ice–ocean model. *Journal of Geophysical Research*, **95**, 15959–15969.

Hanna, E. (2001) Anomalous peak in Antarctic sea ice area, winter 1998. *Geophysical Research Letters*, **28**, 1595–1598.

Holland, M.M. & Bitz, C.M. (2003) Polar amplification of climate change in coupled models. *Climate Dynamics*, **21**, 221–232.

Jacobs, S.S. & Comiso, J.C. (1997) A climate anomaly in the Amundsen and Bellingshausen Seas. *Journal of Climate*, **10**, 697–709.

Johannessen, O.M., Shalina, E.V. & Miles, M.W. (1999) Satellite evidence for an Arctic sea ice cover in transformation. *Science*, **286**, 1937–1939.

Jones, P.D., New, M., Parker, D.E., Martin, S. & Rigor, I.G. (1999) Surface air temperature and its changes over the past 150 years. *Reviews in Geophysics*, **37**, 173–199.

Johannessen, O.M., Shalina, E.V. & Miles, M.W. (1999) Satellite evidence for an Arctic sea ice cover in transformation. *Science*, **286**, 1937–1939.

King, J.C. (1994) Recent climate variability in the vicinity of the Antarctic peninsula. *International Journal of Climatology*, **14**, 357–369.

Kukla, G.J. & Gavin, J. (1981) Summer ice and carbon dioxide. *Science*, **214**, 497–503.

Kwok, R. & Comiso, J.C. (2002a) Southern ocean climate and sea ice anomalies associated with the Southern Oscillation. *Journal of Climate*, **15**, 487–501.

Kwok, R. & Comiso, J.C. (2002b) Spatial patterns of variability in Antarctic surface temperature: connections to the southern hemisphere annular mode and the southern oscillation. *Geophysical Research Letters*, **29**, doi: 10.1029/2002GL015415.

Kwok, R., Schweiger, A., Rothrock, D.A., Pang, S. & Kottmeier, C. (1998) Sea ice motion from satellite passive microwave imagery assessed with ERS SAR and buoy motions. *Journal of Geophysical Research*, **103**, 8191–8214.

Laxon, S., Peacock, N. & Smith, D. (2003) High interannual variability of sea ice thickness in the Arctic region, *Nature*, **425**, 947–950.

Ledley, T.S. & Huang, Z. (1997) A possible ENSO signal in the Ross Sea. *Geophysical Research Letters*, **24**, 3253–3256.

Lefebvre, W., Goose, H., Timmerman, R. & Fichefet, T. (2004) Influence of the Southern Annular Mode on the sea ice–ocean system. *Journal of Geophysical Research*, **109**, 10.1029/2004JC002403.

Lubin, D. & R. Massom (2006) *Polar Remote Sensing, Volume 1, Atmosphere and Oceans*. Springer-Praxis Books, Germany.

Manabe, S., Spelman, M.J. & Stouffer, R.J. (1992) Transient responses of a coupled ocean–atmosphere model to gradual changes of atmospheric CO2. Part II, Seasonal response. *Journal of Climate*, **5**, 105–126.

Markus, T., Kottmeier, C. & Fahrback, E. (1998) Ice formation in coastal polynyas in the Weddell Sea and their impact on oceanic salinity. In: A*ntarctic Sea Ice: Physical Processes, Interactions and Variability* (Ed. M.O. Jeffries). American Geophysical Union, Washington, D.C. *Antarctic Research Series*, **74**, 273–291.

Massom, R.A. (1991) *Satellite Remote Sensing of Polar Regions*. Belhaven Press, London.

Massom, R.A., Comiso, J.C., Worby, A.P., Lytle, V. & Stock, L. (1999) Satellite and *in situ* observations of regional classes of sea ice cover in the East Antarctic pack in winter. *Remote Sensing of the Environment*, **68**, 61–76.

Nghiem, S.V., Rigor, I.G., Perovich, D.K., Clemente-Colon, P., Weatherly, J.W. & Neumann, G. (2007) Rapid reduction of Arctic perennial sea ice. *Geophysical Research Letters* **34**, L19504, 10.1029/2007GL031138.

Parkinson, C.L. & Comiso, J.C. (2008) Antarctic sea ice from AMSR-E from two algorithms and comparisons with sea ice from SSM/I. *Journal of Geophysical Research*, **113**, C02S06, 10.1029/2007JC004253.

Parkinson, C.L., Comiso, J.C., Zwally, H.J., Cavalieri, D.J., Gloersen, P. & Campbell, W.J. (1987) *Arctic Sea Ice 1973–1976 from Satellite Passive Microwave Observations*. National Aeronautics and Space Administration, Washington, DC. *NASA Special Publication*, **489**, 296 pp.

Parkinson, C.L., Cavalieri, D.J., Gloersen, P., Zwally, H.J. & Comiso, J.C. (1999) Arctic Sea ice extents, areas, and trends, 1978–1996. *Journal of Geophysical Research*, **104**, 20837–20856.

Petersen, R.G. & White, W.B. (1998) Slow oceanic teleconnections linking the Antarctic Circumpolar Wave with tropical El-Niño–Southern Oscillation. *Journal of Geophysical Research*, **103**, 24573–24583.

Rothrock, D.A., Yu, Y. & Maykut, G.A. (1999) Thinning of the Arctic sea ice cover. *Geophysical Research Letters*, **26**, 3469–3472.

Serreze, M.C., Holland, M.M. & Stroeve, J. (2007) Perspective on the Arctic's shrinking sea ice cover. *Science*, **315**, 1533–1536.

Shuchman, R.A. & Onstott, R.G. (1990) Remote sensing of the polar oceans. In: *Polar Oceanography*: Part A Physical Science (Ed. W.O. Smith, Jr.), pp. 123–169. Academic Press, San Diego, California.

Smith, Jr. W. & Comiso, J.C. (2008) The influence of sea ice primary production in the Southern Ocean: a satellite perspective. *Journal of Geophysical Research*, **113**, 10.1029/2007JC004251.

Stammerjohn, S. & Smith, R. (1997) Opposing southern ocean climate patterns as revealed by trends in regional sea ice coverage. *Climatic Change*, **37**, 617–639.

Stammerjohn, S.E, Martinson, D.G., Smith, R.C., Yuan, X. & Rind, D. (2008) Trends in Antarctic annual sea ice retreat and advance and their relation to El Nino-Southern Oscillation and Southern Annular Mode variability. *Journal of Geophysical Research*, **113**, C03S90, 10.1029/2007JC004269.

Steig, E.J., Schneider, D.P., Rutherford, S.D., Mann, M.E., Comiso, J.C. & Shindell, D.T. (2009) Warming of the Antarctic ice sheet surface since the 1957 International Geophysical Year. *Nature*. **457**, 459–462.

Stroeve, J., Holland, M.M., Meier, W., Scambos, T. & Serreze, M. (2007) Arctic sea ice decline: faster than forecast. *Geophysical Research Letters*, **34**, L09501, doi:10.1029/2007GL029703.

Sullivan, C.W., Arrigo, K.R., McClain, C.R., Comiso J.C. & Firestone, J. (1993) Distributions of phytoplankton blooms in the Southern Ocean. *Science*, **262**, 1832–1837.

Thompson, D.W.J. & Solomon, S. (2002) Interpretation of recent Southern Hemisphere climate change. *Science*, **296**, 895–899.

Toudal, L., Hansen, K.Q., Valeur, H., Wadhams, P., Aldworth, E. & Comiso, J.C. (1999) Mapping of ice in the Odden by satellite and airborne remote sensing, *Deep-Sea Research*, **46**, 1255–1274.

Tucker, W.B., III, Perovich, D.K., Gow, A.J., Weeks, W.F. & Drinkwater, M.R. (1992) Physical properties of sea ice relevant to remote sensing. In: *Microwave Remote Sensing of Sea Ice* (Ed. F. Carsey). American Geophysical Union, Washington, DC. *Geophysical Monograph*, **68**, 9–28.

Wadhams, P. & Davis, N.R. (2000) Further evidence of ice thinning in the Arctic Ocean. *Geophysical Research Letters*, **27**, 3973–3975.

Walsh, J.E. & Johnson, C.M. (1979) Analysis of Arctic sea ice fluctuations 1953–77. *Journal of Physical Oceangraphy*, 9, 580–591.

Walsh, J.E., Chapman, W.L. & Shy, T.L. (1996) Recent decrease of sea level pressure in the Central Arctic. *Journal of Climate*, **9**, 480–486.

Weeks, W.F. & Ackley, S.F. (1986) The growth, structure, and properties of sea ice. In: *The Geophysics of Sea Ice* (Ed. N. Unterstiener), Plenum Press, New York. *NATO ASI Series B: Physics*, **146**, 9–164.

White, W.B. & Peterson, R.G. (1996) An Antarctic circumpolar wave in surface pressure, wind, temperature, and sea ice extent. *Nature*, **380**, 699–702.

Worby, A.P. & Comiso, J.C. (2004) Studies of Antarctic sea ice edge and ice extent from satellite and ship observations. *Remote Sensing of the Environment*, **92**, 98–111.

Yuan, X. & Li, C. (2008) Climate modes in southern high latitudes and their impacts on Antarctic sea ice. *Journal of Geophysical Research*, **113**, C06S91, 10.1029/2006JC004067.

Zwally, H.J., Comiso, J.C., Parkinson, C.L., Campbell, W.J., Carsey, F.D. & Gloersen, P. (1983) *Antarctic Sea Ice 1973–1976 from Satellite Passive Microwave Observations*. National Aeronautics and Space Administration, Washington, DC. *NASA Special Publication*, **459**.

Zwally, H.J., Comiso, J.C. & Gordon, A.L. (1985) Antarctic offshore leads and polynyas and oceanographic effects. In: *Oceanology of the Antarctic Continental Shelf* (Ed. S.S. Jacobs). American Geophysical Union, Washington, DC. *Antarctic Research Series*, **43**, 203–226.

Zwally, H.J., Comiso, J.C., Parkinson, C.L., Cavalieri, D.J. & Gloersen, P. (2002) Variability of the Antarctic sea ice cover. *Journal of Geophysical Research*, **107**, 1029–1047.

Zwally, H.J., Yi, D., Kwok, R. & Zhao, Y. (2008) ICESat measurements of ice freeboard and estimates of sea ice thickness in the Weddell Sea. *Journal of Geophysical Research*, **113**, C02S15, 10.1029/2007JC004284.

7 Sea Ice Bacteria and Viruses

Jody W. Deming

7.1 Introduction and historical perspective

The existence of bacteria[1] in sea ice, from both Arctic and Antarctic samples, was first reported in the late 1960s, when a number of isolates were cultured from melted samples (reviewed by Baross & Morita, 1978; Sullivan & Palmisano, 1984). The discovery came well after recognition that eukaryotic diatoms and other photosynthetic algae bloom within the ice, supporting a complex and dynamic ecosystem of higher trophic levels (reviewed by Horner, 1985). In the 1970s, with the advent of epifluorescence microscopy, which allows the enumeration of all bacteria in a sample whether they are culturable or not, and of radioisotopes as tracers for measuring microbial activity, studies of Arctic sea ice revealed that bacterial densities and their rates of heterotrophic activity or organic carbon consumption could be as high or higher in (melted) sea ice than in underlying seawater (Horner & Alexander, 1972; Kaneko et al., 1978; Griffiths et al., 1978). Similar work on Antarctic sea ice began with expeditions in the 1980s, the decade when sea ice bacteria were studied intensively for their heterotrophic responses to the ice-algal bloom and competitive use and recycling of nutrients (Sullivan & Palmisano, 1981; Sullivan et al., 1982; Sullivan & Palmisano, 1984; Garrison et al., 1986; Kottmeier et al., 1987; Smith et al., 1989). Emerging as a common theme was the prevalence of physical associations between bacteria and sea ice algae, or particulate matter in general, in sea ice (Grossi et al., 1984; Sullivan & Palmisano, 1984), exceeding that typically observed in seawater. Bacteria were considered to incorporate into growing sea ice primarily as riders attached to algae and other particles (Garrison et al., 1983; Grossmann & Gleitz, 1993; Grossmann & Dieckmann, 1994). Their successional stages, at least in relatively warm or lower latitude sea ice, were tracked accordingly with respect to the presence of ice algae (Delille et al., 1995; reviewed by Kaartokallio et al., 2008).

In the decade of the 1990s, several groups took a renewed interest in culturing heterotrophic bacteria from sea ice, this time to acquire uniquely cold-adapted strains and explore their specific ecological, evolutionary and applied significance (Delille, 1992; Helmke & Weyland, 1995; Bowman et al., 1997, 1998; Gosink et al., 1997, 1998; Junge et al., 1998; Nichols et al., 1999). As high densities of both total and culturable bacteria in sea ice continued to be documented, the presence of their viruses[2] at even higher densities was finally discovered (Maranger et al., 1994). The detection of Archaea in sea ice, often curiously attributed to a study in which only seawater samples were collected (Delong et al., 1994), was only recently verified by molecular techniques and then only for Arctic winter sea ice (Junge et al., 2004;

Collins & Deming, 2006; Collins et al., unpublished data). No sea ice Archaea have yet been brought into culture.

Molecular phylogenetic analyses, based on 16S rRNA gene sequences, came late to sea ice relative to other environments. The first application was to collections of Bacteria cultured from sea ice (Bowman et al., 1997, 1998); it was quickly followed by a series of phylogenetic studies targeting the uncultured bacterial populations in sea ice. Clone libraries were generated from extracts of sea ice DNA to identify the dominant inhabitants, fluorescent *in situ* hybridization (FISH) probes were applied to quantify specific bacterial groups microscopically, and DNA fingerprints were generated via a number of methods, from temperature and denaturing gradient gel electrophoresis (TGGE and DGGE) to terminal restriction fragment length polymorphisms (T-RFLP) and amplified ribosomal intergenic spacer analysis (ARISA), to conduct comparative studies across time and space. Questions on microbial diversity, biogeography, seasonal succession, and even responses to hydrocarbon spills in sea ice have now been addressed in more powerful ways than before (Staley & Gosink, 1999; Brown & Bowman, 2001; Junge et al., 2002, 2004; Brinkmeyer et al., 2003, 2004; Gerdes et al., 2005; Kaartokallio et al., 2008; Collins et al., unpublished data). Other recently developed technologies and approaches, including micro-electrodes that can be frozen into the ice to record oxygen changes (Mock et al., 2002) and clever use of cameras (Rysgaard et al., 2008), have contributed to the discovery of zones of anoxia and active microbial denitrification at levels approaching those classically detected in marine sediments (Rysgaard & Glud, 2004), giving new microbial meaning to the sea ice ecosystem as an inverted benthos or 'upside-down counterpart of the bottom life' (Mohr & Tibbs, 1963, p. 246).

Investigators with ideas and methods from disciplines other than polar marine microbiology have regularly expanded knowledge of sea ice bacteria and are beginning to do the same for viruses. Biochemists have discovered cold adaptations in bacterial enzymes, lipids and other cellular constituents that make life in ice possible (reviewed by Feller & Gerday, 2003; D'Amico et al., 2006; Deming, 2009) and, in the process, have encouraged the pursuit of sea ice bacteria and their gene products for biotechnology (Mancuso Nichols et al., 2005b). Genomicists have obtained the first whole-genome sequences for bacteria known to occur in sea ice, *Psychroflexus torquis* and *Colwellia psychrerythraea*, and deduced a remarkable list of attributes that both reflect and enable life in ice (Methé et al., 2005; Bowman, 2008), including the role of viruses as agents of lateral gene transfer. Geophysicists have pushed the observational scale of sea ice to the micrometre level, revealing the *in situ* habitats of microbes in unmelted sea ice (Eicken et al., 2000; Eicken, 2003; Chapter 2) and bacteria within them (Junge et al., 2001), whether as isolated inhabitants (Fig. 7.1) or sharing pore space with diatoms and other particles (Fig. 7.2). Astrobiologists have asked if more study of the coldest winter sea ice formations and their inhabitants, including cold-active viruses (Fig. 7.3; Wells & Deming, 2006a), can contribute to understanding the possible habitability of extraterrestrial ices (Deming & Eicken, 2007). Those examining scientific and philosophical questions on the definition, origin and evolution of life have not missed the relevance of saline ice formation as a process that concentrates otherwise dilute elements and biopolymers (and microbes in Earth ice today) into highly interactive liquid-filled space (Vajda & Hollosi, 2001; Kanavarioti et al., 2001; Wells, 2006; Price, 2007).

In the following sections, I elaborate approaches to studying bacteria and viruses in sea ice, the smallest and most abundant of sea ice inhabitants and key aspects of what has been learned about them in light of both historical work and areas awaiting advancement.
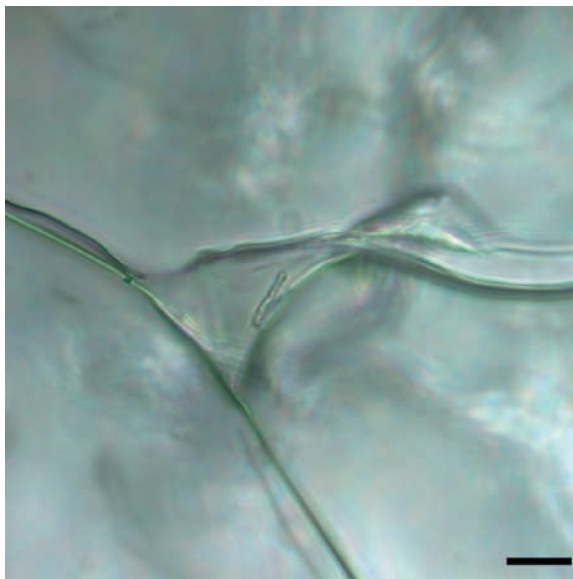
Fig. 7.1 Transmitted light image, taken at −15°C, of a rod-shaped bacterium (apparently dividing on close inspection) along the ice wall of a brine inclusion within a thin section of Arctic winter sea ice (bar = 20 μm; from Junge et al., 2001). Reprinted from the *Annals of Glaciology* with permission of the International Glaciological Society.
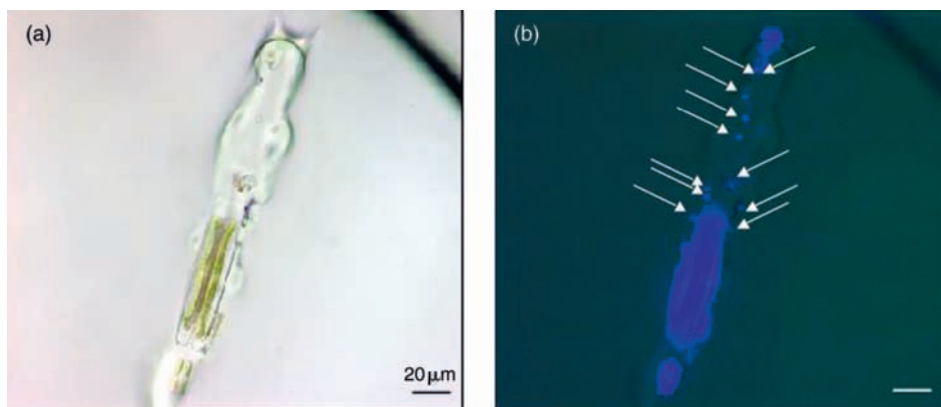
Fig. 7.2 Transmitted light image (a), taken at −15°C, of particles and diatoms with their autofluorescing green chloroplasts in a brine inclusion of a thin section of Arctic winter sea ice; epifluorescent image (b) of the same frame, showing the diatoms stained blue with the DNA-specific stain DAPI and revealing DAPI-stained bacteria (white arrows) associated with the diatoms and clustered at the top of the image (bars = 20 μm; from Junge et al., 2001). Reprinted from the *Annals of Glaciology* with permission of the International Glaciological Society.

The first-edition chapter of this book that included bacteria and viruses within the larger framework of primary production (Lizotte, 2003) served as an initial guide, while other reviews and book chapters specific to bacteria and viruses (Pomeroy & Wiebe, 2001; Mock & Thomas, 2005; Moyer & Morita, 2007; Wells, 2008; Bowman, 2008) and the latest research papers, themselves containing scholarly reviews (Kaartokallio et al., 2008;

Meiners et al., 2008; Różańska et al., 2008), helped to expand my reading of the literature and shape this chapter. It is intended to be read along with other chapters in this book that provide the physical, chemical and ecological context for considering bacteria and viruses in sea ice. My understanding of the subject has also benefited greatly from interactions with numerous students and colleagues who have spent time with me in the field and elsewhere, helping to broaden my focus on extremophiles from those that inhabit the depths of the ocean and its subsurface realm (Deming & Baross, 1993; Deming, 2007a) to those that dwell within its ice-covered surface (Deming, 2002; 2007b). Any errors in presenting published work or flaws in thinking about life in sea ice are mine, not those who have tried to educate me. Enthusiasm over the study of bacteria and viruses in sea ice continues unabated as new investigators discover the wonders of this frozen environment, even as – and perhaps because – climate change threatens to take it from us.

7.2 Sampling issues

Methods

Means to sample sea ice for the study of bacteria and viruses borrow from methods developed first for the larger inhabitants of the ice, from algae and protozoa to macrofauna (Chapters 8–10). The typical sample, when the ice has reached a thickness of 10 cm or more, is an ice core from which sequential sections are cut and melted for analysis, using aseptic technique to the extent possible. All types of thinner and unconsolidated ice (Chapter 2 for definitions of ice by age and formation process) have also been collected using a variety of study-specific techniques to examine bacteria in relation to the ice formation process in fall (Grossmann & Dieckmann, 1994; Gradinger & Ikävalko, 1998). Returning samples of sea ice to the liquid phase has been standard and convenient: all methodologies and analyses developed for pelagic bacteria can be applied to a melted sample. Unfortunately, simply allowing sea ice to melt exposes microbes in the liquid brine phase of the ice to much fresher salinities that can lead to osmotic stress and cell lysis (loss), in spite of cellular adaptations to salinity stress (see Section 7.6). If not also melted with attention to avoiding warm temperatures, cold-adapted microbes can succumb to thermal shock.

   The melting dilemma was recognized years ago for fragile flagellates and ciliates (Garrison & Buck, 1986). An accepted solution for most spring and summer sea ice (relatively warm ice, with a higher volume fraction of seawater-derived brine) has been to melt the ice into a measured volume of seawater first filtered to remove pelagic microbes. The brine inclusions still become diluted as the solid phase of the ice melts, but the drop in salinity and consequent cell losses are minimized. This seawater-melting approach has also been adopted for the study of bacteria (with some exceptions; Kaartokallio, 2004; Kaartokallio et al., 2008). The laboratory melting of sea ice samples, however, can create salt gradients more rapidly than experienced in nature; it also alters the *in situ* physical associations that bacteria may have had with each other while inhabiting a brine inclusion, as well as with other organisms and particles, including gelatinous material, and the ice itself. The study of viruses in sea ice requires additional attention to the melting solution, either to account for viruses present in the solution (Maranger et al., 1994; Wells & Deming, 2006a) or to remove them from it prior to use (Gowing et al., 2002).

An alternative approach to melting sea ice into seawater has been to attempt to collect the brine phase directly. If the ice is warm, unconsolidated or very thin, the brine will drain from it immediately upon recovery, making the collection of a quantitative or representative sample a challenge. If the ice is thicker, sections can be centrifuged at sub-zero temperature to collect the brine phase, though the volume collected and the match between *in situ* and centrifugation temperature are rarely optimal. The more common practice for thick ice involves drilling an ice core partway into the ice sheet and leaving the empty hole to accumulate brine at its base for later sampling. This 'sack-hole' approach is effective in terms of the volume of brine that can accumulate, but the locational origin in the ice sheet of the sampled brine cannot be known with any precision. Although each of these methods has its limitations, their use has verified that many if not most organisms, including bacteria and viruses, live within the brine inclusions of sea ice rather than frozen into its solid phase.

If the ice is very cold with a greatly reduced brine volume fraction, as in winter near the interface with snow or the atmosphere, direct collection of the brine is no longer feasible. Melting, even into seawater, is problematic because the salinity gradients between highly concentrated winter ice brines and seawater are steep (e.g. from 21% salt at −20°C to 3.5% salt at −1°C), again inducing osmotic losses. In exploring ways to circumvent this problem, we developed an isothermal–isohaline melting approach, whereby winter sea ice is melted into an artificial brine solution of higher salinity than the natural brines of interest (Junge et al., 2004). The equations of Cox and Weeks (1983) can be used, along with the volume and temperature of the ice to be melted, to calculate how much salt needs to be in the melting brine such that the final melted sample has approximately the same salinity (and sub-zero temperature) as the original brine inclusions. In testing this melting strategy to determine its effectiveness against cell loss relative to seawater melting, we found that bacterial abundance in the seawater melts were only half the level in isothermal–isohaline melts (unpublished work). We now regularly use this approach for the study of both bacteria and viruses (Wells & Deming, 2006a; Collins et al., 2008, unpublished data).

A further advance in the study of colder sea ice has been the development of means to examine micrometre-scaled features of unmelted ice sections microscopically (Junge et al., 2001). The approach is suitable for studies of ice at temperatures below −5°C, given that above this thermal threshold ice becomes permeable (Golden et al., 1998) and brine will drain from it, compromising efforts to evaluate the *in situ* conditions experienced by microbes (Sullivan & Palmisano, 1984). A freezer laboratory equipped with ice-sectioning tools and an epifluorescence microscope, factory-modified to operate at sub-zero temperatures, is required for the approach, although a cold stage on a microscope may be adaptable (so far used to examine unmelted freshwater or glacial ice, not sea ice; Mader et al., 2006). Initial use of the freezer-microscope approach with winter sea ice yielded the first images of bacteria and diatoms inhabiting an undisturbed brine-filled ice pore at −15°C. In some cases, if the microbe was large enough (a rarity; Fig. 7.1) or contained autofluorescent chloroplasts (occasional diatoms; Fig. 7.3), the use of transmitted light was sufficient to see the organism; no staining was required. For enumeration of bacteria, however, the DNA-specific stain DAPI was prepared in an isothermal–isohaline solution, applied directly to the cut surface of a thin ice section and allowed to diffuse into the open brine inclusions. Patient and thorough examination of sea ice sections (and artificially prepared sections in control experiments) using this approach revealed that the vast majority (95%) of microbes do indeed inhabit the liquid brine phase of the ice. As had been observed in melted samples from earlier studies
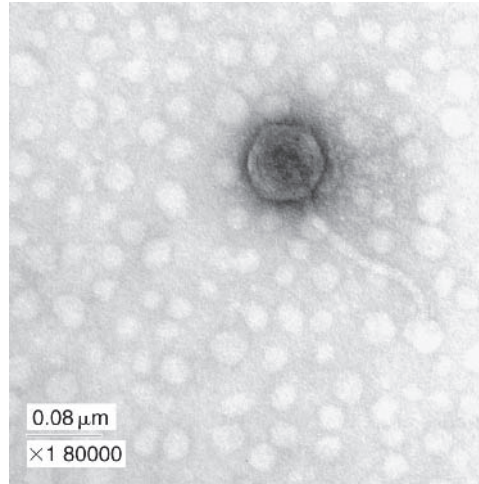
Fig. 7.3 Transmission electron micrograph of the *Siphoviridae* phage 9A that infects two species of the γ-Proteobacterial genus *Colwellia* at sub-zero temperatures, including the sea ice bacterium *C. demingiae*. Reproduced from Wells and Deming (2006b) with permission from Inter-Research.

of sea ice microbial communities (Garrison et al., 1983; Grossi et al., 1984; Sullivan & Palmisano, 1984; Grossmann & Gleitz, 1993; Grossmann & Dieckmann, 1994), as well as more recent ones (Meiners et al., 2003, 2004, 2008; Junge et al., 2004), the bacteria were often associated with particles, aggregates and algal cells. Some appeared to adhere to the face of an ice-crystal framing the inhabited pore (Fig. 7.1), though by what mechanism is not clear. Although particle-associated bacteria are well studied in other environments and eukaryotic inhabitants of sea ice have long been identified as 'thigmotactic' (Mohr & Tibbs, 1963, p. 246) or surface-seeking, the study of bacterial thigmotaxy in sea ice is in its infancy (see Section 7.3).

A major contributor to the development of this freezer-microscope method took it a step further by adapting a second stain, Alcian Blue, to sea ice brine (Krembs et al., 2002). This stain binds to organic polymers, called extracellular polysaccharide (sugar) substances (EPS), already known from earlier melt studies to be present in high concentrations in bottom sea ice, near the ice–water interface (Krembs & Engel, 2001). What the unmelted approach revealed was that virtually every pore space within the ice, and throughout the length of an ice core, contains EPS, and whether or not the pore also contains microbes (Krembs et al., 2009). The many implications of this finding, which include cryoprotection, buffering against osmotic shock and viral attack, stabilizing enzymes and providing fuel for heterotrophic activity (Krembs & Deming, 2008), are addressed later (Section 7.6), but the very presence of EPS as focal points for bacterial location in sea ice has become abundantly clear from the detailed work of Meiners et al. (2003, 2004).

Developing a third stain for use with unmelted ice, one that would address microbial activity *in situ*, was inevitable. The CTC stain, which allows detection of bacteria actively respiring oxygen after an incubation period, was an obvious choice. It had first been applied to melted summer sea ice, revealing higher percentages of active cells in sea ice than in underlying seawater (Junge et al., 2002), and then to isothermal–isohaline melts of winter sea ice (Junge et al., 2004), revealing active bacteria associated with particles, and increasingly so

the colder the temperature (down to –20°C). Meiners et al. (2008) advanced the field by applying CTC to unmelted spring and summer sea ice sections that were returned to the ice sheet for *in situ* (core hole) incubation, mimicking an *in situ* primary production method that two of the authors had developed earlier (Mock & Gradinger, 1999). Activity was stopped in the ice sections by providing fixative in the melting solution, after which DAPI and Alcian Blue stains were applied to subsamples of the melted ice. Using all three stains in this way, which bypasses the need for a freezer-adapted microscope, gel-like particles of EPS were shown not only to be concentrated loci of bacteria, but also to be hot spots of *in situ* bacterial activity.

The stains available for detecting viruses or bacteriophage in seawater have not yet been applied to unmelted sea ice. As a result, we continue to assume, based in part on sack-hole brine collections (Gowing et al., 2002; Gowing, 2003), that viruses partition into the brine phase along with their microbial hosts. Nor have fluorescently labelled gene probes, already effective at quantifying specific phylogenetic types of Bacteria in melted ice samples (Brinkmeyer et al., 2004), been adapted for use in unmelted ice. A fluorescently labelled protein substrate analog (L-leucine 7-amido-4-methylcoumarin), however, has been used to measure extracellular enzyme (protease) activity in unmelted winter sea ice sections, and to a record low temperature of –18°C (Deming, 2007b), suggesting that more promising work using a variety of fluorescent stains in sea ice lies ahead. In spite of earlier concerns about achieving a homogeneous distribution of an added tracer to unmelted sea ice for subsequent incubation (Helmke & Weyland, 1995), renewed efforts to adapt this general approach for use with radioisotope or stable-isotope tracers, and thus revisit available rates of bacterial activity in sea ice, may be worthwhile. Current views on bacterial activity in sea ice are based largely on the results of incubating diluted-melted samples (see Section 7.2).

Scaling

Confirmation that almost all bacteria inhabit the liquid brine phase of sea ice, rather than freezing into the solid phase, has brought renewed attention to the issue of scaling. How should bacterial (and viral) parameters be scaled – to area or volume of ice sampled, to volume of sample after melting (corrected for dilution) or to volume of the brine phase? An earlier recommendation to improve comparative analyses between studies was to scale all biological abundance or biomass measurements to area (m^2) of the ice sheet examined (Horner et al., 1992), implying the need to sample the entire, or at least consistently same, thickness of ice. If not the whole core, then the algal-rich bottom of spring and summer ice where higher trophic levels feed has often been the targeted ice horizon for study. A fundamental difference between bacteria and eukaryotic inhabitants of sea ice, however, is the presence of bacteria in significant numbers throughout the ice, regardless of ice age, thickness or season (Section 7.3). The depth-integrated biomass of bacteria in an ice core can exceed algal (and other) biomass not only during the cold dark winter (Collins et al., 2008), when shrinking pore space and encroaching ice crystals limit the size of sea ice inhabitants to the smallest organisms (Krembs et al., 2000, 2002), but also during the algal bloom season (Gradinger et al., 1999). In some studies, bacterial parameters have been scaled simply to meltwater volume, without converting (or providing required details to convert) to initial volume of ice sampled, much less area, thus preventing intercomparisons. Scaling parameters to the depth-specific volume of the sea ice sampled appears to be the more useful approach for comparative purposes than scaling to meltwater or reporting only the areal values (Horner et al., 1992; Deming & Eicken, 2007).

Ultimately, the research question determines the scaling units. When bacterial numbers from melted samples are scaled to brine volume, the calculated densities invariably exceed those scaled to ice volume. The discrepancy is greater the colder the ice (and smaller the brine volume fraction). If the research question concerns bacterial interactions with each other or with other organisms, viruses, organic compounds or inorganic salts also partitioned into brine, then scaling to brine volume is not only sensible but also yields more significant relationships between bacterial and other parameters than when all are scaled to ice volume (compare brine-scaled findings in Junge et al., 2004, with melted ice scaling in Gowing et al., 2004). Though we must still largely assume that viruses partition into the brine phase along with their hosts, scaling viruses to brine volume has revealed the high contact rates between viruses and hosts that are possible within the brines of very cold sea ice (Wells & Deming, 2006a).

7.3 Abundance and distribution

Ubiquity

Unlike other inhabitants of sea ice, bacteria have been found in significant numbers, as visualized by epifluorescence microscopy, in every ice sample, whether melted or not, that has been examined for this purpose. Reported densities, scaled to volume of ice sampled, range from 4×10^3 ml^{-1} in upper horizons of the coldest sea ice yet examined, in Arctic winter (Collins et al., 2008), to nearly 3×10^7 ml^{-1} in summer bottom ice following the ice-algal bloom in both Arctic and Antarctic sea ice (Krembs & Engel, 2001; Thomas et al., 2001). The latter rivals or exceeds the maxima found in most aquatic environments. Considering data from many Arctic and Antarctic studies led me to develop a generalized depiction of this wide range of observed bacterial densities according to season (Fig. 7.4; revisited for its other details Section 7.4). Early reports of bacterial abundance falling below detection limit in sea ice samples were based on highly selective culturing assays at temperatures foreign to sea ice, rather than on direct microscopy. When quantitative culturing assays have closely mimicked *in situ* sea ice conditions, culturable numbers have approached 60% of the direct count, making sea ice a striking exception to the 'bacterial enumeration anomaly' (Junge et al., 2002; Brinkmeyer et al., 2003), which holds that only 0.01% or less of the total bacteria present in an environmental sample can be cultured. This unusual degree of culturability, matched only by that observed in sewage samples, is attributed to the availability of high concentrations of dissolved, labile organic matter, a general characteristic of sea ice (Thomas et al., 1995, 2001), which, in turn, helps select for a predominance of cold-adapted heterotrophic bacteria (Helmke & Weyland, 1995).

Although relatively few sea ice samples have been examined to quantify viruses microscopically (Maranger et al., 1994; Gowing et al., 2002, 2004; Gowing, 2003; Wells & Deming, 2006a), bacteria are always accompanied by bacteriophage throughout Earth's environments, including other extreme ones (Ortmann & Suttle, 2005), and almost invariably in higher numbers than their hosts. A typical virus to bacteria ratio in aquatic environments is 10 (or less). Bacterial viruses are defined for microscopic purposes as the smallest of DNA-staining viral particles, less than 110 nm in diameter, while an ability to infect bacteria meets the formal definition. In sea ice, and again scaled to volume of ice sampled, the
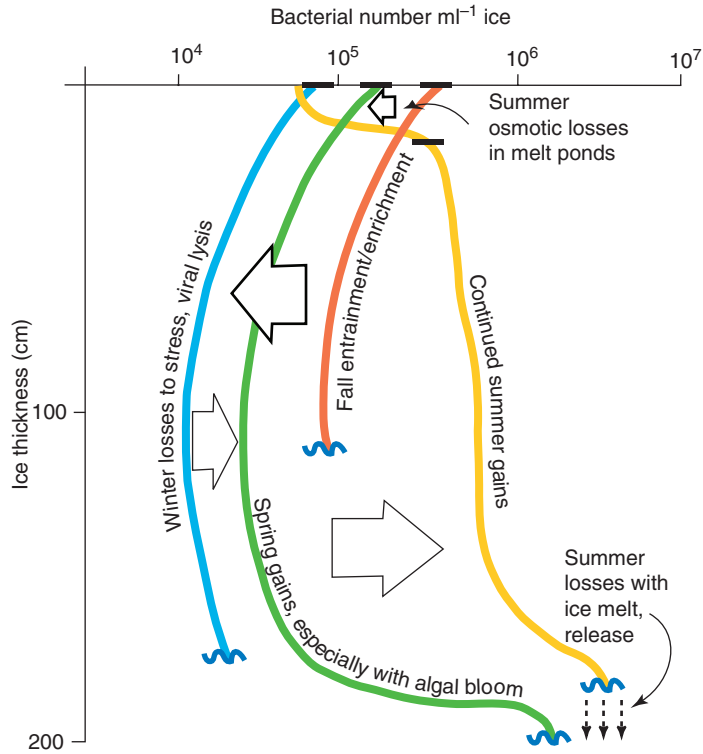
Fig. 7.4 Idealized depth profiles of seasonal changes in bacterial abundance in sea ice: autumn cell entrainment and enrichment (relative to seawater) into new ice (orange line); winter losses (blue line); spring gains, greatest where algae bloom (green line) and continued summer gains prior to ice melt, with osmotic losses in surface melt ponds and releases from bottom ice during ice melt (from data and concepts in Grossmann & Dieckmann, 1994; Gradinger & Zhang, 1997; Delille et al., 2002; Brinkmeyer et al., 2004; Meiners et al., 2004, 2008; Collins et al., 2008).

densities of bacteriophage range from 4×10^5 ml^{-1} in Arctic winter sea ice (Wells & Deming, 2006a) to 1.3×10^8 ml^{-1} in bottom ice during the spring ice-algal bloom (Maranger et al., 1994). The even less well-studied eukaryotic viruses, microscopically defined as greater than 110 nm in diameter, usually account for less than 10% of the total number of viruses of all sizes detected in a sea ice sample (Gowing et al., 2002), in keeping with the general observation that bacterial abundance (though not necessarily biomass) also usually exceeds ice-algal abundance (Gradinger & Zhang, 1997; Delille et al., 2002). Information on eukaryotic viruses in sea ice appears limited to the pioneering microscopic work presented in two recent reports (Gowing, 2003; Gowing et al., 2002).

The ubiquity of microbes and their viruses in any environment is, of course, a matter of scale. With the diameter of most bacteria in sea ice being less than 1 µm (they can be larger in some cases, especially in the midst of the ice-algal bloom), finding a micrometre-scale brine pore in unmelted winter sea ice (Fig. 7.1) devoid of bacteria is possible (though rare; Junge et al., 2001). Finding a typical sea ice sample – a core section several centimeters thick – to be bacteria-free would not be reasonable. Consider that surface seawater in the fall prior to freezing contains bacteria in densities that range from 3×10^5 ml^{-1} to 2×10^6 ml^{-1} (Gradinger & Ikävalko, 1998; Riedel et al., 2007). In spite of brine expulsion as sea ice

forms, young sea ice is usually enriched in bacteria relative to seawater, as discussed below, and most of them survive even a severe winter (Collins et al., 2008).

Physical enrichment

The idea that planktonic organisms, particularly algae and other protists, are incorporated into growing sea ice in numbers disproportionate to those in surface seawater was first suggested many years ago (reviewed by Ackley & Sullivan, 1994; Różańska et al., 2008). The proposed mechanism that has best survived observational and experimental scrutiny involves the physical scavenging of particles, including organisms, by frazil ice crystals that form in underlying waters and rise to concentrate at the surface, forming sea ice (Garrison et al., 1983; Ackley & Sullivan, 1994). From the bacterial perspective, comparative observations of densities in source seawater and new ice soon after its formation have often (Grossmann, 1994; Gradinger & Ikävalko, 1998; Delille et al., 2002; Riedel et al., 2007), though not always (Grossmann & Dieckmann, 1994), indicated a physical enrichment of bacteria in the ice. Evidence that bacteria require an initial adjustment period to ice conditions before growth can occur (Grossmann & Dieckmann, 1994) reinforces that the enrichment mechanism is physical. The bacterial enrichment factor for ice over seawater is typically 5–10, but ranges widely from 2 to 54 (Sullivan & Palmisano, 1984; Gradinger & Ikävalko, 1998; Riedel et al., 2007), likely reflecting the random and complex processes involved in ice formation (see Chapter 2). The densities achieved can approach those observed at the end of the summer season as a result of *in situ* bacterial production (Delille et al., 1995, 2002; Fig. 7.4). Even so, the physical enrichment effect for bacteria during ice formation is almost always less than that observed for algae and other protists.

Because particle size influences entrainment, with larger particles entraining preferentially into sea ice (Grossmann & Gleitz, 1993, Reimnitz et al., 1993), the enrichment of bacteria in new ice is often explained by their attachment to larger particles, especially algal cells with a 'sticky' exterior coating (Grossmann & Dieckmann, 1994; Gradinger & Ikävalko, 1998; Weissenberger & Grossmann, 1998). Organic detritus and sediment grains and aggregates, which also partition into the liquid phase of the ice matrix (Stierle & Eicken, 2002), can deliver large numbers of attached bacteria into the ice (Junge et al., 2004; Deming & Eicken, 2007). DNA-stained bacteria have been observed attached to organic debris (Sullivan & Palmisano, 1984) and gelatinous exopolymer particles (Meiners et al., 2003, 2004, 2008) in melted sea ice samples, including in isothermal–isohaline melts (Junge et al., 2004), as well as directly in the brine pores of unmelted ice (Junge et al., 2001). While only a few percent of bacteria in seawater may be attached to particulate matter, up to 50% of bacteria in sea ice are attached to one surface or another. Whether specific phylogenetic or phenotypic types of bacteria entrain into sea ice more readily than others has not been tested directly, but the obvious candidates are those that associate physically with algal cells or produce their own gelatinous exopolymers or EPS (Mancuso Nichols et al., 2004, 2005b; Marx et al., 2009), a known means to attach. Many of the genera of Bacteria that have been cultured from sea ice or detected in direct phylogenetic analyses of sea ice fit these categories (see below). In spite of the general view that bacteria entrain into sea ice by association with larger particles readily scavenged by rising ice crystals, the possibility of preferential entrainment or retention as individual cells merits reconsideration, given recent findings that some bacteria produce

external coatings that have an affinity for ice itself (Wilson et al., 2006; Kawahara, 2007; Raymond et al., 2007; Ewert Sarmiento & Deming, 2008).

Are viruses also physically enriched into sea ice during its formation? The issue has not been examined experimentally, but comparative analyses of the abundance of both bacteriophage and eukaryotic viruses in underlying seawater and new sea ice indicate substantial enrichment factors of 10–100 (Maranger et al., 1994; Gowing et al., 2004). Interpreting these results as a physical enrichment is complicated by the (unexplored) possibility that virally infected hosts succumb upon entrainment into the ice, releasing large bursts (numbers) of viruses into the ice in the process. On the other hand, if viruses embed in gelatinous particles or cell coatings, ice enrichment may occur in the same way as for particle-attached bacteria. Supporting the concept of physical enrichment of viruses via passive association with larger particles are observations of particle-associated bacterial viruses in polar surface waters prior to ice formation (Yager et al., 2001) and of eukaryotic viruses embedded in organic detritus and small faecal pellets in sea ice melts and brines (Gowing et al., 2002; Gowing, 2003). Whether or not the protein capsids of individual viruses (Fig. 7.3) express an affinity for ice remains to be explored.

Physical losses

The reverse process – physical losses of bacteria (and presumably viruses) from sea ice – takes several forms, both at the bottom and top of the ice cover. When biomass in general is released from bottom sea ice into the water column following the ice-algal bloom or the onset of ice melt (Krembs & Engel, 2001), substantial numbers of bacteria and viruses can also be expected to leave the ice. This issue was examined recently, both experimentally and with comparative field measurements of bottom ice and underlying seawater, from the perspective of the role of EPS as 'sticky' exopolymers (Riedel et al., 2006). EPS alone did not explain the loss of bacteria from the ice (exopolymers may have been more responsible for their retention); instead, EPS-rich algae appeared to be the transport mechanism, mirroring how their bacterial predecessors may have entered the ice when it first formed. Unknown is the extent to which bacteria may hydrolyse and degrade the transport EPS in which they are embedded, whether in the ice following enrichment or after release, as a source of nutrition (but see Riedel et al., 2007). How viruses may be transported or otherwise affected by EPS is also unexplored territory.

At the surface of the ice, physical losses of bacteria and their viruses may occur during ice growth through winter, when brine is expelled upwards from the surface ice due to pressure gradients, and in the summer as solar radiation increases, air temperatures warm, snow melts and surface ponds form (Fig. 7.4; Chapter 2). Although brine expulsion is well documented in the former case, the literature appears absent of any measurements of corresponding losses of bacteria or viruses. Recent work suggests that the expulsion of both bacteria and viruses in brine from surface sea ice may be substantial (see Section 7.7). In the case of summer melt ponds, primarily a surface feature of Arctic sea ice, their freshwater nature and exposure to UV make them an oligotrophic (nutrient-poor) and unfriendly environment to many forms of life (Wickham & Carstens, 1998). Although a separate microflora, characterized as freshwater to estuarine, exists in these ponds (Brinkmeyer et al., 2004), the drop in bacterial densities from surface sea ice into overlying snow-melt waters (Fig. 7.4) suggests

that many sea ice bacteria, released into ponds as the surface ice itself begins to melt, succumb to osmotic shock. The fate of viruses in melt ponds is unknown.

Within the ice cover itself, physical displacements of bacteria and viruses can be expected to occur as brine moves via gravity drainage and expulsion. Although such displacements can help to explain the variability commonly observed in ice core profiles of bacterial content (Sullivan & Palmisano, 1984; Gradinger & Zhang, 1997; Collins et al., 2008), studies examining the potential for bacterial transport within the ice are rare (Krembs et al., 2000). Depending on the temporal and spatial scale of brine transport, the ability of cold-adapted bacteria to swim at sub-zero temperatures (Junge et al., 2003) may complicate the matter (larger eukaryotic organisms are well known to migrate towards more clement conditions in the ice). Nevertheless, depth profiles of bacteria in first-year sea ice prior to the spring algal bloom (Fig. 7.4; Collins et al., 2008) assume the classic 'C'-shape of salinity profiles (Chapter 2), implying that physical processes, from initial enrichment to gravity drainage and brine expulsion, may be the primary determinants of initial bacterial distributions in sea ice before the passage of time and change in conditions allow biological processes to come to the fore.

7.4 Bacterial and viral dynamics

Unlike the study of algal dynamics in sea ice, which has benefited from *in situ* incubation approaches for unmelted sea ice (Mock & Gradinger, 1999), *in situ* fluorometry (Rysgaard et al., 2001) and the establishment of unique microcosms (Mock et al., 2003), the study of bacterial and viral dynamics in sea ice has, with rare exception, relied upon the incubation of melted sea ice samples (see Section 7.2). Although much has been learned from such incubations, the degree to which the rates obtained may reflect *in situ* activity, within the ice matrix, remains uncertain. In what follows, both rates derived from incubation experiments with melted ice and patterns of comparative stocks over time or space are used in an attempt to develop a seasonal perspective on bacterial and viral dynamics in first-year sea ice (depicted schematically for bacteria in Fig. 7.4). The available information on bacterial and viral dynamics in multiyear ice is too limited to attempt a parallel analysis, but hints of seasonal changes have been detected in bacterial diversity (lower in winter; Brinkmeyer et al., 2003) and in the balance between bacterial and algal production rates (shifting towards bacteria in summer; Kottmeier & Sullivan, 1990). Sea ice that has survived more than one annual cycle in the Arctic appears to continue to provide a dynamic environment for heterotrophic bacteria, given the detection of larger cell sizes than usual in late summer (Gradinger & Zhang, 1997) and high levels of ammonia indicating active recycling of organic nitrogen even during winter (Thomas et al., 1995). By summer in Antarctic multiyear ice, neither bacterial nor viral abundances in summer could be distinguished from first-year ice (Gowing et al., 2004).

Autumn

As sea ice forms in autumn, the bacteria entrained from seawater into early stages of young ice (Chapter 2) appear to suffer a temporary reduction in activity, with a resurgence in cellular production once the ice has consolidated (Grossmann & Dieckmann, 1994). Little is

known of the initial 'adjustment' period, but obvious physiological responses to enclosure within an ice matrix and segregation into a brine phase that is saltier and richer in dissolved organic substrates than seawater include regulatory shifts in the substrate affinity of membrane uptake systems and the induction of defenses against osmotic and thermal stress (Section 7.6). Some bacteria may not adjust to ice sufficiently to survive or flourish within it, but the overall success of the adjustment is reflected in rates of ice-bacterial production that exceed ice-algal production, as well as bacterioplankton production in open water (Grossman & Dieckmann, 1994). A shift in the production balance towards sea ice bacteria at this stage is consistent with their access to elevated concentrations of dissolved organic matter in the ice (Thomas et al., 1995, 2001) and with the seasonal onset of light limitation for the ice algae, both as solar radiation diminishes and as the ice (and snow cover) thickens above the bottom ice zone where the algae reside.

The dominance of bacterial production over algal production in fall sea ice is also consistent with observations that conventional limits on bacterial production, set by protistan grazing and viral infection, do not appear to increase in young sea ice relative to those in seawater (but see later seasons below). For heterotrophic protists, the negative effects of decreasing inhabitable space within the sea ice may reduce their relative grazing impacts on ice bacteria (difficult to measure *in situ* for any form of ice), except near the ice–water interface (Krembs et al., 2000), or religate more important grazing impacts to warmer ice seasons (Laurion et al., 1995). For viruses, the 'common' ratio of viruses to bacteria in fall sea ice (Gowing et al., 2004) is not higher in newly formed ice but instead matches the average of 10 for seawater. The limited amount of information available on bacterial or viral dynamics in fall sea ice, however, leaves open many scenarios to explore. For example, what happens to the viral–host relationship when seawater bacteria are newly encased in sea ice and experience temporarily stressful conditions is not known. Reports of some very high virus-to-bacteria ratios in fall sea ice samples (up to 119; Gowing et al., 2004) suggest that bulk measurements may be masking important activities occurring at the scale of the organism.

Winter

The onset and progress of the winter season brings increasingly severe temperatures, especially in the Arctic. Below about −5°C, when sea ice effectively becomes a closed system (Golden et al., 1998), dropping temperatures simultaneously reduce the fraction of the ice that remains liquid. This volume reduction means that bacteria and viruses, along with sea salts, become increasingly concentrated in the brine inclusions, as do any other particulate, gelatinous or dissolved organic and inorganic components. Algal cells and other eukaryotes, given their larger sizes and greater cellular fragility, rarely appear intact in the upper zones of the ice (see exceptions in Fig. 7.2), where conditions are most severe; instead, they occupy the larger brine inclusions at ice depths approaching the interface with seawater, where conditions support their existence (Krembs et al., 2000; Krembs & Engel, 2001). Given the ubiquity of bacteria in sea ice and their relative hardiness under extreme conditions, the fate of bacteria in winter sea ice has drawn interest, in the Arctic Ocean where conditions tend to be most severe (Krembs et al., 2002; Junge et al., 2004; Collins et al., 2008), and in Antarctic seas (Delille et al., 1995, 2002; Helmke & Weyland, 1995) and the Baltic Sea (Kaartokallio et al., 2008) under milder conditions. Regardless of location, minima in bacterial abundance have been observed during the winter season (Fig. 7.4).

The physical effects of encroaching ice crystals in winter Arctic ice were first suspected to damage cells and reduce bacterial numbers as temperatures dropped. This idea lost favour when gelatinous exopolymers were found throughout winter sea ice brines, apparently serving as a physical buffer against ice-crystal damage to eukaryotic cellular structures more vulnerable than bacteria (Fig. 7.2; Krembs et al., 2002, 2009; Krembs & Deming, 2008). Because EPS was observed to increase in winter sea ice largely devoid of algal cells, both in laboratory incubations and in the field over the course of a winter season (Fig. 7.5), bacterial EPS production was invoked to explain why bacterial losses were not greater than observed in winter sea ice (from an undetectable loss to a 50% loss in some ice horizons; Collins et al., 2008). The most obvious biological process to explain why the lowest bacterial abundances in sea ice are measured in winter is virally mediated cell death (Collins et al., 2008). Although bacterivorous protists become important agents of mortality during the warmer seasons (Różańska et al., 2008), they are not known to inhabit the restricted brine space of Arctic winter sea ice in sufficient numbers to alter the abundance of their bacterial prey (Krembs et al., 2000, 2002). Bacteriophage, however, are present in winter ice, have high contact rates with their potential hosts due to the winter brine-concentrating factor, and appear capable of reducing bacterial numbers in sea ice brines (at −12°C and 16% salt, the most extreme conditions tested; Wells & Deming, 2006a). Although the reported winter ratios of viruses to bacteria, a proxy for viral activity (higher ratios imply greater viral production), are not as high as in the warmer seasons (Maranger et al., 1994), they support the notion of modest rates of infection and cell loss.

That an overall reduction in bacterial numbers characterizes the dynamic in winter sea ice does not translate to cellular inactivity. To be infected virally and produce new viruses, the bacterial host had to have been actively synthesizing organic compounds for the new viruses
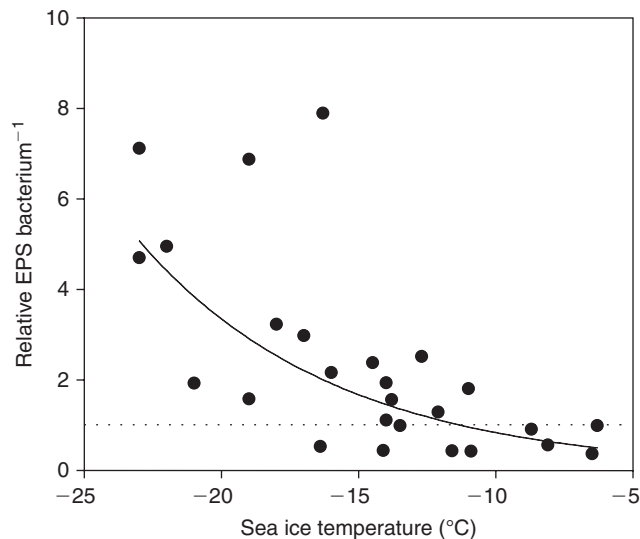
Fig. 7.5 Wintertime increases in EPS concentration per bacterium in Arctic sea ice as a function of ice temperature *in situ*. Increases are relative to concentration at the warmest temperature, highlighted by the dotted line at unity. Data are from upper ice depths of 40–70 cm over a 3-month period from January to March 2004 (Collins et al., 2008), best fit to an exponential curve where $r^2 = 0.46$.

prior to its demise. The use of the CTC stain and fluorescent 16S rRNA probes for Bacteria (see Section 7.2) has revealed that up to 4% of the bacteria in Arctic winter sea ice are actively respiring oxygen and up to 86% have maintained their machinery for protein synthesis at temperatures as low as –20°C (and corresponding brine salinities as high as 209‰; Junge et al., 2004). In studies of warmer (from -1°C to -10°C) Antarctic winter sea ice, bacterial production has been readily measured in melted samples (mainly of bottom ice) held at -1°C to -2°C. The average rates of $1-5$ mg C m^{-3} d^{-1} can be considered annual minima (Kottmeier & Sullivan, 1987a, b; Helmke & Weyland, 1995), since rates (albeit from other studies) will increase considerably come spring and summer. On the other hand, these winter bacterial production rates equal or exceed rates of primary production measured in the same ice, giving winter sea ice its reputation for net heterotrophy.

The transition from winter to spring sees a reversal in the winter trends of bacterial losses and reduced activity with the onset of renewed heterotrophic growth and production (Fig. 7.4). The organic substrates to support this resurgence derive from new and old resources. Bacterial increases near the seawater interface, observed in both Arctic and Antarctic bottom sea ice, are attributed to the onset of the ice-algal bloom and its early release of dissolved organic matter for ready bacterial consumption (Horner & Alexander, 1972; Stewart & Fritsen, 2004). In upper regions of the ice, where algae are not blooming or even present, bacterial increases during this seasonal transition period may be attributed to the consumption of dissolved organic carbon and possibly EPS, concentrated in the ice during fall formation or produced during winter to protect against cell losses (Krembs et al., 2002; Riedel et al., 2007; Collins et al., 2008). The bacterial consumption of dissolved substrates for growth is direct, but the consumption of EPS first requires enzymatic hydrolysis or breakdown of the component polysaccharides to molecular sizes readily transported across the bacterial membrane. The presence of cold-active extracellular enzymes in sea ice that could begin this process, even during winter, has been demonstrated (Helmke & Weyland, 1995; Huston et al., 2000; Deming, 2007b), but evidence to link their activities to the breakdown of EPS has not.

Spring

As spring arrives, bacterial numbers are already on the rise throughout sea ice (Fig. 7.4), in some regions and zones (bottom ice) at an exponential pace. Seasonal (winter–spring) transition studies of viruses in sea ice are not available, but a study by Maranger et al. (1994) provides a remarkably complete data set for evaluating bacterial–viral dynamics in Arctic spring sea ice. At the start of the ice-algal bloom, densities of bacterial viruses in bottom ice are already very high (9×10^7 ml^{-1} ice; Maranger et al., 1994), and much higher than densities reported for underlying seawater and, in another study, for winter sea ice (>100-fold; Wells & Deming, 2006a). Both bacteria and viruses then appear to follow the progress of the ice-algal bloom, increasing in abundance as chlorophyll concentrations rise (Fig. 7.6a). The ratios of viruses to bacteria in spring sea ice, however, are among the highest reported for any environment, up to 72 (Fig. 7.6b; Maranger et al., 1994). To achieve such high ratios, in a defined laboratory setting, requires the presence of actively growing bacteria, prior to their demise upon the release of new viruses. The results of bacterial production assays (also reported by Maranger et al., 1994), when scaled to the individual cell (Fig. 7.6b), are consistent with applying that explanation to spring sea ice: the highest virus-to-bacteria ratios correspond to the presence of the most active cells. Other measures of individual cellular
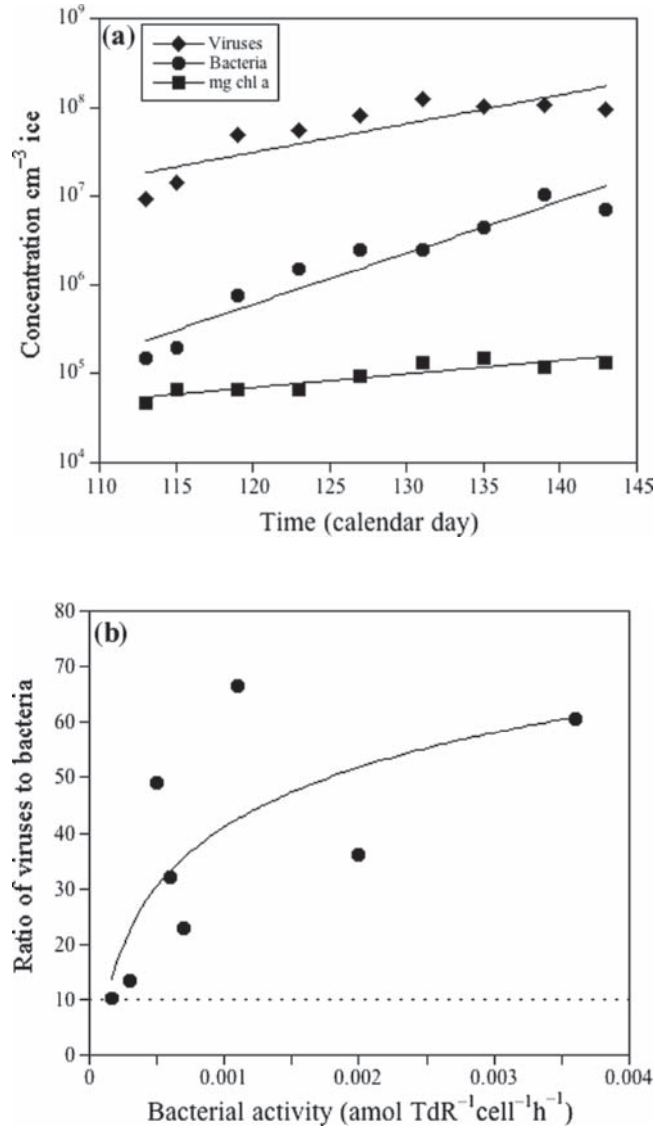
Fig. 7.6 (a) Springtime increases in concentrations of chlorophyll *a*, bacteria and viruses in melted sea ice samples. Data are best fit to linear regressions where $r^2 = 0.74$, 0.71 and 0.53, respectively. (b) Springtime relationship between ratio of viruses to bacteria (the dotted line highlights the typical ratio of 10 in seawater) and cell-specific bacterial growth (measured by thymidine incorporation). Data are best fit to a logarithmic curve where $r^2 = 0.53$. Replotted from Maranger et al. (1994) with permission from Inter-Research.

activity (by CTC stain) support this idea, given the marked increase in the percentage of active bacteria in spring sea ice (up to 17% in bulk ice and 38% in EPS aggregates within the ice; Meiners et al., 2008) compared to winter sea ice (1–4%; Junge et al., 2004). (Note that the CTC stain only allows visualization of the most active cells in a sample; many others may be active but fall below the detection limit of the method.) Whereas modest rates of viral production (and bacterial activity) may explain bacterial losses in winter sea ice, viral

production (and host death) simply accompanies the more robust bacterial production that occurs in spring sea ice, as readily consumable dissolved substrates become plentiful. Again, the importance to bacterial–viral dynamics of 'stored' organic substrates from fall or enzymatically hydrolysed EPS prior to the spring bloom remains to be determined.

The traditional roles of heterotrophic bacteria in aquatic ecosystems come into full play in the network of brine channels that characterize bottom sea ice through the warmer seasons of spring and summer, in all geographic regions of sea ice. Concentrated and labile dissolved organic matter (Thomas et al., 1995, 2001) derived largely from ice algae ensure active and robust bacterial assemblages (Cota et al., 1990; Smith & Clement 1990; Grossmann & Dieckmann 1994; Helmke & Weyland 1995), with production rates on the order of 20–30 mg C m^{-3} d^{-1}. Although these rates are considerably higher than reported fall–winter rates, bacterial production typically represents less than 10% of primary production during spring and summer (Grossi et al., 1984; Kottmeier & Sullivan, 1987a,b; Kottmeier et al., 1987; Smith & Clement, 1990; Grossmann & Dieckmann, 1994) and often peaks post-bloom in summer ice (Gowing et al., 2004). Some data sets lead to the suggestion that more bacterial production than is measured must have been transferred to higher trophic levels, lost to viral infection, or physically expelled from the ice (Smith & Clement, 1990; Laurion et al., 1995; Gowing et al., 2004). Limited data, in part for lack of ideal methods, on the role of both viruses and grazing protists in controlling bacterial production leaves open the possibility that bacteria are more important geochemically, in cycling carbon and other elements, than comparative production rates in carbon units would suggest. They may be more important biologically than realized, if their well-documented physical associations with ice algae involve specific nutrient provisions/exchanges that characterize symbioses. Another important caveat when considering bacterial activity in relation to the ice-algal bloom is that integrating measurements over the full thickness of the ice, rather than only the bottom layers, reveals a dominance of bacterial production over primary production (Gradinger & Zhang, 1997) in many cases. Spring sea ice may be net heterotrophic in spite of intensive algal blooms at its base.

Heterotrophic bacteria are clearly involved in nitrogen cycling in sea ice, and particularly in regenerating nitrogen in the form of ammonia, potentially aiding an extension of the bloom season. A new twist on ammonia production in sea ice comes from a study of EPS concentrations in the ice, which decreased as ammonia increased (Riedel et al., 2007). The classical view of bacteria regenerating nutrients as they consume small molecular weight organic compounds released directly by algae likely needs to be amended for sea ice, to include the enzymatic hydrolysis and consumption of EPS now well known to be lodged in its brine inclusions (Krembs et al., 2002, 2009; Meiners et al., 2008). Variability and lags in the relationship between bacterial abundance and chlorophyll concentration, as often observed (Kottmeier et al., 1987; Stewart & Fritsen, 2004), including apparent independence of bacterial production from primary production (Haecky & Andersson, 1999), may be partially explained not only by the impacts of viral infection but also by a greater dependence on EPS than previously realized. The ice matrix itself, in providing a physical structure with multiple sorptive sites to contain enzymes and EPS, may be responsible for the achievement of useful degradative results, as happens in other porous support structures like particle aggregates and sediments (Vetter et al., 1998).

The general fate of nitrogen in sea ice has come under new scrutiny as a result of the discovery of zones of anoxia in sea ice that support both denitrification and anaerobic ammonia

oxidation or 'anammox' (Rysgaard & Glud, 2004; Rysgaard et al., 2008). For some coastal ice formations, ice-algal blooms sufficiently stimulate heterotrophic bacterial activity so that oxygen is fully consumed, even prior to peak algal activity, leaving pockets of anoxia in the ice. Because bacteria remove nitrogen through the respiratory pathways inherent to denitrification and anammox, these processes can be expected to influence the availability of nutrients for ice algae and thus affect overall primary productivity. Other anaerobic processes, not yet explored, may also be relevant to these organic-rich stages of sea ice, as they appear to be in lower latitude Baltic Sea ice based on the presence of fermenting and other anaerobic bacteria (Petri & Imhoff, 2001; see Section 7.5).

Summer

During summer, the physical demise of sea ice begins, including the melting of the bottom ice layer rich in organic compounds, especially EPS, as well as organisms, from bacteria and algae to various grazers, including viruses. The release of bacteria (and viruses) from the ice has not been easy to document, given ongoing production in the ice, currents beneath the ice and the potential buoyancy of released EPS aggregates in which bacteria are embedded (Krembs & Engel, 2001; Riedel et al., 2006; Meiners et al., 2008), but the potential amounts and rates of transfer are expected to be high. By late summer, the physical demise of sea ice is well underway, even as the system remains highly active microbially. Rates of bacterial production in 'crack pools' of the disintegrating ice cover, believed to represent the 'climax' community leaving the ice (Gleitz et al., 1996), rank among the highest rates detected for the sea ice environment; they also tend to exceed concurrent rates of primary production. Still intact portions of the sea ice cover can support sizeable snow-melt ponds on its surface, of considerable importance to the physics and albedo of the ice (Chapter 2). Though virtual death traps for sea ice microbes due to osmotic shock (as depicted in Fig. 7.4), these melt ponds eventually develop distinctive microbial ecosystems, supported by freshwater algae (Brinkmeyer et al., 2004), in which the bacteria can be very active, with production rates up to 1 g C m^{-3} d^{-1}, surpassing all other values reported for sea ice (Kottmeier & Sullivan, 1987a, b, 1990; Kottmeier et al., 1987; Grossmann & Dieckmann, 1994). The fate of this new biomass includes drainage to underlying seawater via cracks in the ice cover, as well as percolation into the increasingly porous ice itself, complicating evaluations of sea ice bacterial dynamics at the end of the annual cycle.

7.5 Diversity and succession

The study of bacterial diversity in sea ice began with culturing work, where the focus was on physiological rather than phylogenetic type of organism. The question of temperature-based selection was often addressed, with the general understanding today that sea ice strongly selects for cold-adapted bacteria (Helmke & Weyland, 1995, 2004; Bowman et al., 1997, 1998; Junge et al., 2002; Brinkmeyer et al., 2003) and, consequently, for cold-active viruses (Borriss et al., 2003; Wells & Deming, 2006a, b). Culturable sea ice populations are often dominated by 'true' psychrophiles that fail to grow at 20°C and express much lower temperature growth optima and minima, lower than other microbes (according to the definition of Morita, 1975). Curiously, efforts to isolate bacteria with requirements for the elevated brine salinities encountered in cold sea ice have not yet been successful (but see Section 7.7). An unexpected physiological feature detected repeatedly in sea ice bacteria, across multiple

genera, is the formation of gas vacuoles (Gosink et al., 1997, 1998). The buoyancy thus conveyed to a cell is hypothesized to facilitate a form of thigmotaxy, whereby cells rise to the surface (without catching a ride attached to larger particles) to entrain into sea ice during its formation (Staley & Gosink, 1999). Whether or not organisms the size of bacteria, with very low Reynolds numbers, can benefit from the proposed buoyancy in a dynamic ocean has not been considered.

When the heterotrophic bacteria cultured from sea ice, typically from spring or summer sea ice, were finally identified phylogenetically by 16S rRNA gene sequence, representatives from specific genera turned up repeatedly in both Arctic and Antarctic sea ice. These genera include *Colwellia*, *Glaciecola*, *Octadecabacter*, and *Polaribacter*, which fall in the Proteobacteria (α or γ) or *Cytophaga–Flavobacterium–Bacteriodes* (CFB) groups (Table 7.1). Two of these genera, *Octadecabacter* and *Polaribacter*, along with *Gelidibacter*, *Psychroflexus* and *Psychromonas*, were new to culture collections. These culturing results indicated

Table 7.1   Genera of Bacteria, Archaea and bacterial viruses with known representatives from sea ice (ordered alphabetically within groups for polar sea ice), including new genera described from sea ice (asterisks). Genera represented only by environmental 16S rRNA gene sequences are in bold. Also indicated are those known only from melt ponds (mp) or low latitude Baltic Sea ice (bs).

Bacteria	Archaea (only from winter ice)	Bacterial viruses (tailed, dsDNA)
α-Proteobacteria	**Crenarchaeota**	*Siphoviridae*
*Octadecabacter**	**Marine Group I**	*Myoviridae*
Roseobacter	**Euryarchaeota**	
Ruegeria	**Group II-b**	
Sphingomonas		
Sulfitobacter		
Devosia (mp)		
Rhodobacter (mp)		
Loktanella (bs)		
β-Proteobacteria (characterize freshwater habitats)		
Polaromonas		
Aquaspirillum (mp)		
Matsuebacter (mp)		
Rhodoferaz (mp)		
Ultramicrobacterium (mp)		
Comamonadaceae (bs)		
Hydrogenophaga (bs)		
γ-Proteobacteria (common to sea ice)		
Acinetobacter		
Alteromonas		
Citrobacter		
Colwellia		
Glaciecola		
Halomonas		
Iceobacter		

(Continued)

Table 7.1   (*Continued*)

Bacteria	Archaea (only from winter ice)	Bacterial viruses (tailed, dsDNA)
Marinobacter		
Marinomonas		
Neptunomonas		
Oceanospirillum		
Pseudoalteromonas		
Pseudomonas		
Psychrobacter		
Psychromonas*		
Shewanella		
Terridinibacter		
Vibrio		
Cytophaga–Flavobacterium–Bacteriodes (CFB) (common to sea ice)		
Polaribacter*		
Cellulophaga		
Flavobacterium		
Salegentibacter		
Psychroflexus*		
Cytophaga		
Gelidibacter*		
Psychroserpens		
Lewinella		
Hymenobacter (mp)		
Cyclobacterium (mp)		
Flexibacteraceae (bs)		
Green non-sulphur bacteria		
Actinobacteria		
Clavibacter (mp)		
*Corynebacterium_*(mp)		
Planctomycetales (mp)		
Verrucomicrobia		
Prosthecobacter		
Purple sulphur bacteria (bs)		
Gram positives (low mole percent G+C)		
Halobacillus		
Planococcus		
(high mole percent G+C)		
Arthrobacter		
Brachybacterium		

Information taken from Bowman et al. (1997, 1998), Staley and Gosink (1999), Brown and Bowman (2001), Junge et al. (1998, 2002), Brinkmeyer et al. (2003), Collins and Deming (2006), Collins et al. (unpublished) for polar sea ice; Brinkmeyer et al. (2004) for melt ponds; and Petri and Imhoff (2001), Kaartokallio (2004), Kaartokallio et al. (2008) for Baltic Sea ice.

the existence of bacterial sea ice specialists and raised questions about biogeography and endemism (Staley & Gosink, 1999). Did the sea ice environment in general select for similar species at both poles, or were the Arctic and Antarctic sufficiently different and geographically removed from each other to have fostered endemism? Although the definition of a bacterial species continues to be debated, given the phylogenetic convention that requires <97% sequence similarity in the 16S rRNA gene to distinguish species, the results of recent analyses have dispelled notions of sea ice endemism. Highly similar 16S rRNA gene sequences have been found for many bacteria in sea ice from both poles (Brown & Bowman, 2001; Brinkmeyer et al., 2003), including 100% similarity between an Arctic isolate of *Shewanella frigidimara* and an Antarctic isolate (Junge et al., 2002).

The environment of sea ice, wherever it forms, must be sufficiently similar to support a common nature and diversity of inhabitants, at least with regards to the heterotrophic Bacteria. Obvious features in support of such bacteria include a ready supply of (algal-derived) organic substrates, whether dissolved, gelatinous or particulate, and ready access to these resources given their concentration and retention (along with the bacteria) within a porous matrix. Perhaps not unexpectedly, given the long observed physical association of sea ice bacteria with algal cells (Horner & Alexander, 1972; Sullivan & Palmisano, 1984), many of the cultured sea ice bacteria fall within bacterial lineages generally associated with marine algae (Staley & Gosink, 1999; Bowman et al., 1997, 1998; Junge et al., 2002; Brinkmeyer et al., 2003). Because organic resources for heterotrophic bacteria can be viewed as non-limiting in sea ice, the bacterioplankton paradigm that specifies a requirement for higher substrate concentration at suboptimal than optimal growth temperature (Pomeroy & Wiebe, 2001) does not hold for sea ice bacteria (see Stewart & Fritsen, 2004 for an alternative view); even if external supplies become limiting, cold-adapted bacteria from sea ice are known to hoard intracellular polymers that act as energy reserves (Bowman, 2008; see Section 7.6). The availability of organic substrates for heterotrophic bacteria in sea ice also explains the high percentage of the total number of bacteria that can be cultured (up to 60%; Junge et al., 2002) and identified microscopically by fluorescent gene probes (~95%; Brinkmeyer et al., 2003), making sea ice a unique microbial habitat relative to almost all other aquatic environments (Junge et al., 2002). Furthermore, the heterotrophic inhabitants of Arctic sea ice appear well poised to confront the concentrated input of a non-algal source of organic compounds, in the form of an oil spill. The bacterial community is observed to shift, by both culturing and non-culturing methods, towards familiar representatives of the γ-Proteobacteria – species of *Marinobacter*, *Shewanella,* and *Pseudomonas*, with the apparent potential to degrade hydrocarbons, though that remains to be verified (Gerdes et al., 2005).

Comparing bacterial diversity in sea ice to other environments at this stage is problematic, given the few data sets available. An earlier (culture-based) phylogenetic view that diversity may be more limited, due to challenging thermal and saline conditions in the inhabited space of sea ice (Junge et al., 2002), is giving way to a different perspective. Indices that reflect the extent of diversity detected by analyses of DNA amplified directly from sea ice samples (bypassing culturing) indicate that much more diversity awaits discovery (Brinkmeyer et al., 2003), especially as different sea ice seasons, formations and features are examined (Brinkmeyer et al., 2004).

Consideration of bacterial succession in sea ice, using comparative phylogenetic techniques, is in its infancy. Only in short-lived, relatively warm, Baltic Sea ice are community DNA fingerprints available to evaluate succession throughout the lifetime of an ice cover (Kaartokallio et al., 2008); the patterns predictably follow the ice-algal bloom. Succession in polar sea ice,

by contrast, can only be pieced together from the results of a few separate seasonal studies. For example, between fall ice formation and a sampling plan initiated in winter, the nature of the bacterial community by ARISA fingerprinting best resembles the bacterioplankton community in fall seawater (Collins et al., unpublished data). Even groups of Archaea (Table 7.1), well known in polar waters (Delong et al., 1994), are present in the winter ice and persist through the severity of that season (Collins & Deming, 2006). Their absence from spring and summer sea ice at both poles suggests that the winter–spring transition, already argued to support highly active bacterial cells (see Section 7.4), so favours heterotrophic Bacteria that Archaea fade to numbers undetectable by the methods that have been applied to sea ice (approaches to capture rare members of the community have not yet been applied; Sogin et al., 2006). For the rest of the sea ice cycle, influenced by the ice-algal bloom, the familiar suite of heterotrophic Bacteria from culturing work along with some additional uncultured phylotypes appear in clone libraries (Table 7.1; Brown & Bowman, 2001; Brinkmeyer et al., 2003).

The largely freshwater melt ponds that form on the surface of sea ice in late summer (see Section 7.3) present sea ice diversity in a different light. Unlike communities within the sea ice, these melt pond communities of Bacteria (no Archaea have been detected) at the surface of the ice are dominated by β-Proteobacteria (Table 7.1), considered to be physiologically adapted to and characteristic of freshwater habitats. Gram-positive species, rarely detected in the interior sea ice, sometimes comprise 10% of the bacterial fraction (Brinkmeyer et al., 2004). On the other hand, melt ponds with attachment surfaces in the form of sediments also contain an important percentage of members of the CFB group, common to sea ice. Downward percolation of meltwater could transport members of the melt pond community into the sea ice brine channel system, readily explaining the presence of β-Proteobacteria in interior samples, while upwards exposure of interior sea ice may introduce its phylotypes (e.g. *Octadecabacter*, *Marinobacter* and *Flavobacterium*) into melt ponds. The net result is the appearance of an estuarine community in summer melt ponds, where β-proteobacteria dominate freshwater zones and α- and γ-proteobacteria prevail in more saline zones (Brinkmeyer et al., 2004), and an expansion of sea ice diversity in general.

Several studies of the size range and morphological diversity of viruses in sea ice are available (Maranger et al., 1994; Gowing et al., 2002, 2004; Gowing, 2003), indicating the overwhelming predominance of bacterial viruses, but the phylogenetic diversity of viruses in sea ice is not known. In only two studies have bacterial viruses been obtained in culture against cold-adapted bacterial hosts known from sea ice (Borriss et al., 2003; Wells & Deming, 2006b). From these efforts, only the presence of common, tailed, double-stranded DNA viruses classified as members of the *Siphoviridae* and *Myoviridae* can be ascribed to sea ice. Given the importance of viruses in the dynamics of sea ice bacteria (see Section 7.4), and potentially of eukaryotic organisms, the absence of direct analyses of extracted viral DNA is glaring.

7.6 Adaptations to sea ice

Hallmarks

Numerous articles, reviews and books have been written on the genetic, biochemical and molecular basis for bacterial adaptation to the cold. Important hallmarks have been deduced from the sum of physiological work with live cultures, biochemical analyses of their cellular

components and *in silico* analyses of whole-genome sequences (Feller & Gerday, 2003; Mock & Thomas, 2005; Moyer & Morita, 2007; D'Amico et al., 2006; Gerday & Glansdorff, 2007; Margesin et al., 2008; Rodriguez & Tiedje, 2008), including for archaeal adaptation to the cold (though in methanogens, not yet known from sea ice; Saunders et al., 2003). Several recent syntheses have considered cold adaptation from perspectives particularly relevant to sea ice – those provided by the whole-genome sequences of *Psychroflexus torques* (strain ATCC700755) and *Colwellia psychrerythraea* (strain 34H), representatives of the γ-Proteobacteria isolated from sea ice or known to occur in it (Bowman, 2008), and by Earth history and the nature of winter sea ice (Deming, 2007b, 2009), with its temperatures below the minimum of –12°C for cellular reproduction in culture (Breezee et al., 2006; Wells & Deming, 2006b). Universal hallmarks of cold adaptation include modification of the amino acid composition of the proteome (Methé et al., 2005; Bowman, 2008; Deming, 2009), conferring flexibility (and usually increased thermolability as a trade-off) to proteins for their enzymatic functions, and adjustments to the lipid compositions of cellular membranes, maintaining fluidity for their transport functions in the cold. Without compositional adjustments, enzymes and membranes become 'rigid' at low temperatures and lose functionality; with them, bacteria become competitive in the cold, even if absolute rates of chemical reactions and diffusive transport slow as temperatures drop (and viscosity rises). A specific hallmark that counters the slowing of reactions involved in nutrient uptake by Bacteria is the storage of various energy reserves intracellularly, in the form of large polymers like glycogen, polyhydroxybutyrate, polyphosphates or neutral lipid globules. Both *P. torquis* and *C. psychrerythraea* show genomic signs of using protein-like polymers as organic nitrogen reserves (Bowman, 2008).

Bacteria in sea ice experience not only sub-zero temperatures but also seasonal extremes in salinity, from the high salt concentrations of winter brine inclusions to the freshwater status of melt ponds (and similar microscale gradients during sample melting). The hallmark defense against osmotic shock, which simultaneously provides a measure of cryoprotection, is to produce or accumulate intracellularly what are called compatible solutes – typically sugars, polyols, and amino acids and their derivatives, like betaine. Both *P. torquis* and *C. psychrerythraea* carry genes involved in the production or transport of betaine; *P. torquis* also appears capable of using the sugar trehalose for osmo- and cryoprotection (Bowman, 2008). By adjusting intracellular concentrations of these compounds, an organism can balance the influx, or efflux as the case may be, of salts that would otherwise occur when external conditions shift; at high interior concentrations, the freezing point is depressed and potentially damaging ice crystals fail to form. Compatible solutes were so named because they can be accumulated to high levels within the cell without compromising its macromolecular functions. Required ionic interactions can be stabilized by compatible solutes as they interact with the hydration sphere around enzymes, nucleic acids and other macromolecules during osmotic shifts.

Because sea ice bacteria inhabit a physical support structure that is porous, to varying degree depending on temperature, cold-adaptive strategies can also effectively involve the production of compounds released into the environment. In open waters, extracellular releases diffuse away from the cell; in enclosed or semi-enclosed spaces like sea ice pores, the secretions are retained in close enough proximity to benefit the organism (Vetter et al., 1998; Krembs & Deming, 2008). Where multiple bacteria (or bacteria and ice algae) are present, all can benefit from the products of one, which lies at the root of biofilm formation in many environments and helps to explain the intimate associations often observed between bacteria

and sea ice algae, referenced earlier. The hallmark extracellular releases by sea ice (and other cold-adapted) bacteria are antifreeze proteins, cold-active enzymes and the EPS discussed throughout this chapter.

Antifreeze proteins, a structurally diverse group, include proteins that bind to ice crystals, altering their morphology in the process, and that inhibit the recrystallization of ice (formation of large crystals over small ones) at temperatures relevant to sea ice formation. The former are thought to favourably modify an icy habitat for its resident bacteria and the latter, to prevent formation of large ice crystals potentially damaging to membranes. Although the whole genome of *C. psychrerythraea* does not contain sequences currently recognizable as coding for antifreeze proteins, another *Colwellia* isolate from sea ice does (Raymond et al., 2007), and recent experiments with exudates from *C. psychrerythraea* indicate the presence of a sugar-bound protein with ice affinity (Ewert Sarmiento & Deming, 2008, unpublished). *P. torquis* carries a gene that codes for a large putative cell surface protein suspected of antifreeze activity, given the sequence match of several of its repeat domains to smaller known antifreeze proteins (Bowman, 2008). The continued study of ice-affine or ice-active proteins, linking experimental work with genomics (Raymond et al., 2007), promises to enlighten further the specific adaptations of bacteria that successfully inhabit sea ice.

A wealth of similar studies on extracellular enzymes released by cold-adapted bacteria, including *C. psychrerythraea* (Huston et al., 2004), has already established the fundamentals of cold activity for an enzyme (Feller & Gerday, 2003; D'Amico et al., 2006), even those released to act freely of the producing organism (Deming & Baross, 2002; Deming, 2007b). What has not been fully explored for sea ice bacteria is the extent to which they benefit nutritionally from extracellular releases of enzymes into the brine inclusions they occupy. Although *C. psychrerythraea* can be triggered by a drop in temperature to produce and release increased amounts of an extracellular protease (Huston et al., 2004), how well do such proteases function in sub-zero brine? Are extracellular stabilizing factors like EPS required for *in situ* protein degradation, as they appear to be for imparting thermal stability to the protease of *C. psychrerythraea* (Huston et al., 2004)? Do the breakdown products help relieve bacteria of possible organic nutrient limitations due to the inaccessible size of many of the polymers found in sea ice and the reduced rates of transport and uptake in the cold? Are extracellular enzymes in general – proteases and carbohydrases – sufficiently active *in situ* to breakdown some fraction of the EPS that fills sea ice pores?

Receiving much attention since the discovery of their prevalence in sea ice (Krembs et al., 2002) are the many possible roles played by EPS (also see Chapter 15), particularly from the perspective of sea ice bacteria (Mancuso Nichols et al., 2004, 2005b; Riedel et al., 2006; Krembs & Deming, 2008; Meiners et al., 2008). In addition to serving as possible extracellular enzyme-stabilizing agents and external reserves of hydrolysable organic compounds, exopolymers can function as cryoprotectants, depressing the freezing point and providing a physical buffer against encroaching ice crystals (Krembs et al., 2002, 2009). In providing a cell coating more hydrated than the surrounding brine, EPS may function as external osmoprotectants (Krembs & Deming, 2008), perhaps in concert with (easing the need for) compatible solutes. In coating a cell, they may also provide a defense against viruses that must make contact with (EPS-hidden) cell surface receptors in order to infect. The study of cold activity in viruses is in its infancy (Wells, 2008), but experimental evidence suggests that some bacteriophage may carry their own extremely cold-active enzymes, enabling cell entry (Wells & Deming, 2006b). If viral enzymes can also sufficiently hydrolyse portions of EPS to
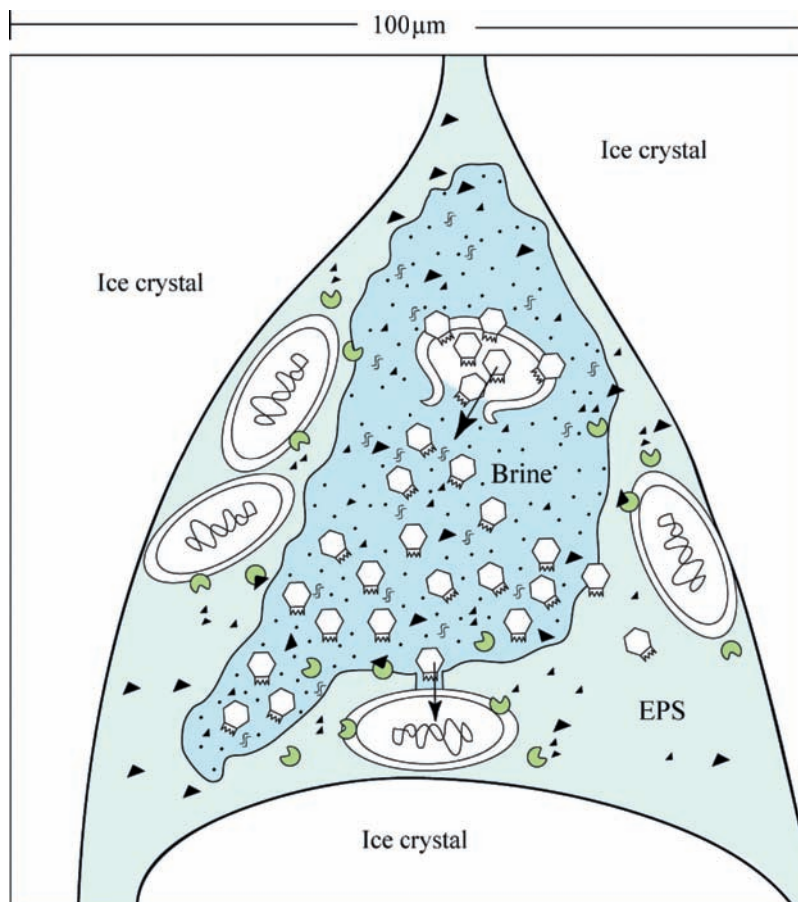
Fig. 7.7 Idealized schematic of a brine inclusion at the juncture of three ice crystals, showing bacteria embedded in exopolymer gels (EPS), liquid brine and dissolved organic substrates concentrated in the interior and extracellular enzymes hydrolysing the substrates. Also shown are cold-active viral enzymes penetrating the EPS and successful viral infection of, reproduction within and lysis of a host bacterium, releasing free DNA and new viruses, potential agents of horizontal gene transfer.

create a channel of attack (Fig. 7.7), then EPS may not always provide an effective defense. Although many of these roles (and others discussed in previous sections) remain to be verified, especially from an *in situ* perspective, what is well established is that many sea ice bacteria in culture produce EPS and often in copious amounts (Mancuso Nichols et al., 2004, 2005b; Marx et al., 2009). The amounts in sea ice itself may pale compared to EPS production by ice algae, but to the individual bacterium lodged in an ice pore (Fig. 7.1), an ability to modify its immediate environment with its own EPS may be critical to its survival.

Like some extracellular enzymes, the production and release of excessive amounts of EPS can be triggered by a drop in temperature (Mancuso Nichols et al., 2004, 2005a), as occurs for both *P. torquis* (Bowman, 2008) and *C. psychrerythraea* (Marx et al., 2009). In the latter case, the specific trigger appears not to be a function of dropping temperature but the event of becoming encased in ice. Maximum production of EPS was observed as a step function
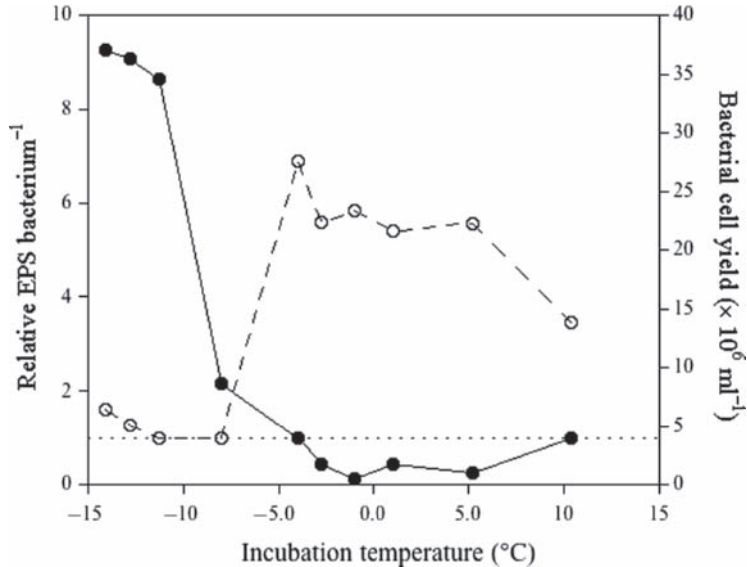
Fig. 7.8 Changes in EPS concentration per bacterium (l) according to incubation temperature when cultures of *Colwellia psychrerythraea* strain 34H were incubated for 4–7 days in saline culture media. Changes are relative to concentration at the warmest temperature, highlighted by the dotted line at unity. Also shown is bacterial abundance or cell yield (m) in the same samples. (Data from Marx et al., 2009.)

concurrent with the freezing of saline growth medium between temperatures of -4°C and -8°C (Fig. 7.8). At the same juncture, detectable bacterial growth in the time frame of the experiment appeared to be suspended. Worth examining further is the apparent switch from investing energy in growth to investing it in a process that could favourably modify the bacterium's immediate pore space for its continued well-being, i.e. EPS production.

Mechanisms

The mechanism usually invoked to explain acquisition of new traits that make an organism better adapted to, and more competitive in its environment, is genetic mutation and the vertical inheritance of beneficial mutations from parent cells. Much of what is known about the hallmarks of cold adaptation, especially regarding proteins, has derived from studies using site-directed mutagenesis and other genetic approaches that take advantage of the vertical inheritance of modified genes. The alternative mechanism is to receive beneficial genes via horizontal or lateral transfer. This mechanism is known to occur in the laboratory via the uptake of free DNA from the medium (transformation), the transfer of DNA between physically connected bacteria (conjugation) and the viral introduction of bacterial DNA from a former host into the genome of its new host (transduction). In the latter case, if an environmental or other trigger does not cause the virus to enter its lytic cycle (to the demise of the host), the viral DNA and bacterial gene(s) brought with it can pass benignly (vertically) to new generations of bacteria, with the virus eventually losing its capacity to become lytic again. With the advent of genomics has come ample evidence that virally mediated gene transfer has been an important evolutionary mechanism for bacteria (Ochman et al., 2000). Even with a limited genomic data for sea ice bacteria, evidence for gene transfer via

transduction is abundant (Methé et al., 2005; Bowman, 2008). *P. torquis* presents a case in point: its genome is rich in insertion elements, including transposases and their remnants, retroviral integrases and phage-like genes, all suggesting a strong influence of viruses in its evolution (Bowman, 2008). In particular, the genome locus for EPS production, so potentially important to life in sea ice, is flanked by sequences suggestive of an assembly process that involves a series of lateral gene transfer events.

In the same time frame of these genomic analyses of sea ice bacteria, work with cold-active virus–host systems in culture has been renewed after a hiatus of decades (Wells, 2008). Several promising systems have recently been obtained from sea ice (Borriss et al., 2003) and the lower temperature limit for viral infectivity of *C. psychrerythraea* has been pushed to −12°C (and 16% salt) in simulated sea ice brines (Wells & Deming, 2006b). The goal of developing a cold-adapted system to demonstrate horizontal gene transfer, whether or not mediated by viruses, has not been achieved. The goal remains, however, motivated by what has been learned from the sea ice environment itself. The concentrating factor inherent to shrinking pore space as sea ice passes through a winter season clearly brings microbes into close proximity with each other in a liquid environment of abundant organic compounds, including EPS that may serve many positive functions for the trapped cells (Fig. 7.7). Model calculations and observed concentrations in melted sea ice indicate that agents of lateral gene transfer, both free DNA (Collins & Deming, unpublished) and viruses (Wells & Deming, 2006a), also surround the encased cells. The virus–bacteria contact rate in winter sea ice brines may be as much as 600 times higher than in underlying seawater. In spite of its seemingly harsh thermal and saline conditions, the interior brine habitats of very cold sea may be more dynamic and important to the evolution of cold adaptation in general than imagined.

7.7 Frontiers

Considering that the ocean represents the bulk of Earth's cold biosphere, today and in the past, the annual freezing of its polar surface waters takes on special significance as an important planetary driver of cold adaptation. Astronomical numbers of bacteria pass through this frozen gauntlet annually, and over extended periods in geological time (Deming, 2009).

Despite all that has been learned about sea ice bacteria since their discovery in the ocean's ice cover more than 50 years ago, these most abundant of all ice inhabitants still represent new biological frontiers from many perspectives, if perhaps especially the molecular and genomic ones. Bacterial viruses, known to exist in sea ice for a brief 15 years, represent the newer frontier. Because they appear to be dynamic entities, infecting and lysing bacteria even in the coldest sea ice brines examined, and because some of their bacterial hosts carry genomic evidence of lateral gene transfer, the continued study of sea ice viruses promises a better understanding of the limits and evolution of life in general. As the Mars research community gets closer and closer to declaring the subsurface realm of the red planet microbially alive (Mumma et al., 2009), questions of the persistence and evolution of microbial life over eons of time in an environment whose surface is deeply frozen loom large (c.f. Chapter 15).

Not even Earth's sea ice, however, has been fully explored from the microbial perspective. As a case in point, consider frost flowers (Perovich & Richter-Menge, 1994), those delicate ice-skeletal structures that form on the surface of new sea ice in both Arctic and Antarctic settings and are most commonly known for their striking beauty, especially when extensive
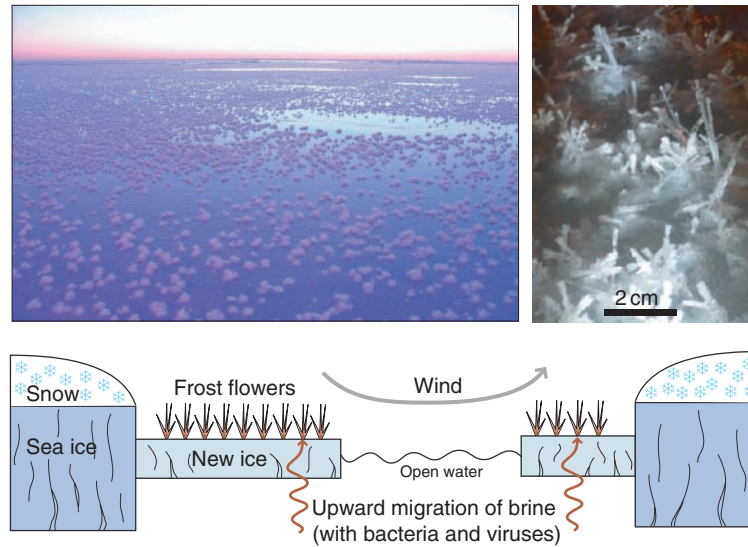
Fig. 7.9 Schematic (not drawn to scale) of a recently opened lead in winter with newly formed sea ice and its surficial frost flowers containing brine (and bacteria and viruses) wicked from the sea ice. Upper left photo shows a field of frost flowers in the Amundsen Gulf of the Canadian Arctic during December 2007 (provided by R.E. Collins); right photo, individual frost flowers (bar = 2 cm) in the same region during the dark month of January 2008 (provided by M. Lin).

fields of them grow overnight (Fig. 7.9). Although these readily airborne structures are the subject of recent scientific scrutiny for their impacts on ice albedo and polar heat budgets (Martin et al., 1996; Grenfell et al., 1998) and their potential roles in atmospheric ozone and mercury depletion events (Schroeder et al., 1998; Rankin et al., 2002; Kaleschke et al., 2004; Douglas et al., 2005), they have not been explored from a biological perspective. A recent doctoral thesis on the growth of frost flowers in both laboratory and field experiments (Style, 2007) clarified the first work of this kind (Martin et al., 1995, 1996) on the formation and life history of frost flowers, from initial nucleation by particles from overlying moist air landing on new sea ice (snowflakes in the field) to rapid ice-skeletal growth over several hours before being dispersed by wind or buried by snowfall. During unimpeded growth, they wick brine from the underlying sea ice by capillary action against a thermal gradient (Wettlaufer & Worster, 1995) until they become weighty with salt at triple the concentration found in seawater and begin to collapse, forming a briny mush on the surface of the new sea ice. Typical temperatures of frost flower formation and the final briny mush fall well below −20°C, making these features prime targets for tests of the thermal and saline limits of microbial dynamics, if they were to contain microbes. During an overwintering icebreaker expedition in the Amundsen Gulf of the Arctic for the International Polar Year, 2007–2008 (Barber et al., 2008), we took the opportunity to sample frost flowers and their immediate environs to determine possible bacterial and viral contents. Given that frost flowers wick brine from the ice below, they should also wick bacteria and viruses present in the brine. The hypothesis seems straightforward, but many outcomes could pertain, including that gelatinous material concentrated in the new ice would retain bacteria and viruses preferentially even as dissolved salts wicked upwards. Frost flowers could be beautiful but lifeless structures. Although this work is ongoing, first results suggest quite the opposite scenario (Deming

et al., unpublished). The saltiest of the frost flowers sampled contained high concentrations of bacteria comparable to those in underlying brine inclusions, while high ratios of viruses to bacteria in some of the younger (fresher) flowers suggested a dynamic (infective) system. Parallel enrichment cultures have yielded bacteria more tolerant of the combined challenge of sub-zero temperature and high salt than other known isolates. Now, even a half-century after the discovery of bacteria in sea ice, much clearly remains to be discovered, debated, elaborated and shared.

End Notes

1 In this chapter, "bacteria" and "microbes" are used as generic terms for the single-celled, micrometre-sized, prokaryotic organisms in the domains of Bacteria and Archaea.
2 Viruses that infect bacteria are also called "bacteriophage", and are typically <110 nm in diameter; larger size classes of viruses infect eukaryotic cells.

References

Ackley, S.F. & Sullivan, C.W. (1994) Physical controls on the development and characteristics of Antarctic sea ice biological communities – a review and synthesis. *Deep-Sea Research Part I*, **41**, 1583–1604.

Barber, D.G, Papakyriakou, T., Macdonald, R. et al. (2008) The International Polar Year (IPY) Circumpolar Flaw Lead (CFL) System Study. *EOS Transactions America Geophysical Union*, **89**, Fall Meeting Supplement, Abstract U23F-02.

Baross, J.A. & Morita, R.Y. (1978) Microbial life at low temperatures: ecological aspects. In: *Microbial Life in Extreme Environments* (Ed. D.J. Kushner), pp. 7–91. Academic Press, New York.

Borriss, M., Helmke, E. Hanschke, R. & Schweder, T. (2003) Isolation and characterization of marine psychrophilic phage-host systems from Arctic sea ice. *Extremophiles*, **7**, 377–384.

Bowman, J.P. (2008) Genomic analysis of psychrophilic prokaryotes. In: *Psychrophiles: from Biodiversity to Biotechnology* (Eds. R. Margesin, F. Schinner, J.-C. Marx & C. Gerday), pp. 265–284. Springer-Verlag, Berlin.

Bowman, J.P., McCammon, S.A., Brown, M.V., Nichols, D.S. & McMeekin, T.A. (1997) Diversity and association of psychrophilic bacteria in Antarctic sea ice. *Applied and Environmental Microbiology*, **63**, 3068–3078.

Bowman, J.P., Gosink, J.J., McCammon, S.A. et al. (1998) *Colwellia demingiae* sp. nov., *Colwellia hornerae* sp. nov., *Colwellia rossensis* sp. nov., and *Colwellia psychrotropica* sp. nov.: psychrophilic Antarctic species with the ability to synthesize docosahexaenoic acid (22:53). *International Journal of Systematic Bacteriology*, **48**, 1171–1180.

Breezee, J., Cady, N. & Staley, J.T. (2006) Subfreezing growth of the sea ice bacterium *Psychromonas ingrahamii*. *Microbial Ecology*, **47**, 300–304.

Brinkmeyer, R., Knittel, K., Jugens, J., Weyland, H., Amann, R. & Helmke, E. (2003) Diversity and structure of bacterial communities in Arctic versus Antarctic pack ice. *Applied and Environmental Microbiology*, **69**, 6610–6619.

Brinkmeyer, R., Glockner, F.-O. Helmke, E. & Amann, R. (2004) Predominance of β-proteobacteria in summer melt pools on Arctic pack ice. *Limnology and Oceanography*, **49**, 1013–1021.

Brown, M. & Bowman, J. (2001) A molecular phylogenetic survey of sea ice microbial communities (SIMCO). *FEMS Microbiology Ecology*, **35**, 267–275.

Collins, R.E. & Deming, J.W. (2006) Persistence of Archaea in sea ice. *Astrobiology*, **6**, 214.

Collins, R.E., Carpenter, S.D. & Deming, J.W. (2008) Spatial heterogeneity and temporal dynamics of particles, bacteria, and pEPS in Arctic winter sea ice. *Journal of Marine Systems*, **74**, 902–917.

Cota, G.F., Kottmeier, S.T., Robinson, D.H., Smith, W.O., Jr. & Sullivan, C.W. (1990) Bacterioplankton in the marginal ice zone of the Weddell Sea: biomass, production and metabolic activities during austral autumn. *Deep-Sea Research Part I*, **37**, 1145–1167.

Cox, G.F.N. & Weeks, W.F. (1983) Equations for determining the gas and brine volumes in sea ice samples. *Journal of Glaciology*, **29**, 306–316.

D'Amico, S., Collins, T., Marx, J.-C., Feller, G. & Gerday, C. (2006) Pscyhrophilic microorganisms: challenges for life. *EMBO Reports*, **7**, 385–389.

Delille, D. (1992) Marine bacterioplankton at the Weddell Sea ice edge, distribution of psychrophilic and psychrotrophic populations. *Polar Biology*, **12**, 205–210.

Delille, D., Fiala, M. & Rosiers, C. (1995) Seasonal changes in phytoplankton and bacterioplankton distribution at the ice-water interface in the Antarctic neritic area. *Marine Ecology Progress Series*, **123**, 225–233.

Delille, D., Fiala, M., Kuparinen, J., Kuosa, H. & Plessis, C. (2002) Seasonal changes in microbial biomass in the first-year ice of the Terre Adelie area (Antarctica). *Aquatic Microbial Ecology*, **28**, 257–265.

DeLong, E.F., Wu, K.Y., Prézelin, B.B. & Jovine, R.V. (1994) High abundance of Archaea in Antarctic marine picoplankton. *Nature*, **371**, 695–697.

Deming, J.W. (2002) Psychrophiles and polar regions. *Current Opinion in Microbiology,* **3**, 301–309.

Deming, J.W. (2007a) Extreme high-pressure marine environments. In: *ASM Manual of Environmental Microbiology* (Eds. C.J. Hurst, R.L. Crawford, J.L. Garland, A.L. Mills & L.D. Stetzenbach), Third Edition, pp. 575–590. ASM Press, Washington, DC.

Deming, J.W. (2007b) Life in ice formations at very cold temperatures. In: *Physiology and Biochemistry of Extremophiles* (Eds. C. Gerday & N. Glansdorff), pp. 133–145. ASM Press, Washington, DC.

Deming, J.W. (2009) Extremophiles: Cold environments. In: *Encyclopedia of Microbiology*, Third Edition (Ed. M. Schaechter), pp. 147–158. Elsevier, Oxford.

Deming, J.W. & Baross, J.A. (1993) Deep-sea smokers: windows to a subsurface biosphere? *Cosmochemica Geochemica Acta*, **57**, 3219–3230.

Deming, J.W. & Baross, J.A. (2002) Search and discovery of microbial enzymes from thermally extreme environments in the ocean. In: *Enzymes in the Environment, Activity, Ecology and Applications* (Eds. R.P. Dick & R.G. Burns), pp. 327–362. Marcel Dekker Publishers, New York.

Deming, J.W. & Eicken, H. (2007) Life in ice. In: *Planets and Life: The Emerging Science of Astrobiology* (Eds. W.T. Sullivan & J.A. Baross), pp. 292–312. Cambridge University Press.

Douglas, T.A., Sturm, M., Simpson, W.R., Brooks, S., Lindberg, S. & Perovich, D.K. (2005) Elevated mercury measured in snow and frost flowers near Arctic sea ice leads. *Geophysical Research Letters* **32**, L04502, 10.1029/2004GL022132.

Eicken, H. (2003) From the microscopic, to the macroscopic, to the regional scale: Growth, microstructure and properties of sea ice. In: *Sea ice – An Introduction to Its Physics, Biology, Chemistry and Geology* (Eds. D.N. Thomas & G.S. Dieckmann), pp. 22–81. Blackwell Science, Oxford.

Eicken, H., Bock, C., Wittig, R., Miller, H. & Poertner, H.-O. (2000) Nuclear magnetic resonance imaging of sea ice pore fluids: methods and thermal evolution of pore microstructure. *Cold Region Science and Technology*, **31**, 207–225.

Ewert Sarmiento, M. & Deming, J.W. (2008) Natural microbial exopolymers: ice affinity and consequent habitat alteration in cold saline ice formations. *Astrobiology*, **8**, 475.

Feller, G. & Gerday, C. (2003) Psychrophilic enzymes: hot topics in cold adaptation. *Nature Reviews*, **1**, 200–208.

Garrison, D.L. & Buck, K.R. (1986) Organism losses during ice melting: a serious bias in sea ice community studies. *Polar Biology*, **6**, 237–239.

Garrison, D.L., Ackley, S.F. & Buck, K.R. (1983) A physical mechanism for establishing algal populations in frazil ice. *Nature*, **306**, 363–365.

Garrison, D.L., Sullivan, C.W. & Ackley, S.F. (1986) Sea ice microbial communities in Antarctica. *BioScience*, **36**, 243–250.

Gerday, C. & Glansdorff, N. (Eds.) (2007) *Physiology and Biochemistry of Extremophiles*. ASM Press, Washington, DC.

Gerdes, B., Brinkmeyer, R., Dieckmann, G. & Helmke, E. (2005) Influence of crude oil on changes of bacterial communities in Arctic sea ice. *FEMS Microbiology Ecology*, **53**, 129–139.

Gleitz, M., Grossmann, S., Scharek, R. & Smetacek, V. (1996) Ecology of diatom and bacterial assemblages in water associated with melting summer sea ice in the Weddell Sea, Antarctica. *Antarctic Science*, **8**, 135–146.

Golden, K.M., Ackley, S.F. & Lytle, V.I. (1998) The percolation phase transition in sea ice. *Science*, **282**, 2238–2241.

Gosink, J.J., Herwig, R.P. & Staley, J.T. (1997) *Octadecabacter arcticus* gen. nov., and *O. antarcticus*, sp. nov., non-pigmented, psychrophilic gas vacuolate bacteria form polar sea ice and water. *Systematic and Applied Microbiology*, **20**, 356–365.

Gosink, J.J., Woese, C.R. & Staley, J.T. (1998) *Polaribacter* gen. nov., with three new species, *P. irgensii*, sp. nov., *P. franzmannii* sp. nov., and *P. filamentus*, sp. nov., gas vacuolate polar marine bacteria of the Cytophaga/Flavobacterium/Bacteroides Group and reclassification of "*Flectobacillus glomeratus*" as *Polaribacter glomeratus*. *International Journal of Systematic Bacteriology,* **48**, 223–235.

Gowing, M.M. (2003) Large viruses and infected microeukaryotes in Ross Sea summer pack ice habitats. *Marine Biology*, **142**, 1029–1040.

Gowing, M.M., Riggs, B.E., Garrison, D.L., Gibson, A.H. & Jeffries, M.O. (2002) Large viruses in Ross Sea late autumn pack ice Habitats. *Marine Ecology Progress Series*, **241**, 1–11.

Gowing, M.M., Garrison, D.L., Gibson, A.H., Krupp, J.M., Jeffries, M.O. & Fritsen, C.H. (2004) Bacterial and viral abundance in Ross Sea summer pack ice communities. *Marine Ecology Progress Series*, **279**, 3–12.

Gradinger, R. & Ikävalko, J. (1998) Organism incorporation into newly forming Arctic sea ice in the Greenland Sea. *Journal of Plankton Research*, **20**, 871–886.

Gradinger, R. & Zhang, Q. (1997) Vertical distribution of bacteria in Arctic sea ice from the Barents and Laptev Seas. *Polar Biology*, **17**, 448–454.

Gradinger, R., Friedrich, C. & Spindler, M. (1999) Abundance, biomass and composition of the sea ice biota of the Greenland Sea pack ice. *Deep-Sea Research Part II*, **46**, 1457–1472.

Grenfell, T.C., Barber, D.G., Fung, A.K. et al. (1998) Evolution of electromagnetic signatures of sea ice from initial formation to the establishment of thick first-year ice. *IEEE Transactions of Geoscience and Remote Sensing,* **36**, 1642–1654.

Griffiths, R.P., Hayasaka, S.S., McNamara, T.M. & Morita, R.Y. (1978) Relative microbial activity and bacterial concentrations in water and sediment samples taken in the Beaufort Sea. *Canadian Journal of Microbiology*, **24**, 1217–1226.

Grossi, S.M., Kottmeier, S.T. & Sullivan, C.W. (1984) Sea ice microbial communities. III. Seasonal abundance of microalgae and associated bacteria, McMurdo Sound, Antarctica. *Microbial Ecology*, **10**, 231–242.

Grossmann, S. (1994) Bacterial activity in sea ice and open water of the Weddell Sea, Antarctica: a microautoradiographic study. *Microbial Ecology*, **28**, 1–18.

Grossmann, S. & Dieckmann, G.S. (1994) Bacterial standing stock, activity, and carbon production during formation and growth of sea ice in the Weddell Sea, Antarctica. *Applied and Environmental Microbiology*, **60**, 2746–2753.

Grossmann, S. & Gleitz, M. (1993) Microbial responses to experimental sea ice formation: implications for the establishment of Antarctic sea ice communities. *Journal of Experimental Marine Biology and Ecology*, **173**, 273–289.

Haecky, P. & Andersson, A. (1999) Primary and bacterial production in sea ice in the northern Baltic Sea. *Aquatic Microbial Ecology*, **20**, 107–118.

Helmke, E. & Weyland, H. (1995) Bacteria in sea ice and underlying water of the Eastern Weddell Sea in midwinter. *Marine Ecology Progress Series*, **117**, 269–287.

Helmke, E. & Weyland, H. (2004) Psychrophilic versus psychrotolerant bacteria – occurrence and significance in polar and temperate marine habitats. *Cellular and Molecular Biology*, **50**, 553–561.

Horner, R. (1985) Ecology of sea ice microalgae. In: *Sea Ice Biota* (Ed. R.A. Horner), pp. 83–103. CRC Press, Boca Raton, FL.

Horner, R. & Alexander, V. (1972) Algal populations in arctic sea ice: an investigation of heterotrophy. *Limnology and Oceanography*, **17**, 454–458.

Horner, R., Ackley, S.F., Dieckmann, G.S. et al. (1992) Ecology of sea ice biota – 1. Habitat, terminology, and methodology. *Polar Biology*, **12**, 417–427.

Huston, A.L., Krieger-Brockett, B.B. & Deming, J.W. (2000) Remarkably low temperature optima for extracellular enzyme activity from Arctic bacteria and sea ice. *Environmental Microbiology*, **2**, 383–388.

Huston, A.L., Methe, B. & Deming, J.W. (2004) Purification, characterization and sequencing of an extracellular cold-active aminopeptidase produced by marine psychrophile *Colwellia psychrerythraea* strain 34H. *Applied and Environmental Microbiology*, **70**, 3321–3328.

Junge, K., Gosink, J.J., Hoppe, H.G. & Staley, J.T. (1998) *Arthrobacter*, *Brachybacterium* and *Planococcus* isolates identified from Antarctic sea ice brine – description of *Planococcus mcmeekinii*. *Systematic and Applied Microbiology*, **21**, 306–314.

Junge, K., Krembs, C., Deming, J., Stierle, A. & Eicken, H. (2001) A microscopic approach to investigate bacteria under in-situ conditions in sea ice samples. *Annals of Glaciology*, **33**, 304–310.

Junge, K., Imhoff, J.F., Staley, J.T. & Deming, J.W. (2002) Phylogenetic diversity of numerically important bacteria in Arctic sea ice. *Microbial Ecology*, **43**, 315–328.

Junge, K., Eicken, H. & Deming, J.W. (2003) Motility of *Colwellia psychrerythraea* strain 34H at subzero temperatures. *Applied and Environmental Microbiology*, **69**, 4282–4284.

Junge, K., Eicken, H. & Deming, J.W. (2004) Bacterial activity at –2 to –20°C in Arctic wintertime sea ice. *Applied and Environmental Microbiology*, **70**, 550–557.

Kaartokallio, H. (2004) Food web components, and physical and chemical properties of Baltic Sea ice. *Marine Ecology Progress Series*, **273**, 49–63.

Kaartokallio, H., Tuomainen, J., Kuosa, H., Kuparinen, J., Martikainen, P. & Servomaa, K. (2008) Succession of sea ice bacterial communities in the Baltic Sea fast ice. *Polar Biology*, **31**, 783–793.

Kaleschke, L., Richter, A., Burrows, J. et al. (2004) Frost flowers on sea ice as a source of sea salt and their influence on tropospheric halogen chemistry. *Geophysical Research Letters*, **31**, L16114, 10.1029/2004GL020655.

Kanavarioti, A., Monnard, P.-A. & Deamer, D.W. (2001) Eutectic phases in ice facilitate nonenzymatic nucleic acid synthesis. *Astrobiology*, **1**, 271–281.

Kaneko, T., Roubal, G. & Atlas, R.M. (1978) Bacterial populations in the Beaufort Sea. *Arctic*, **31**, 97–107.

Kawahara, H. (2007) Cryoprotectants and ice-binding proteins. In: *Psychrophiles: from Biodiversity to Biotechnology* (Eds. R. Margesin, F. Schinner, J.-C. Marx & C. Gerday), pp. 229–246. Springer-Verlag, Berlin.

Kottmeier, S.T. & Sullivan, C.W. (1987a) Sea ice microbial communities. VIII. Bacterial production in annual sea ice of McMurdo Sound, Antarctica. *Marine Ecology Progress Series*, **35**, 175–186.

Kottmeier, S.T. & Sullivan, C.W. (1987b) Late winter primary production and bacterial production in sea ice and seawater west of the Antarctic Peninsula. *Marine Ecology Progress Series*, **36**, 287–298.

Kottmeier, S.T. & Sullivan, C.W. (1990) Bacterial biomass and production in pack ice of Antarctic marginal ice edge zones. *Deep-Sea Research*, **37**, 1311–1330.

Kottmeier, S.T., McGrath-Grossi, S. & Sullivan, C.W. (1987) Sea ice microbial communities. VIII. Bacterial production in annual sea ice of McMurdo Sound, Antarctica. *Marine Ecology Progress Series*, **35**, 175–186.

Krembs, C. & Deming, J.W. (2008) The role of exopolymers in microbial adaptation to sea ice. In: *Psychrophiles: from Biodiversity to Biotechnology* (Eds. R. Margesin, F. Schinner, J.-C. Marx & C. Gerday), pp. 247–264. Springer-Verlag, Berlin.

Krembs, C. & Engel, A. (2001) Abundance and variability of microorganisms and transparent exopolymer particles across the ice–water interface of melting first-year sea ice in the Laptev Sea (Arctic). *Marine Biology,* **138**, 173–185.

Krembs, C., Gradinger, R. & Spindler, M. (2000) Implications of brine channel geometry and surface area for the interaction of sympagic organisms in Arctic sea ice. *Journal of Experimental Marine Biology and Ecology*, **243**, 55–80.

Krembs, C., Deming, J.W., Junge, K. & Eicken, H. (2002) High concentrations of exopolymeric substances in wintertime sea ice: implications for the polar ocean carbon cycle and cryoprotection of diatoms. *Deep-Sea Research Part I*, **49**, 2163–2181.

Krembs, C., Deming, J.W. & Eicken, H. (2009) Effects of exopolymeric substances on sea ice microstructure and salt retention. *Marine Ecology Progress Series* (submitted).

Laurion, I., Demers, S. & Vezina, A.F. (1995) The microbial food web associated with the ice algal assemblage: biomass and bacterivory of nanoflagellate protozoans in Resolute Passage (High Canadian Arctic). *Marine Ecology Progress Series,* **120**, 77–89.

Lizotte, M. (2003) Microbiology. In: *Sea Ice: An Introduction to its Physics, Chemistry, Biology and Geology* (Eds. D.N. Thomas & G. Dieckmann), pp. 184–210. Blackwell Science, Oxford.

Mader, H.M., Pettitt, M.E., Wadham, J.L., Wolff, E.W. & Parkes, R.J. (2006) Subsurface ice as a microbial habitat. *Geology*, **34**, 169–172.

Mancuso Nichols, C., Garon, S., Bowman, J.P., Raguénès, G. & Guézennec, J. (2004) Production of exopolysaccharides by Antarctic marine bacterial isolates. *Journal of Applied Microbiology*, **96**, 1057–1066.

Mancuso Nichols, C., Bowman, J.P. & Guezennec, J. (2005a) Effects of incubation temperature on growth and production of exopolysaccharides by an Antarctic sea ice bacterium grown in batch culture. *Applied and Environmental Microbiology*, **71**, 3519–3523.

Mancuso Nichols, C., Guezennec, J. & Bowman, J.P. (2005b) Bacterial exopolysaccharides from extreme marine environments with special consideration of the Southern Ocean, sea ice, and deep-sea hydrothermal vents: a review. *Marine Biotechnology*, **7**, 253–271.

Maranger, R., Bird, D.F. & Juniper, K. (1994) Viral and bacterial dynamics in Arctic sea ice during the spring algal bloom near Resolute, N.W.T., Canada. *Marine Ecology Progress Series*, **111**, 121–127.

Margesin, R., Schinner, F., Marx, J.-C. & Gerday, C. (Eds.) (2008) *Psychrophiles: From Biodiversity to Biotechnology*. Springer-Verlag, Berlin.

Martin, S., Drucker, R. & Fort, M. (1995) A laboratory study of frost flower growth on the surface of young sea ice. *Journal of Geophysical Research*, **100**, 7027–7036.

Martin, S., Yu, Y. & Drucker, R. (1996) The temperature dependence of frost flower growth on laboratory sea ice and the effect of the flowers on infrared observations of the surface. *Journal of Geophysical Research*, **101**, 12111–12126.

Marx, J.G., Carpenter, S.D. & Deming, J.W. (2009) Production of cryoprotectant extracellular polysaccharide substances (EPS) by the marine psychrophilic bacterium *Colwellia psychrerythraea* strain 34H under extreme conditions. *Canadian Journal of Microbiology*, **55**, 10.1139/W08-130.

Meiners, K., Gradinger, R., Fehling, J., Civitarese, G. & Spindler, M. (2003) Vertical distribution of exopolymer particles in sea ice of the Fram Strait (Arctic) during autumn. *Marine Ecology Progress Series*, **248**, 1–13.

Meiners, K., Brinkmeyer, R., Granskog, M.A. & Lindfors, A. (2004) Abundance, size distribution and bacterial colonization of exopolymer particles in Antarctic sea ice (Bellingshausen Sea). *Aquatic Microbial Ecology*, **35**, 283–296.

Meiners, K., Krembs, C. & Gradinger, R. (2008) Exopolymer particles: microbial hotspots of enhanced bacterial activity in Arctic fast ice (Chukchi Sea). *Aquatic Microbial Ecology*, **52**, 195–207.

Methé, B.A., Nelson, K.E., Deming, J.W. et al. (2005) The psychrophilic lifestyle as revealed by the genome sequence of *Colwellia psychrerythraea* 34H through genomic and proteomic analyses. *Proceedings of the National Academy of Sciences USA*, **102**, 10913–10918.

Mock, T. & Gradinger, R. (1999) Determination of Arctic ice algal production with a new in situ incubation technique. *Marine Ecology Progress Series*, **177**, 15–26.

Mock, T. & Thomas, D.N. (2005) Recent advances in sea ice microbiology. *Environmental Microbiology*, **7**, 605–619.

Mock, T., Dieckmann, G.S., Haas, C. et al. (2002) Micro-optodes in sea ice: a new approach to investigate oxygen dynamics during sea ice formation. *Aquatic Microbial Ecology*, **29**, 297–306.

Mock, T., Kruse, M. & Dieckmann, G.S. (2003) A new microcosm to investigate oxygen dynamics at the sea ice water interface. *Aquatic Microbial Ecology*, **30**, 197–205.

Mohr, J.L. & Tibbs, J. (1963) Ecology of ice substrates. *Proceedings of the Arctic Basin Symposium October 1962*, pp. 245–248. The Arctic Institute of North America, Tidewater Publishing, Centreville, MD.

Morita, R.Y. (1975) Psychrophilic bacteria. *Bacteriological Reviews*, **39**, 144–167.

Moyer, C.L. & Morita, R.Y. (2007) Psychrophiles and psychrotrophs. *Encyclopedia of Life Sciences*, doi:10.1002/9780470015902.a0000402.pub2. John Wiley and Sons, New York.

Mumma, M.J., Villanueva, G.L., Novak, R.E., Hewagama, T., Bonev, B.P., DiSanti, M.A., Mandell, A.M. & Smith, M.D. (2009) Strong release of methane on Mars in northern summer 2003. *Science*, **323**, 1041–1045.

Nichols, D., Bowman, J., Sanderson, K., Mancuso Nichols, C., Lewis, T., McMeekin, T. & Nichols, P.D. (1999) Developments with Antarctic microorganisms: culture collections, bioactivity screening, taxonomy, PUFA production and cold-adapted enzymes. *Current Opinion in Biotechnology*, **10**, 240–246.

Ochman, H., Lawrence, J.G. & Grolsman, E.A. (2000) Lateral gene transfer and the nature of bacterial innovation. *Nature*, **405**, 299–304.

Ortmann, A.C. & Suttle, C.A. (2005) High abundances of viruses in a deep-sea hydrothermal vent system indicates viral mediated microbial mortality. *Deep-Sea Research Part I*, **52**, 1515–1527.

Perovich, D.K. & Richter-Menge, J.A. (1994) Surface characteristics of lead ice. *Journal of Geophysical Research*, **99** (C8), 16,341–16,350.

Petri, R. & Imhoff, J.F. (2001) Genetic analysis of sea ice bacterial communities of the Western Baltic Sea using an improved double gradient method. *Polar Biology*, **24**, 252–257.

Pomeroy, L.R. & Wiebe, W.J. (2001) Temperature and substrates as interactive limiting factors for marine heterotrophic bacteria. *Aquatic Microbial Ecology*, **23**, 187–204.

Price, P.B. (2007) Microbial life in glacial ice and implications for a cold origin of life. *FEMS Microbial Ecology*, **59**, 217–231.

Rankin, A.M., Wolff, E.W. & Martin, S. (2002) Frost flowers: implications for tropospheric chemistry and ice core interpretation. *Geophysical Research*, **107**, 4683–4694.

Raymond, J.A., Fritsen, C. & Shen, K. (2007) An ice-binding protein from an Antarctic sea ice bacterium. *FEMS Microbiology Ecology*, **61**, 214–221.

Reimnitz, E., Clayton, J.R., Kempema, E.W., Payne, J.R. & Weber, W.S. (1993) Interaction of rising frazil with suspended particles: tank experiments with applications to nature. *Cold Regions Science and Technology*, **21**, 117–135.

Riedel, A., Michel, C. & Gosselin, M. (2006) Seasonal study of sea ice exopolymeric substances on the Mackenzie shelf: implications for transport of sea ice bacteria and algae. *Aquatic Microbial Ecology*, **45**, 195–206.

Riedel, A., Michel, C., Gosselin, M. & LeBlanc, B. (2007) Enrichment of nutrients, exopolymeric substances and microorganisms in newly formed sea ice on the Mackenzie shelf. *Marine Ecology Progress Series*, **342**, 55–67.

Rodriguez, D.F. & Tiedje, J.M. (2008) Coping with our cold planet. *Applied and Environmental Microbiology*, **74**, 1677–1686.

Różańska, M., Poulin, M. & Gosselin, M. (2008) Protist entrapment in newly formed sea ice in the Coastal Arctic Ocean. *Journal of Marine Systems*, **74** (3–4), 887–901.

Rysgaard, S. & Glud, R.N. (2004) Anaerobic N₂ production in Arctic sea ice. *Limnology and Oceanography,* **49** (1), 86–94.

Rysgaard, S., Kuhl, M., Glud, R.N. & Hansen, J.W. (2001) Biomass, production and horizontal patchiness of sea ice algae in a high-Arctic fjord (Young Sound, NE Greenland). *Marine Ecology Progress Series*, **223**, 15–26.

Rysgaard, S. Glud, R.N., Sejr, M.K., Blicher, M.E. & Stahl, H.J. (2008) Denitrification activity and oxygen dynamics in Arctic sea ice. *Polar Biology*, **31**, 527–537.

Saunders, N.F., Thomas, T., Curmi, P.M. et al. (2003) Mechanisms of thermal adaptation revealed from the genomes of the Antarctic Archaea *Methanogenium frigidum* and *Methanococcoides burtonii*. *Genome Research*, **13**, 1580–1588.

Schroeder, W.H., Anlauf, K.G., Barrie, L.A, Lu, J.Y., Steffen, A., Schneeberger, D.R. & Berg, T. (1998) Arctic springtime depletion of mercury. *Nature*, **394**, 331–332.

Smith, R.E.H. & Clement, P. (1990) Heterotrophic activity and bacterial productivity in assemblages of microbes from sea ice in the high Arctic. *Polar Biology*, **10**, 351–357.

Smith, R.E.H., Clement, P. & Cota, G.F. (1989) Population dynamics of bacteria in Arctic sea ice. *Microbial Ecology*, **17**, 63–76.

Sogin, M.L., Morrison, H.G., Huber, J.A. et al. (2006) Microbial diversity in the deep sea and the under-explored "rare biosphere." *Proceedings of the National Academy of Sciences*, **103**, 12115–12120.

Staley, J.T. & Gosink, J.J. (1999) Poles apart: biodiversity and biogeography of sea ice bacteria. *Annual Reviews in Microbiology*, **53**, 189–215.

Stewart, F.J. & Fritsen, C.H. (2004) Bacteria–algal relationships in Antarctic sea ice. *Antarctic Science*, **16**, 143–156.

Stierle, A.P. & Eicken, H. (2002) Sediment inclusions in Alaskan coastal sea ice: spatial distribution, interannual variability, and entrainment requirements. *Arctic Antarctic and Alpine Research*, **34** (4), 465–476.

Style, R.M. (2007) The Formation and Evolution of Frost Flowers and Related Phenomena. PhD Thesis, 146 pp. University of Cambridge, Cambridge, UK.

Sullivan, C.W. & Palmisano, A.C. (1981) Sea ice microbial communities in McMurdo Sound, Antarctica. *Antarctic Journal US*, **16**, 126–127.

Sullivan, C.W. & Palmisano, A.C. (1984) Sea ice microbial communities: distribution, abundance, and diversity of ice bacteria in McMurdo Sound, Antarctica in 1980. *Applied Environmental Microbiology*, **47**, 788–795.

Sullivan, C.W., Palmisano, A.C., Kottmeier, S. & Moe, R. (1982) Development of the sea ice microbial community (SIMCO) in McMurdo Sound, Antarctica. *Antarctic Journal US*, **17**, 155–157.

Thomas, D.N., Lara, R.J., Eicken, H., Kattner, G. & Skoog, A. (1995) Dissolved organic matter in Arctic multi-year sea ice during winter: major components and relationship to ice characteristics. *Polar Biology*, **15** (7), 477–483.

Thomas, D.N., Engbrodt, R., Giannelli, V., Kattner, G., Kennedy, H., Haas, C. & Dieckmann, G.S. (2001) Dissolved organic matter in Antarctic sea ice. *Annals of Glaciology*, **33**, 297–303.

Vajda, T. & Hollosi, M. (2001) Cryo-bioorganic chemistry: freezing effect on stereoselection of L- and DL-leucine cooligomerization in aqueous solution. *Cellular & Molecular Life Science*, **58**, 343–346.

Vetter, Y.-A., Deming, J.W., Jumars, P.A. & Krieger-Brockett, B.B. (1998) A predictive model of bacterial foraging by means of freely-released extracellular enzymes. *Microbial Ecology*, **36**, 75–92.

Weissenberger, J. & Grossmann, S. (1998) Experimental formation of sea ice: importance of water circulation and wave action for incorporation of phytoplankton and bacteria. *Polar Biology*, **20**, 178–188.

Wells, L.E. (2006) *Viral Adaptations to Life in the Cold.* PhD Thesis, 370 pp. University of Washington, Seattle.

Wells, L.E. (2008) Cold-active viruses. In: *Psychrophiles: from Biodiversity to Biotechnology* (Eds. R. Margesin, F. Schinner, J.-C. Marx & C. Gerday), pp. 157–173. Springer-Verlag, Berlin.

Wells, L.E. & Deming, J.W. (2006a) Modelled and measured dynamics of viruses in Arctic winter sea ice brines. *Environmental Microbiology*, **8**, 1115–1121.

Wells, L.E. & Deming, J.W. (2006b) Characterization of a cold-active bacteriophage on two psychrophilic marine hosts. *Aquatic Microbial Ecology*, **45**, 15–29.

Wettlaufer, J.S. & Worster, M.G. (1995) Dynamics of premelted films: frost heave in a capillary. *Physics Reviews*, **E 51**, 4679–4689.

Wickham, S. & Carstens, M. (1998) Effects of ultraviolet-B radiation on two arctic microbial food webs. *Aquatic Microbial Ecology*, **16**, 163–171.

Wilson, S.L., Kelley, D.L. & Walker, V.K. (2006) Ice-active characteristics of soil bacteria selected by ice-affinity. *Environmental Microbiology*, 10.1111/j.1462-2920.2006.01066.x.

Yager, P.L., Connelly, T.L., Mortazavi, B. et al. (2001) Dynamic bacterial and viral response to an algal bloom at subzero temperatures. *Limnology and Oceanography*, **46**, 790–801.

8 Primary Producers and Sea Ice

Kevin R. Arrigo, Thomas Mock and Michael P. Lizotte

8.1 Introduction

The extensive pack and fast ice that forms in both Antarctic and Arctic regions provides a unique habitat for polar microbial assemblages (reviewed by Mock & Thomas, 2005). Algal communities, in particular, are known to flourish within the distinct micro-habitats which are created when sea ice forms and ages. The primary advantage afforded by sea ice is that it provides a platform from which sea ice algae can remain suspended in the upper ocean where light is sufficient for net growth. These autotrophic organisms play a critical role in polar marine ecology in both the Arctic and the Antarctic. For example, although rates of primary production (photosynthetic carbon assimilation) by sea ice algae are generally low compared to their phytoplankton counterparts, they are often virtually the sole source of fixed carbon for higher trophic levels in ice-covered waters. In fact, sea ice algae have been shown to sustain a wide variety of organisms (Chapter 10), including krill, through the winter months when other sources of food are lacking.

8.2 Sea ice as a habitat

In the early stages of pack ice formation in both the Arctic and the Antarctic, dense concentrations of frazil ice can develop rapidly under turbulent conditions as large quantities of heat are extracted from the near-surface ocean during strong wind events (for more detail see Chapters 2 and 4). As winds diminish and the sea surface calms, ice crystals float to the sea surface where they coalesce into semi-consolidated grease ice, and eventually, into thicker nilas and pancake ice (Ackley & Sullivan, 1994). Additional freezing and horizontal movement fuses ice pancakes together to form a continuous ice pack. Historically, frazil ice has been much more common in the Antarctic than in the Arctic, due primarily to the fact that more first-year ice forms in the southern hemisphere. This may be changing, however, as the proportion of annual ice formed in the Arctic has been increasing in recent years. In summer, the Arctic is covered by approximately 4.5–9.0 million km² of persistent multiyear ice, compared to only 3.5 million km² of multiyear ice in the Antarctic (Chapter 6). During the winter, the Arctic adds 7–12 million km² of annual ice, bringing the total sea ice extent to approximately 16 million km². The Antarctic, in contrast, produces more than twice as

much first-year ice as the Arctic, averaging 15.5 million km² of new ice per year, and has a greater total sea ice extent of 19 million km² (Gloersen et al., 1992).

The initial stage of sea ice formation generally begins in the autumn when there are still substantial microbial populations left over in surface waters from the preceding spring blooms. As a result, during frazil ice formation, particles such as microalgae, heterotrophic protists and bacteria are often scavenged from the water column as the newly formed frazil ice crystals rise to the surface (Garrison et al., 1990). In some cases, particle concentrations in very young frazil ice have been found to be over 50 times greater than in the underlying sea water, with the incorporation of large diatoms being observed most commonly.

Subsequent ice growth beyond the consolidated pancake stage proceeds vertically as heat is extracted from the sea ice surface by the cold atmosphere. This is also true for land-fast ice which does not have an initial frazil ice stage. Columnar ice crystals extend from the lower ice margin into the water column (Fig. 8.1). The lower margin of the growing columnar ice, referred to as the skeletal layer, is highly porous and has a temperature that is just below the freezing point of sea water. Rafting of ice floes as sea ice is moved by the wind and tides
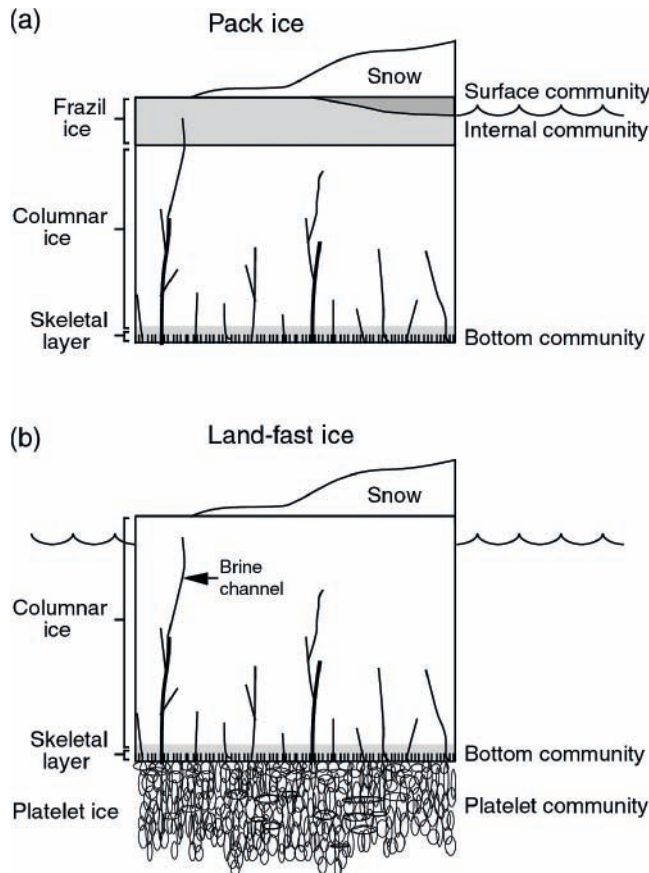
Fig. 8.1 Highly idealized schematic illustration of (a) pack ice and (b) land-fast ice ecosystems in the Arctic and Antarctic showing the location of the major ice algal communities. Whether a given community is found in a particular location is highly variable and dependent on the sea ice structure and formation history.

causes breakage and occasionally forces parts of the floe below freeboard, flooding the ice surface with sea water. Similarly, heavy snow cover can also force the ice floe below freeboard, resulting in surface flooding.

It is in those regions of the ice floe that are most tightly coupled to the underlying sea water that sea ice microalgae flourish. This is because one of the primary factors controlling the growth of algae in sea ice is access to nutrients (Chapter 12). Except for those areas where snow cover is extremely thick, light is usually sufficient for net photosynthesis during the polar spring and summer (Grossi et al., 1987). Sea ice habitats are often characterized by steep gradients in temperature, salinity, light and nutrient concentration. The greatest fraction of sea ice microalgae often reside in the bottom 20 cm of the ice sheet where environmental conditions are generally stable and more favourable for growth, with the rare exception of those areas where sea ice growing in the vicinity of rivers is exposed to low salinities, impacting the ecosystem structure (Kaartokallio et al., 2007). Bottom ice communities form in the skeletal layer and extend upwards as far as 0.2 m, their upward distribution generally being limited by nutrient availability and high brine-salinity characteristic of the sea ice interior when temperatures are low (Arrigo & Sullivan, 1992).

Under certain conditions, microalgae also may be found in internal layers, where they are often subjected to large environmental fluctuations (Lizotte & Sullivan, 1991). For example, brines with salinities as high as 173 and temperatures as low as −16°C have been collected from the upper 1.0–1.5 m of the sea ice in McMurdo Sound (Kottmeier & Sullivan, 1988), high enough to prevent detectable metabolic activity in most sea ice algae (Grant & Horner, 1976; Arrigo and Sullivan, 1992). Internal communities are generally associated with a frazil ice layer or can be found at the freeboard level where sea water can infiltrate the ice floe (Kattner et al., 2004). These communities are seeded by the particles scavenged during frazil ice formation and are especially dependent upon nutrient availability and salinity. They are more common in the Antarctic than the Arctic.

Although the surface and near-surface communities often have adequate light levels for growth, the availability of nutrients for these communities is often restricted. Measurements of salinity in the cavity of the freeboard layer indicate that this layer is infiltrated by sea water that provides the nutrients required by the algal community (Kattner et al., 2004). However, this supply of nutrients depends on the porosity of the surrounding ice. For the algal communities growing at the snow–ice interface, surface flooding, caused by snow loading and submersion of the ice pack, is an important source of nutrients. Such surface flooding occurs over 15–30% of the ice pack in Antarctica (Wadhams et al., 1987). Thus, although snow cover has the negative effect of reducing the amount of light available for algal growth, it is also responsible for providing nutrients to the surface community (Arrigo et al., 1997).

Less common sea ice assemblages include those that grow in a 'strand' layer just beneath the sea ice, and within a sub-ice platelet layer. Mat and strand communities, where algae are loosely attached to the underside of the sea ice but extend well into the water column, are found mainly in Arctic regions (Melnikov & Bondarchuk, 1987; Johnsen & Hegseth, 1991). Conversely, platelet ice, a semi-consolidated layer of ice ranging from a few centimetres to several metres in thickness, is commonly observed beneath sea ice in regions adjacent to floating ice shelves in the Antarctic where 45% of the continental margin is associated with an ice shelf (Bindschadler, 1990; Kipfstuhl, 1991). Platelet ice is the most porous of all sea ice types, being composed of approximately 20% ice and 80% sea water by volume, and harbours some of the highest concentrations of sea ice algae found anywhere on Earth.

8.3 Algae inhabiting sea ice

Quantitative sampling of sea ice is difficult due to the heterogeneous distribution of organisms among the liquid and solid matrices. The first challenge is to capture a representative volume. The most common tool used to sample sea ice is a vertical coring device. Corers function best on thicker ice (capable of supporting the human operator) when the ice is young and cold (with minimal drainage channels). Because the corer is not leak-proof, liquids can drain from the core. This makes it difficult to capture a representative sea ice sample from ice that is porous, has liquid-filled voids or drainage features, is loosely consolidated, is melting or has organisms loosely attached at the ice–sea water interface. Difficult-to-core environments have been sampled from below by SCUBA divers, reticulated arms and undersea robotic devices.

The second challenge in quantitative sampling is to produce a liquid sample containing the sea ice organisms. This is straightforward when the sampling technique extracts liquids from the sea ice. For example, larger volumes of liquids enclosed by sea ice, located within internal or platelet layers, can be sampled directly by pumping. In addition, brine can be removed from a sea ice core sample by gravity drainage or centrifugation. These samples retain the chemical and temperature conditions experienced by sea ice organisms, which are critical for physiological studies. However, liquid sampling is not a comprehensive sampling method because attached or larger sea ice organisms often remain with the ice matrix. To recover a complete community sample, the ice must be melted. Organisms in a melting sea ice sample will experience a shift in salinity from marine or hypersaline (>34) to brackish (salinities as low as 3), which will produce an osmotic shock that can cause cells to lyse. An extreme salinity shift could kill sea ice microbes and leave little trace of fragile cells. To avoid these osmotic losses, the ice can be melted into sufficient sea water (prefiltered to remove planktonic organisms) to keep salinity near 35. While this approach produces a highly disturbed chemical environment and involves temperatures above freezing, it produces samples that can be analysed for microbial abundance and biomass using routine methods developed for marine plankton.

Microbial cell counting is most commonly accomplished by microscopy. Light microscopy was the first analytical technique applied in sea ice biology, when diatoms were first described in the 1840s. The development of epifluorescence microscopy has been an important development because it makes it possible to distinguish algae with fluorescing pigments (e.g. the red fluorescence of chlorophyll *a*) from other microbes. Electron microscopy also has been instrumental in elucidating fine structures. Flow cytometry (which can include microscopy in addition to other optical detection methods) has not been widely applied in sea ice studies, but holds promise for rapid quantification of smaller cells, particularly with the development of species or group-specific fluorescent molecular probes. Finally, methods have recently been developed for microscopy on cells while still enclosed in sea ice (Deming, 2002), which will be particularly useful for observing *in situ* spatial organization of microbial communities.

Abundance and biomass

The abundance of sea ice micro-organisms can be quantified as the concentration of cells or biomass per volume of ice or liquid environments. Organisms are also quantified per unit area; this is particularly useful for quantifying photosynthetic organisms that depend on

solar radiation (which is also quantified in terms of flux per unit area) and for comparisons with planktonic or terrestrial communities.

Algae cell concentrations in sea ice vary by up to six orders of magnitude (from $<10^4$ to $>10^9$ cells per litre), ranging from low values typical of oceanic waters to some of the highest values recorded for any aquatic environment. Low abundance is more typical of newly formed ice or the upper ice column where environmental conditions are extreme. The highest concentrations are found at ice–sea water interfaces, ice-enclosed pockets of sea water (e.g. platelet layers, brash ice and crack pools) and surface ponds.

The biomass of microbes can be derived from microscopic observations and from chemical analyses. The most widely applied chemical method for biomass estimation is algal pigment concentration. Chlorophyll *a* (Chl *a*) is present in all photosynthetic organisms in sea ice. For a chemical marker to be a useful estimator of biomass, it must be present in living organisms at a fairly constant ratio to carbon or cell number. While the ratio of Chl *a* to carbon or Chl *a*/cell can vary amongst species and in response to changes in light (cells become enriched in Chl *a* to increase their ability to harvest light), it serves as a first-order estimate of biomass for photosynthetic organisms. Carbon-to-Chl *a* ratios (ca. 20–40 for sea ice algae) have been used to estimate algal carbon based on Chl *a* concentrations. For pigment analysis, cells are collected on filters and the pigments are extracted with solvents and quantified by various optical techniques (fluorometry or spectrophotometry).

The Chl *a* biomass in sea ice varies by geographic region, ice type and over seasons. To explore these variations, the maximum accumulations of Chl *a* recorded in sea ice have been tabulated (Tables 8.1 and 8.2). Land-fast bottom ice communities have received the most attention from scientists, followed by studies in the pack ice. Platelet ice is much more common in Antarctic coastal waters due to its relationship to ice shelves, and surface communities dependent on tides and surface flooding have drawn more attention in the south. Interior communities have received the most attention in Antarctic pack ice regions.

Volumetric Chl *a* concentrations range from 3 to 800 mg m^{-3} (= µg l^{-1}) in the Arctic and 3 to 10,100 mg m^{-3} in the Antarctic. Given that sea ice may start with only minimal algal biomass from sea water (e.g. 0.01 mg m^{-3}), the extreme values represent changes of 5–7 orders of magnitude. To accumulate this biomass from algal growth via cell division would require 16–20 generations. Most of the reported biomass data are from first-year ice, so this growth will occur in a single growth season of a few months. The accumulated biomass per unit area ranges from 1 to 340 mg m^{-2} in the Arctic and <1 to 1090 mg m^{-2} in the Antarctic.

Across the independent studies of algal biomass accumulation (Tables 8.1 and 8.2), the median values for the Arctic are lower (25 mg m^{-3} and 31 mg m^{-2}; $n > 30$) than for the Antarctic (170 mg m^{-3} and 47 mg m^{-2}; $n > 50$). These differences may be attributed to major oceanographic differences, such as the potential for higher nutrient availability in Antarctic seas, or the lower annual light availability at extreme polar latitudes in the Arctic. However, the differences also may be due to sampling bias, as much of the work in the Antarctic has focused on high biomass platelet and surface ice communities.

Seasons should have an effect on the concentrations of sea ice algae, particularly in first-year ice, increasing from winter through a spring bloom, and possibly continuing into summer or subsequent blooms in summer and autumn. Low-latitude sites may only have sea ice during winter (Chapter 14). Chl *a* accumulations in the Baltic Sea, Labrador Sea and Sea of Okhotsk in the north are approximately an order of magnitude lower than those at higher-latitude sites (Table 8.1). The South Orkney Islands hold a similar position in the south, but

Table 8.1 Maximum algal biomass as chl *a* reported for independent studies of Arctic sea ice.

Ice type	Region	Season	mg m^{-3}	mg m^{-2}	References
Bottom	Canadian Arctic Archipelago	Spring	704	14, 23, 55, 80, 89, 110, 130, 140, 160, 260, 300, 320, 340	Apollonia (1965); Dunbar and Acreman (1980); Smith et al. (1987, 1988); Cota and Horne (1989); Cota et al. (1990); Smith and Herman (1991); Herman et al. (1993); Maranger et al. (1994); Michel et al. (1996); Suzuki et al. (1997); Welch and Bergmann (1989); Apollonia et al. (2002); Lavoie et al. (2005)
	Hudson Bay	Spring	>800	21, 40, 170	Gosselin et al. (1986); Legendre et al. (1987); Welch et al. (1991); Monti et al. (1996)
	Labrador Sea	Spring		5, 8	Grainger (1977); Hsiao (1980)
	Baffin Bay	Spring		25, 56	Nozais et al. (2001); Michel et al. (2002)
	Beaufort Sea	Spring–summer	427, 600, 711	24, 26, 30, 31, 64	Meguro et al. (1967); Alexander (1974); Horner (1976); Alexander and Chapman (1981); Horner and Schrader (1982); Jin et al. (2006); Riedel et al. (2006)
	Chukchi Sea	Summer	123		Ambrose et al. (2005)
	Sea of Okhotsk	Winter	20, 153	6, 8, 30, 36, 119	Kudoh (1997); Robineau et al., (1997); Asami and Imada (2001); Nishi and Tabeta (2006); McMinn et al. (2008)
	White Sea	Spring	35		Krell et al. (2003)
	Baltic Sea	Winter–spring	6, 15, 17, 19, >60	3	Meiners et al. (2002); Granskog et al. (2003); Kaartokallio (2004); Steffens et al. (2006); Kaartokallio et al. (2007)
	Barents Sea	Spring	84		Mock and Gradinger (1999)
	Spitzbergen	Spring–summer	3, 67		Dobrzyn and Tatur (2003); Schunemann and Werner (2005)
	Greenland Sea	Spring	15, 30, 260	2	Buck et al. (1998); Mock and Gradinger (1999); Rysgaard et al. (2001)
Surface	Bering Sea			70	Niebauer et al. (1981)
Pack	Central Arctic Ocean	Summer–autumn	9	7, 15	Gosselin et al. (1997); Gradinger (1999); Melnikov et al. (2002)
	Labrador Sea	Spring	191		Irwin (1990)
	Sea of Okhotsk	Winter	3		McMinn et al. (2008)
	Laptev Sea	Autumn	17	2	Gradinger and Zhang (1997)
	Barents Sea	Summer	17	1	Gradinger and Zhang (1997)
	Greenland Sea	Summer	57	3	Gradinger et al. (1999)
	Fram Strait	Autumn	17		Meiners et al. (2003)
Median			**25**	**31**	

Table 8.2 Maximum algal biomass as chl *a* reported for independent studies of Antarctic sea ice.

Ice type	Region	Season	mg m^{-3}	mg m^{-2}	References
Bottom	McMurdo Sound	Spring	656, >1000, 10,100	9, 170, 170, 173, 252, 294, 309, 378	Sullivan et al. (1982, 1985); Palmisano and Sullivan (1983); Palmisano et al. (1985, 1988); Grossi et al. (1987); Lizotte and Sullivan (1992b); Arrigo et al. (1995); Trenerry et al. (2002); Ryan et al. (2006)
	Terra Nova Bay	Spring	430, 2480		Guglielmo et al. (2000, 2004)
	Cape Hallett	Spring		36	Ryan et al. (2006)
	Adelie Coast	Spring	24, 3100	>500	Riaux-Gobin et al. (2000, 2005)
	Prydz Bay	Spring		15, 96, 110	McConville et al. (1985); Archer et al. (1996); McMinn and Ashworth (1998)
	Lutzow-Holm Bay	Spring	>1000, 2980, 5320	35, 125	Hoshiai (1977, 1981); Watanabe and Satoh (1987)
		Autumn	>829, 944	65	Hoshiai (1977, 1981)
	Weddell Sea	Summer–autumn	540	9	Dieckmann et al. (1990); Lizotte and Sullivan (1991)
Platelet	McMurdo Sound	Spring	132, 250, 430, >6000	76, 125, 164, 1076, 1090	Bunt (1963, 1968); Bunt and Lee (1969, 1970); Grossi et al. (1987); Lizotte and Sullivan (1992b); Arrigo et al. (1993a, 1995)
	Terra Nova Bay	Spring	360		Guglielmo et al. (2004)
	Weddell Sea	Spring	36	20	Smetacek et al. (1992)
Internal	McMurdo Sound	Summer		10	Stoecker et al. (2000)
	Prydz Bay	Spring		6	Archer et al. (1996)
	Weddell Sea	Summer–autumn	4, 5, 10, 440	1, 1, 10, 29	Ackley et al. (1979); Garrison and Buck (1982); Clarke and Ackley (1984); Lizotte and Sullivan (1991); Hegseth and von Quillfeldt (2002); Kattner et al. (2004)
Surface	McMurdo Sound	Spring	730	51	Lizotte and Sullivan (1992b); Robinson et al. (1997)
	Lutzow-Holm Bay	Summer	670	97	Meguro (1962)
	Weddell Sea	Winter–spring	43	80	Clarke and Ackley (1984); Kottmeier and Sullivan (1990)
	Palmer Peninsula	Summer	407	117	Burkholder and Mandelli (1965)
	South Orkney Islands	Winter	7500	244	Whitaker and Richardson (1980)
New	Weddell Sea	Summer–autumn	5, 6, 27	4	Garrison et al. (1983); Lizotte and Sullivan (1991); Mock (2002)
Pack	Weddell Sea	Winter	14, 15, 19, 23	16, 18, 23, 29, 53	Quetin and Ross (1988); Kottmeier et al. (1987); Schnack-Schiel (1987); Augstein et al. (1991); Garrison and Close (1993)
		Spring	15, 23, 27	18, 19, 35, 47	Ainley and Sullivan (1984); Schnack-Schiel (1987); Hempel (1989); Gradinger (1999)

(Continued)

Table 8.2   (*Continued*)

Ice type	Region	Season	mg m^{-3}	mg m^{-2}	References
		Summer	43, 59, 202	73, 77, 99, 453	Hempel (1985); Bathmann et al. (1992); Miller and Grobe (1996); Gradinger (1999)
		Autumn	10, 16, 37	11, 19, 30, 32, 38	Garrison and Buck (1982); Spindler et al. (1993); Fritsen et al. (1994); Lemke (1994); Gradinger (1999)
	Bransfield Strait	Winter	1300		Lizotte et al. (1998)
	Bellingshausen–Amundsen Sea	Summer–autumn	230, 400	60	Thomas et al. (1998); Meiners et al. (2004)
	Ross Sea	Spring	18	11	Arrigo et al. (2003)
		Summer–autumn	84, 97, 1456	12	Fritsen et al. (2001); Garrison et al. (2003); Gowing (2003)
	Prydz Bay	Spring		8	McMinn et al. (2007)
Median			**170**	**47**	

the surface ice diatom blooms recorded there in the 1970s are amongst the highest biomass ever recorded for sea ice (Table 8.2). Most sea ice studies have been conducted during spring at higher latitudes, when ice is a relatively stable (growing or melting slowly) substrate for algal communities. Spring also may begin as a season with relatively low grazer pressure, if invertebrate grazers have an annual life cycle timed to the accumulation and release of ice algae. In general, summer and autumn biomass levels are lower than the spring peaks. Pack ice of the Weddell Sea is the only ice type–region combination for which numerous observations have been made in all seasons; summer appears to be the peak season in this high-latitude basin (Table 8.2).

Biodiversity of photosynthetic organisms

The organisms responsible for photosynthetic production in sea ice are nearly always diatoms, though blooms of other algae have been observed. Extensive reviews of the dominant species were assembled by Horner (1985) and Garrison (1991). These reviews and more recent studies (Table 8.3) imply that diatoms make up most (>90%) of the photosynthetic organism diversity, which probably exceeds 500 species. However, improved methods in taxonomy have increased recognition of flagellate species. Recent studies in the Arctic (Table 8.3) have recorded non-diatom diversity nearly as great as the compilation of Horner (1985). Overall, species diversity appears to be higher in the Arctic than in the Antarctic. Possible explanations for higher Arctic diversity include the greater extension south along continental shelves of the Atlantic and Pacific oceans, and the greater potential for terrestrial species introductions (via rivers, winds and migrating animals).

Amongst the diatoms, species with a pennate form (longer in one axis) are most common (e.g. species of the genera *Nitzschia*, *Fragilariopsis* and *Navicula*), and many form chains of cells. Unicellular forms tend to be large, thus, as either cells or chains, the sea ice diatoms make up large food particles (>20 μm) compared to oceanic phytoplankton. Blooms of pennate diatoms are very common in bottom ice, but also have been noted in surface

Table 8.3 Number of species reported for sea ice as diatoms and other photosynthetic species*, with the latter as per cent of total species reported.

Region	Diatom species	Other species	Other (% total)	References
Arctic	288	32	10	Horner (1985)
	115	6	5	Okolodkov (1993)
	24	37	61	Ikävalko and Thomsen (1997)
	36	11	23	Booth and Horner (1997)
	16	9	36	Tuschling et al. (2000)
	15	7	32	Druzhkov et al. (2001)
	68	20	23	Melnikov (2002)
	231	7	3	Von Quillfeldt et al. (2003)
	26	24	48	Werner et al. (2007)
Antarctic	223	22	9	Horner (1985)
	137	16	10	Garrison (1991)
	71	2	3	Hegseth and von Quillfeldt (2002)

*From most to least common: dinoflagellates, chlorophytes, prymnesiophytes, prasinophytes, silicoflagellates, chrysophytes, cryptophytes, cyanobacteria and ciliates.

ice (Whitaker & Richardson, 1980; Lizotte & Sullivan, 1992b), infiltration communities (Garrison, 1991) and platelet ice (Arrigo et al., 1995). In the Arctic, species of *Fragilaria*, *Cylindrotheca* and *Achnanthes* are relatively common, with some species common with riverine and benthic habitats. In the Antarctic, large species of *Amphiprora*, *Pinnularia*, *Pleurosigma*, *Synedra* and *Tropidoneis* are commonly reported, especially in land-fast ice.

Centric diatoms are also common in sea ice, but only dominate species composition under certain circumstances. In recently formed sea ice, it is possible that centric diatoms that are dominating the water column (e.g. autumn phytoplankton blooms of *Thalassiosira* or *Chaetoceros* species) are simply entrained into the sea ice. Further growth by these planktonic species may be limited within the sea ice. In the Antarctic, dense blooms of centric diatoms (species of *Porosira* and *Thalassiosira*) have been observed to grow in platelet ice habitats (Lizotte & Sullivan, 1992b; Smetacek et al., 1992).

A few species of diatoms are associated with sea ice as attached sub-ice forms with extensive extracellular matrix material that can extend centimetres to metres below the ice bottom. In the Arctic, colonies of the centric diatom *Melosira arctica* can reach lengths of several metres below the ice (Melnikov, 1997; Ambrose et al., 2005). In the Antarctic, the most common strand-forming species are from the genus *Berkeleya*, which only reach lengths of up to 15 cm (McConville & Wetherbee, 1983).

Flagellate species of algae also have been reported for sea ice, especially in surface ice and ponds of trapped sea water or meltwater. Prymnesiophytes (*Phaeocystis* spp.), dinoflagellates (e.g. *Gymnodinium* spp.), prasinophytes (species of *Mantoniella* and *Pyramimonas*), chlorophytes (species of *Monoraphidium* and *Chlamydomonas*), chrysophytes and cryptophytes are reported from both poles. Silicoflagellates (species of *Dictyocha*) have been reported in Arctic sea ice.

Photosynthetic organisms other than eukaryotic algae have been reported only sporadically in sea ice. Photosynthetic ciliates (species of *Mesodinium*) have been reported in

sea ice in the Antarctic (Garrison, 1991) and Arctic (Michel et al., 2002). Photosynthetic prokaryotes, probably of terrestrial freshwater origin, have been recorded occasionally for the Arctic, including cyanobacteria (Horner, 1985; Ikävalko & Thomsen, 1997) and purple sulphur bacteria (Petri & Imhoff, 2001).

8.4 Physiological ecology

Because the abundance and diversity of sea ice algal communities is often determined by the environmental factors, it is important to understand how ice algae respond physiologically to changing conditions within the sea ice environment.

Response to salinity

The physiological activity of sea ice microalgae is known to be sensitive to changes in ambient salt concentrations, with reductions in photosynthetic efficiency, photosynthetic capacity and growth rate as salinity diverges further from sea water values (Bunt, 1964; Grant & Horner, 1976; Bates & Cota, 1986; Vargo et al., 1986, Kottmeier & Sullivan, 1988; Arrigo & Sullivan, 1992; Krell et al., 2007). Recently, Ralph et al. (2007) extended these observations and found that sea ice algae exposed to extreme salinities exhibited substantial closure of photosystem II (PSII) reaction centres when irradiance was applied. These results are consistent with those of Krell et al. (2007) who showed that the efficiency of PSII dropped from 0.61 to 0.24 after an increase in salinity from 34 to 70. Salinity stress may result in limited reduction of the primary electron receptor and the plastoquinone pool, which ultimately inhibits both quantum yield of PSII and electron transport (Ralph et al., 2007).

However, studies investigating either short-term (minutes) photosynthetic responses (Bates & Cota, 1986) or very long-term (weeks) growth responses (Grant & Horner, 1976; Vargo et al., 1986) have shown that acclimation to either high or low salinity is possible. For instance, Vargo et al. (1986) reported that microalgae were capable of adapting their growth rates fully within 1–2 weeks after introduction to salinity regimes ranging from 19.5 to 31.5 while Grant and Horner (1976) reported similar observations over a much wider range of salinities (5–60). In both of these studies, the initial 3 days of the experiment were characterized by a reduction in algal biomass or growth rates that were more extreme as salinity diverged from 35. In addition, Ryan et al. (2004) showed that sea ice algal communities exposed to salinities between 30 and 10 exhibited a progressive decline in maximum quantum yield, relative electron transfer rate ($rETR_{max}$) and photosynthetic efficiency (α) with decreasing salinity. While all diatom species investigated showed a drop in these parameters, *Fragilariopsis curta* and *Entomoneis kjellmannii* showed the least inhibition. However, after their initial decline, there was a steady increase in both $rETR_{max}$ and α over 5 days after melting, especially in the samples melted into the highest salinities (Ryan et al., 2004), suggesting that acclimation was taking place.

One important way that sea ice microalgae acclimate to changes in salinity is by altering their osmolyte concentration. A widely used osmolyte is dimethylsulphoniopropionate (DMSP), which is a precursor of dimethylsulphide (DMS), a climate-active gas. Diatoms appear to be the largest producers of DMSP, with concentrations as high as 1478 nM being

observed in the fast ice of Prydz Bay, Antarctica (Trevena et al., 2003). DMSP concentrations in rafted ice have been reported to be as high as 2910 nM (Trevena & Jones, 2006). It has been suggested that sea ice is a large source of DMSP and DMS to the surrounding ocean and atmosphere (Trevena & Jones, 2006; Delille et al., 2007). Thus, changes in sea ice distributions, and in populations of ice algae acclimating to suboptimal salinity via production of DMSP, may exert important feedbacks on the climate system (Charlson et al., 1987).

Response to temperature

In general, the rate of physiological processes increases with temperature, up to the point where macromolecules become denatured and metabolic rates decline. For example, Ralph et al. (2005) reported effective quantum yield of PSII and $rETR_{max}$ of halotolerant brine microalgae that were higher at $-1.8°C$ than at $-10°C$. Similarly, growth rates of the chlorophyte *Chlamydomonas* sp. ARC, isolated from land-fast sea ice in the Chukchi Sea, Alaska, were significantly higher at 5°C than at $-5°C$ (Eddie et al., 2008). These metabolic rate changes with temperature are often quantified in terms of the Q_{10}, defined the ratio of the metabolic rates at temperature T°C and T+10°C. The photosynthetic Q_{10} for ice algae has been reported to range from 1.0 to 6.0 (Palmisano et al., 1987; Kottmeier & Sullivan, 1988; Arrigo & Sullivan, 1992) and is generally higher than those observed for field collected temperate phytoplankton, which generally range from 1.9 to 2.3 (Talling, 1955; Ichimura & Aruga, 1964; Eppley, 1972; Williams & Murdoch, 1966).

Sensitivity to temperature seems to be higher at the lower end of the temperature range. Palmisano et al. (1987) reported a non-linear Q_{10} response of the maximum photosynthetic rate (P_m^*) that decreased from 6 at the temperature range of $-2-2°C$, to 3 for the temperature range of 2–8°C. Arrigo and Sullivan (1992) reported similar changes in Q_{10} with temperature. If the Q_{10} response of microalgal photosynthesis is indeed non-linear within this temperature range, as both studies suggest, a simple two-parameter model like the one developed by Eppley (1972) may be inadequate to describe algal growth at low temperatures. This response can be attributed to the observation that rates of carbon fixation and growth for polar microalgae are greatest between 4°C and 14°C (Kottmeier & Sullivan, 1988). As a consequence, the sensitivity to changes in temperature would be expected to diminish as the treatment temperature interval approaches the temperature of maximum growth.

However, not all algal rate processes are impacted equally by changes in temperature. Priscu et al. (1989) reported Q_{10} values for nitrate assimilation (approximately 10) that were much larger than those measured for CO_2 fixation. Conversely, when the sea ice diatom *Fragilariopsis cylindrus* (Grunow) was grown under steady-state conditions at $-1°C$ and $+7°C$, no differences in quantum yield of PSII (Fv/Fm) and relative electron transport rates could be detected at either temperature after 4 months of acclimation (Mock & Hoch, 2005). The same was true for relative light utilization efficiency ($\alpha = 0.57$ and 0.60 at $-1°C$, and $+7°C$, respectively) and expression of PSII and the Rubisco large subunit genes. In contrast, Mock and Hoch (2005) did observe a temperature effect in the photoacclimation irradiance (E_k), P_m^*, and the degree of non-photochemical quenching (NPQ). NPQ differences were possibly related to a twofold increase in the concentration of the xanthophyll cycle pigment diatoxanthin and a ninefold up-regulation of a gene encoding a fucoxanthin–Chl *a,c*–binding protein (fcp). It appears that polar microalgae can acclimate photosynthesis over a wide range of polar temperatures given enough time (Mock & Hoch, 2005).

In addition to their physiological response to temperature, the success of sea ice microalgae at growing at the low-temperatures characteristic of sea ice is due in part to their ability to secrete macromolecules that interfere with the growth of ice (Raymond & Knight, 2003; Janech et al., 2006). Structural similarities in these compounds may exist across phytoplankton taxa, since one of these macromolecules produced by the sea ice diatom *Navicula glaciei* Vanheurk is similar to a 25-kDa ice-binding protein (IBP) from *Fragilariopsis cylindrus* (Janech et al., 2006). These macromolecules have a strong ability to inhibit the recrystallization of ice, indicating a cryoprotectant function (Raymond & Knight, 2003). In addition, both proteins closely resemble antifreeze proteins from psychrophilic snow molds that are distinct from those found in fish, insects and plants, and bacteria (Janech et al., 2006). Exopolymeric substances (EPS) secreted primarily by ice diatoms (Meiners et al., 2003; Riedel et al., 2006, 2007), which have been measured at very high concentrations in sea ice, also may serve a cryoprotectant function (Krembs et al., 2002; Chapters 7, 12 and 15).

Response to light

Like all photoautotrophs, sea ice algae must acclimate to the light conditions of their environment. Algae near the sea ice surface or within thin ice cover usually have photosynthetic characteristics similar to nearby surface phytoplankton populations (Lizotte & Sullivan, 1992a). However, in thicker ice or ice with appreciable snow cover, sea ice algae have been reported to have some of the most extreme low-light adaptations ever recorded (Palmisano et al., 1985; Arrigo et al., 1993a, 1995; Robinson et al., 1995). These algae flourish beneath several metres of ice and snow, receiving >1% of the surface solar irradiance (Arrigo et al., 1995; Lazzara et al., 2007).

Extreme low-light acclimation is accomplished by an increase in photosynthetic efficiency (α^*) along with an even larger reduction in P_m^* (Palmisano et al., 1985, 1986, 1987; Arrigo et al., 1993a; Robinson et al., 1995; Lazzara et al., 2007). Under nutrient-sufficient conditions, these diatom communities can approach theoretical maximum light absorption efficiencies and quantum efficiencies for photosynthesis (0.1 mol C fixed per mol photons absorbed). Thus, light harvesting and electron transport are peaked (maximizing α^*), and P_m^* is reduced to a level that will utilize the energy supplied by light harvesting at typical irradiances. In multiyear ice where nutrients are often deficient, the quantum yield of photosynthesis is relatively low (McMinn & Hegseth, 2004) and thylakoid stability is reduced due to a reduction in pigment protein complexes (Mock & Kroon, 2002a,b).

Under low-light conditions, the photosynthetic apparatus of sea ice algae can acclimate on the timescale of hours (McMinn et al., 2003). Accessory photosynthetic pigments (e.g. fucoxanthin and Chl *c* for diatoms) are increased relative to the main photosynthetic pigment, Chl *a*. This adaptation allows the cell to enhance light harvesting at the wavelengths of light penetrating the ice and snow (e.g. green light that Chl *a* is less efficient at absorbing). Accessory pigments that serve a photoprotective role (e.g. β-carotene) are less important in this environment, and concentrations are low relative to Chl *a*. With decreasing light intensity, sea ice diatoms have been observed to increase carbon allocation to glycolipids, which are a component of thylakoid membranes in chloroplasts. Sea ice diatoms also acclimate to low irradiance by increasing the number of photosynthetic units per cell and the concentration of components of the photosynthetic electron transport chain (e.g. plastoquinone).

Because of these low-light adaptations, ice algae can show severe photoinhibition at modest light levels (Arrigo et al., 1993a; Robinson et al., 1995; Rintala et al., 2006), although this photoinhibition can be reversible. For instance, in an ice algal bloom dominated by *Nitzschia frigida*, the sea ice community showed mild inhibition at 490 µmol photons m^{-2} s^{-1}, but after 10 min the quantum yield had recovered 99.5% of its original value (McMinn & Hattori, 2006). In many situations, however, ambient light levels never get sufficiently high to result in photoinhibition (McMinn & Hattori, 2006).

Ultraviolet light (UV; 280–400 nm) reaching the sea ice surface is attenuated strongly by ice and detritus and by algal cells containing mycosporine-like amino acid (MAA) sunscreens. The responses of sea ice diatoms to enhanced UV light include increased concentrations of photoprotective pigments, as well as MAAs, though regulation of the latter is not well understood. Fluorescence-based studies also show that UV, particularly UV-B (280–320 nm), inhibits photosynthesis in sea ice diatoms by diminishing PSII performance, presumably via direct impacts on its binding protein or the primary electron acceptor. During high-UV events, such as the spring development of the Antarctic ozone hole, increased DNA damage has also been detected (Karentz & Spero, 1995), which could also impact recovery of the photosynthetic apparatus. However, algae growing at the base of the sea ice, where these microbial communities are most common, are well adapted to their low-light environment, exhibiting increased Chl *a* per cell and reduced photosynthetic rates. UV damage can be difficult to detect in these habitats (McMinn et al., 2003). Not surprisingly, previous studies of sea ice algae, although few, concluded that MAAs are produced in low amounts by sea ice algae (Karentz, 1994; Ryan et al., 2002) and therefore play only a minor role in UV photoprotection within this habitat.

Response to nutrients and dissolved organic matter

The availability and accumulation of chemical constituents in sea ice habitats is reviewed elsewhere in this volume (Chapter 12), thus the focus in this chapter will be on algal responses and their roles in transforming materials. Sea ice algae utilize inorganic nutrients and carbon dioxide, materials that can be remineralized by the activity of grazers and decomposers. Growth of sea ice algae requires acquisition of relatively large amounts of C, N, P and, for diatoms, Si. The main forms available are the inorganic forms carbon dioxide, nitrate, phosphate and silicic acid. Dissolved organic matter (DOM) may also serve algae as sources of C, N and P, if they have the enzymes and uptake systems specific to these substrates.

There is evidence that Si is the nutrient most likely to limit diatom growth in advanced stages of a bloom (Gosselin et al., 1990), particularly after a diverse microbial community (capable of recycling C, N and P) has formed. Observations also support occasional limitation of sea ice algae by insufficient nitrogen (Lizotte & Sullivan, 1992b; Smith et al., 1997). Nitrogen uptake and assimilation by sea ice diatoms has been studied in some detail (Priscu & Sullivan, 1998). Nitrate uptake shows much higher affinity (low half-saturation coefficients), in the µM range, compared to mM range for intracellular nitrate reductase affinity. The latter matches measurements of mM nitrate intracellular concentrations. This indicates that uptake and assimilation of nitrate are uncoupled, and that incorporation of this N source into cellular components is limited by transport into the cell. The nitrate reductase enzyme in sea ice diatoms also shows weak inhibition (ca. 20% decrease) at environmental ammonium concentrations of approximately 1 µM, which could lead to

a shift from nitrate to ammonium as the primary N source as ammonium accumulates in older sea ice. However, high nitrate utilization has been observed in sea ice with much higher ammonium concentrations, implying that some sea ice diatoms are less susceptible to suppression of nitrate reductase by ammonium. High (mM) intracellular concentrations of ammonium and phosphate relative to low environmental concentrations (µM) suggest that uptake and assimilation might be uncoupled for these nutrients as well (Chapter 12).

The production and utilization of DOM includes contributions from all members of the sea ice microbial community. Overall, the rate of DOM production (as a fraction of primary production) in sea ice communities appears to be high (Gosselin et al., 1997). Photosynthesizing algae excrete a portion of their photosynthate as DOM. The proportion excreted increases under high-light stress due to photorespiration, in which high intracellular oxygen favours RUBISCO oxidation (rather than carboxylation) of C-cycle intermediates. Products of photorespiration include low molecular weight compounds such as glycolate. Sea ice diatoms also can take up DOM (sugars, amino acids) in the light and dark (Palmisano & Garrison, 1993). DOM uptake could recover materials previously released by the algae, and would be advantageous under conditions of light limitation for photosynthesis or overwinter survival.

8.5 Sea ice primary production

Primary production via photosynthesis (as distinct from chemosynthesis) is a complex suite of processes that includes light harvesting, electron transport and carbon fixation, each with different sensitivities to environmental conditions and cellular controls. The environmental conditions that have been studied thus far include light intensity and spectral quality, temperature, salinity and nutrient depletion. Because of its importance in understanding the biology, ecology and biogeochemistry of the ice algal community, a variety of approaches have been developed to measure primary production in sea ice.

Standard techniques: algal biomass accumulation

Early estimates of primary production in sea ice were based on the accumulation of algal biomass, generally either Chl *a* or particulate organic carbon, during the growing season. To derive an estimate of production in this way, a station would be sampled repeatedly over time. Because a single core cannot be sampled more than once, multiple cores would be taken from a small area of interest at each point in time. In this way, the spatial variation in a particular location could be quantified, allowing better characterization of changes in algal biomass over time. However, primary production derived from changes in standing crop are underestimates because loss of material due to respiration, exudation and grazing are not accounted for by this method. Estimating production via changes in algal biomass accumulation is still of value, however, because it is a direct, simple, straightforward measurement that does not require invasive techniques and because it yields a reliable minimum estimate for net primary production, a quantity that itself is of value.

Standard techniques: photosynthesis versus irradiance (PE) determinations

One of the most widely used methods for estimating primary production in sea ice is to collect ice algae from the field, bring them into the laboratory and measure, via ^{14}C-uptake, the maximum photosynthetic rate (or assimilation rate, P_m^*) and the photosynthetic efficiency (α^*) as a function of light intensity. When these photosynthetic parameters are combined with measurements of algal biomass (Chl a) and light (E) from the field, estimates of primary production (PP) can be obtained using the equation:

$$PP = \text{Chl } a\ P_m^* \left[1 - \exp\left(-\frac{\alpha^* E}{P_m^*} \right) \right] \qquad \text{(Equation 8.1)}$$

A significant problem with estimating primary productivity in sea ice using this approach is that the spectral quality of the light source used to estimate P_m^* and α^* is often very different from that within the sea ice. Incubation light sources are usually weighted towards the red end of the visible spectrum, while *in situ* radiation is dominated by blue or green wavelengths. Even though the amount of PAR measured under both circumstances may be equal, photosynthetic pigments produced by the algae are much more efficient at absorbing blue light than red light. As a result, the value derived for α^* (P_m^* is insensitive to spectral quality) is often underestimated during PE determinations. To compensate for this effect, a spectral filter can be applied to the light source used during the incubations so that it mimics the light field the algae would be exposed to *in situ*. Although this correction is simple to implement, it cannot completely account for the fact that the spectral light distribution changes with depth within the ice. A better, albeit more difficult, approach to correct this problem is to apply a spectral correction to the PE-derived estimate of α^* so that it better represents values *in situ* (Arrigo & Sullivan, 1992). This correction requires, however, that both the spectral output of the incubator light source and the *in situ* spectral irradiance distribution, as well as the absorption spectrum of the algae, are reasonably well known.

Minimally invasive techniques: oxygen microelectrodes

The ideal approach, but one that does not currently exist, would be to directly measure primary productivity *in situ*, without disrupting the algae or their sea ice habitat. New developments are coming closer to this ideal (Glud et al., 2002), although it has not yet been attained. Oxygen (O_2) microelectrodes have been used to measure the photosynthetic rates of Antarctic fast ice algae in virtually intact cores, without having to seriously disrupt the algal community (McMinn & Ashworth, 1998; Rysgaard et al., 2001; Glud et al., 2002; Mock et al., 2002, 2003). Measured O_2 profiles are used to estimate the O_2 flux from the sea ice using Fick's first law of diffusion:

$$J = D_0 \frac{\partial C}{\partial X} \qquad \text{(Equation 8.2)}$$

where D_0 is the molecular diffusion coefficient (1.14 e^{-5} cm^{-2} s^{-1} at $-1°C$), ∂C is the change in O_2 concentration across the diffusive boundary layer and ∂X is the effective thickness of the diffusive boundary layer (0.5–1.0 mm, Mock et al., 2003), as deduced from the vertical O_2 profile. By repeating the experiments at a variety of light intensities, and by using dark

controls to correct for respiration, PE relationships can be evaluated just as they are using the ^{14}C approach.

There are a number of shortcomings to this method, however. First, algae in the sea ice are distributed heterogeneously and it is assumed that the O_2 profile generated by this method averages over this variability, although this has not yet been demonstrated (Glud et al., 2002; Mock et al., 2003). Second, the act of inserting the sampling apparatus through the diffusive boundary layer reduces by 25–45% the thickness of that layer, altering the actual O_2 flux. Fortunately, this effect is minimized where O_2 gradients are small and when there is no fluid flow around the tip of the O_2 probe. Third, this method is only effective at measuring productivity in bottom ice communities. However, considering that the majority of algal biomass in both the Arctic and the Antarctic is found in the bottom layers of the congelation ice, this method is likely to prove valuable in the future. Early results using this technique were at the lower end of productivity estimates for fast ice and suggest that conventional ^{14}C techniques may overestimate sea ice algal productivity. Finally, primary productivity by sea ice algae can be depressed at high O_2 concentrations (McMinn et al., 2005), due to the generation of oxygen radicals, complicating quantification of the relationship between O_2 gradients and rates of photosynthesis.

Minimally invasive techniques: in situ ^{14}C incorporation

A truly *in situ* incubation technique was developed to measure primary production in a wider variety of sea ice habitats than had been possible previously (Mock & Gradinger, 1999). The concept behind this method is that an ice core can be extracted from either fast or pack ice, and sectioned into appropriate segments that are placed into individual petri dishes for inoculation with ^{14}C bicarbonate. These petri dishes are then stacked in the order they were collected, placed in an acrylic-glass barrel and returned to their original position in the ice floe where they are incubated. This method provides fine-scale (1 cm) resolution of primary productivity throughout the ice column without severe disruption of sea ice morphology and ambient light field. Rapid deployment is required, however, to minimize brine drainage and associated nutrient loss.

The primary advantage of this approach is that the algae are incubated under as natural a light field as possible, eliminating the need to correct for spectral quality as is required by the more widely used PE method. In addition, because the algae are incubated *in situ*, they are exposed to the same vertical gradients in temperature and brine salinity as undisturbed populations, resulting in more realistic productivity estimates. Under conditions where nutrient concentrations are not limiting, this method is likely to yield estimates of primary production that are superior to most other methods. The major drawback to this technique is the disruption of the ambient nutrient field. Severing brine channels by sectioning the core could alter the nutrient field and result in unrealistic rates of primary production.

Interestingly, two of the most recently developed, minimally invasive *in situ* techniques came to very different conclusions concerning the accuracy of standard ^{14}C incubation techniques used most often for estimating primary production in sea ice. Estimates of photosynthetic carbon fixation made using microelectrodes to measure diffusion of oxygen through the boundary layer were very low, with P_m^* values ranging only from 0.02 to 0.05 mg C mg^{-1} Chl *a* h^{-1} and hourly production rates of 0–1.78 mg C m^{-2} h^{-1}. As can be seen from

Table 8.4   Photosynthesis rates per unit Chl *a* biomass (mg C mg^{-1} Chl *a* h^{-1}) rates reported for Arctic sea ice.

Ice type	Region	Season	Rate (mg C mg^{-1} Chl *a* h^{-1})	References
Bottom	Canadian Arctic Archipelago	Spring	0.03–0.08	Cota (1985)
			0.01–0.33	Bates and Cota (1986)
			0.60–1.17	Smith et al. (1988)
			0.20–4.9	Cota and Horne (1989)
			0.01–0.60	Cota and Smith (1991)
			0.08–0.41	Smith and Herman (1991)
			0.10–0.20	Herman et al. (1993)
			0.40–2.2	Apollonia et al. (2002)
	Hudson Bay	Spring	0.10–1.2	Gosselin et al. (1985)
			1.8–5.2	Gosselin et al. (1986)
	Davis Strait	Spring	0.10–1.2	Cota and Smith (1991)
	Beaufort Sea	Spring	0.01–0.38	Cota and Smith (1991)
	Baltic Sea	Winter	0.90	Kaartokallio et al. (2007)
	Barents Sea	Spring	0.16–0.24	Johnsen and Hegseth (1991)
			0.05–0.90	Mock and Gradinger (1999)
	Greenland Sea	Spring	0.01–0.40	Mock and Gradinger (1999)
Pack	Labrador Sea	Spring	1.4–3.1	Irwin (1990)
Strand	Barents Sea	Summer	0.03–0.09	Johnsen and Hegseth (1991)

Tables 8.4 and 8.5, these estimates are on the low end for Antarctic sea ice, particularly in the spring when rates are generally the highest. Because this technique is the least invasive of all known methods for estimating sea ice primary production, the low values obtained by this technique have led the developers to speculate that previous estimates of sea ice production may be too high. In contrast, the *in situ* ^{14}C technique (whereby core sections are placed into individual petri dishes that are inoculated with ^{14}C bicarbonate, placed in an acrylic-glass barrel and returned to their original position in the ice floe for incubation) showed that production within the sea ice interior was much higher than previously reported and that estimates of primary production based on bottom ice communities were likely severely underestimating production in both the Antarctic and the Arctic. Clearly, additional data need to be collected to evaluate the relative ability of these two approaches to estimate sea ice primary productivity. Using both approaches in the same study would provide valuable insights in this regard.

Numerical modelling

One of the more complex methods for determining, and understanding, primary production in sea ice is through numerical modelling of the sea ice ecosystem. This technique requires a thorough knowledge of both the physics and biology of the sea ice system, and to date, has been applied to very few sea ice habitats, although models for the Arctic (Lavoie et al., 2005; Jin et al., 2006), Antarctic (Arrigo et al., 1993b, 1997, 1998; Arrigo & Sullivan, 1994) and Lake Saroma (Hokkaido, Japan; Nishi & Tabeta, 2005) have now been developed. Using such

Table 8.5 Photosynthesis rates per unit Chl *a* biomass (mg C mg^{-1} Chl *a* h^{-1}) rates reported for Antarctic sea ice.

Ice type	Region	Season	Rate (mg C mg^{-1} Chl *a* h^{-1})	References
Bottom	McMurdo Sound	Spring	0.06–0.32	Palmisano and Sullivan (1985)
			0.05–0.22	Palmisano et al. (1985)
			0.11–0.83	Palmisano et al. (1987)
			0.17–1.9	Grossi et al. (1987)
			0.3–3.0	Kottmeier and Sullivan (1988)
			0.04–0.38	Cota and Sullivan (1990)
			0.1	Arrigo and Sullivan (1992)
			0.02–0.05	McMinn et al. (1999)
			0.29–2.0	McMinn et al. (2000)
	Terra Nova Bay	Spring	0.11–0.12	Guglielmo et al. (2000)
			0.09–0.24	Lazzara et al. (2007)
	Prydz Bay	Spring	0.01–0.05	McMinn and Ashworth (1998)
Platelet	McMurdo Sound	Spring	0.15	Palmisano and Sullivan (1985)
			0.10–0.76	Grossi et al. (1987)
			0.09–0.28	Lizotte and Sullivan (1991)
			0.05–0.20	Arrigo et al. (1993b)
			0.04–0.21	Robinson et al. (1995)
Surface	McMurdo Sound	Spring	3.9±1.5	Palmisano and Sullivan (1985)
			0.40–0.42	Lizotte and Sullivan (1991)
			0.50–1.2	Robinson et al. (1997)
	Bransfield Strait	Summer	2.6–2.7	Burkholder and Mandelli (1965)
New	Bransfield Strait	Winter	0.12–1.4	Lizotte and Sullivan (1991)
	Weddell Sea	Autumn	0.02–1.2	Mock (2002)
Pack	Ross Sea	Spring	0.41–0.81	Arrigo et al. (2003)
	Prydz Bay	Spring	0.05–5.4	McMinn et al. (2007)
	Weddell Sea	Autumn–winter	0.17–4.6	Lizotte and Sullivan (1991)
			0.04–8.6	Lizotte and Sullivan (1992a)
	Bransfield Strait	Winter	0.11–8.6	Lizotte and Sullivan (1991)
			0.12–1.4	Lizotte and Sullivan (1992a)

numerical models, the complete annual cycle of primary production can be simulated as a function of temperature, salinity, nutrient and light availability to gain a better understanding of the processes controlling algal distributions in sea ice as well rates of primary production.

Measured rates of primary production

Owing to the difficulty of the measurement, estimates of primary production in sea ice, even indirect ones, are relatively rare. More common are estimates of photosynthetic rate, which when combined with measured light distributions in the ice, can be used to calculate sea ice primary production. Unfortunately, photosynthetic measurements are rarely used in this way because the data on light distributions in sea ice that are needed for the calculation are

even less common than the photosynthetic measurements. Measurements of photosynthetic rate, in particular, P_m^*, do exhibit some interesting patterns, however, that, when combined with biomass accumulation patterns, can provide some insight into the factors responsible for regulating primary production in sea ice.

Unlike the hemispheric pattern exhibited by Chl a accumulation in sea ice, whereby values in the Antarctic are substantially higher than in the Arctic, data on P_m^* display no such bias, although the data set available for evaluation is somewhat small, particularly in the Arctic (Tables 8.4 and 8.5). While these two observations may seem initially to be inconsistent, they can be explained in part by the different habitats that dominate each region. A major reason for the difference in biomass accumulation between the two poles was that platelet ice, which contains so much more algal biomass than any other habitat, is restricted to the Antarctic. Ignoring the contribution by platelet ice brings algal biomass accumulation in the two hemispheres more closely in line.

An obvious pattern in P_m^* that does emerge from the data is the consistently higher values measured in pack ice relative to land-fast ice in both the Antarctic (Table 8.5; Lizotte and Sullivan, 1992a) and possibly the Arctic (Table 8.4). Values of P_m^* for the fast ice are consistently below 2 mg C mg^{-1} Chl a h^{-1} and often much lower. In contrast, estimates of P_m^* for the pack ice can be as high as >8 mg C mg^{-1} Chl a h^{-1}. The differences in P_m^* between these two habitats can probably be attributed to variation in sea ice thickness. Pack ice tends to be much thinner than land-fast ice in both polar regions and as a result, light levels are substantially higher. Because the P_m^* of algae is highly dependent upon previous light history, fast ice, with its reduced irradiance, exhibits lower values for P_m^* than that of the pack.

The fact that photosynthetic rates are greater in the pack ice is in apparent conflict, however, with the observation that land-fast ice accumulates more algal biomass than pack ice. These observations can be reconciled only if losses of algal biomass from the pack ice are greater than from land-fast ice. This provides strong, albeit indirect, evidence that grazing by zooplankton on sea ice algae is greater in pack ice than in the land-fast ice. Although quantitative data with which to compare relative grazing effort in pack and land-fast ice data are lacking, structural characteristics of the two habitats support a higher grazing rate within pack ice. Pack ice tends to be composed of a mixture of congelation and frazil ice, whereas land-fast ice is predominantly congelation ice. As a result, pack ice tends to be more porous, and therefore, more susceptible to grazers. Consistent with this notion, there have been numerous reports of herbivores such as copepods, amphipods, protists, etc., actively grazing within pack ice in both the Arctic and the Antarctic (Chapter 10). These organisms appear to be less common in the more consolidated congelation ice type characteristic of land-fast ice until much later in the season when the ice begins to melt and the brine volume increases dramatically (Stoecker et al., 2000). Losses due to sinking of algal material must also be considered, but because pack ice has a higher fraction of surface and internal communities that tend to be more resistant to sinking, differences in sinking are unlikely to be important. In addition, fast ice, at least in the Antarctic, is often associated with an under-ice platelet layer that would tend to further minimize losses from the ice due to sinking and grazing.

Therefore, pack ice may represent the more important sea ice habitat in terms of providing a food source for upper trophic-level organisms. Having production rates as much as fourfold higher than land-fast ice and accumulating only half the algal biomass (with little expected difference in sinking losses) implies that a much larger fraction of the primary production in pack ice is being consumed by higher trophic levels. The importance of these

Table 8.6   Primary production rates reported for Arctic sea ice.

Ice type	Region	Season	Daily (mg C m^{-2} d^{-1})	Annual (g C m^{-2} y^{-1})	References
Bottom	Canadian Arctic Archipelago	Spring	21–463	3–23	Smith et al. (1988)
			20–157	2–14	Smith and Herman (1991)
				5	Bergmann et al. (1991)
	Baffin Bay	Spring	26–317		Nozais et al. (2001)
		Spring	2–150		Michel et al. (2002)
				5	Horner (1976)
	Beaufort Sea			0.001	Horner and Schrader (1982)
	Sea of Okhotsk	Winter	60–208		Nishi and Tabeta (2006)
	Barents Sea	Spring	3–7		Mock and Gradinger (1999)
				5	Hegseth (1998)
	Greenland Sea	Spring	0.2		Rysgaard et al. (2001)
Pack	Central Arctic Ocean	Summer	0.5–310	15	Gosselin et al. (1997)
	Labrador Sea	Spring	58		Irwin (1990)
	Davis Strait	Spring	0.03–2.4		Booth (1984)
	Bering Sea	Spring	2.2–4.8		McRoy and Goering (1974)

differences in food web structure is further magnified by the fact that pack ice is so much more prevalent than fast ice in both the Arctic and the Antarctic.

Estimates of annual sea ice primary production from direct ^{14}C uptake rate measurements are uncommon. The few studies that have been conducted indicate that annual production in the Arctic and Antarctic are similar in magnitude, ranging from 2 to 15 g C m^{-2} y^{-1} and from 0.3 to 38 g C m^{-2} y^{-1}, respectively (Tables 8.6 and 8.7). These values are consistent with biomass accumulation data from the two regions that represent a minimum estimate of annual production. For example, assuming a carbon:Chl a ratio for sea ice diatoms of 40, then annual production estimated from maximum spring/summer Chl a abundance ranges from 0.2 to 12 g C m^{-2} y^{-1} for the Arctic and from 0.04 to 44 g C m^{-2} y^{-1} for the Antarctic. Ignoring production in the platelet ice reduces the range for the Antarctic to 0.04–20 g C m^{-2} y^{-1}. Despite the small sample sizes, it is still probably fair to conclude that even in the most productive sea ice habitats, annual production is below 50 g C m^{-2} y^{-1}, an amount similar in magnitude to the oligotrophic central gyres of the open oceans.

Even rarer still are estimates of total primary production integrated over both the entire Arctic and Antarctic regions. Because of the paucity of data used to make such estimates, they are necessarily crude and provide little or no information about either regional patterns of production or its annual cycle. Nevertheless, these estimates can be a useful tool when evaluating the contribution of the sea ice habitat to total regional (ice + water column) production, and that has generally been the context in which they have been made. Measurements made in near-shore sea ice led to early estimates of 1–6 g C m^{-2} y^{-1} (Bunt & Lee, 1970; Horner, 1976), suggesting that sea ice production was several orders of magnitude lower than that being reported for phytoplankton. As a result, the contribution of primary production

Table 8.7 Primary production rates reported for Antarctic sea ice.

Ice type	Region	Season	Daily (mg C m^{-2} d^{-1})	Annual (g C m^{-2} y^{-1})	References
Bottom	McMurdo Sound	Spring	0.5—85	0.3—3.4	Grossi et al. (1987)
				1—6	Bunt and Lee (1970)
	Prydz Bay	Spring	140	4.6	Archer et al. (1996)
Platelet	McMurdo Sound	Spring	2—1250	4—38	Grossi et al. (1987)
			200—1200		Arrigo et al. (1995)
Internal	McMurdo Sound	Summer	0.5—12		Stoecker et al. (2000)
New	Weddell Sea	Autumn	0.02—0.25		Mock (2002)
Pack	Bransfield Strait	Winter	42—60		Kottmeier et. al. (1987)

in sea ice was dismissed as insignificant. More recent estimates of basin-wide production in both the Arctic and Antarctic regions (Legendre et al., 1992; Arrigo et al., 1997; Lizotte, 2001) are much higher and in general agreement, suggesting that approximately 70 Tg C are fixed annually.

Recent large-scale estimates of annual primary production by pelagic phytoplankton in the Arctic range from 329 Tg C y^{-1} (Sakshaug, 2003) to between 350 and 500 Tg C y^{-1} (Pabi et al., 2008). This latter estimate includes interannual variability in productivity resulting from recent losses of Arctic sea ice (Arrigo et al., 2008a). These estimates for the pelagic environment suggest that Arctic sea ice contributes approximately 15–20% of total primary production in Arctic waters (ice + water column). In Antarctic waters (south of 50°S), phytoplankton primary production averaged 1949 ± 70.1 Tg C y^{-1} between 1997 and 2006 (Arrigo et al., 2008b). Assuming that sea ice algae contributed an additional 70 Tg C y^{-1}, then sea ice ecosystems could account for approximately 4% of total annual production in Antarctic waters. This fraction would increase substantially if the analysis were restricted to the sea ice zone of the Southern Ocean (Arrigo et al., 1997).

8.6 Genetics and genomics of sea ice algae

Environmental genetics and genomics have revolutionized our view on how organisms have evolved and are adapted to their specific habitat (Armbrust et al., 2004; Schloss & Handelsman, 2005; Rusch et al., 2007; Palenik et al., 2007). The identification of genes and their activity provide an unbiased view on phylogenetic relationships among organisms and their metabolism that might explain speciation by differences in metabolic processes leading to adaptation (Frias-Lopez et al., 2008; Mock et al., 2008; Bowler et al., 2008). A major speciation event in the Earth's history was the development of surface low-temperature ecosystems such as the Antarctic continent with its seasonal sea ice formation (Crame, 1997). The Antarctic continent experienced the first cycles of glaciation during the Eocene (42 Myr BP). This dramatic environmental change from a tropical climate to an 'icehouse' caused an allopatric speciation in Antarctic taxa, explaining the high degree of endemism (up to 100% for some groups), particularly for phylogenetically more evolved groups, including marine crustaceans

and vertebrates. However, there also is evidence of many endemic microbes in the Antarctic. Most of them live in the Southern Ocean, with the highest number of psychrophiles likely being found in sea ice due to its extreme conditions. Although genetic and genomic studies on these organisms are still in their infancy, considerable effort has been made over the last decade and we certainly are at the beginning of a steep exponential increase in fundamental new understanding about these unique microbes (Hoag, 2003; Grzymski et al., 2006; Mock et al., 2005; Hwang et al., 2008). So far, molecular-based work mainly has focused on sea ice bacteria and only in the last ca. 5 years have the first studies on eukaryotic sea ice microbes, mainly algae, been published. Below, we summarize results from these new studies and provide a guideline for future molecular research on sea ice algae.

Molecular species diversity

Molecular surveys of protistan assemblages from sea ice or other polar marine habitats have been conducted only rarely (Gast et al., 2004; Lovejoy et al., 2006). Most of our knowledge in this field for polar regions traditionally comes from microscopic and morphological studies done by taxonomists. These studies often required the organisms to be in culture, which is difficult for polar organisms because of their specific temperature needs. Thus, undersampling of these communities is common. The first culture-independent survey of sea ice protists was done by Rebecca Gast and colleagues. They used denaturing gradient gel electrophoresis (DGGE) to obtain the genetic composition of protists in different types of sea ice (surface and bottom) and sea water. Although DGGE is not able to cover the full diversity of species, this study clearly showed a high degree of uniqueness among the protistian assemblages within different micro-habitats of sea ice and between sea ice and seawater. This finding was contrary to former studies which suggested that ice crystals forming in the water column harvest sea water microbes and incorporate them into the ice to establish a very similar sea ice microbial community. The primary source of sea ice protists is still the underlying sea water column, but the study of Gast et al. (2004) indicated that either there are major shifts in the dominance of species after incorporation into the ice or that morphologically similar, but genetically distinct, strains were present. The latter assumption implies that Antarctic protists may have developed specific ecotypes for different sub-polar habitats, such as sea water and sea ice, that were not identified by morphological studies. This concept is well known from niche adaptation in marine cyanobacteria, where different ecotypes are adapted to different light and temperature regimes (Rocap et al., 2003), and by the first evidence from eukaryotic phytoplankton (Palenik et al., 2007).

   Physical differences between sea ice and sea water are very strong, particularly for temperature and salinity, which may cause the development of distinct strains. Sequence analysis of selected DGGE bands revealed the presence of major groups such as diatoms, dinoflagellates, ciliates, flagellates and several unidentified eukaryotes. The same groups formerly were identified by microscopic surveys but this culture-independent molecular approach also was able to discover novel phylotypes. One of them was a very abundant clone in the 18S libraries from sea water and ice slush (Gast et al., 2006). A BLAST search indicated that this dominant clone was derived from a dinoflagellate because it shared 97.6–98.3% sequence similarity with both *Karenia* and *Karlodium* species. This novel sea ice–associated dinoflagellate phylotype could be brought into culture and morphological studies confirmed its placement as a relative of the *Karenia/Karlodinium* group (Fig. 8.2; Gast et al., 2006).

An 18S survey on small marine microbial eukaryotes in the Arctic Ocean also revealed many novel lineages and extended the geographic record of recently discovered lineages known only from environmental sequences from other cold-water habitats such as the deep ocean (Lovejoy et al., 2006). In total, 42% of their sequenced 18S genes were <98% (benchmark of genus-level diversity) similar to publicly available sequences. They even reported new representatives from five of the eight major marine eukaryotic lineages. One of them was a group of novel stramenopiles, a sister group to the bolidophytes (Lovejoy et al., 2006). This cluster may be bipolar *Parmales*, which have distinct siliceous plates. However, none of them has been cultivated yet, although there are reports from environmental samples obtained via microscopy. Most diatom sequences in this study were related to the sea ice species *Fragilariopsis cylindrus*. However, they also identified eight novel genotypes closely clustering with *F. cylindrus*, probably indicating that there are many different subspecies. Although this is the first and only study so far of the molecular diversity of eukaryotic phylogeny in the Arctic Ocean, it has already shown that even the geologically younger Arctic Ocean harbours many endemic species among invaders from adjacent oceans (Lovejoy et al., 2006). However, no such study has yet been conducted specifically on Arctic sea ice, despite the fact that the environmental pressure to select organisms specifically adapted to sea ice might even be stronger in the Arctic Ocean due to the presence of multiyear sea ice. Unfortunately, the proportion of multiyear sea ice has been greatly reduced over the last decade, suggesting that unique polar phylotypes may already be threatened and might possibly be extinct before they have been identified. Consequently, a strong effort is urgently needed to intensify our molecular research on the largely underexplored microalgal diversity in polar oceans.

Gene discovery

Physiological studies on how sea ice algae are adapted to their extreme habitat have been conducted over the last couple of decades and have provided important information about their temperature, light and nutrient requirements, as well as adaptation to high salinities in their brine channel habitat. Only for the last 5 years have modern molecular tools been used to discover the molecular bases of their adaptation and their gene composition (Mock and Valentin, 2004; Mock et al., 2005; Hwang et al., 2008). The availability of genome sequences has revolutionized marine science over the last few years because they provide an unbiased view of evolutionary adaptation and metabolism of the sequenced organisms (Armbrust et al., 2004; Palenik et al., 2007; Bowler et al., 2008). The genomic era for marine algae began with the publication of the genome sequence for *Thalassiosira pseudonana* in 2004. Since then, other algal genome projects followed and the Joint Genome Institute (JGI, USA) recently approved genome projects for polar microalgae. The genome of the sea ice diatom *Fragilariopsis cylindrus* is already being sequenced and will be released to the public domain soon, whereas a genome project for *Phaeocystis antarctica* was very recently approved by JGI. However, in the era of high-throughput sequencing, which no longer requires cloning (e.g. GS-FLX, Illumina, SOLID), genome sequencing has become decentralized as the costs per sequenced nucleotide continue to decline. This has opened the door for many more algal genome projects in small sequencing facilities. Even more cost-effective is the sequencing of complementary DNA (cDNA). These sequences are derived from messenger RNA (mRNA) and therefore represent only the expressed parts of a genome (coding and non-coding RNA). *Fragilariopsis cylindrus* was selected to conduct the first cDNA sequencing project with
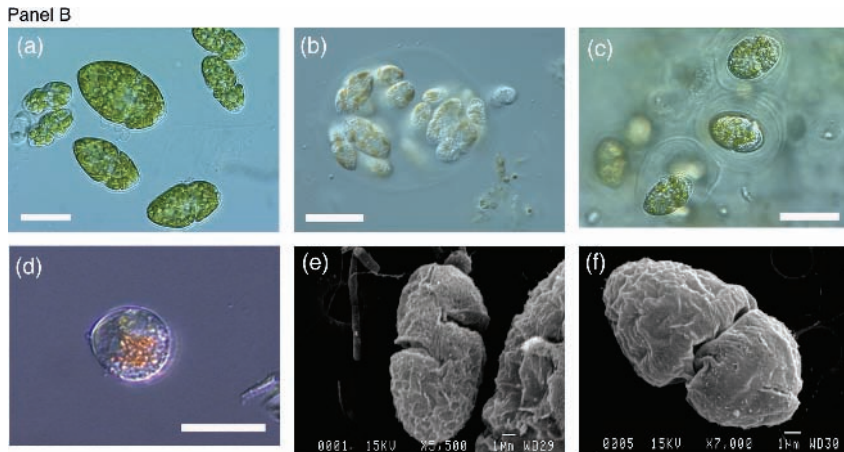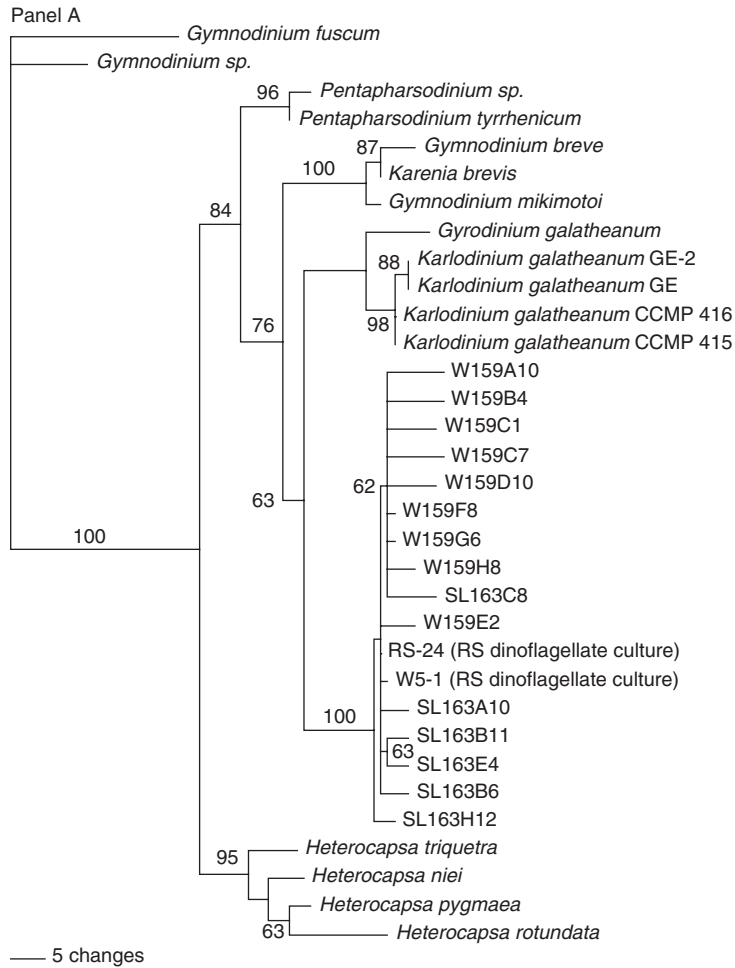
Fig. 8.2 (Panel A) Unrooted phylogenetic reconstruction (maximum likelihood) of novel dinoflagellate sequence taxonomic affiliations. (Panel B) Light (a–d) and SEM (e–f) images of a novel dinoflagellate culture. (a) Vegetative cells, scale bar 20 μm; (b) temporary cyst, scale bar 25 μm; (c) resting stage with mucilage, scale bar 30 μm; (d) cyst, scale bar 30 μm; (e) and (f) SEMs of vegetative cells. Reproduce from Gast et al. (2006) with permission from Wiley-Blackwell.

a polar alga (Mock et al., 2005). *Chaetoceros neogracile*, another polar diatom, followed a couple of years later (Jung et al., 2007).

The Fragilariopsis cylindrus EST libraries

Fragilariopsis cylindrus is considered to be an indicator for cold water because it is found only in the Arctic Ocean and Southern Ocean (von Quillfeldt, 2004). *Fragilariopsis cylindrus* can form large ice-edge blooms (Kang & Fryxell, 1992; Arrigo et al., 2003), and because of its widespread distribution in polar oceans, this diatom is an ideal candidate for the investigation of adaptations to the polar environment. Consequently, *F. cylindrus* was selected to prepare the first EST (expressed sequence tag) libraries for a polar marine alga (Mock et al., 2005). In this study, diatom cells were grown either at freezing temperatures (cold stress) or with added salt (salt stress), both environmentally relevant conditions. For cold stress, RNA was obtained 5 days after chilling the cells to the freezing point of sea water; for salt stress, RNA was taken at different time points after adding salt (final salinity of 60). To date, 4256 *F. cylindrus* EST sequences have been generated: 1376 from the cold-stress library and 2880 sequences from the salt-stress library. All ESTs have been deposited at the dbEST-databank at NCBI. Furthermore, about 200 gene-specific oligonucleotides (70mers) for functional gene-array experiments are available. All EST sequences were compared against the genome of *Thalassiosira pseudonana* and *Phaeodactylum tricornutum* and 11 additional algae and plant databanks were consulted to annotate those sequences that were not found in the genomes of both diatoms. Nevertheless, <50% of all sequences displayed similarity to known sequences in these databanks and to both diatom genomes, even when using a comparatively high *e*-value of $\leq 10^{-4}$ (Mock et al., 2005).

In the cold-stress library, the most abundant functional categories were related to translation, post-translational modification of proteins and transport of amino acids and peptides by ABC-transporters. Some of these ABC-transporters displayed homology to bacterial permeases, whereas others appeared to be involved in translational control or post-translational processes. However, most of them have no assigned function at this point. The presence of six different DNA/RNA helicases in the cold-stress library indicated that DNA and RNA coiling and uncoiling are important under freezing temperatures. Minimizing the likely formation of secondary structures and duplexes of mRNAs under low-temperature stress is necessary to initiate translation. However, protein domains of DNA/RNA helicases also are the eighth most abundant protein domain in the genome of *T. pseudonana* and, therefore, more evidence is necessary to determine if these enzymes are essential to cope with freezing temperatures (Armbrust et al., 2004). The most abundant sequences in this library in terms of their redundancy were those that were related either to light harvesting (e.g. fucoxanthin–Chl *a*, *c*–binding proteins) or completely unknown sequences (Mock et al., 2005). In the salt-stress library, the most abundant functional categories of sequences were related to post-translational modification of proteins (e.g. heat-shock proteins) and ion transport (Krell, 2006). Most of them were heat-shock proteins (hsps) and different ion transporter genes, reflecting the requirement to re-establish homeostasis under salt stress.

Several sequences of different kinds of V-type H+-ATPases and antiporters for various ions such as sodium, potassium and calcium were found in this library. V-type H+-ATPases are of great importance to the establishment of an electrochemical proton gradient across the tonoplast to drive sodium sequestration into the vacuole (Shi et al., 2003).

One important organic osmolyte under salt stress in diatoms is the amino acid proline. Many genes involved in proline synthesis were found in the salt-stress EST library, indicating that this pathway was active under the experimental conditions. The gene pyrroline-5-carboxylate reductase (*P5CR*, catalyzing the final step in proline synthesis) could be identified among the most abundant sequences in the salt-stress library, which indicates that this gene was at least moderately expressed under salt stress and therefore important for salt acclimation (Krell, 2006).

The salt-stress cDNA library also contained a number of genes encoding proteins involved in the detoxification and scavenging of reactive oxygen species (ROS), e.g., glutathione synthetase, peroxiredoxin and thioredoxin. Glutathione content has been shown to increase in higher plants subjected to salt stress (Ruiz & Blumwald, 2002) and in algae under high light intensities, since it acts as an intermediate in ROS removal during light saturation of photosynthesis (Dupont et al., 2004). Taken together, these results imply that ROS scavenging pathways play a role in the salt tolerance of *F. cylindrus* as they do in higher plants, where oxidative stress-related genes were highly abundant in EST libraries established under salt stress (Wang et al., 2006). In contrast to higher plants, some sea ice diatoms live in a mutual relationship with epiphytic bacteria, which make a significant contribution to the diatom's antioxidant defence. They are able to produce different ROS scavenging enzymes (catalase, superoxide dismutase and glutathione reductase) that might help to eliminate ROS produced by these diatoms. On the other hand, these bacteria benefit from organic substances secreted from diatoms (Huenken et al., 2008). This interspecies H_2O_2 reduction might benefit diatom growth under high-light stress when most of the H_2O_2 is being produced.

One of the most interesting discoveries in the salt-stress library was a gene involved in antifreeze processes. The protein sequence (translated from the nucleotide sequence) of this gene showed high sequence similarity to an isoform protein of the snow mold *Typhula ishikariensis*. The *T. ishikariensis* protein has been shown to reduce the freezing point of sea water by approximately 0.1°C (Hoshino et al., 2003). However, this is not a strong freezing point depression when compared to the antifreeze ability from numerous antifreeze proteins identified from fish, insects, plants and bacteria. Thus, they might represent a new class of ice-binding proteins (IBPs).

Using a proteomics approach and another polar diatom (*Navicula glaciei*), the corresponding protein also was discovered (Janech et al., 2006). This protein is probably unique in polar diatoms since none of the temperate diatoms tested so far had this class of genes and neither did the two whole genomes available for temperate diatoms (Janech et al., 2006). Furthermore, in contrast to polar diatoms with IBPs, temperate diatoms when subjected to freeze-thaw cycles were not able to survive (Janech et al., 2006). The amplification of the *Navicula* gene revealed strong similarity to the gene from *F. cylindrus* and the corresponding *T. ishikariensis* genes (Fig. 8.3; Krell et al., 2008). The N-terminal sequences of the identified IBPs of *N. glaciei*, *F. cylindrus* and each of the *T. ishikariensis* antifreeze isoforms are most likely signal peptides and have low probabilities of being mitochondrial- or chloroplast-targeting peptides.

These IBPs also show some similarity (between 43% and 58% amino acid sequence identity) to hypothetical proteins from gram-negative bacteria such as *Cytophaga hutchonsonii* and *Shewanella denitrificans*, genera that have frequently been isolated from Arctic and Antarctic sea ice (Chapter 7; Junge et al., 2002). The former species belongs to the Cytophaga–Flavibacterium–bacterioides (CFB) phylum group – a bacterial group that
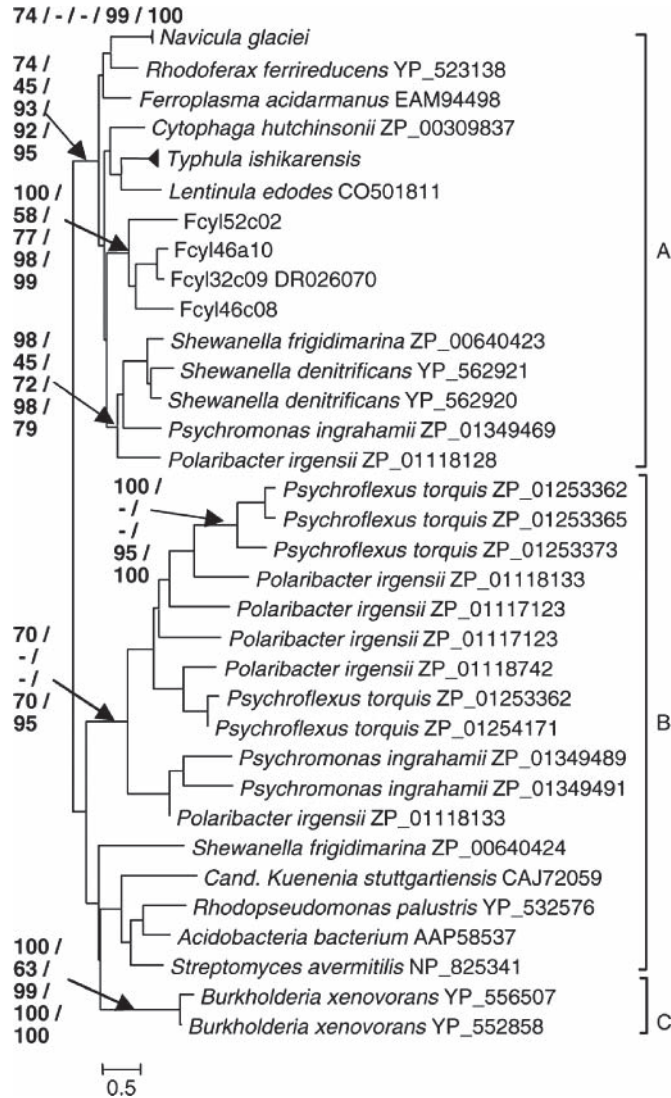
Fig. 8.3 Maximum likelihood phylogenetic tree of the candidate ice-binding protein sequences from EST library and homologues (including Accession number) found in the Genbank database. *Typhula ishikariensis* comprises seven homologues (BAD02891–BAD02897) and four homologues from another diatom *Navicula glaciei* (AAZ76250–AAZ76254, Janech et al., 2006). These sequences were found with primers based on the *F. cylindrus* 32c09 sequence (DR026070). Numbers on the nodes indicate bootstrap values from neighbour joining analyses with uncorrected, JTT and ScoreDist distances, maximum parsimony and maximum likelihood analysis, respectively (only bootstrap values above 60% are shown). The three groups marked A, B and C are the 'subfamilies' identified by SciPhy. Reprinted from Krell et al. (2008) with permission from Taylor & Francis.

appears to be especially important in well-established sea ice algal assemblages (Bowman et al., 1997) and the coldest (winter) sea ice (Junge et al., 2004). Several psychrophilic species of *Shewanella* have been isolated from sea ice, often in association with algal assemblages (Bowman et al., 1997). Whether polar sea ice bacteria also express IBPs remains to be explored. The sequence similarity to bacterial and fungal IBPs also invites questions about the

origin of these genes. Horizontal gene transfer from fungi is one possibility because basidio-mycotic fungi (which include *Typhula*) are also known to inhabit sea ice and are believed to have arisen hundreds of millions of years before diatoms appeared. Horizontal gene transfer from members of the CFB group of bacteria is another possibility because of their known association with algal assemblages in sea ice and their relation to species with IBP-like genes. In other organisms, antifreezes appear to have arisen from a variety of proteins with other functions, although some retain their original functions (Cheng, 1998). Overall, the evolution of IBPs needs to be explored further.

The Chaetoceros neogracile EST library

The genus *Chaetoceros* is one of the largest genera of diatoms, with approximately 400 described species. They are distributed worldwide from tropical to polar marine systems and some of them are even psychrophilic. Jung et al. (2007) selected the Antarctic species *C. neogracile* to construct a cDNA library from cultures grown at $+4°C$ and 40 µmol photons m^{-2} s^{-1} continuous light. A total of 2500 ESTs were sequenced, resulting in a set of 1694 unique genes after clustering. Putative functions were assigned to 55.4% of these sequences. Most of these genes fell into the functional category of metabolism (16.6%), followed by genes involved in genetic information processing (7.6%), photosynthesis (4.2%) and defence and stress resistance. The most highly expressed genes in terms of EST redundancy (4–80 ESTs per gene) accounted for 18% of the non-redundant EST set. As for *Fragilariopsis cylindrus* and other non-polar diatoms, fucoxanthin and Chl *a*/*c*–binding proteins were among the genes with the most abundant ESTs, indicating a very complex gene family where different genes seem to have different functions required for regulation of light harvesting under various environmental conditions.

A glutathione *S*-transferase (GST), not reported from a polar diatom before, was among the genes with most EST coverage. GSTs catalyze the conjugation of reduced glutathione via the sulphhydryl group, to electrophilic centres on a wide variety of substrates. This activity is useful in the detoxification of endogenous compounds such as peroxidized lipids and the metabolism of xenobiotics. Glutathione, the substrate of GST, has diverse functions in defence and sulphur metabolism. It also can react with ROS as part of the ascorbate–glutathione cycle to detoxify H_2O_2. Whether the identified GST in *C. neogracile* is also present in other sea ice diatoms and whether it is of advantage to thrive in sea ice remains to be seen. However, diverse molecular detoxification mechanisms are present in *F. cylindrus* and *C. neogracile*, and the mutualistic relationship to epibiontic bacteria for detoxification of ROS indicates the importance of this process for sea ice diatoms.

In summary, these EST libraries provide a first glimpse of the gene diversity of sea ice algae and general conclusions cannot yet be drawn until we increase our sequencing efforts and include species from other major lineages of sea ice algae (e.g. dinoflagellates, prymnesiophytes, chlorophytes). However, there is the possibility that defence against oxidative stress is of general importance due to their exposure to freezing temperatures that causes light stress under relatively low-light intensities. Furthermore, only environmental sequencing projects (e.g. metatranscriptomes) on samples collected directly from sea ice can reveal the significance of this process. About 50% of the genes from these organisms have no assigned function and between ca. 15% and 30% of the genes seem to be species-specific. This is entirely different from higher plants where genome sequences from different species

exhibit greater similarity. The genome diversity in diatoms is probably indicative of the multilineage evolutionary history of these organisms, as recently revealed by a genome-wide comparison between the temperate diatoms *Phaeodactylum tricornutum* and *Thalassiosira pseudonana* (Bowler et al., 2008). These resources, as well as the EST projects with *F. cylindrus* and *C. neogracile*, already have shown a huge potential for gene discovery (e.g. IBPs, GST) that can generate novel hypotheses about how these organisms are adapted to their extreme environment.

Gene expression

These small-scale preliminary EST projects provided the functional capacity but not much information about the actual metabolic activity of sea ice algae. However, this information is essential to link genes to physiology, a necessary step to understand acclimation and adaptation to conditions in sea ice. A commonly used molecular method to investigate acclimation responses of organisms to diverse kinds of stimuli is the analysis of gene expression. Gene expression can be studied on single genes, entire genomes and even metagenomes (Mock et al., 2008; Friaze-Lopez et al., 2008). Highly appropriate is the use of gene arrays because many different genes from an organism can be investigated simultaneously, which enables a more global analysis of the acclimation response. This might lead to a selection of genes most important for acclimation due to their expression intensity, temporal dynamic, or clustering according to specific conditions. Only two major studies have been conducted so far where gene arrays (macro- and microarrays) were used to investigate the response of sea ice algae to environmental conditions (Mock & Valentin, 2004; Hwang et al., 2008). A macroarray with 44 genes (gene-specific oligonucleotides, 50mers) was used to investigate the response of *F. cylindrus* to temperature reduction (+5 to –1.8°C) at two different light intensities (3 and 35 µmol photons m^{-2} s^{-1}, Mock & Valentin, 2004) and a microarray with 1744 amplified PCR products from the EST library of *C. neogracile* was used to study its response to temperature increase (+4 to +10°C, Fig. 8.4; Hwang et al., 2008). Both studies focussed on temperature, the most fundamental physical condition in polar environments, and studied transient responses of the algae to temperature shifts that occur during sea ice formation and warming of ocean. Although a shift from +4°C to +10°C represents a rather high-temperature stress for polar oceans, it may give new insights into the acclimation to general temperature increases. The study with *F. cylindrus* was focussed on photosynthesis, whereas the one with *C. neogracile* revealed a more global acclimation response, although the most interesting changes in gene expression also occurred for photosynthesis genes.

  The short-term response (up to 13 days) of *F. cylindrus* to freezing temperatures, which simulates the incorporation into newly formed sea ice during fall, was characterized by down-regulation of genes encoding proteins for photosystem II (psbA and psbC) and carbon fixation (RUBISCO large subunit, rbcL), regardless of light intensity used (3 and 35 µmol photons m^{-2} s^{-1}). However, under the higher irradiance (35 µmol photons m^{-2} s^{-1}), up-regulation of genes encoding chaperons (heat-shock protein 70) and genes for plastid protein synthesis and turnover (elongation factor EfTs, ribosomal rpS4 and plastidial ftsH protease) was observed. Freezing accompanied by a reduction in irradiance (from 35 to 3 µmol photons m^{-2} s^{-1}) showed a typical response to low-light acclimation by up-regulation of genes encoding specific fcps without signs of a cold-stress response. Fcps are a diverse gene family composed of genes involved in light harvesting as well as dissipation of light.
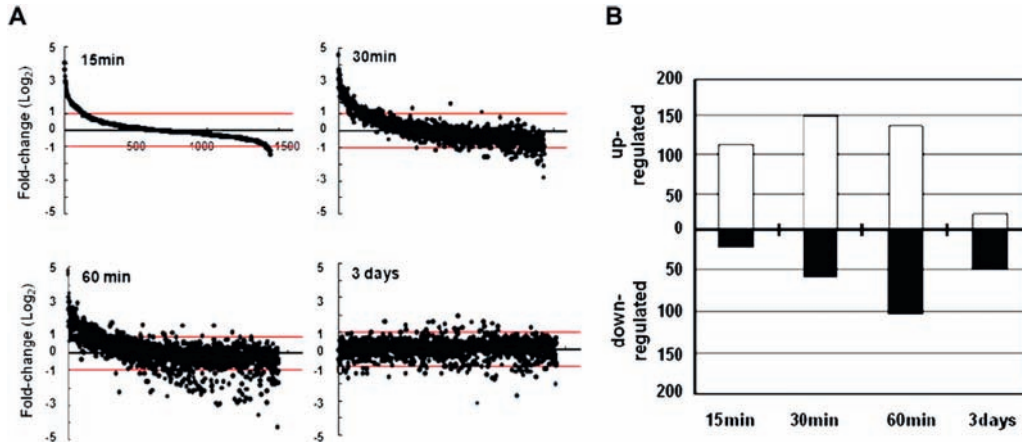
Fig. 8.4 Transcriptional profiling analysis relative to the duration of thermal stress. (a) Time course dependent changes in RNA profiling of *Chaetoceros neogracile* in response to thermal stress. The fold change is expressed as the log2 scale of the relative expression ratio for each gene between the 4°C and 10°C cultures at the indicated time. Genes were ranked in a descending order of the fold change beginning after 15 min of thermal stress. (b) Total number of genes differentially expressed by thermal stress (≥ twofold) at the indicated time. Reproduced from Hwang et al. (2008) with permission from Elsevier.

Up-regulation of stress response genes and genes for protein turnover only under higher light intensities and decreasing temperatures indicates that a decrease in temperature at such light intensities mimics a further increase in light that could be more stressful than the decrease in temperature alone. This phenomenon is probably part of a cold-shock response that also is known from temperate plants when they are exposed to lower temperatures (Allen & Ort, 2001). In contrast to temperate plants and diatoms, psychrophilic plants and diatoms are able to acclimate to higher irradiances under low temperatures (Streb et al., 1998; Mock & Hoch, 2005; Ralph et al., 2005; Morgan-Kiss et al., 2006). Long-term acclimation experiments to higher irradiances at freezing temperatures when compared to the same light intensity but higher temperatures (+5°C) revealed that cells kept at lower temperatures showed a response typical of high-light acclimation: higher NPQ, up-regulation of the gene psbA and up-regulation of high-light fcps that are involved in energy dissipation (Mock & Hoch, 2005).

A reduction in expression of other photosynthesis-related genes (such as rbcL) was not observed after several months under freezing conditions, indicating that long-term acclimation had been achieved. Temperature effects that are less dependent on adjustments of the energy flow under freezing temperatures could also be identified by gene expression analysis. The short-term (up to 3 days) heat-shock response of *C. neogracile* caused a differential regulation (≥twofold up or down) of 21.5% of all 1439 genes on the array. These data furthermore revealed a rapid establishment of molecular homeostasis at 10°C, in contrast to the cold-shock experiments with *F. cylindrus* where homeostasis was only established after several weeks, likely caused by a strongly reduced metabolism under freezing temperatures. After 1 hour at 10°C, 57% of the differentially regulated genes (309) in *C. neogracile* were up-regulated and 43% were down-regulated (Fig. 8.5). Three days of culturing at
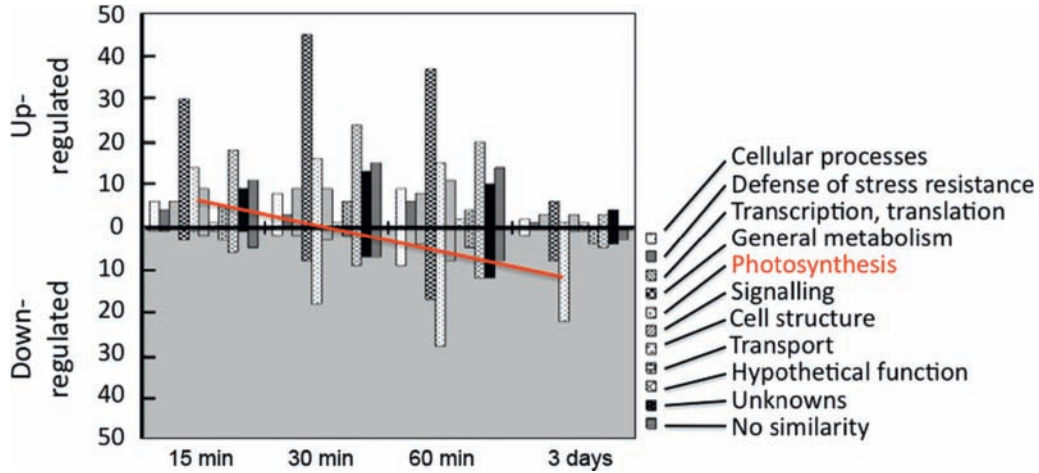
Fig. 8.5 Number of genes that are up- or-down regulated by thermal stress at indicated time displayed by each functional category in *Chaetoceros neogracile*. Genes of differential expression were dissected on the basis of their functional categories. The time periods depicted are as in Fig. 8.4. Reproduced from Hwang et al. (2008, supplementary material) with permission from Elsevier.

10°C reduced the total number of differentially expressed genes to 74 of which 68% were down- and 32% were up-regulated. Most of the transiently fast up-regulated genes were associated with protein folding and unfolding (heat-shock protein 90, co-chaperon Hsc20 and GrpE), protein degradation (26S proteosome regulatory subunit S2, ubiquitin protein ligase, FtsH and FtsH2) and oxidative stress-related genes (monoascorbate reductase, glutarredoxin, glutathione peroxidase, GST). Interestingly, many of the down-regulated genes were related to photosynthesis and most of them remained down-regulated even after 3 days of acclimation, which is in contrast to the homeostatic acclimation observed for other thermal stress-responsive genes. Down-regulation of photosynthetic genes may, therefore, have been partially responsible for the reduction in growth and cell yield at 10°C compared to 4°C.

The *Chaetoceros neogracile* population increased fivefold in cell number when cultured at 4°C for 10 days but only doubled during the same time period at 10°C. The reduction of growth is well known during a downshift of temperatures but not a reduction in total cell number at the end of exponential growth. The largest group of photosynthetic genes that were down-regulated in *C. neogracile* belonged to the group of fcps, although other light harvesting proteins (LHCs) and PSII extrinsic proteins also were down-regulated. However, four LHCs and five fcps were up-regulated more than fourfold within 15–30 min after the first exposure to 10°C. It seems that these genes might have a function in photoprotection rather than in light harvesting. Cluster analysis of these fcps revealed that they fall into the same cluster with a fcp from *Cyclotella cryptica* that is known to be involved in photoprotection under high-light conditions.

These array studies with *Fragilariopsis cylindrus* and *Chaetoceros neogracile* reveal for the first time how Antarctic sea ice algae respond to different thermal conditions on a molecular level. As expected for sychrophilic organisms, the acclimation to lower temperature seems physiologically less stressful, although more time is required, compared to high-temperature

stress that already begins at 10°C for sea ice algae. Photosynthesis is strongly negatively affected under higher temperatures and probably is not able to fully recover after a longer time of acclimation, leading to a reduced growth rate and population size. The molecular basis of this phenomenon in sea ice algae is not yet known but the consequences might be dramatic if polar sea water temperatures rise due to global climate change. These organisms will then be the first to disappear in a changing polar environment. Consequently, genetic and genomic studies with these organisms are required to discover their gene diversity and to understand their evolution and adaptation. Understanding this evolution is essential to predict the impact that climate change will have on polar regions.

References

Ackley, S.F. & Sullivan, C.W. (1994) Physical controls on the development and characteristics of Antarctic sea ice biological communities – a review and synthesis. *Deep-Sea Research I*, **41**, 1583–1604.

Ackley, S.F., Buck, K.A. & Taguchi, S. (1979) Standing crop of algae in the sea ice of the Weddell Sea region. *Deep-Sea Research*, **26**, 269–281.

Ainley, D. & Sullivan, C.W. (1984) AMIEREZ 1983: a summary of activities on board the R/V Mellville and USCGC Westwind. *Antarctic Journal of the United States*, **19**, 177–179.

Alexander, V. (1974) Primary productivity regimes of the nearshore Beaufort Sea, with reference to potential roles of ice biota. In: *The Coast and Shelf of the Beaufort Sea* (Ed. by J.C. Reed & J.E. Sater), pp. 609–632, Arctic Institute of North America, Arlington, VA.

Alexander, V. & Chapman, T. (1981) The role of epontic algal communities in Bering Sea ice. In: *The eastern Bering Sea shelf: Oceanography and resources, vol.2* (Eds. D.W. Hood & J.A. Calder), pp. 773–780. Univ. Washington Press, Seattle.

Allen, D.J. & Ort, D.R. (2001). Impacts of chilling temperatures on photosynthesis in warm-climate plants. *Trends in Plant Science*, **6**, 36–42.

Ambrose, W.G., Jr., von Quillfeldt, C., Clough, L.M., Tilney, P.V.R. & Tucker, T. (2005) The sub-ice algal community in the Chukchi Sea: Large- and small-scale patterns of abundance based on images from a remotely operated vehicle. *Polar Biology*, **28**, 784–795.

Apollonia, S. (1965) Chlorophyll in Arctic sea ice. *Arctic*, **18**, 118–122.

Apollonia, S., Pennington, M. & Cota, G.F. (2002) Stimulation of phytoplankton photosynthesis by bottom-ice extracts in the Arctic. *Polar Biology*, **25**, 350–354.

Archer, S.D., Leakey, R.J.G., Burkill, P.H., Sleigh, M.A. & Appleby, C.J. (1996) Microbial ecology of sea ice at a coastal Antarctic site; community composition; biomass and temporal change. *Marine Ecology Progress Series*, **135**, 179–195.

Armbrust, E.V., Berges, J.A., Bowler, C. et al. The genome of the diatom *Thalassiosira pseudonana*: ecology, evolution, and metabolism. *Science*, **306**, 79–86.

Arrigo, K.R. & Sullivan, C.W. (1992) The influence of salinity and temperature covariation on the photophysiological characteristics of Antarctic sea ice microalgae. *Journal of Phycology* **28**, 746–756.

Arrigo, K.R. & Sullivan, C.W. (1994) A high resolution bio-optical model of microalgal growth: Tests using sea ice algal community time series data. *Limnology and Oceanography*, **39**, 609–631.

Arrigo, K.R., Robinson, D.H. & Sullivan, C.W. (1993a) A high resolution study of the platelet ice ecosystem in McMurdo Sound, Antarctica: photosynthetic and bio-optical characteristics of a dense microalgal bloom. *Marine Ecology Progress Series*, **98**, 173–185.

Arrigo, K.R., Kremer, J.N. & Sullivan, C.W. (1993b) A simulated Antarctic fast-ice ecosystem. *Journal of Geophysical Research*, **98**, 6929–6946.

Arrigo, K.R., Dieckmann, G., Gosselin, M., Robinson, D.H., Fritsen, C.H. & Sullivan, C.W. (1995) A high resolution study of the platelet ice ecosystem in McMurdo Sound, Antarctica: biomass,

nutrient, and production profiles within a dense microalgal bloom. *Marine Ecology Progress Series*, **127**, 255–268.

Arrigo, K.R., Lizotte, M.P., Worthen, D.L., Dixon, P. & Dieckmann, G. (1997) Primary production in Antarctic sea ice. *Science*, **276**, 394–397.

Arrigo, K.R., Worthen, D.L., Dixon, P. & Lizotte, M.P. (1998) Primary productivity of near surface communities within Antarctic pack ice. In: *Antarctic Sea Ice Biological Processes, Interactions, and Variability* (Eds. M.P. Lizotte & K.R. Arrigo). *Antarctic Research Series*, **73**, 23–43.

Arrigo, K.R., Robinson, D.H., Dunbar, R.B., Leventer, A.R. & Lizotte, M.P. (2003) Physical control of chlorophyll *a*, POC, and PON distributions in the pack ice of the Ross Sea, Antarctica. *Journal of Geophysical Research,* **108** (C10), 3316, 10.1029/2001JC001138.

Arrigo, K.R., van Dijken, G.L. & Pabi, S. (2008a) The impact of a shrinking Arctic ice cover on marine primary production. *Geophysical Research Letters*, **35**, L19603, 10.1029/2008GL035028.

Arrigo, K.R., van Dijken, G.L. & Bushinsky, S. (2008b) Primary Production in the Southern Ocean, 1997–2006. *Journal of Geophysical Research*, **113**, C08004, 10.1029/2007JC004551.

Asami, H. & Imada, K. (2001) Ice algae and phytoplankton in the late ice-covered season in Notoro Ko lagoon, Hokkaido. *Polar Bioscience*, **14**, 24–32.

Augstein, E., Bagriantsev, N. & Schenke, H-W. (1991) Die expedition Antarktis VIII/1-2, 1989 mit der Winter Weddell Gyre study der Forschungsschiffe Polarstern and Akademik Federov. *Berichte zum Polarfurschung*, **84**, 134 pp.

Bates S.S. & Cota G. F. (1986) Fluorescence induction and photosynthetic responses of arctic ice algae to sample treatment and salinity. *Journal of Phycology*, **22**, 421–429.

Bathmann, U., Schulz-Baldes, M., Farbach, E., Smetacek, V. & Hubberten, H-W. (1992) Die expedition Antarktis IX/1-4 des Forschungsschiffes Polarstern. *Berichte zum Polarfurschung,* 100 pp.

Bergmann, M.A., Welch, H.E., Butler-Walker, J.E. & Silfred, T.D. (1991) Ice algal photosynthesis at Resolute and Saqvaqjuac in the Canadian Arctic, *Journal of Marine Systems*, **2**, 43–52.

Bindschadler, R. (1990) SeaRISE: a multidisciplinary research initiative to predict rapid changes in global sea level caused by collapse of marine ice sheets. *NASA Conference Publication* 3075, 47 pp.

Booth, J.A. (1984) The epontic algal community of the ice edge zone and its significance to the Davis Strait ecosystem. *Arctic*, **37**, 234–243.

Booth, B.C. & Horner, R.A. (1997) Microalgae on the Arctic Ocean Section, 1994; species abundance and biomass. *Deep-Sea Research II*, **44**, 1607–1622.

Bowler, C., Allen, A.E., Badger, J.H. et al. (2008) The *Phaeodactylum* genome reveals the dynamic nature and multi-lineage evolutionary history of diatom genomes. *Nature*, **456**, 239–244.

Bowman, J.P., McCammon, S.A., Brown, M.V., Nichols, D.S. & McMeekin, T.A. (1997). Diversity and association of psychrophilic bacteria in Antarctic sea ice. *Applied and Environmental Microbiology,* **63**, 3068–3078.

Buck, K.R., Nielsen, T.G., Hansen, B.W., Gastrup-Hansen, D. & Thomsen, H. (1998) Infiltration phyto- and protozooplankton assemblages in the annual sea ice of Disko Island, West Greenland, spring 1996. *Polar Biology*, **20**, 377–381.

Bunt, J.S. (1963) Diatoms of Antarctic sea ice as agents of primary production. *Nature*, **199**, 1254–1257.

Bunt, J.S. (1964) Primary productivity under sea ice in Antarctic waters: influence of light and other factors on photosynthetic activities of Antarctic marine microalgae. *Antarctic Research Series*, **1**, 27–31.

Bunt, J.S. (1968) Some characteristics of microalgae isolated from Antarctic sea ice. *Antarctic Research Series*, **11**, 1–14.

Bunt, J.S. & Lee, C.C. (1969) Observations within and beneath Antarctic sea ice in McMurdo Sound and the Weddell Sea, methods and data. *Institute of Marine Science Technical Report*, **69-1**, 32 pp.

Bunt, J.S. & Lee, C.C. (1970) Seasonal primary production in Antarctic sea ice at McMurdo Sound in 1967. *Journal of Marine Research*, **28**, 304–320.

Burkholder, P.R. & Mandelli, E.F. (1965) Productivity of microalgae in Antarctic sea ice. *Science*, **149**, 872–874.

Charlson, R.J., Lovelock, J.E., Andrea, M.O. & Warren, S.G. (1987) Oceanic phytoplankton, atmospheric sulfur, cloud albedo and climate. *Nature*, **326**, 655–661.

Cheng, C.H.C. (1998). Evolution of the divers antifreeze proteins. *Current Opinions in Genetics and Development*, **8**, 715–720.

Clarke, D.B. & Ackley, S.F. (1984) Sea ice structure and biological activity in the Antarctic marginal ice zone. *Journal of Geophysical Research*, **89**, 2087–2095.

Cota, G.F. (1985) Photoadaptation of high Arctic ice algae. *Nature,* **315**, 219–222.

Cota, G.F. & Horne, E.P.W. (1989) Physical control of Arctic ice algal production. *Marine Ecology Progress Series*, **52**(2), 111–121.

Cota, G.F. & Smith, R.E.H. (1991) Ecology of bottom ice algae: II. Dynamics, distributions and productivity, *Journal of Marine Systems,* **2**, 279–295.

Cota, G.F. & Sullivan, C.W. (1990) Photoadaptation, growth and production of bottom ice algae in the Antarctic. *Journal of Phycology*, **26**, 399–411.

Cota, G.F., Anning, J.L., Harris, L.R., Harrison, W.G. & Smith, R.E.H. (1990) Impact of ice algae on inorganic nutrients in seawater and sea ice in Barrow Strait, N.W.T., Canada, during spring *Canadian Journal of Fisheries and Aquatic Sciences*, **47**, 1402–1415.

Crame, J.A. (1997) An evolutionary framework for the polar regions. *Journal of Biogeography*, **24**, 1–9.

Delille, B., Jourdain, B., Borges, A.V., Tison, J.L. & Delille, D. (2007) Biogas (CO_2, O_2, dimethylsulfide) dynamics in spring Antarctic fast ice. *Limnology and Oceanography*, **52**, 1367–1379.

Deming, J.W. (2002) Psychrophiles and polar regions. *Current Opinion in Microbiology*, **5**, 301–309.

Dieckmann, G., Sullivan, C.W. & Garrison, D.L. (1990) Seasonal standing crop of ice algae in pack ice of the Weddell Sea, Antarctica. *EOS, Transactions of the American Geophysical Union*, **71**, 79.

Dobrzyn, P. & Tatur, A. (2003) Algal pigments in fast ice and under-ice water in an Arctic fjord. *Sarsia*, **88**, 291–296.

Dunbar, M.J. & Acreman, J.C. (1980) Standing crops and species composition of diatoms in sea ice from Robeson Channel to the Gulf of St. Lawrence. *Ophelia*, **19**, 61–72.

Dupont, C.L., Goepfert, T.J., Lo, P., Wei, L. & Ahner, B.A. (2004) Diurnal cycling of glutathione in marine phytoplankton: Field and culture studies. *Limnology and Oceanography,* **49**, 991–996.

Druzhkov, N.V., Druzhkova, E.I. & Kuznetsov, L.L. (2001) The sea-ice algal community of seasonal pack ice in the southwestern Kara Sea in late winter. *Polar Biology,* **24**, 70–72.

Eddie, B., Krembs, C. & Neuer, S. (2008) Characterization and growth response to temperature and salinity of psychrophilic, halotolerant *Chlamydomonas* sp ARC isolated from Chukchi Sea ice. *Marine Ecology Progress Series*, **354**, 107–117.

Eppley, R.W. (1972) Temperature and phytoplankton growth in the sea. *Fish Bulletin*, **70**, 1063–1085.

Frias-Lopez J., Shi, Y., Tyson, G.W., Coleman, M.L., Schuster, S.C., Chisholm, S.W. & DeLong, E.F. (2008) Microbial community gene expression in ocean surface waters. *Proceedings of the National Academy of Science, USA,* **105**, 3805–3810.

Fritsen, C.H., Lytle, V.I., Ackley, S.F. & Sullivan, C.W. (1994) Autumn bloom of Antarctic pack-ice algae. *Science*, **266**, 782–784.

Fritsen, C.H., Coale, S., Neenan, D., Gibson, A. & Garrison, D.L. (2001). Biomass, production and microhabitat characteristics near the freeboard of ice floes in the Ross Sea during the austral summer. *Annals of Glaciology*, **33**, 280–286.

Garrison, D.L. (1991) Antarctic sea ice biota. *American Zoologist*, **31**, 17–33.

Garrison, D.L. & Buck, K.R. (1982) Sea ice algae in the Weddell Sea. I. Biomass distribution and the physical environment. *EOS, Transactions of the American Geophysical Union*, **63**, 47.

Garrison, D.L. & Close, A.R. (1993) Winter ecology of the sea ice biota in Weddell Sea pack ice. *Marine Ecology Progress Series*, **96**, 17–31.

Garrison, D.L., Ackley, S.F. & Buck, K.R. (1983) A physical mechanism for establishing algal populations in frazil ice. *Nature*, **306**, 363–365.

Garrison, D.L., Close, A.R. & Reimnitz, E. (1990) Microorganisms concentrated by frazil ice: evidence from laboratory experiments and field measurements. In *Sea Ice Properties and Processes*, (Eds S.F. Ackley & W.F. Weeks), U.S. Army Corps of Engineers, Cold Regions Research and Engineering Laboratory, Monograph 90–1, 92–96.

Garrison, D.L., Jeffries, M.O., Gibson, A. et al. (2003) Development of sea ice microbial communities during autumn ice formation in the Ross Sea. *Marine Ecology Progress Series*, **259**, 1–15.

Gast, R.J., Dennett M.R. & Caron D.A. (2004) Characterization of protistan assemblages in the Ross Sea, Antarctica, by denaturing gradient gel electrophoresis. *Applied and Environmental Microbiology*, **70**, 2028–2037.

Gast R.J., Moran, D.M., Beaudoin, D.J., Blythe, J.N., Dennett, M.R. & Caron, D.A. (2006) Abundance of a novel dinoflagellate phylotype in the Ross Sea, Antarctica. *Journal of Phycology*, **42**, 233–242.

Gloersen, P., Campbell, W.J., Cavalieri, D.J., Comiso, J.C., Parkinson, C.L. & Zwally, H.J. (1992) *Arctic and antarctic sea ice, 1978–1987: Satellite Passive-Microwave Observations and Analysis.* NASA, Washington, DC, USA, 290 pp.

Glud, R.N., Rysgaard, S. & Kuhl, M. (2002) A laboratory study on O_2 dynamics and photosynthesis in ice algal communities: quantification by microsensors, O_2 exchange rates, ^{14}C incubations and a PAM fluorometer. *Aquatic Microbial Ecology*, **27** (3), 301–311.

Gosselin, M., Legendre, L., Demers, S. & Ingram, R.G. (1985) Responses of sea ice microalgae to climatic and fortnightly tidal energy inputs (Manitounuk Sound, Hudson Bay). *Canadian Journal of Fisheries and Aquatic Sciences*, **42**, 999–1006.

Gosselin, M., Legendre, L., Therriault, J.C., Demers, S. & Rochet, M. (1986) Physical control of the horizontal patchiness of sea ice microalgae. *Marine Ecology—Progress Series*, **9** (3), 289–298.

Gosselin, M., Legendre, L., Therriault, J.-C. & Demers, S. (1990) Light and nutrient limitation of sea ice microalgae (Hudson Bay, Canadian Arctic). *Journal of Phycology*, **26**, 220–232.

Gosselin, M., Levasseur, M., Wheeler, P.A., Horner, R.A. & Booth, B.C. (1997). New measurements of phytoplankton and ice algal production in the Arctic Ocean. *Deep-Sea Research Part II*, **44**, 1623–1644.

Gowing, M.M. (2003) Large viruses and infected microeukaryotes in Ross Sea summer pack ice habitats. *Marine Biology*, **142**, 1029–1040.

Gradinger, R. (1999) Integrated abundance and biomass of sympagic meiofauna in Arctic and Antarctic pack ice. *Polar Biology*, **22**, 169–177.

Gradinger, R. & Zhang, Q. (1997) Vertical distribution of bacteria in Arctic sea ice from the Barents and Laptev Seas. *Polar Biology*, **17**, 448–454.

Gradinger, R., Friedrich, C. & Spindler, M. (1999) Abundance, biomass and composition of the sea ice biota of the Greenland Sea pack ice. *Deep-Sea Research Part II*, **46**, 1457–1472.

Grainger, E.H. (1977) The annual nutrient cycle in sea ice. In: *Polar Oceans* (Ed. M.J. Dunbar), pp. 285–299. Arctic Institute of North America, Calgary, Canada.

Granskog, M.A., Kaartokallio, H. & Shirasawa, K. (2003) Nutrient status of Baltic Sea ice: evidence for control by snow-ice formation, ice permeability, and ice algae. *Journal of Geophysical Research*, **108**, 9-1–9-9.

Grant, W.S. & Horner, R.A. (1976) Growth responses to salinity variation in four arctic ice diatoms (*Melosira juergensii, Porosira glacialis, Navicula transitans derasa, Coscinodiscus lacustris*). *Journal of Phycology*, **12**, 180–185.

Grossi, S.M., Kottmeier, S.T., Moe, R.L., Taylor, G.T. & Sullivan, C.W. (1987) Sea ice microbial communities. VI. Growth and primary production in bottom ice under graded snow cover. *Marine Ecology Progress Series*, **35**, 153–164.

Grzymski, J.J., Carter, B.J., DeLong, E.F., Feldman, R.A., Ghadiri, A. & Murray, A.E. (2006) Comparative genomics of DNA fragments from six Antarctic marine planktonic bacteria. *Applied and Environmental Microbiology*, **72**, 1532–1541.

Guglielmo, L., Carrada, G.C., Catalano, G. et al. (2000) Structural and functional properties of sympagic communities in the annual sea ice at Terra Nova Bay (Ross Sea, Antarctica). *Polar Biology*, **23**, 137–146.

Guglielmo, L., Carrada, G.C., Catalano, G. et al. (2004) Biogeochemistry and algal communities in the annual sea ice at Terra Nova Bay (Ross Sea, Antarctica). *Chemistry and Ecology*, **20**, 43–55.

Hegseth, E.N. (1998) Primary production of the northern Barents Sea. *Polar Research*, **17**, 113–123.

Hegseth, E.N. & von Quillfeldt, C.H. (2002) Low phytoplankton biomass and ice algal blooms in the Weddell Sea during the ice-filled summer of 1997. *Antarctic Science*, **14**, 231–243.

Hempel, G. (1985) Die expedition Antarktis III/3 mit F.S. Polarstern 1984/85. *Berichte zum Polarfurschung*, **25**, 222 pp.

Hempel, I. (1989) The expedition Antarctic VII/1 and 2 (EPOS 1) of R.V. Polarstern in 1988/89. *Berichte zum Polarfurschung*, **62**, 184 pp.

Herman, A.W., Knox, D.F., Conrad, J. & Mitchell, M.R. (1993) Instruments for measuring subice algal profiles and productivity in situ. *Canadian Journal of Fisheries and Aquatic Sciences*, **50**, 359–369.

Hoag, H. (2003) Genomes take pole position in the icy wastes. *Nature*, **421**, 880.

Horner, R.A. (1976) Sea ice organisms. *Oceanography and Marine Biology, An Annual Review*, **14**, 167–182.

Horner, R.A. (1985) Taxonomy of sea ice microalgae. In: *Sea Ice Biota*. (Ed. R. Horner) CRC Press, Boca Raton, 147–158.

Horner, R.A. & Schrader, G.C. (1982) Relative contributions of ice algae, phytoplankton, and benthic microalgae to primary production in nearshore regions of the Beaufort Sea. *Arctic*, **35**, 485–503.

Hoshiai, T. (1977) Seasonal change of ice communities in the sea ice near Syowa Station, Antarctica. In: *Polar Oceans* (Ed. M.J. Dunbar.), pp. 307–317. Arctic Institute of North America, Calgary, Canada.

Hoshiai, T. (1981). Proliferation of ice algae in the Syowa Station area, Antarctica. *Memoirs of the National Institute of Polar Research, Series E*, **34**, 1–12.

Hoshino, T., Kiriaki, M., Ohgiya, S. et al. (2003). Antifreeze proteins from snow mold fungi. *Canadian Journal of Botany*, **81**, 1175–1181.

Hsiao, S.I.C. (1980) Quantitative composition, distribution, community structure and standing stock of sea ice microalgae in the Canadian Arctic. *Arctic*, **33**, 768–793.

Hünken, M., Harder, J. & Kirst, G. O. (2008) Epiphytic bacteria on the Antarctic ice diatom *Amphprora kufferathii* Manguin cleave hydrogen peroxide produced during algal photosynthesis. *Plant Biology*, **10**, 519–526.

Hwang, Y-S., Jung, G. & Jin, E. (2008) Transcriptome analysis of acclamatory responses to thermal stress in Antarctic algae. *Biochemical and Biophysical Research Communications*, **367**, 635–641.

Ichimura, S. & Aruga Y. (1964) Photosynthetic natures of natural algal communities in Japanese waters. In: *Recent Researches in the Field of Hydrosphere, Atmosphere, and Nuclear Geochemistry* (Ed. Y. Miyake & T. Koyama), Maruzen, Tokyo, 13–37.

Ikävalko, J. & Thomsen, H.A. (1997) The Baltic Sea ice biota (March 1994): a study of the protistan community. *European Journal of Protistology*, **33**, 229–243.

Irwin, B.D. (1990) Primary production of ice algae on a seasonally-ice-covered, continental shelf. *Polar Biology*, **10**, 247–254.

Janech, M.G., Krell, A., Mock, T., Kang, J.S. & Raymond, J.A. (2006) Ice-binding proteins from sea ice diatoms (Bacillariophyceae). *Journal of Phycology*, **42**, 410–416.

Jin, M., Deal, C.J., Wang, J. et al. (2006) Controls of the landfast ice-ocean ecosystem offshore Barrow, Alaska. *Annals of Glaciology*, **44**, 63–72.

Johnsen, J. & Hegseth, E.N. (1991) Photoadaptation of sea ice microalgae in the Barents Sea. *Polar Biology*, **11**, 179–184.

Jung, G., Lee, C.-G., Kang, S.-H. & Jin, E. (2007) Annotation and expression profile analysis of cDNA from the Antarctic diatom *Chaetoceros neogracile*. *Journal of Microbiology and Biotechnology*, **17**, 1330–1337.

Junge, K., Eicken, H. & Deming, J.W. (2004). Bacterial activity at −2 to −20°C in Arctic wintertime sea ice. *Applied and Environmental Microbiology*, **70**, 550–557.

Junge, K., Imhoff, F., Staley, J.T. & Deming. J.W. (2002) Phylogenetic diversity of numerically important arctic sea-ice bacteria cultured at subzero temperature. Microbiai Ecology, 43, 315–328.

Kaartokallio, H. (2004) Food web components, and physical and chemical properties of Baltic Sea ice. *Marine Ecology Progress Series*, **273**, 49–63.

Kaartokallio, H., Kuosa, H., Thomas, D.N., Granskog, M.A. & Kivi, K. (2007) Biomass, composition and activity of organism assemblages along a salinity gradient in sea ice subjected to river discharge in the Baltic Sea. *Polar Biology*, **30** (2), 183–197.

Karentz, D. (1994) Considerations for evaluating ultraviolet radiation-induced genetic damage relative to Antarctic ozone depletion. *Environmental Health Perspectives*, **102** (12), 61–63.

Karentz, D. & Spero, H.J. (1995) Response of natural *Phaeocystis* population to ambient fluctuation of UVB radiation caused by Antarctic ozone depletion. *Journal of Plankton Research*, **17** (9), 1771–1789.

Kang, S.H. & Fyxell, G.A. (1992) *Fragilariopsis cylindrus* (Grunow) Krieger: The most abundant diatom in the water column assemblages. In: Antarctic marginal ice-edge zones. *Polar Biology,* **12**, 609–627.

Kattner, G., Thomas, D.N., Haas, C., Kennedy, H. & Dieckmann, G.S. (2004) Surface ice and gap layers in Antarctic sea ice: highly productive habitats. *Marine Ecology Progress Series*, **277**, 1–12.

Kipfstuhl, J. (1991) On the formation of underwater ice and the growth and energy budget of the sea ice in Atka Bay, Antarctica. *Reports on Polar Research*, **85**, 1–89.

Kottmeier, S.T. & Sullivan, C.W. (1988) Sea ice microbial communities. IX. Effects of temperature and salinity on metabolism and growth of autotrophs and heterotrophs. *Polar Biology*, **8**, 293–304.

Kottmeier, S.T. & Sullivan, C.W. (1990) Bacterial biomass and bacterial production in pack ice of Antarctic marginal ice edge zones. *Deep-Sea Research*, **37**, 1311–1330.

Kottmeier, S.T., Grossi, S.M. & Sullivan, C.W. (1987) Late winter primary production and bacterial production in the sea ice and seawater west of the Antarctic Peninsula. *Marine Ecology Progress Series*, **36**, 287–298.

Krell, A. (2006). *Salt Stress Tolerance in the Psychrophilic Diatom* Fragilariopsis cylindrus. Dissertation, University of Bremen, Germany.

Krell, A., Ummenhofer, C., Kattner, G., Naumov, A., Evans, D., Dieckmann, G.S. & Thomas, D.N. (2003) The biology and chemistry of land fast ice in the White Sea, Russia: a comparison of winter and spring conditions. *Polar Biology*, **26**, 707–719.

Krell, A., Funck, D., Plettner, I., John, U. & Dieckmann, G. (2007) Regulation of proline metabolism under salt stress in the psychrophilic diatom *Fragilariopsis cylindrus* (Bacillariophyceae). *Journal of Phycology*, **43**, 753–762.

Krell, A., Beszteri, B., Dieckmann, G., Glöckner, G., Valentin, K. & Mock, T. (2008) A new class of ice-binding proteins discovered in a salt stress induced cDNA library of the psychrophilic diatom *Fragilariopsis cylindrus* (Bacillariophyceae). *European Journal of Phycology*, **43**, 423–433.

Krembs, C., Eicken, H., Junge, K. & Deming, J.W. (2002) High concentrations of exopolymeric substances in Arctic winter sea ice: Implications for the polar ocean carbon cycle and cryoprotection of diatoms. *Deep-Sea Research Part I*, **49**, 2163–2181.

Kudoh, S., Robineau, B., Suzuki, Y., Fujiyoshi, Y. & Takahashi, M. (1997) Photosynthetic acclimation and the estimation of temperate ice algal primary production in Saroma-ko Lagoon, Japan. *Journal of Marine Systems*, **11**, 93–109.

Lavoie, D., Denman, K. & Michel, C. (2005) Modeling ice algal growth and decline in a seasonally ice-covered region of the Arctic (Resolute Passage, Canadian Archipelago). *Journal of Geophysical Research*, **110**, C11009, 10.1029/2005JC002922.

Lazzara, L., Nardello, I., Ermanni, C., Mangoni, O. & Saggiomo, V. (2007) Light environment and seasonal dynamics of microalgae in the annual sea ice at Terra Nova Bay, Ross Sea, Antarctica. *Antarctic Science*, **19**, 83–92.

Legendre, L., Demers, S. & Gosselin, M. (1987) Chlorophyll and photosynthetic efficiency of size-fractionated sea ice microalgae (Hudson-Bay, Canadian Arctic). *Marine Ecology Progress Series*, **40**, 199–203.

Legendre, L., Ackley, S.F., Dieckmann, G.S. et al. (1992) Ecology of sea ice biota: 2. Global significance. *Polar Biology*, **12**, 429–444.

Lemke, P. (1994) Die expedition Antarktis X/4 mit F.S. Polarstern 1992. *Berichte zum Polarfurschung*, **140**, 90 pp.

Lizotte, M.P. (2001) The contribution of sea ice algae to Antarctic marine primary production. *American Zoologist*, **41**, 57–73.

Lizotte, M.P. & Sullivan, C.W. (1991) Photosynthesis-irradiance relationships in microalgae associated with Antarctic pack ice: evidence for *in situ* activity. *Marine Ecology Progress Series*, **71**, 175–184.

Lizotte, M.P. & Sullivan, C.W. (1992a) Photosynthetic capacity in microalgae associated with Antarctic pack ice. *Polar Biology*, **12**, 497–502.

Lizotte, M.P. & Sullivan, C.W. (1992b) Biochemical composition and photosynthate distribution in sea ice algae of McMurdo Sound: evidence for nutrient deficiencies during the bloom. *Antarctic Science,* **4**, 23–30.

Lizotte, M.P., Robinson, D.H. & Sullivan, C.W. (1998) Algal pigment signatures in Antarctic sea ice. In: *Antarctic Sea Ice: Biological Processes, Interactions and Variability* (Eds. M.P. Lizotte & K.R. Arrigo). American Geophysical Union, Washington. *Antarctic Research Series*, **73**, 93–106.

Lovejoy, C., Massana, R. & Pedros-Alio, C. (2006) Diversity and distribution of marine microbial eukaryotes in the Arctic Ocean and adjacent seas. *Applied Environmental Microbiology*, **72**, 3085–3095.

Maranger, R., Bird, D.F. & Juniper, S.K. (1994) Viral and bacterial dynamics in Arctic sea ice during the spring algal bloom near Resolute, N.W.T., Canada. *Marine Ecology Progress Series*, **111**, 121–127.

McConville, M.J. & Wetherbee, R. (1983) The bottom-ice microalgal community from annual ice in the inshore waters of East Antarctica. *Journal of Phycology*, **19**, 431–439.

McConville, M.J., Mitchell, C. & Wetherbee, R. (1985) Patterns of carbon assimilation in a microalgal community from annual sea ice, East Antarctica. *Polar Biology*, **4**, 135–141.

McMinn, A. & Ashworth, C. (1998) The use of oxygen microelectrodes to determine the net production by an Antarctic sea ice algal community. *Antarctic Science*, **10**, 39–44.

McMinn, A. & Hattori, H. (2006) Effect of time of day on the recovery from light exposure in ice algae from Saroma Ko lagoon, Hokkaido. *Polar Bioscience*, **20**, 30–36.

McMinn, A. & Hegseth, E.N. (2004) Quantum yield and photosynthetic parameters of marine microalgae from the southern Arctic Ocean, Svalbard. *Journal of the Marine Biological Association of the United Kingdom*, **84** (5), 865–871.

McMinn A., Ashworth, C. & Ryan, K. (1999) Growth and productivity of Antarctic Sea ice algae under PAR and UV irradiances. *Botanica Marina*, **42**, 401–407.

McMinn, A., Ryan, K. & Gademann, R. (2003) Diurnal changes in photosynthesis of Antarctic fast ice algal communities determined by pulse amplitude modulation fluorometry. *Marine Biology*, **143**, 359–367.

McMinn, A., Pankowski, A. & Delfatti, T. (2005) Effect of hyperoxia on the growth and photosynthesis of polar sea ice microalgae. *Journal of Phycology*, **41**, 732–741.

McMinn, A., Ryan, K.G., Ralph, P.J. & Pankowski, A. (2007) Spring sea ice photosynthesis, primary productivity and biomass distribution in eastern Antarctica, 2002–2004. *Marine Biology*, **151**, 985–995.

McMinn, A., Hattori, H., Hirawake, T. & Iwamoto, A. (2008) Preliminary investigation of Okhotsk Sea ice algae; taxonomic composition and photosynthetic activity. *Polar Biology*, **31**, 1011–1015.

McRoy, C.P. & Goering, J.J. (1974) The influence of ice on the primary productivity of the Bering Sea. In: *Oceanography of the Bering Sea with Emphasis on Renewable Resources* (Ed. D.W. Hood & E.J. Kelley), pp. 403–421. Institute of Marine Science, University of Alaska, Fairbanks, Alaska.

Meguro, H. (1962) Plankton ice in the Antarctic Ocean. *Antarctic Record*, **14**, 1192–1199.

Meguro, H., Ito, K. & Fukushima, H. (1967) Ice flora (bottom type): a mechanism of primary production in polar seas and the growth of diatoms in sea ice. *Arctic*, **20**, 114–133.

Meiners, K., Fehling, J., Granskog, M.A. & Spindler, M. (2002) Abundance, biomass and composition of biota in Baltic Sea ice and underlying water (March 2000). *Polar Biology*, **25**, 761–770.

Meiners, K., Gradinger, R., Fehling, J., Civitarese, G. & Spindler, M. (2003) Vertical distribution of exopolymer particles in sea ice of the Fram Strait (Arctic) during autumn. *Marine Ecology Progress Series*, **248**, 1–13.

Meiners, K., Brinkmeyer, R., Granskog, M.A. & Lindfors, A. (2004) Abundance, size distribution and bacterial colonization of exopolymer particles in Antarctic sea ice (Bellingshausen Sea). *Aquatic Microbial Ecology*, **35**, 283–296.

Melnikov, I.A. (1997) *The Arctic Sea Ice Ecosystem*. Gordon and Breach Science Publishers, Amsterdam.

Melnikov, I.A. & Bondarchuk, L.L. (1987) To the ecology of the mass aggregations of colonial diatom algae under the Arctic drifting sea ice. *Oceanology*, **27**, 317–321.

Melnikov, I.A., Kolosova, E.G., Welch, H.E. & Zhitina, L.S. (2002) Sea ice biological communities and nutrient dynamics in the Canada Basin of the Arctic Ocean. *Deep-Sea Research Part I*, **49**, 1623–1649.

Michel, C., Legendre, L., Ingram, R.G., Gosselin, M. & Levasseur, M. (1996) Carbon budget of sea ice algae in spring: Evidence of a significant transfer to zooplankton grazers. *Journal of Geophysical Research*, **101**, 18345–18360.

Michel, C., Nielsen, T.G., Nozais, C. & Gosselin, M. (2002) Significance of sedimentation and grazing by ice micro- and meiofauna for carbon cycling in annual sea ice (northern Baffin Bay). *Aquatic Microbial Ecology*, **30**, 57–68.

Miller, H. & Grobe, H. (1996) Die expedition Antarktis X1/3 mit F.S. Polarstern 1994. *Berichte zum Polarfurschung*, **188**.

Mock, T. (2002) In situ primary production in young Antarctic sea ice. *Hydrobiologia*, **470**, 127–132.

Mock, T. & Gradinger, R. (1999) Determination of Arctic ice algal production with a new *in situ* incubation technique. *Marine Ecology Progress Series*, **177**, 15–26.

Mock, T. & Kroon, B.M.A. (2002a) Photosynthetic energy conversion under extreme conditions: I: important role of lipids as structural modulators and energy sink under N-limited growth in Antarctic sea ice diatoms. *Phytochemistry*, **61**, 41–51.

Mock, T. & Kroon, B.M.A. (2002b) Photosynthetic energy conversion under extreme conditions: II: the significance of lipids under light limited growth in Antarctic sea ice diatoms. *Phytochemistry*, **61**, 53–60.

Mock, T. & Hoch, N. (2005) Long-term temperature acclimation of photosynthesis in steady-state cultures of the polar diatom *Fragilariopsis cylindrus*. *Photosynthesis Research*, **85**, 307–317.

Mock, T. & Thomas, D.N. (2005) Recent advances in sea ice microbiology. *Environmental Microbiology*, **7**, 605–619.

Mock, T. & Valentin, K. (2004). Photosynthesis and cold acclimation, molecular evidence from a polar diatom. *Journal of Phycology*, **40**, 732–741.

Mock, T., Dieckmann, G.S., Haas, C. et al. (2002) Micro-optodes in sea ice: a new approach to investigate oxygen dynamics during sea ice formation. *Aquatic Microbial Ecology*, **29**, 297–306.

Mock, T., Kruse, M. & Dieckmann, G.S. (2003) A new microcosm to investigate oxygen dynamics at the sea ice water interface. *Aquatic Microbial Ecology*, **30**, 197–205.

Mock, T., Krell, A., Glöckner, G., Kolukisaoglu, U. & Valentin, K. (2005). Analysis of expressed sequence tags (ESTs) from the polar diatom *Fragilariopsis cylindrus*. *Journal of Phycology*, **42**, 78–85.

Mock, T., Samanta, M.P., Iverson, V. et al. (2008) Whole genome expression profiling of the marine diatom *Thalassiosira pseudonana* identifies genes involved in silicon bioprocesses. *Proceedings of the National Academy of Science, USA*, **105**, 1579–1584.

Monti, D., Legendre, L., Therriault, J.C. & Demers, S. (1996) Horizontal distribution of sea ice microalgae: environmental control and spatial processes (southeastern Hudson Bay, Canada). *Marine Ecology Progress Series*, **133**, 229–240.

Morgan-Kiss, R.M., Priscu, J.C., Pocock, T., Gudynaite-Savitch, L. & Huner, N.P.A. (2006) Adaptation and acclimation of photosynthetic microorganisms to permanently cold environments. *Microbial Molecular Biology Review*, **70**, 222–252.

Niebauer, H.J., Roberts, J. & Royer, T.C. (1981) Shelf break circulation in the northern Gulf of Alaska. *Journal of Geophysical Research*, **86**, 4231–4242.

Nishi, Y. & Tabeta, S. (2005) Analysis of the contribution of ice algae to the ice-covered ecosystem in Lake Saroma by means of a coupled ice-ocean ecosystem model. *Journal of Marine Systems*, **55** (3–4), 249–270.

Nishi, Y. & Tabeta, S. (2006) Estimation of the physical release of organic matter from ice using observational data and a coupled ice–water box model. *Polar Bioscience*, **19**, 1–10.

Nozais, C., Gosselin, M., Michel, C. & Tita, G. (2001) Abundance, biomass, composition and grazing impact of the sea ice meiofauna in the North Water, northern Baffin Bay. *Marine Ecology Progress Series*, **217**, 235–250.

Okolodkov, Y.B. (1993) A checklist of algal species found in the East Siberian Sea in May 1987. *Polar Biology*, **13**, 7–11.

Pabi, S., van Dijken, G.L. & Arrigo, K.R. (2008) Primary production in the Arctic Ocean, 1998–2006. *Journal of Geophysical Research*, **113**, C08005, 10.1029/2007JC004578.

Palenik, B., Grimwood, J., Aerts, A. et al. (2007) The tiny eukaryote *Ostreococcus* provides genomic insights into the paradox of plankton speciation. *Proceedings of the National Academy of Science, USA*, **104**, 7705–7710.

Palmisano, A.C. & Sullivan, C.W. (1983) Sea ice microbial communities (SIMCO). I. Distribution, abundance, and primary production of ice microalgae in McMurdo Sound, Antarctica in 1980. *Polar Biology*, **2**, 171–177.

Palmisano, A.C. & Sullivan, C.W. (1985) Pathways of photosynthetic carbon assimilation in sea ice microalgae from McMurdo Sound, Antarctica. *Limnology and Oceanography*, **30**, 674–678.

Palmisano, A.C. & Garrison, D.L. (1993) Microorganisms in Antarctic sea ice. In: *Antarctic Microbiology* (Ed. E.I. Friedmann), pp. 167–218, Wiley-Liss, New York.

Palmisano, A.C., SooHoo, J.B. & Sullivan, C.W. (1985) Photosynthesis-irradiance relationships in sea ice microalgae from McMurdo Sound, Antarctica. *Journal of Phycology*, **21**, 341–346.

Palmisano, A.C., SooHoo, J.B., SooHoo, S.L., Kottmeier, S.T. Craft, L.L. & Sullivan, C.W. (1986) Photo-adaption in *Phaeocystis pouchetii* advected beneath annual sea ice in McMurdo Sound, Antarctica. *Journal of Plankton Research*, **8**, 891–906.

Palmisano, A.C., SooHoo, J.B. & Sullivan, C.W. (1987) Effects of four environmental variables on photosynthesis–irradiance relationships in Antarctic sea ice microalgae, *Marine Biology*, **94**, 299–306.

Palmisano, A.C., Lizotte, M.P., Smith, G.A., Nichols, P.D., White, D.C. & Sullivan, C.W. (1988) Changes in photosynthetic carbon assimilation in Antarctic sea-ice diatoms during a spring bloom: variation in synthesis of lipid classes. *Journal of Experimental Marine Biology and Ecology*, **116**, 1–13.

Petri, R. & Imhoff, J.F. (2001) Genetic analysis of sea-ice bacterial communities of the Western Baltic Sea using an improved double gradient method. *Polar Biology*, **24**, 252–257.

Priscu, J.C. & Sullivan, C.W. (1998) Nitrogen metabolism in Antarctic fast-ice microalgal assemblages. In: *Antarctic Sea Ice: Biological Processes, Interactions and Variability* (Ed. M.P. Lizotte & K.R. Arrigo). *Antarctic Research Series*, **73**, 147–160.

Priscu, J.C., Palmisano, A.C., Priscu, L.R. & Sullivan, C.W. (1989) Temperature dependence of inorganic nitrogen uptake and assimilation in Antarctic sea ice microalgae. *Polar Biology*, **9**, 443–446.

Quetin, L. & Ross, R. (1988) Summary of WINCRUISE II to the Antarctic Peninsula during June and July, 1987. *Antarctic Journal of the United States*, **23**, 149–151.

Quillfeldt, von C.H. (2004). The diatom *Fragilariopsis cylindrus* and its potential as an indicator species for cold water rather than for sea ice. *Vie Milieu*, **54**, 137–143.

Quillfeldt, von C.H., Ambrose, W.G., Jr., & Clough, L.M. (2003) High number of diatom species in first year ice from the Chukchi Sea. *Polar Biology*, **26**, 806–818.

Ralph, P.J., McMinn, A., Ryan, K.G. & Ashworth, C. (2005) Short-term effect of temperature on the photokinetics of microalgae from the surface layers of Antarctic pack ice. *Journal of Phycology*, **41**, 763–769.

Ralph, P.J., Ryan, K.G., Martin, A. & Fenton, G. (2007) Melting out of sea ice causes greater photosynthetic stress in algae than freezing in. *Journal of Phycology*, **43**, 948–956.

Raymond, J.A. & Knight, C.A. (2003) Ice binding, recrystallization inhibition, and cryoprotective properties of ice-active substances associated with Antarctic sea ice diatoms. *Cryobiology*, **46** (2), 174–181.

Riaux-Gobin, C., Treguer, P., Poulin, M. & Vetion, G. (2000) Nutrients, algal biomass and communities in land-fast ice and seawater off Adelie Land (Antarctica). *Antarctic Science*, **12**, 160–171.

Riaux-Gobin, C., Treguer, P., Dieckmann, G., Maria, E., Vetion, G. & Poulin, M. (2005) Land-fast ice off Adelie Land (Antarctica): short-term variations in nutrients and chlorophyll just before ice break-up. *Journal of Marine Systems*, **55**, 235–248.

Riedel, A., Michel, C., Gosselin, M. & Leblanc, B. (2007) Enrichment of nutrients, exopolymeric substances and microorganisms in newly formed sea ice on the Mackenzie shelf. *Marine Ecology Progress Series*, **342**, 55–67.

Riedel, A., Michel, C. & Gosselin, M. (2006) Seasonal study of sea ice exopolymeric substances on the Mackenzie shelf: implications for transport of sea ice bacteria and algae. *Aquatic Microbial Ecology*, **45** (2), 195–206.

Rintala, J.-M., Piiparinen, J., Ehn, J., Autio, R. & Kuosa, H. (2006) Changes in phytoplankton biomass and nutrient quantities in sea ice as responses to light/dark manipulations during different phases of the Baltic winter 2003. *Hydrobiologia*, **554**, 11–24.

Robineau, B., Legendre, L., Kishino, M. & Kudoh, S. (1997) Horizontal heterogeneity of microalgal biomass in the first-year sea ice of Saroma-ko Lagoon (Hokkaido, Japan). *Journal of Marine Systems*, **11**, 81–91.

Robinson, D.H., Arrigo, K.R., Iturriaga, R. & Sullivan, C.W. (1995) Adaptation to low irradiance and restricted spectral distribution by Antarctic microalgae from under-ice habitats. *Journal of Phycology*, **31**, 508–520.

Robinson, D.H., Kolber, Z. & Sullivan, C.W. (1997) Photophysiology and photoacclimation in surface sea ice algae from McMurdo Sound, Antarctica. *Marine Ecology Progress Series*, **147**, 243–256.

Rocap, G., Larimer, F.W., Lamerdin, J. et al. (2003). Genome divergence in two *Prochlorococcus* ecotypes reflects oceanic niche differentiation. *Nature*, **424**, 1042–1047.

Ruiz, J.M. & Blumwald, E. (2002) Salinity-induced glutathione synthesis in *Brassica napus*. *Planta*, **214**, 965–969.

Rusch, D.B., Halpern, A.L., Sutton, G. et al. (2007) The Sorcerer II global ocean sampling expedition: Northwest Atlantic through eastern tropical Pacific. *PloS Biology*, **5**, e77.

Ryan, K.G., McMinn, A., Mitchell, K.A. & Trenerry, L. (2002) Mycosporine-like amino acids in Antarctic Sea ice algae, and their response to UVB radiation. *Zeitschrift fuer Naturforschung Section C Journal of Biosciences*, **57**, 471–477.

Ryan, K.G., Ralph, P. & McMinn, A. (2004) Acclimation of Antarctic bottom-ice algal communities to lowered salinities during melting. *Polar Biology*, **27** (11), 679–686.

Ryan, K.G., Hegseth, E.N., Martin, A. et al. (2006) Comparison of the microalgal community within fast ice at two sites along the Ross Sea coast, Antarctica. *Antarctic Science*, **18**, 583–594.

Rysgaard, S., Kuhl, M., Glud, R.N. & Hansen, J.W. (2001) Biomass, production and horizontal patchiness of sea ice algae in a high-Arctic fjord (Young Sound, NE Greenland). *Marine Ecology Progress Series*, **223**, 15–26.

Sakshaug, E. (2003) Primary and secondary production in the Arctic Seas. In: *The Organic Carbon Cycle in the Arctic Ocean* (Eds. R. Stein & R.W. Macdonald) pp. 57–81. Springer-Verlag, Berlin.

Schloss, P.D. & Handelsman, J. (2005) Metagenomics for studying unculturable microorganisms: cutting the Gordian knot. *Genome Biology*, **6**, 229.

Schnack-Schiel, S. (1987) The winter expedition of RV Polarstern to the Antarctic (ANT V/1-3). *Berichte Reports on Polar Research*, **39**, 1–258.

Schunemann, H. & Werner, I. (2005) Seasonal variations in distribution patterns of sympagic meiofauna in Arctic pack ice. *Marine Biology*, **146** (6), 1091–1102.

Shi, H., Lee, B., Wu, S. & Zhu, J. (2003) Overexpression of a plasma membrane Na^+/H^+ antiporter gene improves salt tolerance in *Arabidopsis thaliana*. *Nature Biotechnology*, **21**, 81–85.

Smetacek, V., Scharek, R. Gordon, L.I., Eicken, H., Fuhrbach, E., Rohardt, G. & Moore, S. (1992) Early spring phytoplankton blooms in ice platelet layers of the southern Weddell Sea, Antarctica. *Deep-Sea Research*, **39**, 153–168.

Smith, R.E.H. & Herman, A.W. (1991) Productivity of sea ice algae: *in situ* vs incubator methods. *Journal of Marine Systems*, **2**, 97–110.

Smith, R.E.H., Clement, P., Cota, G. & Li, W.K.W. (1987) Intracellular photosynthate allocation and the control of Arctic marine ice algal production. *Journal of Phycology*, **23**, 124–132.

Smith, R.E.H., Anning, J., Clement, P. & Cota, G. (1988) Abundance and production of ice algae in Resolute Passage, Canadian Arctic. *Marine Ecology Progress Series*, **48**, 251–263.

Smith, R.E.H., Gosselin, M. & Taguchi, S. (1997) The influence of major inorganic nutrients on the growth and physiology of high Arctic ice algae. *Journal of Marine Systems*, **11**, 63–70.

Spindler, M., Dieckmann, G. & Thomas, D.N. (1993) Die expedition Antarktis X/3 mit F.S. Polarstern. *Berichte zum Polarfurschung*, **121**, 1–122.

Steffens, M., Granskog, M.A., Kaartokallio, H., Kuosa, H., Luodekari, K., Papadimitriou, S. & Thomas, D.N. (2006) Spatial variation of biogeochemical properties of landfast ice in the Gulf of Bothnia, Baltic Sea. *Annals of Glaciology*, **44**, 80–87.

Streb, P., Shang, W., Feierabend, J. & Bligny, R. (1998). Divergent strategies of photoprotection in high mountain plants. *Planta*, **207**, 313–324.

Stoecker, D.K., Gustafson, D.E., Baier, C.T. & Black, M.M.D. (2000) Primary production in the upper sea ice. *Aquatic Microbial Ecology*, **21**, 275–287.

Sullivan, C.W., Palmisano, A.C., Kottmeier, S.T. & Moe, R. (1982) Development of the sea ice microbial community in McMurdo Sound. *Antarctic Journal of the United States*, **17**, 155–157.

Suzuki, Y., Kudoh, S. & Takahashi, M. (1997) Photosynthetic and respiratory characteristics of an Arctic ice algal community living in low light and low temperature conditions. *Journal of Marine Systems*, **11**, 111–121.

Talling, J.F. (1955) The relative growth rates of three plankton diatoms in relation to underwater radiation and temperature. *Annals of Botany London*, **19**, 329–341.

Thomas, D.N., Lara, R.J., Haas, C. et al. (1998) Biological soup within decaying summer sea ice in the Amundsen Sea, Antarctica. In: *Antarctic Sea Ice: Biological Processes, Interactions and Variability* (Eds. M.P. Lizotte & K.R. Arrigo). American Geophysical Union, *Antarctic Research Series,* **73**, 161–171.

Trenerry, L.J., McMinn, A. & Ryan, K.G. (2002) In situ oxygen microelectrode measurements of bottom-ice algal production in McMurdo Sound, Antarctica. *Polar Biology*, **25**, 72–80.

Trevena, A.J. & Jones, G.B. (2006) Dimethylsulphide and dimethylsulphoniopropionate in Antarctic sea ice and their release during sea ice melting. *Marine Chemistry*, **98**, 210–222.

Trevena, A.J., Jones, G.B., Wright, S.W. & van den Enden, R.L. (2003) Profiles of dimethylsulphonio-propionate (DMSP), algal pigments, nutrients, and salinity in the fast ice of Prydz Bay, Antarctica. *Journal of Geophysical Research*, **108** (C5), 14-1–14-11.

Tuschling, K., Juterzenka, K.V., Okolodkov, Y.B. & Anoshkin, A. (2000) Composition and distribution of the pelagic and sympagic algal assemblages in the Laptev Sea during autumnal freeze-up. *Journal of Plankton Research*, **22**, 843–864.

Vargo, G.A., Fanning, K., Heil, C. & Bell, L. (1986) Growth rates and the salinity response of an antarctic ice microflora community. *Polar Biology*, **5**, 241–247.

Wadhams, P., Lange, M.A. & Ackley, S.F. (1987) The ice thickness distribution across the Atlantic Sector of the Antarctic Ocean in midwinter. *Journal of Geophysical Research*, **92**, 14,535–14,552.

Wang, Y. Yang, C.P., Liu, G.F., Jiang, J. & Wu, J.H. (2006) Generation and analysis of expressed sequence tags from a cDNA library of *Tamarix androssowii*. *Plant Science*, **170**, 28–36.

Watanabe, K. & Satoh, H. (1987) Seasonal variations of ice algal standing crop near Syowa Station, East Antarctica, in 1983/84. *Bulletin of Plankton Society of Japan*, **34**, 143–164.

Welch, H.E. & Bergmann, M.A. (1989) Seasonal development of ice algae and its prediction from environmental factors near Resolute, N.W.T., Canada. *Canadian Journal of Fisheries and Aquatic Sciences*, **46**, 1793–1804.

Welch, H.E., Bergmann, M.A., Silferd, T.D. & Amarualik, P.S. (1991) Seasonal development of ice algae near Chesterfield inlet, NWT, Canada. *Canadian Journal of Fisheries and Aquatic Sciences*, **48**, 2395–2402.

Werner, I., Ikävalko, J. & Schunemann, H. (2007) Sea ice algae in Arctic pack ice during late winter. *Polar Biology*, **30**, 1493–1504.

Williams, R.B. & Murdoch, M.B. (1966) Phytoplankton and chlorophyll in the Beaufort Channel, North Carolina. *Limnology and Oceanography*, **11**, 73–82.

Whitaker, T.M. & Richardson, M.G. (1980) Morphology and chemical composition of a natural population of an ice-associated Antarctic diatom *Navicula glaciei*. *Journal of Phycology*, **16**, 250–257.

This page intentionally left blank

9 Heterotrophic Protists Associated with Sea Ice

David A. Caron and Rebecca J. Gast

9.1 Introduction

Sea ice makes up a physically complex, geographically extensive but often seasonally ephemeral biome on Earth. Despite the extremely harsh environmental conditions under which it forms and exists for much of the year, sea ice can serve as a suitable, even favourable, habitat for dense assemblages of microorganisms. Our knowledge of the existence of high abundances of microalgae (largely diatoms) in sea ice spans at least a century, but for many years, it remained unknown whether these massive accumulations were metabolically active cells or merely inactive cells brought together through physical processes associated with ice formation. Work begun approximately a quarter century ago began to fill this void in our knowledge of sea ice microbiota.

Observations and experimental studies have now demonstrated that microalgal communities of sea ice are both taxonomically diverse and metabolically active. These algal populations and their attendant bacterial assemblages were initially believed to exist largely in the absence of grazing mortality from herbivorous and bacterivorous organisms. Research during the last few decades has dramatically changed our perception of these microbial assemblages, and it is now clear that sea ice supports highly enriched, taxonomically diverse and trophically active microbial consumers in Arctic and Antarctic environments (Laurion et al., 1995; Sime-Ngando et al., 1997a; Thomas & Dieckmann, 2002; Kaartokallio, 2004; Riedel et al., 2008).

Aspects of the biology of sea ice bacteria and microalgae have been detailed in Chapters 7 and 8, respectively, of this book. The present chapter focuses on the microbial consumers that characterize these unique marine habitats. Within the complex microbial communities of sea ice, single-celled eukaryotic microorganisms displaying heterotrophic ability (usually phagotrophy) are the major consumers of bacterial and algal biomass. The term 'protozoa' has traditionally been employed and is still commonly used to describe these species. However, the recent application of DNA sequence information for constructing taxonomies and testing hypotheses of phylogeny has resulted in radical and frequent changes in our perception of the evolutionary relationships among eukaryotic organisms (Simpson & Roger, 2004; Adl et al., 2005; Burki et al., 2007).

One realization arising from these studies has been that older, descriptive terms or taxonomic groupings that have been commonly employed for single-celled, eukaryotic microbes possess some obvious inconsistencies with our present knowledge of eukaryotic phylogeny

and ecology. Most significantly for this article, closely related taxa of phototrophic protists (i.e. unicellular microalgae) were historically placed into separate taxonomic groupings from their heterotrophic counterparts (protozoa). These older terms have biased our interpretation of the ecology of these species by inferring that phototrophy and heterotrophy are mutually exclusive nutritional modes, but they are not. Technically, the term 'protozoa' adequately describes truly heterotrophic protists, but it does not recognize that phagotrophy is a common behaviour among many microscopic algae, nor does it recognize that some apparently photosynthetic species of protists are actually heterotrophic forms that consume photosynthetic prey and retain the chloroplasts of their prey in a functional state. Due to the existence of these mixotrophic species, the term 'phagotrophic protists' provides a more accurate description of many protistan species that employ heterotrophic nutrition, regardless of the presence or absence of chloroplasts. These deficiencies having been noted, the term 'protozoa' will be used synonymously with 'heterotrophic protists' (which includes mixotrophic species) in this text for the sake of brevity.

Scientific understanding of the diversity, abundances and trophic activities of these sea ice consumers has only emerged within the past few decades, and much remains to be learned. Although their ecology is still not as thoroughly described or investigated as that of many photosynthetic taxa, bacteria and even some metazoa from polar ecosystems, a basic understanding of the breadth of their abundances and activities now exists. Protozoan populations in sea ice reduce bacterial and algal abundances, remineralize major nutrients contained in their biomass and constitute additional sources of nutrition for metazoa within or associated with the ice. The available information, complemented by a wealth of information regarding the ecology of heterotrophic microbial eukaryotes from temperate and tropical marine ecosystems, is beginning to clarify the pivotal role played by protozoa.

9.2 Origins and fates of sea ice protists

The processes giving rise to sea ice protozoan assemblages presumably are the same as those for phytoplankton, bacteria and invertebrates. Entrainment into ice platelets formed in subsurface waters and lifted to the surface where ice is forming, populations trapped at the surface during the formation of frazil ice or invasion of existing ice through brine channels or fissures may all play roles in the formation of sea ice microbial communities (Garrison et al., 1986). It has been conjectured that these processes may selectively concentrate certain microbial taxa because of size selection or other characteristics of the microbes (e.g. pennate diatoms may attach to ice, while foraminifera possess sticky pseudopodia that may result in their scavenging by ice crystals). Thus, the initial assemblages present in sea ice may represent a 'biased' sampling of the water column microorganisms (Eicken, 1992).

The collection of free-living and particle-associated microbes that are incorporated into the ice experiences chemical and physical characteristics that are vastly different than the surrounding sea water environment. Therefore, following introduction into the ice, the community structure of the ice microbial community is dictated by the growth and mortality of species contained within the initial colonizing assemblage (or invading from the water column), under selective pressures that differ greatly from those in the surrounding water column. These selective pressures result in a divergence in community composition from that

in the water as the ice ages. There are reports that protistan assemblages in newly formed sea ice are similar to the assemblage in the water column initially (Gradinger & Ikavalko, 1998; Garrison et al., 2003), but only one actually documented that this similarity decreased as the assemblages adapted to growth conditions and food availability in the ice (Rózanska et al., 2008).

Even when the same protistan species are present in ice and water, the dominant taxa from sea ice may be quite different from the dominant taxa observed in the water column underlying or adjacent to the ice at the site of collection. Gast et al. (2004) observed very different dominant eukaryotic taxa in samples collected from sea ice and the surrounding water column in the Ross Sea. Microbial eukaryotic assemblages in ice samples collected from different sites were more similar to each other than to the assemblages from water samples collected at the same sites as the ice samples. The conclusion that the assemblages of eukaryotes of ice and water were distinct was supported by subsequent work (Gast et al., 2006) comparing the frequency of DNA sequences in clone libraries from ice and water (Fig. 9.1). The genetic analysis of eukaryote community structure in those studies included phototrophic and heterotrophic protists (and some minute multicellular eukaryotes). Similarly, a microscopical study of sea ice protistan assemblages collected from different locations in the Ross Sea showed a relatively high degree of similarity in major biomass components, presumably indicating the dominance of specific forms that were more adapted to existence within the sea ice than in the water (Garrison et al., 2005).

Gradients of environmental conditions within sea ice can also create microhabitats within the ice that differ significantly in their chemical/physical characteristics (Fig. 9.2). For example, snow cover on ice dramatically affects light penetration, an important variable controlling algal biomass within and especially at the bottom of the ice (Grossi & Sullivan, 1985). In turn, this variability in algal abundance and activity affects the total amount of organic matter entering the microbial food web. Gradients of temperature and salinity also affect small-scale spatial heterogeneity in the ice. Sea water infiltration and/or melting of snow and ice at the surface of sea ice can result in a wide range of salinities in these meltwater (slush) microbial communities.

These microenvironmental differences can lead to dramatic differences in the composition and magnitude of the microbial communities growing there. Densities of microbial populations can range from extremely low abundances to communities that are present as visible, discolourations of the ice. Horizontal bands of colour within the ice are sometimes apparent, but brine channels, compression ridges, meltwater (slush) at the snow/ice interface and the bottom of the ice are often microhabitats of exceptionally high microbial biomass (Fig. 9.2c,d,f–k). Dramatic differences in the dominant taxa within these microhabitats can exist over small spatial scales, presumably due to snow cover, nutrient supply or the exclusion of specific consumer populations (Fig. 9.2g–k). Gast et al. (2004, 2006) observed that the meltwater microbial eukaryote assemblages were distinct not only from the ones in the water column near the ice, but also from the assemblages collected from the interior of the ice (Fig. 9.1). We presently know little about the rates (growth, grazing, encystment, death) at which protozoan assemblages respond to differences in the physical/chemical gradients in sea ice.

In addition to environmental conditions, sea ice protozoan communities are influenced by the tremendous spatial variability of the algal assemblages in sea ice (Gosselin et al., 1986; Laurion et al., 1995). Spatial (horizontal) variability in these communities also appears to be affected by wind-driven advection of pack ice (Garrison et al., 2003). Interannual
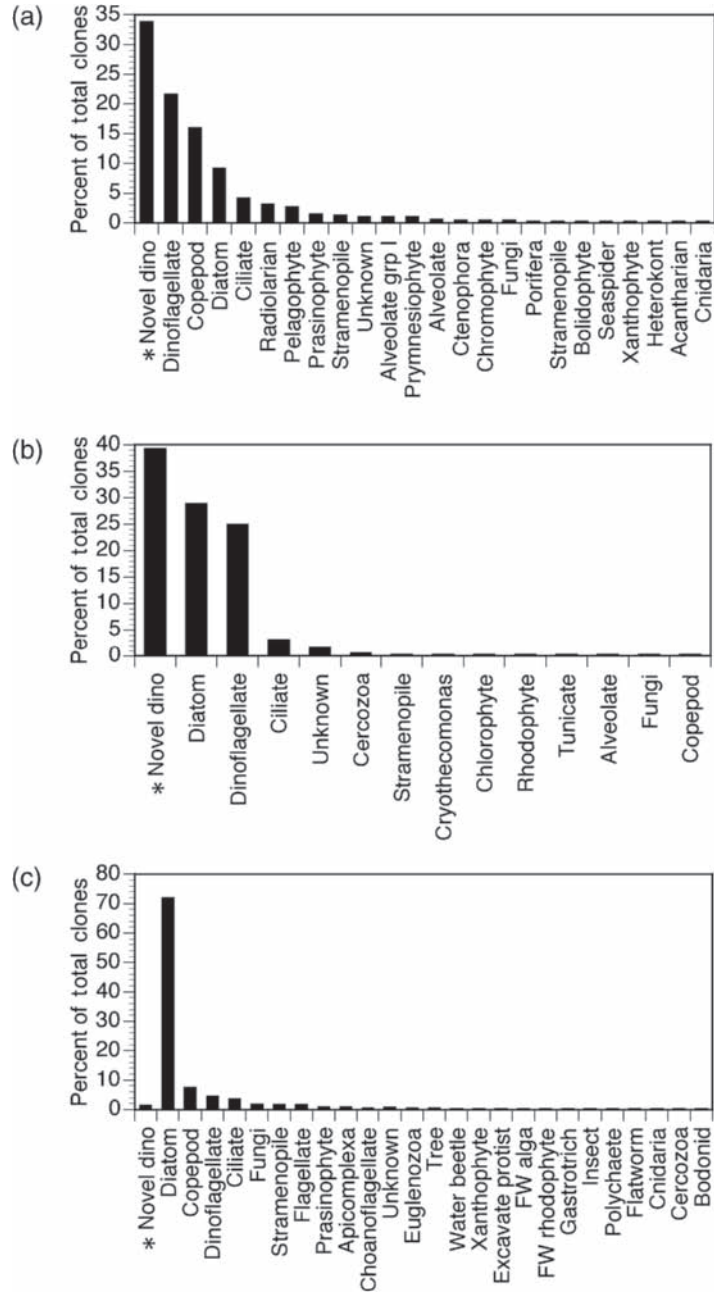
Fig. 9.1   Rank abundance curves of microbial eukaryotic taxa from the water column (a), slush (b, meltwater at the ice/snow interface) and ice cores (c) of pack ice in the Ross Sea, Antarctica. Rank abundances indicate the frequency of phylotypes of rDNA sequences in clone libraries. From Gast et al. (2006). The asterisk indicates the occurrence of a novel, mixotrophic dinoflagellate that steals the chloroplasts from the abundant prymnesiophyte *Phaeocystis antarctica* (Gast et al., 2007).
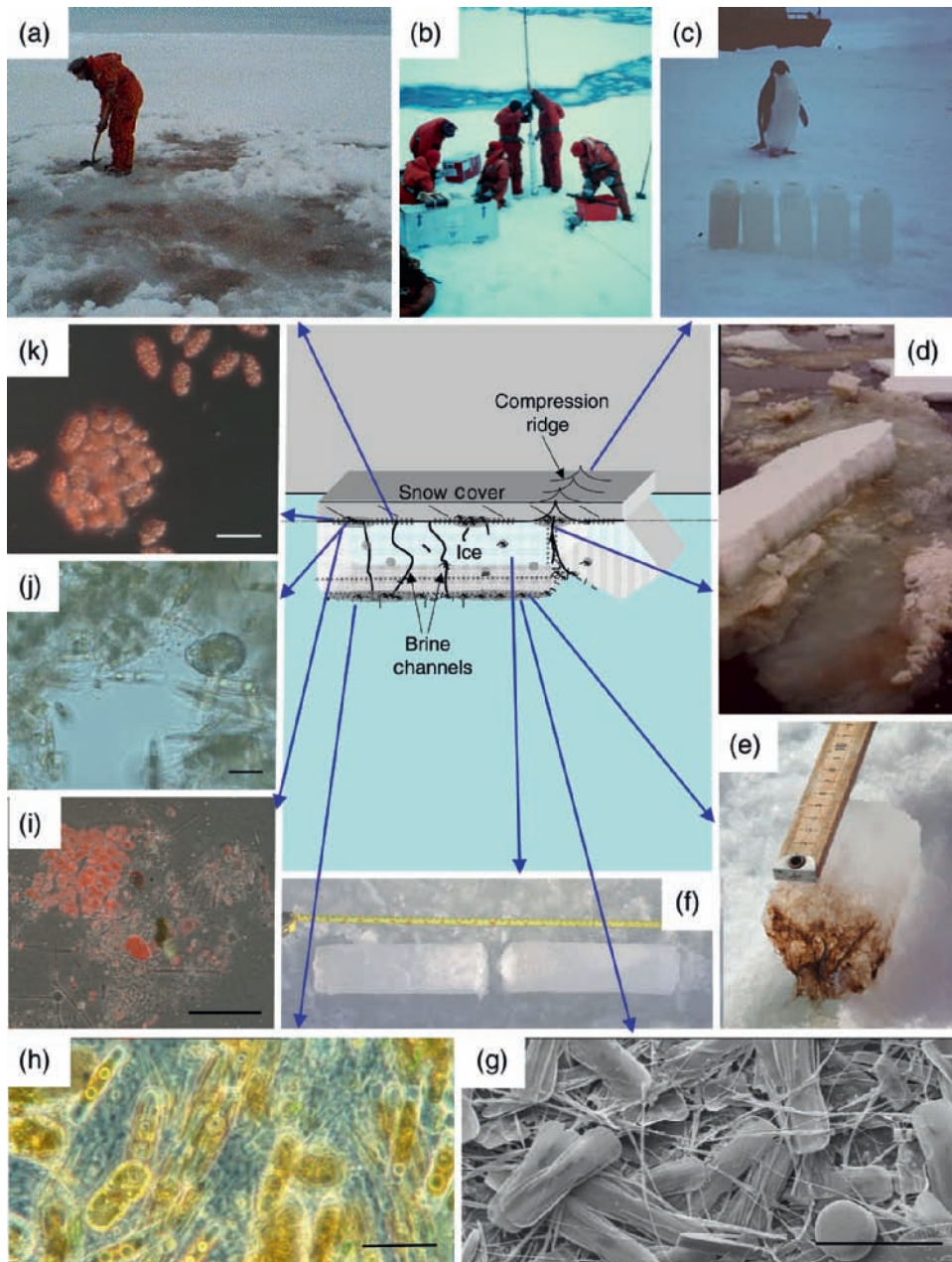
Fig. 9.2 A schematic (centre) of some of the microhabitats of sea ice colonized by protozoa, and the macroscopic manifestations and dominant taxa of these microhabitats (surrounding pictures). From top left: (a) Removal of several centimetres of snow cover reveals dense assemblages of microorganisms (coloured patches) at the tops of brine channels on Antarctic pack ice. (b) Collecting ice core samples from pack ice. (c) Samples of slush (meltwater and infiltration sea water) collected across a ridge compression on pack ice. High concentrations of microorganisms (brown colour in left-hand bottles) found at the fissure between ice fragments decrease rapidly away from the axis of the ridge. (d) Pack ice overturned by a ship reveals densely coloured microbial communities of the snow/ice meltwater microhabitat. (e) Dense mat of diatoms and associated bacteria and protozoa from the bottom of a core of land-fast ice in the Ross Sea, Antarctica. (f) A core of pack ice showing low microbial biomass (no visible colour). (g) Scanning electron micrograph and (h) transmitted light micrograph of diatoms from the bottom of sea ice. (i,j,k) Light micrographs showing the dominance of different taxa in the different meltwater microhabitats from Antarctic pack ice. These communities may contain large amounts of phototrophic and heterotrophic populations (bacteria and protozoa) and debris (i), be dominated by diatoms (j) or phototrophic dinoflagellates (k). Red colour in (i) and (k) is due to chlorophyll fluorescence by phototrophic protists, predominantly dinoflagellates. Scale bars are 100 μm (g,h,i) or 20 μm (j,k).

variability in algal biomass has also been reported (Fritsen et al., 2008). Heterotrophic protists often mirror these spatial distributions, or demonstrate a lagged response to increases and decreases in the abundance of phototrophic protists and bacteria (Sime-Ngando et al., 1997a, 1999; Riedel et al., 2008). Seasonal successions within sea ice appear to be similar to classical patterns observed for water column microbes (Parsons et al., 1984; Strom, 2000), but there are few complete data sets because of the logistical issues of obtaining such time series in polar environments.

The AMERIEZ program (Antarctic Marine Ecosystem Research in the Ice Edge Zone) has probably provided one of the most complete data sets for examining temporal relationships among sea ice microbial communities (Garrison & Buck, 1989). These studies revealed that high abundances of phototrophic protists during spring and early summer gave way to higher abundances of bacteria as organic substrate concentrations increased due to primary production and grazing activities. In turn, heterotrophic protistan abundances increased during summer as prey abundances increased (bacteria and algae) and temperature increased. Changes in abundance were extreme in brine and slush forming at the surface of the floes.

The tremendous accumulation of phototrophic biomass that is often observed in sea ice prior to the build-up of substantial numbers of heterotrophs may be explained in part by the differential effect of temperature on phototrophic and heterotrophic processes (see Section 9.4). In addition, Gradinger et al. (1992) noted that the successional stages of pack ice microbial communities in the lower portions of Arctic pack ice were strongly affected by light and its effect on the development of the ice alga assemblage.

The physical structure of the ice is presumably a major determinant for the survival and growth of heterotrophic protists because food acquisition for these species is dependent on movement and prey capture. Approaches for studying the physical structure of sea ice are still limited, but some generalities are known. Active microbes in ice appear to be relegated to the brine, and liquid water maintained through the production of ice-retarding substances (Janech et al., 2006). The size and three-dimensional structure of these regions may be a strong selective pressure on phagotrophic protists in ice. Price (2003) proposed that 'ice veins' are likely microhabitats for survival and growth of sea ice microbes. The existence of 'microaggregations' of bacteria in sea ice support the hypothesis that ice veins serve as concentration points for bacteria in sea ice, and therefore as sites of elevated abundances of prey for bacterivorous protozoa.

The physical dimensions of brine channels in sea ice have been examined using a water-soluble resin (Weissenberger et al., 1992). These studies indicated a typical diameter of 200 μm for many of the channels, creating highly convoluted, complex microhabitats of narrow passageways and a high surface area. For this reason, many of the protozoa commonly observed in sea ice display morphological or behavioural features that are more characteristic of protozoa from sediment rather than from planktonic ecosystems.

The potential influence of the physical structure of sea ice on microbial colonization has been examined experimentally (Krembs et al., 2000). These researchers estimated that 6–41% of the brine channel surface area may be covered by microorganisms. The authors compared that range to the less than 1% of the surface area of soil that might be colonized by microorganisms, and concluded that the surfaces of interstitial spaces in ice were important determinants of prey location, and that the size of these interstices placed constraints on the size of microbial predators that could survive in the ice. However, while physical refuge from motile protozoa and their prey appeared to play a role in structuring the microbial

community in sea ice, the presence of small spaces (that could exclude consumers) in the proximity of larger channels that might support renewal of nutrients or organic substrates was also important.

The high abundances of protozoa that develop in sea ice constitute a significant fraction of the total microbial biomass in these microhabitats (see next section) and often in the water column as a whole. As a consequence, the fate of this biomass constitutes an important aspect of the flux of energy and elements in coastal polar ecosystems. Insight can be gained from the fate of sea ice algae, for which more information is available, but even there, the fate of the microbial biomass is more conjecture than hard data.

Sea ice microbiota have been hypothesized to serve as 'seed populations' for spring phytoplankton blooms in polar ecosystems (Kuosa et al., 1992). A similar role could be hypothesized for protozoa. Sea ice protozoa could contribute to microbial grazing pressure in the water column upon release from melting sea ice during spring/summer thaws. As noted above, however, many of the protozoa in sea ice are adapted to consuming prey that are attached to surfaces within the ice, or present in microhabitats of the ice at highly elevated abundances relative to abundances in the plankton. It is therefore unclear if protozoan species released from ice could capture a sufficient amount of prey to grow when preying upon microbial assemblages in the water column.

Aggregations of microbes in sea ice also presumably contribute to the vertical flux of carbon and other elements in coastal ecosystems. Sime-Ngando et al. (1997a) reported that net production by heterotrophic protists in sea ice was 2–4 times greater than reported for sea ice bacteria, but how that carbon is used remains a question. Protozoan biomass in sea ice would be expected to be at its maximum during late summer when ice melt is maximal, and thus the contribution of protozoan biomass and protozoan waste materials could be a significant source of sinking particles during this period.

Sea ice protozoa also serve as prey for metazoa either within the ice or in the surrounding water, but we know virtually nothing of the consumption of sea ice protozoa by metazoa. In the water column of the south-central polynya of the Ross Sea, Antarctica, *Phaeocystis antarctica* dominates phytoplankton biomass during austral summer. This alga is a poor food source for some metazoa, but protozoa that consume the alga directly, or consume bacterial biomass supported by the breakdown of *P. antarctica* and algal detritus, may be important intermediates in the food chain between primary production and metazoan zooplankton in this region (Caron et al., 1997). Whether protozoa in sea ice occupy a similar niche between sea ice algae and metazoa is presently unknown.

Some protozoa trapped during ice formation may encyst (flagellates and dinoflagellates) or form resting spores (diatoms) (Garrison & Buck, 1989; Buck et al., 1992; Stoecker et al., 1992, 1997; Ikavalko & Gradinger, 1997; Okolodkov, 1998; Montresor et al., 1999). Many photosynthetic sea ice protists occur as dormant forms in sea ice (Fig. 9.3). The incorporation of cysts into sea ice by some dinoflagellates and chrysophytes (hypnozygotes, statocysts) may allow retention in surface waters during the winter until daylight is sufficient for vegetative growth. Such a cycle has been documented for some phototrophic protistan taxa in the land-fast ice of McMurdo Sound, Antarctica (Stoecker et al., 1997, 1998). Alternatively, cyst formation by some protistan taxa may enable overwintering in sea ice for species whose vegetative life stages take place in the water column during the spring–fall period.

One additional, potential fate of sea ice protozoa that has recently emerged is infection and lysis by eukaryotic viruses. Viral infection of some sea ice heterotrophic protists in pack
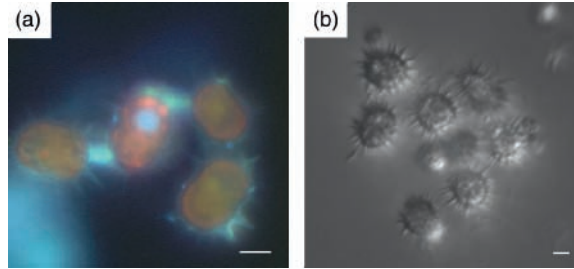
Fig. 9.3 Epifluorescence micrograph (a) and transmitted light micrograph (b) of spined cysts of a phototrophic dino-flagellate (likely *Polarella glacialis*) from sea ice of the Ross Sea, Antarctica. The red colour in (a) is due to the chlorophyll fluorescence, the whitish blue colour is from the fluorochrome DAPI. Scale bars are 10 μm.

ice habitats of the Ross Sea has been demonstrated (Gowing, 2003). The high abundances and constrained mobility of sea ice microbial eukaryotes may make sea ice a particularly suitable condition for viral infection and transmission.

9.3 Diversity and abundances

As noted in previous chapters, the unique physical and chemical conditions of sea ice create a variety of extreme conditions for the microbial assemblages inhabiting it. Extremes of salinity exist, ranging from highly saline brine to nearly freshwater that can occur near the top of the ice under snow cover. Extremely low temperatures can also occur in the upper portions of sea ice, and high light intensities can occur seasonally. There is little doubt that sea ice protistan species have evolved adaptations to these extreme conditions. However, it is presently unclear if these adaptations imply strain-specific adaptations, or the presence of large numbers of unique, endemic species in these polar microhabitats. Much of this confusion is rooted in the changing species concept applied to protists, which has traditionally used primarily morphological criteria but now includes physiological information. There is considerable disagreement at this time over how much physiological difference must exist between two morphologically similar strains of protists in order to consider them different species (Caron, 2009). This uncertainty makes the characterization of protistan species diversity a topic of lively debate.

  Sea ice communities are often dominated by photosynthetic protists. Visible discolourations can be the result of extremely high abundances of diatoms, dinoflagellates, *Phaeocystis* (the latter primarily in Antarctic waters) and other taxa. These accumulations are commonly observed at specific depths within the ice column, in the meltwater habitat at the surface of the ice or on the bottom of the ice (Fig. 9.2). The magnitude of these accumulations on the bottom of some regions of fast ice can be remarkable (Michel et al., 2002).

  Notwithstanding the conspicuous presence of phototrophs, protozoa can contribute a significant fraction of the overall biomass of sea ice communities. Archer et al. (1996b) noted that sea ice protozoa contributed up to nearly 20% of the total integrated microbial biomass at a coastal Antarctic site and up to approximately 10% of the biomass attached to the bottom of the ice. Similar proportions of phototrophic and heterotrophic biomass in Antarctic

sea ice were observed by Garrison and co-workers (Garrison & Buck, 1991; Garrison et al., 2005). Euglenoid flagellates, heterotrophic dinoflagellates, ciliates and 'nanoheterotrophs' (small heterotrophic flagellates) constituted major components of the heterotrophic protistan assemblages in the latter studies, and pack ice and land-fast ice assemblages usually differed in species composition. Euglenoid flagellates alone (Fig. 9.6d) contributed up to 20% of the biomass in coastal Antarctic sea ice, while heterotrophic dinoflagellates such as *Protoperidinium* (Fig. 9.6a) were also abundant (Archer et al., 1996a). In Greenland Sea pack ice, heterotrophic flagellates alone constituted an average of 20% of the total microbial biomass (Gradinger et al., 1999).

These and other comparisons of photosynthetic and heterotrophic protists in Arctic and Antarctic sea ice have indicated that, at certain times, heterotrophs attain accumulations of biomass that are comparable to or even exceed the biomass of phototrophs (Garrison & Buck, 1989; Buck et al., 1998; Rózanska et al., 2008). Seasonal shifts in the proportion of phototrophic and heterotrophic microbial biomass are also typical of assemblages in the water column of polar ecosystems (Dennett et al., 2001). It is noteworthy that these studies have not yet considered the contribution of mixotrophic algae, which would increase estimates of the overall contribution of phagotrophic protists in these habitats.

Relative abundances of phototrophic and heterotrophic protists in planktonic microbial communities of polar regions (Garrison, 1991; Sherr et al., 1997) are generally similar to the relative abundances of these groups within sea ice communities. However, absolute abundances of these species in sea ice (cells per volume of sea ice versus cells per volume of sea water) that are 1–2 orders of magnitude higher than in the surrounding water column are not unusual (Garrison, 1991; Davidson & Marchant, 1992; Garrison & Close, 1993; Garrison et al., 1993; Sime-Ngando et al., 1997a,b; Vaqué et al., 2004; Fonda Umani et al., 2005). For example, studies of Arctic sea ice have reported protozoan abundances up to four times greater than abundances in the surrounding water (Sime-Ngando et al., 1997a). These findings are indicative that sea ice is composed of favourable microhabitats for the survival and growth of protozoa (although some scavenging by ice as it forms may contribute to elevated abundances in sea ice).

Obtaining accurate abundances of sea ice heterotrophic protistan populations has been challenging. Similar challenges exist for sea ice microalgal populations, and many of the approaches employed to collect sea ice microalgae have been used for protozoa (Chapter 8). Thawing of sea ice can produce water of low salinity relative to full-strength sea water, and dramatically less than the salt concentrations in the brine in which many sea ice protists may exist. Cell lysis as a consequence of osmotic shock undoubtedly affected early studies to examine protistan diversity and abundance in sea ice and biased perceptions of the importance of robust taxa such as diatoms and many dinoflagellates. Modern approaches to obtain these populations now generally thaw ice in much larger volumes of filtered sea water in order to minimize osmotic damage to delicate cells.

Estimates of the total diversity of protozoa in sea ice do not yet exist. This situation is in part a consequence of the difficulties associated with sampling these assemblages as noted above, and partly a consequence of the fact that the diversity of protists in general is still hotly debated (Finlay & Fenchel, 1999; Foissner, 1999; Finlay et al., 2004). Controversy surrounding the species concept for protists prevents an accurate assessment of their species richness and their geographical distribution on Earth (Caron, 2009).

Nevertheless, a wide diversity of protozoa have been documented from polar ecosystems and specifically from sea ice (see next section and Palmisano & Garrison, 1993). Studies of

microbial diversity in polar ecosystems prior to the last few decades have focused largely on diatoms, phototrophic dinoflagellates and a few other phytoplankton groups from the water column. Studies since then have begun to provide more complete taxonomic or ecological analyses for specific protozoan groups such as ciliates (Petz et al., 1995) or choanoflagellates (Marchant, 1985; Marchant & Perrin, 1990). One recent compendium of phototrophic and heterotrophic Antarctic protists exists (Scott & Marchant, 2005). These studies, using traditional approaches of microscopy and culture, have concluded that polar ecosystems are characterized by high species diversity (Vørs, 1993; Petz et al., 1995). The description of a number of previously undescribed species of protozoa from sea ice may indicate that these microhabitats support unique protozoan assemblages and endemic species (Song & Wilbert, 2000).

Genetic approaches for characterizing and studying protistan species diversity have begun to complement traditional approaches, and to expand our knowledge of the breadth of microbial diversity in sea ice as they have in other ecosystems (Caron, 2005; Vaulot et al., 2008). Gene sequencing methods have been applied to studies of protistan diversity only within the last decade, but they have already resulted in the discovery of several novel, previously undescribed lineages of protists. Genetic methods have the advantage that they can characterize species composition across a wide taxonomic range of organisms. Traditional morphology-based taxonomies for protists are highly taxon-specific, and their application is dependent on considerable taxonomic expertise. Moreover, molecular approaches can differentiate small, phylogenetically distinct protists even if they exhibit few distinctive morphological features by light microscopy (Slapeta et al., 2006; Stoeck et al., 2008).

However, it is not yet possible to easily distinguish some protozoa (heterotrophic protists) from some microalgae (phototrophic protists) using DNA sequence information alone, for primarily two reasons. First, many of the sequences obtained thus far represent protistan species that have not yet been described and sequenced. This situation will change in the future as DNA sequence information is slowly integrated with existing morphology-based taxonomies. Second, the distinction of a heterotrophic protist from a phototrophic one by gene sequences is difficult for some protistan species because of close phylogenetic relatedness. For example, chrysomonads and chrysophytes are closely related, despite the absence of a plastid in chrysomonads.

These caveats aside, genetic studies of protistan diversity conducted by Gast et al. (2006) on samples collected from pack ice and water in the Ross Sea, Antarctica, demonstrated the presence of a wide diversity of protistan phylotypes (Fig. 9.1). These approaches have begun to characterize the phylogenetically diverse protistan assemblages present in sea ice habitats, particularly in the dense microbial communities that occur in slush at the water/snow interface of pack ice (Fig. 9.1b,c). Similar molecular analyses of Arctic waters are now beginning to be conducted, although not yet on sea ice microbial communities (Lovejoy et al., 2006; Hamilton et al., 2008).

Ciliates

Ciliated protozoa constitute a conspicuous component of the protozoan assemblages colonizing sea ice (Fig. 9.4). Taxonomic studies of these taxa have been largely morphology-based until recent years. Those studies have documented a very wide diversity of morphological types from ice habitats of this monophyletic protistan lineage (Corliss & Snyder, 1986; Stoecker et al., 1993; Petz et al., 1995). Ciliate taxonomic diversity is presumably reflective of physical and chemical complexity of sea ice microhabitats.
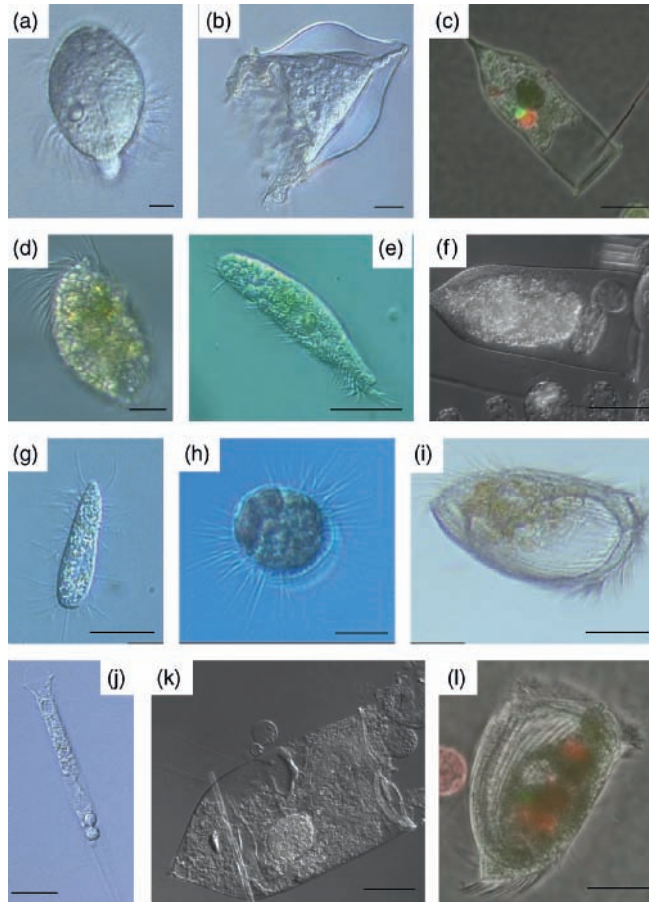
Fig. 9.4   Ciliates of sea ice habitats in the Ross Sea, Antarctica. (a) *Didinium*, a predatory ciliate. (b,c,f,j,k) Species of tintinnids often encountered in the meltwater assemblages at the ice/snow interface of pack ice are also common in the plankton. (d) An unidentified hypotrich ciliate possessing many food vacuoles filled with algal prey. (e) A heterotrich species with elongated shape characteristic of benthic ciliates. (g) A scuticociliate that displays bacterivory in culture. (h) *Mesodinium* sp., a chloroplast-retaining ciliate. (i,l) Algal prey in food vacuoles in two large ciliates, possibly *Chlamydonella* sp., is evidence of herbivory in sea ice habitats. Red colour in (l) is chlorophyll fluorescence from ingested algae. Scale bars are 10 (a,g), 20 (b,c,d,f,h,k) and 40 (e,i,j,l) μm.

A number of the ciliates associated with sea ice are also common inhabitants of the water column at the same locations (Garrison, 1991). For example, several tintinnid species (Fig. 9.4b,c,f,j,k) and strombidiid ciliates are typical filter-feeding 'planktonic' forms whose presence in ice presumably indicates the existence of significant quantities of water within some ice microhabitats. *Mesodinium rubrum*, a kleptoplastidic ciliate, is commonly observed, and can sometimes comprise up to 25% of the ciliate assemblage, and over a third of the assemblage in neighbouring waters (Sime-Ngando et al., 1997a). Some brine channels, and the slush habitats that develop at the ice–snow interface of summer sea ice may provide environmental conditions that adequately mimic conditions in many planktonic (i.e. non-ice) ecosystems in the ocean. Indeed, species of tintinnids and strombidiid taxa (e.g. *Strombidium*) are abundant in the marine plankton worldwide (Pierce & Turner, 1992).

Petz et al. (2007) conducted taxonomic studies of ciliates from freshwater ecosystem in the Arctic and Antarctic and concluded that at least some of the species (i.e. morphotypes) had bipolar distributions.

In contrast to these truly 'planktonic' morphotypes, many of the ciliate species described from sea ice are forms that are commonly associated with surfaces, the benthos or eutrophic conditions that are not typical of oceanic plankton (Fig. 9.4d,e,g,i,l). For example, species of *Lacrymaria* and *Condylostoma* are large ciliates often observed within dense accumulations of microbial cells and debris. These species possess highly elongated bodies that facilitate movement and prey capture in confined spaces. Spirotrich, heterotrich and hypotrich ciliates that possess fused ciliary structures such as membranelles and cirri allow these species mobility along surfaces and enable the collection of surface-associated prey. Such taxa have been commonly observed in the pack ice in the Ross Sea, Antarctica (Fig. 9.4d,e,i,l), and in land-fast ice of Baffin Bay (Michel et al., 2002), but rarely are they observed in the plankton. Many of these latter species show evidence of a herbivorous mode of nutrition (Fig. 9.4c,d,e,h,i,k,l). Species of *Chlamydonella* consume fairly large algal prey such as pennate diatoms (Petz et al., 1995).

Oligohymenophorean ciliates comprise a group of predominantly bacterivorous species that are often found in sea ice (Petz et al., 1995; Song & Wilbert, 2000). *Pseudocohnilembus* sp. isolated from Arctic Sea ice preferentially ingested bacteria-sized particles when offered particles of different size (Scott et al., 2001). These species are capable of rapid growth, but they are best adapted for feeding at relatively high prey (bacteria) concentrations (Fig. 9.4g). They are only occasionally observed at significant abundances in most planktonic ecosystems.

Many of the ciliate ice taxa noted above are rarely encountered in the water column near the ice. Prey abundances presumably are not sufficiently dense or the pelagic habitat conducive to the development of significant populations of some of the larger, robust ciliates. Thus, it is not clear where the 'seed' populations of ciliate assemblages in ice originate, although it is possible that low numbers rafted on particles through the water column serve as an inoculum but are too rare to appear commonly in routine surveys of water samples. One exception to this generality is the existence of substantial ciliate populations that are frequently observed associated with large algal colonies of the prymnesiophyte *Phaeocystis antarctica* in the Ross Sea, Antarctica. These large (>1 mm) hollow colonies reach extraordinary abundances during austral spring and summer (Smith et al., 1996; Smith & Gordon, 1997). The colonies are often inhabited by heterotrophic flagellates and ciliates living on or within them that presumably feed on the algal cells of the colonies or on bacteria and other protists associated with the colonies (Fig. 9.5). These large structures may provide a mechanism for inoculating sea ice with particle-associated ciliate taxa through their incorporation into sea ice.

The morphological and behavioural adaptations of many of the ice ciliates imply that sea ice microhabitats create a 'false benthos' in the water column of polar regions that are analogous to microhabitats created by large detrital aggregates in most marine ecosystems, the so-called 'marine snow' (Caron et al., 1986). Marine snow particles are colonized by ciliated protozoa whose morphologies are equipped for movement on surfaces and in confined spaces. Similarly, the ciliates of sea ice display morphologies that presumably reflect a strong selection for robust forms capable of movement in physically complex, nutritionally rich microhabitats. Therefore, with regard to ciliated protozoa, sea ice habitats in polar seas create microcosms of physical, chemical and biological conditions that enable the establishment and proliferation of assemblages that are highly unique for pelagic ecosystems.
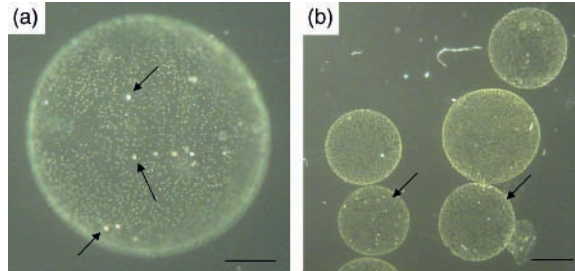
Fig. 9.5 Colonization of *Phaeocystis antarctica* colonies by protozoa in the Ross Sea, Antarctica. Individual algal cells are visible in a single colony (a) as minute green dots. Arrows point to several heterotrophic protists associated with the colony. (b) Several colonies from a water sample. The interior of two of the colonies (arrows) are colonized with several heterotrophic protists each (white dots). Scale bars are 200 (a) and 500 (b) μm.

Heterotrophic and mixotrophic flagellates

The heterotrophic flagellates are a phylogenetically diverse group of protistan taxa with representatives from no fewer than six different protistan supergroups (Simpson & Roger, 2004; Burki et al., 2007). Among these disparate taxa, our knowledge of the diversity is probably most complete for the heterotrophic dinoflagellates because these species often display high abundances, large size and conspicuous morphologies. Species of the genera *Protoperidinium*, *Gymnodinium*, *Gyrodinium* and *Polykrikos* are conspicuous members of sea ice communities (Stoecker et al., 1993; Archer et al., 1996a; Michel et al., 2002), and are large enough to be easily visualized using a dissecting microscope.

Heterotrophic dinoflagellates (including mixotrophic species that retain the chloroplasts of ingested algal prey) are important herbivores in planktonic marine ecosystems (Lessard, 1991; Sherr & Sherr, 2007). These species exhibit similar trophic activities in sea ice, although quantitative estimates of their importance in ice microhabitats are virtually non-existent because most heterotrophic dinoflagellates are sensitive to physical disturbance. Also, many of these species feed using delicate pseudopodial projections to surround prey (e.g. diatoms) that are often larger than themselves (Jacobson & Anderson, 1986, 1996; Strom, 1991). These feeding structures are easily disrupted by sample handling and preparation for microscopy.

The existence and trophic activity of kleptoplastidic dinoflagellates is now emerging in temperate ecosystems (Jeong et al., 2005), and these species presumably are also common in polar ecosystems. For example, species of *Dinophysis* (Fig. 9.6b) have recently been shown to retain the chloroplasts of *Mesodinium rubrum*, which in turn steals its chloroplasts from its cryptophyte prey (Park et al., 2006). One dominant dinoflagellate from the Ross Sea has been shown to prey on *Phaeocystis antarctica* and retain its chloroplasts for several months (Gast et al., 2007). This species has been shown to be exceptionally abundant in the water column and some sea ice microhabitats (Fig. 9.1).

Choanoflagellates have been established as frequent and abundant components of the heterotrophic plankton of Arctic and Antarctic coastal waters (Buck, 1981; Marchant, 1985; Caron et al., 1997; Tong et al., 1997; Lovejoy et al., 2006). Blooms of these minute (usually <10 μm) bacterivorous species often appear in Antarctic coastal seas following maxima in bacterial abundances during austral summer. These species are also found in sea ice
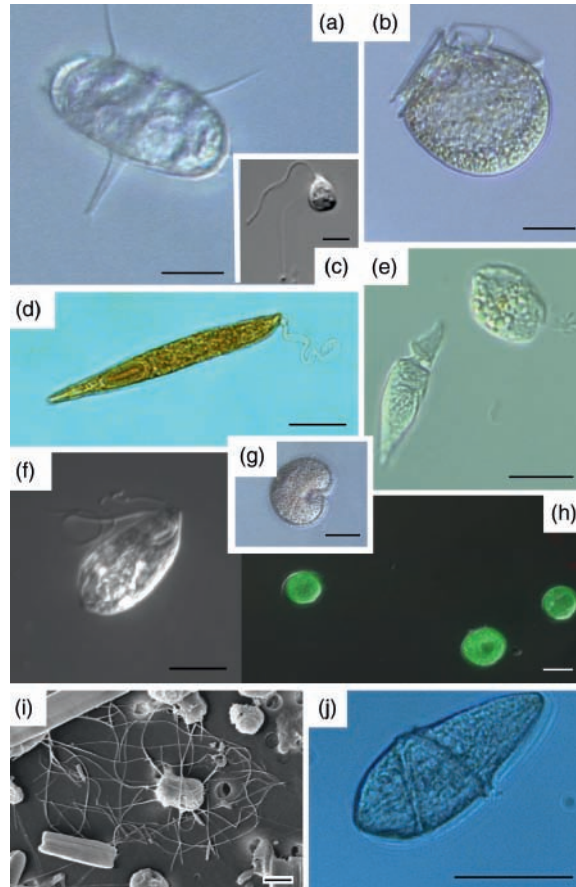
Fig. 9.6 Heterotrophic flagellates are taxonomically diverse and often numerically dominant within sea ice. Heterotrophic dinoflagellates (a,b,e,g,h,j) such as *Protoperidinium* (a), *Dinophysis* (b), *Katodinium* (e, left), *Protoperidinium* (g) and *Gyrodinium* (j) may be major consumers of phytoplankton in the ice. (h) An unidentified dinoflagellate displaying a distinctive apple-green fluorescence with blue light excitation. Many heterotrophic dinoflagellates exhibit this fluorescent signal, making them very conspicuous when viewed by epifluorescence microscopy. (c) *Pseudobodo* sp., a small bacterivorous species. (d) A heterotrophic euglenoid flagellate stained with Lugol's iodine to visualize the cell and flagellum. (f) An unidentified flagellate cultured from the Ross Sea, Antarctica. (i) Scanning electron micrograph of the choanoflagellate *Diaphanoeca* sp. showing the cell and the lattice of the lorica (thin structure of bars surrounding the cell). Choanoflagellates are often extremely abundant in the plankton of high-latitude ecosystems, and are also common in sea ice microbial communities. Scale bars are 5 (c,f,i), 20 (a,b,d,e,g,h) or 50 (j) μm.

(Fig. 9.6i), and our knowledge of their diversity is aided by the intricate and taxonomically informative skeletal structures produced by these species. Together with *Cryothecomonas*-like cercozoa, choanoflagellates dominated the heterotrophic flagellate assemblages in the ice communities of Saroma-ko lagoon in Japan (Sime-Ngando et al., 1997b).

Cercozoan flagellates of the genus *Cryothecomonas* are also ubiquitous heterotrophic flagellates of Antarctic sea ice (Garrison & Buck, 1989; Thomsen et al., 1991; Garrison & Close, 1993; Stoecker et al., 1993; Gast et al., 2006), and in Arctic polar waters (Sime-Ngando et al., 1997a; Lovejoy et al., 2006). These species appear to be particularly well adapted for survival and growth at extreme temperatures in sea ice.

Much less information is known regarding the abundance and diversity of the many small, morphologically nondescript groups of heterotrophic flagellates in sea ice. These species contribute significantly to bacterial mortality in aquatic ecosystems worldwide (Strom, 2000; Sherr & Sherr, 2002), but even for those ecosystems, their overall species diversity is not well known because of the relative absence of taxonomically informative morphological features for most of these species (the choanoflagellates are an exception because they possess distinctive collar structures and loricae) and the increasing tendency to incorporate physiological information into the species concept (Boenigk, 2008). In any event, chrysomonad (especially *Paraphysomonas* spp.), bodonid (Fig. 9.6c) and heterotrophic euglenoid flagellates (Fig. 9.6d) are commonly observed in enrichment cultures established from samples of sea ice and slush microbial communities.

Amoeboid forms

Amoeboid protozoan species are a collection of phylogenetically diverse taxa that span a range from some of the least to the most conspicuous protozoan forms observed in sea ice (Fig. 9.7). Gymnamoebae or 'naked' amoebae (i.e. lacking skeletal structure) and heliozoa are easily enriched from sea ice samples, and occasionally observed by microscopy (Garrison & Buck, 1989; Moran et al., 2007), but these species are often extremely difficult to distinguish when they are entangled with debris and other microbial taxa in natural samples of sea ice communities (Fig. 9.7a,b,g). Amoebae are not unique to sea ice but are present in non-ice environments around Antarctica (Mayes et al., 1997; Tong et al., 1997). Yet, they are typically rare in marine planktonic ecosystems, and are representative of species whose distributions and survival are strongly linked to particles and other surfaces (Davis et al., 1978).

Larger, much more noticeable amoeboid protozoa in sea ice include the foraminifera, acantharia and radiolaria. The foraminifera bear calcium carbonate tests that have been noted in Antarctic sea ice for more than three decades (Lipps & Krebs, 1974; Spindler & Dieckmann, 1986). At least one of these species, *Neogloboquadrina pachyderma* is a consistent inhabitant of sea ice where it can attain significant abundances (Fig. 9.7e), and some planktonic foraminifera apparently have bipolar distributions in the plankton (Darling et al., 2000).

Acantharia also appear infrequently in sea ice (Fig. 9.7c,d,f,i). These species are common constituents in the plankton of most epipelagic marine ecosystems. Species identifications are based on their distinctive skeletons of strontium sulphate. These structures dissolve rapidly in most preservatives if special precautions are not taken, and acantharia can be easily overlooked in preserved samples if the skeletons have dissolved. For this reason, the taxonomy of these species is difficult, and their overall diversity is not well known. Most of these species possess symbiotic algae that are held within the cytoplasm of the host and which supplement the nutrition of these phagotrophic protists. Acantharian host–symbiont associations are abundant in low-latitude ecosystems where the acantharia can contribute significantly to primary productivity and to the vertical distribution of elements such as strontium (Michaels, 1991; Caron et al., 1995). It is unclear if the acantharia associated with sea ice habitats are actively growing and reproducing, but specimens in apparently good physiological condition are present in sea ice.

Phaeodarian radiolarians are common in the ice edge regions of Antarctic coastal seas where they can reach abundances comparable to other larger sarcodine protozoa such as foraminifera and polycystine radiolaria (Gowing, 1989; Gowing & Garrison, 1992). These populations are omnivorous in the water column, consuming prey ranging from bacteria to
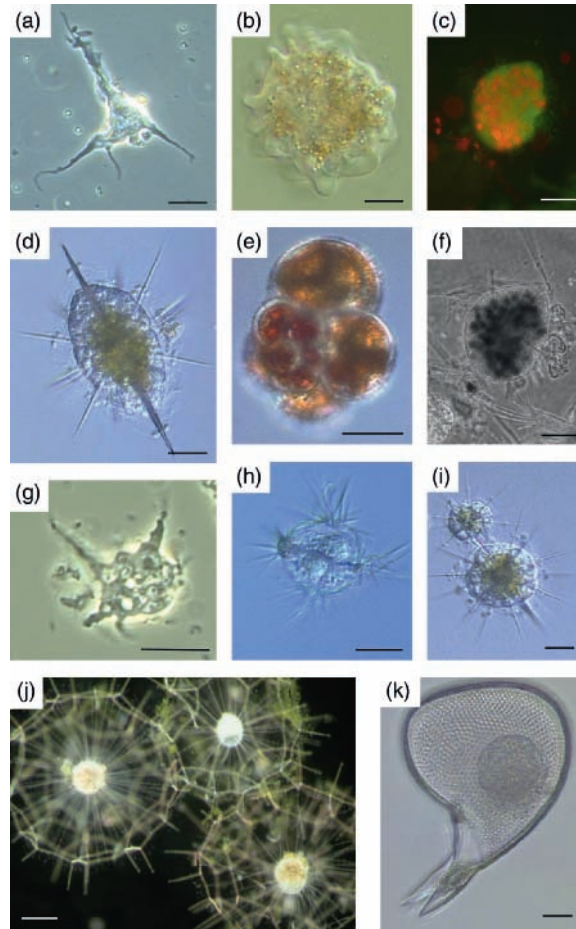
Fig. 9.7 Amoeboid protozoa of the plankton and sea ice of the Ross Sea, Antarctica. Gymnamoebae (a,b,g) are inconspicuous, particle-associated protozoa. Acantharia (c,d,f,i) occur in the water column but are also observed in slush microhabitats in apparently good physiological condition. Red-fluorescing structures in a specimen observed by epifluorescence microscopy (c) indicate the presence of endocellular symbiotic algae in the same specimen examined by transmitted light microscopy (f). Endosymbionts are also present as yellowish brown areas in the light micrographs of specimens in (d) and (i). (e) The 'planktonic' foraminifer *Neogloboquadrina pachyderma* is often present in sea ice. (h,j,k) Heliozoa and radiolaria. The unusual heliozoan *Sticholonche* sp. (h), and phaeodarian radiolaria (j,k) are occasionally observed in sea ice, but are more commonly found at the pack ice edge. (k) *Protocystis* sp. Scale bars are 10 (a,b,g,i), 20 (d,h,k), 50 (c,f,j) and 100 (e) µm.

algae and other protozoa, based on analyses of food vacuole contents. As for other larger amoeboid protozoa, it is not clear whether they are metabolically active within sea ice microhabitats.

9.4 Ecology and biogeochemistry of sea ice protozoa

Trophic activities (herbivory, bacterivory and mixotrophy)

Many of the trophic activities ascribed to protozoa in sea ice have been derived from observations of food vacuole contents of recently collected specimens. Some information has

also been obtained from experimental work conducted on sea ice microbes thawed into sea water, but the results of these experiments are difficult to interpret due to potential stresses on microbes of removing them from the ice, and changes in the physical structure of the medium. Investigations of intact sea ice microbial community activities are very difficult; therefore, observations and experiments performed on samples collected from the water column near sea ice have also been extrapolated to provide information on the probable trophic activity of these species in ice microhabitats. As noted above, some of the same species that characterize the water column may also be encountered in sea ice so there is reason to believe that many of the same processes take place in both habitats.

Direct measurements of the grazing activities of phagotrophic protists in sea ice typically require the introduction of marker cells for tracing and quantifying consumption, which in turn causes drastic changes in the physical matrix of the sea ice habitat. Generally, these experiments have been conducted by carefully melting sea ice in a larger volume of full-strength sea water to minimize osmotic shock when the ice melts, and then applying routine protocols for the measurement of bacterivory or herbivory (Caron, 2000a). The physical constraints imposed by sea ice, the lower temperatures that can be experienced in sea ice at certain times of year and the considerable dilution that microbial populations undergo during thawing and experimental manipulations may alter the rates and perhaps the very nature of the trophic interactions between heterotrophic protists and potential prey populations.

There have been very few quantitative measurements of herbivory in sea ice, and virtually no work on this topic until approximately the last decade. Indeed, some early reports hypothesized that algal growth took place largely in the absence of grazing pressure. This hypothesis is not surprising given that chlorophyll concentrations in excess of 1000 μg l^{-1} have been observed (see Table 8.1), indicating an enormous accumulation of algal biomass. However, the high abundances of heterotrophic protists in some samples of sea ice are evidence that herbivory and/or bacterivory does occur in sea ice. A strong correlation between ciliate abundances and those of pennate diatoms in Artic sea ice also implies a predator–prey relationship (Gradinger et al., 1992). Moreover, the growth of sea ice protozoa in cultures has confirmed herbivorous and/or bacterivorous modes of nutrition for many of these species. Their existence at high abundance within sea ice habitats is consistent with significant rates of prey consumption. Anecdotal information that grazing takes place is also provided by shifts in the proportion of phototrophic to heterotrophic protists in sea ice during summer and autumn (Gradinger et al., 1992; Stoecker et al., 1993; Garrison et al., 2003, 2005).

Heterotrophic dinoflagellates are important herbivores in polar ecosystems (Archer et al., 1996a; Becquevort, 1997). These species are particularly well suited for consuming large diatoms that often dominate coastal polar ecosystems. As noted earlier, ingestion by these species is often accomplished using a pseudopodial veil. Unfortunately, these feeding structures can be easily disrupted and therefore are not often observed or documented in samples of sea ice. Nevertheless, dinoflagellate species reach high abundances in sea ice habitats, and do leave tangible evidence of herbivory. Buck et al. (1990) reported an abundant (>10^5 l^{-1}), novel heterotrophic dinoflagellate that produced 'faecal pellets' containing large numbers of diatom frustules (Fig. 9.8). These faecal pellets are commonly encountered in sea ice samples, indicating that the species producing these pellets are probably important consumers of diatom biomass in sea ice (compare Fig. 9.8 with Figure 1E in Nöthig and von Bodungen (1989)).

Heterotrophic dinoflagellates also play a role as consumers of *Phaeocystis antarctica* biomass in the water column of the Ross Sea, although the quantitative significance of this trophic activity has not been established. These protozoa are commonly found in association
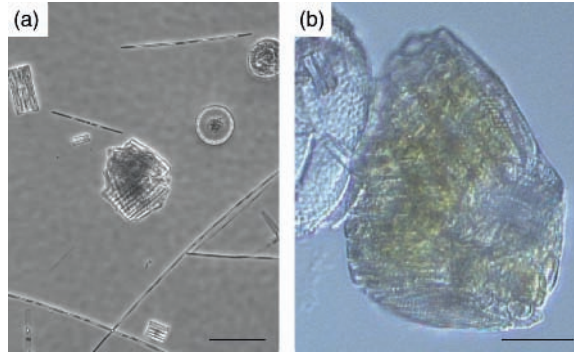
Fig. 9.8   Light micrographs of the faecal pellets of heterotrophic dinoflagellates. These membrane-bound pellets are often encountered in samples of sea ice containing high abundances of diatoms. Scale bars are 100 (a) and 50 (b) μm.

with *P. antarctica* colonies and often exhibit evidence of ingested photosynthetic prey. As noted above, one dinoflagellate steals and maintains the chloroplasts of this prymnesiophyte alga (Gast et al., 2007). The presence of high abundances of *P. antarctica* and heterotrophic dinoflagellates such as the species noted by Gast et al. (2007) imply that significant rates of consumption of this prymnesiophyte are probable in sea ice.

Observations of the microbial communities of land-fast ice in McMurdo Sound, Antarctica, implicate the potential importance of flagellate taxa other than dinoflagellates as herbivores in sea ice. Stoecker et al. (1993) noted high numbers of the cysts of some phototrophic protists in sea ice during austral winter. The cysts of phototrophic dinoflagellates and other algae are often observed in sea ice samples (Fig. 9.3). Stoecker et al. noted that many of these cysts excysted during austral spring as day length became sufficient for vegetative growth of the algae. The appearance of large populations of heterotrophic protists, in particular the cercozoan *Cryothecomonas*, coincided with high abundances of the phototrophic protists that were its probable prey (Stoecker et al., 1997, 1998). *Cryothecomonas* spp. use pseudopodia to feed on large photosynthetic prey such as diatoms (Schnepf & Kühn, 2000).

Larger ciliates are also potentially important herbivores within sea ice (note ingested prey in Fig. 9.4). Most of these species appear better adapted for the consumption of non-diatom prey based on the structure of the oral apparatus and the fact that these consumers typically completely engulf their prey during phagocytosis. For example, many of the diatom species comprising the dense diatom assemblages at the bottom of land-fast ice may not be suitable prey for *Strombidium* spp. which typically consume small algae and bacteria (Michel et al., 2002). In addition, some ciliate taxa are better adapted for consuming bacteria-sized particles (Fig. 9.4g) or are specialized predators of other protozoa (Fig. 9.4a).

Massive accumulations of biomass within some microhabitats of the sea ice would be expected to support significant rates of herbivory by sea ice protozoa. However, the dominant taxa within these algal assemblages are often species that may be difficult prey to consume by some herbivores. In the Ross Sea, Antarctica, large, chain-forming diatoms often dominate in coastal waters, while the colony-forming prymnesiophyte *P. antarctica* often dominates in the central polynya. Herbivory in these waters is generally low relative to rates observed at similar standing stocks of phytoplankton in other regions of the ocean

(Caron et al., 2000). These finding have indicated that these algal species are not palatable, or cannot be as easily captured and ingested by protozoa. Additionally, these issues may be exacerbated by extremely low temperature which appears to retard heterotrophic processes relative to photosynthetic processes (Rose & Caron, 2007; Caron & Rose, 2008; López-Urrutia, 2008). As a result, much of the production produced by these algal assemblages may become available to higher trophic levels through decomposition and conversion into bacterial biomass, and the subsequent repackaging of bacterial biomass into bacterivorous protozoa. Such speculation implicates the importance of bacterivory by protozoa in coastal polar ecosystems.

A number of studies of bacterivory have been conducted on sea water samples collected in polar ecosystems (Leakey et al., 1996; Becquevort, 1997; Vaqué et al., 2004). Choano-flagellates appear to be particularly abundant bacterivores in these ecosystems (Becquevort, 1997; Caron et al., 1997). However, these minute bacterivores are adapted for feeding on small, free-living planktonic bacteria, while many of the bacteria associated with sea ice are attached and filamentous forms. It is not clear how effective bacterivores adapted for feeding on bacteria in the plankton are at feeding on sea ice bacteria, and thus the primary consumers of bacteria in sea ice are not well known. Nevertheless, heterotrophic flagellates are believed to be a major source of bacterial mortality in sea ice. Gradinger et al. (1992) noted a ratio of bacteria to heterotrophic flagellates in Arctic sea ice of approximately 1000:1, a relationship typical of pelagic ecosystems where these protozoan assemblages exhibit strong predator:prey coupling (Sanders et al., 1992).

Measurements of bacterial ingestion in sea ice are rare. Laurion et al. (1995) and Sime-Ngando et al. (1999) examined bacterivory in Arctic ice and sea ice from a Japanese lagoon, respectively. These studies employed fluorescently labelled bacteria (FLB) to examine bacterial grazing by small protozoa. Both studies noted that bacterivory was an important trophic activity among small ice protozoa.

Omnivory is suspected but unconfirmed in many sea ice protozoa, although some feeding specialists undoubtedly exist. For example, the predatory ciliate *Didinium* (Fig. 9.4a) is adapted primarily for preying on other ciliates, while veil-feeding heterotrophic dinoflagellates use their feeding apparatus to capture and consume diatoms that are often larger than themselves. However, several strains of sea ice protozoa cultured in the laboratory have been shown to consume a mixture of algae, bacteria and other small protozoa (Caron et al., unpublished). Such behaviour would be expected to take place in nature within the complex microbial communities of sea ice.

Phaeodarian radiolarians are particularly well known for their omnivorous diet (Gowing, 1986, 1989; Nöthig & Gowing, 1991; Gowing & Garrison, 1992). These species contain numerous food vacuoles that contain the remains of recently captured prey items. Examination of the contents of these vacuoles by transmitted light and epifluorescence microscopy and especially by electron microscopy has indicated the consumption of a wide variety of prey. Although they are limited to the sea ice edge, they may be responsible for significant grazing impact on assemblages released from melting ice. Foraminifera, polycystine radiolaria and acantharia are also known to be feeding generalists, and may play active grazing roles within the sea ice (Anderson, 1983; Hemleben et al., 1988; Caron & Swanberg, 1990).

The significance of mixotrophic nutrition in Antarctic food webs is still emerging at this time. This behaviour encompasses phototrophic algae that are capable of ingesting food particles, heterotrophic protists (predominantly ciliates and dinoflagellates) that consume

algae and retain the functional chloroplasts of their prey and symbiont-bearing heterotrophic protists, including many of the radiolaria, acantharia and foraminifera (Jones, 1994; Stoekker, 1998, 1999; Caron, 2000b). The importance of these nutritional modes has now been firmly established in a range of aquatic realms (Stoecker et al., 1987; Sanders & Porter, 1988; Sanders, 1991).

Chloroplast-retaining ciliates, including *Strombidium* spp. and *Mesodinium rubrum* have been observed in significant abundances in the brine of Antarctic and Arctic sea ice (Stoecker et al., 1993; Archer et al., 1996b; Michel et al., 2002). *M. rubrum* was often the most frequently occurring ciliate species in these studies. These ciliate taxa were also common in such disparate locales as the pack ice of the Ross Sea and Weddell Sea, and in sea ice of Saroma-ko lagoon (Japan) and Baffin Bay (Garrison & Buck, 1989; Michel et al., 2002; Garrison et al., 2005).

The recent documentation of kleptoplastidy in a Ross Sea heterotrophic dinoflagellate indicates the infancy of our ability to assess the importance of this nutritional strategy in polar microbial ecology (Gast et al., 2007). This dinoflagellate was originally believed to be a phototrophic species (i.e. true chloroplast-bearing form) based on long-term survival of the dinoflagellate in mixed protistan enrichment cultures and the observation of robust chloroplasts within the organism. However, attempts to obtain pure cultures resulted in diminished growth and eventual death of the dinoflagellate. Molecular analysis revealed that 16S gene sequences of the chloroplasts of this organism were identical to the chloroplasts of the prymnesiophyte, *Phaeocystis antarctica*. Growth of the dinoflagellate in the presence of the prymnesiophyte, but not other microalgae, confirmed the hypothesis that predation on the prymnesiophyte and retention of its chloroplasts was sustaining the mixotrophic dinoflagellate. The potential importance of this nutritional strategy is evidenced by the fact that sequences of this kleptoplastidic heterotrophic dinoflagellate dominated samples collected from the water column and the microbial communities developing in the slush at the snow/ice interface of Ross Sea pack ice (Fig. 9.1b).

The presence of symbiont-bearing acantharia in sea ice has been noted previously (Fig. 9.7c,d,f,i). These symbiont–host associations are exceptionally abundant at some tropical and subtropical locations where they can form a significant fraction of the total primary production of the water column (Caron et al., 1995). Polar regions appear to have substantially smaller contributions of these associations, but this strategy still appears to be important for the autecology of some polar taxa.

Phagotrophic nutrition by phototrophic protists in polar regions has, to our knowledge, been uninvestigated until the recent study by Moorthi et al. (2009). These investigators demonstrated the presence of significant abundances of mixotrophic flagellates (phagotrophic algae) in sea ice and the plankton of the Ross Sea, Antarctica. This approach employed FLB as tracers of bacterial ingestion by flagellated protists, and the fluorescence of chloroplasts to identify which of these individuals were phototrophic. The study revealed that up to 15% of the small flagellates ingesting bacteria in ice cores were chloroplast-containing protists (i.e. mixotrophs), while up to 10% of all small, chloroplast-bearing protists ingested FLB (i.e. 10% of small algae were mixotrophic). These percentages are substantial, given that the method is believed to provide a lower limit estimate of bacterivory taking place because not all cells that are capable of consuming prey are necessarily ingesting bacteria during the incubation period. These results are also supported by recent reports of phagotrophy among algae that were not previously known to ingest prey. For example, *Pyramimonas gelidicola*

is an abundant, minute prasinophyte that is easily isolated from sea water samples and sea ice off Antarctica (McFadden et al., 1982). This species has recently been reported to ingest small prey (Bell & Laybourn-Parry, 2003).

Biogeochemical processes and rates

Protozoa play significant biogeochemical roles in all natural ecosystems on Earth. Their trophic activities result in the repackaging of (usually) smaller prey such as bacteria, small algae and small protozoa into larger cells that serve as food for other protozoa and metazoa. In the process, some percentage of the prey biomass is released as dissolved and particulate organic compounds that serve as substrates for bacterial growth, or remineralized completely to inorganic nutrients that can fuel primary productivity (Sherr et al., 2007). These species undoubtedly play similar roles in sea ice, but our understanding of the magnitude of their activities is only beginning to develop and few models of energy or elemental flow within sea ice communities have thus far been constructed. Vézina et al. (1997) developed a model to examine carbon flow through the sea ice microbial community of Resolute Passage, Canadian High Arctic. The approach used changes in standing stocks of microbial assemblages to infer carbon flow. An important role of herbivory by flagellates and ciliates was indicated by the results of their modelling effort.

   The effect of low environmental temperature on the physiological processes of sea ice protists has been, and continues to be, a central theme in polar biology. Temperature directly affects metabolic rates of microorganisms over the range of temperatures experienced in nature, and might also change the eventual fate of biomass moving through microbial food webs by affecting the growth efficiencies of microbial consumers. There is no question that many species of protozoa can survive and grow at low environmental temperature. However, it is not probable that many sea ice protozoa exhibit true physiological compensation, maintaining constant physiological rates in the face of changing temperature (Peck, 2002). Studies with Antarctic ciliates more than 30 years ago did not indicate any significant degree of physiological compensation (Fenchel & Lee, 1972; Lee & Fenchel, 1972). Growth at low temperature was substantially slower than growth at higher temperatures. Low temperature has also been reported to greatly depress the growth rates of Antarctic amoebae (Mayes et al., 1997). However, Choi and Peters (1992) reported little effect of low temperature on the growth of a strain of the heterotrophic flagellate *Paraphysomonas imperforata*.

   Rose and Caron (2007) summarized information on the growth rates of phototrophic and heterotrophic protists from a wide variety of studies. They concluded that the effect of temperature on maximal potential growth rates is not the same for phototrophic and heterotrophic protists species (Fig. 9.9). Maximal growth rates for heterotrophic protists (both bacterivorous and herbivorous) decrease more rapidly with decreasing temperature than maximal growth rates for phototrophic protists. Differences between maximal potential growth rates of phototrophs and heterotrophs are most acute at the temperatures experienced by sea ice (left-hand portion of Fig. 9.9). Thus, dense algal accumulations and the dominance of total microbial biomass by algae in sea ice during spring may be due, in part, to more rapid growth during spring as algal growth is stimulated but protozoan growth is constrained by extremely low temperatures. Estimates of the net growth rates of Antarctic sea ice heterotrophic protists based on changes in abundances in the ice have indicated relatively slow rates 0.005–0.5 d^{-1} (Laurion et al., 1995; Archer et al., 1996b; Levinsen et al.,
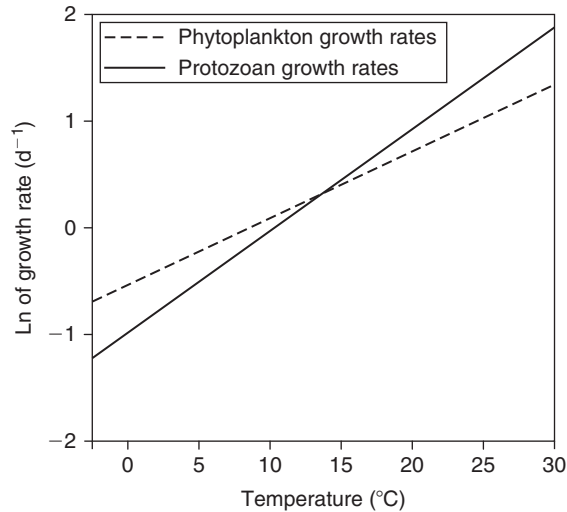
Fig. 9.9 The effect of environmental temperature on the maximal growth rates of phototrophic and herbivorous protists. Lines represent the maximal growth rates observed from more than 2000 measurements. Separate regressions for herbivorous and bacterivorous protists are displayed. All other factors removed, low environmental temperature appears to constrain heterotrophic processes to a greater degree than phototrophic processes. Data taken from Rose and Caron (2007).

2000), in general agreement with the overall constraint of low temperature on metabolic rates as reported in the meta-analysis of Rose and Caron. However, these net growth rates must be considered rough approximations because they do not take into account changes in the assemblages due to immigration/emigration or consumption by larger organisms.

Studies of the rates of bacterivory and herbivory in sea ice and in coastal polar waters also support the controlling effect of temperature on overall protozoan rate processes. Decreasing environmental temperature was shown to significantly decrease microzooplankton (predominantly protistan) herbivory when this process was compared over a large range of environmental temperatures (see summary and references in Caron et al., 2000). Experiments to characterize bacterivory in sea ice (Laurion et al., 1995; Sime-Ngando et al., 1999) have also yielded low rates. These low grazing rates are commensurate with rates expected from other ecosystems with low environmental temperatures (Berninger et al., 1991; Leakey et al., 1996; Becquevort, 1997; Caron et al., 1997; Vaqué et al., 2004), but there are presently too few measurements to accurately determine the impact of sample handling in these experiments on rates of bacterivory in sea ice specifically.

While the general pattern of decreasing protozoan growth and grazing rates with decreasing temperature seems clear, there are conflicting views at present on the direction and magnitude of the effect of temperature on the overall fate of microbial biomass consumed by protozoa in polar ecosystems. Growth at low environmental temperatures has been reported to increase (Choi & Peters, 1992) or dramatically decrease (Mayes et al., 1997) the gross growth efficiencies of protozoa. Other studies have observed no significant effect on gross growth efficiency of a polar protozoan (Rose et al., 2009). The latter study noted that gross growth efficiency at 0°C of an Antarctic strain of a common heterotrophic flagellate

was greater than 30%, similar to efficiencies observed for this and other strains of the same species growing at much warmer temperatures.

The effect of low environmental temperature on protozoan growth efficiency has important implications for energy flow and elemental recycling in sea ice. Low growth efficiencies imply that protozoa act primarily as agents for the decomposition of organic matter and the remineralization of nutrients contained in their microbial prey. On the other hand, high growth efficiencies would suggest a much more important role for protozoa as intermediate steps in the food webs of sea ice microbial communities. Resolution of these apparently conflicting data sets await further study, and may reveal that different protistan species have different strategies or physiological responses to low temperature.

9.5 Conclusions and future directions

Studies of sea ice protozoan assemblages during the past few decades have begun to provide a basic understanding of the major taxa occurring in sea ice and their contribution to total microbial biomass. Many of the important trophic interactions involving these species have been at least crudely characterized, derived either from observations of protozoa in natural samples of sea ice, extrapolated from our knowledge of the activities of the same or similar species in the water column or established from observations and experimental studies of cultured species.

Major gaps in our knowledge still remain, however, regarding the physiological rates (feeding, growth and mortality rates) of sea ice microbial communities in intact ice microhabitats. Evidence of feeding activity such as food vacuole content and feeding behaviour in laboratory cultures provides information on the types of prey consumed by protozoa, but it is unclear how this information extrapolates to rates of consumption in the ice. Similarly, information on the growth efficiencies of protozoa at environmentally relevant temperatures must be obtained for species of protozoa that are ecologically important in ice microhabitats in order to establish the impact of their activities on decomposition, nutrient remineralization and food web processes. These goals are not without significant methodological hurdles and potential artefacts, but this information is fundamental in order to understand the overall biogeochemical importance of protozoa to sea ice microbial community structure and function.

Studies of physiological adaptation by sea ice protozoan species, and protozoan diversity of sea ice microhabitats will continue to improve our understanding of community structure of polar ecosystems, provide insights into physiological adaptations among microbes, contribute genetic fodder for biotechnological exploitation of unique biochemical abilities and contribute to a larger discussion of global protistan biogeography (Caron, 2009). As noted in this chapter, the morphology-based species concept for protists is somewhat confused by our lack of knowledge of the physiological flexibility associated with a protistan morphotype. Additional information from protistan species living at one extreme of environmental temperature in sea ice will help address the difficult issues of the morphology-based species concept, the existence of cryptic species, and the distribution of protistan species on our planet. Future studies of diversity will undoubtedly continue to incorporate genetic approaches for assessing diversity, but these findings must be interpreted in conjunction with traditional approaches of microscopy and culture rather than replace them.

Acknowledgements

References

Adl, S.M., Simpson, A.G.B., Farmer, M.A. et al. (2005) The new higher level classification of eukaryotes with emphasis on the taxonomy of protists. *Journal of Eukaryotic Microbiology*, **52**, 399–451.

Anderson, O.R. (1983) *Radiolaria*. Springer-Verlag, New York.

Archer, S.D., Leakey, R.J.G., Burkill, P.H. et al. (1996a) Microbial dynamics in coastal waters of east Antarctica: herbivory by heterotrophic dinoflagellates. *Marine Ecology Progress Series*, **139**, 239–255.

Archer, S.D., Leakey, R.J.G., Burkill, P.H., Sleigh, M.A & Appleby, C.J. (1996b) Microbial ecology of sea ice at a coastal Antarctic site: community composition, biomass and temporal change. *Marine Ecology Progress Series*, **135**, 179–195.

Becquevort, S. (1997) Nanoprotozooplankton in the Atlantic sector of the Southern Ocean during early spring: biomass and feeding activities. *Deep-Sea Research Part II*, **44**, 355–373.

Bell, E.M. & Laybourn-Parry, J. (2003) Mixotrophy in the Antarctic phytoflagellate, *Pyramimonas gelidicola* (Chlorophyta: Prymnesiophyceae). *Journal of Phycology*, **39**, 644–649.

Berninger, U.-G., Caron, D.A., Sanders, R.W. & Finlay, B.J. (1991) Heterotrophic flagellates of planktonic communities, their characteristics and methods of study. In: *The biology of free-living heterotrophic flagellates,* (Eds. D.J. Patterson & J. Larsen), pp. 39–56. Clarendon Press, Oxford.

Boenigk, J. (2008) The past and present classification problem with nanoflagellates exemplied by the genus *Monas*. *Protist*, **159**, 319–337.

Buck, K. (1981) A study of choanoflagellates (Acanthoecidae) from the Weddell Sea, including a description of *Diaphanoeca multiannulata* n.sp. *Journal of Protozoology*, **28**, 47–54.

Buck, K.R., Bolt, P.A. & Garrison, D.L. (1990) Phagotrophy and fecal pellet production by an athecate dinoflagellate in Antarctic sea ice. *Marine Ecology Progress Series*, **60**, 75–84.

Buck, K.R., Bolt, P.A., Bentham, W.N. & Garrison, D.L. (1992) A dinoflagellate cyst from Antarctic sea ice. *Journal of Phycology*, **28**, 15–18.

Buck, K.R., Nielsen, T.G., Hansen, B.W., Grastrup-Hansen, D. & Thomsen, H.A. (1998) Infiltration phyto- and protozooplankton assemblages in the annual sea ice of Disko Island, West Greenland, spring 1996. *Polar Biology*, **20**, 377–381.

Burki, F., Shalchian-Tabrizi, K., Minge, M., Skjaeveland, Å., Nikolaev, S.I., Jakobsen, K.S. & Pawlowski, J. (2007) Phylogenomics reshuffles the eukaryotic supergroups. *PLoS One*, **8**, E790.

Caron, D.A. (2000a) Protistan herbivory and bacterivory. In: *Marine microbiology: methods in microbiology* (Ed. J. Paul), pp. 289–315. Academic Press, London.

Caron, D.A. (2000b) Symbiosis and mixotrophy among pelagic microorganisms. In: *Microbial ecology of the oceans* (Ed. D.L. Kirchman), pp. 495–523. Wiley-Liss, New York.

Caron, D.A. (2005) Marine microbial ecology in a molecular world: what does the future hold? *Scientia Marina*, **69**(**S**), 97–110.

Caron, D.A. (2009) Protistan biogeography: why all the fuss? *Journal of Eukaryotic Microbiology*, **56**, 105–112.

Caron, D.A. & Rose, J.M. (2008) The metabolic theory of ecology and algal bloom formation (Reply to comment by López-Urrutia). *Limnology and Oceanography*, **53**, 2048–2049.

Caron, D.A. & Swanberg, N.R. (1990) The ecology of planktonic sarcodines. *Reviews in Aquatic Sciences*, **3**, 147–180.

Caron, D.A., Davis, P.G., Madin, L.P. & Sieburth, J.M. (1986) Enrichment of microbial populations in macroaggregates (marine snow) from the surface waters of the North Atlantic. *Journal Of Marine Research*, **44**, 543–565.

Caron, D.A., Michaels, A.F., Swanberg, N.R. et al. (1995) Primary productivity by symbiont-bearing planktonic sarcodines (Acantharia, Radiolaria, Foraminifera) in surface waters near Bermuda. *Journal of Plankton Research*, **17**, 103–129.

Caron, D.A., Lonsdale, D.J. & Dennett, M.R. (1997) Bacterivory and herbivory play key roles in fate of Ross Sea production. *Antarctic Journal of the United States*, **32**, 81–83.

Caron, D.A., Dennett, M.R., Lonsdale, D.J., Moran, D.M. & Shalapyonok, L. (2000) Microzooplankton herbivory in the Ross Sea, Antarctica. *Deep-Sea Research Part II*, **47**, 15–16.

Choi, J.W. & Peters, F. (1992) Effects of temperature on two psychrophilic ecotypes of a heterotrophic nanoflagellate, *Paraphysomonas imperforata*. *Applied and Environmental Microbiology*, **58**, 593–599.

Corliss, J.O. & Snyder, R.A. (1986) A preliminary description of several new ciliates from Antarctica, including *Cohnilembus grassei* n. sp. *Protistologica*, **22**, 39–46.

Darling, K.F., Wade, C.M., Stewart, I.A., Kroon, D., Dingle, R. & Leigh Brown, A.J. (2000) Molecular evidence for genetic mixing of Arctic and Antarctic subpolar populations of planktonic foraminifers. *Nature*, **405**, 43–47.

Davidson, A.T. & Marchant, H.J. (1992) Protist abundance and carbon concentration during a *Phaeocystis*-dominated bloom at an Antarctic coastal site. *Polar Biology*, **12**, 387–395.

Davis, P.G., Caron, D.A. & Sieburth, J.M. (1978) Oceanic amoebae from the North Atlantic: culture, distribution, and taxonomy. *Transactions of the American Microscopical Society*, **96**, 73–88.

Dennett, M.R., Mathot, S., Caron, D.A., Smith, W.O. & Lonsdale, D.J. (2001) Abundance and distribution of phototrophic and heterotrophic nano- and microplankton in the southern Ross Sea. *Deep-Sea Research Part II*, **48**, 4019–4037.

Eicken, H. (1992) The role of sea ice in structuring Antarctic ecosystems. *Polar Biology*, **12**, 3–13.

Fenchel, T. & Lee, C.C. (1972) Studies on ciliates associated with sea ice from Antarctica: I. The nature of the fauna. *Archiv für Protistenkunde*, **114**, 231–236.

Finlay, B.J. & Fenchel, T. (1999) Divergent perspectives on protist species richness. *Protist*, **150**, 229–233.

Finlay, B.J., Esteban, G. & Fenchel, T. (2004) Protist diversity is different? *Protist*, **155**, 15–22.

Foissner, W. (1999) Protist diversity: estimates of the near-imponderable. *Protist*, **72**, 6578–6583.

Fonda Umani, S., Monti, M., Bergamasco, A., Cabrini, M., de Vittor, C., Burba, N. & del Negro, P. (2005) Plankton community structure and dynamics versus physical structure from Terra Nova Bay to Ross Ice Shelf (Antarctica). *Journal of Marine Systems*, **55**, 31–46.

Fritsen, C.H., Memmmott, J. & Stewart, F.J. (2008) Inter-annual sea ice dynamics and micro-algal biomass in winter pack ice of Marguerite Bay, Antarctica. *Deep-Sea Research Part II*, **55**, 2059–2067.

Garrison, D.L. (1991) An overview of the abundance and role of protozooplankton in Antarctic waters. *Journal of Marine Systems*, **2**, 317–331.

Garrison, D.L. & Buck, K.R. (1989) The biota of Antarctic pack ice in the Weddell Sea and Antarctic peninsula regions. *Polar Biology*, **10**, 237–239.

Garrison, D.L. & Buck, K.R. (1991) Surface-layer sea ice assemblages in Antarctic pack ice during the austral spring: environmental conditions, primary production and community structure. *Marine Ecology Progress Series*, **75**, 161–172.

Garrison, D.L. & Close, A.R. (1993) Winter ecology of the sea ice biota in Weddell Sea pack ice. *Marine Ecology Progress Series*, **96**, 17–31.

Garrison, D.L., Ackley, S.F. & Buck, K.R. (1986) A physical mechanism for establishing algal populations in frazil ice. *Nature*, **306**, 363–365.

Garrison, D.L., Buck, K.R. & Gowing, M.M. (1993) Winter plankton assemblage in the ice edge zone of the Weddell and Scotia Seas: composition, biomass and spatial distribution. *Deep-Sea Research*, **40**, 311–338.

Garrison, D.L., Jeffries, M.O., Gibson, A. et al. (2003) Development of sea ice microbial communities during autumn ice formation in the Ross Sea. *Marine Ecology Progress Series*, **259**, 1–15.

Garrison, D.L., Gibson, A., Coale, S.L., Gowing, M.M., Okolodkov, Y.B., Fritsen, C. & Jefferies, M.O. (2005) Sea ice microbial communities in the Ross Sea: autumn and summer biota. *Marine Ecology Progress Series*, **300**, 39–52.

Gast, R.J., Dennett, M.R. & Caron, D.A. (2004) Characterization of protistan assemblages in the Ross Sea, Antarctica by denaturing gradient gel electrophoresis. *Applied and Environmental Microbiology*, **70**, 2028–2037.

Gast, R.J., Moran, D.M., Beaudoin, D.J. Blythe, J.N. & Dennett, M.R. (2006) Abundance of a novel dinoflagellate phylotype in the Ross Sea, Antarctica. *Journal Of Phycology*, **42**, 233–242.

Gast, R.J., Moran, D.M., Dennett, M.R. & Caron, D.A. (2007) Kleptoplasty in an Antarctic dinoflagellate: caught in evolutionary transition? *Environmental Microbiology*, **9**, 39–45.

Gosselin, M., Legendre, L., Therriault, J.-C. , Demers, S. & Rochet, M. (1986) Physical control of the horizontal patchiness of sea ice microalgae. *Marine Ecology Progress Series*, **29**, 289–298.

Gowing, M.M. (1986) Trophic biology of phaeodarian radiolarians and flux of living radiolarians in the upper 2000 m of the North Pacific central gyre. *Deep-Sea Research*, **33**, 655–674.

Gowing, M.M. (1989) Abundance and feeding ecology of Antarctic phaeodarian radiolarians. *Marine Biology*, **103**, 107–118.

Gowing, M.M. (2003) Large viruses and infected microeukaryotes in Ross Sea summer pack ice habitats. *Marine Biology*, **142**, 1029–1040.

Gowing, M.M. & Garrison, D.L. (1992) Abundance and feeding ecology of larger protozooplankton in the ice edge zone of the Weddell and Scotia Seas during the austral winter. *Deep-Sea Research*, **39**, 893–919.

Gradinger, R. & Ikavalko, J. (1998) Organism incorporation into newly forming Arctic sea ice in the Greenland Sea. *Journal of Plankton Research*, **20**, 871–886.

Gradinger, R., Friedrich, C. & Spindler, M. (1999) Abundance, biomass and composition of the sea ice biota of the Greenland Sea pack ice. *Deep-Sea Research Part II*, **46**, 1457–1472.

Gradinger, R., Spindler, M. & Weissenberger, J. (1992) On the structure and development of Arctic pack ice communities in Fram Strait: a multivariate approach. *Polar Biology*, **12**, 727–733.

Grossi, S.M. & Sullivan, C.W. (1985) Sea ice microbial communities. V. The vertical zonation of diatoms in an Antarctic fast ice community. *Journal of Phycology*, **21**, 401–409.

Hamilton, A.K., Lovejoy, C., Galand, P.E. & Ingram, R.G. (2008) Water masses and biogeography of picoeukaryote assemblages in a cold hydrographically complex system. *Limnology and Oceanography*, **53**, 922–935.

Hemleben, C., Spindler, M. & Anderson, O.R. (1988) *Modern planktonic foraminifera*. Springer-Verlag, New York.

Ikavalko, J. & Gradinger, R. (1997) Flagellates and heliozoans in the Greenland Sea ice studied alive using light microscopy. *Polar Biology*, **17**, 473–481.

Jacobson, D.M. & Anderson, D.M. (1986) Thecate heterotrophic dinoflagellates: feeding behavior and mechanisms. *Journal of Phycology*, **22**, 249–258.

Jacobson, D.M. & Anderson, D.M. (1996) Widespread phagocytosis of ciliates and other protists by marine mixotrophic and heterotrophic thecate dinoflagellates. *Journal of Phycology*, **32**, 279–285.

Janech, M.G., Krell, A., Mock, T., Kang, J.-S. & Raymond, J.A. (2006) Ice-binding proteins from sea ice diatoms (Bacillariophyceae). *Journal of Phycology*, **42**, 410–416.

Jeong, H.J., Yoo, Y.D., Park, J.Y. et al. (2005) Feeding by red-tide dinoflagellates: five species newly revealed and six species previously known to be mixotrophic. *Aquatic Microbial Ecology*, **40**, 133–150.

Jones, R.I. (1994) Mixotrophy in planktonic protists as a spectrum of nutritional strategies. *Marine Microbial Food Webs*, **8**, 87–96.

Kaartokallio, H. (2004) Food web components, and physical and chemical properties of Baltic sea ice. *Marine Ecology Progress Series*, **273**, 49–63.

Krembs, C., Gradinger, R. & Spindler, M. (2000) Implications of brine channel geometry and surface area for the interaction of sympagic organisms in Arctic sea ice. *Journal of Experimental Marine Biology and Ecology*, **243**, 55–80.

Kuosa, H., Borrman, B., Kivi, K. & Brandini, F. (1992) Effects fo Antarctic sea ice biota on seeding as studied in aquarium experiments. *Polar Biology*, **12**, 333–339.

Laurion, I., Demers, S. &Vézina, A.F. (1995) The microbial food web associated with the ice algal assemblage: biomass and bacterivory of nanoflagellate protozoans in Resolute Passage (High Canadian Arctic). *Marine Ecology Progress Series*, **120**, 77–87.

Leakey, R.J.G., Archer, S.D. & Grey, J. (1996) Microbial dynamics in coastal waters of East Antarctica: bacterial production and nanoflagellate bacterivory. *Marine Ecology Progress Series*, **142**, 3–17.

Lee, C.C. & Fenchel, T. (1972) Studies on ciliates associated with sea ice from Antarctica. II. Temperature responses and tolerances in ciliates from antarctic, temperate and tropical habitats. *Archiv für Protistenkunde*, **114**, 237–244.

Lessard, E.J. (1991) The trophic role of heterotrophic dinoflagellates in diverse marine environments. *Marine Microbial Food Webs*, **5**, 49–58.

Levinsen, H., Gissel Nielsen, T. & Winding Hansen, B. (2000) Annual succession of marine pelagic protozoans in Disko Bay, West Greenland, with emphasis on winter dynamics. *Marine Ecology Progress Series*, **206**, 119–134.

Lipps, J.H. & Krebs, W.N. (1974) Planktonic foraminifera associated with Antarctic sea ice. *Journal of Foraminiferal Research*, **4**, 80–85.

López-Urrutia, Á. (2008) The metabolic theory of ecology and algal bloom formation. *Limnology and Oceanography*, **53**, 2046–2047.

Lovejoy, C., Massana, R. & Pedros-Alio, C. (2006) Diversity and distribution of marine microbial eukaryotes in the Arctic Ocean and adjacent seas. *Applied and Environmental Microbiology*, **72**, 3085–3095.

Marchant, H.J. (1985) Choanoflagellates in the Antarctic marine food chain. In: *Antarctic nutrient cycles and food webs* (Eds. W.R. Siegfried, P.R. Condy & R.M. Laws), pp. 271–276. Springer-Verlag, Berlin.

Marchant, H.J. & Perrin, R. (1990) Seasonal variation in abundance and species composition of choanoflagellates (Acanthoecidae) at Antarctic coastal sites. *Polar Biology*, **10**, 499–505.

Mayes, D.F., Rogerson, A., Marchant, H. & Laybourn-Parry, J. (1997) Growth and consumption rates of bacterivorous Antarctic naked marine amoebae. *Marine Ecology Progress Series*, **160**, 101–108.

McFadden, G.I., Moestrup, O. & Wetherbee, R. (1982) *Pyramimonas gelidicola* sp. nov. (Prasinophyceae), a new species isolated from Antarctic sea ice. *Phycologia*, **21**, 103–111.

Michaels, A.F. (1991) Acantharian abundance and symbiont productivity at the VERTEX seasonal station. *Journal of Plankton Research*, **13**, 399–418.

Michel, C., Gissel Nielsen, T., Nozais, C. & Gosselin, M. (2002) Significance of sedimentation and grazing by ice micro- and meiofauna for carbon cycling in annual sea ice (northern Baffin Bay). *Aquatic Microbial Ecology*, **30**, 57–68.

Montresor, M., Procaccini, G. & Stoecker, D.K. (1999) *Polarella glacialis*, Gen. Nov. Sp. Nov. (Dinophyceae): Suessiaceae are still alive! *Journal of Phycology*, **35**, 186–197.

Moorthi, S.D., Caron, D.A., Gast, R.J. & Sanders, R.W. (2009) Mixotrophic nanoflagellates in plankton and sea ice of the Ross Sea. *Aquatic Microbial Ecology,* **54**, 269–277.

Moran, D.M., Anderson, O.R., Dennett, M.R., Caron, D.A. & Gast, R. (2007) A description of seven Antarctic marine Gymnamoebae including a new species and a new genus: *Platyamoeba contorta* n. sp. and *Vermistella antarctica* n. gen. n. sp. *Journal of Eukaryotic Microbiology*, **54**, 169–183.

Nöthig, E.-M. & von Bodungen, B. (1989) Occurrence and vertical flux of faecal pellets of probably protozoan origin in the southeastern Weddell Sea (Antarctica). *Marine Ecology Progress Series*, **56**, 281–289.

Nöthig, E.-M. & Gowing, M.M. (1991) Late winter abundance and distribution of phaeodarian radiolarians, other large protozooplankton and copepod nauplii in the Weddell Sea, Antarctica. *Marine Biology*, **111**, 473–484.

Okolodkov, Y.B. (1998) A check list of dinoflagellates recorded from the Russian arctic seas. *Sarsia*, **83**, 267–292.

Palmisano, A.C. & Garrison, D.L. (1993) Microorganisms in antarctic sea ice. In: *Antarctic microbiology,* (Ed. E.I. Friedmann), pp. 167–218. Wiley-Liss, New York.

Park, M.G., Kim, S., Kim, H.S., Myung, G, Kang, Y.G. & Yih, W. (2006) First successful culture of the marine dinoflagellate Dinophysis. *Aquatic Microbial Ecology*, **45**, 101–106.

Parsons, T.R., Takahashi, M. & Hargrave, B. (1984) *Biological Oceanographic Processes*. Pergamon Press, Elmsford.

Peck, L.S. (2002) Ecophysiology of Antarctic marine ectotherms: limits of life. *Polar Biology*, **25**, 31–40.

Petz, W., Song, W. & Wilbert, N. (1995) Taxonomy and ecology of the ciliate fauna (Protozoa, Ciliophora) in the endopagial and pelagial of the Weddel Sea, Antarctica. *Stapfia*, **40**, 1–223.

Petz, W., Valonesi, A., Schiftner, U. Quesada, A. & Ellis-Evans, C. (2007) Ciliate biogeography in Antarctic and Arctic freshwater ecosystems: endemism or global distribution of species? *FEMS Microbiology Ecology*, **59**, 396–408.

Pierce, R.W. & Turner, J.T. (1992) Ecology of planktonic ciliates in marine food webs. *Reviews in Aquatic Sciences*, **6**, 139–181.

Price, P.B. (2003) Life in solid ice on Earth and other planetary bodies. In: *Bioastronomy 2002: Life Amongst the Stars* (Eds. R. Norris & F. Stootman). Astronomical Society of the Pacific, IAU Symposium Series, 2003, Symposium 213, pp 363–366.

Riedel, A., Michel, C. & Gosselin, M. (2008) Grazing of large-sized bacteria by sea ice heterotrophic protists on the Mackenzie Shelf during the winter–spring transition. *Aquatic Microbial Ecology*, **50**, 25–38.

Rose, J.M. & Caron, D.A. (2007) Does low temperature constrain the growth rates of heterotrophic protists? Evidence and implications for algal blooms in cold water. *Limnology and Oceanography*, **52**, 886–895.

Rose, J.M., Vora, N.M., Countway, P.D., Gast, R.J. & Caron, D.A. (2009) Effects of temperature on growth rate and gross growth efficiency of an Antarctic bacterivorous protist. *The ISME Journal*, **3**, 252–260.

Rózanska, M., Poulin, M. & Gosselin, M. (2008) Protist entrapment in newly formed sea ice in the coastal Arctic Ocean. *Journal of Marine Systems*, **74**, 887–901.

Sanders, R.W. (1991) Mixotrophic protists in marine and freshwater ecosystems. *Journal of Protozoology*, **38**, 76–81.

Sanders, R.W. & Porter, K.G. (1988) Phagotrophic phytoflagellates. *Advances in Microbial Ecology*, **10**, 167–192.

Sanders, R.W., Caron, D.A. & Berninger, U.-G. (1992) Relationships between bacteria and heterotrophic nanoplankton in marine and fresh water: an inter-ecosystem comparison. *Marine Ecology Progress Series*, **86**, 1–14.

Schnepf, E. & Kühn, S.F. (2000) Food uptake and fine structure of *Cryothecomonas longipes* sp. nov., a marine nanoflagellate incertae sedis feeding phagotrophically on large diatoms. *Helgoland Marine Research*, **54**, 18–32.

Scott, F.J. & Marchant, H.J. (2005) *Antarctic Marine Protists*. Australian Biological Resources, Canberra and ADD, Hobart.

Scott, F.J., Davidson, A.T. & Marchant, H.J. (2001) Grazing by the Antarctic sea ice ciliate *Pseudocohnilembus*. *Polar Biology*, **24**, 127–131.

Sherr, E.B. & Sherr, B.F. (2002) Significance of predation by protists in aquatic microbial food webs. *Antonie Van Leeuwenhoek International Journal of General and Molecular Microbiology*, **81**, 293–308.

Sherr, E.B. & Sherr, B.F. (2007) Heterotrophic dinoflagellates: a significant component of microzooplankton biomass and major grazers of diatoms in the sea. *Marine Ecology Progress Series*, **352**, 187–197.

Sherr, E.B., Sherr, B.F. & Fessenden, L. (1997) Heterotrophic protists in the Central Arctic Ocean. *Deep-Sea Research Part II*, **44**, 1665–1682.

Sherr, B.F., Sherr, E.B., Caron, D.A., Vaulot, D. & Wordon, A.Z. (2007) Oceanic protists. *Oceanography*, **20**, 130–134.

Sime-Ngando, T., Gosselin, M., Juniper, S.K. & Levasseur, M. (1997a) Changes in sea ice phagotrophic microprotists (20–200 µm) during the spring bloom, Canadian Arctic Archipelago. *Journal of Marine Systems*, **11**, 163–172.

Sime-Ngando, T., Juniper, S.K. & Demers, S. (1997b) Ice-brine and planktonic microheterotrophs from Saroma-ko Lagoon, Hokkaido (Japan): quantitative importance and trophodynamics. *Journal of Marine Systems*, **11**, 149–161.

Sime-Ngando, T., Demers, S. & Juniper, S.K. (1999) Protozoan bacterivory in the ice and water column of a cold temperate lagoon. *Microbial Ecology*, **37**, 95–106.

Simpson, A.G.B. & Roger, A.J. (2004) The real 'kingdoms' of eukaryotes. *Current Biology*, **14**, 693–696.

Slapeta, J., López-Garcia, P. & Moreira, D. (2006) Global dispersal and ancient cryptic species in the smallest marine eukaryotes. *Molecular Biology and Evolution*, **23**, 23–29.

Smith, W.O. Jr. & Gordon, L.I. (1997) Hyperproductivity of the Ross Sea (Antarctica) polynya during austral spring. *Geophysical Research Letters*, **24**, 233–236.

Smith, W.O. Jr., Nelson, D.M., DiTullio, G.R., Giacomo, R. & Leventer, A.R. (1996) Temporal and spatial patterns in the Ross Sea: Phytoplankton biomass, elemental composition productivity and growth rates. *Journal of Geophysical Research*, **101**, 18,455–18,466.

Song, W. & Wilbert, N. (2000) Ciliates from Antarctic sea ice. *Polar Biology*, **23**, 212–222.

Spindler, M. & Dieckmann, G.S. (1986) Distribution and abundance of the planktic foraminifera *Neogloboquadrina pachyderma* in sea ice of the Weddell Sea (Antarctica). *Polar Biology*, **5**, 185–191.

Stoeck, T., Jost, S. & Boenigk, J. (2008) Multigene phylogenies of clonal *Spumella*-like strains, a cryptic heterotrophic nanoflagellate, isolated from different geographical regions. *International Journal of Systematic and Evolutionary Microbiology*, **58**, 716–724.

Stoecker, D.K. (1998) Conceptual models of mixotrophy in planktonic protists and some ecological and evolutionary implications. *European Journal of Protistology*, **34**, 281–290.

Stoecker, D.K. (1999) Mixotrophy among dinoflagellates. *Journal of Eukaryotic Microbiology*, **46**, 397–401.

Stoecker, D., Michaels, A.E. & Davis, L.H. (1987) Large proportion of marine planktonic ciliates found to contain functional chloroplasts. *Nature*, **326**, 790–792.

Stoecker, D.K., Buck, K.R. & Putt, M. (1992) Changes in the sea ice brine community during the spring–summer transition, McMurdo Sound, Antarctica. 1. Photosynthetic protists. *Marine Ecology Progress Series*, **84**, 265–278.

Stoecker, D.K., Buck, K.R. & Putt, M. (1993) Changes in the sea ice brine community during the spring–summer transition, McMurdo Sound, Antarctica. 2. Phagotrophic protists. *Marine Ecology Progress Series*, **95**, 103–113.

Stoecker, D.K., Gustafson, D.E., Merrell, J.R., Black, M.M.D. & Baier, C.T. (1997) Excystment and growth of chrysophytes and dinoflagellates at low temperatures and high salinities in Antarctic sea ice. *Journal of Phycology*, **33**, 585–595.

Stoecker, D.K., Gustafson, D.E., Black, M.M.D. & Baier, C.T. (1998) Population dynamics of microalgae in the upper land-fast sea ice at a snow-free location. *Journal of Phycology*, **34**, 60–69.

Strom, S.L. (1991) Growth and grazing rates of the herbivorous dinoflagellate *Gymnodinium* sp. from the open subarctic Pacific Ocean. *Marine Ecology Progress Series*, **78**, 103–113.

Strom, S.L. (2000) Bacterivory: interactions between bacteria and their grazers. In: *Microbial ecology of the oceans* (Ed. D.L. Kirchman), pp. 351–386. Wiley-Liss, New York.

Thomas, D.N. & Dieckmann, G.S. (2002) Antarctic sea ice – a habitat for extremophiles. *Science*, **295**, 641–644.

Thomsen, H.A., Buck, K.R., Bolt, P.A. & Garrison, D.L. (1991) Fine structure and biology of *Cryothecomonas* gen. nov. (Protista incertae sedis) from the ice biota. *Canadian Journal of Zoology*, **69**, 1048–1070.

Tong, S., Vørs, N. & Patterson, D.J. (1997) Heterotrophic flagellates, centrohelid heliozoa and filose amoebae from marine and freshwater sites in the Antarctic. *Polar Biology*, **18**, 91–106.

Vaqué, D., Agustí, S. & Duarte, C.M. (2004) Response of bacterial grazing rates to experimental manipulation of an Antarctic coastal nanoflagellate community. *Aquatic Microbial Ecology*, **36**, 41–52.

Vaulot, D., Eikrem, W., Viprey, M. & Moreau, H. (2008) The diversity of small eukaryotic phytoplankton (≤3 µm) in marine ecosystems. *FEMS Microbiology Reviews*, **32**, 792–820.

Vézina, A.F., Demers, S., Laurion, I., Sime-Ngando, T., Juniper, S.K. & Devine, L. (1997) Carbon flows through the microbial food web of first-year ice in Resolute Passage (Canadian High Arctic). *Journal of Marine Systems*, **11**, 173–189.

Vørs, N. (1993) Heterotrophic amoebae, flagellates and heliozoa from Arctic marine waters (North West Territories, Canada and West Greenland). *Polar Biology*, **13**, 113–126.

Weissenberger, J., Dieckmann, G.S., Gradinger, R. & Spindler, M. (1992) Sea ice: a cast technique to examine and analyse brine pockets and channel structure. *Limnology and Oceanography*, **37**, 179–183.

10 Sea Ice Meio- and Macrofauna

Bodil A. Bluhm, Rolf R. Gradinger and Sigrid B. Schnack-Schiel

10.1 Introduction

Sea ice is a habitat, feeding ground, refuge, breeding and/or nursery ground for a number of metazoan species, in addition to harbouring a diverse group of autotrophs, bacteria and protozoans (Gradinger, 2002; Chapters 7–9). Metazoans live in association with sea ice either permanently (autochthonous fauna) or temporarily (allochthonous fauna). Allochthonous fauna may originate from pelagic and/or benthic habitats depending mainly on region and water depth. In addition, colonization of newly formed ice can occur from older pieces of sea ice in the region. Some metazoan species live within the sea ice, e.g. turbellarians, nematodes, rotifers and copepods, and are summarized as in-ice fauna or sea ice meiofauna. Other taxa, particularly larger-bodied ones such as euphausiids, amphipods and fish, are found in close association with the under-ice habitat and are referred to as under-ice or sea ice macrofauna (Gradinger & Bluhm, 2004). The majority of ice meio- and macrofauna appears to be feeding on ice algae, but some prey on other sea ice–related or pelagic animals (Grainger & Hsiao, 1990; Werner, 1997; Brierley & Thomas, 2002). In turn, ice-associated metazoans and specifically the under-ice fauna form a key component of the diet of many 'top trophics' (Chapter 11). Thereby, they are fundamental to the mediation of particulate fluxes from sea ice to water column and benthos and therefore to processes associated with bentho-pelagic coupling, especially in shallow shelf regions.

Current belief is that species richness of sea ice fauna is low compared to water column and interstitial sediment faunas with only a few species per higher taxonomic rank, suggesting high specialization (Table 10.1; e.g. rotifers: Friedrich & De Smet, 2000; nematodes: Tchesunov & Riemann, 1995; hydrozoans: Bluhm et al., 2007; crustaceans: Schnack-Schiel et al., 1998; Arndt & Swadling, 2006; Macnaughton et al., 2007). Environmental conditions in sea ice can vary widely with location and season, requiring wide ecological tolerances of the fauna (Gradinger & Schnack-Schiel, 1998). Extreme temperatures (below −10°C) and brine salinities (>100) occur specifically in the ice interior during winter and early spring, while temperature and salinity conditions close to the ocean–ice interface are less extreme and relatively constant (Gradinger, 2002). Spatial constraints through the dimensions of the brine channel network also limit the occurrence of larger metazoans within the sea ice interior (Krembs et al., 2000). The combination of these unique environmental conditions and the high-latitude seasonality caused the dominance of only a few species of sympagic fauna (Table 10.1). It should, however, be noted that the sea ice biotic inventory is not yet complete as indicated by recent discoveries of new metazoan species in both the Arctic (hydrozoan

Table 10.1 Characteristic metazoan species found within Arctic and Antarctic sea ice.

Taxon	Arctic	Antarctic
Cnidarians	*Sympagohydra tuuli*	Unknown
Ctenophores	Unknown	*Callianira antarctica*
Turbellarians	Several unidentified species	Several unidentified species
Nematodes	*Theristus melnikovii, Cryonema tenue, C. crassum*	*Geomonhystera glaciei*
Rotifers	*Synchaeta hyperborea, Encentrum graingeri*	Unknown
Polychaetes	*Scolelepis squamata* (juveniles), *Unidentified hesionid*	Unknown
Gastropodes	Unidentified larvae	*Tergipes antarcticus*
Calanoid copepods	*Pseudocalanus* sp.	*Paralabidocera antarctica, Stephos longipes*
Harpacticoid copepods	*Halectinosoma sp., Harpacticus superflexus, Tisbe furcata, Microsetella norvegica*	e.g. *Drescheriella glacialis, Idomene antarctica, Harpacticus furcifer, Diarthrodes cf. lilacinus*
Cyclopoid copepods	*Cyclopina gracilis, C. schneideri, Oithona similis*	*Oncaea curvata, Oithona similis*
Others	*Tunicate larvae, amphipod juveniles*	

Source: Grainger and Hsiao (1990); Grainger (1991); Carey (1992); Riemann and Sime-Ngando (1997); Friedrich (1997); Schnack-Schiel et al. (1998); Blome and Riemann (1999); Swadling et al. (2001); Bluhm et al. (2007); Kiko et al. (2008a).

Sympagohydra tuuli; Bluhm et al., 2007; Piraino et al., 2008; Siebert et al., 2008) and Antarctica (ctenophores *Callianira antarctica*, Kiko et al., 2008a) and the still lacking identification of dominant taxa such as turbellarians occurring in both Arctic and Antarctic sea ice (Janssen & Gradinger, 1999; Friedrich & Hendelberg, 2001).

The contrasting characteristics of Arctic and Antarctic sea ice (Chapter 1) resulted in differences in the role of sea ice for the ecology, life history strategies and seasonal dynamics of metazoans in both polar oceans. Most of the sea ice area in the Antarctic is annual (about 80%), whereas a significant portion (about 50%) of the Arctic Ocean has been permanently covered by sea ice, at least prior to the changes in the last decades. Consequently, sympagic metazoans in most of Antarctica and parts of the Arctic, specifically in large parts of the shelves, had to adapt to the seasonal melt and growth of the ice cover and must be able to survive parts of the life cycle in the water column or at the sea floor. In contrast, unique ice endemic species evolved in regions with permanent sea ice cover like the central Arctic deep water regions, where ice-associated fauna can complete their entire life cycles in association with the multiyear ice cover.

10.2 Sea ice metazoan communities

In-ice fauna species diversity

Sea ice fauna is a mixture of ice endemic, pelagic and benthic species. Pelagic taxa include, for example, calanoid and cyclopoid copepods and rotifers and benthic taxa include, for
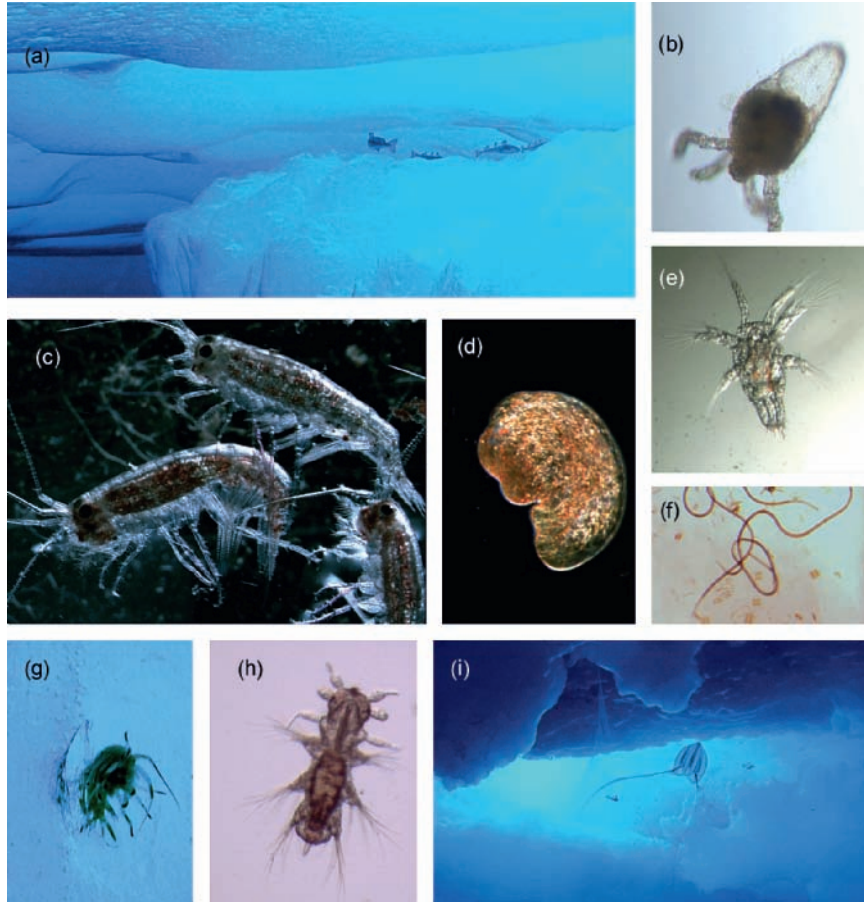
Fig. 10.1   Arctic ice-associated fauna. (a) Arctic cod, *Boreogadus saida* (about 15 cm), (b) *Sympagohydra tuuli* (350 µm), (c) *Apherusa glacialis* (18 mm), (d) turbellarian (500 µm), (e) Copepod nauplius (70 µm), (f) nematode (650 µm), (g) *Gammarus wilkitzkii* (3 cm), (h) Hesionidae juvenile (460 µm), (i) *Mertensia* sp. (several cm). Photographs by Bodil Bluhm (c–f, h), Rolf Gradinger (b), and Katrin Iken (a, g, i; all at University of Alaska Fairbanks). Photographs reproduced with permission from Katrin Iken.

example, turbellarians, nematodes, polychaete and gastropod juveniles and harpacticoid copepods (Figs 10.1 and 10.2). Distinct differences exist in the taxonomic composition of the dominant ice meiofauna of Arctic and Antarctic sea ice fauna (Fig. 10.3) (Gradinger, 1999; Schnack-Schiel et al., 2001a; Arndt & Swadling, 2006). Most obvious, rotifers and nematodes occur regularly only in Arctic sea ice, while calanoid copepods are dominants only in Antarctic sea ice (Fig. 10.3; Gradinger, 1999; Gradinger et al., 1999; Schnack-Schiel et al., 2001a; Gradinger et al., 2005; Schünemann & Werner, 2005; Arndt & Swadling, 2006). Cnidarians have so far only been reported from Arctic fast ice (Bluhm et al., 2007), while ctenophores, recently found in the pack ice of the western Weddell Sea (Kiko et al., 2008a), represent a taxon not found in the Arctic hitherto. Nudibranchs, inhabiting Antarctic sea ice, are not known from Arctic sea ice, but larval gastropods do occur in coastal Arctic fast ice.

Fig. 10.2 Antarctic ice-associated fauna. (a) *Euphausia superba* (4 cm), (b) *Stephos longipes* (900 µm), (c) *Eusirus tridentatus* (1 cm), (d) *Callianira antarctica* (6 cm), (e) *Drescheriella glacialis* (700 µm), (f) *Tergipes antarcticus* (3 mm). Photographs by Cheryl Hopcroft (a; University of Alaska Fairbanks), Ingo Arndt (b–e; GEO/AWI), Rainer Kiko (f; Kiel University from Kiko et al. (2008)). Reproduced with kind permission from Springer Science + Business Media and Hopcroft, Arndt and Kiko.

Species richness in each of the ice meiofauna taxa appears to be low (Table 10.1), although not all known species have been described yet. Only one species each of sympagic cnidarians (*Sympagohydra tuuli*; Fig. 10.1; Piraino et al., 2008) and ctenophores (*Callianira antarctica*; Fig. 10.2; Kiko et al., 2008a) is known. Eight rotifer species were identified in sea ice of the Barents, Laptev and Greenland Seas, with *Synchaeta hyperborea* being the most abundant followed by *S. tamara* (Friedrich & De Smet, 2000). Three Arctic ice endemic nematode species, *Teristus melnikovii*, *Cryonema crassum* and *C. tenue*, plus several undescribed species were recorded in the Arctic (Tchesunov & Riemann, 1995; Riemann & Sime-Ngando, 1997), and only a single observation reports the occurrence of a sea ice monhysteroid species (*Geomonhystera glaciei*) plus three not-to-species-level-identified nematodes in Antarctic ice (Blome & Riemann, 1999).

Within the copepods, three species clearly dominate the Antarctic sea ice metazoan fauna: the harpacticoid *Drescheriella glacialis* and the calanoids *Paralabidocera antarctica* and *Stephos*
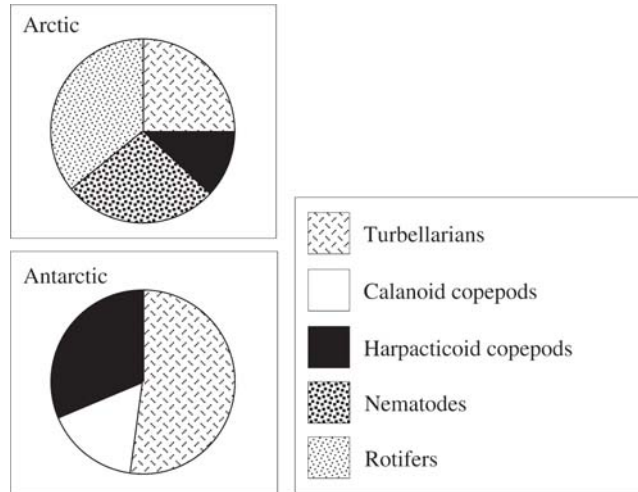
Fig. 10.3 Examples of relative contribution of ice metazoans to mean abundance in sea ice of the central Arctic and the Antarctica Weddell Sea. Taxonomic composition varies among locations at both poles, but some taxa such as rotifers and nematodes are common only in Arctic sea ice, while others such as calanoid copepods are more dominant in Antarctic sea ice. Data from Gradinger (1999) and Schnack-Schiel et al. (2001a).

longipes (Table 10.1). Several other harpacticoids occur sporadically in sea ice cores, typically in low numbers, although some such as *Idomene antarctica*, *Ectinosoma* sp., *Harpacticus furcifer* and *Diarthrodes* cf. *lilacinus* occasionally reach relatively high abundances. The calanoids *Ctenocalanus citer* and *Metridia gerlachei*, and the cyclopoids *Oncaea curvata* and *Oithona similis* are occasionally present in Antarctic sea ice cores in very low numbers (Swadling et al., 1997, 2001; Schnack-Schiel et al., 1998, 2008; Guglielmo et al., 2007). In the Arctic, the cyclopoid copepods *Cyclopina gracilis* and *C. schneideri*, as well as the harpacticoids *Harpacticus* spp., *Halectinosoma* sp. and *Tisbe furcata*, are common in sea ice samples (Carey & Montagna, 1982; Grainger, 1991). Commonly found calanoid species from the water column, such as *Acartia longiremis*, *Pseudocalanus* sp., *Calanus glacialis* and the cyclopoid *Oithona similis*, occasionally reach noteworthy densities in coastal fast ice (Carey & Montagna, 1982; Gradinger & Bluhm, 2005 and unpublished).

In nearshore and shallow waters (depth <50 m) larvae and juveniles of benthic organisms such as polychaetes and gastropods can contribute at certain times of the seasonal cycle. They occur in high numbers in coastal fast ice in the Arctic (Carey, 1992; Gradinger & Bluhm, 2005), and to a lesser degree in Antarctic sea ice over the relatively deep shelf (Andriashev, 1968). Not all species have been identified yet, because larval and juvenile stages do not have all distinguishing features, but the polychaete *Scolelepis squamata* is a common taxon in coastal fast ice in at least the Chukchi and Beaufort Seas.

Spatial and temporal variability of in-ice fauna

The spatial distribution of sea ice biota in general is tightly linked to the physical properties of sea ice, including ice thickness, snow depth, light (Steffens et al., 2006) and, for herbivorous sea ice fauna, ice-algal biomass (Swadling et al., 2000). Similarly, migration and

reproduction events cause considerable temporal changes in the abundance and composition of the sea ice biota with changes of several orders of magnitude (Kern & Carey, 1983; Gradinger & Bluhm, 2005). On small spatial scales (millimetres to centimetres), inhabitable space availability within the ice determines the size, taxonomic composition and distribution of metazoans within the sea ice matrix. The total volume of brine-filled pockets, pores and channels is a function of sea ice temperature and bulk salinity and typically ranges between less than 5% in cold winter ice and greater than 20% in warm summer ice. Typical dimensions of inhabitable and interconnected brine channels are in the submillimetre diameter range (Weissenberger et al., 1992). Sympagic metazoans differ greatly in their morphology and plasticity: small, elongated, plastic life forms such as turbellarians and rotifers are able to enter and traverse narrow brine channels, whereas larger animals such as copepods and amphipods are restricted by their size and inflexible exoskeletons. In an experiment using capillary tubes of different sizes, rotifers and turbellarians penetrated channels 57% and 60%, respectively, smaller than their usual body diameter by stretching and flexing their bodies (Krembs et al., 2000). Harpacticoid copepods, in contrast, only entered the tubes of diameters similar to their body diameters. Amphipods avoided narrow passages, and are only found in larger brine pockets and channels in the bottom layer of the ice and at the ice underside (Cross, 1982). Diving observations (Iken et al., personal communication) documented that amphipods utilized tiny depressions or large brine-drainage channels within the ice, likely to minimize predation pressure.

Ice exhibits pronounced vertical gradients in its physical and biological properties. The bottom layers are most suitable for sea ice meio- and macrofauna due to least extreme and relatively stable environmental conditions and the highest food availability. From autumn to spring, ice temperature and brine salinity in the skeletal layers and brine channels at the ice–water interface are most similar to those of the underlying water (Figs 10.4 and 10.5). The organisms in the ice bottom layer, therefore, do not need to undergo any energetically costly physiological or metabolic acclimation during periods of ice growth. During extensive ice melt, low salinity water layers with salinities below 5 can form under ice floes (Gradinger & Bluhm, 2004) and exert osmotic stress on sympagic organisms. Typically, sea ice fauna abundances match the vertical gradients of environmental conditions and are highest in the bottom 0–5 cm of the sea ice (Smith et al., 1988; Tanimura et al., 1996; Schnack-Schiel et al., 2001a; Swadling et al., 2001; Gradinger et al., 2005), except during melt periods with low salinity layers (Gradinger et al., 2005). High concentrations of metazoans at the bottom of ice floes typically coincide with high ice-algal biomass on which many metazoans feed (Hoshiai et al., 1987; Grainger & Hsiao, 1990; Schnack-Schiel et al., 1995; Janssen & Gradinger, 1999; Figs 10.4 and 10.5). Additionally, owing to the warmer temperatures towards the bottom of the ice, brine volume and channel diameter are larger and permit the colonization by larger species.

In the ice interior, colder temperatures specifically during the periods of ice growth result in narrow brine channels, possibly crushing or trapping organisms as well as exposing them to high-salinity stress. In newly forming sea ice, metazoans are rarely found (Schnack-Schiel et al., 1995, 2001b; Gradinger & Bluhm, 2005), suggesting that colonization occurs at later stages of the seasonal ice cycle. In the highly porous sea ice during late summer and autumn, ice sympagic metazoans can easily migrate to virtually all layers in the ice floes, and high concentrations may also be encountered in upper and intermediate layers. This phenomenon has been observed both in Arctic multiyear summer sea ice (Friedrich, 1997) as well as in
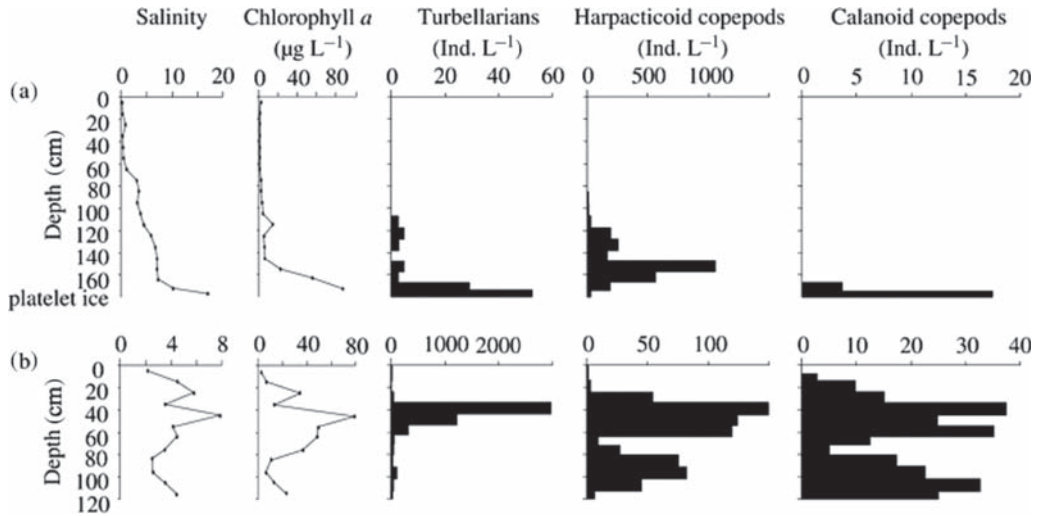
Fig. 10.4 Example of vertical distribution of salinity, chlorophyll *a* and abundances of turbellarians, harpacticoid and calanoid copepods in Antarctic sea ice: (a) in an ice core with an underlying platelet ice layer and (b) in an ice core without platelet ice.
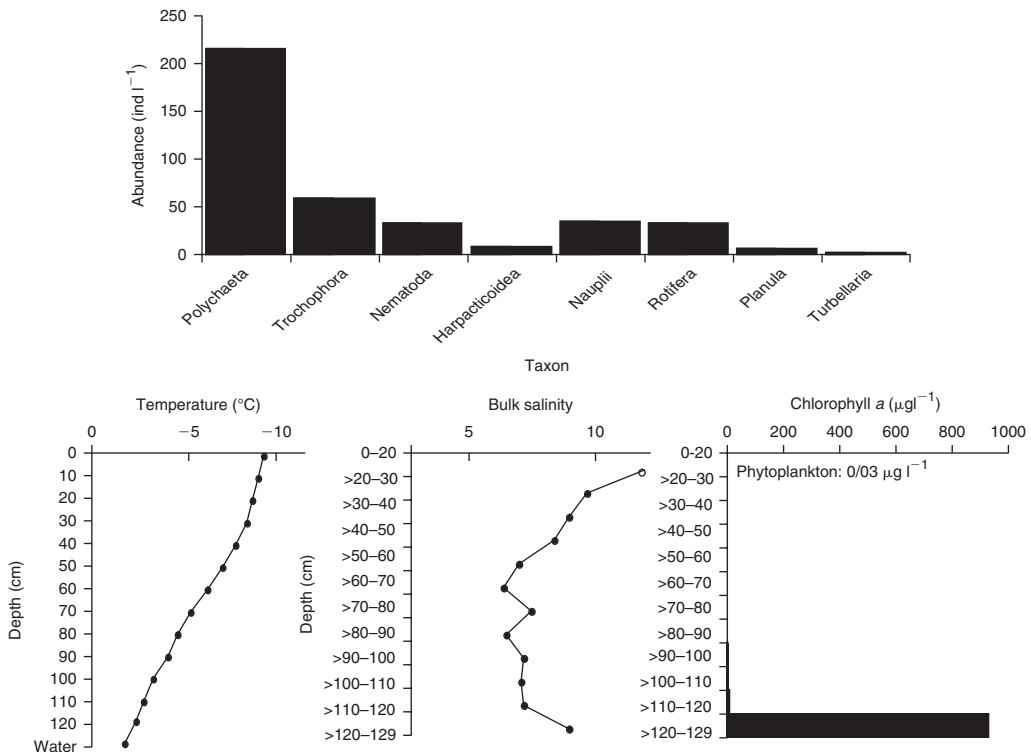
Fig. 10.5 Example of ice meiofauna abundance in the 10 cm at the ice–water interface and vertical distribution of temperature, bulk salinity and chlorophyll *a* (whole cores) in Arctic ice cores taken near the island of Little Diomede in Bering Strait in April 2004. 0 cm represents the ice–snow interface, 129 cm represents the ice–water interface.

Antarctic ice. Here, peak faunal abundances in rotten slush surface layers were flooding with seawater leads to high salinity and nutrient replete conditions and dense algal concentrations (Schnack-Schiel et al., 1998, 2001b; Thomas et al., 1998; Chapter 12).

The regional trends in sea ice meiofauna abundances follow, to a large extent, the available sea ice-algal food availability, causing regional differences by several orders of magnitude. In oligotrophic Arctic offshore pack ice regions, mean integrated abundances of sympagic metazoans range from less than 1000 to 10,000 individuals m^{-2} (Gradinger et al., 2005), but are typically one or more orders of magnitude higher in nearshore fast ice regions where peak abundances may be over 250,000 individuals m^{-2} (Cross, 1982; Nozais et al., 2001; Wiktor & Szymelfenig, 2002; Gradinger & Bluhm, 2005). One comparative study documented considerable regional differences in the abundances of summer Arctic sea ice meiofauna with highest concentrations in the Greenland Sea (mean 119,000 individuals m^{-2}) followed by the Laptev Sea (14,300 individuals m^{-2}) and the Barents Sea (6800 individuals m^{-2}) (Friedrich, 1997). In the Antarctic Weddell Sea, the integrated abundance of sea ice metazoans quantified at similar times of the year ranged between less than 10,000 and more than 120,000 individuals m^{-2} (Gradinger, 1999; Schnack-Schiel et al., 2001a) with no clear seasonal trend.

On local scales, ice meiofauna densities are patchy as a result of variable ice thickness, snow depth, sediment loads and resulting light conditions that control ice-algal primary production (Gradinger et al., 1991; Chapter 8). For example, meiofauna abundance in sediment-loaden coastal fast ice was an order of magnitude lower than in clean ice in spring, likely related to the dramatic reduction of light penetration and consequent lack of ice-algal bloom development in 'dirty' ice (Gradinger & Bluhm, 2005). Relationships of ice meiofauna with ice thickness are less clear due to the limited amount of information available from pressure ridges. First evidence suggests that for Arctic summer ice, meiofauna abundance may be higher at pressure ridges than level ice, but this may be related to more favourable salinity conditions at ridges during ice melt rather than to ice thickness (Gradinger et al., unpublished). Small-scale patchiness within a given sampling site of rather homogeneous conditions tends to be much lower than local and regional variability (Gradinger & Bluhm, 2005).

Temporal variability at any location can also be substantial with increases in abundance from winter to spring–early summer by a factor of 1–4 orders of magnitude in coastal fast ice (Grainger et al., 1985; Gradinger & Bluhm, 2005). Temporal changes may be related to migration and reproductive events in response to the build-up of a rich food sources in the ice in the spring and can include changing composition of ice meiofauna. For example, the apparently herbivorous juveniles of the spionid polychaete *Scolelepis squamata* appear in coastal fast ice in March, feed and grow through periods of high ice-algal biomass when they can be the dominant taxon and leave the ice in May (Fig. 10.6) (Bluhm & Gradinger, unpublished). This seasonal change in dominance and abundance was also recorded for other taxa; e.g. nauplii contributed >90% to total abundance in Arctic pack ice in March/April but less than 10% in later summer (Schünemann & Werner, 2005). In that study, absolute abundances changed little between September and March/April.

The diversity and variability of under-ice fauna

The morphology of the ice underside is an important factor for colonization, and the variety of under-ice structures provides a wide range of different microhabitats (Hop et al., 2000;
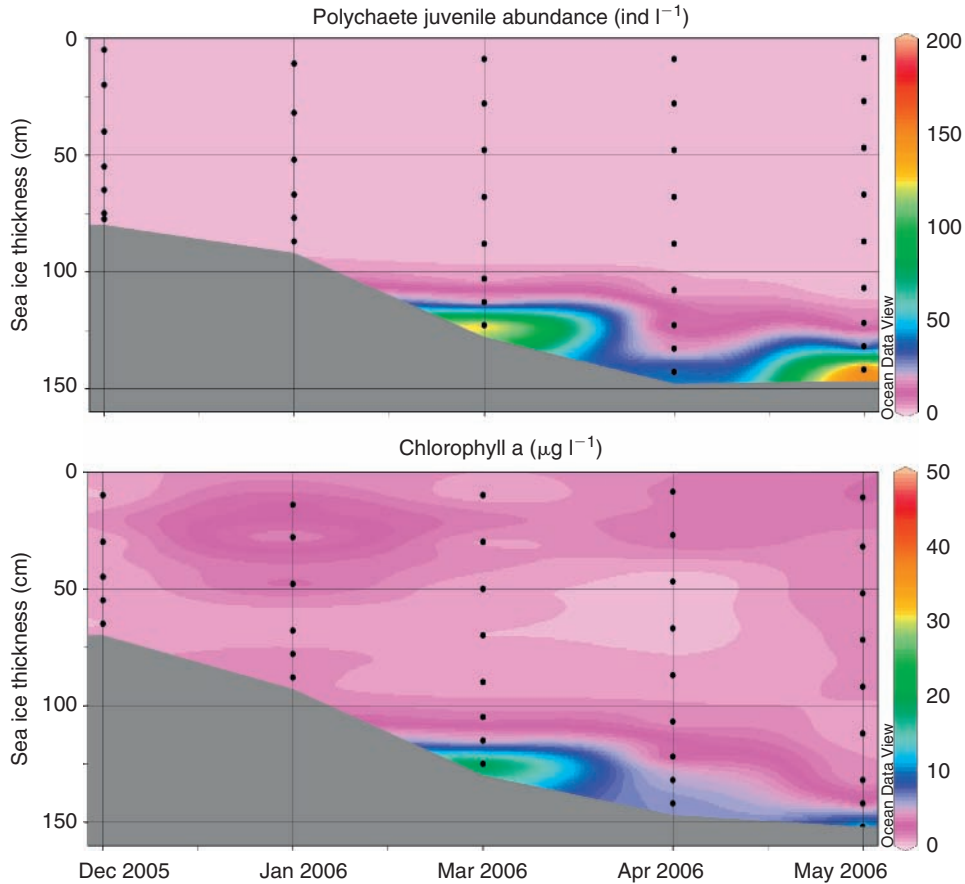
Fig. 10.6 Example for the seasonality in abundance of a temporally sea ice–associated, herbivorous taxon in coastal fast ice: juveniles of the spionid polychaete *Scolelepis squamata*. Black dots represent sampling locations.

Krembs et al., 2001). Small-scale refuges are highly dependent on ice thickness profiles, the prevailing water current direction and speed, and because of this are rather changeable in nature. For example, swarms of the amphipod *Parathemisto libellula* concentrated in hydrodynamically calm regions of pressure ridges and relocated when currents increased (Melnikov, 1997). Large-scale structures such as pressure ridges are in constant evolution because of ice drift and friction. Under level sea ice, areas of hundreds of square metres can exhibit minor thickness changes in the centimetre range with typically small associated variability in the biological properties. In contrast, pressure ridges may include huge complex surfaces of nooks and crannies with changes in ice thickness of several metres. Consequently, the fauna in the sub-ice layer is patchily distributed and their abundance can vary greatly between sampling sites, even on the scales of centimetres to metres (Daly & Macaulay, 1988; Hop et al., 2000; Arndt & Swadling, 2006).

The dominant under-ice macrofauna organisms that live attached to sea ice at least part of the time are euphausiids in Antarctica (Figs 10.2 and 10.7) (O'Brien, 1987; Nicol, 2006)
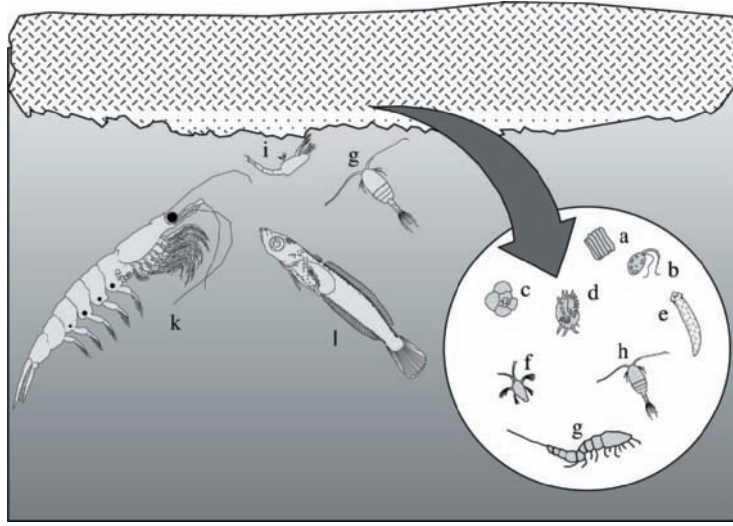
Fig. 10.7   Food web in the Antarctic pack ice. (a) Pennate diatoms; (b) autotrophic flagellates; (c) foraminifera; (d) ciliates; (e) turbellarians; (f) copepod nauplii; (g) harpacticoid copepods; (h) calanoid copepods; (i) euphausiid larvae; (k) adult Antarctic krill; and (l) young notothenoid fish, *Pagothenia borchgrevinki*.

and gammarid amphipods in the Arctic (Fig. 10.1) (Beuchel & Lønne, 2002; Macnaughton et al., 2007). Within the euphausiids, *Euphausia superba* and, to some extent, *Euphausia crystallorophias* are important members of the Antarctic sub-ice community. SCUBA and ROV (remotely operated vehicles) observations revealed dense swarms of these species at the ice–water interface region, feeding on ice-algal biomass (O'Brien, 1987; Marschall, 1988) specifically in winter and early spring, when phytoplankton abundances are still low. *E. superba* occurs directly at the undersurface of the ice in densities between 1 and 100 individuals m^{-2} or in free-swimming aggregations in the water column directly beneath the sea ice, while *E. crystallorophia*s occurs in swarms of 100 to greater than 10,000 individuals m^{-3} mainly in the water column 1–5 m below the sea ice (O'Brien, 1987). We are unaware of published reports of Euphausiids found in association with Arctic ice although our recent observations (spring 2008) for *Thysanoessa raschii* from the Bering Sea suggest euphausiids may actually be very abundant under sea ice, at least in that area (Gradinger et al., unpublished).

Gammarid amphipods are the dominant members underneath Arctic sea ice where they occur in abundances of less than 5 to greater than 100 individuals m^{-2} (Carey, 1985, 1992; Poltermann, 1997; Werner, 1997; Gradinger & Bluhm, 2004; summary tables in Hop et al., 2000 and Arndt & Swadling, 2006). Dominant species in offshore pack ice include *Apherusa glacialis*, *Gammarus wilkitzkii*, *Onisimus nanseni* and *O. glacialis* and in nearshore areas include *O. litoralis*, *Gammarus setosus*, *Gammaracantus loricatus* and others (Table 10.2) (Arndt & Swadling, 2006).

The few available studies on pressure ridges observed higher abundances associated with pressure ridges versus level sea ice (Hop et al., 2000; Gradinger et al., submitted). Carey (1985) distinguished five different amphipod associations in the Arctic ranging from near-shore regions (both fast ice and pack ice), where benthic species like *Onisimus litoralis* frequent the under-ice habitat to ice endemic species associations formed by authochthonous

Table 10.2 Dominant metazoan species found in the ice–water interface including the under-ice (mostly amphipods and euphausiids) and sub-ice (mostly copepods and fish) faunas.

Taxon	Arctic	Antarctic
Calanoid copepods	*Pseudocalanus* sp., *Calanus glacialis*	*Stephos longipes, Paralabidocera antarctica*
Harpacticoid copepods	*Halectinosoma finmarchicum, Tisbe* spp., *Harpacticus superflexus*	*Drescheriella glacialis, Ectinosoma* sp., *Idomene antarctica, Diarthrodes* cf. *lilacinus*
Cyclopoid copepods	*Cyclopina schneideri, Oithona similis, Oncaea borealis*	*Oithona similis, Oncaea curvata*
Euphausiids	*Thysanoessa raschii*	*Euphausia superba, E. crystallorophias*
Gammarid amphipods	*Aperusa glacialis, Gammarus wilkitzkii, Onisimus nanseni, O. glacialis, O. litoralis, Gammaracantus loricatus, Ischyocerus anguipes, Weyprechtia pinguis, Eusirus holmii*	*Paramoera walkeri, Cheirimedon foungeri, Pontogoneia antarctica, Eusirus antarcticus, E. laticarpus, Orchomene plebs, Probolisca* sp.
Other invertebrates	Meroplanktonic stages of polychaetes, bivalves, echinoderms; turbellarians, ctenophores	Turbellarians, ctenophores (*Callianira antarctica*), gastropods
Fish	*Boreogadus saida, Arctogadus glacialis*	*Pagothenia* (= *Trematomus*) *borchgrevinki, Dissostichus mawson*

Source: Richardson and Whitaker (1979); Carey and Montagna (1982); Cross (1982); Conover et al. (1986); O'Brien (1987); Runge and Ingram (1988); Waghorn and Knox (1988); Gulliksen and Lønne (1989); Grainger and Hsiao (1990); Gulliksen and Lønne (1991); Carey (1992); Menshenina and Melnikov (1995); Schnack-Schiel et al. (1995); Tanimura et al. (1996); Poltermann (1997); Siferd et al. (1997); Kiko et al. (2008a); Krapp et al. (2008); Gradinger et al., personal observation)

species (e.g. *Gammarus wilkitzkii* and *Apherusa glacialis*) existing in the multiyear sea ice regions (Cross, 1982; Carey, 1985; Poltermann, 1997; Siferd et al., 1997; Werner, 1997; Gradinger & Bluhm, 2004).

Gammarid amphipods have also been found locally in high concentration (up to about 13,000 individuals m^{-3}) in Antarctica, both at under ice surfaces in shallow (Andriashev, 1968; Richardson & Whitaker, 1979; Gulliksen & Lønne, 1991; Günther et al., 1999) and deep waters. In deeper Antarctic waters, six under-ice amphipod species were recorded in the Weddell and Lazarev Seas where *Eusirus antarcticus* and *E. laticarpus* were most numerous (Krapp et al., 2008). *Eusirus antarcticus* and *E. tridentatus* were observed in abundances of 0–70 individuals m^{-2} in both the ice surface community and the ice water interface (Kiko et al., 2008a). Hyperiid amphipods have only rarely been found beneath sea ice at either pole. A notable exception is *Parathemisto libellula*, which is probably not a true sympagic species, but occurs regularly in low numbers on the undersides of Arctic ice (Gulliksen & Lønne, 1991; Melnikov, 1997).

Copepods can be highly concentrated directly under the ice both in the Arctic and Antarctica (Conover et al., 1986; Schnack-Schiel et al., 1995, 1998; Tanimura et al., 1996; Kiko et al., 2008a). The calanoids *Stephos longipes* and *Paralabidocera antarctica* and the harpacticoids *Drescheriella glacialis*, *Ectinosoma* sp., *Idomene antarctica* and *Diarthrodes* cf. *lilacinus*, which are dominant within Antarctic sea ice (Table 10.2), are also abundant members of the sub-ice fauna in the Antarctic (Table 10.2; Schnack-Schiel et al., 1998; Swadling

et al., 2001; Kiko et al., 2008a). Other copepod species, such as the calanoid *Ctenocalanus citer*, the cyclopoids *Oithona similis, Pseudocyclopina belgicae* and *Oncaea curvata*, as well as other harpacticoid species, are also occasionally captured near the sea ice–water interface (Menshenina & Melnikov, 1995; Günther et al., 1999; Swadling et al., 2001; Kiko et al., 2008a). In one Antarctic study, nauplii of cyclopoid copepods were most abundant (up to 2390 individuals m^{-3}) followed by several pelagic crustacean taxa (Kiko et al., 2008a).

In the Arctic, the calanoids *Pseudocalanus* sp., *Calanus glacialis* and various nauplii have been collected in high concentrations in the water directly adjacent to the ice undersurface (Conover et al., 1986). The small copepods *Acartia longiremis* (calanoid) and *Oithona similis* (cyclopoid) occur in variable numbers, although regularly, at the ice–water interface (Runge & Ingram, 1988; Conover et al., 1990; Werner & Martinez-Arbizu, 1999). Total abundance of Arctic sub-ice fauna is on the order of 200–30,000 individuals m^{-3} (Werner & Martinez-Arbizu, 1999). An extensive review of all crustacean species collected in or under Arctic and Antarctic sea ice is given by Arndt and Swadling (2006).

At times, siphonophores, ctenophores, appendicularians, chaetognaths, mysids and the pelagic polychaete *Tomopteris carpenteri* have also been reported in significant numbers in the sea ice–water boundary layer (Gulliksen & Lønne, 1989; Menshenina & Melnikov, 1995; Kiko et al., 2008a; Purcell et al., in press). High numbers of benthic invertebrate larvae, such as cirripede nauplii, can seasonally inhabit the underside of sea ice in shallow areas in the Arctic (Conover et al., 1990).

In the Arctic, the arctic cod (*Boreogadus saida*) and the glacial cod (*Arctogadus glacialis*) live in close association with the ice underside (Carey, 1985; Melnikov, 1997). Young arctic cod utilize cavities and narrow wedges of sea water along the edges of melting ice floes (Carey, 1985; Gradinger & Bluhm, 2004; Fig. 10.1), whereas older specimens of *B. saida* are only rarely found just beneath the ice (Gulliksen & Lønne, 1989). Observed school sizes of *B. saida* associated with sea ice were small (one to a few dozens; Gradinger & Bluhm, 2004; Iken et al., unpublished), but it is unclear if the huge schools occurring during the open water season (Welch et al., 1993) also utilize the under-ice habitat. In the Antarctic, swarms of young and adult broadhead fish, *Pagothenia borchgrevinki* and young giantfish *Dissostichus mawsoni* live immediately under the ice (Andriashev, 1968).

Platelet ice

Platelet ice layers form a unique ice habitat, found mainly along the Antarctic coast underlying fast ice adjacent to ice shelves, and only seldom found underlying pack ice (Thomas, 2004). These layers consist of accumulations of disc-shaped plates of ice ranging from a few centimetres up to 20 metres in thickness. The loose platelets trap interstitial sea water between the ice plates, and owing to the turbulence of the underlying water, the interstitial water is exchanged periodically. Hence, temperature and salinity are similar to the underlying sea water. The surfaces of platelets are irregular, providing extensive surfaces for bacteria and phytoplankton growth, and dense ice-algal blooms can occur within these layers (Dieckmann et al., 1992). The Antarctic platelet ice is the most productive sea ice habitat, and harbours chlorophyll *a* concentrations up to greater than 1000 mg chl *a* m^{-2}, more than two times greater than that reported for any other sea ice type either in the Arctic or the Antarctic (Chapter 8).

The standing stock of algae and bacteria within sea ice provides a valuable food source for zooplankton, especially during times of the year when food in the water column is severely

limited. However, the association of metazoans with platelet layers is not yet clearly under-
stood, and evidence for their occurrence and significance is somewhat controversial. Several
investigators did not find metazoans in platelet ice layers (Smetacek et al., 1992; Arrigo
et al., 1995; Grossmann et al., 1996). In contrast, around 30 species, mainly copepods, were
found in platelet layers in the Ross and Weddell Seas (Waghorn & Knox, 1988; Günther
et al., 1999; Schnack-Schiel et al., 2004, Guglielmo et al., 2007). Species numbers were parti-
cularly high in platelet ice layers at Drescher Inlet, eastern Weddell Sea, including species new
to science (Günther et al., 1999; Gleitz, personal communication and video). Crustaceans,
mainly copepods, were the most numerous and diverse group in that study, with harpacti-
coids contributing most species (16). The most abundant species were the same commonly
found in sea ice cores from the Weddell Sea, *Drescheriella glacialis* and *Stephos longipes*,
confirming the match of high abundance of *S. longipes* in ice and platelet layers elsewhere in
the eastern Weddell Sea (Kurbjeweit et al., 1993; Schnack-Schiel et al., 1995).

Eggs and larval stages of the Antarctic silverfish *Pleuragramma antarcticum* occur in pla-
telet ice at Terra Nova Bay in spring. The stomach of the larvae contained large quanti-
ties of the ice-associated copepods *S. longipes* and *Harpacticus furcifer*. Hence, the platelet
layer also provides a breeding and nursery ground for *P. antarcticum* (Vacchi et al., 2004;
Guglielmo et al., 2007).

High ammonium concentrations, up to ~200 μM, are reported from numerous sea
ice types, including platelet ice and slush ice layers (Chapter 12). These high values are
particularly remarkable since the surface sea water values are generally less than 1 μM in
ice-covered regions. A highly significant correlation between ammonium values (up to 9 μM)
and total copepod abundance in the platelet ice at Drescher Inlet in February 1998 supports
the hypothesis that zooplankton excretion can at least partly be responsible for the high
ammonium values in platelet ice (Schnack-Schiel et al., 2004). This source of regenerated
nitrogen, in turn, may be a preferential nitrogen source for photo-autotrophs within the
ice and has been suggested as one of the reasons for high standing stocks of algae accumu-
lating within the sea ice matrix (Dieckmann et al., 1992; Thomas et al., 1998). This pos-
sibility has been especially stressed since modelling of nitrogen uptake by sea ice diatoms
clearly indicates that nitrate within the matrix is not enough to sustain massive algal growth
(Kennedy et al., 2002). This hypothesis is an alternative to the idea that the absence of
grazers causes the high algal biomass (Smetacek et al., 1992). The role of metazoan excre-
tion is probably an important pathway in the biogeochemical cycling of nitrogen within the
sea ice.

Sampling the sea ice community

A wide range of sea ice types and structures, depending on different growth processes, occur
over the course of the year and in different regions. This, combined with the inherent differ-
ences of the in-ice, under-ice and sub-ice habitat and the substantial size range of sympagic
taxa (from micrometres to centimetres) makes adequate and standard sampling procedures
difficult and requires a set of techniques if all subhabitats are to be sampled (Gradinger &
Bluhm, in press). Patchiness of biota at any given location can be extreme even (reviewed
by Brierley & Thomas, 2002; Steffens et al., 2006) and is closely linked to environmental
parameters like ice thickness, snow depth, algal biomass etc. An adequate, typically high
number of replication and spatial resolution are necessary to study such high levels of spatial

heterogeneity. Coupled with this is the challenge of year-round sampling needed to understand the role of seasonal sea ice changes in the life cycles of sympagic heterotrophs.

Fast ice and coastal pack ice can be sampled from land bases. Offshore pack ice is, however, difficult to access and requires an ice-going research vessel, drifting ice camps and/or air support. Sampling of the organisms inside sea ice is carried out using standard ice-coring techniques with a barrel-type corer (Horner et al., 1992), typically of the types SIPRE (Snow, Ice and Permafrost Research Establishment) or CRREL (Cold Regions Research and Engineering Laboratory). Cores of a known diameter (around 10 cm) are typically sectioned into pieces, melted with the addition of filtered sea water to avoid osmotic shock and lysis (Garrison & Buck, 1986) and analysed after concentration over gauze of various mesh sizes (depending on target group). Densities are then reported per square metre or per cubic metre, often only for layers that contained dense ice-algal concentrations.

A general problem is to retain brine and interstitial organisms associated with the bottom layer of the ice during extraction of the core to the ice surface, in particular when coring porous and rotten ice with large brine channels or pockets. Care has to be taken to avoid brine drainage and contamination with sea water although these losses are inevitable with current techniques. Close attention also needs to be paid to the careful sampling of highly porous sea water-filled gaps and voids that can occur within the ice mainly at or just below the water level (Schnack-Schiel et al., 2001b; Kattner et al., 2004). These freeboard layers can contain considerable metazoan biomass, and can only be sampled by carefully coring the overlying ice and sampling the gap water by immersing sampling devices into the gap layer.

The under-ice fauna is best sampled by optical techniques including submerged camera systems and by SCUBA divers and pumps (Horner et al., 1992; Hop et al., 2000; Gradinger & Bluhm, 2004; Gradinger et al., submitted). A diverse set of tools are used by divers: Fauna can be 'vacuumed' with an electrical suction pump (Lønne, 1988) from a set area using sampling quadrates place on the underside of the ice. Alternatively, fauna gets counted in those quadrates *in situ* with representatives of all species occurring collected in mesh bags (Gradinger et al., submitted). During counts and suctioning, divers do not exhale to avoid dislocation or disturbance caused by air bubbles. Alternatively, divers record video transects under the ice with a scale included in the imagery, though species identifications are less accurate from video than *in situ* counts or collections (Gradinger & Bluhm, 2004). Other investigators deployed stationary video instrumentation through an ice hole (Werner & Gradinger, 2002), resulting in reasonable abundance estimates limited to a small area. Metazoans can also be sampled through a core hole by using pumps (Schnack-Schiel et al., 1998; Werner & Martinez Arbizu, 1999; Kiko et al., 2008a) and small gear such as the NIPR-I sampler in which water is sucked into the sampler by a current caused by a rotating propeller and collected by the net attached to the sampler (Tanimura et al., 1996). The 'Surface and Under Ice Trawl' (SUIT) is a new development, which just has been deployed in Antarctica. It is towed sideways of a ship, allowing to sample under undisturbed ice at a distance of about 150 m from the water channel produced by the towing vessel (Krapp et al., 2008). Under-ice nets are used by Arctic native peoples and researchers to fish for ice-associated fish (Hill et al., 1996). The boundary layer between the sea ice and the underlying water gets disturbed to some extent during any deployment of gear, making high vertical resolution of sampling difficult.

Besides scuba divers, ROV and autonomous underwater vehicles (AUVs) are increasingly useful tools for the direct observations of the under-ice environment. These vehicles can be equipped with video cameras, upward-looking sonar, radiometers and other sensors and

have, for example, been used to characterize under-ice topography and estimate Antarctic krill abundance (Hop et al., 2000; Brierley & Thomas, 2002).

10.3 Biochemical adaptations

Ectothermic invertebrates and most fish have body temperatures corresponding to ambient temperature. If the ambient temperature drops below the freezing point of the body fluids, the animals face the problem of internal ice formation. Any drop in ice temperature also increases brine salinity in sea ice. Consequently, adaptations to low temperature and high salinity together with freezing resistance are prerequisites for the survival of sympagic organisms in sea ice and influence species diversity (Gradinger & Schnack-Schiel, 1998). In addition, ice fauna is also exposed to seasonal changes in their physical environment as the sea ice melts and freezes. In general, many invertebrates avoid freezing by supercooling, where the body fluids are cooled below the equilibrium freezing point without freezing, or they have the potential to actually tolerate ice formation in their tissues (Aarset, 1991; Waller et al., 2006).

The Arctic amphipod *Gammarus oceanicus* and juveniles of the Antarctic krill *Euphausia superba* survived experimentally freezing into sea ice for several hours, in case of Antarctic krill at temperatures as low as –4°C and a corresponding salinity of 69 (Aarset & Torres, 1989; Aarset, 1991). The Arctic sympagic crustaceans studied to date had slightly higher supercooling points (e.g. –7.9°C for *A. glacialis*; Kiko et al., 2008c) than Antarctic species (e.g. –9.0°C for *E. superba*; Aarset & Torres, 1989), possibly an indication that Antarctic species may have a greater supercooling capacity than those from the Arctic (Aarset, 1991). The Arctic gammarid amphipods *Gammarus wilkitzkii* and *Onismus glacialis* and the Antarctic *Eusirus antarcticus* do not tolerate freezing into solid sea ice.

Another adaptation to thriving in polar seas is the accumulation of large lipid depots that help buffer the strong seasonal variability in food supply. For example, in a study of krill in the Lazarev Sea at the onset of winter, juvenile and adult krill had very high lipid contents of 36 and 44% of their dry mass, respectively (Atkinson et al., 2002). The dominant type of lipid classes indicates certain feeding behaviours (Sargent et al., 1981; Lee et al., 2006). Wax esters are stored as long-term energy reserves, and such wax ester storage is known for many pelagic species that cease feeding in autumn and overwinter in a resting stage. These include the herbivorous Arctic copepods *Calanus hyperboreus* and *C. glacialis*, and the Antarctic *Calanoides acutus* (Kattner & Hagen, 1995; Schnack-Schiel & Hagen, 1995). In contrast, species that continue feeding during the dark season on alternative food sources store mostly triacylglycerols instead of wax esters. Accordingly, ice-associated crustaceans and fish that feed opportunistically and throughout the year are primarily triacylglycerol-storing. Examples include the copepods *Stephos longipes* (Schnack-Schiel et al., 1995), *Paralabidocera antarctica* (Swadling et al., 2000), the euphausiid *Euphausia superba* (Falk-Petersen et al., 2000), and the notothenioid fish *Pagothenia borchgrevinki* (Clarke et al., 1984) in the Antarctic, and the gammarid amphipods *Apherusa glacialis*, *Gammarus wilkitzkii*, *Onismus nanseni* (Scott et al., 1999) and the gadiform fish *Boreogadus saida* in the Arctic (Scott et al., 1999).

One of the most critical requirements at low temperatures is maintenance of functional lipid membranes. The fatty acid composition of membrane phospholipids regulates the degree of membrane fluidity, and the combination of a high proportion of unsaturated fatty

acids, low average chain length and high levels of polyunsaturated fatty acids (PUFAs) are important for retaining membrane fluidity at low temperatures. The amount of PUFAs in ice diatoms increases with decreasing temperature and light intensity and increasing nutrient concentrations (Mock & Kroon, 2002a,b), and can be higher than in phytoplankton (McMahon et al., 2006), making ice algae a valuable and preferred food source compared to phytoplankton. Hence, released ice algae from melting ice in spring are important for herbivores not only in terms of food quantity when phytoplankton biomass is still low, but also because of their high nutritional quality.

Sea ice–related fauna is also exposed to a wide range of salinities that can be higher than 60 in the brine channels during cold temperatures and below 2 at the ice–water interface regions during periods of summer ice melt. The Arctic sympagic amphipods *Gammarus wilkitzkii*, *Onismus glacialis* and *Apherusa glacialis* are hyperosmotic regulators at low salinity values (<30), regulating extracellular concentrations of sodium and chloride in the haemolymph. At higher salinities (>30), they are osmoconformers over the tolerated salinity range (34–60) (Aarset & Aunaas, 1987; Aarset, 1991; Kiko et al., 2008c). The Antarctic sympagic amphipod *Eusirus antarcticus* and juveniles of the Antarctic krill, *Euphausia superba*, are osmoconformers with a much lower salinity range tolerance (26–40 and 25–45, respectively; Aarset & Torres, 1989). Contrary to these findings, adult krill were observed moving from the water column through rotten ice into low-salinity (<15) surface ponds to graze on strands of algae in summer (Schnack-Schiel et al., 2001b; D.N. Thomas, personal communication).

Survival in a supercooled state can result from thermal hysteresis agents in body fluids. In a range of crustaceans from both poles, no such thermal hysteresis agents have been found (Aarset, 1991). Instead, these species were adapted to living in the vicinity of ice by lowered melting points of their body fluids that in turn prevented internal ice formation at low temperatures (Aarset & Aunaas, 1987; Aarset & Torres, 1989; Aarset, 1991; Kiko et al., 2008c). In contrast, various classes of macromolecular antifreezes have been found in polar fish. Almost all teleost fish are hyposmotic to seawater and, hence, the freezing point of the blood of polar species is about 1°C higher than that of the surrounding seawater. All of the macromolecular antifreezes found in fish are proteins (AFPs) or glycoproteins that also have carbohydrate moieties (AFGPs) (DeVries, 1971, 1997; Praebel & Ramlov, 2005). Macromolecular antifreezes lower the freezing point of the solution as efficiently as NaCl, i.e. solutions containing these macromolecular antifreezes exhibit thermal hysteresis and decrease the blood serum's freezing point of many polar fish to approximately −2°C. For *Boreogadus saida*, the hysteresis freezing point is at −3.3°C (Praebel & Ramlov, 2005). The content of antifreeze molecules in a body fluid varies greatly between species and depends upon the habitat of the fish with species living close to sea ice possessing the highest amounts (Jin & DeVries, 2006).

Antarctic notothenioid fish such as the cryopelagic species *Pagothenia borchgrevinki* and *Dissostichus mawsoni* have glycoprotein macromolecules (AFGP), which are composed of repeating tripeptide units. In many non-notothenioid Antarctic fish and most Arctic fish, freezing is inhibited by AFPs. The Arctic cryopelagic gadiforms *Boreogadus saida* and *Arctogadus glacialis* have, however, glycoproteins similar in structure to the Antarctic ice-associated fish, posing interesting questions on molecular evolution of such compounds (Enevoldsen et al., 2003). In Antarctic fish, antifreeze glycopeptides are synthesized year-round, whereas in Arctic fish, where summer water temperatures can be well above

freezing, the synthesis of antifreeze molecules often occurs only during winter (Cheng & DeVries, 1991; DeVries, 1997; Wöhrmann, 1997). The Antarctic *P. borchgrevinki* decrease their AFGP concentrations in response to warm acclimation. After 16 weeks acclimation at +4°C, the total AFGP level decreased by 53% (Jin & DeVries, 2006).

Only recently, thermal hysteresis was also detected in the sympagic nudibranch *Tergipes antarcticus* (Kiko et al., 2008b) and in the ice-associated calanoid copepod *Stephos longipes*. The latter is the first report of thermal hysteresis activity for a crustacean (Kiko, 2009). Thermal hysteresis was not observed in a second species of ice-associated calanoid copepod, *Paralabidocera antarctica* (Kiko, 2009). The difference between the two copepods is probably due to the difference in their distribution patterns. *S. longipes* occurs throughout the sea ice inhabiting all habitats including refrozen gaps and surface layers (Schnack-Schiel et al., 2001b; Kiko et al., 2008a). This species, therefore, has to be adapted to strong gradients in temperature and salinities. In contrast, *P. antarctica* occurs preferentially in the lowermost parts of the sea ice where temperature and salinities are similar to those of the open water (Kiko, 2009). In *S. longipes*, two isoforms of an ice-active protein were found (Kiko, 2009). The author suggests that due to the high homology to ice-binding proteins from sea ice diatoms, bacteria and a mold, *S. longipes* obtained the gene through horizontal gene transfer.

10.4 Sea ice as a feeding ground

Sea ice fauna is the primary consumer of the organic carbon produced by sea ice algae during periods of ice cover. The fauna, in particular the under-ice taxa, also plays a major role as mediator between sea ice and pelagic and benthic habitats in at least two aspects. First, under-ice fauna produces faecal pellets that can contribute to the carbon flux from the ice into the plankton and benthos (Carey & Boudrias, 1987; Werner, 2000; Michels et al., 2008) and second, it is important food for higher trophic levels like birds, fish and seals (Bluhm & Gradinger, 2008). Consequently, sea ice fauna is important to the food web of the ice-covered oceans (Chapter 11).

Relatively little is actually known about the nutrition and carbon consumption by metazoan in-ice fauna. Grainger and Hsiao (1990) studied the stomach content of 16 Arctic ice meiofauna taxa in the spring including turbellarians, nematodes, rotifers, polychaetes, copepod nauplii and various harpacticoid copepods and concluded, on the basis of the dominance of diatoms as identifiable particles, that most taxa were mainly herbivorous. Stable isotope work confirms the dominance of herbivory for turbellarians, juveniles of the polychaete *Scolelepis squamata* and harpacticoid copepods but a second unidentified hesionid polychaete species and copepod nauplii had more enriched δ^{15}N signatures, suggesting feeding on a higher trophic level (Bluhm & Gradinger, unpublished).

Tchesunov and Riemann (1995) suggested that Arctic ice nematodes ingest dissolved organic material as the authors did not observe any particles in the guts of the nematodes studied. Nematodes might also consume other exudates like EPS, which can occur in high concentrations in sea ice (Krembs & Deming, 2008; Meiners et al., 2008). The ice endemic nematodes' closest relatives live in the baleen of whales, where they likely also live on ingestion of DOM. A recently discovered new sea ice hydroid is likely carnivorous and potentially the top predator within the Arctic brine channel network (Bluhm et al., 2007; Siebert

et al., 2008). The Antarctic ctenophore *Callianira antarctica* is also a predator feeding on krill under sea ice (Hammer et al., 1989; Hammer & Hammer, 2000; Scolardi et al., 2006).

Although sea ice meiofauna can be very abundant, estimates of their impact on the ice-algal standing stock and production, based on the application of size specific allometric equations, suggest that as little as 1% of the ice-algal stock and less than 10% of the daily ice-algal production are consumed and that ice meiofauna, therefore, does not appear to limit ice-algal production in the Arctic or Antarctic (Gradinger, 1999; Nozais et al., 2001; Michel et al., 2002; Gradinger et al., 2005). However, recent feeding experiments have shown that the ingestion rates of the Antarctic ice copepods *Stephos longipes* and *Drescheriella* spp. feeding on ice protists were very high, with ingestion rates varying between less than 1 and 74 ng Chl *a* µg C^{-1} d^{-1} and 2 and 133 ng Chl *a* µg C^{-1} d^{-1}, respectively, depending on the food concentration and the copepod developmental stages (Michels & Schnack-Schiel, unpublished). The estimated gazing impact was extremely high, reaching a maximum population impact of 31.4% of the ice algae stock per day in the infiltration layers.

Various under-ice taxa also take advantage of the high ice-algal biomass, providing a densely packed food source when phytoplankton concentrations are low in the spring. The Antarctic amphipod *Pontogeneia antarctica* and the Arctic amphipod *Apherusa glacialis* are predominately herbivorous, feeding mainly on ice algae (Richardson & Whitaker, 1979; Werner, 1997; Nicol, 2006). In contrast, detritus–algae aggregates that develop at the ice underside, together with animal remains, are probably the major food source for the more omnivorous Arctic species *Onismus nanseni* and *O. glacialis* (Poltermann, 1997; Werner, 1997). The nearshore amphipod *Onismus litoralis* almost exclusively feeds on ice algae when they are abundant, but switches to other food sources later in the year (Carey & Boudrias, 1987; Gradinger & Bluhm, 2005). Although ice algae have been found in the guts of the Antarctic *Paramoera walkeri* and the Arctic *Gammarus wilkitzkii*, these species clearly exhibit predatory behaviour. Under fast ice, *P. walkeri* actively preyed on the newly hatched young of *Pontogeneia antarctica*. Gut content studies and fatty acid markers of *G. wilkitzkii* also revealed strong preference mainly for crustaceans (Gulliksen & Lønne, 1989; Scott et al., 1999; Werner et al., 2002) and even cannibalism was documented (Poltermann, 1997).

The calanoids *Pseudocalanus* sp., *Calanus glacialis* (Arctic), *Paralabidocera antarctica* and *Stephos longipes* (Antarctic) graze heavily on ice algae, the latter two species within ice floes as well as underneath the ice (Conover et al., 1986; Hoshiai et al., 1987; Runge & Ingram, 1988; Schnack-Schiel et al., 1995; Guglielmo et al., 2007). *C. glacialis* and *Pseudocalanus* spp. migrate to the ice water interface for feeding on ice algae during night-time, likely to minimize predation pressure during day hours (Fortier et al., 2001). Experiments have shown size-selective feeding in *S. longipes* and *Drescheriella* spp. with preferential grazing on small-sized protist species (>30 µm) such as *Fragilariopsis cylindrus*, *F. curta*, *Cylindrotheca closterium*, *Phaeocystis antarctica* and small dinoflagellates (Michels & Schnack-Schiel, unpublished).

The two Antarctic ice-associated euphausiids, *Euphausia superba* and *E. crystallorophias*, seem to exploit different food sources under the ice. They also differ in the major depot lipids they produce: *E. superba* stores triacylglycerols while *E. crystallorophias* stores wax esters (Falk-Petersen et al., 2000; Ju & Harvey, 2004). During summer, the main food resource of *E. superba* is phytoplankton, while in winter both omnivorous/carnivorous feeding in the water column and scraping off sea ice algae from the ice underside has been reported (O'Brien, 1987; Marschall, 1988; Daly, 2004; Nicol, 2006). In contrast, *E. crystallorophias*

Table 10.3 Relation of body size of *Pagothenia borchgrevinki* and its food items.

Length	Food item
5 cm	Copepods, small amphipods, ostracods
5–10 cm	Calanoid copepods, amphipods, euphausiids
10–15 cm	Calanoid copepods, amphipods, euphausiids
>15 cm	Amphipods, euphausiids, gastropods and smaller fish

Source: Andriashev (1968); Gulliksen and Lønne (1991).

has never been observed scraping algae off the ice underside. Detrital material derived from ice algae and sinking faecal pellets from other sympagic animals are probably a major food source for this species (O'Brien, 1987; Falk-Petersen et al., 2000). In winter, high levels of 20:1 and 22:1 fatty acids, typical for calanoid copepods, indicate also a carnivorous diet of *E. crystallorophias* at this time (Nicol et al., 2004). Recent observations (March/April 2008) suggest that the common Arctic euphausiid *Thysanoessa raschii* may feed on ice-algal matter under first-year ice in the Bering Sea (Gradinger et al., unpublished).

The Arctic sea ice–associated fish, *Boreogadus saida*, is an opportunistic feeder in the sub-ice habitat, eating a wide range of food items including copepods and the hyperiid amphipod *Parathemisto libellula* under first-year ice, and various gammarid amphipod species except *Gammarus wilkitzkii* under multiyear ice. *G. wilkitzkii* is probably avoided because of its large size coupled with the spiny morphology (Gulliksen & Lønne, 1989). Much like *B. saida* in the Arctic, the circumantarctic nothothenioid fish, *Pagothenia borchgrevinki*, utilizes the under-ice habitat as both a feeding ground and a refuge from predators (Gulliksen & Lønne, 1991). *P. borchgrevinki* is probably amongst the most important carnivores to feed on the metazoans of the accessible Antarctic ice assemblages. The diet of *P. borchgrevinki* becomes more diverse with increasing body size of the fish (Table 10.3).

In summary, the seasonally high biomass within the sea ice as well as at the ice–water interface clearly serves as food for the larger metazoan grazers and is a key food source in early spring when algal concentrations in the water column below are scarce.

10.5 Colonization of sea ice and life history cycles

There are several mechanisms by which metazoans may be incorporated into sea ice:

(1) Planktonic organisms maybe trapped during frazil ice formation in the upper metres of the water column (Garrison et al., 1983).
(2) Ice platelets, only occurring regularly in Antarctica, formed at great water depth and often in large quantities, potentially act as vectors for lifting organisms from the depths to overlying waters (Dieckmann et al., 1986).
(3) Benthic species may be lifted up with anchor ice formed on the sea bottom as found in shallow waters in McMurdo Sound (Dayton et al., 1969).

(4) Sea ice turbellarians and nematodes could attach to free-swimming migrating inverte-brates such as crustaceans and use these animals as vectors to arrive at or leave the ice habitat (Riemann & Sime-Ngando, 1997; Janssen & Gradinger, 1999).

(5) Metazoans may migrate to existing ice, simply by moving into large brine channels with seed populations coming from other sea ice, the pelagic or benthic realms.

While these mechanisms are plausible means for the colonization of ice in shallow waters, it still remains a mystery as to how ice overlying water several thousand metres deep is colo-nized by metazoans with relatively poor swimming abilities (Brierley & Thomas, 2002).

When the sea ice melts in summer, organisms are released into the water column. In seaso-nal sea ice regions, ice fauna therefore must tolerate rapidly changing environmental conditi-ons and undergo or tolerate a pelagic or benthic period as part of their life cycles. However, although nematode and turbellarian species are able to swim, no genuinely planktonic life stages of these taxa have been found in polar seas, and how or if they survive the ice-free periods is unknown. For ice endemic Arctic taxa like under-ice amphipods, it is still under discussion whether they can maintain their buoyancy in the water column for extended peri-ods during the summer melt or whether they sink to the sea floor (Werner et al., 1999).

Owing to major differences in sea ice formation, age and structure, the number of taxa with an autochthonous life history is greater in the Arctic compared to the Antarctic (Gulliksen & Lønne, 1991). Both sexes and all developmental stages of the Arctic gammarid species *Gammarus wilkitzkii*, *Apherusa glacialis*, *Onismus nanseni* and *O. glacialis* as well as the mysid *Mysis polaris* have been found under sea ice (Gulliksen & Lønne, 1991). The listed gammarids are endemic to sea ice and evidently require multiyear ice to successfully complete their life cycles (Gulliksen & Lønne, 1991; Poltermann, 1997; Werner, 1997; Pol-termann, 2000; Poltermann et al., 2000; Beuchel & Lønne, 2002). Other Arctic sea ice fauna such as the nearshore amphipod *Onismus litoralis* and larvae/juveniles of benthic fauna are allochthonous. Likewise, the ice-associated metazoans in the Antarctic are probably allo-chthonous in their majority. The life cycle of sea ice-related fauna is correlated with the seasonal growth and melt dynamics in sea ice cover. For instance, when the sea freezes, the Antarctic amphipods *Paramoera walkeri* and *Pontogeneia antarctica* migrate from the seabed, their summer habitat, to the sea ice undersurface. Here, hatchlings are released and the next generation is protected in the bottom skeletal ice layers of floes (Rakusa-Suszczew-ski, 1972; Richardson & Whitaker, 1979). Truly autochthonous species in the Antarctic seem to be the nudibranch *Tergipes antarcticus* and the harpacticoid copepod *Drescheriella glacialis* since all developmental stages occur concurrently within the ice (Dahms et al., 1990; Swadling, 2001; Kiko et al., 2008b). In the following, we provide examples demonstrating this close connection to sea ice for several sympagic copepods and a benthic invertebrate.

Case studies: Life cycles of three ice-associated Antarctic copepods and an Arctic polychaete

The life cycles of the three dominant ice-associated Antarctic copepod species (*Stephos lon-gipes, Paralabidocera antarctica* and *Drescheriella glacialis*) show close ties to sea ice forma-tion and temporal evolution. However, the links between survival and/or life history strategy, and the seasonal sea ice cycle, are very different for these three species.

Stephos longipes is a small neritic calanoid copepod with a generally circumantarctic dis-tribution, with higher numbers found in the Weddell, Bellingshausen and Amundsen Seas

compared to the Indian Ocean sector (Schnack-Schiel et al., 1995, 1998; Swadling et al., 2001). *S. longipes* is adapted to live in all different sea ice habitats, including surface ponds, gap water, sea ice proper, sub-ice layer and platelet ice (Schnack-Schiel et al., 1995, 1998, 2008; Guglielmo et al., 2007; Kiko et al., 2008a). In winter and spring, *S. longipes* mainly inhabits the lowermost regions of ice floes and the ice–water interface, where it may reach abundances up to five orders of magnitude greater than those in the underlying water column (Schnack-Schiel et al., 1995). In porous rotten sea ice that is easily accessible and occurs mainly from late spring to early autumn, *S. longipes* is distributed throughout the sea ice thickness as well as in the surface and the sub-ice layers. The mean abundance of *S. longipes* in the sea ice varies between less than 1 and 55 ind. l^{-1} depending on region and season, with lowest values in the eastern Weddell Sea in summer and highest in spring at Terra Nova Bay. Nauplii outnumber copepodids and adults in the sea ice and account for between 43% and 100% of the total population (Schnack-Schiel et al., 1995, 1998, 2001b, 2008; Guglielmo et al., 2007). Nauplii dominate the population also in surface layers (52% and 94% of the total) (Schnack-Schiel et al., 2001b; Kiko et al., 2008a). Adults occur in higher numbers in the ice/water interface and in the water column throughout the year (Schnack-Schiel et al., 1995, 1998; Guglielmo et al., 2007), but also in surface layers in spring (Kiko et al., 2008a). The abundance of copepodids in the sea ice and the ice/water interface is low in winter and spring, but reaches relatively equal numbers in summer and autumn with early stages dominating (Kurbjeweit et al., 1993; Schnack-Schiel et al., 1995, 1998).

This distribution pattern suggests that breeding takes place in the surface layers and in the uppermost layers of the water column and that the eggs or nauplii are transported or incorporated into the ice, or that *S. longipes* females attach their sticky eggs directly onto frazil ice crystals or ice platelets (Kurbjeweit et al., 1993; Schnack-Schiel et al., 1995; Kiko et al., 2008a). The nauplii develop to copepodids within the ice. In summer, *S. longipes* is most abundant in the upper-water layers of the water column, where copepodite stages rapidly develop, even though some adults remain in rotten sea ice (Schnack-Schiel et al., 1998). With new ice formation in autumn, *S. longipes* begins to accumulate in the sea ice and at the ice–water interface where it attains abundances comparable to those observed in spring, and again, nauplii and the first copepodite stage dominate in the ice. Late copepodite stages, in contrast, are numerous in mid-water layers. In summary, *S. longipes* has two overwintering stages, a nauplius/first copepodite stage overwintering in the first-year sea ice, and an older population migrating deep into the water column (Fig. 10.8). It is possible that at least a portion of the latter population has a benthic phase in winter, living in or on top of the sediment. Nauplii in sea ice cores had food in their guts in winter, but whether or not the older copepodite stages overwintering near the sediment continue to feed is unknown. Since *S. longipes* stores triglycerols rather than wax esters as energy resources, it likely feeds year-round.

The small calanoid species *Paralabidocera antarctica* is strongly associated with fast ice, mainly in the Indian and Pacific Sector, and occurs in the sea ice for most of the year except summer when this species concentrates just beneath the ice (Tanimura et al., 1996, 2002; Swadling et al., 1997, 2000). In early summer, maturation and mating occur in the ice–water interface, and in late summer eggs are spawned. Resting eggs occur in the sediment until approximately late summer when hatching to nauplia stage NI takes place. With the onset of ice formation in early autumn, the nauplii enter the bottom part of the sea ice. Nauplii develop in the sea ice to NIV, at which stage they stay throughout the winter (>5 months) with slow development. In early spring, the nauplii develop rapidly to early copepodids. As copepodite stage CIV, the population then shifts its habitat again from the sea ice to the
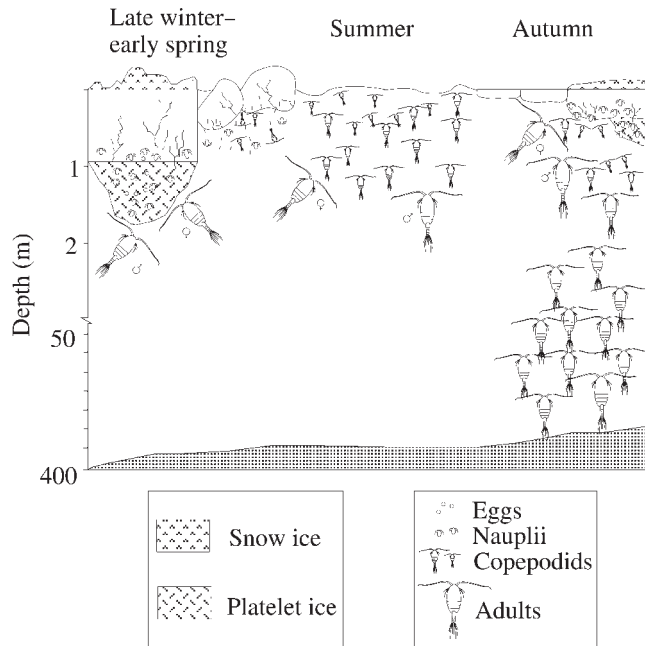
Fig. 10.8 Schematic diagram of the life cycle of the Antarctic calanoid copepod *Stephos longipes*. From Schnack-Schiel et al. (1995).

underlying water (Tanimura et al., 1996). *P. antarctica* utilizes ice algae throughout its life cycle of 1 year, and synthesize almost exclusively triacylglycerols, indicating that it stays active during winter (Hoshiai et al., 1987; Swadling et al., 2000).

All instars (including females with egg sacs) of the dominant harpacticoid *Drescheriella glacialis* (Schnack-Schiel et al., 1998, 2001b; Swadling et al., 2001) are found in the ice, suggesting that this species reproduces and develops within the ice matrix. *D. glacialis* seems to spend most of its life in coastal ice where fast ice is often a perennial feature, although it has also been found in annual pack ice offshore in the northern Weddell Sea (Dahms et al., 1990). In those deep areas, recolonization from the benthos is unlikely. While nauplii of *D. glacialis* are not able to swim, adults and copepodids are and are therefore, capable of surviving in the water column after annual melting of sea ice (Dahms et al., 1990). Since nauplii are poor swimmers, colonization apparently occurs by copepodids and/or adults. *D. glacialis* exploits all sea ice habitats and has a wide distribution within the cores (Schnack-*Schiel* et al., 1998, 2001b). In the western Weddell Sea in spring, adults and nauplii occurred in surface layers in high numbers (maximum 32 and 1280 ind. l^{-1}, respectively), while nauplii and copepodids dominated in the sea ice proper. Adults occur only rarely in the sea ice (Kiko et al., 2008a; Schnack-Schiel et al., 2008). Kiko et al. (2008a) concluded that adults migrate actively to the surface layer using this habitat as breeding and nursery ground.

A second *Drescheriella* species, *D. racovitzai*, can reach high concentrations in the spring ice in the western Weddell Sea (Kiko et al., 2008a; Schnack-Schiel et al., 2008). In contrast to *D. glacialis*, *D. racovitzai* mainly occurs in the lowermost parts of the sea ice and the ice–water interface, where an exchange with the underlying water occurs (Kiko et al., 2008a; Schnack-Schiel et al., 2008). This suggests that *D. glacialis* is better adapted to the low temperature and high salinities within the sea ice than *D. racovitzai*.
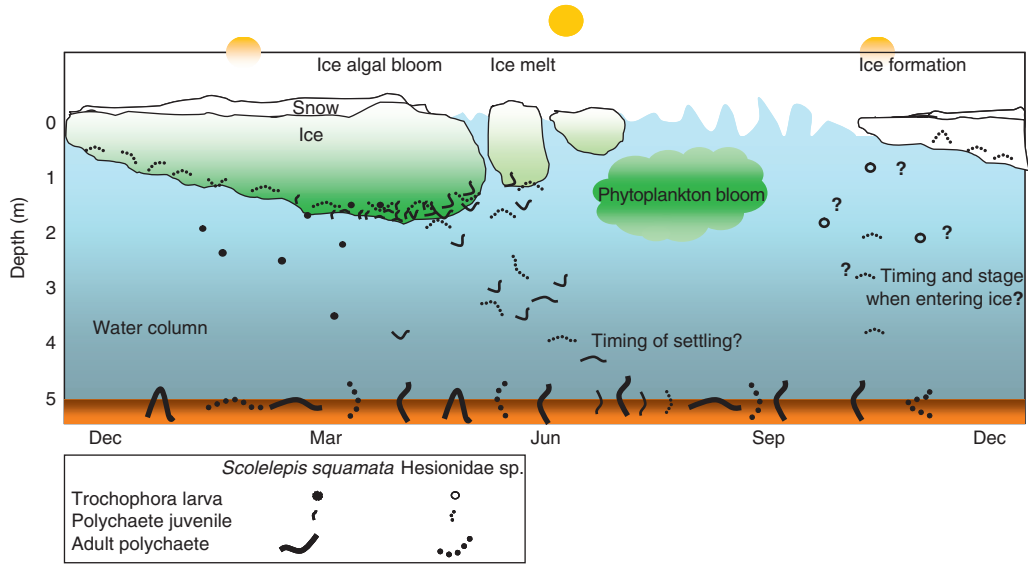
Fig. 10.9 Schematic diagram of the life cycles of two Arctic benthic polychaete species, *Scolelepis squamata* and a hesionid species. The schematic is based on data collected in coastal fast ice in the Alaskan Chukchi Sea (Gradinger & Bluhm, 2005; Bluhm & Gradinger, unpublished).

Two Arctic copepod species, the cyclopoid *Cyclopina schneideri* and the harpacticoid *Tisbe furcata*, found in the annual ice-covered coast of Baffin Island in the Canadian Arctic, have a similar life cycle to *S. longipes*. Both Arctic species occur in the sea ice during winter. After ice melt, only small numbers of the copepods appear in the water column; instead they descend to near the bottom of the water column and live close to the seabed during summer (Grainger, 1991).

In the Arctic, the polychaete *Scolelepis squamata* has a life cycle that is an example of cryo-benthic coupling (Bluhm & Gradinger, unpublished). Juveniles of that species start appearing in coastal fast ice in March at the onset of the algal bloom and feed, likely on ice algae, and grow in the ice until May when ice begins to melt (Fig. 10.9). At that time, they either get released or actively migrate to the sea floor and resume a benthic life style as adults. Densities of *S. squamata* larvae in the water column are orders of magnitude lower than within the ice throughout most of the ice-covered season. Morphological and physiological studies showed that spionid larvae in general are well adapted to feeding on surfaces and are tolerant to various environmental conditions in the Atlantic and North Pacific where the species occurs in high abundances in sandy beaches (Amaral, 1979; Shanks & del Carmen, 1997; Souza & Borzone, 2000; Van Hoey et al., 2004). These traits may have resulted in the species ability to utilize the sea ice habitat for parts of its life cycle.

The role of sea ice for the Antarctic krill, Euphausia superba

The distribution of *Euphausia superba* is primarily restricted to the region covered by ice in winter with a close correspondence between krill abundance and sea ice cover (Brierley & Thomas, 2002). Krill has developed specific behaviour for foraging and predator avoidance

associated with pack ice, both important for overwintering survival (Meyer et al., 2002; Nicol, 2006). Larvae, juveniles and adult krill have all been observed directly beneath sea ice (O'Brien, 1987; Daly & Macaulay, 1988; Marschall, 1988; Hammer et al., 1989; Quetin et al., 1996; Brierley et al., 2002; Daly, 2004), but the degree of association with the sea ice differs between seasons and developmental stages. In spring and summer, adults aggregate at the underside of sea ice (O'Brien, 1987; Marschall, 1988; Quetin & Ross, 1991) as indicated by acoustic surveys (Brierley et al., 2002). During ice melt, they take advantage of the tremendous concentrations of ice algae released from the ice (Huntley et al., 1994). Krill were concentrated within a narrow band under the ice 1–13 km south of the ice edge, and their abundance increased southward of 40% ice concentration (Fig. 10.10). In winter, adults seem not to be tightly coupled to the underside of the sea ice, but prefer the water column in ice-covered regions with highest concentrations near the ice edge (Daly & Macaulay, 1991; Ross et al., 1996).

Foraging and predatory behaviour can explain swarm distribution underneath the ice. Krill concentrate in the vicinity of the keels of pressure ridges and in ice interstices under thick and rafted multiyear ice. In regions of relatively smooth level ice, adult krill swarms are not immediately underneath the ice but in deeper and darker waters. Reasons for this behaviour could be either lower food concentration and/or lack of spatial structure to avoid predation compared to ridge structures. Krill swarms evidently adjust their depth to remain shallow enough to exploit algal standing stocks, but sufficiently deep to avoid visual predators (Quetin & Ross, 1991; Brierley & Watkins, 2000).

Euphausia superba adults have several different strategies for overwintering. They do not depend directly on sea ice algae for winter survival (Quetin et al., 1996; Atkinson et al., 2002), and mostly seem not to move beneath the ice before late winter when sea ice has begun to disintegrate. Lowered metabolic rate (hibernation) is apparently by far the most
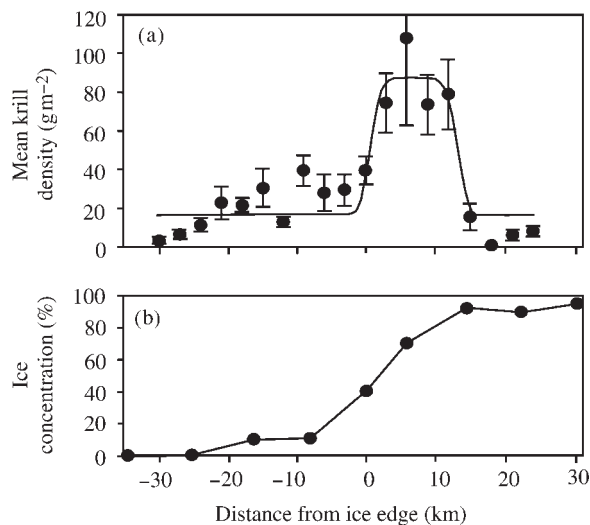
Fig. 10.10 Krill distribution relative to the sea ice edge and ice concentration. (a) Krill density by distance (in 3 km bins, positive is under sea ice) from the local sea ice edge. The line is a highly significant regression function, error bars are ± 1 SEM. (b) Sea ice concentration. Modified after Brierley et al. (2002). Antarctic krill under sea ice: Elevated abundance in a narrow band just south of ice edge. Science 295:1890–1892. Reprinted with permission from AAAS.

important strategy of the adult krill for successfully surviving winter (Quetin & Ross, 1991; Pape et al., 2008). Adults are also capable of surviving long periods of starvation (up to 212 days, Ikeda & Nixon, 1982; Atkinson et al., 2002; Fach et al., 2008) through utilization of body reserves and shrinkage. However, it is uncertain how frequently krill really encounter food shortages sufficient to induce shrinkage in nature (Nicol, 2000). Other overwintering mechanisms include metabolic reduction and lipid depletion (Quetin & Ross, 1991; Hagen et al., 2001; Teschke et al., 2007; Pape et al., 2008), switching to carnivorous feeding on lipid-rich metazoans such as copepods (Huntley et al., 1994; Atkinson et al., 1999, 2002; Ju & Harvey, 2004), and migration down to the seabed (Quetin et al., 1996). Atkinson et al. (2002) report a variety of changes in krill feeding strategies in the autumn including a transition to a non-feeding mode.

The distribution of krill larvae and juveniles is even more closely coupled to sea ice. In winter through spring, krill larvae shift their habitat from the water column to the sea ice to take advantage of ice algae (Daly& Macaulay, 1988; Quetin & Ross, 1991). During this time, food supply in the water column is low and larvae exploit the ice biota to fulfil their metabolic demands (Meyer et al., 2002). Their small size probably allows larvae to take refuge from predation even within seemingly smooth ice surfaces. However, larvae and juveniles, like adults, are more often concentrated in areas around pressure ridge keels, and rafted and/or eroded ice surfaces, which all provide better refuge from predators than level ice (Daly & Macaulay, 1988; Melnikov & Spiridonov, 1996; Frazer et al., 1997).

Krill larvae, unlike adults, do not accumulate large lipid stores during the short summer periods, and therefore can only starve for shorter periods in autumn and winter (Quetin et al., 1996; Fach et al., 2008). Daly (2004) found that furcilia could survive starvation for 1 month by combusting body reserves. Ice-algal assemblages are a vital nutrient resource (Daly, 1990; Hofman & Lascara, 2000) of which young krill can ingest 2–44% of their body carbon per day, covering the metabolic requirements for growth and development (Daly, 1990). However, more recent studies show that furcilia appeared to be food-limited during winter (Daly, 2004; Ross et al., 2004), and larvae were opportunistic, feeding on a variety of items such as phytoplankton, sea algae, microzooplankton and detritus (Daly, 2004). In winters with a great pack ice cover, larval and juvenile krill may be in better physiological condition, have higher growth and development rates and higher survival rates than in winters with low ice cover (Quetin et al., 1996). In summary, the different distribution patterns of adults and larvae during the winter are a result of differences in starvation tolerance coupled with the need to avoid predation.

Interannual changes in krill abundances have been linked to oscillations in sea ice extent (Loeb et al., 1997). Abundance and duration of food availability is evidently greater after winters with a long sea ice cover and a large spatial extent compared to conditions following winters of low and short ice cover. Food availability is not only relevant for the timing of reproduction, but also for the proportion of the population that reproduces and for the number of broods per female. A specific combination of the timing and magnitude of ice biota, ice edge blooms and open water phytoplankton blooms seems to be optimal for meeting the spring and summer food requirements of reproducing female krill (Quetin et al., 1996; Siegel, 2000). Larvae hatching early in summer show a high rate of survival during the feeding and growth season and are well conditioned for their first winter. A second winter of extensive sea ice cover further enhances survival of larvae spawned the previous year as well as promoting early spawning in this generation. Protection from predation in winters with

greater ice cover may also promote high survival rates, and may hence affect krill recruit-
ment and stock size (Loeb et al., 1997; Siegel, 2000).

10.6 Climate variability and change and (potential) consequences to sympagic fauna

Sea ice plays a vital role in the ecosystems of both polar oceans. Therefore, changes in
ice extent and duration will strongly influence their character and percolate all the way to
higher trophic levels. The response of sympagic metazoans to changes in sea ice extent and
character is still poorly understood and may range from species extinctions, shift in habitats
to range extensions (Bluhm & Gradinger, 2008). In the following, we summarize what is
known or can be hypothesized about the effects of sea ice and environmental variability and
change on examples of Arctic and Antarctic sympagic species, on the basis of observed or
predicted changes.

Krill stocks appear to have decreased in the Antarctic Peninsula region since the 1980s
(Siegel & Loeb, 1995; Loeb et al., 1997). Reductions in krill densities have major conse-
quences as krill is the primary food source for a large number of 'higher trophic' species
(Chapter 11), and many investigators consider it a *keystone species* in the Southern Ocean
ecosystem (Quetin et al., 1996). Any decrease in krill abundance will have subsequent effects
on the predators. Many potential links are obvious between sea ice, krill and breeding suc-
cess of krill predators (Brierley & Thomas, 2002 and chapters above). However, krill stocks
display large interannual fluctuations in abundance, and it remains to be proven whether or
not the observed changes in krill demography are simply representative of a high degree of
interannual variability or the beginning of a downward trend (Siegel, 2000).

A close relationship has been documented between krill, the pelagic tunicate *Salpa thomp-
soni* and sea ice extent and duration (Loeb et al., 1997; Siegel, 2000; Atkinson et al., 2004).
Following winters with low sea ice cover, extensive blooms of salps tend to form and krill
recruitment is low. Salps are opportunistic feeders competing with krill for food and salps
exploit the spring phytoplankton bloom, resulting in rapid population growth. Hence, salp
blooms can severely affect the reproduction and survival of krill larvae (Fig. 10.11). In con-
trast, after long periods of extensive sea ice cover that favours krill recruitment and also
induces a delayed seasonal spring phytoplankton bloom, krill outcompete salps.

Owing to the uneven distribution of krill under sea ice, the reduction in persistence of win-
ter sea ice cover does not necessarily directly lead to reductions in krill stocks. Instead, reduc-
tions in krill stock are thought to be proportional to the reduction of ice edge length (Brierley
et al., 2002). The suggested decline of 25% of the area covered by sea ice (De la Mare, 1997)
equates to only a 9% decline in ice edge length. Therefore, the reduction of sea ice cover may
be less responsible for the reduction of krill than previously thought (Brierley et al., 2002).

Another possible but not well-understood factor influencing the apparent decline in
krill populations around the Antarctic Peninsula might be the increased ultraviolet-B (UV-B)
irradiation due to seasonal depletions in atmospheric ozone. Krill have relatively high con-
centrations of absorbing mycosporine-like amino acids, which may act as a natural ultra-
violet (UV) filter system (Karentz et al., 1991). However, krill also have a high frequency
of (T)n arrays in their DNA, which are the primary targets of damage by UV-B irradiation
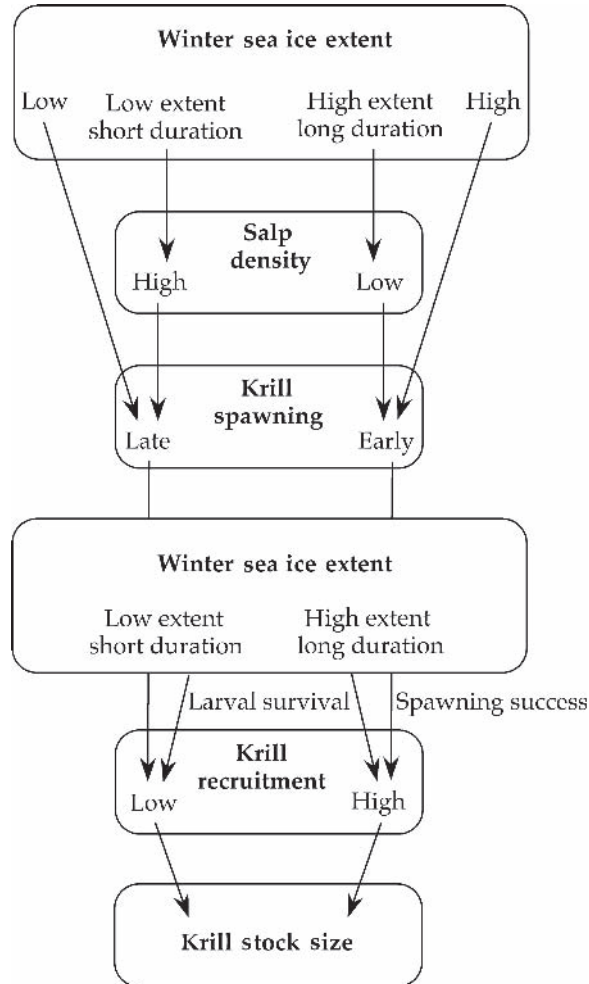
Fig. 10.11 Hypothetic relationship between krill recruitment success and sea ice condition and biological factors (salp abundance, spawning time). Reproduced from Siegel V (2000) Krill (Euphausiacea) life history and aspects of propulation dynamics. Can. J. Fish Aquat. Sci. 57(S3): 130–150. With permission from NRC Research Press.

(Jarman et al., 1999). Ozone depletion could also have other indirect effects as increases to UV-B exposure are likely to also cause changes in phytoplankton, bacterioplankton and protozoan species composition as more tolerant species replace sensitive ones (Brierley & Thomas, 2002). Hence, the ability of krill to exploit a wider range of food sources than competitive organisms will be important for maintaining its dominant role in the Southern Ocean ecosystem.

   The recent changes in Arctic ice conditions appear to support the predicted complete loss of summer sea ice for the Arctic Ocean within the next century (Comiso et al., 2008), and we recently discussed likely implications of such and other changes for the entire Arctic ecosystem (Bluhm & Gradinger, 2008). From the perspective of sea ice macrofauna, two major impacts are likely: (a) the loss of critical habitat for ice endemic taxa and (b) a

mismatch between the needs of certain life stages and the ice regime for allochthonous fauna. *Gammarus wilkitzkii*, for example, is only found in the Arctic and is unique to the multiyear ice regions of the central Arctic. This amphipod completes its entire life cycle with sea ice. As outlined above, it might be able to survive for several weeks within the water column before sinking to the sea floor, from where it is likely unable to colonize newly forming ice in the next winter. *G. wilkitzkii* tends to concentrate at pressure ridges in summer (Hop et al., 2000), and if those massive structures at least partially survive the summer melt, individuals could recolonize adjacent newly forming ice in fall and winter.

Changes in the ice regime will also impact the allochthonous Arctic ice fauna even if ice remains present for part of the year. Compared to the 1970s, the coastal fast ice off Alaska forms a month later and breaks up about 1 week earlier (Mahoney et al., 2007). Currently, the spring bloom of sea ice algae in this region occurs in March–May, while break-up typically happens in June/July. The juveniles of sympagic polychaetes have their abundance maximum in the ice tightly linked to the ice-algal bloom, which currently occurs well before ice break-up (Figs 10.6 and 10.9). A continued downward trend in ice presence could lead to a scenario where reproductive events of allochthonous taxa occur at a time when ice is already gone. In the polychaete example, the currently tight link between ice and benthic life stage for the polychaetes would be decoupled. It remains to be seen whether juveniles of this and other species might find suitable habitat in the pelagic or benthic realms or whether it would bring them into a competitive disadvantage with other taxa.

In conclusion, changes in the sea ice regime due to interannual variability and long-term change will impact the life cycles of ice-associated fauna that currently plays a critical role in both Arctic and Antarctic marine food webs. Changes ice fauna productivity will likely propagate through the food web and may also influence higher trophic levels (Chapter 11).

References

Aarset, A.V. (1991) The ecophysiology of under-ice fauna. *Polar Research*, **10**, 309–324.

Aarset, A.V. & Aunaas, T. (1987) Physiological adaptations to low temperature and brine exposure in the circumpolar amphipod *Gammarus wilkitzkii. Polar Biology*, **8**, 129–133.

Aarset, A.V. & Torres, J.J. (1989) Cold resistance and metabolic responses to salinity variations in the amphipod *Eusirus antarcticus* and the krill *Euphausia superba. Polar Biology*, **9**, 491–497.

Amaral, A.C.Z. (1979) Ecologia e contribuição dos anelídeos poliquetos para a biomassa bêntica da zona das marés, no litoral norte do Estado de São Paulo. *Boletim Do Instituto Oceanografico Sao Paulo*, **28**, 1–52.

Andriashev, A.P. (1968) The problem of the life community associated with the Antarctic fast ice. In: *Symposium on Antarctic Oceanography* (Ed. R.I. Currie), pp. 147–155. Scott Polar Research Institute, Cambridge.

Arrigo, K.R., Dieckmann, G., Gosselin, M., Robinson, D.H., Fritsen, C.H. & Sullivan, C.W. (1995) High resolution study of the platelet ice ecosystem in McMurdo Sound, Antarctica: biomass, nutrient, and production profiles within a dense microalgae bloom. *Marine Ecology Progress Series*, **127**, 255–268.

Arndt, C.E & Swadling, K.M. (2006) Crustacea in Arctic and Antarctic sea ice: distribution, diet and life history strategies. *Advances in Marine Biology*, **51**, 197–315.

Atkinson, A., Ward, P., Hill, A., Brierley, A.S. & Cripps, G.C. (1999) Krill–copepod interactions at South Georgia, Antarctica, II. *Euphausia superba* as a major control on copepod abundance. *Marine Ecology Progress Series*, **176**, 63–79.

Atkinson, A., Meyer, B., Stübing, D., Hagen, W., Schmidt, K. & Bathmann, U.V. (2002) Feeding and energy budgets of Antarctic krill *Euphausia superba* at the onset of winter – II. Juveniles and adults. *Limnology and Oceanography*, **47**, 953–966.

Atkinson, A., Siegel, V., Pakhomov, E. & Rothery, P. (2004) Long-term decline in krill stock and increase in salps within the Southern Ocean. *Nature,* **432**, 100–103.

Beuchel, F. & Lønne, O. (2002) Population dynamics of the sympagic amphipods *Gammarus wilkitzkii* and *Apherusa glacialis* in sea ice north of Svalbard. *Polar Biology*, **25**, 241–250.

Blome, D. & Riemann, F. (1999) Antarctic sea ice nematodes, with description of *Geomonhystera glaciei* sp. nov. (Monhysteridae). *Mitteilungen aus dem Hamburgischen Zoologischen Museum und Institut*, **96**, 15–20.

Bluhm, B.A. & Gradinger, R. (2008) Regional variability in food availability for Arctic marine mammals. *Ecological Applications* **18,** S77–S96.

Bluhm, B.A., Gradinger, R. & Piraino, S. (2007). First record of sympagic hydroids (Hydrozoa, Cnidaria) in Arctic coastal fast ice. *Polar Biology,* **30**, 1557–1563.

Brierley, A.S. & Thomas, D.N. (2002) On the ecology of Southern Ocean pack ice. *Advances in Marine Biology*, **43**, 171–278.

Brierley, A.S. & Watkins, J.L. (2000) Effects of sea ice cover on the swarming behaviour of Antarctic krill, *Euphausia superba. Canadian Journal of Fisheries and Aquatic Sciences*, **57** (Suppl. 3), 24–30.

Brierley, A.S., Fernandes, P.G., Brandon, M.A. et al. (2002) Antarctic krill under sea ice: elevated abundance in a narrow band just south of ice edge. *Science*, **295**, 1890–1892.

Carey, A.G., Jr. (1985) Marine ice fauna. In: *Sea Ice Biota* (Ed. R.A. Horner), pp. 173–190. CRC Press, Boca Raton, FL.

Carey, A.G., Jr. (1992) The ice fauna in the shallow southwestern Beaufort Sea, Arctic Ocean. *Journal of Marine Systems*, **3**, 225–236.

Carey, A.G.J. & Boudrias, M.A. (1987). Feeding ecology of *Pseudalibrotus* (=*Onisimus*) *litoralis* Krøyer (Crustacea: Amphipoda) on the Beaufort Sea inner continental shelf. *Polar Biolog*y, **8**, 29–33.

Carey, A.G. & Montagna, P.A. (1982) Arctic sea ice formation assemblage: first approach to description and source of the underice meiofauna. *Marine Ecology Progress Series*, **8**, 1–8.

Cheng, C.C. & DeVries, A.L. (1991) The role of antifreeze glycopeptides and peptides in the freezing avoidance of cold-water fish. In: *Life Under Extreme Conditions. Biochemical adaptation* (Ed. G. di Prisco), pp. 1–15. Springer-Verlag, Berlin.

Clarke, A., Doherty, N., DeVries, A.L. & Eastman, J.T. (1984) Lipid content and composition of three species of Antarctic fish in relation to buoyancy. *Polar Biology*, **3**, 77–83.

Comiso, J.C., Parkinson, C.L. Gersten, R. & Stock, L. (2008) Accelerated decline in the Arctic sea ice cover, *Geophysical Research Letters* **35**, 10.1029/2007GL031972.

Conover, R.J., Herman, A.W., Prinsenberg, S.J. & Harris, L.R. (1986) Distribution of and feeding by the copepod *Pseudocalanus* under fast ice during the Arctic spring. *Science*, **232**, 1245–1247.

Conover, R.J, Cota, G.F., Harrison, W.G., Horne, E.P.W. & Smith, R.E.H. (1990) Ice/water interactions and their effect on biological oceanography in the Arctic Archipelago. In: *Canada's Missing Dimension: Science and History in the Canadian Arctic Islands* (Ed. C.R. Harington), pp. 204–228. Canadian Museum of Nature, Ottowa.

Cross, W.E. (1982) Under-ice biota at the Pond Inlet ice edge and in adjacent fast ice areas during spring. *Arctic*, **35**, 13–27.

Dahms, H.U., Bergmann, M. & Schminke, H.K. (1990) Distribution and adaptations of sea ice inhabiting Harpacticoida (Crustacea, Copepoda) of the Weddell Sea (Antarctica). *Marine Ecology*, **11**, 207–226.

Daly, K.L. (1990) Overwintering development, growth, and feeding of larval *Euphausia superba* in the Antarctic marginal ice zone. *Limnology and Oceanography*, **35**, 1564–1576.

Daly, K.L. (2004) Overwintering growth and development of larval *Euphausia superba*: an interannual comparison under varying environmental conditions west of the Antarctic Peninsula. *Deep-Sea Research Part II*, **51**, 2139–2168.

Daly, K.L. & Macaulay, M.C. (1988) Abundance and distribution of krill in the ice edge zone of the Weddell Sea, austral spring 1983. *Deep-Sea Research Part I*, **35**, 21–41.

Daly, K.L. & Macaulay, M.C. (1991) Influence of physical and biological mesoscale dynamics on the seasonal distribution and behavior of *Euphausia superba* in the Antarctic marginal ice zone. *Marine Ecology Progress Series*, **79**, 37–66.

Dayton, P.K., Robilliard, G.A. & DeVries, A.L. (1969) Anchor ice formation in McMurdo Sound, Antarctica, and its biological effects. *Science*, **163**, 273–274.

De la Mare, W.K. (1997) Abrupt mid-twentieth-century decline in Antarctic sea ice extent from whaling records. *Nature*, **389**, 57–59.

DeVries, A.L. (1971) Glycoproteins as biological antifreeze agents in Antarctic fish. *Science*, **172**, 1152–1155.

DeVries, A.L. (1997) The role of antifreeze proteins in survival of Antarctic fish in freezing environments. In: *Antarctic Communities. Species, Structure and Survival* (Eds. B. Battaglia, J. Valencia & D.W.H. Walton), pp. 202–208. Cambridge University Press, Cambridge.

Dieckmann, G.S., Rohardt, G., Hellmer, H. & Kipfstuhl, J. (1986) The occurrence of ice platelets at 250 m near the Filchner Ice Shelf and its significance to sea ice biology. *Deep-Sea Research*, **33**, 141–148.

Dieckmann, G.S., Arrigo, K. & Sullivan, C.W. (1992) A high resolution sampler for nutrient and chlorophyll *a* profiles of the sea ice platelet layer and underlying water column below fast ice in polar oceans: preliminary results. *Marine Ecology Progress Series*, **80**, 291–300.

Enevoldsen, L.T., Heiner, I., DeVries, A.L. & Steffensen, J.F. (2003) Does fish from the Disco Bay area of Greenland possess antifreeze proteins during the summer? *Polar Biology*, **26,** 365–370.

Fach, B.A., Meyer, B., Wolf-Gradow, D. & Bathmann, U. (2008) Biochemically based modeling study of Antarctic krill *Euphausia superba* growth and development. *Marine Ecology Progress Series,* **360**, 147–161.

Falk-Petersen, S., Hagen, W., Kattner, G., Clarke, A. & Sargent, J. (2000) Lipids, trophic relationships, and biodiversity in Arctic and Antarctic krill. *Canadian Journal of Fisheries and Aquatic Sciences*, **57** (Suppl. 3), 178–191.

Fortier, M., Fortier, L., Hattori, H., Saito, H. & Legendre, L. (2001) Visual predators and the diel vertical migration of copepods under Arctic sea ice during the midnight sun. *Journal of Plankton Research*, **23**, 1263–1278.

Frazer, T.K., Quetin, L.B. & Ross, R.M. (1997) Abundance and distribution of larval krill, *Euphausia superba*, associated with annual sea ice in winter. In: *Antarctic Communities, Species, Structure and Survival* (Eds. B. Battaglia, J. Valencia & D.W.H. Walton), pp. 107–111. Cambridge University Press, Cambridge.

Friedrich, C. (1997) Ecological investigations on the fauna of the Arctic sea ice. *Berichte zur Polarforschung*, **246**, 1–211 (in German).

Friedrich, C. & De Smet, W.H. (2000) The rotifer fauna of Arctic sea ice from the Barents Sea, Laptev Sea and Greenland Sea. *Hydrobiologia*, **432**, 73–90.

Friedrich, C. & Hendelberg, J. (2001). On the ecology of Acoela living in the Arctic sea ice. *Belgian Journal of Zoology* (Suppl. 1) **131**, 213–216.

Garrison, D.L. & Buck, K.R. (1986) Organism losses during ice melting: a serious bias in sea ice community studies. *Polar Biology,* **6**, 237–239.

Garrison, D.L., Ackley, S.F. & Buck, K.R. (1983) A physical mechanism for establishing algal populations in frazil ice. *Nature*, **306**, 363–365.

Gradinger, R. (1999) Integrated abundance and biomass of sympagic meiofauna in Arctic and Antarctic pack ice. *Polar Biology*, **22**, 169–177.

Gradinger, R. (2002) Sea ice microorganisms. In: *Encyclopedia of Environmental Microbiology* (Ed. G.E. Bitten), pp. 2833–2844. Wiley & Sons.

Gradinger, R.R. & Bluhm, B.A. (2004) *In situ* observations on the distribution and behavior of amphipods and Arctic cod (*Boreogadus saida*) under the sea ice of the high Arctic Canadian Basin. *Polar Biology,* **27**, 595–603.

Gradinger, R. & Bluhm, B. (2005) Susceptibility of sea ice biota to disturbances in the shallow Beaufort Sea: Phase 1: Biological coupling of sea ice with the pelagic and benthic realms. Final Report. OCS Study MMS 2005-062, p. 87.

Gradinger, R.R. & Bluhm, B.A. (2009) Assessment of the abundance and diversity of sea ice biota. In: *Handbook on field techniques in sea ice research (a sea ice system services approach)* (Eds. H. Eicken, R. Gradinger, M. Salganek, K. Shirasawa, D.K. Perovich & M. Leppäranta), University of Alaska Press.

Gradinger, R. & Schnack-Schiel, S.B. (1998) Potential effect of ice formation on Antarctic pelagic copepods: salinity induced mortality of *Calanus propinquus* and *Metridia gerlachei* in comparison to sympagic acoel turbellarians. *Polar Biology*, **20**, 139–142.

Gradinger, R., Spindler, M. & Henschel, D. (1991*)*. Development of Arctic sea ice organisms under graded snow cover. *Polar Research* **10,** 295–307.

Gradinger, R., Friedrich, C. & Spindler, M. (1999) Abundance, biomass and composition of the sea ice biota of the Greenland Sea pack ice. *Deep-Sea Research Part I*, **46**, 1457–1472.

Gradinger, R.R., Meiners, K., Plumley, G., Zhang, Q. & Bluhm, B.A. (2005) Abundance and composition of the sea ice meiofauna in off-shore pack ice of the Beaufort Gyre in summer 2002 and 2003. *Polar Biology,* **28**, 171–181.

Gradinger, R., Bluhm, B.A. & Iken, K. (unpublished) Arctic sea ice ridges – safe havens for sea ice fauna during periods of extreme ice melt? *Deep-Sea Research Part II*,

Grainger, E.H. (1991) Exploitation of arctic sea ice by epibenthic copepods. *Marine Ecology Progress Series*, **77**, 119–124.

Grainger, E.H. & Hsiao, S.I.C. (1990) Trophic relationship of the sea ice meiofauna in Frobisher Bay, Arctic Canada. *Polar Biology*, **10**, 283–292.

Grainger, E.H., Mohammed, A.A. & Lovrity, J.E. (1985) The sea ice fauna of the Frobisher Bay, Arctic Canada. *Arctic*, **38**, 23–30.

Grossmann, S., Lochte, K. & Scharek, R. (1996) Algal and bacterial processes in platelet ice during late austral summer. *Polar Biology*, **16**, 623–633.

Guglielmo, L., Zagami, G., Saggiimo, V., Catalano, G. & Granata, A. (2007) Copepods in spring annual sea ice at Terra Nova Bay (Ross Sea, Antarctica). *Polar Biology*, **30,** 747–758.

Gulliksen, B. & Lønne, O.J. (1989) Distribution, abundance, and ecological importance of marine sympagic fauna in the Arctic. *Rapports et Process-Verbaux des Réunions. Conseil Permanent International pour l'Exploration de la Mer*, **188**, 133–138.

Gulliksen, B. & Lønne, O.J. (1991) Sea ice macrofauna in the Antarctic and the Arctic. *Journal of Marine Systems*, **2**, 53–61.

Günther, S., George, K.H. & Gleitz, M. (1999) High sympagic metazoan abundance in platelet layers at Drescher-Inlet, Weddell Sea, Antarctica. *Polar Biology*, **22**, 82–89.

Hagen, W., Kattner, G., Terbrüggen, A. & Van Vleet, E.S. (2001). Lipid metabolism of the Antarctic krill *Euphausia superba* and its ecological implications. *Marine Biology*, **139**, 95–104.

Hammer, W.M. & Hammer, P.P. (2000) Behavior of Antarctic krill (*Euphausia superba*): schooling, foraging, and antipredatory behavior. *Canadian Journal of Fishery and Aquatic Science*, **57** (Suppl. 3), 192–202.

Hammer, W.M., Hammer, P.P. & Obst, B.S. (1989) Field observations on the ontogeny of schooling of *Euphausia superba* furciliae and its relationship to ice in Antarctic waters. *Limnology and Oceanography*, **34**, 451–456.

Hill, T.D., Lynott, S.T., Bryan, S. & Duffy, W.G. (1996) An efficient method for setting gill nets under-ice. *North American Journal of Fisheries Management*, **16**, 960–962.

Hofman, E.E. & Lascara, C.M. (2000) Modeling the growth dynamics of Antarctic krill Euphausia superba. *Marine Ecology Progress Series*, **194**, 219–231.

Hop, H., Poltermann, M., Lønne, O.J., Falk-Petersen, S., Kornes R. & Budgell, W.P. (2000) Ice amphipod distribution relative to ice density and under-ice topography in the northern Barents Sea. *Polar Biology*, **23**, 357–367.

Horner, R., Ackley, S.F., Dieckmann, G.S. et al. (1992) Ecology of sea ice biota. 1. Habitat, terminology, and methodology. *Polar Biology*, **12**, 417–427.

Hoshiai, T., Tanimura, A. & Watanaba, K. (1987) Ice algae as food of an Antarctic ice-associated copepod, *Paralabidocera antarctica* (I.C. Thompson). *Proceedings of the NIPR Symposium on Polar Biology*, **1**, 105–111.

Huntley, M.E., Nordhausen, W. & Lopez, M.D.G. (1994) Elemental composition, metabolic activity and growth of Antarctic krill *Euphausia superba* during winter. *Marine Ecology Progress Series*, **107**, 23–40.

Ikeda, T. & Nixon, P. (1982) Body shrinkage as a possible overwintering mechanism of the Antarctic krill, *Euphausia superba* Dana. *Australian Journal of Marine and Freshwater Research*, **33**, 71–76.

Janssen, H.H. & Gradinger, R. (1999) Turbellaria (Archoophora: Acoela) from Antarctic sea ice endofauna – examination of their micromorphology. *Polar Biology*, **21**, 410–416.

Jarman, S., Elliott, N., Nicol, S., McMinn, A. & Newman, S. (1999) The base composition of the krill genome and its potential susceptibility to damage by UV-B. *Antarctic Science*, **11**, 23–26.

Jin, Y. & DeVries, A.L. (2006) Antifreeze glycoprotein levels in Antarctic notothenioid fish inhabiting different thermal environments and the effect of warm acclimation. *Biochemistry and Physiology*, Part B, **144**, 290–300.

Ju, S.-J. & Harvey, H.R. (2004) Lipids as markers of nutritional condition and diet in the Antarctic krill *Euphausia superba* and *Euphausia crystallorophias* during austral winter. *Deep-Sea Research II*, **51**, 2199–2214.

Karentz, D., McEuen, F.S., Land, M.C. & Dunlap, W.C. (1991) Survey of mycosporine-like amino acid compounds in Antarctic marine organisms: potential protection from ultraviolet exposure. *Marine Biology*, **108**, 157–166.

Kattner, G. & Hagen, W. (1995) Polar herbivorous copepods – different pathways in lipid biosynthesis. *ICES Journal of Marine Science*, **51**, 329–335.

Kattner, G., Thomas, D.N., Haas, C., Kennedy, H. & Dieckmann, G.S. (2004) Surface ice and gap layers in Antarctic sea ice: highly productive habitats. *Marine Ecology Progress Series*, **277**, 1–12.

Kennedy, H., Thomas, D.N., Kattner, G., Haas, C. & Dieckmann, G.S. (2002) Particulate organic carbon in Antarctic summer sea ice: concentration and stable carbon isotopic composition. *Marine Ecology Progress Series*, **238**, 1–13.

Kern, J.C. & Carey, A.G. (1983) The faunal assemblage inhabiting seasonal sea ice in the nearshore Arctic Ocean with emphasis on copepods. *Marine Ecology Progress Series*, **10**, 159–167.

Kiko, R., Michels, J., Mizdalski, E., Schnack-Schiel, S.B. & Werner, I. (2008a) Living conditions, abundance and composition of the metazoan fauna in surface and sub-ice layers in pack ice of the western Weddell Sea during late spring. *Deep-Sea Research Part II*, **55**, 1000–1014.

Kiko, R., Kramer, M., Spindler, M. & Werner, I. (2008b) *Tergipes antarcticus* (Gastropoda, Nudibranchia): distribution, life cycle, morphology, anatomy and adaptation of the first mollusk known to live in Antarctic sea ice. *Polar Biology*, **31**, 1383–1395.

Kiko, R., Werner, I. & Wittmann, A. (2008c). Osmotic and ionic regulation in response to salinity variations and cold resistance in the Arctic under-ice amphipod *Apherusa glacialis*. *Polar Biology*, **32**, 393–398.

Kiko, R. (2009) Ecophysiology of Antarctic sea-ice meiofauna. Doctoral thesis. Institute for Polar Ecology, Kiel University, Kiel, Germany, 116 pp.

Krapp, R.H., Berge, J., Flores, H., Gulliksen, B. & Werner, I. (2008) Sympagic occurrence of eusirid and lysianassoid amphipods under Antarctic pack ice. *Deep-Sea Research Part II*, **55,** 1015–1023.

Krembs, C. & Deming, J.W., 2008. The role of exopolymers in microbial adaptation to sea ice. In: *Psychrophiles: from Biodiversity to Biotechnology* (Eds. R. Margesin, F. Schinner, J.-C. Marx & C. Gerday), pp. 247–264. Springer, Heidelberg.

Krembs, C., Gradinger, R. & Spindler, M. (2000) Implications of brine channel geometry and surface area for the interaction of sympagic organisms in Arctic sea ice. *Journal of Experimental Marine Biology and Ecology*, **243**, 55–80.

Krembs, C., Tuschling, K. & von Juterzenka, K. (2001) The topography of the ice water interface – its influence on the colonisation of sea ice by algae. *Polar Biology*, **25**, 106–117.

Kurbjeweit, F., Gradinger, R. & Weissenberger, J. (1993) The life cycle of *Stephos longipes* – an example for cryopelagic coupling in the Weddell Sea (Antarctica). *Marine Ecology Progress Series*, **98**, 255–262.

Lee, R.F., Hagen, W. & Kattner, G. (2006) Lipid storage in marine zooplankton. *Marine Ecology Progress Series*, **307**, 273–306.

Loeb, V., Siegel, V., Holm-Hansen, O., Hewitt, R., Fraser, W., Tivelpiece, W. & Trivelpiece, S. (1997) Effects of sea ice extent and krill or salp dominance on the Antarctic food web. *Nature*, **387**, 897–900.

Lønne, O.J. (1988) A diver-operated electric suction sampler for sympagic (=underice) invertebrates. *Polar Research*, **6**, 135–136.

Macnaughton, M.O., Thormar, J. & Berge, J. (2007) Sympagic amphipods in the Arctic pack ice: redescriptions of *Eusirus holmii* Hansen, 1887 and *Pleusymtes karstensi* (Barnard, 1959). *Polar Biology*, **30**, 1013–1025.

Mahoney, A., Eicken, H., Gaylord, A.G. & Shapiro, L. (2007) Alaska landfast sea ice: Links with bathymetry and atmospheric circulation. *Journal of Geophysical Research*, **112**, doi:10.1029/2006JC003559.

Marschall, P. (1988) The overwintering strategy of Antarctic krill under the pack ice of the Weddell Sea. *Polar Biology*, **9**, 129–135.

McMahon, K.W., Ambrose Jr., W.G., Johnson, B.J., Sun, M.-Y., Lopez, G.R., Clough, L.M. & Carroll, M.L. (2006) Benthic community response to ice algae and phytoplankton in Ny Ålesund, Svalbard. *Marine Ecology Progress Series* **310,** 1–14.

Meiners, K., Krembs, C. & Gradinger, R. (2008). Exopolymer particles: microbial hotspots of enhanced bacterial activity in Arctic fast ice (Chukchi Sea). *Aquatic Microbial Ecology*, **52**, 195–207.

Melnikov, I.A. (1997) *The Arctic Sea Ice Ecosystem*. Gordon Breach Science Publishers, Amsterdam.

Melnikov, I.A. & Spiridonov, V.A. (1996) Antarctic krill under perennial sea ice in the western Weddell Sea. *Antarctic Science*, **8**, 323–329.

Menshenina, L.L. & Melnikov, I.A. (1995) Under-ice zooplankton of the western Weddell Sea. *Proceedings of the NIPR Symposium on Polar Biology*, **8**, 126–138.

Meyer, B., Atkinson, A., Stübing, D., Oettl, B., Hagen, W. & Bathmann, U. (2002) Feeding and energy budgets of Antarctic krill *Euphausia superba* at the onset of winter – I. Furcilia III larvae. *Limnology and Oceanography*, **47**, 943–952.

Michel, C., Nielsen, T.G., Nozais, C. & Gosselin, M. (2002) Significance of sedimentation and grazing by ice micro- and meiofauna for carbon cycling in annual sea ice (northern Baffon Bay). *Aquatic Microbial Ecology*, **30**, 57–68.

Michels, J., Dieckmann, G.S., Thomas, D.N. et al. (2008) Short-term biogenic particle flux under late spring sea ice in the western Weddell Sea. *Deep-Sea Research Part II*, **55**, 1024–1039.

Mock, T. & Kroon, B.M.A. (2002a) Photosynthetic energy conversion under extreme conditions. I. Important role of lipids as structural modulators and energy sink under N-limited growth in Antarctic sea ice diatoms. *Phytochemistry*, **61**, 41–51.

Mock, T. & Kroon, B.M.A. (2002b) Photosynthetic energy conversion under extreme conditions. II. The significance of lipids at low temperature and low irradiances in Antarctic sea ice diatoms. *Phytochemistry*, **61**, 53–60.

Nicol, S. (2000) Understanding krill growth and aging: the contribution of experimental studies. *Canadian Journal of Fisheries and Aquatic Sciences*, **57** (Suppl. 3), 168–177.

Nicol, S. (2006) Krill, currents, and sea ice: *Euphausia superba* and its changing environment. *BioScience* **56**, 111–120.

Nicol, S., Virtue, P., King, R., Davenport, S.R., McGaffin, A.F. & Nichols, P. (2004) Condition of *Euphausia crystallorophias* off East Antarctica in winter in comparison to other seasons. *Deep-Sea Research Part II*, **51**, 2215–2224.

Nozais, C., Gosselin, M., Michel, C. & Tita, G. (2001) Abundance, biomass, composition and grazing impact of the sea ice meiofauna in the North Water, northern Baffin Bay. *Marine Ecology Progress Series*, **217**, 235–250.

O'Brien, D.P. (1987) Direct observations of the behaviour of *Euphausia superba* and *Euphausia crystallorophias* (Crustacea: Euphausiacea) under pack ice during the Antarctic spring. *Journal of Crustacean Biology*, **7**, 437–448.

Pape, C., Teschke, M. & Meyer, B. (2008) Melatonin and its possible role in mediating seasonal metabolic changes of Antarctic krill, *Euphausia superba*. *Comparative Biochemistry and Physiology*, **A149**, 426–434.

Piraino, S., Bluhm, B.A., Gradinger, R. & Boero, F. (2008) *Sympagohydra tuuli* gen. nov. et sp. nov. (Cnidaria: Hydrozoa) a cool hydroid from the Arctic sea ice. *Journal of the Marine Biological Association of the U.K.*, **88**, 1637–1641.

Poltermann, M. (1997) Biologische und ökologische Untersuchungen zur kryopelagischen Amphipodenfauna des arktischen Meereises. *Berichte zur Polarforschung*, **225**, 1–170 (in German).

Poltermann, M. (2000) Growth, production and productivity of the Arctic sympagic amphipod *Gammarus wilkitzkii*. *Marine Ecology Progress Series*, **193**, 109–116.

Poltermann, M., Hop, H. & Falk-Petersen, S. (2000) Life under Arctic sea ice – reproduction strategies of two sympagic (ice-associated) amphipod species, *Gammarus wilkitzkii* and *Apherusa glacialis*. *Marine Biology*, **136**, 913–920.

Praebel, K. & Ramlov, H. (2005) Antifreeze activity in the gastrointestinal fluids of *Arctogadus glacialis* (Peters 1874) is dependent on food type. *Journal of Experimental Biology*, **208**, 2609–2613.

Purcell J.E., Hopcroft, R.R., Kosobokova, K.N. & Whitledge, T.E. Distribution, abundance, and predation effects of epipelagic ctenophores and jellyfish in the western Arctic Ocean. *Deep-Sea Research Part II*, in press.

Quetin, L.B. & Ross, R.M. (1991) Behavioral and physiological characteristics of the Antarctic krill, *Euphausia superba*. *American Zoologist*, **31**, 49–63.

Quetin, L.B., Ross, R.M., Frazer, T.K. & Haberman, K.L. (1996) Factors affecting distribution and abundance of zooplankton, with an emphasis on Antarctic krill, *Euphausia superba*. *Antarctic Research Series*, **70**, 357–371.

Rakusa-Suszczewski, S. (1972) The biology of *Paramoera walkeri* Stebbing (Amphipoda) and the Antarctic sub-fast ice community. *Polish Archives of Hydrobiology*, **19**, 11–36.

Richardson, M.G. & Whitaker, T.M. (1979) An Antarctic fast-ice food chain: observations on the interaction on the amphipod *Pontogeneia antarctica* Chevreux with ice-associated micro-algae. *British Antarctic Survey*, **47**, 107–115.

Riemann, F. & Sime-Ngando, T. (1997) Note on sea ice nematodes (Monhysteroidea) from Resolute Passage, Canadian High Arctic. *Polar Biology*, **18**, 70–75.

Ross, R.M., Quetin, L.B. & Lascara, C. (1996) Distribution of Antarctic krill and dominant zooplankton west of the Antarctic Peninsula. In: *Foundations for Ecological Research West of the Antarctic Peninsula* (Eds. R.M. Ross, E.E. Hofmann & L.B. Quetin). American Geophysical Union, Washington, DC. *Antarctic Research Series*, **70**, 199–217.

Ross, R.M., Quetin, L.B., Newbergen, T. & Oakes, S.A. (2004) Growth and behavior of larval krill (*Euphausia superba*) under the ice in late winter 2001 west of the Antarctic Peninsula. *Deep-Sea Research Part II*, **51**, 2169–2184.

Runge, J.A. & Ingram, R.G. (1988) Underice grazing by planktonic, calanoid copepods in relation to a bloom of ice microalgae in southeastern Hudson Bay. *Limnology and Oceanography*, **33**, 280–286.

Sargent, J.R., Gatten, R.R. & Henderson, R.J. (1981) Lipid biochemistry of zooplankton from high latitudes. *Océanis*, **7**, 623–632.

Schnack-Schiel, S.B. & Hagen, W. (1995) Life cycle strategies of *Calanoides acutus*, *Calanus propinquus and Metridia gerlachei* (Copepoda: Calanoida) in the eastern Weddell Sea, Antarctica. *ICES Journal of Marine Science*, **51**, 541–548.

Schnack-Schiel, S.B., Thomas, D., Dieckmann, G.S. et al. (1995) Life cycle strategy of the Antarctic calanoid copepod *Stephos longipes*. *Progress in Oceanography*, **36**, 45–75.

Schnack-Schiel, S.B., Thomas, D.N., Dahms, H.U., Haas, C. & Mizdalski, E. (1998) Copepods in Antarctic Sea ice. In: *Antarctic Sea Ice Biological Processes, Interactions and Variability* (Eds. M.P. Lizotte & K. Arrigo). American Geophysical Union, Washington, DC. *Antarctic Research Series*, **73**, 173–182.

Schnack-Schiel, S.B., Dieckmann, G.S., Gradinger, R., Melnikov, I.A., Spindler, M. & Thomas, D.N. (2001a) Meiofauna in sea ice of the Weddell Sea (Antarctica). *Polar Biology*, **24**, 724–728.

Schnack-Schiel, S.B., Thomas, D.N., Haas, C., Dieckmann, G.S. & Alheit, R. (2001b) On the occurrence of the copepods *Stephos longipes* (Calanoida) and *Drescheriella glacialis* (Harpacticoida) in summer sea ice in the Weddell Sea. *Antarctic Science*, **13**, 150–157.

Schnack-Schiel S.B., Dieckmann, G.S., Kattner, G. & Thomas, D.N. (2004) Copepods in summer platelet ice in the eastern Weddell Sea (Antarctica). *Polar Biology*, **27**, 502–506.

Schnack-Schiel, S.B., Haas, C., Michels, J., Mizdalski, E., Schünemann, H., Steffens, M. & Thomas, D. (2008) Copepods in sea ice of the western Weddell Sea during austral spring 2004. *Deep-Sea Research Part II*, **55,** 1056–1067.

Schünemann, H. & Werner, I. (2005) Seasonal variations in distribution patterns of sympagic meiofauna in Arctic pack ice. *Marine Biology*, **146**, 1091–1102.

Scolardi, K.M., Daly, K.L., Pakhomov, E.A. & Torres, J.J. (2006) Feeding ecology and metabolism of the Antarctic cydippid ctenophore *Callianira antarctica*. *Marine Ecology Progress Series*, **317**, 111–126.

Scott, C.L., Falk-Petersen, S., Sargent, J.R., Hop, H., Lønne, O.J. & Poltermann, M. (1999) Lipid and trophic interactions of ice fauna and pelagic zooplankton in the marginal zone of the Barents Sea. *Polar Biology*, **21**, 65–70.

Shanks, A.L. & del Carmen, K.A. (1997) Larval polychaetes are strongly associated with marine snow. *Marine Ecology Progress Series*, **154**, 211–221.

Siebert, S., Anton-Erxleben, F., Kiko, R. & Kramer, M. (2009) *Sympagohydra tuuli* (Cnidaria, Hydrozoa): first record from sea ice of the central Arctic Ocean and insights into histology, reproduction and locomotion. *Marine Biology,* **156**, 541–554.

Siegel, V. (2000) Krill (Euphausicea) life history and aspects of population dynamics. *Canadian Journal of Fisheries and Aquatic Sciences*, **57**, 130–150.

Siegel, V. & Loeb, V. (1995) Recruitment of Antarctic krill *Euphausia superba* and possible causes for its variability. *Marine Ecology Progress Series*, **123**, 45–56.

Siferd, T.D., Welch, H.E., Bergmann, M.A. & Curtis, M.F. (1997) Seasonal distribution of sympagic amphipods near Chesterfield Inlet, N.W.T., Canada. *Polar Biology*, **18**, 16–32.

Smetacek, V., Scharek, R., Gordon, L.I., Eicken, H., Fahrbach, E., Rohardt, G. & Moore, S. (1992) Early spring phytoplankton bloom in ice platelet layers of the southern Weddell Sea, Antarctica. *Deep-Sea Research Part I*, **39**, 153–168.

Smith, R.E.H., Anning, J., Clement, P. & Cota, G. (1988). Abundance and production of ice algae in Resolute Passage, Canadian Arctic. *Marine Ecology Progress Series*, **48**, 251–263.

Souza, J.R.B. & Borzone, C.A. (2000) Population dynamics and secondary production of *Scolelepis squamata* (Polychaeta: Spionidae) in an exposed sandy beach of southern Brazil. *Bulletin of Marine Science*, **67**, 221–233.

Steffens, M., Granskog, M.A., Kaartokallio, H., Kuosa, H., Luodekari, K., Papadimitriou, S. & Thomas, D.N. (2006) Spatial variation of biogeochemical properties of landfast sea ice in the Gulf of Bothnia (Baltic Sea). *Annals of Glaciology*, **44**, 80–87.

Swadling, K.M. (2001) Population structure of two Antarctic ice-associated copepods. *Drescheriella glacialis* and *Paralabidocera antarctica*, in winter sea ice. *Marine Biology*, **129**, 597–603.

Swadling, K.M., Gibson, J.A.E., Ritz, D.A. & Nichols, P.D. (1997) Horizontal patchiness in sympagic organisms of the Antarctic fast ice. *Antarctic Science*, **9**, 399–406.

Swadling, K.M., Nichols, P.D., Gibson, J.A.E. & Ritz, D.A. (2000) The role of lipid in the life cycles of ice-dependent and ice-independent populations of the copepod *Paralabidocera antarctica*. *Marine Ecology Progress Series*, **208**, 171–182.

Swadling, K.M., McPhee, A.D. & McMinn, A. (2001) Spatial distribution of copepods in fast ice of eastern Antarctica. *Polar Bioscience*, **13**, 55–65.

Swadling, K.M., McKinnon, A.D., De'ath, G. & Gibson, J.A.E. (2004) Life cycle plasticity and differential growth and development in marine and lacustrine populations of an Antarctic copepod. *Limnology and Oceanography*, **49**, 644–655.

Tanimura, A., Hoshiai, T. & Fukuchi, M. (1996) The life cycle strategy of the ice-associated copepod *Paralabidocera antarctica* (Calanoida, Copepoda), at Syowa Station, Antarctica. *Antarctic Science*, **8**, 257–266.

Tanimura, A., Hoshiai, T. & Fukuchi, M. (2002) Change in habitat of the sympagic copepod *Paralabidocera antarctica* from fast ice to seawater. *Polar Biology*, **25**, 667–671.

Tchesunov, A.V. & Riemann, F. (1995) Arctic sea ice nematodes (Monhysteroidea) with descriptions of *Cryonema crassum* gen. n. sp. n. and *C. tenue* sp. n. *Nematologica*, **41**, 35–50.

Teschke, M., Kawaguchi, S. & Meyer, B. (2007) Simulated light regimes affect feeding and metabolism of Antarctic krill, *Euphausia superba*. *Limnology and Oceanography*, **52**, 1046–1054.

Thomas, D.N. (2004) *Frozen Ocean*, 224pp. Natural History Museum, London.

Thomas, D.N., Lara, R.J., Haas, C. et al. (1998) Biological soup within decaying summer sea ice in the Amundsen Sea, Antarctica. In: *Antarctic Sea Ice Biological Processes, Interactions and Variability* (Eds. M.P. Lizotte & K. Arrigo). American Geophysical Union, Washington, DC. *Antarctic Research Series*, **73**, 161–171.

Vacchi, M., LaMesa, M., Dalu, M. & MacDonald, J. (2004) Early life stages in the life cycle of Antarctic silverfish, *Pleuragramma antarcticum* in Terra Nova Bay, Ross Sea. *Antarctic Science*, **16**, 299–305.

Van Hoey, G., Degraer, S. & Vincx, M. (2004) Macrobenthic community structure of soft-bottom sediments at the Belgian continental shelf. *Estuarine and Coastal Shelf Science*, **59**, 599–613.

Waghorn, E.J. & Knox, G.A. (1988) Summer tide-crack zooplankton at White Island, McMurdo Sound, Antarctica. *New Zealand Journal of Marine and Freshwater Research*, **22**, 577–582.

Waller, C., Worland, M., Convey, P. & Barnes, D. (2006) Ecophysiological strategies of Antarctic intertidal invertebrates faced with freezing stress. *Polar Biology*, **29**, 1077–1083.

Weissenberger, J., Dieckmann, G., Gradinger, R. & Spindler, M. (1992) Sea ice: a cast technique to examine and analyze brine pockets and channel structure. *Limnology and Oceanography*, **37**, 179–183.

Welch, H.E., Crawford, R.E. & Hop, H. (1993) Occurrence of Arctic cod (*Boreogadus saida*) schools and their vulnerability to predation in the Canadian high arctic. *Arctic* **46**, 331–339.

Werner, I. (1997) Grazing of Arctic under-ice amphipods on sea ice algae. *Marine Ecology Progress Series*, **160**, 93–99.

Werner, I. (2000) Faecal pellet production by Arctic under-ice amphipods – transfer of organic matter through the ice/water interface. *Hydrobiologia*, **426**, 89–96.

Werner, I. & Gradinger, R. (2002) Under-ice amphipods in the Greenland Sea and Fram Strait (Arctic): environmental controls and seasonal patterns below the pack ice. *Marine Biology* **140**, 317–326.

Werner, I. & Martinez-Arbizu, P.M. (1999) The sub-ice fauna of the Laptev Sea and the adjacent Arctic Ocean in summer 1995. *Polar Biology*, **21**, 71–79.

Werner, I., Auel, H. & Friedrich, C. (2002) Carnvorous feeding and respiration of the Arctic under-ice amphipod *Gammarus wilkitzkii*. *Polar Biology*, **25**, 523–530.

Werner, I., Auel, H., Garrity, C. & Hagen, W. (1999) Pelagic occurrence of the sympagic amphipod *Gammarus wilkitzkii* in ice-free waters of the Greenland Sea – dead end or part of life-cycle? *Polar Biology*, **22**, 56–60.

Wiktor, J. & Szymelfenig, M. (2002) Patchiness of sympagic algae and meiofauna from the fast ice of North Open Water (NOW) Polynya. *Polish Polar Research*, **23**, 175–184.

Wöhrmann, A.P.A. (1997) Freezing resistance in Antarctic fish. In: *Antarctic Communities. Species, Structure and Survival* (Eds. B. Battaglia, J. Valencia & D.W.H. Walton), pp. 209–216. Cambridge University Press, Cambridge.

This page intentionally left blank

11 Sea Ice: A Critical Habitat for Polar Marine Mammals and Birds

Cynthia T. Tynan, David G. Ainley and Ian Stirling

11.1 Introduction

Marine birds and mammals, which we will refer to collectively as 'top trophics' (members of the top trophic level in marine food webs), relate to sea ice in two ways. They either have evolved ways to exploit the opportunities its presence affords (often, increased through specialized access to food) or they find it merely a barrier that must recede or break into open leads and floes before they can move into a previously ice-covered area. In a bit of irony, some resident populations of prey grow large or otherwise benefit from the presence of ice during the period of the predators' forced absence. Modern, industrial humans are among the organisms that find sea ice a hindrance; sea ice, particularly before the era of motorized icebreakers, was a major deterrent to human exploration of polar regions. Sea ice certainly dissuaded the pre-eminent explorer James Cooke, and others before, from discovering *terra incognita*. On the other hand, in his journal, James Clarke Ross (1847), upon his first encounter of Antarctic sea ice, writes of the specialized type of organism:

At 6 P.M. a fine breeze sprang up from the eastward, and we carried a press of sail all night, passing a great many bergs, and much loose ice in long narrow streams, as we advanced to the southward. A beautiful white petrel was seen in the evening, giving notice of our approach to a large body of ice, although we were not at the time aware that these birds never wander far from the main pack.

Though Cooke and others must have observed a similar association of petrel with sea ice, it was Ross, the sailor-scientist, who first made note of it and repeated his observations, including those of other species (certain seals and penguins), several times in his journals. To this day, the snow petrel *Pagodroma nivea* is mentioned in the *Antarctic Pilot* to warn mariners of the immediate presence of ice in the fog-enshrouded seas that often exist at the large-scale sea ice edge. The snow petrel is highly adapted for existence in ice-covered waters and is one of those species classified as an obligate associate of sea ice. We now know that ice-obligate whales, seals and birds exist in both polar regions as well as, in the Arctic only, the polar bear (Table 11.1).

The unique nature of the Antarctic sea ice avifauna has been especially well studied and offers insights into the nature of what being a 'sea ice–obligate species' entails among the top trophics. An analysis of seabird communities in the South Pacific, based on many thousands of kilometres of surveys criss-crossing the entire basin, found the most distinctive of all communities to be the one comprising that associated with the Antarctic pack ice. It was

Table 11.1   A list of polar marine mammals and birds whose presence is characteristic of sea ice–covered waters. Those marked with an asterisk (*) are obligate associates never found far from sea ice; those with a plus (+) are not of the latter, but have evolved specific morphological, physiological or behavioural adaptations to exploit sea ice habitat. The remainder is found often in the open ice pack but ice is largely a barrier to them.

MAMMALS

Antarctic	*Crabeater seal	*Lobodon carcinophagus*
	*Leopard seal	*Hydrurga leptonyx*
	*Weddell seal	*Leptonychotes weddellii*
	*Ross seal	*Ommatophoca rossii*
	Antarctic fur seal	*Arctocephalus gazella*
	+Minke whale	*Balaenoptera bonaerensis*
	+Killer whale	*Orcinus orca*
	Sperm whale	*Physeter macrocephalus*
Arctic		
	*Ringed seal	*Phoca hispida*
	+Harp seal	*Pagophilus groenlandicus*
	+Hooded seal	*Cystophora cristata*
	*Bearded seal	*Erignathus barbatus*
	+Walrus	*Odobenus rosmarus*
	*Polar bear	*Ursus maritimus*
	*Bowhead whale	*Balaena mysticetus*
	+Minke whale	*Balaenoptera acutorostrata*
	Gray whale	*Eschrichtius robustus*
	*Narwhal	*Monodon monoceros*
	+Beluga	*Delphinapterus leucas*
	Killer whale	*Orcinus orca*

BIRDS
Antarctic

	*Emperor penguin	*Aptenodytes forsteri*
	*Adélie penguin	*Pygoscelis adeliae*
	Southern giant fulmar	*Macronectes giganteus*
	Antarctic fulmar	*Fulmarus glacialoides*
	*Snow petrel	*Pagodroma nivea*
	+Antarctic petrel	*Thalassoica antarctica*
	Blue petrel	*Halobaena caerulea*
	Wilson's storm-petrel	*Oceanites oceanicus*
	+South Polar skua	*Catharacta maccormicki*

Arctic

	Northern fulmar	*Fulmarus glacialis*
	*Ivory gull	*Pagophila eburnea*
	*Ross's gull	*Rhodostethia rosea*
	Eider spp. (4)	*Somateria spp.*
	Oldsquaw duck	*Clangula hyemalis*
	+Thick-billed murre	*Uria lomvia*
	+Black guillemo**t**	*Cepphus grylle*
	Dovekie	*Alle alle*

composed of five species (those marked by an asterisk or cross in Table 11.1; Ribic & Ainley, 1988, 1989). In contrast, composition among lower-latitude species communities included much overlap, with community composition much less defined. Following on that study was another that investigated the shift in bird communities as the extent of Antarctic sea ice waxed and waned seasonally (Ainley et al., 1994). The pack ice community remained robust year-round, whereas most species in the open-water community departed high latitudes when winter arrived. Apparently, the lack of sunlight reduced productivity and food availability in open waters, and along with the ice and cold temperatures, forced open-water species to migrate north for the winter. These species, while able to exploit Antarctic waters during summer after the sea ice retreated, did not possess the adaptations to exploit opportunities in the pack ice during winter (or summer). Obligate pack ice species did not then stray into the seasonally vacated open waters; apparently, the pack ice offered sufficient foraging opportunities to satisfy their needs. Indeed, body mass of these birds reached its heaviest of the entire year during winter. The contrast was further demonstrated by a smaller-scale 'natural experiment', when during winter the rapid passing of weather fronts along the large-scale ice edge changed the wind direction from southerlies (very cold, off continent) to northerlies (off warmer waters; Ainley et al., 1993). Under cold, southerly conditions, seas froze northwards hundreds of kilometres 'overnight'; but with the passing of the front and a switch in wind direction a few days later, the new sea ice melted and retreated, leaving the same wide band free of ice. In accord, what remained of the open-water avifauna flip-flopped with that of the pack ice within this zone of dynamic ice cover with the passing of each front.

A somewhat analogous pattern is demonstrated each year among large baleen whales both in the Antarctic and Arctic (Brown & Lockyer, 1984). These are open-water creatures that can forage under ice only as far as their breath-holding abilities allow. It has been well known since the commercial whaling days that the great whales would follow the seasonal retreat of the pack ice. As the ice disappeared, new prey concentrations would become available. Thus, there was a sequential replenishment of feeding opportunities, with the whales and their pursuers being led ever farther south following the retreating ice. However, all but the minke whale in the Antarctic and the bowhead whale, narwhal, and beluga in the Arctic vacate the ice-covered polar waters before the autumn advance of sea ice. Prior to freeze-up each year, the whaling ships (the lucky ones) departed as well.

In this chapter, we explore the adaptations that allow warm-blooded, air-breathing vertebrates to remain in ice-covered waters throughout the year.

11.2 Polynyas

Before proceeding much further, we must first explore the subject of areas of predictable or persistent open water surrounded by ice. These open-water areas, called polynyas (Chapters 1 and 3), are very important to all top trophics and the need to access them drives the life-history patterns of several species. The reader wishing to explore the subject of polynyas in even greater detail should refer to Smith and Barber (2007).

Hypothetically, in the 'purest' definition of the word, a polynya exists only during that time of the year when sea water should be actively freezing. In some areas, especially along headlands and fast ice edges, such as in coastal Antarctica or the North Water of northern Baffin Bay, strong, near-continual winds sweep new ice clear, along with the heat expelled

from continually freezing surface water, creating what is known as a 'latent-heat' polynya. Similarly, along coastal areas such as in much of the Arctic Basin or Hudson Bay and the southern Beaufort Sea, offshore winds alternate with onshore winds that alternately create open leads parallel to the shoreline or cause them to close up.

In other areas, warmer subsurface waters are brought to the surface, usually a function of currents rising over ridges and rising shelf topography. The result is that surface waters remain above the freezing point. These are 'sensible-heat' polynyas. However, even after air temperatures become warm in the late spring and surface waters are no longer cool enough to freeze, predictable open-water areas still occur within the sea ice–covered region. Often, these areas are the same as those present during winter as 'true' polynyas. In the larger sense of the word, then, these areas too qualify as polynyas or temporal extensions there of. After the freezing period, these ice-free areas within the pack are then known as 'post-polynyas'.

Recurring polynyas are those that remain open throughout the winter, or open at the same time each spring, at the same location and time every year. While any polynya may be used opportunistically by top trophics at any time of year, recurring polynyas are of the greatest biological importance because overwintering or migrating species can depend on being able to breathe and feed while there. They do not just find these areas in a random way; they 'know' of their existence from past experience and rely on them to be present. This sort of tradition or knowledge can be lost to birds and mammals when their populations become severely reduced by the actions of man, and its loss is one reason why it becomes so difficult for these cognitive creatures to recover their numbers should the deleterious factors be controlled. Polynyas differ in the extent and processes of their production and, thus, they are not equally productive or attractive to all species (Stirling, 1997; Karnovsky et al., 2007), another important bit of a species' 'knowledge'.

In the Antarctic, the importance of polynyas to top trophics is not well understood. While physicists have launched major investigations of Antarctic polynyas, for the most part, this is not the case among biologists. There are many latent-heat polynyas, generated along the coast by fierce katabatic winds. Most of the Antarctic coast is far enough south (well below the Antarctic Circle) that almost all of these polynyas are in total darkness from late fall to early spring. For that reason, they are of little interest to birds and mammals at that time, most of which need daylight to locate prey. Only the distribution of (winter-breeding) emperor penguin nesting colonies is affected by them, as they provide access to open water (Massom et al., 1998; Fig. 11.1). On the other hand, these open areas continue to persist as post-polynyas well into the spring (beyond the freezing period) and then affect the location of Adélie penguin colonies as well (Ainley, 2002; Fig. 11.1). In the autumn, before it becomes dark below the Antarctic Circle, as the sea ice expands, sensible-heat polynyas aid the northward migration of Adélie penguins in the Ross Sea region (Fig. 11.2); they act like 'stepping stones' for the penguins to frequent before darkness forces them to move to the large-scale pack ice edge for the mid-winter period. On the other hand, in the Antarctic Peninsula region, Adélie penguins have to migrate south to remain in the pack ice. The sensible-heat polynyas in Marguerite Bay are very important to them (Fraser & Trivelpiece, 1996).

Ecologically, the situation is different in the Arctic. There, the existence of polynyas, many of which occur well to the south of the Arctic Circle (and in sunlight), is the major feature that affects life-history patterns of top trophics (Brown & Nettleship, 1981; Stirling, 1997). The distribution of most bird and mammal colonies in the Arctic, and in turn the villages (especially prehistoric ones) of native peoples, is strongly related to the presence of polynyas
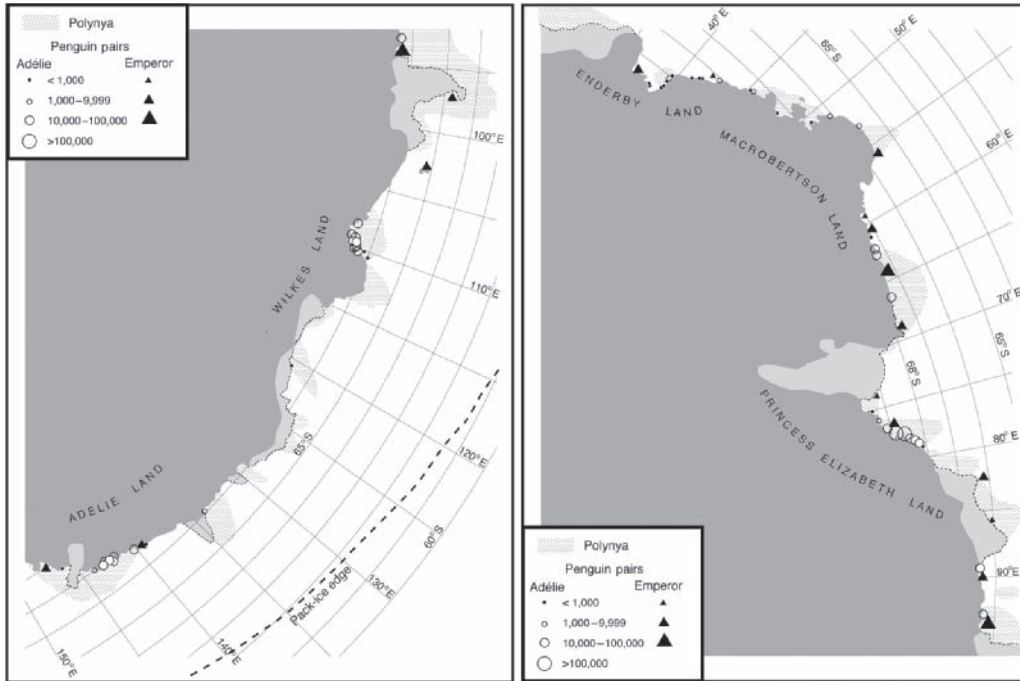
Fig. 11.1 Association of emperor and Adélie penguin nesting colonies with coastal polynyas: East Antarctica. (a) 95°E–150°E and (b) 25°E–95°E. Figure redrawn from Ainley (2002, Fig. 3.1), where data sources also identified. Réproduced from Siegel, V. (2000), with permission from NRC Research Press.

Fig. 11.2 Movement of Adélie penguins from summer breeding colonies on Ross Island north to the pack ice edge, using polynyas as 'stepping' stones during their trip.

(Schledermann, 1980; Fig. 11.3). Major physical–biological investigations have taken place to deduce the processes that enhance their value, both in bringing access to open water and in stimulating biological productivity. The North Water of Baffin Bay provides valuable winter habitat for belugas, bowhead whales, bearded seals and walruses (Stirling, 1997; Richard et al., 1998b; Karnovsky et al., 2007). Studies of other polynyas, such as the Northeast
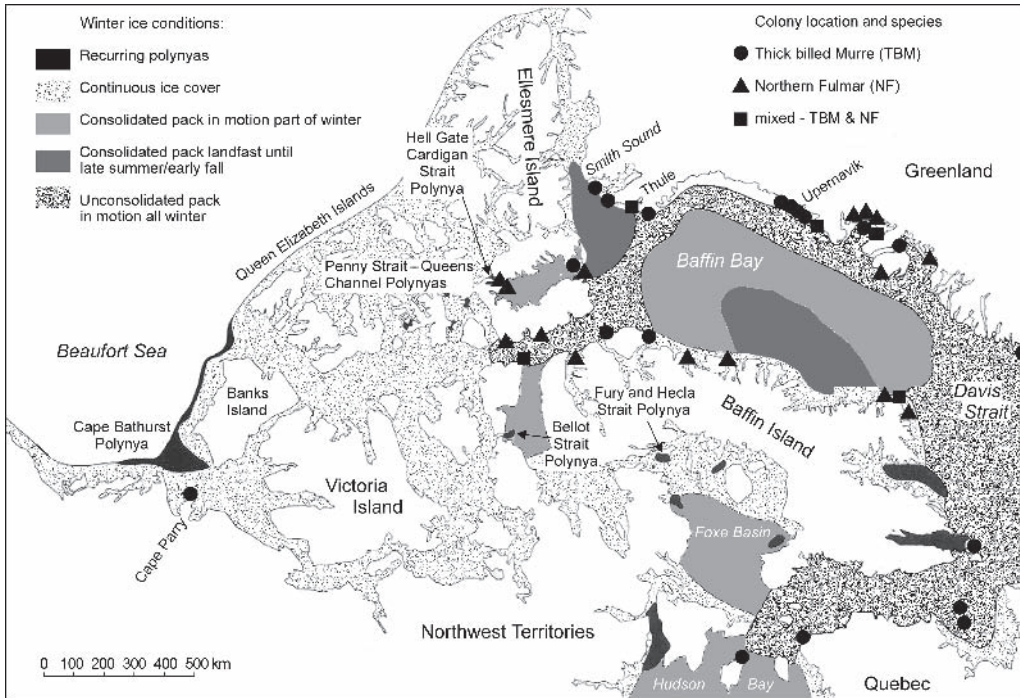
Fig. 11.3 Distribution of seabird colonies in correspondence to polynyas in the Canadian Arctic (reprinted with permission from Brown & Nettleship, 1981).

Water Polynya (Falk et al., 1997; Karnovsky et al., 2007), the Cape Bathhurst Polynya (Harwood & Stirling, 1992), the major polynyas south of the Chukchi Peninsula, St. Lawrence and St. Matthew islands in the Bering Sea (Niebauer et al., 1999; Petersen et al., 1999) and polynyas of the Belcher Islands in southeast Hudson Bay (Gilchrist & Robertson, 2000), all testify to the biological importance of these persistent open-water areas to overwintering mammals and birds. Unlike the Antarctic, where the large-scale ice edge, well to the north of the continent and the Antarctic Circle, first experiences the onset of increased spring production, in the Arctic production gets a faster start in polynya areas. The critical elements are sunlight and open water. So critical are polynyas to top trophics in the Arctic that large dieoffs of seabirds or sea ducks occur when, in rare cases, a usually predictable polynya is not open by the time migrating birds arrive to feed in spring (Stirling et al., 1981). These major mortalities of adults can alter population growth of affected species for decades. The hunting success of polar bears and humans increases as the amount of open water decreases to narrow leads (thereby confining prey), making the hunted seals more vulnerable to predation.

Considering the present trend towards rapidly warming temperatures in the Arctic and some Antarctic regions (Overland et al., 2008; Steig et al., 2009), the large-scale loss of the sea ice (Overland et al., 2008; Stroeve et al., 2008) will likely have significant detrimental effects on marine mammals (Tynan & DeMaster, 1997; Kovacs & Lydersen, 2008; Laidre et al., 2008; Nicol et al., 2008) and birds as well. As yet, it is still unclear what all the consequences of these changes are likely to be. However, the patterns of use of areas that were

formerly polynyas is likely to change to some degree as may the diets of seabirds dependent on feeding in polynyas near their breeding colonies (Gaston et al., 2003). These changes will likely also impact the traditional activities of people in Arctic villages, many of which were originally established because of their proximity to marine resources.

11.3 Habitat preferences and adaptions in sea ice

Antarctic

A major requirement for several marine mammal and bird species is a platform for reproduction, and sea ice does very well in providing this. Included are the pack ice seals (crabeater, leopard, Ross and Weddell; Table 11.1) and the emperor penguin. Almost all middle- or high-latitude top trophic species time their reproductive cycles so that young become independent of parents when food availability is highest – late summer and early fall – thus providing the best conditions for them to learn foraging techniques well enough that they can survive the winter. This means that pups must be born and eggs laid in very early spring or winter depending on the amount of time needed to raise young from birth or egg-laying to independence. Most phocid seals, with the exception of the leopard seal, have small flippers (in itself, probably an adaptation to retard heat loss in cold water), and are far less agile on land or on ice than the larger-flippered fur seals and sea lions of warmer latitudes (Fig. 11.4). Although it is not impossible for the phocids, they tend not to haul out on steep, rocky terrain or move very far inland. The same is true of the emperor penguin, which is very clumsy on land compared to its smaller relatives, such as the Adélie penguin. In middle and lower latitudes, phocid seals breed more on beaches (easily accessed); fur seals and sea lions breed on both beaches and rocky headlands. Beaches exist only for a very short time each year in the Antarctic (and always in the fall). In the spring – the time when young are produced and mating occurs – the only accessible breeding habitat for many top trophics is sea ice, because at that time beaches are layered with ice floes pushed into high ridges (5–10 m or even higher) by winter winds. In the case of Antarctic seals, pups are born on the surface of the fast ice or stable floes where they can be nursed until weaned and at the same time avoid predators. Most seals mate in the water except for crabeater seals, which appear to mate on the surface of the floes, possibly to reduce the risk of predation by leopard seals and killer whales (Siniff et al., 1979). In the case of the emperor penguin, successful breeding requires sea ice attached to the land, known as land-fast ice, which will remain locked in place by capes, rocks and grounded icebergs well into summer. Weddell seals have evolved to the land-fast ice as well but only in places where tidal action and glacial movement help to maintain cracks that can be enlarged by the seals for use as breathing holes. This provides a stable environment far from predators until well after the pups have been weaned.

Later in the year, ice as a platform comes into play again in the annual cycle of Antarctic mammals and birds because they renew their pelage and feathers annually. For the birds, the insulating properties of feathers are critical for survival in cold weather; for seals, it is the blubber layer beneath the coarse coat of hair and skin that keeps them warm. However, rather than replacing fur or feathers gradually, as some related lower-latitude species do, these animals complete their moult within a few weeks. Polar top trophics do this by laying on huge stores of fat on which they live while coats are being replaced quickly at considerable

Fig. 11.4 A female Weddell seal and her pup lying together on fast ice during a gale; McMurdo Sound, Antarctica (Photo D. Ainley).

energetic cost. They cannot afford the heat loss of partly moulted pelage or feathers, and normally abundant food of the pack ice region allows them to accumulate pre-moult fat. During the moult, penguins remain on large ice floes, fasting. In the case of emperor penguins in the Ross Sea, they must travel in the range of 2000 km from their breeding colonies to reach floes of sufficient size and stability to ensure they will be able to complete their moult prior to break-up (Kooyman et al., 2004).

The pack ice is also of importance to the flighted birds. For example, snow and Antarctic petrels, given that food is so abundant, lose so many flight feathers at once that without the strong, persistent winds of the Southern Ocean, they would become practically flightless during the moult. As it is they spend a lot of time sitting on icebergs or large ice floes. Most seals, on the other hand, continue to feed (mostly at night) while moulting but spend longer periods of the day hauled out during the moult. A possible exception is the Ross seal, which appears to remain on the ice through most of the time required to moult and may not feed, or at least not as often as other ice-breeding seals (Ackley et al., 2003). Like elephant seals on islands, Ross seals appear to remain hauled out on large stable ice floes deep in the pack ice that will not disintegrate until after the moult is complete. At that time of year (February–March), all these moulting birds as well as pack ice seals (see below) are concentrated in just six areas where sea ice remains year-round (Chapter 6). Only the flighted birds have access, for roosting and moulting, to the tops of many tabular icebergs that occur where food is abundant. Many icebergs also occur where food is not abundant, but the birds are not interested in these.

The other aspect of sea ice that is important to Antarctic top-trophic species is the rich under-ice community of fish and invertebrates that become prey, if these predators have the ability to exploit it (Ainley et al., 1991; Hopkins et al., 1993). The obligate species are able to do so. Emperor and Adélie penguins, and Weddell seals, can hold their breath much longer than comparably sized, related species that occur in open waters or even other ice-obligate species in the case of seals (Kooyman, 1981; Ainley, 2002; Fig. 11.5). This allows them to swim for appreciable distances under ice floes to forage. The availability of prey in ice-covered waters is often a function of the epontic (under-ice) area that is accessible or available. Thus, the more under-ice habitat that can be accessed, the better chance they have of finding food. Obviously, large floes, if the predator can get farther from the edge, offer the best potential pickings. This is especially true during winter when the only growing phytoplankton (food of the prey) is contained within the ice on the underside of floes (Ainley

Fig. 11.5   Adélie penguins congregating on an ice floe at the edge of a polynya, maintained by persistent winds, in the Ross Sea (Photo D. Ainley).

et al., 1991, Chapter 8). These epontic algae grow deep into the subsurface ice layers, seeking the light that filters through; in that position, the algae are immune, too, of being mixed downwards into the water column (and away from the light) by wind-generated turbulence and mixing. The epontic prey of the top trophics, mainly euphausiids (krill), graze the phytoplankton in this under-ice habitat. The predators either eat the euphausiids or the fish in turn preying on them.

The two obligate-ice penguins, emperor and Adélie as well as the Weddell seal, thus associate with sea ice for several differing reasons. It is not often clear, but presumably, they can exploit open-water habitats as well as any other penguin or seal species. Ultimately, their association comes down to what might be analogous to the question of why songbirds associate with forests. Simply put, it is just that they evolved in association with or to exploit that habitat while other species have not. If the forests are cut down, the songbirds disappear; if the sea ice disappears, so do these two penguin and perhaps the seal species (see below, Section 11.4 on effects of climate change). To summarize the above discussion, the emperor and Weddell seals require stable fast ice for breeding, and these species require reliable ice floes for moulting (although Weddell seals are also able to moult on beaches when they become ice free). These species feed on epontic organisms to a great extent; all, however, can also dive deeply (especially the emperor and Weddell seals) to exploit prey further down in the water column and much farther under ice than can other birds and most other ice-breeding seals.

Snow petrels have perfected what has become known as 'ambush feeding' (Ainley et al., 1994). Their entirely white plumage allows them to sit at the edge of floes or on small bits of ice waiting for an unsuspecting fish to venture out from the edge, at which point the bird dives in to capture it. Sometimes it may catch fish that are too large to be carried away but, because of the concealing nature of their white plumage, they are usually able to consume the prey without gaining the notice of skuas. The latter are in the business of stealing prey from other birds (kleptoparasites). The Antarctic petrel, on the other hand, which is boldly coloured black and white, is the only high-latitude bird that feeds by pursuit plunging. They fly quickly and along the edges of rapidly expanding leads, dive into the water and pursue prey 'without missing a beat' by swimming using their wings for propulsion. Although the feeding strategies of these two flighted predators of the pack ice ecosystem are dramatically different, both effectively exploit different opportunities offered within the pack ice.

Fig. 11.6   Ringed seal looking out of the hole it maintains for breathing using its claws for excavation (Photo by C. Lydersen, presented with permission)

Unlike penguins (and the flighted antarctic birds), antarctic seals rely on a thick blubber layer to provide the insulation needed to conserve heat (Fig 11.4). Seals, of course, which can dive deeper and longer than most birds (the emperor penguin, which can dive to between 300 and 500 m, is an exception), are less constrained by sea ice in their foraging within the pack ice zone compared to most polar birds. On the other hand, except for the Weddell seal, pack ice seals (crabeater, leopard, Ross) tend to avoid areas of consolidated pack ice where freeze-ups (of leads) are more frequent and therefore problematic (Laws, 1984; Ribic et al., 1991).

The Weddell seal is highly adapted to annual fast ice during summer and both fast ice and consolidated pack ice during winter (Laws, 1984; Fig. 11.4). There they search for fish, particularly the Antarctic toothfish (*Dissostichus mawsoni*) and Antarctic silverfish (*Pleuragramma antarcticum,* Plötz et al., 2001). In fast ice areas, they must keep their breathing holes from freezing over by frequently abrading the ice with their canine teeth. They maintain their breathing holes on cracks in the ice that are sustained in the same place each year by tidal action or by glacier fronts that constantly push the annual ice away from shore or around small offshore islands. These cracks are critical to the existence of Weddell seals in land-fast ice areas. Even though several individual seals may cooperate in keeping a breathing hole open, older Weddell seals exhibit worn teeth from abrading the sea ice. Breakage of teeth, followed by root canal infections that spread into the bone of the upper jaw, appears to be a significant cause of mortality (Stirling, 1969).

A recent 'natural experiment' illustrated the importance of these cracks to the survival of Weddell seals. In 2000, a large iceberg grounded cross the entrance to McMurdo Sound for 5 years, precluding the normal pattern of break-up of the annual ice each summer. Because the fast ice was prevented from breaking up, it became progressively thicker each winter and many of the cracks were no longer large enough to allow Weddells seals to maintain breathing holes on them. Consequently, the seal population in McMurdo Sound declined by about half, but recovered soon after the iceberg disappeared and the normal pattern of freezing and break-up of the annual fast ice returned (Siniff et al., 2008).

A unique group of Weddell seals at White Island, about 20 km into the Ross Ice Shelf from the southern extent of of McMurdo Sound, Ross Sea, has been isolated by extensive, uncrakked, persistent sea ice between them and the main population for so long that they have become genetically distinct (Gelatt, 2001). This population probably became established during a period when fast ice in the Sound was less extensive. The combination of their relatively sedentary nature and fidelity to breeding sites has contributed to the genetic separation of Weddell seals in the southern Ross Sea from other Antarctic populations (Davis et al., 2000, 2008).

The primary habitat for overwintering and breeding adult Weddell seals is the coastal fast ice. However, more recent research has indicated the importance of pack ice as well to both adults and pups (especially during winter, Testa, 1994; Stewart et al., 2000). The Weddell seals in McMurdo Sound are the most southern breeding mammal in the world and rely on the annual fast ice for breeding. Most pups leave the breeding colonies at 6 weeks of age and young seals are rarely seen again until they are 5–6 years old. Young seals, tracked with satellite telemetry, left McMurdo Sound in January and headed to the pack ice or open-water polynyas of the Ross Sea during winter (Stewart et al., 2000). Foraging success may be enhanced at polynyas (see above). Although young Weddell seals may be vulnerable to a small amount of predation by leopard seals in the pack ice during winter, killer whales avoid that habitat. Weddell seals have also evolved or learned specific behavioural tactics to help them hunt for small nototheniid fish (e.g. *P. antarcticum*) and larger Antarctic toothfish (Davis et al., 1999), both of which occur mainly in waters overlying the continental shelf (and therefore areas overlain extensively by sea ice). Foraging tactics under the ice may include silhouetting their prey against the under-ice surface, perhaps helping to hide the predator, and attacking from below. Weddell seals have also been observed to expel fish from ice crevices by expelling a blast of air through their muzzle or by prodding the ice with their muzzle (Davis et al., 1999), though it is unclear how often they do this or how important it is to their total dietary intake. They also 'cache', in shallow water or in their ice holes, prey that they have caught elsewhere (Kim et al., 2005), perhaps another adaptation needed in a habitat that requires a long breath-holding capacity to exploit.

Crabeater seals (perhaps the most numerous pinniped in the world, along with the ringed seal in the Arctic; see below) and leopard seals are predominantly species of deep pack ice through most of the year, although subadults also haul out on coastal fast ice, and occasionally land, during summer. During winter, they occur mainly in the divergent ice of the peripheral sea ice zone, and in the deep pack during summer are associated with ice cover of 60–70% and evenly distributed ice floes (Ribic et al., 1991). As crabeaters feed almost exclusively on krill, linkages between sea ice dynamics and krill life history and distribution would be expected to impact their foraging ecology. As the krill occur beneath ice floes to a great extent, the crabeater is not known as a particularly deep-diving species. The leopard seal, another species of the looser pack ice, has the most catholic of diets among the ice seals. They feed heavily on krill, but also take significant numbers of penguins and other seals (particularly pups) as well (Siniff & Bengtson, 1977). During spring and summer, Ross seals appear to prefer heavier pack ice than the above two species because they appear to remain hauled out for an extended period, possibly the whole time, while moulting and thus require stable floes that will not disintegrate before they are finished. They may also give birth to their young and wean them in the deep stable pack away from predators as well but this aspect of their life history remains unknown. Their predominant prey is squid (Laws, 1984).

For the rest of the year, they appear to use floes at the outer edge of the fast ice only for periodic resting (similar to the use of islands by elephant seals) between extended periods in open waters to feed (Blix & Norday, 2007).

The pack ice seals, as noted above, depend on ice as a floating substrate for resting, breeding, weaning pups and refuge from marine predators. Initially at least, in the Weddell Sea, seasonal reduction in ice cover (Chapter 6) is likely to lead to increases in ice seal densities, due to the fidelity of ice seals to the pack ice despite seasonal and annual changes in its distribution (Bester & Odendaal, 2000). During El Niño 1998, the virtual absence of pack ice in the eastern Weddell Sea led to very high densities of pack ice seals hauled out on the available ice. Whether or not such an increase in seal density affects the foraging efficiency of the ice seals over the longer term, or possibly has negative effects on their prey in such areas is not known. However, when areas of pack ice are reduced, it is likely that resident seals spend more time swimming in transit between haul-out sites and productive foraging grounds, which might be predicted to result in a greater expenditure of energy than during conditions where pack ice is located over sufficiently dense prey (see below).

During the austral winter, some southern elephant seals (*Mirounga leonina*) occur along the outer edge of the Antarctic sea ice. For example, satellite transmitters deployed on adult female elephant seals from King George Island revealed that the seals ranged in the sea ice zone of coastal shelf waters along the Antarctic Peninsula (Bornemann et al., 2000). During winter, some female elephant seals with satellite radios spent several months in heavy but divergent pack ice. The availability of the Antarctic silverfish, as well as perhaps Antarctic toothfish, may explain why elephant seals are attracted to the pack ice to forage. In contrast to the adults, juvenile elephant seals from King George Island appear to avoid the sea ice and range in ice-free waters (Bornemann et al., 2000).

The only cetaceans that occur, regularly, deep into the pack ice of the Southern Ocean are the Antarctic minke whale (*Balaenoptera bonaerensis*), and to a lesser degree what are termed the 'type C' and 'type B' killer whales (*Orcinus orca*). Some portion of the minke whale population is known to inhabit the Antarctic pack ice zone year-round. This, the smallest of the baleen whales, has a very long, narrow and hard rostrum (Fig. 11.7), which they use to break through young ice in order to breathe. When the ice begins to freeze in late autumn, seals and penguins may also use the whales' breathing holes to aid in their own

Fig. 11.7   Antarctic minke whale at the ice edge (Photo by D. Ainley).

escape to areas of sparser ice cover. Thus, movements of some of the pagophilic, top trophics in the Southern Ocean, in some respects, are facilitated by the minke whale. Minke whales are associated with small floes, pancake and new ice (Ribic et al., 1991; Theile et al., 2004; Ainley et al., 2007a). In waters off the west Antarctic Peninsula, humpback whales (*Megaptera novaeangliae*) concentrate at the ice edge during late summer and autumn, whereas minke whales occupy ice-covered areas along the entire shelf in winter as well (Theile et al., 2004). The abundance of minke and humpback whales was related to a threshold density of zooplankton prey, as well as the ice edge (Friedlaender et al., 2006). The whales feed primarily on Antarctic krill (*Euphausia superba*) in most areas; however, the ice or crystal krill (*Euphausia crystallorophias*) appears to be an important prey for minke whales in waters overlying the continental shelf of the Ross Sea and other shelves. Greater food availability near the ice edge appears to significantly attract minke whales (Ichii et al., 1998; Fig 11.7). In 1994–95, extensive sea ice conditions in the Ross Sea covered the typically krill-rich slope region during summer and restricted the availability of this habitat to minke whales. This was reflected in the poor body fat condition of the whales (Ichii et al., 1998). It is unknown how warming trends in the Ross Sea area since the 1960s (Taylor & Wilson, 1990) may have affected the biomass and distribution of their euphausiid prey. Long-term declines, over two decades, in the energy storage and body condition of Antarctic minke whales have been observed (Konishi et al., 2008), coincident with declines in Antarctic krill density in the Southwest Atlantic sector (Atkinson et al., 2004, 2008), regional increase in water temperature (Meredith & King, 2005) and a decrease in sea ice (Parkinson, 2002).

Of the toothed whales (Odontocetes), the killer whale and sperm whale are most closely associated with sea ice. In the pack ice habitat, killer whales, 'type B', stalk seal and penguin prey; 'type C' feed on Antarctic silverfish and toothfish (Pitman & Ensor, 2003; Ainley et al., 2006). Sperm whales observed near the ice edge are probably feeding on mesopelagic squid, as well as toothfish, associated with Circumpolar Deep Water shoaling especially along shelf breaks (Tynan, 1997; Collins et al., 2007). During summer, the distribution of migratory large baleen whales reflects the circumpolar position of the Southern Boundary of the Antarctic Circumpolar Current; as summer progresses with the southward retreat of the ice and concurrent evolution of the productive marginal ice edge zone, these whales move closer to the continent (Tynan, 1998). Linkages between sea ice dynamics and the southernmost extent and depth of warm Upper Circumpolar Deep Water are expected to affect the productivity of the Antarctic ecosystem and the related food web.

Small cetaceans appear to avoid 'type A' killer whales (Pitman & Ensor, 2003) by remaining in extensive sea ice when possible. For example, the behaviour of bowhead whales, belugas and narwhals in the Arctic (see below), and minke whales in the Antarctic, may be strongly influenced by fear of predation by killer whales. Whether sea ice serves to shelter the cetaceans from killer whales more by visual versus acoustic reduction of detection is not known. 'Type A' killer whales, a known and frequent predator of minke whales, avoid the sea ice (Pitman & Ensor, 2003).

Arctic

Ross's and ivory gulls are as highly adapted to life in the Arctic sea ice zone, as is their analog, the snow petrel, in the Antarctic. Neither of these species remains for long in areas without sea ice. In fact, they are rarely found far from drifting sea ice at any time of the year.

They are white or near-white in colour, an effective adaptation (as long as their background is white!) by which they avoid the notice of predators and kleptoparasites. In addition, white colouration allows them to approach their prey more closely. Like the snow petrel, ivory gulls nest in ice-free terrain, which often means the tops of nunataks (mountains projecting through an ice sheet; Haney & MacDonald, 1995; Gilchrist & Mallory, 2005). Not only do they find in those localities the ice-free terrain in or on which to nest early in the spring, but the expanse of ice surrounding their colonies protects them from predators (skuas – Antarctic; foxes and polar bears – Arctic). Ross's gulls often nest on islands within lakes and, in that regard, are less associated with sea ice.

Several top trophics throughout the Arctic rely to a large degree on Arctic cod (*Boreogadus saida*), a small fish that feeds on epontic crustaceans that, in turn, graze the ice algae on the underside of ice floes. Ivory and Ross's gulls forage at the surface, near floe edges, often looking for prey (fish and zooplankton) washed onto floes (Haney & MacDonald, 1995). Black guillemots and thick-billed murres, on the other hand, are strong subsurface divers that forage in epontic habitat where cod and some of the larger crustaceans are their usual targets (Bradstreet, 1980). The guillemot is an almost all-black species, while murres are dark brown on their upper side. Such colouration is cryptic to prey looking down from the ice into the murky depths from which this predator approaches.

Among the Arctic ice seals, the ringed seal is almost certainly the best barometer of changes in ice conditions. This species, like its southern ecological counterpart the Weddell seal, prefers coastal land-fast ice for overwintering and reproduction. In particular, ringed seals depend on stable annual ice, sufficient snow accumulation for subnivean lairs and proximity of productive feeding areas to their breeding habitat (Smith & Stirling, 1975; Hammill & Smith, 1989). They are particularly associated with coastal or between-island fast ice but also occur in offshore areas having large stable annual ice floes such as Baffin Bay and the Barents Sea (Finley et al., 1983; Wiig et al., 1999). Sufficient sea ice deformation is needed to facilitate formation of a snowdrift under which ringed seals maintain breathing holes and excavate haul-out lairs. Ringed seals use the heavy claws on their foreflippers to maintain 2–4 breathing holes in ice up to 2 m or more thick (Fig. 11.6). During spring, ringed seals give birth to their pups inside their subnivean lairs. The pups are born with a white coat of lanugo (soft, first coat) to make them less visible to predators should they be exposed on the ice before they are able to escape predators by entering the water. Ringed seals mate in the water after the pups are weaned, and haul out on the ice beside a breathing hole or crack to moult. The timing of ice formation and therefore of pupping and moulting varies with latitude. Although in most Arctic regions ringed seals typically rely on subnivean lairs for pupping, in the Sea of Okhotsk, pups are born on the ice without any shelter of snow (Gjertz & Lydersen, 1983). In the Canadian Arctic, ringed seals show a preference for annual fast ice with greater than 75% ice cover over water 50–175 m deep (Kingsley et al., 1985) and ice deformation of less than 40% pressure ridging of the total ice cover (Frost et al., 1988). Ringed seals dive near or under the ice in search of arctic cod, other pelagic schooling fish, pelagic amphipods of the genus *Parathemisto* and amphipods associated with the benthos or undersurface of the sea ice (Finley et al., 1983; Welch et al., 1992).

The effect of changes in ice conditions and otherwise undetected fluctuations in the arctic marine ecosystem can be monitored by reproductive success of ringed seals (Smith & Harwood, 2001; Stirling, 2002). The holes made by ringed seals allow for rapid drainage of surface water, such as meltpond water, creating a dendritic pattern around white circular areas

that can be detected by remote sensing (Digby, 1984). The breathing holes of ringed seals can become further enlarged by the flow of meltwater, which often forms a vortex (Holt & Digby, 1985). Processes that redistribute or change the prevalence of surface meltwater are of critical importance for the ice energy and mass balance as it affects ice albedo and heat fluxes through the ice cover (Eicken et al., 2002). Therefore, in regions of the Arctic where first-year ice has few non-biogenic flaws or perturbations, the drainage of meltwater through seal holes may be especially important. Drainage of large meltponds should increase albedo and consequently help to conserve the ice. Further, the freshwater that drains through the seal holes may form new ice at the freshwater–sea water interface under the ice. In this way, the seals contribute to positive feedback loops that promote ice maintenance. No studies, however, have considered possible linkages between ice seals and ocean–ice–atmosphere processes.

Complex linkages between climate change and the extent, structure and associated productivity of sea ice may impact ringed seals (Tynan & DeMaster, 1997). Severity of ice conditions have been related to reduced ovulation rates and reduced body condition of ringed seals (Stirling et al., 1977; Harwood et al., 2000; Stirling, 2002). For example, heavy sea ice conditions in the Beaufort Sea during the winter of 1973–74 coincided with the subsequent decline of ringed seals in 1974 and 1975 (Stirling et al., 1977; Stirling 2002). In Prince Albert Sound, Northwest Territories, Canada severe ice conditions in 1974 appeared to have led to a reduction in the prey available to seals (Harwood et al., 2000). In contrast, the earlier clearance of ice during spring1998 provided greater availability of prey to all ages of ringed seals. Despite the apparent availability of prey, the early disruption of fast ice had a significant negative effect on the growth, condition and survival of pups still dependent on their mothers. With earlier spring warming and early break-up of the sea ice, many pups were apparently separated from their mothers, had shorter lactation and were prematurely forced to enter the water for extended periods, resulting in slower growth and higher mortality (Smith & Harwood, 2001). Early collapse of lairs from rain or warm temperatures can also expose pups to high levels of predation by polar bears and arctic foxes (Stirling & Smith, 2004).

Bearded seals have a circumpolar distribution in the open drift ice and tend to avoid regions of continuous, thick land-fast ice (Burns, 1981). They do, however, sometimes maintain breathing holes in relatively thin ice. Bearded seals rely on drift ice over relatively shallow regions (< 100 m depth) where they feed on benthic prey (Kingsley et al., 1985). Soon after birth, the pups enter the water as capable swimmers (Burns, 1981). In the northern Barents Sea, the distribution and movements of bearded seals tend to track the seasonal advance and retreat of the sea ice cover, with high densities of mother–pup pairs occurring near the ice edge in late April to early May (Wiig & Isaksen, 1995). Similar observations have been recorded in the Beaufort Sea (Stirling, unpublished observations). In order to stay near suitable feeding areas, mother–pup pairs in Kongsfjorden, Svalbard, appear to move away from offshore drifting pack ice and back into the head of the fjord during May (Hammill et al., 1994). There, at the flaw zone, at the edge of the fast ice, they may find more sheltered conditions with suitable ice for hauling out.

Another ice seal, the hooded seal, is a migratory, pelagic species (Bowen et al., 1987). Pups are born during March on heavy ice floes close to the ice edge in three regions of the North Atlantic: near Jan Mayen Island, off northeastern Newfoundland and in the Davis Strait. After only 4 days of lactation, pups are weaned abruptly, their mothers leave and they are left alone on the ice while they adapt to independent life (Bowen et al., 1987). Adults migrate to pack ice off southern Greenland to moult during June and July (Sergeant, 1976).

In spring, harp seals (*Pagophilus groenlandicus*) migrate from pelagic feeding areas in the High Arctic to give birth in vast herds in pack ice areas further south. There they seek regions of extensive drifting pack ice that is not adjacent to land, using floes further in from the ice edge than those used by hooded seals (Lydersen & Kovacs, 1999). Pups are weaned at 12 days of age, having not yet entered the water in most cases. Hooded seals have a broad diet and forage on capelin and the amphipod *Parathemisto libellula* close to the ice edge in the Barents Sea.

The walruses comprise three currently recognized subspecies (i.e. the Atlantic walrus *Odobenus rosmarus rosmarus*, the Laptev walrus *O. r. laptevi* and the Pacific walrus *O. r. divergens*), all of which associate with drift ice, upon which they rest. Polynyas allow some groups to overwinter and breed in winter at high latitude (Sjare & Stirling, 1996). Their long tusks, for which they are renowned, serve as convenient ice axes for hauling out onto the ice floes; hence the derivation of one of their nicknames, the 'tooth-walker'. They are also capable of using their heads to break through young ice up to 20 cm thick (Fay, 1982). After break-up, if ice is not available, they will haul out on land (Fay, 1981). As a highly social and gregarious species, they haul out together in large numbers, lying closely packed together. During the summer moulting period, they reside on either ice or land. Their prey consists mainly of mollusks and, therefore, they must find haul-outs near shallow regions (<80 m) having high benthic production. In the Bering and Chukchi Seas, walruses may spend more than 85% of their time feeding (Fay, 1982). Near Svalbard, walruses feed primarily on the bivalve *Mya truncata* and the gastropod whelk *Buccinum* sp. (Gjertz & Wiig, 1992). Walruses that haul out on drifting pack ice may be passively carried to new benthic feeding grounds. Without drift ice, walruses lose this convenient connection between motile haul-outs and new benthic foraging grounds; when confronted with heavy consolidated ice, the walruses must rely on polynyas and the restricted benthic foraging grounds near them (Sjare & Stirling, 1996). Some walruses winter in the southern parts of Svalbard, as well as within the winter pack ice (Wiig et al., 1996), possibly due to the abundance of open leads within the Barents Sea ice during winter (Vinje & Kvambekk, 1991). Males in northeastern Greenland disperse in autumn and winter in the pack ice along Fram Strait and northeastern Greenland. Sea ice conditions can affect more than foraging success. Studies in the Canadian High Arctic suggest that mating systems and breeding behaviour of walruses are also strongly influenced by variability in sea ice habitat (Sjare & Stirling, 1996). Furthermore, walruses in the Bering Sea, especially females with calves and younger animals, rely on sea ice in the summer over the continental shelf to feed from while nursing. As the summer ice retreats further over deeper water, this is now creating difficulties for walruses, which are shallow-water benthic feeders, by extending the distances between the ice they rest upon and where they need to go to feed (Grebmeier et al., 2006).

Polar bears are confined to seasonally ice-covered areas of the Arctic and sub-Arctic where they search for prey: ringed, bearded, harp, hood and harbour seals; walruses, belugas and occasional narwhals. The dynamics of sea ice can affect their access to these prey species; without ice, the bears often are unable to forage. Polar bears depend on fast ice to search for ringed seals (especially pups). In some regions, such as the Barents Sea, they also hunt for ringed seals, as well as bearded and harp seals, along lead systems or ridged ice on larger floes of drifting pack ice (Wiig et al., 1999). Tracking of polar bears, with satellite radio collars, has shown that bears are more active and range further in active pack ice than in consolidated pack ice (Ferguson et al., 2001). Productivity, and consequently seal availability,

may be higher (albeit less predictable) in active ice than in consolidated pack, but this has not been confirmed.

Among the whales, belugas, narwhals and bowhead whales, as well as minke whales, are capable of breaking new ice with their backs (minke whales their rostrum; see above) in order to make breathing holes. All of these whales, with the exception of the minke, lack a dorsal fin, an adaptation thought to derive from the need to break sea ice with their back. In the case of the minke, its dorsal fin is very small and is located far along towards the tail. These cetaceans, too, however are mostly found in the leads and open-water areas at the periphery of the pack ice zone. Their presence in the sea ice zone during winter is confined to persistent polynyas and shore leads.

Belugas, also called white whales (or belukhas in Alaska), engage in diverse migratory patterns in the Arctic, often travelling far into the permanent pack ice (see Richard et al., 2001b). For example, the Beaufort Sea stock of belugas winters in the Bering Sea and migrates to summering areas in the Beaufort Sea and Amundsen Gulf. Belugas off northern Alaska during summer select slope and basin regions of moderate-to-heavy ice; during autumn, belugas occur over the slope in all ice conditions (Moore et al., 2000). Perhaps most remarkable was the discovery that belugas summering along the north coast of Alaska move great distances well offshore, in deep (>3000 m) water and beneath areas where there is almost complete ice cover to reach their spring feeding areas (Suydam et al., 2001). The whales were able to cover 59–79 km per day through waters having an ice cover of greater than 90%. Belugas overwintering in the Bering Sea are thought to disperse in the seasonal ice, though no data exist (Harwood et al., 1996). For many populations, such as the Cook Inlet and the Beaufort Sea belugas, their winter distribution, movements and habitats are poorly known. For other populations, such as those that summer in the central Canadian Arctic, seasonal migratory patterns have been established. Thousands of belugas that summer around Somerset Island in the Canadian Arctic Archipelago later migrate eastwards along the southern coast of Devon Island and eventually winter primarily in the North Water and, to a lesser extent, off West Greenland (Doidge & Finley, 1993; Richard et al., 1998a, 2001a). Belugas may select a migratory route that relates to the availability of their prey, such as arctic cod. They are capable of deep (>300 m) dives during which they are thought to pursue benthic prey (Martin & Smith, 1999). A system of predictably recurring leads and polynyas, such as the North Water, can provide valuable winter habitat (see Fig. 11.3). For most of the winter, the thickness of the pack ice surrounding the North Water probably prevents the belugas from leaving the region (Heide-Jørgensen et al., 1998). However, belugas may be far more frequent denizens of the thick pack ice than was previously thought. It is unknown how climate-induced changes in extent and thickness of sea ice might affect the foraging success, migratory patterns and consequently the population structure of belugas (Tynan & DeMaster, 1997).

Unlike belugas, narwhals appear to rely little on the North Water during winter. Instead, narwhals occur throughout the pack ice in southern Baffin Bay and southern Davis Strait down to 68°N (Dietz et al., 2001). Although this species may utilize leads or polynyas during winter, no clear areas of concentration have yet been found. Factors that affect the distribution and density of their prey (e.g. arctic cod, Greenland halibut and squid) would likely affect their migratory patterns and selected wintering grounds as well. During the fall, narwhals move from their coastal summer habitat and head towards deeper water. Some individuals visit deep fjords, while others move to the edge of the continental shelf and slope in Baffin

Bay. Here, over steep complex undersea terrain, narwhals may be focusing on deep-water cephalopod prey (Dietz et al., 2001). In November, narwhals from both Canada and Greenland converge in the northern part of Davis Strait, an area where the shelf drops off abruptly and the water is 1000–1500 m deep. During winter, this area is completely covered with pack ice except for shifting cracks and leads. Narwhals remain and make some of the deepest dives ever recorded for a mammal (M. P. Heide-Jørgensen, personal communication).

The bowhead whale and the Antarctic minke whale (the latter discussed above) are the only baleen whales truly adapted to sea ice-covered regions. Morphological adaptations of the bowhead include an elevated blowhole or rostrum for pushing through the ice to breathe (Fig. 11.8). Its migration is shorter than that of many other baleen whale species and is closely linked to climate-driven conditions of sea ice. Heavy ice or a prolonged ice season can delay the arrival of bowheads on their summer foraging grounds in the Arctic. Bowhead whales migrate northwards through systems of leads during spring in order to forage on concentrations of Arctic copepods (e.g. *Calanus glacialis* and *C. hyperboreus*), though regional differences in diet occur and euphausiids and hyperiid amphipods are also consumed during summer and fall (Lowry et al., 2004). Linkages between *Calanus* production and sea ice conditions are likely to have a major impact on bowhead whale foraging (Finley, 2001). For the bowhead population wintering in the eastern Canadian Arctic, their range includes Labrador, Davis Strait and Hudson Strait; during summer, these whales occur in Baffin Bay, Foxe Basin and west into Lancaster Sound and inlets of the Northwest Passage (Finley, 2001). Bowhead whales tend to remain farther south during seasons of heavy ice conditions. In winter, they occur within the margin of the pack ice and in polynyas between 60° and 70°N. The shelter provided by the pack ice may enable bowheads to endure winter storms at high latitude, as well as provide protection from killer whales (Payne, 1995). During summer, bowhead whales off northern Alaska appear to select moderate ice cover over the continental slope (Moore et al., 2000); during autumn, bowheads select inner shelf waters during light and moderate ice conditions, but occur in deeper slope habitat in heavy ice conditions (Moore et al., 2000). The reduction in Arctic sea ice may enhance feeding opportunities for bowhead whales in their summer and autumn habitats (Moore & Laidre, 2006), providing that trophic pathways to their preferred copepod prey remain unaltered.
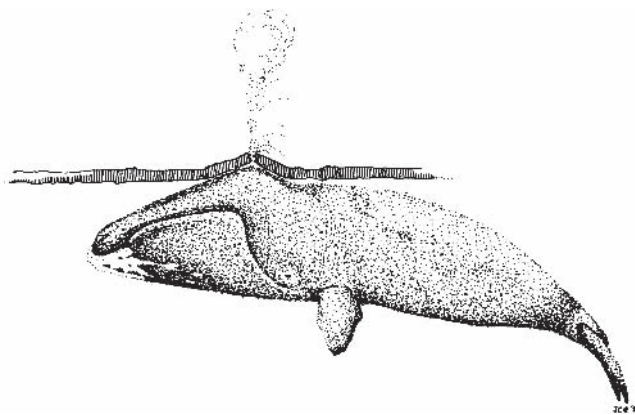
Fig. 11.8   Bowhead whale pushing upwards through new ice in order to breathe (drawing by J. C. George, presented with permission).

Changes in the thickness of ice and availability of leads affect the migratory paths of Arctic cetaceans. Although bowhead whales are able to break through sea ice (18 cm maximum thickness) in order to breathe (George et al., 1989), thicker and continuous multiyear ice can be a deterrent. By pushing up against the ice with their heads, in the area of the blowholes, they fracture the ice and generate a hummock through which to breathe (Fig. 11.8). It has been hypothesized that bowhead whales use sound to acoustically determine the thickness of ice in their migratory path, thereby avoiding regions where the ice is too thick for them to fracture. Despite these abilities, entrapments of bowheads and other Arctic cetacean species occur (Stirling et al., 1981). The possible importance of bowhead icebreaking to air–sea heat exchange (e.g. observations by George et al. (1989) of 50–100 hummocks per km^2), sea ice dynamics and Arctic ecology has not been examined.

Gray whales (*Eschrichtius robustus*), as with other baleen whales, migrate to open waters of the northern Bering and Chukchi Seas to forage during summer, but unlike other whales, they feed on benthic infauna (especially ampelicid amphipods; Grebmeier & Barry, 1991). The seasonal extent of the sea ice therefore affects the length of time these whales can spend on preferred summer foraging grounds. In addition, complex linkages between the biophysical coupling of sea ice, ice-associated production and carbon flux to the benthos would be expected to impact the benthic organisms upon which gray whales depend for food. Such changes have been observed in the Northern Bering Sea, where a reduction in the benthic prey populations upon which gray whales depend has occurred, concomitant with an increase in pelagic fish and a reduction in sea ice (Grebmeier et al., 2006). It is through such complex interactions that ultimately the effects of Arctic and sub-Arctic atmospheric pressure patterns on regional weather and sea ice conditions could impact the condition of gray whales and other benthic foragers, such as bearded seals and walruses.

11.4 The changing scene: global climate change and implications for pagophilic species

Observations and predictions of climate change, as they relate to sea ice and the potential effects on Arctic marine mammals, have received recent consideration (Stirling & Derocher, 1993; Tynan & DeMaster, 1997; Stirling et al., 1999; Derocher et al., 2004; Kovacs & Lydersen, 2008). Changes in the thickness and concentration of sea ice, as well as variability in the seasonal and spatial extent of ice cover, all have ecological consequences for mammals and seabirds. Such changes may produce species-specific alterations in demography, range and population size. Polar bears represent a highly specialized case in that they evolved into existence only because of the presence of an unexploited niche for a surface predator on the sea ice. They are dependent on the presence of sea ice as a platform from which to hunt the seals they depend upon, so, as the availability of sea ice declines, so will polar bear populations in the areas affected. Already, negative effects on population size, body condition and reproduction have been documented in three populations as a result of negative effects of climate warming on ice (Obbard et al., 2007; Regehr et al., 2007a,b). In some areas such as the multiyear ice of the northern Canadian Arctic Archipelago, a change to annual ice as a result of climate warming may create improved habitat, temporarily at least, for species such as polar beears, ringed seals and bearded seals (Krajick, 2001; Derocher et al., 2004; Laidre

et al., 2008). However, if the Arctic climate continues to warm as predicted, any such benefit will be emphemeral.

The loss of ice suitable for resting, moulting and breeding seals has a direct and immediate effect. Less easy to observe and evaluate are ecosystem changes in productivity, species composition and community structure that relate to changes in sea ice extent, volume and thickness. On the Bering Sea shelf, the duration and extent of the seasonal sea ice has important consequences for the timing and magnitude of the spring ice edge bloom of phytoplankton, and consequently, the ensuing cascade of spring and summer productivity of middle and upper trophic levels. Similarly, in the Barents Sea, where more than 15 species of whales and seals forage, a high proportion of the plankton biomass is found near the ice edge and oceanic Polar Front (Sakshaug et al., 1994). In the high Arctic and Barents Sea, alteration of sea ice extent and structure is expected to affect Arctic cod, a pivotal prey for many top trophics (see above) and one that preys on ice amphipods (such as *Parathemisto libellula*, Chapter 10). Factors that affect the productivity and availability of ice-associated amphipods would likely cascade up the Arctic food web to seabirds, cetaceans, ice seals and polar bears.

In western Hudson Bay, a significant positive relationship exists between the time of sea ice break-up and the condition of adult polar bears (e.g. the earlier the break-up, the poorer is the condition of the bears; Stirling et al., 1999). This trend is in accord with rising spring temperatures for the period 1950–1990 and has been continuing since. It has been suggested that this region, which includes the southern edge of the bears' range, may show the earliest and largest impacts of global warming on polar bears (Tynan & DeMaster, 1997). Between 1981 and 1998, polar bears in this region have experienced a 15% decline in the average weight and number of cubs. As the sea ice in western Hudson Bay now breaks up, on average, 3 weeks earlier than it did 30 years ago, bears are forced to head for land by mid-July or earlier, a time when they normally are hunting seal pups on the ice (Stirling et al., 1999, 2008). Conversely, particularly heavy ice conditions, such as in the winters of 1973–1974 and 1984–1985 in the eastern Beaufort Sea, coincided with a decline in ringed seal pupping rate and consequently in polar bear numbers as well (Stirling, 2002). Therefore, there appears to be an optimal range of sea ice conditions that foster polar bear well-being. Too little ice and the polar bears are unable to forage successfully on ice seals for long enough; too much winter and spring ice and the food web sustaining ice seals may be reduced as well as access to the seals themselves. While consolidated pack ice has lower interannual spatial and seasonal variability, and is also associated with less productivity, divergent sea ice has higher interannual variability and greater productivity. Due to the immediate effect of ringed seal pupping rate on polar bear reproduction and cub survival, the polar bear is an excellent indicator species for changes in sea ice conditions and changes in the marine ecosystem generally (Stirling, 2002; Stirling & Parkinson, 2006; Wiig et al., 2008).

The recent retreat of Arctic sea ice has had a dual effect on such avian species as black guillemot and others (e.g. horned puffin *Fratercula corniculata*, a species that frequents ice-free polar waters; Krajick 2001, reporting data from G.J. Divoky). Initially, the retreat encouraged northward extensions of range as the ice-free period lengthened sufficiently to include the long nesting period of these species. Especially the black guillemot then exploited the epontic prey in the under-ice habitat that was easily accessible nearby. Subsequently, however, continued warming has caused the sea ice to retreat so far away from limited suitable nesting habitat that it no longer is in range of the foraging birds, which must feed their chicks

often enough that growth and development are ensured. As a result, reproductive success has declined and populations have begun to decline. Similarly, populations of ivory gulls are also declining as their sea ice foraging habitat has disappeared and moved farther from nesting sites.

The effects of interannual and decadal shifts in atmospheric pressure patterns on sea ice are also reflected in top trophic levels of both northern and southern polar ecosystems. The Arctic Oscillation (AO) appears to have altered ocean circulation, ice drift and air temperatures in the Arctic during the early 1990s (Morison et al., 2000). The effects of atmospheric pressure systems and coupled ocean response can be far reaching, such as:

(1) The significant correlation between the Pacific Decadal Oscillation (PDO) and ice in the Bering Sea (Niebauer et al., 1999).
(2) The significant negative correlation between the El Niño–Southern Oscillation (ENSO) and sea ice conditions in the Baffin Bay–Labrador Sea region (Wang et al., 1994).
(3) The linkage between the Southern Annular Mode (SAM) and sea ice extent in the Southern Ocean (Stammerjohn et al., 2008).

A number of correlations between marine mammal condition and the effects of large-scale atmospheric forcing on sea ice have been observed, but the mechanisms at the ecosystem level are often not well understood. During El Niño, the pupping rate of Weddell seals in McMurdo Sound (Ross Sea) is lower (Proffitt et al., 2007), as is the pup weaning mass of southern elephant seals at King George Island (Bellingshausen Sea; Vergani et al., 2001) compared to non-ENSO years, but why these patterns exist is not understood.

Two seal species of the outer Antarctic pack ice (crabeater, leopard) exhibit quasi-cyclic 4- to 5-year patterns in their biology (Testa et al., 1991). These are in accord with ENSO, which with the SAM, effects sea ice extent in a see-sawing fashion between the Ross Sea and the Weddell Sea sectors of the Southern Ocean (Stammerjohn et al., 2008). The loss of sea ice in the Antarctic Peninsula region appears to have led to a reduction in the abundance of krill in that region (Atkinson et al., 2004). Krill, which is a key prey species for top trophics, exhibits high reproductive output during conditions of high winter sea ice concentration (Siegel & Loeb, 1995; Fraser & Hofmann, 2003; Nicol, 2006). Moreover, winter sea ice also provides a source of food (e.g. ice algae) and under-ice refuge for krill (Ross & Quetin, 1991). Therefore, it might be expected that mammals and birds that inhabit the northern portion of the sea ice zone should benefit from years of higher winter ice concentration.

The two ice-obligate penguin species in the Austro-Pacific sector of Antarctica (emperor, Adélie) have shown opposite population trajectories since the mid-1950s. The fast-ice breeding emperor penguin population at Pointe Géologie declined during the 1970s (Barbraud & Weimerskirch, 2001) while the pack ice–frequenting Adélie penguin on Ross Island increased in number through the same period (Wilson et al., 2001; Ainley et al., 2007b). The emperor penguin trends are responses to decreased productivity as well as increased mortality of males, which must recover from their wintertime fasts that extend for 2 months while incubating eggs. Their nesting depends on stable fast ice and then access to food through the presence of polynyas nearby. The increased winds evident in the Antarctic (see below), might well have decreased the stability of the fast ice on which this species depends for nesting; indeed an increasing frequency of premature blowout of fast ice has been observed at Pt. Géologie with concomitant loss of eggs and chicks (Barbraud & Weimerskirch, 2001; Ainley

et al., 2005). The Adélie penguin, on the other hand, appears to be favoured by decreased sea ice extent during winter, at least initially. This allows the naïve juveniles an easier effort to forage effectively in the rich waters south of the Southern Boundary of the ACC. Extensive sea ice shifts them north of that boundary to unproductive waters. This pattern is evident on an interannual scale as position of the outer sea ice boundary varies in accord with the SAM. Unfortunately, the sea ice record before 1974, when the first sea ice sensing satellite was launched, is non-existent. As a proxy for ice conditions during previous decades, however, numbers of penguins indicate that sea ice characteristics differed during the 1950s and 1960s; likely the factor involved was the growing size of coastal polynyas in recent decades (Ainley et al., 2005). The high take of minke whales by whaling during the 1970s and early 1980s may have been involved in these penguin trends as well (Ainley et al., 2007b).

When winter ice consolidates, covering and restricting access to summer feeding grounds in the Arctic, polynyas and leads associated with rich pelagic and benthic communities sustain populations of top trophics as noted above. However, the present ability of general circulation models to simulate changes in the size and productivity of these recurring, regional features is rather limited. In the Antarctic, coastal polynyas have been growing (Parkinson, 2002), ostensibly in response to the increased strength and persistence of winds, in turn a response to global warming (Russell et al., 2006). Changes in the timing, size and subsequent ocean productivity in and adjacent to polynyas would have profound effects on polar marine birds and mammals, as already indicated by Antarctic penguins.

In the future, researchers will be keeping a close eye on the extension and retreat of sea ice coupled to changes in weather and longer-term climate signals in both polar regions. Record minima of Arctic sea ice coverage in the past few years (Walsh, 2008) have important ecological implications for mammals and birds. A species-sensitivity analysis suggests that the hooded seal, the polar bear and the narwhal may be the three most sensitive marine mammal species to Arctic warming, due to reliance on sea ice and specialized feeding (Laidre et al., 2008). In the Antarctic, analyses of air-temperature trends indicate warming not only along the Antarctic Peninsula but over most of western Antarctica (Steig et al., 2009). Though the ecological impacts of warming may have first been observed along the Antarctic Peninsula, warming trends in western Antarctica (0.17 ± 0.06°C per decade between 1957 and 2006) and eastern Antarctica (0.10 ± 0.07°C per decade) are also significant (Steig et al., 2009). Simulations using a general circulation model suggest that changes in sea ice and regional circulation are required to produce the observed warming. Thus, long-term monitoring of linkages between top trophics, sea ice, ice-associated productivity and ecosystem structure and function is of vital importance. Without such monitoring, it is doubtful that meaningful assessments and predictions of climate-induced impacts on polar marine ecosystems will be achieved. Diverse and healthy polar marine ecosystems should be part of our world heritage.

Acknowledgements

References

Ackley, S.F., Bengtson, J.L., Boveng, P. et al. (2003) A top-down multidisciplinary study of the structure and function of the pack-ice ecosystem in the eastern Ross Sea, Antarctica. *Polar Record*, **39**, 219–230.

Ainley, D.G. (2002) *The Adélie Penguin: Bellwether of Climate Change*. Columbia University Press, NY.

Ainley, D.G., Fraser, W.R., Smith, W.O., Hopkins, T.L. & Torres, J.J. (1991) The structure of upper level pelagic food webs in the Antarctic: effect of phytoplankton distribution. *Journal of Marine Systems*, **2**, 111–122.

Ainley, D.G., Ribic, C.A. & Spear, L.B. (1993) Species–habitat relationships among Antarctic seabirds: a function of physical of biological factors. *Condor*, **95**, 806–816.

Ainley, D.G., Ribic, C.A. & Fraser, W.R. (1994) Ecological structure among migrant and resident seabirds of the Scotia-Weddell Confluence region. *Journal of Animal Ecology*, **63**, 347–364.

Ainley, D.G., Clarke, E.D., Arrigo, K., Fraser, W.R., Kato, A., Barton K.J. & Wilson P.R. (2005) Decadal-scale changes in the climate and biota of the Pacific sector of the Southern Ocean, 1950s to the 1990s. *Antarctic Science*, **17**, 171–182.

Ainley, D., Toniolo, V., Ballard, G. et al. (2006) Managing ecosystem uncertainty: critical habitat and dietary overlap of top-predators in the Ross Sea. *CCAMLR Document EMM 06 – 07*, Hobart.

Ainley, D.G., Dugger, K.M., Toniolo, V. & Gaffney, I. (2007a) Cetacean occurrence patterns in the Amundsen and southern Bellingshausen Sea sector, Southern Ocean. *Marine Mammal Science*, **23**, 287–305.

Ainley, D.G., Ballard, G., Ackley, S. et al. (2007b) Paradigm lost, or, is top-down forcing no longer significant in the Antarctic Marine Ecosystem? *Antarctic Science* **19**, 283–290.

Atkinson, A., Siegel, V., Pakhomov, E. & Rothery, P. (2004) Long-term decline in krill stock and increase in salps within the Southern Ocean. *Nature*, **432**, 100–103.

Atkinson, A., Siegel, V., Pakhomov, E.A. et al. (2008) Oceanic circumpolar habitats of Antarctic krill. *Marine Ecology Progress Series*, **362**, 1–23.

Barbraud, C. & Weimerskirch, H. (2001) Emperor penguins and climate change. *Nature*, **411**, 183–186.

Bester, M.N. & Odendaal, P.N. (2000) Abundance and distribution of Antarctic pack ice seals in the Weddell Sea. In: *Antarctic Ecosystems: Models for Wider Ecological Understanding* (Ed. W. Davison, C. Howard-Williams & P. Broady), pp. 51–55. The Caxton Press, Christchurch, New Zealand.

Blix, A.S. & Norday, E.S. (2007) Ross seal (*Ommatophoca rossii*) annual distribution, diving.behaviour, breeding and moulting, off Queen Maud Land, Antarctica. *Polar Record*, **30**, 1449–1458.

Bornemann, H., Kreyscher, M., Ramdohr, S., Martin, T., Carlini, A., Sellmann, L. & Plötz, J. (2000) Southern elephant seal movements and Antarctic sea ice. *Antarctic Science*, **12**, 3–15.

Bowen, W.D., Myers, R.A. & Hay, K. (1987) Abundance estimation of a dispersed, dynamic population: hooded seals (*Cystophora cristata*) in the Northwest Atlantic. *Canadian Journal of Fisheries and Aquatic Science*, **44**, 282–295.

Bradstreet, M.S.W. (1980) Thick-billed murres and black guillemots in the Barrow Strait areas, N.W.T., during spring: diets and food availability along ice edges. *Canadian Journal of Zoology*, **58**, 2120–2140.

Brown, S.G. & Lockyer, C.H. (1984) Whales. In: *Antarctic Ecology*, Vol. 2 (Ed. R.M. Laws), pp. 717–782. Academic Press, London.

Brown, R.G.B. & Nettleship, D.N. (1981) The biological significance of polynyas to arctic colonial seabirds. In: *Polynyas in the Canadian Arctic* (Eds. I. Stirling & H. Cleator), pp. 59–66. *Canadian Wildlife Service Occasional Paper* **45**, Ottawa.

Burns, J.J. (1981) Bearded seal *Erignathus barbatus* Erxleben, 1777. In: *Handbook of Marine Mammals*, Vol. 2. (Ed. by S.H. Ridgway & R.J. Harrison), pp. 145–170. Academic Press, London.

Collins, M.A., Ross, K.A., Belchier, M. & Reid, K. (2007) Distribution and diet of juvenile Patagonian toothfish on the South Georgia and Shag Rocks shelves (Southern Ocean). *Marine Biology*, **152**, 135–147.

Davis, C.S., Stirling, I. & Strobeck, C. (2000) Genetic diversity of Antarctic pack ice seals in relation to life history characteristics. In: *Antarctic Ecosystems: Models for Wider Ecological Understanding*. (Ed. W. Davison, C. Howard-Williams & P. Broady), pp. 56–62. The Caxton Press, Christchurch, New Zealand.

Davis, R.W., Fuiman, L.A., Williams, T.M. et al. (1999) Hunting behavior of a marine mammal beneath the Antarctic fast ice. *Science*, **283**, 993–996.

Davis, C.S., Stirling, I., Strobeck, C. & Coltman, D.W. (2008) Population structure of ice-breeding seals. *Molecular Ecology*, **17**, 3078–3094.

Derocher, A.E., Lunn, N.J. & Stirling, I. (2004) Polar bears in a warming climate. *Integrative and Comparative Biology*, **44**,163–176.

Dietz, R., Heide-Jørgensen, M.P., Richard, P.R. & Acquarone, M. (2001) Summer and fall movements of narwhals (*Monodon monoceros*) from northeastern Baffin Island towards northern Davis Strait. *Arctic*, **54**, 244–261.

Digby, S.A. (1984) Remote sensing of drained ice areas around the breathing holes of ice-inhabiting seals. *Canadian Journal of Zoology*, **62**, 1011–1014.

Doidge, D.W. & Finley, K.J. (1993) Status of the Baffin Bay population of beluga, *Delphinapterus leucas*. *Canadian Field Naturalist*, **107**, 533–546.

Eicken, H., Krouse, H.R., Kadko, D. & Perovich, D.K (2002) Tracer studies of pathways and rates of meltwater transport through Arctic summer sea ice. *Journal of Geophysical Research*, **107**, 10.1029/2000JC000583.

Falk, K., Hjørt, C., Andreasen, C. et al. (1997) Seabirds utilizing the Northeast Water polynya. *Journal of Marine Systems*, **10**, 47–65.

Fay, F.H. (1981) Walrus. In: *Handbook of Marine Mammals*, *Vol. 1* (Ed. S.H. Ridgeway & R.J. Harrison), pp 1–23. Academic Press, London.

Fay, F.H. (1982) Ecology and biology of the Pacific walrus, *Odobenus rosmarus divergens* Illiger. *North American Fauna*, **74**, 1–279.

Ferguson, S.H., Taylor, M.K., Born, E.W., Rosing-Asvid, A. & Messier, F. (2001) Activity and movement patterns of polar bears inhabiting consolidated versus active pack ice. *Arctic*, **54**, 49–54.

Finley, K.J. (2001) Natural history and conservation of the Greenland whale, or bowhead, in the Northwest Atlantic. *Arctic*, **54**, 55–76.

Finley, K.J., Miller, G.W., Davis, R.A. & Koski, W.R. (1983) A distinctive large breeding population of ringed seals (*Phoca hispida*) inhabiting the Baffin Bay pack ice. *Arctic*, **36**, 162–173.

Fraser, W.R. & Hofmann, E.E. (2003) A predator's perspective on causal links between climate change, physical forcing and ecosystem response. *Marine Ecology Progress Series,* **265**, 1–15.

Fraser, W.R. & Trivelpiece, W.Z. (1996) Factors controlling the distribution of seabirds: winter–summer heterogeneity in the distribution of Adélie penguin populations. In: *Foundations for Ecological Research West of the Antarctic Peninsula* (Eds R.M. Ross, E.E. Hofmann & L.B. Quetin), American Geophysical Union, Washington, DC. *Antarctic Research Series*, **70**, 257–272.

Friedlaender, A.S., Halpin, P.N., Qian, S.S., Lawson, G.L., Wiebe, P.H., Thiele, D. & Read, A.J. (2006) Whale distribution in relation to prey abundance and oceanographic processes in shelf waters of the Western Antarctic Peninsula. *Marine Ecology Progress Series*, **317**, 297–310.

Frost, K.J., Lowry, L.F., Gilbert, J.R. & Burns, J.J. (1988) Ringed seal monitoring: relationships of distribution and abundance to habitat attributes and industrial activities. Alaska Outer Continental Shelf Environmental Assessment Program, U. S. Minerals Management Service and Department of Interior, NOAA Project RU No. 667.

Gaston, A.J., Woo, K. & Hipfner, J.M. (2003) Trends in forage fish populations in northern Hudson Bay since 1981, as determined from the diet of nestling thick-billed murres *Uria lomvia*. *Arctic*, **56**, 227–233.

Gelatt, T.S. (2001) *Male reproductive success, relatedness, and the mating system of Weddell seals in McMurdo Sound, Antarctica*. PhD Dissertation, University of Minnesota.

George, J.C., Clark, C., Carroll, G.M. & Ellison, W.T. (1989) Observations on the ice-breaking and ice navigation behavior of migrating bowhead whales (*Balaena mysticetus*) near Point Barrow, Alaska, spring 1985. *Arctic*, **42**, 24–30.

Gilchrist, H.G. & Mallory, M.L. (2005) Declines in abundance and distribution of the ivory gull (*Pagophila eburnea*) in Arctic Canada. *Biological Conservation*, **121**, 303–309.

Gilchrist, H.G. & Robertson, G.J. (2000) Observations of marine birds and mammals wintering at polynyas and ice edges in the Belcher Islands, Nunavut, Canada. *Arctic*, **53**, 61–68.

Gjertz, I. & Lydersen, C. (1983) *Phoca hispida* pupping in the Svalbard area. *Fauna*, **36**, 65–67.

Gjertz, I. & Wiig, Ø. (1992) Feeding of walrus *Odobenus rosmarus* in Svalbard. *Polar Record*, **28**, 57–59.

Grebmeier, J.M. & Barry, J.P. (1991) The influence of oceanographic processes on pelagic–benthic coupling in polar regions: a benthic perspective. *Journal of Marine Systems*, **2**, 495–518.

Grebmeier, J.M., Overland, J.E., Moore, S.E. et al. (2006) A major ecosystem shift in the northern Bering Sea. *Science*, **311**, 1461–1464.

Hammill, M.O. & Smith, T.G. (1989) Factors affecting the distribution and abundance of ringed seal structures in Barrow Strait, Northwest Territories. *Canadian Journal of Zoology*, **67**, 2212–2219.

Hammill, M.O., Kovacs, K.M. & Lydersen, C. (1994) Local movements by nursing bearded seal (*Erignathus barbatus*) pups in Kongsfjorden, Svalbard. *Polar Biology*, **14**, 569–570.

Haney, J.C. & MacDonald, S.D. (1995) Ivory Gull (*Pagophila eburnean*). In: *The Birds of North America, No. 175* (Eds. A. Poole & F. Gill). The Academy of Natural Sciences, Philadelphia, The American Ornithologists' Union, Washington, DC.

Harwood, L.A. & Stirling, I. (1992) Distribution of ringed seals in the southeastern Beaufort Sea during late summer. *Canadian Journal of Zoology*, **70**, 891–900.

Harwood, L.A., Innes, S., Norton, P. & Kingsley, M.C.S. (1996) Distribution and abundance of beluga whales in the Mackenzie estuary, southeast Beaufort Sea, and west Amundsen Gulf during late July 1992. *Canadian Journal of Fisheries and Aquatic Science*, **53**, 2262–2273.

Harwood, L.A., Smith, T.G. & Melling, H. (2000) Variation in reproduction and body condition of ringed seal (*Phoca hispida*) in Western Prince Albert Sound, NT, Canada, as assessed through a harvest-based sampling program. *Arctic*, **53**, 422–431.

Heide-Jørgensen, M.P., Richard, P.R. & Rosing-Asvid, A. (1998) Dive patterns of belugas (*Delphinapterus leucas*) in waters near Eastern Devon Island. *Arctic*, **51**, 17–26.

Holt, B. & Digby, S.A. (1985) Processes and imagery of first-year fast sea ice during the melt season. *Journal of Geophysical Research*, **90**, 5045–5062.

Hopkins, T.L., Ainley, D.G., Torres, J.J. & Landcraft, T.M. (1993) Trophic structure in open waters of the marginal ice zone in the Scotia-Weddell confluence region during spring (1983). *Polar Biology*, **13**, 389–397.

Ichii, T., Shinohara, N., Kujise, Y., Nishiwaki, S. & Matsuoka, K. (1998) Interannual changes in body fat condition index of minke whales in the Antarctic. *Marine Ecology Progress Series*, **175**, 1–12.

Karnovsky, N., Ainley, D.G. & Lee, P. (2007) The impact and importance of production in polynyas to top-trophic predators: three case histories. In: *Polynyas: Windows to the World* (Ed. by W.O. Smith, Jr. & D.G. Barber). Elsevier Publishers, London.

Kim, S.L., Conlan, K., Malone, D.P. & Lewis, C.V. (2005) Possible food caching and defence in the Weddell seal: observations from McMurdo Sound, Antarctica. *Antarctic Science*, **17**, 71–72.

Kingsley, M.C.S., Stirling, I. & Calvert, W. (1985) The distribution and abundance of seals in the High Arctic, 1980–1982. *Canadian Journal of Fisheries and Aquatic Science*, **42**, 1189–1210.

Konishi, K., Tamura, T., Zenitani, R., Bando, T., Kato, H. & Walløe, L. (2008) Decline in energy storage in the Antarctic minke whale (*Balaenoptera bonaerensis*). *Polar Biology*, DOI: 10.1007/s00300-008-0491-3.

Kooyman, G.L. (1981) *Weddell Seal: Consummate Diver*. Cambridge University Press, London.

Kooyman, G.L., Siniff, D.B. & Stirling, I. (2004) Moult habitat, pre- and post-moult diet and post-moult travel of Ross Sea emperor penguins. *Marine Ecology Progress Series*, **267**, 281–290.

Kovacs, K.M. & Lydersen, C. (2008) Climate change impacts on seals and whales in the North Atlantic Arctic and adjacent shelf seas. *Science Progress*, **91** (2), 117–150.

Krajick, K (2001) Arctic life, on thin ice. *Science*, **291**, 424–425.

Laidre, K.L., Stirling, I., Lowry, L.F., Wiig, Ø., Heide-Jørgensen, M.P. & Ferguson, S.H. (2008) Quantifying the sensitivity of Arctic marine mammals to climate-induced habitat change. *Ecological Applications*, **18** (2), Supplement S97–S125.

Laws, R.M (1984) Seals. In: *Antarctic ecology*, Vol. 2 (Ed. R.M. Laws), pp. 621–715. Academic Press, London.

Lowry, L.F., Sheffield, G. & George, J.C. (2004) Bowhead whale feeding in the Alaskan Beaufort Sea, based on stomach contents analyses. *Journal of Cetacean Research and Management*, **6**, 215–223.

Lydersen, C. & Kovacs, K.M. (1999) Behaviour and energetics of ice-breeding, North Atlantic phocid seals during the lactation period. *Marine Ecology Progress Series*, **187**, 265–281.

Martin, A.R. & Smith, T.G. (1999) Strategy and capability of wild belugas *Delphinapterus leucas* during deep, benthic diving. *Canadian Journal of Zoology*, **77**, 1783–1793.

Massom, R.A., Harris, P.T., Michael, K.J. & Potter, M.J. (1998) The distribution and formative processes of latent-heat polynyas in East Antarctica. *Annals of Glaciology*, **27**, 420–426.

Meredith, M.P. & King, J.C. (2005) Rapid climate change in the ocean west of the Antarctic Peninsula during the second half of the 20th century. *Geophysical Research Letters*, **32**, 1–5.

Moore, S.E. & Laidre, K.L. (2006) Trends in sea ice cover within habitats used by bowhead whales in the western Arctic. *Ecological Applications*, **16**, 932–944.

Moore, S.E., DeMaster, D.P. & Dayton, P.K. (2000) Cetacean habitat selection in the Alaskan Arctic during summer and autumn. *Arctic*, **53**, 432–447.

Morison, J., Aagaard, K. & Steele, M. (2000) Recent environmental changes in the Arctic: a review. *Arctic*, **53**, 359–371.

Nicol, S. (2006) Krill, currents, and sea ice: *Euphausia superba* and its changing environment. *BioScience*, **56**, 111–120.

Nicol, S, Worby, A. & Leaper, R. (2008) Changes in the Antarctic sea ice ecosystem: potential effects on krill and baleen whales. *Marine and Freshwater Research*, **59**, 361–382.

Niebauer, H.J., Bond, N.A., Yakunin, L.P. & Plotnikov, V.V. (1999) An update on the climatology and sea ice of the Bering Sea. In: *Dynamics of the Bering Sea: A Summary of Physical, Chemical and Biological Characteristics and a Synopsis of Research* (Eds. T.R. Loughlin & K. Ohtani), pp. 29–59. North Pacific Marine Science Organization, PICES, Alaska Sea Grant.

Obbard, M.E., McDonald, T.L., Howe, E.J., Regehr, E.V. & Richardson, E.S. (2007) *Polar Bear Population Status in Southern Hudson Bay, Canada*. U.S. Geological Survey, Washington, DC. Administrative Report, 32 pp.

Overland, J., Turner, J., Francis, J., Gillett, N., Marshall, G. & Tjernstöm, M. (2008) The Arctic and Antarctic: two faces of climate change. *EOS*, **89** (19), 177–178.

Parkinson, C.L. (2002) Trends in the length of the Southern Ocean sea ice season, 1979–99. *Annals of Glaciology*, **34**, 435–440.

Payne, R.S. (1995) *Among Whales*. Scribner, New York.

Petersen, M.R., Larned, W.W. & Douglas, D.C. (1999) At-sea distribution of spectacled eiders: a 120-year-old mystery solved. *Auk,* **116**, 1009–1020.

Plötz, J., Bornemann, H., Knust, R., Schröder, A. & Bester, M. (2001) Foraging behavior of Weddell seals, and its ecological implications. *Polar Biology*, 24, 901–909.

Pitman, R.L. & Ensor, P. (2003) Three forms of killer whales in Antarctic waters. *Journal of Cetacean Research and Management*, **5**, 1–9.

Proffitt, K. M., Garrott, R.A., Rotella, J.J., Siniff, D.B. & Testa, J.W. (2007) Exploring linkages between abiotic oceanographic processes and a top-trophic predator in an Antarctic ecosystem. *Ecosystems*, **10**, 119–126.

Regehr, E. V., Lunn, N. J., Amstrup, S. C. & Stirling, I. (2007a) Population decline of polar bears in Western Hudson Bay in relation to climatic warming. *Journal of Wildlife Management*, **71**, 2673–2683.

Regehr, E.V., Hunter, C.M., Caswell, H., Amstrup, S.C. & Stirling, I. (2007b) *Polar Bears in the Southern Beaufort Sea I: Survival and Breeding in Relation to Sea Ice Conditions, 2001–2006*. U.S. Geological Survey, Washington, DC. Administrative Report, 45 pp.

Ribic, C.A. & Ainley, D. G. (1988/89) Constancy of seabird species assemblages: an exploratory look. *Biological Oceanography*, **6**, 175–202.

Ribic, C.A., Ainley, D. G. & Fraser, W. R. (1991) Habitat selection by marine mammals in the marginal ice zone. *Antarctic Science*, **3**, 181–186.

Richard, P.R., Heide-Jørgensen, M.P. & St. Aubin, D. (1998a) Fall movements of belugas (*Delphinapterus leucas*) with satellite-linked transmitters in Lancaster Sound, Jones Sound, and Northern Baffin Bay. *Arctic*, **51**, 5–16.

Richard, P.R., Orr, J.R., Dietz, R. & Dueck, L. (1998b) Sightings of belugas and other marine mammals in the North Water, late March 1993. *Arctic*, **51**, 1–4.

Richard, P.R., Heide-Jørgensen, M. P., Orr, J.R., Dietz, R. & Smith, T.G. (2001a) Summer and autumn movements and habitat use by belugas in the Canadian High Arctic and adjacent areas. *Arctic*, **54**, 207–222.

Richard, P.R., Martin, A.R. & Orr, J.R. (2001b) Summer and autumn movements of belugas of the eastern Beaufort Sea stock. *Arctic*, **54**, 223–226.

Ross, J.C. (1847) *Voyage of Discovery and Research in the Southern and Antarctic Regions during the Years 1839–43, Vol. 1*. John Murray, London.

Ross, R.M. & Quetin, L.B. (1991) Ecological physiology of larval euphausiids, *Euphausia superba* (Euphausiacea). *Memoirs of the Queensland Museum*, **31**, 321–333.

Russell, J.L., Dixon, K.W., Gnanadesikan, A., Stouffer, R.J. & Toggweiler, J.R. (2006) The Southern Hemisphere westerlies in a warming world: propping open the door to the deep ocean. *Journal of Climate*, **19**, 6382–6390.

Sakshaug, E., Bjørge, A., Gulliksen, B., Loeng, H. & Mehlum, F. (1994) Structure, biomass distribution, and energetics of the pelagic ecosystem in the Barents Sea: a synopsis. *Polar Biology*, **14**, 405–411.

Schledermann, P. (1980) Polynyas and prehistoric settlement patterns. *Arctic*, **33**, 292–302.

Sergeant, D.E (1976) Research on hooded seals *Cystophora cristata* Erxleben in 1976. *ICNAF Res. Doc*. 76/126, Ser. No. 4012.

Siegel, V. & Loeb, V. (1995) Recruitment of Antarctic krill *Euphausia superba* and possible causes for its variability. *Marine Ecology Progress Series*, **123**, 45–56.

Siniff, D.B. & Bengtson, J.L. (1977) Observations and hypotheses concerning interactions among crabeater seals, leopard seals, and killer whales. *Journal of Mammalogy*, **58**, 414–416.

Siniff, D.B., Stirling, I., Bengtson, J.L. & Reichle, R.A. (1979) Social and reproductive behavior of crabeater seals (*Lobodon carcinophagus*) during the austral spring. *Canadian Journal of Zoology*, **57**, 2243–2255.

Siniff, D.B., Garrott, R.A., Rotella, J.J., Fraser, W.R. & Ainley, D.G. (2008) Projecting the effects of environmental change on Antarctic seals. *Antarctic Science*, **20**, 425–435.

Sjare, B. & Stirling, I. (1996) The breeding behavior of Atlantic walruses, *Odobenus rosmarus rosmarus*, in the Canadian High Arctic. *Canadian Journal of Zoology*, **74**, 897–911.

Smith, T.G. & Harwood, L.A. (2001) Observations of neonate ringed seals (*Phoca hispida*) after early breakup of sea ice in Prince Albert Sound, Northwest Territories, Canada, Spring 1998. *Polar Biology*, **24**, 215–219.

Smith, T.G. & Stirling, I. (1975) The breeding habitat of the ringed seal (*Phoca hispida*): the birth lair and associated structures. *Canadian Journal of Zoology*, **53**, 1297–1305.

Smith, R.C., Stammerjohn, S.E. & Baker, K.S. (1996) Surface air temperature variations in the western Antarctic Peninsula region. *Antarctic Research Series*, **70**, 105–121.

Smith, W.O. Jr. & Barber, D.G. (Eds.) (2007) *Polynyas: Windows to the World*. Elsevier, London.

Stammerjohn, S.E., Martinson, D.G., Smith, R.C., Yuan, X. & Rind, D. (2008) Trends in Antarctic annual sea ice retreat and advance and their relation to ENSO and Southern Annular Mode variability. *Journal of Geophysical Research*, **113**, CO3S90, 10.1029/2007JC004269.

Steig, E.J., Schneider, D.P., Rutherford, S.D., Mann, M.E., Cominso, J.C. & Shindell, D.T. (2009) Warming of the Antarctic ice-sheet surface since the 1957 International Geophysical Year. *Nature*, **457**, 459–463.

Stewart, B.S., Yochem, P.K., Gelatt, T.S. & Siniff, D.B. (2000) First-year movements of Weddell seal pups in the Western Ross Sea, Antarctica. In: *Antarctic Ecosystems: Models for Wider Ecological Understanding*. (Eds. W. Davison, C. Howard-Williams & P. Broady), pp. 71–76. The Caxton Press, Christchurch, New Zealand.

Stirling, I. (1969) Tooth wear as a mortality factor in the Weddell seal (*Leptonychotes weddellii). Journal of Mammalogy*, **50**, 559–565.

Stirling, I (1997) The importance of polynyas, ice edges, and leads to marine mammals and birds. *Journal of Marine Systems*, **10**, 9–21.

Stirling, I. (2002) Polar bears and seals in the Eastern Beaufort Sea and Amundsen Gulf: a synthesis of population trends and ecological relationships over three decades. *Arctic*, **55** (Supplement 1), 59–76.

Stirling, I. & Derocher, A.E. (1993) Possible impacts of climatic warming on polar bears. *Arctic*, **46**, 240–245.

Stirling, I. & Parkinson, C.L. (2006) Possible effects of climate warming on selected populations of polar bears (*Ursus maritimus*) in the Canadian Arctic. *Arctic*, **59**, 261–275.

Stirling, I. & Smith, T.G. (2004) Implications of warm temperatures and an unusual rain event for the survival of ringed seals on the coast of southeastern Baffin Island. *Arctic*, **57(1)**, 59–67.

Stirling, I., Archibald, W.R. & DeMaster, D. (1977) Distribution and abundance of seals in the Eastern Beaufort Sea. *Journal of the Fisheries Research Board of Canada*, **34**, 976–988.

Stirling, I., Cleator, H. & Smith, T.G. (1981) Marine mammals. In: *Polynyas in the Canadian Arctic* (Eds. I. Stirling& H. Cleator), pp. 45–58, *Canadian Wildlife Service Occasional Paper*, **45**, Ottawa.

Stirling, I., Lunn, N. J. & Iacozza, J. (1999) Long-term trends in the population ecology of polar bears in western Hudson Bay in relation to climatic change. *Arctic*, **52**, 294–306.

Stirling, I., Derocher, A.E. Rode, K. & Gough, W.A. (2008) Response to Dyck et al. (2007) on polar bears and climate change in western Hudson Bay. *Ecological Complexity* 5, 193–201.

Stroeve, J, Serreze, M., Drobot, S. et al. (2008) Arctic sea ice extent plummets in 2007. *EOS*, **89** (2), 13–14.

Suydam, S., Lowry, L. F., Frost, K.J., O' Corry-Crowe, G.M. & Pikok, D. Jr. (2001) Satellite tracking of eastern Chukchi Sea beluga whales into the Arctic Ocean. *Arctic*, **54**, 237–243.

Taylor, R.H. & Wilson, P.R. (1990) Recent increase and southern expansion of Adelie penguin populations in the Ross Sea, Antarctica, related to climate warming. *New Zealand Journal of Zoology*, **14**, 25–29.

Testa, J.W (1994) Over-wintering movements and diving behavior of female Weddell seals (*Leptonychotes weddellii*) in the southwestern Ross Sea, Antarctica. *Canadian Journal of Zoology*, **72**, 1700–1710.

Testa, J.W., Oehlert, G., Ainley, D.G., Bengtson, J.L., Siniff, D.B., Laws, R.M. & Rounsevell, D. (1991) Temporal variability in Antarctic marine ecosystems: periodic fluctuations in the phocid seals. *Canadian Journal of Fisheries and Aquatic Science*, **48**, 631–639.

Thiele, D., Chester, E.T., Moore, S.E., Širovic, A., Hildebrand, J.A. & Friedlaender, A.S. (2004) Seasonal variability in whale encounters in the Western Antarctic Peninsula. *Deep-Sea Research Part II*, **51**, 2311–2325.

Tynan, C.T. (1997) Cetacean distributions and oceanographic features near the Kerguelen Plateau. *Geophysical Research Letters*, **24**, 2793–2796.

Tynan, C.T. (1998) Ecological importance of the Southern Boundary of the Antarctic Circumpolar Current. *Nature*, **392**, 708–710.

Tynan, C.T. & DeMaster, D.P. (1997) Observations and predictions of Arctic climatic change: potential effects on marine mammals. *Arctic*, **50**, 308–322.

Vergani, D.F., Stanganelli, Z.B. & Bilenca, D. (2001) Weaning mass variation of southern elephant seals at King George Island and its possible relationships with "El Niño" and "La Niña" events. *Antarctic Science*, **13**, 37–40.

Vinje, T. & Kvambekk, A.S. (1991) Barents Sea drift ice characteristics. *Polar Research*, **10**, 59–68.

Walsh, J. E. (2008) Climate of the Arctic marine environment. *Ecological Applications*, **18** (2), Supplement, S3–S22.

Wang, J., Mysak, L. A. & Ingram, R. G. (1994) Interannual variability of sea-ice cover in the Hudson Bay, Baffin Bay and Labrador Sea. *Atmosphere Ocean*, **32**, 421–447.

Welch, H.E., Bergmann, M.A., Siferd, T.D. et al. (1992) Energy flow through the marine ecosystem of the Lancaster Sound region, arctic Canada. *Arctic*, **45**, 343–357.

Wiig, Ø. & Isaksen, K. (1995) Seasonal distribution of harbour seals, bearded seals, white whales and polar bears in the Barents Sea. *Norsk Polarinstitutt Meddelelser*, **136**, 47–59.

Wiig, Ø., Gjertz, I. & Griffiths, D. (1996) Migration of walruses (*Odobenus rosmarus*) in the Svalbard and Franz Josef Land area. *Journal of Zoology (London)*, **238**, 769–784.

Wiig, Ø., Derocher, A.E. & Belikov, S.E. (1999) Ringed seal (*Phoca hispida*) breeding in the drifting pack ice of the Barents Sea. *Marine Mammal Science*, **15**, 595–598.

Wiig, Ø., Aars, J. & Born, E. W. (2008) Effects of climate change on polar bears. *Science Progress*, **91** (2), 151–173.

Wilson, P.R., Ainley, D.G., Nur, N., Jacobs, S.S., Barton, K.J., Ballard, G. & Comiso, J.C. (2001) Adélie Penguin population change in the Pacific sector of Antarctica: relation to sea-ice extent and the Antarctic Circumpolar Current. *Marine Ecology Progress Series*, **213**, 301–309.

This page intentionally left blank

12 Biogeochemistry of Sea Ice

David N. Thomas, Stathys Papadimitriou and Christine Michel

12.1 Introduction

The study of the chemistry of the oceans has been at the forefront of oceanographic endeavours ever since the first expeditions took their first water samples. During the past 50 years, there have been dramatic advances in the suite of analytical tools available for measuring dissolved constituents down to trace levels. Marine chemists have readily adopted these tools, although often considerable effort has had to be expended in adapting methodologies to the very pertinent problem of working in a highly saline matrix. The challenge of working on a hyposaline to hypersaline medium at sub-zero temperatures still remains unresolved as far as making reliable *in situ* process measurements are concerned.

In the past 25 years, the rapid advances in our knowledge of the chemistry of the marine environment have been paralleled by equally dramatic advances in our appreciation of the dominant biological processes of the open oceans and coastal waters. Among the most far-reaching developments has been our increased understanding of the dynamics and role of small organisms, such as viruses, bacteria, micro-algae and protozoans, as well as the complex biochemical interactions associated with this microbial network. It has been the harnessing of state-of-the-art analytical methodologies, including flow cytometry and molecular techniques, that has enabled the biologists to unravel the complex growth patterns and interactions at the microscopic level.

Organisms are greatly influenced by the chemistry of the medium surrounding them and, in turn, modify it. Some organisms are typically adapted to specific ranges of chemical conditions within which they are physiologically viable, and growth and reproduction can take place. Some organisms can tolerate a wide range of conditions (e.g. euryhaline species), while others exhibit narrow tolerance to changes in the chemical environment in which they thrive (e.g. stenohaline species). It is also clear that microbial processes in the ocean drive much of the spatial and temporal gradients measured by the chemists. This realization has led to an ever-increasingly closer union between biologists and chemists in their study of the oceans, the dynamics of biology and the elemental flow between the living and non-living reservoirs.

The basis of much of the life in the oceans is the harvest of energy from sunlight and the assimilation of a suite of major and minor biophilic elements, such as carbon, nitrogen, phosphorus, silicon and iron, into biomass by phototrophic organisms through photosynthesis or primary production (Chapter 8). Just as the grasslands in terrestrial systems, the

aquatic primary producers, predominantly phytoplankton, are food for secondary producers, i.e. grazing organisms. Primary production can only take place in the sunlit part of the water column (i.e. euphotic zone) and is therefore generally restricted to the upper 50 m of the ocean.

The organic material produced in the upper ocean is ultimately recycled through microbial transformations. Only a small fraction of the primary production in the euphotic zone eventually makes its way to the sediments accumulating on the sea floor, and an even smaller amount escapes recycling by benthic organisms within the upper sediment layers and is buried with sediment accumulation. This buried organic matter is nevertheless sufficient to provide clues used by geologists to reconstruct detailed descriptions of environmental constraints and their change over time. These geological clues include signature biochemical components developed by organisms in response to the prevailing abiotic conditions at the time of their growth. In turn, a specific set of abiotic conditions may favour selection of particular species, or groups of species, which, together with their biochemical signatures, will be preserved in the sediments. These processes make for a large study area for both geologists and geochemists alike, but the fact that biochemical signatures are ultimately tied with metabolism has resulted in 'biogeochemistry' becoming a leading field of research over the past decade or so. The term ideally describes the multidisciplinary approach needed to fully understand the complex chemical and biological interactions in the oceans, and the implications for the geological record.

We have been studying the biology of sea ice since the mid-19th century, and in earnest in the past 50 years (Chapter 1). The complexity of the microbial network in sea ice, although not always fully appreciated, is well studied (Chapters 7–9), as are the implications for the wider ecosystem dynamics (Chapters 9–11). The chemical environment has only really been studied in terms that are pertinent to the biogeochemical processes within the ice since the early 1980s, and in any comprehensive way since the 1990s (Thomas & Dieckmann, 2002). Despite the apparent lag behind other disciplines interested in sea ice, the biogeochemistry of sea ice is a rapidly growing research area, unifying biologists, chemists and geologists with a common goal. Naturally their research is underpinned by, and cannot advance without, the complementary research of the physicists: it is the unique physical structure of sea ice and the physical–chemical processes influencing its formation and decay that determine the chemistry and biology of the sea ice matrix.

12.2 Sea ice chemistry

Abiotic modification of the chemical composition of sea water during freezing

Salinity and temperature

Large salinity and temperature shifts are the major physical–chemical transformations within sea ice during its seasonal cycle of formation and decay. Chapter 2 has described in detail the phase relations in sea ice and the effect of sea water freezing on the concentration of dissolved salts during sea ice formation. The dramatic change in the concentration of dissolved salts during the freezing of sea water translates into modification of the ionic strength of the residual brine that is expelled from, and is partially trapped within, the ice crystal matrix.

A large part of the hypersaline brine escapes the growing ice column by gravity drainage into the underlying oceanic water column, with the remaining brine residing in pockets and channels within the sea ice (Chapter 2). The size of the brine inclusions in sea ice is directly related to ice temperature, which bears on their connectivity within the ice and with the atmosphere above or the underlying water column (Perovich & Gow, 1996; Chapter 2). Ice temperature and brine salinity in thermally equilibrated sea ice follow a well-constrained functional relationship (Assur, 1960; Chapter 2), which has also been documented in field measurements of sea ice brines (Fig. 12.1). Sea ice and its brine inclusions transit large temperature and salinity spectra during an annual period, from the freezing point of sea water at the ice–water interface (−1.85°C, salinity of 34) to the much colder conditions at the top of ice floes (−10°C, salinity of 155), the latter depending on air temperature (Fig. 12.1).

Dissolved gases

The coupled variations in brine salinity (S) and temperature (T) accompanying the structural changes during the seasonal formation–decay cycle of sea ice have direct bearing on the thermodynamic parameters that describe the solubility of gases such as CO_2 and O_2. The speciation in solution of the dissolved weak acids and bases, such as carbonic acid (H_2CO_3), which control the buffering capacity of aqueous media and influence pH, is similarly influenced. The S–T functions which describe the relevant thermodynamic equilibria are well established in the temperature range of 0–45°C and in the salinity range of 0–45 (Weiss, 1974; Gacia & Gordon, 1992; Millero, 1995; Mojica-Prieto & Millero, 2002). A wealth of experimental and field data exists for hypersaline solutions ($S>45$) at $T = 25$°C, or higher, from sea water evaporation systems (Lazar et al., 1983; Sherwood et al., 1991; Lazar & Erez, 1992; Barkan et al., 2001; Millero et al., 2002). The empirical S–T functions indicate that the solubility of gases in sea water at equilibrium with air increases as the temperature drops, while an
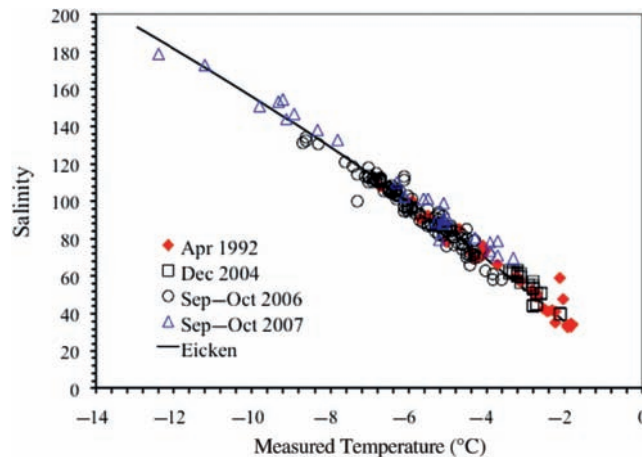
Fig. 12.1 Measured temperature (°C) and salinity of sea ice brines collected from bore holes (sack holes) drilled at different depths into first- and multi-year ice floes in the Weddell Sea, Antarctica, in austral autumn (April 1992, Gleitz et al., 1995), spring (September–October 2006, unpublished data) and summer (December 2004, Papadimitriou et al., 2007), and in the Indian Ocean sector of the Southern Ocean in austral spring (September–October 2007, unpublished data). The trend line illustrates the functional relationship of salinity with temperature in sea ice, taken from Chapter 2.

increase in salinity has the opposite effect, i.e. decreased gas solubility. The combined effect of the strongly coupled S–T changes in sea ice on gas solubility, in the absence of biological activity, is based on extrapolation of the existing S–T function to the low temperature and high salinity field of sea ice brines. This indicates the salinity effect on gas solubility to be the strongest in sea ice, i.e. net decline in the brine during sea ice formation and growth, with the reverse during sea ice decay.

The solubility of gaseous CO_2 is described by Henry's law constant (K_H). The change in gaseous CO_2 solubility in sea ice brine is predicted from the empirical S–T function of Weiss (1974), as illustrated in Fig. 12.2, along with the concentration of dissolved CO_2, $[CO_2(aq)]$, in the medium when at equilibrium with the atmosphere, $[CO_2(aq)]_{eq} = K_H pCO_2$, where pCO_2 = partial pressure of gaseous CO_2. A similar trend is predicted for the solubility of dissolved molecular oxygen (O_2) in sea ice brine, ranging from an O_2 concentration at atmospheric equilibrium of $[O_2]_{eq} = 370$ μmol kg^{-1} at the freezing point of sea water of $S = 34$ ($T_{freezing} = -1.85$) to $[O_2]_{eq} < 169$ μmol kg^{-1} at $S > 155$ and $T < -10°C$ based on the extrapolation of the empirical thermodynamic S–T function in Gacia and Gordon (1992).

The relationship between salinity and O_2 (and presumably other gases) found in the work of Mock et al. (2002) and Glud et al. (2002) indicates that O_2 responds similarly to the major dissolved salts in sea ice, i.e. being expelled from the forming ice matrix during freezing and concentrated in the residual brine. Therefore, the physical concentration of dissolved gases in the residual brine will be superimposed to the thermodynamic trend described above, leading to an increased concentration of dissolved gas relative to that at thermodynamic equilibrium of the brine with air (supersaturation). Consequent on the physical concentration of dissolved gases above air saturation during sea water freezing is the nucleation of gas bubbles and their entrapment within the ice matrix, as has been demonstrated in experimental low ionic strength media (Killawee et al., 1998). A considerable amount of gas will be incorporated into sea ice as bubbles during ice formation, especially in turbulent water conditions (Killawee et al., 1998; Mock et al., 2002; Tison et al., 2002). In short, the net
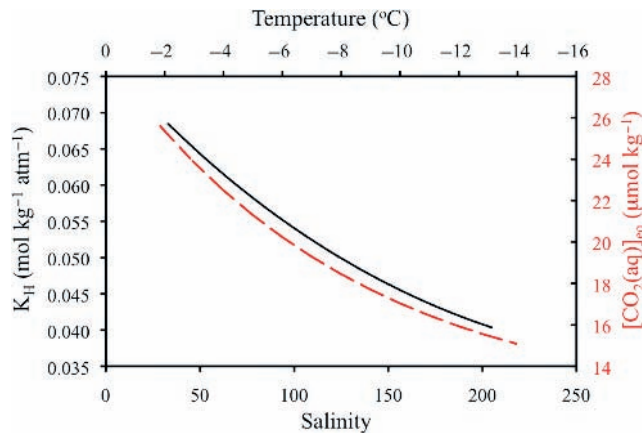
Fig. 12.2   The solubility of CO_2 in sea water–derived hypersaline solutions at sub-zero temperatures expressed as Henry's law constant (K_H), derived from Weiss (1974), and the concentration of dissolved CO_2 $[CO_2(aq)]_{eq}$ at equilibrium with the current partial pressure of atmospheric CO_2 ($pCO_2 = 374$ μatm).

decrease in gas solubility and the physical expulsion of dissolved constituents in the parent sea water mass under sea ice conditions results in degassing of sea ice as it gets colder and older via physical accumulation of total gas within the brine followed by subsequent migration into gas bubbles (brine degassing) and ultimate release of the gaseous component to the atmosphere above or in the underlying water (Mock et al., 2002).

To date, there have been very few studies to measure the total gas content and gas composition of sea ice. Tison et al. (2002) review our current knowledge on major gas inclusions found in sea ice in the absence of biological activity. Existing measurements range from 2 to 25 ml of total (gaseous + dissolved) gas per kilogram of ice (equivalent to 89–1125 mmol kg^{-1}), with a composition that tends to reflect origin from sea water saturated with air. However, there is significant variability, especially considering the concentrations of two biologically important gases, O_2 and CO_2. To date, relevant measurements, made in artificial sea ice for O_2, indicate that the brine released from sea ice tends to be supersaturated with O_2, as expected from the physical–chemical thermodynamics of the system, whereas melting ice is undersaturated with respect to O_2. Glud et al. (2002) speculate that the O_2 depletion in thawing ice can create favourable conditions for anaerobic bacteria to develop, such that anoxic processes, such as sulphate reduction and denitrification, possibly occur within the ice matrix. In the Baltic Sea, Petri and Imhoff (2001) reported the presence of anoxygenic phototrophic purple sulphur bacteria, and Kaartokallio (2001) reported evidence of denitrification in first-year ice, indicating the occurrence of O_2-deficient or anoxic zones within the ice. Rysgaard and Glud (2004) later quantified denitrification and anaerobic ammonium oxidation in Arctic first-year sea ice. It is fascinating that the presence of sea ice allows for anaerobic processes to take place over the top metre, or so, over many millions of square kilometres, of the surface ocean.

Available observations of the gas content and ionic composition of sea ice have often deviated from predictions based on theoretical solubility. This discrepancy may be because sea ice rarely forms and grows under constant abiotic forces but is rather a historical record of a large number of diverse climatic conditions. To complicate matters further, there is also an overriding dissolved gas signature in the ice due to biological production and consumption of dissolved gases such as O_2 and CO_2 (see below). Indeed, most of the available field observations are taken during, or directly after, periods of high biological activity within the sea ice.

Mineral authigenesis

Similar to dissolved gases, thermodynamic *S–T* constraints on mineral solubility coupled with the physical concentration of their ionic species in the expelled brine can lead to precipitation of minerals during the freezing of sea water. The propensity for a mineral A_xB_y to precipitate from, or dissolve in, a solution (i.e. mineral solubility) is controlled by the state of saturation of the solution with respect to the mineral, which is described by the dimensionless saturation index Ω (after Berner, 1980):

$$\Omega = \frac{ICP}{K_{sp}^*}$$

(Equation 12.1)

where ICP = $[A]^x[B]^y$ is the ion concentration product in the given solution, and K_{sp}^* is the ICP of the solution at thermodynamic equilibrium with the mineral phase (i.e. the stoichiometric solubility constant), which is a function of the salinity and temperature (as well as

pressure) of the solution (Millero, 1995; Marion, 2001). Once K_{sp}^* is exceeded by the ICP of the solution ($\Omega > 1$), the solution is supersaturated with respect to the mineral, mineral crystals will begin to nucleate, and the ions will precipitate out of solution as an authigenic mineral phase. When $\Omega < 1$, the solution is undersaturated with respect to the mineral, and precipitation does not occur. Further in this case, the undersaturated solution is corrosive towards the mineral, i.e. the mineral dissolves upon contact with the solution.

Mineral precipitation from sea ice brine has been well characterized by thermodynamic models from the freezing point to the eutectic point of sea water (Marion & Farren, 1999; Marion, 2001). The most thermodynamically consistent sequence of minerals precipitating from sea water-derived brines during freezing is known as the Gitterman pathway and consists of calcite ($CaCO_3$) at $-2.2°C$, mirabilite ($Na_2SO_4 \cdot 10H_2O$) at $-6.3°C$, gypsum ($CaSO_4 \cdot 2H_2O$) at $-22.9°C$, hydrohalite ($NaCl \cdot 2H_2O$) at $-22.9°C$, sylvite (KCl) at $-33.0°C$ and $MgCl_2 \cdot 12H_2O$ at $-36.2°C$ (Marion & Farren, 1999). Documented observations of mineral authigenesis in sea ice are still scarce in natural settings, but there is field evidence for mirabilite (Chapter 2) and calcium carbonate mineral formation (Dieckmann et al., 2008).

Carbonate minerals in sea ice

There are two main drivers for $CaCO_3$ precipitation from sea ice brines: the first and primary driver is the physical concentration of ions during freezing, which results in the increase of the Ca^{2+} and CO_3^{2-} concentrations in the brine, thus exceeding the thermodynamic equilibrium concentrations of $CaCO_3$ phases at the sub-zero temperature and high ionic strength of the sea ice system. The second driver is the concentration of $CO_2(aq)$ (i.e. pCO_2) of the brine, which is superimposed on the physical concentration effect on the Ca^{2+} and CO_3^{2-} concentrations, because it affects the pH of the medium and, thus, the concentration of CO_3^{2-} based on the set of chemical thermodynamic equilibrium equations that control the speciation of H_2CO_3 in aqueous media (after Stumm & Morgan, 1996):

$$CO_2 + H_2O \leftrightarrow H_2CO_3 \leftrightarrow H^+ + HCO_3^- \leftrightarrow 2H^+ + CO_3^{2-} \qquad \text{(Equation 12.2)}$$

Reduction of the pCO_2 of the brine due to degassing during sea ice formation (Killawee et al., 1998; Papadimitriou et al., 2004), biological activity (Gleitz et al., 1995; Arrigo & Thomas, 2004; Papadimitriou et al., 2007), or both, can lead to thermodynamically favourable conditions for carbonate mineral authigenesis in sea ice (Papadimitriou et al., 2007). In general, heterotrophic activity in sea ice will have the opposite effect on the reactions pertaining to the carbonate system (e.g. increase in internal pCO_2, shifts in carbonate mineral precipitation and dissolution equilibria) in the enclosed brine. Finally, because biological activity and the freezing and melting of sea ice are driven by air temperature and solar radiation, the conditions conducive to carbonate precipitation and dissolution will have a strong seasonal component.

Although $CaCO_3$ precipitation in sea ice has been proposed for more than 100 years, actual evidence has until recently only been from laboratory-made artificial sea ice (Gitterman, 1937; Killawee et al., 1998; Tison et al., 2002; Papadimitriou et al., 2004), with uncertainty as to the actual mineral phase likely to precipitate in field sea ice brines (Marion, 2001). Calcite ($CaCO_3$) is thermodynamically predicted to precipitate at $-2.2°C$ from sea ice

brine (with a corresponding salinity of 39) at equilibrium with current atmospheric $p\mathrm{CO}_2$ (Marion, 2001). Ikaite, a metastable hydrated CaCO_3 mineral ($\mathrm{CaCO}_3 \cdot 6\mathrm{H}_2\mathrm{O}$), is also thermodynamically viable in sea ice brine at $-4.5°\mathrm{C}$ (corresponding to a brine salinity of 77) at equilibrium with current atmospheric $p\mathrm{CO}_2$ and in the absence of calcite formation (Marion, 2001). The lack of calcite formation as a prerequisite for ikaite formation is equivalent to the kinetic inhibition of the former mineral in favour of the latter.

The presence of ikaite in sea ice was recently documented in natural sea ice in the Weddell Sea, Antarctica (Dieckmann et al., 2008). The ikaite crystals (Fig. 12.3) were unevenly distributed throughout the ice column in a range of sea ice types in early spring, covering a wide ice temperature spectrum of $-8.9°\mathrm{C}$ to $-2.0°\mathrm{C}$. This discovery clearly indicates that the natural brine was sufficiently supersaturated with respect to ikaite for precipitation of the mineral to occur. It also indicates that the formation of the anhydrous carbonate mineral phases (calcite, aragonite, vaterite) appears to be kinetically inhibited. Ikaite is thought to be the most likely dominant calcium carbonate mineral phase in sea ice because of its insensitivity to the presence of major ($\mathrm{Mg^{2+}}$, $\mathrm{SO_4^{2-}}$) and minor (dissolved organic matter [DOM], dissolved inorganic phosphorus [DIP]) dissolved species, which are known to inhibit calcite formation in ionic media (Dickens & Brown, 1970; Bischoff et al., 1993).

The physical–chemical dynamics of sea ice brine (gravity drainage) and ikaite precipitation have been proposed as the driving force for a sea ice–driven carbon pump in ice-covered oceanic waters (Jones & Coote, 1981; Rysgaard et al., 2007) and as a factor in the control of tropospheric ozone depletion events at the poles (Sander et al., 2006). At the moment, little is known on the spatial and temporal occurrence of ikaite precipitates in polar sea ice. Subsequent discovery of mineral crystals in fast ice off Adélie Land, Antarctica, in November 2007, identical to those from the north-western Weddell Sea (G. S. Dieckmann, unpublished data), indicates that ikaite formation in sea ice is not a localized phenomenon, although the significance of ikaite authigenesis in sea ice on processes of global relevance can as yet not be fully assessed.

The existing laboratory-derived direct (Killawee et al., 1998; Tison et al., 2002) and indirect (Marion, 2001; Papadimitriou et al., 2004, 2007) thermodynamic and geochemical
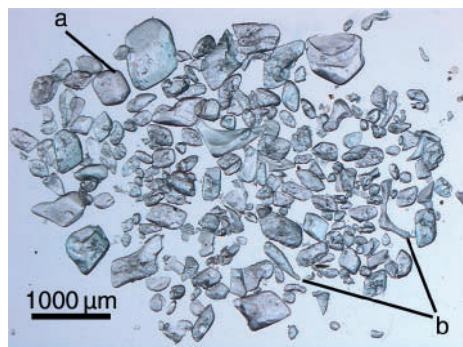
Fig. 12.3 Photograph of ikaite crystals taken from a single bulk sea ice sample showing various crystal shapes and sizes. (a) Idiomorphic and (b) shape of brine pockets or channels. Photo from gerhard Dieckmann.

evidence for this process in sea ice is insufficient to address the key aspects of mineral dynamics, such as the stability field and the precipitation and dissolution rates of ikaite, which would allow full integration into existing models of carbon cycling in sea ice (Chapter 8). The first direct field evidence for ikaite authigenesis in sea ice (Dieckmann et al., 2008) indicates a large stability field under sea ice *S–T* conditions. To date, the production of carbonate minerals in sea ice remains a poorly documented and, crucially, unquantified component of the polar carbon cycle. Key aspects of the dynamics of these minerals need to be studied before a true appreciation of their role can be assessed.

The pH of sea ice

The changes in the chemistry of carbon can result in significant shift in the pH of the sea ice brine, or the interstitial waters of platelet systems and rotten ice. Once again, the number of studies citing pH in sea ice is rather limited and is based on spring and summer measurements. The collection of undisturbed sea ice brine samples, as well as complications in measuring stable pH values at the elevated salinity of concentrated brine solutions, both hinder the collection of realistic pH values from sea ice. Any intrinsic shift in the pH during the freezing of sea water is masked by the pH effect of photosynthetic activity within the ice with reports generally describing biologically driven elevated pH in closed sea ice systems or within dense standing stocks of sea ice organisms. In natural sea ice brines from ice floes in the Weddell Sea, pH values (on the sea water pH scale; Millero, 1995) ranging from 8.4 to 8.8 were measured during early austral summer (December 2004; Papadimitriou et al., 2007), with pH measurements ranging from 8.2 to 9.9 and from 7.8 to 8.9 later in the austral summer (January–March 1991) and autumn (April–May 1992), respectively (Gleitz et al., 1995). The observed pH increase in colonized sea ice habitats results from the decline in the concentration of dissolved inorganic carbon, with concomitant depletion of CO_2(aq) as a result of photosynthetic carbon assimilation.

Molecular diffusion

As described by Eicken (1992) and in Chapter 2, sea ice is characterized by large temporal and spatial gradients in brine channel volume, temperature and salinity, even within a single ice floe. These gradients in physical conditions are reflected in corresponding gradients in the chemical composition of the sea ice, which can lead to diffusive migration of dissolved species and their exchange with sea water. The possibility for sea water exchange is greater at the margins of ice floes, or in under-ice accumulations of platelet ice, resulting in replenishment of biologically important dissolved gases and inorganic nutrients. Also, in young sea ice, or in warm and rotten porous ice, the interior of ice floes is rarely isolated from the influence of sea water exchange. In these cases, the exchange of solutes between sea ice and sea water will be constrained by ion diffusion across diffusive boundary layers (DBL) similar to what is commonly described at the sediment–water interface and only recently studied at the water–ice interface during O_2 micro-sensor studies (Rysgaard et al., 2001; Mock et al., 2002). It is only in older consolidated sea ice, especially at low ambient temperature, that the brine channel network becomes isolated and can be regarded as a closed chemical environment. This compromises issues such as categorization and chemical classification for various ice types or ice ages (Weeks & Ackley, 1982; Meese, 1989; Dieckmann et al., 1991).

12.3 Biological activity: the modification of the chemical composition of sea ice by sympagic organisms

The metabolic balance

Several researchers have looked at the effects on sea ice chemistry of the high standing stocks of sea ice algae observed in the growing season from spring to autumn, and of the associated high rates of photosynthesis (O_2-producing, CO_2-consuming) and heterotrophic respiration (O_2-consuming, CO_2-producing). It is important to note that algae both photosynthesize and respire, while heterotrophic bacteria and grazers (including protozoans and metazoans) only respire, relying on the photosynthetically produced biogenic matter for growth and cell maintenance. The vast standing stocks of algae and, at times, of bacteria and grazers (Gradinger et al., 1999; Kaartokallio, 2004; Riedel et al., 2008) can alter the gaseous composition predicted under abiotic conditions.

The existing data on dissolved gases in sea ice brine and platelet ice systems show that where high primary production and concomitant accumulation of large algal standing stocks have occurred, the brine is characterized by substantial reductions in total dissolved inorganic carbon (ΣCO_2), exhaustion of $CO_2(aq)$, highly alkaline pH (range: 8–10) and O_2 supersaturation (Gleitz et al., 1995, 1996a; Günther et al., 1999; Thomas et al., 2001b; Papadimitriou et al., 2007). These dramatic chemical changes indicate that photosynthetic activity by the algae exceeds respiration by all of the organisms within the ice. Naturally, this metabolic imbalance can only hold at times of the year when significant photosynthesis and growth of ice algae takes place. It is expected that, in winter, or in thick or heavily snow-covered ice, where irradiance is too low for photosynthesis, the biological assemblages will tend towards being net heterotrophic. Indeed, a recent seasonal study of microbial processes in Arctic first-year sea ice described a predominantly heterotrophic assemblage in late winter (i.e. prior to the ice algal bloom) at low irradiance (i.e. high snow cover), with dominance of a non-diatom based food web. In this case, heterotophic bacteria were estimated to contribute, on average, ~80% of the total sea ice biomass, followed by autotrophic and heterotrophic protists (Riedel et al., 2008). This agrees with previous observations of high bacterial biomass in Arctic land fast and pack ice in winter (Gradinger & Zhang, 1997; Gradinger et al., 1999; Kaartokallio, 2004). Heterotrophic processes continue during the period of the ice algal bloom, but their effect on the chemical composition of the sea ice brine is overridden by that of the growth and accumulation of the dense sea ice diatom assemblages (Riedel et al., 2008).

The possibility that sea ice algae switch from photoautotrophy to heterotrophy as a means for winter survival has been postulated in the past (Palmisano & Sullivan, 1985; Rivkin & Putt, 1987). Zaslavskaia et al. (2001) have shown that all the necessary activities for glucose metabolism exist in certain diatom cells, and the potential to transform from obligate photoautotrophy to full heterotrophy can be achieved. However, the dominance of flagellates in late winter sea ice, many of which are not obligate autotrophs, and the fact that diatoms dominate the sympagic microbial community only at times or sites of increased irradiance (Riedel et al., 2008; Różańska et al., 2009) suggest that mixotrophic flagellates, rather than diatoms, play a key part in transitions between autotrophy and heterotrophy in sea ice. Overwintering strategies of diatoms in sea ice may include resting spores and cysts, which were found to be more abundant in newly formed sea ice than in surface waters in the Arctic, but such strategy has been assessed to be of minor importance for sea ice protists in the

Arctic (Różańska et al., 2008). In Antarctic sea ice, encystment of dinoflagellates has been reported (Buck et al., 1992; Stoecker et al., 2000).

Altogether, the existing studies show that, during the annual cycle of first-year ice formation and decay, heterotrophy dominates the microbial processes in sea ice from autumn to early spring, while, during the ice algal bloom in the growing season, intense autotrophy super-imposes on the active heterotrophic food web present in the ice. The influence of hetereotrophic activity on the composition of sea ice still warrants further investigation, especially as the agent for anaerobic microbial production of molecular nitrogen (N_2) via denitrification, i.e. the stepwise reduction of nitrate to N_2 (Rysgaard & Glud, 2004; Rysgaard et al., 2008). Denitrifying bacterial strains have been isolated from Antarctic sea ice (Staley & Gosink, 1999), and the potential for bacterial denitrification has recently been shown for Artic sea ice in various locations (Kaartokallio, 2001; Rysgaard & Glud, 2004; Rysgaard et al., 2008). Oxygen inhibits the activity of denitrifying enzymes, and denitrification takes place at low oxygen concentrations and under anoxic conditions. Glud et al. (2002) showed that oxygen is expelled along with brine during ice growth and that oxygen depletion can occur during ice melt. Recent field observations have also revealed anoxic conditions in the lower parts of first-year ice and low bulk oxygen concentrations in melted sea ice samples (Rysgaard et al., 2008). The presence of localized sites supersaturated or undersaturated with oxygen creates a 'mozaic-like O_2 distribution pattern' in the sea ice (Rysgaard et al., 2008). The co-occurrence of microenvironments, where denitrification and its reverse microbial process, nitrification (the stepwise oxidation of ammonium to nitrite and nitrate), can take place, may explain the high concentrations of nitrate and ammonium frequently measured at the same time in sea ice samples. Ammonium-oxidizing bacteria have been found in sea ice assemblages (Priscu et al., 1990b). The activity of nitrifiers and denitrifiers alike is likely to be enhanced by attachment to surfaces, such as ice crystals, polysaccharide gels or organisms, since ammonium- and nitrite-oxidizing activity in other marine systems is induced by attachment.

Photosynthetic quotient

The photosynthetic quotient (PQ = moles of O_2 produced/moles of CO_2 fixed) is a measure of carbon metabolism and photosynthetic performance within a biological assemblage. Photosynthetic organisms growing under nutrient-replete conditions tend to exhibit PQs between 1.0 and 1.4. The relative proportions of O_2 and CO_2 found within a closed sea ice matrix will therefore provide a record of the dominant carbon metabolism. In the few studies that have examined both O_2 and ΣCO_2 concentrations in sea ice, the calculated PQs tend to fall within a range of 1.2–1.4, therefore well within the 'typical range' (Gleitz et al., 1995; Günther et al., 1999; Glud et al., 2002). These measurements have been made over a wide range of ice types and biological standing stocks but are biased towards periods of significant algal growth. As mentioned earlier, there is a need to obtain more data at times of the year when a switch in metabolism and in the community composition results in net heterotrophy, which may alter significantly the chemical composition of sea ice inherited from the preceding, predominantly autotrophic stage in perennial sea ice.

Dissolved oxygen and carbon dioxide

Low CO_2 conditions, although rare, can occur in sea water after periods of dense phyto-plankton blooms, while situations when hyperoxia develops are seldom found in marine
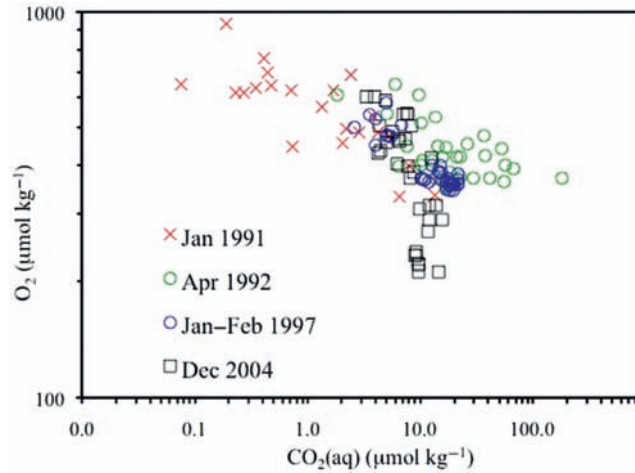
Fig. 12.4   Dissolved molecular oxygen (O_2) versus dissolved carbon dioxide CO_2(aq) observations from sea ice brines collected from sack holes in first-year and multi-year ice floes in the Weddell Sea, Antarctica, in austral autumn (Data from April 1992, Gleitz et al., 1995) and summer (Data from January 1991, Gleitz et al., 1995; January–February 1997, Kennedy et al., 2002; December 2004, Papadimitriou et al., 2007).

systems (Raven et al., 1994). Yet, available measurements (Fig. 12.4) show that hyperoxic conditions ($[O_2] > 300$–$350\ \mu$mol kg^{-1}) coupled with low CO_2(aq) concentration are quite common in predominantly autotrophic-dominated sea ice habitats (Gleitz et al., 1995; Kennedy et al., 2002; Papadimitriou et al., 2007). Oxygen is a competitive inhibitor of the CO_2 carboxylation by ribulose bisphosphate carboxylase/oxygenase (RUBISCO), the key enzyme in photosynthetic carbon assimilation by algae (Chapter 8). To suppress the oxygenase activity of the enzyme, many algal species have carbon-concentrating mechanisms (CCM), thereby ensuring that there is a high supply of dissolved inorganic carbon in the forms of CO_2(aq) and HCO_3^- at the RUBISCO site within the cell.

   The expression of CCM is not found in all algae but has been observed in some sea ice diatoms, possibly providing a competitive advantage over those species without such mechanism, being an important feature when exposed to low extracellular CO_2(aq) concentrations (Gleitz et al., 1996b; Mitchel & Beardall, 1996). Although O_2 is not toxic *per se*, potentially harmful reactive oxygen species, such as hydrogen peroxide and hydroxyl radicals, may accumulate at very high concentrations of O_2 (Vincent & Roy, 1983; Raven, 1991; Prézelin et al., 1998). Toxic photochemical products are also produced by the interaction of UV-B radiation, O_2 and certain organic molecules. Little is known about how sea ice organisms cope with oxidative stress, but isolated sea ice diatoms have been shown to have high activities of protective antioxidative enzymes such as catalase, glutathione peroxidise and glutathione reductase (Schriek, 2000). The dimethyl-sulphoniopropionate (DMSP) produced by sea ice diatoms (see below) may also serve as an antioxidant.

Dimethyl sulphide

The diffusion limitation that results in the build up of O_2 and the depletion of CO_2(aq) in sea ice will apply to other dissolved gases produced by sea ice organisms. One of the few to be studied in any detail is dimethyl sulphide (DMS), which is derived from dimethylsulfonioproprionate (DMSP). In remote ocean regions, DMS accounts for most of the non-sea salt

sulphate in the atmosphere, and its atmospheric chemistry is closely linked to the production of aerosol particles that serve as cloud condensation nuclei as part of a complex system of localized and global climate control (Malin & Kirst, 1997; Stefels et al., 2007). Of particular interest is the breakdown of DMSP to DMS and subsequently into methanesulphonic acid (MSA) which can be used as a proxy in glacial ice cores for past sea ice extent estimations (Curren et al., 2003; Dixon et al., 2005; Chapter 13).

The concentration of DMSP within sea ice organisms can be orders of magnitude higher than that measured in the open ocean water and in the under-ice sea water (Kirst et al., 1991; DiTullio et al., 1998; Trevena & Jones, 2006; Trevena et al., 2000, 2003; Chapters 7–9). Light, temperature and nutrient supply all influence the production of DMSP (Malin & Kirst, 1997; Stefels et al., 2007). Hefu and Kirst (1997) showed that ultraviolet (UV) radiation significantly reduced the production of DMSP by *Phaeocystis antarctica*, a prymnesiophyte and prolific DMSP producer, responsible for large pelagic blooms in Antarctic and Arctic waters (Arrigo et al., 1999; DiTullio et al., 2000). In sea ice, however, salinity is the dominant factor influencing DMSP production by the ice algae, with DMSP being synthesized and accumulating internally in the cells in hypersaline conditions. DMSP is broken down to release DMS and acrylic acid into the surrounding medium when ambient salinity decreases. Furthermore, DMSP is also broken down to release DMS in alkaline conditions, such that the biology-induced shifts of pH up to ~10 that have been measured in sea ice brine (Gleitz et al., 1995) may enhance this reaction within the sea ice habitat. Lastly, DMSP is broken down to DMS and acrylic acid through the action of the algal and bacterial enzyme DMSP-lyase and, also, from grazing by protozoans and metazoans, as well as viral infection. An increase in the conversion rate of DMSP to DMS and acrylic acid was observed to accompany its reduced production rate by UV radiation (Hefu & Kirst, 1997).

To date, observations indicate great variation in the distribution of DMSP in sea ice, largely reflecting the variability in species composition of the local biological assemblages. However, the small-scale spatial heterogeneity of the physical factors that influence the production of DMSP by ice algae, namely light, salinity and temperature, are also responsible for the observed variability in the DMSP distribution within sea ice. Brine channel morphology, which determines the extent of grazing activity within the ice (Krembs et al., 2000), will determine the degree of grazing-induced release of DMS under sea ice conditions. As most of the particulate organic material that accumulates in the sea ice during the ice algal bloom is released into surface waters at the time of ice melt (Michel et al., 2002; Juul-Pedersen et al., 2008), a large input of particulate DMSP ($DMSP_p$) from the sea ice into surface oceanic waters is expected to occur during the melt period and at ice edges. Increased heterotrophy and bacterial activity at the end of ice algal blooms (Haecky & Andersson, 1999; Kaartokallio, 2004), and the fact that periods and sites of ice ablation are usually associated with high grazing activity, point to a high release of DMSP in surface waters and, potentially, of DMS to the atmosphere. Whether DMSP is mainly transferred from the sea ice to the surface waters in particulate or dissolved form at the time of melt, and how much bacterial DMSP-lyase activity takes place in the sea ice versus surface waters, warrants closer investigation.

Other climate-relevant volatile compounds

DMS is not the only volatile compound produced by marine algae, which may be incorporated into the dynamics of sea ice, with potential consequences for atmospheric chemistry.

Reactive halogen species significantly contribute to the destruction of ozone in the polar stratosphere and underlying troposphere. The origins of the increased halogen concentrations, and the spatial and temporal extents of their influence, remain unclear. However, tropospheric air enrichment of reactive bromine species closely associated with sea ice has been observed (Wagner & Platt, 1998). Both Arctic and Antarctic sea ice algae produce significant quantities of a suite of brominated hydrocarbons, including bromoform, dibromomethane, bromochloromethanes and methyl bromide, all of which may be converted photochemically into active forms of bromine (Sturges et al., 1992, 1993). The levels of production evidently have important implications for the chemistry of the polar oceans and may be of similar orders of magnitude to the influence of anthropogenic and macrophyte sources on a global scale (Sturges et al., 1992). It has also been speculated that short-term high concentrations of BrO in the troposphere are due to autocatalytic bromine release from sea salts in sea ice rather than due to degradation of unstable organic compounds containing halogens. The investigation into the mechanism of the abiotic sea ice–associated bromine release is ongoing (Sanders et al., 2006; Morin et al., 2008).

Inorganic macro-nutrients

By far, the greatest attention to the chemistry of sea ice has been given to the dynamics of inorganic macro-nutrients such as nitrate (NO_3^-), nitrite (NO_2^-), ammonium (NH_4^+), DIP and silicic acid ($Si(OH)_4$). In abiotic systems, as ice forms and consolidates, the concentration of these compounds will change in a conservative manner, i.e. in proportion to the salinity change. For example, macro-nutrient concentrations measured in bulk ice will decrease linearly with decreasing bulk salinity of the ice, or, conversely, their concentration will increase proportionally to salinity when measured directly in brine pockets. In reality, such straightforward scenarios are rarely encountered. Major ions, such as sodium, potassium, magnesium, calcium, chloride and sulphate, in different types and ages of ice generally follow closely their theoretical dilution line predicted from salinity changes in sea ice (Meese, 1989). However, when concentrations of macro-nutrients are compared with their theoretical dilution line, there is often significant deviation from this trend, indicating depletion, or even complete exhaustion, of these nutrients (Fig. 12.5; Meese, 1989; Dieckmann et al., 1991; Gleitz & Thomas, 1993; Gleitz et al., 1995; Thomas et al., 1998; Kennedy et al., 2002; Arrigo et al., 2003; Papadimitriou et al., 2007). As with dissolved gases discussed above, these deviations are clearly associated with the biological activity occurring within the ice, which introduces a high degree of spatial and temporal heterogeneity.

Several workers have tried to categorize ice age and/or type by the concentration of these nutrients, only to be confounded by the large-scale variability within and between ice cores (Meese, 1989; Dieckmann et al., 1992). In the Antarctic, nutrient exhaustion has only rarely been reported in assemblages within platelet ice underlying more consolidated ice (Dieckmann et al., 1992; Günther & Dieckmann, 1999, 2001; Arrigo et al., 1995), because replenishment of nutrients is possible even in dense aggregates of platelets that can extend tens of metres under the ice (Thomas et al., 2001a). Similarly, in porous summer sea ice and surface sea ice layers, such as gap, infiltration and freeboard layers (Ackley & Sullivan, 1994; Fritsen et al., 1998, 2001; Haas et al., 2001; Ackley et al., 2008), the high algal standing stocks often recorded will be supported to a large degree by continuous or intermittent replenishment of nutrients from the surrounding sea water by wave action (Garrison & Buck, 1991; Fritsen
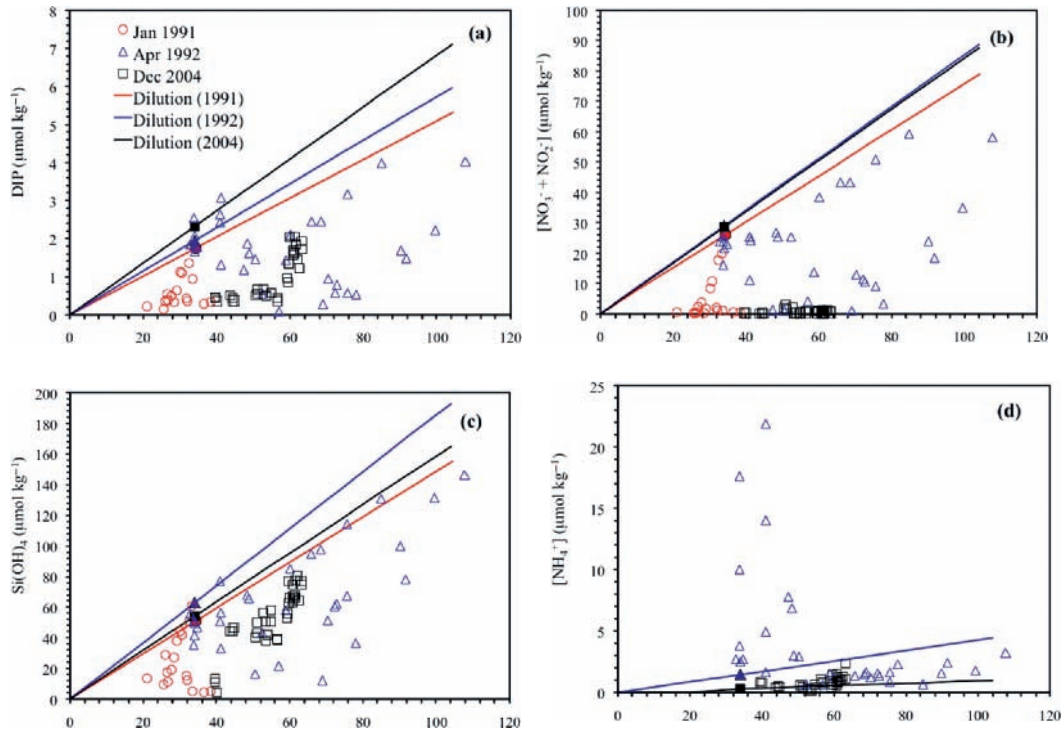
Fig. 12.5 (a) DIP, (b) nitrate plus nitrite, (c) silicic acid and (d) ammonium concentrations as a function of salinity in sea ice brines collected from sack holes in first-year and multi-year ice floes in the Weddell Sea, Antarctica, in austral autumn (Data from April 1992, Gleitz et al., 1995) and summer (Data from January 1991, Gleitz et al., 1995; December 2004, Papadimitriou et al., 2007). Dilution lines were constructed based on the concentrations of the solutes reported in the surface sea water on each occasion.

et al., 1994; Thomas et al., 1998; Kennedy et al., 2002). Surface gap, freeboard and infiltration layers are often not continuous throughout a floe. In some regions in the ice, such layers can be cut off from nutrient re-supply, resulting in overall nutrient depletion locally (Fritsen et al., 2001), even within a few centimetres from that part of the floe which exchanges fully with the surrounding sea water. The zones of highest productivity within ice floes are clearly governed by the degree of re-supply of nutrients (Syvertsen & Kristiansen, 1993; Gleitz et al., 1996a; Kennedy et al., 2002).

In contrast to situations where significant biological standing crops are supported by continuous exchange of inorganic nutrients between sea ice and the surrounding sea water (open systems), several comprehensive studies have shown that nitrate-based primary production within closed or semi-enclosed sea ice habitats proceeds in general stoichiometric balance, with nitrate, DIP and $Si(OH)_4$ decreasing with decreasing ΣCO_2 and increasing O_2 (Gleitz et al., 1995; Günther et al., 1999; Fritsen et al., 2001; Kennedy et al., 2002). However, as is discussed below, sea ice assemblages are not universally nitrate based due to high accumulation of ammonium within the sea ice matrix.

Even after the exhaustion of the dissolved inorganic nitrogen compounds, photosynthetic activity continues, with synthesis and accumulation of low nitrogen compounds (lipids,

carbohydrates). In these cases, the resulting rise in pH and depletion of SCO_2 are much greater than can be accounted for by including inorganic nitrogen pools in the stoichiometric mass balance (Gleitz et al., 1996a,b; Günther et al., 1999; Kennedy et al., 2002). The presence of conspicuous lipid droplets within the cells and changes in lipid class abundances are two of the biochemical observations most commonly reported for nutrient-limited sea ice algae (Nichols et al., 1989; Priscu et al., 1990a; Fahl & Kattner, 1993; Gleitz et al., 1996a; McMinn et al., 1999; Mock & Gradinger, 2000). Nutrient limitation coupled with low temperature and low incident light has been shown to influence significantly the fatty acid composition of the cell membrane in sea ice diatoms (Mock & Kroon, 2002a,b). During periods of nitrogen limitation, protein biosynthesis is affected, and the loss of bilayer-stabilizing proteins and pigments could disrupt chloroplast membranes and, consequently, photosynthesis. In sea ice diatoms, loss of membrane protein caused by nutrient limitation can be compensated for by the production of bilayer-forming fatty acids such as digalactosyldiaglycerol and phosphatidylglycerol (Mock & Kroon, 2002b). These processes affect the quality of sea ice assemblages as a food source for grazing protozoans and metazoans, as well as for the chemotaxonomy and organic geochemistry of algal assemblages and associated sediments (Nichols et al., 1989). In particular, the use of lipid composition as a biomarker for identifying the source of organic matter in sediments will be influenced greatly by the changes induced within the nutrient-depleted sea ice system (Volkman et al., 1998).

In the Arctic, nutrient limitation of ice algal growth has often been reported, with different nutrient species being considered limiting. In Hudson Bay, it was proposed that nitrogen limitation of ice algal growth occurs in estuarine waters influenced by a river plume whereas in marine waters, silicic acid was considered limiting (Gosselin et al., 1990). Silicic acid has also been suggested to limit the growth of the very high standing stocks of bottom ice algae observed near Resolute, in the Canadian Arctic Archipelago (Cota et al., 1990; Smith et al., 1990; Lavoie et al., 2005). However, nitrogen enrichment bioassays have also shown nitrogen limitation of bottom ice algae in the same region (Smight et al., 1997). In the Baltic Sea, phosphorus has been proposed to limit ice algal growth in the spring (Haecky & Andersson, 1999; Meiners et al., 2002; Chapter 14).

In many cases, however, these nutrients are present far in excess of what would be predicted from simple conservative behaviour during the freezing of sea water. Specifically, they often exhibit concentrations more akin to those found in heterotrophic environments, such as in sedimentary pore waters, where these nutrients are liberated into solution by the oxidation of organic matter during microbial respiration. In particular, nitrate concentrations up to 300 $\mu mol\ l^{-1}$, $Si(OH)_4$ concentrations up to 320 $\mu mol\ l^{-1}$, ammonium concentrations up to 200 $\mu mol\ l^{-1}$ and DIP concentrations up to 70 $\mu mol\ l^{-1}$ have been recorded in sea ice (Arrigo et al., 2002). Nitrite levels are generally low in sea ice, although in some studies, elevated concentrations of this nutrient have been reported (Thomas et al., 1995; Gradinger & Ikävalko, 1998; Kaartokallio, 2001). Unusually high inorganic nutrient concentrations are frequently found in association with dense, actively growing algal and bacterial standing stocks. This feature is not restricted to sea ice from high latitude regions but is also a characteristic of Baltic sea ice (Mock et al., 1997; Kaartokallio, 2001). Such high nutrient concentrations, equivalent to nutrient regeneration rates of 35 $\mu mol\ l^{-1}\ d^{-1}$ for DIP and in excess of 31 $\mu mol\ l^{-1}\ d^{-1}$ for ammonium, were considered to be due to high rates of (heterotrophic) bacterial metabolism and/or excretion by metazoan grazers (Arrigo et al., 1995; Grossmann et al., 1996), which can reach high population abundance in these ammonium- and DIP-rich

systems (Chapter 10). Several diatom species also release ammonium at high rates under conditions of excess cellular energy (Lomas & Glibert, 2000). Further, algal mortality and cell lysis, amplified by inefficient metazoan grazing within high algal standing stocks, can liberate considerable DOM and inorganic nutrients (Günther et al., 1999). However, it seems unlikely that the extraordinarily high concentrations of DIP and ammonium can be explained by the release of internal pools alone. The most probable explanation is that large nutrient reserves result from a combination of some of the above factors. Regardless of the processes responsible for excess nutrient accumulation in sea ice, their production is clearly greater than the apparent capacity for utilization within such systems. Excess nutrient accumulation also indicates that exchange with the surrounding water must be limited or entirely absent, otherwise the high concentrations would be diluted by the relatively less nutrient-loaded sea water. However, the systems in which high nutrient concentrations develop cannot always be isolated from external exchange, because algal biomass, which serves as a repository of inorganic nutrients via assimilation and remineralization, could never reach levels higher than the starting concentrations of oxygen, carbon, nitrogen and phosphorus permit without some exchange with sea water. The fact that these levels are so often grossly exceeded indicates biomass increase that, in this case, has been supported by both external supply of nutrients and nutrients released by regeneration processes within the system (Arrigo et al., 1995; Thomas et al., 1998; Arrigo et al., 2002; Kennedy et al., 2002).

The degree to which there is possible exchange with the surrounding sea water is one of the key factors influencing the nutrient dynamics of sea ice. In biological assemblages at the periphery of ice floes, especially bottom ice assemblages, nutrient depletion is only seldom reported as being a growth-limiting factor, because exchange with the underlying water is readily possible. Small-scale differences in the topography of the ice–water interface were shown to be conducive to an increased fluid and, hence, nutrient exchange across irregular undersides of sea ice floes (Krembs et al., 2001b). The small-scale exchange rates in bottom ice skeletal layers were measured to be 100 times those for pore water exchange in sandy sediments and more than enough to satisfy algal nutrient demands (Krembs et al., 2001b). The transient nature of such small topographical features is one of the key factors determining not only the variability of nutrient and gas fluxes across the ice–water interface, but also the localized variability in the accumulation (abundance) of organisms that depend on these nutrient supplies to grow. Exchange processes decrease away from the ice–water interface and further into the ice. There can be significant nutrient depletion and limitation of algal growth even within 5–10 cm from the ice–water interface (McMinn et al., 1999). The existence of steep vertical gradients in nutrient concentrations and the associated challenges to assumptions of small-scale homogeneity in sea ice studies were eloquently articulated almost two decades ago (Smith et al., 1990).

One aspect of sea ice nutrient loading that has not been studied in detail yet is the role of atmospheric deposition into surface ice layers. High NO_3^- and NH_4^+ concentrations have been measured in precipitation (NO_3^-: 49–80 µmol l^{-1}; NH_4^+: 27–32 µmol l^{-1}) and in the uppermost (10–20 cm) layer of sea ice in the Baltic Sea (Kaartokallio, 2004), supporting the hypothesis that atmospheric nutrient loading can play an important role in sea ice–covered regions. Various inorganic compounds, such as nitrate, ammonium and sulphate, are well known for being deposited and stored in snow. These will be added to the nutrient pool of the surface sea ice layers as snow is transformed and incorporated into the gross structure of ice floes (Eicken et al., 1994; Haas et al., 2001; Massom et al., 2001).

With respect to essential micro-nutrients, such as iron, the contribution of atmospheric deposition to their stocks in sea ice appears to be variable. For example, Antarctic studies report iron concentrations in the snow higher (Edwards et al., 1998) or lower (Lannuzel et al., 2007) than in the sea ice. It has been proposed that iron released from melting sea ice can increase surface water iron concentrations by almost an order of magnitude (Sedwick & DiTullio, 1997; Sedwick et al., 2000; Lannuzel et al., 2007, 2008). This release may be an efficient mechanism for stimulating phytoplankton production because it adds Fe at the sea surface in the austral spring (Thomas, 2003).

Nitrate and ammonium affinity at low temperature

Marine algae and bacteria have a lower affinity for inorganic and organic substrates at low temperatures below their optimum growth temperature (reviewed by Nedwell, 1999; Pomeroy & Wiebe, 2001). In order for the organisms to grow, it is vital that the necessary substrates are present in high enough concentrations to counterbalance the reduced affinity. The high levels of ammonium, DIP and DOM in sea ice will fulfil such temperature-affected metabolic constraints. Similarly, and in slight contrast to this line of thought, low substrate affinity has also been proposed as the reason that available substrates are not always exploited despite the high concentrations in the ice (Pomeroy & Wiebe, 2001). Although not working with sea ice isolates, Reay et al. (1999) measured a consistent decrease in the specific affinity of microorganisms from polar regions for nitrate with decreasing temperatures. Priscu and Sullivan (1998) further showed that it is the slower nitrate transport into the cell relative to the efficiency of enzymatic nitrate reduction that is the limiting factor at low temperature. This is not the case for ammonium, for which the specific affinity is evidently independent of temperature (Reay et al., 1999). The difference is attributable to the fact that active uptake processes, as is the case for nitrate, are more influenced by the changes in membrane structure that occur at low temperatures than passive uptake as is the case for ammonium transport into the cells. These differences in the uptake of dissolved inorganic nitrogen species, therefore, have profound effects on which source of inorganic nitrogen is used by photosynthetic organisms at low temperatures.

The first stage in the reduction of nitrate into a form that can be used for cellular metabolism involves the enzyme nitrate reductase (NR) that converts nitrate to nitrite. Priscu and Sullivan (1998) showed that the extra nitrate did not increase protein-specific NR activity in sea ice algae and that the NR activity was significantly suppressed at ammonium concentrations below 1 mM. Ammonium inhibition of nitrate assimilation is well reported for marine phytoplankton (Thompson et al., 1989; Flynn, 1991). Further, there is an increase in the proportion of ammonia (NH_3) compared to ammonium (NH_4^+) at high (alkaline) pH, the former compound diffusing directly into cells (Flynn, 1991; Raven et al., 1992; Reay et al., 1999). The high levels of ammonium frequently measured in sea ice will inhibit nitrate assimilation by algae, while the elevated ambient pH often measured in sea ice brine will be favourable to ammonium assimilation via increased NH_3 availability in the extracellular medium. In other words, sea ice may be one of the few marine environments where ammonium-dominated nitrogen metabolism prevails (Raven et al., 1992).

In diatoms, the dominant algal group within sea ice systems, nitrate can be stored intracellularly, whereas ammonium is generally not stored. The transport of ammonium into the

cell is inactivated if the intracellular levels of ammonium are excessive (Flynn, 1991). In contrast, flagellates can store high amounts of ammonium within their cells (Lomas & Glibert, 2000). Possibly, differences in nitrogen assimilation patterns within sea ice assemblages play a role in determining the species composition of photosynthesizing organisms within the sea ice. Studies of seasonal shifts in the primary nitrogen uptake (Kristiansen et al., 1992, 1998) reported nitrate to be the main nitrogen source for infiltration algae in spring, whereas ammonium became a much more important nitrogen source during summer.

Silicic acid in sea ice

The availability of silicic acid is fundamental to the dominance of diatoms in sea ice habitats, because it is essential for the formation of their frustules. As for other nutrients, replenishment of silicic acid to the bottom skeletal layer, where most of the ice algal biomass is found, is through exchange with the water column and is ultimately controlled by diffusion across the molecular sublayer immediately adjacent to the ice (Cota et al., 1987). In the Arctic, $Si(OH)_4$ limitation of ice algae has been frequently reported (Cota et al., 1990; Gosselin et al., 1990; Smith et al., 1990) but nitrogen (Smith et al., 1997a) and DIP (Haecky & Andersson, 1999; Meiners et al., 2002) limitation can also occur. There is no evidence of significant dissolution of diatom frustules (i.e. biogenic silicon) taking place in the ice matrix, which would explain that $Si(OH)_4$ is often the limiting nutrient for ice algal growth at high biomass. Using a coupled snow–ice and ice–algae model, Lavoie et al. (2005) showed that tidal mixing can modulate bottom ice algal growth through $Si(OH)_4$ replenishment but that the oceanic heat flux plays a key role in controlling the ice algal biomass. Fripiat et al. (2007) used the fractionation of silicon isotopes to characterize Antarctic sea ice. Their study shows that brine channels and skeletal layers behave as semi-enclosed systems where diatoms used a significant part of the pool of silicic acid, the latter being only partially replenished by convection or diffusion from the $Si(OH)_4$ pool in the underlying sea water. Snow ice and brine pockets of frazil or congelation ice behaved as a closed system, where diatoms use a significant part of the small dissolved silicon pool available. This supports the general view that $Si(OH)_4$ in sea ice is replenished by exchange with underlying waters rather than by dissolution of diatom frustules (Harrison & Cota, 1991).

In general terms, the specific rate of silicon uptake (V_{Si}) by diatoms follows a Michaelis–Menten function:

$$V_{Si} = \frac{V_{max}[Si(OH)_4]}{K_s^{Si} + [Si(OH)_4]} \qquad \text{(Equation 12.3)}$$

where V_{max} = maximum rate of uptake at infinite $Si(OH)_4$ concentration, K_s^{Si} = half-saturation constant for $Si(OH)_4$ uptake and $[Si(OH)_4]$ = substrate concentration in the external medium. Typically, the half-saturation constant for growth is lower than K_s^{Si}, such that diatoms can maintain optimum division rates at $Si(OH)_4$ concentrations that limit its uptake (Paascche, 1973; Brzezinski et al., 1990; Nelson & Dortch, 1996). Diatoms also have intracellular pools of $Si(OH)_4$ and maintain supersaturated concentrations of intracellular silicon, probably in the form of mono- or poly-silicic acid complexed with organic material (Martin-Jézéquel et al., 2000). The size of the internal pool varies between diatom species

(Chisholm et al., 1978) and is influenced by environmental or physiological factors such as temperature, light intensity, nitrogen or phosphorus limitation and growth rate. However, a very small extractable pool mesaured in bottom ice algae in the High Canadian Arctic suggests that ice diatoms may not be able to maintain substantial intracellular pools of $Si(OH)_4$ (Smith et al., 1990). This would explain potential silicon limitation of sea ice algal growth in this environment. The silicification of diatom walls occurs through silica polymerization in specialized compartments enclosed in an organic casing presumably formed with proteins and glycoproteins (Martin-Jézéquel et al., 2000). Silicification is affected by various factors, including cell growth rate, the concentration of $Si(OH)_4$ and other nutrients in the external medium and temperature. Silicification is typically higher at low temperature; the frustules of ice algal cells are highly silicified (Smith & Nelson, 1985; Nelson et al., 1989). Iron limitation can also increase silicification in some diatom species (Hutchins & Bruland, 1998; De La Rocha et al., 2000) but may not be a factor in sea ice habitats as indicated by the high iron concentrations measured in Arctic (Measures, 1999) and Antarctic (Grotti et al., 2005; Lannuzel et al., 2007) sea ice.

DOM

Central to the concept of a closely coupled microbial network is that there is often a considerable amount of DOM within the sea ice. This pool of diverse organic compounds is operationally defined as the organic matter that is smaller than 0.2 μm. In practice, DOM characterization is routinely done after filtration through GF/F glass fibre filters, which have a nominal pore size of ~0.7 μm. This technical aspect of DOM measurements may have significant bearing on the operational characterization of the dissolved, gel-like and particulate organic matter pools in the sea ice, and in the ocean in general, as current methodologies produce some overlap in the continuum of sizes that organic matter spans. The DOM pool comprises a diverse mixture of compounds, such as carbohydrates, amino acids, proteins and complex humic substances of undefined and highly changeable structure, ranging in size from simple monomers through to large biopolymers. Some of this material will be readily broken down by biological activity (biologically labile), whereas some of the other components of the DOM pool will only slowly be broken down and have a long residence time in the water column (biologically refractory). In marine systems, DOM is derived from excretion, as well as the death and lysis, of organisms ranging from bacteria through to whales, and as a result of inefficient feeding by grazers. Rivers can be a significant source of DOM in coastal waters, as is the case in the Arctic Ocean, which is under the influence of large riverine input. Most of the work to date in marine systems has focused on the dynamics of dissolved organic carbon (DOC) and dissolved organic nitrogen (DON), and to a lesser extent on the dynamics of dissolved organic phosphorus (DOP). Hansell and Carlson (2002) provide a comprehensive review of DOM research in the marine environment.

In the microbial network of sea ice, algae are sinks for dissolved inorganic nutrients, as discussed above, whereas the heterotrophic protozoans and metazoans are sources of dissolved organic and inorganic compounds via excretion (Chapters 7–9). Heterotrophic bacteria utilize inorganic nutrients and DOM as substrates for their growth and cell maintenance (respiration), competing with algae for inorganic nutrients depending on the elemental composition of the organic substrate available for bacterial growth. Heterotrophic bacteria also

release nutrients in order to maintain a steady state elemental composition. The degree of nutrient regeneration depends largely on the composition of the organic matter source to which the bacteria are exposed.

The obvious importance of DOM to the sea ice system has spawned a number of studies investigating this pool of organic compounds within the ice in recent years. This was spurred on by the realization that the production and transformation of DOM would be central to the biogeochemical cycling within the ice and that large amounts of DOM were needed to mediate the observed ecology of algae, bacteria and protozoans within the ice (Gleitz et al., 1996a; Grossmann et al., 1996; Günther et al., 1999). Thus, there has been a concerted effort to measure the DOC and, to a lesser extent, the DON content within the sea ice in both the Antarctic (Thomas et al., 1998; Herborg et al., 2001; Thomas et al., 2001a,b; Carlson & Hansell, 2003; Papadimitriou et al., 2007) and the Arctic (Thomas et al., 1995; Smith et al., 1997b; Amon et al., 2001; Krembs et al., 2002; Junge et al., 2004; Riedel et al., 2008). It has been shown experimentally that DOM incorporated from the sea water into a growing sea ice matrix behaves conservatively during sea ice formation and is released from the ice following similar dynamics as inorganic salts and dissolved gases (Giannelli et al., 2001; Amon, 2004). Low concentrations of DOC in first-year sea ice compared to surface oceanic water in winter in the Arctic have been interpreted in terms of exclusion of DOM during ice formation (Krell et al., 2003; C. Michel, unpublished data). Exclusion of DOM and coloured dissolved organic matter (CDOM) has been reported from freshwater lake ice in Canadian lakes and rivers, with specific retention of low molecular weight molecules in the ice (Belzile et al., 2002).

Despite the loss of DOM from the sea ice during formation via brine expulsion, many field investigations have shown significant accumulation of DOM within the ice, with DOC concentrations up to 280 mg Cl^{-1}, 450-fold greater than in surface oceanic water (Smith et al., 1997b; Thomas et al., 2001b; Riedel et al., 2008; Carlson & Hansell, 2003). The high concentrations of DOC in sea ice are often associated with the highest standing stocks of organisms. Strong correlations between DOC with proxies for ice algal biomass (Chl *a* and POC) have been observed during the spring ice algal bloom in the Arctic (Bunch & Harland, 1990; Smith et al., 1997b; Riedel et al., 2008), indicating an algal origin for sea ice DOC. There are, however, other instances of a poor correlation between DOM and chlorophyll or particulate material, while high DOM concentrations have been found on occasions in the absence of living ice organisms, suggesting that it could be a remnant of past biological activity (Thomas et al., 2001a; Krell et al., 2003).

The few published studies that have measured both the DOC and the DON components of the DOM pool in first-year sea ice report variable DOC to DON ratios, ranging from 3 to 50 (Thomas et al., 2001a,b; Krell et al., 2003; Papadimitriou et al., 2007). High DOC to DON ratios in Arctic multi-year ice have been attributed to an uncoupling of the carbon and nitrogen metabolism, such that a nitrogen-rich pool of amino acids would be hydrolysed and utilized faster than carbon-rich polysaccharide pools (Thomas et al., 1995). Guglielmo et al. (2000) have also shown preferential turnover of nitrogen-enriched organic matter in Antarctic sea ice, estimating potential utilization of the entire protein pool within 3 h in comparison with up to 102 h for the complete utilization of the carbohydrate pool in the studied sea ice system. Arrigo et al. (1995) showed that amino acids and sugars accumulated in platelet layers, although the reported concentrations were at sub-millimolar level, which is very low compared with the levels of DOC and DON reported above. The work of Herborg

et al. (2001) indicates that up to 99% of the DOC pool can be composed of carbohydrates, with the majority of this being mono- rather than poly-carbohydrates. Amon et al. (2001) showed that DOM from Arctic ice samples was characterized by a high neutral sugar and amino acid content, with a dominance of glucose and glutamic acid, which pointed to fresh DOM presumed to be produced by ice algae. Calace et al. (2001) found a large accumulation of DOM in Antarctic sea ice and refered to the ice acting as 'an organic matter tank', with elevated content of proteinaceous material, carbohydrates and humic substances, the latter suggesting active humification of algal-derived DOM *in situ*. Humic substances have largely undefined chemical structure but are generally thought to be biologically refractory.

Accumulation of DOM in sea ice indicates that there is an uncoupling between production and consumption or loss. Pomeroy and Wiebe (2001) concluded that a reduced substrate affinity of bacteria (as discussed above for nutrient uptake) at low temperatures may be responsible for the uncoupling, resulting in poor exploitation of the high concentrations of available organic compounds in the ice. However, recent observations from Arctic sea ice revealed the presence of active bacteria, mainly attached to particles and surfaces, at temperatures as low as –20°C (Junge et al., 2004). It was found that, contrary to expectations of metabolic inhibition at these low temperatures, the proportion of active bacteria did not decrease with decreasing temperatures. Riedel et al. (2008) found that the bacterial carbon requirement accounted for <5% of the net accumulation rate of DOC during the algal bloom in Arctic first-year ice. Direct utilization of DOC by heterotrophic flagellates can also take place in sea ice, channelling a small fraction of DOM to grazers (Vézina et al., 1997). The accumulation of DOC during the spring ice algal bloom in bottom ice layers makes this pool of carbon readily available for export to the water column at the time of ice melt. The DOM derived from sea ice, either upon ice melt, or through exchange between ice and sea water, has been considered to be an important source of organic matter for stimulating microbial activity in the under-ice oceanic waters (Kähler et al., 1997; Krembs & Engel, 2001). Due to large dilution, it is likely that this will only be pertinent to the oceanic waters very close to the ice, or where stabilized melt water lenses persist for some time (Krembs & Engel, 2001).

There is great potential for photochemical reactions to take place within sea ice floes. Belzile et al. (2000) showed a strong absorption of UV radiation in Arctic sea ice by DOM and concluded that significant photochemical reactions could occur. Sea ice is an effective barrier to UV radiation and, thus, photochemical modification of the DOM pool is likely to be important near the ice surface. Photochemical reactions have the potential to change the chemical characteristics and biological lability of the DOM pool (Mopper et al., 1991; Kieber & Mopper, 1996). Photochemical effects are dependent on the nature of the DOM before exposure to UV radiation (Tranvik & Kokalj, 1998). Thomas and Lara (1995) found that an Antarctic diatom-derived DOM pool was resistant to photodegradation. Obernosterer et al. (1999) have shown that freshly released labile DOM might be rendered more biologically refractory by photochemical reactions, whereas the bioavailability of refractory DOM can be actually enhanced upon exposure to solar radiation. More recently, photooxidation of DOC into carbon monoxide (CO) has been shown to occur in sea ice, with CO concentrations more than one order of magnitude higher than those in underlying waters increasing rapidly in the bottom, alga-rich ice layer (Xie & Gosselin, 2005). These results suggest that substantial photooxidation of organic matter can take place in sea ice, with consequences for the cycling of carbon in ice-covered seas.

Gel-like organic substances in sea ice

Over the past decade, it has become unambiguously clear that polymer gels play a profound role in marine systems, as they are integral to microbial food webs, biogeochemical cycling of carbon and other elements and particle dynamics in the oceans. The widespread abundance of gel-like substances in the ocean has challenged the traditional separation of organic matter into a dissolved and particulate pool. Evidence of the spontaneous assembly of DOM into polymer gels (Chin et al., 1998) has provided new insights into the transfer of dissolved material to the particulate pool, highlighting alternative pathways in carbon cycling in the ocean. Marine gels span over a size spectrum ranging from colloids in the size range of one nanometre to macro-gels several micrometres in size, which are actually POM (Verdugo et al., 2004). The term exopolymeric substances (EPS) is used to refer to high molecular weight polymers produced primarily by bacteria and algae in marine and benthic environments (Decho, 2000; Passow, 2002). The term transparent exopolymeric particles (TEP) originally refers to particle-size gels (also called gel-like particles) formed from precursors in the dissolved pool and containing acidic polysaccharides, which can be stained with Alcian Blue (Passow & Alldredge, 1995). Gels can undergo reversible phase transitions from condensed to hydrated phases with changes of pH, temperature and ionic conditions (Li & Tanaka, 1992; Chin et al., 1998). These phase transitions can drastically change the physico-chemical properties of the gels, e.g. their size, dielectric properties, chemical reactivity and permeability (Li & Tanaka, 1992), and, therefore, their role in biological processes and interactions.

All polymers released by bacteria and algae are hydrocolloids that can hold a large amount of water and can form gels, aided by the presence of cations such as K^+, H^+ and Ca^+ (Verdugo et al., 2004). Large amounts of EPS can be produced by benthic diatoms (Smith & Underwood, 1998) and phytoplankton, especially at the end of blooms, when cells are nutrient-limited (Corzo et al., 2000; Engel et al., 2002). The role of EPS in microbial food webs is diverse. EPS aid in cell locomotion and protect the cell against harsh environmental conditions (Cooksey & Wigglesworth-Cooksey, 1995). Also, they can provide a carbon-rich substrate and defence against grazing, while, importantly, they can create microhabitats which influence microbial processes and nutrient cycling (Simon et al., 2002; Mari & Rassoulzadgan, 2004). These microhabitats, where bacterial attachment is favoured by the sticky EPS surfaces, are sites of intense bacterial activity and increased bacteria-mediated processes.

It is only recently that attention has been given to the presence and role of gels in sea ice. The terms TEP (Krembs & Engel, 2001), EPS (Krembs et al., 2002; Meiners et al., 2003; Riedel et al., 2006, 2007a) and exopolymer particles (EP; Meiners et al., 2004, 2008) have all been used to describe gels present in sea ice (reviewed by Krembs & Deming, 2008; Chapter 7). High concentrations of EPS have been measured in Arctic sea ice throughout the year (Krembs et al., 2001b, 2002; Meiners et al., 2003, 2008; Riedel et al., 2006, 2007a). The highest EPS concentrations were measured in bottom first-year sea ice during the ice algal bloom, with EPS-carbon values up to 6.6 mg l^{-1}, two orders of magnitude higher than in the underlying oceanic water (Riedel et al., 2006). The high EPS concentrations in sea ice have been linked to production by sea ice diatoms (Krembs & Engel, 2001; Krembs et al., 2002; Meiners et al., 2003, 2008; Riedel et al., 2006, 2008), whereas bacteria were not found to be significant producers of EPS in sea ice (Riedel et al., 2006). Note that even if the EPS produced by bacteria do not constitute a large proportion of the EPS found in sea ice, it can significantly influence bacterial processes and dynamics. Hahn et al. (2004) have shown

that production of an exopolymer matrix by colony-forming bacteria serves as a protection against protistan grazing. A similar mechanism may be found to hold in sea ice, supported by genomic evidence of the ability of sea ice bacteria to produce exopolymers (Methé et al., 2005) and by studies indicating that heterotrophic grazing does not control bacterial biomass in sea ice (Gowing et al., 2004).

Very little is known about the characteristics of Coomassie stained particles (Long and Azam, 1996) and other potential micro- and macro-gels (Kerner et al., 2003) in sea ice. While sea ice studies have quantified gels using the Alcian Blue method, which originally identifies TEP, recent studies have used the terms EP and EPS for gels found in sea ice in recognition that the formation processes of exopolymers are largely unknown in sea ice and that sea ice exopolymers are predominantly produced by diatoms (Meiners et al., 2003, 2008; Mancuso Nichols et al., 2004; Riedel et al., 2006). However, although field or laboratory evidence is still lacking, we surmise that exopolymer phase transitions may take place in sea ice. The role of ions in determining the structure and properties of gels is an important aspect to consider with respect to exopolymer phase transitions in the sea ice. Strong correlations between DOC and EPS have been found in sea ice (Krembs et al., 2002; Meiners et al., 2004; Riedel et al., 2008), indicating a tight coupling between these two carbon pools. In addition, strong correlations between algal biomass, DOC and EPS-carbon indicate that DOC and EPS of algal origin can undergo reversible phase transitions between the polymer gel and dissolved matter pools (Riedel et al., 2008). DOC produced by diatoms, especially diatom species with benthic life history, has been found to adhere to filters and to be retained in the particulate pool (Wetz & Wheeler, 2007). Such finding is particularly relevant to those sea ice communities which are dominated by benthic diatom species in spring. Altogether, these findings challenge our current understanding of organic matter pools in the sea ice. In an environment defined by microscale heterogeneity in physical and chemical conditions in the brine channel network and sudden changes associated with specific periods or events (e.g. ice melt), polymer phase transitions are likely to be an integral part of organic matter cycling and microbial dynamics.

EPS are an important carbon pool in sea ice, contributing as much as 72% of the total POC at the end of the ice algal bloom. They also are an essential and fundamental component of microbial food webs in sea ice and play a key role in structuring sea ice microbial assemblages (Krembs & Deming, 2008). EPS influence biogeochemical cycling in sea ice through various processes, such as cryogenic protection against harsh conditions in brine channels (Krembs et al., 2002), acting as a substrate for bacterial colonization and a carbon-rich source for grazers (Meiners et al., 2004; Riedel et al., 2006, 2007b), as well as for incorporation of cells into the ice matrix during ice formation and nutrient remineralisation (Riedel et al., 2007a). By means of non-invasive microscope techniques, it was shown that diatoms in the ice are often within EPS-filled pockets or channels (Krembs et al., 2002). It has been suggested that the EPS surrounding algal cells would allow them to adhere to ice crystals. The presence of high EPS within the ice also alters the viscosity of the brine and its properties with respect to diffusive transport of ions and gases. The consequences for bacterial–algal interactions, as well as effects on hindering efficient feeding by algal and bacterial grazers can be profound. Recent studies have shown that EPS facilitates bacterial attachment to particles and increases bacterial activity (Meiners et al., 2004; Junge et al., 2004; Riedel et al., 2006), and that high EPS concentrations in sea ice may interfere with grazing by heterotrophic protists (Riedel et al., 2007b). EPS may also play a role in the cycling of contaminants in sea ice and ice-associated fauna as it has been shown that EPS-coated silica

sorbed more cadmium than non-coated silica, and that this effect was increased at low salinity (Schlekat et al., 1999). Production of EPS coupled with the narrow channel space might also help explain the apparent breakdown of the classic microbial loop in the sea ice matrix and the high accumulation of DOM.

Over the annual cycle of ice formation and decay, ice-associated EPS can play various roles. EPS have been found to be enriched in newly formed sea ice compared to surface oceanic waters, with EPS enrichment correlated with the enrichment of large autotrophs (Riedel et al., 2007a). These authors suggested that the presence of EPS enhanced the incorporation of large cells in the newly formed ice matrix in line with the view that cell stickiness can influence cell selectivity during sea ice formation (Gradinger & Ikävako, 1998). Furthermore, ammonium regeneration was strongly correlated with EPS concentrations in newly formed sea ice, suggesting that EPS enhanced the regeneration of ammonium by acting as a carbon source for sea ice heterotrophs. During spring melt, a rapid increase has been observed in the EPS to Chl *a* and the EPS-carbon to POC ratios in bottom Arctic sea ice, suggesting that a substantial part of the EPS remained in the ice matrix while the POM (dominated by ice algae) was released into the surface oceanic waters (Riedel et al., 2006; Juul-Pedersen et al., 2008). The preferential retention of EPS in the sea ice matrix relative to POM has various implications for food web dynamics and the biochemical and physical processes in the ice and surface waters. For example, in the ice, the presence of EPS can continue to support the high bacterial activity typically found at the end of ice algal blooms, and can also modify optical and physical properties of the ice, thus influencing radiative and thermal transfer, as well as ablation. In surface waters, a delayed input of exopolymeric organic material from the sea ice would sustain microbial food webs for an extended period, possibly bridging the gap between the ice algal bloom release into the surface oceanic waters and the phytoplankton bloom. As EPS might be a vector for contaminant cycling due to their sorptive properties (Schlekat et al., 1999; Bhaskar & Bhosle, 2006), their behaviour and incorporation by grazers in surface waters will influence bioaccumulation along marine food chains.

12.4 Stable carbon isotopes in sea ice

The measurement of the ratio of the stable carbon isotopes (R = ^{13}C:^{12}C) at their natural abundance level has been used as a tool to trace metabolic processes. The stable carbon isotope ratio is commonly reported on a per mil basis in the δ notation relative to the international standard Vienna Pee Dee Belemnite (VPDB) as $\delta^{13}C$ = 1000 [(R/R_{VPDB}) − 1]. A negative $\delta^{13}C$ value indicates ^{13}C depletion, with positive values indicating the reverse. Photosynthetic carbon assimilation proceeds with slower reaction kinetics for ^{13}C than ^{12}C resulting in a measurable isotope effect (ε), defined as the isotopic difference between substrate (CO_2) and product (POC). As a result, the produced biomass becomes enriched in ^{12}C, and the residual ΣCO_2 pool can become enriched in ^{13}C in closed or semi-closed systems. The largest contribution to the isotopic effect during photosynthetic carbon assimilation into biomass occurs at the RUBISCO site within the cell (Fogel & Cifuentes, 1993). The isotope effect attributable to RUBISCO (ε_R) is −27‰ in photosynthetic algae (Burkhardt et al., 1999). In other words, the RUBISCO effect, when it is fully expressed, will result in a $\delta^{13}C$ of the photosynthetically produced organic carbon (hereafter, $\delta^{13}C_{POC}$) that is more enriched in ^{12}C (i.e. isotopically lighter) than the CO_2 available for assimilation at the intracellular site of

enzymatic assimilation by an amount equivalent to ε_R. A large isotope effect can be observed during growth in CO_2-replete conditions. However, the biological isotope fractionation during photosynthesis and, hence, the final $\delta^{13}C_{POC}$ are a complex function of a number of factors, such as the concentration of extracellular $CO_2(aq)$, the type of carboxylating enzyme, induction of active dissolved inorganic carbon transport into the cell, growth rate and cell size and geometry (Popp et al., 1998; Burkhardt et al., 1999; Cassar et al., 2006). The above factors conspire to reduce the isotope effect during photosynthesis to values close to 0‰ on occasions, when the $\delta^{13}C_{POC}$ essentially reflects the isotopic composition of the substrate (CO_2). This can occur in extracellular CO_2-limiting conditions, such as those imposed by high growth rates and, hence, high intracellular CO_2 demand. By comparison, the isotope effect during biological respiration is minimal, with the CO_2 produced during this process having the same stable isotope ratio as that of the bulk organic carbon respired.

The restricted CO_2 exchange with the external sea water combined with high rates of algal growth in spring results in dramatic reduction of the ΣCO_2 concentration in brine pockets in sea ice. This is likely to be compounded by the initial expulsion of CO_2 during the consolidation of the ice as discussed above. Due to sampling constraints, there have been only very few coupled measurements of the concentration and the stable isotopic composition of the internal pool of total dissolved inorganic carbon in sea ice brines (Papadimitriou et al., 2007). The most comprehensive study to date, in which such measurements have been made on samples from surface ponds and gap waters from freeboard layers, showed that variations in the $\delta^{13}C$ of the ΣCO_2 pool were commensurate with the changes predicted from nitrate deficits caused by algal growth (Kennedy et al., 2002). Overall, the existing field and laboratory observations indicate coupling of depleted concentration with ^{13}C enrichment of the ΣCO_2 pool in sea ice, indicative of the photosynthetic isotope effect (Gleitz et al., 1996a; Gibson et al., 1999; Thomas et al., 2001a; Kennedy et al., 2002; Papadimitriou et al., 2007). In general, the $\delta^{13}C_{POC}$ in open oceanic waters from polar latitudes ranges from -20‰ to -30‰ (Schubert & Calvert, 2001; Kennedy et al., 2002). In contrast, $\delta^{13}C_{POC}$ values up to -8‰ have been measured in samples from sea ice habitats, consistent with the hypothesis that these samples represent algal populations that grew in a CO_2-limiting environment (Fischer, 1991; Rau et al., 1991; Dunbar & Leventer, 1992; McMinn et al., 1999; Thomas et al., 2001b; Schubert & Calvert, 2001; Kennedy et al., 2002; Arrigo et al., 2003). Several of these studies concluded that high algal biomass with the most ^{13}C-enriched values occurred in the sea ice habitats with maximal degree of limitation of CO_2 exchange with the external sea water. However, the work of Kennedy et al. (2002) has shown that some of the highest algal standing stocks in sea ice are associated with semi-closed rather than closed systems, such that replenishment of nutrients, in particular dissolved inorganic carbon and nitrate, is possible. This means that the link between inorganic carbon limitation and increased values of $\delta^{13}C_{POC}$ in sea ice habitats is far from being satisfactorily addressed at the present time. The implications of the stable carbon isotope composition of sea ice diatoms and their ^{13}C enrichment as a sedimentary proxy for past CO_2 concentrations in surface waters and sea ice distribution is discussed in Chapter 13.

12.5 Arctic river inputs into sea ice

The Southern Ocean is largely cut off from terrestrial influence, except for limited aerial deposition. In contrast, the Arctic Basin is characterized by a high input of fresh water – almost

10% of global river discharge – from many large river systems such as the Ob', Lena, Yenisey, MacKenzie and Yukon (Anderson, 2001; Holmes et al., 2001; Anderson, 2002). This translates into high riverine discharge of suspended solids, DOM and dissolved inorganic nutrients (Kattner et al., 1999; Holmes et al., 2001; Anderson, 2002; Amon, 2004), and naturally these are incorporated into sea ice formed in the coastal regions of freshwater influence. These rivers also convey pollutants to the Arctic Ocean, such as PCBs and heavy metals, which will be absent from the Southern Ocean. As a result of such large amounts of freshwater input, much of the surface waters of the Kara, Laptev, East Siberian and Beaufort Sea shelves in the Arctic Ocean exhibit low salinity. Estimates of riverine total organic carbon (TOC) fluxes into the Arctic Ocean reveal that, for the Eurasian Arctic only, DOC represents 75% of the 25.7×10^6 t y^{-1} TOC discharge (Rachod et al., 2004). Recent studies indicate that slightly more than 50% of the terrestrial DOM carried onto the Beaufort Sea shelf (western Canadian Arctic) is subject to degradation (Hansell et al., 2004) and that ~3% of the DOC carried by the Mackenzie river onto that same shelf is photomineralized (Bélanger et al., 2006). Lara et al. (1998), Kattner et al. (1999), Lobbes et al. (2000) and Amon (2004) measured the organic matter at the mouths of Arctic rivers and have concluded that much of the DOM is soil-derived material with a high degree of degradation. The DOC and DON inputs are very large, with concentrations up to 1000 μmol l^{-1} and 30 μmol l^{-1}, respectively, in the freshwater discharge. Furthermore, during the process of sea ice formation DOM will be rejected from the growing ice (Giannelli et al., 2001) and Amon (2004) calculates that just by this process alone there may be up to a 0.52 Tg carbon enrichment of DOC into the Kara Sea.

Much of this organic material will be biologically refractory (Amon & Benner, 2003) and, therefore, available to be transported long distances through transarctic drift. The chemical composition of the particulate and dissolved lignin phenols, which are exclusively of terrestrial origin, in river discharge waters of 12 Russian rivers is significantly correlated with the proportion of tundra and taiga in the drainage areas. The contribution of lignin to the overall carbon flux from Russian rivers is only 0.3% of the total carbon export but is a useful tracer for organic matter fluxes from tundra and taiga regions (Lobbes et al., 2000). Anderson (2002) gives a more comprehensive discussion of the processes controlling DOC in the Arctic Ocean.

Arctic ice formed in coastal areas can be heavily laden with sediments, which can be transported large distances in the moving ice fields carried by transpolar currents (Chapter 4). Even allochthonous material, such as tree trunks and soil turfs, becomes encased in Arctic ice floes, eventually being released many thousands of kilometres from the place it was initially caught up in the ice. Although the dynamics of freshwater input into the Arctic significantly influence large-scale sea ice formation processes, it is unclear how the high organic matter and nutrient loading of the riverine run-off influences the biogeochemical processes in the ice. Little is known about the biogeochemical processes in ice formed in areas subjected to large river discharge, especially the influence of riverine discharge during ice formation, the effects of river plumes under the ice and the seasonal flooding of ice sheets with terrestrially derived organic and inorganic nutrient-rich waters. In general, it can be conceived that Arctic sea ice has a far greater potential for carbon loading than ice in the Antarctic. Of course, the Arctic Ocean is not the only ice-covered region that is influenced by significant freshwater inputs. The Baltic Sea is also a semi-enclosed water body receiving large riverine discharge, and Hudson Bay is a large inland sea which receives a cumulative annual discharge of about

700 km^3 from a large number of rivers (Prinsenberg, 1986; Dery et al., 2005) and is completely ice-covered in winter. Many of the biogeochemical processes occurring in the ice formed in weakly saline Arctic coastal waters will be pertinent to the ice formed in the low salinity waters of the Baltic and in coastal areas of Hudson Bay and other ice-covered inland seas.

12.6 Data collection and *in situ* measurements: some challenges

One of the greatest difficulties in the measurement of dissolved gases and realistic pH values within sea ice, especially in brines, is the collection of undisturbed samples. While this limitation also applies to the study of microbial processes, such as bacterial activity, which are likely to change rapidly in disturbed samples, the potential bias is especially important for dissolved gases which will equilibrate with ambient conditions. Total gas content of the ice is relatively easy to sample, since the total gas can be trapped from disrupted whole pieces of ice (Tison et al., 2002). However, the *in situ* chemistry of brines and different phases of ice is not so straightforward.

Brine collection

To date, most of the chemical analyses in the sea ice are performed on bulk melted ice core sections and brines collected by centrifugation or by drainage into 'sack holes' cored into the ice. In the latter, the ice is partially cored to leave a core hole in its surface. When this is done carefully to a depth in the ice that ensures that sea water from below does not enter the hole, brine drains from the surrounding ice into the hole and can be collected.

   Clearly, there are significant problems with each of these sampling strategies when looking at the biogeochemical composition (gas content, particles, dissolved materials) of the ice. Sack holes do not fill immediately, and in cold ice where brine volumes are small, it can take considerable time to collect enough solution for analyses. Therefore, during the accumulation of the brine, there is scope for changes in the brine chemistry by equilibration with the atmosphere. The brines collected in sack holes derive from an undefined area of the surrounding ice, representing a mixture of localized brine pockets. This, of course, can be viewed from a positive perspective as the method integrates the biogeochemical composition of sea ice brine over distances around the sack hole much larger than the size of individual brine pockets, thus facilitating general estimates and characterization of ice chemistry. However, the uncertainty regarding the origin of the collected brine within the ice column is also a downfall of the method. Furthermore, sack hole brine collection is hardly useful in very cold ice or in warm porous ice; only minimal brine drainage will occur in the former, whereas there is increased possibility for contamination with sea water in the latter.

   The centrifugation of ice cores at *in situ* temperatures has been a valuable addition to the methodologies for sampling sea ice brines (Weissenberger et al., 1992; Krembs et al., 2000, 2001a,b). Typically, the ice core is placed on the porous grid of a centrifuge bucket, and the brine drained during centrifugation is collected underneath the grid. When care is taken, and long enough centrifugation times are used, the percentage brine recovery can be high. However, the more efficient centrifugation times, the longer the time for gas equilibration in the collecting brines. In the same vein, this method is particularly unsuitable for measurements of the carbonate system and its isotopic composition in sea ice (Papadimitriou et al., 2004).

Melted sea ice samples

The slow melting of ice core sections at low temperature is by far the method employed most often to measure routinely the chemical and biological components of sea ice cores. Because organisms pass from a highly saline brine to a low salinity melted ice solution, there is loss of fragile organisms due to osmotic shock during the melting process (Garrison & Buck, 1986). For this reason, it is recommended to melt the sea ice samples in filtered sea water, usually collected at the time of sampling, for biological analyses. Considering the internal cellular pools within these organisms of the main nutrients and chemicals routinely measured by sea ice biogeochemists, the input of dissolved chemicals into the sample from cell disruption is often insignificant relative to the concentrations usually measured within sea ice (Thomas et al., 1998). It is only in the very highest biological standing stocks measured in sea ice that such artifacts will become a problem. This method maintains better the full spectrum of the biological assemblage but does not confer any advantage to the measurement of the dissolved chemical constituents and is inappropriate for the measurement of dissolved gases and the pH.

Microelectrodes and sea ice

Microelectrode technology is amongst the most sophisticated analytical tools to have been developed in aquatic sciences in the past 20 years. It has revolutionized the study of small-scale gradients of nutrients, gas, light, and pH in aquatic biofilms, sediments and across diffusion boundary layers. It was only natural that effort should be taken to utilize micro-electrodes for the study of biogeochemical processes in sea ice. This technology can generate highly pertinent measurements for describing the photosynthetic and respiratory dynamics in bottom ice communities, which are common features in both the Antarctic and the Arctic (McMinn & Ashworth, 1998; McMinn et al., 2000; Trenerry et al., 2001). To date only oxygen electrodes have been employed in sea ice studies, although it cannot be long until other electrodes are also used in conjunction with high resolution irradiance sensors. Most of the successful microelectrode studies in sea ice environments offered unparalleled insight into oxygen exchange at the ice–water interface through millimetre-scale micro-profiles (McMinn & Ashworth, 1998; Kühl et al., 2001; Rysgaard et al., 2001). However, the semi-solid sea ice matrix significantly restricts the use of these probes to the ice–water interface and porous ice, typically at best in the bottommost few centimetres of ice floes, where ice crystals are still loose, and electrode tips are not so easily damaged. Although such measurements are highly informative for the bottom ice communities, these assemblages are dominated by dissolved gas and inorganic nutrient regimes where exchange with the surrounding sea water is possible. They are not at all representative of those biological assemblages growing in the interior of ice floes and surface gap layers where exchange is limited to some degree or another.

Despite the rapid advances in micro-sensor technology in recent years, robust methodologies for measuring the *in situ* gas dynamics in the interior of the ice have remained illusive, which is frustrating since it is within closed or semi-enclosed parts of the ice that the greatest changes to the sea ice chemistry will take place. The microelectrode studies to date in sea ice have relied on deployment methodologies that are not well suited to the long term (weeks, months) under extreme field conditions. This is because the electrodes are fragile and inflexible, a major problem in a dynamic ice matrix. Oxygen microelectrodes also consume

oxygen, a methodological hindrance when measuring the O_2 dynamics in confined spaces. Finally, microelectrodes also measure the partial pressure of O_2, and so changes in temperature and salinity affect the sensor signal even when the O_2 concentration remains constant (Glud et al., 2002). Recent developments in micro-optode design have allowed the freezing of optode arrays into ice as it forms (Mock et al., 2002). These optical fibre–based sensors proved robust enough to withstand being frozen into the ice, can be temperature and salinity compensated for and do not consume O_2. Therefore, they overcome many of the methodological constraints imposed by the 'traditional' microelectrodes. Microscopic analysis of the optode tips in the ice showed that they remained in brine pockets within the ice, and were able to record realistic changes in dissolved O_2 over several weeks of deployment in a growing ice sheet (Mock et al., 2002). Oxygen micro-profiles at the sea–ice interface revealed DBL which varied significantly in thickness, which is related to a small-scale horizontal variability. The small-scale patchiness of algae and the differences in DBL thickness seem to be caused by physico-chemical processes (e.g. turbulence, water flow velocity), which in turn were influenced by ice lamellar structure at the ice–water interface (Mock et al., 2003). Sensor measurements in a sea ice microcosm over 24 h (continuous illumination) directly in one brine channel of the ice–water interface at $-3°C$ indicated a highly dynamic flux of dissolved oxygen, which was possibly related to activity changes of the diatom community and/or morphological changes of the brine channel (Mock et al., 2003). As further optical sensors are developed, it can be envisioned that these will be the 'next step' in elucidating dissolved gas dynamics in the sea ice matrix.

12.7 Future perspectives

The study of sea ice biogeochemistry has largely evolved from the study of sea ice ecology and in particular the extensive investigations devoted to the understanding of photosynthesis within the ice (Chapter 8). A major focus of the ecological studies was sea ice microbial dynamics (Chapters 7–9), with sea ice algal growth being central to these studies. Because of these research roots, the progress in our understanding has largely been led by a desire to understand the biology of sea ice. It is only in recent years that the chemical processes dominant within sea ice have been considered in 'their own right'.

Ice tank facilities

In reviewing the subject, it is evident that our understanding of 'geochemical' processes within sea ice remains limited. One of the main reasons for this is that studies of abiotic sea ice are limited and can only take place in facilities that allow the formation of realistic sea ice in laboratory conditions. This is not a trivial task and involves considerable logistical costs and difficulties. Recently, the adaptation of large-scale ice tank facilities, such as those at the Ship Model Basin in Hamburg, Germany (www.hsva.de), have gone far to address this issue (Eicken et al., 1998; Haas et al., 1999; Giannelli et al., 2001; Tison et al., 2002; Papadimitriou et al., 2004). As our experience with such facilities grows, much will be learnt about the fundamental changes in sea ice chemistry, which are often masked by the effects of biology in sea ice sampled in the field. There has also been some success in introducing biology into these 'artificial' sea ice systems (Weissenberger, 1998; Krembs et al., 2001a;

Mock et al., 2002) to produce experiments in which the biology can be investigated under controlled abiotic conditions. Similar large-scale mesocosms will make it much easier for biogeochemists in the future to unravel the complexity of biological and chemical processes taking place in the ice.

Variability and the problem of scale

It is likely that microelectrodes and optodes will be more often deployed during studies to measure nutrient and gas fluxes in sea ice, especially at the ice–water interface. Such technology gives highly defined measurements on scales (micrometre) that are relative to the organisms living within the sea ice brine channel system. These are important findings, of course, but present problems in scaling up the findings to consider processes on the scale of tens of metres. The sea ice habitat is notoriously patchy, and the variability of both chemical and biological parameters is a problem that vexes the establishment of general paradigms being formed within sea ice biogeochemistry. More and more sophisticated technology is being developed to examine microscale processes within sea ice (Krembs & Deming, 2008; Chapter 15). It is important that future studies that use such techniques also employ resources and time to find ways of extrapolating small-scale dynamic events to larger, and arguably, ecologically more important scales.

The biochemical characterization of the DOM pools within sea ice is a major requirement for our understanding of the biogeochemistry of sea ice. To date, we know very little about what actually makes up the DOM and how biologically labile this material is in sea ice. In addition, there is much need to characterize the enzyme and bacterial activities that control the turnover of this material. In particular, the biochemical basis of reduced substrate affinity of sea ice organisms needs to be further linked to measurements of organic and inorganic nutrient pools within the ice (Pomeroy & Wiebe, 2001). For these studies to be successful, there is a pressing need for the study of sea ice biogeochemistry to move forward and harness biochemical and molecular techniques that are now routinely used for the study of biogeochemistry of comparable marine systems such as sediments and biofilms.

Our understanding of the role and dynamics of gel-like substances in the sea ice may still be at its infancy, but their potential to alter physical–chemical conditions in brine channels and of their significance for biochemical and microbial processes has been recognized in recent sea ice studies. There is need to develop innovative biogeochemical approaches in sea ice research as our conceptual thinking of nutrient and gas exchange within the brine channel system needs to be revisited in terms of the presence of heterogeneous microsites, organic biofilms and potential phase transitions in the organic matter pool. The general concepts already developed from biofilm studies in aquatic microbiology and the effect of EPS on the permeability and solute transport in other porous media, especially sediments, are also highly pertinent to future sea ice studies (Meyer-Reil, 1994; Decho, 1990, 2000).

Time-series measurements

Of paramount need is the study of the changes in biogeochemistry within growing ice sheets with dynamic biological assemblages, where succession of species and organism type develops in step with changes in the physical–chemical characteristics of the ice. Time-series type of measurements is one of the main positive aspects of mesocosm or abiotic ice tank

experiments. The only way that such measurements will happen in natural sea ice systems will be logistically difficult long-term field campaigns, either from land-based stations or during drift experiments with research ships, such as the 2004 ISPOL experiment in the western Weddell Sea (Papadimitriou et al., 2007; Haas et al., 2008; Hellmer et al., 2008; Lannuzel et al., 2008; Tison et al., 2008). Most of the biogeochemical measurements we have to date come from 'spot samples' of sea ice. It is impossible to separate the 'historical' chemical signature of developing ice from the present composition of the biological assemblage in the sample. The adoption of stable isotope methodologies can go part of the way to divulging such historical processes during the evolution of a piece of ice, but far more will be learnt from actually being able to follow these processes as they take place.

It is highly pertinent that future sea ice studies concentrate on defining what type of physical–chemical system is encountered by the organisms recruited in sea ice. Up to now, we have considered the sea ice matrix as a labyrinthine network of brine-filled channels and pores, containing attached and free organisms. We may have to rethink this perspective and to rather consider biofilms on the surfaces of pores and channels, and viscous gel-filled spaces, in which organisms are embedded as opposed to simply being suspended within a liquid brine.

Acknowledgements

References

Ackley, S.F. & Sullivan, C.W. (1994) Physical controls on the development and characteristics of Antarctic sea ice biological communities – a review and synthesis. *Deep-Sea Research Part I*, **41**, 1583–1604.

Ackley, S.F., Lewis, M.J., Fritsen, C.H. & Xie, H. (2008) Internal melting in Antarctic sea ice: development of 'gap layers'. *Geophysical Research Letters*, **35**, L11503, 10.1029/2008GL033644.

Amon, R.M.W. (2004) The role of dissolved organic matter for the organic carbon cycle in the Arctic Ocean. In: *The Organic Carbon Cycle in the Arctic Ocean*. (Eds. R. Sten & R.W. Macdonald), pp. 83–99. Springer Verlag, Berlin.

Amon, R.M.W. & Benner, R. (2003) Combined neutral sugars as indicators of the diagenic state of dissolved organic matter in the Arctic Ocean. *Deep-Sea Research Part I*, **50**, 151–169.

Amon, R.M.W., Fitznar, H.P. & Benner, R. (2001) Linkages among the bioreactivity, chemical composition, and diagenetic state of marine dissolved organic matter. *Limnology and Oceanography*, **46**, 287–297.

Anderson, L.G. (2001) Chemical oceanography in polar oceans. In: *Physics of Ice-covered Seas*, Vol. 2 (Ed. M. Leppäranta), pp. 787–810. Helsinki University Press, Helsinki, Finland.

Anderson, L.G. (2002) DOC in the Arctic Ocean. In: *Biogeochemistry of Marine Dissolved Organic Matter* (Eds. D.A. Hansell & C.A. Carlson), pp. 665–683. Academic Press, San Diego.

Arrigo, K.R. & Thomas, D.N. (2004) Large scale importance of sea ice biology in the Southern Ocean. *Antarctic Science*, **16**, 471–486.

Arrigo, K.R., Dieckmann, G.S., Gosselin, M., Robinson, D.H., Fritsen, C.H. & Sullivan, C.W. (1995) High resolution study of the platelet ice ecosystem in McMurdo Sound, Antarctica – biomass, nutrient, and production profiles within a dense microalgal bloom. *Marine Ecology Progress Series*, **127**, 255–268.

Arrigo, K.R., Robinson, D.H., Worthern, D.L. et al. (1999) Phytoplankton community structure and the drawdown of nutrients and CO_2 in the Southern Ocean. *Science*, **283**, 365–367.

Arrigo, K.R., Robinson, D.H, Dunbar, R.B., Leventer, A.R. & Lizotte, M.P. (2003) Physical control of Chlorophyll *a*, POC and TPN distributions in the pack ice of the Ross Sea, Antarctica. *Journal of Geophyical Research*, **108** (**C10**), 3316, 10.1029/2001JC001138.

Assur, A. (1960) Composition of sea ice and its tensile strength. *SIPRE Research Report*, **44**.

Barkan, E., Luz, B. & Lazar, B. (2001) Dynamics of the carbon dioxide system in the Dead Sea. *Geochimica et Cosmochimica Acta*, **65**, 355–368.

Bélanger, S., Xie, H., Krotkov, N., Larouche, P., Vincent, W.F. & Babin, M. (2006) Photomineralization of terrigenous dissolved organic matter in Arctic coastal waters from 1979 to 2003: internannual variability and implications of climate change. *Global Biogeochemical Cycles* 20, GB4005, 10.1029/2006GB002708.

Belzile, C., Johannessen, S.C., Gosselin, M., Demers, S. & Miller, W.L. (2000) Ultraviolet attenuation by dissolved and particulate constituents of first-year ice during late spring in an Arctic polynya. *Limnology and Oceanography*, **46**, 1265–1273.

Belzile, C., Gibson, J.A.E. & Vincent, W.F. (2002) Colored dissolved organic matter and dissolved organic carbon exclusion from lake ice: implications for irradiance transmission and carbon cycling. *Limnology and Oceanography*, **47**, 1283–1293.

Berner, R.A. (1980) *Early Diagenesis: A Theoretical Approach*. Princeton University Press, Princeton, NJ.

Bhaskar, P.V. & Bhosle, N.B. (2006) Bacterial extracellular polymeric susbtance (EPS): a carrier of heavy metals in the marine food-chain. *Environment International*, **32**, 191–198.

Bischoff J.L., Fitzpatrick, J.A. & Rosenbauer, R.J. (1993) The solubility and stabilization of ikaite ($CaCO_3 \cdot 6H_2O$) from 0°C to 25°C: environmental and paleoclimatic implications for thinolite tufa. *Journal of Geology*, **101**, 21–33.

Brzezinski, M.A., Olson R.J. & Chisholm, S.W. (1990) Silicon availability and cell-cycle progression in marine diatoms. *Marine Ecology Progress Series*, **67**, 83–96.

Buck, K.R., Bolt, P.A., Bentham, W.N. & Garrison, D.L. (1992) A dinoflagellate cyst from Antarctic sea ice. *Journal of Phycology*, **28**, 15–18.

Bunch, J.N. & Harland, R.C. (1990) Bacterial production in the bottom surface of sea ice in the Canadian subarctic. *Canadian Journal of Fisheries and Aquatic Science*, **47**, 1986–1995.

Burkhardt, S., Riebesell, U. & Zondervan, I. (1999) Effects of growth rate, CO_2 limitation and cell size on the stable carbon isotope fractionation in marine phytoplankton. *Geochimica et Cosmochimica Acta*, **63**, 3729–3741.

Calace, N., Castrovinci, D., Maresca, V., Petronio, B.M., Pietroletti, M. & Scardala, S. (2001) Aquatic humic substances in pack ice–seawater–sediment system. *International Journal of Environmental Analytical Chemistry*, **79**, 315–329.

Carlson, C.A. & Hansell, D.A. (2003) The contribution of DOM to the biogeochemistry of the Ross Sea. In: *Biogeochemical Cycles in the Ross Sea* (Eds. G. DiTullio & R. Dunbar), American Geophysical Union, Washington, DC. *Antarctic Research Series*, **78**, 123–142.

Cassar, N., Laws, E.A. & Popp, B.N. (2006) Carbon isotopic fractionation by the marine diatom *Phaeodactylum tricornutum* under nutrient- and light-limited growth. *Geochimica et Comsochimica Acta*, **70**, 5323–5335.

Chin, W.-C., Orellana, M.V. & Verdugo, P. (1998) Spontaneous assembly of marine dissolved organic matter into polymer gels. *Nature*, **391**, 568–572.

Chisholm, S.W., Azam, F. & Eppley, R.W. (1978) Silicic acid incorporation in marine diatoms on light: dark cycles: use of an assay for phased cell division. *Limnology and Oceanography*, **23**, 518–529.

Cooksey, K.E. & Wigglesworth-Cooksey, B. (1995) Adhesion of bacteria and diatoms to surfaces in the sea: a review. *Aquatic Microbial Ecology*, **9**, 87–96.

Corzo, A., Morillo, J.A. & Rodriguez, S. (2000) Production of transparent exopolymer particles (TEP) in cultures of *Chaeoceros calcitrans* under nitrogen limitation. *Aquatic Marine Ecology*, **23**, 63–72.

Cota, G.F., Prinsenberg, S.J., Bennett, E.B. et al. (1987) Nutrient fluxes during extented blooms of Arctic ice algae. *Journal of Geophysical Research*, **92** (C2), 1951–1962.

Cota, G.F., Anning, J.L., Harris, L.R., Harrison, W.G. & Smith, R.E.H. (1990) The impact of ice algae on inorganic nutrients in seawater and sea ice in Barrow Strait, NWT, Canada during spring. *Canadian Journal of Fisheries and Aquatic Sciences*, **47**, 1402–1515.

Curren, M.A.J., van Ommen, T.D., Morgan, V.I., Phillips, K.L. & Palmer, A.S. (2003) Ice core evidence for Antarctic sea ice decline since the 1950s. Science, **302**, 1203–1206.

Decho, A.W. (1990) Microbial exopolymer secretions in ocean environments – their roles in food webs and marine processes. *Oceanography and Marine Biology An Annual Review*, **28**, 73–153.

Decho, A.W. (2000) Microbial biofilms in intertidal systems: an overview. *Continental Shelf Research*, **20**, 1257–1273.

De La Rocha, C.L., Hutchins, D.A. & Brzezinski, M.A. (2000) Effects of iron and zinc deficiency on elemental composition and silica production by diatoms. *Marine Ecology Progress Series*, **195**, 71–79.

Dery, S.J., Stieglitz, M., McKenna, E.C. & Wood, E.F. (2005) Characteristics and trends of river discharge into Hudson, James, and Ungava Bays, 1964–2000. *Journal of Climate*, **18**, 2540–2557.

Dieckmann, G.S., Lange, M.A., Ackley, S.F. & Jennings, J.C., Jr (1991) The nutrient status in sea ice of the Weddell Sea during winter: effects of sea ice texture and algae, **11**, 449–456.

Dieckmann, G.S., Arrigo, K. & Sullivan, C.W. (1992) A high resolution sampler for nutrient and chlorophyll *a* profiles of the sea ice platelet layer and underlying water column below fast ice in Polar oceans: preliminary results. *Marine Ecology Progress Series*, **80**, 291–300.

Dieckmann, G.S., Nehrke, G., Papadimitriou, S. et al. (2008) Calcium carbonate as ikaite crystals in Antarctic sea ice. *Geophysical Research Letters*, **35**, L08501, 10.1029/2008GL033540.

Dickens, B. & Brown, W.E. (1970) The crystal structure of calcium hexahydrate at ~120°. *Inorganic Chemistry*, **9**, 480–486.

DiTullio, G., Garrison, D.L. & Mathot, S. (1998) Dimethylsulfoniopropionate in sea ice algae from the Ross Sea polynya. In: *Antarctic Sea Ice Biological Processes, Interactions and Variability* (Eds. M.P. Lizotte & K.R. Arrigo), American Geophysical Union, Washington, DC. *Antarctic Research Series*, **73**, 139–146.

DiTullio, G.R., Grebmeier, G.M., Arrigo, K.R. et al. (2000) Rapid and early export of *Phaeocystis Antarctica* blooms in the Ross Sea, Antarctica. *Nature*, **404**, 595–598.

Dixon D., Mayewski, P.A., Kaspari, S. et al. (2005) A 200 year sulfate record from 16 Antarctic ice cores and associations with Southern Ocean sea-ice extent. *Annals of Glaciology*, **41**, 155–166.

Dunbar, R.B. & Leventer, A. (1992) Seasonal variation in carbon isotopic composition of Antarctic sea ice and open water plankton communities. Antarctic *Journal of the United States*, **27**, 79–81.

Edwards, R., Sedwick, P.N., Morgan, V., Boutron, C.F. & Hong, S. (1998) Iron in ice cores from Law Dome, East Antarctica: implications for past deposition of aerosol iron. *Annals of Glaciology*, **27**, 365–370.

Eicken, H. (1992) The role of sea ice in structuring Antarctic ecosystems. *Polar Biology*, **12**, 3–13.

Eicken, H., Lange, M.A., Hubbertan, H.-W. & Wadhams, P. (1994) Characteristics and distribution patterns of snow and meteoric ice in the Weddell Sea and their contribution to the mass balance of sea ice. *Annales Geophysicae*, **12**, 80–93.

Eicken, H., Weissenberger, J., Cottier, F. et al. (1998) Ice tank studies of physical and biological sea ice processes. In: *Ice in Surface Waters, Proceedings of the 14th International Symposium on Ice*, (Ed. H.T. Shen), pp. 363–370. Potsdam, New York.

Engel, A., Goldthwait, S., Passow, U. & Alldredge, A. (2002) Temporal decoupling of carbon and nitrogen dynamics in a mesocosm diatom bloom. *Limnology and Oceanography*, 47, 753–761.

Fahl, K. & Kattner, G. (1993) Lipid content and fatty acid composition of algal communities in sea ice and water from the Weddell Sea (Antarctica). *Polar Biology*, 13, 405–409.

Fischer, G. (1991) Stable carbon isotope ratios of plankton carbon and sinking organic matter from the Atlantic sector of the Southern Ocean. *Marine Chemistry*, 35, 581–596.

Flynn, K.J. (1991) Algal carbon–nitrogen metabolism: a biochemical basis for modelling the interactions between nitrate and ammonium uptake. *Journal of Plankton Research*, 13, 373–382.

Fogel, M.L. & Cifuentes, L.A. (1993) Isotope fractionation during primary production. In: *Organic Geochemistry* (Eds. M.H. Engel & S.A. Macko), pp. 73–98. Plenum, New York.

Fripiat, F., Cardinal, D., Tison, J.-L., Worby, A & André, L (2007) Diatom-induced silicon isotopic fractionation in Antarctic sea ice, Journal of Geophysical Research, 112, G02001, doi: 10.1029/2006JG000244.

Fritsen, C.H., Lytle, V.I., Ackley, S.F. & Sullivan, C.W. (1994) Autumn bloom of Antarctic pack-ice algae. *Science*, **266**, 782–784.

Fritsen, C.H., Ackley, S.F., Kremer, J.N. & Sullivan, C.W. (1998) Flood–freeze cycles and microalgal dynamics in Antarctic pack ice. In: *Antarctic Sea Ice Biological Processes, Interactions and Variability*, (Eds. M.P. Lizotte & K.R. Arrigo), American Geophysical Union, Washington, DC. *Antarctic Research Series*, **73**, 1–21.

Fritsen, C.H., Coale, S.L., Neenan, D.R., Gibson, A.H. & Garrison, D.L. (2001) Biomass, production and microhabitat characteristics near the freeboard of ice floes in the Ross Sea, Antarctica, during the austral summer. *Annals of Glaciology*, **33**, 280–286.

Garcia, H.E. & Gordon, L.I. (1992) Oxygen solubility in seawater: better fitting equations. *Limnology and Oceanography*, **37**, 1307–1312.

Garrison, D.L. & Buck, K.R. (1986) Organism losses during ice melting: a serious bias in sea ice community studies. *Polar Biology*, **6**, 237–239.

Garrison, D.L. & Buck, K.R. (1991) Surface-layer sea ice assemblages in Antarctic pack ice during the austral spring: environmental conditions, primary production and community structure. *Marine Ecology Progress Series*, **75**, 161–172.

Giannelli, V., Thomas, D.N., Haas, C., Kattner, G., Kennedy, H.A. & Dieckmann, G.S. (2001) Behaviour of dissolved organic matter and inorganic nutrients during experimental sea ice formation. *Annals of Glaciology*, **33**, 317–321.

Gibson, J.A.E., Trull, T., Nichols, P.D., Summons, R.E. & McMinn, A. (1999) Sedimentation of C-13 rich organic matter from Antarctic sea ice algae: a potential indicator of past sea ice extent. *Geology*, **27**, 331–334.

Gitterman, K.E. (1937) Thermal analysis of seawater. *CRREL TL 287*. USA Cold Regions Research and Engineering Laboratory, Hanover, New Hampshire.

Gleitz, M. & Thomas, D.N. (1993) Variation in phytoplankton standing stock, chemical composition and physiology during sea ice formation in the southeastern Weddell Sea, Antarctica. Journal of *Experimental Marine Biology and Ecology*, **173**, 211–230.

Gleitz, M., Rutgers van der Loeff, M., Thomas, D.N., Dieckmann, G.S. & Millero, F.J. (1995) Comparison of summer and winter inorganic carbon, oxygen and nutrient concentrations in Antarctic sea ice brine. *Marine Chemistry*, **51**, 81–91.

Gleitz, M., Grossmann, S., Scharek, R. & Smetacek, V. (1996a) Ecology of diatom and bacterial assemblages in water associated with melting summer sea ice in the Weddell Sea, Antarctica. *Antarctic Science*, **8**, 135–146.

Gleitz, M., Kukert, H., Riebesell, U. & Dieckmann, G.S. (1996b) Carbon acquisition and growth of Antarctic sea ice diatoms in closed bottle incubations. *Marine Ecology Progress Series*, **135**, 169–177.

Glud, R.N., Rysgaard, S. & Kühl, M. (2002) A laboratory study in O_2 dynamics and photosynthesis in ice algal communities: quantification by microsensors, O_2 exchange rates, ^{14}C incubations and a PAM fluorometer. *Aquatic Microbial Ecology*, **27**, 301–311.

Gowing, M.M., Garrison, D.L., Gibson, A.H., Krupp, J.M., Jeffries, M.O. & Fritsen, C.H. (2004) Bacterial and viral abundance in Ross Sea summer pack ice communities. *Marine Eoclogy Progress Series*, **279**, 3–12.

Gosselin, M., Legendre, L., Therriault, J.C., & Demers, S. (1990) Light and nutrient limitation of sea ice microalgae (Hudson Bay, Canadian Arctic). *Journal of Phycology*, **26**, 220–232.

Gradinger, R. & Zhang, Q. (1997) Vertical distribution of bacteria in Arctic sea ice from the Barents and Laptev seas. *Polar Biology*, **17**, 448–454.

Gradinger, R. & Ikävalko, J. (1998) Organisms incorporation into newly forming Arctic sea ice in the Greenland Sea. *Journal of Plankton Research*, **20**, 871–886.

Gradinger, R., Friedrich, C. & Spindler, M. (1999) Abundance, biomass and composition of the sa ice biota of the Greeland Sea pack ice. *Deep-Sea Research Part II*. **46**, 1457–1472.

Grossmann, S., Lochte, K. & Scharek, R. (1996) Algal and bacterial processes in platelet ice during late austral summer. *Polar Biology*, **16**, 623–633.

Grotti, M., Soggia, F., Ianni, C. & Frache, R. (2005) Trace metals distributions in coastal sea ice of Terra Nova Bay, Ross, Sea, Antarctica. *Antarctic Science*, **17**, 289–300.

Guglielmo, L., Carrada, G.C., Catalano, G. et al. (2000) Structural and functional properties of sympagic communities in the annual sea ice at Terra Nova Bay (Ross Sea, Antarctica). *Polar Biology*, **23**, 137–146.

Günther, S. & Dieckmann, G.S. (1999) Seasonal development of algal biomass in snow-covered fast ice and the underlying platelet layer in the Weddell Sea, Antarctica. *Antarctic Science*, **11**, 305–315.

Günther, S. & Dieckmann, G.S. (2001) Vertical zonation and community transition of sea ice diatoms in fast ice and platelet layer, Weddell Sea, Antarctica. *Annals of Glaciology*, **33**, 287–296.

Günther, S., Gleitz, M. & Dieckmann, G.S. (1999) Biogeochemistry of Antarctic sea ice: a case study on platelet ice at Drescher Inlet, Weddell Sea. *Marine Ecology Progress Series*, **177**, 1–13.

Haas, C., Cottier, F., Smedsrud, L.H. et al. (1999) Multidisciplinary ice tank study shedding new light on sea ice growth processes. *EOS, Transactions of the American Geophysical Union*, **80**, 507–513.

Haas, C., Thomas, D.N. & Bareiss, J. (2001) Surface properties and processes of perennial Antarctic sea ice in summer. *Journal of Glaciology*, **47**, 613–625.

Haas, C., Nicolaus, M., Willmes, S., Worby, A. & Flinspach, D. (2008) Sea ice and snow thickness and physical properties of an ice floe in the western Weddell Sea and their changes during spring warming. *Deep-Sea Research Part II*, **55**, 963–974.

Haecky, P & Andersson, A. (1999) Primary and bacterial production in sea ice in the northern Baltic Sea. *Aquatic Microbial Ecology*, **20**, 107–118.

Hahn, M., Lünsdorf, H. & Janke, L. (2004) Exopolymer production and microcolony formation by planktonic freshwater bacteria: defence against protistan grazing. *Aquatic Microbial Ecology*, **35**, 297–308.

Hansell, D.A. & Carlson, C.A. (Eds.) (2002) *Biogeochemistry of Marine Dissolved Organic Matter*. Academic Press, San Diego.

Hansell, D.A., Kadko, D. & Bates, N.R. (2004) Degradation of terrigenous dissolved organic carbon in the western Arctic Ocean. *Science*, **304**, 858–861.

Harrison, W.G. & Cota, G.F. (1991) Primary production in polar waters: relation to nutrient availability. *Polar Research*, **10**, 87–104.

Hefu, Y. & Kirst, G.O. (1997) Effect of UV-radiation on DMSP content and DMS formation of *Phaeocystis antarctica*. *Polar Biology*, **18**, 402–409.

Hellmer, H.H., Schroder, M., Haas, C., Dieckmann, G.S. & Spindler, M. (2008) The ISPOL drift experiment. *Deep-Sea Research Part II*, 55, 913–917.

Herborg, L.-M., Thomas, D.N., Kennedy, H., Haas, C. & Dieckmann, G.S. (2001) Dissolved carbohydrates in Antarctic sea ice. *Antarctic Science*, **13**, 119–125.

Holmes, R.M., Peterson, B.J., Zhulidov, A.V. et al. (2001) Nutrient chemistry of the Ob' and Yenisey Rivers, Siberia: results from June 2000 expedition and evaluation of long-term data sets. *Marine Chemistry*, **75**, 219–227.

Hutchins, D.A. & Bruland, K.W. (1998) Iron-limited diatom growth and Si:N uptake ratios in a coastal upwelling regime. *Nature*, **393**, 561–564.

Jones, E.P. & Coote, A.R. (1981) Oceanic CO_2 produced by the precipitation of $CaCO_3$ from brines in sea ice. *Journal of Geophysical Research*, **86**, 11041–11043.

Junge, K., Eicken, H. & Deming, J.W. (2004) Bacterial activity at −2 to −20°C in Arctic wintertime sea ice. *Applied Environmental Microbiology*, **70**, 550–557.

Juul-Pedersen, T., Michel, C., Gosselin, M. & Seuthe, L. (2008) Seasonal changes in the sinking export of particulate material under first-year sea ice on the Mackenzie Shelf (western Canadian Arctic). *Marine Ecology Progress Series*, **353**, 13–25.

Kaartokallio, H. (2001) Evidence for active microbial nitrogen transformations in sea ice (Gulf of Bothnia, Baltic Sea) in midwinter. *Polar Biology*, **24**, 21–28.

Kaartokallio, H. (2004) Food web components, and physical and chemical properties of Baltic sea ice. *Marine Ecology Progress Series*, **273**, 49–63.

Kähler, P., Bjørnsen, P.K., Lochte, K. & Antia, A. (1997) Dissolved organic matter and its utilisation by bacteria during spring in the Southern Ocean. *Deep-Sea Research*, **44**, 341–353.

Kattner, G., Lobbes, J.M., Fitzner, H.P., Engbrodt, R., Nöthig, E.-M. & Lara, R.J. (1999) Tracing dissolved organic substances and nutrients from the Lena river through Laptev Sea (Arctic). *Marine Chemistry*, **65**, 25–39.

Kennedy, H., Thomas, D.N., Kattner, G., Haas, C. & Dieckmann, G.S. (2002) Particulate organic carbon in Antarctic summer sea ice: concentration and stable carbon isotopic composition. *Marine Ecology Progress Series*, **238**, 1–13.

Kerner, M., Hohenberg, H., Ertl, S., Rechermann, M. & Spitzy, A. (2003) Self-organization of dissolved organic matter to micelle-like microparticles in river water. *Nature*, **422**, 150–154.

Kieber, D.J. & Mopper, K. (1996) Photochemistry of Antarctic waters during the 1994 austral summer. *Antarctic Journal of the United States*, **30**, 150–151.

Killawee, J.A., Fairchild, I.J., Tison, J.-L., Janssens, L. & Lorrain, R. (1998) Segregation of solutes and gases in experimental freezing of dilute solutions: implications for natural glacial systems. *Geochimica et Cosmochimica Acta*, **62**, 3637–3655.

Kirst, G.O., Thiel, C., Wolff, H., Nothangel, J., Wanzek, M. & Ulmke, R. (1991) Dimethylsulfonioproprionate (DMSP) in ice-algae and its possible biological role. *Marine Chemistry* **35**, 381–388.

Krell, A., Ummenhofer, C., Kattner, G., Naumov, A., Evans, D., Dieckmann, G.S., & Thomas, D. N. (2003) The biology and chemistry of land fast ice in the White Sea, Russia – A comparison of winter and spring conditions. *Polar Biology*, **26**, 707–719.

Krembs, C. & Deming, J.W. (2008) The role of exopolymers in microbial adaptation to sea ice. In: *Psychrophiles: from Biodiversity to Biotechnology* (Eds. R. Margesin, F. Schinner, J.-C. Marx & C. Gerday), pp. 247–264. Springer-Verlag, Berlin.

Krembs, C. & Engel, A. (2001) Abundance and variability of microorganisms and transparent exopolymer particles across the ice–water interface of melting first-year sea ice in the Laptev Sea (Arctic). *Marine Biology*, **138**, 173–185.

Krembs, C., Gradinger, R. & Spindler, M. (2000) Implications of brine channel geometry and surface area for the interaction of sympagic organisms in Arctic sea ice. *Journal of Experimental Marine Biology and Ecology,* **243**, 55–80.

Krembs, C., Mock, T. & Gradinger, R. (2001a) A mesocosm study of physical–biological interactions in artificial sea ice: effects of brine channel surface evolution and brine movement on algal biomass. *Polar Biology*, **24**, 356–364.

Krembs, C., Tuschling, K. & von Juterzenka, K. (2001b) The topography of the ice water interface – its influence on the colonisation of sea ice by algae. *Polar Biology*, **25**, 106–117.

Krembs, C., Eicken, H., Junge, K. & Deming, J.W. (2002) High concentrations of exopolymeric substances in Arctic winter sea ice: implications for the polar ocean carbon cycle and cryoprotection of diatoms. *Deep-Sea Research Part I*, **49**, 2163–2181.

Kristiansen, S., Syvertsen, E.E. & Farbrot, T. (1992) Nitrogen uptake in the Weddell Sea during late winter and spring. *Polar Biology*, **12**, 245–251.

Kristiansen, S., Farbrot, T., Kuosa, H., Myklestad, S. & Quillfeldt, C.H. (1998) Nitrogen uptake in the infiltration community, an ice algal community in Antarctic pack-ice. *Polar Biology*, **19**, 307–315.

Kühl, M., Glud, R.N., Borum, J., Roberts, R. & Rysgaard, S. (2001) Photosynthetic performance of surface-associated algae below sea ice as measured with a pulse-amplitude-modulated (PAM) fluorometer and O_2 microsensors. *Marine Ecology Progress Series*, **223**, 1–14.

Lannuzel, D., Schoemann, V., de Jong, J., Tison, J.-L. & Chou, L. (2007) Distribution and biogeochemical behavior of iron in the East Antarctic sea ice. *Marine Chemistry* **106**, 18–32.

Lannuzel, D., Schoemann, V., de Jong, J., Chou, L., Delille, B., Becquevort, S. & Tison, J.-L. (2008) Iron study during a time series in the western Weddell pack ice. *Marine Chemistry*, **108**, 85–95.

Lara, R.J., Rachold, V. Kattner, G., Hubberten, H.W., Guggenberger, G., Skoog, A. & Thomas, D.N. (1998) Dissolved organic matter and nutrients in the Lena River, Siberian Arctic: characteristics and distribution. *Marine Chemistry*, **59**, 301–309.

Lavoie, D., Denman, K. & Michel, C. (2005) Modelling ice algal growth and decline in a seasonally ice-covered region of the Arctic (Resolute Passage, Canadian Archipelago). *Journal of Geophysical Research*, **110**, C11009, doi: 10.1029/2005JC002922.

Lazar, B. & Erez, J. (1992) Carbon geochemistry of marine-derived brines: I. ^{13}C depletion due to intense photosynthesis. *Geochimica et Cosmochimica Acta*, **56**, 335–345.

Lazar, B., Starinsky, A., Katz, A. & Sass, E. (1983) The carbonate system in hypersaline solutions: alkalinity and $CaCO_3$ solubility of evaporated seawater. *Limnology and Oceanography*, **28**, 978–986.

Li, Y. & Tanaka, T. (1992) Phase transitions of gels. *Annual Review of Material Science*, **22**, 243–277.

Lobbes, J.M., Fitzner, H.P. & Kattner, G. (2000) Biogeochemical characteristics of dissolved and particulate organic matter in Russian rivers entering the Arctic Ocean. *Geochimica et Cosmochimica Acta*, **64**, 2973–2983.

Lomas, M.W. & Glibert, P.M. (2000) Comparisons of nitrate uptake storage and reduction in marine diatoms and flagellates. *Journal of Phycology*, **36**, 903–913.

Long, R.A. & Azam, F. (1996) Abundant protein-containnig particles in the sea. *Aquatic Microbial Ecology*, **10**, 213–221.

McMinn, A. & Ashworth, C. (1998) The use of oxygen microelectrodes to determine the net production by an Antarctic sea ice algal community. *Antarctic Science*, **10**, 39–44.

McMinn, A., Skerratt, J., Trull, T., Ashworth, C. & Lizotte, M. (1999) Nutrient stress gradient in the bottom 5 cm of fast ice, McMurdo Sound, Antarctica. *Polar Biology*, **21**, 220–227.

McMinn, A., Ashworth, C. & Ryan, K.G. (2000) *In situ* net primary productivity of an Antarctic fast ice bottom algal community. *Aquatic Microbial Ecology*, **21**, 177–185.

Mancuso Nichols, C.A., Caron, S., Bowman, J.P., Raguenes, G. & Guezennec, J. (2004) Production of exopolysaccharides by Antarctic marine bacterial isolates. *Journal of Applied Microbiology*, **96**, 1057–1066.

Mari, X. & Rassoulzadegan, F. (2004) Role of TEP in the microbial food web structure. I. Grazing behavior of a bacterivorous pelagic ciliate. *Marine Ecology Progress Series*, **279**, 13–22.

Malin, G. & Kirst, G.O. (1997) Algal production of dimethyl sulfide and its atmospheric role. *Journal of Phycology*, **33**, 889–896.

Marion, G.M. (2001) Carbonate mineral solubility at low temperatures in the Na–K–Mg–Ca–H–Cl–SO$_4$–OH–HCO$_3$–CO$_3$–CO$_2$–H$_2$O system. *Geochimica et Cosmochimica Acta*, **65**, 1883–1896.

Marion, G.M. & Farren, R.E. (1999) Mineral solubilities in the Na–K–Mg–Ca–Cl–SO$_4$–H$_2$O system: a re-evaluation of the sulphate chemistry in the Spencer–Moller–Weare model. *Geochimica et Cosmochimica Acta*, **63**, 1305–1318.

Martin-Jézéquel, V., Hildebrand, M. & Brezinski, M.A. (2000) Silicon metabolism in diatoms: implications for growth. *Journal of Phycology*, 36, 821–840.

Massom, R.A., Eicken, H., Haas, C. et al. (2001) Snow on Antarctic Sea ice. *Reviews of Geophysics*, **39**, 413–445.

Measures, C.I. (1999) The role of entrained sediments in sea ice in the distribution of aluminium and iron in the surface waters of the Arctic Ocean, *Marine Chemistry*, **68**, 59–70.

Meese, D.A. (1989) The chemical and structural properties of sea ice in the southern Beaufort Sea. *CRREL Report*, **89–25**, 1–97.

Meiners, K., Brinkmeyer, R., Granskog, M.A. & Lindfors, A. (2004) Abundance, size distribution and bacterial colonization of exopolymer particles in Antarctic sea ice (Bellingshausen Sea). *Aquatic Microbial Ecology*, **35**, 283–296.

Meiners, K., Fehling, J., Granskog, M.A. & Spindler, M. (2002) Abundance, biomass and composition of biota in Baltic sea ice and underlying waters (March 2000). *Polar Biology*, **25**, 761–770.

Meiners K., Gradinger, R., Fehling, J., Civitarese, G. & Spindler, M. (2003) Vertical distribution of transparent exopolymer particles (TEP) in sea ice of the Fram Strait (Arctic) during autumn. *Marine Ecology Progress Series*, **248**, 1–13.

Meiners, K., Krembs, C. & Gradinger, R. (2008) Exopolymer particles: microbial hotspots of enhanced bacterial activity in Arctic fast ice (Chukchi Sea). *Aquatic Microbial Ecology*, **52**, 195–207.

Methé, B.A., Nelson, K.E., Deming, J.W. et al. (2005) The psychrophilic lifestyle as revealed by the genome sequence of *Colwellia pshychrerythraea* 34H through genomic and proteomic analyses. *Proceedings of the National Academy of Science, USA*, **102**, 10913–10918.

Meyer-Reil, L.-A. (1994) Microbial life in sedimentary biofilms – the challenge to microbial ecologists. *Marine Ecology Progress Series*, **112**, 303–311.

Michel, C., Nielsen, T.G., Nozias, C. & Gosselin, M. (2002) Significance of sedimentation and grazing by ice micro- and meiofana for carbon cycling in annual sea ice (northern baffin Bay). *Aquatic Microbial Ecology*, **30**, 57–68.

Millero, F.J. (1995) Thermodynamics of the carbon dioxide system in the ocean. *Geochimica et Cosmochimica Acta*, **59**, 661–677.

Millero, F. J., Huang, F. & Laferiere, A.L. (2002) Solubility of oxygen in the major sea salts as a function of concentration and temperature. *Marine Chemistry*, **78**, 217–230.

Mitchell, C. & Beardall, J. (1996) Inorganic carbon uptake by an Antarctic sea ice diatom, *Nitzschia frigida*. *Polar Biology*, **16**, 95–99.

Mock, T. & Gradinger, R. (2000) Changes in photosynthetic carbon allocation in algal assemblages of Arctic sea ice with decreasing nutrient concentrations and irradiance. *Marine Ecology Progress Series*. **202**, 1–11.

Mock, T. & Kroon, B.M.A. (2002a) Photosynthetic energy conversion under extreme conditions. I. Important role of lipids as structural modulators and energy sink under N-limited growth in Antarctic sea ice diatoms. *Phytochemistry*, **61**, 41–51.

Mock, T. & Kroon, B.M.A. (2002b) Photosynthetic energy conversion under extreme conditions. II. The significance of lipids at low temperature and low irradiances in Antarctic sea ice diatoms. *Phytochemistry*, **61**, 53–60.

Mock, T., Meiners, K.M. & Giesenhagen, H.C. (1997) Bacteria in sea ice and underlying brackish water at 54° 26′ 50″ N (Baltic Sea, Kiel Bight). *Marine Ecology Progress Series*, **158**, 23–40.

Mock, T., Dieckmann, G.S., Haas, C. et al. (2002) Micro-optodes in sea ice: a new approach to investigate oxygen dynamics during sea ice formation. *Aquatic Microbial Ecology*, **29**, 297–306.

Mock, T., Kruse, M. & Dieckmann, G.S. (2003) A new microcosm to investigate oxygen dynamics at the sea–ice water interface. *Aquatic Microbial Ecology*, **30**, 197–205.

Mojica-Prieto, F.J. & Millero, F.J. (2002) The values of $pK_1 + pK_2$ for the dissociation of carbonic acid in seawater. *Geochimica et Cosmochimica Acta*, **66**, 2529–2540.

Mopper, K., Zhou, X., Kieber, R.J., Kieber, D. J., Sikorski, R.J. & Jones, R.D. (1991) Photochemical degradation of dissolved organic carbon and its impact on the oceanic carbon cycle. *Nature*, **353**, 60–62.

Morin, S., Marion, G. M., von Glasow, R., Voisin, D., Bouchez, J. & Savarino, J. (2008) Precipitation of salts in freezing seawater and ozone depletion events: a status report. *Atmospheric Chemistry and Physics*, **8**, 7317–7324.

Nedwell, D.B. (1999) Effect of low temperature on microbial growth: lowered affinity for substrates limits growth at low temperature. *FEMS Microbiology Ecology*, **30**, 101–111.

Nelson, D.M. & Dortch, Q. (1996) Silicic acid depletion and silicon limitation in the plume of the Mississippi River: evidence from kinetic studies in spring and summer. *Marine Ecology Progress Series*, 136, 163–178.

Nelson, D.M., Smith, W.O., Muench, R.D., Gordon, L.I., Sullivan, C.W. & Husby, D.M. (1989) Particulate matter and nutrient distribution in the ice-edge zone of the Weddell Sea: Relationship to hydrography during late summer. *Deep-Sea Research Part I*, **36**, 191–209.

Nichols, P.D., Palmisano, A.C., Rayner, M.S., Smith, G.A. & White, D.C. (1989) Changes in the lipid composition of Antarctic sea ice diatom communities during a spring bloom: an indication of community physiological status. *Antarctic Science*, **1**, 133–140.

Obernosterer, I., Reitner, B. & Herndl, G.J. (1999) Contrasting effects of solar radiation on dissolved organic matter and its bioavailability to marine bacterioplankton. *Limnology and Oceanography*, **44**, 1645–1654.

Paasche, E. (1973) The influence of cell size on growth rate, silica content, and some other properties of four marine diatom species. *Norwegian Journal of Botany*, **20**, 197–204.

Palmisano, A.C. & Sullivan, C.W. (1985) Growth, metabolism, and dark survival in sea ice microalgae. In: *Sea Ice Biota* (Ed. R.A. Horner), pp. 131–146. CRC Press, Boca Raton, FL.

Papadimitriou, S., Kennedy, H., Kattner, G., Dieckmann, G.S. & Thomas, D.N. (2004) Experimental evidence for carbonate precipitation and CO_2 degassing during sea ice formation. *Geochimica et Cosmochimica Acta*, **68**, 1749–1761.

Papadimitriou, S., Thomas, D.N., Kennedy, H., Hass, C., Kuosa, H., Krell, A., & Dieckmann, G.S. (2007) Biochemical composition of natrual sea ice brines from the Weddell Sea during early austral summer. *Limnology and Oceanography*, **52**, 1809–1823.

Passow, U. (2002) Transparent exopolymer particles (TEP) in aquatic environments. *Progress in Oceanography*, **55**, 287–333

Passow, U. & Alldredge, A.L. (1995) A dye-binding assay for the spectrophotometric measurement of transparent exopolymeric substances. *Limnology and Oceanography*, **40**, 1326–1335.

Perovich, D.K. & Gow, J.K. (1996) A quantitative description of sea ice inclusions. *Journal of Geophysical Research*, **101**, 18327–18343.

Petri, R. & Imhoff, J.F. (2001) Genetic analysis of sea ice bacterial communities of the Western Baltic Sea using an improved double gradient method. *Polar Biology*, **24**, 252–257.

Pomeroy, L.R. & Wiebe, W.J. (2001) Temperature and substrates as interactive limiting factors for marine heterotrophic bacteria. *Aquatic Microbial Ecology*, **23**, 187–204.

Popp, B.N., Laws, E.A., Bidigare, R.R., Dore, J.E., Hanson, K.L. & Wakeham, S.G. (1998) Effect of phytoplankton cell geometry on carbon isotopic fractionation. *Geochimica et Cosmochimica Acta* **62**, 69–77.

Prézelin, B., Moline, M.A. & Matlick, H.A. (1998) ICECOLORS '93: Spectral UV radiation effects on Antarctic frazil ice algae. In: *Antarctic Sea Ice Biological Processes, Interactions and*

Variability (Eds. M.P. Lizotte & K.R. Arrigo). American Geophysical Union, Washington, DC. *Antarctic Research Series*, **73**, 45–83.

Prinsenberg, S.J. (1986) The circulation pattern and current structure of Hudson Bay. In: *Canadian Inland Seas. Elsevier Oceanography Series, Vol. 44* (Ed. I.P. Martini) , pp. 187–204. Elsevier, NewYork.

Priscu, J.C. & Sullivan, C.W. (1998) Nitrogen metabolism in Antarctic fastice microalgal assemblages. In: *Antarctic Sea Ice Biological Processes, Interactions and Variability* (Eds. M.P. Lizotte & K.R. Arrigo). American Geophysical Union, Washington, DC. *Antarctic Research Series*, **73**, 147–160.

Priscu, J.C., Priscu, L.R., Palmisano, A.C. & Sullivan, C.W. (1990a) Estimation of neutral lipid levels in Antarctic sea ice microalgae by nile red fluorescence. *Antarctic Science*, **2**, 149–155.

Priscu, J.C., Downes, M.T., Priscu, L.R., Palmisano, A.C. & Sullivan, C.W. (1990b) Dynamics of ammonium oxidizer activity and nitrous oxide (N_2O) within and beneath Antarctic sea ice. *Marine Ecology Progress Series*, **62**, 37–46.

Rachold, V., Eicken, H., Gordeev, V.V. et al. (2004) Modern terrigeneous organic carbon input to the Arctic Ocean. In: *The Organic Carbon Cycle in the Arctic Ocean* (Eds. R. Sten & R.W. Macdonald), pp. 33–55, Chapter 2.

Rau, G.H., Sullivan, C.W. & Gordon, L. (1991) $\delta^{13}C$ and $\delta^{15}N$ variations in Weddell Sea particulate organic matter. *Marine Chemistry*, **35**, 355–369.

Raven, J.A. (1991) Plant responses to high O2 concentrations: relevance to previous high O_2 episodes. *Palaeogeography, Palaeoclimatology, Palaeoecology*, **97**, 19–38.

Raven, J.A., Wollenweber, B. & Handley, L.L. (1992) A comparison of ammonium and nitrate as nitrogen sources for photolithotrophs. *New Phytologist*, **121**, 19–32.

Raven, J.A., Johnston, A.M., Parsons, R. & Kübler, J. (1994) The influence of natural and experimental high O_2 concentrations on O_2-evolving phototrophs. *Biological Review*, **69**, 61–94.

Reay, D.S., Nedwell, D.B., Priddle, J. & Ellis-Evans, J.C. (1999) Temperature dependence of inorganic nitrogen uptake: reduced affinity for nitrate at suboptimal temperatures in both algae and bacteria. *Applied and Environmental Microbiology*, **65**, 2577–2584.

Riedel, A., Michel, C. & Gosselin, M. (2006) Seasonal study of sea ice exopolymeric substances (EPS) on the Mackenzie shelf: implications for the transport of sea ice bacteria and algae. *Aquatic Microbial Ecology*, **45**, 195–206.

Riedel, A., Michel, C.,Gosselin, M. & LeBlanc, B. (2007a) Enrichment of nutrients, exopolymeric substances and microorganisms in newly formed sea ice on the Mackenzie shelf. *Marine Ecology Progress Series*, **342**, 55–67.

Riedel, A., Michel, C. & Gosselin, M. (2007b) Grazing of large-sized bacteria by sea ice heterotrophic protists on the Mackenzie shelf during the winter-spring transition. *Aquatic Microbial Ecology*, **50**, 25–38.

Riedel, A., Michel, C., Gosselin M. & LeBlanc, B. (2008) Winter–spring dynamics in sea ice carbon cycling in the coastal Arctic Ocean. *Journal of Marine Systems*, **74**, 918–932.

Rivkin, R.B. & Putt, M. (1987) Heterotrophy and photoheterotrophy in Antarctic microalgae: light-dependent incorporation of amino acids and glucose. *Journal of Phycology*, **23**, 442–452.

Różańska, M., Poulin, M. & Gosselin, M. (2008) Protist entrapment in newly formed sea ice in the coastal Arctic Ocean. *Jounal of Marine Systems*, 74, 887–901.

Różańska, M., Poulin, M., Gosselin, M., Wiktor, J.M. & Michel, C. (2009) Influence of environmental factors on the development of bottom ice protist communities during the winter-spring transition. *Marine Ecology Progress Series,* **386**, 43–59.

Rysgaard, S. & Glud, R.N. (2004) Anaerobic N_2 production in Arctic sea ice. *Limnology and Oceanography*. **49**, 86–94.

Rysgaard, S., Kühl, M., Glud, R.N. & Hansen, J.W. (2001) Biomass, production and horizontal patchiness of sea ice algae in a high-Arctic fjord (Young Sound, NE Greenland). *Marine Ecology Progress Series*, **223**, 15–26.

Rysgaard, S., Glud, R.N., Sejr, M.K., Bendtsen, J. & Christensen, P.B. (2007) Inorganic carbon transport during sea ice growth and decay: a carbon pump in polar seas. *Journal of Geophysical Research*, **112**, C03016, 10.1029/2006jc003572.

Rysgaard, S., Glud, R.N., Sejr, M.K., Blicher, M.E. & Stahl, H.J. (2008) Denitrification activity and oxygen dynamics in Arctic sea ice. *Polar Biology*, **31**, 527–537.

Sander, R., Burrows, J. & Kaleschke, L. (2006) Carbonate precipitation in brine – a potential trigger for tropospheric ozone depletion events. *Atmospheric Chemical Physics*, **6**, 4653–4658.

Sedwick, P.N. & DiTullio, G.R. (1997) Regulation of algal blooms in Antarctic shelf waters by the release of iron from melting sea ice. *Geophysical Research Letters*, **24**, 2515–2518.

Sedwick, P.N., DiTullio, G.R. & Mackey, D.J. (2000) Iron and manganese in the Ross Sea, Antarctica: Seasonal iron limitation in Antarctic shelf waters. *Journal of Geophysical Research*, **105**, 11321–11336.

Schlekat, C.E., Decho, A.W. & Chandler, G.T. (1999) Dietary asimilation of cadmium associated with bacterial exopolymer sediment coatings by the estuarine amphipod *Leptocheirus plumulosus*: effectsof Cd concentration and salinity. *Marine Ecology Progress Series*, **183**, 205–216.

Schriek, R. (2000) Effects of light and temperature on the enzymatic antioxidative defense systems in the Antarctic ice diatom *Entomoneis kufferathii* Manguin. *Reports on Polar Research*, **349**, 1–130.

Schubert, C.J. & Calvert, S.E. (2001) Nitrogen and carbon isotopic composition of marine and terrestrial organic matter in Arctic Ocean sediments: implications for nutrient utilization and organic matter composition. *Deep-Sea Research Part I*, **48**, 789–810.

Sherwood, J.E., Stagnitti, F., Kokkinn, M.J. & Williams, W.D. (1991) Dissolved oxygen concentration in hypersaline waters. *Limnology and Oceanography*, **36**, 235–250.

Simon, M., Grossart, H.P., Schweitzer, B. & Ploug, H. (2002) Microbial ecology of organic aggregates in aquatic ecosystems. *Aquatic Microbial Ecology*, **28**, 175–211.

Smith, D.J. & Underwood, G.J.C. (1998) Exopolymer production by intertidal epipelic diatoms. *Limnology and Oceanography*, **43**, 1578–1591.

Smith, R.E.H., Harrison, W.G., Harris, L.R. & Herman, A.W. (1990) Vertical fine structure of particulate matter and nutrients in sea ice of the high Arctic. *Canadian Journal of Fisheries and Aquatic Science*s, **47**, 1348–1355.

Smith, R.E.H., Gosselin, M. & Taguchi, S. (1997) The influence of major inorganic nutrients on the growth and physiology of high Arctic ice algae. *Journal of Marine Systems*, **11**, 63–70.

Smith, R.E.H., Gosselin, M., Kudoh, S., Robineau, B. & Taguchi, S. (1997) DOC and its relationship to algae in bottom ice communities. *Journal of Marine Systems*, **11**, 71–80.

Smith, W.O. & Nelson, D.M. (1985) Phytoplankton bloom proudced by a receding ice edge in the Ross Sea: spatial coherence with the density field. *Science*, **227**, 163–166.

Staley, J.T. & Gosink, J.J. (1999) Poles apart: biodiversity and biogeography of sea ice bacteria. *Annual Reviews in Microbiology*, 53, 189–215.

Stefels, J., Steinke, M., Turner, S., Malin, G. & Belviso, S. (2007) Environmental constraints on the production and removal of the chemically active gas dimethylsuphide (DMS) and implcations for ecosystem modelling. *Biogeochemistry*, **83**, 245–275.

Stoecker, D.K., Gustafson, D.E., Baier, C.T. & Black, M.M.D. (2000) Primary production in the upper sea ice. *Aquatic Microbial Ecology*, **21**, 275–287.

Stumm, W. & Morgan, J.J. (1996) *Aquatic chemistry: Chemical Equilibria and Rates in Natural Waters, Third edition*. John Wiley & Sons, New York.

Sturges, W.T., Cota, G.F. & Buckley, P.T. (1992) Bromoform emission from Arctic ice algae. *Nature*, **358**, 660–662.

Sturges, W.T., Sullivan, C.W., Schnell, R.C., Heidt, L.E. & Pollock, W.H. (1993) Bromoalkene production by Antarctic ice algae. *Tellus*, **45**, 120–126.

Syvertsen, E.E. & Kristiansen, S. (1993) Ice algae during EPOS leg 1: assemblages, biomass, origin and nutrients. *Polar Biology*, **13**, 61–65.

Thomas, D.N. (2003) Iron limitation in the Southern Ocean. *Science*, **302**, 565.

Thomas, D.N. & Dieckmann, G.S. (2002) Antarctic sea ice – a habitat for extremophiles. *Science*, **295**, 641–644.

Thomas, D.N., Lara, R.J., Eicken, H., Kattner, G. & Skoog, A. (1995) Dissolved organic matter in Arctic multi-year sea ice during winter: major components and relationship to ice characteristics. *Polar Biology*, **15**, 477–483.

Thomas, D.N., Lara, R.J., Haas, C. et al. (1998) Biological soup within decaying summer sea ice in the Amundsen Sea, Antarctica. In: *Antarctic Sea Ice Biological Processes, Interactions and Variability* (Eds. M.P. Lizotte & K.R. Arrigo). American Geophysical Union, Washington, DC. *Antarctic Research Series*, **73**, 161–171.

Thomas, D.N., Engbrodt, R., Giannelli, V., Kattner, G., Kennedy, H., Haas, C. & Dieckmann, G.S. (2001a) Dissolved organic matter in Antarctic sea ice. *Annals of Glaciology*, **33**, 297–303.

Thomas, D.N., Kennedy, H., Kattner, G., Gerdes, D., Gough, C. & Dieckmann, G.S. (2001b) Biogeochemistry of platelet ice: its influence on particle flux under fast ice in the Weddell Sea, Antarctica. *Polar Biology*, **24**, 486–496.

Thompson, P.A., Levasseur, M.E. & Harrison, P.J. (1989) Light-limited growth on ammonium vs. nitrate: what is the advantage for marine phytoplankton. *Limnology and Oceanography*, **34**, 1014–1024.

Tison, J.-L., Haas, C., Gowing, M.M., Sleewaegen, S. & Bernard, A. (2002) Tank study of physico-chemical controls on gas content and composition during growth of young sea ice. *Journal of Glaciology*, **48**, 177–191.

Tison, J.-L., Worby, A., Delille, B. et al. (2008) Temporal evolution of decaying summer first-year sea ice in the Western Weddell Sea. *Deep-Sea Research Part II*, **55**, 975–987.

Tranvik, L. & Kokalj, S. (1998) Decreased biodegradability of algal DOC due to interactive effects of UV radiation and humic matter. *Aquatic Microbial Ecology*, **14**, 301–307.

Trenerry, L.J., McMinn, A. & Ryan, K.G. (2001) *In situ* oxygen microelectrode measurements of bottom-ice algal production in McMurdo Sound, Antarctica. *Polar Biology*, **25**, 72–80.

Trevena, A.J. & Jones, G.B. (2006) Dimethylsulphide and dimethylsulphonioproprionate in Antarctic sea ice and their release during sea ice melting. *Marine Chemistry*, **98**, 210–222.

Trevena, A.J., Jones, G.B., Wright, S.W. & van den Enden, R.L. (2000) Profiles of DMSP, algal pigments, nutrients and salinity in pack ice from eastern Antarctica. *Journal of Sea Research*, **43**, 265–273.

Trevena, A.J., Jones, G.B., Wright, S.W. & van den Enden, R.L. (2003) Profiles of dimethylsuphonio-proprionate (DMSP), algal pigments, nutrients and salinity in th efast ice of Prydz bay, Antarctica. *Journal of Geophysical Research*, **108**, 3145,10.1029/2002JC001369.

Verdugo, P., Alldredge, A.L., Azam, F. et al. (2004) The oceanic gel phase: a bridge in the DOM–POM continuum. *Marine Chemistry*, **92**, 67–85.

Vézina, A.F., Demers, S., Laurion, I., Sime-Ngando, T., Juniper, S.K. & Devine, L. (1997) Carbon flows through the microbial food web of first-year ice in Resolute Passage (Canadian High Arctic). *Journal of Marine Systems*, **11**, 173–189.

Vincent, W.F. & Roy, S. (1993) Solar ultraviolet-B radiation and aquatic primary production: damage, protection and recovery. *Environment Review*, **1**, 1–12.

Volkman, J.K., Barrett, S.M., Blackburn, S.I., Mansour, M.P., Sikes, E.L. & Gelin, F. (1998) Microalgal biomakers: a review of recent research developments. *Organic Geochemistry*, **29**, 1163–1179.

Wagner, T. & Platt, U. (1998) Satellite mapping of enhanced BrO concentrations in the troposphere. *Nature*, **395**, 486–490.

Weeks, W.F. & Ackley, S.F. (1982) The growth, structure and properties of sea ice. *CRREL Monograph*, **82** (1), 1–130.

Weiss, R. (1974). Carbon dioxide in water and seawater: the solubility of a non–ideal gas. *Marine Chemistry*, **2**, 203–215.

Weissenberger, J. (1998) Arctic sea ice biota: design and evaluation of a mesocosm experiment. *Polar Biology*, **19**, 151–159.

Weissenberger, J., Dieckmann, G.S., Gradinger, R. & Spindler, M. (1992) Sea ice: a cast technique to examine and analyse brine pockets and channel structure. *Limnology and Oceanography*, **37**, 179–183.

Wetz, M.S. & Wheeler, P.A. (2007) Release of dissolved organic matter by coastal diatoms. *Limnology and Oceanography*, **52**, 798–807.

Xie, H. & Gosselin, M. (2005) Photoproduction of carbon monoxide in first-year sea ice in Franklin Bay, southeastern Beaufort Sea. *Geophysical Research Letters*, **32**, L12606, doi:10.1029/2005GL022803.

Zaslavskaia, L.A., Lippmeier, J.C., Shih, C., Ehrhardt, D., Grossman, A.R. & Apt, K.E. (2001) Trophic conversion of an obligate phototrophic organism through metabolic engineering. *Science*, **292**, 2073–2075.

This page intentionally left blank

13 Palaeo Sea Ice Distribution and Reconstruction Derived from the Geological Record

Leanne K. Armand and Amy Leventer

13.1 Introduction

Since the 1970s, oceanographers have worked towards reconstructing past oceanographic conditions. One of the most significant studies of its time, the CLIMAP (Climate, Long-Range Investigation, Mapping and Prediction) project, had the goal of reconstructing earth's climate at specific time slices of the past, such as the Last Glacial Maximum (LGM) 21,000 years ago (CLIMAP Project Members, 1976, 1981). The field of palaeoceanographic research has subsequently thrived, employing increasingly sophisticated methods, more highly resolved records and a wider suite of proxies. Reconstruction of past sea-surface temperatures (SST) and salinities, the position of oceanographic boundaries, palaeoproductivity and palaeo sea ice distribution has become a standard field of research. Specific interest in reconstructing sea ice distribution through time rests upon the major role sea ice plays in climate, oceanographic and ecological systems and it's increasing significance in modelling the Earth's oceanographic climatology.

Sea ice plays a key role in moderating the exchange of both heat and gases, e.g. carbon dioxide, oxygen and dimethylsulphide, between the atmosphere and the ocean in polar latitudes (Maykut, 1978). First, it impacts climate by virtue of its high albedo, since the reflectivity of sea ice greatly exceeds that of open water, and because it forms an insulating barrier to turbulent heat transfer between the atmosphere and the ocean (Maykut, 1978; Grenfell, 1983; Chapters 2 and 4). Decreased sea ice extent may thus have a positive feedback effect on climate change, through the greater absorption of heat by exposed sea water. The location of the ice edge has been shown to influence regional weather patterns in polar regions (Gloersen et al., 1989; Chapter 6). Second, the formation of sea ice and consequent brine rejection affects oceanic circulation through the formation of dense water masses (Gordon, 1978; Killworth, 1983; Broecker et al., 1998; Rintoul, 1998; Chapters 1 and 3). This vertical convection of the polar oceans has important consequences on the ventilation of deep waters. Conversely, sea ice melt produces a low-salinity meltwater layer that stratifies the upper water column and decreases vertical circulation. Third, polar regions are globally significant sites of primary productivity, located in the sea ice, open water and in regions of sea ice melt known as marginal ice zones (Smith & Sakshaug, 1990; Chapter 8). Changes in the overall levels and nature of production that govern the transfer of organic material

to the sea floor may have significantly influenced global carbon and silica budgets through time (Kumar et al., 1995). These changes are most likely to have included varying proportions of overall production in each of these different settings: the sea ice, ice edge and open ocean.

Palaeoceanographic reconstructions that include estimates of palaeo sea ice extent are, therefore, of great interest to researchers ranging from global climate and ocean circulation modellers to palaeoclimatologists. These reconstructions are particularly significant today as most models of global warming predict that polar regions will warm more rapidly than most of the globe (Budd & Wu, 1998; Warner & Budd, 1998; Matear & Hirst, 1999; Bi et al., 2001, Jansen et al., 2007), with profound consequences for the sea ice regime. Significantly, sea ice thickness and extent in the Arctic appears to be decreasing (Lemke et al., 2007; Stroeve et al., 2007; Chapters 4 and 6), though not all researchers have confidence in the trends in thickness given the large amount of interannual variability in sea ice (McLaren et al., 1992; Parkinson, 2000). However, this finding of decreased sea ice thickness also reflects instrumental data that cover only several decades. Whether Antarctic sea ice is changing due to global warming is uncertain as there are no statistically significant trends in sea ice extent over the satellite era, and few data on Antarctic sea ice thickness (Watkins & Simmonds, 2000; Comiso & Steffen, 2001; Zwally et al., 2002; Lemke et al., 2007; Chapters 4 and 6). Palaeo sea ice distribution data allow scientists to develop a better and very necessary understanding of the relationship between climate change and sea ice, within the context of a longer-term perspective.

The objective of this updated review chapter is to cover the growth and establishment of methods for reconstructing past sea ice distribution and its seasonal variability based on microfossil assemblage distribution, and geochemical and sedimentological tracers (e.g. ice-rafted debris) that have been established for polar regions since our original review (Armand & Leventer, 2003). In addition, the instigation of sea ice over time is outlined, and palaeo sea ice reconstruction on time slices, such as the LGM, and in time series during the Quaternary (last 1.8 Ma) and Neogene (last 23 Ma) will be reviewed.

In general, in both the northern and southern high latitudes, the primary method through which sea ice cover is reconstructed is by using the microscopic remains of marine organisms in marine sediments. For example, the CLIMAP project inferred past sea ice cover by tracking the relative distribution of biosiliceous versus clay-rich sediments, assuming that permanent sea ice cover would inhibit light penetration and the ability of siliceous-tested diatoms to photosynthesize and grow (CLIMAP Project Members, 1976, 1981). This approach has continued to the present, with diatom data from the Arctic (e.g. the northernmost Pacific – Sancetta, 1983; the Nordic Seas – Koç et al., 1993 and Baffin Island – Williams, 1990) and in the circum-Antarctic (most recently Crosta et al., 1998a,b; Armand, 2000; Gersonde & Zielinski, 2000; Gersonde et al., 2005). A complete revision of the LGM sea ice proxies was recently undertaken for both hemispheres under MARGO (Multiproxy Approach for the Reconstruction of the Glacial Ocean surface; Kucera et al., 2005; de Vernal et al., 2005a; Gersonde et al., 2005). The results of these efforts are now used for the testing of palaeoclimate models (MARGO Project Members, 2009).

Although diatom assemblage data have been most useful in the Antarctic, in the Arctic (including the northern North Atlantic and Pacific), quantitative analysis of dinocyst assemblages has been a more powerful tool (Rochon et al., 1998, 1999; de Vernal et al., 2000, 2001, 2005a).

Given the large differences in the utility of types of palaeo sea ice proxies that are useful in the northern versus southern polar regions, the Arctic and the Antarctica are reviewed separately.

13.2 Antarctic

Methods for reconstructing past sea ice distribution and seasonal variability

Unlike the Arctic, the Antarctic is surrounded by ocean and is, thus, subjected to asymmetric and zonally defined atmospheric and oceanographic climatic forcing (Chapter 3). Both atmospheric and oceanic circulation systems bring warmth from the tropics to the polar regions. The transfer of this heat along with insolation variability in response to changes in the orbital rotations of the earth around the sun affect the cover and extent of annual sea ice from the Antarctic coast into the Southern Ocean. In turn, the cover of sea ice feeds back upon the climate system by reducing heat transfer between the ocean and the atmosphere through its high reflectivity (albedo) and insulating affect. We know from modern satellite observations that sea ice extent, thickness and duration undergo considerable variation from year to year (Chapters 4–6). Pre-satellite data, predominantly reports from whaling records and recently Antarctic continental ice core atmospheric records, also indicate that the sea ice edge may have been located farther northwards in the past (Parkinson, 1990; de la Mare, 1997; Vaughan, 2000; Ackley et al., 2003; Curran et al., 2003; Wolff et al., 2006; Iizuka et al., 2008; Röthlisberger et al., 2008). Yet, of all the climate variables fundamental to our understanding of climate change, particularly in the southern hemisphere, sea ice remains the least documented and modelled (Parkinson et al., 2006; Massom et al., unpublished data). There is a lack of historical knowledge of the Antarctic sea ice regime (Watkins & Simmonds, 2000) that has been the root of poor understanding. Although satellite sea ice records have only been available for the past ~30 years, it is upon these annually combined records that reconstruction of the Holocene and Quaternary periods must rely.

   Estimates of sea ice in the Southern Ocean have evolved from sedimentological and micro-palaeontological studies in the 1970s and are now linked to the study of either fossil diatom remains from the Southern Ocean sea floor or from aerosol proxies captured in Antarctic ice cores. The ice core records currently provide a higher time resolution than the marine core records. Correlation between both types of core proxies for sea ice cover has been subjective (Wolff et al., 2006) and is a new focus of research effort (Iizuka et al., 2008; Röthlisberger et al., unpublished data). Marine core-derived proxies have focused on single-celled microscopic organisms, diatoms, as indicators of sea ice conditions. Their success as a proxy is a product of their abundance in the fossil record and their dominance within the sediments surrounding Antarctica. Yet it is their relationship with the sea ice environment upon which many individual species are ecologically associated that holds the key to this proxy success (Horner, 1985; Armand, 1997; Zielinski & Gersonde, 1997; Crosta et al., 1998a; Armand et al., 2005; Chapter 8). Diatoms alone are not the only organisms to have distinguishing distributions in the water column (Chapters 7–11) or sea floor as a consequence of the sea ice boundary; another indicator group is dinoflagellate cysts (Harland & Pudsey, 1999). Ice core proxies rely on the record of two aerosols, methanesulphonic acid (MSA) and sea salt sodium, and both records are considered representative of the average extent of the

aerosol's source region, which is linked to sea ice cover (Curran & Jones, 2000; Rankin et al., 2000; Wolff et al., 2003; Iizuka et al., 2008). In the following sub-sections, we describe the approaches undertaken to document past sea ice cover before examining the results of these methods under time-slice scenarios.

Sedimentological tracers

Lithological changes in the sediments surrounding Antarctica provided the first evidence of the effects of overlying sea ice cover on the sea floor (Lisitzin, 1972). The belt of diatomaceous ooze that surrounds Antarctica (Burckle, 1984) is dominant between 50° and 60°S, and extends both south- and northwards of the modern maximum winter sea ice edge (Fig. 13.1). The earliest sea ice estimates combined biological and lithological evidence, such that summer sea ice extent was determined by mapping core locations with siliceous clay and silt overlain by Holocene diatomaceous ooze, and winter sea ice extent was delineated by a mid-way point between a faunally identified Polar Front and the summer sea ice boundary (CLIMAP Project Members, 1976; Hays et al., 1976).

The southern lithological boundary has still yet to be conclusively related to an observed physical oceanographic boundary. In contrast to the CLIMAP compilations, the southern boundary has been variously identified as representing three entities: the winter sea ice edge in the South Atlantic (DeFelice, 1979; DeFelice & Wise, 1981); a region experiencing greater than 35% annual sea ice cover (Crowley & Parkinson, 1988); or linked with pack ice cover in late spring (i.e. >65% concentration in November, Burckle et al., 1982). It would appear that sea ice cover might not be the only determinant of the southern lithological boundary. A simple overlay of the southern limit of the Upper Circumpolar Deep Water boundary (Orsi et al., 1995; Fig. 13.1) suggests that oceanographic and linked primary productivity responses in regions external to the Ross and Weddell Seas may have some bearing on the positioning of the southern lithological boundary.

Hays (1978) believed that maximum winter sea ice extent was best estimated from records of sea ice–transported volcanic ejecta in the sediments. He was less concise in describing methods of estimating winter sea ice extent in later work, citing a mixture of ice-rafted debris (IRD) distribution, lithological and sediment rate changes (Cooke & Hays, 1982). There is some evidence that correlations between IRD and abundance of the diatom *Eucampia antarctica* (Fig. 13.2) were used for winter sea ice estimates as well as stratigraphic control for glacial periods (Cooke et al., 1977; Burckle, 1984; Burckle & Burak, 1988). *Eucampia* abundance has been considered unrepresentative of sea ice extent (Fryxell & Prasad, 1990; Armand, 1997; Zielinski & Gersonde, 1997; Gersonde et al., 2003) and also diachronous (i.e. dating from different periods) for stratigraphic control in cores south of the Polar Front (Burckle & Abrams, 1986). Yet as discussed in later sections, study on the varieties of *Eucampia antarctica* have lead to the reinstigation of the species as a sea ice cover proxy.

The northern lithological silica boundary appears unlikely to be linked directly to sea ice cover. This boundary most likely indicates the summer position of the sub-Antarctic Front (SAF), having been tied to diatom thermal tolerances and subsequent low primary productivity north of this oceanographic feature (Burckle, 1983; Burckle & Cirilli, 1987). Silica and iron availability (Sedwick et al., 1997; Clementson et al., 1998; Takeda, 1998) are among other factors that are likely to define the northern lithological boundary. The relationship between the northern lithological boundary and the SAF is evident when viewed against the oceanographic frontal positions of Orsi et al. (1995; Fig. 13.1).
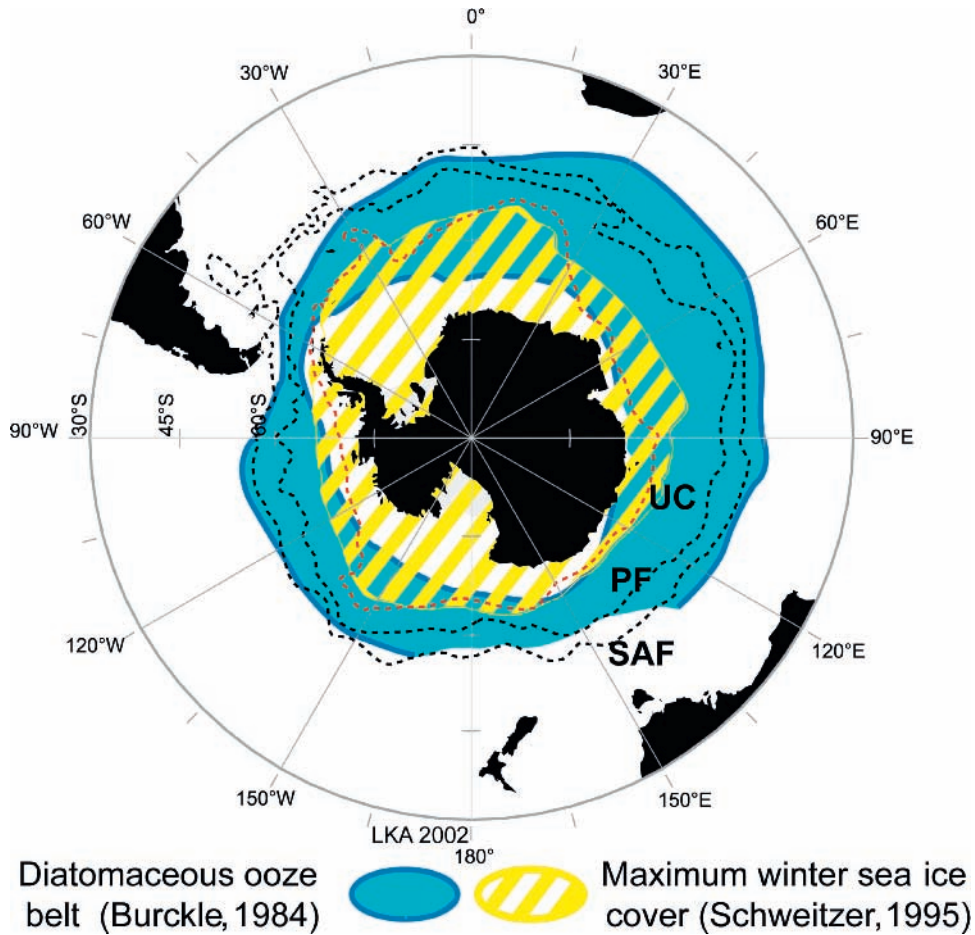
Fig. 13.1 Potential physical relationships between the circumpolar opal ooze belt (Burckle, 1984) with respect to major oceanographic fronts (Orsi et al., 1995) and present-day maximum winter sea ice edge (13.25-year compilation of satellite data, Schweitzer, 1995). The northern boundary of siliceous ooze on the sea floor may be related to the position of the SAF and decreases in primary productivity. The southern siliceous boundary appears unrelated to maximum winter sea ice extent, and is northwards of the maximum summer sea ice extent (not shown). In regions exterior to the Ross and Weddell Seas' influence, the southern limit of Upper Circumpolar Deep Water (UC) has some coincidental relationship to the southern siliceous boundary. In the Ross and Weddell Seas vicinity, winter sea ice extent appears related to the southern limit of Upper Circumpolar Deep Water. Abbreviations: SAF = Sub-Antarctic Front; PF = Polar Front; UC = southern limit of Upper Circumpolar Deep Water.

IRD abundances were a successful tool in providing additional evidence for sea ice cover in the early stages of this research field. A resurgence of the IRD abundance method has taken place in recent times with two methods of analysis being adopted. The first of these is X-ray analysis of core material and counts of IRD particles greater than 2 mm in size being counted in 1 cm intervals (Grobe, 1987; Kunz-Pirrung et al., 2002; Whitehead & McMinn, 2002). The second method relies on counting particles remaining in >150 µm sieved fractions (Kanfoush et al., 2000; Hodell et al., 2001; Carter et al., 2002; Nielsen et al., 2007).
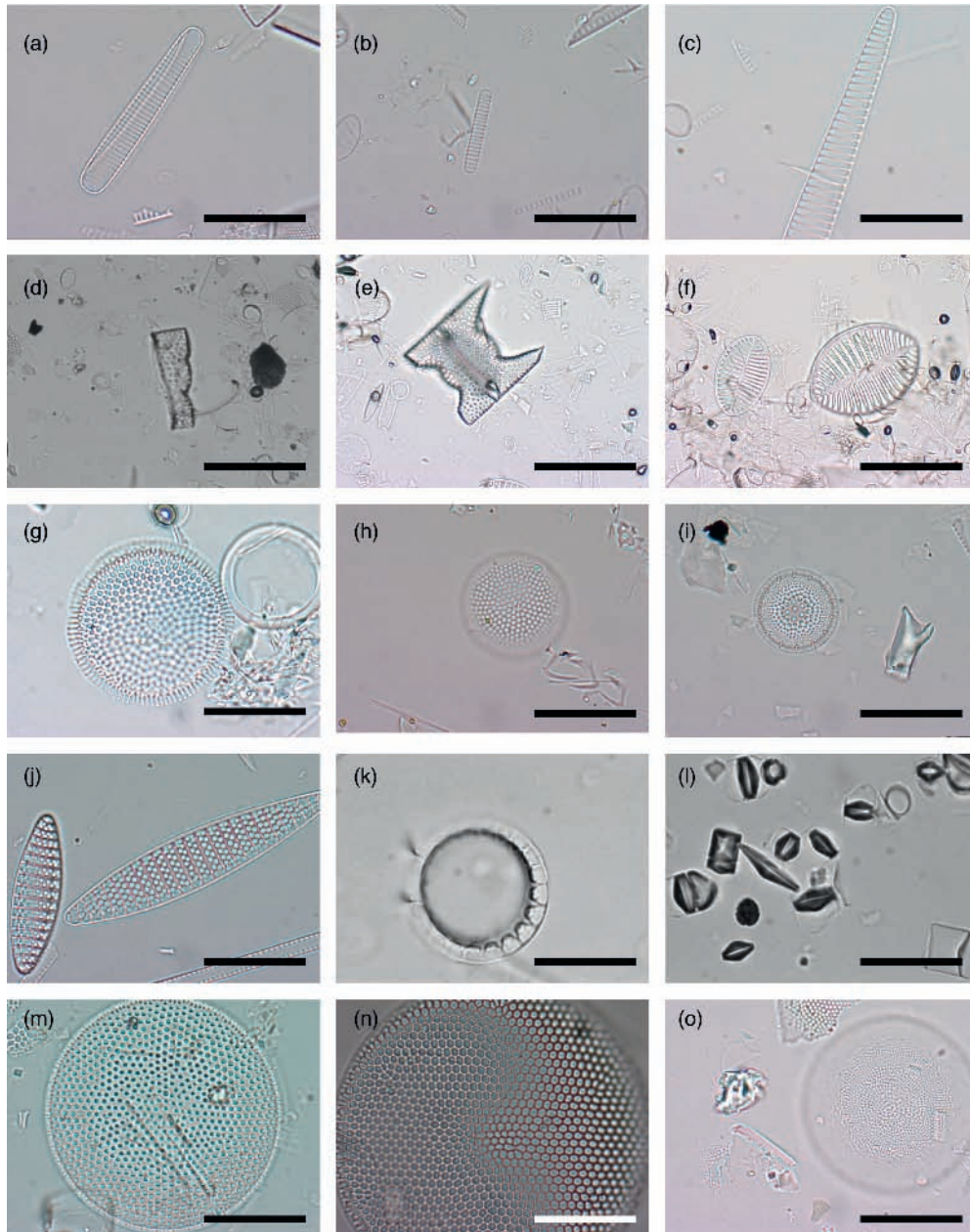
Fig. 13.2   Images of Antarctic diatom species relevant to the definition of sea ice and open ocean conditions in Holocene and Quaternary sea ice reconstructions. Key: (a) *Fragilariopsis curta*, (b) *F. cylindrus*, (c) *F. obliquecostata*, (d) *Eucampia antarctica* variation *antarctica* (Sub-Antarctic form, intercalary frustule valve), (e) Eucampia antarctica variation *recta* (Antarctic form, flat intercalary and pointy terminal frustule valves), (f) *Cocconeis* species, (g) *Thalassiosira antarctica* (warm form), (h) *Thalassiosira antarctica* (cold form), (i) *Thalassiosira gracilis*, (j) *Fragilariopsis kerguelensis*, (k) *Corethron inermis* (valve cap only shown), (l) *Chaetoceros* sub-genus *Hyalochaete* resting spores, (m) *Thalassiosira lentiginosa*, (n) *Thalassiosira tumida* and (o) *Porosira glacialis*. Scale bars in d–f represent 50 µm, all other scale bars are 20 µm. Photos A. Leventer.

An evolving consensus from IRD research in the South Atlantic region has exposed the volcanic provenance and dominance of South Sandwich Island IRD in regions of the South Atlantic influenced by highly extended sea ice during glacial periods (Kanfoush et al., 2002; Nielsen & Hodell, 2007; Nielsen et al., 2007). This is in contrast to earlier hypotheses for heightened Antarctic ice shelf dynamics and iceberg-dominated IRD provenances (Grobe & Mackensen, 1992; Kanfoush et al., 2000). The effect of far more extensive ice shelves around South Georgia, even as recently as the last glacial, may provide an alternative source for recent iceberg rafting of IRD into the South Atlantic (Graham et al., 2008). IRD observations in the South-west Pacific (Carter et al., 2002; Quilty, unpublished data) and the South Indian Ocean (Labeyrie et al., 1986; Whitehead & McMinn, 2002) have varying concentrations of IRD that appear related to regionally sourced iceberg pulses, the northerly expanse of sea ice cover or lags that identify erosional disconformities dependent on the study location.

Diatom proxies of sea ice conditions

Studies of diatom associations with respect to sea ice cover, primarily pioneered by DeFelice and Burckle in the early 1980s, have since evolved into a major research effort to define past sea ice conditions. A list of diatom studies relevant to palaeo sea ice reconstruction in the Southern Ocean is given in Table 13.1. Almost all the methods employed today rely on the recent biogeographic sea-floor distributions of diatoms and, therefore, their modern relationship to the sea ice environment for the reconstruction of Antarctic sea ice. To determine sea ice conditions beyond the Late Quaternary when either extinct taxa or precursor species appear in the sediment records, the continued use of proxy species for the sea ice condition relies on the evaluation of concurrent sea ice assemblage occurrences and/or the extension of specific fossil lineages (Leventer et al., 2007). Specific examples of sea ice palaeoenvironmental taxa back to the upper Oligocene (~28 Ma) are now being published from the McMurdo–Ross Sea sector under the auspices of the ANDRILL programme and its predecessors (Harwood & Bohaty, 2007; Scherer et al., 2007; Olney et al., in press).

The use of diatom proxies can now be divided into two fields of research endeavour. Those documenting sea ice extent in the open ocean with more or less low-resolution records across the Quaternary period (<1.8 Ma BP) and those that are largely confined to the Antarctic continental shelf regions, which represent high-resolution Holocene or deglacial sequences of sea ice absence/presence over the last ~17,000 years before present (ka BP).

Two approaches have been employed for the open ocean Quaternary record: the use of *Fragilariopsis* taxa proxies and the statistical Modern Analogue Technique (MAT). The former determines latitudinal summer and winter sea ice extents (Gersonde & Zielinski, 2000; Frank et al., 2000; and others identified on Table 13.1), whereas the latter provides sea ice duration, as a month per year coverage estimate (Crosta et al., 1998a,b, 2004; Hodell et al., 2001; Table 13.1). These methods are briefly described below, while a table summarizing the major proxies and their interpretations is given in Table 13.2.

The winter sea ice edge proxy relies on the combined abundance data of *Fragilariopsis curta* and *F. cylindrus* (Fig. 13.2). Both species exist in sea ice and sea ice melt-back environments (reviewed in Zielinski & Gersonde, 1997; Armand et al., 2005). The abundance of these species in moderate-to-well-preserved core records was calibrated by Gersonde and Zielinski (2000) from the South Atlantic sector so that combined relative abundances in

Table 13.1   List of diatom studies relevant to palaeo Antarctic sea ice reconstruction.

Reference/year	Region	Method	Time period (BP*)
Circumpolar			
Burckle (1984)	Circum-Antarctic	IKM	LGM
Crosta et al. (1998a)	Circum-Antarctic	MAT	LGM
Crosta et al. (1998b)	Circum-Antarctic	MAT	LGM
Gersonde et al. (2005)	Circum-Antarctic	MAT	LGM (23,000–19,000 year)
South Atlantic Sector (including Weddell and Scotia Seas)			
DeFelice (1979)	South Atlantic	Total diatom relative abundance	Late Quaternary (<300,000 year)
Burckle et al. (1982)	South Atlantic and Pacific	Sediment type	LGM
Burckle and Burak (1988)	South Atlantic	*Eucampia* abundances and IKM	LGM
Burckle and Mortlock (1998)	South Atlantic and Pacific	% opal proxy	LGM
Gersonde and Zielinski (2000)	South Atlantic	*Fragilariopsis* proxies	Late Quaternary (~138,000 year)
Frank et al. (2000)	South Atlantic	*Fragilariopsis* proxies	Late Quaternary (<150,000 year)
Hodell et al. (2001)	South Atlantic	MAT	Holocene (<10,000 year)
Bianchi and Gersonde (2002)	South Atlantic and west Indian	*Fragilariopsis* proxies	Late Quaternary (70,000–140,000 year)
Kunz-Pirrung et al. (2002)	South Atlantic	*Fragilariopsis* proxies	Mid-Late Pleistocene (423,000–362,000 year)
Shemesh et al. (2002)	South Atlantic	MAT	Holocene–Late Quaternary (<35,000 year)
Gersonde et al. (2003)	South Atlantic	*Fragilariopsis* proxies	LGM (23,000–18,000 year)
Nielsen et al. (2004)	South Atlantic	MAT	Holocene (<12,500 year)
Stuut et al. (2004)	South Atlantic and SW Pacific	MAT	Late Quaternary (<45,000 year)
Bianchi and Gersonde (2004)	South Atlantic	*Fragilariopsis* proxies	Holocene–Late Quaternary (<25,000 year)
Schneider-Mor et al. (2005)	South Atlantic	*Fragilariopsis* proxies	Late Quaternary (<640,000 year)
Abelmann et al. (2006)	South Atlantic	*Fragilariopsis* proxies	Late Quaternary (<70,000 year)
Collins et al. (2007)	Scotia Sea	*Fragilariopsis* proxies	Late Quaternary (<60,000 year)
Schneider-Mor et al. (2008)	South Atlantic	*Fragilariopsis* proxies	Late Quaternary (<660,000 year)
South Indian Sector (including Kerguelen Plateau, Prydz Bay, East Antarctica)			
Kaczmarska et al. (1993)	Kerguelen Plateau	*Eucampia* ratio proxy	Quaternary (< 800,000 year)
Rathburn et al. (1997)	Mac. Robertson Shelf, Prydz Bay	Diatom assemblages	Late Holocene (<8000 ^{14}C years BP)
McMinn (2000)	Vestfold Hills, Prydz Bay	Fast ice, benthic and snow indices	Late Holocene (<3233 ^{14}C years BP)
Cremer et al. (2001)	Windmill Islands, East Antarctica	Diatom assemblages	Late Quaternary

Table 13.1 (*Continued*)

Reference/year	Region	Method	Time period (BP*)
Taylor and McMinn (2001)	Mac. Robertson Shelf, Prydz Bay	PCA	Holocene (<10,700 ^{14}C years BP)
Taylor and McMinn (2002)	Prydz Bay	PCA	Late Pleistocene (<21,320 ^{14}C years BP)
Whitehead and McMinn (2002)	Kerguelen Plateau	Sea ice versus open ocean diatom assemblage ratio	Quaternary–Pliocene
Cremer et al. (2003)	Windmill Islands, East Antarctica	Diatom spp.	Modern Holocene
Escutia et al. (2003)	Wilkes Land, East Antarctica	Diatom abundances, sediment type	Quaternary
Crosta et al. (2004)	Southeast Indian	MAT	Late Quaternary (<220,000 year)
Whitehead et al. (2005)	South Indian	GLM – New *Eucampia* proxy	Modern, Early-Late Pliocene
Stickley et al. (2005)	Mac. Robertson Shelf, Prydz Bay	Diatom lamination types	Holocene (~11,000 year)
Maddison et al. (2006)	George V Coast, East Antarctica	Diatom lamination types	Holocene (9809–13,267 ^{14}C year)
Denis et al. (2006)	Adélie Land, East Antarctica	Diatom lamination types	Holocene (1000–9600 year)
Crosta et al. (2007a)	Adélie Land, East Antarctica	% *F. curta*, *Thalassiosira antarctica* and *Chaetoceros Hyalochaete* resting spores	Holocene (<9000 year)
Crosta et al. (2007b)	Adélie Land, East Antarctica,	% *F. curta*	Holocene (<9000 year)

South Pacific Sector (including Ross Sea, Antarctic Peninsula)

Burckle et al. (1987)	NZ to Ross Sea transect	IKM, % *F. curta* and *F. kerg.*	Modern
Leventer and Dunbar (1988)	McMurdo Sound, Ross Sea	% *F. curta* and *Thalassiosira* spp.	Modern–Late Holocene (<500 ^{14}C years BP)
Leventer et al. (1993)	Granite Harbor, Ross Sea	% *F. curta*, *F. cylindrus*, *Corethron* and *Chaetoceros* spp.	Modern–Late Holocene (<1250 ^{14}C years BP)
Leventer et al. (1996)	Palmer Deep, Antarctic Peninsula	Low-salinity meltwater proxy	Late Holocene (< 3700 ^{14}C years BP)
Shevenell et al. (1996)	Lallemand Fjord, Antarctic Peninsula	Total organic carbon, centric-pennate diatom ratio	Late Holocene (< 9700 ^{14}C years BP)
Nishimura et al. (1998)	Ross Sea	Diatom abundances, sediment type	Late Quaternary (<38,000 ^{14}C years BP)
Bárcena et al. (1998)	Bransfield Strait, Antarctic Peninsula	% Sea ice taxa, *Thalassiosira antarctica/T. scotia*	Late Holocene (<2810 ^{14}C years BP)
Cunningham et al. (1999)	Ross Sea	PCA	Holocene (≤ c.12,000 ^{14}C years BP)
Taylor et al. (2001)	Lallemand Fjord, Antarctic Peninsula	Cluster analysis, ANOVA regression, *Thalassiosira antarctica* sea ice regime proxy	Late Holocene (<10,500 ^{14}C years BP)
Bárcena et al. (2002)	Bransfield Strait, Antarctic Peninsula	% Sea ice taxa, *Thalassiosira antarctica/T. scotia*	Late Holocene (<6000 ^{14}C years BP)

Table 13.1   (*Continued*)

Reference/year	Region	Method	Time period (BP*)
Yoon et al. (2002)	Western Antarctic Peninsula	Low-salinity meltwater and *Fragilariopsis* proxies	Holocene–Late Quaternary (<15,000 ^{14}C years BP)
Leventer et al. (2002)	Palmer Deep, Antarctic Peninsula	*Eucampia antarctica* varieties	Holocene (<13,000 year)
Sjunneskog and Taylor (2002)	Palmer Deep, Antarctic Peninsula	Total diatom abundance	Holocene (<13,200 year)
Taylor and Sjunneskog (2002)	Palmer Deep, Antarctic Peninsula	Cluster analysis, ANOVA regression *Thalassiosira antarctica* sea ice regime proxy	Holocene (<13,200 year)
Maddison et al. (2005)	Palmer Deep, Antarctic Peninsula	Diatom lamination types	Holocene (11,460–13,180 year)
Finocchiaro et al. (2005)	Ross Sea	Diatom lamination types	Holocene (<9500 year)
Heroy et al. (2007)	Bransfield Basin, Antarctic Peninsula	Cluster analysis, ANOVA regression,	Holocene (<10,650 year)

Relevant modern sea-floor database distributions

DeFelice and Wise (1981)	South Atlantic	Q-mode analysis, abundance distribution	Modern
Pichon et al. (1987)	South Atlantic	Q-mode analysis, IKM	Modern
Leventer and Dunbar (1988)	Ross Sea	Abundance distribution	Modern
Leventer (1992)	East Antarctica, George V Land	Abundance distribution	Modern
Taylor et al. (1997)	East Antarctica, Prydz Bay	PCA	Modern
Zielinski and Gersonde (1997)	South Atlantic	Abundance versus SST	Modern
Cunningham and Leventer (1998)	Ross Sea	PCA	Modern
Armand et al. (2005)	South Atlantic and South Indian	Abundance versus sea ice parameters	Modern
Crosta et al. (2005)	South Atlantic and South Indian	Abundance versus sea ice parameters	Modern
Whitehead et al. (2005)	South Indian	GLM-New *Eucampia* proxy	Modern
Buffen et al. (2007)	Western Antarctic Peninsula	PCA, *Thalassiosira antarctica* sea ice regime proxy	Modern
Pike et al. (2008)	Western Antarctic Peninsula	DCA, PCA	Modern

*Ages are given as calendar years before present, unless stated otherwise. All ages are indicative only due to independent age models that may include reservoir corrections. Species listed are illustrated in Fig. 13.2. Explanation of statistical methods listed are described in the supporting references, major methods are described in this chapter. Key: IKM: Imbrie and Kipp Methodology; MAT: Modern Analogue Technique; PCA: Principal Component Analysis; GLM: Generalized Linear Model with logit link; DCA: Detrended Correspondence Analysis; LGM: Last Glacial Maximum.

Table 13.2 Summary of Antarctic sea ice proxies, their interpretation and source references.

Proxy	Sea ice interpretation	References
Fragilariopsis curta and *F. cylindrus* relative abundance*	>3% indicates 'averaged maximum' extent of winter sea ice obtained	Gersonde and Zielinski (2000)
	>1% indicates maximum winter sea ice extent	Gersonde et al. (2003)
Fragilariopsis obliquecostata relative abundance*	>3% and with low sedimentation rate indicates average summer sea ice edge and near or total year-round sea ice cover	Gersonde and Zielinski (2000)
Grouped sea ice taxa abundances	>3% means sea ice cover	Bárcena et al. (1998)
Modern Analogue Technique	Statistical average and standard error of modern analogue sea ice conditions (annual sea ice cover in months per year) based on diatom assemblage comparisons	Prell (1985), Crosta et al. (1998a)
Eucampia ratio	Ratio of intercalary and terminal valves, decreasing ratio indicates increasing sea ice cover	Kaczmarska et al. (1993)
Eucampia variety ratio	Ratio of sub-polar to polar variety, increasing ratio indicates colder water masses	Leventer et al. (2002)
Eucampia Generalized Linear Model	Statistical estimates of September sea ice concentrations based on entries of the *Eucampia* ratio	Whitehead et al. (2005)
Biogenic opal %	Increase in opal % linearly attributed to the decrease in annual sea ice cover	Burckle and Mortlock (1998)
^{13}C organic matter	Increase in isotope value indicative of increasing sea ice hosted algae, sea ice cover	Gibson et al. (1999)
Methanesulphonic Acid (MSA)	Increases in MSA are interpreted as increases in winter sea ice extent – valid in East Antarctic, negative correlation in Weddell Sea	Curran et al. (2003), Abram et al. (2007)
Sea salt sodium (ssNa)	Increases in flux are interpreted as increases in winter sea ice areal extent within oceanic source area	Wolff et al. (2006), Iizuka et al. (2008)

*Combined, these two proxies are referred to as the *Fragilariopsis* proxies in this chapter.

excess of 3% were considered representative of the averaged maximum extent of winter sea ice in the Weddell Sea. The 1% minimum abundance level has recently been used to indicate the maximum winter sea ice extent in the South Atlantic (Gersonde et al., 2003). The summer sea ice edge was defined by relative abundances of *Fragilariopsis obliquecostata* exceeding 3% relative abundance (Fig. 13.2). Application of this latter proxy is based on evidence that the abundances of the thickly silicified *F. obliquecostata* are coincident with markedly low sedimentation rates as a result of near or total year-round sea ice cover (Gersonde &

Zielinski, 2000; Frank et al., 2000). Often, these two *Fragilariopsis* proxies are shown in contrast to the abundance of the open ocean species, *Fragilariopsis kerguelensis* (Bianchi & Gersonde, 2004; Abelmann et al., 2006; Fig. 13.2). In other instances, grouped sea ice taxa (i.e. *F. curta*, *F. cylindrus*, *F. obliquecostata*, *F. sublinearis* and *F. vanheurkii*) are used to define the sea ice proxy (Bárcena et al., 1998, 2002, personal communication).

Annual sea ice cover and maximum sea ice extents (summer and winter) are determined from application of the MAT to take into account species abundances and their individual relationships to sea ice cover. The basis of this approach is to avoid single representation of the sea ice condition by one or two species, and to use all diatom data available (i.e. generally species with more than 2% relative abundance) with the purpose of extracting subtle variations through statistical analysis (Crosta et al., 1998a,b). The MAT compares the diatom assemblage data down-core to a subset of modern core-top analogues within a larger Southern Ocean data set by calculating a dissimilarity coefficient between the down-core sample and the core-top analogue (Prell, 1985; Crosta et al., 1998a). The sea ice estimates provided by MAT are weighted averages of the core-top analogues and each estimate is reported with a standard error of the estimate, an improvement over the Imbrie and Kipp (1971) statistical method used in the past (Table 13.1). The main disadvantages of MAT are the need for an extensive distribution of core-top samples for the analogue situations, and problems associated with the dissolution of frustules and the winnowing of an assemblage by sea-floor currents relative to modern and past conditions.

Although some studies have relied on using simple assemblage abundances or selected abundance ratios to indicate a dominance of sea ice taxa over time, none of these methods provides quantitative estimates of sea ice cover or extent (Tables 13.1 and 13.2). The only other significant Open Ocean Quaternary/Pliocene method utilizing an indicator species has been the *Eucampia* proxy. Kaczmarska et al. (1993) employing knowledge of chain length differences between the short-chained polar and long-chained sub-polar varieties of *E. antarctica* devised a ratio of flat-apexed intercalary valves to pointy-apexed terminal valves (Fig. 13.2) to define the northern limit of winter sea ice. A decrease in the *Eucampia* ratio indicated increasing winter sea ice cover. Although the *Eucampia* ratio held much promise, it was rarely employed in sea ice estimation studies, and was criticized for a lack of ground-truthing in respect to modern sea-floor distributions of *Eucampia* varieties (Armand, 2000; Gersonde & Zielinski, 2000). One study used the *Eucampia* proxy, referred to as the *Eucampia* index method, to infer SST <4°C (Gersonde et al., 2003). Leventer et al. (2002), however, took another approach and used the morphological differences between the two varieties, the sub-polar variety asymmetrically shaped in contrast to the polar variety symmetrically formed (Fig. 13.2), to determine a ratio that indicated the presence of cold or warm water masses. Similarly, Taylor and Sjunneskog (2002) used the incidence of the sub-polar variety to indicate incursion of warm water to the Antarctic coast. Nonetheless, Whitehead et al. (2008) reapplied the *Eucampia* proxy in a more statistical manner from Prydz Bay and Kerguelen Plateau region after calibrating the method from 12 modern sea-floor samples against a 9-year averaged series of September sea ice concentrations. They used a new statistical approach, a bootstrapped Generalized Linear Model, to define the relationship and entered the Kaczmarska-based *Eucampia* ratio to provide estimates of Pliocene winter sea ice concentrations.

In earlier work on the Kerguelen Plateau, Whitehead and McMinn (2002) produced a ratio of two Principal Component Analyses (PCA)-determined assemblages and on a summer–spring sea ice cover interpretation across the Quaternary-Late Neogene. They interpreted

extended spring–summer sea ice across the southern Kerguelen Plateau consisting of open pack ice capable of supporting two species currently associated with different habitats (*Fragilariopsis curta* – sea ice, *Thalassiosira lentiginosa* – open ocean, Fig. 13.2) and thus called into question the retreat of summer sea ice to modern extents during the LGM (Crosta et al., 1998a). Whitehead and McMinn (2002) supported their sea ice cover analogy by arguing that the use of modern species assemblages could lead to erroneous environmental estimations for glacial conditions because non-analogue mixed assemblages, which they had encountered, could be overlooked. The influence of bottom water pathways and winnowing, which were considered instrumental to their IRD lag deposits in the same cores, might also displace *F. curta* into an otherwise open ocean assemblage sediment accumulation and could be an alternative interpretation for their conclusions. Transport of *F. curta* northwards along the Kerguelen Plateau was shown recently by Armand et al. (2008).

Holocene-aged, Antarctic shelf sediment investigations have required different solutions to describe past sea ice cover, or perhaps more precisely absence of sea ice, due to the lack of significant coastal sea-floor databases or local sediment trap surveys upon which to draw calibrations. These investigations depend on ecological occurrence proxies in place of statistical methodologies, with exception of the PCA (Taylor & McMinn, 2001; Table 13.1). The PCA, however, does not lead to quantitative estimates of sea ice cover, but rather provides statistically meaningful assemblages that are either representative of the presence or absence of sea ice cover.

Many Holocene records include very high resolution laminated or varved sediment layers, indicating periods of rapid sedimentation from enhanced primary productivity events in the surface waters (Leventer et al., 2006). Lamination studies including scanning electron imagery and X-ray scanning have relied on teasing apart the faunal assemblage compositions and terrigenous input to sediments. These fine-scale analyses have elucidated regional seasonal and sub-seasonal changes from the laminations, the results of which are seasonal diatom signatures tied to likely physical conditions including sea ice onset and retreat (Cunningham et al., 1999; Taylor et al., 2001; Leventer et al., 2002; Taylor & Sjunneskog 2002; Stickley et al., 2005, 2006; Maddison et al., 2005, 2006; Denis et al., 2006; Buffen et al., 2007). Examples of signature species include: *Chaetoceros Hyalochaete* resting spores as indicators of earliest spring productivity after spring sea ice melt, *Porosira glacialis* resting spores representative of autumn sea ice formation and *Corethron* species as indicative of a nearby sea ice edge (Maddison et al., 2006; Fig. 13.2) or an autumn phytoplankton bloom fallout (Leventer et al., 2002). These associations have not, however, been calibrated against annual cycle data from sediment traps. *Thalassiosira tumida* laminae are also considered indicators of conditions in late autumn prior to significant sea ice formation (Stickley et al., 2006; Fig. 13.2). *Cocconeis* spp. and *Thalassiosira gracilis* have been used to indicate increased storm frequency and sea ice duration (Taylor & Sjunneskog, 2002; Heroy et al., 2007; Fig. 13.2). The presence of *Thalassiosira antarctica* has been used as a proxy of late summer/early autumn salinity change or an autumn/winter sea ice formation marker (Cunningham et al., 1999; Leventer et al., 2002; Stickley et al., 2005; Denis et al., 2006; Crosta et al., 2007a,b; Fig. 13.2). This last species has been proved additionally useful in the understanding of past climatic conditions due to its morphological plasticity under differing environmental conditions (Taylor et al., 2001; Taylor & Sjunneskog, 2002; Domack et al., 2003; Buffen et al., 2007). Two forms are recognized: a smaller, tight aerolated form considered representative of greater seasonal duration of sea ice cover and lower productivity and a larger, more ornate form indicative of warmer waters and elevated productivity (Fig. 13.2). Some have used *Thalassiosira*

antarctica (open ocean indicator) in a ratio with *Fragilariopsis curta* and *F. cylindrus* (sea ice) to determine increases and decreases in the volume of low-salinity sea ice meltwater (Leventer et al., 1996; Yoon et al., 2002).

Regardless of these various species associations during the absence of sea ice, the determination of extensive sea ice conditions and the potential period of sea ice cover over the Antarctic shelf remains firmly in the observation of the 'iconic' sea ice indicator species, *Fragilariopsis curta*. The abundances of this species could now be statistically calibrated against the extent of sea ice along the Adélie Land coast given the detailed understanding of their abundance variations over warm and cold phases of the Holocene (Crosta et al., 2007a,b). A need for supplementary observations from sediment trap, culture and surface water studies on their bloom and fallout periods, and life cycle traits with respect to environmental conditions are nevertheless required in this region.

Modern sea ice satellite data used in diatom proxy statistical analyses

In earlier proxy estimations, several authors (Pichon et al., 1987; Bárcena et al., 2002; Stuut et al., 2004; Crosta et al., 2004) relied on the Naval Oceanography Command Detachment (1985) data maps to determine sea ice cover parameters. These maps used mainly visible and infrared satellite data, primarily from AVHRR (Advanced Very High Resolution Radiometer – Chapter 6) to determine the ice edge. Current transfer function methods now use a 13.25-year series (1978–1991) of monthly sea ice concentration averages derived from SMMR and SSM/I satellites via the NASA Team algorithm (Schweitzer, 1995). Schweitzer's compilation is based entirely on passive-microwave data and defines the sea ice edge as 15% sea ice concentration. This 15% concentration definition of the ice edge is routinely used by sea ice researchers (Gloersen & Cavalieri, 1986; Cavalieri et al., 1995; Worby & Comiso, 2004; Chapter 6). Biases between the visible and passive-microwave sea ice databases are thus expected, not only because of the difference in technique, but also because the ice edge was defined differently (J.C. Comiso, pers. comm.). This has implications because sea ice extent estimated using the different methodologies may vary.

There is a need for a new source sea ice database to support palaeoproxy research. This should be constructed with consensus between sea ice observers and palaeo sea ice researchers. The database would need to allow the user to define an appropriate algorithm (NASA Team or Bootstrap; see Chapter 6) and the period over which the source data are averaged (the current first ~13 years of data may be too small in determining the average concentration). We need to ask ourselves, will a certain year eventually be described as the turning point for the effects of global warming, and therefore confine a sea ice concentration database for palaeoceanographic purposes? An option to vary the ice concentration value at which the sea ice edge is defined conservatively for palaeoceanographic purposes (e.g. 15% current definition for the unconsolidated sea ice edge or 40% modern interpretation of the consolidated sea ice edge) would also be valuable.

Continental ice core sea salt proxies

Ice core records, from coastal and inland Antarctic sites, are also used to determine sea ice cover via aerosol proxies. Two major proxies, MSA and sea salt sodium, are currently employed and are likely to provide the highest resolution sea ice histories. They also provide regional averages of sea ice extent, in contrast to the point location histories given by the diatom sediment core records.

Dimethylsulphide (DMS) is produced in the surface ocean predominately by phytoplankton and large amounts are released to the atmosphere during sea ice decay where it is oxidized to MSA (Curran & Jones 2000; Chapters 8 and 12). MSA is transported south and inland where it is deposited with snow precipitation on the Antarctic continent. MSA concentrations in Antarctic ice cores are linked to the amount of open ocean within the sea ice zone available for primary productivity, and at some sites this gives a good proxy for maximum sea ice extent (Curran et al., 2003). An MSA proxy for maximum winter sea ice extent (August–October) was developed by Curran et al. (2003) following observations linking sea ice extent with MSA concentrations (Welch et al., 1993). The proxy MSA record from Law Dome (66.7°S, 112.8°E) was calibrated against 21 years of overlapping satellite ice extent observations for the atmospheric source region between 80° and 140°E, where the strongest correlation occurred. When this proxy was applied to a longer 54-year Law Dome ice core MSA record, it showed a 20% decrease in maximum sea ice extent for the region since the 1950s, from 59.3°S to 60.8°S.

MSA records from other Antarctic coastal sites (Ross Sea, Amundsen-Bellingshausen Sea, East Antarctic coast) were also found to be good proxies for sea ice extent (Welch et al., 1993; Steig et al., 1998; Foster et al., 2006; Abram et al., 2007). At some sites in the Weddell Sea sector, negative correlations were found between MSA and sea ice extent (Pasteur et al., 1995; Abram et al., 2007). A number of factors can confuse the MSA proxy including atmospheric transport strength, type of precipitation (wet = with water such as snow and crystals, dry = as a precipitate without water), presence of multiyear ice, the amount of open ocean in summer and movement of sea ice in gyres (Curran et al., 2003; Abram et al., 2007). The use of MSA as a proxy for sea ice extent thus becomes dependent on region. Given the wet deposition, atmospheric patterns and modern warm interglacial conditions under which the MSA sea ice extent proxy has been developed, the extension of the proxy for use during glacial periods remains a challenge. In particular, precipitation at most coastal locations during colder glacial periods is thought to be analogous to current dry deposition at inland Antarctic sites (van Ommen et al., 2004).

Petit et al. (1999) hypothesized that variations in the Vostok ice core sodium concentrations are related to sea ice extent. This was confirmed by a comparison between the Vostok record and diatom-derived, sea ice cover estimates from a South Atlantic deep sea core (Shemesh et al., 2002). Sea salt tracers derived from continental ice cores, particularly sea salt sodium (ssNa), have subsequently been proposed as a potential proxy source of information on past sea ice coverage (Wolff et al., 2003, 2006). A doubling of ssNa flux values in the European Project for Ice Coring in Antarctica (EPICA) Dome C ice core and the concomitant approximate doubling of circumpolar sea ice extent, estimated from diatom–sea ice proxies, during the EPILOG (Environmental Processes of the Ice Age: Land, Oceans, Glaciers programme) time slice provided some evidence for this (Gersonde et al., 2005). Wolff and colleagues, however, concluded that the ssNa proxy was only useful over millennial timescales, where ssNa flux is synchronous with temperature. The relationship between ssNA flux and temperature did not hold at shorter timescales. Discussion on the validity of this approach hotly ensured, since this sea ice proxy was not strictly validated against the sea ice extent within the source area for sea salts to Dome C (Abram et al., 2007; Curran et al., 2008). This was very recently corrected in a study of ssNa fluxes from an ice core and snow pit samples from Dome Fuji (Iizuka et al., 2008). This study revealed that the annual average ssNa flux from 1980 to 2000 was in clear linear proportion with the

summed annual extent of new sea ice in the Indian and Weddell Sea sectors, which are the combined source areas for Dome Fuji precipitation. As with the MSA proxy, this validation does not cover glacial conditions and interpreting the ssNA proxy beyond warm intervals requires caution. This said, Röthlisberger and colleagues (2008) found threshold limitations between air temperature (from ice core deuterium records) and the response of the ssNA flux record across the glacial-interglacial transitions at Dome C. They showed that saturation of the ssNA record occurred at temperatures 5°C below (δD of –420‰) current Antarctic plateau temperatures. This results in a decreased sensitivity between sea ice extent in the source area and sea salt during maximum glacial conditions, and a delayed response of ssNa against temperature during terminations. The same decrease in sensitivity is also apparent in the Dome Fuji ssNa flux record as it extends back into the LGM(Iizuka et al., 2008).

Sea salts have traditionally been thought to be sourced from bubbles bursting in the open ocean (Curran et al., 2008). However, the development of frost flowers on newly formed sea ice has recently been proposed as a significant source (Rankin et al., 2000, 2002). Release of bromide from snow-covered sea ice may also contribute as a source of sea salt tracers (Yang et al., 2008). Debate exists regarding the source of aerosol input of ssNa from the sea ice to inland Antarctic core sites such as EPICA Dome C, particularly in glacial periods when continental sources of sodium have been shown to represent a third of the sodium ions and the input of frost flower–sourced ssNa is limited away from the coast (Bigler et al., 2006; Curran et al., 2008). Research into the use of sea salt tracers as sea ice markers from Antarctic ice core sites is an ongoing research theme (Weller & Wagenbach, 2007; Curran et al., 2008; Röthlisberger et al., unpublished data).

Other tracers

Other methods of determining Antarctic sea ice extent or concentration have also been attempted. Bromwich (1984; personal communication) used correlations between stable-isotope changes in early Antarctic ice core records, modern snow $\delta^{18}O$ observations and the diatom-based sea ice estimates of Burckle et al. (1982) to define the summer and winter sea ice extent. The method requires fresh evaluation in light of advances in ice core recovery and interpretation. Burckle and Mortlock (1998) hypothesized that the percentage of biogenic opal in surface sediments could be used to estimate annual sea ice cover as a percentage over a site. They based this approach on the role sea ice plays in manipulating surface water productivity and export in regions partly covered by annual sea ice. Gibson et al. (1999) observed increasing carbon isotope values with the presence of sea ice–hosted phytoplankton, and hence proposed the use of ^{13}C-rich organic matter as an indicator of past sea ice cover. New research into various isotopic, trace element and biomarker signatures of the sea ice environment are gaining momentum and may lead to new proxies of sea ice cover during the Holocene (Carson & Ganeshram, 2006; Belt et al., 2007).

Time-slice palaeo sea ice reconstructions

We break up the Antarctic record into several time periods for the remaining discussion. Figure 13.3 indicates the location of many of the cores or studies (ice and sediment) referred to in the text.

Pre-satellite – Last 1000 years

Satellite sea ice coverage has been available for a little over 30 years now and thus we have a reasonable indication of sea ice extent and variability in the most recent past (Cavaleri & Parkinson 2008; Chapter 6). Pre-satellite records of sea ice that cover the past 100 years have been derived from whaling records (Parkinson, 1990; de la Mare, 1997; Ackley et al., 2003), penguin population records (Barbraud & Weimerskirch, 2001; Wilson et al., 2001; Massom et al., 2009; Chapter 11) and aerosol tracers (MSA, ssNa) from ice cores (Curran et al., 2003; Iizuka et al., 2008). de la Mare's (1997) summer sea ice extent determined from whaling ship records suggests a 25% decrease between the mid-1950s and early 1970s. The use of whaling records alone, with lack of reference to historically reported sea ice edge data, was questioned by Vaughan (2000), opening the discussion of whether or not summer sea ice extent had indeed extended so far northwards. The topic was pursued by Ackley et al. (2003) who concluded that the 25% decrease was untenable over the 1950s to 1970s. They argued that on one hand, the whaling reports were biased and that on the other hand the sea ice extent was influenced by decadal changes in the Southern Annual Mode.

Adélie penguin population changes in the Ross Sea region, covering roughly the same period of time as the de la Mare study, are presented as a proxy for winter sea ice extent by Wilson et al. (2001). In this study, smaller penguin population numbers were found to be highly correlated to a greater ice extent 5 years earlier, the offset between the parameters being related to the 3–7-year sub-adult survival to breeding capability. The penguin population study suggests that sea ice extent was greater in the winter seasons from the 1950s to the early 1970s, whereas in the overlapping satellite record era, penguin populations increased relative to a decreased winter sea ice extent. Emperor penguin studies covering the past 50 years expose links between decreased adult survival and diminished annual sea ice extent, and conversely, decreased hatching success with increased winter sea ice extension (Barbraud & Weimerskirch, 2001). Other Antarctic birds have shifted arrival and breeding times by several days due to the decrease in east Antarctic sea ice extent (Barbraud & Weimerskirch, 2006). The relationship between short-term pack ice and fast ice anomalies and biotic responses have been investigated by Massom et al. (2006, 2009). The link between sea ice cover and higher predator success is potentially an area that can provide further information on the historical regional sea ice and climate conditions in the Antarctic.

Most of the pre-satellite records imply that sea ice conditions were more extensive than over the past 30 years. Yet, unlike the Arctic, Antarctic historical records of the most recent large potential sea ice expansion, the Little Ice Age (LIA, maximum cold conditions ~200 years BP, Fig. 13.4), remain lacking and inconclusive (Parkinson, 1990). Indications from the Law Dome $\delta^{18}O$ ice core record suggest both greater cooling and more variability in winter temperatures coincident with the LIA. This was hypothesized as owing to a change in winter sea ice extent (Morgan & van Ommen, 1997). Several investigations along the Antarctic Peninsula continental shelf and within embayments of the Ross Sea have conclusively (Leventer and Dunbar, 1988; Bárcena et al., 1998, 2002) or cautiously (Shevenell et al., 1996; Leventer et al., 1993, 1996) identified the LIA from increases in sea ice taxa. In general, increases in abundances of sea ice taxa, particularly *F. curta*, and notable decreases in productivity-associated taxa, such as *Chaetoceros* resting spores, provide evidence of this cooling event. An exception occurs in McMurdo Sound. There a decrease in *F. curta* and increase in *Thalassiosira antarctica* abundances are interpreted as being due to an activation of the Ross Polynya from increased winds during the LIA (Leventer & Dunbar, 1988).
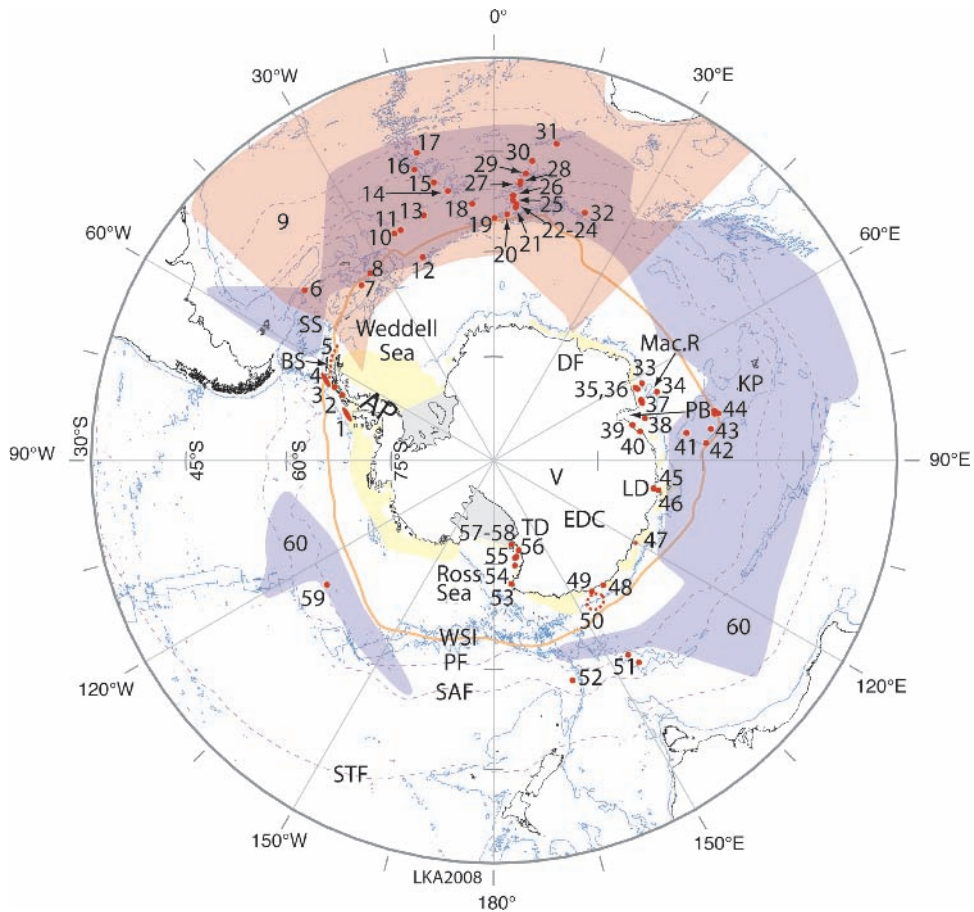
Fig. 13.3 Location of studies or core sites discussed in the text relevant to sea ice histories around Antarctica, excluding the study of Gersonde et al., 2005 (see Fig. 13.5). 3000 m bathymetric contour from GEBCO, Oceanic Fronts Orsi et al. (1995). Red shading = 9 in Key. Abbreviations: STF = Sub-Tropical Front; SAF = Sub-Antarctic Front; PF = Polar Front; WSI = maximum winter sea ice edge as yellow line; Yellow shading = maximum summer sea ice extent; AP = Antarctic Peninsula; BS = Bransfield Strait; SS = Scotia Sea; Mac.R = Mac.Roberston Shelf; PB = Prydz Bay; KP= Kerguelen Plateau; DF = Dome Fuji; LD = Law Dome; EDC = EPICA Dome C; V = Vostok; TD = Taylor Dome. Key: 1 = 15 cores: Villa et al. (2003); 2 = Lallemand Fjord, PD92-II-01GC1: Shevenell et al. (1996), Taylor et al. (2001); 3 = Palmer Deep ODP 1098B, PD92-30: Leventer et al. (1996), Leventer et al. (2002), Sjunneskog and Taylor (2002), Taylor and Sjunneskog (2002), Maddison et al. (2005); 4 = GC03,-02, NCS09: Yoon et al. (2002); 5 = Bransfield Strait and Basin: G-1 and G2, A-3 and A-6: Báarcena et al. (1998, 2002); S-2 and S-19: Yoon et al. (2000); GC00-13 and EB-2: Bahk et al. (2003); NBP0201-PC61: Heroy et al. (2007); 6 = PC063: Collins et al. (2007); **7** = PS2603-3: Bianchi and Gersonde (2002); 8 = PS2305-6: Gersonde and Zielinski (2000), Bianchi and Gersonde (2002); 9 = 50 core coverage zone: Gersonde et al. (2003); 10 = PS22-76-4: Gersonde and Zielinski (2000), Bianchi and Gersonde (2002); 11–14 = RC11-76, IO1578-4, RC11-77, RC11-78: Burckle and Mortlock (1998); 15–17 = PS1778-5, PS2499-5, PS2498-1: Gersonde and Zielinski (2000); 18 = PS2102-2: Bianchi and Gersonde (20020; 19 = PS1772-8: Gersonde and Zielinski (2000), Frank et al. (2000), Bianchi and Gersonde (2002); 20–21 = PS1649-2, PS1652-2: Gersonde and Zielinski (2000); 22 = ODP1094: Bianchi and Gersonde (2002, 2004),Kunz-Pirrung et al. (2002), Schneider-Mor et al. (2005, 2008); 23 = TTN057-13: Hodell et al. (2001), Shemesh et al. (2002), Stuut et al. (2004); 24= PS2089-2: Kunz-Pirrung et al. (2002); 25 = PS1768-8: Gersonde and Zielinski (2000), Frank et al. (2000), Bianchi and Gersonde (2002); 26 = RC13-271: Burckle and Mortlock (1998); 27 = TN057-17: Nielsen et al. (2004); 28 = PS1756-5: Frank et al. (2000); 29 = ODP1093: Kunz-Pirrung et al. (2002), Bianchi and Gersonde (2004), Schneider-Mor et al. (2008); 30–31 = PS1754-1, PS2082-1: Frank et al. (2000); 32 = IO1277-10 Burckle and Mortlock (1998); 33 = GC1: Taylor and McMinn (2001); 34 = ODP1165: Whitehead et al. (2005); 35 = GC2: Taylor and McMinn (2001); 36 = NBP01-0143B: Stickley et al. (2005, 2006);. 37 = GC5 and GC35: Rathburn et al. (1997); 38 = ODP1166: Whitehead et al. (2005); 39 = GC29: Taylor and McMinn (2002); 40 = Abel and Platcha Bays: McMinn (2000); 41 = GC34: Whitehead and McMinn (2002); 42 = ODP119 745B: Kaczmarska et al. (1993); 43 = GC48: Whitehead and McMinn 2002);

A continuous MSA record from the Law Dome ice core currently provides an insight into maximum winter sea ice extent since the 1840s (Curran et al., 2003). MSA data show a significant positive relationship with remotely sensed September sea ice extent records between 1973 and 1995. A drop in MSA levels is observed in the Law Dome ice core since the 1950s and, thus, in the region 80–140°E the September sea ice extent is thought to have decreased by approximately 20%. The data suggest that years with greater sea ice extent (in September) produce more MSA (in summer) as a result of the increased ice-covered ocean area, which 'captures' a greater area for the summer biological activity (Curran et al., 2003). Ice core aerosol records are likely to be the best high-resolution solution to confirm and interrelate historical records, satellite data and some of the laminated diatom remains in sediment core records.

Holocene (11,000–1000 year BP)

The Holocene epoch was a period of early warming followed by oscillating periods of Neoglacial cooling events prior to the last cooling (LIA) and the subsequent warming of our current times. Diatom records from the Antarctic continental shelves commonly reveal an early Holocene climatic warming, often identified as the Antarctic Early Holocene Climatic Optimum, ~11.5–9 ka BP (Fig. 13.4). This period was after deglaciation and retreat of the extensive ice shelves around the Antarctic continent from the LGM. Ross Sea studies indicate that during this time sea ice was reduced and open ocean conditions prevailed, but the deposition of terrigenous material from the retreating ice shelves continued (Cunningham et al., 1999; Finocchiaro et al., 2005). In the environs of Prydz Bay and Mertz Glacier, diatom records suggest very high productivity resulting in true seasonal varves or event laminations. These unique environmental records are now thought to be derived from the establishment of ice shelf calving bay re-entrant systems along the continental margin during the deglaciation (Stickley et al., 2005; Leventer et al., 2006; Maddison et al., 2006). Under this scenario, ice shelves retreated into bays gouged by previously advancing ice tongues and released accumulated particles such as iron-rich dust into the generally deeply scoured bays during the meltback of the ice shelf. These pulses were conducive to large productivity blooms and led to the rapid deposition of sediments as laminations. Prydz Bay sea ice cover remained seasonal with spring and summer ice-free. This suggests conditions either close to today's sea ice cover off the shelf or with more open ocean conditions in the bay (Taylor & McMinn, 2001, 2002; Stickley et al., 2005). Along the Adélie Coast and in the Mertz Glacier region, sea ice cover persisted from late autumn through to spring, with a suggestion that the Mertz Polynya played a role in enhancing primary productivity (Denis et al., 2006; Maddison et al., 2006). Some studies

---

Fig. 13.3 (*cont'd*)
44 = GC49 to 51: Whitehead and McMinn (2002); 45 = Bunger Hills-Mumiyo records: Ainley et al. (2006); 46 = Windmill Islands: Cremer et al. (2001, 2003); 47 = E17-17: Burckle and Mortlock (1998); 48 = MD03-2601: Denis et al. (2006), Crosta et al. (2007a,b); 49 = NBP01-01JPC10: Maddison et al. (2006); 50 = Multiple core study region, DF79-13: Escutia et al. (2003); 51 = MD88-787: MD88-784: Armand (1997), Gersonde et al. (2005); 52 = SO136-111: Crosta et al. (2004), Stuut et al. (2004), Ainley et al. (2006); 53 = ANTA02-CH41: Finocchiaro et al. (2005);. 54 = GC1604: Nishimura et al. (1998); 55 = GC1605 and GC1606: Nishimura et al. (1998); 56 = KC208-09, DF89WG35,-17: Leventer et al. (1993) and NBP9501-31,-37,-39: Cunningham et al. (1996); 57 = 8 cores: Leventer and Dunbar (1988); 58 = ANDRILL AND-1B: Scherer et al. (2007); 59 = E20-10: Burckle and Mortlock (1998); 60 = 106 cores: Crosta et al. (1998a,b).
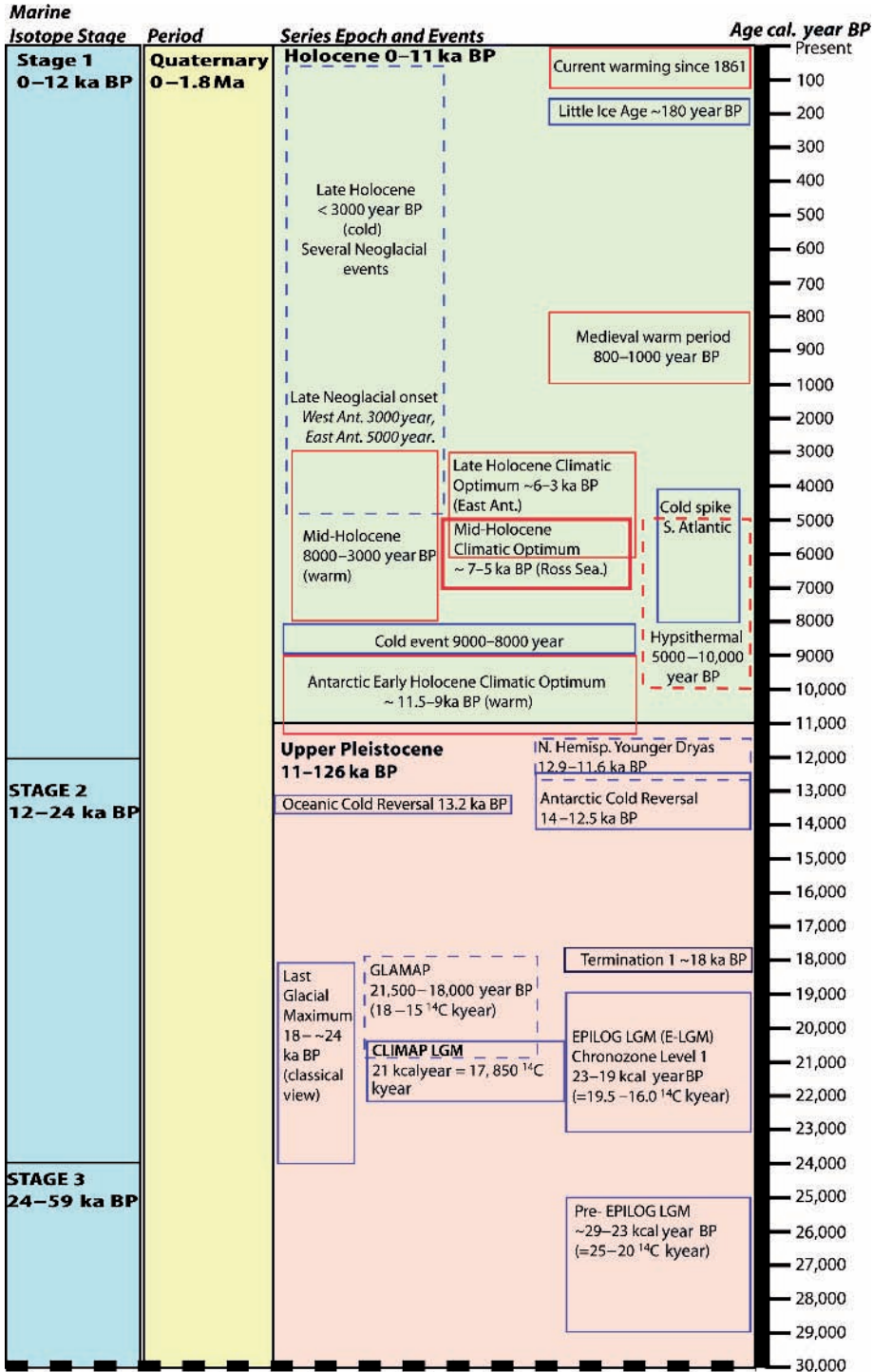
Fig. 13.4 A Holocene and late Quaternary timeline incorporating Antarctic climatological events described in the text.

along the Antarctic Peninsula provide indications of high productivity via elevated *Chaetoceros* resting spores and low sea ice taxa abundances, therefore implying seasonal sea ice cover with spring and summer sea ice–free in the Early Holocene (Yoon et al., 2002; Maddison et al., 2005; Heroy et al., 2007). However, two studies indicate that the first of the cold climatic reversals following the Early Holocene Climatic Optimum had already commenced around 11–9 cal kyears BP (Sjunneskog & Taylor, 2002; Taylor & Sjunneskog, 2002; Fig. 13.4). Nevertheless, the preceding warm phase reveals laminations and elevated abundances of *Chaetoceros* resting spores, indicative of sea ice absence in the spring–summer period. South Atlantic quantitative sea ice estimates based on the *Fragilariopsis* proxies and the MAT suggest this climatic optimum as a period lacking sea ice cover even in the winter months between 53° and 49°S (Hodell et al., 2001; Shemesh et al., 2002; Gersonde et al., 2003; Nielsen et al., 2004; Bianchi & Gersonde, 2004; Schneider-Mor et al., 2008). There are currently no published high-resolution Holocene sea ice estimates from the open ocean regions of the East Antarctic or Pacific sectors of the Southern Ocean.

Extensive sea ice cover and decreased seasonality along the continental margins during the Holocene appears to have occurred on at least two other occasions interrupted by the Mid- (Ross Sea) or Late (East Antarctic) Holocene Climatic Optimum (Fig. 13.4). This optimum is sometimes called the Hypsithermal warming. The earliest of these cold climatic reversals producing increased sea ice has been reported around ~11–8 kyears BP at Palmer Deep, Bransfield Basin and Lallemand Fjord in the Antarctic Peninsula from evidence of increased sea ice taxa and other species linked to polynya-enhanced conditions (Shevenell et al., 1996; Taylor et al, 2001; Sjunneskog & Taylor, 2002; Taylor & Sjunneskog, 2002; Heroy et al., 2007). In the Ross Sea, the cooling is interpreted from increases in *F. curta* and *Eucampia antarctica* abundances suggesting persistent sea ice cover with shorter cool summers (Cunningham et al., 1999; Finocchiaro et al., 2005), whereas along the Adélie coast, increases of *F. curta* and other sea ice taxa compared with the decreases of *F. kerguelensis* and open ocean taxa imply cooler conditions (Crosta et al., 2007a,b). Carbon isotope analyses of snow petrel mumiyo (spit) from the Bunger Hills suggest sea ice is extensive due to the change in the $\delta^{13}C$ composition of the petrel diet. An explanation of the enrichment of the $\delta^{13}C$ signatures is that the petrel's food is sourced further from the shelf (Ainley et al., 2006).

The Mid-Holocene Climatic Optimum/Hypsithermal period (~8000–3000 years BP dependent on sector, Fig. 13.4) is generally distinct as the major warm period of the Holocene. Yet some investigations have suggested conditions were warmer than today and summer sea ice cover was reduced (Crosta et al., 2007a,b; Heroy et al., 2007). In some regions, a minor cold reversal is evident from distinct increases in *F. curta*, *Cocconeis* taxa and lithic inputs (Ross Sea, Finocchiaro et al., 2005, Windmill Islands, Cremer et al., 2001; Antarctic Peninsula, Shevenell et al., 1996; Taylor et al., 2001; Sjunneskog & Taylor, 2002; Taylor & Sjunneskog, 2002).

This interruption of the Mid-Holocene Optimum by a spike of cooler conditions appears to have been registered in cores from the South Atlantic where the *Fragilariopsis* winter proxy exceeds 3% between 8–5 kyearrs BP at ODP site 1094 (53°S, 5°E) and a MAT estimate of 0.5 month of ice cover per year at the same ODP site survey core site, TN057-13PC4, at ~6.5 kyears (Hodell et al., 2001; Bianchi & Gersonde, 2004). Nielsen et al. (2004) also estimate a brief 1 month per year of sea ice cover at a slightly more northern site (50°S) at earlier timings (9.3 and 10.3 kyears BP) yet well within their double-phased Mid-Holocene Climatic Optimum period of little or no winter sea ice cover in this region.

The next major cooling and sea ice advance, in which many consider modern sea ice seasonality patterns were generally established, occurred in the subsequent Late Holocene Neoglacial period (<~5000 years BP East Antarctic, <3000 years BP West Antarctic, Fig. 13.4). Neoglacial oscillating conditions appear best detailed in the Antarctic Peninsula work of Bárcena et al. (1998, 2002) where up to six Neoglacial events are recorded from changes in the mean total abundance of several sea ice taxa against the dominance of *Chaetoceros* resting spore abundances. The former sea ice group exceeds 6%, while the *Chaetoceros* resting spores are diminished to ≤80% of the total community during these Neoglacial episodes. Bárcena et al. (1998, 2002) find that Neoglacial episodes 1 (the LIA) and 3 (~1000–1300 corrected ^{14}C years BP) have the highest levels of sea ice indicator species. The record of sea ice indicator species over the last 3000 years reveals consistent climatic cooling and increase in sea ice generally in the Bransfield Strait.

Other studies covering the Neoglacial period of the Antarctic Peninsula (<~4000 years BP), in less precise detail, also indicate cooler conditions with the decrease in *Chaetoceros* resting spores and increases in sea ice taxa such as *F. curta*, *Eucampia antarctica* and *Thalassiosira antarctica* winter varieties/forms, and ratios of species or diatom categories (Shevenell et al., 1996; Taylor et al., 2001; Leventer et al., 2002; Taylor & Sjunneskog, 2002; Yoon et al., 2002; Heroy et al., 2007). Perhaps, more importantly, some of these studies identify, from the elevated incidence of two diatoms (*Cocconeis* spp. and *Thalassiosira gracilis*), windier conditions and greater wave action as a result of increased storminess (Taylor & Sjunneskog, 2002; Heroy et al., 2007). Sea ice conditions in the Antarctic Peninsula are described as representing a protracted winter particularly at the onset of the Neoglacial but with shorter periods of meltwater stratification in spring due to the increasing winds (Taylor & Sjunneskog, 2002; Heroy et al., 2007). In the South Atlantic open ocean, most Holocene diatom profiles indicate conditions largely representative of the modern condition, particularly from ~3000 year BP (Hodell et al., 2001; Shemesh et al., 2002; Bianchi & Gersonde, 2004; Nielsen et al., 2004). Nonetheless, two studies indicate winter sea ice extent, estimated from MAT and the *Fragilariopsis* winter proxy, as having reached 53°S from onset of the Neoglacial until ~1–2 ka BP (Gersonde & Zielinski, 2000; Hodell et al., 2001; Bianchi & Gersonde, 2004). These observations were in phase with SST decreases and an increase in IRD (Hodell et al., 2001). Bianchi and Gersonde (2004) were able to postulate from other diatom occurrences that the extended sea ice extent afforded a prolonged summer growing season after early spring melting.

In the East Antarctic sector within and nearby the environs of Prydz Bay, several diatom records from the fjords and along the Mac.Roberston Land shelf indicate a period of climatic instability and more permanent sea ice cover at the onset of the Neoglacial followed by establishment of modern sea ice conditions with summer sea ice–free period of up to 2 months per year in place by ~2000 years BP (Rathburn et al., 1997; McMinn, 2000; Taylor & McMinn, 2001, 2002). Adélie Land shelf records clearly indicate the Neoglacial inception with an abrupt increase in *F. curta* abundances and suggested increases in SST by 1°C and annual sea ice cover by an additional month per year (Denis et al., 2006; Crosta et al., 2007a,b) The detailed lamination study of Denis et al. (2006) suggests that, based on the observation of thinner summer and thicker spring laminations, the 1-month increase in sea ice cover is due to late break-up and earlier return of sea ice to the D'Urville Trough region. Nearby, snow petrel mumiyo δ^{13}C records also point to enlarged foraging patterns out to the pelagic zone due to increases in sea ice cover between 4500 and 900 cal. years BP (Ainley et al., 2006).

In the south-east Indian Ocean sector of the Southern Ocean, a core along the 56°S meridian and within the modern Permanently Open Ocean Zone details variability in maximum sea ice cover during the Holocene (MIS 1 – Armand, 1997, 2000). Early Holocene sea ice extent at this site was estimated at nearly 4 months per year cover with a maximum of 30% September sea ice concentration. Sea ice is thought to have decreased through the mid-Holocene with a subsequent rebound to 2 months per year and ~25% September sea ice concentration and then later a decrease to modern conditions of no sea ice cover (i.e. <15% concentration = no sea ice cover). Sea ice taxa abundances throughout the Holocene were <0.5% in a nearby core at a similar latitude from the Emerald Basin, SO136-111. Crosta et al. (2004) therefore concluded that this location never experienced Holocene sea ice cover.

Finally, sediment core records of the Neoglacial in the Ross Sea focus on the change of stability of the system, suggesting increased wind and a decrease in *F. curta* abundances as a result of increased polynya activity. The earlier polynya activation is considered to have sped up the spring sea ice break-up and thus was detrimental to the development of *F. curta* blooms due to the disruption to the timing of the sea ice melt. The polynya most likely enhanced *Chaetoceros* abundances with a shallower surface mixed layer (Leventer et al., 1993; Cunningham et al., 1999).

Three Antarctic ice core studies report MSA or sodium profiles clearly identifying the impact of the Neoglacial onset. At Taylor Dome (inland of the Transantarctic Mountains, ~158°E, Fig. 13.3), a relationship between increasing MSA and an increase in the abundance of the sea ice–related diatom, *F. curta*, from western Ross Sea sediment cores, occurs around 6000 years BP (Steig et al., 1998). At Law Dome, (East Antarctica, ~112°E, Fig. 13.3), stepped increases in sodium ion concentrations over the Holocene from the LGM minimum are evident (van Ommen et al., 2004). One such step occurs around ~5500–6000 years BP and may also be related to increased cooling as also indicated by diatom observations in this East Antarctic sector (Escutia et al., 2003; Crosta et al., 2007a,b), and for which van Ommen et al. (2004) interpret changes in the meridional circulation (e.g. cyclonic track, frequency, moisture delivery). Implications of such circulation changes on the sea ice regime (break-up, snow loading, compaction of sea ice; Chapters 3 and 5) are very likely to influence the diatom community and structure, and therefore the record preserved in the coastal sediments. Finally, at Dome Fuji (Dronning Maud Land, ~39°E, Fig. 13.3), Iizuka et al. (2008) observe a significant change in the ssNa flux profile, implying that the Neoglacial commenced at 5400 years BP. The flux of ssNa increases significantly from earlier Holocene levels and is considerably more variable than the rest of the Holocene. These workers suggest, with comparison to records of the *Fragilariopsis* proxy in the South Atlantic (Bianchi & Gersonde, 2004), that the increased flux reflects increases in sea ice cover and variability. Overall, the Neoglacial reveals increased circumpolar cooling, increased sea ice cover and a change to atmospheric circulation patterns. These changes are evident from Antarctic continental ice cores and from sediment records along the continental shelf and in the wider open ocean.

The future development of Holocene records will depend on the associations that can be drawn between the sediment/biological and ice/atmospheric records, not just in reconstructing sea ice cover and seasonality, but also for inferring climatic forcing such as solar variability. Solar cycles on centennial timescales (200 years) have been invoked to explain the climatic changes inferred from some of the diatom records in Neoglacial periods described above (Leventer et al., 1996; Bárcena et al., 1998; Crosta et al., 2007b).

Quaternary (11,000 years–1.8 Ma BP)

Quaternary studies of sea ice cover in the Antarctic are focused at two levels: continuous records of sea ice extent and percentage cover; and time-slice events such as the LGM. In this sub-section, we first concentrate on the time-slice LGM records (18,000–21,000 years BP, Fig. 13.4) and subsequent deglaciation records (11,000–17,000 years BP), then continue back into the earlier Quaternary period with records generally described under the Marine Isotopic Stage (MIS) age scale framework.

The CLIMAP Project Members (1976, 1981) undertook the first major combined effort to describe global conditions of the LGM on earth. Winter sea ice extent was estimated to have migrated northwards to the approximate position of the modern Polar Front (Fig. 13.5a). Summer sea ice was also projected significantly northwards (Fig. 13.5b). In more recent assessments of the CLIMAP diatom data (Crosta et al., 1998b) and in other studies (Bromwich, 1984; Armand, 1997; Gersonde & Zielinski, 2000), CLIMAP's northward summer sea ice extent was considered overestimated. Regional studies concluded that the summer sea ice extent in the LGM was similar to today's position (Bromwich, 1984; Crosta et al., 1998b). In the South Atlantic, it is estimated to have been somewhere between the modern maximum winter sea ice extent and the modern maximum summer sea ice extent (Gersonde & Zielinski, 2000; Fig. 13.5b).

A modern evaluation of the LGM sea ice extents was undertaken through the MARGO initiative (Gersonde et al., 2005). This work brought together 122 diatom and radiolarian sea ice proxy estimates from all sectors of the Southern Ocean, assessing the estimate and source data via tiered quality-control levels. This effort provided an updated reconstruction of summer and winter sea ice extents at the EPILOG-LGM time-slice definition of 23,000–19,000 cal. years BP (= 19,500–16,000 ^{14}C years BP) as proposed by the Environment Processes of the Ice age: Land, Ocean, Glaciers (EPILOG) working group (Mix et al., 2001). The results of the new assessment are reproduced from Gersonde et al. (2005) in Fig. 13.5a,b. The winter sea ice extent was found to have approximately doubled (39×10^6 km^2) from the modern coverage of 19×10^6 km^2 (Chapter 6), yet the increase in extent was not equal in all major sectors of the Southern Ocean. A limited number of sites provided estimates for the Pacific sector where the winter extent expanded out to 57°S, whereas in the comparatively more densely sampled Atlantic and Indian sectors, winter sea ice reached ~47°S (Fig. 13.5a). Estimates of summer sea ice extent were limited due to the difficultly in recovering suitable sediment samples south of 60°S (within the zone of modern winter sea ice extent) and also because summer sea ice determination is difficult due to reduced sedimentation and a smaller window of open ocean conditions in which sea ice taxa can develop and reach the sea floor. In the MARGO reconstruction, Gersonde et al. (2005) confirmed an increasing number of reports that the CLIMAP summary for summer sea ice extent was largely exaggerated (Fig. 13.5b). The MARGO team's best interpretations from both MAT and the *Fragilariopsis obliquecostata* proxies combined was that the Atlantic sector had sporadic summer sea ice cover just north of the modern winter sea ice edge, whereas in the East Antarctic region between 90° and 120°E, summer sea ice was likely to have been mid-way between the modern summer and winter extents (Fig. 13.5b). They suggested that the EPILOG-LGM sea ice extent increased from the modern summer cover of 4×10^6 km^2 (Chapter 6) to 5–6 $\times 10^6$ km^2. Ambiguity over the actual summer extent of Antarctic sea ice remains today since few suitable high-resolution deep-sea sediment records have been retrieved south of the winter sea ice edge to document summer sea ice variability over the Quaternary and Holocene periods.
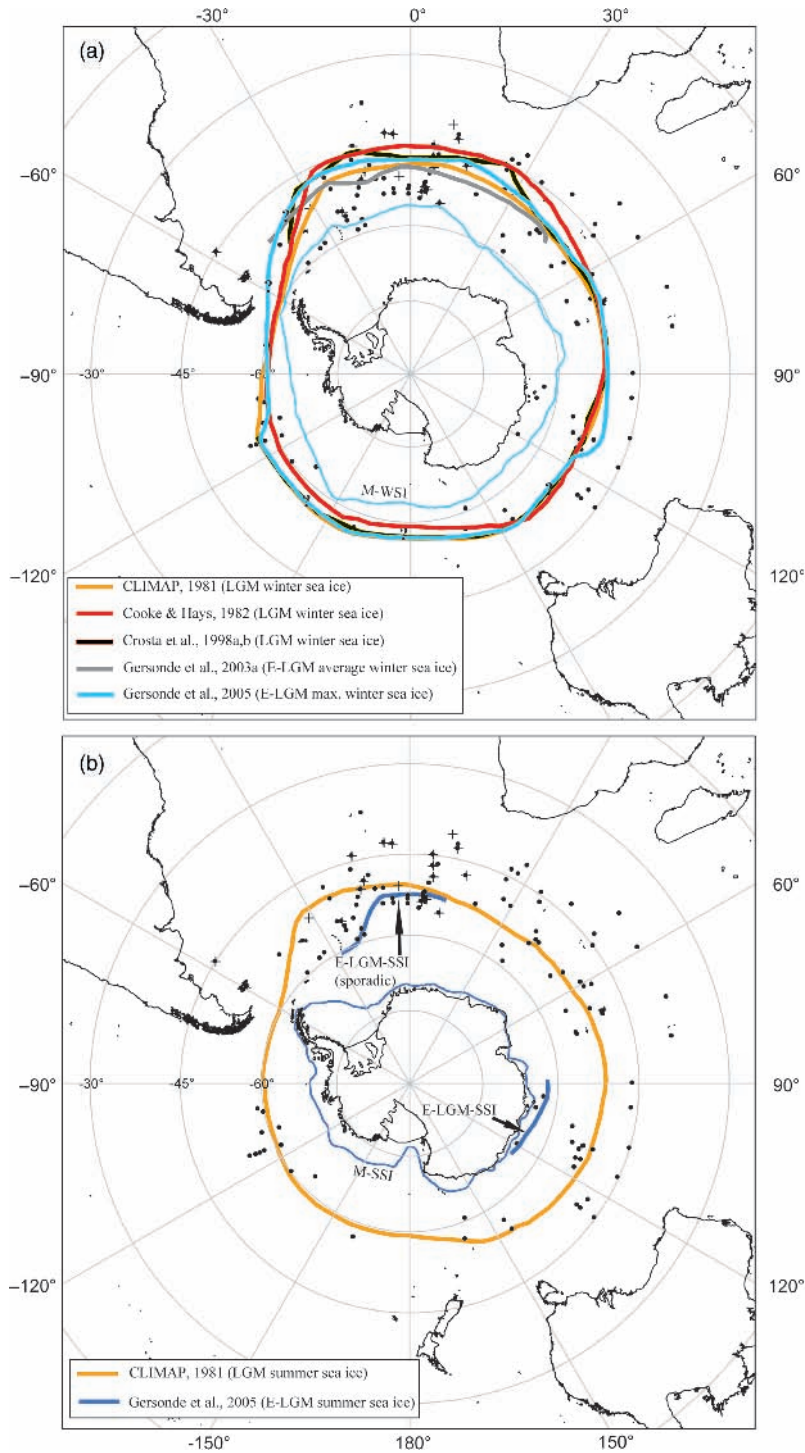
Fig. 13.5 (a) Comparison of the LGM winter sea ice edge reconstructions presented by various studies identified in the key. (b) Comparison of the LGM summer sea ice edge reconstructions from CLIMAP (1981) and Gersonde et al. (2005). Reprinted from Gersonde et al. (2005) with permission from Elsevier.

Other studies in the Atlantic sector have also reported more severe LGM sea ice conditions in a pre-EPILOG LGM event (~29,000–23,000 cal. years BP, = 25,000–20,000 ^{14}C ka BP, = transition between MIS 3 and 2, Fig. 13.4) (Shemesh et al., 2002; Gersonde et al., 2003; Bianchi & Gersonde, 2004; Collins et al., 2007; Schneider-Mor et al., 2008). These studies, at varying degrees of age resolution, all suggest extensive sea ice cover of some form during this time; viz, out to the modern Polar Front in the Scotia Sea, winter sea ice out to 50°S and up to 5 months per year cover at 53°S in the South Atlantic. Two studies from the South-west Pacific report maximum abundances of sea ice taxa that indicate winter sea ice cover out to 54–56°S for between 2 and 6 months per year (Armand, 1997; unpublished data; Crosta et al., 2004). Neither of these core samples retains evidence for summer sea ice extent. In both studies, the coolest environment (from SST and sea ice estimates) appeared in the pre-EPILOG LGM period. In the Western Ross Sea, sea ice conditions are presumed to be persistent with the local or nearby presence of grounded ice as the sediment records from several cores contain elevated percentages of reworked diatoms alongside *Chaetoceros* resting spores and reduced abundances of *Fragilariopsis curta* (Nishimura et al., 1998; Cunningham et al., 1999). The sediment records from the Windmill Islands further along the East Antarctic margin also indicate grounded ice masses were a major feature prior to deglaciation (Cremer et al., 2001).

Termination I (the transition from the LGM to the Holocene interglacial, Fig. 13.4) appears as an abrupt warming in open ocean–located sediment cores and is interpreted as a rapid retreat of sea ice cover between 18,000 and 16,000 cal. years BP (Frank et al., 2000; Crosta et al., 2004; Schneider-Mor et al., 2008). Antarctic margin records during this time suggest conditions were largely affected or under the influence of grounded ice until 11,500–9000 cal. years BP (Cunningham et al., 1999; Cremer et al., 2001; Taylor & Sjunneskog, 2002; Stickley et al., 2005; Heroy et al., 2007). An exception has been noted from the Mertz Glacier region where diatom occurrences suggest that ice shelf retreat may have occurred 1000 or 2000 years earlier (Maddison et al., 2006). Leventer et al. (2006) provide a detailed summary of deglacial conditions along the East Antarctic margin. They propose an ice shelf calving bay re-entrant scenario. This scenario has been developed to account for the high productivity evidenced in the very high resolution laminae deposited subsequent to the ice shelf retreat. The laminations vary in duration from 10 to 200 years and are indicative of the supply of previous ice trapped iron and fresh water necessary to sustain elevated levels of diatom productivity (as seen in *Chaetoceros* resting spore dominance) and varved seasonal units.

Beyond the LGM time slice, records of estimated Quaternary sea ice conditions are less common and are generally focused on open ocean records reported from the Atlantic sector. Marine Isotope Stage 3 (24,000–59,000 cal. years BP), although an interglacial stage, appears to have been subjected to glacial-like conditions. Evidence from the Windmill Islands in East Antarctica reveals an early onset of ice shelf coverage leading into the Last Glacial (< 38,000 uncor. ^{14}C years BP), while the preceding diatom assemblage indicates winter sea ice cover and short, cold, non-stratified waters during summer season (Cremer et al., 2001). Similar ice shelf grounding is reported in the western Ross Sea (Nishimura et al., 1998). In the South-west Pacific, sea ice species and the MAT-derived sea ice duration estimates increase over MIS 3 with the major sea ice advance from ~35,000 cal. years BP where 1–2 months per year cover is observed at 56°S (Crosta et al., 2004). Concomitantly, South Atlantic records indicate increasing sea ice cover from both MAT and *Fragilariopsis* species proxies

(Shemesh et al., 2002; Frank et al., 2000; Gersonde & Zielinski, 2000; Schneider-Mor et al., 2005, 2008). The only MAT estimates (core TTN057-13PC4, ~53°S, 5°E, Fig. 13.3) (Shemesh et al., 2000) suggest relatively stable cool Holocene-like sea ice cover of 1.5 months per year from 35,000 to 30,000 cal. years BP followed by increased annual sea ice cover of 3–4 months per year through to the MIS 2. The remaining studies rely on the *Fragilariopsis* proxies to determine the proximity of the winter and summer sea ice extents, generally between the narrow longitude range of 1–7°E. Each study projected the winter extent out to ~53°S (Frank et al., 2000; Gersonde & Zielinski, 2000), and in some instances intermittently reaching 48–49°S (loc. cite.; Schneider-Mor et al., 2008). Summer sea ice extent was estimated out to ~55°S (Frank et al., 2000; Gersonde & Zielinski, 2000). Records for MIS 4 (59,000–74,000 cal. years BP) from these reported Atlantic sources provide a similar picture to that presented in MIS 3, with winter sea ice extent reaching at least ~53°S and from time to time 47–49°S. In the South-west Pacific, sea ice extent is considered to have commenced a slow increase northwards from ~78 ka BP, but it persisted for only 1–1.5 months per year at 56°S, 160°E (SO136-111, Fig. 13.3) (Crosta et al., 2004).

Sporadic occurrences of sea ice have been reported from cores in both the South Atlantic and South-west Pacific during sub-stages of MIS 5. At MIS 5 sub-stage b (83–93 cal. kyears BP), ice persistence of 1 month per year was reported from the core SO136-111 (Crosta et al., 2004), while evidence of sea ice cover in the E–W Atlantic transect cores (33°W–4°E, 58–52°S, Gersonde & Zielinski, 2000) was documented from elevated abundance of the winter *Fragilariopsis* proxy. Later studies by Frank et al. (2000) and Bianchi and Gersonde (2002), however, report no sea ice during MIS 5 sub-stage b. Only two reports of sea ice cover in the cold MIS 5 sub-stage d (103–115 cal. kyears BP) are known, both from the South Atlantic. Sea ice appeared to be similar to the modern Holocene coverage (Gersonde & Zielinski, 2000) with maximum extent reaching ODP 1094 (53°S) and PS1768 (52°S) at ~110 cal. kyears BP (Bianchi & Gersonde, 2002; Fig. 13.3). Recent reanalysis by Schneider-Mor et al. (2008) of ODP 1094 reports no evidence of sea ice during the whole of MIS 5.

Marine Isotope Stage 6 (130–190 cal. kyears BP) would appear, based on the *Fragilariopsis* proxies in cores PS1772-8, PS1649-2, PS1768-8 and PS1756-5 from the South Atlantic (Frank et al., 2000; Gersonde & Zielinski, 2000; Fig. 13.3), to have experienced similar sea ice advance as suggested in both MIS 4 and MIS 2. Research on seven cores in the Atlantic and western Indian Ocean specifically target sea ice conditions across Termination 2 (~138 cal. kyears BP) between MIS 5 and late MIS 6 (Bianchi & Gersonde, 2002; Fig. 13.3). These observations also suggest sea ice advance conditions in the late MIS 6 not unlike that of the LGM. Bianchi and Gersonde (2002) conclude that the reduced sedimentation rate and occurrence of *F. obliquecostata* at 3% abundance levels imply an expansion of summer sea ice cover, and hence that sea ice seasonality was reduced during late MIS 6. Another notable finding in the Bianchi & Gersonde study was regional differences in sea ice response: locations under the influence of the Weddell Gyre show a strong extension of sea ice, whereas those to the east of the gyre, in the south-west Indian Ocean, experienced more stable and less northward extension at the same time. Recent results from the ODP core 1094 also indicate a strong winter sea ice cover response throughout MIS 6, whereas further north at ODP 1093, only at ~132 and 178 ka BP did winter sea ice play any influence at 49°S (Schneider-Mor et al., 2005, 2008). The only record outside the Atlantic, at 56°S in the South-west Pacific, reveals sea ice duration slightly reduced than the maximum obtained at the LGM, but nevertheless still persisting for 1 month per year during this stage. The maximum

duration of 1.5 months per year was obtained at ~161 cal. kyears BP and this coverage remained relatively constant through to 133 cal. kyears BP where, upon Termination II, sea ice abruptly disappears from the record (Crosta et al., 2004).

Beyond MIS 6, seven studies report on the diatom record of sea ice cover back to various times in the Quaternary (Kaczmarska et al., 1993; Gersonde & Zielinski, 2000; Kunz-Pirrung et al., 2002; Whitehead & McMinn, 2002; Crosta et al., 2004; Schneider-Mor et al., 2005; 2008). We do not detail all of these records here, but highlight some of the studied intervals.

The MIS 11 warm period is another time-slice event where sea ice extent has been estimated because of its analogue to modern and future climate conditions. A South Atlantic study by Kunz-Pirrung et al. (2002) covering MIS 12 to MIS 10 (450–340 cal. kyears BP) using the *Fragilariopsis* abundance indicators of Gersonde and Zielinski (2000) suggests variations in seasonal sea ice cover. Sea ice–free conditions during the warm MIS 11 (containing the Mid-Brunhes Event at 400 ka BP) are derived from decreases in the abundance of sea ice taxa, increases in open ocean species, decreases in IRD content and an SST estimated to be ~2°C warmer than present. Winter sea ice cover during both MIS 10 and MIS 12 extended out to the Polar Front similar to reconstructions for other more recent glacial periods. Two additional cores in the South Atlantic (PS1772-8, PS1649-2) also indicate, from application of the *Fragilariopsis* proxies, extensive sea ice cover in both summer and winter to 54–55°S during MIS 10 (Gersonde & Zielinski, 2000). Recent use of the winter *Fragilariopsis* proxy on the ODP 1093 and 1094 records suggests sea ice was a common occurrence back to 650 cal. kyears BP, whereas at site 1093 sea ice occurs less often (Schneider-Mor et al., 2005, 2008).

On the Kerguelen Plateau at ODP Leg 119 Site 745B (59°S, 85°E, Fig. 13.3), the *Eucampia* ratio proxy was first employed back to 800 ka BP (Kaczmarska et al., 1993). This proxy suggested that the first northward expansion of sea ice over the Kerguelen site since 800 ka BP commenced around 500 ka BP. A decrease in the *Eucampia* ratio, as an indicator of increasing winter sea ice cover, continued until 100,000 cal. years BP at which point the index remains near or below the ratio levels observed in present-day surface water plankton. Kaczmarska et al. (1993) also reported that the diatom-derived sea ice estimates showed a response to oscillations in the Earth's obliquity.

The EPICA Dome C ice core sea salt sodium record provides the only continuous record of potential sea ice cover back to 740 cal. years BP (Wolff et al., 2006; Röthlisberger et al., 2008; Fig. 13.3). The record, although oscillating between typical peaks and troughs of glacial-interglacial events, remains controversial due to the lack of understanding sources of ssNa to the inner continent (Bigler et al., 2006). There is a need to firmly establish the relationship between the source area of ssNa and the sea ice areal cover (see earlier methods discussion). Wolff et al. (2006) suggest that proxy indicates sea ice cover mid-way between the LGM maximum extent and modern interglacial conditions for weak interglacial periods before 440 cal. kyears BP. Their results also imply that the strongest response for sea ice cover in the south Indian sector occurred between 300 and 250 kyears BP. Resolving the sediment and ice core proxies for sea ice independently and then in concert will require thoughtful investigation.

Beyond the Quaternary

Whitehead and McMinn (2002) in their study of the Quaternary and Pliocene records from a N–S transect along a southern Kerguelen Plateau (Fig. 13.3) employed a sea ice to open

ocean assemblage ratio to determine the reduction of summer sea ice in glacial periods. Their proxy was less reliable in the Pliocene sections due to the introduction (exit) of extinct (modern) taxa and therefore relied on the ratio of silicoflagellate species abundance within the genera *Dictyocha*. From the mid-Pliocene to around 2.6 million years ago (Ma), summer sea ice extent was considered intermittent with open water conditions across most of the southern Kerguelen Plateau. An intense cold interval is assumed to have led to erosion and, consequently, deposition of an IRD lag deposit between 3.1 and 2.2 Ma. Their ratio suggests summer sea ice dominated the region at ~2.2 Ma. Within the lower Pleistocene, the first major warming across the southern Plateau was recorded in a distinct period within a 1.5–1.6 Ma interval that otherwise experienced summer pack ice cover. Erosion, again considered representative of extreme glacial conditions, interrupts deposition of sediments across the plateau until after the LGM at ~0.62 Ma. These subsequent ratio records are representative of modern sea ice and oceanographic conditions. Closer to Prydz Bay (Whitehead et al., 2005; Fig. 13.3), this time employing the *Eucampia* Generalized Linear Model for winter sea ice concentrations clearly revealed winter sea ice concentrations throughout the Pliocene (~5.0–2.0 Ma) that were significantly reduced from present. Whitehead and his colleagues concluded the northern winter sea ice edge was in the vicinity of 64°38'S, slightly north of the modern summer sea ice edge, and therefore represented a decrease in area of ~45% from the modern winter sea ice edge.

Preliminary diatom assemblage analysis from the ANDRILL AND-1B core site (Fig. 13.3) suggests sea ice/intermediate open ocean conditions dominated two Pliocene sequences: mid-Pliocene to late Pliocene and mid-lower to early lower Pliocene. The late lower Pliocene to mid-lower Pliocene sequence is represented by a warm open ocean assemblage (Scherer et al., 2007). It is likely that the origins of Antarctic sea ice regime and the history of sea ice diatom taxa will be derived from the future results of ANDRILL.

13.3 Arctic

Methods for reconstructing past sea ice distribution and seasonal variability

As with records of Antarctic sea ice, historical data on sea ice extent in the Arctic are temporally limited, hence our need to rely on proxy indicators of sea ice extent in order to gain a long-term perspective on changes in the distribution of ice over time. General concern over the 'state of sea ice' in the Arctic has been highlighted by recent reports of decreases in both ice extent (Gloersen & Campbell, 1991; Chapman & Walsh, 1993; Johannessen et al., 1995, 2004; Bjørgo et al., 1997; McPhee et al., 1998; Johannessen et al., 1999; Vinnikov et al., 1999; Meier et al., 2006; Serreze et al., 2007) and ice thickness (Rothrock et al., 1999; Lindsay & Zhang, 2005; Chapter 4) over the past several decades, decreases that have raised an alarm over the possible impact of human-induced climate change. For example, based on satellite passive-microwave observations, Meier et al. (2006) note an 8.4±1.5% per decade decrease in Arctic sea ice extent in September, over the years from 1979 to 2005. Extension of this number back to 1953 results in a decrease of 7.74±0.6% per decade; these data reflect the recent acceleration in the loss of Arctic sea ice (Meier et al., 2006). Data on sea ice thickness measured from US nuclear submarine missions in 1958 and 1976, and supplemented by more recent data in 1993, 1996 and 1997 from the Scientific Ice Expeditions (SCICEX),

demonstrate a mean decrease in ice thickness of 1.3 m, from 3.1 m to 1.8 m, over less than 50 years (Rothrock et al., 1999). In addition to concern over changes in total areal extent of sea ice, and in ice thickness, the timing of spring ice melt is also a concern, as discussed by Stabeno and Overland (2001), who note the impact of the ice edge zone on primary and secondary productivity in the Bering Sea and point out the role of sea ice as a platform for walrus, polar bears and a hunting ground for northern natives.

Satellite-derived records of sea ice extent, however, go back only to the early 1970s, with continuous microwave-derived satellite records from the Nimbus-7 Scanning Multichannel Microwave Radiometer (SMMR) and from the Special Sensor Microwave/Imagers (SSM/I) (Chapter 6). Due to this relatively short timescale, the relationship of changes in sea ice extent and thickness to natural cycles, such as the North Atlantic and Arctic Oscillations, versus anthropogenically induced warming, are not completely clear (Johannessen et al., 1999; Rothrock et al., 1999). Modelling work by Vinnikov et al. (1999) suggests that the observed changes over the past century are larger than would be expected as a consequence of natural climate variability alone. In addition, a decrease in sea ice extent is not observed universally in the Arctic (Parkinson, 1995). Given these uncertainties, it is clear that longer, detailed records of sea ice extent, thickness and dynamics in the Arctic are necessary, with proxy records as the most likely source of information.

Similar to work in the Antarctic, estimates of sea ice in the high northern latitudes were first put forward by CLIMAP (1976, 1981). These estimates were based on a variety of evidence, including the absence of coccoliths, low accumulation rates of planktonic foraminifera, reduced bulk sedimentation rates and the occurrence of IRD. The conclusions of CLIMAP have since been revised dramatically by more extensive work using sedimentological, geochemical and micropalaeontological tracers of sea ice. While a variety of microfossil groups have provided data on palaeo sea ice distribution, including diatoms, coccolithophorids and foraminifera, dinoflagellate cyst assemblages have been utilized most successfully in these studies, due to their diversity and abundance in sediments from both the Arctic and sub-Arctic seas. As with our presentation of data from the Antarctic, we first describe the approaches undertaken when documenting past sea ice cover and then examine the results of these methods under time-slice scenarios.

Ice core data

Physical and geochemical properties of glacial ice in the Arctic have been related to sea ice cover, though it seems that their full potential remains to be utilized. Koerner (1977), e.g., found a positive relationship between melt layers in glacial ice of the Devon Island Ice Cap and maximum open water in the nearby Queen Elizabeth Islands region. This relationship is driven by warmer summers that produce both surface melting on the ice cap that subsequently refreezes as a melt layer, and less summer sea ice. Consequently, the number and thickness of melt layers in glacial ice hold potential as a palaeo sea ice proxy.

The concentration of sea salts in glacial ice may also provide a record of sea ice cover, through the transport and deposition of marine aerosols from open water to glacial ice. However, this relationship is only applicable in situations in which aerosol transport is more a function of the area of open water, though other factors may also be important. In the case of the Greenland Ice Core, strength of polar atmospheric circulation has a stronger control on the concentration of sea salts in the glacial ice, so even when sea ice concentration increases, increased strength of atmospheric transport can result in a greater amount of sea

salt being deposited in the glacial ice (Mayewski et al., 1994; O'Brien et al., 1995). However, in the Penny Ice Cap, on Baffin Island, Grumet et al. (2001) demonstrated the existence of an inverse relationship between spring sea ice extent in Baffin Bay and the concentration of sea salt in the glacial ice. More recently, Kinnard et al. (2006) correlated the concentration of sea salts in an ice core from the Devon Ice Cap and sea ice cover in Baffin Bay; greater transport of sea salts occurred during times of greater open water during the spring and fall, when the weather was stormier.

Sedimentological tracers: IRD including driftwood

Both sea ice and icebergs carry lithogenic material that is released as the ice melts (IRD) and is consequently fluxed to the sea floor. While icebergs are able to transport material of all sizes (Clark & Hanson, 1983; Dowdeswell & Dowdeswell, 1989), more than 90% of the lithogenic material carried by sea ice is clay to silt-sized particles (Pfirman et al., 1989; Wollenburg, 1993). For this reason, particles >500 µm that are randomly distributed at the sea floor are generally considered to be iceberg rafted, though it is possible for these coarser grains to be transported by sea ice (Darby et al., 2006). A large body of literature exists concerning changes in the volume and source of iceberg-rafted material over time (Ruddiman, 1977, 1997; Heinrich, 1988; Henrich et al., 1989; Bischof, 1990; Bond et al., 1992; Hebbeln & Wefer, 1997; Hebbeln et al., 1998; Darby et al., 2002).

Distinction of sea ice versus iceberg-rafted material, however, is not always clear, even though in some settings such material can dominate mass flux (Hebbeln, 2000). Difficulty in tracking the exact transport mode of fine-grained lithogenic particles, which can be ice rafted by either icebergs or sea ice, has resulted in few studies that utilize fine-grained IRD as a proxy for sea ice extent. One exception is work by Bond et al. (1997) who demonstrate that the concentration of volcanic glass (>100 µm) erupted onto drifting ice, from either Iceland or Jan Mayen, can be used as a tracer for drifting sea ice through the Holocene. Their rationale for this distinction is the probable absence of Icelandic tidewater glaciers during the middle- to late Holocene and the large size of the grains, ruling out both iceberg rafting and aeolian transport. Work by Darby (2003) presents a 'geochemical fingerprinting' technique to trace the drift path of Arctic sea ice. Elemental composition of Fe oxide mineral grains as determined by microprobe analysis was used to match grains collected from sea ice floes to coastal source regions. This technique has been used in several studies. Darby and Bischof (2004), e.g., evaluate changes in the Arctic Oscillation during the late Holocene through its influence on the Transpolar Drift and related variability in the provenance of grains rafted by sea ice.

Recent work by St John (2008) has attempted to address the problem of distinguishing transport modes through the observation of surface features of sand-sized quartz grains. Glacially transported grains will have features associated with mechanical breakage that can be observed via SEM imaging; these features include conchoidal fractures, angular edges and step fractures. Surface features associated with chemical weathering, including more rounded edges, were assumed to be associated with sea ice transport. Application of these criteria to sand-sized grains from IODP 302 cores from the central Arctic supports the major findings of this project regarding the timing of the initiation of both sea ice and glacial ice in the Arctic at 46 Ma, and is used to track changes in ice extent since its initial appearance (St John, 2008).

Larger objects such as wood also are transported by drifting ice. River bank erosion in North America and Eurasia results in the delivery of wood to the Arctic that is then transported,

with moving sea ice, via surface currents such as the Transpolar Drift and Beaufort Gyre (Dyke et al., 1997; Tremblay et al., 1997). After several years of drift as part of the moving pack ice, the wood can be stranded on the distant coastlines of the Canadian Arctic, Iceland, Greenland and Svalbard. Although not directly supplying information on the distribution of sea ice over time, radiocarbon dating of stranded wood has been used to identify changes in sea ice drift patterns over time that are then related to changes in atmospheric circulation patterns (Dyke et al., 1997; Tremblay et al., 1997).

Geochemical tracers: clay minerals and biomarkers

As with the work on driftwood, clay mineral studies of particles transported by sea ice do not provide direct data on sea ice distribution through time, but provide information on both the source of the sediments and the transport path of the sea ice. For example, Dethleff et al. (2000) have traced different branches of the Transpolar Drift originating in the Laptev Sea, based on the transport of specific clay minerals with the sea ice. In this study, the incorporated sediment is delivered to the ocean via rivers, and is then frozen into the sea ice. Pfirman et al. (1997), interested in the role of sea ice in distributing both contaminants and sediments in the Arctic, have developed a method to backtrack ice motion in the Eurasian Arctic, based on historical drift data. To verify their trajectories, they link clay mineralogical data of the sediment carried within the sea ice to sea-floor sediments in the suspected sources.

Geochemical work using photosynthetic biomarker pigments (Rosell-Melé & Koç, 1997) and C_{37} alkenones (Rosell-Melé, 1998; Rosell-Melé et al., 1998) has been used to address the question of variable sea ice cover in the Nordic seas since the last glacial. In both cases, the principle guiding the use of these proxies is the association of the chemistry with photosynthetic organisms. Consequently, their presence in marine sediment cores suggests the lack of permanent ice cover. More specifically, Rosell-Melé and Koç (1997) measured the concentration of chlorins and porphyrins, diagenetic products of the photosynthetic pigment chlorophyll, in sediment cores from the Nordic seas, in order to assess whether these seas were permanently ice covered during the LGM, as indicated by the CLIMAP (1976, 1981) project. The presence of these compounds during the end of the last glacial and the Younger Dryas shows that seasonally ice-free conditions must have existed at those times. The C_{37} alkenones are associated with the coccolithophorid *Emiliani huxleyi*, a photosynthetic organism common in waters that are ice-free for at least part of the year. As with the chlorins and porphyrins, the presence of C_{37} alkenones indicates the lack of permanent ice cover in the Nordic seas during the Younger Dryas (Rosell-Melé et al., 1998).

A newly developed geochemical tracer is the biomarker IP_{25}, a monounsaturated hydrocarbon with a 25-carbon skeleton (Belt et al., 2007). One of its most critical characteristics is its identification as a biomarker that is specific to sea ice diatoms, found in diatoms that live within the sea ice but not in the nearby phytoplankton. Belt et al. (2007) note that IP_{25} also can be measured in both surface and down-core sediment samples, indicating that it is stable enough and occurs in sufficient quantities to allow detection; consequently, it has a great deal of promise as a sea ice proxy. Belt et al. (2007), however, caution that for now, IP_{25} can be used as an indicator only of the presence or absence of sea ice, and that more work needs to be done to derive quantitative estimates of sea ice cover. Subsequent work by Massé et al. (2008) analysed IP_{25} in a core from just north of Iceland to demonstrate the reliability of the method in reconstructing sea ice cover over the past 1000 years. The authors observed an excellent correspondence between not only the IP_{25} data and the historical document-based

record of sea ice extent, but also with the diatom-based SST reconstruction of Jiang et al. (2005) from the same core, and the northern hemisphere temperature reconstruction of Crowley and Lowery (2000).

Geochemical tracers: stable isotope

Hillaire-Marcel and de Vernal (2008) provide a novel interpretation of planktonic foraminiferal stable isotopic data to evaluate the history of sea ice growth. One reason their approach is so important is that, as the authors point out, most sea ice proxies are used to assess the presence or absence of sea ice; their approach provides information on the rate of sea ice growth. They interpret 'off-equilibrium, low $\delta^{18}O$ values in mesopelagic planktonic foraminiferal species' (p. 143) as the result of sea ice formation and the production of isotopically light brines. This rationale forms the framework for their reinterpretation of $\delta^{18}O$ data from the LGM and from Heinrich layers in cores from the north-western North Atlantic. Heavy isotopic data from the LGM indicate little sea ice formation, while light isotopic data from the Heinrich layers suggest high rates of production of sea ice at that time (Hillaire-Marcel & de Vernal, 2008).

Microfossil assemblage distribution: calcareous microfossils

Calcareous microfossils, such as coccolithophorids and planktonic foraminifera, have been used to track sea ice cover over time in the high northern latitudes, with the caveat that there is greater dissolution of calcium carbonate as water temperature decreases and reduced species diversity as latitude increases. For example, only a single species of planktonic foraminifera, *Neogloboquadrina pachyderma*, is common in the polar setting. Coccolithophorid diversity is slightly higher, although dominated by two species, *Emiliani huxleyi* and *Coccolithus pelagicus* (Braarud, 1979; Samtleben & Schroder, 1992; Baumann et al., 2000). The productivity and downward flux of coccoliths is greatly decreased in polar waters with seasonal ice cover (Eide, 1990). In addition, since planktonic foraminifera can live deeper in the water column, their distribution is not as directly linked to the presence or absence of sea ice as that of the phytoplanktonic coccolithophorids.

That said, work with both microfossil groups has provided useful information on the variability of permanent sea ice cover in the Arctic and sub-Arctic seas. As with the biomarker methods, the presence of coccoliths in marine sediments suggests seasonally ice-free conditions, since the algae need enough light to photosynthesize. For example, Rahman and de Vernal (1994) used the presence versus absence of calcareous nannofossils to trace the history of sea ice in the Labrador Sea over the past 31,000 years. Hebbeln and Wefer (1997) do the same for the Fram Strait, though their data go back farther in time, to oxygen isotope stage 5 at 128 ka. This concept is expanded upon by Hebbeln et al. (1998) in their review of the 200,000-year record of palaeoceanographic conditions in the North Atlantic.

Large-scale work with planktonic foraminifera is in progress through the use of an MAT with a similarity index, SIMMAX, which is being used to develop maps of SST that can be used to infer palaeo sea ice extent (Pflaumann et al., 1996). One of the principal advantages of this statistical method, over previously used techniques such as the MAT alone, or the CLIMAP transfer function method (Imbrie & Kipp, 1971), is the ability to estimate very low SST (–1.4°C for caloric winter and 0.4°C for caloric summer; Pflaumann et al., 1996). This ability is critical for work in the higher latitudes, where these SST estimates will be used to reconstruct sea ice distribution.

Microfossil assemblage distribution: diatoms

Based on their abundance and diversity in the sea ice, water column and sediments, and the associations of certain species with specific habitats, diatoms have proven to be excellent palaeo sea ice proxies in the Southern Ocean, as presented earlier in this chapter. However, their use in the northern high latitudes is more limited, primarily as a result of the more lightly silicified and more easily dissolved frustules found in the nutrient-poor Arctic (Machado, 1993; Kohly, 1998). As a result, although diatoms are relatively diverse and abundant in Arctic surface waters, their distribution in surface sediments is patchy enough that a circum-Arctic database is unlikely to be developed. However, in specific regions – the Bering Sea and Sea of Okhotsk (Sancetta, 1979, 1981, 1982, 1983), the Greenland, Iceland and Norwegian Seas (Koç Karpuz & Schrader, 1990; Koç et al., 1993; Jiang et al., 2001; Justwan & Koç, 2008), the Labrador Sea (De Sève, 1999), Baffin Bay, Frobisher Bay and the Davis Strait (Williams, 1990), and the Laptev Sea (Cremer, 1999; Bauch & Polyakova, 2000) – diatoms are abundant enough in sediments that their records have provided important palaeoceanographic insights. Note that with the exception of the Laptev Sea, these sites are all outside the enclosed Arctic Ocean.

In the northern Pacific, including both the Bering Sea and the Sea of Okhotsk, diatoms are common in surface sediments (Jousé, 1962) and have been worked on extensively by Sancetta (1979, 1981, 1982, 1983). Sancetta (1981) presents quantitative diatom data, from 200 surface sediment samples from this region, that link distinct diatom assemblages to specific oceanographic conditions, including an assemblage from the Bering Sea associated with 'shelf waters covered by sea ice for six months of the year, with productivity occurring in very early spring at the margin of the melting ice'. This sea ice assemblage is dominated by *Thalassiosira nordenskioldii* and species of *Nitzschia* such as *Nitzschia grunowii* (now *Fragilariopsis grunowii*) and *Nitzschia cylindrus* (now *Fragilariopsis cylindrus*), which are commonly associated with sea ice (Gran, 1904; Horner & Alexander, 1972). Notably, *F. cylindrus* holds a similar ecological position in the Southern Ocean.

Sancetta (1983) applies this understanding of the modern distribution of diatoms in the northern Pacific to five sediment cores from the North Pacific and Bering Sea that span the past 40,000 years. The most obvious change in assemblage down-core is the increased abundance of the two sea ice species, *F. grunowii* and *F. cylindrus*, during the last glacial, indicating increased sea ice cover at that time, in the Bering Sea. These species are rarely found in the two North Pacific cores she studied, even during the last glacial, which indicates that sea ice expansion did not extend that far south. Additionally, the diatom data show that the prolonged sea ice cover characteristic of the Sea of Okhotsk today was more widespread during the last glacial. This is based on the greater distribution of diatom species associated with sea ice melt and cool, low-salinity surface water layers.

Koç et al. (1993) reconstruct the palaeoceanographic history of the Greenland, Iceland and Norwegian Seas over the past 14,000 years based on diatom assemblage work initially developed by Koç Karpuz and Schrader (1990). Like Sancetta's (1983) work in the high-latitude Pacific, Koç et al. (1993) note the association of species as *Nitzschia cylindrica* (now *Fragilariopsis cylindrus*), *F. grunowii* and *Thalassiosira hyalina* with sea ice, and use this information to track sea ice distribution over time. More simply, they also trace the ice margin through the first occurrence of diatoms in the nine sediment cores they analysed. Similarly, Jiang et al. (2001) identify a sea ice diatom assemblage characterized by the species *F. cylindrus*, *Fragilariopsis oceanica* and *Thalassiosira antarctica/gravida* resting spores, based on analysis of surface sediment samples from around Iceland.

More recently, Justwan and Koç (2008) developed a diatom-based sea ice transfer function for the North Atlantic, based on 99 surface sediment samples. Their quantitative approach, which allows for the reconstruction of May sea ice concentration, was then applied to specific case studies of sea ice concentration at the LGM, during the Younger Dryas and through the Holocene. The results of their diatom-based transfer function compare favourably to those obtained via alternative proxies, indicating the reliability of this new technique.

Similarly, De Sève (1999) used Q-mode factor analysis on 66 surface sediment samples from the Labrador Sea to develop transfer functions relating assemblage information to August and February SST and salinities. De Sève's (1999) Factor 2 dominated by *T. gravida* is associated with cold Arctic surface waters 'indicative of heavy and prolonged ice coverage'. Factor 6 dominated by *N. frigida* is indicative of the sea ice assemblage. Based on the results of her factor analysis, it is likely that down-core reconstruction of sea ice distribution over time is possible for the Labrador Sea.

Slightly to the north in the Baffin Bay–Davis Strait region, Williams (1986, 1990, 1993) used diatom abundance data to look at both the recent and deglacial/Holocene history of the area. Using CABFAC factor analysis, Williams was able to distinguish several assemblages associated with sea ice. Her Baffin Current assemblage, dominated by *T. gravida*, is associated with prolonged and heavy ice cover, as was found by De Sève (1999). Her summer pack ice assemblage has high concentrations of *Actinocyclus curvatulus* and *Thalassiosira trifulta*, and a third assemblage is associated with fast ice (*Porosira glacialis*). In her down-core work, Willliams (1990, 1993) notes that initial ice break-up at the end of the glacial is generally indicated by the appearance of *T. gravida*. In addition, *N. grunowii* (*F. grunowii*) and *N. cylindra* (*F. cylindrus*), not *P. glacialis*, are used to track sea ice extent through the Holocene.

Finally, in the Arctic Ocean, data on diatom assemblages are presented by Polyakova (1989 – Barents Sea, White Sea, Kara Sea, East Siberian Sea, Chukchi Sea and the Canadian Arctic), Polyakova et al. (1992 – Barents Sea), Cremer (1999 – Laptev Sea) and Bauch & Polyakova (2000 – Laptev Sea). As was found with the previous studies, *F. grunowii* and *F. cylindrus* (and *Fossula arctica*) are used as indicators of sea ice.

Clearly, as in the Southern Ocean, specific diatoms can be, and are, used to trace the distribution of sea ice over time. However, for large portions of the central and marginal Arctic Ocean, diatom abundances are so low, and preservation so poor, that other proxies must be utilized.

Microfossil assemblage distribution: foraminifera and tintinnids

Use of foraminiferal assemblage data as a proxy for sea ice in the Arctic has been limited. Scott et al. (2008), however, used a combination of foraminiferal and planktonic ciliate (tintinnids) data from the surfaces of 51 box cores from the Beaufort Sea to evaluate their use in palaeo sea ice reconstruction. They note that the presence of both tintinnids and abundant agglutinated benthic foraminifera suggests freshwater input to the marine setting, a condition that is not possible with perennial sea ice cover. In addition, since freshwater input results in decreased abundance of planktonic foraminifera, the planktonic (P) to benthic (B) foram ratio can be used to evaluate if there was perennial ice, with a P:B ratio of ~1:1 indicative of permanent ice cover. Schell et al. (2008) utilize these strategies in four box cores from the Amundsen Gulf to reconstruct the history of sea ice over the past century.

Sarnthein et al. (2003a) took another approach to the use of foraminifera towards reconstructing sea ice extent in the North Atlantic. Their strategy, which used a Similarity

Maximum Modern-Analog Technique, was based on a sequence of steps whereby SST were reconstructed first, based on planktonic foraminiferal assemblage data; this effort was part of GLAMAP 2000 (Glacial Atlantic Ocean Mapping, see Sarnthein et al., 2003b). The authors then noted that 'today, almost 100% of all sites with SST >2.5°C during summer, >0.4° for winters 1978–1987, and >0.75°C for LIA winters lie seaward of the sea ice margin' (Sarnthein et al., 2003). Consequently, SST data were used to define 'the minimum extent of ice-free regions during past summer and winter times'. This strategy was applied towards an assessment of sea ice extent during the LGM in the northern North Atlantic. Their results, which are in contrast to those presented by CLIMAP (1981), reveal that sea ice covered a smaller area of the North Atlantic during the LGM summer than indicated by the CLIMAP reconstruction, while winter sea ice was quite extensive.

Microfossil assemblage distribution: dinoflagellate cysts

In the high northern latitudes, dinoflagellate cysts have proven to be the most powerful proxy recorder of palaeo sea ice, with reconstructions using best analogue techniques capable of estimating past sea ice cover with an error of prediction of ±1.3 months/year (de Vernal et al., 2005a). Their utility of these cysts, which form as a normal part of the dinoflagellate life cycle, is the result of several factors. As with other microorganisms living within the photic zone such as diatoms and coccolithophorids, dinoflagellate distribution is sensitive to changes within the upper water column, including fluctuations in SST and salinity, and of course, sea ice cover. Annual sea ice cover restricts the amount of light available for photo-synthesis, thus forcing a disruption of metabolic activities. In the case of the dinoflagellates, this interruption influences the life stage of the dinoflagellate.

Dinoflagellate populations are relatively diverse (~30 dinocyst species and 10 distinctive morphotypes have been recorded in Arctic surface samples, Rochon et al., 1999; de Vernal et al., 2001, 2005a) and widespread in the Arctic, with changes in assemblage composition directly a function of changes in surface water conditions (Table 13.3). This is ideal for transfer function analyses, since the resolution of transfer functions increases as both species diversity and the range of ecological niches represented increases (Mudie et al., 2001). Species commonly found in regions with extensive sea ice cover include *Brigantedinium* spp. and *Operculodinium centrocarpum*, both of which tolerate a broad range of environmental conditions, and others such as *Islandinium minutum*, which is more specifically adapted to colder and ice-covered conditions (de Vernal & Hillaire-Marcel, 2000; Head et al., 2001). In contrast, the extremely low diversity exhibited by planktonic foraminiferal populations (essentially only left-coiling *N. pachyderma*) and the coccolithophorids (primarily *E. hux-leyi* and *C. pelagicus*) in the Arctic makes it difficult to track changes in sea ice cover by examining variability in the microfossil assemblage. Moreover, dinoflagellates and dinocysts are euryhaline, existing in environments with salinities ranging from estuarine to normal marine, while planktonic foraminifera are stenohaline, living under only normal marine salinities. In addition, while dominantly photosynthetic, many dinoflagellates are capable of heterotrophic behaviour. This, in combination with their ability to encyst, results in their ability to survive even under very harsh environmental conditions (Mudie et al., 2001; de Vernal et al., 2001).

Finally, many of the dinocysts are composed of dinosporin, a complex and refractory organic compound that is very resistant to dissolution (de Vernal et al., 2001; Zonneveld et al., 2001). Even when siliceous and calcareous microfossils have dissolved, dinocysts are

Table 13.3   List of dinocyst studies relevant to Arctic palaeo sea ice reconstruction.

Reference/year	Region	Time period
Boessenkool et al. (2001)	South-east Greenland Margin	Modern
Grøsfjeld et al. (1999)	Western Norway fjords	Late glacial–Holocene
Head et al. (2001)	Arctic/Kara and Laptev Seas	Modern
Kunz-Pirrung (2001)	Arctic/Laptev Sea	Modern
Kunz-Pirrung et al. (2001)	Arctic/Laptev Sea	Late Holocene
Levac and de Vernal (1997)	Labrador Coast	Postglacial
Levac et al. (2001)	Baffin Bay	Postglacial
Matthiessen and Knies (2001)	Barents Sea	Oxygen Isotope Stage 5
Mudie (1992)	Circum-Arctic	Neogene and Quaternary
Mudie and Rochon (2001)	Canadian Arctic	Modern
Mudie et al. (2001)	Arctic and high-latitude circum-Arctic basins	Introduction to special volume
Peyron and de Vernal (2001)	Arctic and sub-Arctic seas	Modern and 25,000-year records
Radi et al. (2001)	Bering and Chukchi Seas	Modern
Rochon and de Vernal (1994)	Labrador Sea	Modern and Holocene
Rochon et al. (1998)	North Sea	Late glacial–deglacial
Rochon et al. (1999)	North Atlantic	Modern
Solignac et al. (2006)	Western North Atlantic	Holocene
de Vernal and Hillaire-Marcel (2000)	North-west North Atlantic	LGM versus modern
de Vernal et al. (1993a)	Gulf of St Lawrence	Late glacial–Holocene
de Vernal et al. (1993b)	North Atlantic	Modern
de Vernal et al. (1997)	North Atlantic	Modern
de Vernal et al. (2000)	North Atlantic	LGM
de Vernal et al. (2001)	North Atlantic, Arctic, sub-Arctic Seas compilation	Modern
de Vernal et al. (2005a)	Arctic Seas compilation	Modern, LGM
de Vernal et al. (2005b)	Chukchi Sea	Holocene
Voronina et al. (2001)	Barents Sea	Holocene

commonly well preserved. Consequently, the records of dinocysts are much more continuous, in both glacial and interglacial sediments (de Vernal & Mudie, 1989), than those of other microfossil groups (Thiede et al., 1989).

Mudie et al. (2001) presents an excellent summary of the progress made in the use of statistical assessments of dinocyst assemblages to reconstruct sea ice cover. Quantitative studies completed by Mudie and Short (1985) and Mudie (1992) were among the first to use Q-mode factor analysis to develop dinocyst-based transfer functions for SST and sea surface, but not sea ice cover. These studies were based on the eastern Canadian continental margin, using less than 100 samples. Later work by Rochon et al. (1999) and de Vernal and Hillaire-Marcel (2000) increased the geographical coverage to include the northern North Atlantic, Gulf of St Lawrence, Hudson Bay and Barents Sea. This larger data set, of almost 400 core tops, was analysed with a Best Analogue Technique (BAT). The primary advantage

of this technique over the Imbrie-Kipp Q-mode factor analysis is in its logarithmic trans-formation of abundance data that allocates greater significance than otherwise to sparsely represented taxa, which do have an ecological significance. In addition, this technique is rela-tively conservative, requiring little manipulation and transformation of the data (de Vernal et al., 2005a). One of the most significant problems, however, with these analyses was the occurrence of non-analogue situations in the palaeo record. In order to address this issue, de Vernal et al. (2001) increased the database to include almost 700 samples that cover a wider range of environmental variability, and even more recently, the calibration database was increased to include 940 reference points, and also analysed with a BAT (de Vernal et al., 2005a). In addition, Peyron and de Vernal (2001) apply another statistical approach to calibrate dinocyst assemblages and specific environmental parameters, Artificial Neuron Net-works (ANN). The advantage of ANN is that it does not assume a unimodal response by taxa to an environmental parameter. Their results show that ANN can be used successfully, and are in good agreement with the results of the BAT work. In summary, over the past two decades, researchers have seen a progression over time that has increased the number of sample sites and the total range of ecological variability, and have worked with these data using increa-singly sophisticated statistical methods. Work still must be done to deal with the problems of non-analogue situations and those related to reconstruction of environmental variables, like sea ice cover, that exhibit a large amount of interannual and/or interdecadal variability.

Mudie et al. (2001) and de Vernal et al. (2001) list several avenues for continued research, in order to improve the accuracy and resolution of dinocyst assemblage-based reconstruc-tions of sea ice cover. Continued work on dinocyst taxonomy is critical. In addition, a better understanding of the ecological framework for each taxon is important. This includes more work on the species distribution and dynamics of Arctic dinoflagellate and dinocyst popu-lations, which can be accomplished through a combination of water column and sediment trap work. The link between dinoflagellates and their cysts needs to be addressed more com-pletely, with incubation studies to confirm taxonomic relationships and the environmental controls on encystment and germination.

Time-slice palaeo sea ice reconstructions

Initiation of Sea Ice and Perennial Ice in the Arctic Basin

A wealth of data concerning the history of sea ice in the Arctic, and in particular, of the initiation of sea ice formation in the Arctic, was realized based on data acquired during the Integrated Ocean Drilling Program (IODP) Arctic Coring Expedition (ACEX) on the Lomonosov Ridge during 2004. The results of this >400-m-long core, which extended back 55 million years, place the initiation of sea ice at ~46 million years, much earlier than previously thought (Moran et al., 2006). Most importantly, the data indicate a synchrone-ity with both the Antarctic record of ice and with records of atmospheric carbon dioxide, suggesting the key role of the atmosphere in driving both northern and southern hemisphere glaciation (Moran et al., 2006).

A variety of proxy data suggest the initiation of sea ice at ~46 MYBP (Sangiorgi et al., 2008). For example, St John (2008) presents the IRD record form IODP 302 cores; these data include both quantitative information on sand accumulation rates and a qualitative

evaluation of surface textures and grain composition. These data support the initiation of both sea ice and glacial ice in the Arctic at ~46 Ma and are in accordance with 'pebble-based interpretation made by the IODP Scientific Party (Backman et al., 2006; Moran et al., 2006)'. Stickley et al. (2008) have observed an increase in the abundance of a form of diatoms (needle-like) that they interpret to be indicative of sea ice, based on morphological similarities to modern sea ice diatoms. Finally, Wadell and Moore (2008) have used $\delta^{18}O$ data from fish bone carbonate recovered in the ACEX core to reconstruct middle-Eocene salinities. Their data show an increase in salinity at ~46 Ma, which they interpret as the result of sea ice formation.

The second major finding of the ACEX project is that perennial ice in the central Arctic developed at ~14 Ma. Geochemical fingerprinting of detrital Fe oxide grains by Darby (2008) demonstrates that perennial sea ice has been present in the Arctic since ~14 Ma. By identifying source regions for the Fe oxide mineral grains <180 µm in size, following likely drift paths, and then estimating if the drift time was either greater than or less than a year, Darby (2008) distinguishes between perennial versus seasonal sea ice cover. Similarly, heavy and clay mineral analysis of the ACEX IODP 302 cores indicates a large scale shift in provenance at ~13 Ma, which Krylov et al. (2008) interpret as a shift to perennial sea ice at that time. Their rationale is similar to that of Darby (2008), that in order for grains from the eastern Laptev–East Siberian seas to have been transported to the ACEX site, sea ice must have survived for more than a single season.

Last Glacial Maximum (~16–20 ka in ¹⁴C years)

Last Glacial Maximum (~16–20 ka in ^{14}C years)

One of the key questions leading the effort to reconstruct sea ice extent in the high northern latitudes has been that of ice extent during the LGM. Based primarily on the sparse distribution of coccoliths in LGM sediments and data from planktonic foraminiferal transfer functions, CLIMAP (1976, 1981) proposed extensive sea ice cover in the northern North Atlantic, with winter sea ice extending as far south at 45°N. This interpretation was further supported by the work of several scientists, including e.g., Gard (1987) and Gard and Backman (1990) in Nordic Seas, Rahman and de Vernal (1994) in the Labrador Sea that described very sparse LGM coccolith assemblages, and foraminiferal studies by Kellogg (1976).

However, since the initial CLIMAP reconstruction, evidence for at least seasonally ice-free waters in the Nordic Seas during the LGM has accumulated (Henrich et al., 1989; Johannessen et al., 1994; Hebbeln et al., 1994; Wagner & Henrich, 1994; Sarnthein et al., 1995; Weinelt et al., 1996; Rosell-Melé, 1997; Norgaard-Pedersen et al., 2003). Hebbeln et al. (1994) and Hebbeln and Wefer (1997) e.g. suggest seasonally ice-free conditions in the Nordic Seas between 27–22.5 ka and 19.5–14.5 ka, based on increased abundances of both coccoliths and planktonic foraminifera, in cores from the Fram Strait. These ice-free periods are termed 'Nordway events'. In addition, evidence points to the growth of the Barents Sea Ice Sheet during the last Ice Age, about 22 ka (Elverhoi et al., 1993). The moisture source for ice growth is problematic, if, as suggested by CLIMAP, the Nordic Seas were permanently ice covered at that time (Hebbeln et al., 1994).

Hebbeln et al. (1998) summarized the state of knowledge concerning palaeo sea ice extent in the North Atlantic at that time, by stating:

> During the last fifteen years the CLIMAP palaeoceanographic view of the glacial Polar North Atlantic as an almost permanently isolated sea covered by heavy sea ice

throughout the year has shifted to a much more dynamic view of the environmental conditions. A meridional current system similar to the present-day conditions secured the exchange of water, ice and heat between the Polar North Atlantic and the Atlantic and Arctic Oceans. Although affected by variations in strength and intensity this meridional current pattern resulted in an almost permanent presence of at least some seasonally ice-free areas, with all the consequences for e.g. marine life and deep water formation.

Given conflicting lines of evidence, the need to further investigate sea ice extent during the LGM became clear. This recognition led to an international open science meeting in 1999, Environmental Processes of the Ice Age: Land, Oceans, Glaciers (EPILOG) (Mix et al., 2001). Participants reviewed the state of knowledge concerning the LGM and identified key issues that needed to be addressed through future work, with a goal of developing a better understanding of the conditions and processes that characterized the LGM.

Several lines of evidence have been pursued aggressively, including dinocyst work (de Vernal & Hillaire-Marcel, 2000; de Vernal et al., 2000, 2005a), oxygen-isotope-based studies (Sarnthein et al., 1995) and multiproxy work (Hebbeln et al., 1994, 1998; Hebbeln & Wefer, 1997; Norgaard-Pedersen et al., 2003; Sarnthein et al., 2003a). For example, de Vernal and Hillaire-Marcel (2000) and de Vernal et al. (2000) have shown that permanent sea ice in the North Atlantic, though much more extensive than today, was as much as 10° further north than indicated by the CLIMAP study. More specifically, de Vernal et al. (2005a) showed that in the North Atlantic, sea ice cover was relatively dense on the eastern continental margins of both Canada and Greenland, while offshore and the sub-polar seas were regions with seasonal sea ice that lasted from several weeks to several months each year. South of 50°N, the eastern North Atlantic was shown to be ice-free. In addition, dinocyst and planktonic foraminiferal isotope data suggest that surface waters were strongly stratified during the LGM (de Vernal & Hillaire-Marcel, 2000), which must have slowed down North Atlantic circulation and reduced heat transport to both the Arctic and western Europe. de Vernal and Hillaire-Marcel (2000) speculate that one of the consequences of this stratification was expansion of winter sea ice extent off eastern North America.

The work of both Norgaard-Pedersen et al. (2003) and Sarnthein et al. (2003a) was part of the GLAMAP 2000 programme, mentioned previously, whose goal was to develop new SST maps for the Atlantic during the LGM. Norgaard-Pedersen et al. (2003) presented a multiproxy-based interpretation of LGM sea ice conditions in Fram Strait, and the eastern and central Arctic, based on a combination of data on sediment composition and flux rates of IRD and planktonic foraminiferal abundance and isotopic data. Their data reveal spatial heterogeneity in the character of sea ice, with seasonal sea ice cover in the eastern Fram Strait and northern Barents Sea, perennial ice cover with occasional open leads in the summer and finally, extensive perennial sea ice cover in the central Arctic Basin. The planktonic foraminiferal-based work of Sarnthein et al. (2003a) from the North Atlantic showed glacial summers were characterized by relatively ice-free Nordic seas, while sea ice extended south to the Iceland Faroe Ridge during the winter. Clearly, our understanding of the sea ice conditions that characterized the LGM in the high northern latitudes has been refined by the many studies, which have been completed following the initial work of the CLIMAP project.

While many studies have been devoted to establishing the geographic limits of sea ice cover during the LGM, few have addressed the character of that ice. An exception is the work by Bradley and England (2008), who bring the term 'paleocrystic ice' back into use. They suggest that during Marine Isotope Stage 2 (MIS 2), most of the Arctic Basin was covered by exceptionally thick, multiyear sea ice with a contribution of firn. They attribute the accumulation of such thick ice primarily to lower sea level that resulted in the relative isolation of the Arctic Basin and access in and out of the basin restricted to the Fram Strait. Combined with colder temperatures, lower ablation rates and refreezing of meltwater, conditions resulted in which paleocrystic ice filled nearly the entire Arctic Basin. Bradley and England (2008) suggest that the loss of this thick floating mass of ice via export and melting, following initial sea level rise and the re-entry of warm waters from the Atlantic at the end of the last glacial, was in part responsible for the Younger Dryas.

Holocene (0–10 ka BP)

Great interest in Holocene climate springs from both the relationship between well-documented human activities and climate over the past 10,000 years and the recognition of recent dramatic change in sea ice over in the high northern latitudes (Serreze et al., 2007). As summarized by Grove (1988), relatively recent climatic events, such as the LIA, a cool climatic interval that lasted from around the mid-1300s to the mid-1800s, had a strong impact on European societies of the time. Cooler temperatures and increased Nordic Sea ice extent at that time are thought to have been a factor in the disappearance of Viking colonies in Greenland (Grove, 2001). This has been investigated by many including Jensen et al. (2004) and Moros et al. (2006), who used variability in the diatoms in marine sediment cores from south and west of Greenland to reconstruct sea ice conditions in the area and to address how that might have impacted Norse societies. Similarly, changes in sea ice cover, based on dinocyst assemblage transfer functions, have been shown to impact Palaeo- and Ne-eskimo settlements and their activities (Mudie et al., 2005). Given the strong impact of sea ice extent on human activities in the area, some of the longest suites of historical data documenting sea ice are from here. In particular, data from Iceland extend back to the earliest days of Iceland's colonization, during the 9th century. These data have been collated by Thoroddsen (1916, 1917), updated by Koch (1945) and re-evaluated more recently by Sigtryggsson (1972) and Ogilvie (1981, 1983). The data can be used to supplement the relatively short instrumental data set, derived from satellites, that goes back only to the early 1970s (Chapter 6). Other methods, through which the instrumental data set can be supplemented, include fishing and ships' logs (Bergthorsson, 1969 and Catchpole, 1992, respectively) and biological data on the distribution of different species of seals, as indicated by the distribution of bones in archaeological sites (Woollett, 1999). In addition, researchers developing new proxies, such as the IP$_{25}$ biomarker, have used comparison of their data to the instrumental record of sea ice extent to test the effectiveness of the proxy in recording sea ice conditions (Massé et al., 2008).

Regional differences in sea ice behaviour, and the need for more quantitative data, have led to research efforts to acquire more information on Arctic sea ice extent through the Holocene. These efforts have multiplied over the past decade with a multitude of recent studies based on a wide variety of proxies, primarily, but not exclusively, multiproxy data from both glacial ice and marine sediment cores (Fisher et al., 2006). These findings are summarized below.

One of the more unusual lines of evidence for changes in sea ice extent during the Holocene is the radiocarbon dating of bowhead whale remains. These data have been used to establish when stocks of whales from the Bering Sea and the Davis Strait could have intermingled. Today, the persistence of ice between the two regions prohibits this kind of exchange, but the data indicate that in the early Holocene, until about 8900 calendar years BP, the absence of blocking ice allowed these two stocks to intermingle (Dyke et al., 1996; Dyke & Savelle, 2001). This observation of reduced sea ice cover in the early Holocene is a feature observed in many records (Levac et al., 2001; de Vernal et al., 2005b). While the whale data provide an important window on sea ice conditions in the early Holocene, they are limited in terms of their temporal and spatial resolution.

Ice core data have provided higher-resolution information regarding changes in sea ice cover, but most of the data cover only the later part of the Holocene. Based on a statistically significant relationship between sea salt concentration in glacial ice from the Penny Ice Cap (Baffin Island) and Baffin Bay spring sea ice extent (90-year data set), Grumet et al. (2001) reconstruct ice distribution over the past 700 years. Their data do show increased sea ice during the LIA. Their data also demonstrate links between sea ice extent and the North Atlantic Oscillation, reinforcing that the behaviour of these oceanic and atmospheric systems are closely coupled and need to be studied in parallel. Similarly, Kinnard et al. (2006) have analysed ion concentration in an ice core from the Devon Ice Cap and used the data to evaluate sea ice cover in Baffin Bay; their record extends back only ~150 years. Both these data sets, from Grumet et al. (2001) and Kinnard et al. (2006) are intriguing, but relatively short; longer records of a similar type are much needed.

To date, single-proxy and multiproxy analysis of marine sediment cores have provided longer records detailing Holocene sea ice extent. For example, diatom data document changes in sea ice cover over the past 10,000 years, though the data are qualitative and geographically discontinuous (Williams, 1990; Koç et al., 1993; Bauch & Polyakova, 2000; Jiang et al., 2005). For example, Williams (1990) links reduced diatom abundance in cores from Baffin Bay to reduced diatom productivity at times when sea ice extent was more severe than today. She links increased sea ice cover to the presence of low-salinity meltwater, as this would freeze more easily than surface waters of normal salinity. The timing of these events is dependent upon location. Koç et al. (1993) note that the eastern Nordic Seas were ice-free by 13.4 ka (oldest part of record), with decreasing ice extent through the mid-Holocene, followed by cooling and increased ice extent until today. Finally, Bauch and Polyakova (2000), working in the Laptev Sea on a relatively short record (>3000 years), find that more severe pack ice marks the earliest part of their record.

Multiproxy work by Bond et al. (1997) in the North Atlantic demonstrate ~1500-year cyclicity in North Atlantic circulation throughout the Holocene, that can be tied to oceanographic cycles of the same frequency during the last glacial (Bond & Lotti, 1995) and to changes in atmospheric circulation recorded in the Greenland Ice Core (O'Brien et al., 1995). Bond et al. (1997) suggest the alternation of two modes of oceanographic circulation. Maximum IRD input and cooler SST occur during periods characterized by southward advection of waters originating from north of Iceland that includes drifting sea ice carrying volcanic glass erupted onto the sea ice. Giraudeau et al. (2000) present a 12,000-year, coccolith-based study of a core from south of Iceland. Both long-term trends and higher-frequency instabilities are noted. Millennial-scale variability in the accumulation of *E. huxleyi* is in phase with associated IRD peaks described by Bond et al. (1997) that have been linked to changes in the advection of

cooler, icy waters from the north. Jennings et al. (2002) also find links to the millennial-scale cycles of Bond et al. (1997) in their multiproxy data set from the East Greenland margin. Millennial- and century-scale variability in sea ice cover also is recorded in multiproxy data sets from western Greenland (Møller et al., 2006; Moros et al., 2006; Seidenkrantz et al., 2007, 2008), where a combination of microfossil and XRF data demonstrates highly variable sea ice conditions through the Holocene, though data coverage is stronger over the past 4400 years. Despite the isolated fjord settings from which these cores were recovered, their records are similar to those from the Labrador Sea. Seidenkrantz et al. (2007, 2008) note that these data are in accordance with the commonly termed 'North Atlantic climate seesaw' that describes the air-temperature differences between Greenland and northern Europe.

Given the success of dinocyst assemblage data in faithfully recording modern sea ice extent (de Vernal et al., 2005a), dinocyst data are the most heavily utilized tools for reconstruction of variations in Holocene sea ice extent. Studies include those from the Labrador Sea (Rochon & de Vernal, 1994; Levac & de Vernal, 1997), Baffin Bay (Levac et al., 2001), the Barents Sea (Voronina et al., 2001), the western North Atlantic (Solignac et al., 2006; de Vernal & Hillaire-Marcel, 2006) and the Chukchi Sea (de Vernal et al., 2005b). These studies demonstrate both temporal and spatial variability in sea ice cover through the Holocene. Perhaps their most important finding is the distinct geographic heterogeneity in patterns of sea ice extent. These regional differences need to be understood in order to evaluate the role of processes that have influenced sea ice cover in the Arctic in the past and continue under warming conditions (Fisher et al., 2006).

Dinocyst-based reconstructions for the Chukchi Sea, western Arctic, indicate minimal sea ice cover in the early Holocene (before 12,000 cal. years BP), followed by extensive sea ice cover from about 12,000 to 6000 cal. years BP and then generally reduced sea ice for the rest of the Holocene, though both century- and millennial-scale oscillations are also observed (de Vernal et al., 2005b). In contrast, Levac et al. (2001) observed a very different trend in dinocyst data from Baffin Bay, in the eastern Arctic, where the relatively ice-free conditions that characterized the early Holocene were followed by increasing sea ice cover through the late Holocene. Similarly, in the north-west North Atlantic, de Vernal and Hillaire-Marcel (2006) observed a sea ice minimum from 11,500 to 6000 cal. years BP, with slightly increased and variable sea ice for the remainder of the Holocene.

Solignac et al. (2006) note similar geographic variability, with cores from the east Greenland and north Iceland shelves documenting decreasing sea ice extent through the Holocene, while a core from south of Greenland shows the opposite trend. Solignac et al. (2006) note that the trend of decreasing sea ice through the Holocene that is recorded from the east Greenland and north Iceland shelves may at first glance appear to be at odds with other data sets that suggest a late Holocene cooling trend (Andrews et al., 1997; Jennings et al., 2002; Moros et al., 2006), primarily based on analysis of terrigenous grains. However, Solignac et al. (2006) propose alternative interpretations for the data that provide a coherent picture of changes in sea ice extent and the subsequent influence on the distribution of ice-rafted material. One possibility is that decreased sea ice could have resulted in a change from a system in which glacial margins were floating to one where the margins were characterized by calving icebergs that were more likely to carry IRD out of fjords. Another possibility is related to the role of sea ice in determining IRD drift patterns. Solignac et al. (2004) suggest that one consequence of decreased sea ice was the increased transport of IRD from sites more distant to the core locations.

The geographic differences of sea ice cover in response to changes in climate during the Holocene that are apparent in these records demonstrate the need for increased temporal and spatial resolution of Holocene sea ice trends in the Arctic, a complex region characterized by dynamic processes. These data will enhance our ability to model and predict the potentially heterogeneous response to modern atmospheric warming that has been observed and which is predicted to continue (Johannessen et al., 2004).

13.4 Conclusion

Palaeo sea ice estimates commenced in both the southern and northern polar regions primarily as a result of SST estimates under CLIMAP. The development of sea ice proxies and statistical modelling is hence still in its infancy. Arctic researchers have taken an active lead in advancing palaeo sea ice estimation using grouped dinocyst databases and advanced, yet comparable, estimation models. Antarctic palaeo sea ice estimation, based primarily on circumpolar diatom distributions, is less advanced. Efforts are hampered by the existence of two seafloor diatom distribution databases, multiple, yet-to-be compared, proxies and the need for a revised satellite sea ice database. Improving estimates of the history and variability of Antarctic sea ice, required by both the modelling community and the ice core community (to cross-validate their aerosol proxies), are being partially addressed by the MARGO project.

Antarctic sea ice variation over the Quaternary is best recorded from the South Atlantic sector, and lightly covered in the south Indian Ocean. There are very few palaeo sea ice records from the South Pacific sector, and reconstructions that are mostly hypothetical. Current studies by German researchers should soon provide new data from the eastern Pacific. An increase in Antarctic climate change records from coastal regions, and a significant increase in the resolution of events down to the annual scale, have highlighted a need for different signature species to provide a record of physical conditions in the sea ice zone. The reconstruction of a Holocene record of sea ice around the Antarctic continental margin has increased the number of potentially useful proxy indicator species for this. Studies determining *Fragilariopsis curta*'s ecological niche, physiological responses and modulation by physical oceanographic conditions may provide the best sea ice duration proxy for the Antarctic coastal margin. Statistical solutions would be the next step in providing useful quantitative estimates.

Arctic sea ice knowledge for the Holocene and the LGM are now well documented and highly advanced, pulling on evidence from many microfossil and lithological sources. Extension of the record to longer-term variation over the Arctic region is within reach and should allow for sea ice boundary conditions over time to be incorporated into GCMs, providing the spatial coverage required by the GCM is attended to.

The relationship between climate and sea ice is a complex and ongoing research area. With additional palaeo sea ice records, and continuing elucidation of the forcings upon the long-term variability of sea ice (e.g. atmosphere, heat flux and isolation), this key climate modulator will eventually be understood. Our understanding of past boundary conditions will be insightful when married to results from modern studies of the physical interactions between the ice, ocean and atmosphere. The study of sea ice and atmospheric phenomena will clarify probable trends in both hemispheres and links to global weather. Global atmospheric responses to Antarctic sea ice variability are also being investigated (Arzel et al., 2006; Holland & Raphael, 2006; Lefebvre & Goose 2008). Although present sea ice characteristics can now

be reasonably modelled in GCMs (Parkinson et al., 2006), simulating the natural variability in the Antarctic is a challenge for coupled ocean/sea ice/atmosphere climate models (Fichefet et al., 2008). Long simulations will help determine mechanisms responsible for Holocene and LGM sea ice conditions and variability (Renssen et al., 2005; Holland et al., 2006; Otto-Bliesner et al., 2006; Toggweiler & Russell, 2008). Gersonde et al. (2003) called for new methods of determining summer sea ice cover so that sea ice seasonality could be better incorporated into the modelling of air–sea exchange of CO_2. Their call remains valid today, and highlights one of many interrelated challenges in determining the history of polar sea ice and its interaction with the climate system.

Acknowledgements

References

Abelmann, A. Gersonde, R., Cortese, G., Kuhn, G. & Smetacek, V. (2006) Extensive phytoplankton blooms in the Atlantic sector of the glacial Southern Ocean. *Paleoceanography*, **21**, PA1013, 10.1029/2005PA001199.

Abram, N., Mulvaney, R., Wolff, E.W. & Mudelsee, M. (2007) Ice core records as sea ice proxies: an evaluation from the Weddell Sea region of Antarctica. *Journal of Geophysical Research*, **112**, D15101, 10.1029/2006JD008139.

Ackley, S., Wadhams, P., Comiso, J.C. & Worby, A.P. (2003) Decadal decrease of Antarctic sea ice extent inferred from whaling records revisited on the basis of historical and modern sea ice records. *Polar Research*, **22**, 19–25.

Ainley, D.G., Hobson, K.A., Crosta, X., Rau, G.H., Wassenaar, L.I. & Augustinus, P.C. (2006) Holocene variation in the Antarctic coastal food web: linking δD and δ13C in snow petrel diet and marine sediments. *Marine Ecology Progress Series*, **306**, 31–40.

Andrews, J.T., Smith, L.M., Preston, R., Cooper, T. & Jennings, A. (1997) Spatial and temporal patterns of iceberg rafting (IRD) along the east Greenland margin, ca. 68°N, over the last 14 cal. ka. *Journal of Quaternary Research*, **12**, 1–13.

Armand, L.K. (1997) The use of diatom transfer functions in estimating sea-surface temperature and sea ice in cores from the southeast Indian Ocean. PhD thesis, Australian National University, Canberra.

Armand, L.K. (2000) An ocean of ice – advances in the estimation of past sea ice in the Southern Ocean. *GSA Today*, **10**, 1–7.

Armand, L.K. & Leventer, A. (2003) Palaeo sea ice distribution – reconstruction and palaeoclimatic significance. In: *Sea Ice: Physics, Chemistry and Biology* (Eds. D. Thomas & G. Dieckmann), pp. 333–372. Blackwell Science Ltd, Oxford.

Armand, L.K., Crosta, X., Romero, O. & Pichon, J.-J. (2005) The biogeography of major diatom taxa in Southern Ocean sediments. 1. Ice-related species. *Palaeogeography, Palaeoclimatology, Palaeoecology*, **223**, 93–126.

Armand, L.K., Crosta, X., Quéguiner, B. Mosseri, J. Garcia, N. (2008) Diatoms in surface sediments of the Kerguelen-Heard region of the South Indian Ocean. *Deep-Sea Research Part II*, **55**, 677–692.

Arzel, O., Fichefet, T. & Goosse, H. (2006) Sea ice evolution over the 20th and 21st centuries as simulated by current AOGCMs. *Ocean Modelling*, **12**, 401–415.

Backman, J., Moran, K., McInroy, D.B., Mayer, L. & Expedition 302 Scientists (2006) *Proceedings of the Integrated Ocean Drilling Program*, **302**, 10.2204/iodp.proc.302.104.2006.

Bahk, J.J., Yoon, H.I., Kim, Y., Kang, C.Y. & Bae, S.H. (2003) Microfabric analysis of laminated diatom ooze (Holocene) from the eastern Bransfield Strait, Antarctic Peninsula. *Geoscience Journal*, **7**, 135–142.

Barbraud, C. & Weimerskirch, H. (2001) Emperor penguins and climate change. *Nature*, **411**, 183–186.

Barbraud, C. & Weimerskirch, H. (2006) Antarctic birds breed later in response to climate change. *Proceedings of the National Academy of Sciences*, **103**, 6248–6251.

Bárcena, M.A., Gersonde, R., Ledsma, S. et al. (1998) Record of Holocene glacial oscillations in Bransfield Basin as revealed by siliceous microfossil assemblages. *Antarctic Science*, **10**, 269–285.

Bárcena, M.A., Isla, E., Plaza, A. et al. (2002) Bioaccumulation record and paleoclimatic significance in the Western Bransfield Strait. The last 2000 years. *Deep-Sea Research Part II*, **49**, 935–950.

Bauch, H.A. & Polyakova, Y.I. (2000) Late Holocene variations in Arctic shelf hydrology and sea ice regime: evidence from north of the Lena Delta. *International Journal of Earth Sciences*, **89**, 569–577.

Baumann, K.-H., Andruleit, H.A. & Samtleben, C. (2000) Coccolithophores in the Nordic Seas: comparison of living communities with surface sediment assemblages. *Deep-Sea Research*, **47**, 1743–1772.

Bergthorsson, P. (1969) An estimate of drift ice and temperature in Iceland in 1000 years. *Joekull*, **19**, 94–101.

Belt, S.T., Masse, G., Rowlands, S.J., Poulin, M., Michel, C. & LeBlanc, B. (2007) A novel chemical fossil of palaeo sea ice: IP_{25}. *Organic Chemistry*, **38**, 16–27.

Bi, D., Budd, W.F., Hirst, A.C. & Wu, X. (2001) Collapse and reorganisation of the Southern Ocean overturning under the global warming in a coupled model. *Geophysical Research Letters*, **28**, 3927–3930.

Bianchi, C. & Gersonde, R. (2002) The Southern Ocean surface between Marine Isotope Stages 6 and 5d: shape and timing of climate change. *Palaeogeography, Palaeoclimatology, Palaeoecology*, **187**, 151–177.

Bianchi, C. & Gersonde, R. (2004) Climate evolution at the last deglaciation: the role of the Southern Ocean. *Earth and Planetary Science Letters*, **228**, 407–424.

Bigler, M., Röthlisberger, R., Lambert, F., Stocker, T.F. & Wagenbach, D. (2006) Aerosol deposited in East Antarctica over the last glacial cycle: detailed apportionment of continental and sea-salt contributions. *Journal of Geophysical Research*, **111**, D08205, DOI:10.1029/2005JD0006469.

Bischof, J. (1990) Dropstones in the Norwegian–Greenland Sea – indications of late Quaternary circulation patterns? In: *Geological History of the Polar Oceans: Arctic versus Antarctic* (Eds. U. Bleil & J. Thiede), NATO ASI Series C, Vol. 308, pp. 499–518. Kluwer Academic Publishers, Dordrecht.

Bjørgo, E., Johannessen, O.M. & Miles, M.W. (1997) Analysis of merged SMMR-SSMI time series of Arctic and Antarctic sea ice parameters 1978–1995. *Geophysical Research Letters*, **24**, 413–416.

Boessenkool, K.P., Van Gelder, M.-J., Brinkhuis, H. & Troelstra, S.R. (2001) Distribution of organic-walled dinoflagellate cysts in surface sediments from transects across the Polar Front offshore southeast Greenland. *Journal of Quaternary Science*, **16**, 661–666.

Bond, G.C. & Lotti, R. (1995) Iceberg discharges into the North Atlantic on millennial time scales during the last glaciation. *Science*, **267**, 1005–1010.

Bond, G., Heinrich, H., Broecker, W.S. et al. (1992) Evidence for massive discharge of icebergs into the North Atlantic ocean during the last glacial period. *Nature*, **360**, 245–249.

Bond, G., Showers, W., Cheseby, M. et al. (1997) A pervasive millennial-scale cycle in North Atlantic Holocene and glacial climates. *Science*, **278**, 1257–1266.

Braarud, T. (1979) The temperature range of the non-motile stage of *Coccolithus pelagicus* in the North Atlantic region. *British Phycological Journal*, **14**, 349–352.

Bradley, R.S. & England, J.H. (2008) The Younger Dryas and the sea of ancient ice. *Quaternary Research*, **70**, 1–10, DOI:10.1016/j.yqres.2008.03.002.

Broecker, W.S., Peacock, S.L., Walker, S. et al. (1998) How much deep water is formed in the Southern Ocean. *Journal of Geophysical Research*, **103**, 15833–15843.

Bromwich, D.H. (1984) A reconstruction of the coastal Antarctic climate and summer sea ice position at 18 ka BP (Abstract). *Annals of Glaciology*, **5**, 201.

Budd, W.F. & Wu, X. (1998) Modelling long term global and Antarctic changes resulting from increased greenhouse gases. In: *Coupled Climate Modelling: Proceedings of the Tenth Annual BMRC Modelling Workshop, 12–13 October 1998, Melbourne, Victoria*, pp. 71–74. Bureau of Meteorology Research Centre, Melbourne.

Buffen, A., Leventer, A., Rubin, A. & Hutchins, T. (2007) Diatom assemblages in surface sediments of the northwestern Weddell Sea, Antarctic Peninsula. *Marine Micropaleontology*, **62**, 7–30.

Burckle, L.H. (1983) Diatom dissolution patterns sediments of the Southern Ocean. *Journal of the Geological Society of America*, **15**, 536–537.

Burckle, L.H. (1984) Diatom distribution and palaeoceanographic reconstruction in the Southern Ocean – present and last glacial maximum. *Marine Micropalaeontology*, **9**, 241–261.

Burckle, L.H. & Abrams, N. (1986) Biotic response to two late Neogene intervals of global climatic change: evidence from the deep-sea record. *South African Journal of Science*, **82**, 69.

Burckle, L.H. & Burak, R.W. (1988) Fluctuations in late Quaternary diatom abundances: stratigraphic and paleoclimatic implications from subantarctic deep sea cores. *Palaeogeography, Palaeoclimatology, Palaeoecology*, **67**, 147–156.

Burckle, L.H. & Cirilli, J. (1987) Origin of diatom ooze belt in the Southern Ocean: implications for late Quaternary paleoceanography. *Micropaleontology*, **33**, 82–86.

Burckle, L.H. & Mortlock, R. (1998) Sea ice extent in the Southern Ocean during the Last Glacial Maximum: another approach to the problem. *Annals of Glaciology*, **27**, 302–304.

Burckle, L.H., Robinson, D. & Cooke, D. (1982) Reappraisal of sea ice distribution in the Atlantic and Pacific sectors of the Southern Ocean at 18,000 yr BP. *Nature*, **299**, 435–437.

Burckle, L.H., Jacobs, S.S. & McLaughlin, R.B. (1987) Late austral spring diatom distribution between New Zealand and the Ross Ice Shelf, Antarctica: hydrographic and sediment correlations. *Micropaleontology*, **33**, 74–81.

Carson, D. & Ganeshram, R. (2006) Reconstructing biogeochemical processes in near shore Antarctic sea ice environment. *Goldschmidt Conference Abstract*, DOI:10.1016/j.gca.2006.06.084.

Carter, L., Neil, H.L., & Northcote, L. (2002) Late Quaternary ice-rafting events in the SW Pacific Ocean, off eastern New Zealand. *Marine Geology*, **191**, 19–35.

Catchpole, A.J.W. (1992) Hudson Bay Company Ships log-books as sources of sea ice data 1751–1870. In: *Climate Since AD 1500* (Eds. R.S. Bradley & P.D. Jones), pp. 17–39. Routledge, London.

Cavaleri, D.J. & Parkinson, C.L. (2008) Antarctic sea ice variabilityand trends, 1979–2006. *Journal of Geophysical Research*, **113**, C07004, 10.1029/2007JC004564.

Cavalieri, D.J., St Germain, K.M. & Swift, C.T. (1995) Reduction of weather effects in the calculation of sea ice concentration with the DMSP SSM/I. *Journal of Glaciology*, **41**, 455–464.

Chapman, W.L. & Walsh, J.E. (1993) Recent variations of sea ice and air temperature in high latitudes. *Bulletin of the American Meteorological Society*, **74**, 33–47.

Clark, D.L. & Hanson, A. (1983) Central Arctic Ocean sediment texture: a key to ice transport mechanisms. In: *Glacial-Marine sedimentation* (Ed. B.F. Molnia), pp. 301–330. Plenum, New York.

Clementson, L.A., Parslow, J.S., Griffiths, F.B. et al. (1998) Controls on phytoplankton production in the Australiasian sector of the subtropical convergence. *Deep-Sea Research*, **45**, 1627–1661.

CLIMAP Project Members (1976) The surface of the ice-age Earth. *Science*, **191**, 1131–1137.

CLIMAP Project Members (1981) *Seasonal reconstructions of the Earth's surface at the last glacial maximum*. Geological Society of America: Map and Chart Series MC-36.

Collins, L.G., Allen, C., Pike, J. & Hodgson, D. (2007) The Scotia Sea: reconstructing glacial climates from diatom assemblages. In: *Antarctica: A Keystone in a Changing World – Online Proceedings of the 10th ISAES X* (Eds. A.K. Cooper et al.). USGS Open File Report-2007-1047, Extended Abstract 136, 6p.

Comiso, J.C. & Steffen, K. (2001) Studies of Antarctic sea ice concentrations from satellite data and their applications. *Journal of Geophysical Research*, **106**, 31361–31385.

Cooke, D.W. & Hays, J.D. (1982) Estimates of Antarctic Ocean seasonal sea ice cover during glacial intervals. In: *Antarctic Geoscience* (Ed. C. Craddock), Series B, No. 4, pp. 1017–1025. International Union of Geological Sciences, The University of Wisconsin Press, Wisconsin.

Cooke, D.W., Burckle, L.H. & Hays, J.D. (1977) Winter sea ice cover during the late Pleistocene in the Antarctic Ocean. *EOS, Transactions of the American Geophysical Union*, **58**, 416.

Cremer, H. (1999) Distribution patterns of diatom surface sediment assemblages in the Laptev Sea (Arctic Ocean). *Marine Micropaleontology*, **38**, 39–67.

Cremer, H., Gore, D., Kirkup, H. et al. (2001) The Late Quaternary environmental history of the Windmill Islands, East Antarctica – initial evidence from the diatom record. In: *Proceedings of the 16th International Diatom Symposium,* Athens 2000 (Ed. A. Economou-Amilli), pp. 471–481. University of Athens, Athens.

Cremer, H., Roberts, D., McMinn, A., Gore, D. & Melles, M. (2003) The Holocene diatom flora of marine bays in the Windmill Islands, East Antarctica. *Botanica Marina*, **46**, 82–106.

Crosta, X., Pichon, J.-J. & Burckle, L.H. (1998a) Application of modern analog technique to marine Antarctic diatoms: reconstruction of maximum sea ice extent at the Last Glacial Maximum. *Palaeoceanography*, **13**, 286–297.

Crosta, X., Pichon, J.-J. & Burckle, L.H. (1998b) Reappraisal of Antarctic seasonal sea ice at the Last Glacial Maximum. *Geophysical Research Letters*, **25**, 2703–2706.

Crosta, X., Sturm, A., Armand, L. & Pichon, J.-J. (2004) Late Quaternary sea ice history in the Indian sector of the Southern Ocean as recorded by diatom assemblages. *Marine Micropaleontology*, **50**, 209–226.

Crosta, X., Romero, O., Armand, L.K. & Pichon, J.-J. (2005) The biogeography of major diatom taxa in Southern Ocean sediments. 2. Open-Ocean related species. *Palaeogeography, Palaeoclimatology, Palaeoecology*, **223**, 66–92.

Crosta, X., Denis, D. & Ther, O. (2007a) Sea ice seasonality during the Holocene, Adélie Land, East Antarctica. *Marine Micropaleontology*, **66**, 222–232.

Crosta, X., Debret, M., Denis, D., Courty, M.A. & Ther, O. (2007b) Holocene long- and short-term climate changes off Adélie Land, East Antarctica. *Geochemistry, Geophysics, Geosystems*, **8**, Q11009, DOI:10.1029/2007GC001718.

Crowley, T.J. & Lowery, T.S. (2000) Northern hemisphere temperature reconstruction. *Ambio*, **29**, 51–54.

Crowley, T.J. & Parkinson, C.L. (1988) Late Pleistocene variations in Antarctic sea ice I: effect of orbital insolation changes. *Climate Dynamics*, **3**, 85–91.

Cunningham, W.L. & Leventer, A. (1998) Diatom assemblages in surface sediments of the Ross Sea: relationship to present oceanographic conditions. *Antarctic Science*, **10**, 134–146.

Cunningham, W.L., Leventer, A., Andrews, J.T., Jennings, A.E. & Litch, K.J. (1999) Late Pleistocene–Holocene marine conditions in the Ross Sea, Antarctica: evidence from the diatom record. *The Holocene*, **9**, 129–139.

Curran, M.A.J. & Jones, G.B. (2000) Dimethyl sulphide in the Southern Ocean: seasonality and flux *Journal of Geophysical Research*, **105**, 20451–20459.

Curran, M.A.J., van Ommen, T.D., Morgan, V.I., Phillips, K.L. & Palmer, A.S. (2003) Ice core evidence for Antarctic sea ice decline since the 1950's. *Science*, **302**, 1203–1206.

Curran, M.A.J., Wong, G., Goodwin, I., van Ommen, T. & Vance, T. (2008) Estimate of sea salt sources to Antarctica: an alternative interpretation of the EPICA sea salt record? *Geophysical Research Abstracts*, **10**, SRef-ID:1607-7962/gra/EGU2008-A-07581.

Darby, D.A. (2003) Sources of sediment found in sea ice from the western Arctic Ocean, new insights into processes of entrainment and drift patterns. *Journal of Geophysical Research*, **108**, 10.1029/2002JC001350.

Darby, D.A. (2008) Arctic perennial ice cover over the last 14 million years. *Paleoceanography*, **23**, 10.1029/2007PA001479.

Darby, D.A. & Bischof, J.F. (2004) A Holocene record of changing Arctic Ocean ice drift analogous to the effects of the Arctic Oscillation. *Paleoceanography*, **19**, PA1027, 10.1029/2003PA000961.

Darby, D.A., Bischof, J.F., Spielhagen, R.F., Marshall, S.A. & Herman, S.W. (2002) Arctic ice export events and their potential impact on global climate during the late Pleistocene. *Paleoceanography*, **17**, 10.1029/2001PA000639.

Darby, D.A., Polyak, L. & Bauch, H.A. (2006) Past glacial and interglacial conditions in the Arctic Ocean and marginal seas – a review. *Progress in Oceanography*, **71**, 129–144.

De Sève, M.A. (1999) Transfer function between surface diatom assemblages and sea-surface temperature and salinity of the Labrador Sea. *Marine Micropalaeontology*, **36**, 249–267.

DeFelice, D.R. (1979) Relative diatom abundance as tool for monitoring winter sea ice fluctuations in southeast Atlantic. *Antarctic Journal of the United States*, **14**, 105–106.

DeFelice, D.R. & Wise, S.W.J. (1981) Surface lithofacies, biofacies and diatom diversity patterns as models for delineation of climatic change in the southeast Atlantic Ocean. *Marine Micropalaeontology*, **6**, 29–70.

Denis, D., Crosta, X., Zaragosi, S., Romero, O., Martin, B. & Mas, V. (2006) Seasonal and sub-seasonal climate changes recorded in laminated diatom ooze sediments, Adélie Land, East Antarctica. *The Holocene*, **16**, 1137–1147.

Dethleff, D., Rachold, V., Tintelnot, M. & Antonow, M. (2000) Sea ice transport of riverine particles from the Laptev Sea to Fram Strait based on clay mineral studies. *International Journal of Earth Sciences*, **89**, 496–502.

Dowdeswell, J.A. & Dowdeswell, E.K. (1989) Debris in icebergs and rates of glaciomarine sedimentation: observations from Spitsbergen and a simple model. *Journal of Geology*, **97**, 221–231.

Domack, E., Leventer, A., Root, S. et al. (2003) Marine sediment record of natural environmental variability and recent warming in the Antarctic Peninsula. *AGU Antarctic Research Series*, Antarctic Peninsula Climate Variability: A historical and palaeoenvironmetal perspective, **79**, 205–244.

Dyke, A.S. & Savelle, J.M. (2001) Holocene history of the Bering Sea bowhead whale (*Balaena mysticetus*) in its Beaufort Sea summer grounds off southwestern Victoria Island, NWT, western Canadian Arctic. *Quaternary Research*, **55**, 371–379.

Dyke, A.S., Hooper, J. & Savelle, J.M. (1996) A history of sea ice in the Canadian Arctic Archipelago based on postglacial remains of the bowhead whale (*Balaena mysticetus*). *Arctic*, **49**, 235–255.

Dyke, A.S., England, J., Reimnitz, E. & Jette, H. (1997) Changes in driftwood delivery to the Canadian Arctic archipelago: the hypothesis of postglacial oscillations of the transpolar drift. *Arctic*, **50**, 1–16.

Eide, L.K. (1990) Distribution of coccoliths in surface sediments in the Norwegian–Greenland Sea. *Marine Micropalaeontology*, **16**, 65–75.

Elverhoi, A., Russwurm, L., Fjeldskaar, W., Solheim, A. & Nyland-Berg, M. (1993) The Barents Sea ice sheet – a model of its growth and decay during the last ice maximum. *Quaternary Science Reviews*, **12**, 863–873.

Escutia, C., Warnke, D., Acton, G.D. et al. (2003) Sediment distribution and sedimentary processes across the Antarctic Wilkes Land margin during the Quaternary. *Deep-Sea Research Part II*, **50**, 1481–1508.

Fichefet, T., Arzel, O. & Goosse, H. (2008) On the ability of current atmosphere-ocean general circulation models to predict the evolution of sea ice. *CLiC Ice and Climate News*, **10**, 5–6.

Finocchiaro, F., Langone, L., Colizza, E., Fontolan, G., Giglio, F. & Tuzzi, E. (2005) Record of the early Holocene warming in a laminated sediment core from Cape Hallett Bay (Northern Victoria Land, Antarctica). *Global and Planetary Change*, **45**, 193–206.

Fisher, D., Dyke, A., Koerner, R. et al. (2006) Natural variability of Arctic sea ice over the Holocene. *EOS, Transactions, American Geophysical Union*, **87**, 10.1029/2006EO280001.

Foster, A.F.M., Curran, M.A.J., Smith, B.T., van Ommen, T.D. & Morgan, V.I. (2006) Covariation of sea ice and methanesulphonic acid in Wilhelm II Land, East Antarctica. *Annals of Glaciology*, **44**, 429–432.

Frank, M., Gersonde, R., Rutgers van der Loeff, M. et al. (2000) Similar glacial and interglacial export bioproductivity in the Atlantic sector of the Southern Ocean: multiproxy evidence and implications for glacial atmospheric CO_2. *Paleoceanography*, **15**, 642–658.

Fryxell, G.A. & Prasad, A.K.S.K. (1990) *Eucampia antarctica* var. *recta* (Mangin) stat. nov. (Biddulphiaceae, Bacillariophyceae): life stages at the Weddell Sea ice edge. *Phycologia*, **29**, 27–38.

Gard, G. (1987) Late Quaternary nannofossil biostratigraphy and sedimentation patterns: Fram Strait, Arctic. *Palaeoceanography*, **2**, 519–529.

Gard, G. & Backman, J. (1990) Synthesis of Arctic and sub-Arctic coccolith biochronology and history of North Atlantic Drift water influx during the last 500,000 years. In: *Geological History of the Polar Oceans: Arctic versus Antarctic* (Eds. U. Bleil & J. Thiede), NATO ASI Series C, Vol. 308, pp. 417–438. Kluwer Academic Publishers, Dordrecht.

Gersonde, R. & Zielinski, U. (2000) The reconstruction of late Quaternary Antarctic sea ice distribution – the use of diatoms as a proxy for sea ice. *Palaeogeography, Palaeoclimatology, Palaeoecology*, **162**, 263–286.

Gersonde, R., Abelmann, A., Brathauer, U. et al. (2003) Last glacial sea surface temperatures and sea ice extent in the Southern Ocean (Atlantic-Indian sector): a multiproxy approach. *Paleoceanography*, **18**, 1061, 10.1029/2002PA000809.

Gersonde, R., Crosta, X., Abelmann, A. & Armand, L. (2005) Sea-surface temperature and sea ice distribution of the Southern Ocean at the EPILOG Last Glacial Maximum – a circum-Antarctic view based on siliceous microfossil records. *Quaternary Science Reviews*, **24**, 869–896.

Gibson, J.A.E., Trull, T., Nichols, P.D., Summons, R.E. & McMinn, A. (1999) Sedimentation of ^{13}C-rich organic matter from Antarctic sea ice algae: a potential indicator of past sea ice extent. *Geology*, **27**, 331–334.

Giraudeau, J., Cremer, M., Manthe, S., Labeyrie, L. & Bond, G. (2000) Coccolith evidence for instabilities in surface circulation south of Iceland during Holocene times. *Earth and Planetary Science Letters*, **179**, 257–268.

Gloersen, P. & Campbell, W.J. (1991) Recent variations in Arctic and Antarctic sea ice covers. *Nature*, **352**, 33–36.

Gloersen, P. & Cavalieri, D.J. (1986) Reduction of weather effects in the calculation of sea ice concentration from microwave radiances. *Journal of Geophysical Research*, **91**, 3913–3919.

Gloersen, P.E., Mollo-Christensen, E. & Hubanks, P. (1989) Observations of Arctic polar lows with the Nimbus 7 Scanning Multichannel Microwave Radiometer. In: *Polar and Arctic Lows* (Eds. P.F. Twitchell, E.A. Rasmussen & K.L. Davidson), pp. 359–371. A. Deepak, Hampton, VA.

Gordon, A.L. (1978) Deep Antarctic convection west of Maud Rise. *Journal of Physical Oceanography*, **8**, 600–612.

Graham, A.G.C., Fretwell, P.T., Larter, R.D. et al. (2008) A new bathymetric compilation highlighting extensive paleo-ice sheet drainage on the continental shelf, South Georgia, sub-Antarctica. *Geochemistry, Geophysics, Geosystems*, **9**, Q07011, 10.1029/2008GC001993.

Gran, H.H. (1904) Diatomaceae from the ice-floes and plankton of the Arctic Ocean. In: *The Norwegian North Polar Expedition 1893–1896, Vol. 4* (Ed. F. Nansen), pp. 1–74. Longmans, London.

Grenfell, T.C. (1983) A theoretical model of the optical properties of sea ice in the visible and near infrared. *Journal of Geophysical Research*, **88**, 9723–9735.

Grobe, H. (1987) A simple method for the determination of ice-rafted debris in sediment cores. *Polarforschung*, **57**, 123–126.

Grobe, H. & Mackensen, A. (1992) Late Quaternary climatic cycles as recorded in sediments from the Antarctic continental margin. *Antarctic Research Series*, **56**, 349–376.

Grøsfjeld, K., Larsen, E., Sejrup, H.P. et al. (1999) Dinoflagellate cysts reflecting surface-water conditions in Voldafjorden, western Norway during the last 11,300 years. *Boreas*, **28**, 403–415.

Grove, J.M. (1988) *The Little Ice Age*. Routledge, London.

Grove, J.M. (2001) The initiation of the 'Little Ice Age' in regions round the North Atlantic. *Climatic Change*, **48**, 53–82.

Grumet, N.S., Wake, C.P., Mayewski, P.A. et al. (2001) Variability of sea ice extent in Baffin Bay over the last millennium. *Climatic Change*, **49**, 129–145.

Harland, R. & Pudsey, C.J. (1999) Dinoflagellate cysts from sediment traps deployed in the Bellingshausen, Weddell and Scotia seas, Antarctica. *Marine Micropaleontology*, **37**, 77–99.

Harwood, D.M. & Bohaty, S.M. (2007) Late Miocene sea ice diatoms indicate a cold polar East Antarctic ice sheet event. *Geophysical Research Abstracts*, **9**, 08078, SRef-ID 1607-7962/gra/EGU2007-A-08078.

Hays, J.D. (1978) A review of the Late Quaternary climatic history of Antarctic Seas. In: *Antarctic Glacial History and World Palaeoenvironments: Proceedings of the 10th INQUA*, (Ed. B. van Zinderen), pp. 57–71. Balkema, Rotterdam.

Hays, J.D., Lozano, J.A., Shackleton, N. & Irving, G. (1976) Reconstruction of the Atlantic and western Indian Ocean sectors of the 18,000 B.P. Antarctic Ocean. *Geological Society of America, Memoir*, **145**, 337–372.

Head, M.J., Harland, R. & Matthiessen, J. (2001) Cold marine indicators of the late Quaternary: the new dinoflagellate cyst genus *Islandinium* and related morphotypes. *Journal of Quaternary Science*, **16**, 621–636.

Hebbeln, D. (2000) Flux of ice-rafted detritus from sea ice in the Fram Strait. *Deep-Sea Research*, **47**, 1773–1790.

Hebbeln, D. & Wefer, G. (1997) Late Quaternary palaeoceanography in the Fram Strait. *Palaeoceanography*, **12**, 65–78.

Hebbeln, D., Dokken, T., Andersen, E.S., Hald, M. & Elverhoi, A. (1994) Moisture supply for northern ice-sheet growth during the last glacial maximum. *Nature*, **370**, 357–360.

Hebbeln, D., Henrich, R. & Baumann, K.-H. (1998) Palaeoceanography of the last interglacial/glacial cycle in the polar North Atlantic. *Quaternary Science Reviews*, **17**, 125–153.

Heinrich, H. (1988) Origin and consequences of cyclic ice-rafting in the northeast Atlantic Ocean during the past 130,000 years. *Quaternary Research*, **29**, 142–152.

Henrich, R., Kassens, H., Vogelsang, E. & Thiede, J. (1989) Sedimentary facies of glacial–interglacial cycles in the Norwegian Sea during the last 350 ka. *Marine Geology*, **86**, 283–319.

Heroy, D.C., Sjunneskog, C. & Anderson, J.B. (2007) Holocene climate change in the Bransfield Basin, Antarctic Peninsula: evidence from sediment and diatom analysis. *Antarctic Science*, **20**, 69–87.

Hillaire-Marcel, C. & de Vernal, A. (2008) Stable isotope clue to episodic sea ice formation in the glacial North Atlantic. *Earth and Planetary Science Letters*, **268**, 143–150.

Hodell, D.A., Kanfoush, S.L., Shemesh, A., Crosta, X., Charles, C.D. & Guilderson, T.P. (2001) Abrupt cooling of Antarctic surface waters and sea ice expansion in the South Atlantic sector of the Southern Ocean at 5000 cal yr B.P. *Quaternary Research*, **56**, 191–198.

Holland, M.M. & Raphael, M.N. (2006) Twentieth century simulation of the southern hemisphere climate in coupled models. Part II: sea ice conditions and variability. *Climate Dynamics*, **26**, 229–245.

Holland, M.M., Bitz, C.M., Hunke, E.C., Lipscomb, W.H. & Schramm, J.L. (2006) Influence of the sea ice thickness distribution on polar climate in CCSM3. *Journal of Climate*, **19**, 2398–2414.

Horner, R.A. (Ed.) (1985) *Sea Ice Biota*. CRC Press, Boca Raton, FL.

Horner, R.A. & Alexander, V. (1972) Algal populations in Arctic sea ice: an investigation of heterotrophy. *Limnology and Oceanography*, **17**, 454–458.

Imbrie, J. & Kipp, N.G. (1971) A new micropalaeontological method for quantitative palaeoclimatology; application to a late Pleistocene Caribbean core. In: *The Late Cenozoic Glacial Ages* (Ed. K.K. Turekian), pp. 71–147. Yale University Press, New Haven.

Iizuka, Y., Hondoh, T. & Jujii, Y. (2008) Antarctic sea ice extent during the Holocene reconstructed from inland ice core evidence. *Journal of Geophysical Research*, **113**, D15114, 10.1029/2007JD009326.

Jansen, E., Overpeck, J., Briffa, K.R. et al. (2007) Palaeoclimate In: *Climate Change 2007: The Phyical Science Basis. Contribution of Working Group 1 to the Fourth Assessment Report of the Intergovernmental Panel on Climate Change* (Eds S. Solomon et al.), pp. 433–497. Cambridge University Press, Cambridge, United Kingdom and New York, NY, USA.

Jennings, A.E., Andrews, J.T., Knudsen, K.L., Hald, M. & Hansen, C.V. (2002) A mid-Holocene shift in Arctic sea ice variability on the East Greenland Shelf. *The Holocene*, **12**, 49–58.

Jensen, K.G., Kuijpers, A., Koç, N., & Heinemeier, J. (2004) Diatom evidence of hydrographic changes and ice conditions in Igaliku Fjord. *The Holocene*, **14**, 152–164.

Jiang, H., Seidenkrantz, M.-S., Knudsen, K.L. & Eiriksson, J. (2001) Diatom surface sediment assemblages around Iceland and their relationships to oceanic environmental variables. *Marine Micropaleontology*, **41**, 73–96.

Jiang, H., Eiriksson, J., Schultz, M., Knudsen, K.L. & Seidenkrantz, M.S. (2005) Evidence for solar forcing of sea surface temperature on the North Icelandic Shelf during the late Holocene. *Geology*, **33**, 73–76.

Johannessen, T., Jansen, E., Flatoy, A. & Ravelo, A.C. (1994) The relationship between surface water masses, oceanographic fronts and palaeoclimatic proxies in surface of the Greenland, Iceland, Norwegian Seas. In: *Carbon Cycling in the Glacial Ocean: Constraints on the Oceans's Role in Global Change* (Eds. R. Zahn, T.F. Pedersen, M.A. Kaminski & L. Labeyrie), pp. 61–85. Springer, Berlin.

Johannessen, O.M., Miles, M. & Bjørgo, E. (1995) The Arctic shrinking sea ice. *Nature*, **376**, 126–127.

Johannessen, O.M., Shalina, E.V. & Miles, M.W. (1999) Satellite evidence for an Arctic sea ice cover in transformation. *Science*, **286**, 1937–1939.

Johannessen O.A., Bengtsson, L., Miles, M.W. et al. (2004) Arctic climate change: observed and modeled temperature and sea ice variability. *Tellus*, **56A**, 328–341.

Jousé, A.P. (1962) *Stratigraphicheskiye I Palaeogeographicheskiye Issledovaniya v Severo-Zapadnoy Chasti Tikhogo Okeana*. Akademia Nauk S.S.S.R.

Justwan, A. & Koç, N. (2008) A diatom based transfer function for reconstructing sea ice concentrations in the North Atlantic. *Marine Micropaleontology*, **66**, 264–278.

Kaczmarska, I., Barbrick, N.E., Ehrman, J.M. & Cant, G.P. (1993) *Eucampia* Index as an indicator of the Late Pleistocene oscillations of the winter sea ice extent at the ODP Leg 119 Site 745B at the Kerguelen Plateau. *Hydrobiologia*, **269/270**, 103–112.

Kanfoush, S. L. Hodell, D.A., Charles, C.D., Guilderson, T.P., Mortyn, P.G. & Ninnemann, U.S. (2000) Millennial-scale instability of the Antarctic ice sheet during the Last Glaciation. *Science*, **288**, 1815–1818.

Kanfoush, S. L. Hodell, D.A., Charles, C.D., Janecek, T.R. & Rack, F.R. (2002) Comparison of ice-rafted debris and physical properties in ODP Site 1094 (South Atlantic) with the Vostock ice core over the last four climatic cycles. *Palaeogeography, Palaeoclimatology, Palaeoecology*, **182**, 329–349.

Kellogg, T.B. (1976) Late Quaternary climatic changes: evidence from deep-sea cores of Norwegian and Greenland Seas. *Geological Society of America Memoir*, **145**, 77–110.

Killworth, P.D. (1983) Deep convection in the world ocean. *Geophysics and Space Physics*, **21**, 1–26.

Kinnard, C., Zdanowicz, C.M., Fisher, Wake, D.A. & Cameron P. (2006) Calibration of an ice-core glaciochemical (sea-salt) record with sea ice variability in the Canadian Arctic. *Annals of Glaciology*, **44**, 383–390.

Koç, N., Jansen, E. & Haflidason, H. (1993) Palaeoceanographic reconstructions of surface ocean conditions in the Greenland, Iceland and Norwegian seas through the last 14 ka based on diatoms. *Quaternary Science Reviews*, **12**, 115–140.

Koç Karpuz, N. & Schrader, H. (1990) Surface sediment diatom distribution and Holocene palaeotemperature variations in the Greenland, Iceland and Norwegian Sea. *Palaeoceanography*, **5**, 557–580.

Koch, L. (1945) The east Greenland ice. *Meddelelser om Grønland*, **130**, 1–374.

Koerner, R.M. (1977) Devon Island ice cap: core stratigraphy and palaeoclimate. *Science*, **196**, 15–18.

Kohly, A. (1998) Diatom flux and species composition in the Greenland Sea and the Norwegian Sea in 1991–1992. *Marine Geology*, **145**, 293–312.

Krylov, A.A., Andreeva, I.A., Vogt, C. et al. (2008) A shift in heavy and clay mineral provenance indicates a middle Miocene onset of a perennial sea ice cover in the Arctic Ocean. *Paleoceanography*, **23**, PA1S06, DOI: 10.1029/2007PA0014979.

Kucera, M., Rosell-Melé, A., Schneider, R., Waelbroeck, C. & Weinelt, M. (2005) Multiproxy approach for the reconstruction of the glacial ocean surface (MARGO). *Quaternary Science Reviews*, **24**, 813–819.

Kumar, N., Anderson, R.F., Mortlock, R.A. et al. (1995) Increased biological productivity and export production in the glacial Southern Ocean. *Nature*, **378**, 675–680.

Kunz-Pirrung, M. (2001) Dinoflagellate cyst assemblages in surface sediments of the Laptev Sea region (Arctic Ocean) and their relationship to hydrographic conditions. *Journal of Quaternary Science*, **16**, 637–649.

Kunz-Pirrung, M., Matthiessen, J. & de Vernal, A. (2001) Late Holocene dinoflagellate cysts as indicators for short-term climate variability in the Eastern Laptev Sea (Arctic Ocean). *Journal of Quaternary Science*, **16**, 711–716.

Kunz-Pirrung, M., Gersonde, R. & Hodell, D.A. (2002) Mid-Brunhes century scale diatom sea surface temperature and sea ice records from the Atlantic sector of the Southern Ocean (ODP Leg 177, sites 1093, 1094 and core PS2089-2). *Palaeogeography, Palaeoclimatology, Palaeoecology*, **182**, 305–328.

Labeyrie, L., Pichon, J.-J., Labracherie, M., Ippolito, P., Duprat, J., & Duplessy, J.C. (1986) Melting history of Antarctica during the past 60 000 years. *Nature*, **322**, 701–706.

Lefebvre, W. & Goose, H. (2008) An analysis of the atmospheric processes driving the large scale winter sea ice variability in the Southern Ocean. *Journal of Geophysical Research*, **113**, C02004, 10.1029/2006JC004032.

Lemke, P., Ren, J., Alley, R.B. et al. (2007) Observations: changes in snow, ice and frozen ground. In: *Climate Change 2007: The Physical Science Basis. Contributions of Working Group 1 to the Fourth Assessment Report of the Intergovernmental Panel on Climate Change* (Eds. S. Solomon et al.), pp. 337–383. Cambridge University Press, Cambridge, United Kingdom and New York, NY, USA.

Levac, E. & de Vernal, A. (1997) Postglacial changes of terrestrial and marine environments along the Labrador coast: palynological evidence from cores 91-045-005 and 91-045-006, Cartwright Saddle. *Canadian Journal of Earth Sciences*, **34**, 1358–1365.

Levac, E., de Vernal, A. & Blake Jr., W. (2001) Sea-surface conditions in northernmost Baffin Bay during the Holocene: palynological evidence. *Journal of Quaternary Science*, **16**, 353–363.

Leventer, A. (1992) Modern distribution of diatoms in sediments from the George V Coast, Antarctica. *Marine Micropaleontology*, **19**, 315–332.

Leventer, A. & Dunbar, R.B. (1988) Recent diatom record of McMurdo Sound, Antarctcica: implications for the history of sea ice extent. *Paleoceanography*, **3**, 259–274.

Leventer, A., Dunbar, R. & DeMaster, D.J. (1993) Diatom evidence for late Holocene climatic events in Granite Harbor, Antarctica. *Paleoceanography*, **8**, 373–386.

Leventer, A., Domack, E.W., Ishman, S.E., Brachfeld, S., McClennen, C.E. & Manley, P. (1996) Productivity cycles of 200–300 years in the Antarctic Peninsula region: understanding linkages among the sun, atmosphere, oceans, sea ice, and biota. *Geological Society of America, Bulletin*, **108**, 1626–1644.

Leventer, A., Domack, E., Barkoukis, A., McAndrews, B. & Murray, J. (2002) Laminations from the Palmer Deep: a diatom-based interpretation. *Palaeoceanography*, **17**, 1–15.

Leventer, A., Domack, E., Dunbar, R. et al. (2006) East Antarctic Margin marine sediment record of deglaciation, *GSA Today*, **16**, 10.1130/GSAT01612A.1.

Leventer, A., Armand, L. Harwood, D., Jordan, R. & Ligowski, R. (2007) New approaches and progress in the use of polar marine diatoms in reconstructing sea ice distribution. In: *Antarctica: A Keystone in a Changing World – Online Proceedings of the 10th ISAES X* (Eds. A.K. Cooper et al.), USGS Open File Report-2007-1047, Extended Abstract 005.

Lindsay, R.W. & Zhang, J. (2005) The thinning of Arctic sea ice, 1988–2003: have we passed a tipping point? *Journal of Climate*, **18**, 4879–4894.

Lisitzin, A.P. (1972) *Sedimentation in the World Ocean*. Special Publication No. 17. Society of Economic Palaeontologists and Mineralogists, Tulsa, OK.

Machado, E. (1993) Production, sedimentation and dissolution of biogenic silica in the northern North Atlantic, pp. 1–123. PhD dissertation, Christian Albrechts University, Kiel, Germany.

McLaren, A.S., Wittmann, W., Walsh, J.E., Bourke, R.H. & Weaver, R.L. (1992) Variability in sea ice thickness over the North Pole from 1977 to 1990. *Nature*, **358**, 224–226.

McMinn, A. (2000) Late Holocene increase in sea ice extent in fjords of the Vestfold Hills, eastern Antarctica. *Antarctic Science*, **12**, 80–88.

McPhee, M.G., Stanton, T.P., Morison, J.H. & Martinson, D.G. (1998) Freshening the upper ocean in Arctic: is perennial sea ice disappearing? *Geophysical Research Letters*, **25**, 1729–1732.

Maddison, E.J., Pike, J., Leventer, A. & Domack, E. (2005) Deglacial seasonal and sub-seasonal diatom record from Palmer Deep, Antarctica. *Journal of Quaternary Science*, **20**, 435–446.

Maddison, E.J., Pike, J., Leventer, A. et al. (2006) Post-glacial seasonal diatom record of the Mertz Glacier Polynya, East Antarctica. *Marine Micropaleontology*, **60**, 66–88.

de la Mare, W.K. (1997) Abrupt mid-twentieth-century decline in Antarctic sea ice extent from whaling records. *Nature*, **389**, 57–60.

MARGO Project Members (2009). Constraints on the magnitude and patterns of ocean cooling at the Last Glacial Maximum, *Nature Geoscience*, **2**, 127–132.

Massé, G., Rowland, S.J., Sicre, M.-A., Jacob, J., Jansen E. & Belt, S.T. (2008) Abrupt climate changes for Iceland during the last millennium: evidence from high resolution sea ice reconstructions, *Earth and Planetary Science Letters*, **269**, 564–568.

Massom, R.A., Hill, K., Barbraud, C. et al. (2009) Fast ice distribution in Adélie Land, East Antarctica: interannual variability and implications for Emperor penguins (*Aptenodytes forsteri)*. *Marine Ecology Progress Series*, **374**, 243–257.

Massom, R.A., Stammerjohn, S.E., Smith, R.C. et al. (2006) Extreme anomalous atmospheric circulation in the west Antarctic Peninsula region in Austral spring and summer 2001/02, and its profound impact on sea ice and biota. *Journal of Climate*, **19**, 3544–3571.

Matear, R. & Hirst, A.C. (1999) Climate change feedback on the future oceanic CO_2 uptake. *Tellus*, **51**, 722–733.

Matthiessen, J. & Knies, J. (2001) Dinoflagellate cyst evidence for warm interglacial conditions at the northern Barents Sea margin during marine oxygen isotope stage 5. *Journal of Quaternary Science*, **16**, 727–737.

Mayewski, P.A., Meeker, L.D., Whitlow, S.I. et al. (1994) Changes in atmospheric circulation and ocean ice cover over the North Atlantic during the last 41,000 years. *Science*, **263**, 1747–1751.

Maykut, G.A. (1978) Energy exchange over young sea ice in the central Arctic. *Journal of Geophysical Research*, **83**, 3646–3658.

Meier, W.N., Stroeve, J.C. & Fetterer, F. (2006) Whither Arctic sea ice? A clear signal of decline regionally, seasonally and extending beyond the satellite record. *Annals of Glaciology*, **46**, 428–434.

Mix, A.C., Bard, E. & Schneider, R. (2001) Environmental processes of the ice age: land, oceans, glaciers (EPILOG). *Quaternary Science Reviews*, **20**, 627–657.

Moran, K., Backman, J., Brinkhuis, H. et al. (2006) The Cenozoic palaeoenvironment of the Arctic Ocean. *Nature*, **441**, 601–605.

Morgan, V. & van Ommen, T.D. (1997) Seasonality in late Holocene climate from ice-core records. *The Holocene*, **7**, 351–354.

Moros, M., Andrews, J.T., Eberl, D.E. & Jansen, E. (2006) Holocene history of drift ice in the northern North Atlantic: evidence for different spatial and temporal modes. *Paleoceanography*, **21**, 10.1029/2005PA001214.

Mudie, P.J. (1992) Circum-Arctic Quaternary and Neogene marine palynofloras: palaeoecology and statistical analysis. In: *Neogene and Quaternary Dinoflagellate Cysts and Acritarchs* (Eds. M.J. Head & J.H. Wrenn), pp. 347–390. American Association of Stratigraphic Palynologists Foundation, Dallas, TX.

Mudie, P.J. & Rochon, A. (2001) Distribution of dinoflagellate cysts in the Canadian Arctic marine region. *Journal of Quaternary Science*, **16**, 603–620.

Mudie, P.J. & Short, S.K. (1985) Marine palynology of Baffin Bay. In: *Quaternary Environments* (Ed. J.T. Andrews), pp. 263–308. Allen & Unwin, Boston.

Mudie, P.J., Harland, R., Matthiessen, J. & de Vernal, A. (2001) Marine dinoflagellate cysts and high latitude Quaternary palaeoenvironmental reconstructions: an introduction. *Journal of Quaternary Science*, **16**, 595–602.

Mudie, P., Rochon, A. & Levac, E. (2005) Decadal-scale sea ice changes in the Canadian Arctic and their impacts on humans during the past 4,000 years. *Environmental Archaeology*, **10**, 113–126.

Naval Oceanography Command Detachment (1985) *Sea Ice Climatic Atlas*. NSTL MS 39529-500, NAVAIR 50-1C-540, ADA-168716. Commander, Naval Ocaenography Command, 1, Antarctic, Asheville.

Nielsen, S.H.H. & Hodell, D.A. (2007) Antarctic ice-rafted detritus (IRD) in the South Atlantic: indicators of iceshelf dynamics or ocean surface conditions? In: *Antarctica: A Keystone in a Changing World – Online Proceedings of the 10th ISAES* (Eds. A.K. Cooper et al.). USGS Open-file Report 2007-1047, Short Research Paper 020,10.3133/of2007-1047.srp020.

Nielsen, S.H.H., Koç, N. & Crosta, X. (2004) Holocene climate in the Atlantic sector of the Southern Ocean: controlled by insolation or oceanic circulation? *Geology*, **32**, 317–320.

Nielsen, S.H.H., Hodell, D.A., Kamenov, G., Guilderson, T. & Perfit, M.R. (2007) Origin and significance of ice-rafted detritus in the Atlantic sector of the Southern Ocean. *Geochemistry, Geophysics, Geosystems*, **8**, Q12005, DOI:10.1029/2007GC001618.

Nishimura, A., Nakasone, T., Hiramatsu, C., & Tanahashi, M. (1998) Late Quaternary paleoenvironment of the Ross Sea continental shelf, Antarctica. *Annals of Glaciology*, **27**, 275–280.

Norgaard-Pedersen, N., Spielhagen, R.F., Erlenkeuser, H. et al. (2003) Arctic Ocean during the Last Glacial Maximum: Atlantic and polar domains of surface water mass distributions and ice cover. *Paleoceanography*, **18**, 1063, 10.1029/2002PA000781.

O'Brien, S., Mayewski, P.A., Meeker, L.D., Meese, D.A., Twickler, M.S. & Whitlow, S.I. (1995) Holocene climate as reconstructed from a Greenland ice core. *Science*, **270**, 1962–1964.

Ogilvie, A.E.J. (1981) Climate and society in Iceland from the medieval period to the late eighteenth century. PhD thesis, University of East Anglia, Norwich, UK.

Ogilvie, A.E.J. (1983) The past climate and sea ice record from Iceland, 1, Data to AD 1780. *Climate Change*, **6**, 131–152.

Olney. M.P., Bohaty, S.M., Harwood, D.M. & Scherer, P. (in press) *Creania lacyae* gen. nov. et sp. nov. and *Synedropsis cheethamii* sp. nov.: fossil indicators of Antarctic sea ice? Diatom Research.

van Ommen, T.D., Morgan, V, & Curran, M.A.J. (2004) Deglacial and Holocene changes in accumulation at Law Dome. *Annals of Glaciology*, **39**, 359–365.

Orsi, A.H., Whitworth, T., III & Nowlin, W.D. (1995) On the meridional extent and fronts of the Antarctic circumpolar current. *Deep-Sea Research*, **42**, 641–673.

Otto-Bliesner, B., Brady, E.C., Clauzet, G., Tomas, R., Levis, S. & Kothavala, Z. (2006) Last Glacial Maximum and Holocene climate in CCSM3. *Journal of Climate*, **19**, 2526–2544.

Parkinson, C.L. (1990) Search for the Little Ice Age in Southern Ocean sea ice records. *Annals of Glaciology*, **14**, 221–225.

Parkinson, C.L. (1995) Recent sea ice advances in Baffin Bay/Davis Strait and retreats in the Bellingshausen Sea. *Annals of Glaciology*, **21**, 348–352.

Parkinson, C.L. (2000) Variability of Arctic sea ice: the view from Space, an 18-year record. *Arctic*, **53**, 341–358.

Parkinson, C.L., Vinnikov, K.Y. & Cavalieri, D.J. (2006) Evaluation of the simulation of the annual cycle of Arctic and Antarctic sea ice coverages by 11 major global climate models. *Journal of Geophysical Research*, **111**, C07012, 10.1029/2005JC003408.

Pasteur, E. C., Mulvaney, R., Peel, D.A. Saltzman, E.S. & Whung, P.-Y. (1995) A 340 year record of biogenic sulphur from the Weddell Sea area, Antarctica. *Annals of Glaciology*, **21**, 169–174.

Petit, J.R., Jouzel, J., Raynaud, D. et al. (1999) Climate and atmospheric history of the past 420,000 years from the Vostok ice core, Antarctica. *Nature*, **399**, 429–436.

Peyron, O. & de Vernal, A. (2001) Application of artificial neural networks (ANN) to high-latitude dinocyst assemblages for the reconstruction of past sea-surface conditions in Arctic and sub-Arctic seas. *Journal of Quaternary Science*, **16**, 699–709.

Pfirman, S.L., Colony, R., Nürnberg, D., Eicken, H. & Rigor, I. (1997) Reconstructing the origin and trajectory of drifting Arctic sea ice. *Journal of Geophysical Research*, **102**, 12575–12586.

Pfirman, S.L., Wollenburg, I., Thiede, J. & Lange, M.A. (1989) Lithogenic sediment on Arctic pack ice: potential aeolian flux and contributions to deep sea sediments. In: *Palaeoclimatology and Palaeometeorology: Modern and Past Pattern of Global Atmospheric Transport* (Eds. M. Sarnthein & M. Leinen), pp. 463–493. Kluwer, Dordrecht.

Pflaumann, U., Duprat, J., Pujol, C. & Labeyrie, L.D. (1996) SIMMAX: a modern analog technique to deduce Atlantic sea surface temperatures from planktonic foraminifera in deep-sea sediments. *Palaeoceanography*, **11**, 15–35.

Pichon, J.-J., Labracherie, M., Labeyrie, L.D. & Duprat, J. (1987) Transfer functions between diatom assemblages and surface hydrology in the Southern Ocean. *Palaeogeography, Palaeoclimatology, Palaeoecology*, **61**, 79–95.

Pike, J., Allen, C.S., Leventer, A., Stickley, C.E. & Pudsey, C.J. (2008) Comparison of contemporary and fossil diatom assemblages from the western Antarctic Peninsula shelf. *Marine Micropaleontology*, **67**, 274–287.

Polyakova, E. (1989) Diatoms in Arctic shallow seas and sediments. In: *The Arctic Sea* (Ed. Y. Herman), pp. 481–496. Van Nostrand Reinhold, New York.

Polyakova, Y., Pavlidis, Y.A. & Levin, A.A. (1992) Factors governing diatom fossil distributions in the surface layer of bottom sediments on the Barents Sea Shelf. *Oceanology*, **32**, 112–119.

Prell, W.L. (1985) The stability of low-latitude sea-surface temperatures: an evaluation of the CLIMAP reconstructions with emphasis on the positive SST anomalies. US Department of Energy Technical Report. DOE/ER/60167. US Department of Energy, Office of Energy Research, Washington, D.C.

Radi, T., de Vernal, A. & Peyron, O. (2001) Relationships between dinoflagellate cyst assemblages in surface sediment and hydrographic conditions in the Bering and Chukchi seas. *Journal of Quaternary Science*, **16**, 667–680.

Rahman, A. & de Vernal, A. (1994) Surface oceanographic changes in the eastern Labrador Sea: nannofossil record of the last 31,000 years. *Marine Geology*, **121**, 247–263.

Rankin, A.M. Auld, V. & Wolff, E.W. (2000) Frost flowers as a source of fractionated sea salt aerosol in the polar regions. *Geophysical Research Letters*, **27**, 3469–3472.

Rankin, A.M., Wolff, E.W. & Martin, S. (2002) Frost flowers: implications for tropospheric chemistry and ice core interpretation. *Journal of Geophysical Research*, **107**, 4683, DOI:10.1029/2002JD002492.

Rathburn, A.E., Pichon, J.-J., Ayress, M.A. & DeDeckker, P. (1997) Microfossil and stable-isotope evidence for changes in Late Holocene palaeoproductivity and palaeoceanographic conditions in the Prydz Bay region of Antarctica. *Palaeogeography, Palaeoclimatology, Palaeoecology*, **131**, 485–510.

Renssen, H., Goosse, H., Fichefet, T., Masson-Delmotte, V. & Koç, N. (2005) Holocene climate evolution in the high latitude southern hemisphere simulated by a coupled atmosphere-sea ice-ocean-vegetation model. *The Holocene*, **15**, 951–964.

Rintoul, S.R. (1998) On the origin and influence of Adélie Land bottom water. In: *Ocean, Ice, and Atmosphere: Interactions at the Antarctic Continental Margin* (Eds. S.S. Jacobs & R. Weiss), American Geophysical Union, Washington, D.C. *Antarctic Research Series*, **75**, pp. 151–171.

Rochon, A. & de Vernal, A. (1994) Palynomorph distribution in recent sediments from the Labrador Sea. *Canadian Journal of Earth Sciences*, **31**, 115–127.

Rochon, A., de Vernal, A., Sejrup, H.-P. & Haflidason, H. (1998) Palynological evidence of climatic and oceanographic changes in the North Sea during the last deglaciation. *Quaternary Research*, **49**, 197–207.

Rochon, A., de Vernal, A., Turon, J.L., Matthiessen, J. & Head, M.J. (1999) Distribution of recent dinoflagellate cysts in surface sediments from the North Atlantic Ocean and adjacent seas in relation to sea-surface parameters. *American Association of Stratigraphic Palynologists, Contribution Series*, **35**, 1–152.

Rosell-Melé, A. (1997) Appraisal of CLIMAP temperature reconstruction in the NE Atlantic using alkenone proxies. *EOS, Transactions of the American Geophysical Union*, **78**, F28.

Rosell-Melé, A. (1998) Interhemispheric appraisal of the value of alkenone indices as temperature and salinity proxies in high-latitude locations. *Palaeoceanography*, **13**, 694–703.

Rosell-Melé, A. & Koç, N. (1997) Palaeoclimatic significance of the stratigraphic occurrence of photosynthetic biomarker pigments in the Nordic seas. *Geology*, **25**, 49–52.

Rosell-Melé, A., Weinelt, M., Sarnthein, M., Koç, N. & Jansen, E. (1998) Variability of the Arctic front during the last climatic cycle: application of a novel molecular proxy. *Terra Nova*, **10**, 86–89.

Röthlisberger, R., Mudelsee, M., Bigler, M. et al. (2008) The southern hemisphere at glacial terminations: insights from the Dome C ice core. *Climate of the Past Discussions*, **4**, 761–789.

Rothrock, D.A., Yu, Y. & Maykut, G.A. (1999) Thinning of the Arctic sea ice cover. *Geophysical Research Letters*, **26**, 3469–3472.

Ruddiman, W.F. (1977) Late Quaternary deposition of ice rafted sand in the subpolar North Atlantic (lat. 40°N to 65°N). *Bulletin of the Geological Society of America*, **88**, 1813–1827.

Ruddiman, W.F. (1997) North Atlantic ice rafting: a major change at 75,000 years before present. *Science*, **196**, 1208–1211.

St John, K. (2008) Cenozoic ice-rafting history of the central Arctic Ocean: terrigenous sands on the Lomonosov Ridge. *Paleoceanography*, **23**, PA1S05, 10.1029/2007PA001483.

Samtleben, C. & Schroder, A. (1992) Living coccolithophore communities in the Norwegian–Greenland Sea and their record in sediment. *Marine Micropalaeontology*, **19**, 333–354.

Sancetta, C. (1979) Oceanography of the North Pacific during the last 18,000 years: evidence from fossil diatoms. *Marine Micropalaeontology*, **4**, 103–123.

Sancetta, C. (1981) Oceanographic and ecologic significance of diatoms in surface sediments of the Bering and Okhotsk seas. *Deep-Sea Research*, **28**, 789–817.

Sancetta, C. (1982) Distribution of diatom species in surface sediments of the Bering and Okhotsk Seas. *Marine Micropalaeontology*, **28**, 221–257.

Sancetta, C. (1983) Effect of Pleistocene glaciation upon oceanographic characteristics of the North Pacific Ocean and Bering Sea. *Deep-Sea Research*, **30**, 851–869.

Sangiorgi, F., van Soelen, E.E., Spofforth, D.J.A. et al. (2008) Cyclicity in the middle Eocene central Arctic Ocean sediment record: orbital forcing and environmental response. *Paleoceanography*, **23**, PA1S08, 10.1029/2007PA001487.

Sarnthein, M., Jansen, E., Weinelt, M. et al. (1995) Variations in Atlantic surface ocean palaeoceanography, 50–80°N: a time-slice record of the last 30,000 years. *Palaeoceanography*, **10**, 1063–1094.

Sarnthein, M., Plaumann, U. & Weinelt, M. (2003a) Past extent of sea ice in the northern North Atlantic inferred from foraminiferal palaeotemperature estimates. *Paleoceanography*, **18**, 10.1029/2002PA000771.

Sarnthein, M., Gersonde, R., Niebler, S. et al. (2003b) Overview of the Glacial Atlantic Ocean Mapping (GLAMAP 2000). *Palaeoceanography*, **18**, 1030, 10.1029/2002PA000769.

Schell, T.M., Moss, T.J., Scott, D.B. & Rochon, A. (2008) Paleo–sea ice conditions of the Amundsen Gulf, Canadian Arctic Archipelago: implications from the foraminiferal record of the last 200 years. *Journal of Geophysical Research*, **113**, 10.1029/2007JC004202.

Scherer, R., Hannah, M., Maffioli, P. et al. (2007) Palaeontologic characterisation and analysis of the AND-1B core, ANDRILL McMurdo Ice Shelf project, Antarctica. *Terra Antartica*, **14**, 223–254.

Schneider-Mor, A., Yam, R., Bianchi, C., Kunz-Pirrung, M. Gersonde, R. & Shemesh, A. (2005) Diatom stable isotopes, sea ice presence and sea surface temperature records of the past 640 ka in the Atlantic sector of the Southern Ocean. *Geophysical Research Letters*, **32**, L10704, 10.1029/2005GL022543.

Schneider-Mor, A., Yam, R., Bianchi, C., Kunz-Pirrung, M. Gersonde, R. & Shemesh, A. (2008) The nutrient regime at the siliceaous belt of the Atlantic sector of the Southern Ocean during the past 660 kyr. *Palaeoceanography*, **23**, PA3217, 10.1029/2007PA001466.

Schweitzer, P.N. (1995) *Monthly averaged polar sea ice concentration*. US Geological Survey Digital Data Series: Virginia. CD, Ed. 1. DDS-27.

Scott, D.B., Schell, T., Rochon, A. & Blasco, S. (2008) Modern benthic foraminifera in the surface sediments of the Beaufort Shelf, Slope and MacKenzie Trough, Beaufort Sea, Canada: taxonomy and summary of surficial distributions. *Journal of Foraminiferal Research*, **38**, 228–250.

Sedwick, P.N., Edwards, P.R., Mackey, D.J., Griffiths, F.B. & Parslow, J.S. (1997) Iron and manganese in surface waters of the Australian subantarctic region. *Deep-Sea Research*, **44**, 1239–1253.

Seidenkrantz, M.-S., Aagaard-Sørensen, S., Sulsbrück, H., Kuijpers, A., Jensen, K.G. & H. Kunzendorf, H. (2007) Hydrography and climate of the last 4400 years in a SW Greenland fjord: implications for Labrador Sea palaeoceanography. *The Holocene*, **17**, 387–401.

Seidenkrantz, M.-S., Roncaglia, L., Fischel, A., Heilmann-Clausen, C., Kuijpers, A. & Moros, M. (2008) Variable North Atlantic climate seesaw patterns documented by a late Holocene marine record from Disko Bugt, West Greenland. *Marine Micropaleontology*, **68**, 66–83.

Serreze, M.C., Holland, M.M. & Stroeve, J. (2007) Perspectives on the Arctic's shrinking sea ice cover. *Science*, **315**, 1533–1536.

Shemesh, A. Hodell, D., Crosta, X., Kanfoush, S., Charles, C. & Guilderson, T. (2002) Sequence of events during the last deglaciation in Southern Ocean sediments and Antarctic ice cores. *Paleoceanography*, **17**, 10.1029/2000PA000599,2002.

Shevenell, A.E., Domack, E.W. & Kernan, G.M. (1996) Record of Holocene palaeoclimate change along the Antarctic Peninsula: evidence from glacial marine sediments, Lallemand Fjord. *Papers and Proceedings of the Royal Society of Tasmania*, **130**, 55–64.

Sigtryggsson, H. (1972) An outline of sea ice conditions in the vicinity of Iceland. *Joekull*, **22**, 1–11.

Sjunneskog, C. & Taylor, F. (2002) Postglacial marine diatom record of the Palmer Deep, Antarctic Peninsula (ODP Leg 178, Site 1098). I: total diatom abundance. *Palaeoceanography*, **17**, 10.1029/2000PA000563.

Smith Jr., W.O. & Sakshaug, E. (1990) Polar phytoplankton. In: *Polar Oceanography, Part B Chemistry, Biology, and Geology* (Ed. W.O. Smith Jr.), pp. 477–525. Academic Press, San Diego, CA.

Solignac, S., de Vernal, A. & Hillaire-Marcel, C. (2004) Holocene sea-surface conditions in the North Atlantic – contrasted trends and regimes in the western and eastern sectors (Labrador Sea vs. Iceland Basin). *Quaternary Science Reviews*, **23**, 319–334.

Solignac, S., Giraudeau, J. & de Vernal, A. (2006) Holocene sea surface conditions in the western North Atlantic: spatial and temporal heterogeneities. *Paleoceanography*, **21**, PA2004, 10.1029/2005PA001175.

Stabeno, P.J. & Overland, J.E. (2001) Bering Sea shifts toward an earlier spring transition. *EOS, Transactions of the American Geophysical Union*, **82**, 317.

Steig, E.J., Hart, C.P., White, J.W.C., Cunningham, W.L., Davis, M.D. & Saltzman, E.S. (1998) Changes in climate, ocean and ice sheet conditions in the Ross embayment, Antarctica, at 6 ka. *Annals of Glaciology*, **27**, 305–310.

Stickley, C.E., Pike, J., Leventer, A. et al. (2005) Deglacial ocean and climate seasonality in laminated diatom sediments, Mac. Robertson Shelf, Antarctica. *Palaeogeography, Palaeoclimatology, Palaeoecology*, **227**, 290–310.

Stickley, C.E., Pike, J. & Leventer, A. (2006) Productivity events of the marine diatom *Thalassiosira tumida* (Janisch) Hasle recorded in deglacial varves from the East Antarctic Margin. *Marine Micropalaeontology*, **59**, 184–196.

Stickley, C. E., Koç, N., Brumsack, H.-J., Jordan, R. W. & Suto, I. (2008) A siliceous microfossil view of middle Eocene Arctic paleoenvironments: a window of biosilica production and preservation. *Paleoceanography*, **23**, PA1S14, 10.1029/2007PA001485.

Stroeve, J., Holland, M.M., Meier, W., Scambos, T. & Serreze. M. (2007) Arctic sea ice decline: faster than forecast. *Geophysical Research Letters*. **34**, L09501, 10.1029/2007GL029703.

Stuut, J.-B.W., Crosta, X., van der Borg, K., & Schnieder, R. (2004) Relationship between Antarctic sea ice and southwest African climate during the late Quaternary. *Geology*, **32**, 909–912.

Takeda, S. (1998) Influence of iron availability on nutrient consumption ratio of diatoms in oceanic waters. *Nature*, **393**, 774–777.

Taylor, F. & McMinn, A. (2001) Evidence from diatoms for Holocene climate fluctuation along the East Antarctic margin. *The Holocene*, **11**, 455–466.

Taylor, F. & McMinn, A. (2002) Late Quaternary diatom assemblages from Prydz Bay, Eastern Antarctica. *Quaternary Research*, **57**, 151–161.

Taylor, F. & Sjunneskog, C. (2002) Postglacial marine diatom record of the Palmer Deep, Antarctic Peninsula (ODP Leg 178, Site 1098) 2. Diatom assemblages. *Palaeoceanography*, **17**, 10.1029/2000PA000564.

Taylor, F., McMinn, A. & Franklin, D. (1997) Distribution of diatoms in surface sediments of Prydz Bay, Antarctica. *Marine Micropalaeontology*, **32**, 209–229.

Taylor, F., Whitehead, J. & Domack, E. (2001) Holocene paleoclimate change in the Antarctic Peninsula: evidence from the diatom, sedimentary and geochemical record. *Marine Micropaleontology*, **41**, 25–43.

Thiede, J., Eldholm, O. & Taylor, E. (1989) Variability of Cenozoic Norwegian–Greenland Sea palaeoceanography and Northern Hemisphere palaeoclimate; synthesis of palaeoenvironmental studies of ODP Leg 104, Voring Plateau, Norwegian continental margin. *Proceedings of the Ocean Drilling Program, Scientific Results*, **104**, 1067–1118.

Thoroddsen, Th. (1916/17) Árferdi á Íslandi í thúsund ár, 432 pp., Hid Íslenska Fraedafjelag í Kaupmannahöfn, S.L. Møller, Copenhagen, 1916 (pt. 1) and 1917 (pt. 2) (in Icelandic).

Toggweiler, J.R. & Russell, J. (2008). Ocean circulation in a warming climate. *Nature*, **451**, 286–288.

Tremblay, L.-B., Mysak, L.A. & Dyke, A.S. (1997) Evidence from driftwood records for century-to-millenial scale variations of the high latitude atmospheric circulation during the Holocene. *Geophysical Research Letters*, **24**, 2027–2030.

Vaughan, S. (2000) Can Antarctic sea ice extent be determined from whaling records? *Polar Record*, **36**, 345–347.

de Vernal, A. & Hillaire-Marcel, C. (2000) Sea ice cover, sea-surface salinity and halothermocline structure of the northwest North Atlantic: modern versus full glacial conditions. *Quaternary Science Reviews*, **19**, 65–85.

de Vernal, A. & Hillaire-Marcel, C. (2006) Provincialism in trends and high frequency changes in the northwest North Atlantic during the Holocene. *Global and Planetary Change*, **54**, 263–290.

de Vernal, A. & Mudie, P.J. (1989) Late Pliocene to Holocene palynostratigraphy at ODP Site 645, Baffin Bay. *Proceedings of the Ocean Drilling Program*, **105**, 401–422.

de Vernal, A., Guiot, J. & Turon, J.-L. (1993a) Late and postglacial palaeoenvironments of the Gulf of St. Lawrence: marine and terrestrial palynological evidence. *Géographie physique et Quaternaire*, **47**, 167–180.

de Vernal, A., Turon, J.-L. & Guiot, J. (1993b) Dinoflagellate cyst distribution in high-latitude marine environments and quantitative reconstruction of sea-surface salinity, temperature, and seasonality. *Canadian Journal of Earth Sciences*, **31**, 48–62.

de Vernal, A., Rochon, A., Turon, J.-L. & Matthiessen, J. (1997) Organic-walled dinoflagellate cysts: palynological tracers of sea-surface conditions in middle to high latitude marine environments. *GEOBIOS*, **30**, 905–920.

de Vernal, A., Hillaire-Marcel, C., Turon, J.-L. & Matthiessen, J. (2000) Reconstruction of sea-surface temperature, salinity, and sea ice cover in the northern North Atlantic during the last glacial maximum based on dinocyst assemblages. *Canadian Journal of Earth Sciences*, **37**, 725–750.

de Vernal, A., Henry, M., Matthiessen, J. et al. (2001) Dinoflagellate cyst assemblages as tracers of sea-surface conditions in the northern North Atlantic, Arctic and sub-Arctic seas: the new 'n = 677' data base and its application for quantitative palaeoceanographic reconstruction. *Journal of Quaternary Science*, **16**, 681–698.

de Vernal, A., Eynaud, F., Henry, M. et al. (2005a) Reconstruction of sea-surface conditions at middle to high latitudes of the Northern Hemisphere during the Last Glacial Maximum (LGM) based on dinoflagellate cyst assemblages. *Quaternary Science Reviews*, **24**, 897–924.

de Vernal, A., Hillaire-Marcel, C. & Darby, D.A. (2005b) Variability of sea ice cover in the Chukchi Sea (western Arctic Ocean) during the Holocene. *Paleoceanography*, **20**, PA4018, 10.1029/2005PA0011575.

Villa, G., Persico, D., Bonci, M.C., Lucchi, R.G., Morigi, C. & Rebesco, M. (2003) Biostratigraphic characterization and Quaternary microfossil palaeoecology in sediment drifts west of the Antarctic Peninsula – implications for cyclic glacial-interglacial deposition. *Palaeogeography, Palaeoclimatology, Palaeoecology*, **198**, 237–263.

Vinnikov, K.Y., Robock, A., Stouffer, R.J. et al. (1999) Global warming and northern hemisphere sea ice extent. *Science*, **286**, 1934–1937.

Voronina, E., Polyak, L., de Vernal, A. & Peyron, O. (2001) Holocene variations of seasurface conditions in the southeastern Barents Sea, reconstructed from dinoflagellate cyst assemblages. *Journal of Quaternary Science*, **16**, 717–726.

Wadell, L.M. & Moore, T.C. (2008) Salinity of the Eocene Arctic Ocean from oxygen isotope analysis of fish bone carbonate, *Paleoceanography*, **23**, PA1S14, 10.1029/2007PA001451.

Wagner, T. & Henrich, R. (1994) Organo- and lithofacies of TOC-lean glacial/interglacial deposits in the Norwegian–Greenland Sea: sedimentary and diagenetic responses to palaeoceanographic and palaeoclimatic changes. *Marine Geology*, **120**, 335–364.

Warner, R.C. & Budd, W.F. (1998) Modelling the long-term response of the Antarctic ice sheet to global warming. *Annals of Glaciology*, **27**, 161–168.

Watkins, A.B. & Simmonds, I. (2000) Current trends in Antarctic sea ice: the 1990s impact on a short climatology. *Journal of Climate*, **13**, 4441–4451.

Weinelt, M., Sarnthein, M., Pflaumann, U., Schulz, H., Jung, S. & Erlenkeuser, H. (1996) Ice-free Nordic seas during the last glacial maximum? Potential sites of deepwater formation. *Palaeoclimates*, **1**, 283–309.

Welch, K.A., Mayewski, P.A. & Whitlow, S.I. (1993) Methanesulfonic acid in coastal Antarctic snow related to sea ice extent. *Geophysical Research Letters*, **20**, 443–446.

Weller, R. & Wagenbach, D. (2007) Year-round chemical aerosol records in continental Antarctica obtained by automatic samplings. *Tellus*, **59**, 755–765.

Whitehead, J.M. & McMinn, A., (2002) Kerguelen Plateau Quaternary-late Pliocene palaeoenvironments: from diatom, silicoflagellate and sedimentological data. *Palaeogeography, Palaeoclimatology, Palaeoecology*, **186**, 335–368.

Whitehead, J.M., Wotherspoon, S. & Bohaty, S.M. (2005) Minimal Antarctic sea ice during the Pliocene. *Geology,* **33**, 137–140.

Williams, K.M. (1986) Recent arctic marine diatom assemblages from bottom sediments in Baffin Bay and Davis Strait. *Marine Micropalaeontology*, **10**, 327–341.

Williams, K.M. (1990) Late Quaternary palaeoceanography of the western Baffin Bay region: evidence from fossil diatoms. *Canadian Journal of Earth Sciences*, **27**, 1487–1494.

Williams, K.M. (1993) Ice sheet and ocean interactions, margin of the East Greenland Ice Sheet (14 ka to present): diatom evidence. *Palaeoceanography*, **8**, 69–83.

Wilson, P.R., Ainley, D.G., Nur, N. et al. (2001) Adélie penguin population change in the Pacific sector of Antarctica: relation to sea ice extent and the Antarctic circumpolar current. *Marine Ecology Progress Series*, **213**, 301–309.

Wolff, E.W., Rankin, A.M. & Röthlisberger, R. (2003) An ice core indicator of Antarctic sea ice production? *Geophysical Researcher Letters*, **30**, 2158, 10.1029/2003GL018454.

Wolff, E.W., Fischer, H., Fundel, F. et al. (2006) Southern Ocean sea ice extent, productivity and iron flux over the past eight glacial cycles. *Nature*, **440**, 491–496.

Wollenburg, I. (1993) Sediment transport durch das arktische Meereis: Die rezente lithogene und biogene Materialfracht. *Berichte zur Polarforschung*, **127**, 1–159.

Woollett, J. (1999) Living in the narrows: subsistence economy and culture change in Labrador Inuit society during the contact period. *World Archaeology*, **30**, 370–387.

Worby, A.P. & Comiso, J.C. (2004) Studies of the Antarctic sea ice edge and ice extent from satellite and ship observations. *Remote Sensing of Environment*, **92**, 98–111.

Yang, X., Pyle, J.A. & Cox, R.A. (2008) Sea salt aerosol production and bromide release: role of snow on sea ice. *Geophysical Research Letters*, **35**, L16815, 10.1029/2008GL034536.

Yoon, H.I., Park, B.-K., Kim, Y., & Kim, D. (2000) Glaciomarine sedimentation and its paleoceanographic implications along the fjord margins in the South Shetland Islands, Antarctica during the last 6000 years. *Palaeogeography, Palaeoclimatology, Palaeoecology*, **157**, 189–211.

Yoon, H.I., Park, B.-K., Kim, Y. & Kim, C.Y. (2002) Glaciomarine sedimentation and its paleoceanographic implications on the Antarctic Peninsula shelf over the last 15 000 years. *Palaeogeography, Palaeoclimatology, Palaeoecology*, **185**, 235–254.

Zielinski, U. & Gersonde, R. (1997) Diatom distribution in Southern Ocean surface sediments (Atlantic sector): implications for palaeoenvironmental reconstructions. *Palaeogeography, Palaeoclimatology, Palaeoecology*, **129**, 213–250.

Zonneveld, K.A.F., Versteegh, G.J.M. & de Lange, G.J. (2001) Palaeoproductivity and postdepositional aerobic organic matter decay reflected by dinoflagellate cyst assemblages of the Eastern Mediterranean S1 sapropel. *Marine Geology*, **172**, 181–195.

Zwally, H.J., Comiso, J.C., Parkinson, C.L., Cavalieri, D.J. & Gloersen, P. (2002) Variability of Antarctic sea ice 1979–1998. *Journal of Geophysical Research*, **107**, 1029–1047, 10.1029/2000JC000733.

This page intentionally left blank

14 Sea Ice in Non-polar Regions

Mats A. Granskog, Hermanni Kaartokallio and Harri Kuosa

14.1 Introduction

There is no need to travel to the ends of the earth to find sea ice. For many people that live in sub-polar areas in the northern hemisphere, e.g. in Alaska USA, Canada, Russia, China, Japan and Scandinavia, at the shores of temperate seas that seasonally freeze over, sea ice has been, and is, a part of daily life for some time of the year.

Detailed aspects of sea ice formation, properties and ecology have been thoroughly described in the earlier chapters. In this chapter, we will therefore only briefly introduce the characteristics and peculiarities of ice in non-polar seas, which often get much less attention than their polar counterparts. In some of these seas, ice has been extensively studied, in others very little is known besides the general knowledge of the seasonal cycle and extent of the ice cover. Nevertheless, in these places, the seasonal sea ice cover does have a significant influence on the local climate, the physical environment and ecosystems, and also economically important human activities, such as shipping and exploitation of marine resources. It is often indeed the economical aspect that has triggered efforts to understand the sea ice in seasonally ice-covered seas, such as in the Baltic and Caspian Seas. These seas are located at lower latitudes than the polar regions, with generally milder climate conditions and thus more restricted sea ice formation and spatio-temporal existence than in polar areas. Subsequently, they may also be very vulnerable both to human activities and climate change, as already a minor shift in the climate regime may result in a considerable reduction in annual ice cover extent and duration.

So far, most attention has been paid to high-latitude seas, around Antarctica and especially in the Arctic, where the recent changes in sea ice extent and thickness have been surprisingly rapid in the past decades. However, in the middle latitudes, temperature and sea ice may respond more sensitively in the context of global warming and the associated changes in atmospheric circulation. On the other hand, a climate signal can be harder to detect, as the natural variability is much larger than at the poles. Looking at the location of the areas with sea ice we have chosen to describe in this chapter (Fig.14.1 and Table 14.1), one can note that they are all surrounded or bordered by continental land masses, a phenomenon that in winter results in below-freezing temperatures which are associated with continental climates, like in continental North America and Eurasia. These terrestrial margins are often located on the continental shelves and are therefore shallow and impacted by continental freshwater run-off, which in turn promotes freezing (but also melting) by affecting the heat content and stratification of the waters.

Fig. 14.1 Map of sea ice extent in the northern hemisphere. Dark grey depicts the extent in the summer when only the perennial ice pack in the Arctic Ocean is frozen, and the lighter grey depicts the seasonal sea ice zone. Modified from Leppäranta (2004).

Table 14.1 Basic features of the sea ice cover in some non-polar seas.

Sea	Total sea area (× 10^6 km²)	Maximum ice extent (% of area)	Highest latitude	Maximum ice thickness range (m)[¥]	Average ice season length (days with ice)
Sea of Okhotsk	1.530	50–90	62°N	0.5–1.5	180
Hudson Bay	0.830	95–100	64°N	1.0–2.0	275
Baltic Sea	0.377	10–100	66°N	0.1–1.2	180
Caspian Sea	0.373	8–22	47°N	0.1–0.4	140
Gulf of St. Lawrence	0.250	90–100	52°N	0.6–1.2	150
Bohai Sea	0.078	15–80+	41°N	0.1–0.6	130
White Sea	0.091	75–100	69°N	0.2–1.0	180
Sea of Azov	0.038	n.a.	47°N	0.1–0.8	130
Aral Sea	0.017[§]	n.a.	47°N	n.a.	140

[§]in 2004 (0.066 in 1960s), [¥]level ice, n.a. = data not available.

What should be considered as non-polar? There are many ways to define the Polar Regions, especially in the northern hemisphere (see for example Arctic Monitoring and Assessment Programme, http://www.amap.no) the definition is ambiguous. Several different criteria can be used, such as latitude (south of the Arctic Circle), temperature, vegetation, permafrost and marine boundaries, among others. Choosing any of these would result in a different set of seas to be defined as non-polar. For practical reasons, we have here simply opted to describe those seasonally ice-covered seas that get less attention than sea ice at the poles and are therefore less well known to the public, despite being close(est) to habited areas and having severe ice conditions at least in parts of the sea for part of the year (Table 14.1).

14.2 Sea of Okhotsk

By far, the largest sea ice extent of the non-polar seas considered here occurs in Sea of Okhotsk (see Table 14.1), a marginal sea in the western Pacific Ocean, located within latitudes of about 44–59°N and longitudes 135–155°E (Fig. 14.1). The Sea of Okhotsk is bordered by the Siberian coast and Sakhalin Island in the west and north, Kamchatka Peninsula and the Kuril Islands (all belonging to Russia) in the east and Hokkaido Island (Japan) in the south. Observational sea ice data from Sea of Okhotsk, mainly from Japanese and Russian sources, is limited (Talley & Nagata, 1995). The thickness of thermodynamically grown ice can range from 30 to 60 cm in Hokkaido in the south up to 150 cm on the north-west shelf (Fukutomi, 1950; Shirasawa et al., 2005; Fig. 14.2). In recent years, however, sea ice investigations have been increasing, much due to the exploitation of oil and gas offshore Sakhalin, where sea ice information is needed for platform construction, for transportation of oil and gas and for environmental risk analysis for oil spills (Shirasawa et al., 2005).

The seasonal cycle of sea ice extent (>15% concentration based on satellite data) is shown in Fig. 14.3 (Ohshima et al., 2006). Ice formation begins from the north-west shelf in November, an area that is less than 200 m deep and is also impacted by run-off from the Amur River (about 350–400 km^3 annually). Especially the region around the northern tip of Sakhalin Island is impacted by run-off. The onset of ice formation is determined by the local heat flux in fall (October–November); the degree to which the ocean is cooled by the atmosphere, which occurs first in the shallow northern parts of the bay with a generally cold continental climate. Maximum ice extent is usually reached in late February or early March, when ice covers 50–90% of the surface area, with about 80% (about 1.2×10^6 km^2) being the average. Most of the ice melts in May and has completely disappeared by beginning of June (Fig. 14.3). The north-west shelf of Sea of Okhotsk is an active ice-production area, mainly because of low temperatures and north-westerly winds that transport ice southward promoting further ice production and the associated dense shelf water formation is considered to be the main source for ventilation of the North Pacific Intermediate Water (NPIW), the densest water mass formed locally in the north Pacific (Shcherbina et al., 2003). Several persistent polynyas, areas with open water despite below-freezing temperatures, are observed along the northern and western parts of the Okhotsk Sea every winter, both along the Siberian coast in the north and in a few locations on the east coast of Sakhalin Island. These polynyas are associated with high ice-production rates in winter, especially under offshore wind conditions (Kimura & Wakatsuchi, 2004). The geographical distribution of the ice-production area agrees well with that of the well-known coastal polynya areas (Kimura &
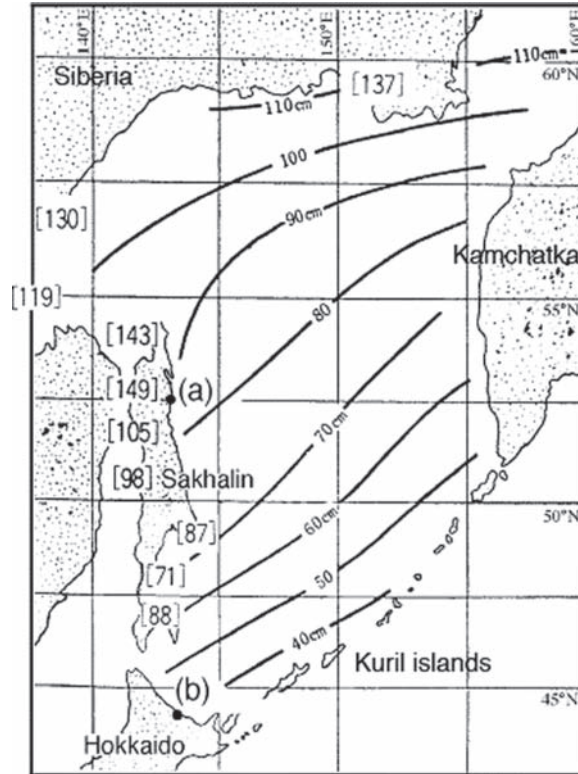
Fig. 14.2   Estimated maximum ice thickness (isolines) in Sea of Okhotsk based on Fukutomi (1950) and Shirasawa et al. (2005). The numbers in brackets [ ] indicate observed maximum ice thickness. Reproduced from Fukutomi (1950).

Wakatsuchi, 2004). The variable ice conditions influence larger-scale atmospheric and oceanic processes in the region, thus, the Okhotsk sea ice extent plays an important role in the global climate system.

The sea ice extents in Sea of Okhotsk show large interannual variability (Parkinson, 1990). Variability in atmospheric circulation patterns is known to cause large fluctuations in ice coverage. For example, fluctuations have been linked with anomalous positions and intensities of the Siberian high and the Aleutian low pressures (Parkinson, 1990). In contrast, the variation in sea ice extent in the Sea of Okhotsk influences atmospheric circulation patterns felt in the Bering Sea, Alaska and North America (Honda et al., 1999). The total extent of sea ice in winter varies interannually by a factor of two, from approximately 1.5×10^6 to 0.8×10^6 km². The maximum ice extent in 1996 was only about half of the maximum extent in 2001, which was the largest ice extent observed in the past 20+ years (Ohshima et al., 2006).

A sea ice radar network that has been operational since 1969 has allowed continuous monitoring of ice coverage along a 250 km stretch of northern Hokkaido as far as 50 km offshore. The sea ice coverage observed by the radar network shows a negative trend for the past years in this region (Shirasawa, 1998). Sea ice advection is important for the ice extent in Sea of Okhotsk. In brief, interannual differences in ice extent are mainly caused by variability in atmospheric conditions such as the surface wind field (Kimura & Wakatsuchi,
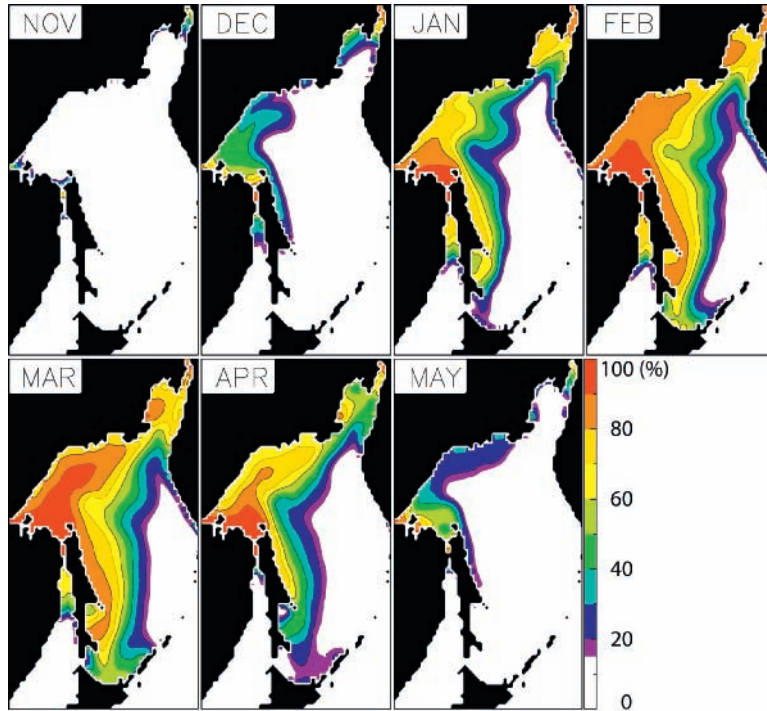
Fig. 14.3   Monthly mean ice concentration in Sea of Okhotsk for the period 1978–2001, derived from SMMR and SSM/I satellite data (modified from Ohshima et al., 2006). Reproduced from Ohshima et al (2006). With permission from the Meteorological Society of Japan.

2004). The advance of the ice cover occurs primarily through ice advection by wind. As a large-scale drifting pattern, the dominant southward flow of sea ice is from the north, where most of the ice is produced, along the eastern coast of Sakhalin approaching Hokkaido in the south. Near Hokkaido and the southern ice edge, the ice movement patterns become more complex. According to Shevchenko et al. (2004), who studied ice motion off the Sakhalin coast, the ice drift is governed by tidal currents and wind-induced drift, which explain from 92% to 95% of the total ice drift variance. Tidal currents dominate off the northern Sakhalin coast, accounting for from 65% to 80% of the variance, while low-frequency wind-induced motions govern off the south-central Sakhalin coast, accounting for over 91% of the variance. Opposite to common belief, Ogi et al. (2001) found evidence that the Amur River discharge is strongly negatively correlated with the ice extent in Sea of Okhotsk. Years with large river discharge are followed by suppressed sea ice formation in the Okhotsk Sea and vice versa. However, there is not necessarily a direct causal relationship, rather atmospheric circulation patterns control both the precipitation in the river basin and ice formation in such a way that summer discharge is larger and winter ice is reduced during positive Arctic Oscillation (AO) years (Ogi & Tachibana, 2006).

Ice thickening in the Sea of Okhotsk is largely governed by dynamical processes (Kimura & Wakatsuchi, 2004; Toyota et al., 2004, 2007; Fukamachi et al., 2006), and is mainly caused by piling-up or rafting and ridging of ice floes. In addition, the ice thickness is difficult

to measure and interannual variability has not been clarified as observations are very sparse and largely limited to the southernmost parts off Hokkaido. Therefore, the ice thickness or ice volume in Sea of Okhotsk as a whole is not well known. In southern Sea of Okhotsk, in the vicinity of Hokkaido Island, where most of the observations of the sea ice in the region has been made by Japanese scientists, the ice thickness is generally less than 0.5 m in the mobile pack ice, based on ship-borne observations (Shimoda et al., 1996; Toyota et al., 2000, 2004; Toyota & Wakatsuchi, 2001). Ship-based ice thickness measurements using an electromagnetic induction device show that video observations of ice thickness (Toyota et al., 2004) underestimate the total thickness (Uto et al., 2006). They describe two character-istics ice thickness ranges for the southern Sea of Okhotsk, namely 0.4–0.6 m for level ice and a 0.9–1.1-m thickness range for moderately deformed ice. In northern Sakhalin, (level) pack ice floes can be 1.0–1.2 m thick (Polomoshnov, 1992; Kharitonov, 2008).

Perhaps the most complete set of data on sea ice thickness in southern Sea of Okhotsk to date is from a recent mooring with sonar measuring ice draft (i.e. the depth of ice below the sea surface; Fukamachi et al., 2006) at a location near the Hokkaido coast. Observations from three consecutive winters (1999–2001) reveal that the mean draft ranged between 0.5 and 0.7 m, while level ice thicknesses were less than 0.3 m, and deformed ice contributed about 80% of the total ice volume. Regardless of the importance of dynamic thickness growth, the small number of deep keels (>10 m or more) suggests that intense deformation events are not very frequent in Sea of Okhotsk (Fukamachi et al., 2006), and it is likely to be rafting rather than ridging, that is the major contributor to dynamic ice thickening. Further evidence for the importance of dynamical growth in pack ice has been gathered from thin-section analysis of crystal structure. Toyota et al. (2007) reported that frazil ice contributed 48% of total ice core length, being more prevalent than congelation ice (39%). Further, it has been proposed that the thickening process of Okhotsk pack ice is as follows: sea ice about 10 cm thick, formed in open water, is thickened through rafting until it attains a thickness of 30–40 cm and then the ice further thickens through ridging (Toyota et al., 2007). Despite the fact that dynamic thickening is important in the Sea of Okhotsk, observations of ice ridges or grounded ridges (stamukhi) are sparse, although it is ice ridges that are especially hazardous both to navigation and marine constructions. Kharitonov (2008) reports on observations of ice ridges on the Sakhalin coast, based on his results that the thickest ice ridges have a keel of up to about 15–16 m, while the sail can be up to 2 m high. From mooring data, the deepest keel observed off the Hokkaido coast in 3 years was about 17 m (Fukamachi et al., 2006), although the occurrence of keels larger than 10 m in depth was very infrequent, and keels that deep were observed only a few times during three winters (1999–2001).

Fast-ice thickness, which is often a result of static thermodynamical thickness growth that reflects the severity of the local winter climate (Fig. 14.2), has been examined for Hokkaido and Sakhalin islands (Shirasawa et al., 2005). In Saroma-ko Lagoon (northern Hokkaido), fast ice grows to 40–50 cm, with snow-ice portion of 10–100% of the total thickness. In a similar semi-enclosed location in northern Sakhalin, the ice grows to about 100 cm, with a remarkable addition (on average 24 cm) during mid-March to mid-April due to snow-ice for-mation (Shirasawa et al., 2005). The contribution of snow-ice to fast-ice thickness in Sea of Okhotsk appears to be much higher than in the Arctic, but with similarities to, for example, the Baltic Sea (Granskog et al., 2004). However, observations in pack ice in southern Sea of Okhotsk indicate a smaller contribution from snow, by mass 8% and 12% on average, based on observations by Ukita et al. (2000) and Toyota et al. (2007), respectively.

Other properties than sea ice thickness measurements in Sea of Okhotsk are rather sparse. Coincident with ice core sampling, salinity and oxygen isotopic composition have been investigated (Toyota et al., 2000, 2007; Ukita et al., 2000). The salinity of Okhotsk sea ice is lower than that reported for Arctic or Antarctic sea ice (about 2–3 units lower), this is thought to be a result of the moderate climate, with melting at daytime (based on heat budget calculations) and the observed salinity is close to multiyear ice salinities from polar regions (Toyota et al., 2000). The average salinity reported for southern Okhotsk by Toyota et al. (2007) is 4.6 ± 1.3. Similarly to Arctic and Antarctic sea ice, bulk salinity of ice is related to ice thickness, salinity decreasing with increasing ice thickness.

14.3 Hudson Bay

Hudson Bay is a large inland sea that includes Hudson Bay and James Bay in Canada. Foxe Basin, Ungava Bay and Hudson Strait are also often considered to belong to the same system, as they provide the connection Hudson Bay has to the world ocean. Although the meridional extension of Hudson Bay (including James Bay) spans roughly 14 degrees of latitude across the Arctic Circle (50–64°N), the entire basin is characterized by typical Arctic (oceanic and atmospheric) conditions and is the southernmost extension of the Arctic region as defined by the Arctic Monitoring and Assessment Programme (AMAP; http:/www.amap.no). The most typical Arctic feature of the basin is perhaps its complete seasonal ice cover, which makes it the largest inland body of water in the world (about 0.83×10^6 km^2) with a complete cryogenic cycle, i.e. to seasonally completely freeze over and then be ice-free in the summer, although for a relatively short period (Prinsenberg, 1988). In summer months, the ice-free Bay creates a marine climate in the surrounding area, while in the winter it is insulated by ice and snow and permits cold polar air masses to extend south towards central Canada (Prinsenberg, 1984). This southern extension of Arctic conditions, well beyond the Arctic Circle, has a large impact on the climate of the surrounding areas, which is exemplified, for example, by the southern displacement of the tree line in eastern Canada. The presence of sea ice until late July in the southern and western Hudson Bay is suggested to contribute to the presence of permafrost in the region, as this is the southernmost location of permafrost in North America (Gough & Leung, 2002). The extreme southerly presence of Arctic marine mammals is also characteristic of the Hudson Bay marine ecosystem. Although belonging to the Arctic, from a climatological point of view, Hudson Bay has seldom received any detailed attention when the Arctic Ocean is considered.

Recently there has been, however, a revitalized interest in the region, through interdisciplinary research programmes such as the Canadian Arctic Net programme. The region provides one important route for Arctic Ocean water, through the Canadian Arctic Archipelago via Hudson Bay, to the North Atlantic where the freshwater transported through and exported from the system (including both run-off and sea ice melt) can influence deep water formation in Labrador Sea (Déry et al., 2005), thereby potentially influencing the thermohaline circulation of the oceans. Research work in Hudson Bay has been summarized by Martini (1986) and an updated account can be found in Stewart and Lockhart (2005).

Sea ice studies in the region are sparse, a result of the quite insignificant economical importance of the area and its inaccessibility (Martini, 1986). However, moving towards ice-free

conditions would allow for increased shipping in the area and could change the situation. The seasonal sea ice cover effectively prevents most year-round research and other human activities in Hudson Bay and the shallow coastal waters make it very difficult to conduct bay-wide research from a single research platform. Consequently, characteristics of the circulation and water mass are not well known, especially outside the open water period (Stewart & Lockhart, 2005). Hitherto, studies of sea ice in Hudson Bay appear only to have been conducted on land-fast sea ice in the vicinity of Kuujjuarapik (Great Whale; Legendre et al., 1981, 1996; Ingram et al., 1996) in south-eastern Hudson Bay, at Churchill (Schwerdtfeger, 1962; Ehn et al., 2006; Kuzyk et al., 2008) and in Chesterfield Inlet (Welch et al., 1991) in western Hudson Bay. However, there is virtually no information on the pack ice, which contributes to the majority of the ice in the Bay, as land-fast ice mainly covers only narrow fringes at the perimeter of the Bay.

Hudson Bay is ice-covered for about 8–9 months every year, with nearly complete ice cover between November and June, and ice-free conditions prevailing only for 2–3 months in summer. This reflects the cold climate in the region, in comparison to, for example, the Baltic Sea which is located roughly at similar latitudes but has on average considerably shorter ice season and less severe ice conditions (Table 14.1). The seasonal cycle of sea ice in the region has been summarized by for example Markham (1986), and ice charts and climatologies (1971–2000) are available from the Canadian Ice Service (CIS, 2002). Conditions referred to hereafter are median conditions and one has to note that there can be significant deviations from the medians in individual years, especially early in the season (CIS, 2002). In mid-October, the Bay is completely ice-free. Ice formation starts in the north-western corner of the Bay in late October and the ice cover generally then spreads southwards along the west coast. By mid-November, ice typically covers only the north-west corner of the Bay around Southampton Island, and along a relatively narrow stretch along the western coast, almost all the way down to the mouth of James Bay. Thereafter, the ice cover subsequently spreads eastwards and within a month, by mid-December, the Bay is ice-covered to 90–100% of its surface area. At this point, ice thickness for level land-fast ice is from 80 cm in the north to 25–30 cm in James Bay in the south. The almost complete ice cover, with the exceptions of leads and openings in the mobile pack ice, is present until late May or early June, when ice starts to break up in James Bay. Fast ice fills bays along the western coast of Hudson Bay and forms around the Ottawa and Belcher Islands in south-eastern parts of the Bay.

There is a steady growth in ice thickness from January until April, and April and May represent the maximum ice conditions as ice thickness is close to its maximum and ice concentration is high. The climatological maximum ice thickness in the region, i.e. thermodynamical growth of level ice, varies from 100 cm in James Bay to 200 cm in north-western Hudson Bay, with 160 cm as averaged over the whole bay (Prinsenberg, 1988). However, it has been shown that dynamic thickening of the ice cover in Hudson Bay is significant, and the volume of ice produced in the bay can be as much as 90% above values based on level ice (Prinsenberg, 1988). However, there is virtually no actual ice thickness data from the mobile ice pack, and many of these estimates have been produced indirectly, for example, by using the estimated amount of sea ice melt in the water column (Prinsenberg, 1988) or by modelling studies (Saucier et al., 2004). Therefore, there is still uncertainty as how much ice is actually produced in the Bay.

In south-eastern Hudson Bay, the consolidation of the fast ice normally occurs between mid-January and mid-March (Larouche & Galbraith, 1989). The largest extent of fast ice in

Hudson Bay develops east of a line from Cape Jones (north-east corner of James Bay), via Belcher Islands to Sleeper Islands (roughly along a line along a longitude of 79°W). Sometimes, this fast ice along the eastern coast may reach almost all the way to Mansel Island, at the exit to Hudson Strait. Western Hudson Bay, north of Churchill, can be regarded as the ice factory of the bay (Saucier et al., 2004). Here, persistent winds from north–north-west drive ice that has formed towards south–south-east, promoting further ice formation. The prevailing winds, together with tides, generate a quite persistent flaw lead in western Hudson Bay throughout the winter. This bears some resemblance to the Sea of Okhotsk, where polynyas and ice advection play an important role. Tidal mixing generated at the ice water interface and salt rejection from the growing ice cover continually deepens the pycnocline until the end of April, when maximum ice-cover thickness and pycnocline depth of 95 m are reached in western Hudson Bay (Prinsenberg, 1986). Despite the significant ice production in western Hudson Bay, accompanied by salt rejection from the forming ice, it is not completely sure if there is any local formation of deep waters within in the bay (Saucier et al., 2004).

On the shallow shelf in western Hudson Bay, salt rejection in the flaw lead can result in salinities as high as 33.8 (at freezing; Kuzyk et al., 2008); on the basis of its density, this cold and saline water would have the potential to replace the deepest waters in the bay, although it has not been verified that this does happen and that these dense shelf waters actually leave the shelf before spring ice melt and dilution by melt and run-off. The winds and general cyclonic circulation in the Bay transport ice from the west and north-west to the south and south-east, and in the latter regions, sea ice advection and dynamic thickening are more important than local thermodynamic growth (Saucier et al., 2004).

Sea ice advection plays also an important role during the melting season, when the last remaining ice in the Bay is usually located in offshore waters west of the Belcher Islands, where the last remaining ice is transported to by the cyclonic circulation and prevailing winds. Melting usually starts in James Bay in late April, where the air temperature increases first above freezing but also because increased run-off caused by snow melt from more southerly watersheds bring additional heat to melt ice. The rapid change in the length of day in northern spring results in that melting occurs over the whole Bay by late June (Markham, 1986). After (southern) James Bay, the first areas to become free of ice are in the north-west, where the combined effect of winds moving pack ice offshore to south/south-east and melting result in widening of the flaw lead. The region along the eastern shore from James Bay to Mansel Island also becomes ice-free relatively early, which is attributed to the northward flow of river waters from spring freshet in James Bay melting the ice (Fig. 14.4). By mid-July, the south-western coast is free of ice, and all remaining ice is generally located in the south-central parts of the bay. By end of July, this pack has shrank considerably with some remains floating in offshore waters between Nelson River and James Bay, and by mid-August all ice has disappeared. Thereafter, the Bay remains essentially ice-free until freezing starts again in late fall in the north-western parts of the bay. Some intrusions of ice from Foxe Basin may occur in the north-eastern part of the bay at any time some years (CIS, 2002). In Hudson Bay, freeze-up has commenced as early as the first week of October and as late as the first week of November, while complete melting has occurred as early as mid-July and as late as the end of August, except for incursions from Foxe Basin (CIS, 2002).

Recent studies have shown that both the extent and the duration of the sea ice cover in Hudson Bay have been decreasing over the past few decades, likely as a result of climate change (e.g. increasing surface air temperature and changes in atmospheric circulation;
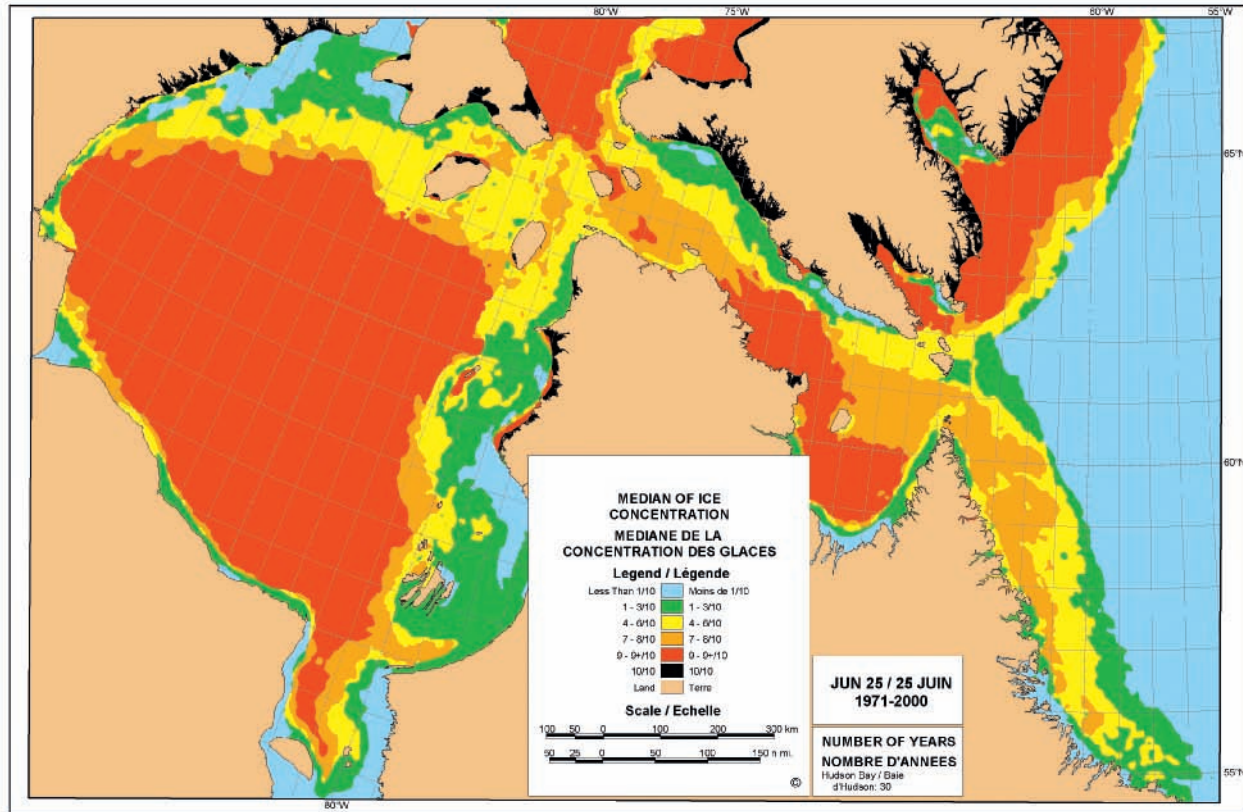
Fig. 14.4   Median ice concentration in Hudson Bay (June 25 1971–2000). Data courtesy of Canadian Ice Service (Environment Canada). Reproduced from Canadian Ice Service (2002) Sea Ice Climatic Atlas. Northern Canadian Waters 1971–2000. With permission from Environment Canada.

Parkinson et al., 1999; Stirling et al., 1999; Falkingham et al., 2002; Gough et al., 2004). Hudson Bay is also considered to be one of the most vulnerable areas for climate change, and could be potentially undergoing a climate shift towards ice-free conditions, although there still are large uncertainties in future scenarios (Gagnon & Gough, 2005). For example, Gough and Wolfe (2001) suggest the cessation of seasonal sea ice in the region as early as 2050. The Intergovernmental Panel on Climate Change (IPCC, 2001) identified the region as one particularly sensitive to climate change, with serious consequences for the native populations which depend on, for instance, sea ice for the traditional hunting of marine mammals. Figure 14.5 shows the severity of ice conditions in Hudson Bay for the spring/summer melt period in 1971–2007, with a trend for less severe ice conditions. Parkinson and Cavalieri (2002) examined sea ice extent over a 21-year period (1979–1999) for Hudson Bay (including Foxe Basin and Hudson Strait) using satellite data. The yearly average extent of sea ice concentrations with over 15% coverage was 798,000 km^2 with a decreasing trend of –4300 ± 1400 km^2 per year. Most recently, Parkinson and Cavalieri (2008) reported a trend of –4500 ± 900 km^2 per year (–5.3 ± 1.1%/decade) for the 1979–2006 period. Similar trends were reported for the 1971–2001 period by Falkingham et al. (2002), with changes of about 13% per decade. The trend is towards earlier break-up in western Hudson Bay (1979–1998), and increasing mean spring temperature is probably largely responsible for the observed trend (Stirling et al., 1999). Gough et al. (2004) investigated the break-up and ice formation dates for the south-western region of the Bay (1971–2003), where the last remains of the ice in the bay melts. They found that one can be 94% confident that the ice in the south-western region of Hudson Bay has been breaking up earlier in recent years and days to break up are decreasing by 0.3 days/year (i.e. 3 days per decade). Break-up appears to occur later during years with Low/Wet El Nino Southern Oscillation (ENSO) episodes (Southern Oscillation Index (SOI) < 0) and strong westerly North Atlantic Oscillation (NAO) episodes associated with strong west–north-west winds over Hudson Bay (NAO > 0) (see Gough et al., 2004). Modelling studies suggest, however, that changes in run-off have a greater effect on interannual variability of the ice cover than temperature changes associated with the NAO, especially in south-eastern Hudson Bay (Saucier & Dionne, 1998). There is evidence for both no change (Stirling et al., 1999; Gough et al., 2004) and later (Parkinson & Cavalieri, 2002) freeze-up dates. Hudson Bay has therefore experienced a shortening of the ice season during the last three decades.

The sea ice cover plays an integral part of the functioning of Hudson Bay, resulting in significant seasonal modifications to, for example, tides, surface circulation, buoyancy fluxes through ice formation and melt and spreading of river run-off. In addition to affecting local and regional climate, sea ice also has significant influences on salt fluxes, which affect thermohaline circulation and vertical mixing in the Bay. The sea ice cover significantly alters offshore spreading of discharge from the numerous rivers (see Ingram, 1981; Freeman et al., 1982; Ingram & Larouche, 1987; Déry et al., 2005; Kuzyk et al., 2008), with subsequent effects, for example, in ice formation and biological production in estuaries. A predominantly level ice cover, such as in the Great Whale River area (Ingram & Larouche, 1987), allows river waters to form large under-ice plumes, that can reach further offshore than in ice-free conditions. On the contrary, formation of ice ridges and/or stamukhi at the edge of the land-fast ice can act as a barrier to run-off transport to the offshore and inshore of these ice barriers under-ice 'lakes' can accumulate run-off depending on the depth of the ice barriers (Kuzyk et al., 2008). These kinds of differences in ice conditions between outlets of

**Historical total accumulated ice coverage
1971–2007 (May 14 – August 6)**
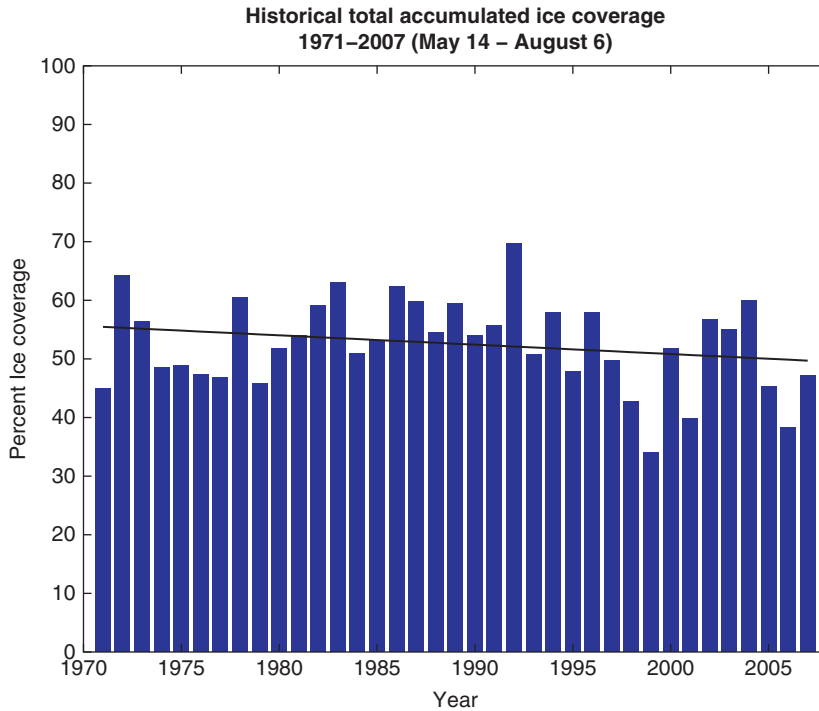
Fig. 14.5 Historical total accumulated ice cover in Hudson Bay for the period from May 14 to August 6, which corresponds well with the spring and summer melt period when the largest changes in ice extent have been observed to take place (see text). Solid line depicts a linear regression to the data. The total amount of ice present is expressed as a per cent of the total sea area. Data courtesy of the Canadian Ice Service (Environment Canada).

major rivers can influence the stability and ice formation in the offshore areas, but also on the functioning of the ecosystem in different estuaries (Kuzyk et al., 2008).

Shipping would be a major gainer of lighter ice conditions. Churchill, on western Hudson Bay, Canada's only deep-water Arctic seaport, has attracted increased attention in recent years as climate change could open the North-west Passage through the Arctic Ocean. Currently, the port's shipping season runs from mid-July to the beginning of November, when the Bay's waters are ice-free, as no icebreakers are used for assistance. A lengthening of the open water season would obviously increase the potential of this Arctic seaport for shipping.

14.4 Baltic Sea

The Baltic Sea is one of the world's largest brackish water basins with a surface area of about 377,000 km^2 and volume of about 21,000 km^3 and spans a relatively large latitudinal zone, from 53°N to 65°N (roughly the same as Hudson Bay). The mean depth of the Baltic Sea is only 55 m, and in the eastern- and northernmost basins, the Gulf of Finland and the Bothnian Bay, respectively, less than 40 m. The surface salinity varies from about 9 in the southern Baltic Proper to less than 1 in the innermost parts of the Gulf of Finland and

the Bothnian Bay and in proximity of larger rivers. The Baltic Sea is heavily influenced by river discharge, and the sea has a positive water balance, meaning that river run-off and precipitation exceeds evaporation. The brackish nature is maintained by intermittent inflows of saline North Sea water through the narrow and shallow Danish Straits, which is the only connection to the world ocean.

Seasonal sea ice plays an important role in the Baltic Sea system, although, as in other seasonally ice-covered seas, the whole importance of the annual ice cover is not well known (see review by Granskog et al., 2006a). There has been a quite keen interest in ice studies in the Baltic Sea (Leppäranta et al., 2001), not least due to the importance of shipping to the trade and economy of countries surrounding the sea. As an example, it can be noted that Finland and Estonia are the only countries in the world where all ports freeze during winter, and therefore a fleet of icebreakers is needed to secure shipping throughout the year.

Ice formation usually begins at the northernmost Bothnian Bay and the easternmost Gulf of Finland in October–November. Ice forms first in the inner skerries and bays where the water is often fresher and shallower, thus has a lower heat content, and where the ice cover can be anchored to islands and shoals. Next to freeze over are the Quark between the Bothnian Bay and Bothnian Sea, the entire Bothnian Bay and the coastal areas of the Bothnian Sea. In average winters, the ice also covers the Archipelago Sea, and the Gulfs of Riga and Finland as well as the northern parts of the Baltic proper. In severe winters, the Danish Straits and the southern Baltic proper are also covered with ice (Granskog et al., 2006a). Annually, sea ice covers a mean of 40% of the Baltic Sea, and the median maximum ice extent for the period 1971–2000 was 157,000 km^2 (Granskog et al., 2006a). Typical ice-covered areas are presented in Fig. 14.6.

The ice conditions in the Baltic Sea can be characterized by the large interannual variability in the severity of the winters (Fig. 14.7), and depending on the severity of the winter, the ice covers 10–100% of the surface area at its maximum annual extent. There is also large variability in the date freezing begins, in ice thickness and break-up dates (Seinä & Palosuo, 1996; Haapala & Leppäranta, 1997; Jevrejeva et al., 2004; Granskog et al., 2006a). The time series of the maximum annual ice extent in the Baltic Sea, reconstructed from historical records from the early 18th to early 20th centuries and thereafter based on observations, is one of the world's longest time series describing ice conditions (Seinä & Palosuo, 1996). It has also received a fair amount of interest in climate studies on the relationships between ice conditions and atmospheric conditions (Tinz, 1995; Jevrejeva & Moore, 2001; Omstedt & Chen, 2001). Also, other historical reconstructions of ice conditions have been made, for example, based on ice break-up in the Port of Riga (Latvia) for the period 1529–1990 (Jevrejeva, 2001). From these investigations, there is considerable evidence that supports that large-scale atmospheric circulation patterns are significantly correlated with the ice conditions. Average and mild winters occur when warm air masses associated with westerly moving cyclones from the Atlantic dominate, while in severe winters, blocking anticyclonic patterns dominate. In very simple terms, the strength of the westerlies, bringing warm and moist air masses to Scandinavia, result in mild ice winters. Further, it is the conditions during the winter months (December–February) that largely control the development of the ice cover, and the climate earlier has little importance on the ice conditions.

Jevrejeva et al. (2004) examined the evolution of ice seasons in the Baltic Sea during the 20th century and indicate a general trend towards milder ice conditions; the largest change being the length of ice season, which has shortened by 14–44 days during the last century.
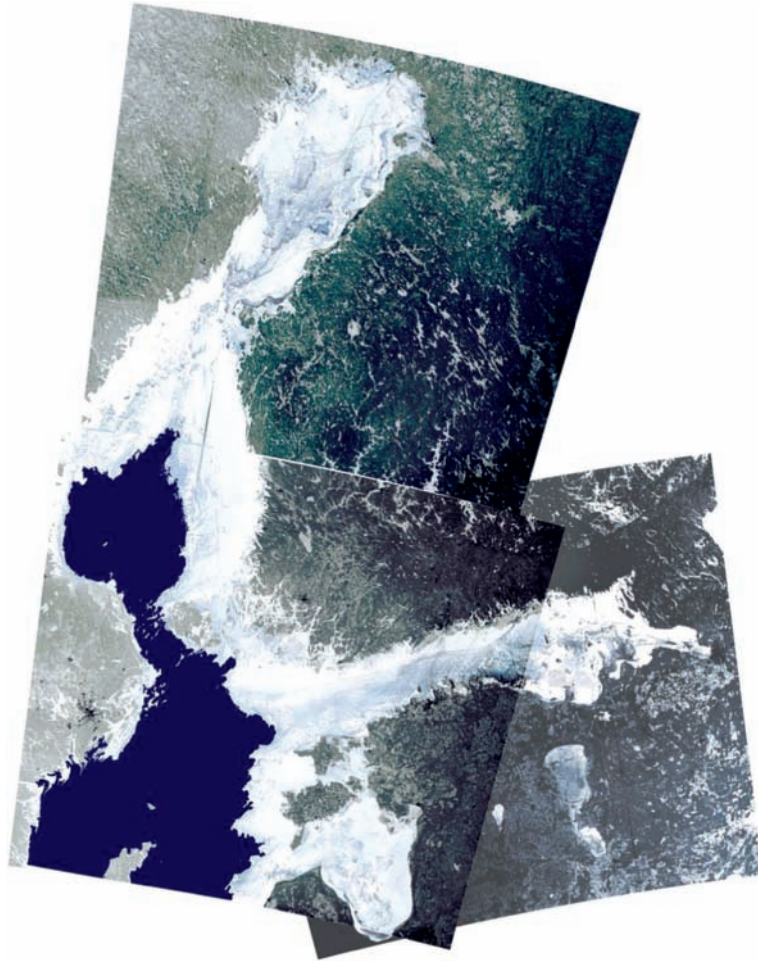
Fig. 14.6   Ice conditions in the Baltic Sea on January 6–7 in 2003. These conditions correspond well with the median maximum ice extent in the period 1971–2000 (see Granskog et al., 2006a). © Canadian Space Agency/Agence spatiale canadienne (2003). Distributed by Kongsberg Satellite Services, KSAT, modified by Jouni Vainio (Finnish Institute of Marine Research).

There has also been a reduction of about 8–20 days per century to earliest ice break-up, which the authors relate to a warming trend in winter air temperatures over Europe. It has been estimated that if the winter air temperature increases about 4°C, the Baltic Sea would become completely ice-free (Omstedt & Hansson, 2006).

The ice regime in the Baltic can be divided into a land-fast ice cover along the coasts and a mobile pack ice regime further offshore. The many islands and skerries bordering the coasts in the northern Baltic play an important role in the extent of land-fast ice, which usually can be said to extend to the 5–15 m isobath, depending on local topography. As the ice becomes anchored to islands, skerries and shoals, it prevents wind break-up, even of thin ice. In the offshore, the ice pack is highly dynamic, and deformation, rafting and ridging, is important for the development of the ice cover.
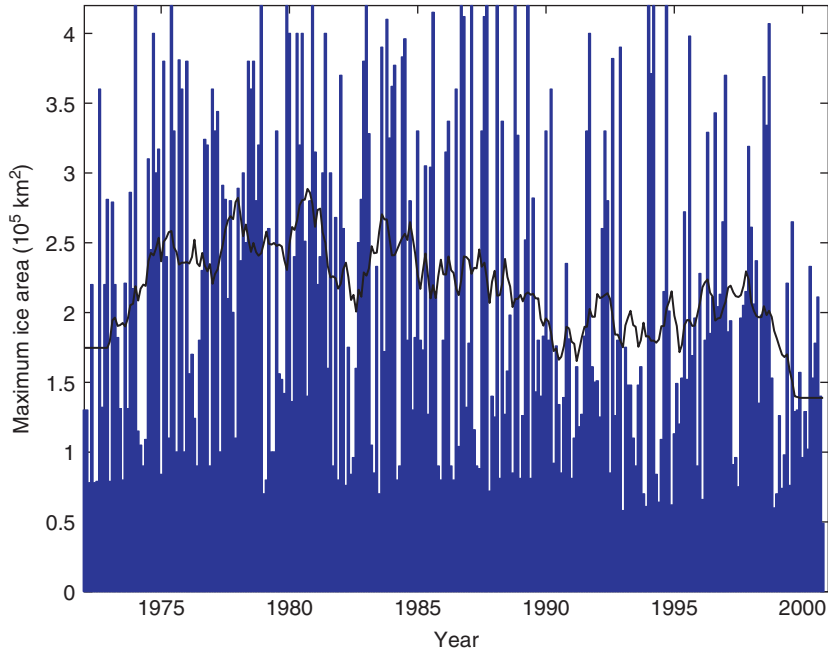
Fig 14.7   Maximum ice extent in the Baltic Sea for winter 1719–1920 to 2007–2008 with a 20-year moving average. Data courtesy of the Ice Service at the Finnish Marine Research Institute (Seinä & Palosuo, 1996; Niskanen et al., 2008).

While there is rather good information on the total ice thickness in the land-fast sea ice domain, Schmelzer et al. (2008), for example, have compiled information on the ice conditions in the Baltic Sea for the period 1956–2005. Similar information is more limited for the pack ice. Mean land-fast ice thicknesses in the southern parts of the Baltic Sea (German and Polish coasts) and Archipelago Sea (northern Baltic proper) are generally less than 0.25 m, about 0.45 m in Gulf of Finland and Bothnian Sea, and 0.55 m or more in the Quark and the Bothnian Bay (see Schmelzer et al., 2008). Maximum (level) ice thickness observed, in the north-eastern part of the Bothnian Bay, is 1.1–1.2 m (Kalliosaari & Seinä, 1987; Schmelzer et al., 2008). Recent observations in Gulf of Bothnia and Gulf of Finland reveal that mean thicknesses in pack ice are much higher, from 0.4 to 1.8 m, due to strong ice deformation (Haas, 2004). Lewis et al. (1993) used a laser system to measure the ice surface profile in the Bothnian Bay, and estimated that 15–40% (which equals 3–28 cm in equivalent ice thickness) of the total ice volume was composed of deformed ice (ridges and rubble). While Kankaanpää (1997) estimated that ridges contributed 6–14 cm equivalent ice thickness in the Bothnian Bay. Observations of sea ice draft in central Bothnian Bay over one ice season (2003–2004, which was an average ice winter) also indicated that ridges make up a large portion, 30–60%, of the total ice volume, and monthly mean ice thicknesses in February–March–April ranged from 0.4 to 1.0 m (Björk et al., 2008). In the Gulf of Finland and Bothnian Sea, the contribution of deformed ice appears to be much smaller (Kankaanpää, 1997). All these observations stress the importance of dynamical processes in thickening of the ice, especially in the Bothnian Bay, and point out that observations in the land-fast ice regime

are only valid for the oldest undeformed ice in any region, and total ice volumes are usually severely underestimated by using level ice thickness alone.

Sea ice contributes also to salt- and freshwater budgets; however, these factors have not received much attention in Baltic Sea studies. Despite the brackish nature of the parent water, sea ice in the Baltic appears to be structurally similar and comparable to sea ice formed in Polar waters, although differences do exist because of the lower parent water salinity, and the ice becomes freshwater ice when the water salinity is lower than about 1 (Granskog et al., 2006a). Baltic Sea ice reflects the low water salinities: the bulk salinities in the northern Baltic Sea are generally less than 2, and even lower depending on the ambient water salinity, growth conditions and thermal history of the ice and therefore much lower than in many other sea ice regions.

Another feature that distinguishes Baltic Sea ice from other regions is the significant contribution of meteoric ice, i.e. precipitation converted to ice, to the thickness growth. Two types of meteoric ice can be distinguished: snow-ice and superimposed ice. Snow-ice is formed when the weight of snow suppresses the ice surface below the water level and sea water that floods the bottom of the snow pack freezes, while superimposed ice forms when snow meltwater drains to the ice surface and refreezes as a solid ice layer. Both mechanisms are important in the Baltic Sea, presumably because of the relatively thin ice cover that easily makes flooding possible (because little snow is needed to submerge the ice surface) and because the mild climate conditions allows for snow melt and even rain to occur anytime during winter. Strong diurnal cycling in the energy balance at the surface also reinforces melt–freeze cycling. Up to 50% of the total ice thickness and 35% of the total ice mass can be composed of meteoric ice in land-fast sea ice (Granskog et al., 2006a), however, there is large interannual variability (Palosuo, 1963; Granskog et al., 2004). In spring, the snow pack on the ice can be completely converted into a superimposed ice layer (Granskog et al., 2006b), before final ice melt. Due to the importance of the snow cover on the development of Baltic Sea ice, the response to future changes is somewhat uncertain as it depends largely on the timing, amount and quality of precipitation during the ice season.

14.5 Caspian and Aral Seas, and Sea of Azov

The Caspian and Aral Seas are landlocked by the Eurasian continent, which also borders the Sea of Azov, located north-east of the Black Sea, through which the Sea of Azov connects to the world ocean (Fig. 14.1). Continental climate in winter is the major reason that these water bodies are partially ice-covered every winter. The ice conditions in these waters are not well known, at least in the western literature, although recently there has been an increased interest, especially caused by the exploitation of marine resources in the Caspian and the Sea of Azov.

Caspian Sea

The Caspian Sea is actually a saltwater lake, albeit the largest lake in the world, covering about 373,000 km² being located between 36°N and 47°N (Fig. 14.1). Because the Caspian sits on top of considerable oil reserves, this lake is of great strategic and economic importance. Another of its valuable attributes is the fact that this is where sturgeon, the source of

beluga caviar, lives and spawns. Every winter, the Caspian Sea is to some extent covered by ice (Kouraev et al., 2004; see also Fig. 14.8). The presence of ice affects navigation, fisheries and other industrial activities (van Gelder et al., 2004). Of special concern is the impact of sea ice on industrial structures located in the coastal zone, such as Russian and Kazakh oil prospecting rigs operating on the Northern Caspian shelf. Ice conditions make it necessary to maintain an icebreaker fleet as well as to use oil-drilling rigs of Arctic-class in the Northern Caspian.

Traditionally, the Caspian Sea is divided into three parts: the deep Southern and Middle Caspian, and shallow Northern Caspian. Ice may form in all three parts of the Sea. However, in the southern part, it appears only in extreme severe winters and in the middle part, ice cover occupies small areas near the coast, while during mild winters it does not appear at all. Only in the Northern Caspian is ice present every year and covers large areas (Kouraev et al., 2004). The northern part of the Sea covers about 80–90,000 km^2. It is relatively shallow, averaging about 5–6 m in depth, thereby promoting ice formation as shallow water freezes more easily due to lower heat-storage capacity of the water column. Salinity in the North Caspian varies markedly, from 0.1 at the mouth of the Volga and Ural rivers increasing to 10–11 near the Middle Caspian. The middle and southern parts of the sea have only small fluctuations of salinity; surface salinity is about 12.6–13.5, increasing from north to south and from west to east. Freezing temperatures are found in the north and in shallow bays along the eastern coast.
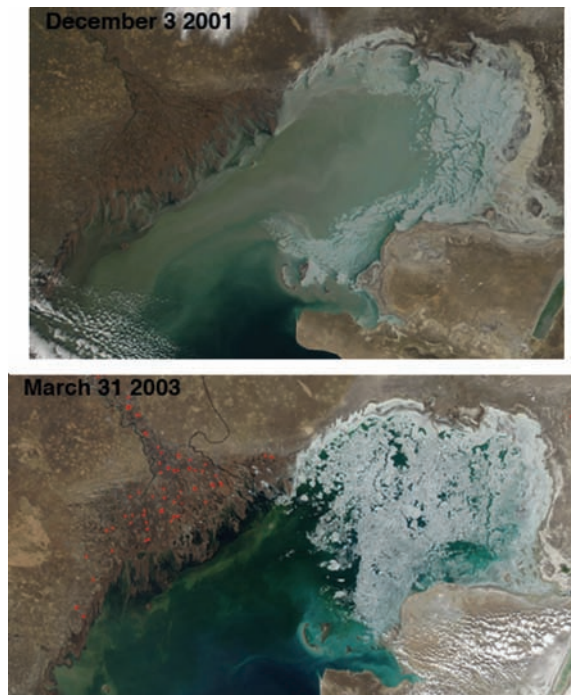
Fig. 14.8   Upper panel: Ice in the North Caspian Sea in early December 2001 and lower panel: in late March 2003, as seen with the MODIS instrument onboard the Terra and Aqua satellites (images courtesy of NASA Visible Earth).

In the north Caspian Sea, ice appears in November. Ice formation in the middle and southern parts of the North Caspian generally occurs in December–January. Near the east coast, the ice is of local origin, whereas near the west coast, the ice mostly drifts in from the northern part of the sea. Along the west coast, drifting ice is found down to the Absheron Peninsula (Azerbaijan) in the middle Caspian. Ice decay starts in March, open areas and shallow regions in the north-western part become ice-free in mid-March and in the region near the Volga delta by late March. In the beginning of April, the ice disappears in the north-eastern part and the last ice resides over the Ural furrow. On average, the duration of the ice period is 120–140 days in the eastern part of the Northern Caspian and 80–90 days or less in the western part (Kouraev et al., 2004).

Kouraev et al. (2003, 2004, 2008a,b) have compiled ice condition data from both historical observations and using recent satellite data. Historical records of ice area have been compiled by Rodionov (1994) and for the period of satellite records, SMMR and SSM/I data have been used to extend the time series (Kouraev et al., 2003, 2004, 2008a,b) and these results are shown in Fig. 14.9 for the period 1927–2007 as average December–January–February (DJF) ice area. However, the reliability of the historical data has to be dealt with caution, as no information on the data source and of the method to calculate ice concentration is provided by Rodionov (1994); although the historical and satellite data on average DJF ice area show reasonable agreement during the overlap period, there are quite significant difference in some years (Fig. 14.9).
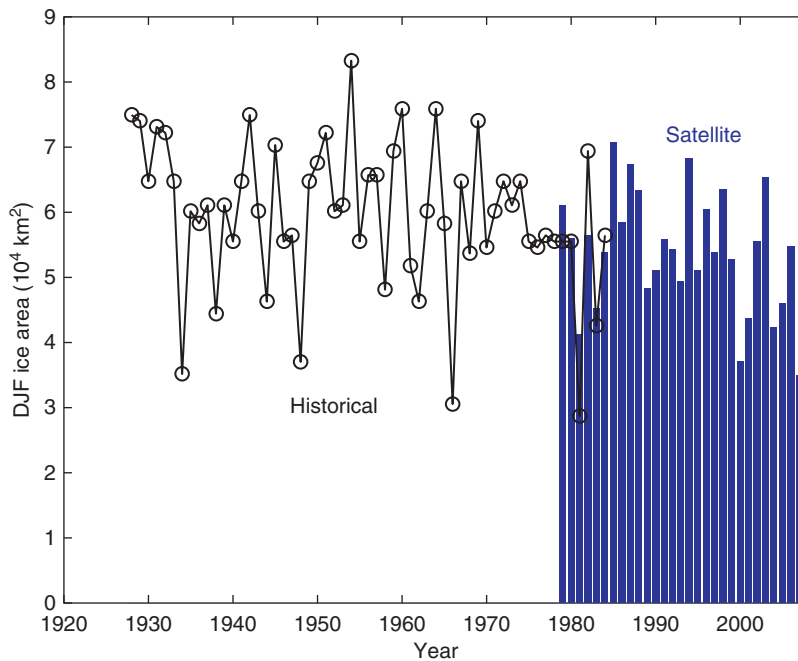
Fig. 14.9   Northern Caspian ice extent. Historical average DJF ice area (km², calculated after Rodionov (1994); and maximum DJF ice coverage (km²) from SMMR–SSM/I satellite data. Data courtesy of Alexei Kouraev.

For the period of 1927–2007, the overall variability shows the complicated structure and existence of various cycles in ice conditions such as a decrease in maxima in average DJF ice concentrations starting from 1950s. Since the late 1980s, there has been a warming tendency observed by satellites. This warming is in relation with the decrease of sum of negative degrees, observed since mid-1960s, but not evident in historical data, probably due to their lower quality since the mid-1970s.

There is quite limited information available on actual properties of Caspian Sea ice besides limited thickness observations. The information that is available is largely related to offshore construction of drilling sites. Winds in this region are very strong and their influence results in intensive deformation of the ice cover and subsequent cracking, fracturing, rafting, as well as the formation of hummocks and ridges. Some hummocks become anchored on the sea floor, reaching 2–4 m (in some cases, 6 m) height (Terziev et al., 1992). The thickest (presumably level) pack ice is observed in the eastern part of the North Caspian in January, averaging 40–50 cm, while in the region of the Volga delta, it is observed in February (20–30 cm). In severe winters, ice thickness may increase up to 75 cm in the western and central regions and 120 cm in the eastern parts (Kouraev et al., 2004 and references therein). Ice keel drafts are generally less than 2 m, while sails are less than 1 m high (Kharitonov, 2008); due to the shallow depths in the northern Caspian, some keels can effectively disturb the bottom and are therefore hazardous to offshore constructions. Comfort et al. (2002) report on ice thickness measurements, where level ice appears to be less than 0.4 m thick and the maximum thickness that was measured was 0.8 m for deformed ice. Barker and Croasdale (2004) made observations of ice pile-up against structures in the northern Caspian Sea, including ridged and rafted ice thickness and geometry, ice pile-up geometry and block size distribution. Mean level ice thickness ranged from 0.3 to 0.5 m. The maximum grounded thickness was approximately 10 m, with a corresponding pile-up height of 6 m in 4 m water depth. It appears that ice pile-ups in the Caspian could be higher than other regions (for the same ice thickness), which was attributed to the shallower water and reduced ice friction between ice blocks due to lack of snow (Barker & Croasdale, 2004).

Besides observations of thickness and extent of ice in the Caspian, there is very little information available. Tsytsarin et al. (1998) report on the salt content and composition in Caspian and Aral Sea ice. Obviously, the composition of the parent water plays an important role in the properties of the ice. As the North Caspian is brackish, the ice formed here is quite low in salinity, Tsytsarin et al. (1998) report that Caspian Sea ice contains usually 1–2 g salts per kg of ice, while in nearby major rivers the ice can be fresh. The brackish nature of the basin is likely to result in ice with similar properties than in the Baltic Sea, although there appears to be much less snow on the ice in the Caspian Sea, which would limit the formation of meteoric ice, which is a rather important factor in the Baltic Sea.

Aral Sea

Formerly the fourth largest inland water body in the world (66,000 km² and >1000 km³ in 1960), the volume and area of the Aral Sea, bordering on Kazakhstan, Uzbekistan and Turkmenistan, have decreased dramatically over the past 30 years, largely as a result of human actions. Nowadays, the Sea is divided into two parts: the northern, shallow Small Aral and the southern, deeper Large (or Big) Aral (see Aladin et al., 2005). The dramatic recession of the Aral Sea witnessed over the past 30 years has brought the world's attention

to the environmental crisis in this extensive and important body of water (Glantz, 1998). Both the level and volume have been severely reduced, primarily by the sustained withdrawal of large quantities of water from the two main feeder rivers, the Amu Darya and the Syr Darya: From 1960 to 1990, the area of the Aral was reduced by 40–60% and the volume by 60–80%. During this period, the salinity rose from 9–10‰ to greater than 30‰ with a dramatic effect on the flora and fauna (Aladin & Potts, 1992; Boomer et al., 2000). However, such dramatic changes in the water level are not unprecedented in the geological record of the basin (Boomer et al., 2000). Since 1988, the Small (northern part) and Large (southern part) Aral became completely divided, actually forming two separate seas. Historical assessment of the ice cover parameters discussed in this section is based on observations made when the Aral Sea was one water body. Due to the rapid changes in sea level and coastline, heterogeneous series of ice conditions can only be obtained for the central part of the Large Aral Sea for the whole period of satellite observations (Kouraev et al., 2004).

The historical and recent satellite record of the ice conditions in the Aral Sea has been compiled in Kouraev et al. (2004). Ice conditions are most severe in the northern and eastern parts of Aral Sea, similar to the Caspian Sea, and are result of the local climate. Ice formation is initiated in the northern and north-eastern coastal regions in mid-November, in the south by the end of November, in the open sea by end of December, while in the western coastal zone, ice forms only in the beginning of January. Variability of the dates of ice formation onset varies from 1 to 2 months depending on region. In moderate winters, by mid-December, the pack ice covers 20–30 km along the northern and north-eastern coast. In January, it covers the whole Small Aral Sea and regions along the eastern and southern coasts. It appears on the western coasts (bands of 4–6 km width) as well. The maximum extent is observed in February, when, in severe winters, ice may cover the whole sea surface. The greatest ice thickness is observed in February (sometimes in March) and it reaches 65–70 cm in the northern and 35–45 cm in the southern parts. As in the northern Caspian, the distribution of drifting ice in the open Aral Sea is influenced by the wind conditions, and the prevailing north-easterly and easterly winds often lead to rapid increase in ice concentration in the southern part of the sea. Ice starts to melt in late February or early March. Southern and south-eastern parts become ice-free by the end of March and the northern coast in mid-April. In severe winters, ice may reside until the end of April or beginning of May. The number of days with ice ranges from 120–140 days in the north to 100–110 in the south, while in the western regions it is minimal, about 70–80 days (Kouraev et al., 2004).

Recently observed trends in the ice duration and extent in the Aral Sea both show generally a decrease in the severity of the ice conditions (Kouraev et al., 2004). The maximal duration of the ice season increased slightly from 90–100 to 120 days in the mid-1990s, the minimal durations, however, dropped from 40 to 10–30 days, especially evident during the last 3–4 winters. Both historical and satellite-derived observations show high interannual variability with many similar features during the overlap period (Fig. 14.10). The estimates of the maximal ice extent during the mild winters of 1980–1981 and 1982–1983 are very close, even in absolute values. Satellite data indicate a recent continuous decrease of ice extent in the Aral Sea, since the winter 1993–1994. In 1999–2000, the values reached the lowest mark for the whole period of satellite observations (until 2002; Kouraev et al., 2004).

The milder ice conditions in recent times may be partly explained by the continuing decrease of sea volume (and thus of heat-storage capacity; Small et al., 2000) and the increase
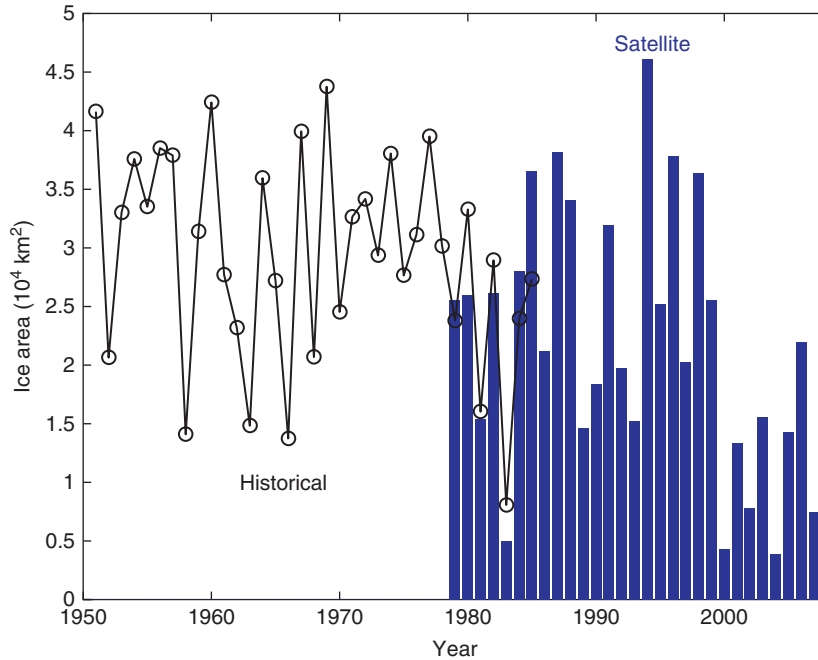
Fig. 14.10 Ice area in the Aral Sea. Historical data is based on records from Bortnik and Chistyayeva (1990). The data from the satellite era (Kouraev et al., 2008) has been corrected to match the historical record, as the area of the Aral Sea has decreased significantly and the satellite can only see a small part of the original Aral Sea area. Data courtesy of Alexei Kouraev.

of salinity, that from 1995 to 2001 increased in the central part of the Large Aral Sea from 42 to 155–166 (see Kouraev et al., 2004). This increase of salinity would have shifted the freezing temperature from –2.3°C to –9.0°C. Such a strong shift in the freezing point may be larger than any influence from changes in local climate. However, since the Aral Sea was divided into two parts, the northern part has had a positive water balance (run-off exceeds evaporation), whilst the southern part has faced continued salinization (Aladin et al., 2004). In the Small Aral, salinity is only about 20, and both lakes have also followed their own hydrobiological evolution (Aladin et al., 2005). The decrease of heat-storage capacity would result in an earlier start of ice formation in autumn and an earlier ice break-up and melting in the spring, while the increase of salinity would lead to a general decrease of ice season length and ice extent. The shrinking of the Aral Sea has affected the local climate, which in turn can then affect the formation of ice in the sea itself. The climate records from around the Aral Sea show dramatic temperature changes between 1960 and 1997, once regionally coherent trends and variability are removed (Small et al., 2000). Mean, maximum and minimum temperatures near the Aral Sea have changed by up to 6°C. Warming is observed during spring and summer and cooling in autumn and winter, which agree with the observed changes in the dates of ice formation and melt in the central part of the Aral Sea. Therefore, local scale changes in the climate are also significant in affecting the ice conditions. Climate warming and the consequent reduction of ice cover could benefit navigation and fisheries. However, it also may result in changes of many environmental parameters, e.g., increasing

the probability of extreme meteorological conditions, such as strong winds and storms. This will negatively affect operating conditions for various industrial activities. Less and thinner ice does not necessarily result in easier navigation as the frequency of ice deformation events may increase.

Sea of Azov

The Sea of Azov is the northernmost part of the Black Sea. It is known for its high productivity and fisheries. It is one of the smallest and shallowest seas in the world (Kosarev et al., 2008). Its area is about 37,600 km^2 and its maximum depth is only 14 m, with generally gently sloping bathymetry and largest depths are in the central basin. Essentially, it is a vast mixing zone between river waters and Black Sea waters, which connects to the Sea of Azov by the shallow (<15 m) and narrow (4 km) Kerch Strait. Two large, Kuban and Don, Rivers and some 200 smaller rivers drain into the Sea of Azov, the two major rivers contributing greater than 90% of the run-off inputs, that result in a lower salinity than in the Black Sea. There is a marked horizontal salinity gradient adjacent to river inflows.

The south-central part of the sea is characterized by salinities of 11–12, while salinities decrease towards the north-east along the relatively shallow Taganrog Bay (only 2–9 m deep), the Don River delta is located at the north-east end of the bay. The average salinity of the Sea of Azov has been between 10 and 13 in the last century, when excluding Taganrog Bay which has a salinity that is about 3 units lower (Matishov et al., 2006). The climate of the sea is continental, characterized by cold winters and hot and dry summers. In winter, the prevailing airflow is from the east or north-east, bringing in cold air masses. This promotes ice formation especially in the shallower and fresher Taganrog Bay (Fig. 14.11). Ice is formed every year, but the ice coverage strongly depends on the severity of the winter (Kosarev et al., 2008).

The average duration of the ice period is 4.5 months (Kosarev et al., 2008). In anomalously warm or severe winters, the times of ice formation and thawing may be shifted by 1–2 months or even greater. The ice first forms and disappears last in Taganrog Bay. Ice usually begins to form at the end of November or the beginning of December in Taganrog Bay, while it disappears completely in late March or early April. Fast ice forms first along the northern coast in December and somewhat later along other coasts. The width of the fast ice is 6–7 km along the north coast and less than 2 km elsewhere (Kosarev et al., 2008). In the central part of the sea, ice is formed only at the end of January or in early February. The Sea of Azov reaches its most complete ice coverage in February, when in severe winters, some ice can also form in the Kerch Strait and nearby areas in the Black Sea. Despite the quite severe ice conditions and length of the ice season, information on the functioning of the ecosystem in winter is virtually non-existent (Matishov et al., 2007).

Maximum thicknesses of level ice were observed in fast ice were within a range of 25–35 cm (Kharitonov, 2008), although when the ice cover is most developed in early February, its thickness reaches 30–40 cm (up to 60–80 cm in Taganrog Bay, Kosarev et al., 2008). The thin ice and variable conditions result in deformed ice with ice ridges up to 1 m high in the central basin, but several metres high when the ice is moved onshore or into shallow water. Due to the shallowness of the area, considerable amounts of sediment are incorporated in the sea ice cover, the sediment load in the ice being larger than the river inputs to the sea (Aibalutov & Grudinova, 1991), the dynamic sea ice cover might therefore contribute significantly to the redistribution of bottom sediments in the Sea of Azov.
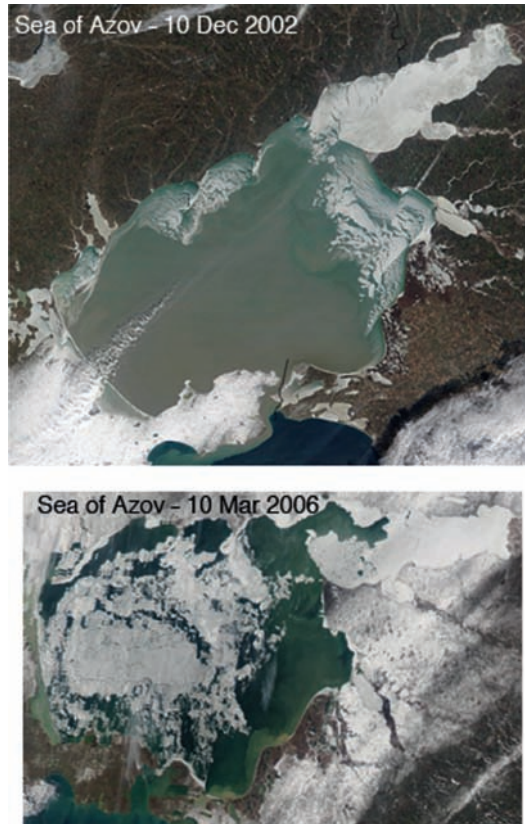
Fig. 14.11 Upper panel: Ice in the northern and north-eastern parts of the Sea of Azov on December 10, 2002 as seen with the MODIS instrument onboard the Terra Satellite. Taganrog Bay, the elongate bay in north-east, is completely ice-covered at this early phase of the ice season. Lower panel: Ice in the Sea of Azov on March 10, 2006 as seen with the MODIS instrument on the Aqua Satellite. (Images courtesy of NASA Visible Earth and the MODIS Rapid Response Project at NASA/GSFC).

Borovskaya and Lomakin (2008) examined the ice conditions in winter 2005–2006, which was the coldest winter in the region for the past 20 years. Especially the months of January and February were cold, and from the onset of ice formation to the time the whole sea was ice-covered took only a period of about 10 days in January, which normally takes place in 5–6 weeks, if the sea gets a complete ice cover at all. The major part of the seawater area was under ice fields 25–40 cm thick, while the ice was 50–70 cm in the Taganrog Bay, somewhat thicker than climatological long-term means. According to Borovskaya and Lomakin (2008), the number of mild winters has considerably increased, the number of temperate winters decreased and no severe winters were observed in last two decades. On the whole, ice winters have become milder but longer.

14.6 Gulf of St. Lawrence

The Gulf of Saint Lawrence (about 250,000 km²), located in North America (Fig. 14.1), is the outlet of the Great Lakes via the Saint Lawrence River into the Atlantic Ocean. The Gulf can therefore be regarded as a large estuary, with considerable influence from freshwater

run-off. It is surrounded in the north by the Labrador Peninsula, in the east by Newfoundland, to the south by the Nova Scotia Peninsula and Cape Breton Island and to the west by the Gaspé Peninsula and New Brunswick. The major connections to the Atlantic Ocean are the Strait of Belle Isle between Labrador and Newfoundland in the north-east, the Cabot Strait between Newfoundland and Cape Breton Island in the east and the Strait of Canso between Cape Breton Island and Nova Scoatia. It should be noted that after the construction of the Canso Causeway in 1955, the Strait of Canso does not permit free-flowing exchange of water between the Gulf and the Atlantic. Due to the limited connection to the world ocean, the Gulf can be considered a semi-enclosed sea. The Gulf is also characterized by complex topography, with shallow areas and deep troughs. Seasonal sea ice is also an important feature in the functioning of the system as during its maximum extent it virtually covers the whole gulf.

Ice formation starts usually in late December or early January, when new ice begins to form along the northern shore of the Gulf while that which has formed in the estuary proper begins to drift eastwards. By the end of January, the western half of the Gulf is ice-covered, at this time ice is also starting to be transported eastwards through the Cabot Strait. The ice cover continues to grow and gradually spreads eastwards to cover most of the remaining areas of the Gulf by the end of February. The ice usually reaches its greatest areal extent during early March (Fig. 14.12) when it also extends over the north-eastern Scotian Shelf (Hill et al., 2002). Land-fast ice in the gulf generally does not extend very far offshore. Ice break-up usually begins around mid-March in the leeward and thinner ice areas and proceeds southwards and south-eastwards through the gulf. The main shipping route through the gulf clears first, normally during early April. The last two areas to clear of sea ice are the southern portions of the gulf between Prince Edward Island and Cape Breton Island and the Northeast Arm.

The extent of sea ice in the Gulf of St. Lawrence area, more exactly the area of ice east of Cabot Strait, has been reconstructed for the period from early 1800s to early 1960s on the basis of historical records (Hill et al., 2002) and more recent records (until 2007) are available from the Canadian Ice Service archives (whole record shown in Fig. 14.13). The trend in the past 50 years has been of decreased ice extent; ice has been observed east of Cabot Strait for all 80 years prior to 1950 but since then there has been 3 years with no ice (Hill et al., 2002). One problem dealing with the earlier historical data is that if there were no ice reports in the Straits or on the Scotian Shelf, is that because there was no ice present or was it because there was no ship present to observe the ice or, just as likely, was ice present and noted but no record of it has yet been found (Hill et al., 2002)? Therefore, one has to be cautious with using the historical record as a precise measure of ice conditions in the area.

Information on the ice thickness in the mobile sea ice in the Gulf is limited. Prinsenberg et al. (2006) studied the drift and deformation of sea ice in the southern part of the gulf, where level ice can grow about 0.65 m thick thermodynamically. Deformation events play an important role in the area, as by the end of the winter, after several winter storms, the mean ice thickness has shifted from less than 0.6 m to about 2.8 m in the southern parts of the gulf. Sea ice dynamics therefore plays an important role in the overall volume and mass of the sea ice in the region. In the northern part of the Gulf, the land-fast ice can reach 0.8–1.2 m in thickness.
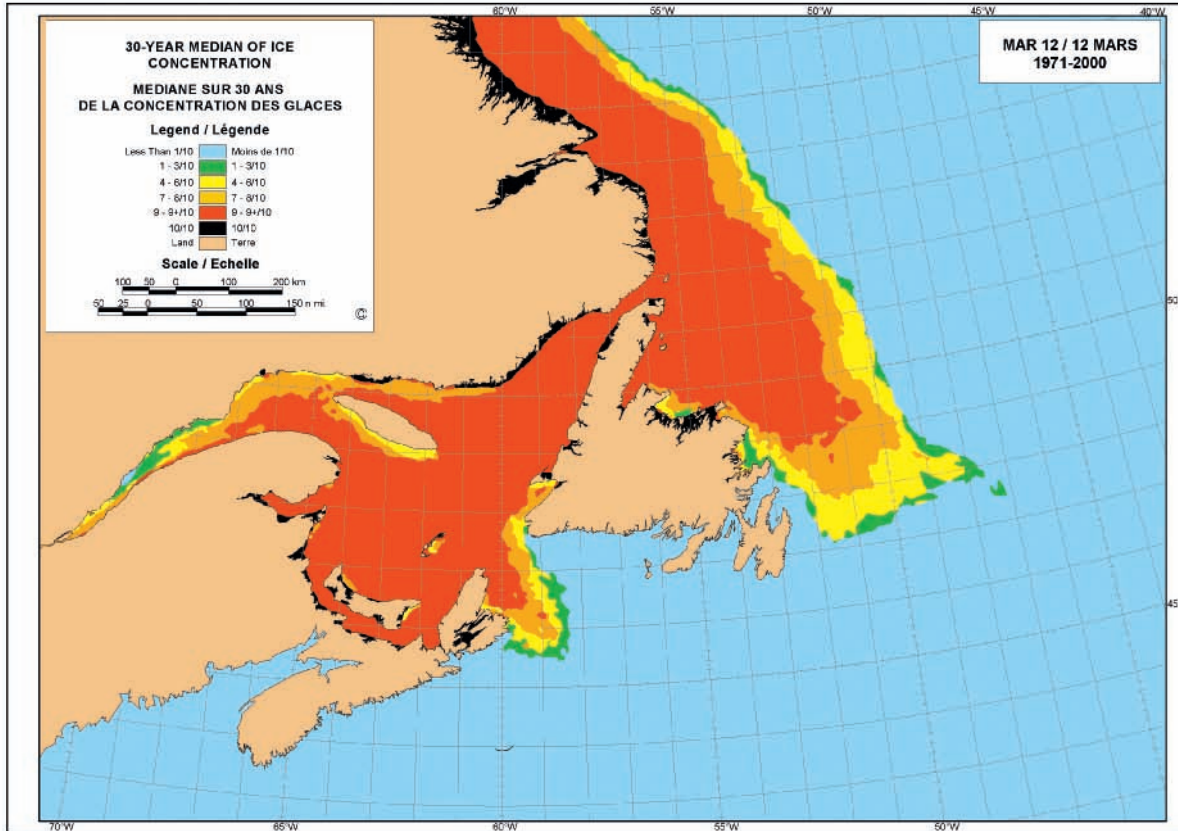
Fig. 14.12 Median ice concentration (12 March 1971–2000) in the St. Lawrence estuary and adjacent areas, which represent the conditions at maximum ice extent in the area. Reproduced from Canadian Ice Service (2002) Sea Ice Climatic Atlas. Northern Canadian Waters 1971–2000. With permission from Environment Canada.
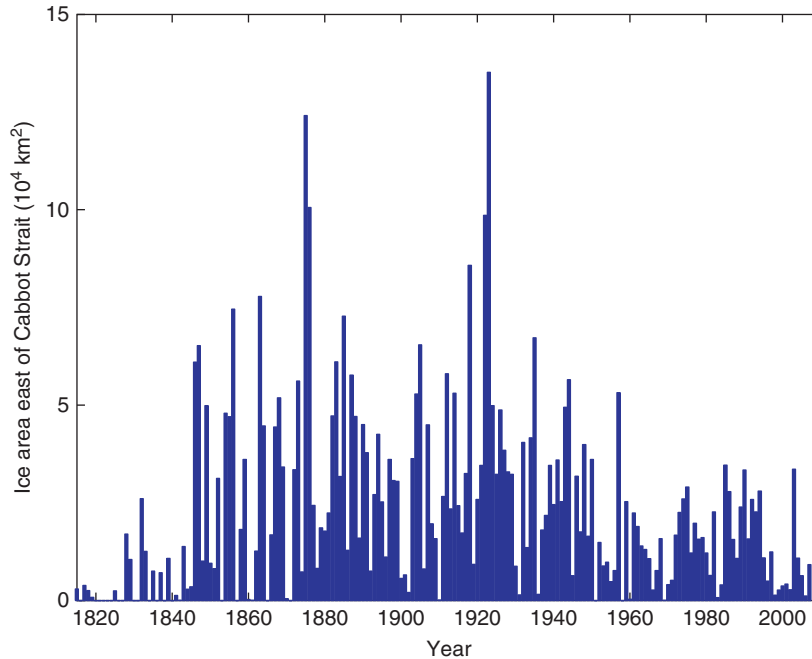
Fig. 14.13 Historical ice extent (1812–1962) east of Cabot Strait from historical records (Hill et al., 2002) and more recent record is based on ice charts from Canadian Ice Service. Data courtesy of Brian Hill.

14.7 White Sea

The White Sea (63–69°N) is a marginal semi-enclosed sea located and surrounded by land masses of northern Europe, with a connection to the Arctic Ocean through the Barents Sea (Fig. 14.1). Essentially, it is an arctic shelf sea. Recently, there has been increased scientific interest in the region, resulting in environmental and socio-economic overviews of the White Sea system (Filatov et al., 2005). The mean depth is about 67 m, the bottom relief is rather irregular and complex, with a maximum depth of 350 m. The White Sea can be divided into three major parts, a northern, a central and a southern part. Furthermore, there are many major bays that divide the complex topography of the system into smaller basins. The seasonal sea ice cover is an important feature, covering most of the White Sea every winter. As other marginal seas, it also receives large inputs from many rivers, the area of the watershed is about 1.1×10^6 km² (about 10 times larger than the sea surface area), and the run-off together with the exchange with the Barent Sea through Voronkin strait are important components for defining the water mass composition in the basin. Run-off exceeds precipitation, run-off totalling about 230 km³ and precipitation about 50 km³ per year, resulting in a freshwater yield of about 3 m if spread evenly over all the surface area. This is a much higher than, for example, the Arctic Ocean, Hudson Bay or Baltic Sea, which also have significant contributions from run-off.

The salinity of the White Sea is therefore lower than in the oceans, but due to the active exchange with Barents Sea waters higher than in, for example, the Baltic Sea. One can also expect considerable gradients in salinity from major freshwater sources towards the Barents

Sea, the complex topography further complicating salinity distributions in the surface waters. Generally, a salinity regime of 14–27 has been cited (Krell et al., 2003), although salinity is considerably lower in near proximity of major rivers (Howland et al., 1999).

The climate regime of the White Sea area can be defined to be between the continental and marine types. The winters are relatively mild for the latitude, as air masses originating from the Atlantic can pass over the area anytime of the year. This resembles the conditions in the (northern) Baltic Sea area. The prevailing atmospheric patterns also bring excessive moisture to the area, which results in high precipitation rates and river run-off. Considerable interannual variation is a typical feature of the conditions in the area.

Sea ice formation and dynamics in White Sea is controlled by many factors, most importantly by the severity of the local winter conditions, wind regime, rate of inflow from the Barents Sea (bringing in heat and salt), morphometric features (enclosed basins, shallowness) and salinity (extent of run-off and Barents Sea inflow). Also, tides play an essential role in the dynamics of the ice cover. Early freezing usually starts in shallow and fresher waters in December as the water column cools fastest in these areas. Ice in the interior basin develops later. Fast ice is the dominant type of ice in many of the bays where ice formation starts first. However, even the fast ice is heavily deformed due to the dynamic nature of the ice cover caused by winds and tides. Especially, deformed ice is found along the eastern coast, as the prevailing winds push the ice towards the coast. Generally, there is a net transport of ice from the south–south-west to the east–north-east. By February, the White Sea is almost completely ice-covered and most of the thickness growth occurs in January and February. Melting usually starts in mid-April, continues rapidly in May and by early June all ice is gone.

The sea ice in the White Sea is first-year sea ice, with thicknesses of about 30–70 cm (Pozdnyakov et al., 2005), however, more than 1 m thick land-fast ice has been observed in the western White Sea (Krell et al., 2003). Heavy deformation is likely to produce fairly thick ice formations, especially along the eastern shores, although rafted and ridged ice are predominant over the entire White Sea (Pozdnyakov et al., 2005). There are only limited reports on the physical properties of sea ice in the area. Obviously, the lower salinity than in polar seas will affect the physical properties of the ice, as in other brackish water areas, like the Baltic Sea. In winter, the bulk salinity of ice therefore varies from close to zero (basically freshwater ice), at proximity of freshwater sources, to 12 in offshore conditions (Fig. 14.14; Krell et al., 2003). The most comprehensive observations on the structure and isotopic composition, which can be used to examine the growth processes of sea ice, were made in the western part of the White Sea (Krell et al., 2003). These observations revealed that congelation growth was less important than either frazil growth or snow-ice or superimposed ice growth late in the season (April). In February, both granular and columnar ice layer were present, although the latter had almost completely disappeared by April. Isotopic evidence suggest that there is considerable upward thickness growth caused by snow-ice or superimposed ice formation, observations of a significant snow load (5–24 cm on top of 20–25 cm of ice) and negative freeboards in February also support this conclusion. The significant drop in ice salinity from February to April (Fig. 14.14), especially in the surface layer at thin ice sites suggests that superimposed ice (pure snow) has been formed. This resembles in many ways the Baltic Sea, where snow contributes significantly to the thickness and mass of sea ice (Krell et al., 2003). Considering the high precipitation rates in White Sea, it would not be surprising that snow-ice and superimposed ice play an important part in the mass balance of sea ice in the White Sea.
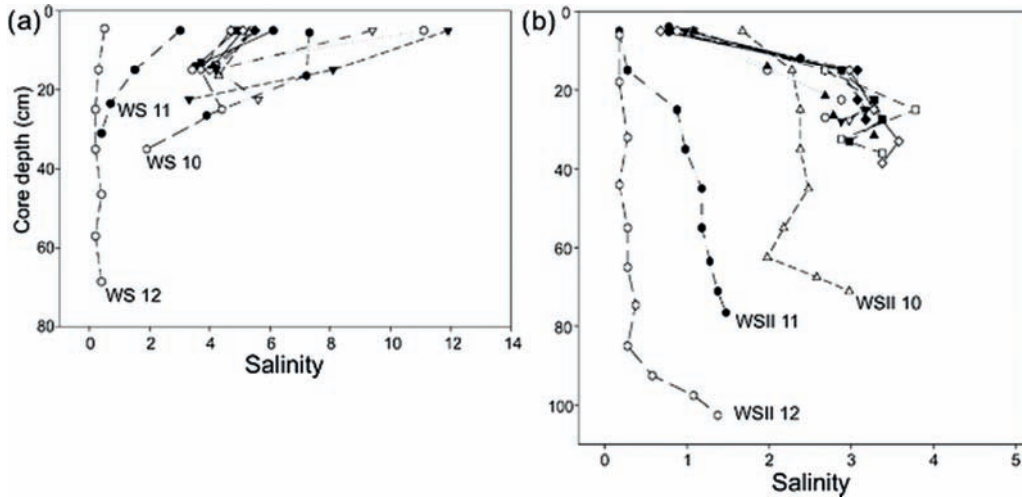
Fig. 14.14   Salinity profiles of sea ice in western White Sea in (a) February and (b) April. Station WS 12 and WSII 12 are in proximity of a small creek, decreasing number means increased distance to this freshwater source. Data is shown at the mid-point of every ice core section measured. With kind permission from Springer Science + Business Media: Polar Biology, Krell et al. (2003).

For the satellite era (1978–1999), the trend overall has been a decrease in the ice extent (8% per decade) in the White Sea, but recently (1992–1999), the ice cover extent has exceeded long-term averages as the negative trend has reversed (see Pozdnyakov et al., 2005). However, a 20-year period of satellite observations is insufficient to confidently establish any long-term variations in the ice cover. Besides ice extent, the changes in thickness are as important, and any information on changes in total ice volume is lacking to make any further conclusions on the nature of the ice conditions in the White Sea. Nevertheless, ice forms every winter and is likely to play an important part of the functioning of the system, and sea ice therefore probably plays a major role in structuring the White Sea ecosystem, since it strongly alters the exchange of energy and material between water and atmosphere (Krell et al., 2003).

14.8 Bohai Sea

The Bohai Sea (37–41°N) off the north-east coast of China is the southernmost sea in the northern hemisphere where seasonal freezing takes place every winter. Its surface area is about 77,000 km². It is surrounded by land to the west, east and north, and it is relatively shallow (18 m on average, 78 m maximum depth). The Bohai Sea is connected to the Yellow Sea in the south by the Bohai Strait. There are several rivers, such as the Yellow River (Huanghe), the Haihe River, the Luanhe River and the Liaohe River, discharging into the Bohai Sea. The total run-off is about 80–90 km³ every year, among which the discharge of the Yellow River is 42 km³ (Yang, 2000; Sündermann & Feng, 2004).

The region belongs to the mid-latitude monsoon climate zone and shows typical continental behaviour. The mean air temperature in January is between –4.0°C and –8.0°C, with

a minimum of –25.0°C (Yang, 2000). In winter, rapidly moving cold fronts from north to south frequently pass the region causing ice formation and rapid changes in ice conditions (Zhang, 2000). The Liaodong Bay in the northern Bohai Sea is normally ice-covered for 3 months in the winter season. Usually, the ice forms in coastal areas and is driven southwards by winds, further promoting new ice production in open leads. As the ice drifts southwards into warmer water, it breaks up and melts (Zhang, 2000). The ice pack in the Bohai Sea has strong mobility due to strong tides and the relatively thin ice and small size of ice floes results easily in ice deformation (rafting and ridging). The maximum mean tidal range along the coast is 2.7 m at the head of the Liaodong Gulf and is about 2 m in the Bohai Strait. The tidal current is predominantly semidiurnal, with a velocity range of 50–100 cm s^{-1} (Yang, 2000). It has been found that ice motion in the Bohai Sea is not only affected by prevailing winds, but also by topographic steering, currents and internal ice stresses (Wu et al., 2005b).

The ice has considerable impact on coastal and near-shore oil- and gas-drilling operations and has caused severe damages to offshore structures and losses of production in this region. Economic development in this area is highly dependent on the sea conditions and is vulnerable to natural disasters such as severe winters (Yang, 2000). The area is one of the major economic development centres in China, accounting for roughly 22% of the nation's Gross Domestic Product in 1999 (Zhang et al., 2006). For example, the severe winter of 1968–1969 is the most remarkable with regard to its impact. Sea ice covered almost the entire Bohai Sea, the only time this has happened since 1954, resulting in great economic loss. More than 400 fishing vessels with about 1500 workers onboard were stranded in the sea by the heavy ice, and one oil-drilling platform was completely destroyed and two others were heavily damaged.

The ice conditions for Bohai Sea have been recently summarized in detail by Yang (2000). Annual maximum ice extent shows large variability in the Bohai Sea (Bai et al., 2001; Gong et al., 2007; Wu et al., 2005a; Zhang, 2000; Zhang et al., 1997). Ice only covers less than 15% of the waters during the warmest winters, while it covers more than 80% during the coldest winters (Yang, 2000), this corresponds to about 10,000 km^2 in very mild winters to almost complete ice coverage in extremely severe winters (once in the period from 1950 to 2000 in 1968–1969) (Wu et al., 2005a). The length of the ice season depends on the severity of the winter and location. In Liaodong Bay, the ice season is on average 100–130 days, with freeze-up in mid- to late November and break-up in late March. In Bohai and Laizhou Bays, the ice season lasts for about 60 days on average (Wu et al., 2005a). The lightest conditions are in the vicinity of the Bohai Strait where ice appears only in very severe winters. Ice also forms in Korea Bay on the northern shores of the Yellow Sea (Fig. 14.15), east of the Bohai Strait towards the Korean Peninsula, where the ice season is almost as long as in Liaodong Bay (see Yang, 2000). In the Korea Bay, the ice extends usually less than 50 km from the coast and covers less than 12,000 km^2 (Wu et al., 2005a).

In Liaodong Bay, level ice thickness has been reported as 30–40 cm (Launiainen & Cheng, 1998) and can reach up to 50 cm at maximum (Li & Wang, 2001). Under normal conditions, the ice thickness ranges from about 40–60 cm in the coastal waters to about 10 cm at the offshore ice edge (Yang, 2000). The ice easily deforms, especially in eastern end of Liaodong Bay and Bohai Bay, in these areas rafted ice can be up to 100 cm thick, while ridge sails can be up to 200 cm high. There appears to be no information on ice ridge keel depths in the area, but ridges certainly affect marine operations in winter. The texture of the sea ice reveals that the sea ice cover often consists of several layers that have been rafted on top of each other (Li et al., 2003), supporting the fact that dynamic thickening is important.
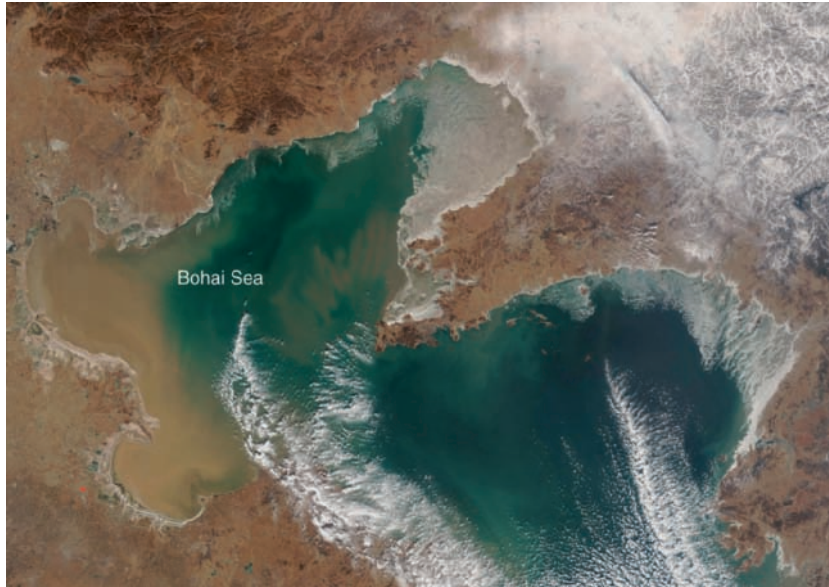
Fig. 14.15   Sea ice in the Bohai Sea (mainly Liaodong Bay) and northern parts of Korea Bay on February 2, 2005 as seen from the MODIS instrument on the Terra satellite (Image courtesy of the MODIS Rapid Response Project at NASA/GSFC).

Climate factors, such as the El Niño/Southern Oscillation, western Pacific subtropical high and AO, have been shown to explain Bohai Sea ice variability (see Gong et al., 2007). It has been shown that the ice severity in Bohai Sea is becoming significantly lighter in the period from 1954 to 2005 (Fig. 14.16), and ice coverage is getting smaller (Gong et al., 2007). This has been accompanied by a general increase in winter temperatures and shorter duration of freezing. Significant trends for the 1954–2005 period include an increase in air temperature in the region by 0.42°C per decade and a decrease in the duration of freezing by 3.8 days per decade. The relation between AO and the severity of Bohai Sea ice conditions is clearly identified by comparing their time series (Fig. 14.16), the two of curves are significantly correlated with a Pearson correlation coefficient of $r = -0.57$ ($r^2 = 32\%$), indicating that ice conditions are closely related by atmospheric circulation patterns that affect the local climate (Gong et al., 2007). Large-scale circulation anomalies associated with the AO play an essential role in local temperatures and ice conditions in the Bohai Sea region. The significant decline of ice severity after the 1970s is unprecedented since at least the 1880s (Gong et al., 2007).

There is not much information available on the physical properties or growth conditions of sea ice in the Bohai Sea. In winter, the surface salinity of the Bohai Sea is about 28.0–30.0, somewhat lower than for the Yellow Sea due to the high river inputs, and is likely to be considerably lower in the vicinity of major rivers. Bulk ice salinities for Bohai Sea have been reported as 4–9 (Yang, 2000; Li & Wang, 2001), which are within the range for polar first-year sea ice. Similarly to its polar counterpart, the salinity significantly decreases with increasing ice thickness (Li & Wang, 2001). The lowest bulk ice salinities in the range appear to be in the vicinity of major river systems, in the Liadong Bay and at the outlet of Yellow
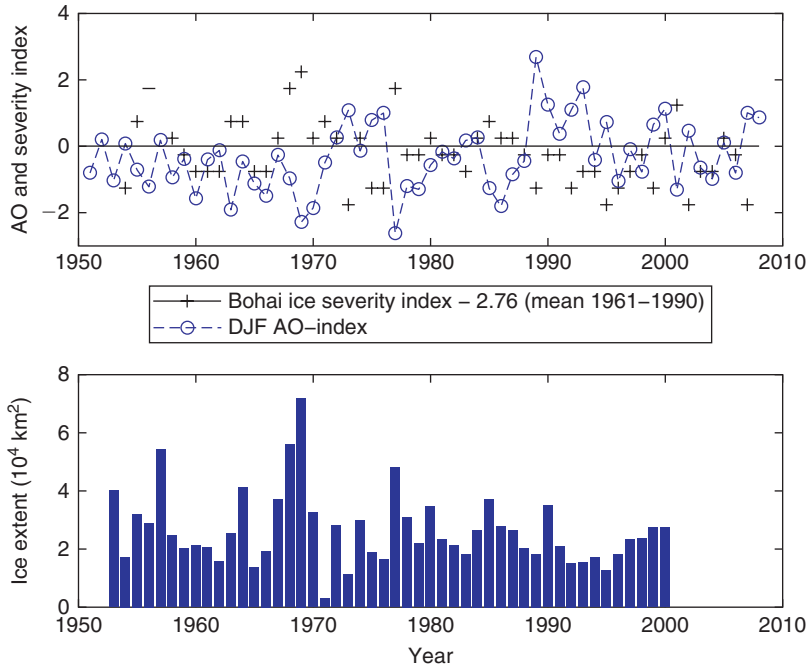
Fig.14.16   Upper panel: Time series of the December–February Arctic-Oscillation index 1951–2008 (dashed line with circles), along with average Bohai Sea ice severity index 1954–2007 (solid line with crosses), the latter as deviation from the average of 1961–1990 (2.76). The ice severity index is divided into five categories that vary from 1.0 to 5.0. Category 1 represents the lightest ice severity, 5 the most severe, 3 the normal, and categories 2 and 4 denote the moderately light and moderately heavy severities, respectively. During extreme conditions (category 5), most of the sea is covered by sea ice (data courtesy of Gong et al., 2007). Bottom panel: Ice cover area (extent) in Bohai Sea from 1953 to 2000 (data from Wu et al., 2005a).

River. Relatively high salinities and temperatures are likely to produce porous ice, reduced in strength, and thereby easily deformed.

14.9 Characteristics of non-polar sea-ice ecosystems

Studies concerning ice organism assemblages and ice food webs in non-polar sea ice are scarcer than studies on physical characteristics. Information on sea ice biota is available only from the Hudson Bay (mainly SE Hudson Bay), the Gulf of St. Lawrence, Baltic Sea (the Gulfs of Finland and Bothnia), White Sea (Chupa inlet in the central White Sea) and the Sea of Okhotsk (mainly Saroma-ko Lagoon in Hokkaido). Most studies have been conducted in land-fast level ice, which is relatively easy to access from land. Studies on open sea pack/drift-ice ecosystems in non-polar seas are still rare.

Whereas extensive research on sea ice biota and assemblages living within the ice has been conducted in polar regions for more than 100 years (reviews by Brierley & Thomas, 2002; Thomas & Dieckmann, 2002; Lizotte, 2003), ice biota in non-polar seas have been studied

only during the last three decades; since 1980s in the SE Hudson Bay (Legendre et al., 1996 and references therein) and 1990s in the Baltic Sea (reviewed by Granskog et al., 2006a) and the Sea of Okhotsk. Most internationally available studies from the White Sea are published within the last 5 years (Krell et al., 2003; Ratkova et al., 2004; Sazhin et al., 2004; Melnikov et al., 2005). From many non-polar sea ice areas, as the Caspian Sea, Sea of Azov and Bohai Sea, information on sea ice assemblages and ice ecosystems in general is to our knowledge not available. In the following section, we will give an overview on the characteristics of non-polar sea ice as a habitat and discuss some of the most important common characteristics of non-polar sea ice ecosystems.

Non-polar sea ice is always seasonal, i.e. it forms in autumn or early winter and completely disappears upon ice melt in spring. The length of the ice season is the most important factor governing the formation and succession of sea ice organism communities because it determines the lifetime of the entire ice habitat in a given year. Geographical location (latitude) and other factors contribute to the length of the ice season in non-polar ice-covered areas and are discussed earlier in this chapter (Table 14.1).

The properties of parent water, from where the ice forms, are also important as they partly determine the properties of sea ice. The most critical parent water property is salinity, which is a key factor determining sea ice bulk salinity and subsequently ice main interior habitat, brine channel system characteristics. Also, other chemical constituents dissolved in the parent water, such as inorganic nutrients and dissolved organic matter (DOM), contribute to the sea ice characteristics (Chapter 12). Initial organism communities incorporated into growing ice (Chapters 7–10) form a basis for sea ice community succession. Once sea ice is formed, its physical characteristics (ice thickness and snow cover) affect the growth of communities, e.g. by regulating amount of light entering the ice (Sime-Ngando et al., 1999; Kuosa & Kaartokallio, 2006).

While the spatial variability of sea ice properties has been investigated by several studies in the Arctic and Antarctic, the topic has been addressed only recently in non-polar areas. In the Baltic Sea (Granskog et al., 2005a; Steffens et al., 2006), there appears to be sub-basin scale variations in the sea ice properties (Meiners et al., 2002; Granskog et al, 2003), but also regional scale variation in coastal sea ice properties (Granskog et al., 2005b), largely controlled by sub-basin differences and inshore–offshore gradients in salinity created by river water inflows. Bulk salinity of the ice bottom, typically reflecting the inshore–offshore salinity gradients in ice parent water, has been suggested to control the amount and distribution of sea ice algal biomass (as chlorophyll) as well as the composition of ice organism assemblages also in the SE Hudson Bay (Legendre et al., 1981, 1996), Saroma-ko Lagoon (Sea of Okhotsk; Robineau et al., 1997) and in the White Sea (Krell et al., 2003; Melnikov et al., 2005).

Typical succession sequence of organism communities in non-polar sea ice is analogous to Polar sea ice (Grossmann & Gleitz, 1993; Günther & Dieckmann, 1999), with the initial colonization during the sea ice formation followed by low-productive midwinter stage, the bloom of the sea ice algae and finally a heterotrophy-dominated stage late in the season (Fig. 14.17). Biomass accumulation of the sea ice algae generally follows the seasonal increase in solar radiation beginning at the transition of winter and spring and lasts until the onset of ice melt (Cota et al., 1991; Norrman & Andersson, 1994; Haecky & Andersson, 1999). The significance of heterotrophic processes increases in late bloom and post-bloom situations late in the sea ice season (Stoecker et al., 1993; Vezina et al., 1997; Kaartokallio, 2004).
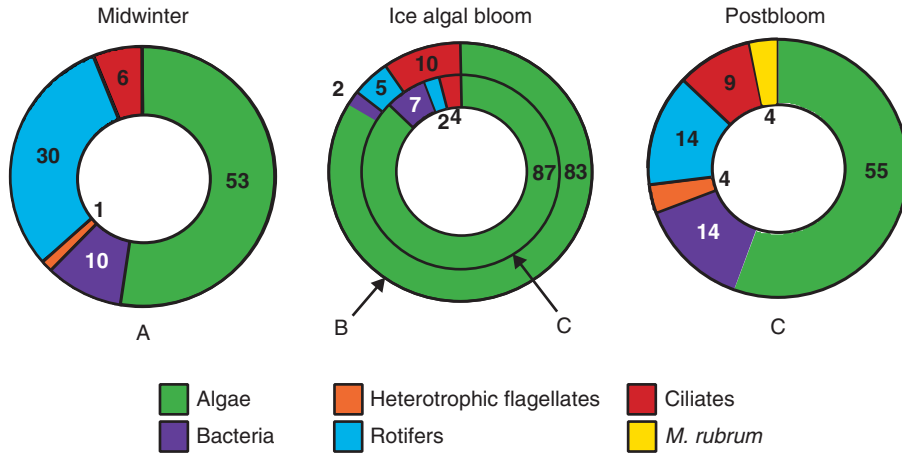
Fig. 14.17 The biomass in percentages of ice organism groups in the Baltic Sea coastal fast ice during low-biomass midwinter period (January), ice algal bloom (early March) and more heterotrophic post-bloom situation (late March–early April). Numbers denote percentages from total organism biomass as mean values for the entire ice column with the ice algal bloom period represented by two winters (b and c). Data from Kuosa and Kaartokallio (2006) (a); Kaartokallio et al. (2007) (b) and Kaartokallio (2004) (c).

    Mass accumulation of ice algae at early spring is typical for all non-polar areas studied (Michel et al., 1993; Legendre et al., 1996; Sazhin, 2004). A full succession sequence beginning with a low-productive midwinter stage followed by an algal bloom inside the ice and a heterotrophy-dominated post-bloom situation has been documented in the Baltic Sea and the Sea of Okhotsk (Sime-Ngando et al., 1997; Haecky & Andersson, 1999; Kaartokallio, 2004). The timing of ice algal bloom seems to be partly related both to amount of solar radiation and length of ice season and ice thickness. Algal bloom inside the sea ice occurs in February in the Saroma-ko Lagoon (located at 44°N) located in the Sea of Okhotsk, and in the Baltic Sea either in March (the Gulf of Finland (60°N)) (Kaartokallio, 2004; Kuosa & Kaartokallio, 2006) or in April (the Gulf of Bothnia (64°N)) (Norrman & Andersson, 1994; Haecky et al., 1998; Haecky & Andersson, 1999) as is the case also in the SE Hudson Bay (55°N) (Michel et al., 1993). In the Gulf of Finland, an occurrence of another, minor algal biomass maximum during a low-light period in January under snow-free ice has also been reported (Kaartokallio, 2004; Kuosa & Kaartokallio, 2006).
    The biomass of sea ice organism varies in non-polar ice localities studied (Table 14.2). It seems that the salinity of underlying water is an important factor determining biomass in ice also on global scale, the low-salinity Baltic Sea having the lowest sea ice algal biomass. Organism biomass in the sea ice of Saroma-ko Lagoon (Sea of Okhotsk) is highest among the localities studied, which may reflect the combination of favourable salinity, latitude (44°N) as well as typically thin snow cover.
    Under-ice algal blooms starting at the ice–water interface before ice break-up and facilitated by stable melting water layer under the ice are a common phenomenon in non-polar sea ice areas (Legendre et al., 1981; Spilling, 2007). These blooms are assumed to contribute to the onset of the major phytoplankton spring bloom after ice break-up in all studied areas. In the Gulf of Finland, the Baltic Sea, these blooms are often dominated by dinoflagellates

Table 14.2 Salinity and biomass (chlorophyll *a*, bacteria and protozooplankton) in non-polar sea ice.

Location	Salinity of UIW	Chl *a* mg m⁻²	Ice season (Bloom)	Bacteria µgC l⁻¹	HNF µgC l⁻¹	Ciliate µgC l⁻¹	Key reference
SE Hudson Bay *Baltic Sea*	15–31[1]	1–18[1] (30)[2]	Dec–Jun (April)				[1]Legendre et al. (1996) [2]Gosselin et al. (1986)
Gulf of Bothnia	3–5[4]	0–2[3] (2)[4]	Dec–May (March)	1–8[4] (12)[4]	0–2[5] (7)[5]	0–5[6] (10)[6]	[3]Granskog et al. (2006a) [4]Kuparinen et al. (2007) [5]Haecky and Andersson (1999) [6]Kaartokallio (unpublished data)
Gulf of Finland	5–6[4]	0–6[3] (6)[3]	Jan–Apr (March)	4–20[4] (115)[4]	0–5[7,8] (25)[8]	0–35[7,8] (290)[8]	[7]Kaartokallio (2004) [8]Kaartokallio et al. (2007)
White Sea	26–27[9]	0–7[9] (13)[9]	Dec–Apr		1–17[10] (25)[10]	0–7[10] (10)[10]	[9]Krell et al. (2003) [10]Sazhin et al. (2004)
Sea of Okhotsk	15–31[11]	6–50[12] (80)[12]	Feb–Apr (Feb)	16–24[13] (39)[13]	70–210[13] (550)[12]	13–23[13] (36)[13]	[11]Shirasawa et al. (1993) [12]Robineau et al. (1997) [13]Sime-Ngando et al. (1999)

UIW = under-ice water; Chl *a* = Chlorophyll *a*; Bacteria = bacterial biomass; HNF = heterotrophic flagellate biomass; Ciliate = ciliate biomass. A typical range and the maximum values (in parenthesis) are given.

(Larsen et al., 1995; Spilling, 2007), whereas in SE Hudson Bay (Michel et al., 1993), in the White Sea (Ratkova et al., 2004) and Sea of Okhotsk (Asami & Imada, 2001), blooms are dominated by the same diatom species also growing inside the ice sheet.

Owing to space limitation in the brine channels, internal sea ice food webs are considered to be truncated, meaning that organisms larger than the upper size limit of channels are lacking (Krembs et al., 2000). Clearly, this may be even more the case for non-polar ice as all studied areas have typically salinity below that of oceanic sea water (Table 14.2). In the Baltic Sea ice, largest metazoan animals are occasional copepods and copepod nauplii (Meiners et al., 2002; Kaartokallio, 2004; Werner & Auel, 2004; Kaartokallio et al., 2007). In White Sea sea ice with higher salinity (Table 14.3) also, nematodes, copepods and poly-chaetes are encountered in ice (Sazhin et al., 2004), although the abundance has been repor-ted to be low (Melnikov et al., 2005). In contrast to the Baltic and White Seas, nematodes and copepods are reported to occur in SE Hudson Bay lower ice layers with 2–3 times higher biomass than in under-ice water (Grainger, 1988). The complete absence, or low significance, of larger metazoans typical for polar sea ice (see Chapter 10) simplifies the eco-system by lowering the number of trophic interactions. Different 'short circuits' in the flow of energy and organic matter are suggested to be typical of microbial food webs inside the sea ice (Fig. 14.18). These include herbivory by ciliates and flagellates, ciliate bacterivory and direct utilization of DOM by heterotrophic flagellates (Marchant & Scott, 1993; Laurion et al., 1995; Sime-Ngando et al., 1997; Vezina et al., 1997; Haecky & Andersson, 1999; Kaartokallio 2004; Kaartokallio et al., 2007). Of these, at least direct utilization of DOM by flagellates (Haecky & Andersson, 1999) and ciliate grazing over several size classes have been suggested to be functional in Baltic Sea ice (Kaartokallio, 2004).
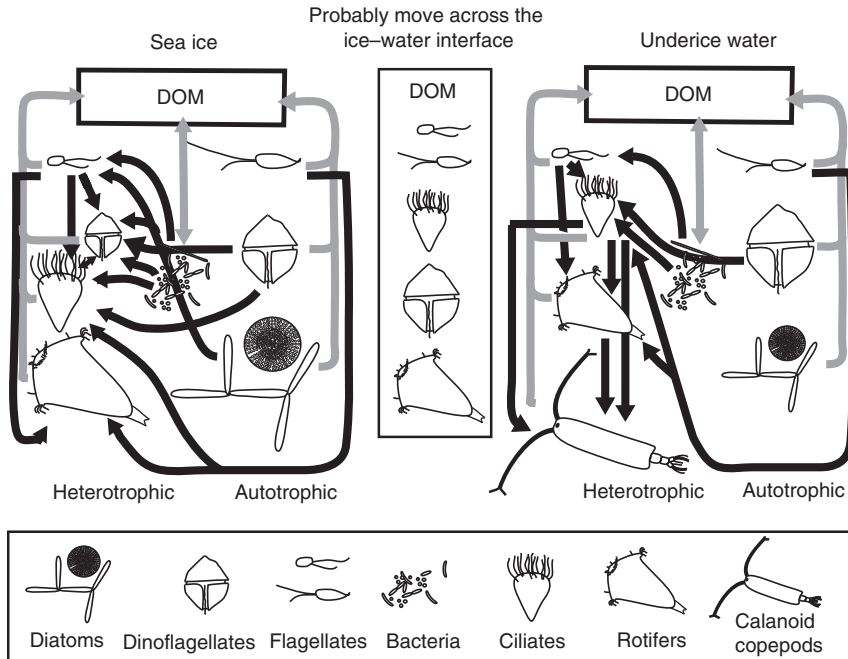
Fig. 14.18 A schematic representation of the Baltic Sea sea-ice and under-ice water food webs. Black lines and arrows stand for trophic interaction, grey lines indicate DOM flow in the food web. Reprinted from Granskog et al. (2006), with permission from Elsevier.

Sparse data existing suggests that there are also differences in sea ice food web structure among non-polar sea ice areas. Mostly, they seem to be related to available space in the brine channels, reflecting ice bulk salinity and salinity of underlying water (Table 14.2). One difference is the presence and importance of larger metazoan animals in ice, but the other seems to be relative importance of heterotrophic flagellates and ciliates as bacterial grazers. In Baltic Sea sea ice, ciliates seem to be more important than in other areas, probably reflecting the paucity of higher animals in ice (Haecky & Andersson, 1999; Meiners et al., 2002; Kaartokallio, 2004), whereas in the White Sea (Sazhin, 2004) and the Sea of Okhotsk, heterotrophic flagellates seem to be more important in terms of biomass (Table 14.2).

14.10 Organism communities in non-polar sea ice

Sea ice assemblages have been studied in detail only in some of the non-polar seas. Thus, we are far away of a concerted view on sea ice community structure or species composition. The most extensive studies are on the diatom flora of the Hudson Bay (Poulin & Cardinal, 1982a,b, 1983), the protists of the Baltic Sea (Ikävalko & Thomsen, 1996, 1997; Ikävalko, 1998) and the sea ice algae in the White Sea (Ratkova & Wassmann, 2005).

The studies from the Baltic and White Seas point at the diversification of land-fast and pack ice algal communities. Ratkova and Wassmann (2005) found land-fast ice communities being dominated by pennate diatoms, with apparent relation to benthic communities, and pack ice communities more by flagellates, dinoflagellates and centric diatoms. Similar

Table 14.3 Examples of representative taxa from sea ice in marginal polar seas.

Organism type	Area
Algae	
Dinophyceae	
Peridiniella catenata (Levander) Balech	BS, WS
Scrippsiella hangoei (Schiller) Larsen	BS
Prymnesiophyceae	
Chrysochromulina birgerii Hällfors & Niemi	BS
Phaeocystis pouchetii (Hariot) Lagerheim	WS
Diatomophyceae	
Pennate	
Achnanthes taeniata Grunow	BS, JL, WS
Cylindrotheca closterium (Ehrenberg) Lewin & Reimann	BS, WS
Fragilaria striatula Lyngbye	JL, WS
Fragillariopsis cylindrus (Grunow) W. Krieger	BS, JL
Melosira arctica (Ehrenberg) Dickie ex Ralfs	BS, JL, WS
Navicula kariana Grunow in Cleve et Grunow	JL, CA
Navicula pelagica P.T. Cleve	BS, JL, WS
Navicula vanhoeffenii Gran	BS, JL, WS
Nitzscia frigida Grunow	BS, JL, WS, CA
Nitzscia cylindrus (Grunow) Hasle	BS, CA
Nitzschia polaris Grunow	WS, CA
Centric	
Attheya septentrionalis (Øestrup) Crawford	WS
Chaetoceros spp.	BS, WS
Detonula confervacea (Cleve) Gran	JL
Odontella aurita Agardh	WS, JL
Thalassiosira hyperborea (Grunow) Hasle & Lange	JL, WS
Thalassiosira nordenskioldii Cleve	JL, WS, CA
Thalassiosira punctigera (Castracane) Hasle	JL
Prasinophyceae	
Mantoniella squamata (Manton and Parke) Desikachary	BS
Pyramimonas grossii Parke	WS
Chlorophyceae	
Monoraphidium contortum (Thuret in Brébisson) Komarék	BS
Oocystis spp.	BS
Protozoa (obligate heterotrophs)	
Chrysophyceae	
Paraphysomonas spp.	BS
Choanoflagellidea	
Diaphanoeca sphaerica Thomsen	BS
Monosiga marina Grøntve	WS
Savillea microporea (Norris) Leadbeater	BS
Incertae sedis	
Cryothecomonas armigera Thomsen et al.	BS

Table 14.3   (*Continued*)

Organism type	Area
Ciliata	
Euplotes spp.	BS, JL, WS
Lacrymaria spp.	JL, WS
Lohmanniella oviformis Leegaard	BS, JL
Mesodinium rubrum Lohmann (**symbiotic**)	BS, JL, WS
Strombidium spp.	BS, WS
Uronema spp.	BS, JL, WS
Metazoa	
Rotatoria	
Keratella spp.	BS
Synchaeta spp.	BS
Copepoda	
Acartia spp.	BS, JL

BS: Haecky et al. (1998); Haecky and Andersson (1999); Ikävalko and Thomsen (1996, 1997); Ikävalko (1998); Kaartokallio et al. (2007); Kuparinen et al. (2007); Meiners et al. (2002); Norrman and Andersson (1994); Werner & Auel (2004).
JL: Asami and Imada (2001); Fortier and Fortier (1997); Ikeya et al. (2001); McMinn et al. (2008); Robineau et al. (1997); Sime-Ngando et al. (1997, 1999); Takahashi (1981); Watanabe et al. (1991).
WS: Krell et al. (2003); Ratkova and Wassmann (2005); Sazhin (2004).
CA: De Sève and Dunbar (1990); Legendre et al. (1996).
BS = Baltic Sea; WS = White Sea; JL = Japanese lagoons; CA = Canadian Arctic.

observation concerning diatoms was made by De Sève and Dundar (1990) in the Gulf of St Lawrence with two clearly different community types. Also, McMinn et al. (2008) found two distinctly different sea ice algal communities in pack ice and land-fast ice in the southern Sea of Okhotsk, and a specific community living in the rafted pack ice has been described from the Baltic Sea (Kuparinen et al., 2007). However, in Japanese lagoons, both communities were mainly composed of centric diatoms, and in the Baltic Sea of a green alga.

Ratkova and Wassmann (2005) found that the pack ice community in White Sea is closely related to open water communities, and originated from the colonization during freezing. Land-fast ice colonization could be related to the motility of pennate diatoms, resulting also in more species-rich land-fast ice communities. The two types of diatom communities in the Gulf of St Lawrence show similar tendency (De Sève & Dunbar, 1990). Though pennate diatoms are also the dominant algae in the sea ice of the different sub-basins of the Baltic Sea (Ikävalko & Thomsen, 1997; Haecky et al., 1998; Haecky & Andersson, 1999), and also, for example, in the Saroma-ko Lagoon (Sea of Okhotsk; Robineau et al., 1997), benthic or ice-benthic pennate diatom communities are not known to great detail. We also lack data on other non-polar sea ice communities and more general studies comparing sea ice and water mass communities during and after the freezing in different sea areas. There are some indications on seeding effect by sea ice communities (Michel et al., 1993), which also should be subject to closer studies.

The extensive work by Ratkova and Wassmann (2005) lists altogether 306 species from the sea ice of White and Barents Seas. It consists of all algal systematic groups, and shows the dominance of diatoms, and also the relative similarity of the two areas. Also, De Sève and Dunbar (1990) show the similarity of real Arctic and non-polar sea ice communities.

Considering the reported low species number of diatoms of, for example, Japanese and Baltic Sea sea ice data, it would be attempting to consider the distance and isolation of non-polar seas from the Arctic sea ice and its communities to be a factor. We could learn more on these aspects by a comparative study on all the marginal sea ice communities. It is, however, interesting to observe that the many of the pennate diatom species in the Japanese lagoons, and the Baltic Sea are the same, but the Baltic Sea lacks the real marine centric diatom element with the exception of *Melosira arctica* (Table 14.3).

The specific characteristics of the Baltic Sea (brackish water, low calcium content) are observed in the lack of coccolithophorids, and the presence of a clear freshwater element including green algae (Ikävalko & Thomsen, 1997; Kuparinen et al., 2007). The role of freshwater element in sea ice communities is likely to be considerable in the Baltic Sea, and it has been found to be present near the St Lawrence River, too (Frenette et al., 2008).

The role of auto- and heterotrophic flagellates in non-polar sea ice is still unclear. Several studies list either flagellates or nanoflagellates, and some point at their importance. However, species composition is not known to great detail, though the works of Ikävalko and Thomsen (1996), Ikävalko (1998) and Ratkova and Wassmann (2005) reveal great diversity of flagellates. Dinoflagellates are also known to be present in all studied areas, but again the species composition of specifically naked dinoflagellates is poorly known. The Baltic Sea appears to be the only non-polar sea region with cyanobacteria incorporated into its sea ice biota.

Ciliates of various sizes have been encountered in sea ice at least in the Japanese lagoons and the Baltic Sea (Sime-Ngando et al., 1999; Kaartokallio 2004; Kaartokallio et al., 2007). They are mostly yet overlooked probably due to their small size and naked cells as tintinnid ciliates are rarely found from sea ice. However, at least several genera of oligotrichs ciliates are found in sea ice. The symbiotic ciliate, *Mesodinium rubrum*, is present at least in the Baltic Sea and Japanese lagoons.

Whereas the diverse metazoan assemblages of oceanic sea ice are relatively well described (Chapter 10), they are poorly known in marginal sea ice. Only rotifers and copepods have been described in Baltic Sea sea ice (Norrman & Andersson, 1994; Meiners et al., 2002; Werner & Auel, 2004), and a rich copepod community is associated to sea ice in Saroma-ko Lagoon (Fortier & Fortier, 1997). The metazoan communities associated with sea ice in the Hudson Bay are more diverse, including nematods and harpacticoid copepods (Grainger, 1988; Tremblay et al., 1989). However, systematic studies in sea ice living or closely associated metazoa are scarce, but specifically the ice underside appears to be an important feeding ground in winter for metazoa. In the Baltic Sea, the dominant species of calanoid copepods, such as *Acartia bifilosa*, have been shown to reproduce, grow and develop under-ice cover (Werner & Auel, 2004).

14.11 Habitat change due to climate change

Non-polar sea ice cover is, alike to Polar sea ice, an important habitat for microorganisms and marine mammals as the polar bear (Hudson Bay) and seals (Hudson Bay, the Baltic, Caspian and White Seas). Stirling et al. (1999) reported that long-term trends in the population ecology of polar bears (*Ursus maritimus*) in the western Hudson Bay region appear to be related to changes in ice conditions in the region (earlier break-up). Their reliance on ice makes ringed and bearded seals, polar bears and walruses vulnerable to changes in the ice

environment of Hudson Bay. In the Baltic Sea, the Baltic grey seal (*Halichoerus grypus*) and Baltic ringed seal (*Phoca hispida botnica*) use sea ice as their primary breeding habitat. The grey seal can also breed successfully on land but ringed seal is dependent on ice for breeding (Meier et al., 2004). Anticipated climate change–induced diminishing of Baltic Sea sea ice cover may lead to survival of Baltic ringed seal in the Bothnian Bay only and thus poses a major threat to all southern populations of Baltic ringed seal (Meier et al., 2004). *Phoca caspica*, the endemic seal of the Caspian Sea breeds on the sea ice in the Northern Caspian, is also vulnerable to changes in the ice cover, although also other natural and anthropogenic factors have strongly affected the population size during the 20th century (see Härkönen et al., 2008). As in the Polar Seas, sympagic species in non-polar seas are also vulnerable to changing ice conditions. However, it is the local changes in the climate that drive any changes, and therefore one coherent picture cannot be presented here, as to what will happen in the future. Regional assessments have to be made in order to understand the potential threats.

Acknowledgements

References

Aibalutov, A.I. & Grudinova, L.Y. (1991) Ice rafting of sedimentary material in the Azov Sea. *Water Resources (Vodnye Resursy)*, **17**, 179–187.

Aladin, N.V. & Potts, W.T.W. (1992) Changes in the Aral Sea ecosystems during the period 1960–1990. *Hydrobiologia*, **237**, 67–79.

Aladin, N.V., Plotnikov, I.S. & Letolle, R. (2004) Hydrobiology of the Aral Sea. In: *Dying and Dead Seas: Climatic Versus Anthropic Causes: Proceedings of th*e NATO Advanced Research Workshop (Eds. J.C.J. Nihoul, P.O. Zavialov & P.P. Micklin), pp. 125–157. Nato Science Series: 4. Earth and Environmental Sciences, 36. Kluwer Academic Publisher, Dordrecht.

Aladin, N.V., Crétaux, J.-F., Plotnikov, I.S. et al. (2005) Modern hydro-biological state of the Small Aral sea. *Environmetrics*, **16**, 375–392.

Asami, H. & Imada, K. (2001) Ice algae and phytoplankton in the late ice-covered season in Notoro Ko lagoon, Hokkaido. *Polar Bioscience*, **14**, 24–32.

Bai S., Liu Q.-Z., Wu H.-D. & Wang Y-L. (2001) Relation of ice conditions to climate change in the Bohai Sea of China. *Acta Oceanologica Sinica*, **20**, 331–342.

Barker, A. & Croasdale, K. (2004) Numerical modelling of ice interaction with rubble mound berms in the Caspian Sea. In: *Proceedings of the 17th IAHR International Symposium on Ice*, Saint Petersburg, Russia, 21–25 June 2004, **2**, 257–264.

Björk, G., Nohr, C., Gustafsson, B.G. & Lindberg, A.E.B (2008) Ice dynamics in the Bothnian Bay inferred from ADCP measurements. *Tellus*, **60A**, 178–188.

Boomer, I., Aladin, N., Plotnikov, I. & Whatley, R. (2000) The palaeolimnology of the Aral Sea: a review. *Quaternary Science Reviews*, **19**, 1259–1278.

Borovskaya, R.V. & Lomakin, P.D. (2008) Specific features of ice conditions in the Sea of Azov and the Kerch Strait in the winter season of 2005/06. *Russian Meteorology and Hydrology*, **33**, 453–457.

Bortnik, V.N. & Chistyayeva, S.P. (Eds.) (1990) *Gidrometeorologiya I Gidrohimiya Morey (Hydrometeorology and Hydrochemistry of Seas) Aral Sea*, Vol. VII. Gidrometeoizdat, Leningrad.

Brierley, A.S. and Thomas, D.N., (2002) Ecology of Southern Ocean pack ice. *Advances in Marine Biology,* **43**, 171–276.

CIS (2002) *Sea Ice Climatic Atlas. Northern Canadian Waters 1971–2000*. Canadian Ice Service, Ottawa, ON, Canada.

Comfort, G., Metge, M., Liddiard, A. & Vincent, P. (2002) Ice environmental data collection for the north Caspian Sea. In: *Proceedings of the 16th IAHR International Symposium on Ice* (Eds. V. Squire and P. Langhorne), Dunedin, New Zealand, 2–6 December, 2002, **3**, 223–230.

Cota, G.F., Legendre, L., Gosselin, M. & Ingram, R.G. (1991) Ecology of bottom ice algae. I. Environmental controls and variability. *Journal of Marine Systems*, **2**, 257–277.

Déry, S.J., Stieglitz, M., McKenna, E.C. & Wood, E.F. (2005) Characteristics and trends of river discharge into Hudson, James, and Ungava Bays, 1964–2000. *Journal of Climate*, **18**, 2540–2557.

De Sève, M.A. & Dunbar, M.J. (1990) Structure and composition of ice algal assemblages from the Gulf of St. Lawrence, Magdalen Islands area. *Canadian Journal of Fisheries and Aquatic Science*, **47**, 780–788.

Ehn, J., Granskog, M.A., Papakyriakou, T., Galley, R. & Barber, D.G. (2006) Surface albedo observations of Hudson Bay land-fast sea ice during melt onset. *Annals of Glaciology*, **44**, 23–29.

Falkingham, J., Chagnon, R. & McCourt, S. (2002) Trends in sea ice in the Canadian Arctic. In: *Proceedings of the 16th IAHR International Symposium on Ice (*Eds. V. Squire and P. Langhorne), Dunedin, New Zealand, 2–6 December, 2002, **1**, 352–359.

Filatov, N., Pozdnyakov, D., Johannessen, O.M., Pettersson, L.H. & Bobylev, L.P. (Eds.) (2005) *White Sea – Its Marine Environment and Ecosystem Dynamics Influenced by Global Change*. Springer Verlag, Berlin.

Fortier, M. & Fortier, L. (1997) Transport of marine fish larvae to Saroma-ko Lagoon (Hokkaido, Japan) in relation to the availability of zooplankton prey under the winter ice cover. *Journal of Marine Systems*, **11**, 221–234.

Freeman, N.G., Roff, J.C. & Pett, R.J. (1982) Physical, chemical, and biological features of river plumes under an ice cover in James and Hudson Bays. *Le Naturaliste Canadien,* **109**, 745–764.

Frenette, J.-J., Thibeault, P., Lapierre, J.-F. & Hamilton, P.B. (2008) Presence of algae in freshwater ice cover of fluvial Lac Saint-Pierre (St. Lawrence River, Canada). *Journal of Phycology*, **44**, 284–291.

Fukamachi, Y., Mizuta, G. Ohshima, K.I., Toyota, T., Kimura, N. & Wakarsuchi, M. (2006) Sea ice thickness in the southwestern Sea of Okhotsk revealed by a moored ice-profiling sonar. *Journal of Geophysical* Research, **111**, C09018, 10.1029/2005JC003327.

Fukutomi, T. (1950) Study of sea ice (The 4th Report). A theoretical study on the formation of sea ice in the central part of the Okhotsk Sea (in Japanese with English summary). *Low Temperature Science, Series A*, **3**, 143–157.

Gagnon, A.S. & Gough, W.A. (2005) Climate change scenarios for the Hudson Bay region: an inter-model comparison. *Climatic Change*, **69**, 269–297.

van Gelder, P.H.A.J.M., Molenaar, W. F., Bolgov, M.V. & Krasnozhon, G.F. (2004) Statistical analysis of icing event occurrences in the northern Caspian Sea based on meteorological satellite data. In: *Proceedings of OMAE04 23rd International Conference on Offshore Mechanics and Arctic Engineering,* paper number: OMAE2004-51560, June 20–25, 2004, Vancouver, British Columbia, Canada.

Gong, D.-Y., Seong-Joong, K. & Ho, C.-H. (2007) Arctic Oscillation and ice severity in the Bohai Sea, East Asia. *International Journal of Climatology*, **27**, 1287–1302.

Gosselin, M., Legendre, L., Therriault, J.L., Demers, S. & Rochet, M. (1986) Physical control of the horizontal patchiness of sea-ice microalgae. *Marine Ecology Progress Series*, **29**, 289–298.

Gough, W.A. & Leung, A. (2002) Nature and fate of Hudson Bay permafrost. *Regional Environmental Change*, **2**, 177–184.

Gough, W.A. & Wolfe, E. (2001) Climate change scenarios for Hudson Bay, Canada from general circulation models. *Arctic,* **54**, 142–148.

Gough, W.A., Cornwell, A.R. & Tsuji, L.T.S. (2004) Trends in seasonal sea ice duration in southwestern Hudson Bay. *Arctic*, **57**, 299–305.

Glantz, M. (Ed.) (1998) *Creeping Environmental Problems and Sustainable Development in the Aral Sea Basin*. Cambridge University Press, Cambridge.

Grainger, E.H. (1988) Influence of a River Plume on the Sea ice Meiofauna in South-eastern Hudson Bay. *Estuar*ine *Coastal and Shelf Science*, **27**, 131–141.

Granskog, M.A., Kaartokallio, H. & Shirasawa, K. (2003a). Nutrient status of Baltic Sea ice: evidence for control by snow-ice formation, ice permeability, and ice algae. *Journal of Geophysical Research,* **108** (C8), 3253, 10.1029/2002JC001386.

Granskog, M.A., Leppäranta, M., Kawamura, T., Ehn, J. & Shirasawa, S. (2004) Seasonal development of the properties and composition of landfast sea ice in the Gulf of Finland, the Baltic Sea. *Journal of Geophysical Research*, **109**, C02020, 10.1029/2003JC001874.

Granskog, M.A., Kaartokallio, H., Kuosa, H., Thomas, D.N., Ehn, J. & Sonninen, E. (2005a) Scales of horizontal patchiness in chlorophyll *a*, chemical and physical properties of landfast sea ice in the Gulf of Finland (Baltic Sea). *Polar Biology*, **28**, 276–283.

Granskog, M.A., Kaartokallio, H., Thomas, D.N. & Kuosa, H. (2005b). The influence of freshwater inflow on the inorganic nutrient and dissolved organic matter within coastal sea ice and underlying waters in the Gulf of Finland (Baltic Sea). *Estuarine and Coastal Shelf Science*, **65**, 109–122.

Granskog, M., Kaartokallio, H., Kuosa, H., Thomas, D.N. & Vainio, J. (2006a) Sea ice in the Baltic Sea – a review. *Estuarine Coastal and Shelf Science*, **70**, 145–150.

Granskog, M.A., Vihma, T., Pirazzini, R. & Cheng, B. (2006b) Superimposed ice formation and surface energy fluxes on sea ice during the spring melt-freeze period in the Baltic Sea. *Journal of Glaciology*, **62**, 119–127.

Grossmann, S. & Gleitz, M. (1993). Microbial responses to experimental sea ice formation: implications for the establishment of Antarctic sea ice communities. *Journal of Experimental Marine Biology and Ecology*, **173**, 273–289.

Günther, S. & Dieckmann, G.S (1999). Seasonal development of algal biomass in snow-covered fast ice and the underlying platelet layer in the Weddell Sea, Antarctica. *Antarctic Science*, **11**, 305–315.

Haapala J. & Leppäranta M. (1997) The Baltic Sea ice season in changing climate. *Boreal Environment Research*, **2**, 93–108.

Haas, C. (2004) Airborne EM sea ice thickness profiling over brackish Baltic sea water. *Proceedings of the 17th International IAHR Symposium on Ice*, June 21–25, 2004, St. Petersburg, Russia, All-Russian Research Institute of Hydraulic Engineering (VNIIG), Saint Petersburg, Russia, **2**, 12–17.

Haecky, P. & Andersson, A. (1999). Primary and bacterial production in sea ice in the northern Baltic Sea. *Aquatic Microbial Ecology*, **20**, 107–118.

Haecky, P., Jonsson, S. & Andersson, A. (1998). Influence of sea ice on the composition of the spring phytoplankton bloom in the northern Baltic Sea. *Polar Biology*, **20**, 1–8.

Härkönen, T., Jüssi, M., Baimukanov, M. et al. (2008) Pup production and breeding distribution of the Caspian Seal (*Phoca caspica*) in relation to human impacts. *Ambio*, **37** (5), 356–361.

Hill, B.T., Ruffman, A. & Drinkwater, K. (2002) Historical record of the incidence of sea ice on the Scotian shelf and the Gulf of St. Lawrence. In: *Proceedings of the 16th IAHR International Symposium on Ice* (Eds. V. Squire and P. Langhorne), Dunedin, New Zealand, 2–6 December, 2002, 16–24.

Honda, M., Yamazaki, K., Nakamura, H. & Takeuchi, K. (1999) Dynamic and thermodynamic characteristics of atmospheric response to anomalous sea ice extent in the Sea of Okhotsk. *Journal of Climate*, **12**, 3347–3358.

Howland, R.J.M., Pantiulin, A.N., Millward, G.E. & Prego, R. (1999) The hydrography of the Chupa estuary, White Sea, Russia. *Estuarine, Coastal and Shelf Science*, **48**, 1–12.

Ikävalko, J. (1998) Further observations on flagellates within sea ice in northern Bothnian Bay, the Baltic Sea. *Polar Biology,* **19,** 323–329.

Ikävalko, J. & Thomsen, H.A. (1996) Scale-covered and loricate flagellates (Chrysophyceae and Synurophyceae) from Baltic Sea ice. *Nova Hedwigia Beihefte,* **114,** 147–160.

Ikävalko, J. & Thomsen, H.A. (1997) The Baltic Sea ice biota (March 1994): a study of the protistan community. *European Journal of Protistology,* **33,** 229–243.

Ikeya, T., Kikuchi-Kawanobe, K. & Kudoh, S. (2001) Floristic examination of diatom assemblage in the dim light-environment of water column and sea ice, Saroma Ko lagoon, Hokkaido, Japan. *Polar Bioscience,* **14,** 33–44.

Ingram, R.G. (1981) Characteristics of the Great Whale River plume. *Journal of Geophysical Research,* **86,** 2017–2023.

Ingram, R.G. & Larouche, P. (1987) Variability of an under-ice river plume in Hudson Bay. *Journal of Geophysical Research,* **92,** 9541–9547.

Ingram, R.G., Wang, J, Lin, C., Legendre, L. & Fortier, L. (1996) Impact of freshwater on a subarctic coastal ecosystem under seasonal sea ice (southeastern Hudson Bay, Canada). I. Interannual variability and predicted global warming influence on river plume dynamics and sea ice. *Journal of Marine Systems,* **7,** 221–231.

IPCC (Intergovernmental Panel on Climate Change) (2001) *Climate Change 2001: The Scientific Basis – Contribution of Working Group 1 to the Third Assessment Report of IPCC.* UNEP and WMO. Cambridge University Press, Cambridge.

Jevrejeva, S. (2001) Severity of winter seasons in the northern Baltic Sea during 1529–1990. *Climate Research,* **17,** 55–62.

Jevrejeva, S. & Moore, J.C. (2001) Singular spectrum analysis of Baltic Sea ice conditions and large-scale atmospheric patterns since 1708. *Geophysical Research Letters,* **28,** 4503–4506.

Jevrejeva, S., Drabkin, V.V., Kostjukov, J. et al. (2004) Baltic Sea ice seasons in the twentieth century. *Climate Research,* **25,** 217–227.

Kaartokallio, H. (2004) Food web components, and physical and chemical properties of Baltic Sea ice. *Marine Ecology Progress Series,* **273,** 49–63.

Kaartokallio, H., Kuosa, H., Thomas, D.N., Granskog, M.A. & Kivi, K. (2007) Changes in biomass, composition and activity of organism assemblages along a salinity gradient in sea ice subjected to river discharge. *Polar Biology,* **30,** 186–197.

Kalliosaari, S. & Seinä, A. (1987) Ice winters 1981–1985 along the Finnish coast. *Finnish Marine Research,* **254,** 5–63.

Kankaanpää, P. (1997) Distribution, morphology and structure of sea ice pressure ridges in the Baltic Sea. *Fennia,* **175** (2), 139–240.

Kharitonov, V.V. (2008) Internal structure of ice ridges and stamukhas based on thermal drilling data. *Cold Regions Science and Technology,* **52,** 302–325.

Kimura, N. & Wakatsuchi, M. (2004) Increase and decrease of sea ice area in the Sea of Okhotsk: ice production in coastal polynyas and dynamic thickening in convergence zones. *Journal of Geophysical Research,* **109,** C09S03, 10.1029/2003JC001901.

Kosarev, A.N., Kostianoy, A.G. & Shiganova, T. A. (2008) The Sea of Azov. In: *Handbook of Environmental Chemistry, Vol. 5, Part Q* (Eds. A.G. Kostianoy and A.N. Kosarev), pp. 63–89. Springer-Verlag, Berlin, Heidelberg.

Kouraev, A.V., Papa, F., Buharizin, P.I, Cazenave, A., Cretaux, J.-F., Dozortseva, J. & Remey, F. (2003) Ice cover variability in the Caspian and Aral Seas from active and passive satellite microwave data. *Polar Research,* **22,** 43–50.

Kouraev, A.V., Papa, F., Mognard, N.M. et al. (2004) Sea ice cover in the Caspian and Aral Seas from historical and satellite data. *Journal of Marine Systems,* **47,** 89–100.

Kouraev A.V., Kostianoy A.G. & Lebedev, S.A. (2008) Recent changes of sea level and ice cover in the Aral Sea derived from satellite data (1992–2006). *Journal of Marine Systems,* 10.1016/j.jmarsys.2008.03.016.

Kouraev A.V., Shimaraev, M.N., Buharizin, P.I. et al. (2008) Ice and snow cover of continental water bodies from simultaneous radar altimetry and radiometry observations. *Surveys in Geophysics*, doi: 10.1007/s10712-008-9042-2.

Krell, A., Ummenhofer, C., Kattner, G. et al. (2003) The biology and chemistry of land fast-ice in the White Sea, Russia – a comparison of winter and spring conditions. *Polar Biology*, **26**, 707–719.

Krembs, C., Gradinger, R. & Spindler, M. (2000). Implications of brine channel geometry and surface area for the interaction of sympagic organisms in Arctic sea ice. *Journal of Experimental Marine Biology and Ecology*, **243**, 55–80.

Kuosa, H. & Kaartokallio, H. (2006). Experimental evidence on nutrient and substrate limitation of Baltic sea ice algae and bacteria. *Hydrobiologia*, **554**, 1–10.

Kuparinen, J., Kuosa, H., Andersson, A. et al. (2007) Role of sea ice biota in nutrient and organic material cycles in the northern Baltic Sea. *Ambio*, **36**, 149–154.

Kuzyk, Z.A., Macdonald, R.W., Granskog, M.A. et al. (2008) Sea ice, hydrological, and biological processes in the Churchill River estuary region, Hudson Bay. *Estuarine, Coastal and Shelf Science*, **77**, 369–384.

Larouche, P. & Galbraith, P.S. (1989) Factors affecting fast-ice consolidation in southeastern Hudson Bay, Canada. *Atmosphere-Ocean*, **27**, 367–375.

Larsen, J., Kuosa, H., Ikävalko, J., Kivi, K. & Hällfors, S. (1995) A redescription of *Scrippsiella hangoei* (Schiller) comb. nov. a 'red tide' dinoflagellate from the northern Baltic. *Phycologia*, **34**, 135–144.

Launiainen, J. & Cheng, B. (1998) Modelling of ice thermodynamics in natural water bodies. *Cold Regions Science and Technology*, **27**, 153–178.

Laurion, I., Demers, S. & Vézina, A.F. (1995) The microbial food web associated with the ice algal assemblage: biomass and bacterivory of nanoflagellate protozoans in Resolute Passage (High Canadian Arctic). *Marine Ecology Progress Series*, **120**, 77–87.

Legendre, L., Ingram, R.G. & Poulin, M. (1981) Physical control of phytoplankton production under sea ice (Manitounuk Sound, Hudson Bay). *Canadian Journal of Fisheries and Aquatic Science*, **38**, 1385–1392.

Legendre, L., Robineau, B., Gosselin, M. et al. (1996) Impact of freshwater on a subarctic coastal ecosystem under seasonal sea ice (southeastern Hudson Bay, Canada) II. Production and export of microalgae. *Journal of Marine Systems*, **7**, 233–250.

Leppäranta, M. (2004) *The Drift of Sea Ice*. Springer-Verlag, Berlin.

Leppäranta, M., Palosuo, E., Kuusisto, E. & Makkonen, L. (2001) Geophysics of snow and ice in Finland during the 1900s. *Geophysica*, **37**, 261–286.

Lewis, J.E., Leppäranta, M. & Granberg, H.B. (1993) Statistical properties of sea ice surface topography in the Baltic Sea. *Tellus*, **45A**, 127–142.

Li, Z. & Wang, Y. (2001) Statistical ice conditions in the Bohai Sea. In: *20th International Conference on Offshore Mechanics and Arctic Engineering*, June 3–8, 2001, Rio de Janeiro, Brazil.

Li, Z., Kang, J. & Pu, Y. (2003) Characteristics of the Bohai Sea and Arctic sea ice fabrics and crystals. *Acta Oceanologica Sinica*, **25**, 48–53.

Lizotte, M.P. (2003). The microbiology of sea ice. In: *Sea Ice: An Introduction to its Physics, Chemistry, Biology and Geology* (Eds. D.N. Thomas & G.S. Dieckmann), pp. 184–210. Blackwell Science, Oxford, UK.

Marchant, H.J. & Scott, F.J. (1993). Uptake of sub-micrometre particles and dissolved organic material by Antarctic choanoflagellates. *Marine Ecology Progress Series*, **92**, 59–64.

Markham, W.E. (1986) The ice cover. In: *Canadian Inland Seas*, (Ed. I.P. Martini), pp. 101–116. Elsevier Oceanography Series 44, Elsevier, New York.

Martini, I.P. (Ed.) (1986) *Canadian Inland Seas*. Elsevier Science Publishers, Elsevier Oceanography Series 44, Amsterdam.

Matishov, G., Matishov, D., Gargopa, G. et al. (2006) Climatic Atlas of the Azov Sea 2006. In: *NOAA Atlas NESDIS 59* (Eds. G. Matishov & S. Levitus). U.S. Government Printing Office, Washington D.C.

Matishov, G.G., Stepanyan, O.V., Povazhnyi, V.V., Kovaleva, G.V. & Kreneva, K.V. (2007) Functioning of the ecosystem in the Sea of Azov in winter. *Doklady Earth Sciences*, **413**, 297–299.

McMinn A., Hattori H., Hirawake T. & Iwamoto A. (2008) Preliminary investigation of Okhotsk Sea ice algae; taxonomic composition and photosynthetic activity. *Polar Biology*, **31**, 10.1007/s00300-008-0433-0.

Meier, H.E.M., Döscher, R. & Halkka, A. (2004) Simulated distributions of Baltic sea-ice in warming climate and consequences for the winter habitat of the Baltic ringed seal. *Ambio*, **33**, 249–256.

Meiners, K., Fehling, J., Granskog, M.A. & Spindler, M. (2002) Abundance, biomass and composition in Baltic sea ice and underlying water (March 2000). *Polar Biology*, **25**, 761–770.

Melnikov, I.A., Dikarev, S.N., Egorov, V.G., Kolosova, E.G. & Zhitina, L.S. (2005) Structure of the coastal ice ecosystem in the zone of sea-river interactions. *Oceanology*, **45**, 511–519.

Michel, C., Legendre, L., Therriault, J.-C., Demers, S. & Vandevelde, T. (1993) Springtime coupling between ice algal and phytoplankton assemblages in southeastern Hudson Bay, Canadian Arctic. *Polar Biology*, **13**, 441–449.

Niskanen, T., Vainio, J., Eriksson, P. & Heiler, I. (2008) Maximum ice extent of the Baltic Sea ice recalculated for the period 1971–2008, Sixth Workshop on Baltic Sea Ice Climate, August 25–28, 2008, Lammi Biological Station, Lammi, Finland.

Norrman, B. & Andersson, A. (1994). Development of ice biota in a temperate sea area (Gulf of Bothnia). *Polar Biology*, **14**, 531–537.

Ogi, M. & Tachibana, Y. (2006) Influence of the annual Arctic Oscillation on the negative correlation between Okhotsk Sea ice and Amur River discharge. *Geophysical Research Letters*, **33**, L08709, 10.1029/2006GL025838.

Ogi, M., Tachibana, Y., Nishio, F. & Danchenkov, M.A. (2001) Does the fresh water supply from Amur River flowing into the Sea of Okhotsk affect sea ice formation? *Journal of the Meteorological Society of Japan*, **79**, 123–129.

Ohshima, K.I., Nihashi, S., Hashiya, E. & Watanabe, T. (2006) Interannual variability of sea ice area in the Sea of Okhotsk: importance of surface heat flux in fall. *Journal of the Meteorological Society of Japan*, **84**, 907–919.

Omstedt, A. & Chen, D. (2001) Influence of atmospheric circulation on the maximum ice extent in the Baltic Sea. *Journal of Geophysical Res*earch, **106** (C3), 4493–4500.

Omstedt, A. & Hansson, D. (2006) The Baltic Sea ocean climate system memory and response to changes in the water and heat balance components. *Continental Shelf Research*, **26**, 236–251.

Palosuo, E. (1963) The Gulf of Bothnia in winter. II. Freezing and ice forms. *Merentutkimuslaitoksen julkaisu / Havsforskningsinstitutets skrift*, **209**, 64pp.

Parkinson, C.L. (1990) The impact of the Siberian high and Aleutian low on the sea ice cover of the Sea of Okhotsk. *Annals of Glaciology*, **14**, 226–229.

Parkinson, C.L. & Cavalieri, D.J. (2002) A 21 year record of Arctic sea ice extents and their regional, seasonal and monthly variability and trends. *Annals of Glaciology,* **34**, 441-446.

Parkinson, C.L. & Cavalieri, D.J. (2008) Arctic sea ice variability and trends, 1979–2006. *Journal of Geophysical Research*, **113**, C07003, 10.1029/2007JC004558.

Parkinson, C.L., Cavalieri, D.J., Gloersen, P., Zwally, H.J. & Comiso, J.C. (1999) Arctic sea ice extents, areas and trends, 1978–1996. *Journal of Geophysical Res*earch, **104** C, 20837–20856.

Polomoshnov, A. (1992) Seasonal variability of sea ice physicomechanical properties. In: *Proceedings of the 7th International Symposium on Okhotsk Sea and Sea Ice*. The Okhotsk Sea and Cold Ocean Research Association, pp. 336–339. Mombetsu, Japan.

Poulin, M. & Cardinal, A. (1982a) Sea ice diatoms from Manitounuk Sound, southeastern Hudson Bay (Quebec, Canada). I. Family Naviculaceae. *Canadian Journal of Botany*, **60**, 1263–1278.

Poulin, M. & Cardinal, A. (1982b) Sea ice diatoms from Manitounuk Sound, southeastern Hudson Bay (Quebec, Canada). II. Naviculaceae, genus Navicula. *Canadian Journal of Botany,* **60**, 2825–2845.

Poulin, M. & Cardinal, A. (1983) Sea ice diatoms from Manitounuk Sound, southeastern Hudson Bay (Quebec, Canada). III. Cymbellaceae, Entomoneidaceae, Gomphonemataceae, and Nitzschiaceae. *Canadian Journal of Botany*, **61**, 107–118.

Pozdnyakov, D.V., Pettersson, L.H., Johannessen, O.M. et al. (2005) Satellite oceanography: new results. In: *White Sea Its Marine Environment and Ecosystem Dynamics Influenced by Global Change* (Eds. A.V. Filatov et al.), pp. 179–239. Springer Verlag, Berlin.

Prinsenberg, S.J. (1984) Freshwater contents and heat budgets of James Bay and Hudson Bay. *Continental Shelf Research*, **3**, 191–200.

Prinsenberg, S.J. (1986) Salinity and temperature distribution of Hudson Bay and James Bay. In: *Canadian Inland Seas*, (Ed. I.P. Martini), pp. 163–186. Elsevier Oceanography Series 44, Elsevier, New York.

Prinsenberg, S.J. (1988) Ice-cover and ice-ridge contributions to the freshwater contents of Hudson Bay and Foxe Basin. *Arctic*, **41**, 6–11.

Prinsenberg, S.J., van der Baaren, A. & Peterson, I.K. (2006) Ice ridging and ice drift in southern Gulf of St. Lawrence, Canada, during winter storms. *Annals of Glaciology*, **44**, 411–417.

Ratkova, T. & Wassmann, P. (2005) Sea ice algae in the White and Barents seas: composition and origin. *Polar Research*, **24**, 95–110.

Ratkova, T.N., Sazhin, A. & Kosobokova, K. (2004) Unicellular inhabitants of the White Sea underice pelagic zone during the early spring period. *Oceanology*, **44**, 240–246.

Rodionov, S.N. (1994) *Global and Regional Climate Interactions: The Caspian Sea Experience*. Kluwer Academic Publishers, Dordrecht/Boston/London, 241pp.

Robineau B., Legendre, L., Kishino, M. & Kudoh, S. (1997) Horizontal heterogeneity of microalgal biomass in the first-year sea ice of Saroma-ko Lagoon (Hokkaido, Japan). *Journal of Marine Systems*, **11**, 81–91.

Saucier, F.J. & Dionne, J. (1998) A 3D coupled ice-ocean model applied to Hudson Bay, Canada: the seasonal cycle and time-dependent climate response to atmospheric forcing and runoff. *Journal of Geophysical Research*, **103**, 27689–27705.

Saucier, F.J., Senneville, S., Prinsenberg, S. et al. (2004) Modelling the sea ice-ocean seasonal cycle in Hudson Bay, Foxe Basin and Hudson Strait, Canada. *Climate Dynamics*, **23**, 303–326.

Sazhin A.F. (2004) Phototrophic and heterotrophic nano- and microorganisms of sea ice and sub-ice water in Guba Chupa (Chupa Inlet), White Sea, in April 2002. *Polar Research*, **23**, 11–18.

Sazhin, A.F., Ratkova, T.N. & Kosobokova, K.N. (2004) Unicellular inhabitants of the White Sea underice pelagic zone during the early spring period. *Oceanology*, **44**, 82–89.

Schmelzer, N., Seinä, A., Lundqvist, J-E. & Sztobryn, M. (2008) Ice. In: *State and Evolution of the Baltic Sea, 1952–2005* (Eds. R. Feistel, G. Nausch & N. Wasmund), pp. 199–240. Wiley, New York.

Schwerdtfeger, P. (1962) Energy exchange through an annual sea ice cover, PhD Thesis, McGill University, Montreal.

Seinä, A. & Palosuo, E. (1996) The classification of the maximum annual extent of ice cover in the Baltic Sea 1720–1995. *Meri – Report Series of the Finnish Institute of Marine Research*, **27**, 79–91.

Shcherbina, A.Y. Talley, L.D. & Rudnick, D.L. (2003) Direct observations of North Pacific ventilation: brine rejection in the Okhotsk Sea. *Science*, **302**, 1952–1955.

Shevchenko, G.V., Rabinovich, A.B. & Thomson, R.E. (2004) Sea ice drift on the Northeastern Shelf of Sakhalin Island. *Journal of Physical Oceanography*, **34**, 2470–2491.

Shimoda, H., Uto, S., Tamura, K. & Narita, S. (1996). Sea ice situations in the Sea of Okhotsk off the coast of Hokkaido by on board ship observations (in Japanese with English summary). In: *Proceedings of the 11th International Symposium on Okhotsk Sea and Sea Ice. The Okhotsk Sea and Cold Ocean Research Association*, pp. 156–160. Mombetsu, Japan.

Shirasawa, K. (1998) Sea ice in the Okhotsk Sea – Effects by global warming? (in Japanese). In: *Hydrology and Water Resources in Snow-Covered Regions* (Ed. by the Japan Society of Hydrology and Water Resources. Editorial Board. Shinzansha Scitech, Tokyo, pp. 191–204.

Shirasawa, K., Leppäranta M., Saloranta, T., Kawamura, T., Polomoshnov, A. & Surkov, G. (2005) The thickness of coastal fast ice in the Sea of Okhotsk. *Cold Regions Science and Technology*, **42**, 25–40.

Small, E.E., Sloan, L.C. & Nychka, D. (200) Changes in surface air temperature caused by desiccation of the Aral Sea. *Journal of Climate*, **14**, 284–299.

Sime-Ngando, T., Gosselin, M., Juniper, K.S. & Levasseur, M. (1997). Changes in phagotrophic micro-protists (20–200 μm) during the spring algal bloom, Canadian Arctic Archipelago. *Journal of Marine Systems*, **11**, 163–172.

Sime-Ngando, T., Demers, S. & Juniper, S.K. (1999) Protozoan bacterivory in the ice and the water column of a cold temperate lagoon. *Microbial Ecology*, **37**, 95–106.

Spilling, K. (2007) Dense sub-ice bloom of dinoflagellates in the Baltic Sea, potentially limited by high pH. *Journal of Plankton Research*, **29**, 895–901.

Steffens, M., Granskog, M.A., Kaartokallio, H. et al. (2006) Spatial variation of biogeochemical properties of landfast sea ice in the Gulf of Bothnia (Baltic Sea). *Annals of Glaciology,* **44**, 80–87.

Stewart, D.B. & Lockhart, W.L. (2005) An overview of the Hudson Bay marine ecosystem. *Canadian Technical Reports on Fisheries and Aquatic Sciences*, **2586**, 1–487.

Stirling, I., Lunn, N.J. & Iacozza, J. (1999) Long-term trends in the population ecology of polar bears in western Hudson Bay in relation to climatic change. *Arctic*, **52**, 294–306.

Stoecker, D., Buck, K.R. & Putt, M. (1993) Changes in the sea-ice brine community during the spring-summer transition, McMurdo Sound, Antarctica. II. Phagotrophic protists. *Marine Ecology Progress Series*, **95**, 103–113.

Sündermann, J. & Feng, S. (2004) Analysis and modelling of the Bohai sea ecosystem – a joint German-Chinese study. *Journal of Marine Systems*, **44**, 127–140.

Takahashi E. (1981) Floristic study of ice algae in the sea ice of a lagoon, Lake Saroma, Hokkaido, Japan. *Memoirs of National Institute of Polar Research Series E Biology and Medical Science*, **34**, 49–56.

Talley, L.D. & Nagata, Y. (1995) The Okhotsk Sea and Oyashio region (Report of Working Group 1). *PICES Scientific Report*, **2**, 1–227.

Terziev, F.S., Kosarev, A.N. & Kerimov, A.A. (Eds.) (1992) *Gidrometeorologiya I Gidrohimiya Morey (Hydrometeorology and Hydrochemistry of Seas. Vol. VI) Caspian Sea, Hydrometeorological Conditions*, Vol. 1. Gidrometeoizdat, St. Petersburg.

Thomas, D.N. and Dieckmann, G.S. (2002) Biogeochemistry of Antarctic sea ice. *Oceanography and Marine Biology: An Annual Review*, **40**, 143–169.

Tinz, B. (1995) On the relation between annual maximum extent of ice cover in the Baltic Sea and sea level pressure as well as air temperature field. *Geophysica*, **32**, 319–341.

Toyota, T. & Wakatsuchi, M. (2001) Characteristics of the surface heat budget during the ice growth season in the southern Sea of Okhotsk. *Annals of Glaciology*, **33**, 230–236.

Toyota, T., Kawamura, T. & Wakatsuchi, M. (2000) Heat budget in the ice cover of the southern Okhotsk Sea derived from in-situ observations. *Journal of the Meteorological Society of Japan*, **78**, 585–596.

Toyota, T., Kawamura, T., Ohshima, K. I., Shimoda, H. & Wakatsuchi, M. (2004) Thickness distribution, texture and stratigraphy, and a simple probabilistic model for dynamical thickening of sea ice in the southern Sea of Okhotsk. *Journal of Geophysical Research*, **109**, C06001, 10.1029/2003JC002090.

Toyota, T., Takatsuji, T., Tateyama, K., Naoki, K. & Ohshima, K.I. (2007) Properties of sea ice and overlying snow in the Southern Sea of Okhotsk. *Journal of Oceanography*, **63**, 393–411.

Tremblay, C., Runge, J.A. & Legendre, L. (1989) Grazing and sedimentation of ice algae during and immediately after bloom at the ice-water interface. *Marine Ecology Progress Series*, **56**, 291–300.

Tsytsarin, A.G., Skorokhod, A. & Lisistyna, L.V. (1998) Vertical distribution of the main salt-forming components in Aral and Caspian Sea ice. *Water Resources*, **25**, 617–622.

Ukita, J., Kawamura, T., Tanaka, N., Toyota, T. & Wakatsuchi, M. (2000) Physical and stable isotopic properties and growth processes of sea ice collected in the southern Sea of Okhotsk. *Journal of Geophysical Research*, **105**, 22083–22093.

Uto, S., Toyota, T., Shimoda, H., Tateyama, K. & Shirasawa, K. (2006) Ship-borne electromagnetic induction soundings of sea ice thickness in the south Okhotsk Sea. *Annals of Glaciology*, **44**, 253–260.

Vezina, A.F., Demers, S., Laurion, I., Sime-Ngando, T., Juniper, K.S. & Devine, L. (1997). Carbon flows through the microbial food web of the first-year ice in Resolute Passage (Canadian High Arctic). *Journal of Marine Systems Systems*, **11**, 173–189.

Watanabe, K., Satoh, H., Yamaguchi, Y. et al. (1991) Ice algal assemblages from lagoons Saroma-Ko, Notoro Ko and Akkeshi-Ko in Hokkaido. *Abstracts of the Sixth International Symposium on Okhotsk Sea and Sea Ice*, 75–79.

Welch, H.E., Bergmann, M.A., Siferd, T.D. & Amarualik, P.S. (1991) Seasonal development of ice algae near Chesterfield Inlet, N.W.T., Canada. *Canadian Journal of Fisheries and Aquatic Sciences*, **48**, 2395–2402.

Werner, I. & Auel, H. (2004) Environmental conditions and overwintering strategies of planktonic metazoans in and below coastal fast ice in the Gulf of Finland (Baltic Sea). *Sarsia*, **89**, 102–116.

Wu, H., Bai, S., Liu, Q. et al. (2005a) Sea ice regime in the Bohai Sea in comparison to the Baltic Sea ice regime. In: *5th Baltic Sea Ice Climate Workshop*, Center for Marine and Atmospheric Research, Hamburg, Germany, August 31–September 2, 2005.

Wu, L., Wu, H., Li, W., et al. (2005b) Sea ice drifts in response to winds and tide in the Bohai Sea. *Acta Oceanologica Sinica*, **27**, 15–21.

Yang, G.-J. (2000) Bohai Sea ice conditions. *Journal of Cold Regions Engineering*, **14**, 54–67.

Zhang, Z. (2000) On modelling ice dynamics of semi-enclosed seasonally ice-covered seas. *Report Series in Geophysics*, University of Helsinki, **43**, 34pp.

Zhang, Z., Wu, H. & Wang, Y. (1997) Variability of climatic and ice conditions in the Bohai Sea, China. *Boreal Environment Research*, **2**, 163–169.

Zhang, Z., Zhu, M., Wang, Z. & Wang, J. (2006) Monitoring and managing pollution load in Bohai Sea, PR China. *Ocean & Coastal Management*, **49**, 706–716.

This page intentionally left blank

15 Sea Ice and Astrobiology

John S. Wettlaufer

15.1 Introduction: a dowser in a freezer – terrestrial laboratories for exobiology

Our laboratory-based scientific experience in the biological and physical sciences is bound to Earth, and hence we believe that liquid water is required for the persistence of all known forms of life. Within our solar system, stable supplies of liquid water are invariably found in close association with ice. Thus, the search for unintelligent[1] life is that of a dowser in an enormous freezer. The most promising and accessible targets in the search for past and present exobiological communities are the frozen surface of Mars and the icy moons of Jupiter. On Earth, microbes inhabit liquid networks at sub-zero temperatures within glacial ice, ice-infiltrated sediments and sea ice, which is clearly the focus of the discussion here. To refine the scope of a search for evidence of unintelligent life in an extraterrestrial setting requires a confluence of approaches drawing on a variety of disciplines. One can approach the problem by analogy or simile with what we can say firmly from our earth-bound perspective. This can involve examining a wide swath of the biological complexity of terrestrial ecosystems using methods ranging from evolutionary theory to modern molecular biology and ecology. It can also proceed by focusing in on a few robust evolutionary features that organisms have incorporated into their repertoire for survival and trying to understand the biological or physicochemical basis for those features and thereby facilitate our generalizations to other planets. One might further study known terrestrial habitats in terms of the robust physical features that rely on conservation laws for their persistence and hence must be obeyed elsewhere in the universe. Dyson advocates 'pit-lamping' (i.e. optical backscattering) which is a modality that can be informed by the understanding of the thermodynamic range in which unintelligent life exists on Earth (Dyson, 2007). All of these approaches and others inform an intelligent search for unintelligent life; in this short chapter, I describe aspects of the latter two approaches that may be of some use. They also happen to be the approaches for which my own background is most useful. I refer the reader to Chapters 7–10 for a complete view of the richness of the ecology of sea ice. This chapter is certainly a limited view from one practitioner in a rapidly growing field involving many disciplines. It is not intended to be comprehensive, rather it is intended to be a reasonable portal to enter into some of the many interesting tendrils that connect ice on Earth to planetary evolution and life.

15.2 The earth context

Two terrestrial settings provide obvious models of extremophiles and exobiology in general; deep-sea hydrothermal vents and the ice forms of the polar regions. The latter is the focus here with the primary goal of answering the questions 'Where is the water in ice?' and 'What is that water good for?', because it is this unfrozen water that provides the potential habitat. For researchers in many areas of science and technology, the existence of unfrozen liquid is most often solely associated with colligative effects, but a rigorous assessment of the potential for habitation of ice-bound liquid reservoirs, as well as their ability to preserve evidence of past and present life, requires a more thorough examination of the means by which water can exist at low temperatures. In other words, the water budget of 'frozen' ice masses. Indeed, one of the primary constraints on the balance between dormancy and viability within polycrystalline ice is the confluence of microbial mobility and the efficiency of the fluid-mediated transport of nutrients and waste products. Hence, polycrystalline ice in all of its terrestrial forms can function as both a safe haven for organisms (perhaps developed under more hospitable conditions) and habitats for active, sustainable life.

On the largest scales, Earth's climate is strongly influenced by the extent of the global ice cover. Much is, and should be, made of the fact that more than two-thirds of the surface of the Earth is covered by water, but on any given day, one of the polar oceans is freezing. Although the waxing and waning of oceanic ice is implicated in ice-albedo feedback-driven climate change, a relatively untouched aspect of the process concerns the coupling between high latitude physical processes and polar ocean ecology. Not only is the issue a key aspect of the food web in Earth's Oceans, but it also serves as a test bed for astrobiology: life in and on the surface of ice. The terrestrial setting in which life has undergone the most extensive ecological cryo-adaptation is within *sea ice*. Indeed, Earth's history has seen ice-free poles and, while it is still a matter of considerable debate, *global glaciation*[2]. Some 13% of the surface area of the ocean surface is seasonally ice covered and thereby comprises an enormous ecosystem exceeding those of the deserts, grasslands or tundra taken alone (Lizotte, 2001).

The dense populations of bacteria, algae and metazoans observed to colonize sea ice (Horner et al., 1992; see also Chapters 7–10) provide the most compelling evidence that, when stressed, elemental and original forms of life have evolved to thrive at the lowest temperatures on earth. Indeed, considering temperature alone does not adequately describe the magnitude of the struggle these organisms embrace, for, as humans, we carry our own osmotic environment, whereas the range of osmotic pressures experienced by sea ice biota from the surface to the underside of sea ice presents an uncontrolled stress. The struggle does not end with those at the low end of the polar food web. Antarctic fish manage to spend their days and nights swimming in waters that, from a thermodynamic point of view, should freeze them instantly. Is it possible that such fish are swimming under the ice cover of Europa or Enceladus? It was a surprise when some of the first photographs of the floor of the Arctic Ocean revealed a fish staring into the lens (Ewing et al., 1969). We now recognize that the blood of fish found in the ice pack contains an antifreeze protein (AFP), crafted by evolution, but we struggle to understand the physics and chemistry that underlie how the protein staves off their demise. Hence, we are compelled to organize our understanding of the influence that surface and size effects have on the phase behaviour of ice in parallel studies of the interaction of biota with equilibrium and nonequilibrium ice forms.

An understanding of the ecological success of these ice-bound extremophiles provides the underlying connections between their existence, the food web in which they live and the environmental factors that influence the system. Indeed, this understanding is crucial in providing a qualitative understanding of the necessities of evolution and a quantitative description of important linkages. However, it is the chemistry and physics that underlie their persistence in the face of extremes that holds clues to the true breadth of what natural biota offer, from exobiology to more 'selfish' matters such as effective pre-emptive crop damage agents to biomineralization and medical applications. Clues lie in the important aspects of the microscopic and the mesoscopic processes associated with the interaction between biopolymers and ice. Quantitative laboratory experiments simultaneously addressing the thermodynamics, dynamics and kinetics underlying the interaction of naturally occurring biopolymers and the surface of ice are of contemporary interest. A principal focus of my own activities concerns the basic mechanisms of organism–ice surface adhesive interactions, and to understand the essential features of how life persists on the surface of ice, we must probe the problem using a biologically and chemically informed physics approach. Sea ice ecology suggests that two crucial biopolymers underlie the ability of organisms to thwart an icy death. However, before we discuss these rather complex issues, a brief discussion of the equilibrium structure of polycrystalline ice is necessary.

15.3 The equilibrium phase behaviour of ice

The *premelting* of any material refers to the range of effects responsible for the stable persistence of the liquid phase at temperatures below the normal melting temperature, T_m. The most commonly encountered effects in the literature are the *Gibbs-Thomson* and *colligative effects*. The former is a statement that a solid phase convex into its melt phase has a lower freezing point than the bulk and the latter originates in the lowering of the chemical potential of a solvent in the presence of a solute[3]. In the absence of a phase boundary curvature or solute, there exists a wide class of premelting phenomena dominated by the nature and range of intermolecular interactions that can attract the liquid phase to a subfreezing interface in the face of the penalty paid by the increase in the bulk free energy of that same liquid. Cumulatively, we refer to these effects as *premelting* phenomena, and they characterize the *equilibrium* structure of the material.

The melting of a solid is described as a first-order phase transition due to the discontinuous change in *bulk* quantities at the transition point. However, all crystals, whether in contact with their vapour phase or another material, have surfaces where the process of melting is initiated: If there were a layer of liquid at the surface, at temperatures below the bulk melting transition, then there is little need to activate the melting process. This deduction was made long ago by Tammann (1909) on the basis of the inability to superheat crystals. The ease with which liquids can be supercooled tells us that the melting process is inherently asymmetrical about the transition point. The interplay between melting and dimensionality is demonstrated in *surface melting* (Dash et al., 2006).

In the absence of *Gibbs-Tho*mson and *colligative effects*, a wide range of experimental methods show that the melting of solids begins at temperatures below the bulk transition. This *interfacial premelting* occurs at the surfaces of solid rare gases, quantum solids, metals,

semiconductors and molecular solids, and is characterized by the appearance of an interfacial thin film of liquid that grows in thickness as T_m is approached from below. Interfacial premelting is driven by polarization forces that shift the equilibrium domain of the liquid phase into the solid region of the bulk phase diagram. The precise relationship between the film thickness and the temperature depends on the nature of the polarization forces in the system, often complicated by the coexistence of several types of interactions driving the process. When interfacial premelting occurs at vapour surfaces, it is referred to as *surface melting* and when it occurs at the interface between a solid and a chemically inert substrate it is called *interfacial melting*, and when at the interface between two grains of the same material, it is called *grain boundary melting*. An essential point to make here is that the transport of unfrozen liquid at planar surfaces is driven by *thermomolecular pressure* gradients and *not* capillarity. The process is central to the sintering, coarsening, transport behaviour and many other bulk phenomena within such a matrix. The physics underlying the effect and these and other applications are described in the reviews of various levels of sophistication (Wettlaufer & Dash, 2000; Dash et al., 2006; Wettlaufer & Worster, 2006).

Most crystalline solids consist not of single crystals but rather of large numbers of crystal grains. Those domains are separated by grain boundaries that are so numerous in most materials that they often play a central role in their physical, thermal and electrical properties; ice is no exception. Premelting is responsible for the fact that naturally occurring polycrystalline ice, such as that of glaciers and ice sheets, is not entirely solid below the bulk melting temperature. Ice is a close-packed hexagonal crystal, interlaced with liquid films threading through its volume. Where three ice grains come together, a thin liquid vein exists, and where four grains join, a node of liquid water forms (Fig. 15.1). In ice, these interfacial liquid structures separating grains facilitate the redistribution of climate proxies (Rempel et al., 2001), influence the permeability to brine flow in sea ice (see below), can supply nutrients to organisms (Price, 2000), scatter Cherenkov radiation used to detect neutrinos (Ackermann et al., 2008), and they define the fabric and flow of the great ice sheets (Wilen, 2000).
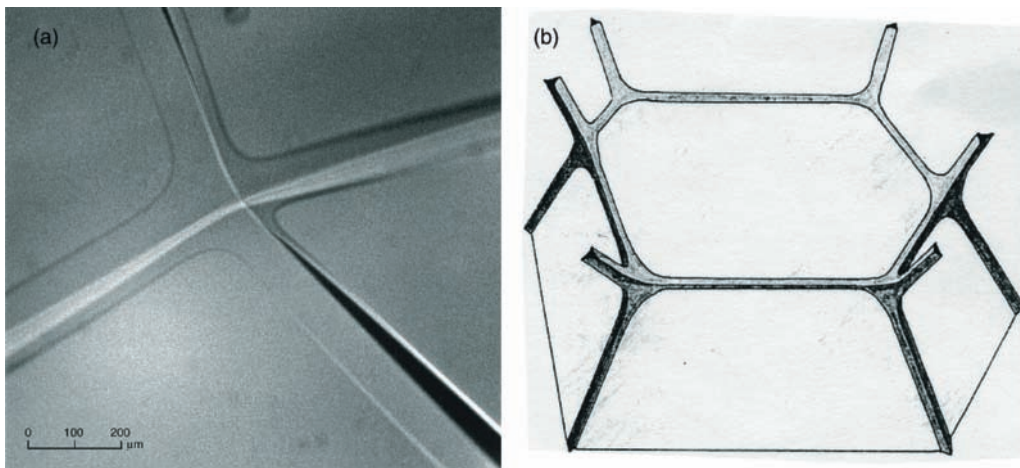
Fig. 15.1   (a) A photograph of four veins intersecting at a node between four grains in polycrystalline ice near the bulk melting temperature. (b) Schematic representation of the vein/node network. From Mader (1992a,b). Reprinted from Mader (1992a) with permission of the International Glaciological Society.

The persistence of liquid water at subfreezing temperatures associated with premelting has many large-scale implications on land, in the polar oceans and throughout the atmosphere and biosphere (Wettlaufer & Dash, 2000; Dash et al., 2006; Wettlaufer & Worster, 2006).

Of particular relevance to the question of such liquid harbouring life is the transport of this unfrozen water in temperature gradients that create thermomolecular pressure gradients driving liquid from high to low temperatures (Dash et al., 2006; Wettlaufer & Worster, 2006). The process has been studied quantitatively at single crystal interfaces but there remains a dearth of experimental information about the structure of ice-grain boundaries, their liquidity, their transport properties and their habitability. How is this structure related to life and liquid water? Because the surface area of a polycrystal such as that shown in Fig. 15.1 is dominated by grain boundaries, the water budget of ice must include information about grain boundary melting. However, the length scale is far smaller than can be seen by the optical methods used to produce the image shown there.

15.4 Biopolymers, disequilibrium phase behaviour of ice and ice-bound habitats

Exopolymeric substances

Because it forms rapidly from the ocean, sea ice consists of an interconnected mixture of nearly pure solid ice bathed in brine. The liquid network spans many orders of magnitude and is the result of the basic phase behaviour and dynamics of the growth process (Dash et al., 2006). The physical mechanisms that govern the solidification patterns are typical of crystal growth from a binary alloy and are fundamental to many systems of interest (Langer, 1980; Cross & Hohenberg, 1993; Dash et al., 2006). The insights gained from their study are broadly applicable to a range of settings, including the growth of semiconductor wafers, the casting of high-performance turbine blades, the solidification of lava and the Earth's iron alloy inner core (Sumita et al., 1996), and the growth of the polar ice sheets among others. But such processes do not occur in isolation of the ecological setting. Between 1% and 20% of the total sea ice volume consists of brine, resulting in an interior surface area of 1–4 $m^2 kg^{-1}$ (Krembs et al., 2000). This liquid system serves as a habitat for the so-called sympagic communities consisting of various groups of organisms like viruses, bacteria, autotrophic and heterotrophic protists and metazoa (Meiners et al., 2002; Horner et al., 1992; Lizotte, 2001). Sympagic organisms are adapted to the extreme environmental conditions of sea ice brine and can use the brine channel walls as sites of locomotion, attachment and grazing. The most important primary producers in sympagic communities are pennate diatoms (Pennales, Bacillariophyceae). In benthic marine environments, pennate diatoms are the most frequent early algal colonizers of submersed natural and artificial substrata. In these environments, attachment of algae to surfaces is driven by the production of exopolymeric substances (EPS) that serve as adhesive mucilage (Wetherbee et al., 1998). Benthic biofilms are also sites of increased microbial activity and exhibit enhanced biogeochemical processing (Romaní & Sabater, 2000).

Recent investigations show that sea ice harbours copious amounts of EPS and that its concentration is closely correlated with the abundance of the pennate diatoms (Krembs & Engel, 2001; Meiners et al., 2003; see also Chapters 7, 8 and 12), which are considered

the main producers of EPS during the construction of primary sea ice biofilms. Krembs and colleagues have described gel-like EPS accumulations around sea ice diatoms serving as extracellular cryoprotective spheres for the cells. The evidence that EPS plays a central role for organisms colonizing the sea ice habitat is clear. However, (a) the physical mechanisms of organism–ice surface adhesive interactions, the development, structure and activity of ice-associated biofilms and the formation of cryoprotective gels are not understood, and (b) the influence of EPS on bulk transport properties, such as brine viscosity, and hence the coupling of the heat and mass transfer between the porous sea ice and the ocean are not understood. These problems are unique in the sense that fundamental biological processes have basic and important physical consequences. Therefore, an understanding of the evolution of the phase fraction of brine in sea ice is in a serious sense, but one yet to be completely quantified, equivalent to understanding the evolution of its ecology. Why should such things matter for the state and fate of this habitat?

The configuration of the phase boundaries that evolve during ocean freezing bear a great deal in common with those formed during the solidification of any binary alloy; in our case the alloy is a salt solution approximated very adequately from this perspective as water and sodium chloride. The formation of sea ice involves a hierarchy of instabilities controlled by, among other effects, molecular diffusion, hydrodynamics and crystallization, all of which result in a complex composite material. Because of these phenomena, such directionally solidified alloys are often referred to as 'mushy layers' (Figs 15.2 and 15.3). As a result of the variety of processes underlying these instabilities, the mushy layer develops a substructure on many length scales. In fact, when viewed on a length scale of millimetres, the patterns on the underside of sea ice bear strong similarities to those typical of snowflakes (Wettlaufer, 1992; Furukawa & Wettlaufer, 2007). Under all conditions of growth on Earth, this instability is operative and hence sea ice will always grow as a two-phase, two-component material, making it among the most dynamic effective media of all terrestrial ice forms (comprehensive reviews include Chapter 2; Weeks, 1998, 2009; Wettlaufer, 1998). Due to the fact that the substructure is grown into sea ice, its bulk thermal and transport properties owe their origin to these microscopic effects. An essential macroscopic transport property is the permeability which describes the resistance to the flow of brine through the porous sea ice matrix.

The importance of the permeability is great; it underlies the process that determines the rate at which dense brine is delivered to the surface of the polar oceans and, importantly, must be dealt with both thermodynamically and dynamically due to the fact that ice grows in a thermal gradient and the interstitial fluid has a density that increases with height in the layer (Wettlaufer et al., 1997). The process is outlined as follows: ice grows because it is colder at its surface than at its base. Thermodynamic equilibrium throughout a growing layer is maintained by the salinity of the brine within the ice substructure increasing towards the surface. Owing to the fact that the density of salt water increases with salinity, buoyancy forces will tend to drive the fluid out of the matrix. The permeability of the layer is decreased if the crystals are sufficiently close to one another and hence the matrix resists the buoyancy forces. As the layer grows, the buoyancy forces and permeability evolve and ultimately the former prevails and the brine trapped within the sea ice is abruptly released into the ocean below. Not only does the microstructure, through its control on the permeability, have a direct influence on the evolution of the water column below, but it also leads to the abrupt change of the overall connectivity of sea ice. In consequence, the porosity varies spatially and hence this convectively driven release of brine leads to focusing of subsequent flow which
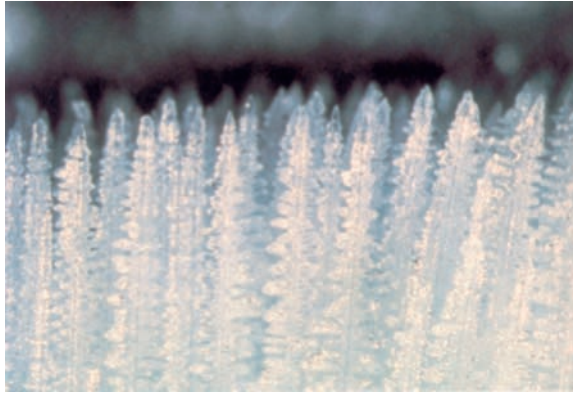
Fig. 15.2   This photograph, taken by Grae Worster and Herbert Huppert at the University of Cambridge, shows the interface between the dendritic crystals of the mushy layer of ammonium-chloride crystals grown from aqueous solution. The crystals are solidified from below the liquid region but the same general mushy layer structure is seen in natural sea ice growing from the surface of the ocean. This example is used to emphasize the generality of the phenomena discussed in the text.
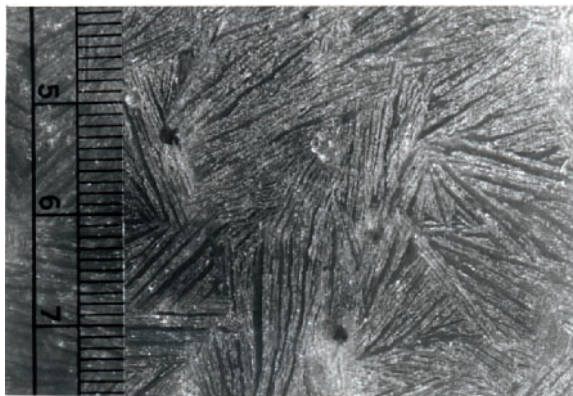
Fig. 15.3   A photograph of the two-phase nature of the ice formed from salt water (Wettlaufer et al., 1997). This is a section that is perpendicular to the growth direction (the numbers on the scale indicate centimetres). Note the linear 'substructure' which separates the solid (white) from the brine. This coexists with channels (or holes) that form due to convective instabilities and thread the material parallel to the growth direction. These channels are the principal conduits through which desalination, nutrient and waste transport occurs.

ultimately creates the brine channels in sea ice. While these channels dictate the brine volume of ice (e.g., Wettlaufer et al., 1997; Notz and Worster, 2009), they are also known to be conduits of nutrient and waste transport as well as active habitats for everything from zooplankton to microorganisms, as discussed above. For example, it is known that the channels in sea ice act as homes for amphipods (Beuchel & Lønne, 2002) and that their lack of mobility (they are shrimp that are not active swimmers) makes channels in the ice not just a home, but a safe haven. Amphipods are a mainstay of the diet of polar sea birds (Lønne & Gabrielsen, 1992) and fish and thus the conditions for the opening, closing and evolution of channels in ice have far-reaching consequences for ecosystem dynamics. Importantly, these diffusive and buoyancy-driven instabilities are general, neither specific to ice nor to Earth. We understand this from a wide range of laboratory and theoretical studies, and one can thus only imagine

that if, for example, a Europan ice cover grew from a saline ocean it will have had to pass through these and related instabilities and hence will have the same substructure and brine channels we understand here on Earth.

Shear flow at the ice–ocean interface can influence these patterns, as well as producing further spatiotemporal patterns in the permeability on larger length scales. This process has been studied theoretically and experimentally (DeVries & Wohlschlag, 1969; Feltham & Worster, 1999; Neufeld et al., 2006; Neufeld & Wettlaufer, 2008a,b) by analysing the effect of a perturbation of a planar mush–liquid interface with an applied external shear flow. These perturbations lead to perturbed flow in the bulk fluid that drive pressure variations along the mush–liquid (sea ice–ocean) interface. These pressure variations in turn drive flow in the sea ice that trigger the convective instability described above, but with a symmetry breaking associated with the external flow. The application of an external flow can significantly reduce the stability of these convective modes and the resultant *forced mushy layer instability* gives rise to the formation of channels of reduced solid fraction aligned perpendicular to the applied flow that are distinct from the platform of brine channels found in the absence of an external flow (Fig. 15.4). Thus, understanding the hydrodynamics and thermodynamics of ice formation underlies the heat and mass balance of the Arctic and Antarctic oceans. Moreover, the finite phase fraction and its spatiotemporal evolution provide an ideal environment for biota. Such an interplay between the topography of the ice–ocean interface and its colonization by algae has been examined qualitatively by Krembs et al. (2002).

Antifreeze proteins

Antifreeze proteins (AFPs) were discovered in fish over 30 years ago (DeVries & Wohlschlag, 1969; DeVries et al., 1970; Ewart & Hew, 2002). Because these fish live in sea water at a typical temperature of –1.9°C (Yeh & Feeney, 1996; Davies et al., 2002), and their blood is about a third of the salinity of the surrounding sea, AFPs are argued to be responsible for the lowering of the freezing point of the fish blood below the colligatively determined melting point. We know that a sufficiently large ice crystal placed in super-cooled melt will always grow rapidly and yet these fish do not freeze because blood-borne AFPs prevent explosive freezing. A wide selection of organisms have developed AFPs, including insects (Tomchaney et al., 1982), plants (Urrutia et al., 1992; Worrall et al., 1998), bacteria (Gilbert et al., 2004), fungi
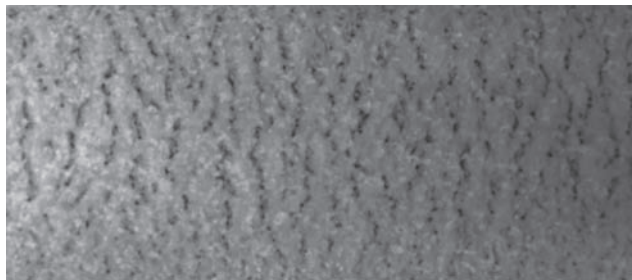
Fig. 15.4   A plan view of the experimental observation of the effects of a shear flow on a growing mushy layer described above. A shear flow from left to right drives an instability wherein the volume fraction of sea ice becomes nearly zero (dark regions) in a transverse direction. The image is 9 by 25 cm. See Neufeld and Wettlaufer (2008a,b) for a detailed description of the experimental and theoretical treatment of this phenomena.

(Robinson, 2001) and vertebrates (Barrett, 2001). AFPs vary greatly in shape and size (Davies & Sykes, 1997) and, for example, the AFP of the spruce budworm is a rigid left-handed beta-helix secured by disulphide bonds (Graether et al., 2000), while fish AFP type I is a simple alpha helix (Chakrabartty et al., 1989; Baardsnes et al., 1999). It is clear that there are few unifying principles for AFP structure because comparison of the DNA sequences that code for these proteins shows that they developed separately (Davies et al., 1988; Chen et al., 1997; Logsdon & Doolittle, 1997; Cheng, 1998; Cheng & Chen, 1999; Ewart et al., 1999). Hence, although strong evolutionary pressures combined with some residual inherent anti-freeze activity have caused parallel development of many AFPs (Davies et al., 2002), we seek understanding of some underlying principles and their effect on the nucleation and growth of ice. A benefit of this approach is the fact that there are some general implications in crop preservation and cryobiology. Indeed, frost damage is one of the main limiting factors to crop production and distribution of horticultural crops (Rodrigo, 2000), and hence a basic understanding of the mechanism of AFP action could potentially have a major impact on agriculture.

Here we describe several new approaches for investigating the activity of these proteins and I will focus on the work in which I have been involved. However, I note that the field is rapidly transforming into a quantitative one with many complimentary techniques. One of the reasons is the increased ability to control single ice crystals or polycrystals in small cells that can be probed optically using a variety of means. Because ice is transparent we can make use of optical wavelengths, birefringence and fluorescence methods. One such experimental apparatus (Fig. 15.5) has been repeatedly modified since first developed by Wilen and Dash (1995a,b). An ice polycrystal is nucleated within a disc-shaped region, ~0.8 mm in width and 18 mm in diameter, created by sandwiching two glass cover slips over a hole bored into a thin wafer. The system is sealed with paraffin and mounted onto a base unit cooled with a thermo-electric device. The centre of one of the glass windows is flush with a cooling finger, while the outside diameter is temperature-regulated by a heating coil. Fill lines are connected to small holes providing continuous water flow and dopant control. Ice is nucleated from pure water at the cooling tip and grows radially outwards, reaching a steady state radius which depends upon the temperature distribution specified. The sample is illuminated and viewed between crossed polarizers to distinguish and measure the grain structure. The entire system is enc-losed within an insulating shell, isolating it from the laboratory, and dry nitrogen is pumped into the shell to prevent anomalous temperature transients due to latent heat effects.

The entire water budget of the ice polycrystal must be scrutinized in the quest to examine the viability of various habitats within the matrix. Hence, the value of such a method is that one can systematically probe the various interfaces while controlling first the chemical and then the biological dopant levels. Thus, first we probe grain boundary melting using optical scattering (Thomson et al., 2005, 2009). The fluid surrounding the polycrystal can then also be replaced with solutions of known impurity/biota concentration. It turns out to be a challenging theoretical consideration to understand the propagation through, and scattering of light from, an anisotropic–isotropic–anisotropic interface (Thomson et al., 2009) but this is an essential aspect of understanding the simplest case of a salt-doped grain boundary for which theoretical considerations indicate a liquidity that is very sensitive to impurity level (Benatov & Wettlaufer, 2004). By scattering the beam of a 4 mW Helium–Neon laser ($\lambda = 632.8$ nm) off the selected grain boundary (Fig. 15.4) and analysing the intensity and phase of the reflected signal, one can engage in a measurement programme to extract the
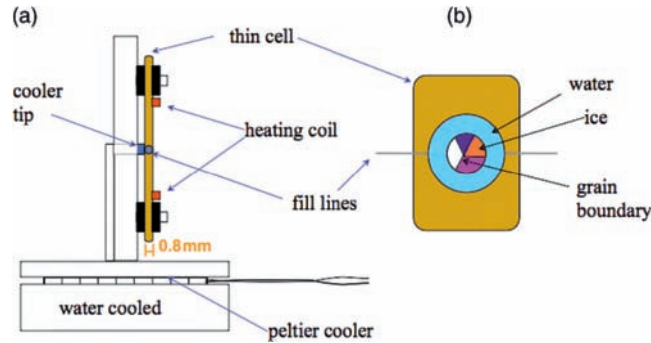
Fig. 15.5 Schematic representation of laboratory apparatus used for controlled studies of biopolymer–ice interactions and grain boundary melting. To the left is (a) the base unit and to the right (b) the thin wafer.

thickness of the grain boundary as a function of temperature, dopant concentration and crystallographic orientation (Thomson et al., 2005, 2009). This is the baseline knowledge for a sequential study of the habitability of an ice polycrystal in the confined spaces away from the vein/node/trijunction system.

Therefore, this same cell allows one to examine a number of effects of both EPS and AFP by introducing these biopolymers into the liquid surrounding the sample once a stable pure ice disc has been established. The biologically doped solution flows around the ice lens to replace the pure water. A qualitative example is displayed in Fig 15.6 that shows an ice disc before (left) and after (right) AFP was introduced. We did not control many parameters, but clearly the AFP influences each grain orientation uniquely. Where one orientation grows faster than an adjacent one, it is observed to wedge out the other grain. In some cases, a new grain orientation is nucleated as the ice grows out.

A complimentary and more quantitative approach is to conjugate the proteins with green fluorescent protein (GFP) and study its affinity for various crystallographic orientations (Pertaya et al., 2007a,b; Zepeda et al., 2008). GFP is a protein that fluoresces green when illuminated under blue or UV light and can then be imagined directly on the surface of an ice crystal in contact with solution using confocal fluorescence microscopy. This provides a quantitative methodology to study the influence of AFPs on crystal growth kinetics and to thereby provide a foundation for how bioadaption functions on a molecular level to thwart freezing. There is presently a great debate regarding the mechanisms by which AFPs actually control the nature of ice crystal growth and there are variations among the varieties of proteins found in living organisms which fuel the confusion and the vigour of the debate. A quantitative approach is necessary to distinguish among the range of theoretical explanations. In Fig. 15.7 we see an example from the spruce budworm AFP (sbwAFP) that appears to attach efficiently to the slow-growing orientations of the ice crystal to insure that they dominate the growth shape.

Somehow, it 'knows' what orientation is dangerous to the organism and what orientation need not be dealt with. The question of reversibility and irreversibility of attachment to the ice surface of various proteins found in organisms is presently an actively engaged question in the laboratory and these optical means are a central technique in the experimental arsenal (Pertaya et al., 2007a,b; Zepeda et al., 2008). Theory lags, for we are unsure about the basic
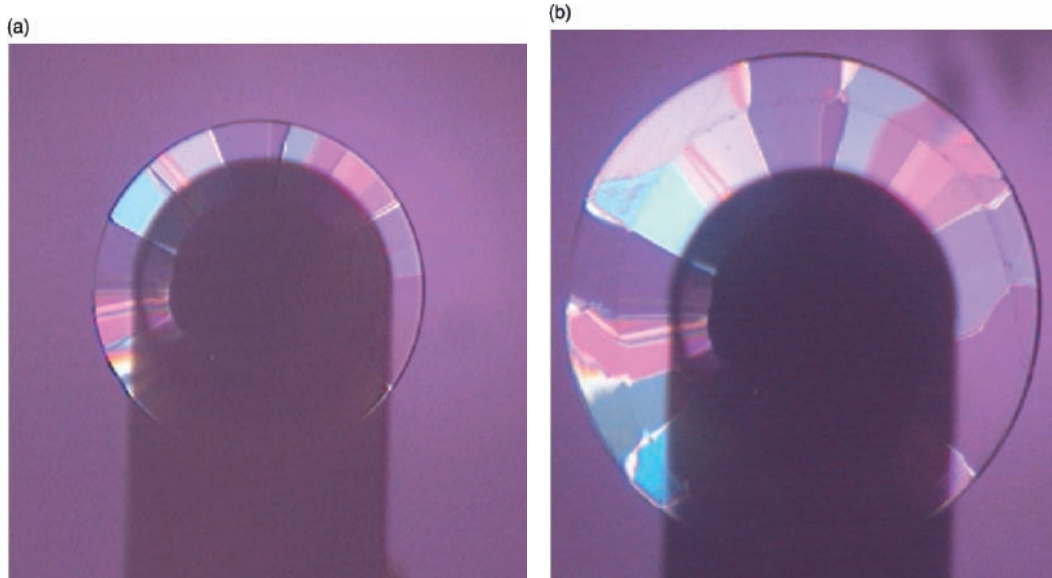
Fig. 15.6 A demonstration of the strong influence of an AFP (a so-called modified AFP type III) on the crystal structure. (a) The ice disc that grew in pure water. (b) The ice disc after growth into the AFP solution. The colours of the different grains are brought out using crossed polarizers and the optical bifringence of the ice. There is clearly an abrupt horizon where the crystallography changes in consequence of the presence of the AFP indicating a strong influence of this biopolymer on the surface energy of the ice–solution interface.
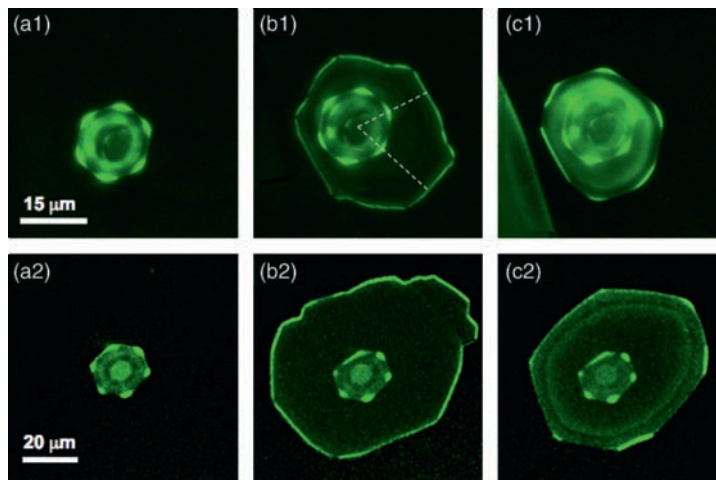
Fig. 15.7 Growth of ice crystals in sbwAFP-GFP solution from Pertaya et al. (2007). The crystallographic c-axis is perpendicular to the plane of the page. The higher the (green) intensity the higher is the surface concentration of protein on the surface. See Pertaya et al. (2007) for a detailed description for how these images are produced. Series 1 (top) and 2 (bottom) show the location of the sbwAFP-GFPs on the ice crystals in two separate experiments. (a) Initial melting shapes. (b) Growing shapes. During subsequent growth the sbwAFP-GFPs are overgrown by the ice, and additional sbwAFP molecules from solution attach to the prism facets that emerge from the corners of the melt shape 30° from the planes therein. (c) Partial melting. The AFPs attach to the same directions as on the original melt shape, accumulating on the centres of the shrinking facets of a hexagonal ice crystal at locations that eventually become corners.

issues concerning how a polymer conforms in the presence of a surface. The surface of ice in contact with a solution has a finite charge density. Hence, during growth, there exists an electric field in the liquid phase, and thus experienced by the polymer, with a decay length that depends on the solute concentration and the solidification rate. How does the polymer conform in that field? Is that conformation essential to the 'decision' it makes regarding where to attach to an ice surface? How strong is the surface affinity as a function of growth rate and orientation? What are the steric effects? How do we treat this system with a sufficient level of theoretical tractability and yet maintain biological complexity? The study of such issues is just beginning (Hansen-Goos and Wettlaufer, 2009).

15.5 Summary

We look out into the universe with the blinds provided by our biology and with the telescopes provided by our chemistry and physics. Namely, if we as scientists believe in the present cosmology then the system specificity of Earth may reside solely in its chemical origin and trajectory of the tree of life. Whereas the periodic table and the laws of physics are universal, biology lacks this rigidity. Life is propitious for life and hence biological adaptation, while constrained by chemistry and physics, is not reigned over by the lack of creativity of our humanity; the nature and number of forms it can take is, frankly, astronomical. The blinds we have are the constraints of our knowledge of how organisms seek out a living here on Earth. The context of this book is the cold end of this spectrum and so I began this chapter by taking the perspective that the cold dark distant potential abodes of unintelligent life, as we understand it here, must have water for survival. The search then becomes one of a dowser in the freezer. Looking around the planet brings us to cold-adapted organisms. What then are some of the questions that remain for us?

The issues and implications are much more broad than may first be apparent. If we understand key aspects of cryo-adaptation, we can contribute to understanding of planetary-scale adaptation over geologic time while also understanding key technical issues that can advance the organic technology of crop preservation and cryobiology. The organisms inhabiting sea ice were not emplaced in their present environment. Rather, they adapted to that environment over the time scales of global change. Indeed, recently, spores from temperate aquatic ferns have been discovered in sediment cores taken near the North Pole suggesting that some 50 million years ago the now ice-covered ocean was ice-free (Appenzeller, 2005). Therefore, understanding the mechanism of AFP and EPS action evolved by natural organisms could potentially have a major impact not only on the basic understanding of the dynamics of life forms during past climate epochs but on those elsewhere in the universe.

Unfortunately, scrutiny of the detailed taxonomy of this large swath of 'freezing inhibition' biopolymers has apparently not unified the understanding of their function. What we do know is that an ice crystal placed in supercooled melt causes explosive crystallization of the water and yet cold-adapted organisms *do not* suffer the same violent fate of freezing. Thus, we ought to seek understanding of underlying principles controlling the action of all such polymers. Essential questions include:

(1) What are the principal features of the interaction between EPS and AFPs with the surface of ice? (a) How do they influence the amount of premelted liquid in ice-grain boundaries? (b) How do they adhere to ice surfaces?

(2)   Is the metabolic activity of organisms attached to crystal surfaces higher than the activity of organisms suspended in the sea ice brine?

(3)   What abiotic and biotic factors control EPS and AFP production *in situ*?

(4)   What are the bulk effects of biopolymers in a growing ice matrix and hence what is their ecological influence? (a) How do EPS and AFPs influence the flow in grain boundaries and the stability of growth fronts? (b) What is the interaction between the external flow and the brine volume? (c) How quickly do instabilities change the ice structure and is it too rapid for biological redistribution? Are these proteins basic to life in the harsh cold environments elsewhere in the universe?

It would seem that the answer to this last question is in the affirmative unless that biology is of an entirely different nature than that which we understand. If we believe in our cosmology, the chemistry and physics will fall in line in support of the biology.

Acknowledgements

End notes

1 The search for intelligent life is a rather different matter involving as it does communication rather than just observation or experimentation.

2 While it is clear that in the Neoproterozoic low-latitude ice existed, the debate about the extent of "Snowball Earth" continues unabated. See Hoffman et al. (2008) and Peltier & Liu (2008).

3 The term *colligative* is generally taken to refer to solute effects in the dilute limit because they depend solely on the number of atoms/molecules rather than their specific nature. Hence, while there is still a solutally controlled freezing point depression when this limit is no longer operative, strictly speaking the effect is not 'colligative'. For ease of delivery we use the term out of this range of strict validity.

References

Ackermann, M. Adams, J., Ahrens, J et al. (2008) Search for ultra-high-energy neutrinos with AMANDA-II. *Astrophysical Journal*, **675**, 1014–1024.

Appenzeller, T. (2005) Great green north: was the icy Arctic once a warm soup of life? *National Geographic*, **207**, 5 May 2005.

Baardsnes, J., Kondejewski, L.H., Hodges, R.S., Chao, H., Kay, C. & Davies, P.L. (1999) New ice-binding face for type I antifreeze protein. *FEBS Letters*, **463**, 87–91.

Barrett, J. (2001) Thermal hysteresis proteins. *International Journal* of Biochemistry and Cell Biology, **33**, 105–117.

Benatov, L. & Wettlaufer, J.S. (2004) Abrupt grain boundary melting in ice. *Physical Review E*, **70**, 10.1103/PhysRevE.70.061606.

Beuchel, F. & Lønne, O.J. (2002) Population dynamics of the sympagic amphipods *Gammarus wilkitzkii* and *Apherusa glacialis* in sea ice north of Svalbard. *Polar Biology*, **25**, 241–250.

Chakrabartty, A., Ananthanarayanan, V.S. & Hew, C.L. (1989) Structure-function relationships in a winter flounder antifreeze polypeptide. I. Stabilization of an alpha-helical antifreeze polypeptide by charged-group and hydrophobic interactions. *Journal of Biological Chemistry*, **264**, 11307–11312.

Chen, L., DeVries, A.L. & Cheng, C.H. (1997) Convergent evolution of antifreeze glycoproteins in Antarctic notothenioid fish and Arctic cod. *Proceeding of the National Academy of Science USA*, **94**, 3817–3822.

Cheng, C.H. (1998) Evolution of the diverse antifreeze proteins. *Current Opinion in Genetics and Development*, **8**, 715–720.

Cheng, C.H. & Chen, L. (1999) Evolution of an antifreeze glycoprotein. *Nature*, **401**, 443–444.

Cross, M.C. & Hohenberg, P.C. (1993) Pattern-formation outside of equilibrium. *Reviews of Modern Physics*, **65**, 851–1112.

Dash, J.G., Rempel, A.W. & Wettlaufer, J.S. (2006) The physics of premelted of ice and its geophysical consequences. *Reviews of Modern Physics*, **78**, 695–741.

Davies, P.L. & Sykes, B.D. (1997) Antifreeze proteins. *Current Opinion in Structural Biology*, 7, 828–834.

Davies, P.L., Hew, C.L. & Fletcher, G.L. (1988) Fish antifreeze proteins – physiology and evolutionary biology. *Canadian Journal of Zoology – Revue Canadienne De Zoologie*, **66**, 2611–2617.

Davies, P.L., Baardsnes, J., Kuiper, M.J. & Walker, V.K. (2002) Structure and function of antifreeze proteins. *Philosophical Transactions of the Royal* Society London B Biological Sciences, **357**, 927–935.

DeVries, A.L. & Wohlschlag, D.E. (1969) Freezing resistance in some Antarctic fish. *Science*, **163**, 1073–1075.

DeVries, A.L., Komatsu, S.K. & Feeney, R.E. (1970) Chemical and physical properties of freezing point-depressing glycoproteins from Antarctic fish. *Journal of Biological Chemistry*, **245**, 2901–2908.

Dyson, F.J. (2007) *A Many Colored Glass: Reflections on the Place of Life in the Universe*. University of Virginia Press, Virginia.

Ewart, K.V. & Hew, C.L. (2002) *Fish Antifreeze Proteins*. World Scientific, River Edge, NJ.

Ewart, K.V., Lin, Q. & Hew, C.L. (1999) Structure, function and evolution of antifreeze proteins. *Cell Molecular and Life Science*, **55**, 271–283.

Ewing, M. Hunkins, K. and Thorndike, E.M. (1969) Some unusual photographs in the Arctic Ocean. *Marine Technology Society Journal*, **3**, 41–44.

Feltham, D.L. & Worster, M.G. (1999) Flow-induced morphological instability of a mushy layer. *Journal of Fluid Mechanics*, **391**, 337–357.

Furukawa, Y. & Wettlaufer, J.S. (2007) Snow and ice crystals. *Physics Today*, **60**, 70–71.

Gilbert, J.A., Hill, P.J., Dodd, C.E., Laybourn-Parry, J. (2004) Demonstration of antifreeze protein activity in Antarctic lake bacteria. *Microbiology*, **150**, 171–180.

Graether, S.P., Kuiper, M.J., Gagne, S.M. et al. (2000) Beta-helix structure and ice-binding properties of a hyperactive antifreeze protein from an insect. *Nature*, **406**, 325–328.

Hansen-Goos, H., & Wettlaufer, J.S. (2009) Solvation structure of ice-binding antifreeze proteins, *Bulletin of the American Physical Society*, **54**, C1.237.

Hoffman, P.F., Crowley, J.W., Johnston, D.T., Jones D.S. & Schrag, D.P. (2008) Snowball prevention questioned. *Nature*, **456**, 10.1038/nature07655.

Horner, R., Ackley, S.F., Dieckmann, G.S. et al. (1992) Ecology of sea ice biota 1. Habitat, terminology, and methodology. *Polar Biology*, **12**, 417–427.

Krembs, C. & Engel, A. (2001) Abundance and variability of microorganisms and transparent exopolymer particles across the ice-water interface of melting first-year sea ice in the Laptev Sea (Arctic). *Marine Biology*, **138**, 173–185.

Krembs, C., Gradinger, R. & Spindler, M. (2000) Implications of brine channel geometry and surface area for the interaction of sympagic organisms in Arctic Sea ice. *Journal of Experimental Marine Biology and Ecology*, **243**, 55–80.

Krembs, C., Tuschling, K. & von Juterzenka, K. (2002) The topography of the ice-water interface—its influence on the colonization of sea ice by algae. *Polar Biology*, **25**, 106–117.

Langer, J.S. (1980) Instabilities and pattern formation in crystal growth. *Reviews of Modern Physics*, **52**, 1–28.

Lizotte, M.P. (2001) The contributions of sea ice algae to Antarctic marine primary production. *American Zoologist*, **41**, 57–73.

Logsdon, J.M. Jr. & Doolittle, W.F. (1997) Origin of antifreeze protein genes: a cool tale in molecular evolution. *Proceedings of the National Academy of Sciences USA*, **94**, 3485–3487.

Lønne, O.J. & Gabrielsen, G.W. (1992) Summer diet of seabirds feeding in sea ice covered waters near Svalbard. *Polar Biology*, **12**, 685–692.

Mader, H. (1992a) Observations of the water-vein system in polycrystalline ice. *Journal of Glaciology*, **38**, 333–347.

Mader, H. (1992b) The thermal behavior of the water-vein system in polycrystalline ice. *Journal of Glaciology*, **38**, 359–374.

Meiners, K., Fehling, J., Granskog, M.A. & Spindler, M. (2002) Abundance, biomass and composition of biota in Baltic sea ice and underlying water. *Polar Biology*, **25**, 761–770.

Meiners, K., Gradinger, R., Fehling, J., Civitarese, G. & Spindler, M. (2003) Vertical distribution of exopolymer particles in sea ice of the Fram Strait (Arctic) during autumn. *Marine Ecology Progress Series*, **248**, 1–13.

Neufeld, J.A. & Wettlaufer, J.S. (2008a) Shear enhanced convection in a mushy layer. *Journal of Fluid Mechanics*, **612**, 339–361.

Neufeld, J.A. & Wettlaufer, J.S. (2008b) An experimental study of shear enhanced convection in a mushy layer. *Journal of Fluid Mechanics*, **612**, 363–385.

Neufeld, J.A., Wettlaufer, J.S., Feltham, D.L., & Worster, M.G. (2006) Corrigendum to flow-induced morphological instability of a mushy layer. *Journal of Fluid Mechanics*, **549**, 442–443.

Notz, D., & Worster, M.G. (2009) Desalination processes of sea ice revisited. *Journal of Geophysical Research*, **114**, 10.1029/2008JC004885.

Peltier, W.R. & Liu, Y. (2008) Brief communication arising: Peltier & Liu reply. *Nature*, **456**, 10.1038/nature07656.

Pertaya, N., Marshall, C.B., DiPrinzio, C.L. et al. (2007a) Fluorescence microscopy evidence for quasi-permanent attachment of antifreeze proteins to ice surfaces. *Biophysical Journal*, **92**, 3663–3673.

Pertaya, N., Celik, Y., DiPrinzio, C.L., Wettlaufer, J.S., Davies, P.L. & Braslavsky, I. (2007b) Growth–melt asymmetry in ice crystals under the influence of spruce budworm antifreeze protein. *Journal of Physics: Condensed Matter*, **19**, 412101.

Price, P.B. (2000) A habitat for psychrophiles in deep Antarctic ice. *Proceedings of the National Academy of Sciences USA*, **97**, 1247–1251.

Rempel, A.W., Waddington, E.D., Wettlaufer, J.S. & Worster, M.G. (2001) Possible displacement of the climate signal in ancient ice by premelting and anomalous diffusion, *Nature*, **411**, 568–571.

Robinson, C.H. (2001) Cold adaptation in Arctic and Antarctic fungi. *New Phytologist*, **151**, 341–353.

Rodrigo, J. (2000) Spring frosts in deciduous fruit trees – morphological damage and flower hardiness. *Scientia Horticulturae*, **85**, 155–173.

Romaní, A.M. & Sabater, S. (2000) Influence of algal biomass on extracellular enzyme activity in river biofilms. *Microbial Ecology*, **41**, 16–28.

Sumita, I., Yoshida, S., Kumazawa, M. & Hamano, Y. (1996) A model for sedimentary compaction of a viscous medium and its application to inner-core growth. *Geophysical Journal International*, **124**, 502–524.

Tammann, G. (1909) Zur überhitzung von kristalen. *Zeitschrift für Physikalische Chemie*, **68**, 257–269.

Thomson, E.S., Wettlaufer, J.S. & Wilen, L.A. (2005) Grain boundary melting in ice. *Bulletin of the American Physical Society*, **50**, 159.

Thomson, E.S., Wilen, L.A. &Wettlaufer, J.S. (2009) Light scattering from an isotropic layer between uniaxial crystals. *Journal of Physics: Condensed Matter*, **21**, 195407, 10.1088/0953-8984/21/19/195407.

Tomchaney, A.P., Morris, J.P., Kang, S.H., Duman, J.G. (1982) Purification, composition, and physical properties of a thermal hysteresis "antifreeze" protein from larvae of the beetle, *Tenebrio molit*or. *Biochemistry*, **21**, 716–721.

Urrutia, M.E., Duman, J.G. & Knight, C.A. (1992) Plant thermal hysteresis proteins. *Biochimicca et Biophysica Acta*, **1121**, 199–206.

Weeks, W.F. (1998) Growth conditions and the structure and properties of sea ice. In: *Physics* of *Ice-Covered Seas*, Vol. I (Ed. M. Leppäranta), pp. 25–104. Helsinki University Press, Helsinki.

Weeks, W.F. (2009) *On Sea Ice*. University of Alaska Press, Fairbanks.

Wetherbee, R., Lind, J.L., Burke, B. & Quatrana, R.S. (1998) The first kiss: establishment and control of initial adhesion by raphid diatoms. *Journal of Phycology*, **34**, 9–15.

Wettlaufer, J.S. (1992) Directional solidification of salt water – deep and shallow cells. *Europhysics Letters*, **19**, 337–342.

Wettlaufer, J.S. (1998) Introduction to crystallization phenomena in natural and artificial sea ice. In: *Physics of Ice-Covered Seas*, Vol. I (Ed. M. Leppäranta), pp. 105–194. Helsinki University Press, Helsinki.

Wettlaufer, J.S. & Dash, J.G. (2000) Melting below zero. *Scientific American*, **282**, 50–53.

Wettlaufer, J.S. & Worster, M.G. (2006) Premelting dynamics. *Annual Review of Fluid Mechanics*, **38**, 427–452.

Wettlaufer, J.S., Worster, M.G. & Huppert, H.E. (1997) Natural convection during solidification of an alloy from above with application to the evolution of sea ice. *Journal of Fluid Mechanics*, **244**, 291–316.

Wilen, L.A. (2000) A new technique for ice-fabric analysis. *Journal of Glaciology*, **46**, 129–139.

Wilen, L.A. & Dash, J.G. (1995a) Frost heave dynamics at a single crystal interface. *Physical Review Letters*, **74**, 5076–5079.

Wilen, L.A. & Dash, J.G. (1995b) Giant facets at ice grain-boundary grooves. *Science*, **270**, 1184–1186.

Worrall, D., Elias, L., Ashford, D. et al. (1998) A carrot leucine-rich-repeat protein that inhibits ice recrystallization. *Scie*nce, **282**, 115–117.

Yeh, Y. & Feeney, R.E. (1996) Antifreeze proteins: structures and mechanisms of function. *Chemical Reviews*, **96**, 601–618.

Zepeda, S., Yokoyama, E., Uda, Y., Katagiri, C. & Furukawa, Y. (2008) *In situ* observation of antifreeze glycoprotein kinetics at the ice interface reveals a two-step reversible adsorption mechanism. *Crystal Growth* & *Design*, **8**, 3666–3672.

Glossary

Abiotic: Non-living, non-biological usually describing factors in an ecosystem such as atmospheric gases, inorganic salts, mineral soil particles and water. This expression is also used to describe the chemical and physical factors, such as temperature, salinity and humidity, which influence organisms.

Ablation: The sum of processes through which an ice cover is losing mass, either to the air (evaporation, erosion and resuspension of snow) or the water (surface melt and run-off, bottom melt).

Acantharia: Amoeboid protozoa that produce strontium sulphate skeletal structures.

Accessory pigment: Photosynthetic pigment that traps light energy and channels it to chlorophyll *a*, the primary pigment, which initiates the reactions of photosynthesis. Accessory pigments include the carotenoids, phycobiliproteins and chlorophylls *b*, *c* and *d*.

Acoel: Lack of a coelom (body cavity).

Aeolian: Processes including the erosion, transport and deposition of material by wind.

Aerobic: Aerobic microorganisms (aerobes) are those that require oxygen for growth; obligate aerobes cannot survive in the absence of oxygen. The opposite are anaerobic organisms, which do not require oxygen for growth; obligate anaerobes cannot survive in the presence of oxygen.

Albedo: The fraction of the incident shortwave radiation (at wavelengths between 0.4 and 1.5 mm) that is reflected from a surface (i.e. the ratio between the upwelling and downwelling shortwave radiation at a reference level above a given surface).

Algae: General term for eukaryotic, chlorophyll-containing, oxygen-producing photosynthetic non-vascular organisms that live almost exclusively in aquatic environments.

Amphipods: A member of an order of crustaceans, Amphipoda, with over 4600 species. They are generally flattened laterally and look hunchbacked, sometimes even swimming on their sides.

Anaerobic: See **aerobic**.

Anoxygenic photosynthetic purple sulphur bacteria: Non-oxygen-evolving bacteria that use energy from sunlight and electrons from hydrogen sulphide to obtain carbon from carbon dioxide for growth. They are anaerobic and are found in illuminated anoxic zones of aquatic environments.

Antarctic Bottom Water (AABW): A cold, relatively saline dense bottom water mass that forms around the edge of the Antarctic continent, particularly in the Ross and Weddell Seas. It spreads northwards into all three ocean basins.

Antarctic Circumpolar Current (ACC): The major current system that flows eastwards around the Antarctic continent under the influence of the strong prevailing winds (sometimes called the West Wind Drift).

Antarctic Circumpolar Wave (ACW): A propagating wave observed to cause disruptions at the sea ice margin and moves around the Antarctic with a period of approximately 8 years and a wave number of 2.

Anticyclonic: Flow around a region of high pressure (whether atmospheric pressure or dynamic height). In the northern hemisphere it is clockwise, in the southern hemisphere it is anticlockwise.

Antifreeze proteins (AFP) and antifreeze glycoproteins (AFGP): Proteins produced by an organism in order to prevent freezing of its tissues or body fluids when subjected to sub-zero environmental temperatures. Many animals living in cold climates adopt a strategy of preventing ice formation in their tissues when subject to freezing conditions. One way of achieving this is to accumulate solutes in their blood, thereby raising the osmotic concentration and so depressing the freezing point.

Archaea: One of the three major domains of life (the other two are the **Bacteria** and the **Eukarya**) and one of two of these domains (the other is the Bacteria) that encompasses only prokaryotic microorganisms. Many of the cultured species of Archaea are associated with extreme environments.

Arctic Oscillation (AO): A pattern of atmospheric circulation related to variation in atmospheric pressure differences between polar and middle latitudes on timescales of weeks to decades. Different phases of the AO bring differing atmospheric circulation patterns in the Arctic.

Atlantic Meridional Overturning Circulation (AMOC): The Atlantic component of the global thermohaline circulation.

Atlantic Water (AW): Warm and saline water mass that originates in the Gulf Stream and is carried northwards in the North Atlantic Current. AW is a major source of heat into the Arctic where it enters through the Fram Strait and the Barents Sea.

Authigenic: Applied to materials, particularly minerals, that formed in place (in the rock of which they are a part) during, or soon after, their deposition.

Autotrophic: The ability to utilize inorganic carbon (usually CO_2) as the sole source of carbon for organic synthesis, based on energy from light (photoautotrophic) or from oxidation of inorganic compounds (chemoautotrophic).

Avifauna: All the bird species that occur in a region.

Bacteria: One of the three domains of life (the other two are the **Archaea** and the **Eukarya**) and one of the two of these domains (the other is the Archaea) that encompasses only prokaryotic microorganisms. Many of the cultured Bacteria are associated with heterotrophy. When not capitalized, the term bacteria is often used to refer to natural microbial assemblages that may contain both Bacteria and Archaea.

Baleen whale: Large cetacean, whose mouth is lined with bristles which are used to strain food from sea water (the larger species are referred to as 'great whales', but the latter also includes sperm whales which have teeth).

Bacterivore: An organism that feeds on bacteria.

Benthic: Refers to the sea floor, or waters in contact with the sea floor; see also **mesopelagic**.

Benthos: In freshwater and marine ecosystems, the collection of organisms attached to, or resting on, the bottom sediments (epifaunal), and those which bore or burrow into the sediments (infaunal).

Biogenic: Applied to material produced by living or once-living organisms; sometimes also applied to the biological processes or activities leading to the production of such material.

Biogeochemistry: Science concerned with the effects of living things on sub-surface geology; or with the distribution and fixation of chemical elements in the biosphere.

Biomass: The total mass of all the organisms of a given type and/or in a given area; may be expressed in terms of wet weight, dry weight or the mass of a key component of the organisms of interest (carbon, chlorophyll, etc.).

Biosiliceous sediment: Sediment derived from the siliceous components of living or once-living organisms.

Bottom water: This is the general term for water which occupies the deepest part of the water column. See **Antarctic Bottom Water**.

Boundary current: An ocean current that is part of a sub-tropical gyre and is close to the boundary of an ocean basin. Western Boundary Currents are relatively intense, warm, narrow and deep currents forming on the western limb of a sub-tropical gyre. Eastern Boundary Currents are generally slow, wide and diffuse and transport cool water towards the equator.

Brackish water: A mixture of freshwater and sea water, with a salinity less than 30; see also **hyposaline**.

Buoyancy: A force generated by differences in density (generated by changes in the temperature or salinity of the water) generally causing water to rise or sink relative to its surroundings.

Carnivore: An animal that feeds largely or exclusively on other animals. The term is used most frequently for members of the order Carnivora, which includes flesh-eating mammals such as dogs, cats, bears and seals, but is also appropriate for some fish, crustacea and other marine animals.

Cascade: The descent of cold dense shelf waters down the continental slope often in a plume.

Chemosynthesis: The use of the energy contained in reduced inorganic compounds to synthesize organic material from carbon dioxide and water. See **autotrophic**.

Chemotaxis: The movement of a cell or a microorganism in response to an external chemical stimulus.

Chlorophyll: A group of green pigments in photosynthetic organisms involved in harvesting light by absorption, excitation and transfer of energy.

Choanoflagellate: Small (usually ≤10 μm), flagellated protozoa that consume bacteria.

Chrysophyte/Chrysomonad: Small (usually ≤10 μm) flagellated protists that include the golden-brown algae and non-pigmented forms that consume bacteria and other small microorganisms.

Ciliates: Protozoans, usually up to 0.15 mm long, which swim actively, engulfing small food particles via mouth and gullet.

Cold Halocline Layer (CHL): The boundary that marks the bottom of the mixed layer in the Arctic Ocean. There is a rapid increase in salinity with depth whilst the temperature remains almost isothermal and usually very close to the freezing point, hence the term Cold Halocline Layer.

Convection: Movement of a fluid resulting from density instabilities. In seawater, convection is usually driven by surface cooling or by increased surface salinity due to evaporation or brine rejection from sea ice. In the snow covering the ice, the fluid is air, and its movement can be the result of buoyancy differences due to variations in temperature, or forced by surface winds.

Copepodids (copepodite stages): Copepods in their larval stage.

Copepods: Small aquatic crustacea of the class Copepoda, without a carapace and with paddle-like feet. Many are minute (<1 mm) but they form a major component of marine plankton.

Cryopelagic: Environment including sea ice and the underlying water.

Cryoprotectant: A compound that prevents freezing of cellular structures. An antifreeze.

Cryosphere: Frozen water, in the form of snow, floating ice (freshwater or saline), permafrost, glaciers and ice sheets, that constitutes a component of the Earth's surface and near-surface layers, interacting with the oceans, atmosphere and crust.

CTD: An oceanographic sensor that measures conductivity, temperature and pressure (the 'D' stands for the implicit conversion to depth). From these three parameters, the salinity and density of the water can be calculated.

Cyclonic: Flow around a region of low pressure (whether atmospheric pressure or dynamic height). In the northern hemisphere it is anticlockwise, in the southern hemisphere it is clockwise.

Cyst: A resistant structure, usually a resting stage, produced by many bacteria and protists.

Denitrification: A microbial, or biochemical, process whereby nitrate from the environment (soil, sediment, water, ice) enters the cell and is reduced to molecular nitrogen which, as a gas, can be released to the atmosphere. This process is mediated only by denitrifying bacteria, which use nitrate in the production of energy (in the chemical form of ATP) for other biochemical reactions in a manner similar to oxygen respiration by aerobic organisms.

Densificiation: The process by which the snow cover compacts and reduces its porosity while increasing its density.

Depth hoar: A type of coarse-grained snow that forms when there is a strong temperature gradient across the snow pack. Depth hoar is typically brittle and weak, therefore a highly insulative type of snow.

Detritivores: Animals that feed on detritus. Detritivores play an important role in the breakdown of organic matter from decomposing animals and plants.

Detritus: Particulate organic material derived from dead organisms.

Diatoms: Bacillariophyceae, unicellular algae with a cell wall of amorphous silica. Adapted to a wide range of pelagic, benthic and sympagic aquatic habitats.

Dimethyl sulphide (DMS): A volatile sulphur compound produced by marine algae (phytoplankton and ice algae) and released to the atmosphere. Following oxidation to sulphate particles, DMS affects the radiative properties of the atmosphere by reflecting solar radiation and by affecting the concentration of cloud condensation nuclei (CCN). DMS is the main natural source of sulphate aerosols and the major route by which sulphur is recycled from the ocean to the continents. The production of dimethylsulphoniopropionate (DMSP, the precursor of DMS) in the ocean is strongly dependant on the algal species.

Dimethylsulphoniopropionate (DMSP): See **dimethyl sulphide (DMS)**.

Dinoflagellate: A single-celled eukaryotic microorganism capable of limited propulsion through use of whip-like flagella.

Dispersal: Movement or transport from an area of birth or growth to another area.

Draft: The thickness of the ice underside below the water level.

Drift ice: Any area of sea ice that is not land fast (fast ice); it is mobile by virtue of not being attached to the shoreline or something else.

Ectotherms: All animals except birds and mammals which exhibit poikilothermy, the passive variation in the internal body temperature of an animal, which depends on the temperature of the environment.

Ekman spiral: A spiral current generated in response to wind stress at the surface of the ocean. At the depth of frictional influence is the bottom of the Ekman layer and the current

direction has rotated to the right in the northern hemisphere and the left in the southern hemisphere. In both cases, at the bottom of the layer, the current is in the opposite direction of the surface current and 1/23 of the surface value.

Emissivity: The ratio of the radiation emitted by a surface to the radiation emitted by a blackbody at the same temperature.

ENSO (El Niño Southern Oscillation) cycle: Refers to the coherent, large-scale fluctuation of ocean temperatures, rainfall, atmospheric circulation, vertical motion and air pressure across the tropical Pacific.

Enthalpy of freezing or melting: The amount of energy that has to be supplied to, or removed from, a system in order for it to undergo a phase change from liquid to solid or vice versa (often also referred to as latent heat of freezing or melting). For pure ice, this amounts to 334 J g^{-1}, i.e. approximately 80 times the amount of heat required to warm a gram of water by 1 K.

Epiphyte: An organism living on the surface of a plant; also used to describe bacteria and other microorganisms living on the surface of photoautotrophic algae.

Epontic organism: An organism physically associated with sea ice, usually within the interstitial spaces between ice crystals or within the brine inclusions of the ice matrix.

Eukaryotes: Organisms belonging to the domain of **Eukarya**. Their cells each contain a nucleus with the DNA typically arranged in multiple chromosomes.

Euphausiids: Relatively large (10–70 mm) shrimp-like, holoplanktonic crustaceans of the phylum Arthropoda.

Euphotic zone: The topmost layer of a lake or sea receiving sufficient light to support net primary production. The depth varies, depending on such factors as turbidity, supply of nutrients in the water, tidal turbulence and temperature. For example, high nutrient levels will encourage a greater biomass of phytoplankton near the surface, which causes shading and consequent reduction in depth of the euphotic zone. It typically ranges from less than 1 m to about 30 m in lakes and coastal waters, and rarely reaches depths greater than 200 m in the open ocean.

Euryhaline: Able to tolerate a wide range of salinities.

Eutectic: When two liquids are mixed, the mixture typically freezes at a lower temperature than either pure substance. The solute composition with the lowest melting point is called the eutectic from the Greek for 'easily melted'.

Extremophile: A microorganism that thrives under extreme environmental conditions, usually specified by temperature, pH, salinity, pressure or nutrient deprivation.

Fast ice: Permanent, often multi-year, ice covering oceanic/fjord water which is literally stuck 'fast' to the continent or to some other fixed objects such as islands, ice shelves, grounded icebergs or peninsulas (also called land-fast ice).

Fatty acid: An organic acid with a long straight hydrocarbon chain and an even number of carbon atoms. Fatty acids are the fundamental constituents of many important lipids, including triglycerides. In aimals, some fatty acids can be synthesized by the body; others, the essential fatty acids, must be obtained from the diet.

First-year ice: Sea ice of not more than one winter's growth, developing from young ice and having a thickness >30 cm and usually with snow cover. Level when undeformed, but where ridges and hummocks occurs, it is rough and sharply angular.

Flagellates: Autotrophic, mixotrophic or heterotrophic protists, which have one or more flagella.

Flaw polynya: Wind-induced openings in the ice cover that usually separate fast ice and drifting ice in coastal areas.

Flooded ice: Sea ice with liquid water at the snow–ice interface caused by negative freeboard due to snow loading.

Fluorescence: Emission of light of a certain wavelength when activated by light of another, lower wavelength.

Foraminifer: A protozoan of the mainly marine order Foraminifera, having a perforated shell through which amoeba-like pseudopodia emerge. The shells eventually drop to the sea bed to form calcareous ooze. Fossil deposits of foraminifers form the main constituent of chalk.

Frazil ice: Fine spicules or plates of ice suspended in water during ice formation.

Freeboard: The height of the ice surface above water level.

Freezing point: Temperature of thermodynamic equilibrium between ice and the surrounding solution (e.g. brine). See **melting point** for the discussion of non-equilibrium and the effect of antifreeze.

Frustule: Silica cell wall of a diatom, generally two per cell.

Gastropods: (Gastropoda) snails of the phylum Mollusca.

Global Circulation Model (GCM): A computer-based model that calculates and predicts what climate patterns will look like in a number of years. The GCM programs use several equations at once and account for conservation of mass, energy and momentum in a grid box system. A given model focuses on each grid box and the transfer of energy between grid boxes. Once calculated you can determine a number of climate patterns, from ocean and wind currents to patterns in precipitation and evaporation rates that could affect lake levels and agricultural levels.

Glycolipid: Organic molecule containing both a sugar and a fat component.

Grazing: The consumption of algae or bacteria by protozoans and/or other fauna.

Grease ice: A soupy layer of ice at the water surface formed from the accumulation of frazil ice.

Gymnamoebae: Amoeboid protozoa lacking rigid skeletal structures that prey on bacteria and other microorganisms.

Halotolerant: Able to withstand large changes in salinity.

Heat flux: The rate at which heat is transported through, or by, a material, e.g. water, air and ice; defined as the flow of energy per unit area per unit time.

Herbivore: An organism that feeds on plants or algae.

Heterotrophic: The ability to obtain carbon for organic synthesis by metabolizing organic materials.

High salinity shelf water (HSSW): A cold salty water mass formed through salt rejection from ice growth on the shallow coastal regions of Antarctica. HSSW is dense enough to cascade down the continental shelf to the sea floor and it is a precursor to AABW. However, the exact mechanism of its modification or contribution to the formation of AABW currently remains undetermined.

Holocene: The last 10,000 years (ka) of post-glacial deposition in the sedimentary record.

Holoplankton: Planktonic organisms that spend their entire lives in the water column, i.e. have a completely pelagic life cycle.

Hyperosmotic: The condition when an organism's total osmotic concentration is higher than that of the environment.

Hypersaline: More saline than sea water.

Hyposaline: Less saline than sea water.

Hyposmotic: The condition when an organism's total osmotic concentration is less than that of the environment.

Ice–albedo feedback: Due to the substantial contrast in albedo between the open and ice-/snow-covered ocean, the former absorbs more than 90% of the incoming solar radiation whereas the latter typically absorbs less than 30%. Hence, changes in the extent or albedo of the ocean's sea ice cover, e.g. triggered by the effects of anthropogenic atmospheric warming, can lead to an amplification of such perturbations, since a reduction in ice extent provides more solar heat to the ocean which in turn helps reduce the ice cover even further (and vice versa in the case of cooling).

Ice area: The actual area covered by ice. It is the sum of the product of the ice concentration and the area of each data element in the ice-covered ocean.

Ice-binding proteins: Proteins produced by an organism that interact with and alter the surfaces of ice crystals.

Ice concentration: The percentage of ice-covered surfaces within the satellite footprint or grid. Often expressed as a fraction of 10, i.e. on a scale from 1/10 to 10/10. (Also sea ice concentration).

Ice edge: The demarcation between ice-free ocean (or sea) and ice-covered ocean (or sea) and is usually set at 15% ice concentration when using satellite microwave data. Definition depends on scale. At smallest scale, refers to the edge of fast ice (where it meets open water) in bays. At the largest scale, the ice edge refers to where the pack ice meets the open sea.

Ice extent: The sum of the area of all data elements which have at least 15% sea ice concentration. (Also sea ice extent).

Ice floe: A discrete section of sea ice that varies in area from a few square metres to the area of a small town.

Ice mass balance: The evolution of ice thickness through growth and melt processes.

Ice-obligate (or ice specific) species: An organism that is always found in the presence of sea ice, and which inhabits only those areas where sea ice is a major feature for most of the year.

Ice-rafted debris (IRD): Sediment transported to the deep sea by the melting of floating icebergs.

Infauna: Aquatic animals that live within the bottom substratum rather than on its surface; see also **benthos**.

Infrared radiation: Electromagnetic radiation whose wavelength lies in the range from 0.75 to 1000 mm. Thermal infrared radiation lies in the range from 9 to 14 mm.

Interannual: Refers to the year-to-year variation in an environmental property, such as wind strength or sea ice cover.

Interstitial fauna: Animals that live in the space between adjacent particles in a porous medium (sea ice or sediment).

Inuit: A member of the indigenous peoples inhabiting northernmost North America from northern Alaska to eastern Canada and Greenland.

Iso-osmotic: The condition when an organism's total osmotic concentration is the same as that of the environment.

Isopycnal: A line or surface joining points of equal density in the oceans (*cf*. isohaline which joins points of equal salinity and isotherm which joins points of equal temperature).

Katabatic wind: A strong wind which carries dense cold air down a slope under gravity. In the polar regions, they are often in an offshore direction. The cold air and strong winds promote sea ice growth.

Kleptoparasite: An animal species that steals food from other species.

Kleptoplastidy: Stealing the functional chloroplasts from algae.

Krill: Norwegian word meaning whale food, usually referring to schooling crustaceans of the family Euphausiacea. Often specifically *Euphausia superba* of the Antarctic Ocean.

Latent heat: The amount of energy in the form of heat released or absorbed by a chemical substance during a change of state (i.e. solid, liquid or gas).

Lead: A linear feature of open water that occurs in the ice pack between ice floes caused by ice break-up (see **ice floe**), which may be covered by new ice, especially in winter.

Lithogenic sediment: Sediment derived from the weathering of rocks. See **terrigenous sediment**.

Lithology: A term applied to sediments, referring to their general characteristics or variation in composition and texture.

Lorica: Protective covering that surrounds an algal cell.

Lower Halocline Water (LHW): The most saline water which exists at the bottom of the Cold Halocline Layer.

Lysis: Rupturing of a cell and loss of cell contents. Cell death often mediated by viruses.

Marginal ice zone: A geographical zone at the ice edge where ice floes are relatively loose and influenced by waves.

Marginal sea: Sea part of an ocean that is partially enclosed by land, such as islands or peninsulas.

Marine snow: Detritus, primarily organic, that aggregates in the upper, photic, layers of the water column and then drifts downwards through the water column.

Meiofauna: Small animals that live between sediment particles in the seabed or between ice crystals in sea ice. See **interstitial fauna**.

Melting point: See **freezing point**; there should be no difference between the freezing and melting temperatures of a solution at equilibrium. In a solution containing molecular antifreeze, however, an ice crystal may not increase in size until the solution is further cooled. The extent of cooling prior to crystal growth depends on, for example, type and concentration of antifreeze. If, subsequent to freezing, the temperature of a solution is increased, melting of the ice does not occur at the freezing point but only at a higher temperature.

Meroplankton: Planktonic organisms that spend only part of their life cycle in the water column, e.g. eggs and larvae of benthic species.

Mesopelagic: Refers to organisms that rarely, if ever, ascend to surface waters, but which also are not found at the seafloor.

Metazoans: Multicellular animals, as opposed to single-celled animals or **protozoans**.

Microstructure: A term commonly used in the study of snow and ice (and other geophysical or geological disciplines) to describe the size, shape and spatial arrangement of component phases in a particular medium. In the case of sea ice, this description would include in particular the size, shape and distribution of brine and gas inclusions, as well as that of individual ice crystals harbouring such inclusions. While usage of this term and the related term of 'texture' varies widely in different fields, microstructure is typically limited to the scale of individual grains or small groups of grains, whereas texture describes features that relate to the larger scale patterns of grain arrangement and orientation.

Microwave radiation: Electromagnetic radiation with wavelength ranging from 0.3 to 30 cm corresponding to frequencies from 1 to 100 GHz.

Mixotroph: An organism with the ability to obtain carbon for organic synthesis from either inorganic sources (autotrophy) or organic materials (heterotrophy).

Molt: the process during which birds renew their feathers and animals their fur; usually done once per year during well-bounded periods (i.e. usually not a continuous process).

Multi-year ice: Ice of more than one year's growth (thickness over 2 m). Hummocks and ridges are smooth and the ice is almost salt-free.

Mycosporine-like amino acid (MAA): A molecule that absorbs light strongly in the UV range. Many organisms produce this molecule for use as a 'sunscreen'.

Mysids: Shrimp-like crustaceans of the phylum Arthropoda.

Natural experiment: A situation where natural forces act to produce a temporary excursion from the 'norm;' the altered patterns that develop provide insight into how processes are normally organized and not otherwise revealed.

Nauplii: Early developmental stage in many crustaceans such as copepods and euphausiids.

Nematodes: (Nematoda) small cylindrical roundworms of the phylum Aschelminthes.

Neritic: Pertaining to shallow waters.

New ice: A general term for newly formed ice, which includes frazil ice, grease ice, shuga and nilas.

Nilas: Undeformed new ice formed in non-turbulent conditions resulting in uniform sheets of ice.

Nitrification: A microbial process whereby nitrogen (usually in the form of ammonia) present in plant and animal wastes, and dead remains, enters the cell and is oxidized to nitrite or nitrate. These reactions are mediated by the nitrifying Bacteria, *Nitrosomonas* and *Nitrobacter* and by the marine Crenarchaeota of the domain Archaea. See **denitrification**.

Non-photochemical quenching (NPQ): Processes that reduce fluorescence via pathways not related to primary phochemistry. Generally restricted to heat production via xanthophyll cycling and degradation of the D1 protein of photosystem II.

Non-polar: Areas outside polar areas. *cf*. **Polar**.

Omnivore: An animal that eats both animal and vegetable matter.

Osmo-conformers: Organisms that allows the solute concentrations of body fluids to vary in parallel with ambient salinity, at least over a certain range of salinity.

Osmolyte: Dissolved ion or organic solute within a cell that helps maintain an osmotic pressure within the cell equal to that outside the cell, thus avoiding cell lysis (too much internal pressure) or shrinkage (too little internal pressure).

Oxygen microelectrode: A small (often platinum) probe capable of measuring dissolved oxygen concentrations in small volumes.

Pack ice: All sea ice except that which is attached to terrestrial ice; see **fast ice**. The pieces of which then can be packed together by currents and winds (to become consolidated pack).

Pagophilic: A technical term meaning 'ice-loving', e.g. pagophilic seals are those which use ice for some period of their life cycle. The ice can be free-floating pack ice or fast ice.

Pancake ice: Predominantly circular pieces of ice from about 3 cm–3 m in diameter, less than 10 cm in thickness and with raised edges.

Pelagic: Describing organisms that swim or drift in a sea or a lake, as distinct from those that live on the bottom (see **benthos**). Pelagic organisms are divided into plankton and nekton.

Percolation: The process by which meltwater moves through the snow cover. It can take place in discreet pipe (called percolation columns) or as a general wetting front.

Perennial ice cover: The region of the Arctic and Southern Oceans which remain ice covered all year around.

Petrel: A seabird of the order Procellariiformes, other than albatrosses.

Phaeophorbide: Specific breakdown product of chlorophyll.

Phaeopigments: Degradation products of chlorophyll.

Phagotrophic: The ability to consume particles to obtain organic materials.

Phase: In the context of thermodynamics, a phase describes a microscopically homogeneous part of a system, with distinct boundaries separating it from other phases in the same system. In sea ice, these typically include the ice, liquid brine, gas inclusions (both in ice and brine) and salt precipitates or other mineral inclusions. A phase diagram delineates the limits of stability of different phases within a system, such as the complete absence of ice in a system composed of pure water at temperatures above 0°C.

Phospholipids: A group of lipids that consist of a phosphate group and one or more fatty acids. They are major components of cell membranes in plants and animals.

Photoacclimation: The ability of algae to respond relatively quickly to changes in light conditions. Photoacclimation responses can include changes in chloroplast configuration, pigment concentration and composition.

Photorespiration: A metabolic pathway that occurs in plants in the presence of light, in which ribulose bisphosphate carboxylase/oxygenase (RUBISCO), the enzyme involved in carbon dioxide fixation with ribulose bisphosphate, accepts oxygen, in place of carbon dioxide, resulting in the formation of a two-carbon compound, glycolate, which is subsequently metabolized to carbon dioxide. Unlike respiration, there is no production of adenosine triphosphate (ATP).

Photosynthesis: The process by which green plants and some unicellular organisms use energy from sunlight to synthesize carbohydrates from carbon dioxide and water.

Photosynthetically available radiation (PAR): Radiation at wavelengths between 400 and 700 nm (visible light) which are absorbed by algae for the process of photosynthesis.

Phytoplankton: The photosynthesizing organisms of the plankton, consisting chiefly of microscopic algae, such as diatoms and dinoflagellates. Near the surface of the sea, there may be many millions of such organisms per cubic metre.

Pisces: (Fish) aquatic vertebrates of the phylum Chordata.

Plankton: Pelagic organisms (mostly microscopic) that drift or float passively with the current in a sea or lake. Plankton includes many microscopic organisms, such as bacteria, algae, protozoans, various animal larvae and some worms. It forms an important food source for many other members of the aquatic community and is divided into **zooplankton** and **phytoplankton and bacterioplankton**.

Plastiquinone pool: Pool of electron acceptors associated with the potosynthetic apparatus. Part of the light reactions of photosynthesis.

Platelet ice: Leaf or disc-like ice crystals either free floating or fixed under sea ice, usually fast ice.

Plume: A column of water of one density which descends through water of a different density. In polar regions, plumes can under certain conditions be dense enough to reach the sea floor. They increase in volume as they descend from their source because the surrounding waters are entrained into the plume. This changes the properties of the plume and the resulting density difference between the plume and the water through which it descends.

Polar: Areas near the geographical poles, such as poleward of the Arctic or Antarctic Circles, although the definition of polar regions can also be made used by vegetation zones, mean annual air temperature, permafrost distribution, etc.

Polar Front (PF): The northern boundary of the Antarctic Circumpolar Current.

Polychaetes: (Polychaeta) marine segmented worms of the phylum Annelida. Some are planktonic, but most are benthic, many with meroplanktonic larvae.

Polynya: A Russian word referring to persistently open area within the pack ice. A non-linear open body of water enclosed by ice that may be formed as a latent heat (or coastal) polynya, formed near coastal areas or islands by wind displacement, or as a sensible heat (or deep ocean) polynya formed by the upwelling of warm water.

Polysaccharide: Any of a group of carbohydrates comprising long chains of monosaccharide (simple sugar) molecules.

Polyunsaturated fatty acids (PUFA): Fatty acids with two or more double bonds. Organic acids consisting of carbon chains with a carboxyl group at the end. The nutritionally important fatty acids have an even number of carbon atoms, commonly between 12 and 22.

Potential temperature: The *in situ* temperature of sea water at depth after correction for the effects of adiabatic compression. It is always lower than the measured *in situ* temperature.

Predation: The consumption of animals (or bacteria). Predators include protozoans and zooplankton. *cf*. **Grazing**.

Pressure ridge: An elongated ridge or wall of broken ice forced up by ice pressure between two ice floes.

Primary production: The photosynthetic carbon fixation per unit area, per unit of time.

Prokaryotes: A term describing the organisms that belong to the Bacteria and Archaea, two of the three domains of life (see **Eukaryotes**), lacking a cellular nucleus and typically having DNA arranged as a single circular chromosome or genome.

Protist: General term for eukaryotic microbes (algae and protozoa). Also used more specifically to refer to species in Protista in a five-kingdom taxonomy (with Monera, Fungi, Planta and Animalia) – but this diverse group is commonly divided into several major groups at this level.

Protozoans: (Protozoa) microscopic unicellular eukaryotic organisms that obtain their nutrition from the ingestion and digestion of preformed organic material.

Prymnesiophyta (Haptopyta): A phylum of algae, of which the bloom-forming genus *Phaeocystis* is a member.

Psychrophilic: Describing an organism that lives and grows optimally at relatively low temperatures, usually below 15°C, and cannot grow above 20°C. Psychrophiles consist mainly of bacteria, algae, fungi and protozoans; extreme psychrophiles can grow at sub-zero temperatures.

Psychrotolerant: Organisms that live and grow best at temperatures of 20–40°C, but are able to tolerate (and, in the case of bacteria, grow under) cold conditions.

Pycnocline: An increase in sea water density over a short depth change. It usually marks the lower boundary of the mixed layer.

Q_{10}: Change in physiological rate or biochemical reaction normalized to a 10°C change in temperature.

Quantum yield of photosynthesis (f_p): The amount of carbon fixed per unit of light absorbed.

Quaternary: The most recent period of geologic time in the stratigraphic column representing the last 2 million years.

Radiolaria: Large protozoa that produce siliceous skeletons.

Remineralize: Transforming organic materials into inorganic forms, such as organic carbon to CO_2.

Remote sensing: The gathering and recording of information concerning the Earth's surface by techniques that do not involve actual contact with the object or area under study. These techniques include photography (e.g. aerial photography), multispectral imagery, infrared imagery and radar. Remote sensing is generally carried out from aircraft and, increasingly, satellites.

Respiration: Utilization and decomposition of organic material by biological oxidation, central energy-gaining process for heterotrophic organisms.

Rheology: Study of deformation and flow of materials.

Ridge keel: The bottom section of a pressure ridge protruding below the level ice underside. Typically, ridge keels are 3–5 times thicker than ridge sails.

Ridge sail: The top section of a pressure ridge rising above the level ice surface.

Rossby radius of deformation: A length scale at which it becomes important to consider the rotation of the ocean in relation to flow. It is typically in the kilometre range but tends to be smaller in the polar regions because it is related to latitude.

Rotifer: A protozoan belonging to the phylum Rotifera (about 2000 species), also called wheel animalcule, found mainly in freshwater. Rotifers vary in shape from spherical to worm-like and range between 0.1 and 0.5 mm in length.

RUBISCO (Ribulose bisphosphate carboxylase/oxygenase): The enzyme that mediates the carboxylation of ribulose bisphosphate in the first stage of the dark reaction of photosynthesis.

Salps: Barrel-shaped planktonic tunicates of the phylum Chordata.

SAR: Synthetic Aperture Radar.

Scintillation counting: The technique used to measure the biological uptake of radionuclides such as ^{14}C-labelled bicarbonate by phytoplankton and algae or ^{3}H-thymidine by bacteria.

Sea ice concentration: The fraction of open water within sea ice cover, e.g. 0–15% = open ocean; 100% = continuous ice cover.

Seal: An animal from the family Phocinidae in the order Pinnipedia that has small front flippers and no visible external ear.

Sea lion: An animal from the family Otaridae in the order Pinnipedia that has large front flippers and has external ears (includes also fur seals).

Secondary production: Amount of new biomass produced by heterotrophic organisms.

Sensible heat: Potential energy in the form of thermal energy or heat.

Shuga: Spongy ice lumps, several centimetres wide, formed from a wind-driven accumulation of grease ice or slush.

Slush: A viscous mixture of snow and water.

Snow-ice: Ice formed from freezing of snow flooded or saturated with sea water; see also **flooded ice** and **slush**.

Snow–ice interface: The ice surface before the first snow fall.

Solute segregation: Ice does not incorporate most common sea salt ions and other impurities into its crystal lattice, hence these solutes are concentrated ahead of a freeze-front in a salt water system in a process referred to as segregation.

Species diversity index: Derived from combining the number of species with the number of individuals per species.

Spectrophotometer: An instrument that measures the absorbance of light by a substance, often at multiple wavelengths.

Stoichiometry: The ratios in which the reactants in a chemical reaction combine to form the products. For example, two moles of hydrogen react with one mole of oxygen, giving two moles of water. The stoichiometric equation summarizes this as $2H_2 + O_2 \rightarrow 2H_2O$. In stoichiometric compounds, the elements are present in simple whole number ratios: for example, the ratio is one to one in hydrogen chloride, HCl. In contrast, iron sulphide, Fe_xS, is a non-stoichiometric compound, x taking a range of values slightly less than one.

Strand community: An ice algal community that extends vertically into the upper water column from an ice floe. They can reach a metre or more in length and are generally restricted to Arctic regions.

Stratigraphy: The sequence of layers and units that constitute a sea ice and snow cover. Typically, the stratigraphy is derived from thick and thin sections produced from ice cores drilled through the entire thickness of a floe or in the case of snow from examination of snow layers in a pit. The stratigraphy is also crucial in establishing the growth history and evolution of an ice cover.

Succession: In ecology, replacement of one community by another.

Sulphate reduction: A process during which dissolved sulphate is reduced to hydrogen sulphide. This process is effected by anaerobic heterotrophic bacteria.

Supercooling: The degree to which the actual temperature of a water body has been lowered to below its equilibrium freezing point without the formation of ice. In the open ocean, with numerous biogenic and inorganic particulates aiding in the process of nucleation and ice formation, supercooling is typically less than 0.1 K. However, pure water in the absence of impurities and other potential sites for ice nucleation and growth, can be supercooled to more than 30 K below its freezing point.

Superimposed ice: Ice formed by the freezing of melted snow after deposition.

Sympagic: Organisms living with sea ice.

Teleosts: (Teleostei) fish with bony skeletons.

Terrigenous sediment: Sediment derived from the weathering of rocks. See **lithogenic sediment**.

Texture: Typically describes the spatial arrangement and orientation of (sea ice) grains at a scale somewhat larger than that relevant for the microstructure. See **microstructure**.

Thermal hysteresis: (Antifreeze activity) refers to the fact that the temperature at which an ice crystal grows in a solution containing the antifreeze is lower than the temperature at which the crystal is observed to melt.

Thermodynamics: The science of the relations between heat and other (mechanical, electrical, etc.) forms of energy, and, by extension, of the relationships and interconvertibility of all forms of energy.

Thermohaline: Referring to the combined impacts of temperature and salinity on sea water density. In the polar oceans, these impacts are dominated typically by salinity, in particular in such areas where the loss of highly saline brine from growing sea ice can substantially increase sea water density and induce convective overturning and amplify thermohaline mixing.

Thermohaline circulation: This is the circulation of the global oceans driven by differences in density. As sea water density is a non-linear function of temperature and salinity, it is called 'thermohaline'. Because of the increased importance of salinity in controlling the density of waters at cold temperatures in the polar oceans, the thermohaline circulation is

dominated by the impact of changes in salinity through processes such as sea ice generation and melt.

Thylakoid membrane: The membranes within a chloroplast that contain the photosynthetic apparatus.

Tintinnid: An order of ciliates whose cell bodies are contained in proteinaceous vase-shaped loricae (shells).

Triacylglycerol: An ester of glycerol (propane-1,2,3-triol) in which all three hydroxyl groups are esterified with a **fatty acid**. Triglycerides are the major constituent of fats and oils and provide a concentrated food energy store in living organisms.

Trophic: Used to describe feeding relationships, such as levels in a food chain.

Turbellarians: (Turbellaria) oval to elongated unsegmented flatworms of the phylum Platyhelminthes.

Turbulence: Small-scale motions in sea water that causes heat, salt and dissolved components to be mixed or dispersed through the water.

ULS: Upward looking sonar.

Vienna Standard Mean Ocean Water (VSMOW): The international standard by which samples of the oxygen isotopes $^{18}O/^{16}O$ are measured. On the scale used for oxygen isotope analysis $\delta^{18}O$ VSMOW has a value of 0‰.

Visible radiation: Electromagnetic radiation with wavelength ranging approximately from 4000 to 7700 Å and is capable of causing sensation to vision.

Wax ester: Organic compounds produced by the reaction of an alcohol with an acid, with the elimination of water.

Wind slab: A type of fine-grained snow that results from the pulverizing action of the wind on snow grains. Typically, wind slabs are structurally strong and therefore not very insulative.

Xenobiotic: Substances foreign to the body.

Young ice: Ice in the transition stage between nilas and first-year ice, 10–30 cm in thickness.

Zooplankton: Animals of the plankton. See **plankton**.

Index

Note: Page numbers in *italics* refer to figures and those in **bold** refer to tables.